

**FACULTAD DE INGENIERIA U.N.A.M.
DIVISION DE EDUCACION CONTINUA**

**CURSOS INSTITUCIONALES
METODOS EXPERIMENTALES DE ANALISIS DE ESFUERZOS**

**COMISION FEDERAL DE ELECTRICIDAD
DEL 28 DE FEBRERO AL 4 DE MARZO
IRAPUATO, GTO.**

- FOTOELECTRICIDAD
- EXTENSOMETRIA ELECTRICA

DR. LUIS FERRER ARGOTE

ING. ALFREDO OLIVARES PONCE

1994

a) Luz y Óptica relacionados a la Fotoelasticidad.

a.1. Comportamiento de la luz.

Hasta la fecha no existe una teoría que explique completamente el comportamiento de la energía radiante. Para describir el fenómeno fotoelástico, la teoría electro-magnética debida a Maxwell, es usualmente usada. Esta teoría establece que la luz es una perturbación electromagnética, donde esta perturbación puede ser expresada como un vector de luz normal a la dirección de propagación. En la luz ordinaria emitida por, digamos un filamento de tungsteno incandescente, el vector luz no está restringido en ningún sentido y puede considerarse que esta formado de un número de vibraciones transversales arbitrarias, como se ilustra en la figura 20.

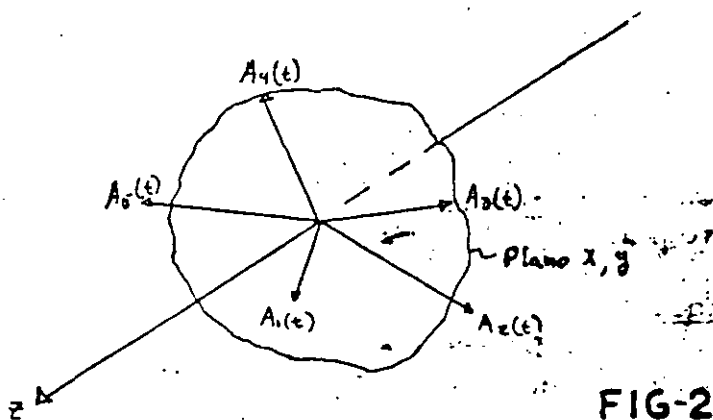


FIG-20

Ya que el disturbio productor de la luz, puede ser considerado como un movimiento ondulatorio, es posible expresar la amplitud del vector luz, en términos de una ecuación de onda unidimensional:

$$A = f(z-ct) + g(z+ct) \quad \text{Ec. 77}$$

donde A : amplitud del vector luz o de uno de sus componentes.

z : la posición a lo largo del eje de propagación.

t : tiempo.

c : velocidad de propagación (3×10^{10} cm/s en el vacío).

Una descripción simple del efecto fotoelástico, se obtiene considerando una componente senoidal de la luz, propagandose en la dirección positiva de z.

De esta manera la ecuación 77 puede escribirse como:

$$A = f(z-ct) = a \text{ Sen } \frac{2\pi}{\lambda}(z-ct) \quad \text{Ec. 78}$$

Una representación gráfica de la amplitud del vector luz (o uno de sus componentes) conforme se propaga en la dirección positiva del eje z está dada en la figura 21.

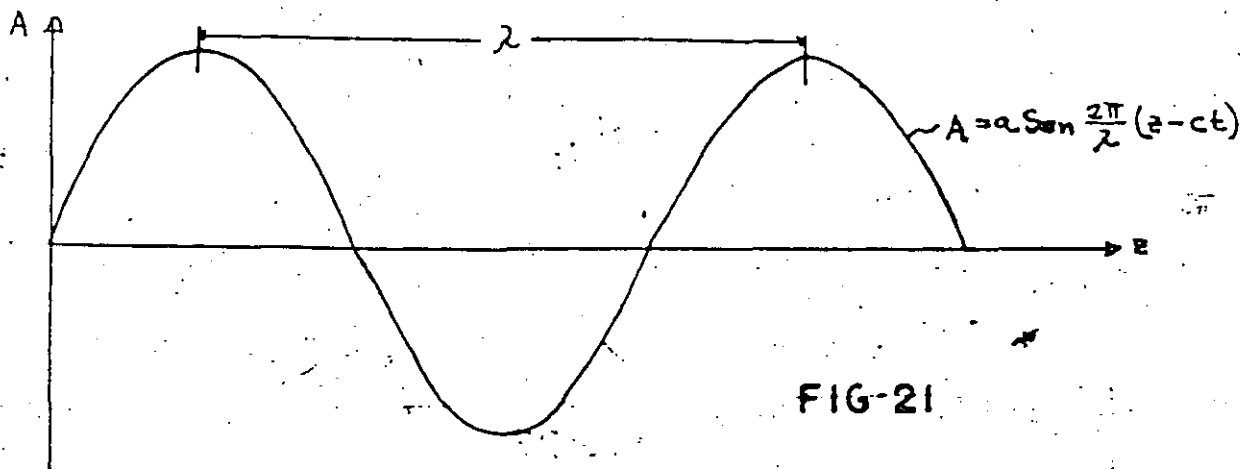


FIG-21

La longitud de pico a pico en la gráfica se define como la longitud de onda λ . El tiempo requerido para el paso de dos picos sucesivos, por algún valor fijo de z , se define como el período T y está dado por:

$$T = \lambda / c \quad \text{Ec. 79}$$

La frecuencia del vector luz o uno de sus componentes, se define como el número de oscilaciones de la amplitud en un segundo, por lo tanto es el inverso del período.

$$f = 1/T \quad \text{Ec. 80}$$

El color de la luz que el ojo humano reconoce, está determinado por la frecuencia de los componentes del vector luz. Los colores en el espectro visible van desde el rojo profundo, con una frecuencia de 390×10^{12} c.p.s., hasta el violeta profundo, con una frecuencia de 770×10^{12} c.p.s.

La mayoría de las investigaciones fotoelásticas se llevan a cabo con luz visible, - pero los principios de la fotoelasticidad son válidos en el rango infrarrojo y ultravioleta de la energía radiante.

Cuando el vector luz está compuesto de vibraciones A_1, A_2, A_3 , que tienen la misma frecuencia, el vector luz es monocromático y su color depende de la frecuencia. Si los componentes son de diferente frecuencia, los colores de los componentes se mezclan y el ojo registra esta mezcla como luz blanca.

a.2. Luz Polarizada.

Desde el punto de vista de la física clásica, la luz ordinaria consiste en ondas electromagnéticas cuya vibración es transversal a la dirección de propagación. Cuando el patrón de vibración de una onda electromagnética exhibe una dirección - preferente de vibración, la luz es considerada como polarizada.

Hay tres diferentes formas de luz polarizada que son actualmente empleadas en los métodos fotoelásticos del análisis de esfuerzos:

- 1) Luz polarizada plana. Se obtiene restringiendo la vibración del vector luz en un solo plano llamado plano de polarización. Figura 22.
- 2) Luz polarizada circular. Se obtiene cuando la punta del vector luz describe una hélice circular conforme se propaga a lo largo del eje z . Figura 23.
- 3) Luz polarizada elíptica. Se obtiene cuando la punta del vector luz describe una hélice elíptica conforme se propaga en la dirección z .

Notese que los casos 1) y 2) son casos particulares del caso 3).

En la práctica la luz polarizada plana puede ser producida con un elemento óptico conocido como polarizador lineal o plano.

La producción de luz polarizada circular o elíptica, requiere del uso de dos elementos ópticos. Estos arreglos se discutirán más adelante.

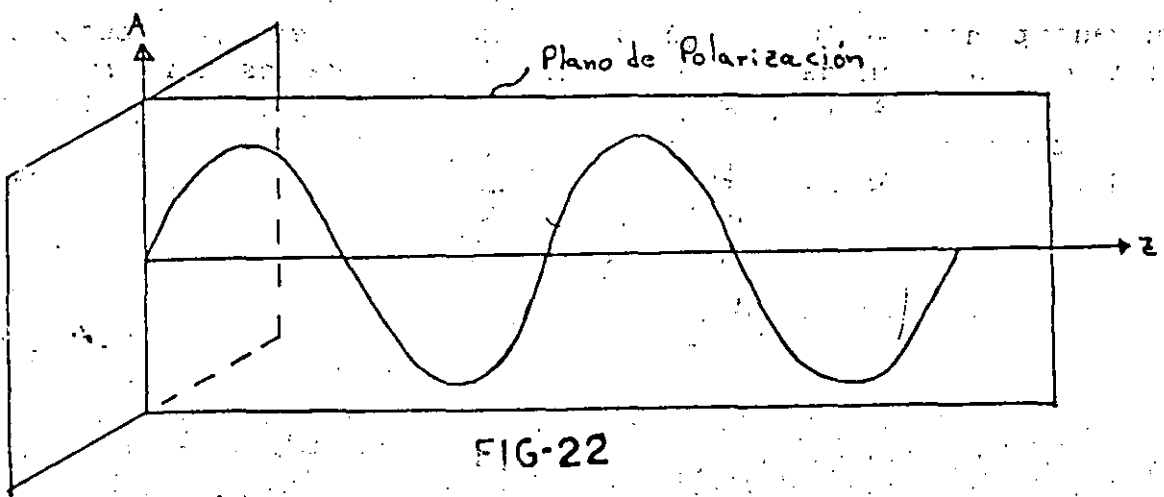


FIG-22

amp, periodo, def. fase $\pm \frac{\pi}{2}$

$$x = a \cos \omega t$$

$$y = a \sin \omega t$$

$$z = ct + e$$

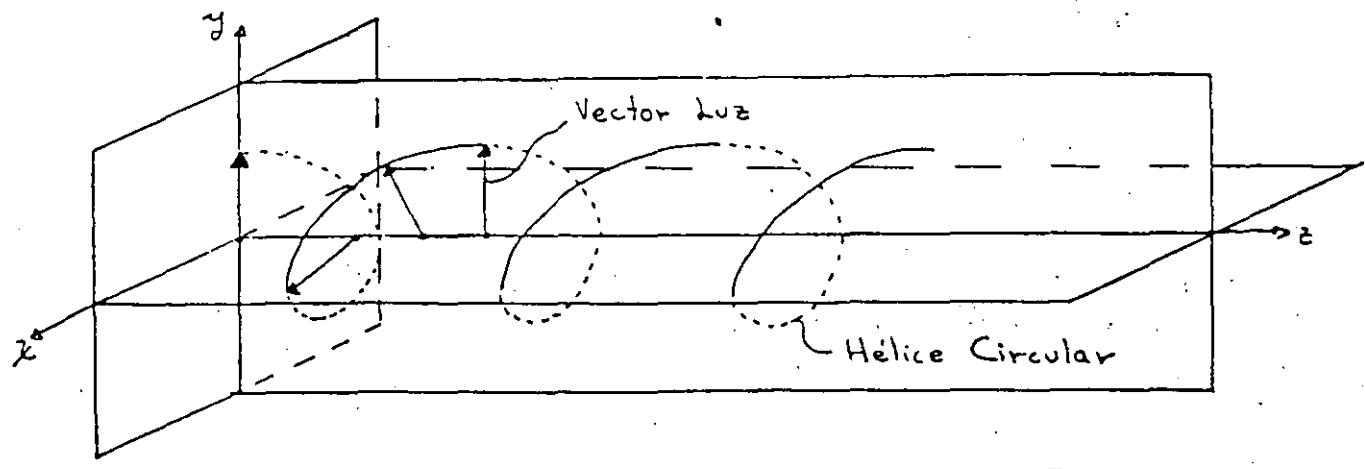


FIG-23

a.3. Polarizadores planos.

Los polarizadores planos son elementos ópticos que absorben los componentes del vector luz que no vibran en la dirección del eje del polarizador.

Cuando un vector luz pasa a través de un polarizador plano, este elemento óptico absorbe la componente perpendicular al eje de polarización y transmite la componente paralela, como se ilustra en la figura 24.

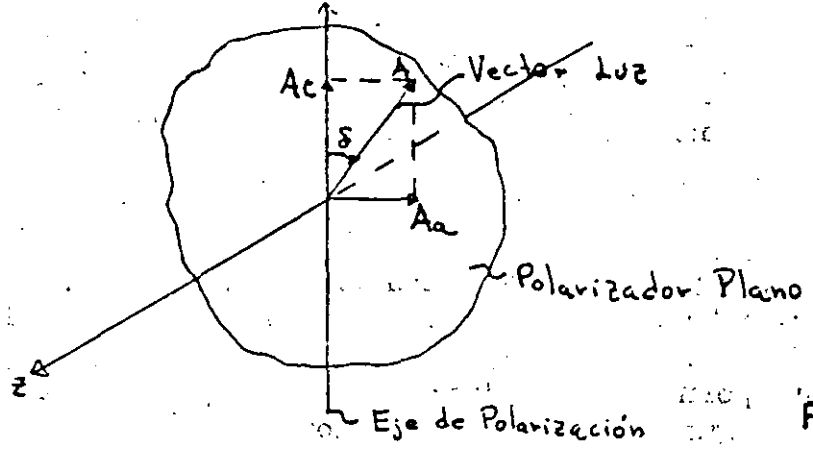


FIG-24

Si el polarizador plano está fijo en algún punto a lo largo del eje z, la ecuación para la amplitud del vector luz dada por la ecuación 78 puede ser escrita como:

$$A = a \text{ Sen } 2\pi/2 ct$$

que puede reducirse a:

$$A = a \text{ Sen } 2\pi ft = \underline{a \text{ Sen } \omega t}$$

Ec. 81

donde $\omega = 2\pi f$ es llamada la frecuencia circular de la luz.

Los componentes absorbido y transmitido del vector luz son:

$$A_a = a \text{ Sen } \omega t \text{ Sen } \delta$$

$$A_t = a \text{ Sen } \omega t \text{ Cos } \delta$$

Ec 82

donde δ es el ángulo entre el vector \vec{E} y el eje de polarización.

En la práctica los filtros polaroid producen un amplio campo de luz muy bien polarizada a un costo relativamente bajo.

En su manufactura, una lámina de alcohol polivinílico se calienta, se alarga, e inmediatamente se deposita en una lámina de acetato o celulosa. La cara de polivinilo de este ensamble, es teñida por un líquido rico en yodo. La cantidad de yodo difuso en la placa determina su calidad. La corporación Polaroid produce tres grados de calidad: HN-22, HN-32, HN-38. La HN-22 es la más recomendada para propósitos fotoelásticos.

a.4. Placas de Onda.

Ciertos materiales tienen la propiedad de descomponer el vector luz en dos componentes ortogonales y transmitir cada uno de ellos a diferentes velocidades. Un material con esta propiedad es llamado birrefringente.

La placa birrefringente mostrada en la figura 25 tiene dos ejes principales marcados como 1 y 2.

La transmisión de la luz a lo largo del eje 1 es a una velocidad C_1 , y a lo largo del eje 2 a una velocidad C_2 . Como $C_1 > C_2$, al eje 1 se le llama eje rápido y al 2 eje lento.

Si la placa birrefringente es colocada en el campo de un polarizador plano, de manera que el vector luz A_t es descompuesto en dos componentes A_{t1}, A_{t2} a lo largo de los ejes 1 y 2 respectivamente, (notese que el ángulo entre A_t y el eje rápido es θ), la magnitud de los componentes A_{t1}, A_{t2} será:

$$A_{t1} = A_t \cos \theta = a \cos \delta \sin \omega t \cos \theta = k \sin \omega t \cos \theta \quad \text{Ec. 8.7}$$

$$A_{t2} = A_t \sin \theta = a \cos \delta \sin \omega t \sin \theta = k \sin \omega t \sin \theta$$

donde $k = a \cos \delta$.

Los componentes A_{t1} y A_{t2} viajan através de la placa con velocidades diferentes C_1 , y C_2 respectivamente. Debido a esta diferencia de velocidades, los dos componentes emergerán de la placa en tiempos diferentes. O sea que un componente se atrasa relativamente al otro.

Este retardo puede ser manejado más eficientemente considerando el cambio relativo de fase entre los dos componentes, como se ve en la figura 26.

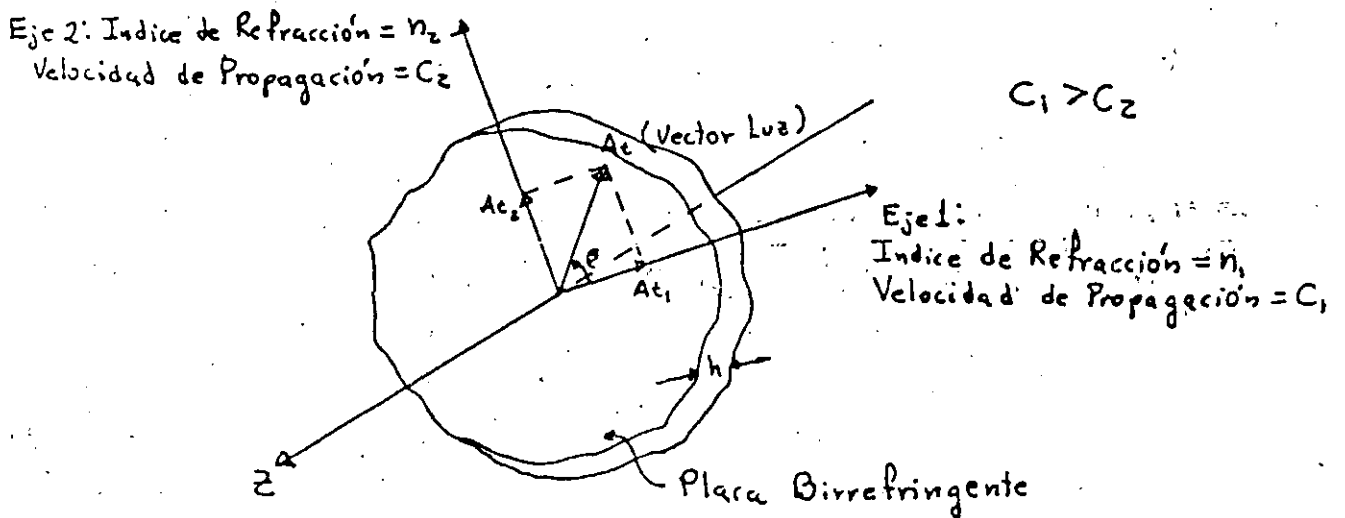


FIG-25

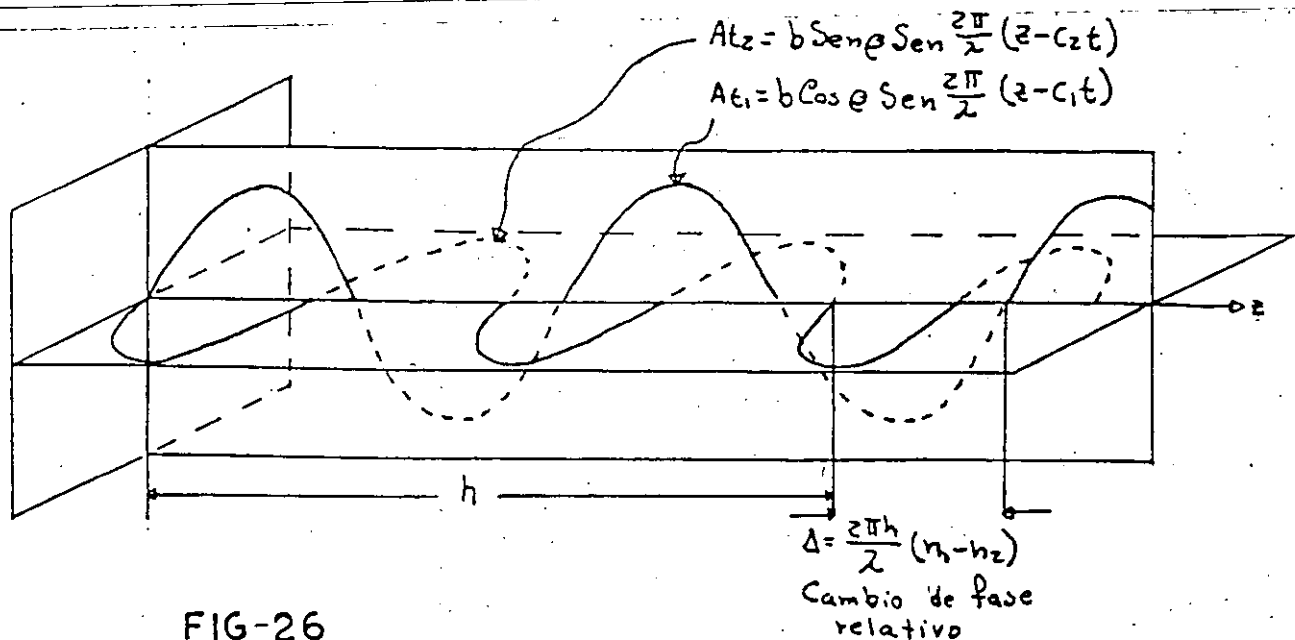


FIG-26

Para obtener este cambio de fase relativo, considere el retardo angular de cada componente, dado a continuación:

$$\Delta_1 = \frac{2\pi h}{\lambda} (n_1 - n) \quad \Delta_2 = \frac{2\pi h}{\lambda} (n_2 - n) \quad \text{Ec. 84}$$

donde n es el índice de refracción del aire.

La diferencia $\Delta_1 - \Delta_2$ representa el cambio de fase o la diferencia entre los dos componentes de luz cuando emergen de la placa de onda. Luego:

$$\Delta = \Delta_1 - \Delta_2 = \frac{2\pi h}{\lambda} (n_1 - n_2) \quad \text{Ec. 85}$$

El cambio de fase relativo producido por una placa birrefringente depende de su espesor h , de la longitud de onda de la luz λ , y las propiedades de la placa $n_1 - n_2$. Cuando la placa se diseña para dar un retardo angular de $\pi/2$, se le llama placa cuarto de onda.

Al emerger de una placa birrefringente, con un retardo Δ , los componentes de la luz serán:

$$A_{te}' = k \text{ Cos } \theta \text{ Sen } (wt + \Delta) \quad \text{Ec. 86}$$

$$A_{tz}' = k \text{ Sen } \theta \text{ Sen } wt$$

La amplitud del vector luz producida por estos dos componentes puede expresarse como:

$$A_{t'} = \sqrt{A_{te}'^2 + A_{tz}'^2} = k \sqrt{\text{Sen}^2 (wt + \Delta) \text{Cos}^2 \theta + \text{Sen}^2 wt \text{Sen}^2 \theta} \quad \text{Ec. 87}$$

El ángulo que el vector luz que emerge de la placa forma con el eje l es:

$$\text{Tan } \gamma = \frac{A_{tz}'}{A_{te}'} = \frac{\text{Sen } wt}{\text{Sen } (wt + \Delta)} \text{ tan } \theta \quad \text{Ec. 88}$$

Es claro que la amplitud y el ángulo de la luz que emerge de la placa, pueden ser controlados por la placa de onda. Los factores de control son Δ y θ . Varias combinaciones de Δ y θ y su influencia en el tipo de polarización de la luz producida se discutirán más adelante.

Las placas de onda empleadas en fotoelasticidad consisten de una simple placa de cuarzo o calcita, cortada paralelamente al eje óptico, una placa de mica, una hoja de celofán, o una hoja de alcohol polivinílico previamente orientada. Estas últimas son fabricadas por Polaroid Corporation, calentando y estirando unidimensionalmente la hoja de alcohol polivinílico. Como esta hoja es de solo 20 micrones de ancho, las placas comerciales son usualmente laminadas entre dos hojas de acetato o celulosa.

a.5. Luz condicionada por una serie de combinaciones de un polarizador lineal y una placa de onda.

La luz que emerge de una combinación en serie de un polarizador plano y una placa de onda, también es polarizada, sin embargo el tipo de polarización puede ser plano, circular o elíptico.

1) Luz polarizada plana:

Si el ángulo θ se escoge de 0° y el retardo relativo Δ no se restringe, la amplitud y dirección del vector luz que emerge será:

$$A_{\epsilon'} = k \sin(\omega t + \Delta) \quad ; \quad \gamma = 0 \quad \text{Ec. 89}$$

Como $\gamma = 0$, el vector luz no rota al pasar através de la placa de onda, luego la luz que emerge sigue siendo luz polarizada plana. La placa de onda sólo retarda la luz un ángulo igual a Δ . Iguales resultados se obtienen si $\theta = \frac{\pi}{2}$.

2) Luz polarizada circular:

Si se selecciona una placa cuarto de onda ($\Delta = \frac{\pi}{2}$) y θ se escoge de $\frac{\pi}{4}$, la amplitud de la luz emergente esta dada por:

$$A_{\epsilon'} = \frac{\sqrt{2}}{2} k \sqrt{\sin^2 \omega t + \cos^2 \omega t} = \frac{\sqrt{2}}{2} k \quad \text{Ec. 90}$$

Así que el vector luz que emerge de la placa tiene una amplitud constante. También se tendría que:

$$\nabla \tan \gamma = \nabla \tan \omega t \Rightarrow \gamma = \omega t \quad \text{Ec. 91}$$

o sea que el ángulo se incrementa continuamente.

De las ecuaciones 90 y 91, se ve que la punta del vector luz describe un círculo. Conforme la luz se propaga en el eje z, el círculo se transforma en una hélice circular con su eje coincidente con el eje z.

3) Luz polarizada elíptica:

Si se selecciona una placa cuarto de onda ($\Delta = \frac{\pi}{2}$), y se permite que θ sea cualquier ángulo menos 0 , $\frac{\pi}{4}$, $\frac{\pi}{2}$, o multiples pares, el vector luz que emerge de la placa tendrá una amplitud:

$$A_{\epsilon'} = k \sqrt{\cos^2 \omega t \cos^2 \theta + \sin^2 \omega t \sin^2 \theta}$$

El ángulo de salida será:

$$\nabla \tan \gamma = \nabla \tan \omega t \tan \theta$$

Ec. 92

Puede demostrarse que el vector luz descrito por las ecuaciones 92 constituyen luz polarizada elíptica.

Ya que la luz polarizada circular es la que se emplea más comunmente en la fotoelasticidad, es importante que la ecuación 85 se reexamine:

$$\Delta = 2\pi h / \lambda (n_1 - n_2)$$

Ec. 85

Recuérdese que la luz polarizada circular requiere una placa cuarto de onda, o sea que $\Delta = \frac{\pi}{2}$. Es claro que el espesor h puede ser determinado para que $\Delta = \frac{\pi}{2}$ una vez que el material ($n_1 - n_2$) y la longitud de onda de la luz han sido seleccionadas. Sin embargo una placa cuarto de onda para una longitud de onda dada, (luz monocromá-

tica) no será muy útil para diferentes longitudes de onda.

También debe notarse que no puede diseñarse una placa cuarto de onda para luz blanca ya que sus componentes poseen diferentes longitudes de onda.

a. 6. Arreglo de los elementos ópticos en un polaroscopio.

1) Polaroscopio plano.

Este es el sistema óptico más sencillo usado en la fotoelasticidad ya que consta de dos polarizadores lineales y una fuente de luz arreglados como se muestra en la figura 27.

El polarizador cercano a la fuente de luz recibe el nombre precisamente de polarizador. El polarizador más alejado de la fuente de luz se llama analizador. En el polaroscopio plano, los dos ejes de polarización están siempre cruzados, de manera que no se transmite luz através del analizador, y éste sistema óptico produce, por lo tanto, un campo oscuro.

Bajo operación, un modelo fotoelástico se introduce entre los dos elementos y se observa através del analizador. El comportamiento del modelo fotoelástico en un polaroscopio plano se verá más adelante.

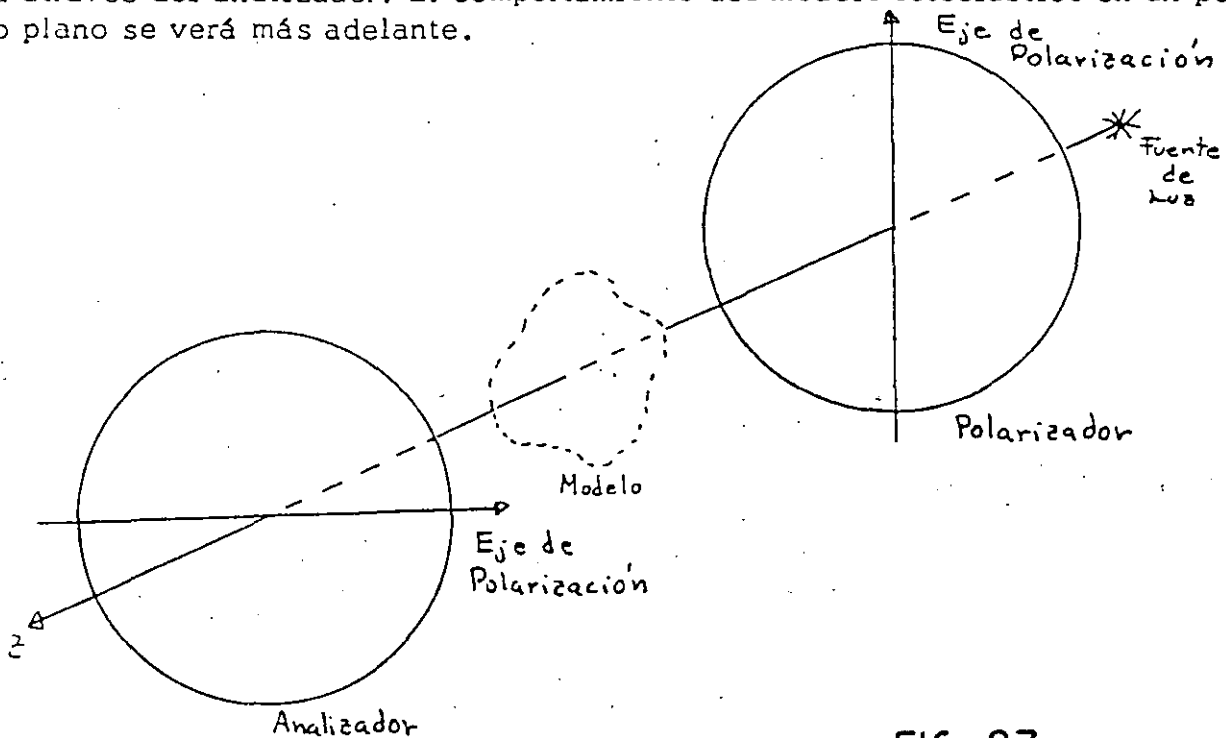


FIG - 27

2) Polaroscopio circular.

Como su nombre lo indica, este polaroscopio emplea luz polarizada circular; consecuentemente el aparato posee cuatro elementos ópticos y una fuente de luz como se observa en la figura 28.

El primer elemento después de la fuente de luz se llama polarizador, el cual convierte la luz ordinaria en luz polarizada plana. El segundo elemento es una placa cuarto de onda con un ángulo $\theta = \frac{\pi}{4}$ con respecto al eje de polarización, convierte la luz polarizada plana en luz polarizada circular. El tercer elemento (placa cuarto de onda) se coloca con su eje rápido paralelo al eje lento de la placa anterior; el propósito de este elemento es convertir la luz polarizada circular en luz polarizada plana que

vibra de nuevo en el plano vertical. El último elemento es el analizador con su eje de polarización horizontal, y su propósito es extinguir la luz. Esta serie de elementos ópticos producen un campo oscuro.

Actualmente se emplean cuatro arreglos de los elementos ópticos del polaroscopio circular, dependiendo de si las placas y los polarizadores son paralelos o cruzados (tabla 2).

Los arreglos A y B se recomiendan para campos oscuros y claros respectivamente, ya que el error introducido por las imperfecciones de las placas cuarto de onda, - (ambas difieren por ejemplo de $\Delta = \pi/2$ una cantidad dada), se cancelan. Ya que las placas cuarto de onda pueden ser de baja calidad, este hecho debe tenerse en cuenta.

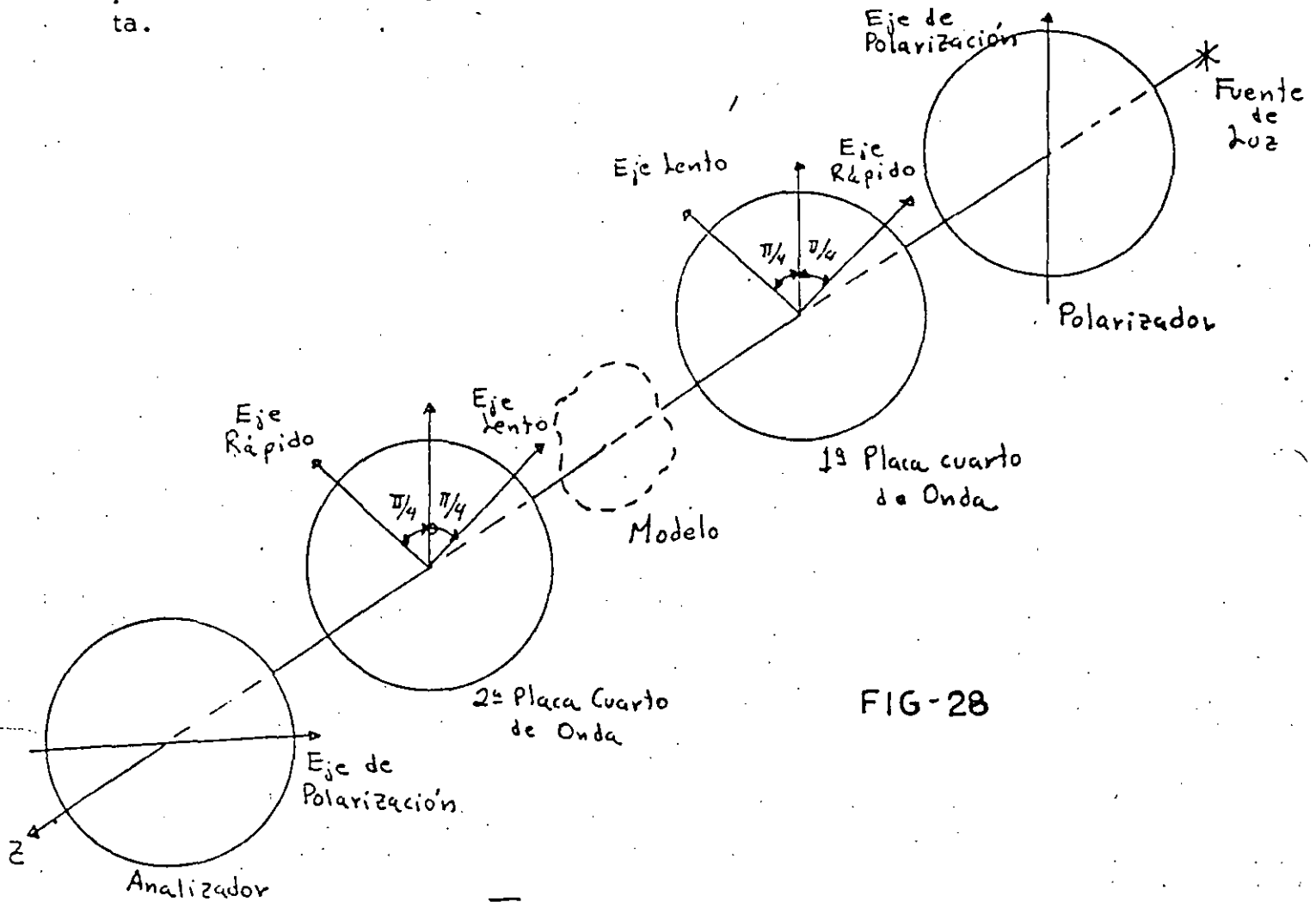


FIG-28

Tabla -2

Arreglo	Placas cuarto de Onda	Polarizador y Analizador	Campo
A*	Cruzadas	Cruzados	Obscuro
B	Cruzadas	Paralelos	Claro
C	Paralelas	Cruzados	Claro
D	Paralelas	Paralelos	Obscuro

* mostrado en la figura 28.

Los arreglos de los elementos ópticos discutidos, no son lo suficientemente completos para un buen polaroscopio de trabajo. El grado de complejidad de un polaroscopio varía desde sistemas complejos de lentes con servomotores para mover los elementos ópticos, hasta arreglos muy simples como los discutidos.

b) Teoría de la Fotoelasticidad.

El propósito es discutir la teoría de la fotoelasticidad, o en otras palabras, discutir lo que pasa en un polaroscopio cuando un modelo fotoelástico es puesto en el polaroscopio y se carga. Esta teoría se mantendrá lo más simple posible, sin embargo lo suficientemente completa para describir la mayoría de los efectos fotoelásticos observables en un polaroscopio.

b.1. La ley del esfuerzo óptico en dos dimensiones con incidencia normal.

Consideremos un modelo bidimensional maquinado de una hoja de plástico transparente. Inicialmente el modelo está libre de esfuerzos y exhibe un índice de refracción n_0 que es el mismo en todos los puntos y planos del modelo.

Sin embargo, cuando se somete a un sistema de fuerzas, un estado de esfuerzos bidimensional se induce en el modelo, y éste cambia sus propiedades ópticas.

Ópticamente el modelo se vuelve birrefringente y exhibe propiedades muy similares a las de las placas de onda.

Los ejes principales de los esfuerzos en cualquier punto del modelo, son los ejes rápido y lento de la placa; luego es evidente que el índice de refracción cambió en relación con el estado de esfuerzos inducido.

Es en esta propiedad óptica poco usual en la que se basa la teoría de la fotoelasticidad. El polaroscopio es el instrumento que nos ayuda a medir estos cambios en el índice de refracción. La teoría que relaciona los cambios del índice de refracción al estado de esfuerzos, se debe a Maxwell en 1853. Maxwell notó que el cambio en los índices de refracción eran linealmente proporcionales a los esfuerzos inducidos en el modelo y seguan las relaciones:

$$\begin{aligned} n_1 - n_0 &= c_1 \sigma_1 + c_2 \sigma_2 \\ n_2 - n_0 &= c_1 \sigma_2 + c_2 \sigma_1 \end{aligned} \quad \text{Ec. 93}$$

donde n_0 : índice de refracción del modelo sin carga.

n_1, n_2 : índices de refracción a lo largo de los ejes principales, asociados con σ_1 y σ_2 .

c_1, c_2 : coeficientes del esfuerzo óptico.

Si restamos las ecuaciones para eliminar n_0 :

$$n_1 - n_2 = (c_1 - c_2)(\sigma_1 - \sigma_2) \quad \text{Ec. 94}$$

Ya que el modelo cargado se comporta como una placa de onda temporal, de la ecuación 85:

$$n_1 - n_2 = \frac{\lambda \Delta}{2\pi h} \quad \text{Ec. 85}$$

De las ecuaciones 85 y 94:

$$\Delta = \frac{2\pi h}{\lambda} (c_1 - c_2)(\sigma_1 - \sigma_2) \quad \text{Ec. 95}$$

Si $c_1 - c_2 = C$: coeficiente relativo del esfuerzo óptico, el retardo relativo Δ será:

$$\Delta = \frac{2\pi h C}{\lambda} (\sigma_1 - \sigma_2) \quad \text{Ec. 96}$$

donde C está expresado en términos del Brewster (1 Brewster = $10^{-13} \frac{\text{cm}^2}{\text{dim}}$).

La ecuación 96 es la clásica descripción de la ley del esfuerzo óptico. El retardo relativo Δ es directamente proporcional a la diferencia de los esfuerzos principales.

Como las unidades asociadas con el Brewster no son comunes en la Ingeniería, es más conveniente escribir la ecuación 96 como:

$$\sigma_1 - \sigma_2 = \frac{N f_\sigma}{h} \quad \text{Ec. 97}$$

donde $N = \frac{\Delta}{2\pi}$: retraso relativo en términos de un ciclo completo de retardo 2π .

$f_\sigma = \frac{\lambda}{C}$: es el valor de franja del material ($\rho_{\sigma_i} \cdot i n$).

h : espesor del modelo ($i n$).

De la ecuación 97 es evidente que la diferencia de esfuerzos principales $\sigma_1 - \sigma_2$ en un modelo bidimensional puede ser determinado si el retardo relativo N puede ser medido y si el valor de franja del material puede ser establecido por calibración. La función del polaroscopio es determinar el valor de N en cada punto del modelo. Si el modelo es perfectamente elástico, puede encontrarse la diferencia entre las deformaciones principales:

$$\frac{N f_\sigma}{h} = \frac{E}{1+\nu} (\epsilon_1 - \epsilon_2) \quad \text{o} \quad \frac{N f_\epsilon}{h} = \epsilon_1 - \epsilon_2 \quad \text{Ec. 98, 99}$$

donde: $f_\epsilon = \frac{1+\nu}{E} f_\sigma$

Luego para un modelo fotoelástico perfectamente elástico, la determinación de N es suficiente para establecer $\sigma_1 - \sigma_2$ y $\epsilon_1 - \epsilon_2$ si las propiedades del material (E, ν, f_σ , o f_ϵ) son conocidas.

b.2. Efectos de un modelo cargado en un polaroscopio plano.

Consideremos el caso de un modelo plano cargado en un campo de un polaroscopio plano con su normal coincidente con el eje del polaroscopio (figura 29).

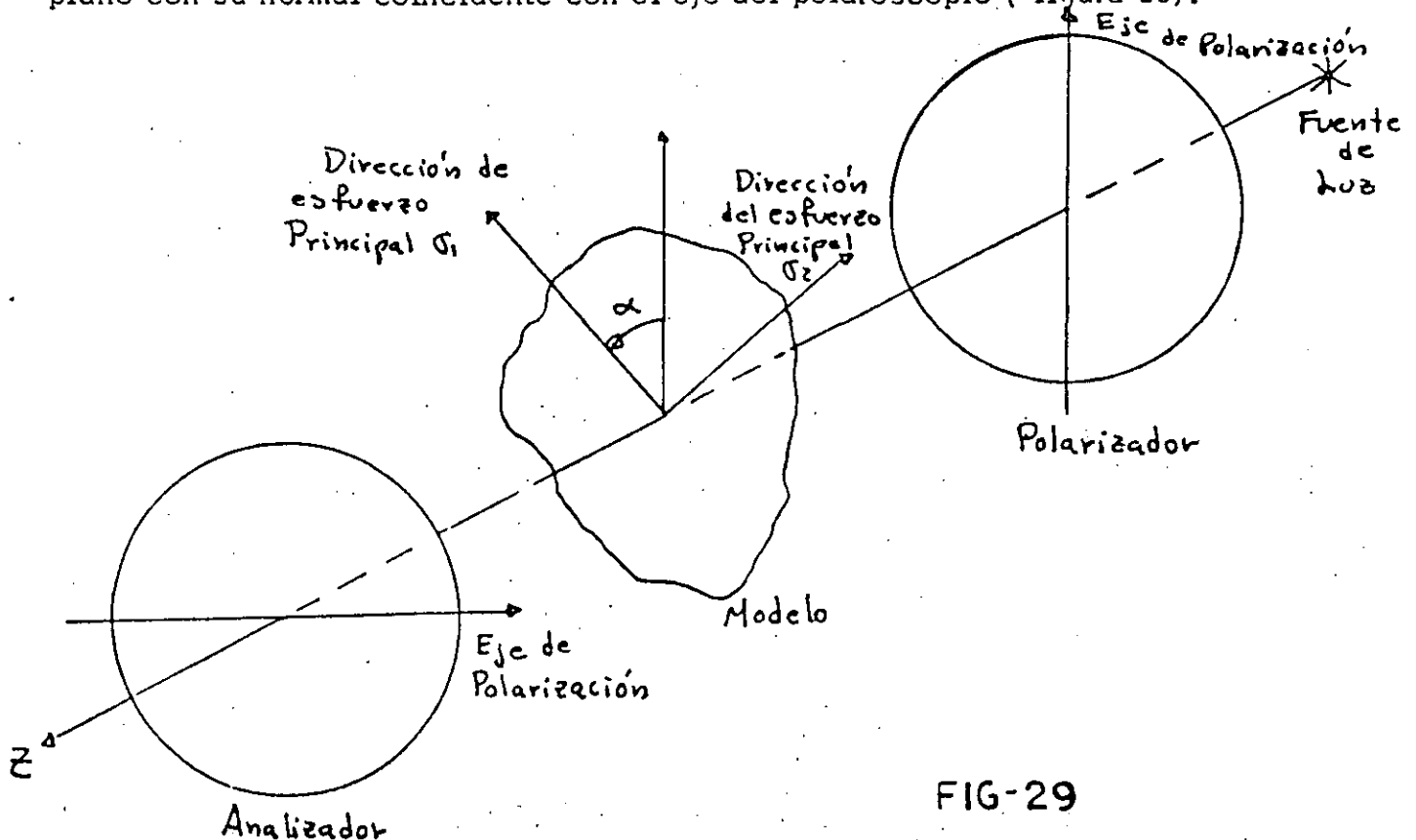


FIG-29

La luz emergente del polarizador en un estado de polarización plana vibrando en el plano vertical con una amplitud que varía con el tiempo de la siguiente manera:

$$A = k \text{ Sen } \omega t$$

(a)

Esta luz polarizada plana penetra al modelo como muestra la figura 30.

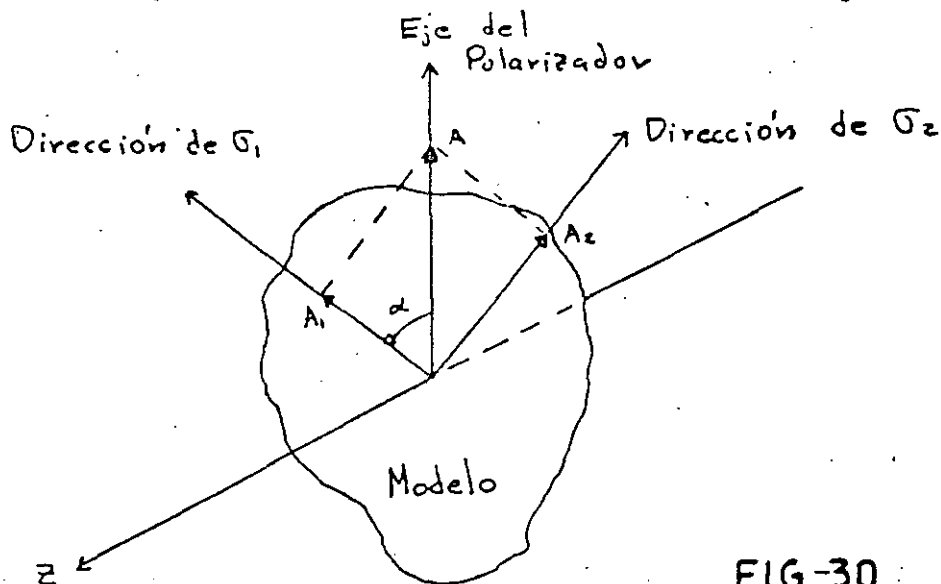


FIG-30

Como el modelo cargado se comporta como una placa de onda, el vector luz es descompuesto en dos componentes A_1 y A_2 .

$$A_1 = k \text{ Sen } \omega t \text{ Cos } \alpha$$

(b)

$$A_2 = k \text{ Sen } \omega t \text{ Sen } \alpha$$

Estos dos componentes se propagan a través del modelo a diferentes velocidades y al salir del modelo estarán defasados. La diferencia relativa de fase entre los dos componentes será, de la ecuación 97:

$$\Delta = 2\pi N = \frac{h}{\rho \sigma} (\sigma_1 - \sigma_2) z \pi$$

(c)

Si esta diferencia de fase relativa se divide por igual entre los dos componentes del vector de luz, al salir los componentes tendrán una amplitud dada por:

$$A_1' = k \text{ Cos } \alpha \text{ Sen } \left(\omega t + \frac{\Delta}{2} \right) \quad A_2' = k \text{ Sen } \alpha \text{ Sen } \left(\omega t - \frac{\Delta}{2} \right)$$

(d)

Los componentes A_1' y A_2' entran al analizador como se muestra en la figura 31.

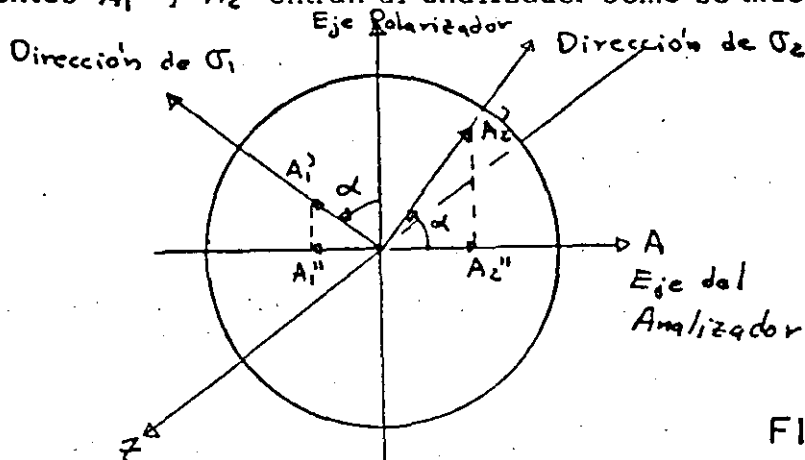


FIG-31

Los componentes A_1' y A_2' se descomponen, cuando entran al analizador, en componentes horizontales A_1'' y A_2'' , y en componentes verticales. Como los componentes verticales se absorben, no se muestran en la figura 31. Los componentes horizontales de la luz, transmitidos a través del analizador se superponen y resultan en un vector luz emergente A cuya magnitud es:

$$A = A_2'' - A_1'' = A_2' \cos \alpha - A_1' \sin \alpha \quad (c)$$

$$A = K \sin \alpha \cos \alpha \left[\sin \left(\omega t - \frac{\Delta}{2} \right) - \sin \left(\omega t + \frac{\Delta}{2} \right) \right] \quad (d)$$

Mediante identidades trigonométricas, puede reducirse a:

$$A = -K \sin 2\alpha \cos \omega t \sin \frac{\Delta}{2} \quad \text{Ec. 100}$$

La intensidad de la luz es proporcional al cuadrado de la amplitud del vector luz emergiendo del analizador; luego, la intensidad de la luz emergente I está dada por:

$$I = K \sin^2 2\alpha \sin^2 \frac{\Delta}{2} \cos^2 \omega t \quad \text{Ec. 101}$$

Esta ecuación muestra que la extinción ($I = 0$) de la luz, puede realizarse de tres maneras:

Caso 1. - Efectos de frecuencia:

Cuando $\omega t = \frac{(2n+1)\pi}{2}$, donde $n=0, 1, 2, \text{etc.}$, el $\cos^2 \omega t = 0$ y la intensidad es cero, produciendo una condición de extinción; sin embargo la frecuencia angular ω es tan alta (por ejemplo del orden de $10^{15} \frac{\text{rad}}{\text{seg}}$) que cualquier tipo de equipo fotográfico de alta velocidad no puede captar esta extinción. Luego para aplicaciones en fotoelasticidad estática, este efecto puede ser completamente ignorado y la ecuación 101 puede ser escrita como:

$$I = K \sin^2 2\alpha \sin^2 \frac{\Delta}{2} \quad \text{Ec. 102}$$

Caso 2. - Efectos de las direcciones principales de los esfuerzos.

Cuando $2\alpha = n\pi$ donde $n=0, 1, 2, \text{etc.}$, el $\sin^2 2\alpha = 0$ y la intensidad I es cero, produciendo una condición de extinción.

Este hecho implica que cuando $\alpha = 0, \frac{\pi}{2}$, ó cualquier múltiplo exacto de $\frac{\pi}{2}$, la dirección principal de σ_1 o σ_2 coincide con el eje del polarizador. Como este análisis puede extenderse para cubrir todos los puntos del modelo, pueden determinarse todos los puntos donde la extinción ocurre debido a este efecto.

Cuando se observa todo el modelo, resulta un patrón de franjas, las cuales se localizan en los puntos donde las direcciones principales (σ_1 o σ_2) coinciden con los ejes del polarizador.

El patrón de franjas producido por el término $\sin^2 2\alpha$ en la ecuación 101 o 102 se conoce como el patrón de franjas Isóclinas.

Este campo de franjas Isóclinas se emplea para determinar las direcciones principales de los esfuerzos en un modelo fotoelástico. Como esto representa una parte muy importante de los resultados o datos obtenidos en un análisis fotoelástico, el tema de las franjas Isóclinas y su interpretación se tratará por separado más adelante.

Caso 3. - Efecto de la diferencia de los esfuerzos principales.

Cuando $\frac{\Delta}{2} = n\pi$, donde $n=0, 1, 2, \text{etc.}$, el $\sin^2 \frac{\Delta}{2} = 0$ y la intensidad es cero produciendo una condición de extinción. Luego es claro que cuando $\frac{\Delta}{2\pi} = n$ la extinción ocurre.

De la ecuación 97 puede verse que $\frac{\Delta}{2\pi} = n = N = \frac{h}{\rho t} (\sigma_1 - \sigma_2)$

Cuando la diferencia de los esfuerzos principales es tal que $\frac{h}{\rho t} (\sigma_1 - \sigma_2) = 0, 1, 2$, las condiciones de extinción son satisfechas. El orden de extinción ($N=0, 1, 2, \text{etc.}$) está co

lado por la magnitud de la diferencia de los esfuerzos principales, por el espesor del modelo y por la sensibilidad del material fotoelástico, mediante el valor de f_{σ} .

En general, la diferencia $\sigma_1 - \sigma_2$ y las direcciones principales varían de punto a punto. El análisis anterior fué hecho con la luz pasando por un solo punto del modelo. Si el análisis se extiende para cubrir cada punto y si los resultados de todos los puntos se combinan para obtener un resultado de todo el campo, las líneas de extinción se obtendrán donde $\sigma_1 - \sigma_2 = \frac{N}{f_{\sigma}} P$ con N variando como 0, 1, 2, 3, etc. y donde una de las dos direcciones principales coincida con el eje de polarización del polarizador.

Los dos patrones de franjas se forman y se superponen uno con otro. Las líneas del primer tipo, llamadas franjas Isocromáticas son líneas en las cuales $\sigma_1 - \sigma_2$ es igual a una constante, dependiente del orden de franja N.

El segundo tipo de líneas, que se relacionan con las direcciones principales de los esfuerzos son llamadas Isóclinas.

Desafortunadamente, los dos patrones de franjas están superpuestos y su separación requiere técnicas especiales que se describirán más adelante.

b.3. Efectos de un modelo cargado en un polaroscopio circular (arreglo en campo obscuro).

El uso de un polaroscopio circular elimina las franjas Isóclinas y mantiene las Isocromáticas, y como resultado es más usado que el polaroscopio plano.

Para ilustrar este efecto, consideremos el modelo cargado en el polaroscopio circular (arreglo A) mostrado en la figura 32.

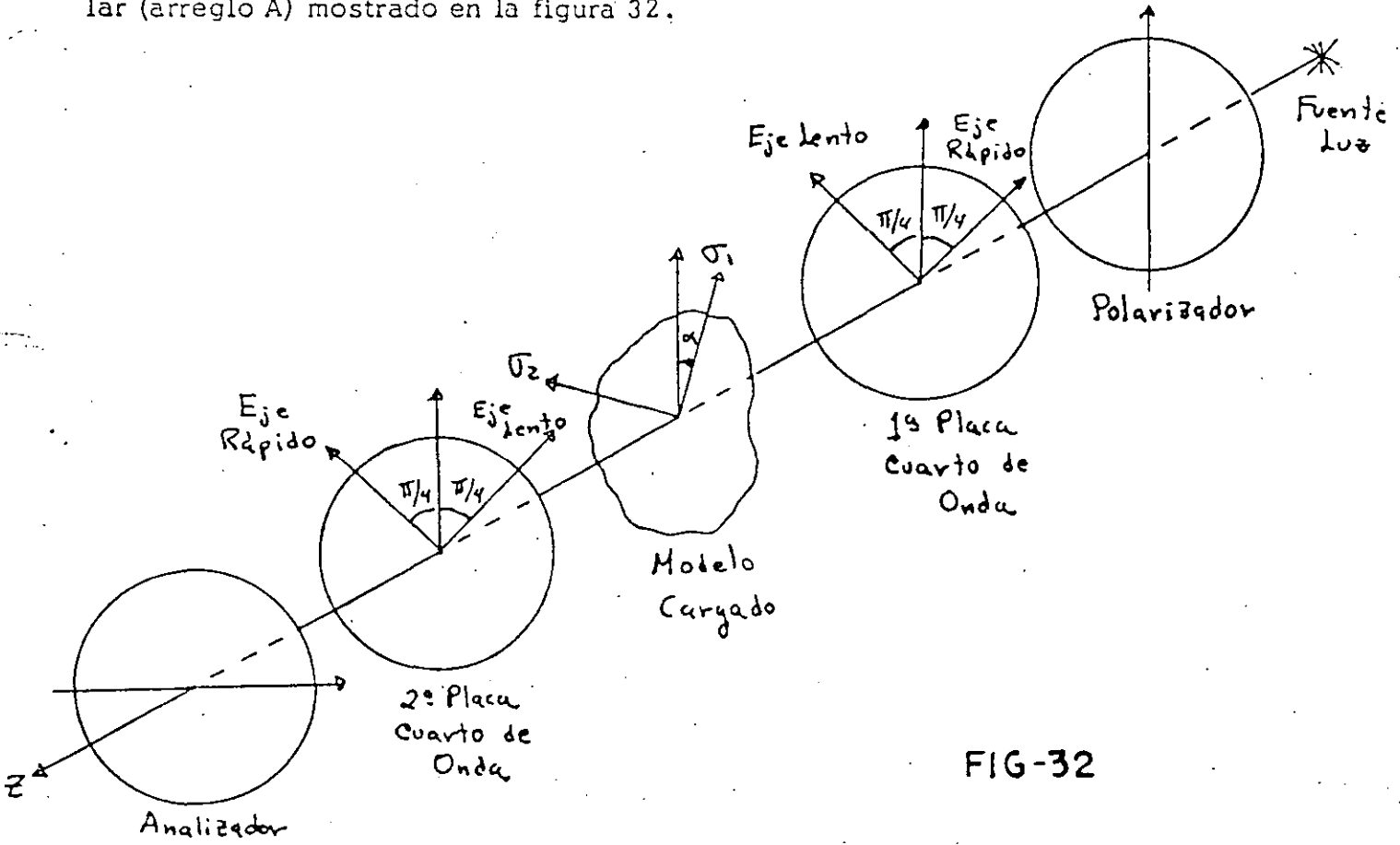


FIG-32

Empleando la ecuación 86 la luz emergente de la primera placa cuarto de onda, puede expresarse como:

$$A_1' = \frac{\sqrt{2}}{2} K \text{Sen}(wt + \frac{\pi}{2}) = \frac{\sqrt{2}}{2} K \text{Cos} wt \quad ; \quad A_2' = K \frac{\sqrt{2}}{2} \text{Sen} wt \quad (a)$$

Como se dijo anteriormente, la luz que emerge de la primera placa cuarto de onda, está polarizada en forma circular. El vector obtenido al combinar los componentes A_1' y A_2' es de amplitud constante y su punta describe una hélice circular conforme se propaga a lo largo del eje del polaroscopio.

Estos componentes entran al modelo como se ilustra en la figura 33.

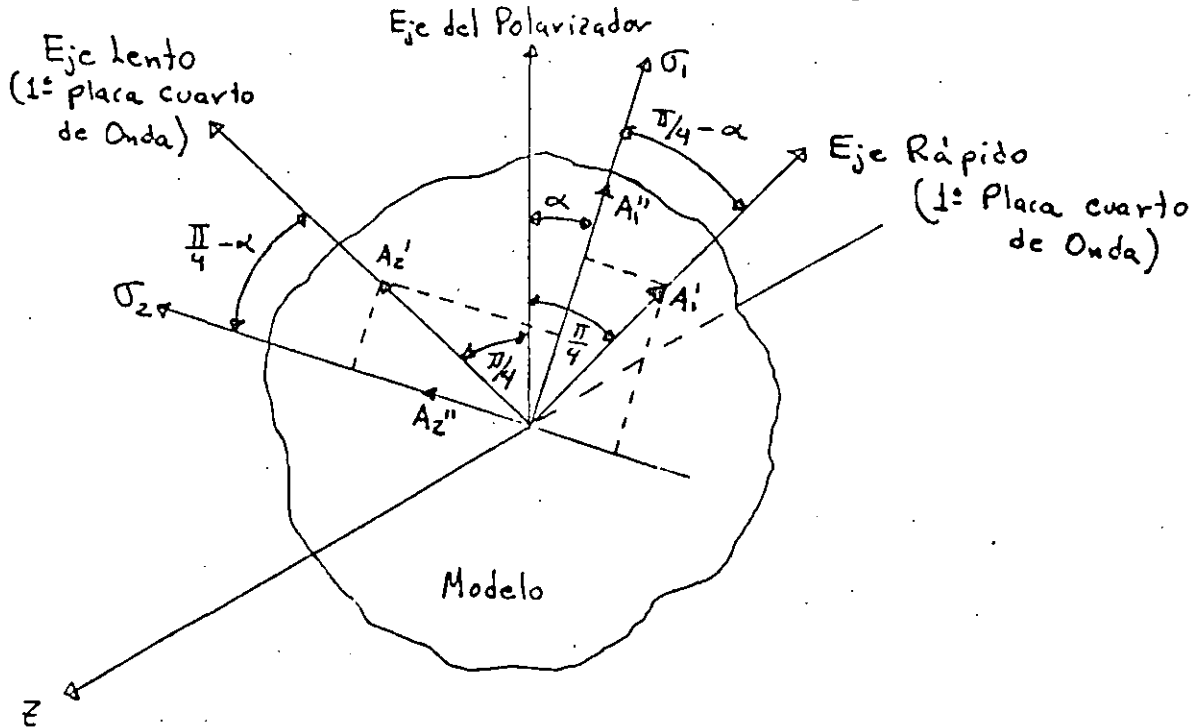


FIG-33

Los componentes A_1' y A_2' son entonces resueltos en dos nuevos componentes A_1'' y A_2'' cuando entran al modelo, a lo largo de los ejes σ_1 y σ_2 .

Los componentes A_1'' y A_2'' son:

$$A_1'' = A_1' \text{Cos}(\frac{\pi}{4} - \alpha) + A_2' \text{Sen}(\frac{\pi}{4} - \alpha) \quad (b)$$

$$A_2'' = A_2' \text{Cos}(\frac{\pi}{4} - \alpha) - A_1' \text{Sen}(\frac{\pi}{4} - \alpha)$$

Combinando las ecuaciones a) y b) :

$$A_1'' = \frac{\sqrt{2}}{2} K [\text{Cos} wt \text{Cos}(\frac{\pi}{4} - \alpha) + \text{Sen} wt \text{Sen}(\frac{\pi}{4} - \alpha)] \quad (c)$$

$$A_2'' = \frac{\sqrt{2}}{2} K [\text{Sen} wt \text{Cos}(\frac{\pi}{4} - \alpha) - \text{Cos} wt \text{Sen}(\frac{\pi}{4} - \alpha)]$$

Como el modelo cargado tiene las características de una placa de onda, las dos componentes A_1'' y A_2'' se propagan a través del modelo con diferentes velocidades y emergen fuera de fase con un ángulo de retraso relativo Δ que es proporcional a la diferencia $\sigma_1 - \sigma_2$ como se indica en la ecuación 96. Si esta diferencia relativa de

fase Δ se divide en los dos componentes, con $+\frac{\Delta}{2}$ aplicado a A_1''' y $-\frac{\Delta}{2}$ aplicado a A_2''' ; las amplitudes de estos componentes cuando emergen del modelo serán:

$$\begin{aligned} A_1''' &= \frac{\sqrt{2}}{2} K \left[\cos(\omega t + \frac{\Delta}{2}) \cos(\frac{\pi}{4} - \alpha) + \sin(\omega t + \frac{\Delta}{2}) \sin(\frac{\pi}{4} - \alpha) \right] \\ A_2''' &= \frac{\sqrt{2}}{2} K \left[\sin(\omega t - \frac{\Delta}{2}) \cos(\frac{\pi}{4} - \alpha) - \cos(\omega t - \frac{\Delta}{2}) \sin(\frac{\pi}{4} - \alpha) \right] \end{aligned} \quad (d)$$

La luz emergente del modelo, entra a la segunda placa cuarto de onda como se ilustra en la figura 34.

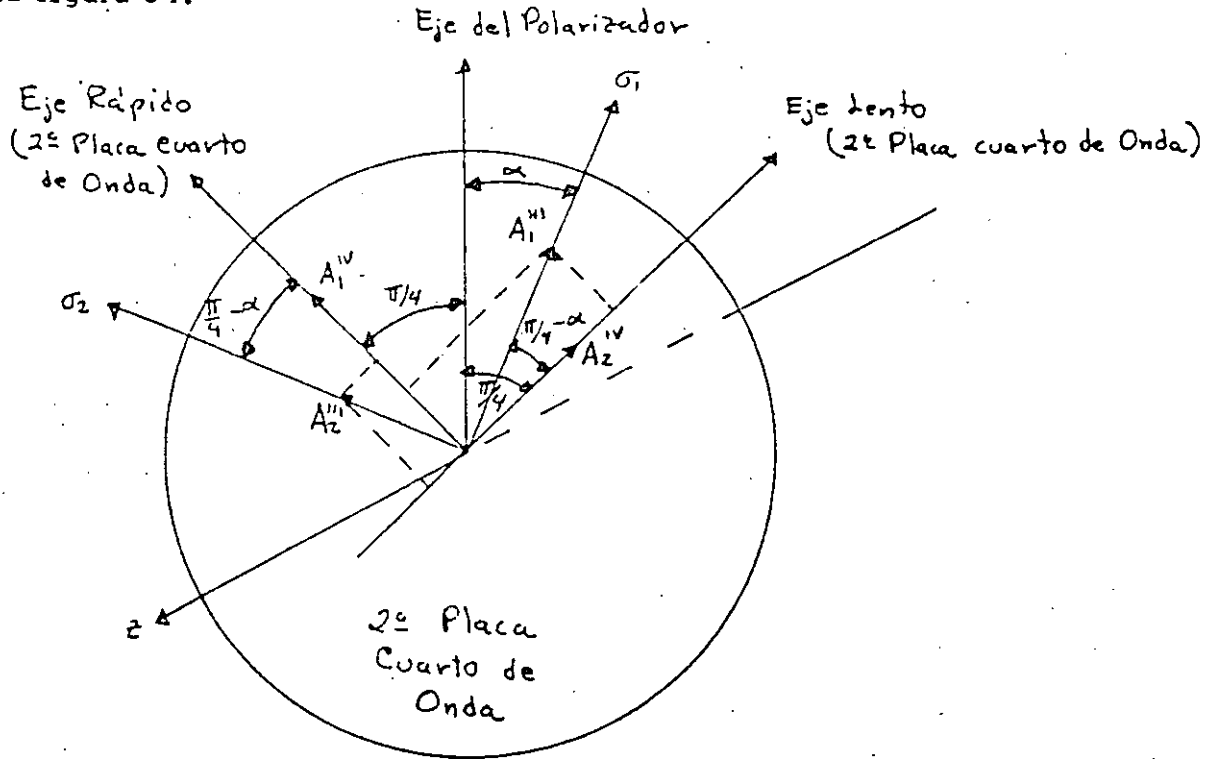


FIG-34

Los componentes A_1''' y A_2''' se descomponen en los ejes rápido y lento de la segunda placa cuarto de onda, y los denotaremos como A_1'''' y A_2'''' que pueden ser descritos por las siguientes ecuaciones:

$$\begin{aligned} A_1'''' &= A_2''' \cos(\frac{\pi}{4} - \alpha) + A_1''' \sin(\frac{\pi}{4} - \alpha) \\ A_2'''' &= A_1''' \cos(\frac{\pi}{4} - \alpha) - A_2''' \sin(\frac{\pi}{4} - \alpha) \end{aligned} \quad (e)$$

Sustituyendo las ecuaciones d) en e):

$$\begin{aligned} A_1'''' &= \frac{\sqrt{2}}{2} K \left[\sin(\omega t - \frac{\Delta}{2}) \cos^2(\frac{\pi}{4} - \alpha) - \cos(\omega t - \frac{\Delta}{2}) \cos(\frac{\pi}{4} - \alpha) \sin(\frac{\pi}{4} - \alpha) + \right. \\ &\quad \left. + \cos(\omega t + \frac{\Delta}{2}) \cos(\frac{\pi}{4} - \alpha) \sin(\frac{\pi}{4} - \alpha) + \sin(\omega t + \frac{\Delta}{2}) \sin^2(\frac{\pi}{4} - \alpha) \right] \\ A_2'''' &= \frac{\sqrt{2}}{2} K \left[\cos(\omega t + \frac{\Delta}{2}) \cos^2(\frac{\pi}{4} - \alpha) + \sin(\omega t + \frac{\Delta}{2}) \sin(\frac{\pi}{4} - \alpha) \cos(\frac{\pi}{4} - \alpha) - \right. \\ &\quad \left. - \sin(\omega t - \frac{\Delta}{2}) \cos(\frac{\pi}{4} - \alpha) \sin(\frac{\pi}{4} - \alpha) + \cos(\omega t - \frac{\Delta}{2}) \sin^2(\frac{\pi}{4} - \alpha) \right] \end{aligned} \quad (f)$$

Si se asume que el cambio de fase relativa de $\frac{\pi}{2}$ que ocurre al pasar la luz a través de esta placa cuarto de onda, es aplicada en sentido positivo a la componente A_1'''' ,

los componentes emergentes de la placa A_1^V y A_2^V pueden expresarse como:

$$A_1^V = \frac{\sqrt{2}}{2} k \left[\cos(\omega t - \Delta/2) \cos^2(\pi/4 - \alpha) + \text{Sen}(\omega t - \Delta/2) \text{Sen}(\pi/4 - \alpha) \cos(\pi/4 - \alpha) - \right. \\ \left. - \text{Sen}(\omega t + \Delta/2) \text{Sen}(\pi/4 - \alpha) \cos(\pi/4 - \alpha) + \cos(\omega t + \Delta/2) \text{Sen}^2(\pi/4 - \alpha) \right]$$

$$A_2^V = \frac{\sqrt{2}}{2} k \left[\cos(\omega t + \Delta/2) \cos^2(\pi/4 - \alpha) + \text{Sen}(\omega t + \Delta/2) \text{Sen}(\pi/4 - \alpha) \cos(\pi/4 - \alpha) - \text{Ec. 103} \right. \\ \left. - \text{Sen}(\omega t - \Delta/2) \cos(\pi/4 - \alpha) \text{Sen}(\pi/4 - \alpha) + \cos(\omega t - \Delta/2) \text{Sen}^2(\pi/4 - \alpha) \right]$$

Finalmente la luz entra al analizador como se muestra en la figura 35.

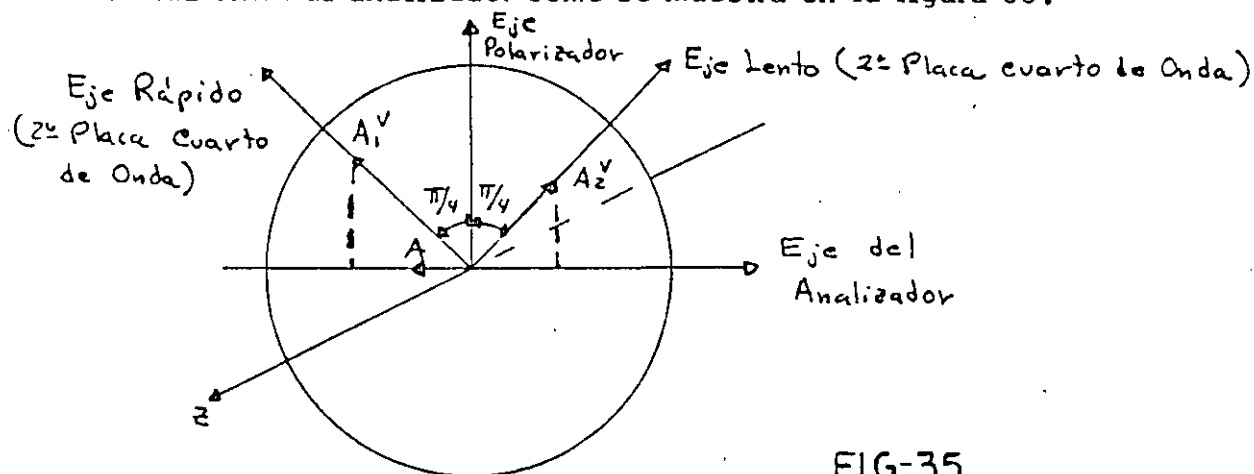


FIG-35

Los componentes A_1^V y A_2^V son descompuestos en componentes horizontales y verticales. Los componentes verticales son absorbidos en el analizador y los horizontales son transmitidos para formar el vector A :

$$A = \frac{\sqrt{2}}{2} (A_2^V - A_1^V) \quad \text{Ec. 104}$$

Sustituyendo la ecuación 103 en la 104 y simplificando:

$$A = \frac{1}{2} k \text{Sen} \frac{\Delta}{2} \left[\cos(\alpha + \omega t) - \text{Sen}(\alpha - \omega t) \right] \quad \text{Ec. 105}$$

La intensidad I de la luz es proporcional al cuadrado de la amplitud, luego:

$$I = k \text{Sen}^2 \frac{\Delta}{2} \left[\cos(\alpha + \omega t) - \text{Sen}(\alpha - \omega t) \right]^2 \quad \text{Ec. 106}$$

Una inspección de la ecuación 106 muestra que la extinción ($I=0$) es posible cuando

$$\text{Sen}^2 \frac{\Delta}{2} = 0 \quad \text{ó} \quad \left[\cos(\alpha + \omega t) - \text{Sen}(\alpha - \omega t) \right]^2 = 0$$

El término $\left[\cos(\alpha + \omega t) - \text{Sen}(\alpha - \omega t) \right]^2$ no produce extinción que pueda ser registrada, ya que la frecuencia angular ω de la luz es demasiada. Por lo tanto, para efectos prácticos, éste término puede ser despreciado y la ecuación 106 puede reescribirse como:

$$I = k \text{Sen}^2 \Delta/2 \quad \text{Ec. 107}$$

Debe notarse que las direcciones de los esfuerzos no producen extinción, ya que el ángulo α está combinado con ωt .

Por lo tanto el polaroscopio circular elimina el patrón de Isóclinas.

Regresando a la ecuación 107, es claro que $I = 0$ cuando $\text{Sen}^2 \frac{\Delta}{2} = 0$. Este hecho implica que la extinción es posible sólo cuando $\frac{\Delta}{2} = n\pi$, donde $n = 0, 1, 2, \text{etc.}$. El tipo de extinción es idéntico al descrito en el caso 3 del polaroscopio plano. La localización de estos puntos de extinción producen un patrón de franjas llamadas Isocromáticas.

b.4. Efectos de un modelo cargado en un polaroscopio circular (arreglo de campo claro).

Un polaroscopio circular es usualmente empleado tanto en un campo oscuro como en uno claro. El polaroscopio puede ser convertido de un campo oscuro a uno claro rotando el analizador 90° . La ventaja de emplear ambos campos es que se obtiene el doble de datos para la determinación de $\sigma_1 - \sigma_2$ en todo el campo.

Recordemos que en el campo obscuro, el número de franja N coincide con n , y las franjas se cuentan en la secuencia 1, 2, 3, etc. Com el arreglo de campo claro, n y N no coinciden. En cambio $N = \frac{1}{2} + n$. Luego con el campo claro el número de línea se cuenta en la secuencia $\frac{1}{2}, 1\frac{1}{2}, 2\frac{1}{2}, 3\frac{1}{2}, \text{etc.}$

Para establecer el efecto de un modelo cargado en un polaroscopio circular con campo claro, sólo es necesario considerar los componentes A_1^V y A_2^V cuando entran al analizador con su nueva orientación, como se muestra en la figura 36.

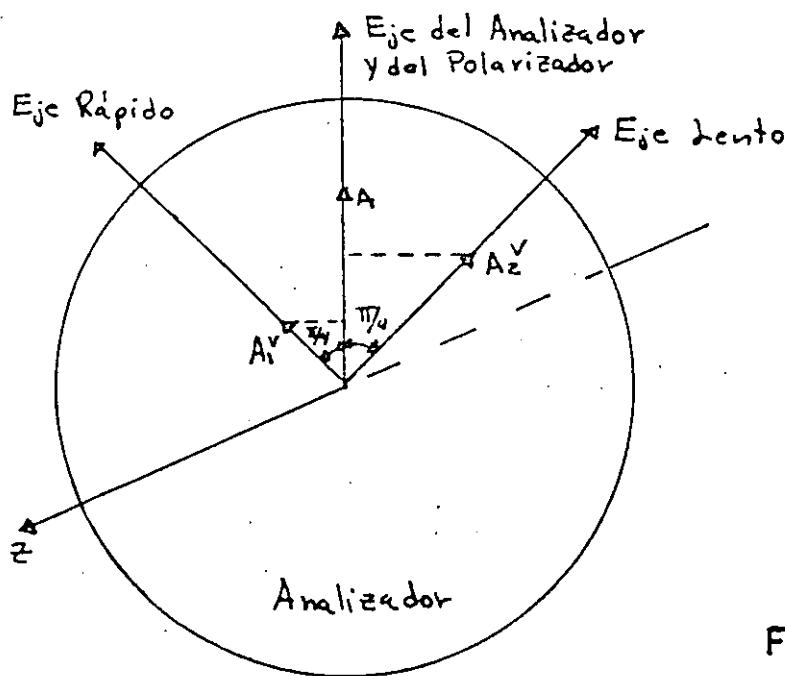


FIG 36

Los componentes horizontales de A_1^V y A_2^V son absorbidos, mientras que los componentes verticales se transmiten. El vector luz emergente estará en el plano vertical con una amplitud dada por:

$$A = \frac{\sqrt{2}}{2} (A_1^V + A_2^V) \quad \text{Ec. 108}$$

Sustituyendo la ecuación 103 en 108 y simplificando tendremos:

$$A = 2K \cos \omega t \cos \frac{\Delta}{2} \quad \text{Ec. 109}$$

y la intensidad:

$$I = K \cos^2 \omega t \cos^2 \frac{\Delta}{2}$$

El término $\cos^2 \omega t$ puede despreciarse por las razones ya expuestas:

$$I = K \cos^2 \frac{\Delta}{2}$$

La extinción ($I=0$) ocurrirá cuando

$$\Delta/2 = \frac{1+2n}{2} \pi ; n = 0, 1, 2, 3, \dots$$

Ec. 110

pero de la ecuación 97:

$$N = \frac{\Delta}{2\pi} = \frac{1}{2} + n$$

Ec. 111

que implica que el orden o número de la primera franja observada en un polaroscopio de campo claro es $\frac{1}{2}$ que corresponde a $n=0$. Usando los dos campos (oscuro y claro), es posible obtener dos fotografías de las franjas isocromáticas resultantes. Los datos así obtenidos, darán una representación del número de franjas separadas por $\frac{1}{2}$ orden. La interpolación entre las franjas permite a menudo una estimación del orden de franja de hasta ± 0.1 que resulta en una aproximación para la diferencia de los esfuerzos principales de $\pm 0.1 \frac{P_0}{h}$. Si se desea mayor exactitud, debe hacerse uso de técnicas más refinadas; algunas se describirán más adelante.

b.5. Fotografía fotoelástica.

En muchos análisis fotoelásticos, se toman fotos de los patrones de franjas Isóclinas e Isocromáticas. Por esta razón es importante establecer los principios básicos de la fotografía.

Una hoja de película fotográfica está preparada con un recubrimiento que contiene plata. Cuando este recubrimiento se expone a la luz, la plata sufre un cambio que es distinguible permanentemente después de un proceso de revelado fotográfico. El cambio es un proceso de oscurecimiento mediante la formación de plata metálica. La cantidad de oscurecimiento es llamada densidad.

La densidad de una película revelada, es simplemente una medida de la habilidad de la plata para prevenir la transmisión de la luz. La densidad de un tipo dado de película, es una función de la exposición (intensidad de la luz \times tiempo). Las características de la función densidad-exposición, fue primeramente establecida por Hurter y Driffield de la manera mostrada en la figura 37. La curva de esta figura define tres características importantes de una película fotográfica, a saber: la densidad de niebla D_0 , la inercia de exposición E_0 , y la pendiente de la curva dada por el número γ de la película.

Cada una de estas características es importante, y deben ser consideradas al seleccionar una película para un análisis fotoelástico.

En una fotografía fotoelástica, la exposición cero ocurre siempre que la intensidad es cero ($N = 0, 1, 2, \dots$). Sin embargo la película registra valores del rango de exposición por encima del valor de inercia E_0 . Es esta exposición "muerta" la que produce las franjas anchas cuando en teoría son líneas.

La pendiente de la densidad vs. $\log E$ dada por γ determina la extensión de la película. La película usual tiene $\gamma \approx 1$. Este relativamente bajo valor de γ da un amplio rango de exposición sobre el cual la película es efectiva y produce un negativo satisfactorio. Este hecho es importante en las fotografías en las que el tiempo correcto de exposición no puede determinarse.

Para fotografías fotoelásticas se emplean películas con valores de γ más altos (de 3 a 6) ya que dan un negativo de más contraste. Esto es deseable ya que las franjas tienden a adelgazar y se definen mejor. El tiempo de exposición es por supuesto más crítico, pero puede establecerse en exposiciones preliminares.

La densidad de niebla es menos importante ya que implica que existe una delgada capa uniformemente distribuida sobre la película, que absorbe la luz. Esto por supuesto va en detrimento de la brillantez del negativo, pero como es un factor relativo, no es objetable.

Para la porción lineal de la curva, densidad vs. log E, la densidad D puede expresarse como:

$$D = D_0 + \gamma (\log E - \log E_0) \tag{Ec. 112}$$

donde $D = \log I_i / I_e$

- I_i : intensidad de la luz incidente sobre un negativo revelado.
- I_e : intensidad de la luz emergente de un negativo revelado.
- D_0 : densidad de niebla = $\log I_i / I_e'$
- I_e' : intensidad de la luz emergente de una parte no expuesta del negativo revelado.
- $E = I t$
- I : intensidad de la luz incidente en la película.
- t : tiempo de exposición.

Empleando las definiciones anteriores, la ecuación 112 puede ser escrita como:

$$\log I_i / I_e = \log I_i / I_e' + \gamma \log E / E_0$$

que puede ser reducida a:

$$1/\beta = I_e' / I_e = (E / E_0)^\gamma \tag{Ec. 113}$$

donde β es llamado el ratio o razón de brillantez $\beta = I_e / I_e'$.

De esta definición se ve que $\beta = 1$ corresponde a la parte más brillante del negativo, mientras que $\beta = 0$ corresponde a un área opaca.

Recordando la ecuación 107:

$$I = K \text{ Sen}^2 \Delta/2$$

La exposición para un negativo en campo oscuro será:

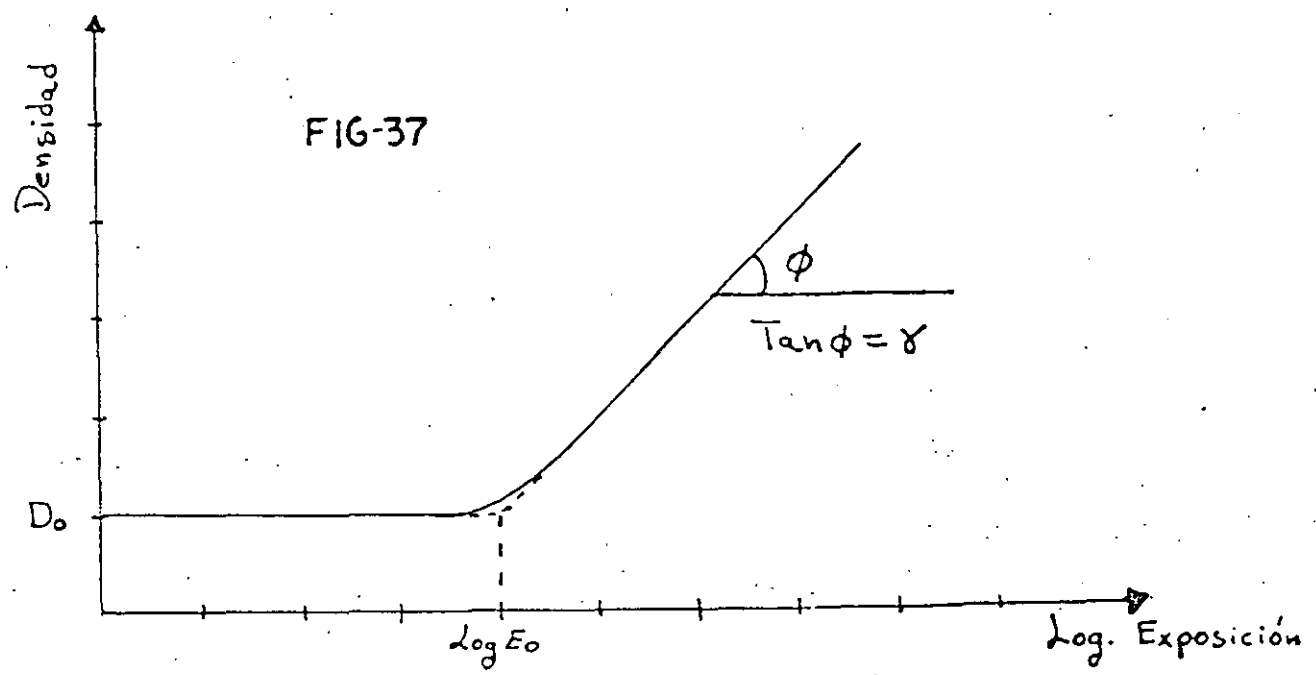
$$E = I t = K t \text{ Sen}^2 \Delta/2 = E_\beta \text{ Sen}^2 \Delta/2 \tag{Ec. 114}$$

donde $E_\beta = K t$ es la exposición uniforme producida por el polaroscopio.

Combinando las ecuaciones 113 y 114:

$$1/\beta = (E_\beta / E_0)^\gamma \text{ Sen}^{2\gamma} \Delta/2 \tag{Ec. 115}$$

La ecuación 115 describe la brillantez de un negativo que resulta de fotografiar un modelo fotoelástico en un polaroscopio de campo oscuro.



b. 6. Multiplicación de franjas por métodos fotográficos.

Empleando procedimientos normales, pueden obtenerse dos fotos de un modelo fotoelástico (una en campo claro y otra en campo oscuro), que permiten la determinación del orden de franja en la siguiente secuencia: $N=0, 1/2, 1, 1 1/2, 2, \text{etc.}$

En algunas aplicaciones es deseable la determinación de ordenes de franja fraccionarios entre los ya listados. Este objetivo puede lograrse de diferentes maneras. En ésta sección se describirá una técnica fotográfica, la cual proporciona, mediante la superposición de patrones de franjas Isocromáticas ordinarias de campo claro y oscuro, un nuevo patrón de franjas de campo mixto.

Este patrón de franjas de campo mixto, junto con los de campo claro y oscuro, permite determinar el orden de franja en la secuencia $0, 1/4, 1/2, 3/4, 1, \text{etc.}$, y representa un factor de incremento de 2 en el número de franjas contables.

Recordando la ecuación 115, que describe la brillantez de un negativo obtenido en un campo oscuro:

$$1/\rho_{\text{osc.}} = (E_f/E_0)^{\gamma} \text{Sen}^{2\gamma} \Delta/2 \quad \text{Ec. 115}$$

Combinando las ecuaciones 113 y 114 con 110, es claro que:

$$1/\rho_{\text{claro}} = (E_f/E_0)^{\gamma} \text{Cos}^{2\gamma} \Delta/2 \quad \text{Ec. 116}$$

Multiplicando estas dos ecuaciones, que es matemáticamente análogo a sobreponer los dos negativos:

$$1/\rho_m = (1/\rho_{\text{osc.}})(1/\rho_{\text{claro}}) = (E_f/E_0)^{2\gamma} \text{Sen}^{2\gamma} \Delta/2 \text{Cos}^{2\gamma} \Delta/2$$

que puede reescribirse como:

$$1/\rho_m = E^{2\gamma} \text{Sen}^{2\gamma} \Delta/2 \text{Cos}^{2\gamma} \Delta/2 \quad \text{Ec. 117}$$

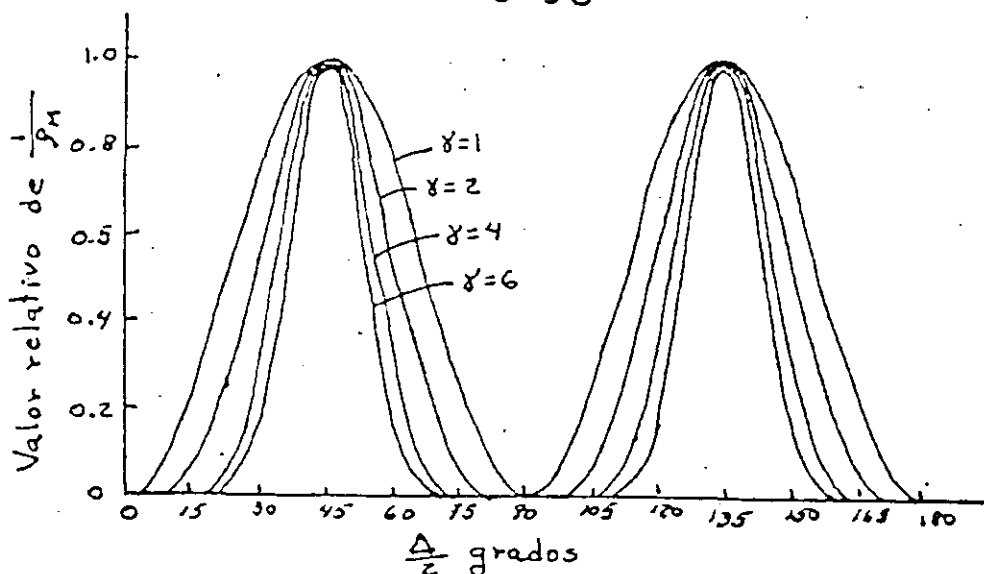
Un exámen de la ecuación 117 muestra que la característica del par de negativos superpuestos está determinado por el factor E (que es controlado por el tiempo de exposición y la velocidad de la película) y el factor γ (que es controlado por la película y las propiedades del revelado). Si se emplea una película con $\gamma=1$ la ecuación 117 se reduce a:

$$1/\rho_m = E^2/8 [1 - \text{Cos} 4(\Delta/2)]$$

Como al término E^2 puede dársele cualquier valor controlando el tiempo de exposición, el término $[1 - \text{Cos} 4(\Delta/2)]$ determina las características de los negativos superpuestos. El término $[1 - \text{Cos} 4(\Delta/2)]$ es uno cuando $\Delta/2 = (2n+1)\pi/4$ donde $n=0, 1, 2, \dots$ indicando que el patrón de franjas se registra en $N/4, 3N/4, 5N/4, \dots$ como se muestra en la figura 38. Luego la posición de los ordenes de franja de $1/4$ pueden registrarse en todo el modelo de una forma simple y directa.

Conforme γ aumenta de valor, la cantidad $[\text{Sen}^{2\gamma}(\Delta/2) \text{Cos}^{2\gamma}(\Delta/2)]$ continúa exhibiendo picos en los valores de franja de $1/4$. Sin embargo estos picos se acentúan y los valles se aplanan. El uso de una película con un γ más alto es preferible ya que adelgaza las franjas y permite mayor exactitud en la determinación de la posición de las franjas.

FIG 38



b.7. Adelgazamiento de franjas con espejos parciales.

El ancho de las franjas Isocromáticas puede ser reducido mediante una técnica debida a Post que emplea espejos parciales en un polaroscopio circular con lentes. Los espejos se insertan en el campo del polaroscopio en ambos lados y paralelos al modelo (figura 39).

El efecto de los espejos es hacer que la luz se propague hacia adelante y hacia atrás através del modelo en la manera ilustrada en la figura 40. Conforme la luz se refleja hacia atrás y hacia adelante entre los espejos, una porción es transmitida en cada punto de reflexión. Luego, la intensidad del rayo es progresivamente reducida. Por ejemplo, el rayo 1 es el más intenso, el 3 es menos intenso, etc. El efecto de los espejos puede ser obtenido modificando la ecuación 107 que es válida si no hubiera espejos.

Consideremos el rayo 1 (figura 40) y reduzcamos la intensidad debido a la pérdida de luz por la reflexión en los puntos A y B. Tendremos:

$$I_1 = K(1-R)^2 \text{Sen}^2 \frac{\Delta}{2} = K T^2 \text{Sen}^2 \frac{\Delta}{2} \quad (a)$$

donde R y T son los coeficientes de transmisión y de reflexión de los espejos.

La intensidad del rayo 3 ha pasado por dos reflexiones y dos transmisiones, luego T y R están al cuadrado. También la luz ha pasado através del modelo tres veces, y el argumento del seno ha sido multiplicado por 3 por este hecho.

$$I_3 = K T^2 R^2 \text{Sen}^2 3\frac{\Delta}{2} \quad (b)$$

Siguiendo este procedimiento, la intensidad del k ésimo rayo será:

$$I_k = K T^2 R^{k-1} \text{Sen}^2 \frac{k\Delta}{2} ; k=1,3,5,7,\dots \quad \text{Ec. 118}$$

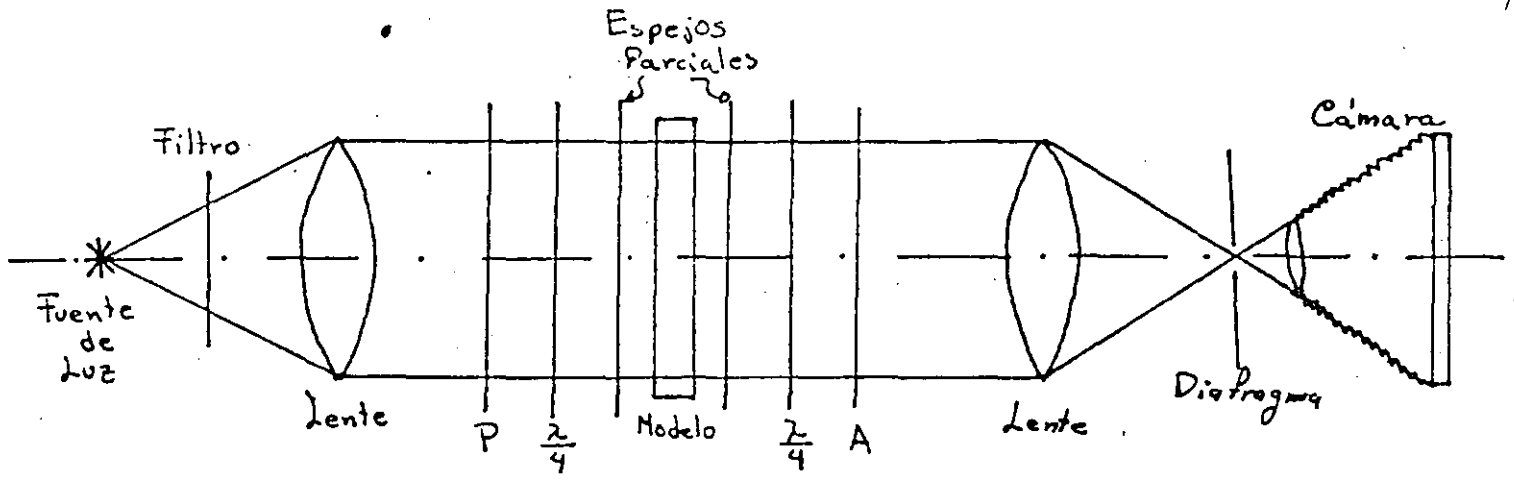


FIG-39

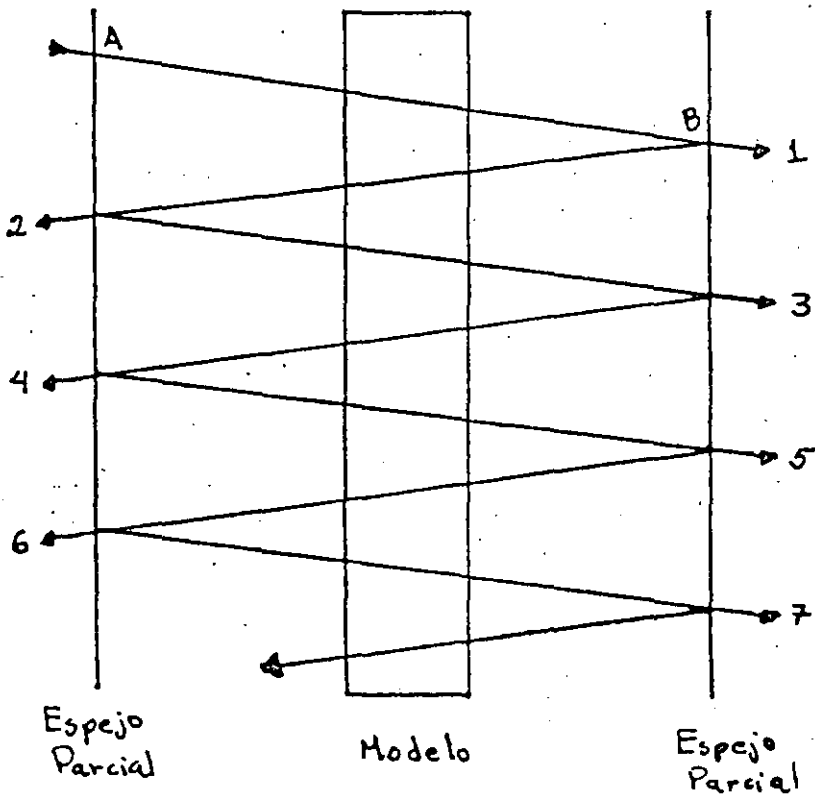


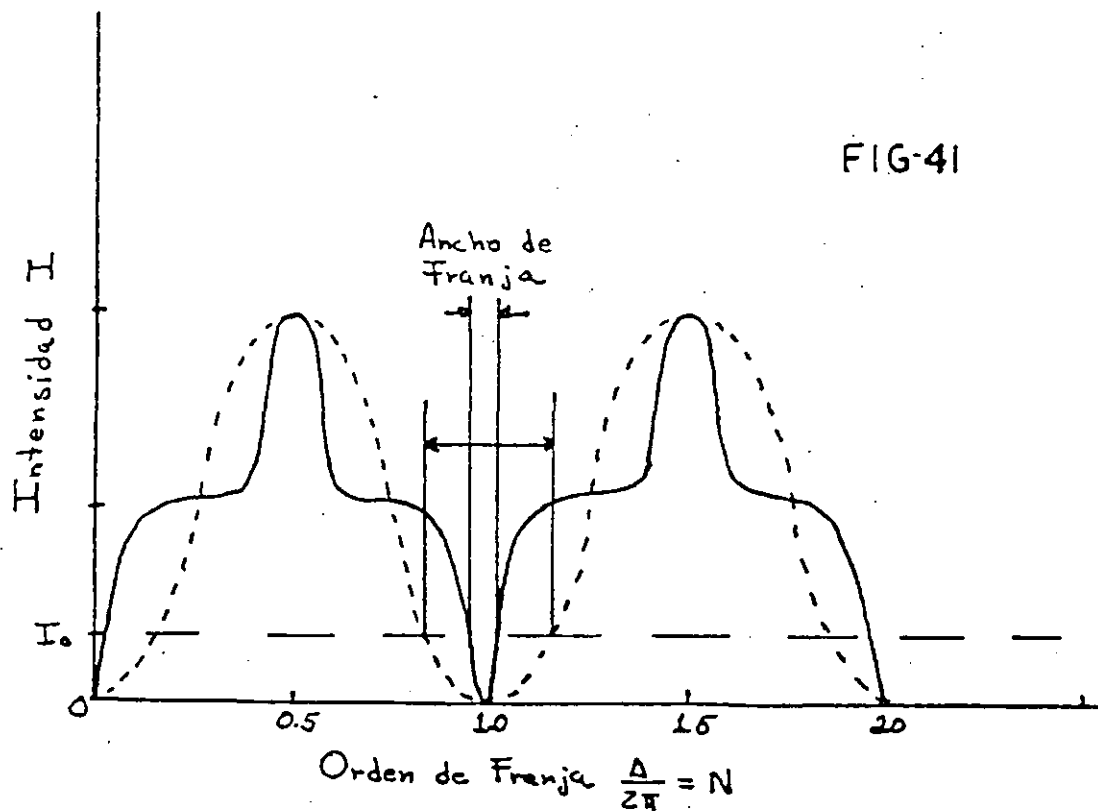
FIG-40

Las intensidades I_1, I_2, I_3, \dots se suman aritméticamente; luego la intensidad resultante de los rayos sobrepuestos está dada por la serie:

$$I = K T^2 \sum_{k=1}^{\infty} R^{k-1} \text{Sen}^2 \frac{k\Delta}{2} \quad \text{Ec. 119}$$

Si ésta relación se expande y se gráfica como función de $\frac{\Delta}{2\pi} = N$, la curva intensidad contra orden de franja es la que se obtiene (figura 41).

Cuando esta gráfica se compara con la curva convencional, se observa que las franjas se adelgazan. El ojo humano empieza a registrar una franja a una cierta intensidad mínima I_0 ; luego la función adelgazada produce una franja mucho más angosta que la función convencional.



En una fotografía obtenida empleando este método, se observan bandas o franjas delgadas claras y oscuras separadas por anchas bandas grises. Las franjas oscuras corresponden a los valles de la figura 41 y las claras a los picos en la misma gráfica. Las bandas grises son producidas por el rango medio de intensidades también mostrado en la figura 41. Las franjas oscuras están ordenadas con una secuencia 0, 1, 2, 3, etc. y las claras con una secuencia $\frac{1}{2}, 1\frac{1}{2}, 2\frac{1}{2}, 3\frac{1}{2}, \dots$. Luego, los datos normalmente obtenidos en campos claro y oscuro convencionales están contenidos en una sola fotografía si se emplean espejos parciales en un polaroscopio circular con lentes.

b.8. Multiplicación de franjas con espejos parciales.

Post también mostró que los espejos parciales pueden ser empleados para multiplicar el número de franjas que pueden ser observadas en un modelo fotoelástico.

Cuando se hace esto, los espejos son nuevamente puestos en el polaroscopio a ambos lados del modelo; sin embargo en esta aplicación uno de los espejos está ligeramente inclinado como se ve en la figura 42.

El efecto del espejo inclinado sobre la luz, al pasar hacia adelante y hacia atrás a través del modelo, se observa en la figura 43. De esta figura es claro que cada rayo de luz que emerge del espejo, sale con un ángulo que es función del número de veces que el rayo pasa a través del modelo. Por ejemplo, los rayos 1, 3, 5, 7 que han atravesado el modelo el mismo número de veces que su número de rayo, emergen con ángulos $0, 2\phi, 4\phi$ y 6ϕ , además que los rayos no pasan por el mismo punto.

En la práctica, multiplicaciones por factores de 5 a 7 pueden ser obtenidos sin introducir grandes errores debido al promedio que es inherente en este método.

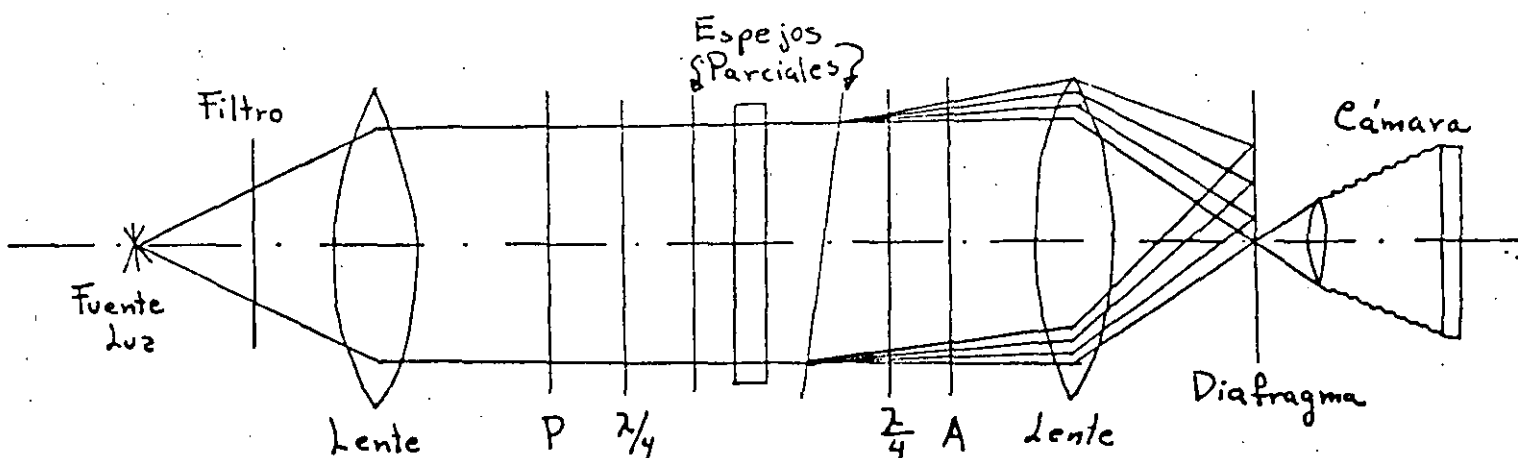


FIG 42

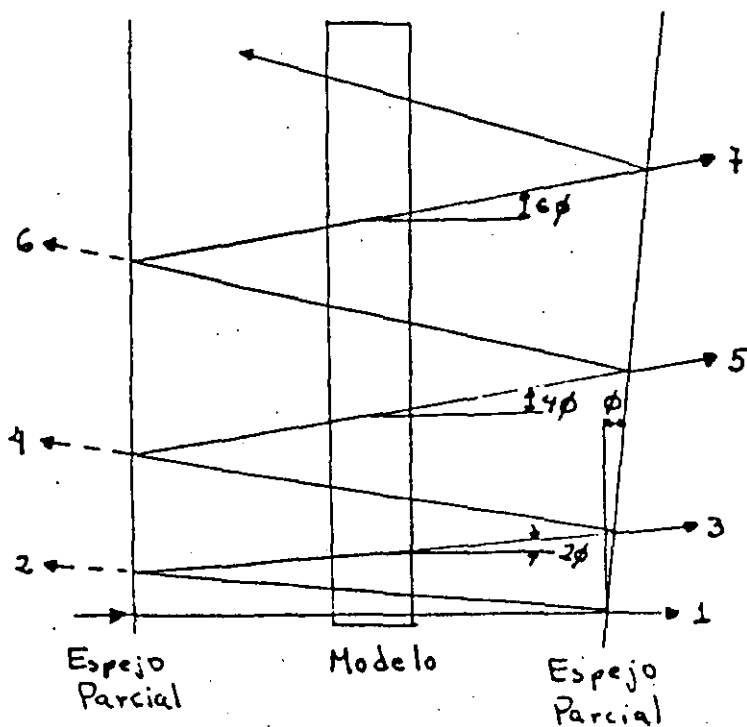


FIG 43

El hecho de que los diferentes rayos de luz estén inclinados diferentes ángulos con respecto al eje del polaroscopio, permite que cada rayo esté aislado. Los rayos son recolectados por los lentes pero enfocados a diferentes puntos en el plano focal de los lentes. Cualquiera de estos rayos pueden ser observados colocando el ojo o un lente de cámara en el punto adecuado.

En la práctica los patrones de Isocromáticas asociados con los rayos 1, 3, 5, 7, etc. pueden ser observados y fotografiados tanto en campo claro como en campo oscuro. Supongase por ejemplo que se obtienen fotografías en ambos campos de los rayos 1, 3 y 5.

El patrón de franjas en las dos fotos del rayo 1 se interpretan de manera convencional, en una secuencia $0, \frac{1}{2}, 1, \frac{3}{2}, \text{etc.}$ Sin embargo, para el rayo 3, para el cual la luz ha pasado tres veces através del modelo, la secuencia de las franjas es $0, \frac{1}{6}, \frac{1}{3}, \frac{1}{2}, \frac{2}{3}, \dots$

Finalmente para el rayo 5, donde la luz ha atravesado el modelo 5 veces, la secuencia será $0, \frac{1}{10}, \frac{1}{5}, \frac{3}{10}, \frac{2}{5}, \frac{1}{2}, \text{etc.}$

Luego la superposición de los resultados obtenidos de estos tres rayos, es suficiente para determinar el orden de franja hasta en $\frac{1}{10}$ de orden sobre todo el modelo.

La relación para la intensidad del m-ésimo rayo, donde m = 1, 3, 5, etc. puede establecerse modificando la ecuación 107.

$$I_1 = K T^2 \text{Sen}^2 \Delta/2$$

$$I_3 = K T^2 R^2 \text{Sen}^2 3\Delta/2$$

$$I_5 = K T^2 R^4 \text{Sen}^2 5\Delta/2$$

Ec. 120

$$I_m = K T^2 R^{m-1} \text{Sen}^2 m\Delta/2$$

Luego, éste método de multiplicación de franjas está acompañado de una considerable pérdida de la intensidad de la luz. La intensidad del patrón multiplicado de franjas, comparado con el patrón convencional, está disminuido por el término $T^2 R^{m-1}$ que es mucho menor que uno.

c) Técnicas de Análisis.

c.1. Introducción.

En un análisis fotoelástico convencional en dos dimensiones, se fabrica un modelo, se carga, y se coloca en un polaroscopio, y los patrones de franjas son analizados y fotografiados. El siguiente paso es la interpretación de los patrones de franjas, que es el verdadero resultado de la prueba. En esta parte del trabajo se discutirán la interpretación de los patrones de franjas Isocromáticas e Isóclinas, las técnicas de compensación, de separación y la escala entre los esfuerzos del modelo y del prototipo.

c.2. Patrón de franjas Isocromático.

El patrón de franjas Isocromático obtenido de un modelo bidimensional, proporciona líneas a lo largo de las cuales la diferencia entre los esfuerzos principales ($\sigma_1 - \sigma_2$) es igual a una constante.

Cuando el orden de franja en cualquier punto del modelo ha sido establecido, es posible valuar ($\sigma_1 - \sigma_2$) de la ecuación 97.

$$\sigma_1 - \sigma_2 = N f \sigma / h$$

donde σ_1 y σ_2 son los esfuerzos principales en el plano del modelo.

El esfuerzo cortante máximo está dado por:

$$\tau_{\max} = \frac{1}{2} (\sigma_1 - \sigma_2) = N f \sigma / 2h$$

Ec. 121

si σ_1 y σ_2 son de signos opuestos y $\sigma_3 = 0$; de otra manera

$$\tau_{\max} = \frac{1}{2} (\sigma_1 - \sigma_3) = \frac{1}{2} \sigma_1$$

si σ_1 y σ_2 son positivos

$$\tau_{\max} = \frac{1}{2} (\sigma_3 - \sigma_2) = \frac{1}{2} \sigma_2$$

si σ_1 y σ_2 son negativos

Ec. 122

La diferencia entre las ecuaciones 121 y 122 está representada gráficamente en la figura 44, donde se ha dibujado el círculo de Mohr para los dos casos. Cuando $\sigma_1 > 0$ y $\sigma_2 < \sigma_3 = 0$, el esfuerzo cortante máximo es la mitad del valor de ($\sigma_1 - \sigma_2$) y puede ser determinado directamente del patrón de Isocromáticas conforme la ecuación 121. Sin embargo, cuando $\sigma_1 > \sigma_2 > \sigma_3 = 0$, el esfuerzo cortante máximo no está en el plano del modelo y la ecuación 121 proporciona τ_p y no τ_{\max} .

Para establecer τ_{\max} en este caso, es necesario determinar σ_1 individualmente y no ($\sigma_1 - \sigma_2$). Este es un punto importante ya que la teoría de falla del cortante máximo se usa con frecuencia en el diseño de elementos mecánicos.

En la superficie libre del modelo, σ_1 o σ_2 son iguales a cero; por lo tanto el esfuerzo tangencial a la frontera puede ser determinado directamente por

$$\sigma_1, \sigma_2 = N f \sigma / h$$

Ec. 123

El signo puede ser usualmente determinado por inspección, particularmente en las áreas críticas donde los esfuerzos en la frontera son máximos.

A lo largo de una frontera que no esté libre, por lo general se conoce la carga aplicada y por lo tanto uno de los esfuerzos, digamos σ_2 ; sea P la carga aplicada.

Luego:

$$\sigma_1 - \sigma_2 = \sigma_1 + P = N f \sigma / h \quad \text{ó} \quad \sigma_1 = N f \sigma / h - P$$

Ec. 124

donde $\sigma_2 = -P$ ya que la presión aplicada se considera positiva.

Concluyendo, es claro que el patrón de franjas Isocromáticas, una vez identificado, puede ser interpretado de la siguiente manera:

1. ($\sigma_1 - \sigma_2$) puede ser determinado en cualquier punto del modelo de la ecuación 97.
2. Si $\sigma_1 > 0$ y $\sigma_2 < 0$, ($\sigma_1 - \sigma_2$) puede ser relacionado al esfuerzo cortante máximo mediante la ecuación 121.

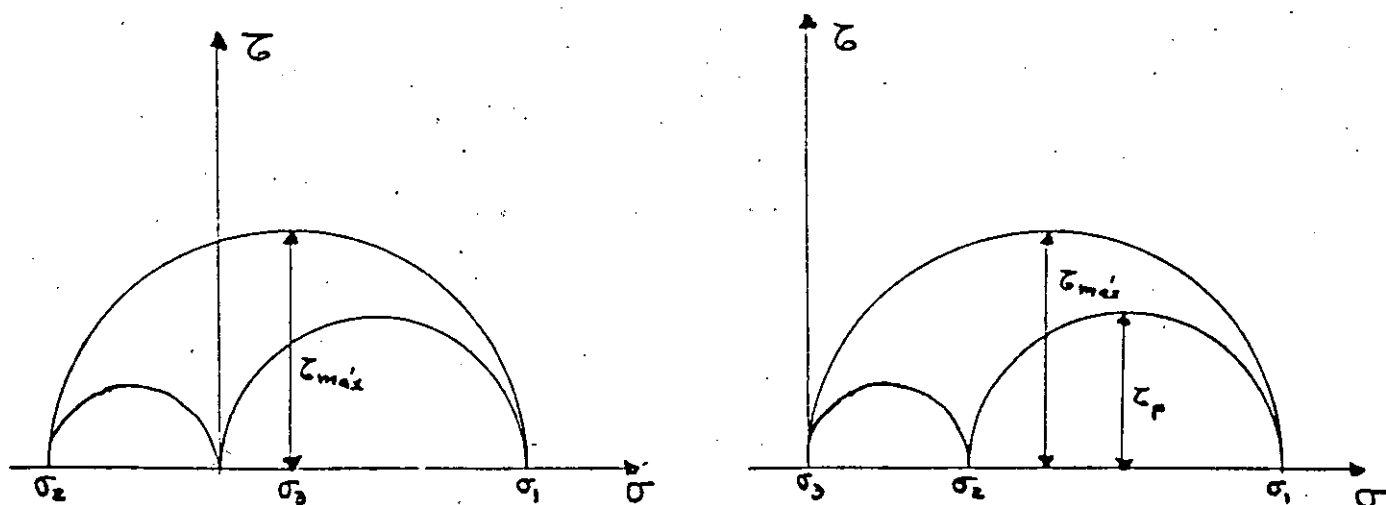


FIG 44

3. Si $\sigma_1 > \sigma_2 > 0$ o si $0 > \sigma_1 > \sigma_2$, $(\sigma_1 - \sigma_2)$ no puede ser referido al esfuerzo cortante máximo y es necesario determinar σ_1 y σ_2 individualmente y referir τ_{max} a σ_1 o a σ_2 , mediante la ecuación 122.
4. Si las fronteras pueden considerarse libres (esto es si σ_1 o $\sigma_2 = 0$) el otro es - fuerza principal puede ser determinado directamente de la ecuación 123.
5. Si la frontera no está libre, pero la carga normal aplicada es conocida, entonces el esfuerzo tangencial a la frontera puede interpretarse utilizando las ecuaciones - 124.
6. Si la frontera no está libre, y la carga aplicada no es conocida, deben aplicarse las técnicas de separación, las cuales se discutirán más adelante, para determinar los esfuerzos en la frontera.

c.3. Patrón de franjas Isóclinas.

El patrón de franjas Isóclinas obtenido en un polaroscopio plano es empleado para dar la dirección de los esfuerzos principales en cualquier punto del modelo. En la práctica esto puede realizarse de dos maneras. La primera es obtener un número de patrones de Isóclinas a diferentes posiciones del polaroscopio y combinar estos patrones para dar los parámetros de las Isóclinas sobre el campo completo del modelo. El segundo procedimiento consiste en aislar los puntos de interés y determinar el parámetro de Isóclinas en cada uno de estos puntos.

Hay varias reglas que deben seguirse al obtener el patrón compuesto de Isóclinas a partir de los patrones individuales. Estas reglas son:

1. Isóclinas de todos los parámetros deben pasar através de los puntos isotropos o singulares.
2. La isóclina de uno de los parámetros debe coincidir con el eje de simetría del modelo si es que existe.
3. El parámetro de una Isóclina que intersecta una superficie libre, es determinado por la pendiente de la frontera en el punto de intersección.

4. Isóclinas de todos los parámetros p en través de los puntos de carga concentrada.

Las líneas Isóclinas, a lo largo de las cuales los esfuerzos principales tienen una inclinación constante, dan las direcciones principales de una manera que no es apreciada en el campo de la ingeniería. Por esto es un procedimiento normal presentar las direcciones principales en forma de un diagrama de Isostáticas o diagrama de trayectorias de esfuerzos, donde los esfuerzos principales son tangentes o normales a las líneas Isostáticas en cada punto.

El diagrama de Isostáticas puede ser construido de una manera directa a partir del patrón de Isóclinas utilizando el procedimiento descrito abajo e ilustrado en la figura 45. En esta técnica de construcción, las trayectorias de los esfuerzos se inician en la Isóclina de 0° a partir de puntos espaciados arbitrariamente. Las líneas marcadas 1 en la figura 45 y orientadas 0° de la normal, se dibujan através de cada uno de éstos puntos, hasta que intersecten la Isóclina de 10° . Las líneas (1) se bisectan y un nuevo set de líneas (2) se dibuja, inclinadas 10° de la vertical, hasta la siguiente Isóclina. Nuevamente estas líneas se bisectan y otro conjunto de líneas (3) se dibujan orientadas un ángulo de 30° con la vertical. Este procedimiento se repite hasta que el campo entero esté cubierto. Las trayectorias de los esfuerzos son trazadas utilizando las líneas 1, 2, 3, etc. como guías. Las trayectorias de los esfuerzos se dibujan tangentes a las líneas construidas en cada intersección de las Isóclinas, como se ve en la figura 45.

Los parámetros Isóclinos también son empleados para determinar los esfuerzos cortantes en un plano arbitrario definido por un sistema coordenado oxy. Recordando el hecho de que los parámetros Isóclinos dan las direcciones entre el eje x del sistema coordenado y las direcciones de σ_1 o σ_2 y recordando el círculo de Mohr y las ecuaciones de transformación de esfuerzos en función de los esfuerzos principales, es claro que:

$$\tau_{xy} = -\frac{\sigma_1 - \sigma_2}{2} \sin 2\theta = -\frac{N \rho}{2h} \sin 2\theta \quad \text{Ec. 125}$$

donde θ es el ángulo entre el eje x y la dirección de σ_1 , dado por el parámetro de la Isóclina. También:

$$\tau_{xy} = \frac{\sigma_1 - \sigma_2}{2} \sin 2\theta_1 = \frac{N \rho}{2h} \sin 2\theta_1 \quad \text{Ec. 126}$$

donde θ_1 es el ángulo entre el eje x y la dirección de σ_2 dado por el parámetro de la Isóclina.

El uso combinado de los datos de las Isocromáticas y las Isóclinas representado en las ecuaciones 125 y 126 permite la determinación de τ_{xy} . Este valor de τ_{xy} es usado en la aplicación del método de diferencia de cortantes (que se verá posteriormente) para la determinación individual de los valores de σ_1 y σ_2 .

c.4. Técnicas de compensación.

El orden de las franjas Isocromáticas puede ser determinado hasta en $\frac{1}{2}$ de orden empleando los patrones de franjas de campo claro y de campo oscuro. Una mayor exactitud en la determinación del orden de franja puede hacerse usando campos compuestos o usando el método de Post para la multiplicación de franjas. Sin embargo cuando se necesita una mayor exactitud deben usarse técnicas de compensación de punto por punto para establecer el orden de franja N. Aquí se discutirá el más común de estos métodos, el método de Tardy.

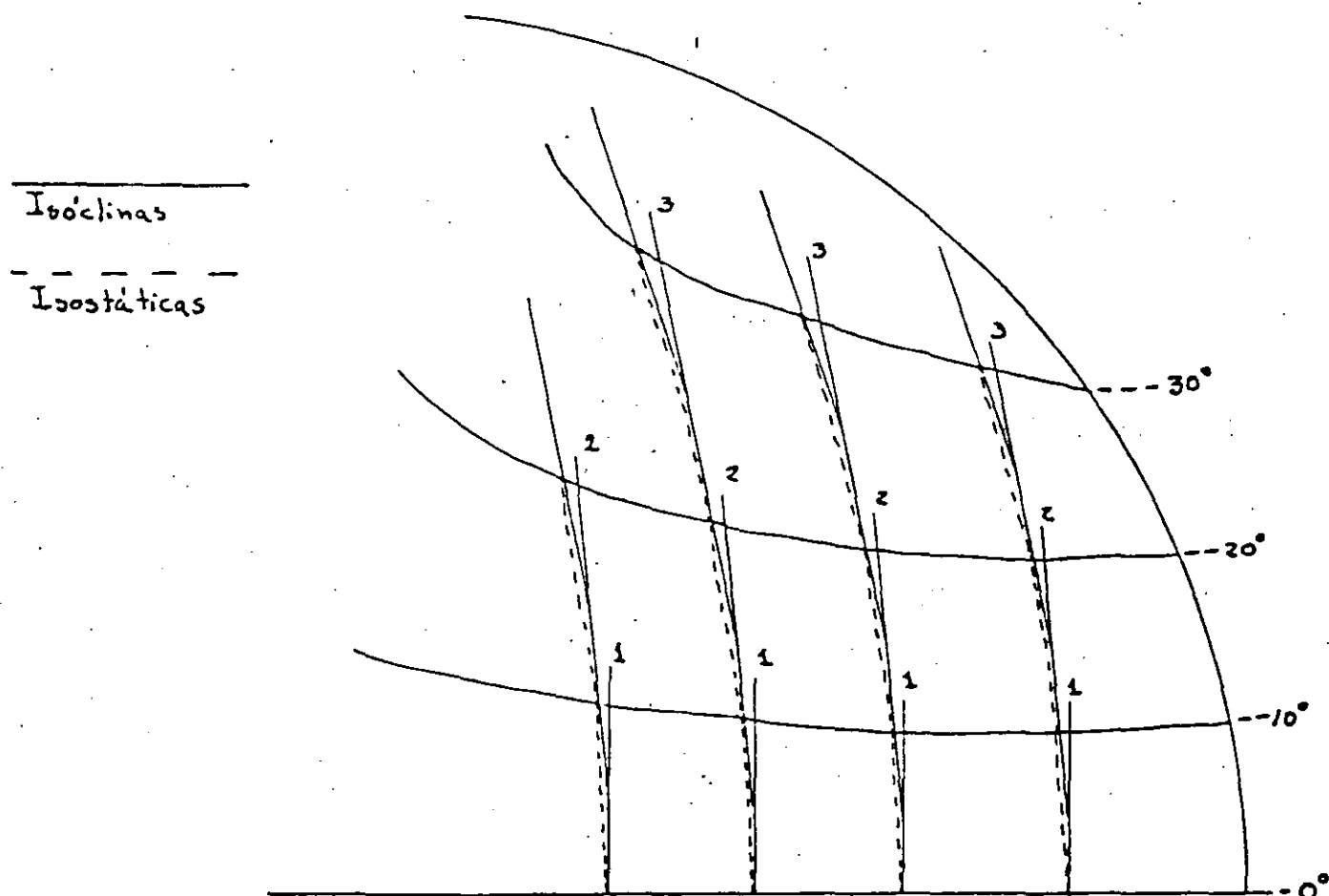


FIG 45

Método de Compensación de Tardy:

El método de compensación de Tardy es muy usado para determinar el orden de franja en un punto arbitrario del modelo. En éste método no se requiere equipo auxiliar y el analizador del polaroscopio sirve de elemento compensador.

Para emplear el método de Tardy, el polarizador del polaroscopio se alinea con la dirección de σ_1 del punto en cuestión, y todos los demás elementos del polaroscopio se rotan para obtener un campo oscuro. En esta posición del polaroscopio, se cumple el análisis presentado en la sección b.3. con el ángulo α igual a cero; por lo tanto las ecuaciones 103, que describen la luz emergente de la segunda placa cuarto de onda, pueden ser escritas como:

$$A_1^V = \frac{\sqrt{2}}{4} k \left[\cos\left(\omega t - \frac{\Delta}{2}\right) + \text{Sen}\left(\omega t - \frac{\Delta}{2}\right) - \text{Sen}\left(\omega t + \frac{\Delta}{2}\right) + \cos\left(\omega t + \frac{\Delta}{2}\right) \right]$$

$$A_2^V = \frac{\sqrt{2}}{4} k \left[\cos\left(\omega t + \frac{\Delta}{2}\right) + \text{Sen}\left(\omega t + \frac{\Delta}{2}\right) - \text{Sen}\left(\omega t - \frac{\Delta}{2}\right) + \cos\left(\omega t - \frac{\Delta}{2}\right) \right]$$

que pueden reducirse a:

$$A_1^v = \frac{\sqrt{2}}{2} k \cos \omega t \left(\cos \frac{\Delta}{2} - \text{Sen} \frac{\Delta}{2} \right)$$

Ec. 127

$$A_2^v = \frac{\sqrt{2}}{2} k \cos \omega t \left(\cos \frac{\Delta}{2} + \text{Sen} \frac{\Delta}{2} \right)$$

Ahora consideremos los componentes de la luz entrando al analizador como se muestra en la figura 46, y determinemos el ángulo γ através del cual hay que rotar el analizador para obtener la extinción (esto es $a_1 = a_2$). La amplitud de los componentes de la luz que pasan por el analizador está dada por:

$$A = A_2^v \cos\left(\frac{\pi}{4} + \delta\right) - A_1^v \cos\left(\frac{\pi}{4} - \delta\right)$$
 Ec. 128

Si δ se selecciona de manera que A sea, cero, y sustituyendo la ecuación 127 en 128, se obtiene:

$$\left(\cos \frac{\Delta}{2} + \text{Sen} \frac{\Delta}{2}\right) (\cos \delta - \text{Sen} \delta) - \left(\cos \frac{\Delta}{2} - \text{Sen} \frac{\Delta}{2}\right) (\cos \delta + \text{Sen} \delta) = 0$$

que se reduce a:

$$\text{Sen} \left(\frac{\Delta}{2} - \delta\right) = 0$$
 Ec. 129

La expresión $\text{Sen} \left(\frac{\Delta}{2} - \delta\right) = 0$ cuando $\frac{\Delta}{2} - \delta = n\pi$, donde $n = 0, 1, 2, \dots$; de manera que el orden de franja N en el punto de interés está dado por:

$$N = \frac{\Delta}{2}\pi = n + \delta/\pi$$
 Ec. 130

Para utilizar la ecuación 130 en el método de Tardy, el valor de n se determina por la posición del punto de interés relativa a el patrón de franjas Isocromáticas en el campo oscuro. Para ilustrar este hecho consideremos el patrón de franjas hipotético y los puntos de interés mostrados en la figura 47.

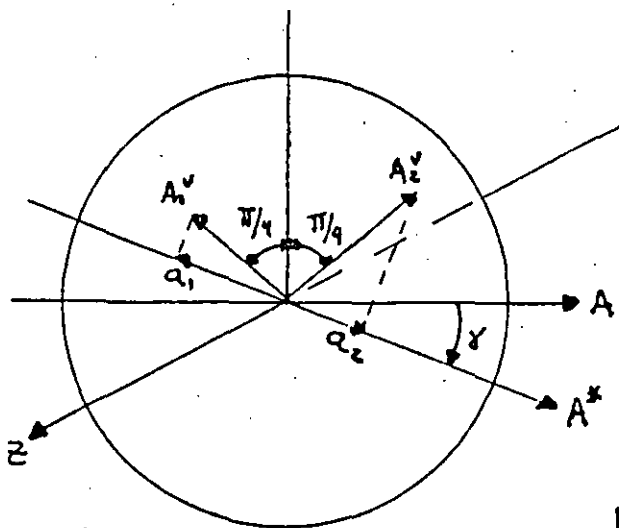


FIG 46

El punto P_1 que está entre los órdenes de franja 2 y 3, el valor asignado a n en ese punto es 2. Conforme el analizador es rotado un ángulo γ , la franja de segundo orden se moverá hacia el punto P_1 hasta que se obtenga la extinción. El orden de franja del punto P_1 será $N = 2 + \gamma/\pi$. Para el punto P_2 el valor de n se toma también como 2, y el analizador es rotado un ángulo γ_1 hasta que la franja de segundo orden provoque la extinción, dando un orden de franja de $N = 2 + \gamma_1/\pi$. En este caso n pudo haberse tomado como 3 y el analizador rotado en la dirección contraria un ángulo $-\gamma_2$, hasta que la franja de tercer orden produzca la extinción en el punto P_2 . En este ca

ha sido evaluada, su influencia en el esfuerzo principal máximo es usualmente menos del 7%.

La segunda excepción de las leyes de similitud es cuando el modelo fotoelástico sufre una distorsión apreciable bajo la acción de la carga, ya que esto altera la distribución de los esfuerzos.

Como el modelo fotoelástico puede diferir del prototipo respecto a la escala, espesor, y carga aplicada, así como las constantes elásticas, es necesario extender este tratamiento para incluir las relaciones de escala. Mucho se ha escrito respecto a esto, empleando números adimensionales y el teorema Π de Buckingham; sin embargo, en la mayoría de las aplicaciones fotoelásticas, relacionar los esfuerzos del modelo al prototipo es relativamente simple cuando los números adimensionales pertinentes pueden ser escritos directamente. Por ejemplo, en el caso de un modelo bidimensional con una carga aplicada P , el número adimensional para los esfuerzos es $\sigma h/P$ y para los desplazamientos $\delta E h/P$.

Luego los esfuerzos del prototipo pueden escribirse como:

$$\sigma_p = \frac{P_p}{P_m} \frac{h_m}{h_p} \frac{l_m}{l_p} \sigma_m \quad \text{Ec. 139}$$

y los desplazamientos del prototipo como:

$$\delta_p = \frac{P_p}{P_m} \frac{E_m}{E_p} \frac{h_m}{h_p} \delta_m \quad \text{Ec. 140}$$

donde σ es el esfuerzo de un punto dado.

δ es el desplazamiento en un punto dado.

P es la carga aplicada.

h es el espesor.

l es una longitud típica.

los subíndices p y m se refieren al prototipo y al modelo respectivamente.

Concluyendo, el módulo de elasticidad no se considera en la determinación de la distribución de los esfuerzos, amén que la deformación cambie la distribución de la carga (esfuerzos de contacto por ejemplo.) También el módulo de Poisson no necesita considerarse cuando el cuerpo sea simplemente conexo y las fuerzas de cuerpo no existen o son uniformes.

d) Materiales fotoelásticos para aplicaciones bidimensionales.

d.1. Criterio para la selección de materiales.

Uno de los aspectos más importantes en el análisis fotoelástico es la selección del material adecuado para el modelo fotoelástico.

Desafortunadamente no existe un material perfectamente fotoelástico y el investigador debe seleccionar de la lista de materiales disponibles el que más se adapte a sus necesidades.

La siguiente lista da las propiedades que el material fotoelástico ideal debería tener:

1. El material debe ser transparente a la luz que se usa en el polaroscopio.
2. El Material debe ser muy sensible a los esfuerzos y deformaciones, indicado por un bajo valor de f_σ o f_ϵ .
3. El material debe tener propiedades lineales con respecto a :
 - Relaciones esfuerzo deformación.
 - Relaciones esfuerzo-orden de franja.
 - Relaciones deformación - orden de franja.
4. El material debe ser isótropo y homogéneo tanto mecánica como ópticamente.

5. El material no debe fluir extensivamente.
6. El material debe tener un alto módulo de elasticidad y un elevado esfuerzo último.
7. La sensibilidad del material (esto es f_{σ} ó f_{ϵ}) no debe cambiar mucho con las variaciones pequeñas de temperatura.
8. El material no debe exhibir efectos "time-edge".
9. El material debe poderse maquinar convencionalmente.
10. El material debe estar libre de esfuerzos residuales.
11. El material no debe ser demasiado caro.

1. Transparencia.

En la mayoría de las aplicaciones, los materiales escogidos son plásticos transparentes. Estos plásticos deben ser transparentes a la luz visible, pero no deben ser claros como el cristal. En ciertas aplicaciones especiales que requieren el estudio de materiales normalmente opacos, un polaroscopio infrarojo es lo que se emplea. Unos pocos materiales son transparentes en las regiones ultravioleta o infraroja. Pueden construirse polaroscopios que operen en estas regiones cuando se necesiten longitudes de onda muy largas o muy cortas. Sin embargo para el análisis de esfuerzos la luz visible es la más adecuada.

2. Sensitividad.

Frecuentemente se desea un material altamente sensitivo ya que esto incrementa el número de franjas que pueden ser observadas en el modelo. Si el valor de f_{σ} para un material es bajo, se puede obtener un patrón de franjas satisfactorio con relativamente bajas cargas. Este hecho reduce la complejidad de los sistemas de carga y la distorsión del modelo.

Materiales fotoelásticos con valores de f_{σ} desde menos de 0.2 hasta más de --- 2000 psi-in, están disponibles. Con respecto a los valores de f_{ϵ} , la situación no es tan satisfactoria, ya que los materiales con un valor suficientemente bajo de f_{ϵ} aún no están disponibles. (Los valores usuales de f_{ϵ} están entre 0.0002 y 0.02 in).

3. Linealidad.

Los modelos fotoelásticos son normalmente empleados para predecir los esfuerzos que ocurrirán en un prototipo de metal. Ya que una escala modelo -prototipo debe ser usada para establecer los esfuerzos del prototipo, el modelo debe exhibir propiedades lineales de esfuerzo-deformación, esfuerzo-óptica, deformaciones-óptica. Muy poco hay en la literatura sobre las relaciones deformación-óptica; sin embargo como el método fotoelástico es usualmente empleado para determinar diferencias de esfuerzos, este hecho no es demasiado serio. Curvas típicas esfuerzo-deformación y esfuerzo-orden de franja se muestran en la figura 50, para mostrar el comportamiento característico de un material polímero fotoelástico. La mayoría de los polímeros exhiben curvas lineales en la porción inicial de la gráfica; sin embargo a valores altos del esfuerzo, el material se comporta de manera no lineal.

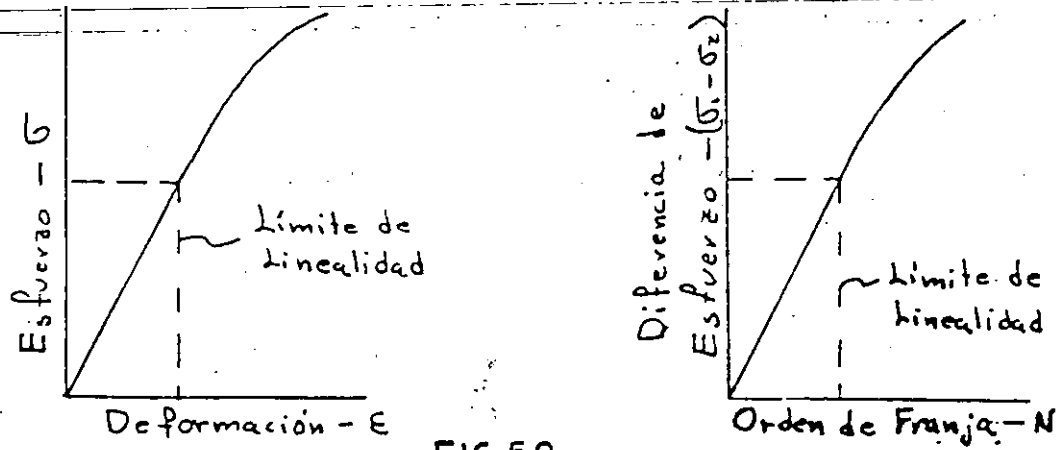


FIG 50

4. Isotropía y Homogeneidad.

Muchos de los materiales fotoelásticos son preparados de polímeros líquidos y vaciándolos entre dos placas de vidrio que forman el molde. Cuando el material fotoelástico es preparado mediante este procedimiento, las cadenas moleculares del polímero se orientan aleatoriamente, y los materiales son esencialmente isótropos y homogéneos. Sin embargo, algunos materiales son rolados o estirados durante el proceso. En ambos casos las cadenas moleculares se orientan en la dirección del rolado o del estirado. Estos materiales exhibirán propiedades no isotrópicas y no deben ser usados.

5. Fluides.

Desafortunadamente, la mayoría de los materiales con base de polímeros fluyen tanto mecánica como ópticamente en el período de el análisis fotoelástico. Debido a esto los polímeros no pueden ser considerados realmente como materiales elásticos, sino como viscoelásticos.

Uno de los primeros intentos para formular una teoría matemática de la fotoviscoelasticidad fué hecha por Mindlin considerando un modelo viscoelástico generalizado consistente de m elementos elásticos con un módulo cortante G_k ($k=1,2,\dots,m$) y m elementos viscosos con un coeficiente viscoso η_k ($k=1,2,\dots,m$) vease figura 51. Asumiendo que los efectos fotoelásticos resultan solamente de la deformación de los elementos elásticos del modelo, Mindlin mostró que el retardo relativo, expresado como $(n_1 - n_2)$ puede relacionarse con los esfuerzos y las deformaciones como:

$$(n_1 - n_2) \cos 2\theta_n = R [(\sigma_1 - \sigma_2) \cos 2\theta_\sigma] + 2S [(\epsilon_1 - \epsilon_2) \cos 2\theta_\epsilon] \quad \text{Ec. 141}$$

donde: $n_1 - n_2$ es el retardo relativo.

$\theta_n, \theta_\sigma, \theta_\epsilon$ son los ángulos entre los ejes ópticos principales, los esfuerzos principales, las deformaciones principales, y el eje respectivamente.

R y S son operadores lineales del tipo que relaciona esfuerzos y deformaciones en la teoría viscoelástica.

Para un modelo standard de 4 elementos (fig. 51), estos operadores son:

$$R = \frac{\eta_0^3}{4} \left[\frac{C_1}{G_1} + \frac{C_2}{G_2} \left(1 + \frac{\eta_2}{\eta_3} + \frac{\eta_2}{G_1} \frac{d}{dt} \right) \right]$$

$$S = \frac{\eta_0^3 C_2 \eta_2}{4 G_2} \frac{d}{dt}$$

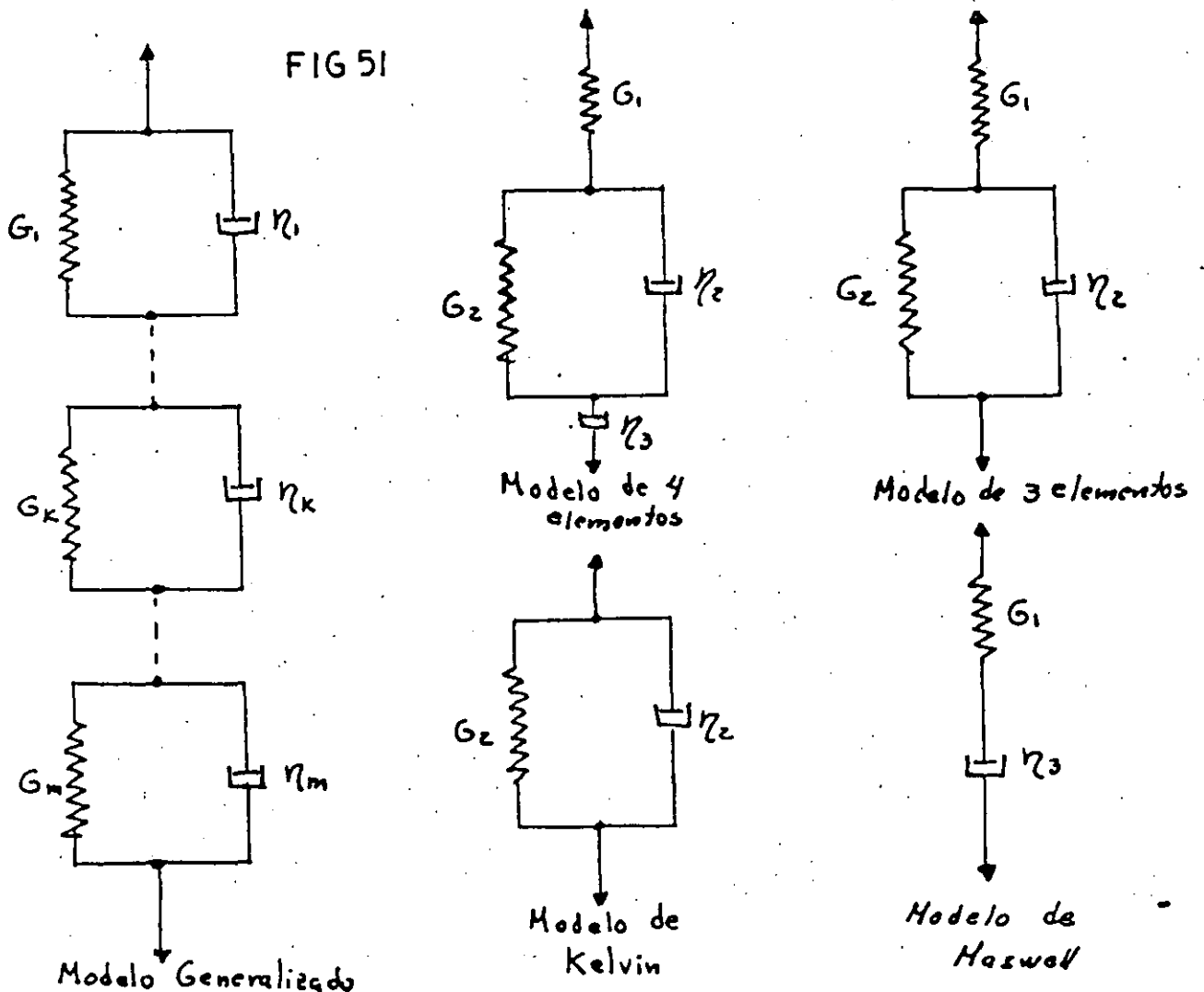
Ec. 142

donde: C_1 y C_2 son las constantes elásticas para los resortes 1 y 2 del modelo
 G_1 y G_2 son los módulos cortantes para los resortes 1 y 2 del modelo.
 η_2, η_3 son los coeficientes viscosos del modelo.

Puede verse de la ecuación 142 que la respuesta fotoelástica de un modelo de 4 elementos se debe a los esfuerzos, la rapidez de deformación, y la variación de los esfuerzos con respecto al tiempo. Para el modelo de tres elementos de la fig. 51 los operadores pueden expresarse como:

$$R = \frac{\eta_0^3}{4G_1} (C_1 - C_2) \quad S = \frac{\eta_0^3}{2} C_2 \quad \text{Ec. 143}$$

Estas ecuaciones muestran que la birrefringencia es debida a los esfuerzos y las deformaciones, pero es independiente de su variación en el tiempo. Coker y Filon encontraron que el material llamado xylonita sigue este modelo viscoelástico particular.



Para el modelo de Kelvin, los operadores se reducen a:

$$R = 0 \quad S = \frac{\eta_0^3}{2} C_2 \quad \text{Ec. 1}$$

Esta ecuación muestra que el efecto fotoelástico es función solamente de la diferencia de deformaciones.

Finalmente para el modelo de Maxwell los operadores son:

$$R = \frac{\eta_0^3 C_1}{4 G_1} \quad S = 0 \quad \text{Ec. 145}$$

Estas ecuaciones muestran que el efecto fotoelástico puede ser expresado como función de los esfuerzos unicamente.

Luego es claro de la discusión anterior, que la interpretación de los efectos de los esfuerzos, las deformaciones y sus variaciones con el tiempo, sobre los patrones de franjas, depende del tipo de modelo que mejor se aproxime al material fotoelástico bajo consideración.

Afortunadamente los materiales fotoelásticos comunmente empleados exhiben una propiedad importante, a saber, que los esfuerzos y las deformaciones que varían con la posición y con el tiempo, pueden representarse por el producto de dos funciones: -- una función exclusiva de las coordenadas y otra función exclusiva del tiempo, como se muestra abajo:

$$\begin{aligned} \sigma^* (x, y, t) &= \sigma(x, y) f(t) \\ \epsilon^* (x, y, t) &= \epsilon(x, y) g(t) \end{aligned} \quad \text{Ec. 146}$$

Cuando se toman las ecuaciones 146 puede demostrarse que:

$$\Theta_n = \Theta_\sigma = \Theta_\epsilon \quad \text{Ec. 147}$$

$$n_z - n_x = C(t) (\sigma_1 - \sigma_2) \quad \text{Ec. 148}$$

$$n_z - n_x = c(t) (\epsilon_1 - \epsilon_2) \quad \text{Ec. 149}$$

donde

$$\begin{aligned} C(t) &= R [f(t)] + \frac{1}{G_0} S [g(t)] \\ c(t) &= G_0 R [f(t)] + S [g(t)] \end{aligned} \quad G_0 = \frac{\sigma_1 - \sigma_2}{2(\epsilon_1 - \epsilon_2)}$$

Lo que esta serie de ecuaciones implica, es que las ecuaciones 97 y 99 pueden reescribirse en la siguiente forma:

$$\begin{aligned} \sigma_1 - \sigma_2 &= N/h f_\sigma(t) \\ \epsilon_1 - \epsilon_2 &= N/h f_\epsilon(t) \end{aligned} \quad \text{Ec. 150}$$

donde f_σ y f_ϵ están escritas como funciones del tiempo en vez de como constantes.

Así los materiales fotoelásticos que exhiben propiedades viscoelásticas pueden ser empleados en el análisis de la distribución de los esfuerzos elásticos si f_σ ó f_ϵ son determinados como función del tiempo. El procedimiento normal es calibrar el material fotoelástico como función del tiempo y graficar f_σ vs. tiempo, como se ilustra en la fig. 52. Inicialmente el valor de f_σ decrece rapidamente con el tiempo pero después de una hora, los cambios en f_σ son muy pequeños en el período de -- tiempo requerido para fotografiar el modelo. En la práctica, un modelo fotoelástico es cargado por una hora aproximadamente, luego es fotografiado y el valor de f_σ correspondiente a la calibración de una hora es usado en el análisis.

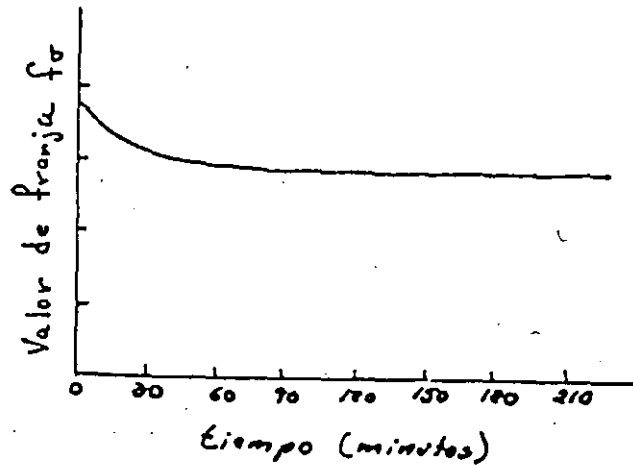


FIG 52

6. Módulo de elasticidad y esfuerzo último.

El módulo de elasticidad es importante en la selección de un material fotoelástico porque el módulo controla la distorsión del modelo debido a los esfuerzos aplicados. Si un modelo se distorsiona apreciablemente, la geometría de su frontera cambiará y la solución fotoelástica ya no será la adecuada. Errores de magnitud considerable son producidos por la distorsión del modelo, donde los cambios en la frontera influyen en la determinación de la distribución de esfuerzos. El factor que puede usarse para juzgar la habilidad del material para resistir la distorsión es $1/\rho_\epsilon$ o $E/\rho_\sigma (1+\nu)$. Los mejores materiales para resistir la distorsión, exhiben altos valores de $1/\rho_\epsilon$.

El esfuerzo último de un material fotoelástico es importante en dos aspectos. Primero, un material con un alto valor del esfuerzo último puede ser cargado a un nivel más alto sin arriesgar la seguridad del modelo. Segundo, un material con un alto valor del esfuerzo último puede ser empleado para producir un patrón de franjas de mayor orden. El esfuerzo último o el límite lineal del esfuerzo se relaciona a la sensibilidad del modelo. El índice de sensibilidad S está dado por:

$$S = \sigma_L / \rho_\sigma$$

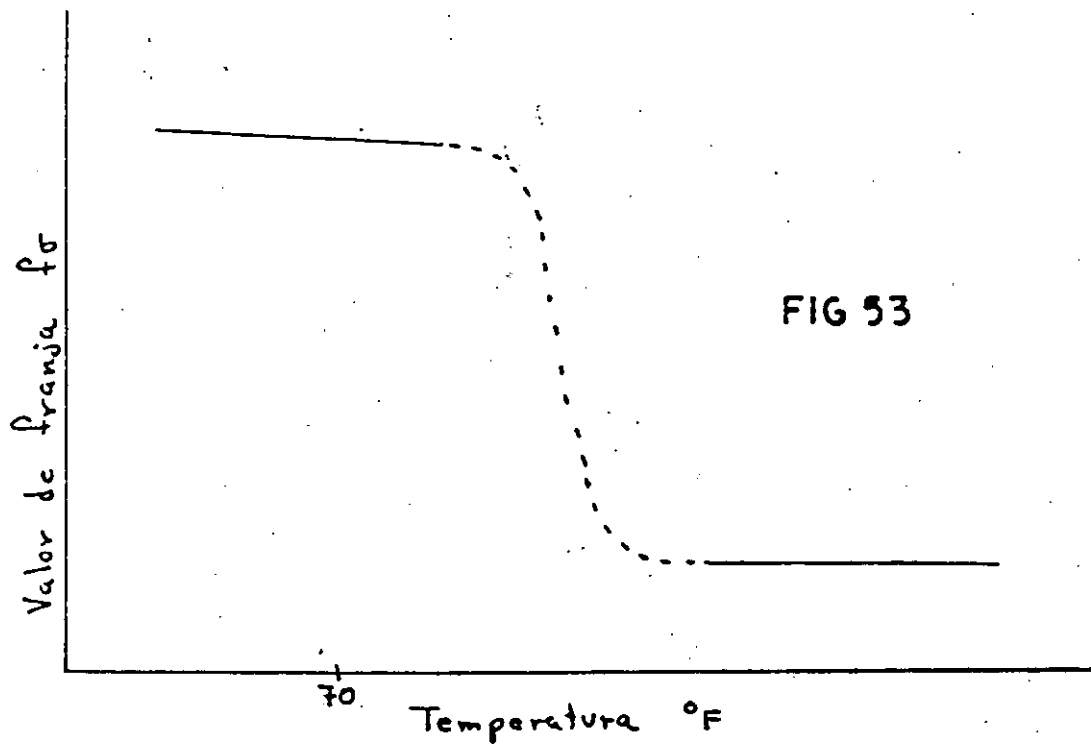
E. 151

donde σ_L es el límite lineal o el esfuerzo último según cual sea el menor.

7. Sensitividad a la temperatura.

Si el valor de franja del material en término de los esfuerzos cambia marcadamente con la temperatura, pueden introducirse errores en el análisis fotoelástico por los cambios de temperatura. Una curva típica que muestra las características generales del cambio del valor de franja con la temperatura se representa en la fig. 53. Para la mayoría de los polímeros hay una región lineal de la curva donde ρ_σ decrece lentamente con la temperatura. Sin embargo a una temperatura suficientemente alta usualmente por encima de 150°F , el valor de ρ_σ empieza a caer rápidamente como función de la temperatura. En este rango de temperaturas, una fase del polímero se vuelve menos viscoso, y como consecuencia el valor de ρ_σ se influye apreciablemente. Para fotoelasticidad convencional en dos dimensiones a una temperatura en

entre 70 y 80° F la pendiente de la curva en la región lineal es la característica importante. Afortunadamente la pendiente de la curva es usualmente modesta, de manera que el cambio producido en el valor de f_{σ} por las variaciones de temperatura del cuarto durante la prueba (usualmente menos de $\pm 5^{\circ}$ F), pueden ser despreciados.



8. Efectos "time- edge".

Cuando un modelo fotoelástico es maquinado de una hoja de plástico y es examinado sin carga como función del tiempo, se nota que se induce un esfuerzo en la frontera que produce franjas paralelas a la frontera. La influencia de estos efectos en un análisis fotoelástico es muy importante. El patrón de franjas observado, es debido a la superposición de dos estados de esfuerzos, uno debido a la carga y otro debido a los efectos "time-edge". Como los esfuerzos debido a el efecto "time-edge" son predominantes en la frontera, los errores introducidos por estos efectos son demasiado grandes en la determinación de los extremadamente importantes esfuerzos de frontera.

Se ha establecido que los efectos "time- edge" son causados por la difusión del agua del aire en el plástico o viceversa.

Para muchos plásticos fotoelásticos, el proceso de difusión, es tan lento a la temperatura ambiente que requiere muchos años para llegar al estado de equilibrio. Por esta razón un modelo recién maquinado estará usualmente en condiciones de aceptar agua

del aire y los efectos "time-edge" comenzarán a revelarse. La rapidez a la cual estos efectos se presentan depende de la humedad relativa del aire y de la temperatura. Las pruebas realizadas a humedades relativas mayores del 80% son difíciles, ya que el efecto "time-edge" es muy alto en 2 o 3 horas. Para la mayoría de los materiales fotoelásticos deben seleccionarse días relativamente secos (humedad relativa menor del 40 o 50%) y fotografiar tan rápido como sea posible.

Las resinas epóxicas son diferentes a los otros materiales fotoelásticos, ya que su condición de saturación puede alcanzarse en 2 o 3 meses. Para estas resinas es posible maquinar un modelo bidimensional de una hoja de material que haya sido mantenida a una humedad constante por varios meses de manera que haya alcanzado su estado de equilibrio. Luego, si el modelo es probado bajo esta misma humedad constante el efecto "time-edge" no se presentará.

9. Maquinabilidad.

Los materiales fotoelásticos deben ser maquinables para fabricar los complejos modelos usados en el análisis fotoelástico.

La acción de una herramienta cortante sobre el plástico, produce frecuentemente calor así como fuerzas relativamente altas de corte. Como consecuencia pueden aparecer esfuerzos en las fronteras lo que hace imposible un buen análisis fotoelástico.

Al maquinar modelos fotoelásticos debe tenerse cuidado de no producir grandes fuerzas o generar mucho calor. Esto puede hacerse empleando herramientas con recubrimientos de carbono, enfriamiento con aire y cortes pequeños con una velocidad de corte mas o menos alta. Para modelos bidimensionales se recomienda emplear un Router fig. 54

10. Esfuerzos residuales.

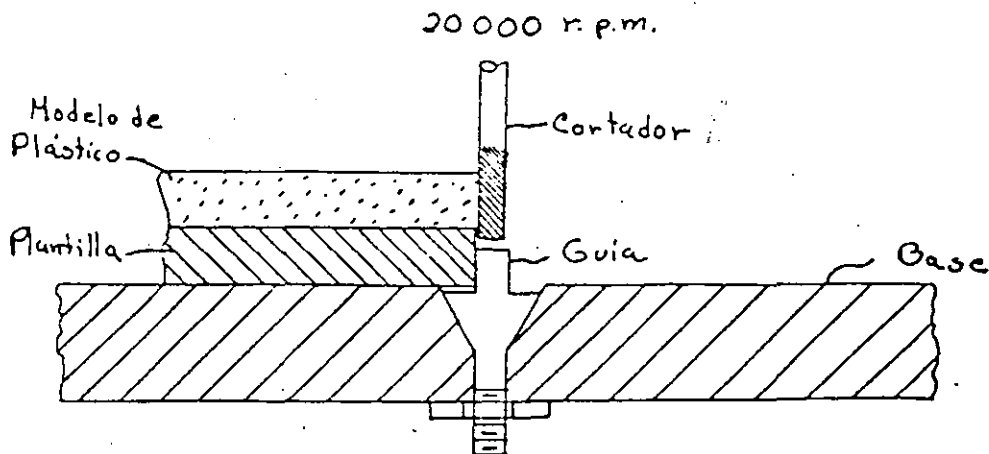
Los esfuerzos residuales se provocan a veces en el proceso de vaciado del material. Pueden observarse simplemente poniendo el material en el polaroscopio y viendo el número de franjas que aparece. La presencia de esfuerzos residuales en un modelo fotoelástico es muy nocivo ya que se superponen a los esfuerzos reales producidos al cargar el cuerpo, y esto introduce serios errores en el análisis.

En ciertos casos es posible reducir el nivel de los esfuerzos residuales templando la hoja de plástico en un baño de aceite caliente, sin embargo es imposible anularlos totalmente.

11. Costo del material

El costo de los materiales más comunmente empleados en fotoelasticidad van desde \$2 hasta \$20 dólares la libra siendo los más baratos el grupo de fenol formaldehidos y los más caros las resinas. Normalmente el costo del material para el modelo representa un muy pequeño porcentaje del costo total de la investigación. Por esto el costo del material no debe ser obstáculo y debe seleccionarse el mejor material disponible. Muy pocos modelos bidimensionales requieren más de una libra de material.

FIG 54



d.2. Conclusiones de la selección del material.

Un sumario de las propiedades ópticas y mecánicas de cinco materiales fotoelásticos se presentan en la tabla 3. Un exámen de esta tabla muestra que la resina epóxica es la que más se acerca a las propiedades ideales de un material fotoelástico. El material Catalin 61-893 también es bueno, pero los efectos "time -- edge" y su escases en grandes cantidades no lo hacen muy deseable.

El Castolite, libre de efectos "time-edge" lo hacen deseable para ciertas aplicaciones, y la altamente pulida superficie del CR-39 no puede ser ignorada en aplicaciones donde los efectos de Creep o la fluidez sean importantes. Finalmente, la goma de uretano puede ser ventajosa en fotoelasticidad dinámica y para la preparación de modelos de demostración.

Tabla 3

Material	Efectos Time-Edge	Fluidez	$P_{0.2}^{0.2}$ Psi-in	$P_{0.2}^{0.2}$ in	E Psi	ν	σ_L Psi	Maquimbilidad	$Q = \frac{E}{P_{0.2}}$	$S = \frac{\sigma_L}{P_{0.2}}$
Catalin 61-893	Malo	Bueno	86	1.91×10^{-4}	615 000	0.365	7 000	Bueno	7 160	81.5
Castolite	Excelente	Bueno	158	3.04×10^{-4}	705 000	0.255	7 400	Bueno	4 450	46.8
CR-39	Regular	Malo	88	5.03×10^{-4}	250 000	0.42	3 000	Malo	2 840	34.2
Epoxy*	Bueno	Bueno	58	1.68×10^{-4}	475 000	0.38	-----	Bueno	8 200	-----
Epoxy†	Bueno	Bueno	64	1.83×10^{-4}	475 000	0.36	8 000	Bueno	7 400	125
Uretano	Excelente	Bueno	0.9	3.24×10^{-3}	450	0.46	-----	Malo	500	-----

* ERL-2774 con 50 partes por cien de anhídrido pentálico.

† ERL-2774 con 42 partes por cien de anhídrido pentálico

« Para luz verde ($\lambda = 5461 \text{ \AA}$)

d.3. Métodos de calibración.

Para determinar la distribución de esfuerzos acertadamente, se requiere una calibración cuidadosa del material, sobre todo del valor de franja del material $f\sigma$. Aunque los valores de $f\sigma$ presentados en la tabla 3 son razonablemente ciertos, los valores de franja de los materiales varían con el proveedor, la temperatura, la edad, etc. Por esta razón es necesario calibrar cada hoja del material en el momento de la prueba. Aquí presento dos métodos de calibración igual de simples y exactos. En cualquier técnica de calibración se debe seleccionar un cuerpo para el cual la distribución teórica de los esfuerzos sea conocida. Preferentemente el modelo debe ser fácil de maquinar y de cargar. El modelo de calibración es cargado en intervalos y el orden de franja y la carga anotados. De estos datos, el valor de franja del material puede ser determinado.

Considere primero un espécimen bajo tensión teniendo una anchura w y un espesor h , que es comunmente usado para calibraciones.

El esfuerzo axial inducido en el espécimen por la carga P puede expresarse como:

$$\sigma_1 = \frac{P}{wh} \quad \text{y} \quad \sigma_2 = 0 \tag{Ec.152}$$

Sustituyendo la ecuación 152 en la ecuación 97 se tendrá:

$$\frac{P}{wh} = \frac{N f\sigma}{h} \quad \text{ó} \quad f\sigma = \frac{P}{wN} \tag{Ec.153}$$

Esta ecuación muestra que el valor de $f\sigma$ obtenido del espécimen a tensión es totalmente independiente del espesor h . En la práctica, se grafica una curva de P como función de N (fig. 55), para 5 o 6 puntos diferentes. La pendiente de la línea recta dibujada a través de estos puntos es usada para el valor de P/N en la ecuación 153. El disco circular cargado bajo compresión diametral es también empleado como modelo de calibración. El disco circular es algo más fácil de maquinar y de cargar que el espécimen a tensión, además, si se requiere pueden obtenerse varios puntos de calibración de una sola carga con este tipo de espécimen.

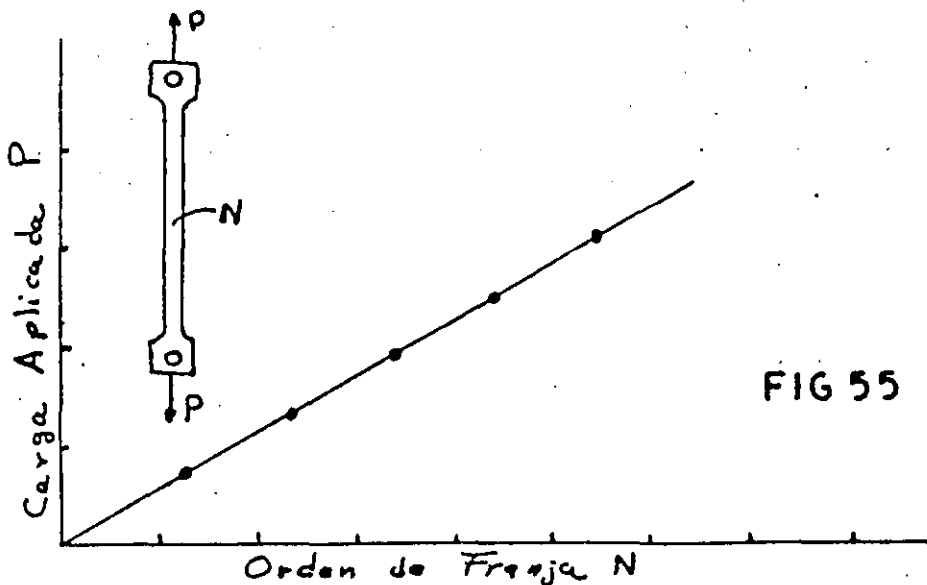


FIG 55

La distribución de esfuerzos a lo largo del diámetro horizontal (o sea $y=0$) está dada por:

$$\sigma_x = \sigma_1 = \frac{2P}{\pi h D} \left(\frac{D^2 - 4x^2}{D^2 + 4x^2} \right)^2$$

$$\sigma_y = \sigma_2 = -\frac{2P}{\pi h D} \left[\frac{4D^4}{(D^2 + 4x^2)^2} - 1 \right]$$

Ec. 154

$$\tau_{xy} = 0$$

donde D es el diámetro del disco.

x es la distancia a lo largo del diámetro horizontal medido desde el centro del disco.

h es el espesor del disco.

La diferencia entre los esfuerzos principales es:

$$\sigma_1 - \sigma_2 = \frac{8P}{\pi h D} \frac{D^4 - 4D^2x^2}{(D^2 + 4x^2)^2} = \frac{Nf_\sigma}{h}$$

Ec. 155

$$f_\sigma = \frac{8P}{\pi D N} \frac{D^4 - 4D^2x^2}{(D^2 + 4x^2)^2}$$

Ec. 156

La ecuación 156 puede ser empleada para calibrar materiales fotoelásticos si una carga simple P es aplicada al disco. En este caso el orden de franja N es determinado como función de x a lo largo del diámetro horizontal. Estos valores de N y x son sustituidos en la ecuación 156 para dar varios valores de f_σ , que se promedian para reducir los errores en la lectura del orden de franja.

Sin embargo es más común usar el centro del disco como punto de calibración y varios valores de la carga se aplican al disco.

Para este caso la ecuación 156 se reduce a:

$$f_\sigma = \frac{8P}{\pi D N}$$

Ec. 157

De nuevo se observa que el valor de f_σ es independiente del espesor del disco h.

El valor de P/N sustituido en esta ecuación se determina graficando varios puntos de P vs. N y estableciendo la pendiente de esta línea recta.

e) Lacas Birrefringentes.

e.1. Introducción.

En esta parte del trabajo, un área especial de la fotoelasticidad será discutida, la cual difiere, en cierto grado, de las aplicaciones más convencionales discutidas anteriormente. Este tópicos especial son las lacas birrefringentes, en donde una delgada capa de plástico fotoelástico se coloca en la superficie de un espécimen metálico. Cuando el espécimen es cargado y deformado, la laca fotoelástica responde y el patrón de franjas resultante observado en un polaroscopio de luz reflejada, puede ser interpretada en términos de las deformaciones superficiales del espécimen -- metálico. Aunque este método fué introducido hace aproximadamente 30 años, ha sido en los últimos años que ha tenido gran publicidad, y que sus aplicaciones se han extendido.

e.2. Lacas Birrefringentes.

El método se basa en la union de una delgada hoja de plástico fotoelástico a la superficie de un espécimen metálico. La laca birrefringente actúa, en efecto, como un "strain gage", y permite la determinación de la diferencia de las deformaciones principales sobre una cierta superficie. La aplicación del método se ilustra en la figura 56, donde dos técnicas diferentes para observar el patrón de franjas en la laca están representadas.

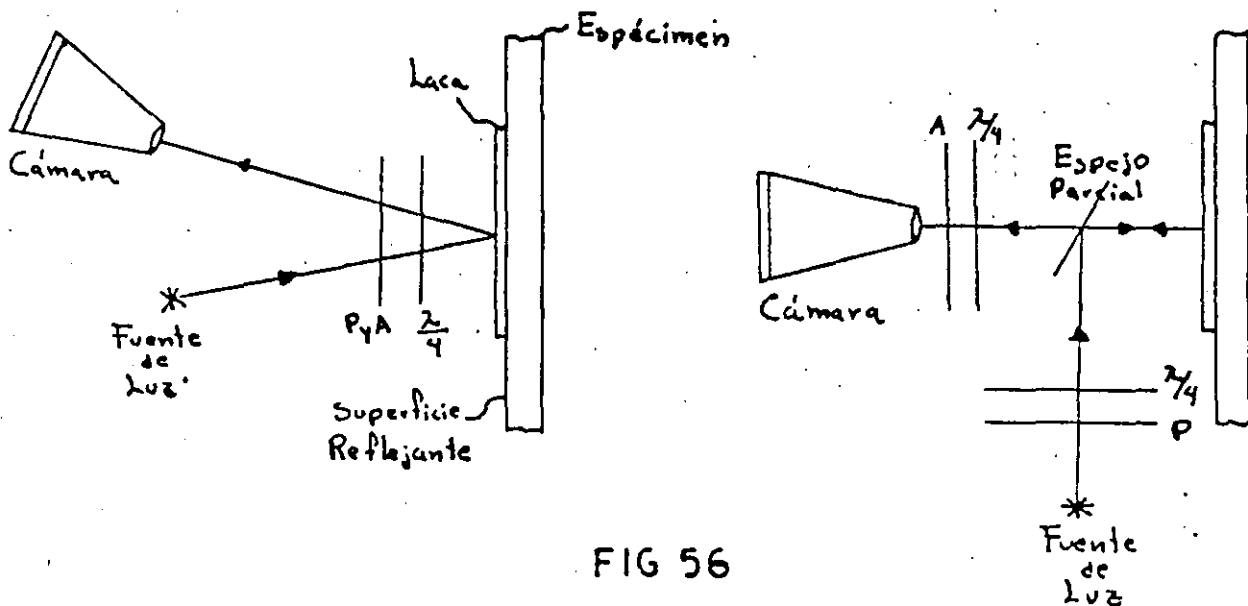


FIG 56

Cuando el espécimen se carga, los desplazamientos superficiales del espécimen se transmiten a la laca birrefringente si la union entre ellos es adecuada, conforme la laca responde a estos desplazamientos transmitidos, se inducen esfuerzos y una birrefringencia asociada. La observación de la laca mediante un polaroscopio de reflexión proporciona un patrón de franjas que se relaciona con las deformaciones superficiales del espécimen.

Si se asume que la laca es lo suficientemente delgada, entonces las deformaciones que ocurren en la superficie del espécimen se transmiten a la laca sin ninguna distorsión. Con esta suposición queda claro que:

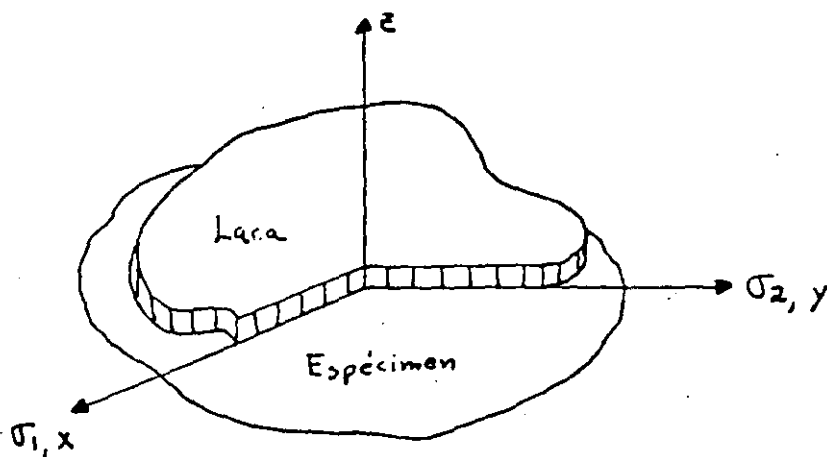
$$\sigma_3 = \sigma_3 = 0 \quad \text{en ambos, espécimen y laca.}$$

$$\epsilon_1^c(x, y) = \epsilon_1^s(x, y) \quad ; \quad \epsilon_2^c(x, y) = \epsilon_2^s(x, y)$$

E.C. 158

donde el sistema de coordenadas es el definido en la figura 57.

FIG 57



De la ley de Hook: $\epsilon_1^s = \frac{1}{E_s} (\sigma_1^s - \nu_s \sigma_2^s)$ $\epsilon_1^c = \frac{1}{E_c} (\sigma_1^c - \nu_c \sigma_2^c)$ E.C. 159

$$\epsilon_2^s = \frac{1}{E_s} (\sigma_2^s - \nu_s \sigma_1^s) \quad \epsilon_2^c = \frac{1}{E_c} (\sigma_2^c - \nu_c \sigma_1^c)$$

Sustituyendo las ecuaciones 158 en éstas ecuaciones anteriores podemos obtener:

$$\frac{1}{E_s} (\sigma_1^s - \nu_s \sigma_2^s) = \frac{1}{E_c} (\sigma_1^c - \nu_c \sigma_2^c) \quad ; \quad \frac{1}{E_s} (\sigma_2^s - \nu_s \sigma_1^s) = \frac{1}{E_c} (\sigma_2^c - \nu_c \sigma_1^c) \quad \text{E.C. 160}$$

Estas ecuaciones pueden resolverse para σ_1^c y σ_2^c como sigue:

$$\sigma_1^c = \frac{E_c}{E_s(1-\nu_c^2)} [(1-\nu_c\nu_s)\sigma_1^s + (\nu_c-\nu_s)\sigma_2^s] \quad \text{E.C. 161}$$

$$\sigma_2^c = \frac{E_c}{E_s(1-\nu_c^2)} [(1-\nu_c\nu_s)\sigma_2^s + (\nu_c-\nu_s)\sigma_1^s]$$

que expresan los esfuerzos de la laca en términos de los esfuerzos en el espécimen.

Restando las dos relaciones dadas en las ecuaciones 161, tenemos:

$$\sigma_1^c - \sigma_2^c = \frac{E_c}{E_s} \frac{1+\nu_s}{1+\nu_c} (\sigma_1^s - \sigma_2^s) \quad \text{E.C. 162}$$

Una inspección de la ecuación 162 muestra que la diferencia de los esfuerzos principales actuantes en la laca ($\sigma_1^c - \sigma_2^c$) está relacionada linealmente a la diferencia de los esfuerzos principales actuantes en la superficie del espécimen ($\sigma_1^s - \sigma_2^s$).

Las constantes elásticas E_c , E_s , ν_c , y ν_s , influyen en la magnitud de ($\sigma_1^c - \sigma_2^c$).

La respuesta fotoelástica de la laca se relaciona a ($\sigma_1^c - \sigma_2^c$) empleando la ecuación

$$\sigma_1^c - \sigma_2^c = \frac{Nf\sigma}{2h} = \frac{E_c}{E_s} \frac{1+\nu_s}{1+\nu_c} (\sigma_1^s - \sigma_2^s) \quad \text{E.C. 163}$$

y la diferencia de los esfuerzos principales en el espécimen está dado por:

$$\sigma_1^s - \sigma_2^s = \frac{E_s}{E_c} \frac{1+\nu_c}{1+\nu_s} \frac{Nf\sigma}{2h} \quad \text{E.C. 164}$$

Es claro que $\sigma_1^s - \sigma_2^s$ puede ser determinado por la observación del patrón de isocromáticas en la laca birrefringente si f_s , E_c , ν_s , ν_c , f_σ , y h , son conocidas. En algunos casos puede ser preferible trabajar en términos de las deformaciones en lugar de los esfuerzos. Esta transformación es muy simple ya que se ha asumido que $\epsilon_1^c - \epsilon_2^c = \epsilon_1^s - \epsilon_2^s$; luego:

$$\epsilon_1^s - \epsilon_2^s = \frac{N f_\epsilon}{2h} = \frac{N}{2h} \left(\frac{1 + \nu_c}{E_c} \right) f_\sigma \quad \text{Ec. 165a}$$

Usando la ecuación 165, la laca birrefringente puede ser empleada como un "strain gage" para dar la diferencia de las deformaciones principales ($\epsilon_1^s - \epsilon_2^s$). La ecuación 165a se representa de una manera diferente por los fabricantes de la laca para permitir la conversión del orden de franja en la diferencia de las deformaciones -- principales sin importar la longitud de onda de la luz empleada para examinar la laca. La forma alternativa de la ecuación 165a es:

$$\epsilon_1^s - \epsilon_2^s = \frac{N}{2h k} \quad \text{Ec. 165b}$$

donde

$$k = \lambda / f_\epsilon$$

En esta expresión la longitud de onda de la luz se expresa en micro pulgadas.

e.3. Sensitividad de las lacas birrefringentes.

El término sensitividad de esfuerzos S_σ^c está dado por:

$$S_\sigma^c = \frac{N}{\sigma_1^s - \sigma_2^s} = \frac{2h}{f_\sigma} \frac{E_c}{E_s} \frac{1 + \nu_s}{1 - \nu_c} \quad \text{Ec. 166}$$

y, similarmente, el término sensitividad de deformaciones S_ϵ^c está dado por:

$$S_\epsilon^c = \frac{N}{\epsilon_1^s - \epsilon_2^s} = \frac{2h}{f_\epsilon} = \frac{2h}{f_\sigma} \frac{E_c}{1 + \nu_c} \quad \text{Ec. 167}$$

Una inspección de las ecuaciones 166 y 167 desde el punto de vista de los parámetros de la laca, indica que h , f_σ , E_c , y ν_c , controla los dos factores de sensitividad. Queda claro que la sensitividad se incrementa linealmente con h . Sin embargo no siempre es posible incrementar h arbitrariamente hasta que se obtenga la suficiente sensitividad. Como veremos más adelante, el incrementar el espesor, produce un efecto de refuerzo, y en algunos casos distorsiona el estado de esfuerzos através del espesor de la laca. Los parámetros del material de la laca que influyen los factores de sensitividad pueden ser agrupados como:

$$Q^c = \frac{E_c}{1 + \nu_c} \frac{1}{f_\sigma} = \frac{1}{f_\epsilon} \quad \text{Ec. 168}$$

donde Q^c se llama figura de mérito de la laca.

La figura de mérito de la laca Q^c puede emplearse efectivamente para medir la utilidad de los materiales polímeros disponibles para aplicaciones de lacas birrefringentes.

Los méritos relativos de varios materiales basados en el valor de Q^c se muestran en la tabla 4. Los epoxis y la Catalin 61-893 son más sensitivos que las lacas comerciales conocidas como Fotostress S. Es también interesante notar que el vidrio, es tan sensitivo como las lacas polímeras comercialmente disponibles hoy en día.

Tabla 4

Material	f_{ϵ}^{\S} in	$Q^c = 1/f_{\epsilon}$
Epoxy*	1.68×10^{-4}	5960
Epoxy†	1.78×10^{-4}	5610
Epoxy**	1.83×10^{-4}	5480
Catalin 61-893	1.91×10^{-4}	5250
Fotostress S	2.58×10^{-4}	3980
Castolite	2.04×10^{-4}	3300
CR-39	5.03×10^{-4}	1980
Vidrio	1.9×10^{-4}	5280

* ERL-2774, 50 partes por 100 de anhídrido pentálico.

† Ciba 6020, 50 partes por 100 de anhídrido pentálico.

** ERL-2774, HEX Pentálico Estandar

§ Para luz verde ($\lambda = 5461 \text{ \AA}$)

La aplicación de las lacas birrefringentes al problema general en el análisis experimental de esfuerzos, está comunmente limitado por la baja sensibilidad inherente del método. Para ilustrar este punto, consideremos un ejemplo en el cual una laca, digamos Photostress S, se une a un espécimen de acero.

Las constantes elásticas pertinentes relacionadas a este problema son:

$$E_0 = 30 \times 10^6 \text{ psi.}$$

$$\nu_0 = 0.3$$

$$E_c = 0.420 \times 10^6 \text{ psi.}$$

$$\nu_c = 0.36$$

$$f_0 = 78 \text{ psi-in.}$$

$$h = 0.10 \text{ in.}$$

Sustituyendo estos valores en la ecuación 166 tendremos:

$$S_0^c = \frac{N}{\sigma_1^s - \sigma_2^s} = 3.42 \times 10^{-5}$$

El resultado de este simple cálculo claramente indica que la respuesta de la laca birrefringente es limitada, y que la laca tiene suficiente sensibilidad para una determinación de pequeños valores de $(\sigma_1^s - \sigma_2^s)$ en el campo completo.

Pueden emplearse métodos de compensación para ampliar la exactitud de la determinación del orden de franja N hasta aproximadamente 0.01, que permite la determinación de $\sigma_1^s - \sigma_2^s$ hasta aproximadamente $\pm 300 \text{ psi}$ o $\epsilon_1^s - \epsilon_2^s$ hasta aproximadamente $\pm 13 \frac{\mu\text{in}}{\text{in}}$. Sin embargo, cuando tienen que emplearse técnicas de compensación, el método no puede seguirse considerando como un método de campo completo ya que la compensación tiene una base de punto por punto.

Comunmente se utiliza luz blanca con las lacas birrefringentes para dar un patrón de isocromáticas de colores. Las franjas coloreadas pueden ser usadas para diferenciar ordenes de franja fraccionarios y compensar hasta aproximadamente 0.1 en una base de campo completo. Aunque la exactitud alcanzada no es tan grande como en el método convencional de compensación de punto por punto, usualmente pueden estimarse los esfuerzos en un 10% del valor real, con el método de campo completo.

La sensibilidad de la laca puede ser duplicada empleando el método fotográfico de multiplicación de franjas.

e.4. Efectos reforzantes de las lacas birrefringentes.

Cuando un espécimen metálico se laquea con una laca birrefringente, y se sujeta a cargas, la laca soporta una porción de esa carga, y consecuentemente la deformación se reduce en una cierta cantidad. Es posible en muchos casos calcular los efectos -- reforzantes de la laca, y establecer factores de corrección que pueden ser empleados de una manera simple para tener en cuenta este refuerzo. En esta sección, el refuerzo debido a la laca será calculado para esfuerzos planos y problemas de flexión. En el problema de esfuerzos planos, un elemento del espécimen laqueado puede aislarse como se muestra en la figura 58.

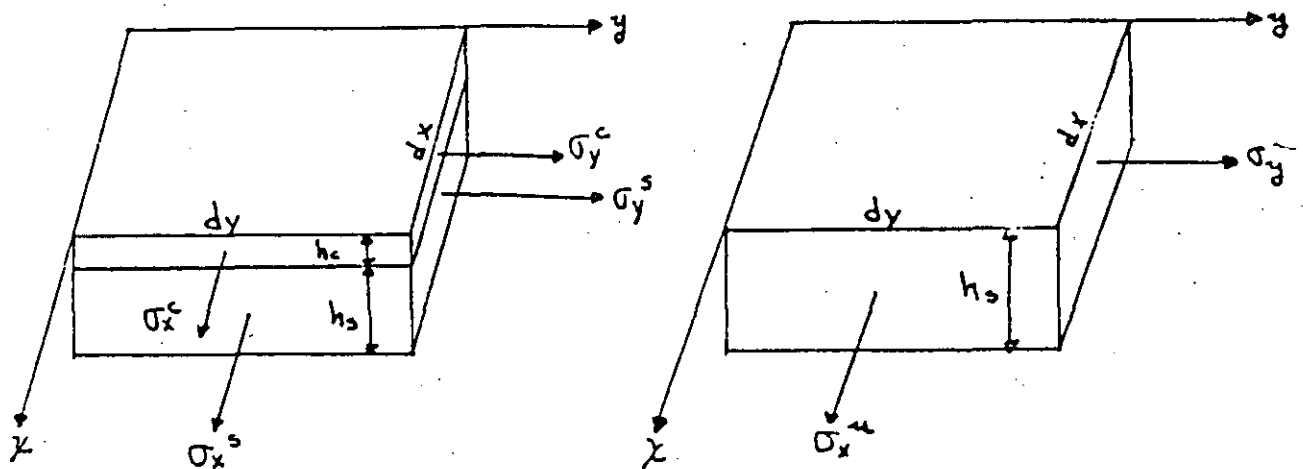


FIG 58

Un elemento similar del espécimen sin laquear también puede aislarse, y la fuerza actuante en la dirección x de ambos elementos puede igualarse para dar:

$$h_s dy \sigma_x^u = h_s dy \sigma_x^s + h_c dy \sigma_x^c$$

$$\sigma_x^u = \sigma_x^s + \frac{h_c}{h_s} \sigma_x^c$$

Ec. 169 a

La expresión correspondiente para las fuerzas en la dirección y es:

$$\sigma_y^u = \sigma_y^s + \frac{h_c}{h_s} \sigma_y^c$$

Ec. 169 b

Si se asume nuevamente que:

$$\begin{aligned} \epsilon_x^c &= \epsilon_x^s & \sigma_z^c &= \sigma_z^s = 0 \\ \epsilon_y^c &= \epsilon_y^s \end{aligned}$$

y como los dos elementos están bajo el estado de esfuerzos plano:

$$\sigma_x = \frac{E}{1-\nu^2} (\epsilon_x + \nu \epsilon_y) \quad \sigma_y = \frac{E}{1-\nu^2} (\epsilon_y + \nu \epsilon_x) \quad \text{Ec. 170}$$

Sustituyendo las ecuaciones 170 en 169, tenemos:

$$\frac{E_s}{1-\nu_s^2} (\epsilon_x^u + \nu_s \epsilon_y^u) = \frac{E_s}{1-\nu_s^2} (\epsilon_x^s + \nu_s \epsilon_y^s) + \frac{h_c}{h_s} \frac{E_c}{1-\nu_c^2} (\epsilon_x^c + \nu_c \epsilon_y^c) \quad (a)$$

$$\frac{E_s}{1-\nu_s^2} (\epsilon_y^u + \nu_s \epsilon_x^u) = \frac{E_s}{1-\nu_s^2} (\epsilon_y^s + \nu_s \epsilon_x^s) + \frac{h_c}{h_s} \frac{E_c}{1-\nu_c^2} (\epsilon_y^c + \nu_c \epsilon_x^c) \quad (b)$$

Restando la ecuación b de la ecuación a y simplificando:

$$\epsilon_x^u - \epsilon_y^u = \left(1 + \frac{h_c}{h_s} \frac{E_c}{E_s} \frac{1+\nu_s}{1+\nu_c} \right) (\epsilon_x^c - \epsilon_y^c) \quad \text{Ec. 171}$$

Esta ecuación puede escribirse como:

$$\epsilon_x^u - \epsilon_y^u = F_{CR} (\epsilon_x^c - \epsilon_y^c)$$

donde

$$F_{CR} = \left(1 + \frac{h_c}{h_s} \frac{E_c}{E_s} \frac{1+\nu_s}{1+\nu_c} \right) \quad \text{Ec. 172}$$

El término F_{CR} representa un factor de corrección que debe ser aplicado al valor de $(\epsilon_x^c - \epsilon_y^c)$ obtenido de la laca birrefringente para establecer el valor real de la diferencia de deformaciones principales en el espécimen sin laquear. El factor de corrección F_{CR} toma en cuenta el efecto de refuerzo debido a la presencia de la laca birrefringente.

Una gráfica que muestra F_{CR} como función de h_c/h_s es presentada para diferentes materiales del espécimen en la figura 59. Estos resultados están basados en un valor de $E_c = 420,000$ psi y $\nu_c = 0.36$, que son representativos del Photostress S, una de las lacas birrefringentes disponibles en el comercio. Una inspección de la figura 59 muestra que el factor de corrección es pequeño para valores de h_c/h_s , menores de 1, si el material del espécimen es metal. Si, sin embargo, el material del espécimen es madera, concreto, o plástico, entonces el factor de corrección es apreciablemente mayor.

Un segundo ejemplo que ilustra la influencia reforzante de la laca en el estado de esfuerzos y deformaciones en el espécimen, es el de una placa sujeta a un momento flexionante M . Considerese un elemento de la región central de ésta placa, como se indica en la figura 60. Si se asume que la distribución de esfuerzos es lineal y que es transmitido a través de la intercara espécimen-laca, entonces, de la teoría elemental de las placas, la deformación en el espécimen y la laca pueden expresarse como una función de z :

$$\epsilon_x^s = \frac{z}{\rho} \quad \text{Para } (h_s - A) \leq z \leq A$$

$$\epsilon_x^c = \frac{z}{\rho} \quad \text{Para } A \leq z \leq (A + h_c)$$

$$\epsilon_y^s = \epsilon_y^c = 0 \quad \text{Para todo } z$$

Ec. 173

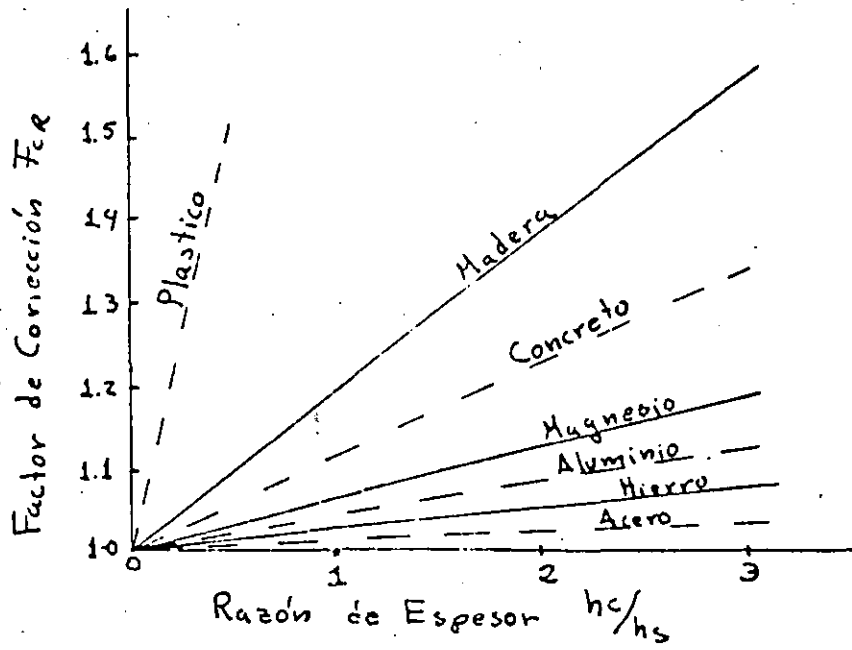


FIG 59

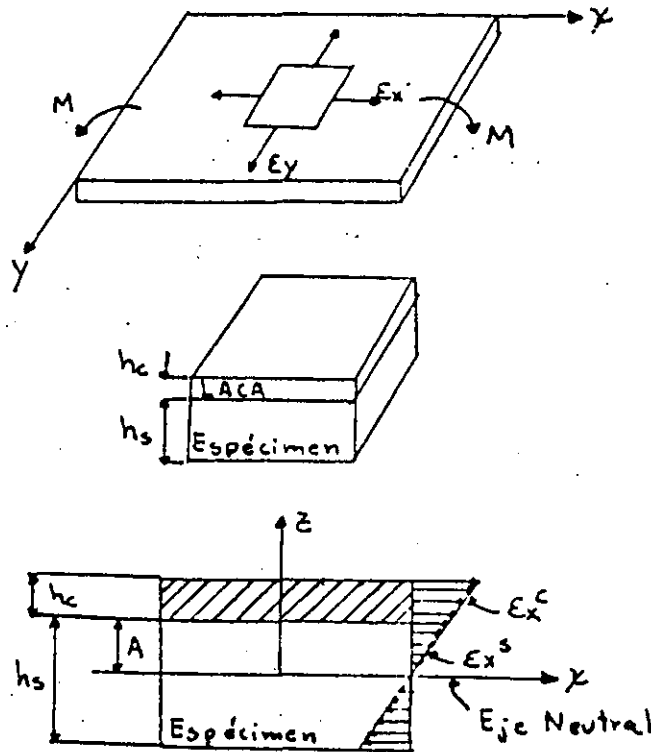


FIG 60

donde z es medido desde el eje neutro.

A es la distancia desde el eje neutro a la intercara.

ρ es el radio de curvatura.

Como se asume que σ_y desaparece para todos los valores de z , las ecuaciones 170 pueden emplearse con las ecuaciones 173 para expresar el esfuerzo σ_x en término de las deformaciones:

$$\sigma_x^s = \frac{E_s}{1-\nu_s^2} \frac{z}{\rho} \quad \text{Para } (h_s - A) \leq z \leq A \quad \text{Ec. 174}$$

$$\sigma_x^c = \frac{E_c}{1-\nu_c^2} \frac{z}{\rho} \quad \text{Para } A \leq z \leq (A + h_c)$$

La posición del eje neutro, descrito por A , puede obtenerse considerando el equilibrio de la placa en la dirección x , como se muestra a continuación:

$$\int_{A-h_s}^A \sigma_x^s dz + \int_A^{A+h_c} \sigma_x^c dz = 0 \quad \text{Ec. 175}$$

Sustituyendo la ecuación 174 en 175, integrando, y resolviendo para A tenemos:

$$A = \frac{h_s}{2} \frac{1 - BC^2}{1 + BC} \quad \text{Ec. 176}$$

donde

$$B = \frac{E_c}{E_s} \frac{1 - \nu_s^2}{1 - \nu_c^2}; \quad C = \frac{h_c}{h_s}$$

El radio de curvatura ρ puede ser calculado considerando el equilibrio de los momentos donde

$$M = \int_{A-h_s}^A \sigma_x^s z dz + \int_A^{A+h_c} \sigma_x^c z dz \quad \text{Ec. 177}$$

Sustituyendo la ecuación 174 en 177, integrando, y usando la ecuación 176 para simplificar los resultados, puede mostrarse que:

$$\frac{1}{\rho} = \frac{12M}{H} \frac{1 - \nu_s^2}{E_s h_s^3}$$

donde

$$H = \left[4(1 + BC^3) - \frac{3(1 - BC^2)^2}{1 + BC} \right] \quad \text{Ec. 178}$$

Si la placa se examina en un polaroscopio de reflexión, el patrón de franjas es proporcional al promedio de la diferencia de deformaciones ($\epsilon_x^c - \epsilon_y^c$) a través del espesor de la placa. Este promedio puede calcularse de las ecuaciones 173, 176, y 177 como sigue:

$$(\epsilon_x^c - \epsilon_y^c)_{av.} = \frac{12M}{H} \frac{1 - \nu_s^2}{E_s h_s^3} \frac{1}{h_c} \int_A^{A+h_c} z dz$$

que da:

$$(\epsilon_x^c - \epsilon_y^c)_{av.} = \frac{6M}{H} \frac{1 - \nu_s^2}{E_s h_s^2} \frac{1 + C}{1 + BC} \quad \text{Ec. 179}$$

Como la diferencia real de las deformaciones en la superficie de una placa no laqueada es:

$$(\epsilon_x^s - \epsilon_y^s) = 6M \frac{1 - \nu_s^2}{E_s h_s^2} \quad \text{Ec. 180}$$

queda claro, mediante una comparación de las ecuaciones 179 y 180, que la laca no indica la diferencia real de las deformaciones superficiales. Es posible, sin embargo, corregir el error introduciendo un factor de corrección de flexión. Luego

$$(\epsilon_x^s - \epsilon_y^s)_{\text{real}} = F_{\epsilon_0} (\epsilon_x^c - \epsilon_y^c)_{\text{av.}}$$

donde el factor de corrección de flexión F_{ϵ_0} es:

$$F_{\epsilon_0} = \frac{H(1+BC)}{1+C} = \frac{1+BC}{1+C} \left[4(1+BC^3) - \frac{3(1-BC^2)^2}{1+BC} \right] \quad \text{Ec. 181}$$

El factor de corrección de flexión, que es función de las razones B y C, se muestra en forma gráfica en la figura 61. Una inspección de estas curvas indica que pueden cometerse grandes errores si los resultados fotoelásticos no son correctamente corregidos. Es interesante notar que el valor de F_{ϵ_0} primero decrece con h_c/h_s y luego crece con posteriores incrementos de h_c/h_s . Primero, conforme el valor de h_c/h_s se incrementa, el plano medio de la laca se separa de la intercara, y la deformación en este plano medio (que es la deformación promedio) se incrementa relativamente a la deformación real en la superficie del espécimen no laqueado. Después, conforme la laca se vuelve más gruesa (esto es h_c/h_s se incrementa), el efecto reforzante baja la deformación promedio en la laca. Para un espécimen de aluminio los dos factores que producen el error se cancelan cuando $h_c/h_s = 1.6$; luego el valor de F_{ϵ_0} es 1.

e.5. Efectos del espesor de las lacas birrefringentes.

En la discusión de las lacas birrefringentes presentada anteriormente se ha asumido que las deformaciones se transmiten del espécimen a la laca de una manera ideal. Desafortunadamente, esta transmisión ideal de las deformaciones entre el espécimen y la laca, no siempre se verifica, y la distribución de deformaciones en la laca está influenciada por el espesor de la laca. La distorsión de la distribución de las deformaciones se conoce como el efecto de espesor. El hecho de que la distribución de deformaciones en la laca se distorsione complica el problema de interpretación del patrón de franjas obtenido de la laca en términos de las deformaciones superficiales. La magnitud del error introducido debido al efecto de espesor, depende de cada problema en particular. A veces el error será pequeño, pero en ocasiones puede ser muy grande.

El señor Duffy y sus asociados (J. Duffy and C. Mylonas, An Experimental Study of the Effects of the Thickness of Birefringent Coatings, in "Photoelasticity"), han aproximado el problema del efecto de espesor en lacas birrefringentes para variaciones bidimensionales en las deformaciones superficiales, empleando la teoría de la elasticidad. La laca se considera como el cuerpo, con desplazamientos superficiales prescritos en la intercara (esto es, $z = 0$, como se define en la figura 57) como:

$$\begin{aligned} u(x, y, 0) &= U \operatorname{Sen} m x \operatorname{Cos} n y \\ v(x, y, 0) &= V \operatorname{Cos} p x \operatorname{Sen} q y \\ w(x, y, 0) &= W \operatorname{Cos} r x \operatorname{Cos} s y \end{aligned}$$

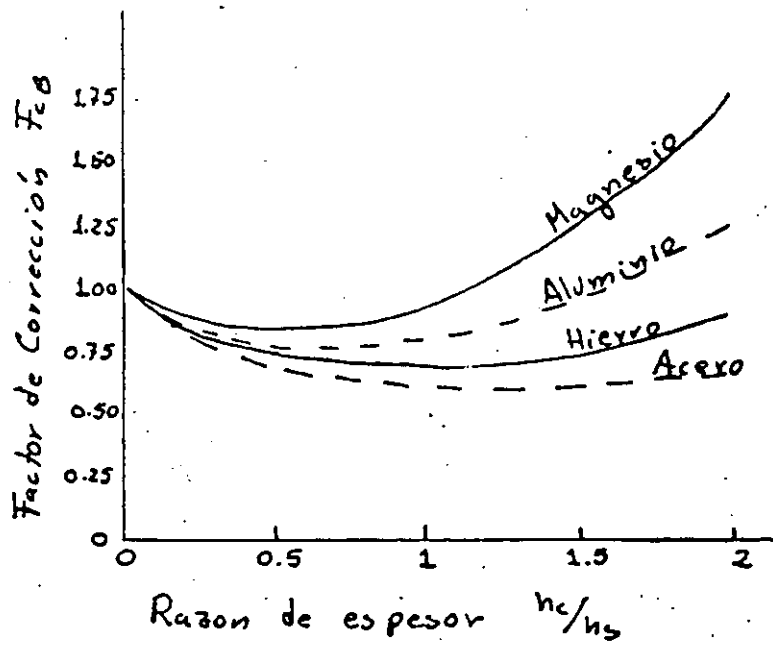


FIG 6I

donde U, V, W, y m, n, p, q, r, y s son constantes arbitrarias usadas para describir el campo de desplazamientos en la intercara. La solución de este problema elástico muestra que el promedio de la diferencia de las deformaciones a través del espesor de la laca y a lo largo del eje x puede representarse como:

$$(\epsilon_x^c - \epsilon_y^c)_{av} = F(mh, nh, \nu) \epsilon_x(x, 0, 0) - F(qh, ph, \nu) \epsilon_y(x, 0, 0) + \frac{r^2 - s^2}{y^2} G(\xi h, \nu) \frac{w(x, 0, 0)}{h} \tag{Ec. 182}$$

donde:

$$G(\xi h, \nu) = \frac{4\nu(1-\nu)(1 - \cosh \xi h) - 2\nu \xi h \operatorname{Senh} \xi h + (\xi h)^2 + \operatorname{Sinh}^2 \xi h}{(\xi h)^2 + (3-4\nu) \cosh^2 \xi h + (1-2\nu)^2}$$

$$F(mh, nh, \nu) = \frac{2n^2}{\xi^2} \frac{\tanh \xi h}{\xi h} + \frac{m^2 - n^2}{\xi^2} \left\{ \frac{2\nu \xi h \operatorname{Cosh} \xi h - 2\nu(1-2\nu) \operatorname{Sinh} \xi h + (1-2\nu)(2\xi h + \operatorname{Sinh} 2\xi h)}{\xi h [(\xi h)^2 + (3-4\nu) \cosh^2 \xi h + (1-2\nu)^2]} \right\}$$

$$\xi = (m^2 + n^2)^{1/2} ; \quad \eta = (r^2 + s^2)^{1/2}$$

En la ecuación 182 se necesitan tres factores de corrección para ajustar el promedio de la diferencia de deformaciones a través del espesor de la laca, a aquellos que ocurren en la superficie del espécimen que está siendo investigada. Los factores de corrección $F(mh, nh, \nu)$ y $F(qh, ph, \nu)$ se usan con los dos componentes de las deformaciones de la intercara.

Los factores de corrección pueden ser calculados para valores arbitrarios de m, n, p, q, r, y s. Un ejemplo típico de la magnitud del factor de corrección $F(\xi h, 0, \nu)$ se muestra en la figura 62 a. Una inspección de esta figura muestra que el factor de corrección varía entre 0 y 0.93 aproximadamente conforme el cociente de la longitud de onda del gradiente sinusoidal de la deformación al espesor de la laca varía de 0 a 30. Este ejemplo particular corresponde a un caso en el cual la deformación varía en la dirección x pero no en la dirección y (esto es $n = 0$). Para evitar los errores asociados con la distorsión de la distribución de las deformaciones a través del espesor de la laca, se requieren espesores de laca muy delgados ($h < \pi/20m$).

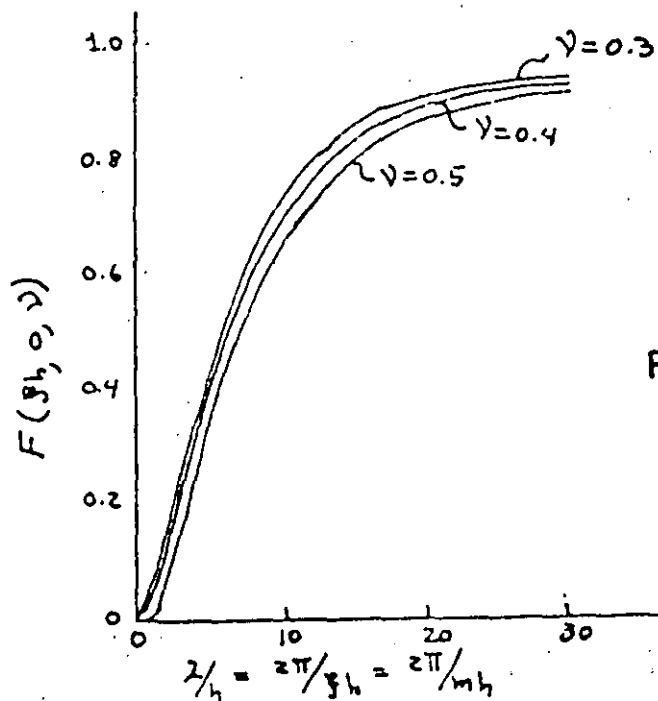


FIG 62 a

1:1 Generalidades

Con el enunciamiento por Robert Hooke en 1.678 de la ley que relaciona las tensiones y deformaciones en materiales sometidos a sollicitaciones mecánicas y el posterior descubrimiento en 1.856 - de Lord Kelvin referente a las variaciones que en su resistencia sufre un conductor eléctrico cuando se modifica su geometría, se establecieron los principios fundamentales de la extensometría eléctrica; si bien su nacimiento ha sido muy posterior, pudiendo decirse - que fué a partir de la II guerra Mundial, cuando su aplicación empezó a vulgarizarse.

En su forma más elemental, una banda extensométrica (Strain-gage; jauge électrique d'extensometrie) está constituida - (fig. 1) por un hilo metálico muy fino en forma de "parrilla" montado sobre un soporte, de tal manera, que la mayor parte de su longitud sea paralela a una dirección fija. Si deseamos conocer las deformaciones de una estructura según una dirección, pegaremos el extensímetro con sus hilos paralelos a dicha dirección y al deformarse aquella, producirá variaciones en la geometría del hilo del extensímetro que originarán una variación de su resistencia; por lo tanto disponiendo de instrumentos capaces de medir variaciones pequeñas de la resistencia original del extensímetro, podemos conocer las deformaciones mecánicas de la estructura en la que se pegó.

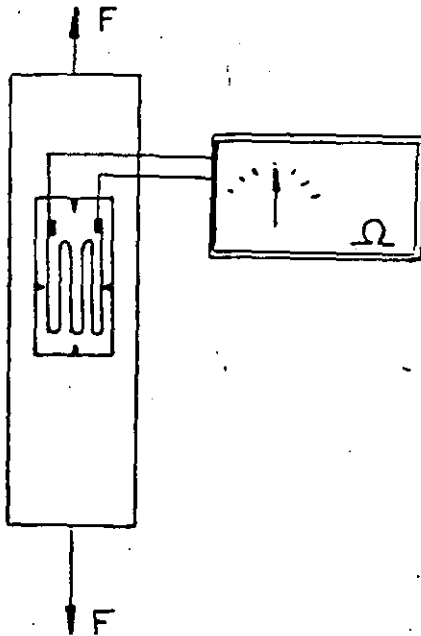


fig 1

La Resistencia de materiales nos enseña las leyes que ligan deformaciones y tensiones, siendo la extensometría la técnica que permitirá conocer el estado de tensiones de un cuerpo a partir de la medida del estado de deformaciones, sin necesidad de recurrir a ensayos destructivos, pudiéndose efectuar un número ilimitado de mediciones. pues si bien el extensímetro una vez pegado es irrecu-

perable, sus cualidades con el tiempo perduran, dentro de los límites de utilización.

Por tanto, una banda extensométrica actúa como elemento transductor, transformando la variación de una magnitud mecánica en la de una eléctrica, facultad ésta que se aprovecha para fabricar captadores sensibles a ciertos parámetros mecánicos, pudiendo así evitarse el inconveniente de su no recuperación.

Actualmente el desarrollo de las técnicas extensométricas, ha alcanzado tal grado de perfección, que normalmente los problemas de medida de deformaciones y tensiones que puedan presentarse en ingeniería tienen solución, determinándose con exactitud la evaluación de fenómenos cuya influencia en la realización de proyectos es primordial, con la ambiciosa meta de fabricación con coeficientes de seguridad próximos a la unidad, sin pérdida de garantías funcionales. Reducción de costos de fabricación, control de calidad, homologación de marcas, investigación, estudios y ensayos, mejores de fabricados, nuevos diseños, etc, etc, son logros, que incluso a corto plazo, se consiguen con equipos sencillos elementales y económicos.

1.2 PRINCIPIOS TEORICOS DEL EXTENSIMETRO OHMICO

Consideremos un extensímetro formado por un solo hilo conductor unido a una estructura, de tal forma, que las deformaciones que pueden producirse sean idénticas en ambos (fig 2).

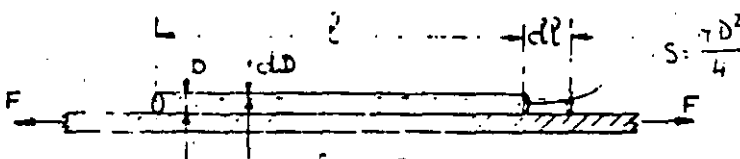


fig 2.

La resistencia R del hilo tiene por valor:

$$R = \rho \frac{l}{S}$$

(ρ = resistividad)

Si el hilo sufre una deformación (alargamiento), la longitud l aumenta, la sección S disminuye y la resistividad varía dando lugar estos cambios a una variación del valor de R que podemos obtener diferenciando (1) y después deducir la relación entre la deformación elástica del hilo y la variación relativa o unitaria de resistencia, en efecto:

$$dR = \frac{\rho}{S^2} (l \, d\rho + \rho \, dl - dS \, l) \quad [2]$$

Dividiendo [2] en [1]:

$$\frac{dR}{R} = \frac{dl}{l} + \frac{d\rho}{\rho} - \frac{dS}{S}$$

Si el hilo es de forma cilíndrica:

$$S = \frac{\pi D^2}{4}; \quad dS = \frac{\pi}{2} D dD \quad \text{y} \quad \frac{dS}{S} = \frac{2dD}{D} \quad \text{sustituyendo en [3]}$$

$$\frac{dR}{R} = \frac{dl}{l} + \frac{d\rho}{\rho} - 2 \frac{dD}{D} \quad [4]$$

La (4) podemos escribirla como:

$$\frac{\frac{dR}{R}}{\frac{dl}{l}} = 1 + \frac{\frac{d\rho}{\rho}}{\frac{dl}{l}} - 2 \frac{\frac{dD}{D}}{\frac{dl}{l}}$$

pero el último término del segundo miembro, es la expresión del coeficiente de Poisson $\frac{dD}{D} : \frac{dl}{l} = -\mu$, luego sustituyendo tenemos el valor de la relación entre la variación de resistencia y la deformación unitaria.

$$\frac{\frac{dR}{R}}{\frac{dl}{l}} = 1 + \frac{\frac{d\rho}{\rho}}{\frac{dl}{l}} + 2\mu \quad [5]$$

al segundo miembro de (5) se llama factor de banda o de sensibilidad K;

$$K = 1 + 2\mu + \frac{\frac{d\rho}{\rho}}{\frac{dl}{l}} \quad [6]$$

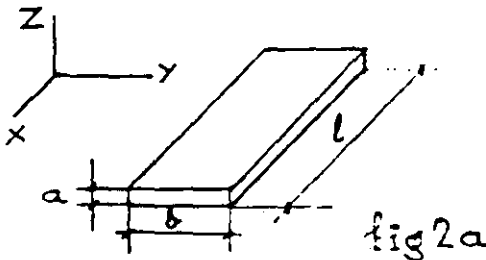
Bridgman enunció que la variación relativa de resistividad de un conductor es proporcional a la variación relativa de volumen de dicho conductor

$$\frac{d\rho}{\rho} = C \frac{dV}{V} \quad (C = \text{Constante de Bridgman}) \dots [7]$$

Si $V = l \cdot S$ y sustituyendo [7] en [5]

$$\frac{dR}{R} = [(1+2\mu) + C(1-2\mu)] \frac{dl}{l} \quad [8]$$

Hasta aquí, hemos considerado la sección del hilo circular, pero en las modernas bandas impresas la sección es rectangular y la variación de resistencia $\frac{dR}{R}$, función de las deformaciones que experimenta la banda en las tres dimensiones se calculará así.



Siendo ρ (fig. 2a)

$$R = \rho \frac{l}{ab} \quad [9]$$

y las deformaciones según los ejes X, Y, Z son:

$$\varepsilon_x = \frac{dl}{l} ; \quad \varepsilon_y = \frac{db}{b} ; \quad \varepsilon_z = \frac{da}{a} = -\mu \frac{dl}{l} - \mu \frac{db}{b} = -\mu (\varepsilon_x + \varepsilon_y)$$

diferenciando logarítmicamente la (1) tendremos

$$\begin{aligned} \frac{dR}{R} &= \frac{dP}{P} + \frac{dl}{l} - \frac{da}{a} - \frac{db}{b} = C \frac{dV}{V} + \frac{dl}{l} - \frac{da}{a} - \frac{db}{b} \\ &= C \left(\frac{dl}{l} + \frac{da}{a} + \frac{db}{b} \right) + \frac{dl}{l} - \frac{da}{a} - \frac{db}{b} \\ &= C (\varepsilon_x - \mu \varepsilon_x - \mu \varepsilon_y + \varepsilon_y) + \varepsilon_x + \mu \varepsilon_x + \mu \varepsilon_y - \varepsilon_y \\ &= \varepsilon_x [C(1-\mu) + 1 + \mu] + \varepsilon_y (C-1)(1-\mu) \end{aligned}$$

y llamando

$$\begin{aligned} K_1 &= C(1-\mu) + 1 + \mu \\ K_2 &= (C-1)(1-\mu) \end{aligned}$$

queda

$$\frac{dR}{R} = \varepsilon_x K_1 + \varepsilon_y K_2 \quad \dots \dots \dots [10]$$

La (10) nos indica que una banda extensométrica es sensible a la deformación longitudinal según la dirección de los hilos activos, pero también a la deformación transversal, siendo esto último un inconveniente que puede introducir errores. Si el valor de la constante de Bridgman se consigue que valga la unidad, $K_2=0$, pero prácticamente es muy difícil de lograr, por lo que se tiende a buscar un compromiso que haga K_2 lo menor posible y por lo menos que permita conocer el error que su presencia introduce en la medida. Veamos como se logra.

La (10) puede escribirse:

$$\frac{dR}{R} = K_1 (\varepsilon_x + K_t \varepsilon_y) \quad \dots \dots \dots [10a]$$

siendo $K_t = \frac{K_2}{K_1}$ = factor de sensibilidad transversal del extensómetro. Sustituyendo:

$$\frac{dR}{R} = K_1 (\varepsilon_x - K_t \mu \varepsilon_x) = K_1 (1 - \mu K_t) \varepsilon_x = K \varepsilon_x \quad \dots \dots \dots [11]$$

El factor de banda dado por el fabricante es $K = K_1 (1 - \mu K_t)$ para $\mu = 0.285$

La expresión:

$$e = \frac{K_t \left(\frac{\varepsilon_y}{\varepsilon_x} + \mu \right)}{1 - \mu K_t} \cdot 100 \quad \dots \dots \dots [11a]$$

nos dá el error en % que sobre la medida de la deformación según ε_x introduce el factor de sensibilidad transversal. Vemos que en el caso en que la dirección de ε_x coincide con la dirección de tensiones unidireccionales (tracción o compresión simple) el error es cero, pues

se cumple que $E_y = -\mu E_x$, (fig 2b).

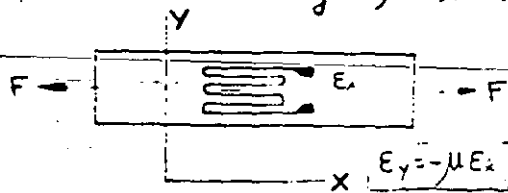


fig 2b

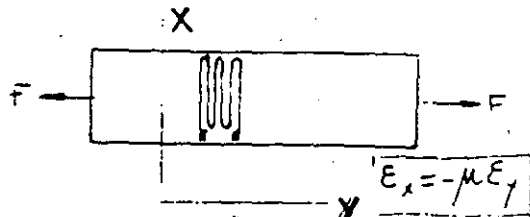


fig 2c

Según la fig. 2c vamos a medir la de formación lateral correspondiente a un estado unidireccional de tensiones, aquí por el giro dado al extensímetro, se cumple que :

$$E_x = -\mu E_y ; \frac{E_y}{E_x} = -\frac{1}{\mu}$$

Si consideramos $\mu = 0,3$ y $k_t = 3\%$ sustituyendo en (11a), el error vale:

$$e = \frac{0,03 \left(-\frac{1}{0,3} + 0,3 \right)}{1 - 0,3 \cdot 0,03} \times 100 = -9\%$$

El error del -9% no puede despreciarse y aún cuando en el ejemplo se ha buscado un caso muy extremo, habrá que evaluar siempre la magnitud del error y considerar si debe o no despreciarse.

El problema en el caso que se conozca la dirección principal de deformaciones (fig. 2b) no tiene importancia; pero como se verá posteriormente en el caso de rosetas de dos o tres direcciones - el error por efecto de la sensibilidad lateral puede tener influencia, pues se estará siempre entre las dos posturas extremas presentadas en las fig. 2b y 2c.

1.3. OBJETO DE LAS MEDIDAS EXTENSOMETRICAS: Unidades

Los materiales empleados en la fabricación de máquinas o cualquier elemento sometido a sollicitaciones externas, sufren en su estructura interna unas tensiones que deben equilibrar las cargas que soportan para que no aparezca la rotura, sobredimensionándose siempre los diseños para obtener un coeficiente de seguridad adecuado. Evidentemente el máximo conocimiento del estado de tensiones ayudará a mejorar el diseño y a reducir el coeficiente de seguridad, pero la medida directa de tensiones no siempre es posible.

Demostraremos en este capítulo, que si conocemos el estado de deformaciones en un punto, podremos calcular el estado de tensiones del mismo y determinar el valor de tensiones críticas (tensiones normales máximas o combinación, en una determinada dirección de tensiones normales y cortantes, que puedan representar un fallo).

El estado de deformaciones se determinará a partir de las medidas, que en una, dos o tres direcciones, que se efectuen con

extensímetros.

Salvo casos muy especiales, la aplicación de las bandas extensométricas será siempre en la superficie de los elementos de ensayo, por lo que solo estudiaremos el estado plano o binaxial de deformaciones y tensiones en un punto.

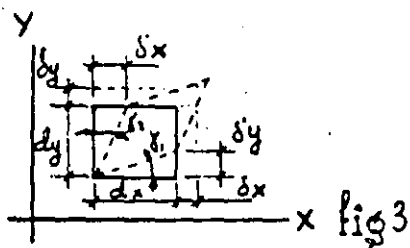
El concepto de deformaciones es análogo al de alargamiento unitario y lo representaremos por ϵ midiéndose en microdeformaciones ($\mu\delta$).

$$\epsilon \cdot 10^6 = \frac{\Delta l}{l} \cdot 10^6 = \mu\delta \quad \dots \text{microdeformación (adimensional)}$$

Diversa literatura suele expresar las deformaciones en micromilímetros/milímetro o micropulgada/pulgada, creando a veces alguna confusión, en realidad es decir lo mismo de una o de otra manera, ya que se trata de la misma unidad por lo que nosotros recomendamos referirse siempre a $\mu\delta$.

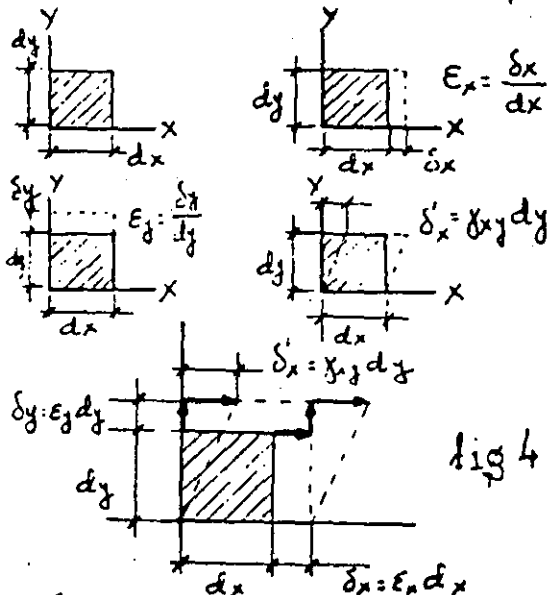
El módulo de elasticidad E y las tensiones se expresarán en daN/cm^2 , aunque en algunas tablas pueden aparecer estos valores en Kp/cm^2 o Kp/mm^2 .

1.4 ESTADO BIAxIAL DE DEFORMACIONES

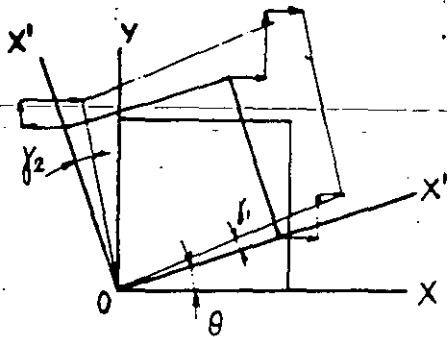


El rectángulo elemental de la fig. 3 de lados dx y dy tiene como posibles las deformaciones lineales según los ejes X e Y ya definidas y de valor:

$$\epsilon_x = \frac{\delta_x}{dx} \quad \epsilon_y = \frac{\delta_y}{dy}$$



originadas cuando la dirección del alargamiento coincide con los ejes X e Y respectivamente y otro tipo de deformación llamada angular que aparece cuando hay un desplazamiento transversal de los lados dx y dy que motiva que la forma rectangular original se convierta en rombic. La deformación angular γ_{xy} se define como la suma de los desplazamientos transversales divididos por las longitudes originales que no le son paralelas es



decir:

$$\gamma_{xy} = \frac{\delta'_x}{dy} + \frac{\delta'_y}{dx} = \text{tg } \gamma_2 + \text{tg } \gamma_1 \approx \gamma_1 + \gamma_2$$

La deformación angular se considera positiva si supone una disminución del ángulo recto original por una extensión.

En un punto arbitrario (fig.4) de la superficie de una pieza cargada podemos aislar un elemento infinitesimal de material para estudiar sus deformaciones en el plano XY y para ello aplicaremos el principio de superposición, por el cual la deformación total será la suma de las deformaciones parciales, es decir, la suma de la deformación lineal según los ejes X e Y respectivamente y la deformación angular γ_{xy} .

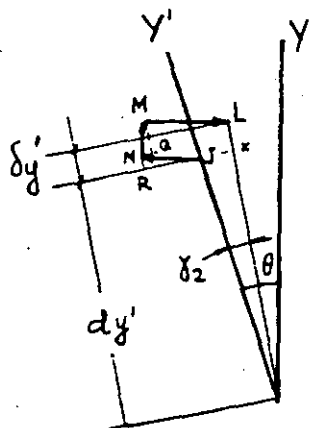
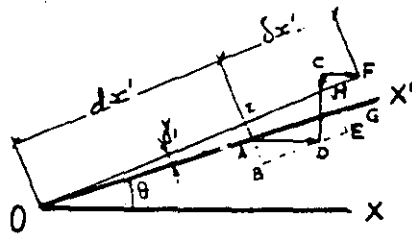


fig 5

Vamos a relacionar los valores de las deformaciones según los X-Y con otro conjunto de ejes X'-Y' que forman un ángulo θ . Al ángulo θ le consideraremos positivo en sentido contrario al de las agujas del reloj.

En la fig. 5 se observa la geometría del elemento infinitesimal referido a los nuevos ejes X'-Y', el alargamiento según el eje X' será: $\epsilon_{x'} = \frac{\delta x'}{dx'}$

$$\begin{aligned} \delta x' &= \epsilon_x dx' = \overline{BD} + \overline{DE} + \overline{FH} \\ \overline{BD} &= \epsilon_x dx' \cos \theta \cos \theta = \epsilon_x dx' \cos^2 \theta \\ \overline{DE} &= \epsilon_y dy' \sin \theta \cos \theta = \epsilon_y dy' \sin \theta \cos \theta \\ \overline{FH} &= dx' \sin \theta \gamma_{xy} \cos \theta \end{aligned}$$

$$\epsilon_{x'} = \epsilon_x \cos^2 \theta + \epsilon_y \sin^2 \theta + \gamma_{xy} \sin \theta \cos \theta \quad [12]$$

$$\epsilon_{y'} = \epsilon_x \cos^2 \left(\theta + \frac{\pi}{2} \right) + \epsilon_y \sin^2 \left(\theta + \frac{\pi}{2} \right) + \gamma_{xy} \sin \left(\theta + \frac{\pi}{2} \right) \cos \left(\theta + \frac{\pi}{2} \right) \quad [13]$$

La deformación angular viene expresada por: $\gamma_{\theta} = \gamma_1 + \gamma_2 = \frac{\overline{AI}}{dx'} + \frac{\overline{JK}}{dy'}$

$$\left. \begin{aligned} \overline{AI} &= -\overline{HC} + \overline{CE} - \overline{AB} \\ \overline{JK} &= -\overline{RJ} + \overline{NQ} + \overline{PL} \\ -\overline{AB} &= -\epsilon_x dx' \sin \theta \cos \theta \end{aligned} \right\} \begin{aligned} -\overline{HC} &= -dx' \gamma_{xy} \sin^2 \theta \\ \overline{CE} &= \epsilon_y dx' \sin \theta \cos \theta \\ \overline{PL} &= dy' \gamma_{xy} \cos^2 \theta \end{aligned}$$

$$\gamma_{\theta} = -2(\epsilon_x - \epsilon_y) \sin \theta \cos \theta + \gamma_{xy} (\cos 2\theta - \sin^2 \theta) \quad [14]$$

Si expresamos la (12) y (14) en función del ángulo doble podemos escribirlas

$$\epsilon_{x'} = \frac{\epsilon_x + \epsilon_y}{2} + \frac{\epsilon_x - \epsilon_y}{2} \cos 2\theta + \frac{\gamma_{xy}}{2} \sin 2\theta \quad [15]$$

$$\frac{\delta \theta}{2} = \frac{\epsilon_x - \epsilon_y}{2} \sin 2\theta + \frac{\gamma_{xy}}{2} \cos 2\theta \quad [16]$$

Por ser funciones periódicas tendrán un máximo y un mínimo que calculemos derivando la (15) respecto a θ e igualando a cero.

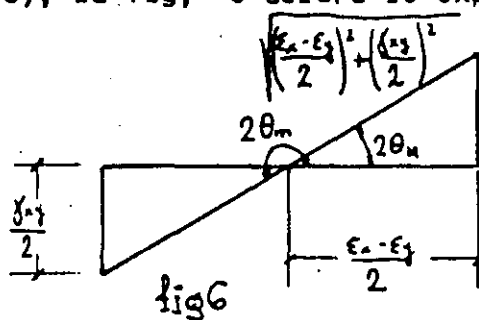
$$\frac{d\epsilon_{x'}}{d\theta} = -2 \frac{\epsilon_x - \epsilon_y}{2} \sin 2\theta + 2 \frac{\gamma_{xy}}{2} \cos 2\theta = 0$$

$$\tan 2\theta_{M-m} = \frac{\gamma_{xy}/2}{\frac{\epsilon_x - \epsilon_y}{2}} = \frac{\sin 2\theta}{\cos 2\theta} \quad [17]$$

de donde sustituyendo en (15) tenemos:

$$\begin{aligned} \epsilon_{x'(M-m)} &= \frac{\epsilon_x + \epsilon_y}{2} + \frac{1}{4 \sqrt{\left(\frac{\epsilon_x - \epsilon_y}{2}\right)^2 + \left(\frac{\gamma_{xy}}{2}\right)^2}} [(\epsilon_x - \epsilon_y)^2 + \gamma_{xy}^2] = \\ &= \frac{\epsilon_x + \epsilon_y}{2} \pm \sqrt{\left(\frac{\epsilon_x - \epsilon_y}{2}\right)^2 + \left(\frac{\gamma_{xy}}{2}\right)^2} \quad [18] \end{aligned}$$

Los subíndices M-m indican los valores máximo y mínimo, en efecto hay dos valores de $2\theta_{M-m}$ que cumplen la ecuación (17) ya que $\tan 2\theta = \tan(2\theta + \pi)$ o sea que las direcciones de las deformaciones máxima y mínima son perpendiculares entre sí, verificándose además que la deformación angular es nula como se demuestra sustituyendo la (17) en la (16), la fig. 6 aclara lo expuesto.



El valor máximo de la deformación angular se obtiene por el mismo procedimiento y tiene por valor:

$$\frac{\gamma_{\theta_{M-m}}}{2} = \pm \sqrt{\left(\frac{\epsilon_x - \epsilon_y}{2}\right)^2 + \left(\frac{\gamma_{xy}}{2}\right)^2} \quad [19]$$

demostrándose que su dirección forma 45° con respecto a las direcciones principales.

Si el ángulo θ_M que el eje arbitrario X' forma con el eje X hacemos que sea nulo las expresiones (18) y (19) se pueden escribir:

$$\left. \begin{aligned} \epsilon_{x'(M-m)} &= \frac{\epsilon_1 + \epsilon_2}{2} \pm \frac{\epsilon_1 - \epsilon_2}{2} \\ \frac{\gamma_{M-m}}{2} &= \pm \frac{\epsilon_1 - \epsilon_2}{2} \end{aligned} \right\}$$

siendo ϵ_1 y ϵ_2 las deformaciones según las direcciones principales.

Para cualquier otra dirección que forme un ángulo α respecto a las principales, las fórmulas quedarán:

$$\epsilon_\alpha = \frac{\epsilon_1 + \epsilon_2}{2} + \frac{\epsilon_1 - \epsilon_2}{2} \cos 2\alpha \quad [20]$$

$$\frac{\gamma_\alpha}{2} = \frac{\epsilon_1 - \epsilon_2}{2} \sin 2\alpha \quad [21]$$

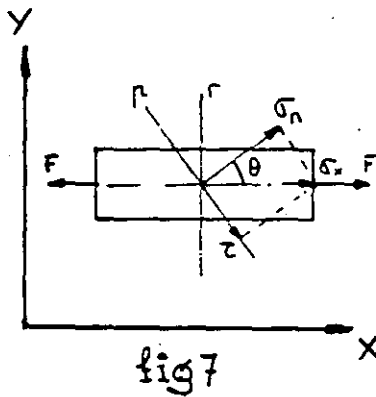
si llamamos:

$$d = \frac{\epsilon_1 + \epsilon_2}{2} \quad \text{y} \quad r = \frac{\epsilon_1 - \epsilon_2}{2}, \quad \text{tendremos que:}$$

$$\epsilon_\alpha = d + r \cos 2\alpha \quad [22]$$

$$\frac{\gamma_\alpha}{2} = r \sin 2\alpha \quad [23]$$

1.5. ESTADO BIAxIAL DE TENSIONES



En una barra prismática sometida a una extensión pura, se llama tensión (esfuerzo o fatiga) a la fuerza que actúa por unidad de superficie;

$$\sigma_x = \frac{F}{S} \quad (S: \text{sección según } r-r')$$

si consideramos otra sección S' (según $p'-p$) cuya normal forma un ángulo θ con el eje de aplicación de fuerzas, la tensión según el eje X valdrá:

$$\sigma_x' = \frac{F}{S'} = \frac{F}{S} \cos \theta = \sigma_x \cos \theta$$

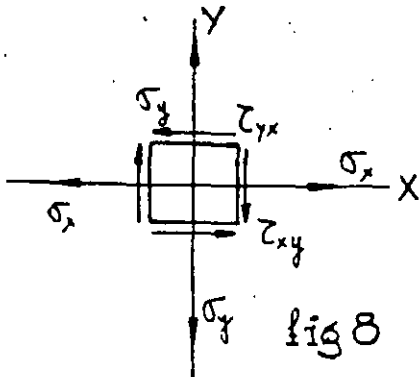
y descomponiéndola en las direcciones normal y tangencial respectivamente de $p-p'$ tendremos que:

$$\sigma_n = \sigma_x \cos \theta \cos \theta = \sigma_x \cos^2 \theta \quad [24]$$

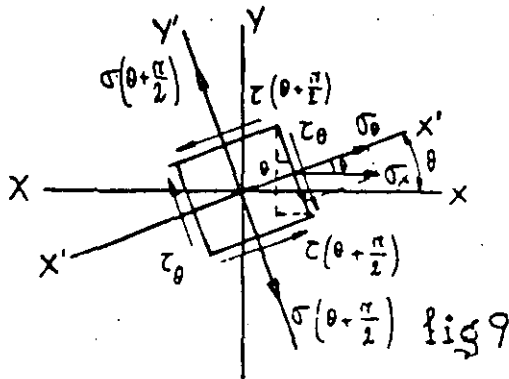
$$\tau = \sigma_x \cos \theta \sin \theta = \frac{1}{2} \sigma_x \sin 2\theta \quad [25]$$

llamándose el valor (24) tensión normal y al (25) tensión cortante.

Estudiaremos el estado biaxial de tensiones en la superficie de un cuerpo que no esté sometido a presiones exteriores; de forma análoga a como se desarrolla el caso de deformaciones, para ello aislemos un elemento infinitesimal de lados paralelos a unos ejes X - Y, las acciones que actúen sobre el elemento originan mas tensiones normales y cortantes que mantienen el equilibrio del sistema. - (fig. 8).



Las tensiones normales serán positivas en caso de tracción y negativas en caso de compresión, así mismo - las tensiones cortantes se consideran positivas cuando producen un par en sentido de las agujas del reloj y negativas en caso contrario.



En la fig. 9, vemos el elemento infinitesimal referenciado a unos ejes que forman un ángulo θ con los $X-Y'$; buscaremos el valor de las tensiones ligadas a la nueva orientación de ejes, para ello tengamos en cuenta que el equilibrio debe ser de fuerzas, en efecto:

$$\begin{aligned} \sigma_{\theta} S &= \sigma_x S \cos \theta \cos \theta + \sigma_y S \operatorname{sen} \theta \operatorname{sen} \theta + \tau_{xy} S \cos \theta \operatorname{sen} \theta + \tau_{yx} S \operatorname{sen} \theta \cos \theta = \\ &= \sigma_x S \cos^2 \theta + \sigma_y S \operatorname{sen}^2 \theta + 2 \tau_{xy} S \operatorname{sen} \theta \cos \theta \end{aligned}$$

$$\sigma_{\theta} = \sigma_x \cos^2 \theta + \sigma_y \operatorname{sen}^2 \theta + 2 \tau_{xy} \operatorname{sen} \theta \cos \theta \quad \dots \dots \dots [26]$$

$$\tau_{\theta} = -(\sigma_x - \sigma_y) \operatorname{sen} \theta \cos \theta \operatorname{sen} \theta \cos \theta + \tau_{xy} (\cos^2 \theta - \operatorname{sen}^2 \theta) \quad \dots \dots \dots [27]$$

ecuaciones que expresadas en función del ángulo doble nos dan:

$$\sigma_{\theta} = \frac{\sigma_x + \sigma_y}{2} + \frac{\sigma_x - \sigma_y}{2} \cos 2\theta + \tau_{xy} \operatorname{sen} 2\theta \quad \dots \dots \dots [28]$$

$$\tau_{\theta} = -\left(\frac{\sigma_x - \sigma_y}{2}\right) \operatorname{sen} 2\theta + \tau_{xy} \cos 2\theta \quad \dots \dots \dots [29]$$

Si derivamos la (28) respecto a θ e igualamos a cero, encontraremos los valores de θ que hacen máximo y mínimo a dicha ecuación:

$$\frac{d\sigma_{\theta}}{d\theta} = -(\sigma_x - \sigma_y) \operatorname{sen} 2\theta + 2 \tau_{xy} \cos 2\theta = 0$$

$$\operatorname{tg} 2\theta_{M.m} = \frac{\operatorname{sen} 2\theta_{M.m}}{\cos 2\theta_{M.m}} = \frac{\tau_{xy}}{\frac{\sigma_x - \sigma_y}{2}}$$

Por consideraciones análogas a las hechas en el estudio de la deformación biaxial, se deducen que hay dos planos perpendiculares que - corresponden a las direcciones en que las tensiones normales son máxima y mínima respectivamente y en las cuales las tensiones cortantes son nulas:

$$\sigma_{M-m} = \frac{\sigma_x + \sigma_y}{2} \pm \sqrt{\left(\frac{\sigma_x - \sigma_y}{2}\right)^2 + (\tau_{xy})^2} \quad [30]$$

De la misma forma encontraremos que:

$$\tau_{M-m} = \pm \sqrt{\left(\frac{\sigma_x - \sigma_y}{2}\right)^2 + (\tau_{xy})^2} \quad [31]$$

El valor máximo y mínimo de la tensión cortante se encuentra defasado 45° respecto a los valores principales de las tensiones normales.

Haciendo que el ángulo $\theta_M = 0$ tenemos que:

$$\sigma_{M-m} = \frac{\sigma_1 + \sigma_2}{2} \pm \frac{\sigma_1 - \sigma_2}{2}$$

$$\tau_{M-m} = \pm \frac{\sigma_1 - \sigma_2}{2}$$

siendo σ_1 y σ_2 el valor de las tensiones normales máxima y mínima; las tensiones en cualquier dirección que formen un ángulo α con las principales, tienen de valor:

$$\sigma_\alpha = \frac{\sigma_1 + \sigma_2}{2} + \frac{\sigma_1 - \sigma_2}{2} \cos 2\alpha \quad [32]$$

Llamando $\tau_\alpha = \frac{\sigma_1 - \sigma_2}{2} \sin 2\alpha \quad [32 \text{ b) }]$

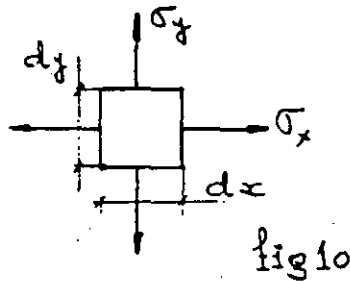
$$\delta = \frac{\sigma_1 + \sigma_2}{2} \quad \text{y} \quad p = \frac{\sigma_1 - \sigma_2}{2}$$

tenemos que:

$$\sigma_\alpha = \delta + p \cos 2\alpha \quad [33]$$

$$\tau_\alpha = p \sin 2\alpha \quad [34]$$

1.6 RELACION ENTRE DEFORMACIONES Y TENSIONES



Supongamos el elemento de la fig. 10, aplicando el teorema de la superposición encontramos que;

$$\left. \begin{aligned} \epsilon_x &= \frac{\sigma_x}{E} - \mu \frac{\sigma_y}{E} \\ \epsilon_y &= \frac{\sigma_y}{E} - \mu \frac{\sigma_x}{E} \end{aligned} \right\}$$

$$\sigma_x = \frac{E}{1 - \mu^2} (\epsilon_x + \mu \epsilon_y) \quad [35]$$

$$\sigma_y = \frac{E}{1 - \mu^2} (\epsilon_y + \mu \epsilon_x) \quad [36]$$

Experimentalmente se demuestra que:

$$\gamma = \frac{\tau}{G} \quad G = \frac{E}{2(1 + \mu)} \quad [37]$$

llamándose a G coeficiente de elasticidad a cortadura.

Recordando las relaciones:

$$d = \frac{\epsilon_1 + \epsilon_2}{2} \quad \delta = \frac{\sigma_1 + \sigma_2}{2}$$

$$r = \frac{\epsilon_1 - \epsilon_2}{2} \quad \rho = \frac{\sigma_1 - \sigma_2}{2}$$

se deduce que:

$$\epsilon_1 + \epsilon_2 = \frac{\sigma_1}{E} - \mu \frac{\sigma_2}{E} + \frac{\sigma_2}{E} - \mu \frac{\sigma_1}{E} = \frac{\sigma_1 + \sigma_2}{E} \left(\frac{1 - \mu}{E} \right)$$

$$\delta = \frac{\sigma_1 + \sigma_2}{2} = \frac{\epsilon_1 + \epsilon_2}{2} \frac{E}{1 - \mu} = d \frac{E}{1 - \mu} \quad \text{--- [38]}$$

$$\epsilon_1 - \epsilon_2 = \frac{\sigma_1}{E} - \mu \frac{\sigma_2}{E} - \left(\frac{\sigma_2}{E} - \mu \frac{\sigma_1}{E} \right) = \frac{\sigma_1 - \sigma_2}{E} \frac{1 + \mu}{E}$$

$$\rho = \frac{\sigma_1 - \sigma_2}{2} = \frac{\epsilon_1 - \epsilon_2}{2} \frac{E}{1 + \mu} = r \frac{E}{1 + \mu} \quad \text{--- [39]}$$

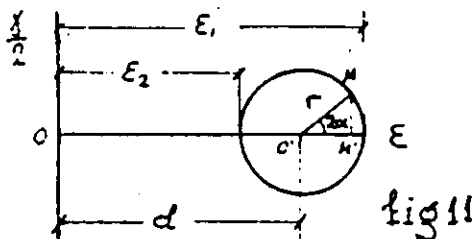
1.7. REPRESENTACION GRAFICA DEL ESTADO BIAxIAL DE TENSIONES Y DEFORMACIONES; CIRCULOS DE MOHR

Una de las formas más sencillas y usuales de representación del estado plano de deformaciones y tensiones es el círculo de Mohr. Recordemos que la deformación en una dirección cualquiera que forma un ángulo α respecto a las direcciones principales tiene por valor:

$$\epsilon_x = \frac{\epsilon_1 + \epsilon_2}{2} + \frac{\epsilon_1 - \epsilon_2}{2} \cos 2\alpha = d + r \cos 2\alpha$$

$$\frac{\delta_x}{2} = \frac{\epsilon_1 - \epsilon_2}{2} \sin 2\alpha = r \sin 2\alpha$$

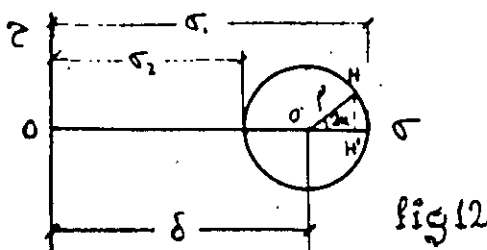
Podemos representar prácticamente éstas ecuaciones según la fig. 11, pues se cumple que:



$$\epsilon_x = \overline{OM'} = d + r \cos 2\alpha$$

$$\frac{\delta_x}{2} = \overline{MM'} = r \sin 2\alpha$$

Observemos que el valor máximo y el mínimo

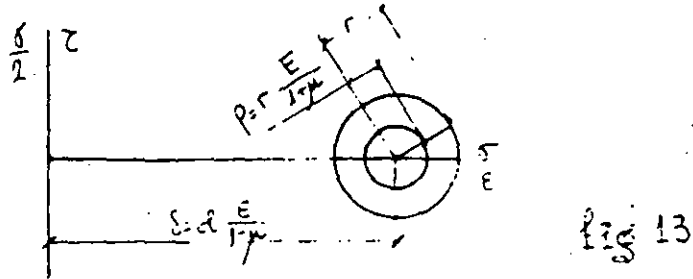


La fig. 12 nos indica el círculo de Mohr para el estado de tensiones y vemos su similitud con el de deformaciones.

$$\sigma_x = \overline{OH} = \delta + \rho \cos 2\alpha$$

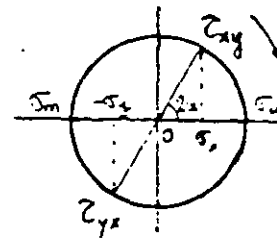
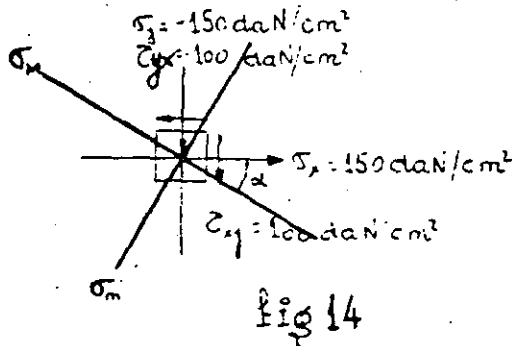
$$\tau_x = \overline{MM'} = \rho \sin 2\alpha$$

En el dominio elástico de los cuerpos isotrópicos, - existe proporcionalidad entre deformaciones y tensiones, por lo que los círculos representativos de ambos valores son concéntricos. Los coeficientes de proporcionalidad han sido deducidos en el apartado 1.6 (fig. 13).



1.8 EJEMPLOS DE APLICACION DE LOS CIRCULOS DE MOHR.

Nº 1. Sobre el elemento de la fig. 14 actúan las tensiones que se indican. Calcular analítica y gráficamente el valor y dirección de los esfuerzos principales.



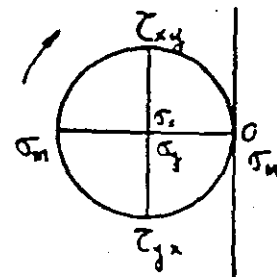
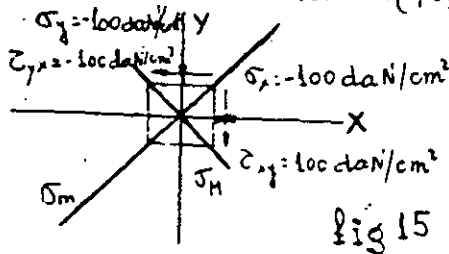
$$\sigma_{M-m} = \frac{150 + (-150)}{2} \pm \sqrt{\left(\frac{150 - (-150)}{2}\right)^2 + 100^2} = \pm 180 \text{ daN/cm}^2$$

$$\tan 2\alpha = \frac{100}{\frac{150 - (-150)}{2}} = 0,66$$

$$2\alpha = \begin{cases} 41^\circ \\ 41^\circ + 180^\circ \end{cases}$$

$$\alpha = \begin{cases} 20,5^\circ \\ 20,5^\circ + 90^\circ \end{cases}$$

Nº 2 Idem al anterior. (fig 15)



$$\delta = \frac{-100 + (-100)}{2} = -100$$

$$p = \pm \sqrt{\left(\frac{-100 - (-100)}{2}\right)^2 + 100^2} = 100$$

$$\tan 2\alpha = \frac{100}{\frac{-100 - (-100)}{2}} = -\infty$$

$$\sigma_M = \delta + p = -100 + 100 = 0$$

$$\sigma_m = \delta - p = -100 - 100 = -200$$

$$\alpha = 45^\circ$$

Casos típicos de aplicación del círculo de Mohr.

TORSION

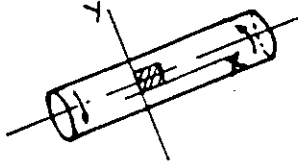
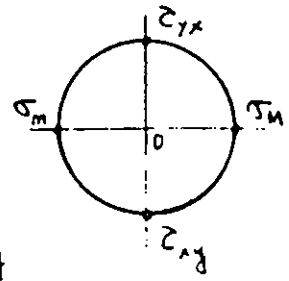
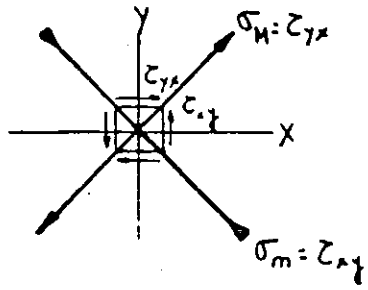


fig 16



TORSION Y TRACCION

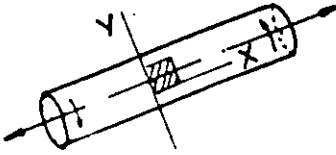
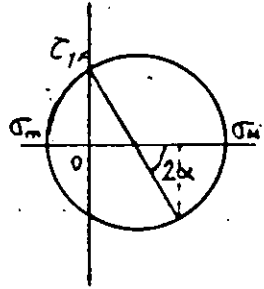
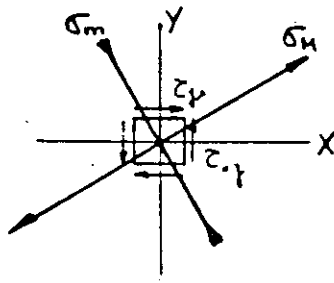


fig 17



TRACCION

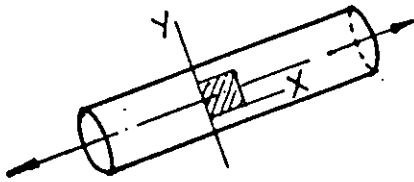
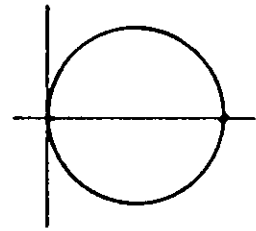
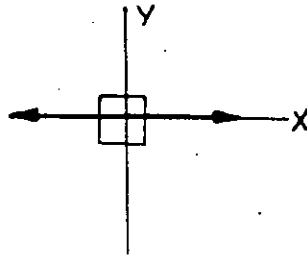


fig 18



CILINDRO BAJO PRESION

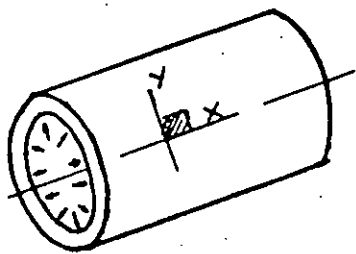
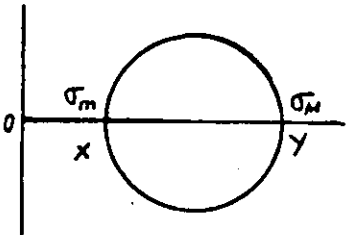
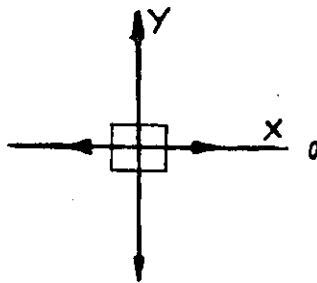


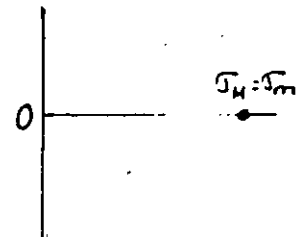
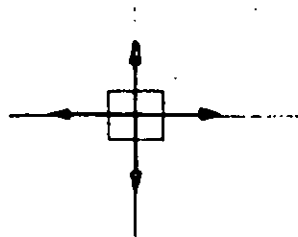
fig 19



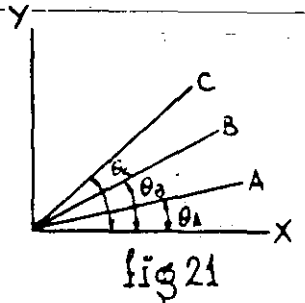
ESFERA BAJO PRESION



fig 20



Consideremos el valor de las deformaciones (fig. 21) en direcciones A, B y C que forman los ángulos θ_A, θ_B y θ_C respectivamente con el eje X de unos ejes arbitrarios X-Y, tendremos:



$$\epsilon_A = \frac{\epsilon_x + \epsilon_y}{2} + \frac{\epsilon_x - \epsilon_y}{2} \cos 2\theta_A + \frac{\gamma_{xy}}{2} \sin 2\theta_A$$

$$\epsilon_B = \frac{\epsilon_x + \epsilon_y}{2} + \frac{\epsilon_x - \epsilon_y}{2} \cos 2\theta_B + \frac{\gamma_{xy}}{2} \sin 2\theta_B$$

$$\epsilon_C = \frac{\epsilon_x + \epsilon_y}{2} + \frac{\epsilon_x - \epsilon_y}{2} \cos 2\theta_C + \frac{\gamma_{xy}}{2} \sin 2\theta_C$$

Si hacemos que:

$$\theta_A = 0 ; \quad \theta_B = \frac{\pi}{4} ; \quad \theta_C = \frac{\pi}{2} \quad \text{nos queda:}$$

$$\left. \begin{aligned} \epsilon_A &= \epsilon_x \\ \epsilon_B &= \frac{\epsilon_x + \epsilon_y}{2} + \frac{\gamma_{xy}}{2} \\ \epsilon_C &= \epsilon_y \end{aligned} \right\} \begin{aligned} \epsilon_x &= \epsilon_A \\ \epsilon_y &= \epsilon_C \\ \gamma_{xy} &= 2\epsilon_B - (\epsilon_A + \epsilon_C) = (\epsilon_B - \epsilon_A) + (\epsilon_B - \epsilon_C) \dots [42] \end{aligned}$$

Sustituyendo las (41) y (42) en (18) y (19) y simplificando tenemos:

$$\epsilon_M = \frac{\epsilon_A + \epsilon_C}{2} + \frac{1}{\sqrt{2}} \sqrt{(\epsilon_A - \epsilon_B)^2 + (\epsilon_B - \epsilon_C)^2} \dots [43]$$

$$\epsilon_m = \frac{\epsilon_A + \epsilon_C}{2} - \frac{1}{\sqrt{2}} \sqrt{(\epsilon_A - \epsilon_B)^2 + (\epsilon_B - \epsilon_C)^2} \dots [44]$$

$$\gamma_{M-m} = \pm \sqrt{2} \sqrt{(\epsilon_A - \epsilon_B)^2 + (\epsilon_B - \epsilon_C)^2} \dots [45]$$

$$\tan 2\theta_M = \left[\frac{(\epsilon_B - \epsilon_A) + (\epsilon_B - \epsilon_C)}{\epsilon_A - \epsilon_C} \right] \dots [46]$$

El ángulo θ_M será el que forma la dirección principal máxima con la dirección A.

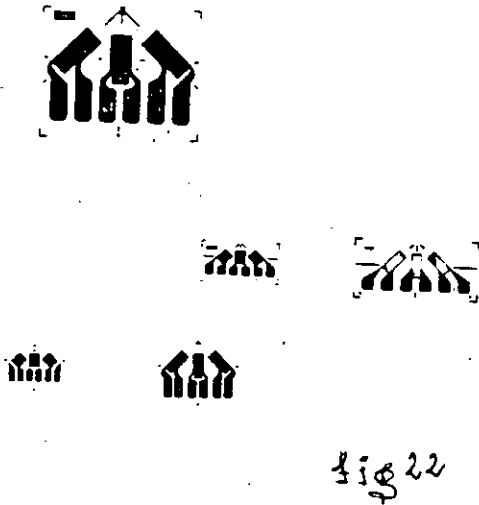
Los valores de las tensiones máxima y mínima

$$\sigma_{M-m} = \frac{E}{2} \left[\frac{\epsilon_A + \epsilon_C}{1-\mu} \pm \frac{\sqrt{2}}{1+\mu} \sqrt{(\epsilon_A - \epsilon_B)^2 + (\epsilon_B - \epsilon_C)^2} \right] \dots [47]$$

$$\tau_M = \frac{E}{\sqrt{2}(1+\mu)} \sqrt{(\epsilon_A - \epsilon_B)^2 + (\epsilon_B - \epsilon_C)^2} \dots [48]$$

Las fórmulas (47) y (48) dan directamente los valores de las tensiones principales a partir de los valores de las deformaciones en las direcciones A, B y C.

Las ecuaciones anteriores corresponden a una banda extensométrica roseta rectangular como la indicada en la fig. 22.



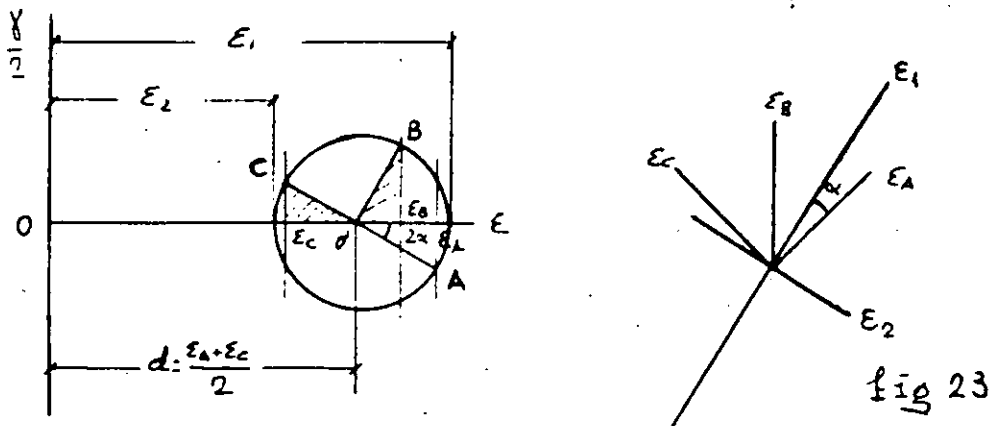
Vamos a ver gráficamente como se determinan las deformaciones principales a partir de las deformaciones $\epsilon_A, \epsilon_B, \epsilon_C$ valiéndonos del círculo de Mohr.

Sobre el eje x (fig. 23) traslademos los valores $\epsilon_A, \epsilon_B, \epsilon_C$. En el círculo ϵ_A y ϵ_C tienen que estar defasados 180° ; por lo que el centro del mismo será: $d = \frac{\epsilon_A + \epsilon_C}{2}$, la dirección de ϵ_B estará en el círculo defasada 90° ; por lo que debe cumplirse la igualdad de los triángulos $\triangle OBB' = \triangle OCC'$ con lo que hemos

determinado $r = \overline{CO'}$

En el círculo observamos que desde el punto A que corresponde a ϵ_A tenemos que correr un ángulo positivo 2α para llegar a $\epsilon_1 = \epsilon_M$; por lo tanto y sobre la banda roseta desplazaremos un ángulo α para la dirección de la deformación principal máxima. El ángulo α es el que forma la dirección principal máxima tomada como referencia y la dirección A, considerando como positivo el sentido contrario al giro de las agujas del reloj.

Conocido el círculo de Mohr de deformaciones fácilmente se deduce el de tensiones (ver. 1.6) de la fig. 23 se deduce:



1.10 CALCULO TABULADO PARA ROSETAS RECTANGULARES

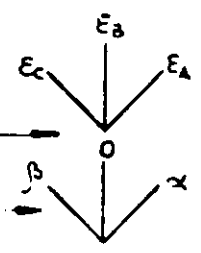
Sean $\epsilon_A, \epsilon_B, \epsilon_C$ las medidas de las bandas, A, B y C.

1) Cálculo de d : $d = \frac{\epsilon_A + \epsilon_C}{2}$ (con su signo)

2) Cálculo de r :

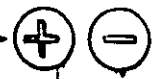
Anotar los 3 valores con su signo

Restar $(-\epsilon_B)$ a los 3 valores, se obtiene



Anotar el signo que corresponda al mayor valor de

α o β en valor absoluto



Sea, por ejemplo, α ese número. Dividir α y β por α con su signo.

Se obtiene



Y puede ser positivo o negativo, pero inferior a 1 en valor absoluto.

Buscar en la tabla I el valor W que corresponde a Y

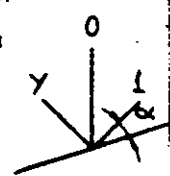
Se tiene que: $r = |\alpha| W$ (Número positivo)

Las deformaciones principales son:

$$\epsilon_1 = d + r$$

$$\epsilon_2 = d - r$$

Buscar en la tabla II, el ángulo que corresponde a Y con su signo. α está comprendido entre 0 y 45°. Llevar el ángulo α en sentido externo (que se aleje de la referencia O) sobre el eje marcado con el i.



La dirección obtenida es:

Máxima si anotamos el signo +

Mínima si anotamos el signo -



TABLA Nº 1
(continuación)

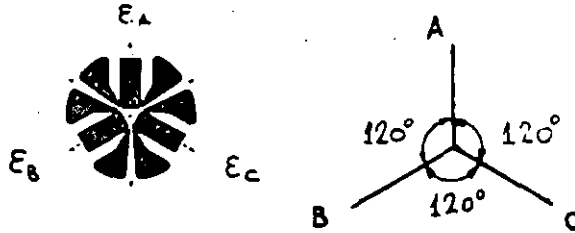
0.65	0.9434	37	41	07	10	14	18	22	26	30
0.66	0.9472	76	40	45	49	53	57	61	65	69
0.67	0.9511	15	19	23	27	31	35	39	04	08
0.68	0.9551	53	56	63	67	71	75	79	83	87
0.69	0.9591	95	59	03	07	11	15	19	23	27
0.70	0.9631	35	39	43	48	52	56	60	64	68
0.71	0.9672	75	60	64	68	73	77	81	85	89
0.72	0.9713	17	21	26	30	34	38	42	46	51
0.73	0.9755	59	63	67	71	76	80	84	88	92
0.74	0.9796	01	05	09	13	17	22	26	30	35
0.75	0.9839	43	47	52	56	60	64	69	73	77
0.76	0.9881	86	90	94	99	03	07	11	16	20
0.77	0.9924	29	33	37	42	46	50	54	58	63
0.78	0.9968	72	76	81	85	89	94	98	03	07
0.79	0.9011	16	20	25	29	33	38	42	47	51
0.80	0.9055	60	64	69	73	77	82	86	91	95
0.81	0.9100	04	09	13	18	22	26	31	35	40
0.82	0.9144	49	53	58	62	67	71	76	80	85
0.83	0.9189	94	98	03	07	12	17	21	26	30
0.84	0.9235	39	44	48	53	57	62	67	71	76
0.85	0.9280	85	90	94	99	03	08	12	17	22
0.86	0.9326	31	36	40	45	49	54	59	63	68
0.87	0.9373	77	82	86	91	96	00	05	10	14
0.88	0.9419	24	28	33	38	43	47	52	57	61
0.89	0.9466	71	75	80	85	90	94	99	04	08
0.90	0.9513	18	23	27	32	37	42	46	51	56
0.91	0.9561	65	70	75	80	84	89	94	99	04
0.92	0.9608	13	18	23	27	32	37	42	47	52
0.93	0.9656	61	66	71	75	80	85	90	95	00
0.94	0.9705	09	14	19	24	29	34	39	43	48
0.95	0.9753	58	63	68	73	78	82	87	92	97
0.96	0.9802	07	12	17	22	27	31	36	41	46
0.97	0.9851	56	61	66	71	76	81	86	91	96
0.98	0.9901	05	10	15	20	25	30	35	40	45
0.99	0.9950	55	60	65	70	75	80	85	90	95
1.00	1.0000									

ht	0	1	2	3	4	5	6	7	8	9
-1.0	0.0									
-0.9	1.5	1.3	1.2	1.0	0.9	0.7	0.6	0.4	0.3	0.1
-0.8	3.2	3.0	2.8	2.7	2.5	2.3	2.2	2.0	1.8	1.7
-0.7	5.0	4.8	4.6	4.4	4.2	4.1	3.9	3.7	3.5	3.3
-0.6	7.0	6.8	6.6	6.4	6.2	6.0	5.8	5.6	5.4	5.2
-0.5	9.2	9.0	8.8	8.5	8.3	8.1	7.9	7.7	7.4	7.2
-0.4	11.6	11.4	11.1	10.9	10.6	10.4	10.1	9.9	9.7	9.4
-0.3	14.1	13.9	13.6	13.4	13.1	12.8	12.6	12.3	12.1	11.8
-0.2	16.8	16.6	16.3	16.0	15.8	15.5	15.2	15.0	14.7	14.4
-0.1	19.7	19.4	19.1	18.8	18.5	18.2	17.9	17.7	17.4	17.1
-0.0	22.5	22.2	21.9	21.7	21.4	21.0	20.8	20.5	20.2	19.9
+0.0	22.5	22.6	23.1	23.3	23.6	24.0	24.2	24.5	24.8	25.1
+0.1	25.3	25.6	25.9	26.2	26.5	26.9	27.1	27.3	27.6	27.9
+0.2	28.2	28.4	28.7	29.0	29.2	29.5	29.8	30.0	30.3	30.6
+0.3	30.9	31.1	31.4	31.6	31.9	32.1	32.4	32.7	32.9	33.2
+0.4	33.4	33.6	33.9	34.1	34.4	34.6	34.9	35.1	35.3	35.6
+0.5	35.6	35.9	36.2	36.5	36.7	36.9	37.1	37.3	37.6	37.8
+0.6	38.0	38.2	38.4	38.6	38.8	39.0	39.2	39.4	39.6	39.8
+0.7	40.0	40.2	40.4	40.6	40.8	40.9	41.1	41.3	41.5	41.7
+0.8	41.8	42.0	42.2	42.3	42.5	42.7	42.8	43.0	43.2	43.3
+0.9	43.5	43.7	43.8	44.0	44.1	44.3	44.4	44.6	44.7	44.9
+1.0	45.0									

TABLA Nº 2

1.11 BANDAS DE TRES DIRECCIONES O ROSETAS (EQUIANGULARES)

Las direcciones arbitrarias de la medida de tres deformaciones en un punto podemos hacer que estén defasados 120° con lo que la banda tiene la geometría indicada en la fig. 24 y por consideraciones análogas al caso de la roseta rectangular encontramos los resultados que se indican



$$\sigma_{M-m} = \frac{E}{3} \left[\frac{\epsilon_A + \epsilon_B + \epsilon_C}{1-\mu} \pm \frac{\sqrt{2}}{1+\mu} \sqrt{(\epsilon_A - \epsilon_C)^2 + (\epsilon_C - \epsilon_B)^2 + (\epsilon_B - \epsilon_A)^2} \right] \quad [49]$$

$$\tau = \frac{\sqrt{2} E}{3(1+\mu)} \sqrt{(\epsilon_A - \epsilon_C)^2 + (\epsilon_C - \epsilon_B)^2 + (\epsilon_B - \epsilon_A)^2} \quad [50]$$

$$\operatorname{tg} 2\theta = \frac{\sqrt{3} (\epsilon_C - \epsilon_B)}{2\epsilon_A - \epsilon_B - \epsilon_C} \quad [51]$$

siendo θ el ángulo de la dirección principal máxima con la dirección A.

Gráficamente podemos encontrar la solución llevando sobre el eje X del diagrama de Mohr los valores de ϵ_A, ϵ_B y ϵ_C (fig. 25).

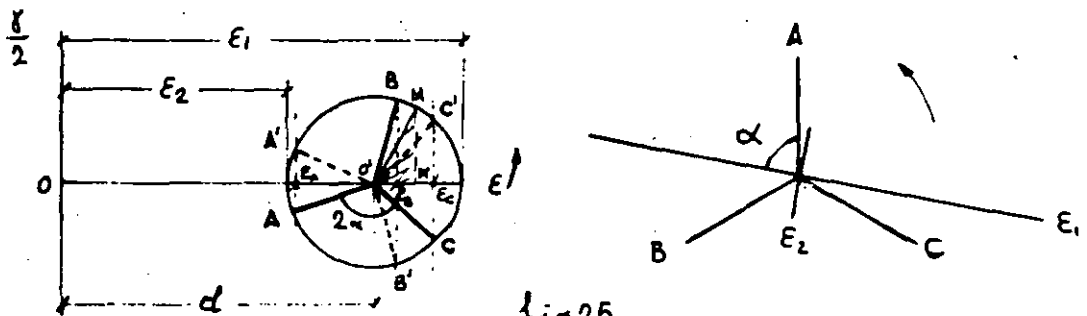


fig 25

El centro del círculo sera $d = \frac{\epsilon_A + \epsilon_B + \epsilon_C}{3}$; sobre las dos proyecciones que queden a la derecha o a la izquierda del centro O; se levanta MM' perpendicular en el punto medio de las dos proyecciones y desde O' se traza una recta que forma 60° con el eje X, el punto de intersección M nos da el radio del círculo $r = \overline{O'M}$. Aparentemente hay dos soluciones pero los puntos A'-B' y C' no guardan en el círculo el defase de 240° de acuerdo con la orientación de las -

De la fig. 25 deducimos:

$$d = \frac{\varepsilon_A + \varepsilon_C + \varepsilon_B}{3} \quad \left. \begin{array}{l} \varepsilon_1 = d + r \\ \varepsilon_2 = d - r \end{array} \right\} \quad \left. \begin{array}{l} \text{tg } 2\alpha = \frac{\sqrt{3} (\varepsilon_a - \varepsilon_b)}{2\varepsilon_A - \varepsilon_B - \varepsilon_C} \\ r = \frac{\varepsilon_a - d}{\cos 2\alpha} \end{array} \right\}$$

$$\left. \begin{array}{l} \sigma_1 = \frac{E}{1 - \mu^2} (\varepsilon_1 + \mu \varepsilon_2) \\ \sigma_2 = \frac{E}{1 - \mu^2} (\varepsilon_2 + \mu \varepsilon_1) \end{array} \right\}$$

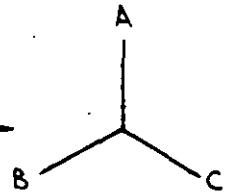
1.12 CALCULO TABULADO PARA ROSETAS EQUIANGULARES

Sean ϵ_A, ϵ_B y ϵ_C las tres medidas con su signo

1) Cálculo de d :
$$d = \frac{\epsilon_A + \epsilon_B + \epsilon_C}{3}$$

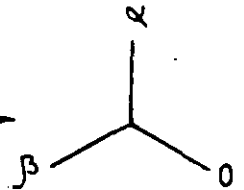
2) Cálculo de r :

Anotar las tres medidas según su dirección



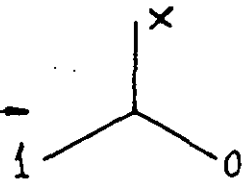
Uno al menos de los valores medios, es algebraicamente igual o menor que los otros dos. Sea por ejemplo ϵ_C . Se suma $(-\epsilon_C)$ a los tres valores.

Se obtiene así 0 y dos números positivos α y β



Dividimos a continuación por el número mayor α o β

sea por ejemplo β



En la tabla III se obtiene un número $U=f(x)$, tal que $r = \beta \cdot U$

$$\epsilon_1 = d + r$$

$$\epsilon_2 = d - r$$

3) Cálculo de ψ

La tabla IV da el ángulo en función de x . Este ángulo comprendido entre 0 y 30° se lleva sobre el esquema de direcciones haciendo girar un ángulo ψ la dirección marcada con 1 en el sentido que se aproxima a la dirección marcada con 0. La dirección obtenida es la algebraicamente máxima.

1.13 ROSETA DE DOS DIRECCIONES

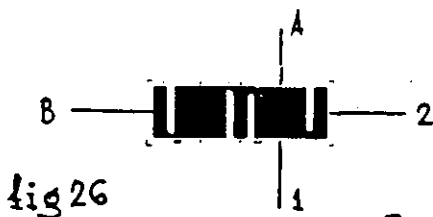
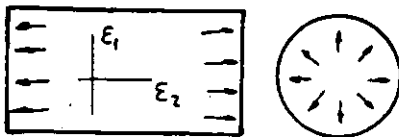


fig 26

Cuando la dirección de los ejes principales es conocida de antemano, como - por ejemplo un cilindro bajo presión (fig. 26), con solo medir las deformaciones en dos direcciones perpendiculares que coincidan con las direcciones principales, será suficiente para determinar el estado de tensiones en un punto

$$\epsilon_1 = \epsilon_A = \epsilon_m; \quad \epsilon_2 = \epsilon_B = \epsilon_m; \quad \gamma_M = \epsilon_A - \epsilon_B$$

$$\sigma_1 = \frac{E}{1-\mu^2} (\epsilon_1 + \mu \epsilon_2) \quad \text{--- --- --- --- ---} \quad [52]$$

$$\sigma_2 = \frac{E}{1-\mu^2} (\epsilon_2 + \mu \epsilon_1) \quad \text{--- --- --- --- ---} \quad [53]$$

$$\tau = G \gamma = G (\epsilon_1 - \epsilon_2) \quad \text{--- --- --- --- ---} \quad [54]$$

Se incluyen ábacos para el cálculo rápido de tensiones a partir de las lecturas en microdeformaciones.

1.14 EXTENSIMETROS UNIDIRECCIONALES

Si se conoce la dirección principal de esfuerzos y ésta es única, como en la tracción pura, la tensión es obtenida aplicando la ley de Hooke.

$$\sigma_1 = \epsilon_1 E \quad \epsilon_2 = \mu \epsilon_1$$

$$\sigma_2 = 0$$

1.15 CORRECCIONES DEBIDAS AL EFECTO DE LA SENSIBILIDAD TRANSVERSAL

Como vimos en el apartado 1.2 el efecto de sensibilidad transversal en el extensímetro, puede tener influencia en los resultados, sobre todo cuando se emplean bandas rosetas. A continuación se indican las correcciones que deben efectuarse sobre los valores de deformaciones principales, así como sobre la distancia del centro y radio del círculo de Mohr.

Sea $\epsilon_M; \epsilon_m$ los valores de las deformaciones principales calculados y K_t el factor de sensibilidad transversal, los ver

dados valores

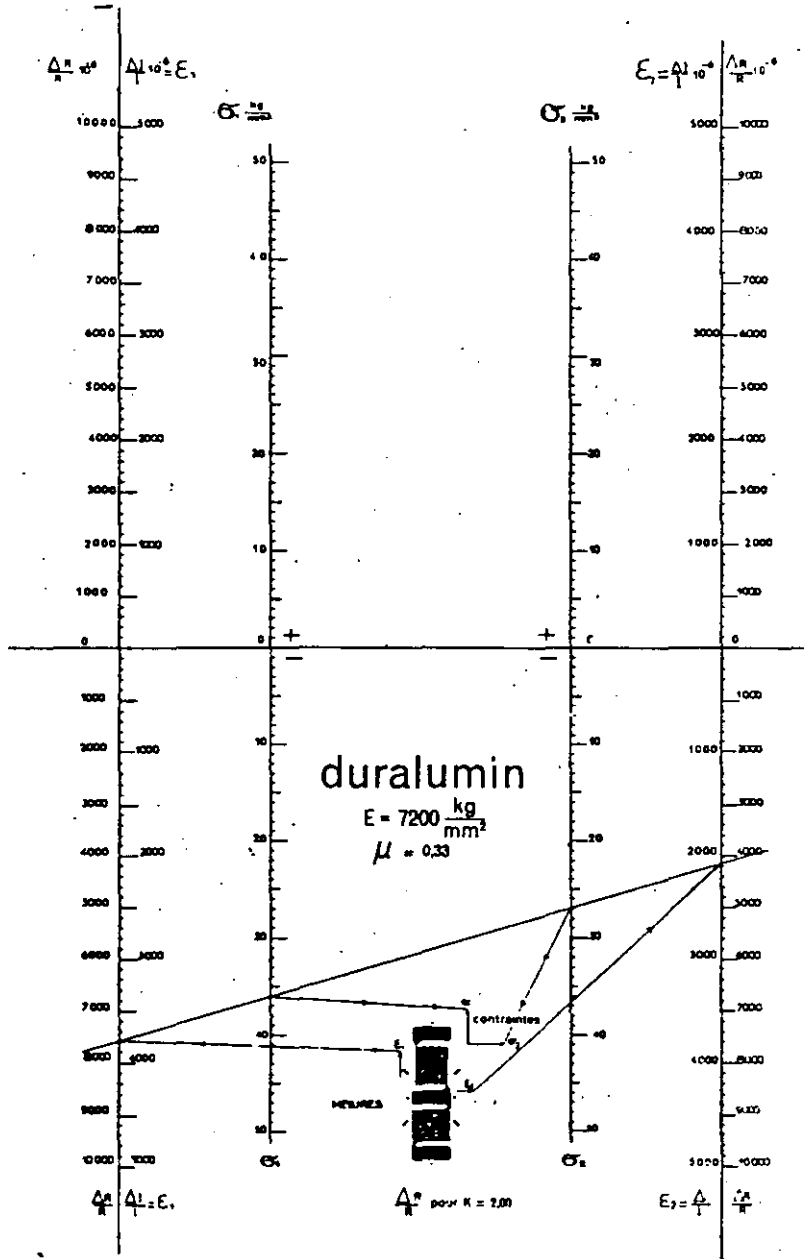
$$\varepsilon'_M = \frac{1 - \mu K_t}{1 + K_t^2} (\varepsilon_M - K_t \varepsilon_m) \dots \dots \dots [55]$$

$$\varepsilon'_m = \frac{1 - \mu K_t}{1 - K_t^2} (\varepsilon_m - K_t \varepsilon_M) \dots \dots \dots [56]$$

$$d' = d (1 - \mu K_t) / (1 + K_t) \dots \dots \dots [57]$$

$$r' = r (1 - \mu K_t) / (1 + K_t) \dots \dots \dots [58]$$

ABACO PARA EL
 CALCULO DE
 TENSIONES
 (Para 2 medidas
 según las direcciones
 principales)



PROPIEDADES DE LOS METALES DE USO MAS CORRIENTE

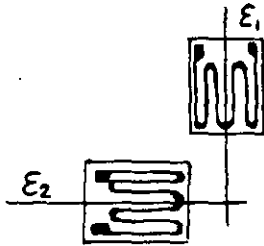
	Modulo #Young (1000 kg/cm ²)	Coefficient de Poisson μ (v/d)	$\frac{E}{1-\mu}$	$\frac{E}{1-\mu}$	$\frac{E}{1-\mu^2}$	α_f	α_s	α_s / α_f	Módulo de torsión (1000 kg/cm ²)	Coeficiente de dilatación 10 ⁻⁶ /°C
Acier de Construcción . . .	21.0	0.285	16.34	29.37	22.87		20 & 60	1	7.80	13
Acier 45 SC 06	22.0	0.285	17.12	30.77	23.97		145	1	7.80	13
Acier resistentes azules . . .	22.0	0.29	17.06	30.99	24.02			1	7.52	25
Acier inoxidable 18-10	20.3	0.29	15.74	28.59	22.16		18 & 22	1	7.30	10.5
Invar	14.1	0.29	10.93	16.86	15.39		40 & 55	1		0.9
Fuentes grises durantes	9 & 12	0.29	7.0 & 9.3	12.7 & 16.9	9.8 & 13.1	7 & 9	16 & 25	3.3	7.1 & 7.2	9 & 11
Fuentes grises azules	10 & 13	0.29	7.7 & 10.0	14.1 & 18.3	10.9 & 14.2	10 & 15	22 & 35	3.4	7.1 & 7.4	9 & 11
Fuentes grises compactadas	5 & 8	0.29	3.9 & 6.7	7.6 & 11.2	5.4 & 8.7		5 & 12	3.5	7.1 & 7.2	9 & 11
Fuente graphite spheroidal	16 & 18	0.29	12.4 & 14.0	22.2 & 25.4	17.5 & 19.6	17 & 35	26 & 60	1.2	7.1 & 7.3	11 & 12
Fuentes blancas non aleras	16 & 20	0.29	12.4 & 15.5	22.2 & 28.2	17.5 & 21.8		24 & 40	5	7.5 & 7.8	9 & 11
Fuentes maleables	17 & 19	0.17	14 & 16	20.5 & 22.9	17.5 & 19.5	16 & 38	20 & 60	1	7.2 & 7.4	9 & 11
Tiame	10.55	0.34	7.67	15.98	11.93	10 & 25	20 & 47	1	4.51	8.9
Aliaje tiame 6Al4V	10.9	0.34	8.13	16.52	12.33					
Aliaje tiame Ti6Al4V	10.5	0.34	7.85	15.91	11.88	60	90	1	4.42	8.0
Aluminium	7.05	0.34	5.26	10.68	7.98					
Aliaje alu AU 4 G	7.5	0.33	5.63	11.19	8.41	12	20	1	2.8	23.5
Aliaje alu AU 2 GN	7.5	0.34	5.60	11.36	8.48	12	37	1	2.8	22 & 24
Aliaje alu AU 5 GT	7.0	0.34	5.22	10.61	7.92	10	22 & 26	1	2.8	23
Zircal AZ80	7.2	0.34	5.37	10.91	8.14		55	1	2.8	23.5
Cobre	10.0	0.33	7.51	14.92	11.22		18	1.3	8.9	17
Latón	9.2	0.33	6.92	13.73	10.33		20	1.4	7.30	18
Bronce ordinario	10.6	0.31	8.09	15.36	11.73		24	3	8.40	17.5
Bronce al beryllium	13	0.34	9.70	19.70	14.71		80	3	8.25	17
Beryllium	30.0	0.05	28.57	31.58	30.68	20	30	1	1.85	12.4
Magnesium	4.60	0.34	3.43	6.97	5.20				1.74	25.0
Marbre	2.6	0.3	2.00	3.71	2.86		50	15	2.3	8
Béton	1.4 & 2.1	0.3	1.1 & 1.6	2.0 & 3.0	1.5 & 2.3		30	11	1.9	14
Vetro	6	0.2 & 0.3	5.0 & 4.6	7.5 & 8.6	6.2 & 6.6		3 & 8	10		
Plexiglass	0.29	0.4	0.207	0.483	0.345		8	1.2	1.8	80 & 90
Acrylate	0.30	0.4	0.214	0.500	0.357		5 & 8	1.2	1.15	90 & 130

Problema nº 1



Una barra de acero está sometida a una tracción pura, montándose una banda en el sentido de la tracción. Calcular las tensiones principales, si leemos $1275/\mu\delta$ y el acero de la barra tiene $E = 21000 \text{ Kg/mm}^2$ y $\mu = 0,28$

Problema nº 2

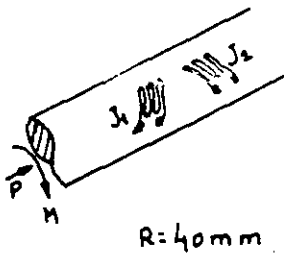


En un depósito cónico de aluminio ($E = 7200 \text{ Kp/mm}^2$; $\mu = 0,33$) se admite que las direcciones principales coinciden con los ejes vertical y horizontal y en tales direcciones se montan dos bandas extensométricas respectivamente. Las lecturas bajo carga son:

para $J_1 \quad \epsilon_1 = 3950/\mu\delta$
 $J_2 \quad \epsilon_2 = 2540/\mu\delta$

Calcular las tensiones en este punto.

Problema nº 3



En un eje cilíndrico de acero ($E = 21000 \text{ Kp/mm}^2$, $\mu = 0,28$) de 80 mm de diámetro se han montado dos bandas, J_1 y J_2 a 45° respecto a su eje. El eje no sufre flexión, pero sí una compresión P y un aumento de torsión M .

En el curso de una primera experiencia, se obtienen como lecturas las siguientes:

$$\epsilon_1 = -\epsilon_2 = 1830/\mu\delta$$

¿Cuales son las tensiones en el punto? ¿Cual la fuerza de compresión y el par?

En una segunda experiencia se obtiene

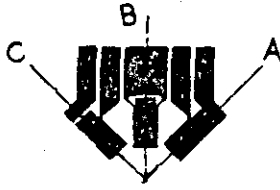
$$\epsilon_1 = 2560/\mu\delta \quad \text{y} \quad \epsilon_2 = -1080/\mu\delta$$

¿Cuales son la fuerza P y momento M ?

Los problemas siguientes, se refieren al cálculo de rosetas, en ellos deberemos calcular:

- Direcciones principales máximas y mínimas
- Deformaciones y tensiones máxima y mínima.

Problema nº 4



Roseta de 45°

$$E = 7200 \text{ Kp/mm}^2 \quad \nu = 0,34$$

$$\text{Lecturas: } A = - 3790 \mu\delta$$

$$B = - 3220 \mu\delta$$

$$C = - 4750 \mu\delta$$

Problema nº 5

$$E = 7200 \text{ Kp/mm}^2 \quad \nu = 0,34$$

$$A = + 2080 \mu\delta$$

$$B = - 1800 \mu\delta$$

$$C = - 1200 \mu\delta$$

Problema nº 6

$$E = 21000 \text{ Kp/mm}^2 \quad \nu = 0,29$$

$$A = + 3580 \mu\delta$$

$$B = + 1930 \mu\delta$$

$$C = + 1370 \mu\delta$$

Problema nº 7

$$E = 21000 \text{ Kp/mm}^2 \quad \nu = 0,29$$

$$A = + 1,792 \mu\delta$$

$$B = 817 \mu\delta$$

$$C = 868 \mu\delta$$

Problema nº 8

$$E = 21000 \text{ Kp/mm}^2 \quad \nu = 0,29$$

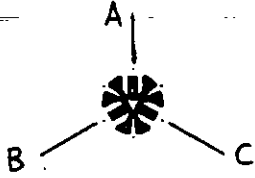
$$A = + 340 \mu\delta$$

$$B = + 520 \mu\delta$$

$$C = - 710 \mu\delta$$

Dar directamente las tensiones, sin pasar por deformaciones.

Problema nº 9



Rosetas de 120°

$$E = 7200 \text{ Kp/mm}^2 \quad \nu = 0,34$$

$$A = + 2400 \mu\delta$$

$$B = + 2010 \mu\delta$$

$$C = + 1370 \mu\delta$$

Problema nº 10

$$E = 7200 \text{ Kp/mm}^2 \quad \nu = 0,34$$

$$A = + 4410 \mu\delta$$

$$B = - 540 \mu\delta$$

$$C = - 1920 \mu\delta$$

Problemas nº 11

$$E = 21000 \text{ Kp/mm}^2 \quad \nu = 0,29$$

$$A = -120 \mu\delta$$

$$B = +540 \mu\delta$$

$$C = +310 \mu\delta$$

Problema nº 12.

$$E = 7200 \text{ Kp/mm}^2 \quad \nu = 0,34$$

$$A = + 1795 \mu\delta$$

$$B = + 1803 \mu\delta$$

$$C = + 1812 \mu\delta$$

2.1. FABRICACIÓN DE BANDAS EXTENSOMÉTRICAS

Una banda extensométrica está formada por dos elementos fundamentales que son el soporte y el conductor eléctrico sensible a las deformaciones, habiendo evolucionado grandemente la constitución y técnicas de fabricación de dichos elementos.

En un principio, se emplearon con gran difusión soportes de papel y conductores de sección circular colocados según la fig. 1,



fig 1

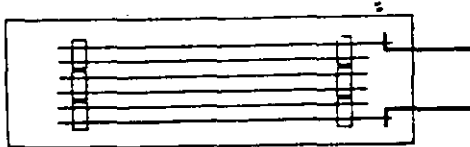


fig 2

pero entre otros, presentaban los graves inconvenientes de la higroscopicidad del papel, que hacía perder el aislamiento de la banda y el elevado factor de sensibilidad transversal en las partes curvas del conductor, intentándose compensar éste último efecto dando forma de zig-zag u otros diseños ingeniosos (fig 2). Actualmente una banda de calidad se fabrica sobre soportes de resinas epóxicas y por el procedimiento de fotograbado, se consiguen formas y dimensiones imposibles por los métodos clásicos (fig 3), ya que los modelos pueden hacerse a escalas muy aumentadas, constituyen

éstas las llamadas bandas de trama pelicular o de film metálico.

Los principios en que se basa la extensometría, suponen que las isostáticas de la estructura bajo ensayo, pasan a través de la parte activa del extensímetro y se ha podido comprobar por fotoelasticidad, que en un extensímetro pegado a una estructura, solo en sus extremidades hay distorsión de aquellas, y nó en la zona central; por dicho motivo, dando a la banda la forma indicada en la fig. 4, conseguimos

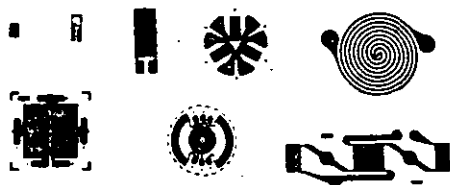
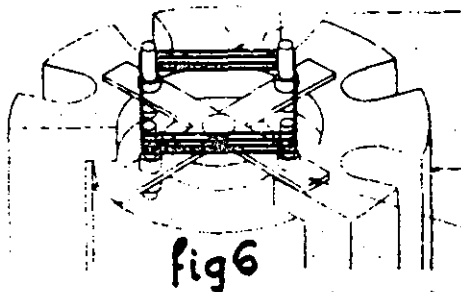
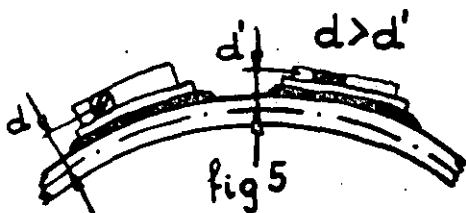


fig 3

establecer en los extremos de los conductores activos una zona de anclaje en la que se inciden las isostáticas y por su mayor sección respecto a la parte activa la variación unitaria de resistencia es menor y despreciables los coeficientes de sensibilidad transversal y longitudinal.

La posibilidad de disponer de superficies adecuadas para la soldadura de los cables y la transparencia de los soportes, que permiten una colocación óptima del extensímetro, añaden ventajas a éste.

Las aleaciones del metal conductor responden a las características específicas de cada tipo, siendo a veces riguroso secreto el proceso de fabricación, en el que se incluyen técnicas sofisticadas para conseguir mejoras en la utilización de extensímetros. A título de ejemplo, en la serie CEA de la casa Vishay-Micromesures, el tratamiento dado a los extremos para soldadura de cables, hace posible que la unión soldada tenga mayor resistencia mecánica a la tracción que el cable que normalmente se utiliza, ventaja ésta que confiere seguridad



a una medida extensométrica. Otras ventajas de las bandas de film metálico residen, en que dado su pequeño es pesor (4 micras), no introducen errores en la medida de deformaciones de secciones delgadas y se adaptan mejor sobre cualquier superficie (fig. 5). Dejando al margen las bandas semiconductoras (de las que nos ocuparemos en otro capítulo) vemos en lo expuesto, que el verdadero sensor de las deformaciones es el conductor, siendo el soporte un medio de transición con la estructura, por lo que exige del pegado a la misma (bonded strain gauge) pero, en aplicaciones para fabricación de transductores, suele emplearse el conductor suelto montado sobre zafros aislantes, (fig.6) que se deforma bajo estímulos mecánicos, sin necesidad del soporte propiamente dicho (unbonded - Strain-gauges).

La banda puede ser posteriormente sometida a recubrimientos y opciones tales como inclusión de hilos de soldadura, que en determinadas aplicaciones resultan de interés.

2.2 CARACTERISTICAS TECNICAS

22.1 Valor óhmico.

El valor de la resistencia óhmica de una banda viene condicionado por motivaciones de tipo eléctrico, y hay razones para

que dicho valor sea elevado de una parte o pequeño de otra, por lo que debe establecerse un compromiso entre las posturas extremas.

Motivos que aconsejan un valor elevado de resistencias:

1. Señales elevadas para debiles deformaciones, en efecto, la señal es función de la tensión de excitación, por lo que conviene que ésta sea elevada, pero para que no circule una corriente excesiva, que por efecto Joule produzca un calentamiento inadecuado, el valor óhmico será alto.
2. Evitar los errores producidos por las resistencias de contacto de los conmutadores y líneas de conexión a los instrumentos, pues siendo éstos valores pequeños su influencia será menor cuando mayor sea la resistencia de la banda.

Motivos que aconsejan valores pequeños de resistencias

1. Evitar la caída de tensión interna considerando a la banda como generador de tensión.
2. Conseguir mejor aislamiento eléctrico entre la banda y la estructura.
3. Mayor robustez, pues resistencias elevadas obligan a conductores de muy pequeña sección y por tanto frágiles.

Por lo expuesto se ha establecido como valor normal y de uso más generalizado el de 120 ohmios, siendo también muy empleados los 350 (generalmente en transductores) 600 y 1000 ohmios.

Las tolerancias de fabricación son muy estrechas 0,15% con el fin de poder equilibrar los circuitos de medida, pero no sería práctico un exceso de dicha tolerancia en límites que puedan confundirse con la variación lógica, que por efecto de montaje, sufriría la banda en su instalación. La exactitud de la medida no será afectada, por ligeras dispersiones del valor nominal.

También se construyen bandas con valores nominales que son fracciones de los indicados para los casos en que la medida requiere un circuito con dos, tres ó cuatro bandas en serie (se hacen de 30, y 60 óhmios u otros valores que no suelen ser standard).

En el estudio teórico de las bandas extensométricas - (1,2) vimos que hay dos factores K_1 y K_2 que relacionan la variación unitaria de resistencia del conductor con la deformación que sufre - en sentido longitudinal y transversal respectivamente por efecto de las sollicitaciones a que esté sometido el elemento donde se instala la banda.

La variación de la resistencia es motivada por el cambio de la geometría del conductor y de la conductividad, pero si bien el primer factor afecta prácticamente igual a todos los metales, el segundo es función de la aleación empleada en la fabricación del extensímetro y es por esta razón por lo que la forma y dimensiones de la banda no influyen sobre el factor de sensibilidad.

Los constructores de bandas, utilizan procesos de fabricación que mantienen el valor del factor de sensibilidad dentro de - unas tolerancias estrechas en una serie, por lo que es importante en medidas con varios extensímetros procurar que no haya dispersión en dichos valores.

Por razones de la instrumentación asociado a las medidas extensométricas, se toma como valor nominal de la sensibilidad longitudinal de las bandas el de 2 y tolerancias admitidas como muy buenas son del $\pm 0,5\%$. El factor de sensibilidad transversal se expresa en tanto por ciento del longitudinal y no debe ser superior al 1%.

El fabricante indica el valor de K obtenido en unas condiciones determinadas de temperatura y sobre medidas efectuadas con probetas de módulo de elasticidad y coeficiente de Poisson conocido, incluyendo curvas (fig. 7) donde se indica la variación del factor K respecto a variaciones de temperatura.

Para medir el factor K se utilizan balanzas de calibración basadas en producir una flexión circular a una probeta en la que se montan bandas correspondientes a una misma serie.

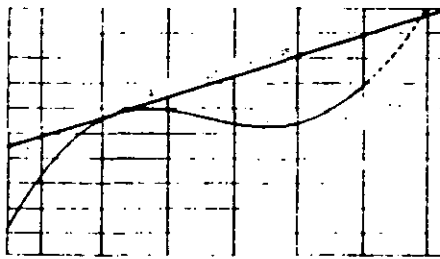
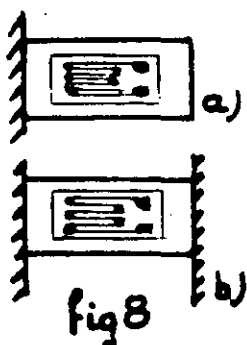


fig 7

Una banda extensométrica mide todas las deformaciones que experimente el elemento sobre el que se monta, pero sabemos que las deformaciones producidas por dilataciones térmicas homogéneas no



crean tensiones, por tanto (fig. 8) si consideramos una viga empotrada en un extremo sin carga alguna y hay variación de temperatura, aquella se dilatará y habrá una deformación que acusará la banda, pero por no originar tensiones, debe ser considerada como error.

El error por variación de temperatura se corrige, dentro de ciertos límites, fabricando el conductor de la banda con coeficientes térmico de variación de la resistividad de igual valor y signo contrario al del coeficiente de dilatación lineal del cuerpo sobre el que montan.

En efecto:

$$R_0 = \rho_0 \frac{l_0}{s} \quad R_t = \rho_0 (1 + \beta t) \frac{l_0 (1 + \alpha t)}{s}$$

$$\Delta R = R_t - R_0 = \frac{l_0}{s} [\rho_0 l_0 \alpha t + l_0 \rho_0 \beta t] = 0$$

$$\alpha = -\beta$$

α = coeficiente dilatación lineal
 β = coeficiente de variación térmico de resistividad

La relación $\alpha = -\beta$ solo es lineal dentro de unos límites de temperatura para los cuales se dice que la banda está autocompensada, los fabricantes indican la curva de respuesta en temperatura de las bandas expresadas como microdeformaciones aparentes (fig.9).

En la fig. 8a vemos que al dilatarse la viga, si la banda es autocompensada, no experimentará variación alguna en su resistencia, por el contrario (fig.8b) si la viga está empotrada en sus extremos, se originan esfuerzos de compresión cuando dilate y la banda por tener el coeficiente $-\beta$ acusará un incremento negativo en la variación unitaria de resistencia, acusando precisamente la compresión habida.

Una banda solo puede ser compensada para materiales que tengan idéntico coeficiente de dilatación. Normalmente se compensan para acero ($\alpha = 11.10^{-6}/^{\circ}C$) y aluminio ($\alpha = 23.10^{-6}/^{\circ}C$).

Veremos en el capítulo de técnicas de Medida, que los efectos de origen térmico pueden compensarse con disposiciones de montaje adecuados.

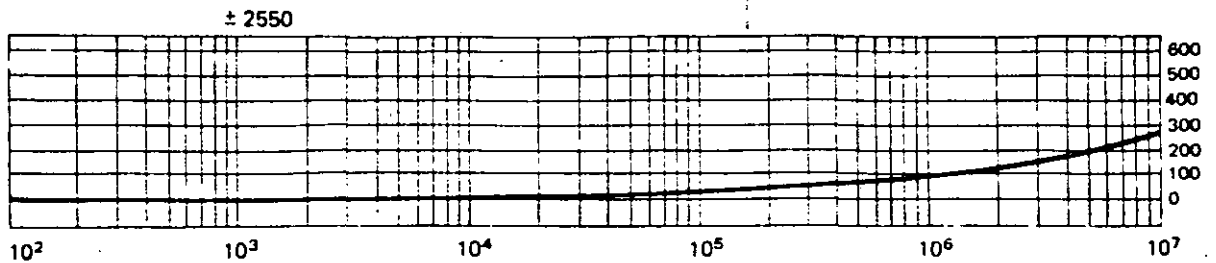


fig 10

2.2.4. LIMITES DE DEFORMACION: ESTATICA Y DINAMICA

La máxima deformación que puede soportar un extensímetro bajo carga estática se expresa en %, de la longitud de su rejilla o parte activa y depende de varios factores, entre ellos:

- a) Temperatura de utilización. El valor indicado por el fabricante se refiere a temperaturas ambientes (24°C) pero a temperaturas criogénicas, la deformación es solo una pequeña fracción de dicho valor.
- b) Ductibilidad de la aleación que constituye el conductor sensible.
- c) Maleabilidad del soporte de la banda y del adhesivo.
- d) Forma y dimensiones del extensímetro.
- e) Calidad del montaje en la estructura

Las bandas impresas de trama pelicular, admiten mayor deformación estática que las de hilo.

El fenómeno de fatiga bajo cargas alterna, presenta aspectos que influyen en las medidas y deben tenerse en cuenta pues pueden introducir errores.

El conductor metálico del extensímetro cuando se monte sobre estructuras sometidas a tensiones alternas, sufre una fatiga - cuyo efecto principal es producir una deriva del valor óhmico de la banda, por éste motivo se ensayan las bandas sometiéndolas a ciclos de amplitud constante ($\pm 1500 \mu\delta; \pm 2250 \mu\delta \dots$) observando cuando la deriva del valor óhmico representa una deformación aparente de $100 \mu\delta$, valor éste admitido como límite (fig. 10).

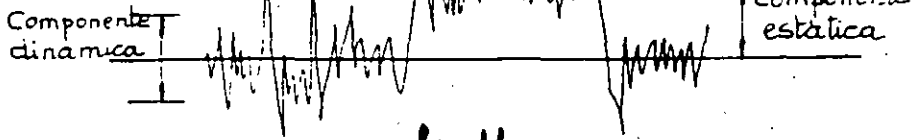


fig 11

Si en una medida dinámica queremos obtener con exactitud los valores de las componentes estáticas y dinámica (fig. 11) prestaremos especial atención en la elección del extensómetro adecuado y sobre todo se cuidará que las soldaduras de los hilos de conexión de los

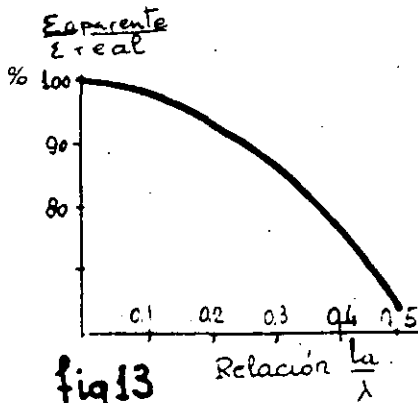


fig 13

instrumentos a la banda sean puntuales para evitar concentración de esfuerzo en la banda y que el tamaño de la misma sea muy pequeño, ya que son los factores más influyentes para evitar llegar al límite de fatiga. En un fenómeno vibratorio la deriva no tiene gran importancia si lo que interesa conocer es solamente la amplitud de la oscilación.

2.2.5. LIMITE DE LA RESPUESTA EN FRECUENCIA

Una banda extensométrica por tener una longitud finita, actúa como un integrador de todas las deformaciones que ocurren a lo largo de la parte activa, por esta razón si la longitud de onda del fenómeno vibratorio que se quiere medir coincide con la longitud activa de la banda (fig. 12) no acusaremos deformación alguna pues la mitad sufrirá alargamiento y la otra mitad compresión.

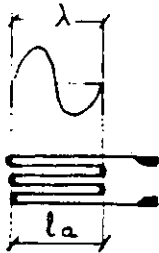


fig 12

Las deformaciones son fenómenos que se propagan a la misma velocidad que el sonido, por tanto conocido éste valor y el de la frecuencia del fenómeno, la longitud de onda $\lambda = \frac{v}{f}$ nos indica el valor límite en el cual una banda de longitud activa $= l_a$ no causaría deformación.

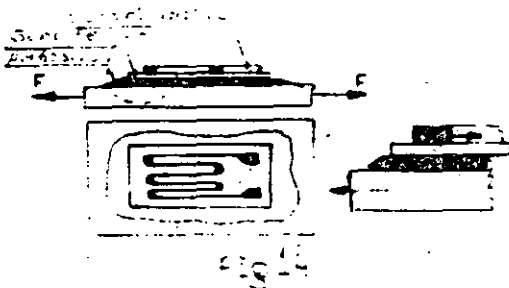
Para evitar la anomalía anterior se admite como valor normal de l_a el 10% de λ con lo que el % de pérdida de sensibilidad es prácticamente nulo (fig. 13).

Se fabrican bandas con longitudes activas de 0,4 mm por lo que se pueden medir en aceros ($v = 5000 \text{ m/seg}$) frecuencias de 10^6 Hz aunque la limitación en éste caso está en los instrumentos de medida.

Otros factores influyen en la limitación de la respuesta en frecuencia de las bandas, pues si bien la debil masa de inercia de la misma favorece el seguir fielmente un fenómeno dinámico, la elasticidad de adhesivos y soportes debe tenerse en cuenta, aunque su valoración es difícil de obtener de forma experimental, debiendo cuidarse la elección de adhesivos en medidas críticas.

2.2.6. FENOMENOS DE FLUENCIA E HISTERESIS

Supongamos que una probeta sobre la que hay montada una banda extensométrica es sometida a esfuerzos de tracción simple (fig 14) las deformaciones de la probeta son entonces transmitidas al conductor activo ^{a través} del adhesivo y del soporte, creandose unas sollicitaciones de cor-



tadura principalmente en los extremos de la banda, que deben compensarse con la fuerza antagonista que se origina en el conductor activo.

La calidad del adhesivo y su elasticidad determinarán la magnitud de la relajación del mismo bajo las sollicitaciones constantes a que esté sometido y por consiguiente que permita al conductor activo un lento retorno a su estado original. El fenómeno descrito es el de fluencia de una banda y tiene importancia considerable en medidas estáticas, no siendolo tanto en medidas dinámicas.

Por la propia naturaleza del fenómeno, se vé que la temperatura juega un papel importante en la fluencia, así como las dimensiones de la banda, participando en razón inversa al tamaño.

Es práctica muy aconsejable, someter las probetas a cargas y descargas sucesivas de magnitud lo mayor posible, antes de efectuar las medidas.

Ligado al concepto anterior puede considerarse el fenómeno de histeresis, el cual ocurre cuando queda una deformación residual después de someter a sollicitaciones la probeta sobre la que está instalada la banda, siendo el principal motivo de este fenómeno que el adhesivo o soporte absorba parte de la energía de deformación y no la

transmita al conductor activo.

2.2.7. NIVELES OPTIMOS DE EXCITACION

La señal eléctrica que obtendremos de cualquier circuito de medida con bandas extensométricas, será proporcional a la tensión de excitación del mismo, lo cual hace presumir el empleo de niveles elevados de excitación, sin embargo hay razones para limitar dichos niveles.

La corriente eléctrica que circula por el conductor de una banda excitada, origina por efecto Joule, una elevación de temperatura al disiparse el calor producido, por cuyo motivo pueden aparecer las perturbaciones siguientes:

- a) Alterar el efecto de autocompensación, cuya estabilidad es mejor con niveles bajos de excitación.
- b) Modificación del estado de tensiones de la estructura bajo ensayo, al absorber ésta el calor disipado por la banda, sobre todo en materiales plásticos.
- d) Derivas del cero, sobre todo en circuitos con varias bandas y en las cuales la disipación de calor no será igual y simultánea.

Los parámetros de mayor incidencia en la determinación del nivel óptimo de excitación de una banda son:

- 1.- Superficie de la rejilla, cuya influencia afecta al poder de disipación de calor.
- 2.- Resistencia óhmica de la banda, que limita el paso de corriente.
- 3.- Coeficiente de conductibilidad térmica de la estructura.
- 4.- Tamaño de la probeta o estructura donde se monta la banda, que determina el poder de absorción de calor.
- 5.- Condiciones ambientales.
- 6.- Calidad del montaje de la banda, cuidándose de que no hayan burbujas de aire entre el soporte y la probeta.

En la tabla I se indica la potencia por cm^2 que pueden disipar las bandas según los materiales donde estén montadas y para precisiones bajas, elevadas o medias (datos cortesía de Vishay-Micro-measures).

POTENCIAS RECOMENDADAS EN WATS/CM²

DISIPACION DE CALOR	PRECISION REQUERIDA					
	ELEVADA	ESTATICAS		DINAMICAS		
		MEDIA	BAJA	ELEVADA	MEDIA	BAJA
<u>Excelente.</u> Piezas grandes de aluminio o de cobre	0,30 á 0,75	0,75 á 1,5	1,5 á 3	0,75 á 3	1,5 á 3	3 á 8
<u>Buena.</u> Piezas grandes de acero.	0,15 á 0,30	0,30 á 0,75	0,75 á 1,5	0,75 á 1,5	1,5 á 3	3 á 8
<u>Media.</u> Piezas pequeñas de acero - inoxidable o titanio.	0,08 á 0,15	0,15 á 0,30	0,30 á 0,75	0,30 á 1,5	0,75 á 1,5	1,5 á 3
<u>Mala.</u> Plásticos, resinas epoxy.	0,01 á 0,03	0,03 á 0,08	0,08 á 0,15	0,08 á 0,15	0,15 á 0,30	0,15 á 0,75
<u>Muy mala.</u> Polies tireno, materiales acrílicos.	0,001 á 0,003	0,003 á 0,008	0,001 á 0,03	0,001 á 0,008	0,003 á 0,015	0,03 á 0,08

La tensión de excitación se deduce a la fórmula:

Potencia disipada: $\frac{V_e^2}{4R} = W_d$ en donde

V_e = Tensión de excitación en Voltios

R = Resistencia nominal de la banda

La potencia por unidad de superficie es

$$\frac{W_d}{S} = w$$

Siendo S la superficie de la rejilla

Si solo disponemos de una fuente de alimentación con tensión fija de tensión y esta es elevada para excitar el circuito de medida se ponen en serie unas resistencias que produzcan una caída de tensión determinada, pero sin olvidar efectuar las correcciones adecuadas por la pérdida de sensibilidad que introducen las mencionadas resistencias.

.3. PRACTICA DE MONTAJE DE BANDAS

.3.1. Preparación de superficies

La instalación de una banda extensométrica tiene como fundamento la perfecta unión entre la banda y el cuerpo de ensayo.

Para el extensometrista cada montaje de circuitos de medida supondrá un aumento de su experiencia y una garantía de que su labor es satisfactoria, solo cuando por un exceso de confianzaomite alguna de las operaciones que se indican como preceptivas, el error aparece, pero desgraciadamente no se manifiesta inutilizando la medida, sino dando como ciertos unos resultados falsos, de ahí que será criterio firme el observar toda la meticulosidad humanamente posible, con la certeza de que, si así se hace, se obtendrán resultados que justificarán el empeño puesto.

La banda puede elegirse, dentro de ciertas opciones que ofrece el fabricante, adaptada a las condiciones de utilización, pero no así la superficie donde deba instalarse, por lo que ésta última deberá ser preparada por el usuario, así como la soldadura de cables que configuran el circuito de medida.

2.5.1. Preparación de superficies

Toda superficie que debe recibir una banda se someterá generalmente a unos tratamientos mecánicos y químicos para conseguir el mayor rendimiento del adhesivo, sin que dichos tratamientos puedan suponer una modificación local de las características del cuerpo a ensayar. Dimensionalmente, se tratará una superficie doble (como mínimo) de la superficie total de la banda.

El proceso previo será el de limpieza y desengrasado, para el que se utilizará preferentemente cloroetileno de calidad, para metales y freón para plásticos, para ello se deposita el desengrasante sobre la superficie (se facilita esta operación si viene envasado en spray) y sin dejarlo evaporar se seca con una gasa limpia y de una sola pasada, repitiéndose esta operación hasta que la gasa aparezca totalmente limpia.

Conviene indicar que siempre que haya que limpiar o secar una superficie debe hacerse con una gasa limpia (no necesariamente esterilizada) o a veces con papel absorbente tipo Kleenex pero nun

ca con algodones que dejarían hebras depositadas. Además la limpieza se hará en una sola pasada y jamás utilizando la misma gasa para pasadas sucesivas, las razones son obvias ya que si la gasa es repuesta sobre la superficie, en vez de limpiar por arrastre, por efecto de estar impregnada de disolvente, la suciedad o grasa existente se disolvería más, entrando en las minúsculas oclusiones que existan.

En montajes sobre metales, recordemos que al estar constituidos por cristales orientados al azar, un pulido superficial presentaría el aspecto de un espejo al quedar incluidas entre los cristales las pequeñísimas partículas arrancadas, por lo que la adhesión y cohesión en estas zonas sería muy dudosa, por tal motivo se comb el tratamiento mecánico por abrasión con un ataque por un ácido de

El proceso de abrasión dependerá del estado inicial la superficie comenzando con papeles de carburo de silicio de gran 400, 200 o 150 respectivamente y que previamente se ha humedecido el ácido, atacando en sentidos alternativos y que formen 90° entre ellos, con el fin de en cada pasada, eliminar las "crestas" que sobre el metal se van marcando; la coloración peculiar que adquiere la superficie y la desaparición de las marcas en un sentido cuando se que a 90°, indican que esta operación está concluida, debiéndose pceder inmediatamente al secado con gasas.

Posteriormente y de inmediato, la superficie se hume ce con un producto neutralizador (solución alcalina detergente) c el fin de que su pH sea adecuado para recibir el adhesivo.

En resumen haremos lo siguiente:

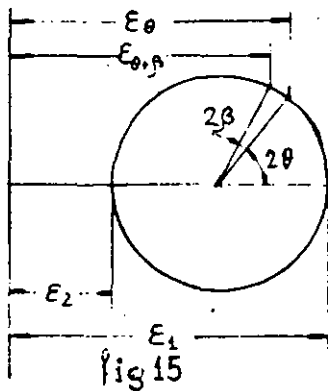
- 1º Limpieza grosera, quitar óxidos pinturas, etc, en una superficie doble que la de la banda.
- 2º Desengrasado absoluto y secado.
- 3º Abrasión progresiva combinada con ácido y secado.
- 4º Neutralización y secado.

Lógicamente el proceso anterior es indicado para ciertos metales, siempre habrá que seguir las indicaciones concretas del fabricante de la propia experiencia.

Si se trata de superficies porosas como el caso del horgón, habrá que impermeabilizar la zona de asentamiento de la banda, consiguiéndose buenos resultados dando después de la limpieza, una capa previa de adhesivo.

En vidrio y plásticos será suficiente el empleo de freón su limpieza con gasas.

3.2. Trazado de ejes de referencia



Una mala alineación de los ejes de la banda con la dirección en la que deseamos medir las deformaciones introduce errores que son función: de la relación entre las deformaciones máximas y mínimas, del ángulo que forma la dirección en la que se desea medir y la dirección de la deformación principal máxima y del ángulo β o error de montaje de la banda (fig. 15).

Como por razones de montaje solo podemos influir sobre β , tendremos que esforzarnos en conseguir que este error sea mínimo, para ello hay que determinar sobre la superficie de asentamiento de la banda, los ejes de la dirección en que deseamos medir, pero tendremos que tener en cuenta que no podemos bajo ningún pretexto, alterar el estado de preparación de la superficie según se explicó en el apartado anterior.

Algunos montadores utilizan (nefastamente) puntas de cero de trazar, que al producir pequeñas incisiones en el material, alteran su estructura, por tanto, nosotros recomendamos siempre que sea posible no trazar sino grabar químicamente los citados ejes.

Con los instrumentos adecuados a la precisión de la medida (escuadras, goniómetros, compás, trazadores ópticos de precisión etc. etc) buscaremos unas referencias ortogonales en los límites de la zona que se ha limpiado procurando que no haya contacto de los trapeles con la superficie limpia, para evitar su contaminación; situadas las referencias tracemos con un bolígrafo de punta fina o con un lápiz de grafito duro (5 ó 6) los ejes completos sobre la superficie reparada. Posteriormente, un palillo cuyo extremo lleve una bolita

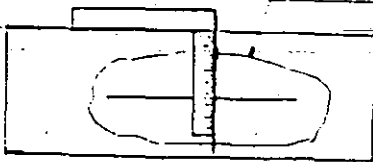


fig 16

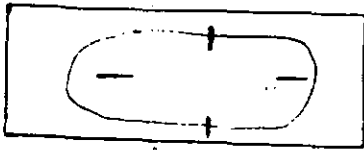


fig 17

de algodón (los utilizados en Pediatría y de venta en farmacias son muy adecuados) se humedece con ácido y se pasa sobre los trazos del bolígrafo o lápiz, secando a continuación y se repite la operación pero humedeciendo un nuevo algodoncito con neutralizador; de esta forma la superficie mecánicamente no se ha modificado y sí veremos que han sido grabados los ejes de referencia, ya que la marca de grafito ha impedido la acción del ácido - sobre la propia línea y a continuación el neutralizador ha limpiado el grafito que se depositó. Este procedimiento tiene una demostrada eficacia por innumerables experiencias y es práctica su aplicación en metales.

Otra solución consiste en marcar con lápiz los ejes, pero sin que estas lleguen a cortarse dejando siempre libre la superficie - del soporte de la banda (fig. 17) pero se ve que conseguir este entraña una pericia grande y no queda exenta de problemas de contaminación de la superficie.

2.3.3. Pegado de extensímetros

El adhesivo utilizado para el pegado de bandas deberá reunir unas características adecuadas a su uso y nunca se pecará por exceso en las exigencias que en su elección hagamos. Tienen preferencia todos aquellos que solidifican por polimerización, es decir que la totalidad de los átomos que forman los componentes (normalmente dos) constituyen el sólido final, a diferencia de los pegamentos normales que solidifican por evaporación de un disolvente.

En general un buen adhesivo tendrá las siguientes características:

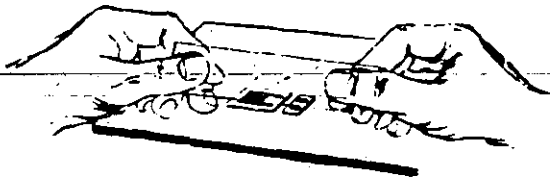
- a) Permitir su aplicación en películas delgadas para no introducir - errores por distanciamiento de la rejilla a la superficie.
- b) Ser neutro a la superficie y al soporte de la banda.
- c) Transmitir los esfuerzos a la banda sin fenómenos de fluencia.
- d) Técnica de aplicación fácil.
- e) Utilización en un margen lo más amplio posible respecto a condiciones ambientales.

Será difícil que un solo adhesivo cumpla en grado óptimo las condiciones anteriores, pero siempre será factible establecer un compromiso para aplicaciones concretas.

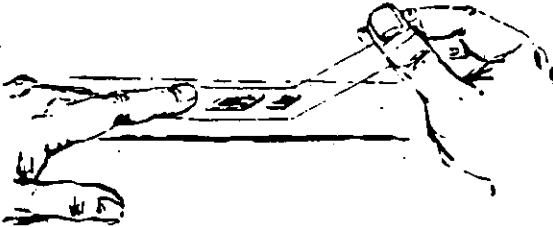
Hay pegamentos de aplicación sencilla y rápida cuyo uso es de interés en piezas grandes y usos generales donde la medida se haga a temperaturas ambientales normales (20° ó 60°C) un ejemplo de aplicación de los mismos se expone gráficamente en la fig. 18, referente al tipo M-200 de la firma Vishay-Micromesures.

Para aplicaciones que exijan una mejor precisión, como puede ser el caso de fabricación de captadores, se utilizarán adhesivos que deben someterse a un tratamiento térmico, operación que no deja de ser engorrosa. En cualquier caso, el fabricante dará normas claras de aplicación. Para usos de condiciones extremas (1000°C) se comprende que los adhesivos se descompondrán, para ello, existen bandas encapsuladas en una vaina metálica que son fijadas por soldadura eléctrica por puntos con utensilios adecuados.

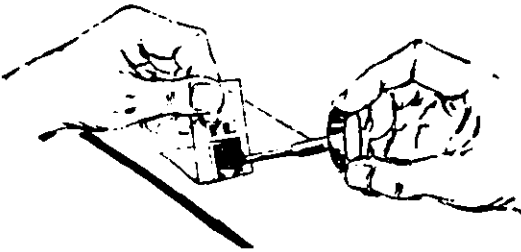
Junto con la banda, es muy práctico pegar unos soportes de terminales impresos que ayudarán a la soldadura e instalación del cableado.



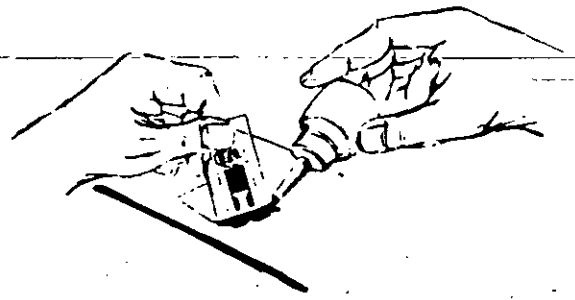
a) la banda y el terminal impreso se colocan sobre un cristal totalmente limpio y con papel transparente autoadhesivo, se cubren y se separan del cristal procurando no doblar la banda.



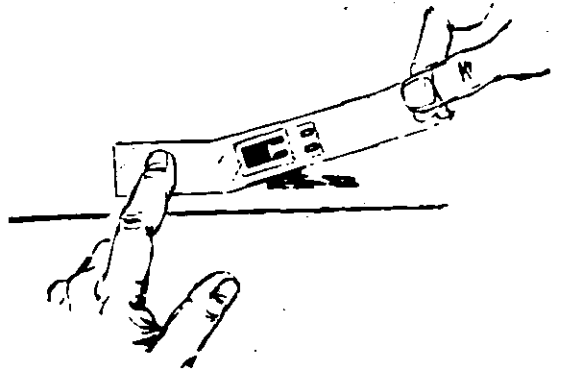
b) se situa la cinta y banda sobre el punto de medida, fijando un extremo y levantando el otro.



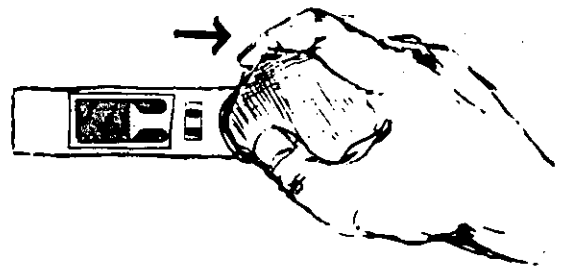
c) con el pincel del acelerador, se aplica éste sobre el reverso de la banda y terminal, procurando no contaminar la banda con adhesivo de la cinta. Dejar secar un minuto.



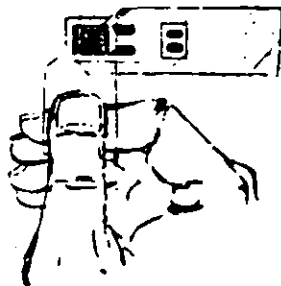
d) depositar una o dos gotas de adhesivo sobre la superficie de asentamiento.



e) se va bajando la cinta y con un dedo se hace ligera presión de izquierda a derecha y evitando tocar directamente el adhesivo.



f) una gasa se pasa varias veces para evitar se formen burbujas de aire.



g) a los 10 minutos como mínimo se puede retirar el papel transparente que ayudó a pegar la banda como se indica.

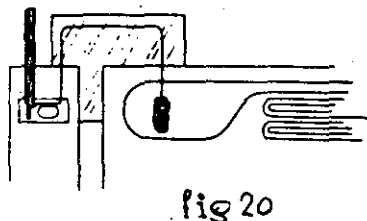
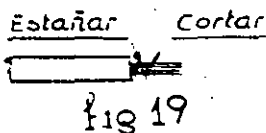
• 2.3.4. Soldadura de cables

La soldadura de las bandas a los hilos de unión de los instrumentos de lectura, requieren una especial atención y el montador necesitará adquirir cierta experiencia para dominar esta operación.

En la composición de las soldaduras se emplean aleaciones de plomo con estaño, plata o antimonio, que llevan o no incorporada una resina y según las proporciones de dichas aleaciones resultan unas características determinadas de conductividad eléctrica, comportamiento a sollicitaciones mecánicas, respuesta en temperatura etc. por todo ello es recomendable el uso de soldaduras comunes en aplicaciones de taller eléctrico o electrónico. Especial atención tiene el conocimiento de la temperatura de fusión que debe ser lo más inmediata superior a la que estará sometida el circuito de medida, con el fin de no tener que aportar más calor del necesario al efectuar las soldaduras.

Según el tipo de soldadura elegido será conveniente o necesario utilizar un fundente, sobre todo para hilos muy delgados, pero será totalmente imprescindible limpiar con un decapante adecuado los puntos de soldadura con el fin de eliminar los residuos de fundente y resina que podrían ocasionar corrosiones y fenómenos parásitos por efecto "pila" ya que evidentemente quedarían dos metales y un electrolito.

El soldador juega un papel muy importante, siendo recomendados aquellos de temperatura regulable; la punta del mismo nunca será cónica sino que tendrá una talla en forma de bisel. Para evitar que los cables puedan ejercer esfuerzos en la banda que pudiesen deteriorarla debe utilizarse siempre que sea posible un terminal impreso que servirá de apoyo al cable (que será de varios hilos) al que previamente se le separó un hilito y se estañó tal y como se indica en la fig. 19.



- En general seguiremos el siguiente proceso:
- 1º Preparar el cable según la fig. 19
 - 2º Proteger con papel autoadhesivo debil la banda, dejando al descubierto solamente los puntos de soldadura.
 - 3º Depositar una gota de soldadura lo más pequeña posible sin aportar excesivo calor

~~que podría desprender la banda del soporte. No debe durar esta operación más de 2 segundos, si no se consiguen el primer intento, dejar enfriar y repetir.~~

4º Presentar el cable ya preparado y sin aporte de soldadura, solamente manteniendo caliente y muy limpio la punta del soldador, fijar los cables a los terminales y a la banda, tal y como se indica en la fig.20.

En la banda conviene que la gota de soldadura sea lo menor posible para evitar concentración de esfuerzos, de ahí que el procedimiento explicado favorezca ésta condición al ser más fino el hilo de unión del terminal a la banda, a la vez que se consiguen dar mayor seguridad al montaje, pues un fuerte tirón del cable rompería el terminal pero no la banda.

Hemos ofrecido unas normas generales ya que el fabricante indicará en cada caso las instrucciones concretas.

2.5.5. Comprobaciones

Una vez instalada una banda deberán efectuarse diversas comprobaciones siendo preceptivas:

- 1º Inspección ocular. Debe hacerse con una lupa de 20 aumentos o más para confirmar que se ha situado correctamente la banda a la vez que se observará que no han quedado bolsas de aire ni "lagunas" (zonas sin adhesivos) bajo el soporte de la misma.
- 2º Comprobación del aislamiento. Se utilizará un megohmetro cuya tensión no exceda los 50 V, si es de válvula mejor y jamás se hará uso de los medidores de aislamiento de tipo magneto que quemarían la banda.

El aislamiento deberá ser mejor que 100 megohms, ya que un aislamiento menor, equivale a introducir un error, por colocar en paralelo con la banda otra resistencia; se puede calcular dicho error, en efecto, consideremos un aislamiento de 2 Mohms.
- 3º Medida del valor óhmico de la banda. Utilizar un instrumento que aprecie decimas de ohmio como mínimo; esta comprobación tiene dos objetos; el primero saber que no está rota ni cortocircuitada la rejilla y el segundo conocer la dispersión del valor nominal, so-

bre todo en circuitos con varias bandas para controlar desequilibrios excesivos.

2.5.6. Protecciones

Desde medidas efectuadas en laboratorio, hasta las difíciles en los conos de cohetes o cascos de barcos, encontraremos una serie de condiciones ambientales que juntamente con la duración de la medida exigirán proteger un elemento delicado con es la banda extensométrica de forma adecuada.

Las bandas, de por sí, son presentadas bajo opciones que aportan una determinada protección, así las hay encapsuladas sobre dos láminas, una inferior que constituye el soporte y otra superior de la misma naturaleza y que deja libre solo los terminales para la soldadura de cables, ésta protección evita la proyección del estaño en la soldadura y mejora enormemente el aislamiento. Otras opciones llevan unos hilos soldados, por lo que el soporte superior cubre totalmente a la banda (fig. 21).

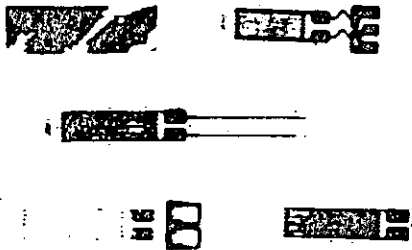


Fig 21

En general la protección la consideramos bajo el aspecto de aislamiento eléctrico y de fortaleza mecánica y previamente a la instalación de la banda tendremos que conocerla, para preparar la superficie adecuadamente antes del pegado de la misma

Los criterios que debemos tener en cuenta para elegir los productos de protección estarán basados en:

- Temperaturas extremas durante la medida, p.e. Probeta en laboratorio $22^{\circ}\text{C} \pm 3^{\circ}\text{C}$; estructura expuesta al sol $0-60^{\circ}\text{C}$ estructura de un avión en vuelo $-50^{\circ}\text{C} + 120^{\circ}\text{C}$.
- Duración de las medidas, p.e. 1 hora en laboratorio; 1 año en un punto sumergido del casco de un buque.
- Ambiente, p.e, aire seco, aire humedo, agua, aceite, chorro de agua, gases corrosivos, hidrocarburos,

No debemos olvidar antes de la aplicación de los protectores, cercionarnos de que no hay restos de adhesivo alrededor de la zona a proteger, que se limpió bien la resina fundente de las soldaduras, que la superficie y los cables están preparados para que el

protector se adhiera, que no hay humedad, etc. en una palabra, no des-
deñar ningún esfuerzo que posteriormente pueda inutilizar varias horas
de laboriosos trabajos.

Una práctica muy aconsejable, siempre que sea posible,
será lo de conectar provisionalmente el instrumento de lectura al cir-
cuito antes de protegerlo y sometiendo aquel a alguna sollicitación,
observar que el funcionamiento es lógico.

Por último, no olvidar tomar datos de posición, fotos,
numeración de cables, esquemas etc. antes de la protección, ya que pos-
teriormente sería imposible, al quedar el circuito tapado por los pro-
tectores.

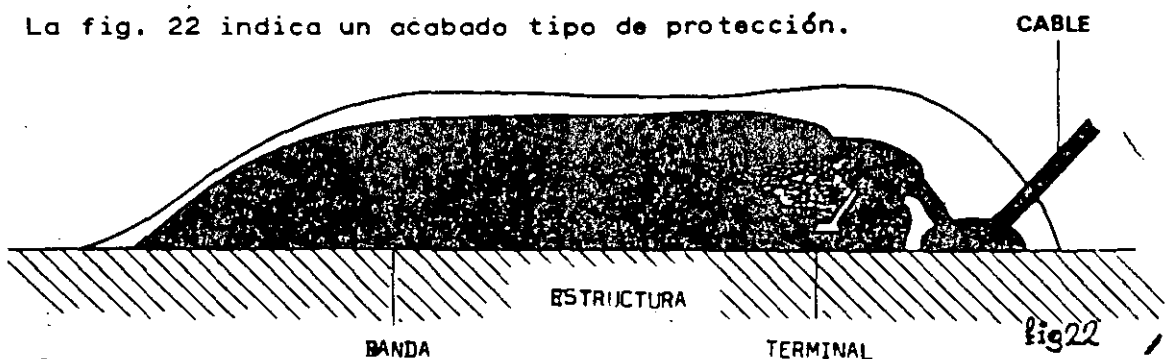
La aplicación del protector la haremos siguiendo siempre
las indicaciones del fabricante pero como orientación tendremos presen-
te:

1º Extender bien el producto sobre la superficie limpia y si hay que
dar varias capas, que la última cubra por completo a las anteriores.
Algunos productos vienen acompañados de un componente previo, que debe
aplicarse sobre la superficie con pincel y dejar secar perfectamente
para luego aplicar el protector y conseguir así la mejor adhesión. Vi-
jilar que no queden bolsas de aire.

2º Cuidar que el espesor del protector sea el adecuado, muchos protec-
tores son blandos y fácilmente las bolitas puntuales de las soldaduras,
pueden atravesar el protector con pequeñas presiones, originando contac-
tos de masa indeseados.

3º Protección del extremo de los cables de unión a instrumentos, pues
de nada sirve esmerarse en la banda si dejamos opción a que por la vai-
na de los cables queden huecos por donde se perdería la protección.

La fig. 22 indica un acabado tipo de protección.



2.6.1. Indicadores de propagación de fisuras

Dos son los motivos que pueden hacer necesario el uso de estos sensores: detectar la aparición de una fisura o determinar la velocidad de propagación de la misma, en ambos casos, si bien el sensor será el mismo, variarán los instrumentos de lectura.

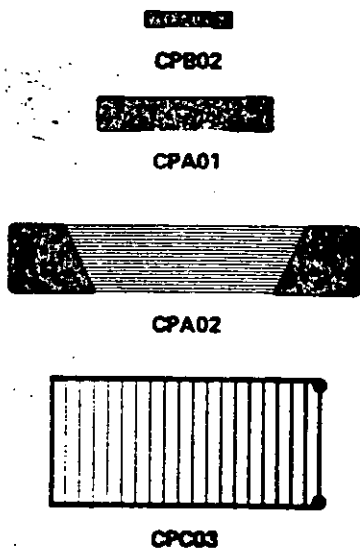


Fig. 23

La aleación de la que están constituidos es suficiente para soportar deformaciones superiores a $\pm 2000 \mu\text{d}$ más de 10^8 ciclos y son montados con técnicas similares a las utilizadas en los extensímetros.

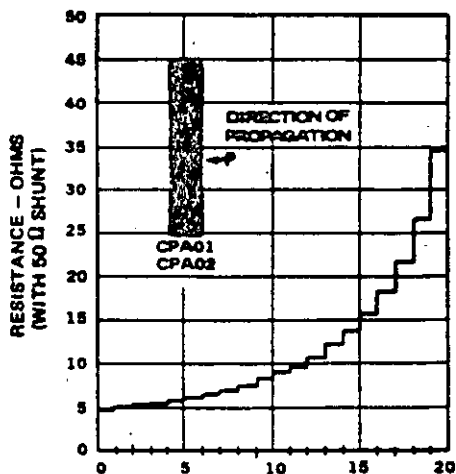


Fig. 24

Estos indicadores están formados por una serie de hilos en paralelo (fig. 23) montados en un soporte similar al de los extensímetros, que se pega en el punto donde se producirá la fisura, y que cuando aparezca romperá un determinado número de conductores, deduciéndose la longitud de la fisura por medida de la resistencia con un ohmetro; si por el contrario el momento de aparición de la fisura es registrado de forma continua por un oscilógrafo, deduciremos la velocidad con que se propaga (fig. 24).

Los efectos de temperatura tienen poca influencia.

2.6.2. Indicadores de fatiga

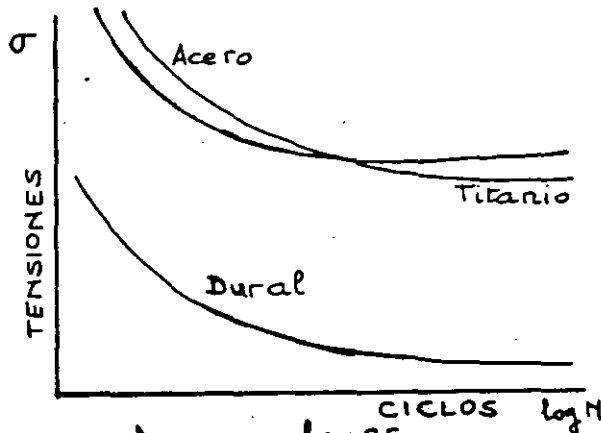
Al contrario que los bandas extensométricas, que miden deformaciones por variaciones instantóneas de su resistencia, los indicadores de fatiga (S/N) guardan "en memoria" todas las deformaciones experimentadas después de su instalación. La memoria aludida viene representada por una modificación permanente del valor nominal de su resistencia, que es función de la amplitud de las deformaciones y de

la frecuencia con que se producen.

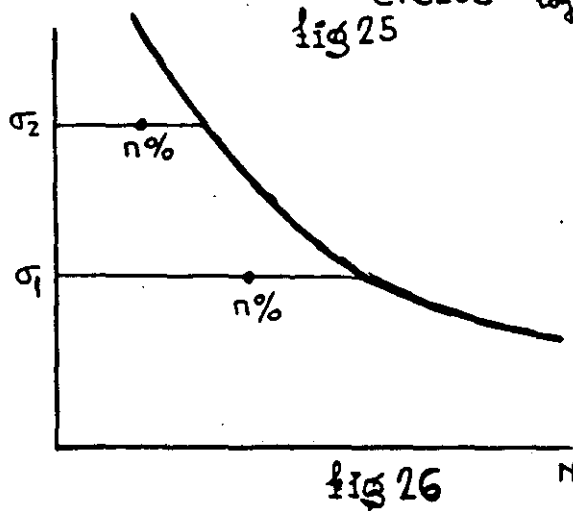
- 1º En una pieza sometida a cargas alternas, la carga de rotura disminuye.
- 2º El número de alternancias que hay que producir para la rotura es tanto menor, cuanto mayor es la amplitud de las mismas.
- 3º Existe un valor de deformación máximo para el cual no se produce rotura sea cual sea el número de ciclos con que se aplique.

En la fig. 25 se expresa gráficamente lo expuesto.

Estudios realizados por Miner, permiten afirmar que el porcentaje de vida de una pieza sometida a tensiones variables, es el mismo si aumentando la amplitud de las tensiones disminuimos su frecuencia o viceversa, siguiendo la proporción obtenida según los criterios de Wöhler.



En la fig. 26 vemos que el tanto por ciento de envejecimiento de una pieza es el mismo sometido a la tensión σ_1 y C_1 ciclos que si se somete a la tensión σ_2 y C_2 ciclos.



Se considera que las tensiones aplicadas oscilan entre un valor σ máximo y un mínimo 0, si así no fuese, lógicamente habrá que considerar los efectos de una componente continua más la carga variable.

Si bien en su aspecto los indicadores de fatiga (fig. 27) son semejantes a las bandas extensométricas, la constitución de su elemento sen-

sible es bien distinta, ya que la aleación de la rejilla persigue aumentar al máximo el efecto que en los extensímetros se trataba de eliminar; en efecto recordemos (2.2.4.) que en las bandas se establece como límite deformaciones dinámicas, aquel que produce una deriva de

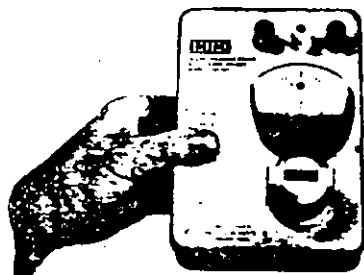


fig 27

100 $\mu\Omega$, equivalente a un incremento de 0,024 ohms en una banda de 120 ohms, mientras que ahora pretendemos que estos valores sean del orden de 7 a 10 ohms. Se constituyen en aleación de constantes con valor nominal de 100 ohms.

La variación de la resistencia del indicador de fatigas es producida por una distorsión de su red cristalina y por la aparición de microfisuras de la aleación de que se compone su rejilla y ha podido demostrarse experimentalmente que en algunos metales, empleados en construcción normalmente, se produce el mismo fenómeno; de ahí que estos sensores cuando son montados sobre piezas mecánicas puedan indicar con gran fidelidad el estado de envejecimiento de los materiales midiendo la desviación del valor nominal de la resistencia del sensor.

Si el envejecimiento de la aleación del sensor es distinto del material sobre el que se monta, la concordancia anterior se pierde y los resultados no tendrán valor alguno, ya que si, por ejemplo la deformación máxima capaz de desviar el valor de la resistencia del sensor, (3ª ley de Wöhler) es superior a la deformación que producirá la rotura de la pieza de ensayo, el indicador de fatiga jamás acusaría desviación de su resistencia; para evitarlo se fabrican sensores multiplicadores los cuales por diversos procedimientos de fabricación se consiguen adaptar la respuesta del sensor a los materiales en que se montan (fig 28a)

Si el envejecimiento de la aleación del sensor es distinto del material sobre el que se monta, la concordancia anterior se pierde y los resultados no tendrán valor alguno, ya que si, por ejemplo la deformación máxima capaz de desviar el valor de la resistencia del sensor, (3ª ley de Wöhler) es superior a la deformación que producirá la rotura de la pieza de ensayo, el indicador de fatiga jamás acusaría desviación de su resistencia; para evitarlo se fabrican sensores multiplicadores los cuales por diversos procedimientos de fabricación se consiguen adaptar la respuesta del sensor a los materiales en que se montan (fig 28a)

La fig. 28 da una respuesta de los sensores FWA de Vishay-Micromesures.

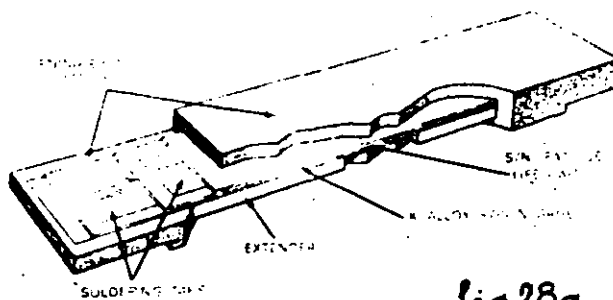


fig 28a



TABLAS PARA
EL CALCULO CON
ROSETAS DE 120°

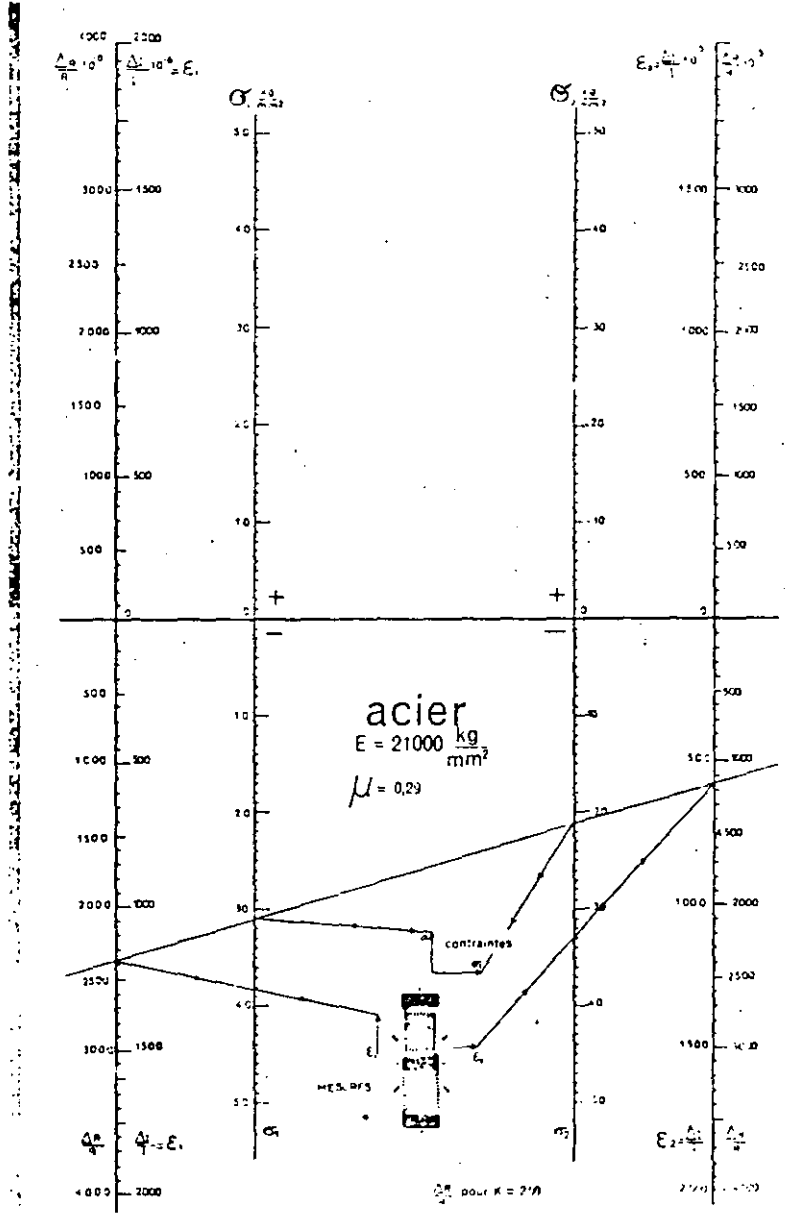
x	0	1	2	3	4	5	6	7	8	9		
0.00	0.6667	63	63	57	53	50	47	43	40	39	0.6634	0.99
0.01	34	30	27	24	20	17	13	10	07	04	01	0.98
0.02	01											
0.03	0.6599	98	95	91	88	85	82	79	75	72	0.6568	0.97
0.04	37	66	63	59	56	53	50	47	44	41	37	0.96
0.05	06	34	31	28	25	22	19	16	13	09	06	0.95
0.06	0.6476	73	70	67	64	61	58	55	52	43	0.6476	0.94
0.07	46	43	40	37	34	31	28	25	22	20	17	0.93
0.08	16	14	11	08	05	02						0.92
0.09	0.6388	85	82	79	76	74	71	68	65	62	0.6387	0.91
0.10	80	57	54	51	48	46	43	40	37	35	32	0.90
0.11	32	29	26	24	21	18	16	13	10	08	04	0.88
0.12	05											
0.13	0.6278	76	73	70	68	65	63	60	58	55	0.6278	0.87
0.14	52	50	47	45	42	40	37	35	32	30	27	0.86
0.15	27	25	22	20	17	15	12	10	07	04	02	0.85
0.16	02											0.84
0.17	0.6178	76	74	71	69	67	64	62	60	57	0.6178	0.83
0.18	55	53	50	48	46	44	41	39	37	34	32	0.82
0.19	32	30	28	26	23	21	19	17	14	12	10	0.80
0.20	10	08	06	04	01							
0.21	0.6089	86	84	82	80	78	76	74	72	70	0.6089	0.79
0.22	68	66	64	62	60	58	56	54	52	50	48	0.78
0.23	48	46	44	42	40	38	36	34	32	30	28	0.77
0.24	28	26	24	22	20	19	17	15	13	11	09	0.75
0.25	09	07	05	03	02	00						
0.26	0.5991	89	88	86	84	82	80	79	77	75	74	0.74
0.27	74	72	70	69	67	65	64	62	60	59	57	0.73
0.28	57	55	54	52	50	49	47	46	44	42	41	0.72
0.29	41	39	38	36	35	33	32	30	28	27	25	0.71
0.30	25	24	22	21	20	18	17	15	14	13	11	0.70
0.31	10	09	08	07	05	04	02	01				0.69
0.32	0.5897	86	94	93	92	90	89	88	86	85	0.5897	0.68
0.33	84	82	81	80	79	77	76	75	74	72	71	0.67
0.34	71	70	69	68	66	65	64	63	62	60	59	0.66
0.35	59	58	57	56	55	54	53	52	51	50	48	0.65
0.36	48	47	46	45	44	43	42	41	40	39	38	0.64
0.37	38	37	36	35	34	33	32	31	30	30	29	0.62
0.38	29	28	27	26	25	24	23	22	22	21	20	0.61
0.39	20	19	18	17	17	16	15	14	13	13	12	0.60
0.40	12	11	10	10	09	08	07	07	06	05	05	0.59
0.41	05	04	03	03	02	01	01	00				
0.42	0.5798	97	97	96	96	95	95	94	93	93	0.5798	0.58
0.43	92	92	91	91	90	90	89	89	88	88	87	0.57
0.44	87	87	86	86	86	85	85	84	84	83	83	0.56
0.45	83	83	82	82	82	81	81	81	80	80	80	0.55
0.46	80	79	79	79	78	78	78	78	77	77	77	0.54
0.47	77	77	77	76	76	76	76	75	75	75	75	0.53
0.48	75	75	75	75	74	74	74	74	74	74	74	0.52
0.49	74	74	74	74	74	74	74	74	74	73	0.51	
											0.5773	0.50

TABLA N° 3

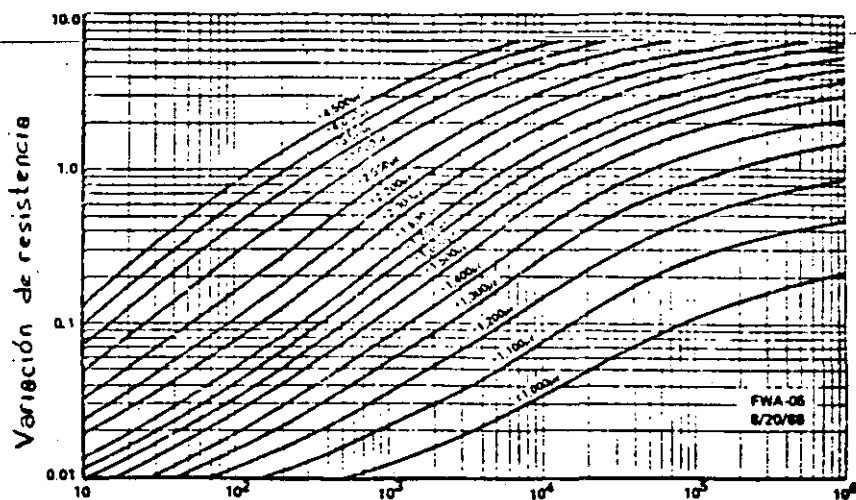
x	0	1	2	3	4	5	6	7	8	9
0.0	0.00	0.25	0.50	0.76	1.01	1.28	1.53	1.80	2.07	2.33
0.1	2.61	2.88	3.16	3.43	3.72	3.99	4.28	4.58	4.87	5.15
0.2	5.45	5.74	6.04	6.34	6.64	6.95	7.26	7.57	7.92	8.18
0.3	8.50	8.82	9.13	9.45	9.77	10.09	10.41	10.73	11.05	11.38
0.4	11.70	12.03	12.36	12.69	13.02	13.35	13.68	14.01	14.24	14.67
0.5	15.00	15.33	15.66	15.99	16.32	16.65	16.98	17.31	17.64	17.97
0.6	18.30	18.62	18.94	19.27	19.59	19.91	20.23	20.55	20.87	21.18
0.7	21.50	21.82	22.08	22.43	22.72	23.05	23.36	23.69	23.95	24.26
0.8	24.55	24.95	25.13	25.42	25.72	26.01	26.28	26.57	26.84	27.12
0.9	27.35	27.67	27.93	28.20	28.47	28.72	28.99	29.24	29.50	29.75
1.0	30.00									

TABLA N° 4

ABACO PARA EL
 CALCULO DE
 TENSIONES
 (Para 2 medidas
 según las direcciones
 principales)



Cortesía de VISHAY MICROMESURES



Nº de ciclos
fig 28

Los indicadores de fatiga son verdaderos integradores de los efectos producidos por cargas alternas, sea cual sea su amplitud así pues, si después de 10.000 ciclos de $\pm 2000 \mu\delta$ producen una desviación de la resistencia de 1,9 ohm y 100 ciclos de $\pm 3000 \mu\delta$ 0,8ohm, la indicación final será de 2,7 ohm.

Al montaje de estos indicadores habrá que tener en cuenta que su eje sensible coincida con el eje de esfuerzo principal máximo, determinado previamente por cualquier procedimiento (extensométrico, fotoelasticidad, etc).

2.6.3. Sensores de temperatura

Siguiendo el mismo procedimiento de fabricación de las bandas extensométricas, pero haciendo que la aleación de la rejilla sea de níquel, se obtienen sensores cuya variación de resistencia es altamente sensible a las variaciones de temperatura siendo este fenómeno muy estable y repetitivo, de ahí que se utilice profusamente en la medida de temperaturas por contacto y utilizando las mismas técnicas de instalación que las expuestas para extensímetros. La curva $\Delta R-t^\circ$ (fig. 29), tiene una pendiente considerable por lo que se obtienen señales de alto nivel, pudiéndose medir con gran precisión, exactitud y poder de resolución, temperaturas comprendidas entre -300 y $+ 500^\circ\text{F}$.

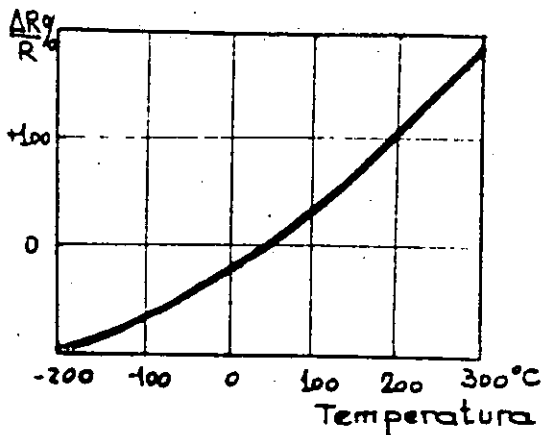


fig 29

nocer los ΔR directamente, no obstante como la respuesta no es lineal siempre tendríamos que tener tablas o curvas de respuesta para conocer el verdadero valor de la temperatura en $^{\circ}\text{C}$ ó $^{\circ}\text{F}$. El inconveniente anterior

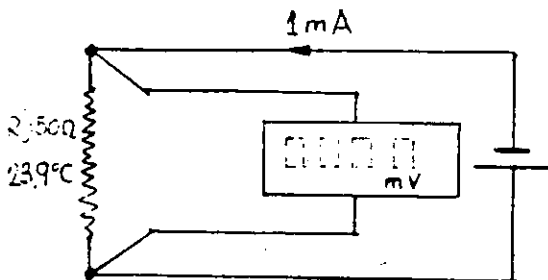


fig 30

ha sido subsanado introduciendo circuitos linealizadores en los cuales, si bien se pierde sensibilidad, la respuesta es lineal, por lo que los instrumentos de lectura pueden ir tarados directamente en escalas termométricas.

Con el fin de utilizar para la medida de temperaturas los mismos instrumentos que para medir deformaciones, los circuitos linealizadores se calculan de tal forma que el sensor constituye una rama de un puente de Wheatstone (fig. 31), de tal forma, que al leer un número entero de microdeformaciones equivalga a la variación de 1 grado centígrado o Fahrenheit. Normalmente se fabrican redes para:

$$10 \mu\delta \leftrightarrow 1^{\circ}\text{C} \leftrightarrow 1^{\circ}\text{F}$$

$$100 \mu\delta \leftrightarrow 1^{\circ}\text{C} \leftrightarrow 1^{\circ}\text{F}$$

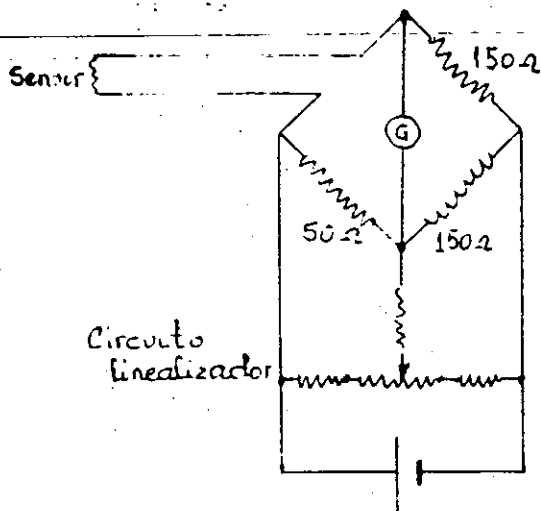


fig 31

por este motivo.

La longitud de los cables puede ser origen de errores - por pérdida de sensibilidad, pero se compensan estos efectos modificando el factor K de sensibilidad en el instrumento de lectura (esto se estudia en el próximo capítulo).

Para medida de muy bajas temperaturas (criogenia) se utilizan sensores (fig. 32) que llevan dos rejillas en serie en aleaciones de manganeso níquel, con lo que se consigue linealizar circuitos desde -400°F .



resistividad cuando son sometidos a tensiones mecánicas, pero en los semiconductores este efecto es mucho más notable y se aprovecha por tanto, como elemento transductor para la medida de deformaciones. El fenómeno

La aleación de níquel, muy sensible a las variaciones de temperatura, obliga a utilizar fuentes de alimentación de baja d.d.p. ya que al circular corriente por el sensor el calor generado por efecto Joule introduce pequeños errores. Por otra parte, si el punto de medida está sometido a deformaciones estas las acusará el sensor, pero dado su insensibilidad a este fenómeno no tendrán gran influencia en la exactitud de la medida, de todas formas el fabricante da con los sensores las curvas de corrección

desde -400°F .

En el montaje de sensores de temperatura no habrá jamás de olvidar utilizar adhesivos soldaduras, cables protectores, etc. cuyo límite de utilización en temperatura sea superior a la que se desea medir.

2.6.4. Bandas semiconductores

Todos los cuerpos tienen, más o menos acusada, la propiedad de sufrir variaciones en el valor de su re-

meno expuesto de la piezoresistividad, no debe ser confundido con el de la piezoelectricidad, que presentan los cristales de cuarzo y otros, de crear cargas eléctricas entre sus caras cuando son deformados, constituyendo elementos activos, mientras a los que aquí nos referimos son elementos pasivos, esto se necesitará una aportación de energía externa (alimentación) para conocer sus variaciones de resistencia.

En un semiconductor la resistividad tiene por valor $\rho = \frac{1}{eNv}$ donde N representa el número de portadores de cargas eléctricas, v su velocidad media y e, es la carga del electrón. La variación de ρ al aplicar cargas al semiconductor dependerá de la concentración específica de portadores y de la orientación cristalográfica respecto a las cargas aplicadas; si aplicamos cargas de tracción o compresión el cambio relativo de resistividad se expresa por:

$$\frac{\Delta \rho}{\rho} = \pi_L \epsilon$$

llamándose a π_L coeficiente de resistividad longitudinal.

Recordemos que un semiconductor es un cristal de silicio o germanio (4 electrones de valencia) al que se le añaden impurezas tipo N (arsenico, 5 electrones de valencia) o Tipo P (galio, 3 electrones de valencia) y dependiendo de la proporción de los agentes contaminantes, podrán obtenerse infinidad de elementos de muy variadas características.

El factor de sensibilidad en los extensímetros de film metálico, hemos visto que tiene de valor 2, pero si empleamos bandas cuyo elemento sensible sea un semiconductor, se pueden obtener valores de K entre 50 y 200 y dado que dimensionalmente pueden fabricarse iguales se establecen las ventajas de:

- 1º Obtener niveles de señal elevadas que pueden evitar una posterior amplificación.
- 2º Mejoran la relación señal-ruido; sin embargo su precio es mucho más elevado y su sensibilidad a la temperatura mucho más acusada que en las bandas convencionales, lo que hace que su uso quede limitado a la medida de muy pequeños valores de deformaciones y a la fabricación de captadores.

El factor de sensibilidad es definido por:

$$K_{sc} = \frac{\Delta R}{R \epsilon} = 1 + 2\mu + \pi_L \epsilon$$

siendo E = Módulo de elasticidad; μ = Coeficiente de Poisson y π_L = coeficiente de resistividad longitudinal del semiconductor.

El término $\pi_L E$ es el equivalente al que por la constante de Bridgman se introduce en las bandas metálicas, con la salvedad de que es bastante más elevado.

La influencia de la temperatura en una banda semiconductor está íntimamente ligada al número de átomos de impurezas que lleve, así para 10^{20} átomos/cm³, el factor K_{sc} es constante prácticamente a las variaciones de temperatura.

$$K_{sc} = \frac{\Delta R}{R E} = \text{Constante}$$

Si la proporción de impurezas es del orden de 10^7 átomos/cm³ el factor de banda se verá afectado en la forma:

$$K_{sc} = \frac{T_0}{T} K_{sc}(0) + C \left(\frac{T_0}{T} \right)^2 E$$

donde T = Temperatura absoluta; $K_{sc}(0)$ = Factor de sensibilidad a la temperatura T_0 ; C = Constante y E = deformación.

Los diferentes niveles de contaminación de los cristales de silicio se denominan por las letras, K, L, C, D, E, F, G y H y determinan las características piezoresistivas del semiconductor. La resistividad según tipos, oscila entre 0,001 ohm/cm y 1ohm/cm, la fig.33, resume la respuesta de las distintas clases.

Para compensar los efectos de variación de temperatura, se emplea un circuito con banda compensadora (ver tema 3) o bien el fabricante adapta el semiconductor para que dentro de ciertos límites de utilización y para determinados materiales, variaciones de temperatura no produzcan deformaciones aparentes.

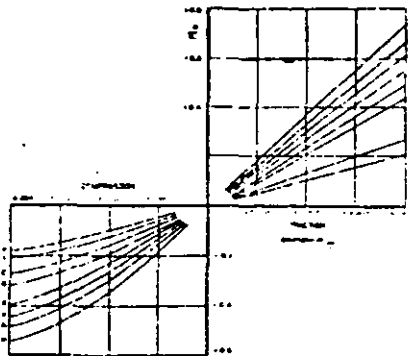


fig 33

En general las técnicas de pegado, protección, etc, serán idénticas a las de los extensímetros metálicos. Añadiremos por último que los monocristales de silicio son perfectamente elásticos, lo que hace que el fenómeno de histeresis y fluencia quede prácticamente reducido al que introdu

2.6.5. Bandas para muy altas presiones y temperaturas

Las necesidades surgidas en la investigación de programas aeroespaciales de armamento, líneas submarinas, grandes obras de ingeniería civil, etc, donde es necesario medir deformaciones en condiciones ambientales francamente adversas, ha motivado el desarrollo de bandas especiales que pueden trabajar bajo elevadísimas presiones y temperaturas, con excelente exactitud.

A título anecdótico señalaremos, que gracias a estas bandas especiales, se han podido medir deformaciones en el cono del fuselaje del avión cohete americano X-15. La tecnología que se expone -- corresponde a la desarrollada por la firma Microdot Inc.

El principio en que se basan es el clásico por el cual la resistencia de un conductor eléctrico varía si se somete a tensiones mecánicas, sin embargo, respecto a las bandas convencionales, se diferencian en que carecen de soporte y su parte activa la constituye un conductor en forma de U introducido en una cápsula metálica de la que está aislado por polvo o presión de óxido de manganeso (fig. 34). Se efectúa su fijación al punto de medición soldando por puntos la base

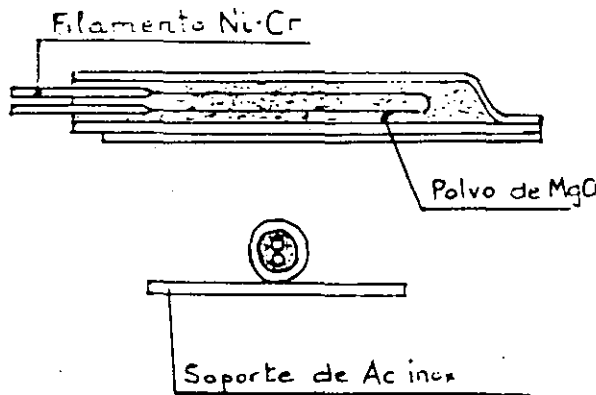


fig 34

Se metálica del sensor. En la construcción del filamento se utilizan aleaciones de Niquel-Cromo para medidas hasta temperaturas de 350°C y Platino-Tungsteno hasta 650°C. Los hilos terminales para unión de los cables a los instrumentos de lectura los constituyen los extremos del propio filamento y así se consigue una resistencia mecánica elevada; esta forma de terminales se realiza actuando por erosión química sobre el hilo constitutivo del sensor de un diámetro igual al del terminal hasta que la parte activa quede al diámetro inferior adecuado.

Las aleaciones Cr-Ni del filamento se someten a tratamientos térmicos, para que la variación de resistencia debida al coeficien

a-0,2-Hz. Un cierto flutter existe siempre debido a imperfecciones en el sistema de transporte δ en el recubrimiento de la cinta. Esto produce perturbaciones en la base de tiempo e introduce ruido en el modo FM.

Se expresa en términos de %, pico a pico. Cuando se comparan especificaciones de flutter en diferentes equipos debe hacerse en el mismo ancho de banda y velocidad de cinta; normalmente a mayor velocidad, el flutter es menor.

El flutter puede reducirse significativamente acoplando un servosistema con control de alta frecuencia a un transporte de baja inercia.

Error de base de tiempos

Cuando se utilizan sistemas de banda ancha, el error de tiempo absoluto es normalmente más significativo que el error de tiempo porcentual. En tales casos, se especifica el TBE, que es la variación del flutter con el tiempo.

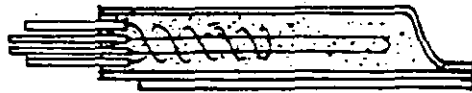
En la comparación de dos registradores de TBE inferiores asegura una reducción proporcional del flutter. Un flutter a baja frecuencia produce proporcionalmente un mayor TBE.

Dynamic Skew

Se define como el error de desplazamiento de tiempo intercanales (ITDE) y es un desplazamiento variable de tiempo entre las pistas de una misma cabeza causado por tensiones no uniformes de cinta δ irregularidades en su dimensionado. Se expresa en /seg. de desplazamiento. Para que sean significativos, deben mencionarse la velocidad de cinta y el número de canales sobre los que se ha medido. Una especificación típica es $\pm 0,25$ /seg. entre pistas adyacentes de la misma cabeza a 120 ips.

te térmico de resistividad, sea de la misma magnitud y signo contrario que la originada por dilatación térmica, con lo que se consigue una - autocompensación en un rango de utilización que especifica el fabricante.

Si la aleación es de Pl-W, un tratamiento térmico de la misma, no ofrecerá una garantía de conseguir una buena compensación - del efecto de temperatura, por estar diseñados para trabajar a eleva- das temperaturas, por tal motivo, se utilizan bandas con coeficiente de sensibilidad a las deformaciones nulo y que se montan en la rama adyacente a la que se monta la banda activa en un circuito de puente Wheatstone (fig. 35); se observa que al construir la banda compensa- dora arrollada en espiral, la sensibilidad a la deformación mecánica es nula, y además se puede fabricar dentro de la misma cápsula de la banda activa; las ventajas que se derivan son enormes, pues se reduce



el tiempo de montaje y se consigue además que los gradientes térmicos incidan con el mismo valor en ambas bandas.

Un pequeño inconveniente de la alea- ción Pl-W se debe a las diferencias que pueden haber entre el coeficiente térmico de resistividad y efecto de dilatación del material de ensayo, por eso se monta en serie una resistencia R_{tc} , que compensan esos errores. Siempre el fabricante incluye las especificaciones de cada tipo.

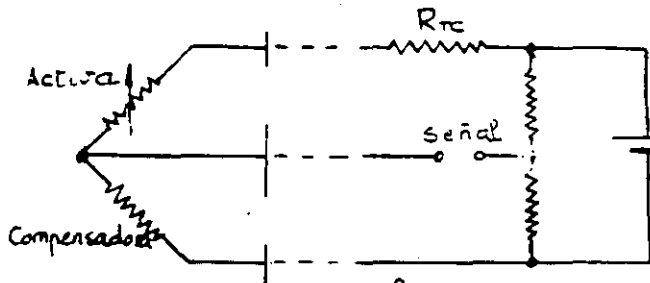


fig 35

La preparación de superficies para montaje, no necesita de la meticulosidad de las bandas clásicas.

El óxido de manganeso es introducido, con suficiente - compactidad, para que pueda transmitir las deformaciones de la extructura al filamento.

3.1. Teoría del Puente Wheatstone

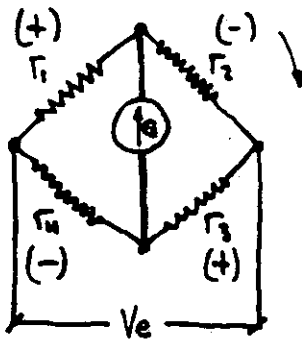


fig.1

La fig. 1 representa el esquema de un circuito en puente de Wheatstone que es el más universalmente utilizado para medidas extensométricas. Las bandas extensométricas podrán ocupar uno, dos o los cuatro brazos del puente, denominándose entonces circuitos de 1/4, 1/2, 1/1, de puente respectivamente.

Se llaman ramas activas las ocupadas por bandas que se deforman por sollicitaciones mecánicas y ramas pasivas aquellas que no intervienen en la medida.

La d.d.p. V_s en la diagonal de G tiene por valor

$$V_s = V_e \left(\frac{r_1}{r_1 + r_2} - \frac{r_4}{r_3 + r_4} \right) \quad [1]$$

para pequeñas variaciones de r_1 ; r_2 ; r_3 y r_4 podemos derivar la [1] entonces:

$$\Delta V_s = V_e \left[\frac{\Delta r_1 (r_1 + r_2) - r_1 (\Delta r_1 + \Delta r_2)}{(r_1 + r_2)^2} - \frac{\Delta r_4 (r_3 + r_4) - r_4 (\Delta r_3 + \Delta r_4)}{(r_3 + r_4)^2} \right] =$$

$$= V_e \left[\frac{r_1 r_2}{(r_1 + r_2)^2} \left(\frac{\Delta r_1}{r_1} - \frac{\Delta r_2}{r_2} \right) - \frac{r_3 r_4}{(r_3 + r_4)^2} \left(\frac{\Delta r_4}{r_4} - \frac{\Delta r_3}{r_3} \right) \right]$$

Si el circuito está equilibrado $\frac{r_1}{r_2} = \frac{r_4}{r_3}$

$$\Delta V_s = V_e \left[\frac{r_1 r_2}{(r_1 + r_2)^2} \left(\frac{\Delta r_1}{r_1} - \frac{\Delta r_2}{r_2} \right) - \frac{r_3}{(1 + \frac{r_4}{r_3})^2} \left(\frac{\Delta r_4}{r_4} - \frac{\Delta r_3}{r_3} \right) \right]$$

$$\Delta V_s = V_e \left[\frac{r_1 r_2}{(r_1 + r_2)^2} \left(\frac{\Delta r_1}{r_1} - \frac{\Delta r_2}{r_2} + \frac{\Delta r_3}{r_3} - \frac{\Delta r_4}{r_4} \right) \right] \quad [2]$$

Si $r_1 = r_2$; $r_3 = r_4$

$$\Delta V_s = \frac{V_e}{4} \left(\frac{\Delta r_1}{r_1} - \frac{\Delta r_2}{r_2} + \frac{\Delta r_3}{r_3} - \frac{\Delta r_4}{r_4} \right) \quad [3]$$

de donde se deduce que la portación a lo d. d. p. de salida V_s de dos ramas adyacentes que experimentan un Δr del mismo signo, tiene sentidos opuestos, propiedad importantísima que por algunos autores es denominado "ley de signos".

Si la expresión $\frac{\Delta r}{r_1} - \frac{\Delta r}{r_2} + \frac{\Delta r}{r_3} - \frac{\Delta r}{r_4}$, la transformamos en otra de forma $p \frac{\Delta r}{r}$ la [3] queda $V_s = \frac{V_e}{4} p \frac{\Delta R}{R}$ -- [3a] en la que el factor de puente "p" incluirá la aportación a la señal de salida de todas y cada una de las ramas, siendo

$$p = \sum a_n b_n c_n = a_1 b_1 c_1 - a_2 b_2 c_2 + a_3 b_3 c_3 - a_4 b_4 c_4 \dots \dots \dots [4a]$$

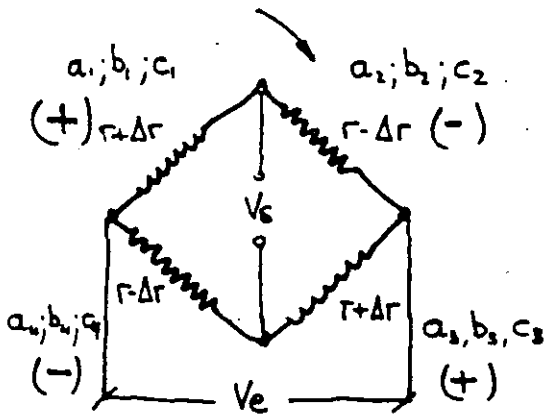


fig 2

Los subíndices indican la posición relativa de las bandas del puente, respecto a un sentido arbitrario y a cada rama le asignaremos tres coeficientes a, b, c, cuyo significado es el siguiente:

El coeficiente a es indicativo de si la rama es activa o pasiva, por lo que tiene de valor:

a = 1 para ramas activas

a = 0 para ramas pasivas

El coeficiente b indicará si una rama activa del puente sufre deformaciones por esfuerzos de tracción o de compresión, por tanto:

b = +1 si $\Delta r > 0$ (tracción)

b = -1 si $\Delta r < 0$ (compresión)

Si las ramas activas del puente no sufren deformaciones absolutas simultáneamente iguales, referiremos la deformación de cada rama al valor máximo de $\frac{\Delta R}{R}$, siendo esto expresado por el coeficiente c, que por tanto tendrá un valor comprendido

$$1 > c > 0$$

Por todo lo anterior, si consideramos el caso de la fig. 2 tendremos que:

$$a_1 = a_2 = a_3 = a_4 = 1$$

$$b_1 = b_3 = +1$$

$$b_2 = b_4 = -1$$

$$c_1 = c_2 = c_3 = c_4 = 1$$

por ser todas las ramas activas

por corresponder a esfuerzos de tracción

por corresponder a esfuerzos de compresión

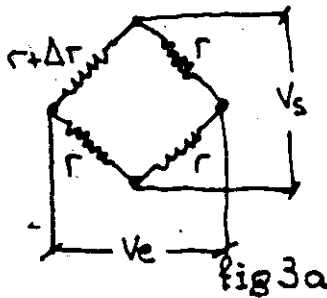
por ser $\frac{\Delta R}{R}$ un valor absoluto el mismo en las cuatro ramas del puente.

por lo que:

$$p = 1.1.1.1 - 1.(-1).1 + 1.1.1.(-1).1 = 0; \quad V_s = \frac{V_e}{4} p \frac{\Delta R}{R} = V_e \frac{\Delta r}{r} \dots \dots \dots [5]$$

Consideremos particularmente el caso del circuito de 1/4 de puente

(fig. 3a) en el se cumple:

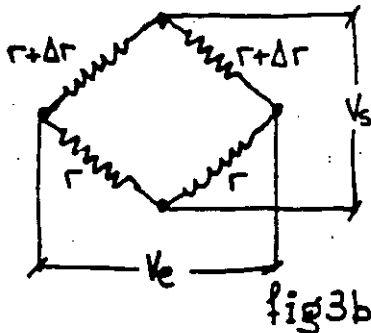


$$\Delta V_s = V_e \left(\frac{r + \Delta r}{2r + \Delta r} - \frac{1}{2} \right) = \frac{\Delta r}{4(R + 0,5\Delta R)} \dots \dots [6]$$

expresión que indica la no existencia de proporcionalidad lineal entre la señal de salida y la deformación; solamente cuando ésta sea muy pequeña, se podría despreciar el término $0,5\Delta R$ del denominador y quedar

$$V_s = \frac{V_e}{4} \frac{\Delta R}{R} \dots \dots \dots [7a]$$

En el circuito de 1/2 de puente (fig. 3b) tenemos que:



$$p = a_1 b_1 c_1 - a_2 b_2 c_2$$

$$a_1 = a_2 = 1$$

$$b_1 = 1$$

$$b_2 = -1$$

$$c_1 = c_2 = 1$$

$$p = 2$$

$$V_s = \frac{V_e}{4} \cdot 2 \frac{\Delta R}{R} = \frac{V_e}{2} \frac{\Delta r}{r} \dots \dots \dots [7b]$$

que es un circuito lineal

3.1.1. Principios básicos en medidas extensométricas

Hemos visto como basándonos en el puente de Wheatstone, podemos - transformar las variaciones que la resistencia que un extensímetro experimenta cuando se deforma, en una variación de diferencia de potencial eléctrico; pero en la materialización de las medidas debemos tener muy en cuenta ciertos principios con el fin de no cometer errores.

En primer lugar consideremos la fig. 4, en la que se representan dos

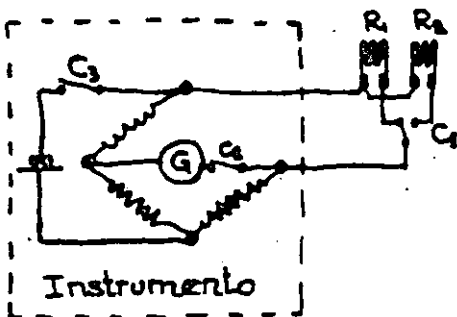


fig 4

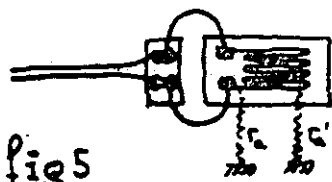
circuitos de medida en 1/4 de puente que son conmutadas al instrumento de lectura a través del conmutador C_1 , si la resistencia de los contactos no es constante, cada vez que conmutemos, a la variación propia de la resistencia de la banda, añadiremos la variación de la resistencia de contacto del conmutador, que introduce un error en la medida, lo que nos dice - que dentro del circuito del puente a, b, c, d no deben producirse más variaciones

de resistencia que las producidas por las bandas.

Si existiesen otros conmutadores C_2 y C_3 que actuasen en el circuito externo del puente, no se introducirían errores, aún cuando las resistencias de contacto fluctuasen entre una y otra actuación, pues en realidad buscamos la condición de equilibrio del puente que no se ve afectada por dichas variaciones.

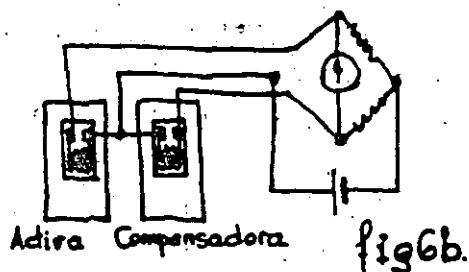
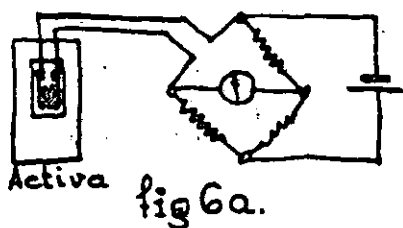
Por tanto en toda medida extensométrica se cuidará rigurosamente, no perturbar las ramas del puente por cambio de cables, contactos defectuosos, resistencias de conmutadores (serán de excelente calidad) etc. etc. sin embargo pequeñas perturbaciones en las diagonales no tendrán influencia.

Otra condición básica será la garantía de un perfecto aislamiento del circuito de medida, ya que defectos del aislamiento (fig. 5) suponen, bien la puesta en cortocircuito de cierta longitud activa de la banda, o bien el acoplamiento en paralelo de una resistencia de elevado valor, y en cualquiera de los casos la medida sería errónea.



3.1.2. Compensación del efecto de variación de temperatura

Los materiales sobre los que se montan las bandas sufren deformaciones por efecto de las variaciones de temperatura (tema 2 apartado 2.2.3) que no crean tensiones y que por lo tanto son origen de errores; si la banda es autocompensada, se vió que, dentro de ciertos límites de temperatura, estos errores son despreciables, no obstante, si el circuito de medida es un puente de Wheatstone, podremos corregir los errores por variación de temperatura en cualquier rango utilizando una banda pasiva o de compensación.



En la fig. 6a la banda montada sobre probeta sufrirá deformaciones cuando hayan variaciones de temperatura, pero si (fig. 6b) sobre un trocito de material idéntico al de la probeta montamos una banda compensadora, haciendo que en el puente de Wheatstone ocupe una rama adyacente respecto a la activa, ocurrirá que por variaciones de temperatura, las dos, activa y compensadora, se deformarán en la mism

magnitud, pero su aportación a la señal de salida es nula por la ley de los signos y por tanto el circuito de medida solo será sensible a las sollicitaciones que sufra la probeta o elemento de ensayo.

Este método presenta el inconveniente de necesitar dos bandas, pero tiene la gran ventaja de compensar los efectos de variación de temperatura en toda la gama de utilización de las bandas. Por otra parte en mediciones de varios puntos, puede emplearse una compensadora común en la mayoría de los casos; así mismo, se podrá buscar la disposición adecuada en ciertas medidas que necesitan dos o cuatro bandas activas, para que los efectos de temperatura queden compensados (Se verá con detalle en el apartado 3.1.6).

3.1.3. Configuración del cableado en diversos montajes

Sea cualquiera el instrumento de medida utilizado, las

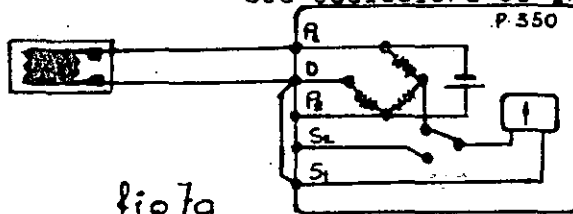


fig 7a

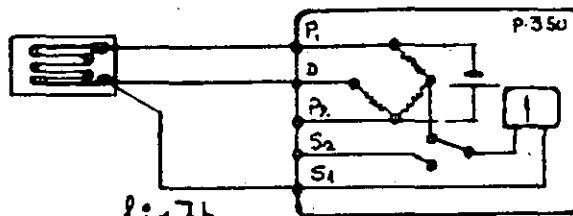


fig 7b

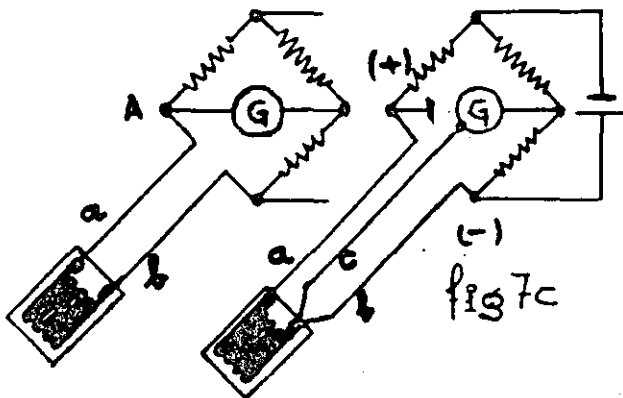


fig 7c

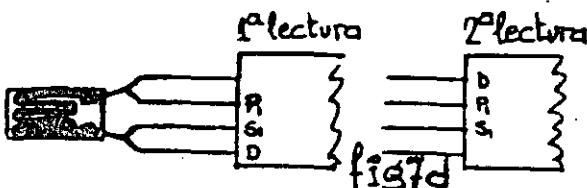


fig 7d

bandas se montan de forma que - constituyen 1, 2 o las 4 ramas de un circuito de puente de Wheatstone, incluyéndose dentro del instrumento las resistencias que - completen el puente según la configuración. Estudiaremos la disposición de los hilos de unión - del circuito de medida a los instrumentos según las diversas configuraciones.

1º Circuito de 1/4 de puente:

En el caso de medidas en las que se pueda considerar la temperatura constante, el montaje de 2 hilos de la fig. 7 se puede utilizar sin más limitaciones que los errores de linealidad, pero si la temperatura varía, aún dentro de los límites de autocompensación, (si la banda está autocompensada) nunca podremos corregir las perturbaciones que se originen en los hilos de unión, ya que éstos

no pueden autocompensarse; por ésta razón se adapta el montaje de 3 hilos (fig. 7b) en los que se consigue una simetría del circuito respecto a dos ramas adyacentes y por la ley de signos, quedan compensadas las perturbaciones en la línea.

En la fig. 7c se resume lo expuesto, viéndose que el traslado del vertice A influye en que los conductores a y b actúen en una sola rama (2 hilos). El conductor c por actuar en la diagonal del puente no influye (3.1.1.) en la medida.

En medidas de gran responsabilidad, se puede utilizar el circuito de 4 hilos (fig. 7d); se harán dos medidas, conectando alternativamente los hilos según el esquema y obteniendo la media aritmética de las dos lecturas. En realidad se han efectuado dos medidas con montaje de 3 hilos para eliminar posibles asimetrías del circuito.

2º Circuito de medio puente.-

El circuito de 1/2 puente es el que se ha indicado para la compensación de los efectos de temperatura. En general se utiliza cuando se quieren eliminar, efectos que actúen ramas adyacentes del puente (fig. 8). Por su simetría, las perturbaciones en la línea quedan compensadas.

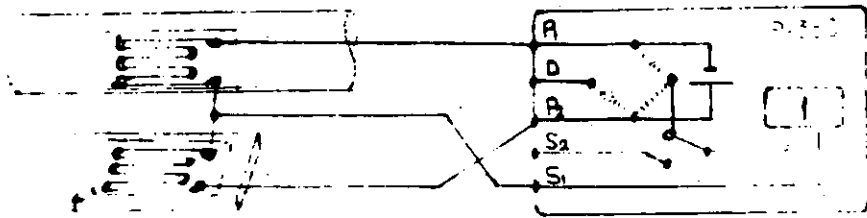


Fig 8

3º Circuito de puente completo (1/1)

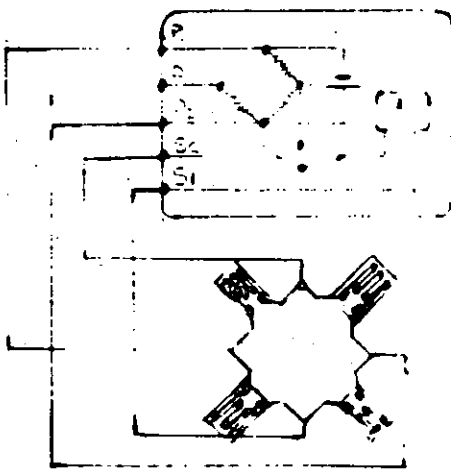
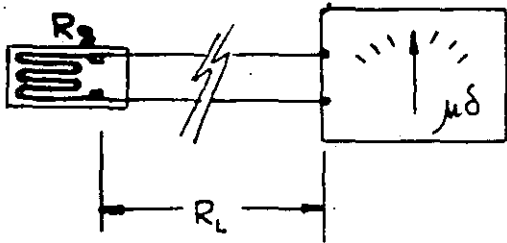


Fig 9

Si utilizamos las 4 ramas como activas, obtendremos la configuración de la fig. 9, en la cual por ser un circuito simétrico se compensan los efectos parásitos que perturban por igual a la línea.

3.1.4. Pérdida de sensibilidad en las líneas de transmisión

Los hilos de unión del circuito de medida extensométrico a los instrumentos de lecturas, añaden resistencias en serie a la banda que afectan al valor del factor de banda K y suponen una pérdida de sensibilidad,



Rg. Valor óhmico nominal de la banda.

Rl = Valor óhmico de la línea de transmisión.

ΔRg. Variación del valor óhmico de la banda.

ε Alargamiento unitario

K. Factor de banda aislada

Kv Factor de banda real

fig 10

El objeto principal de la Extensometría es el conocimiento del estado de deformaciones, pero en el estudio de los circuitos de medida hemos visto que las deformaciones del material donde se monta la banda, producen una variación de la resistencia de la misma y que al ser ésta parte activa de un puente de Wheatstone, origina una d.d.p. en una de sus diagonales proporcional a la deformación, es decir que será necesario establecer la relación entre el estímulo (deformación) y la respuesta (d.d.p. en el puente).

Recordando [3a]: $V_s = \frac{V_e}{4} \mu \frac{\Delta R}{R}$; y la [7a] $K = \frac{\Delta R/R}{\epsilon}$

deducimos que: $\frac{V_s}{\epsilon} = \frac{V_e}{4} \mu K$ [10]

Relación importante sobre todo cuando la lectura se efectúa con instrumentos que no dan lecturas directas en microdeformaciones.

Ejemplo: El elemento de la fig. 11 está sometido a un esfuerzo de tracción simple; si medimos al aplicar la carga, a la salida del puente

en efecto, por definición, el valor del factor de banda teórico K vale (fig. 10)

$$K = \frac{\frac{\Delta R_g}{R_g}}{\epsilon} = \frac{\frac{\Delta R_g}{R_g}}{\Delta l/l} \quad [7]$$

pero el factor verdadero será:

$$K_v = \frac{\frac{\Delta R_g}{R_g + R_l}}{\epsilon} \quad [7a]$$

Dado que el fabricante de bandas ignora cual será la resistencia de los hilos utilizados, habrá que introducir un factor de corrección de valor:

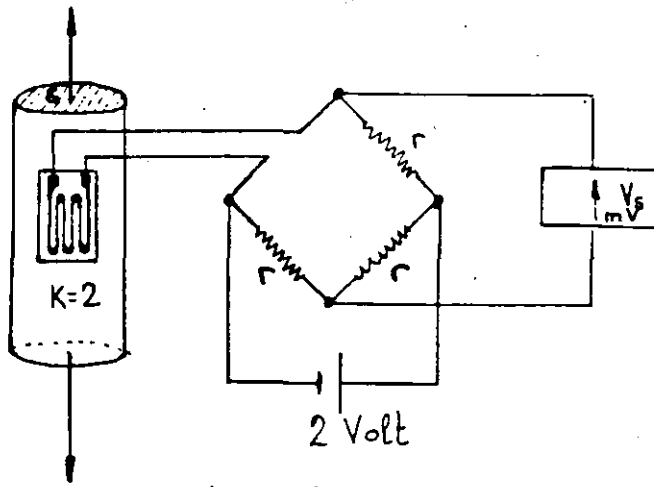
$$D = \frac{K_v}{K} = \frac{R_g}{R_g + R_l} \quad [8]$$

D se llama coeficiente de desensibilización y será prácticamente 1 con líneas muy cortas, pero si éstas son superiores a unos 10 metros, es aconsejable hacer la corrección, para lo cual si no conocemos la resistencia del conductor deberá hallarse experimentalmente.

3.1.5. Relación entre deformación y señal de salida

El objeto principal de la Extensometría

una $V_s = 1 \text{ mV}$, calcular la fuerza F .



$$E = 20,10^6 \text{ N/cm}^2$$

$$S = 0,5 \text{ cm}^2$$

fig 11

$$V_s = \frac{V_e}{4} \cdot K \cdot \epsilon = \frac{2}{4} \cdot 2 \cdot \epsilon = 1000 \mu\text{V} \quad (\mu=1)$$

$$\epsilon = \frac{V_s}{4} = 1 \mu\text{V}$$

$$\epsilon = 1000 \mu\text{S}$$

$$F = \epsilon E S = 1000 \cdot 20 \cdot 10^6 \cdot 0,5 \cdot 10^{-6} = \underline{\underline{10 \text{ KN}}}$$

3.1.6. Estudio de diversos circuitos de medida

Es muy frecuente, que en el punto objeto de medida incidan esfuerzos compuestos y sin embargo, solo nos interese conocer la influencia individual de dichos esfuerzos como veremos estudiando casos particulares.

Tracción o compresión simple

Si el elemento de ensayo está sometido simultáneamente a flexión, tracción compresión y variaciones de temperatura amplias, el circuito de la fig. 12 solo será sensible a los esfuerzos de tracción ó compresión; en efecto, la variación de resistencia de cada una de las bandas es (llamando R_0 = valor nominal de la banda; ΔR_T = incremento de R_0 por la componente tangencial; ΔR_N = idem, normal y ΔR_t efecto variación de temperatura

TRACCION O COMPRESION PURA

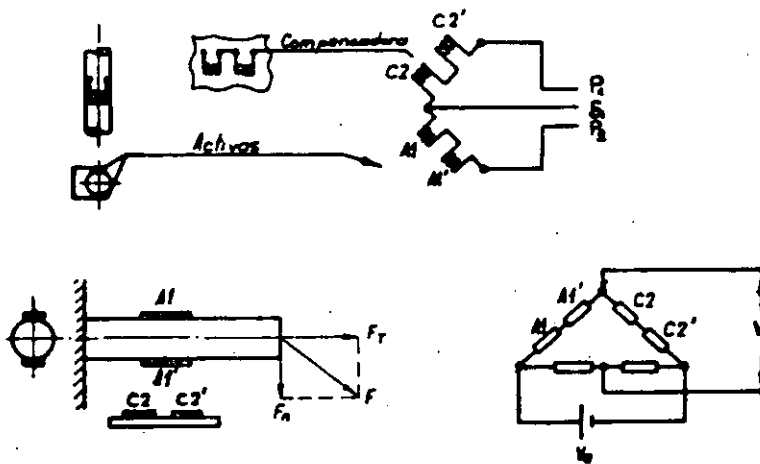


fig 12

$$R_{A1} = R_0 + \Delta R_T + \Delta R_N + \Delta R_t$$

$$R_{A1'} = R_0 + \Delta R_T - \Delta R_N + \Delta R_t$$

$$R_{C2} = R_0 + \Delta R_t$$

$$R_{C2'} = R_0 + \Delta R_t$$

si aplicamos la [3]

$$V_s = \frac{V_0}{4} \left(\frac{\Delta R_T}{2R_0} + \frac{\Delta R_N}{2R_0} + \frac{\Delta R_t}{2R_0} + \frac{\Delta R_T}{2R_0} - \frac{\Delta R_N}{2R_0} + \frac{\Delta R_t}{2R_0} - \frac{\Delta R_t}{2R_0} - \frac{\Delta R_t}{2R_0} \right) = \frac{V_0}{4} \frac{\Delta R_T}{R_0} \quad [11]$$

$$V_s = \frac{V_0}{4} \frac{\Delta R_T}{R_0} = \frac{V_0}{4} K \epsilon_T$$

$$\epsilon_T = \frac{\Delta l}{l} = \frac{4 V_s}{K V_0} \quad [12]$$

Lo anteriormente expuesto es válido siempre que por el eje de aplicación de cargas pase un plano de simetría de la pieza, y exige el montaje de dos bandas por rama del puente, siendo aquí de aplicación el utilizar valores fraccionados (ver 2.2.1.) p.e. 60 ohms, para que la impedancia del circuito sea 120 ohm, siendo esto último preceptivo si no se montan compensadoras y se utiliza montaje de 1/4 de puente.

Flexión simple

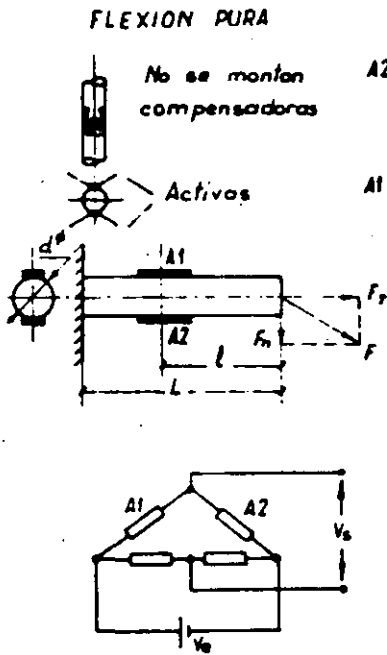


Fig 13

Para medir una flexión simple (fig. 13) eliminando otras influencias, no es necesario montar bandas compensadoras, ya que el propio circuito compensa los efectos de variación de temperatura. Se cumple que:

$$R_{A1} = R_0 + \Delta R_T + \Delta R_N + \Delta R_F$$

$$R_{A2} = R_0 - \Delta R_T - \Delta R_N + \Delta R_F \text{ aplicando [3]}$$

$$V_s = \frac{V_0}{4} \left(\frac{\Delta R_T + \Delta R_N + \Delta R_F}{R_0} + \frac{\Delta R_T + \Delta R_N + \Delta R_F}{R_0} - \frac{\Delta R_T - \Delta R_N - \Delta R_F}{R_0} - \frac{\Delta R_T - \Delta R_N - \Delta R_F}{R_0} \right) = \frac{V_0}{2} \frac{\Delta R_N}{R_0} \text{ [13]}$$

$$V_s = \frac{V_0}{2} \frac{\Delta R_N}{R_0} = \frac{V_0}{2} K \epsilon_N$$

$$\epsilon_N = \frac{2 V_s}{V_0 K} = \frac{4 F N l}{\pi E r^3} = \frac{3 l r}{L^3} f \text{ [14]}$$

$$N = 0,56 \frac{r}{L^2} \frac{E}{\rho}$$

N= frecuencia natural

f= flecha

E= Modulo elasticidad

ρ = densidad

Torsión.

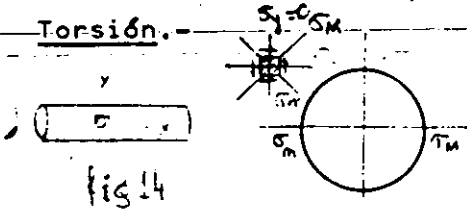


fig 14

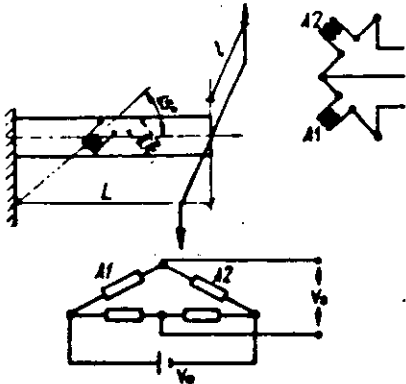


fig 15a

Podemos considerar que:

$$R_{A1} = R_0 + \Delta R_c + \Delta R'_T + \Delta R_c$$

$$R_{A2} = R_0 - \Delta R_c + \Delta R'_T + \Delta R_c$$

$$V_s = \frac{V_0}{4} \left(\frac{\Delta R_c}{R_0} + \frac{\Delta R_c}{R_0} + \frac{\Delta R'_T}{R_0} + \frac{\Delta R_c}{R_0} + \frac{\Delta R_c}{R_0} - \frac{\Delta R'_T}{R_0} - \frac{\Delta R_c}{R_0} \right)$$

$$= \frac{V_0}{2} \frac{\Delta R_c}{R_0} \quad [15]$$

siendo τ el esfuerzo cortante y $G = \frac{E}{2(1+\mu)}$

$$\frac{\Delta R_c}{R_0} = K \frac{\Delta d}{d} ; V_s = \frac{V_0}{2} K \frac{\tau}{2G} \quad [16]$$

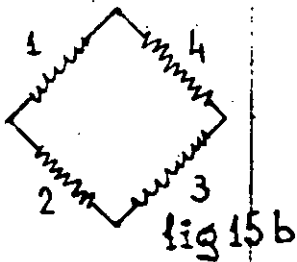
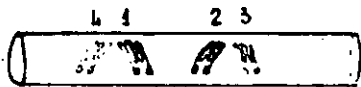


fig 15b

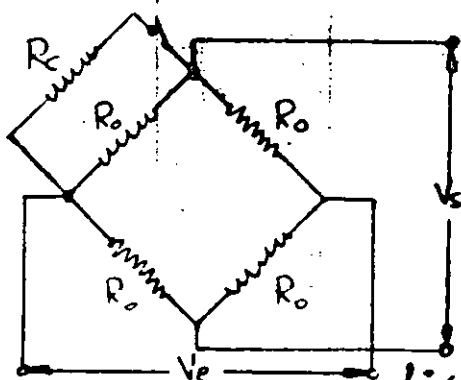


fig 16 (fig. 16).

El efecto de la resistencia de calibración R_c , es equivalente a una compresión sobre la rama que actúa. Supongamos que deseamos calcular el valor de R_c para que tengamos un efecto equivalente a $500 \mu\delta$ en un circuito de bandas de $R_0 = 120 \text{ ohm}$, $K = 2$, excitado con $V_0 = 2 \text{ V}$; tenemos que:

Recordemos (fig. 14) que un eje sometido a un par de torsión experimenta sus máximas deformaciones en una dirección que forma 45° con la dirección de sus generatrices, y que dichas deformaciones son iguales y de signo contrario; por tal motivo si situamos las bandas a 45° según la fig. 15a, tenemos que:

En el montaje de 1/2 se eliminan los efectos de tracción y compresión - pero no la flexión, se puede demostrar que en la configuración de 1/1 de puente, el circuito de medida solo es sensible a esfuerzos producidos - por torsión (fig. 15b).

3.2. Circuitos de calibración y equilibrado

La técnica de calibración de un puente de Wheatstone para extensometría, consiste en producir en una rama del puente, por shuntado de una resistencia, un desequilibrio igual al que se produciría al someter o determinadas sollicitaciones el elemento de ensayo

$$\frac{\Delta R}{R} = \frac{R_c R_0}{R_c + R_0} - R_0 = - \frac{R_0^2}{R_c + R_0} \quad [17]$$

$$E = \frac{R_0}{R_c + R_0} \frac{l}{K} \quad [18]$$

$$R_c = - \frac{R_0 (1 + EK)}{EK} = - 120.000 \text{ ohm.} \quad [19]$$

El signo (-) indica que se trata de compresión. En la fig. 16 se supone que un solo brazo del puente es activo, en general y teniendo en cuenta el nº de brazos activos del circuito, encontramos la expresión general

$$R_c = - \frac{R_0}{N \epsilon K} \quad [20]$$

en la que:

R_c = Resistencia de calibración

R_0 = Valor nominal de la resistencia de una rama del puente.

K = Factor longitudinal de sensibilidad de la banda.

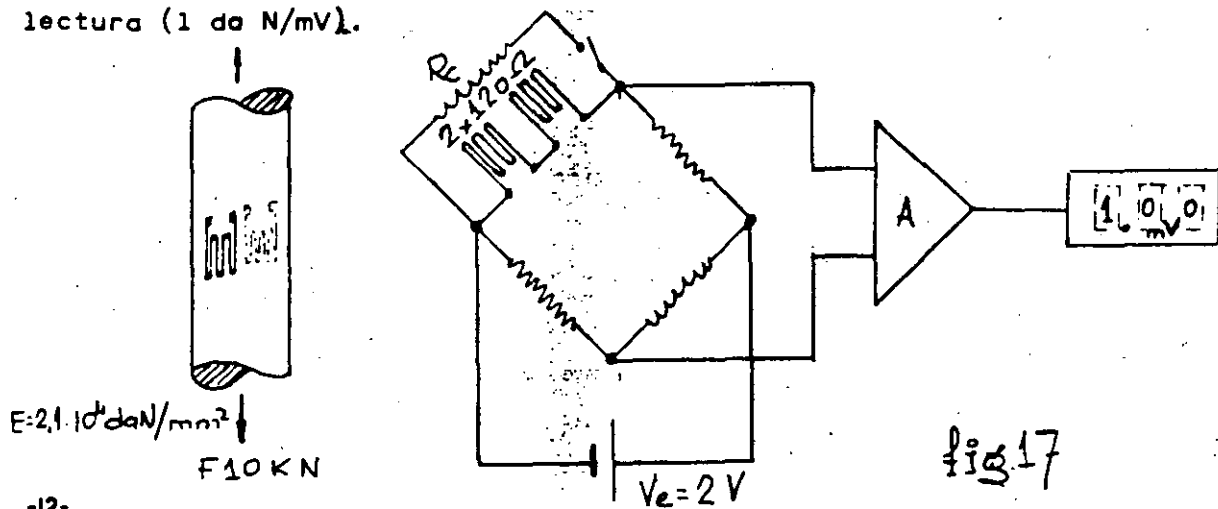
ϵ = Alargamiento unitario equivalente que produce R_c .

N = Nº de brazos activos del circuito del puente.

(El termino ϵK en el numerador se desprecia por ser muy pequeño).

Si el instrumento de lectura da indicaciones directas en microdeformaciones, lo explicado es suficiente, pero ocurre, sobre todo en medidas dinámicas, que tendremos que establecer una relación entre deformaciones y d.d.p. a la salida de los amplificadores que elevan de nivel las débiles señales del puente de medida; siendo regla práctica, buscar escalas enteras. Ejemplo.

En la fig. 17 se representa el circuito para medida de tracción simple en una barra circular de 500mm² de sección, se desea que una carga 10 KN dé una indicación de 100 mV en el instrumento de lectura (1 da N/mV).



$$E = \frac{F}{E} = \frac{\frac{F}{S}}{E} = \frac{10 \cdot 10^2 \cdot 10^6}{500 \cdot 2 \cdot 1 \cdot 10^4} = 476 \mu S$$

$$V_s = \frac{1}{2} \varepsilon K = \frac{1}{2} 476 = 238 \mu V$$

$$G = \frac{100 \text{ (mV)}}{0.238} = 420 \text{ (Ganancia amplificador)}$$

$$R_c = \frac{2 \cdot 120}{476 \cdot 10^6 \cdot 2} = \underline{\underline{252 \text{ } 100 \text{ ohm}}}$$

Luego si colocando una $R_c = 252100 \text{ ohm}$, ajustamos la ganancia del amplificador para leer -100 mV , tendremos el circuito preparado para leer las fuerzas F con una escala de 1 da N/mV .

Observese que se ha empleado circuito de $1/4$ de puente con 2 bandas de 120 ohm en serie para eliminar efectos de flexión y torsión.

La calibración de un circuito extensométrico por shunt de una resistencia es casi universalmente aceptada, no obstante presenta el inconveniente de insertar la señal de referencia en registros dinámicos, ya que dicha señal se superpone a la componente dinámica y la suma puede salirse del rango de medida por saturación de instrumento para paliar esto, se puede utilizar una resistencia en serie tal y como

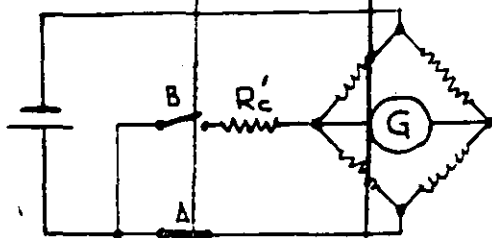


fig 18

se indica en la fig. 18, así abriendo el interruptor A dejamos sin excitación el circuito y nos marcará el cero (correspondiente a carga nula) y si a continuación cerramos B, obtendremos una señal de referencia independiente del estado de carga del circuito.

Se demuestra que para producir la misma señal la relación entre los valores de las resistencias shunt y serie son $R_c = 2R_c$.

Hasta aquí hemos supuesto siempre que el puente de Wheatstone estaba completamente equilibrado para cargas nulas en el circuito de medida, pero debido a las pequeñas variaciones de resistencia que se originan al montaje, (por soldaduras, variaciones de la propia resistencia de la banda al ser pegada, etc.) la señal de salida V_s tendrá un

pequeño valor que conviene anular para hacer lecturas directas.

El desequilibrio inicial del puente en medidas estáticas, con instrumentos que dan lectura directa en microdeformaciones, obliga a hacer una lectura inicial estando sin carga la pieza de ensayo que será restada de las lecturas posteriores bajo carga. En el caso de medidas dinámicas, partir con un desequilibrio, equivale a introducir una componente de continua constante.

Varios con los procedimientos que pueden utilizarse para corregir un desequilibrio inicial pero el más universal, consiste en colocar un potenciómetro de alto valor óhmico en la diagonal de alimentación del puente con el contacto móvil unido a través de una resistencia R_A al vértice intermedio tal y como se indica en la fig. 19.

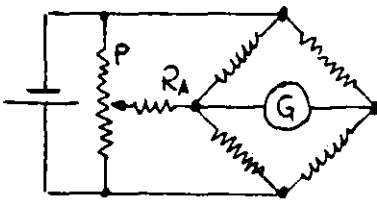


fig 19

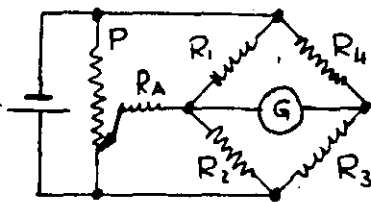


fig 20

La resistencia R_A limita el tanto por ciento de desequilibrio capaz de corregir y el potenciómetro P da el poder de resolución de dicho ajuste. En efecto, supongamos que en el circuito de la fig. 20 queremos calcular R_A para poder corregir desequilibrios de un 2% o lo que es lo mismo suponer que:

$$R_2 = R_3 = R_4 = 120 \text{ ohm}$$

$$R_1 = 117,6 \text{ ohm}$$

La resistencia total de la rama 2 tiene que ser igual a la de la rama 1 por tanto:

$$\frac{1}{R_1} = \frac{1}{R_2} + \frac{1}{R_A} \rightarrow \frac{1}{117,6} = \frac{1}{120} + \frac{1}{R_A}$$

$$R_A = \frac{R_1 \cdot R_2}{R_2 - R_1} = \underline{5880 \text{ ohm}}$$

Para el cálculo hemos supuesto que el cursor del potenciómetro está en un extremo, por lo que si P es de valor elevado, al estar en paralelo con R_1 , no le influye; para desequilibrios inferiores al 2% desplazando el cursor se consigue la posición en la que por G no circula corriente.

Otros procedimientos pueden consistir en añadir resistencias en serie en las ramas hasta conseguir el equilibrio, pero si bien este método es aconsejable para la construcción de captadores, no es práctico en medidas extensométricas salvo casos muy especiales.

En instrumentación para medidas dinámicas, los desequilibrios de los circuitos de medida se compensan introduciendo una contratensión en la entrada de amplificación, con lo que se consigue no desensibilizar en absoluto el circuito e incluso producir "falsos ceros" cuando las condiciones de la medida lo aconsejen (fig. 21).

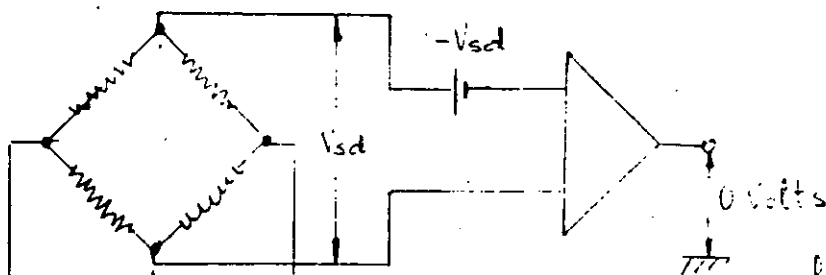


fig 21

Sea cual sea el procedimiento con el que corriamos el desequilibrio, los componentes utilizados serán de precisión y estabilidad idéntica a la exigida al circuito de medida. El potenciómetro P será de 10 vueltas y provisto de duodial, que permitirá reestablecer las condiciones iniciales de equilibrado de manera fácil, aún cuando las condiciones originales hayan variado.

3.3. Captadores extensométricos

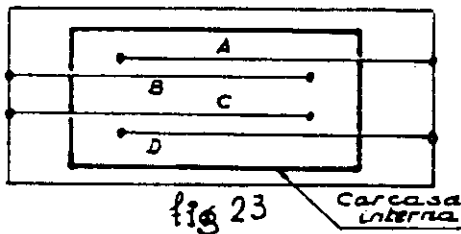
El conocimiento de las técnicas extensométricas abre la posibilidad de construir captadores que efectuen la transducción de cierta energía mecánica en eléctrica, pero no obstante hay que advertir que los problemas que en éste cometido se presentan, son tan complejos, que solo verdaderos especialistas serán capaces de conseguir resultados aceptables, por lo que todo lo expuesto a continuación, debe considerarse solo a título informativo, para mejor comprender el funcionamiento de estos instrumentos indispensables en un laboratorio de ensayos dinámicos.

Un captador estará formado por un dispositivo mecánico que sea sensible de forma mayoritaria a determinados parámetros físicos (fuerza, presión, aceleración, etc) y prácticamente insensible al resto de fenómenos que incidan simultáneamente sobre él. Si sobre el elemento sensible del captador montamos bandas extensométricas, podremos medir las deformaciones de éstas relacionándolas con el parámetro que las originó, como es lógico, podremos conseguir la independencia del captador a solicitaciones no deseadas valiéndonos del adecuado diseño mecánico y de la disposición de las bandas.

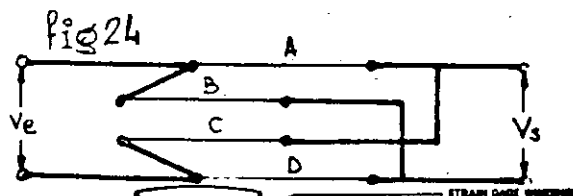
La elección de los materiales que constituyen la parte mecánica del captador es de vital importancia y se tendrá muy en cuenta que el módulo de elasticidad E , sea totalmente constante en el margen de utilización y jamás sobrepasar la zona lineal de trabajo, exenta en lo posible, de fenómenos de histeresis y fluencia, siendo normativamente sobrepasar en las cargas $1/10$ del límite elástico. El coeficiente de dilatación tiene menos importancia una vez que las dilataciones serán homogéneas y se utilizarán bandas autocompensadas.

A título de ejemplo en la fig. 22 se ofrecen esquemáticamente algunos montajes para medidas de los parámetros que se indican. Nunca habrá límite en diseñar cualquier disposición mecánica que añada mejoras para determinados fines.

Hasta aquí nos referimos a bandas extensométricas pegadas (Bonded Strain-gages) pero en captadores se utiliza generalmente otro tipo de extensímetro en el cual, el elemento sensible es un hilo sin soporte y apoyado sobre unos zafiros (unbonded strain-gages), que si bien cumple todos los principios hasta ahora expuestos, es muy distinto. En efecto, consideremos la fig. 23 en la que las bandas extensométricas tal y como las hemos concebido hasta ahora son sustituidas -



por hilos conductores A, B, C y D sometidos a una tensión previa; si la carcasa interna se mueve por cualquier sollicitación mecánica (ej. aceleración) a derecha o izquierda respecto a la carcasa externa, los hilos A y D y los B y C sufren deformaciones de signos contrarios respectivamente. La conexión eléctrica del circuito para constituir el puente de Wheatstone se indica en la fig. 24.



A título de ejemplo la fig. 25 indica la disposición adoptada por B & H en sus captadores de aceleración.

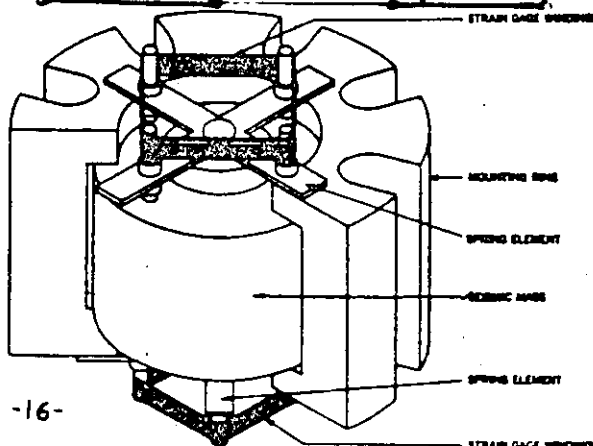
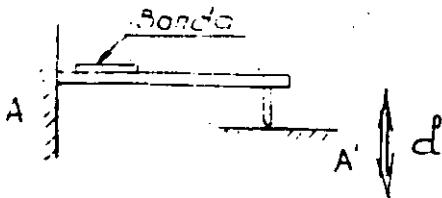


Fig 25

Desplazamiento



Los desplazamientos relativos entre A (fijo) y A' (móvil) producen una deformación en la lámina por flexión, proporcional al desplazamiento d .

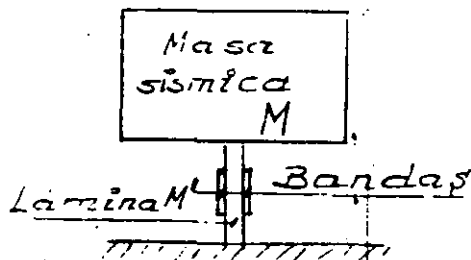
Fuerzas. Pesos



Una barra cilíndrica en tracción y/o compresión (evitar pandeo).

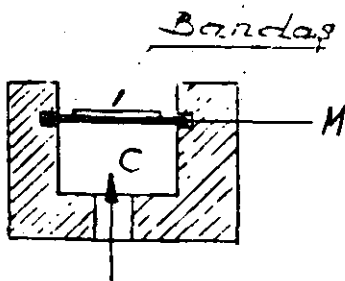
Anillo dinamométrico en tracción.

Aceleración-vibración

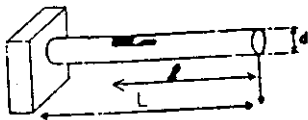


La masa sísmica M es sensible a las fuerzas de aceleración y habrá proporcionalidad con la deformación que sufra a flexión la lámina M' . Si la frecuencia propia de la lámina es superior a la del movimiento la respuesta será a la aceleración y si inferior a la velocidad del desplazamiento de M .

Presión



La membrana M se deforma si en la cámara C hay variaciones de presión.



$$\begin{aligned}
 \epsilon_1 &= \frac{4 F l}{\pi E r^3} = \frac{31 f}{L^3} \\
 \epsilon_2 &= \frac{-4 \mu F l}{\pi E r^3} = \frac{-3 \mu f}{L^3} \\
 f &= \frac{4 F L^3}{3 \pi E r^3} \\
 N &= 0,56 \frac{r}{L^3} \frac{E}{p}
 \end{aligned}$$

Lámina cilíndrica en flexión

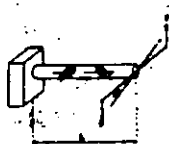
- F fuerza aplicada
- d = 2.r. diámetro
- l brazo fuerza-banda
- L brazo fuerza-encastamiento
- N primera frecuencia propia
- f flecha (desplazamiento de F)
- ϵ_1 deformación longitudinal
- ϵ_2 deformación transversal



$$\begin{aligned}
 \epsilon_2 &= \frac{3 F R}{E e b^2} \left(1 - \frac{2}{\pi}\right) \\
 \epsilon_1 &= \frac{-3 F R}{E e b^2} \left(1 - \frac{2}{\pi}\right) \\
 f &= 1,79 \frac{F R^3}{E e b^2}
 \end{aligned}$$

Anillo dinamométrico

- F fuerza aplicada
- e espesor
- b anchura
- R radio medio
- f flecha total
- ϵ_2 deformación longitudinal exterior
- ϵ_1 deformación longitudinal interior



$$\begin{aligned}
 \epsilon_1 &= -\epsilon_2 = \frac{M}{\pi G R^3} = \frac{R}{2L} \alpha \\
 \alpha &= \frac{2 M L}{\pi G R^4} \\
 \text{avec } G &= \frac{E}{2(1 + \mu)}
 \end{aligned}$$

Arbol en torsión

- M=Fl momento aplicado
- L longitud total del arbol
- α ángulo de giro en radiones
- La distancia de las bandas no afecta
- ϵ_1 deformación de una de las bandas
- ϵ_2 deformación de la otra banda

FORMULAS PARA EL CALCULO DE TRANSDUCTORES



$$\epsilon_1 = \frac{F}{E a e}$$

$$\epsilon_2 = -\frac{\mu F}{E a e}$$

Lámina en Tracción

- F fuerza aplicada
- a anchura
- e espesor
- ϵ_1 deformación longitudinal
- ϵ_2 deformación transversal



$$\epsilon_1 = \frac{4 F}{\pi E (D^2 - d^2)}$$

$$\epsilon_2 = -\frac{4 \mu F}{\pi E (D^2 - d^2)}$$

Toro circular en Tracción y compresión

- F fuerza repartida
- D diámetro exterior
- d diámetro interior
- ϵ_1 deformación longitudinal
- ϵ_2 deformación transversal

$$\epsilon_1 = \frac{6 F l}{E a e^2} = \frac{3 \rho l}{2 L^2} f$$

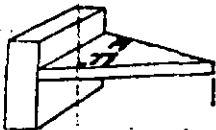
$$\epsilon_2 = -\frac{6 \mu F l}{E a e^2} = -\frac{3 \mu \rho l}{2 L^2} f$$

$$f = \frac{F L^2}{3 E I} = \frac{4 F L^2}{E a e^3}$$

$$N = 0.58 \frac{1}{L^2} \frac{E I}{\rho S} = 0.16 \frac{\rho}{L^2} \frac{E}{\rho}$$

Lámina en flexión

- F fuerza aplicada
- a anchura
- e espesor
- l brazo fuerza-banda
- L brazo fuerza-empotramiento
- N primera frecuencia propia
- f flecha
- ϵ_1 deformación longitudinal
- ϵ_2 deformación transversal



$$\epsilon_1 = \frac{6 F L}{E b e^2} = \frac{\rho}{L^2} f$$

$$\epsilon_2 = -\frac{6 \mu F L}{E b e^2} = -\frac{\mu \rho}{L^2} f$$

$$f = \frac{6 F L^2}{E b e^2}$$

Lámina triangular en isoflexión

- F fuerza aplicada (en el vértice)
- b anchura base
- L brazo fuerza-encastamiento (altura)
- f flecha
- La distancia de las bandas no afecta
- ϵ_1 deformación longitudinal
- ϵ_2 deformación transversal

Para la fabricación de captadores de presión se suele emplear como elemento mecánico sensible una membrana encastrada y conviene recordar como se reparten las deformaciones consideradas como placa (fig. 25) en la que vemos que la deformación tangencial es nula en los bordes y máxima en el centro y que la deformación radial es máxima en los bordes y luego cambia de sentido para adquirir un valor en el centro igual al máximo tangencial.

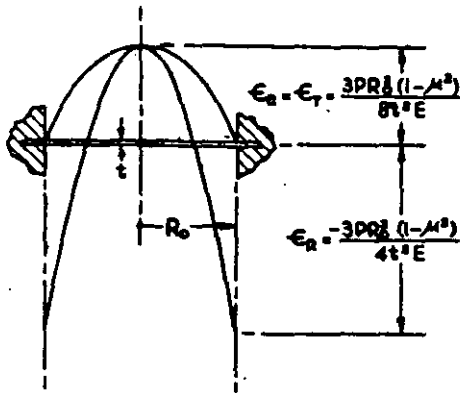


fig 25

Wheatstone, y se fabrican en varios tamaños de acuerdo con diferentes diámetros de membrana (fig. 26). De las formulas de la fig. 25 se deduce que el espesor de la membrana es decisivo en la sensibilidad, pero

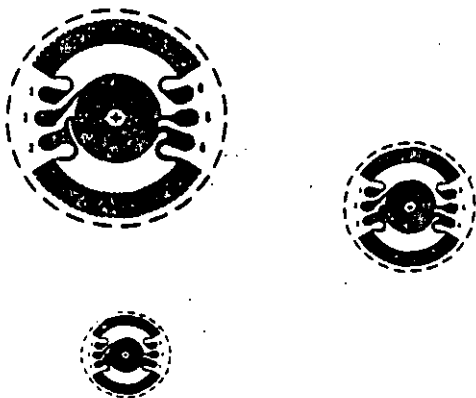


fig 26

Se comprende, por tanto, que una banda extensométrica normal no sería adecuada para conseguir una señal de elevado nivel. Vishay Micromesures ha desarrollado una amplia gama de geometrías en las cuales se combina una disposición radial de la parte activa del extensómetro y otra tangencial, de tal manera, que abarquen aquellas zonas de la membrana de mayor deformación radial y tangencial respectivamente, constituyendo así una roseta de cuatro bandas que configuran un puente completo de

Wheatstone, y se fabrican en varios tamaños de acuerdo con diferentes diámetros de membrana (fig. 26). De las formulas de la fig. 25 se deduce que el espesor de la membrana es decisivo en la sensibilidad, pero habrá que dimensionarlo de acuerdo con el rango de presiones que se deseen medir.

3.3.3. Corrección de la deriva térmica del cero

Si las variaciones de temperatura inciden de forma sensiblemente igual sobre las cuatro ramas del puente, la compensación de los efectos térmicos se corrige bien en circuitos de medida extensométricos, pero cuando se trata de captadores las

especificaciones deben ser más elevadas, ya que por la propia geometría del captador, las variaciones de temperatura no serán homogéneas en t

das las ramas. Con bandas autocompensadas y para usos industriales, se consiguen desviaciones del orden del 1% en empleo a temperaturas próximas a la normal ambiental (24°) pero para mejores prestaciones se tienen que tener en cuenta y corregir las desviaciones en la sensibilidad del puente y la deriva del cero (equilibrio) que la variación de temperatura introduce.

Recordemos que la señal de salida es función de la tensión de excitación y de la variación relativa de resistencia ($V_s = V_e \frac{\Delta R}{R}$) si por variación de temperatura y no por cargas, se modifica la relación $\frac{\Delta R}{R}$ tendremos una señal V_s que al no ser producida por cargas será fuente de error, para evitarlo (fig. 27) se colocan en serie con la alimentación resistencias con un coeficiente térmico que, para las variaciones de la relación $\frac{\Delta R}{R}$ por temperatura, (dentro de un rango de utilización) mantengan constante la relación $\frac{V_s}{V_e} \left(\frac{\Delta R}{R} \right)$ al producirse en R_s una c.d.t. de efecto antagónico al que se produce en el puente.

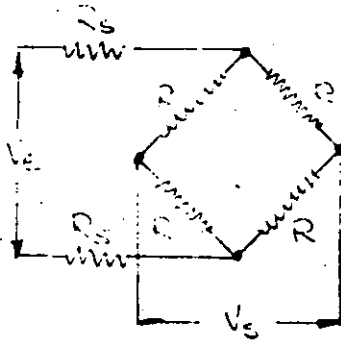


fig 27

más o menos sobre la rama AB o la AD, existiendo una posición en la

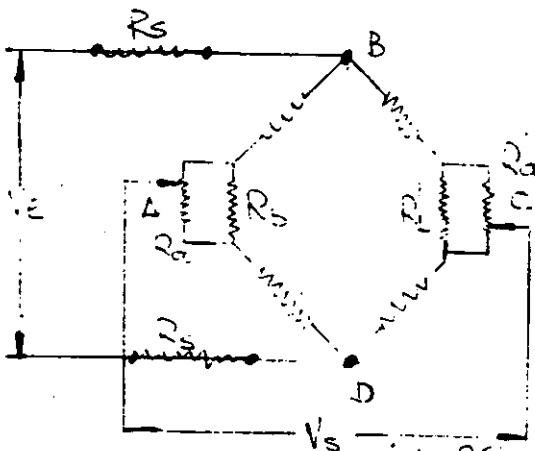


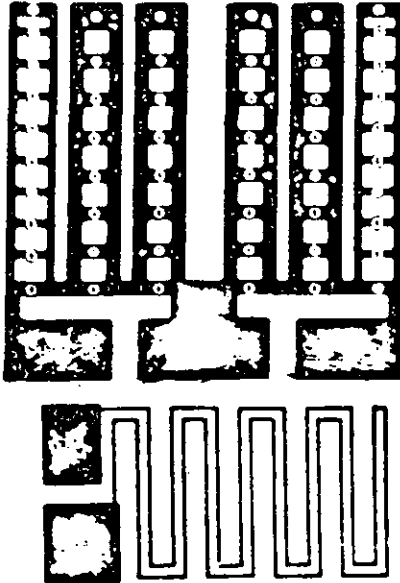
fig 28

Por otra parte, si partimos de un circuito equilibrado, los efectos térmicos pueden producir una desviación del punto cero de equilibrio que se corrige colocando (fig. 28) en un vertice la resistencia R_b sensible a la temperatura y por estar asociada a la R_a , que actúa como divisor de tensión, según la posición del hipotético cursor, se influirá más o menos sobre la rama AB o la AD, existiendo una posición en la que los efectos de variación de temperatura son compensados, pero en el que el equilibrio eléctrico del puente se ha perdido. Para restablecer el equilibrio eléctrico se repite de forma simétrica el circuito de compensación en el vertice C. La relación práctica de lo expuesto puede llevarse a cabo de forma experimental y se comprende que es un proceso laborioso, delicado y caro.

Existen resistencias de constitución análoga a las bandas que facilitan los ajustes mencionados (fig. 29) pues, bien desplazando una gota de soldadura (a), o cortando los circulitos de referencia (b) se consigue un determinado valor en ohmios.

de soldadura (a), o cortando los circuitos de referencia (b) se consigue un determinado valor en ohmios.

AR 222



(Tamaño aumentado)

fig 29

3.4 TERMINOLOGIA EN CAPTADORES.

Carga (Load).- Valor físico aplicado a un captador para obtener una señal eléctrica.

Carga nominal (Full Scale Load).- Valor máximo de carga que puede soportar indefinidamente un captador sin perder sus características.

Escala total de salida (Output Full Scale or Span).- Diferencia algebraica entre señales de salida obtenidas con carga nula y nominal.

Señal de Salida (Output).- Variaciones

de la magnitud eléctrica dadas por un captador cuando varía la carga. Pueden darse bajo la forma de una d.d.p., intensidad o resistencia.

Excitación (Excitation).- F.em. de la fuente destinada a alimentar un captador.

Resistencia de entrada (Input Resistance).- Resistencia eléctrica entre los hilos a los cuales es aplicada la excitación, estando los hilos de salida en circuito abierto.

Resistencia de salida (Output Resistance).- Resistencia eléctrica entre los hilos de conexión a los instrumentos, estando en circuito abierto los hilos de entrada.

Curvas de calibración (Calibration curves).- Curvas representativas de la señal de salida en función de la carga aplicada, obtenidas por la aplicación de cargas conocidas tomadas como patrones.

Resistencia de aislamiento (Insulation Resistance).- Resistencia eléctrica entre el circuito y masa del captador. Debe referenciarse a las condiciones del medio ambiente.

Sensibilidad (Sensitivity).- Relación entre una variación de la señal,

Límite de sensibilidad (Resolution).- Menor variación de carga capaz de crear una variación perceptible de la señal de salida.

Exactitud (Tolerance).- El mínimo valor del cual se está seguro es superior a la diferencia entre la carga real aplicada y el valor obtenido de la curva de calibración. Se expresa en porcentajes de la carga nominal.

Desequilibrio inicial (Zero Balance).- En el caso de una salida de tensión relativa () expresa la señal de salida para una carga nula.

Deriva (Drift).- Variaciones con el tiempo de la señal de salida a carga constante. Se expresa en porcentaje de la escala de salida para un tiempo definido.

Deriva de equilibrio (Zero Drift).- En ausencia de carga y sin causa térmica, variaciones de desequilibrio inicial para un tiempo indefinido.

No retorno a cero (NRZ).- Diferencia entre dos señales de salida a carga nula, antes de la aplicación de la carga y después de la supresión de la misma y su estabilización. (No confundir con histeresis).

Fidelidad (Repeatability).- Máxima divergencia entre las dos señales de salida obtenidas por aplicaciones sucesivas de la misma carga en las mismas condiciones. Se expresa en porcentaje de la escala total de salida.

Linearidad (Linearity).- Divergencia máxima obtenida entre la curva de calibración y una recta trazada entre los puntos representativos de la carga nula y carga nominal. Se expresa en porcentaje de la escala total de salida y no es dada más que para una carga creciente.

Histeresis (Hysteresis).- Divergencia máxima obtenida entre las señales indicadas para una misma carga, pero por dos modos de aplicación diferentes: carga creciente a partir de cero y carga decreciente a partir de la carga nominal. Es dada, salvo indicación en contra, para una carga igual a la mitad de la nominal y se expresa en porcentaje de la escala total de salida. Estas medidas deben ejecutarse lo más rápidas posible para diferenciarlas del fenómeno de fluctuación.

Temperaturas extremas de compensación.- Temperaturas inferior y superior, que no deben sobrepasarse, para que, empleando la compensación, las características del captador se mantengan dentro de los límites definidos para los mismos.

Temperaturas extremas de empleo.- Temperaturas inferior y superior - que, en caso de sobrepasarse, determinan la pérdida definitiva de las características del captador.

Impedancia.- Sensibilidad a fenómenos para los cuales el captador no ha sido realizado, p.e.: Sensibilidad de un acelerómetro para aceleraciones perpendiculares a su eje primario (Cross Axis Sensitivity).

Desplazamiento (Deflection).- Distancia entre las dos posiciones de un punto después de cargado, comprendido dentro de la que existe a carga nula y nominal.

Ambiente (Standard Test Conditions).- Conjunto de aquellos valores característicos del medio ambiente que pueden influenciar las propiedades de un captador y que deben ser definidas en la calibración.

Frecuencia natural (Natural frequency).- Frecuencia de oscilaciones libres en ausencia de cargas.

Sobrecargas eléctricas admisibles.- Potencias límites para el circuito de alimentación y que no deben sobrepasarse, bajo el riesgo:

- a) De pérdida de características de captador.
- b) Destrucción total del captador.

Eje primario (Primory Axis).- Eje según el cual las cargas deben ser aplicadas.

3.5. Determinación de las tensiones residuales

Introducción

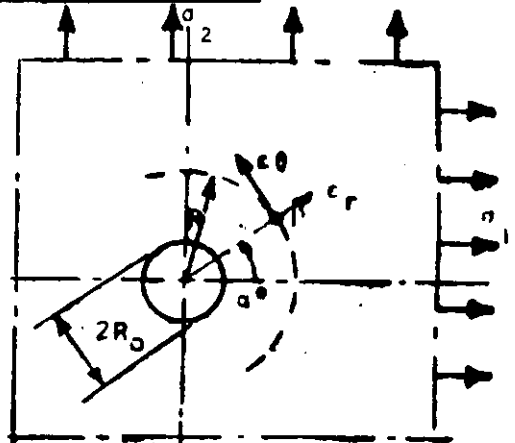
Con los extensímetros ohmicos lo único que puede evaluarse son cambios de deformación. Por consiguiente, si se desea determinar el estado de deformación existente en alguna pieza es necesario poder cambiar esa deformación una cantidad medible después de que se haya pegado la banda. A continuación, interpretar adecuadamen

Las tensiones residuales determinadas por relajación son un ejemplo de este método. En él, una banda se fija a la pieza y se mide su resistencia eléctrica. Luego se perfora o corta un trozo de la pieza teniendo cuidado de que no se produzca calentamiento; y se vuelve a medir la resistencia de la banda.

Si se produce una variación correspondiente a una tracción lo que habría es una compresión y recíprocamente.

Teoría. Para el caso de relajación por taladro (fig. 29)

Si se hace un taladro de pequeño diámetro ($2R_0$) en una región con tensiones residuales, se produce una relajación de deformaciones. Las deformaciones suprimidas en el punto P a una distancia R del centro del taladro cuando solo existe la tensión σ_1 son:



$$\epsilon_r = -\sigma_1 \frac{(1+\mu)}{2E} \left(\frac{1}{r^2} - \frac{3}{4r^4} \cos 2\alpha + \frac{1}{1+\mu} \frac{1}{r^2} \cos 2\alpha \right) \rightarrow r = \frac{k}{R_0}$$

$$\epsilon_\theta = -\sigma_1 \frac{1+\mu}{2E} \left(-\frac{1}{r^2} + \frac{3}{r^4} \cos 2\alpha - \frac{4\mu}{1+\mu} \frac{1}{r^2} \cos 2\alpha \right)$$

$$\gamma_{r\theta} = \frac{\sigma_1}{2G} \left(\frac{3}{r^4} - \frac{2}{r^2} \right) \sin 2\alpha$$

$$\epsilon_r - \epsilon_\theta = -\sigma_1 \frac{1+\mu}{2E} \left(\frac{2}{r^2} - \frac{6}{r^4} \cos 2\alpha + \frac{4}{r^2} \cos 2\alpha \right)$$

que son funciones sinusoidales de la orientación. Por ejemplo la deformación radial suprimida puede escribirse

$$\epsilon_r = (A + B \cos 2\alpha) \sigma_1$$

Y si existen simultáneamente σ_1 y σ_2 será

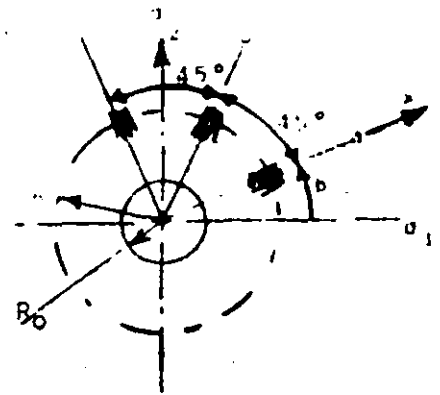
$$\epsilon_r = (A + B \cos 2\alpha) \sigma_1 + [A + B \cos 2(\alpha + 90^\circ)] \sigma_2$$

Los coeficientes A y B pueden calcularse fácilmente a partir de las constantes μ y E del material en cuestión y para cualquier distancia R.

También se pueden determinar experimentalmente los coeficientes A y B haciendo ensayos sin tensiones residuales en los materiales σ_1 y σ_2 conocidos, por ejemplo $\sigma_M = \sigma_1$ y $\sigma_m = 0$

Caso de la roseta (fig. 30)

Con tres bandas pegadas a una distancia R y en las direcciones a, b y c a 45° pueden medirse tres deformaciones ϵ_a, ϵ_b y ϵ_c que llevadas a la ecuación anterior (2) nos permiten despejar σ_1, σ_2 y $\text{tg } 2\beta$



$$\sigma_1 = \frac{(A+B \cos 2\beta) \epsilon_a - (A-B \cos 2\beta) \epsilon_c}{4AB \cos 2\beta}$$

$$\sigma_2 = \frac{(A+B \cos 2\beta) \epsilon_c - (A-B \cos 2\beta) \epsilon_a}{4AB \cos 2\beta}$$

$$\text{tg } 2\beta = \frac{\epsilon_a - 2\epsilon_b + \epsilon_c}{\epsilon_a - \epsilon_c}$$

fig. 30

Estas expresiones son buenas si las direcciones a y c corresponden aproximadamente con las principales. En caso de que no sea así y los a y b den las deformaciones más distintas son más satisfactorias las ecuaciones siguientes:

$$\sigma_1 = \frac{(A+B \text{sen } 2\beta) \epsilon_c - (A-B \cos 2\beta) \epsilon_b}{2AB(\text{sen } 2\beta + \cos 2\beta)}$$

$$\sigma_2 = \frac{(A+B \cos 2\beta) \epsilon_b - (A-B \text{sen } 2\beta) \epsilon_c}{2AB(\text{sen } 2\beta + \cos 2\beta)}$$

Técnicas experimentales

Como en todo lo experimental, las herramientas apropiadas, la instrumentación y la cuidadosa aplicación de los procedimientos son esenciales para obtener resultados ciertos.

Saladrado

Con brocas cilíndricas, no cónicas. La parte cortante sólo en el frente. El diámetro del cilindro se reduce a una distancia de $0,16 \phi$ a un diámetro menor en un 12% del de la punta para dejar sitio entre la broca y el agujero para la salida de virutas.

Rosetas de bandas especialmente bien espaciadas en el círculo y con el centro de este bien definido. (fig. 31)

Puente de medida

Puente portable de baterías con potenciómetros de equilibrio.

Centrado del taladro

Soporte centrador de un microscopio sustituible por una taladradora. (fig. 32)

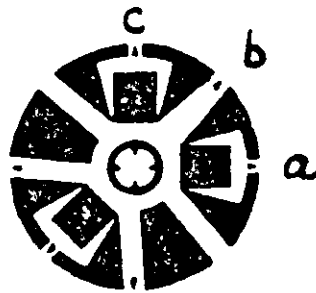


fig 31

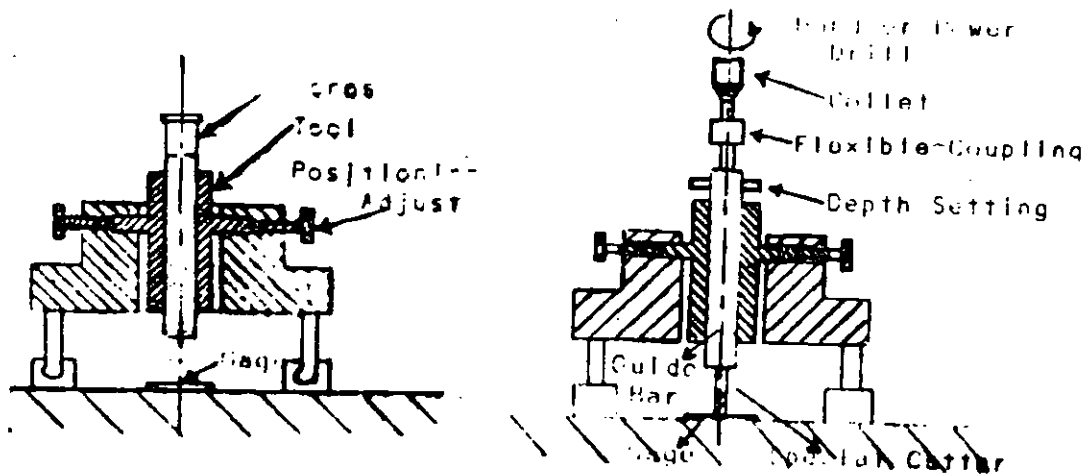


fig 32

4.1. Instrumentos para medidas estáticas.-

Aceptando como universal el circuito de puente de Wheatstone en medidas extensométricas, dos son los procedimientos que se pueden emplear para medir el desequilibrio que en una diagonal se produce cuando las bandas se deforman.

El "Método de oposición" introduce en la diagonal del puente (fig. 1) una tensión opuesta a la de desequilibrio, siendo el instrumento G el que controla la posición de equilibrio. Si el potenciómetro P está graduado en la escala deseada (microdeformaciones) e incluso va dotado de un indicador numérico y dispositivos de pre-equilibrado, podremos hacer las lecturas directas. Se comprende que para no introducir error las tensiones

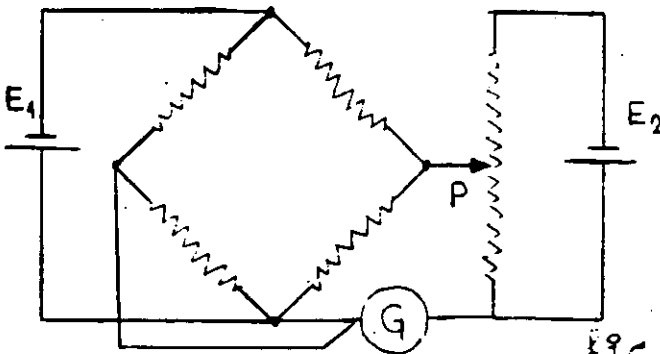


fig 1

deben estar estabilizadas en alto grado o bien que sus variaciones sean totalmente proporcionales, pero según el esquema de la fig. 1, eso es muy difícil de conseguir, de ahí, que se utilice la disposición indicado en la fig. 2 en las que la solución si bien es satisfactoria en un aspecto, crea problemas en otros, en efecto, si alimentamos los puentes en corriente continua, y dada su polaridad, los instrumentos nos indicarán las deformaciones producidas por esfuerzos de tracción o compresión según las desviaciones de la aguja sea en uno u otro sentido respectivamente, pero al ser excitados en corriente alterna es necesario introducir un circuito llamado detector de fase que discrimine cuando las deformaciones son de tracción o de compresión en efecto:

(fig. 3)

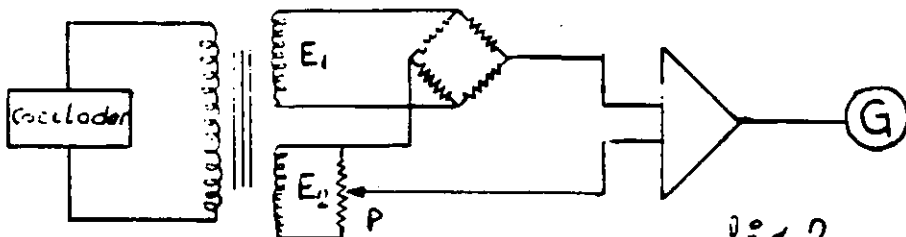


fig 2

si el puente está en equilibrio:

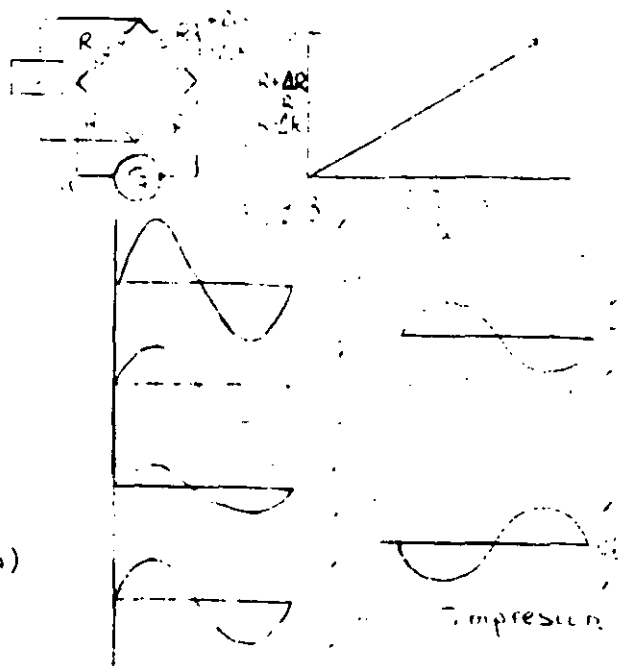
$$v_B - v_A = v_S = 0$$

si hay tracción en una rama:

$$v_B - v_A = v_S \text{ (Tracción)}$$

si hay compresión en una rama

$$v_B - v_A = v'_S \text{ (compresión)}$$



Por otra parte, para conseguir la oposición entre las tensiones E_1 y E_2 es necesario que estén defasadas 180° y para lograrlo hay que introducir ajustes capacitivos, lo cual representa otro inconveniente; por tal motivo la casa Vishay-Micromesures, en su puente P-350, emplea como portadora una onda cuadrada, en vez de senoidal, y la oposición de fase se consigue de forma automática sin necesidad de ajustes capacitivos, ventaja que le confiere una gran aceptación por extensometristas experimentados.

En el "Método de cero" (fig. 4) el equilibrio del puente

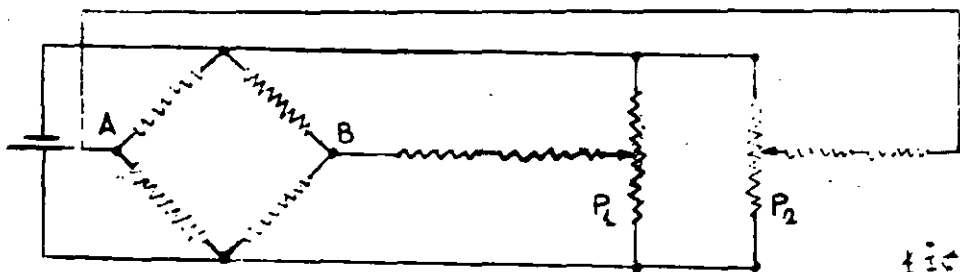


fig 4

se consigue introduciendo resistencias en las ramas del puente hasta conseguir el equilibrio inicial; los potenciómetros P_1 y P_2 se desplazan conjuntamente en sentido inverso hasta anular tensión de desequilibrio entre A y B. graduando adecuadamente los mandos de P_1 y P_2 podremos hacer lecturas directas. El mando de P_1 y P_2 puede hacerse a través de un servomecanismo y constituir así una unidad de lectura automática.

Otro procedimiento, que actualment está siendo cada vez mas empleado, consiste en leer directamente la señal de salida del puente por medio de un voltímetro digital de precisión y exactitud elevada. Este procedimiento exige a su vez que la fuente de excitación sea muy estable (fig. 5)

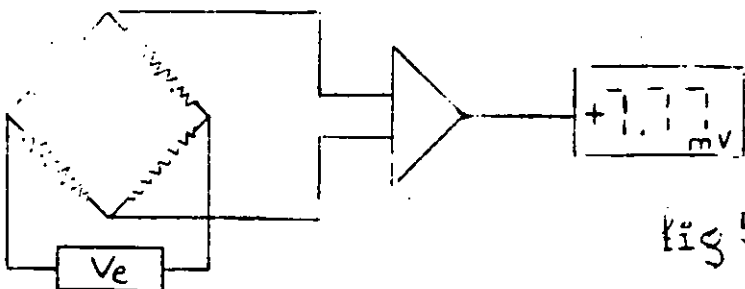


fig 5

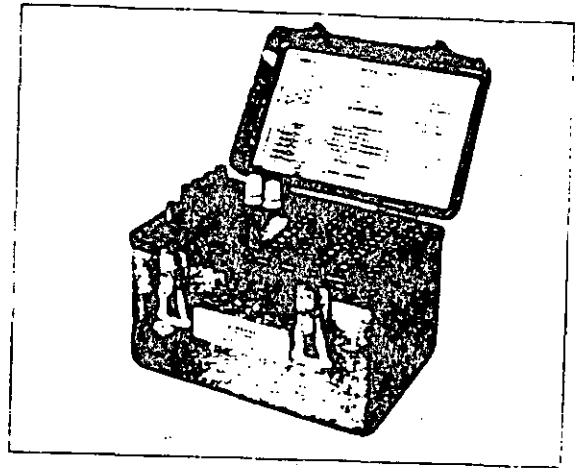
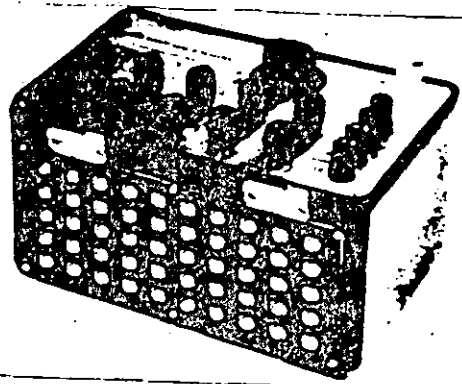
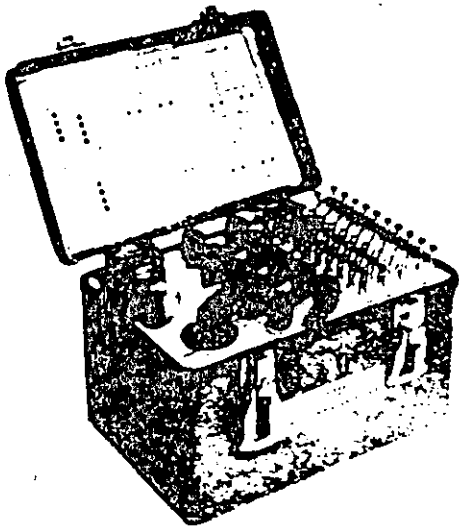
4.1.1. Cajas de conmutación manual

Normalmente, las medidas extensométricas, habrá que efectuarlas en varios puntos, si estos son muy numerosos (se estima que superiores a 25) una unidad automática será conveniente, pero para una cantidad inferior se utilizan unidades de conmutación manual con resultados prácticos satisfactorios; ya que el mayor tiempo de lectura que será necesario emplear justifica su uso por razones meramente económicas, pues lógicamente los equipos manuales son de bajo precio.

El problema que se plantea es conmutar diversos circuitos de medida a un solo instrumento de lectura de lo que se deduce que el conmutador será de una calidad que garantice un mínimo de error en la medida (Ver 3.1.1.). Por otra parte la unidad de conmutación debe ofrecer la posibilidad de un equilibrado previo de los circuitos de medida, para que cuando ensayemos bajo carga la pieza en estudio, las lecturas puedan ser directas.

En la fig. 6 se indica la disposición adoptada por Vishay-Micromesures en su unidad S-B1 en la que se consigue una adaptación completa de los circuitos de $1/1$; $1/2$ ó $1/4$ de puente, asociada al instrumento P-350 o cualquier otro similar.

El potenciómetro P de equilibrado, será de precisión y de 10 vueltas para conseguir una buena resolución, si a su vez va provisto de un mando con contador numérico de vueltas (Duodial) podremos reestablecer las condiciones previas del equilibrado, aún cuando se hubiese utilizado en otros circuitos distintos la unidad de conmutación en el curso de experiencias diversas.



4.1.2. Instrumentos de calibración

Los instrumentos de lectura son contrastados por el fabricante en sus factorías, pero el uso y la degeneración de sus componentes con el tiempo, hace necesario una contrastación periódica de los mismos, para ello pueden seguirse varios procedimientos uno de los cuales se explicó en el apartado 3.2. y consistía en colocar resistencias en paralelo en una rama del puente, que produjesen un desequilibrio - equivalente al que experimentase el mismo circuito sometido a solicitudes concretas. Este método si bien es recomendado para calibrar los circuitos de medida no es idóneo para contrastar el instrumento de lectura, ya que nunca sabremos si al colocar la resistencia en paralelo - observamos alguna anomalía, si el error es del circuito o del instrumento, por tal motivo se recomiendan dos procedimientos: 1º Simulador de deformaciones y 2º Patrón primario de deformaciones.

Simulador de deformaciones. Consiste en una caja de décadas de alta precisión y estabilidad que comprende 5 décadas que pueden obtener valores en pasos de 0,01; 0,1; 1; 10 y 100 ohm. con precisión total de $\pm 0,02\%$ sobre cualquier lectura. Su estabilidad es superior a ± 50 ppm por año. A estas características responde la unidad -

Para calibrar un instrumento de lectura en extensometría, suponfremos que el simulador de deformaciones constituye la banda propiamente dicha y para ello ajustaremos un valor igual al de extensímetro p.e. 120. Efectuaremos posteriormente su conexión al instrumento en montaje de 1/4 de puente en la configuración de 3 hilos (fig. 7).

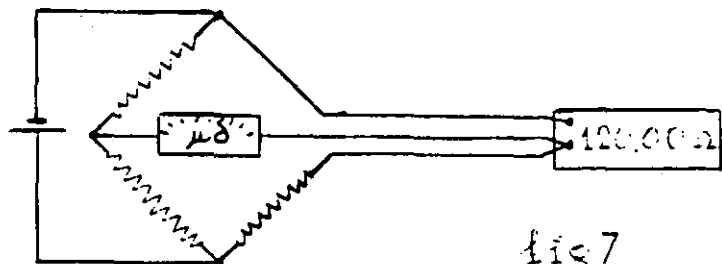


fig 7

Recordando que:

$$AR = K.R.$$

tenemos que para

$$\begin{aligned} \epsilon = 1500 / \mu\delta & \quad \Delta R = 0,36 \text{ ohm} \\ \epsilon = 2000 / \mu\delta & \quad \Delta R = 0,48 \text{ " } \\ \epsilon = 2500 / \mu\delta & \quad \Delta R = 0,60 \text{ " } \end{aligned}$$

Si $K=2$ y $R=120 \text{ ohm}$.

Por tanto si el instrumento de lectura está bien tarado, leemos los valores indicados de microdeformaciones, si en el simulador vamos paulatinamente fijando los valores de 120,36; 120,48 ohm etc. Te ner presente que así simulamos tracciones, si disminuimos el valor 120 ohm, en la misma proporción leeríamos compresiones.

Patrón de deformaciones

Una viga de sección rectangular $b \cdot c$ toma forma de arco de anillo circular, al ser sometida a flexión pura. El valor absoluto de la deformación longitudinal que sufren sus caras horizontales es

$$\epsilon = \frac{6Pa}{bc^2E}$$

La flecha del arco de circunferencia así producido es

$$f = \frac{Pa^3}{\frac{2}{3}bc^3E}$$

La relación entre flecha y deformación es

$$\epsilon = \frac{4c}{3a^2} f$$

lo que nos dice que podemos conocer la deformación en fun

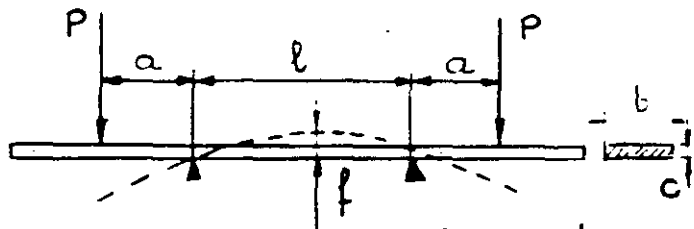


fig 8

ción de la flecha y de cons tantes geométricas, indepen dientemente de las cargas y del módulo de elasticidad del material.

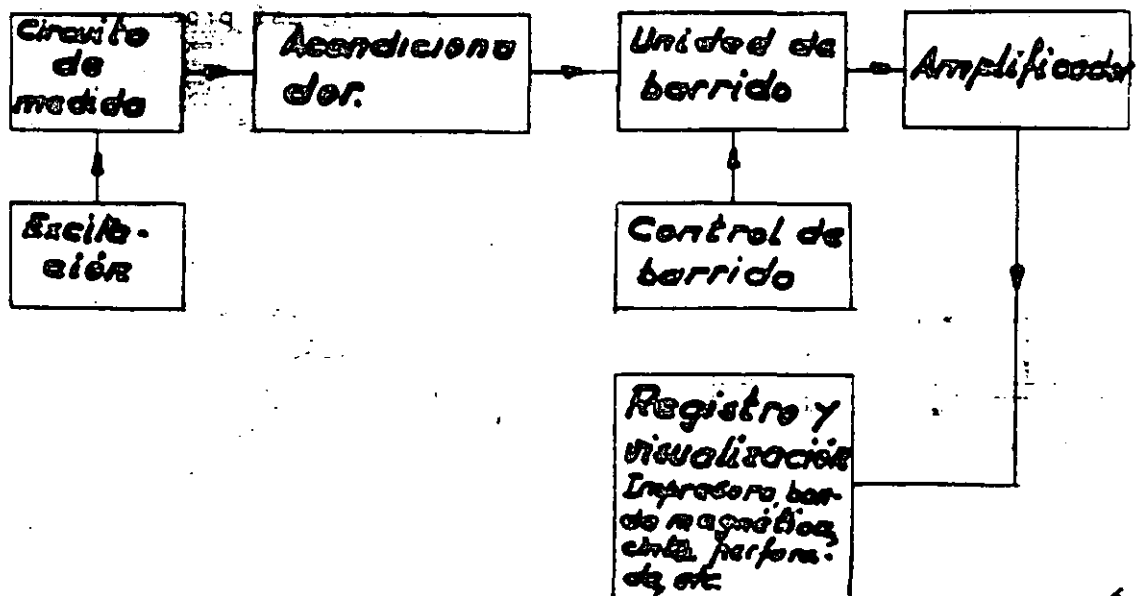
El Patrón de Deformaciones permite fijar la flecha f con lo que se puede calcular la deformación E correspondiente. Si además se mide la deformación E por medio de extensómetros óhmicos, se puede calcular un coeficiente de corrección para este método o comprobar sistemas extensométricos.

4.2. Sistemas automáticos de adquisición de datos.

Estos sistemas son necesarios cuando por el número de puntos de registro, el tiempo requerido para un barrido manual fuese tal que las condiciones del ensayo variasen dentro de él, y por consiguiente no fuesen datos adquiridos en igualdad de condiciones los de una misma lectura; o bien cuando la magnitud y frecuencia de medidas múltiples haga tedioso y propenso a errores de anotación las lecturas manuales.

El avance tecnológico de la electrónica ha facilitado el diseño de equipos muy sofisticados, y a veces, no justifican las pequeñas ventajas que introducen el elevado precio que adquieren. Por tal motivo juzgamos oportuno describir el conjunto para que el usuario futuro, tenga elementos de juicio para configurar el Sistema idóneo a sus necesidades, pero no entraremos en la descripción de circuitos, que se escapan del alcance de este artículo.

4.2.1. Diagrama bloque



Circuito de medida.

Será cualquier circuito extensométrico, ya descrito, -
bién en el aspecto de bandas extensométricas, o bién bajo el concepto
de captador. Generalmente podrá ser cualquier elemento transductor de
energía mecánica en eléctrica.

Excitación.-

Por ser circuitos pasivos, tendremos que aportar ener-
gía, generalmente para excitar un circuito de puente de Wheatstone.

Acondicionador.-

Debe permitir equilibrar el circuito de medida e intro-
ducir señales de calibración.

Unidad de barrido.-

Esta unidad está destinada a conectar cada uno de los
circuitos de medida a la unidad central de lectura, con una secuencia
predeterminada. Sus características principales son: velocidad de con-
mutación; fiabilidad de los contactos, número de polos conmutados, etc.

Amplificador.-

Aumenta el nivel de tensión de las señales débiles que
se crean en los circuitos de medida.

Control de barrido y registro.-

Lo forman circuitos electrónicos, más o menos complejos,
que permiten programar las secuencias de las lecturas y de la impre-
sión.

4.3. Sistemas analógicos de registro continuo

Podríamos definir un sistema como el conjunto de instrumentos, debidamente acoplados, para la adquisición de datos en forma predeterminada, de las magnitudes físicas a medir.

4.3.1. Diagrama bloque

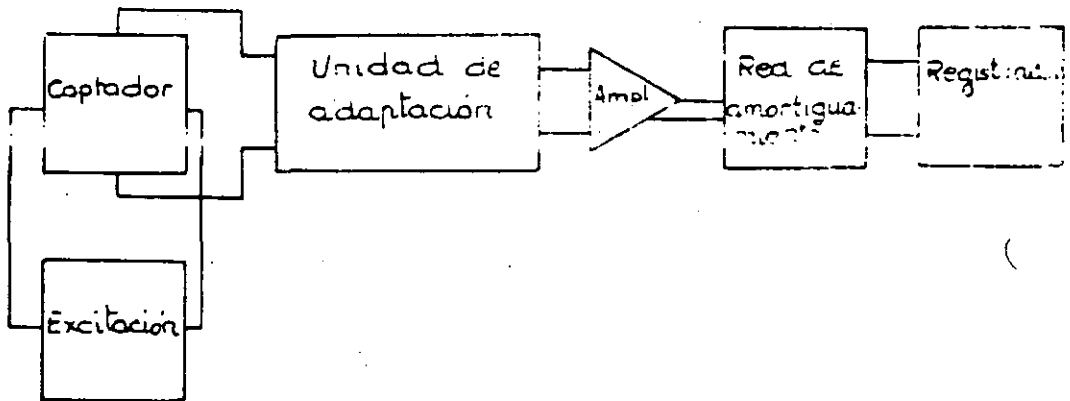


Diagrama bloque de un sistema elemental

El esquema de la figura responde a los elementos funcionales del sistema, que son:

- a) **Captador:** Es un elemento capaz de convertir una magnitud física en eléctrica. Se basa en fenómenos resistivos, capacitivos, inductivos, piezoeléctricos, termoelectrónicos, semi-conductores, etc, etc,
- b) **Unidad de excitación:** Si el captador no autogenera su propia señal (p.e.: termopares) es necesario alimentarlo con una fuente de energía adicional.
- c) **Unidad de adaptación y calibración:** Permite corregir y compensar los desequilibrios en los circuitos e introducirles una señal que permita la calibración de los mismos.
- d) **Amplificador:** Las señales emitidas por los captadores pueden ser tan débiles que no sean capaces de excitar los instrumentos de lectura ó registro. Es necesario entonces el empleo de unidades intermedias que aumenten el nivel de la señal de salida.
- e) **Registrador ó unidades de lectura:** Pueden ser cualquiera de los instrumentos clásicos destinados a registros analógicos ó digitales ó bien osciloscopios, milivoltímetros, etc,

f) Red de amortiguamiento: Sirve para adaptar las impedancias de entrada y salida de los diferentes amplificadores e instrumentos de lectura ó registro. En el caso de galvanómetros, tiene una influencia decisiva referente a la respuesta en presencia de los mismos.

4.3.2. Descripción

A Captadores

Un captador ó transductor es aquel elemento que, bajo estímulos físicos, da origen a señales eléctricas. La mayoría de los captadores proporcionan salidas analógicas en forma de d.d.p. eléctrico. Muy idealizado, podemos suponerlo tal y como se muestra esquemáticamente:

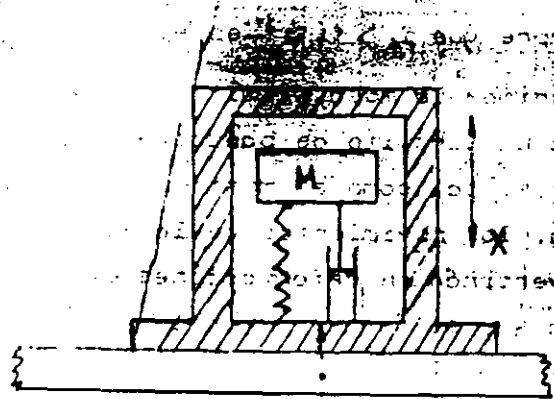
Si una viga elástica y empotrada recibe en su extremo libre un golpe, se producirá un movimiento oscilatorio amortiguado, pues bien, el transductor nos dará una d.d.p. analógica del estímulo recibido.

Los captadores los clasificaremos bajo diversos aspectos:

- Estímulo físico, al que son sensibles: captadores de aceleraciones, vibraciones, presiones, fuerzas, desplazamientos, torsión, calor, etc.
- Principio de la transducción: Resistivos (P. de Wheatstone y potenciométricos) inductivos, piezoeléctricos, fotoeléctricos, capacitivos, semiconductores, etc.
- Alimentación de su circuito interno: Autoexcitados, excitados, en c.c. y excitados en c.a (portadora).

Captadores más usuales son:

- 1º Acelerómetros:** Supongamos una masa sísmica M montada en una caja con un muelle y sistema amortiguador como el representado esquemáticamente. Si la caja es solidaria con un elemento sometido a vibraciones, se creará un movimiento relativo entre masa M y caja y entre caja y un punto fijo del espacio. Si llamamos " X " e " Y " a los desplazamientos de M respecto a caja y de caja respecto al punto fijo, respectivamente, tendremos que ante cualquier excitación aparecerá dentro de la caja una energía de valor: $dE = (x^2 + y^2) dz$.



$$E = \int_0^y M(x'' + y'') dy = \int_0^y M(x'' + y'') y' dt \quad (1)$$

Energía que se manifiesta en tres formas: cinética, deformadora del muelle y disipada en forma de calor por el sistema amortiguador. Por tanto:

$$E = \frac{1}{2} M(x' + y')^2 + \frac{1}{2} Kx^2 + \int_0^t C x'^2 dt \quad (2)$$

siendo $K =$ característica del muelle
 $C =$ constante de amortiguamiento

Si el muelle es totalmente elástico se cumple que $\frac{K}{M} = 4\pi^2 f_n^2$, y si el amortiguamiento es el ideal $\frac{C}{M} = 4\pi f_n$ de donde igualando (1) y (2), simplificando y sustituyendo, obtenemos que:

$$x'' + 4\pi f_n x' + 4\pi^2 f_n^2 x = -y'' \quad (3)$$

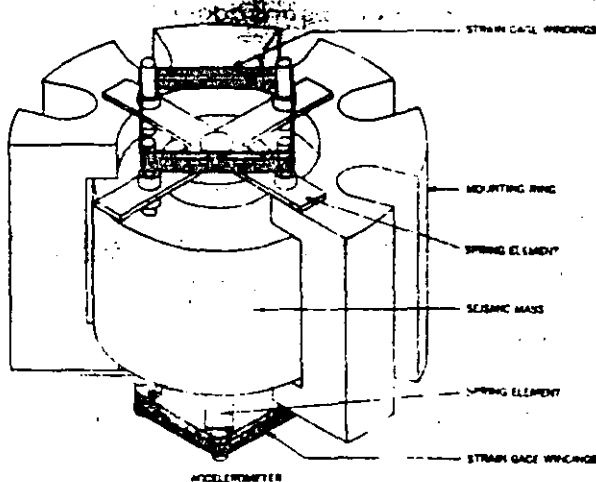
El desplazamiento "Y" varía con el tiempo y no tiene por qué ser periódico. Su armónico principal sería de la forma $y = Ae^{j\omega t}$ siendo A la amplitud y $\omega = 2\pi f$; de esta forma la solución de X sería: $x = Be^{j\omega t}$ en donde B es función compleja de ω ; sustituyendo en (3) queda simplificado que:

$$-B^4 \pi^2 f^2 + jB(2\pi f) + B(2\pi f_n)^2 = -A$$

donde los dos primeros términos pueden despreciarse si $f_n > f$ es decir, si la frecuencia natural del resorte es mayor que la frecuencia del movimiento de la caja, entonces:

$$\left. \begin{aligned} B(2\pi f_n)^2 &= -A \\ x(2\pi f_n)^2 &= -y'' \end{aligned} \right\} x = \frac{-y''}{(2\pi f_n)^2}$$

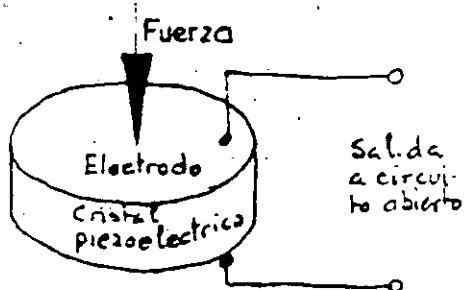
Vemos, por tanto, que el desplazamiento de la masa es proporcional a la aceleración a que se somete la caja, siempre que $f_n > f$ ($\approx f$ es el 60% de f_n)



Si unimos la masa sísmica adecuadamente a un circuito de bandas extensométricas, tal como el mostrado en la figura, los movimientos de la masa se convertirán en deformaciones de las bandas y si éstas forman los cuatro brazos activos de un puente de Wheatstone, el desequilibrio que producen origina una d.d.p. proporcional a la aceleración a que se somete la caja.

Los acelerómetros se construyen de forma que sean sensibles en una sola dirección y con la propiedad que giros de $\pm 90^\circ$ respecto a su posición de equilibrio equivalen a producir los mismos efectos que si se someten a una aceleración de $\pm 1 g$, respectivamente ($g = 9,8 \text{ m/seg}^{-2}$).

El tipo descrito corresponde a un acelerómetro resistivo, que son más utilizados, ya que con un margen de frecuencia, relativamente amplio, permiten medir desde $f = 0 \text{ Hz}$. Son, además, de muy fácil acople en el sistema por su baja impedancia de salida y proporcionan señales altas, no existiendo problemas de ruido ó descompensación especiales cuando haya que utilizarlos a distancias relativamente grandes.



Acelerómetro piezoeléctrico.

Si a un cristal piezoeléctrico le aplicamos entre sus caras una fuerza F , se genera en las mismas una carga q , incorporándole íntimamente una masa al cristal, tenemos un acelerómetro, en efecto: $q = dF = dMa$.

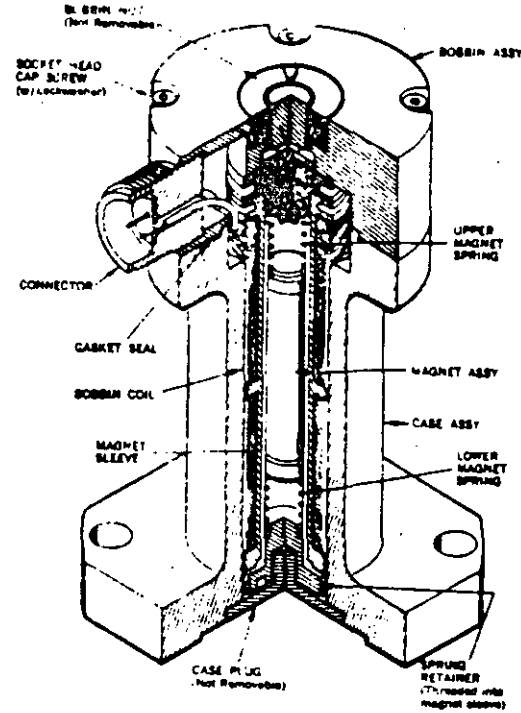
donde la d.d.p. V_s originada entre caras del cristal vale:

$$V_s \propto \frac{q}{C} \propto \frac{dF}{C} \propto \frac{dMa}{C} = K_a$$

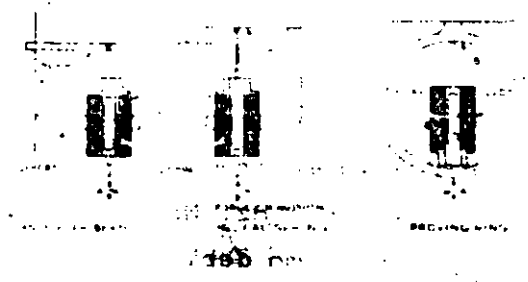
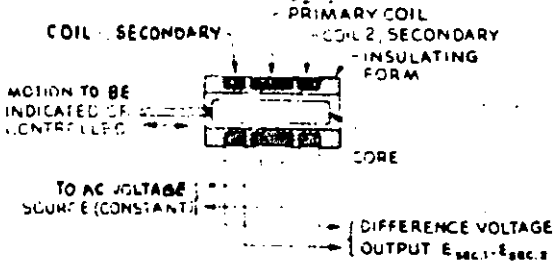
es decir, la d.d.p. V_s es proporcional a las aceleraciones que es sometida la masa M .

Los acelerómetros piezoeléctricos no necesitan alimentación, ya que son autoexcitados. Tienen una respuesta en frecuencia alta, aunque no responden bien a frecuencias próximas a 0 Hz . Necesitan un adaptador de impedancias para su acople en el sistema debido a su muy alta impedancia de salida y pueden dar problemas cuando haya que emplear cableado a distancia.

29) Captadores de vibraciones.- Para los acelerómetros resistivos decimos que la frecuencia del movimiento debía ser menor que la frecuencia natural del resorte, pues bien, si hacemos ahora que $f = f_n$, tendremos un captador de vibración.



Cutaway View of Vibration Transducer



En efecto, si la caja se mueve por encima de la frecuencia de resonancia del muelle, la masa sísmica permanece "quieta" en el espacio y la corriente que se origina en las bobinas es proporcional a la velocidad de los desplazamientos de la caja.

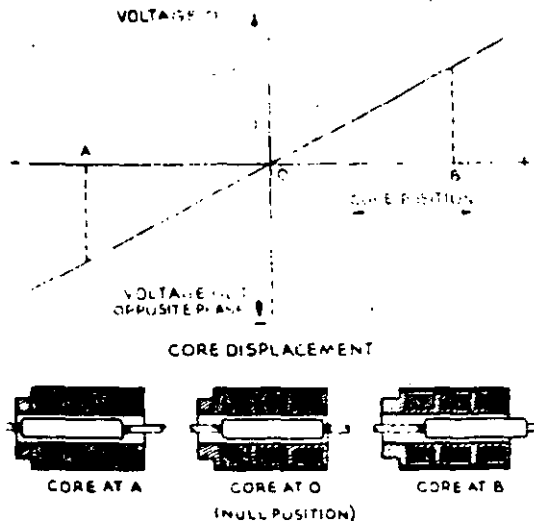
Estos captadores tienen la ventaja de que son autoexcitados.

32) Captadores de presión.- El fundamento es el mismo que en los acelerómetros resistivos, salvo que la masa sísmica es sustituida por un diafragma, que es el elemento sensible a las presiones.

Pueden hacerse medidas absolutas y diferenciales.

42) Captadores basados en transformadores lineales.- Ha sido muy desarrollada la técnica del transformador diferencial lineal para su uso en transductores. Básicamente, está constituido por devanado primario y dos devanados secundarios idénticos y montados en oposición; los tres devanados constituyen la parte estática del captador y un núcleo magnético forma la parte dinámica.

Al excitar el primario con una corriente alterna constante, si el núcleo se encuentra en su posición media, no habrá d.d.p. en los terminales del secundario, pero para cualquier desplazamiento del núcleo aparecerá una d.d.p. entre terminales del secundario proporcional al



Vemos que un transductor basado en el anterior principio, puede convertir cualquier magnitud mecánica (desplazamiento, presión, fuerza, vibración, etc) en magnitud eléctrica.

Las ventajas de estos transductores son:

- Salida exactamente proporcional al desplazamiento del núcleo.
- Alta sensibilidad y nivel elevado a la salida.

Característica lineal de la respuesta en toda su escala.

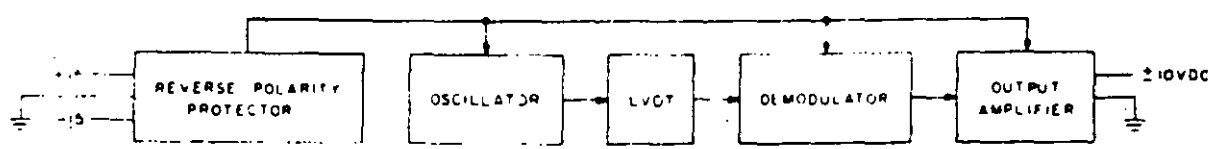
Variación de la d.d.p, de salida desde cero, sin necesidad de equilibrar el circuito.

Estabilidad del cero.

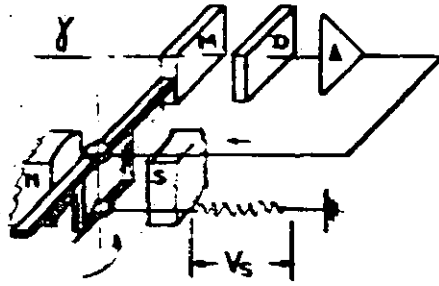
Permiten la suma ó producto de varios desplazamientos - montándolos en serie ó tandem, respectivamente,

Por el contrario, presentan el inconveniente de que necesitan demodular y filtrar la salida y de que su excitación no puede ser en corriente continua.

Para paliar el anterior inconveniente, la firma Schaevitz, ha desarrollado un modelo que puede ser excitado en c.c.; su esquema es el indicado y toda la electrónica la constituye un circuito integrado de estado sólido, de dimensiones reducidísimas, incluido dentro del propio captador. El resultado es francamente favorable.



Servoacelerómetros



Constituyen un avance enorme en la medida de aceleraciones por las elevadas prestaciones que ofrecen. Su principio está basado en la restauración del equilibrio de una masa sísmica pendular cuando éste es desplazado de su posición de reposo por una fuerza aceleradora. En efecto, de la ecuación $Mr = (Momento de tensión) = I$ (Momento de iner

cia) (aceleración) deducimos que una aceleración angular aplicada al acelerómetro y actuando sobre una masa equilibrada montada en un eje giratorio, origina un par de tensión sobre dicho eje; de la misma forma, si la masa no está equilibrada (pendular) y es sometida a una aceleración lineal producirá en el eje de rotación un momento de tensión.

El fenómeno de la transducción aceleración-señal, se consigue disponiendo de un sensor de posición, capaz de detectar los movimientos de la masa sísmica pendular el cual da una señal eléctrica a dichos movimientos y que es amplificada hasta conseguir el nivel adecuado para alimentar la bobina montada dentro de un campo magnético que originará el par antagonista al de torsión que creó la fuerza aceleradora. El circuito es cerrado, de ahí que la señal se obtiene como caída de tensión en R_1 .

La señal de estos acelerómetros es de ± 5 VDC y en la mayoría de aplicaciones no necesitarán posterior amplificación para su registro. Son alimentados normalmente a ± 15 VDC.

B Módulos de excitación

Módulo de excitación es un elemento capaz de suministrar la energía adecuada al captador para obtener señales eléctricas propor

cionales a los estímulos físicos a los que se someta. Podremos utilizar, desde una simple pila seca, hasta una sofisticada fuente de alimentación, siendo la calidad del captador y las características del sistema quienes impondrán el tipo adecuado de módulo.

Nos referiremos siempre a módulos de excitación en c.c. ya que la utilización de excitación en c.a. (portadora) cada vez está más en desuso y, cuando se utiliza, son los propios amplificadores los que llevan incorporados un oscilador que proporciona la excitación con d.d.p. de 0-10 V en frecuencias de 2 a 8 KHz, normalmente.

Un buen módulo de excitación debe suministrar una d.d.p. constante; se comprende esto, ya que cualquier variación en la d.d.p. de la excitación introducirá errores en la señal de salida del captador, que es proporcional a la excitación y a la variación del estímulo físico.

En general, la elección de un módulo de excitación se hará considerando dos aspectos:

1º) Características del captador.- Impondrán el valor de la d.d.p., intensidad de corriente y potencia; deberán considerarse los casos en que sean varios los captadores alimentados en paralelo por un solo módulo.

Especificaciones propias del módulo de excitación.- Serán índice de la calidad del mismo. Deben considerarse como importantes:

Posibilidad de ajuste sobretensiones (cortocircuitos, electromagnética, térmica, electrónica, etc).

Limitador electrónico de la corriente de salida.

Reversibilidad de la polaridad.

Rizo residual de la tensión de salida.

Aislamiento de bornes de salida a masa ó tierra.

Corrientes de fugas.

Rechazo de interferencias.

Voltímetro incorporado de control.

Deriva de la salida respecto a tiempo y temperatura.

Márgenes de la temperatura de utilización.

Posibilidad de alimentación por c.a. ó por baterías.

Incorporación de acumuladores autorrecargables.

Conectores, caja de montaje, pero, etc, etc.

C. Unidades de adaptación

Una unidad de adaptación incorpora en el sistema los elementos necesarios para equilibrar el circuito de medida, es decir, para que una carga nula en el captador dé como señal de salida cero, compensando las asimetrías propias del captador, ó producidas por cables, - conexionado, etc. Si los captadores son resistivos, la compensación - será solo con potenciómetros, siendo necesario un ajuste capacitivo en el caso de captadores inductivos ó cuando se emplee el sistema de excitación por "onda portadora". Opcionalmente, pueden incluir un sistema de excitación y elementos pasivos (resistencias) para completar el circuito de medida de captadores, generalmente cuando se utilizan puentes de Wheatstone.

Normalmente, las especificaciones de una unidad de adaptación son referidas a circuitos con 350 ohmios y excitados con 10 V, pero no hay razón para ampliar estas especificaciones a otros valores, por ejemplo, si una unidad de adaptación permite compensar desequilibrios de ± 4 mV en un circuito de 350 ohmios con 10 V de excitación, - Utilizando un circuito de 1.000 ohmios y la misma excitación, la cobertura de ajuste sería:

$$\frac{1.000}{350} \times (\pm 4) = \pm 11,4 \text{ mV.}$$

El poder de resolución debe ser del orden de 5 microvolts para una buena unidad.

Es frecuente utilizar una resistencia fija de precisión para calibrar un circuito, conmutándolo en paralelo con una rama del puente de Wheatstone. La señal así obtenida es equivalente a la que produciría el captador sometido a cierto estímulo físico. La carta que acompaña a los captadores indica el valor de la resistencia, que produce una señal equivalente a la del captador con el 80% de su nominal. Con el fin de evitar la utilización de numerosas resistencias de calibración, se montan unas bornas exteriores que permiten conectar una caja de décadas y, de esta forma, seleccionar el valor adecuado para cada captador ó circuito de medida.

En medidas de Extensometría se presenta, con frecuencia la necesidad de utilizar 1,2 ó 4 brazos activos de un circuito de puente Wheatstone. Para estos casos ó similares, las unidades de adaptación suelen llevar incorporadas las resistencias que completan los

brazos pasivos del circuito, facilitando el montaje con una economía notable al disminuir el número de extendímetros por circuito de medida.

Se tendrá muy en consideración que no exista un punto común (masa), pues provocaría un cortocircuito en una rama del puente.

D Amplificadores

El amplificador es una unidad intermedia entre el circuito de medida y el registrador y su utilización será justificada por dos razones: una cuando la señal del captador sea insuficiente para excitar los instrumentos de lectura ó registro y otra en el caso de fenómenos cuya presencia sea superior a los 350 Hz, ya que los galvanómetros capaces de dar respuestas a estas frecuencias son de baja sensibilidad.

La tecnología electrónica de un amplificador para sistemas de medida ha evolucionado grandemente en los últimos años y del primitivo tipo de onda portadora (carrier), se ha pasado a las actuales de tipo diferencial, con circuitos transistorizados sencillos, estando desarrollándose actualmente técnicas más avanzadas con empleo de circuitos integrados y del amplificador operacional.

Describir circuitos electrónicos de un amplificador no es objeto de este artículo, pues no olvidemos que, desde el punto de vista de instrumentación, su uso, y no su constitución, es necesario conocer. Sí es preciso, sin embargo, interpretar correctamente las especificaciones que de ellos se dan, para poder elegir y utilizar siempre el modelo más idóneo para un determinado sistema.

Especificaciones de un amplificador.

Configuración (Configuration).- Indica generalmente la disposición de la entrada y salida, diciéndose que es verdaderamente "diferencial" cuando están totalmente aisladas y "single ended" cuando hay una entrada y salida común. La salida de un amplificador puede tener un punto a tierra ó estar totalmente aislada. En este caso se dice que tiene "salidas flotantes".

Ganancia en tensión (Voltage Gain).- Normalmente será por pasos fijos (10, 20, 50, 100, 200, 500, etc) y ajuste fino entre pasos. Es importante el grado de exactitud entre pasos.

Respuesta en frecuencia (Frequency Response).- Nos indicará el % de variación de la ganancia en un determinado ancho de banda.

Tiempo de recuperación contra sobrecargas (Overload Recovery Time).- Si a un amplificador lo sometemos a una sobrecarga de 10 veces el valor final de escala, nos indicará el tiempo que transcurre desde que cesa la sobrecarga hasta que se alcanza el 90% del valor total de escala.

Linearidad (Linearity).- Idealmente, un amplificador deberá dar salidas totalmente proporcionales a las señales de entrada. El error de proporcionalidad expresado en % del valor máximo de la señal de salida lo da esta especificación.

Derivas (Drifts).- Se entiende por derivas las variaciones de la señal de salida con señal de entrada nula y puede referirse al tiempo y/o temperatura. Las variaciones de la salida por este motivo deben mantenerse en el entorno dado en esta - especificación.

Ruido (Noise).- El ruido inherente a circuitos electrónicos (agitación térmica) limita el poder de resolución, que no podrá ser mayor que la especificación dada para ruido.

Modo común de rechazo (Common Mode Rejection).- Es índice del poder de rechazar señales indeseadas. Se expresa, en dB, como la relación entre el voltaje en modo común (CMV) y la señal que dicho CMV originaría en la entrada.

$$CMR (dB) = 20 \log \frac{CMV}{IS}$$

Sensibilidad (Sensitivity).- Relaciona los niveles de la señal de entrada y los máximos de la señal de salida.

Máxima impedancia del circuito de medida (Maximum Source Impedance).- Es el límite superior del valor de la impedancia del circuito de medida.

Impedancia de entrada (Input Impedance).- Es la medida a la entrada del amplificador.

Impedancia de salida (Output Impedance).- Es la medida a la salida del amplificador.

Capacidad (Capability).- Máximos valores en tensión y corriente capaces de obtenerse a la salida.

Ajuste Zero Offset.- Indica la capacidad del amplificador de obtener una salida nula con las entradas conectadas a un circuito de impedancia cero.

Mínima impedancia de carga (Minimum Load Impedance).- Mínima carga que debe conectarse a la salida del amplificador para obtener la máxima salida.

Como conclusión, diremos que las especificaciones del amplificador deberán cumplir, como mínimo, las propias exigidas al sistema en conjunto. Características superiores sólo producirían un encarecimiento innecesario.

E Registadores

El registrador es el instrumento que recibe las informaciones transmitidas por los captadores a través de los módulos intermedios para ser grabadas de forma que permitan el cálculo ó procesamiento de datos.

La elección del registrador, al igual que los demás componentes del sistema, estará condicionada por el parámetro a medir.

Si los fenómenos a registrar son de muy bajas frecuencias un registrador potenciométrico será suficiente. Por el contrario, si las frecuencias son de algunos hercios, tendremos que utilizar un registrador oscilográfico de haz luminoso, microfilm, placas osciloscópicas ó cinta magnética. En general, varios serán los factores que intervendrán en la elección y convendrá considerar:

Fidelidad, ó sea, distorsión que experimenta la señal en la grabación.

Valor mínimo de señal que puede ser grabado y posteriormente interpretado dentro de los límites de exactitud y precisión exigidos en la medida.

Banda de frecuencias con respuesta plana.

Número de canales simultáneos de registro.

Tratamiento posterior de la información.

En medidas dinámicas son muy utilizados los registradores oscilográficos de haz luminoso y los registradores magnéticos de cinta.

Registradores oscilográficos de haz luminoso.

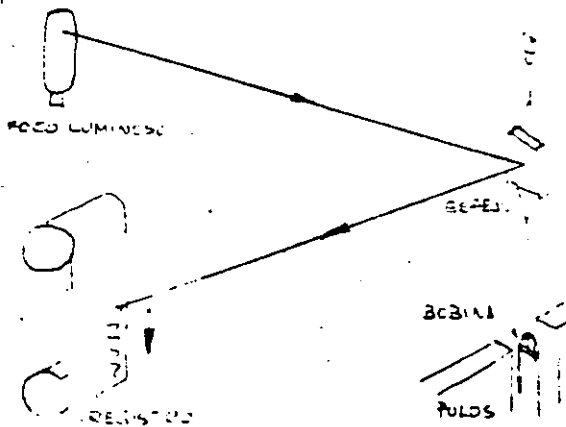
La señal eléctrica procedente del captador excita un galvanómetro que refleja el haz procedente de una fuente luminosa capaz de impresionar un papel fotosensible, grabando en forma analógica la magnitud física objeto de la medida.

Cuatro son los elementos fundamentales de un oscilógrafo: mecanismo de transporte de papel, fuente luminosa de alta intensidad, sistema óptico y galvanómetros. El mecanismo de transporte de papel debe permitir varias velocidades de registro y asegurar la constancia de cada una de ellas. Una de las limitaciones de registrar fenómenos de frecuencias elevadas la impondrá la capacidad de transporte del papel para conseguir la velocidad adecuada que permita una grabación legible, con un consumo mínimo de papel.

La fuente luminosa está también íntimamente ligada a la frecuencia de los fenómenos a registrar y se comprende que, para frecuencias elevadas, el tiempo de exposición del haz luminoso sobre el papel será muy breve, de ahí que la intensidad del mismo tendrá que ser grande. Se utilizan focos de lámparas de tungsteno, arco, halógenos vapor de mercurio, etc. El límite está en frecuencias de unos 25 KHz.

El sistema óptico de su oscilógrafo está formado por una serie de espejos y lentes que conducen el haz luminoso hasta el papel fotosensible, consiguiendo que la grabación sea legible. La calidad de sus componentes, su facilidad de ajuste, así como la precisión de su montaje, serán el índice de la bondad de este sistema.

El galvanómetro es el elemento fundamental de un registrador y su misión es convertir una determinada energía eléctrica en movimiento de rotación.



Los galvanómetros tipo D'Arsonval son los más utilizados y están constituidos por una pequeña bobina con una suspensión torsional sometida a un campo magnético constante; la suspensión es portadora de un espejo que recibe un haz de luz y lo refleja sobre papel fotosensible; el paso de una corriente por la bobina crea un campo electromagnético, cuya resultante con el campo magnético del imán permanente originará el giro de la bobina y, por tanto, el del espejo de la suspensión.

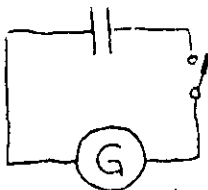
El valor T del par de torsión de la suspensión tiene por valor $T = NBi \cdot a \cdot \cos \phi$ siendo:

- N = Número de espiras
- B = Densidad de flujo
- i = Corriente en la bobina
- a = Ancho de la bobina
- ϕ = Angulo de deflexión

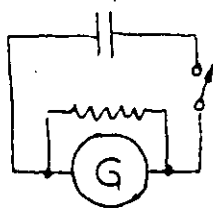
La deflexión del haz luminoso es proporcional al número de espiras de la bobina e inversamente proporcional a la constante de torsión K de la suspensión; un incremento del número de espiras y un decrecimiento de la constante K , aumentará la sensibilidad, pero también el período de la oscilación, disminuyendo, por tanto, la frecuencia natural. De aquí se deduce que un galvanómetro con amplia respuesta en frecuencia implicará sacrificio en la sensibilidad.

Un galvanómetro balístico se usa para medir la cantidad de carga desplazada por una corriente de corta duración. Supongamos (fig. a) que se cierra el interruptor e inmediatamente se abre, por G circulará una corriente de descarga que origina un giro de la suspensión. Este giro de la bobina en un campo magnético induce una f.e.m. pero, como el circuito está abierto no circula corriente por G y éste oscila indefinidamente existiendo

a)



b)



como único amortiguamiento, la fricción de la suspensión.

En la (fig. b) la corriente debida a la f.e.m., inducida por el giro, se cierra por el shunt y esta corriente origina un par de torsión que se opone al movimiento producido por la descarga del condensador. El valor de la resistencia shunt limita el valor de la corriente antagonista, existiendo un valor para el -

cual G retorna a cero sin entrar en oscilación. Este valor de shunt se denomina resistencia externa crítica de amortiguamiento (Critical External Damping Resistance, CSDR).

Galvanómetros utilizados para frecuencias bajas necesitan el amortiguamiento indicado en el párrafo anterior. Por el contrario, para altas frecuencias el amortiguamiento se consigue introduciendo la bobina en un tubo capilar con un fluido (Silicona).

Terminología de galvanómetros

Frecuencia natural (Natural Frequency). - Es la frecuencia a la que un galvanómetro sin amortiguamiento responde con la máxima amplitud.

Sensibilidad en c.c. sin amortiguamiento (Undamped d-c - Sensitivity). -

Deflexión por unidad de corriente del punto luminoso sobre un plano situado perpendicularmente a un brazo óptico determinado.

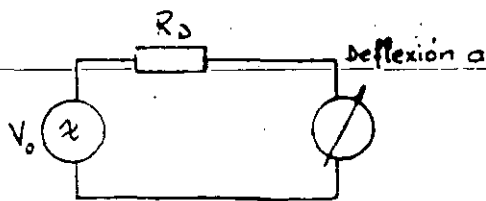
Sensibilidad en tensión (Voltage Sensitivity). - Relación de la deflexión con un determinado brazo óptico a la d.d.p. aplicada al circuito del galvanómetro, teniendo éste una resistencia interna equivalente a la resistencia de amortiguamiento.

Ejemplos

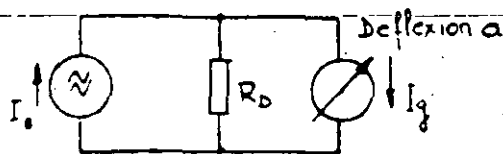
$$\text{Sensibilidad de corriente} = \frac{a}{I_0}$$

$$\text{Sensibilidad de corriente sin amortiguamiento} = \frac{a}{I_g}$$

$$\text{Sensibilidad de tensión} = \frac{a}{V_0}$$



CIRCUITO DE TENSION



CIRCUITO DE CORRIENTE

Resistencia de amortiguamiento (Damped Resistance).- Valor de resistencia requerido para el 0,64 del amortiguamiento crítico.

Desequilibrio (Galvanometer Unbalance).- Máxima deflexión que se produce en un galvanómetro al someterse a una aceleración de 1 g. en cualquier plano.

Linearidad (Linearity).- Grado de concurrencia entre una posición del punto luminoso y valor teórico dividido por deflexión específica al valor total de escala, expresado en %.

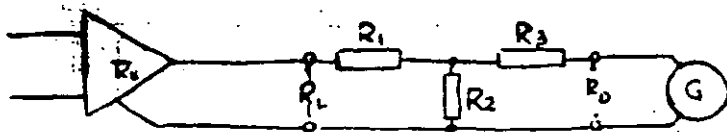
Error tangencial (Tangential Error).- Error causado al registrar en una superficie plana, en vez de una circular de radio igual al brazo óptico.

Respuesta en frecuencia (Frequency Response).- Frecuencia a la cual la respuesta es plana.

Corriente de seguridad (Safe Current).- Máxima corriente que puede pasar permanentemente por el galvanómetro sin dañarlo.

Resistencia interna (Internal Resistance).- Resistencia interna de la suspensión y bobina media con corriente continua.

Cálculo de redes de amortiguamiento.



Al conectar un galvanómetro a un amplificador ó circuito de medida se presenta el problema de acoplamiento de impedancias, ya que el amplificador tendrá un valor óptimo R_L y, a su vez, para un amortiguamiento determinado, el galvanómetro requerirá una cierta R_D . En todos los galvanómetros CEC el valor R_D indicado en sus especificaciones se refiere al 64% de su amortiguamiento crítico, equivalente a una respuesta plana hasta el 60% de su frecuencia natural.

Fijándonos en el esquema, siempre habrá unos valores $R_1 - R_2 - R_3$, que permitan un acoplo y las ecuaciones que establecen dichos valores son:

$$R_2 = K (R_g + R_D) \left[\frac{1}{1 - K^2 (R_g + R_D) / (R_L + R_S)} \right]$$

$$R_3 = \frac{(1-K)}{K} R_2 - R_g$$

$$R = SD/I_0$$

Donde

R_L = Optima impedancia de carga para el amplificador. ()

R_S = Resistencia de salida del amplificador.

R_D = Resistencia de amortiguamiento requerida por el galvanómetro.

S = Sensibilidad del galvanómetro (mA/cm).

R_g = Resistencia interna del galvanómetro

D = Deflexión deseada (cm).

I_0 = Corriente de salida del amplificador para el total de escala.

K = Constante.

En galvanómetros amortiguados electromagnéticamente, el valor h = amortiguamiento total, es la suma de dos valores, uno constante, (amortiguamiento viscoso = h_v) y otro variable (amortiguamiento magnético = h_m). Las especificaciones CEC indican estos valores para cada tipo. En ellos se cumple:

$$h = h_m + h_v$$

$$\frac{h_{m1}}{h_{m2}} = \frac{R_{D1} + R_g}{R_{D2} + R_g}$$

$$R_{D2} = \frac{h_m (R_{D1} + R_g) - h_{m2} R_g}{h_{m2}}$$

Donde

h_{m1} = Componente magnética de amortiguamiento para el 64% de amortiguamiento crítico.

h_{m2} = Componente magnética de amortiguamiento para el nuevo amortiguamiento deseado.

R_{D1} = Resistencia del amortiguamiento (64%)

R_{D2} = Nueva resistencia de amortiguamiento.

Eligiendo un determinado valor de h , (CEC incluye las curvas de respuesta de un galvanómetro para diversos h), podremos uti

F REGISTRADORES ANALÓGICOS DE CINTA MAGNÉTICA

Hace aproximadamente 30 años, Marvin Camras presentó al Navy's Bureau of Ships un instrumento que podría ser utilizado por la industria naval. Era el primer registrador en cinta magnética basado en los mismos principios que hoy se siguen utilizando.

Consideraciones teóricas

Una cinta de material ferro-magnético es el soporte de este registro. La señal eléctrica de entrada se aplica a las bobinas del circuito magnético de registro por el que pasa la cinta, el cual es sometido a una inducción proporcional al valor de entrada.

La inducción remanente forma el dato memorizado en la cinta que, al pasar por un circuito de lectura crea, por variación del flujo, una f.e.m. inducida.

Ventajas del registro magnético

Veamos primero las ventajas del registro en cinta magnética respecto a otros sistemas tradicionales, principalmente gráficos, que han hecho esta técnica indispensable en ciertos campos de aplicación y una de las más utilizadas y de más posibilidades.

1º) Permite registrar un vasto campo de frecuencias, desde c.c. hasta varios MHz.

2º) Un ~~amplificador~~ ~~campo~~ ~~de~~ ~~medida~~ ~~superior~~ ~~a~~ ~~50~~ ~~dB~~. Se conoce ~~por~~ ~~campo~~ ~~de~~ ~~medida~~ la razón, medida generalmente en dB, entre ~~la~~ ~~máxima~~ ~~señal~~ ~~medible~~ ~~sin~~ ~~distorsión~~ ~~ó~~ ~~señal~~ ~~fondo~~ ~~de~~ ~~escala~~ y la mínima señal distinguible del ruido. En otros términos, es una relación señal/ruido referida al valor fondo de escala.

Considerando la señal a medir, un campo de medida superior a 50 dB indica una resolución del orden del 0,3% del valor máximo medible.

3º) En caso de sobrecarga, los posibles desperfectos son mínimos si lo comparamos con los que se pueden suceder a galvanómetros ú otros sistemas mecánicos.

67) La información se recoge y reproduce en su forma eléctrica. Ello permite utilizar el registrador, no solo como instrumento de medida sino también para recrear el fenómeno original, utilizando en su salida un transductor inverso al utilizado en la entrada. Esta capacidad única le hace insustituible en experiencias simuladas.

La memorización de la señal en su forma eléctrica posibilita los trabajos de adquisición de datos en el laboratorio cuando las condiciones de medida no permiten hacerlo in situ.

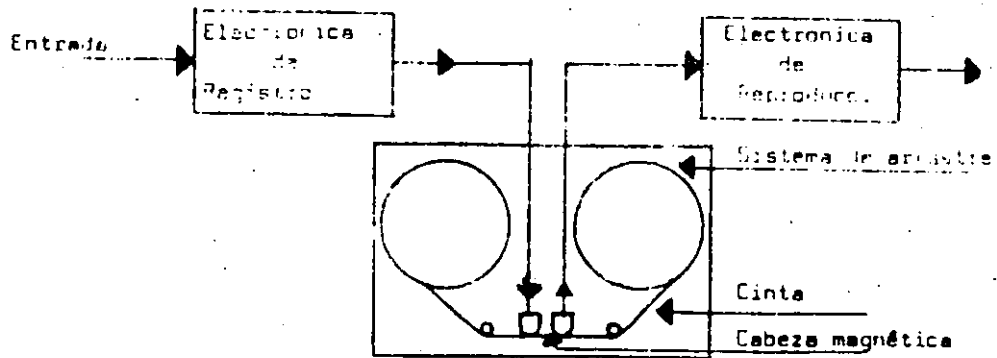
- 59) La cinta magnética puede borrarse y utilizarse de nuevo, lo que representa una gran economía frente a otros métodos.
- 69) El fenómeno registrado puede reproducirse miles de veces, lo que asegura la obtención de la máxima información para el análisis de datos.
- 72) La densidad de información obtenible en un registrador de cinta magnética no es posible con otros métodos. Cientos de canales pueden registrarse mediante técnicas de multiplexing.
- 89) Otra característica, y no la menos importante, es su facilidad para variar la base de tiempo, reproduciendo el fenómeno a distinta velocidad de la del registro.

Descripción de un registrador magnético

Con objeto de conocer alguno de los principios del diseño de estos registradores, pensados para utilización instrumental, estableceremos cuatro grupos básicos en su construcción:

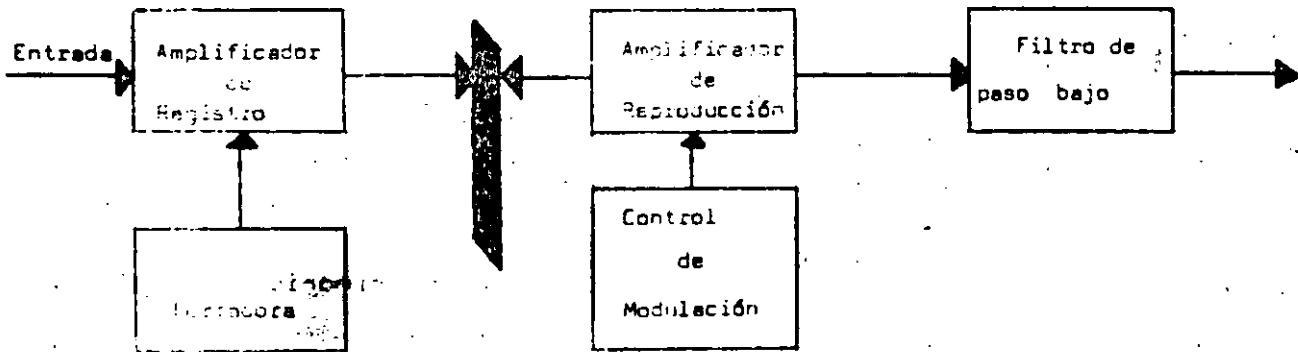
- 1º) Electrónica de registro y reproducción, que codifica la señal, prepara una forma adecuada para registro óptimo y la descodifica para dar lugar a la señal en su forma eléctrica original.
- 2º) Cabezas magnéticas que durante el registro convierten la señal eléctrica en diversos estados de magnetización de la cinta y durante la reproducción realiza el proceso inverso.
- 3º) Sistemas de arrastre cuya función es mover la cinta con la máxima suavidad y a velocidad constante. La precisión de este movimiento condiciona grandemente la calidad y coste del registrador.
- 4º) Cinta magnética constituida por un soporte delgado, magnéticamente neutro, (plástico, poliéster, generalmente) lo más resistente posi

ble a la tracción mecánica sobre la que se ha depositado una suspensión de óxido férrico.



Sistema de registro en Modulación de Frecuencia

Para compensar los inconvenientes implícitos del registro directo, se utiliza la modulación de la señal en frecuencia y así la inestabilidad de amplitud no produce trastornos en cuando que la información va contenida en la frecuencia. La imposibilidad de registrar señales de frecuencias muy bajas no existe, ya que señales en continua son, en realidad, representadas por frecuencias más ó menos altas. En todo sistema FM, el demodulador debe ir seguido por un filtro pasabajo, cuya frecuencia de corte debe ser cerca de 1/5 de la portadora.



La técnica FM lleva la señal a través de un amplificador de c.c. a un oscilador controlado por voltaje. La amplitud de la señal se convierte así en una desviación de frecuencia y la frecuencia de la señal en una velocidad de desviación. Esta portadora de frecuencia ondulada se registra en la saturación. El amplificador de reproducción demodula y filtra la señal para recoger el dato.

Una primera desventaja, inmediatamente observable, comparando los diagramas bloque, es su más compleja electrónica. Asimismo, el sistema de transporte debe ser más perfeccionado y preciso, ya que si la velocidad no es rigurosamente constante, se traduce, no en un

26. Igualmente, la respuesta de frecuencia es inferior que en el registro directo.

Sus ventajas más destacables son:

- a) Posibilidad de registrar señales en continua.
- b) Insensibilidad a las variaciones de amplitud, así como al ruido originado en la cinta. La relación señal/ruido es superior en algunas decenas de dB a la obtenible en el sistema directo.

Especificaciones de un registrador magnético

Respuesta en frecuencia

Viene determinada por la longitud del entrehierro de las cabezas reproductoras, la velocidad de transporte y el método de registro.

El límite superior de frecuencia lo alcanza cuando la longitud de onda registrada (velocidad cinta/frecuencia) equivale al entrehierro. Los registradores de instrumentación actuales operan a velocidades comprendidas entre 1 7/8 y 240 in/rec. Las versiones modernas pueden establecerse en dos categorías de bandas intermedia y de bandas anchas.

Relación señal-ruido

Es una indicación del margen dinámico de señales de entrada que pueden registrarse, reproducirse y separarse del ruido del sistema.

Se expresa en dB y en una función primaria de la electrónica de reproducción y del ruido de la cinta.

Distorsión armónica

Es la medida de la no linealidad del sistema. Se expresa como porcentaje de uno ó todos los armónicos respecto a la frecuencia fundamental sinusoidal.

Flutter

En los registradores de cinta de instrumentación se considera flutter como cualquier forma de variación de velocidad superior



**FACULTAD DE INGENIERIA U.N.A.M.
DIVISION DE EDUCACION CONTINUA**

CURSOS INSTITUCIONALES

METODOS EXPERIMENTALES DE ANALISIS DE ESFUERZOS

COMISION FEDERAL DE ELECTRICIDAD

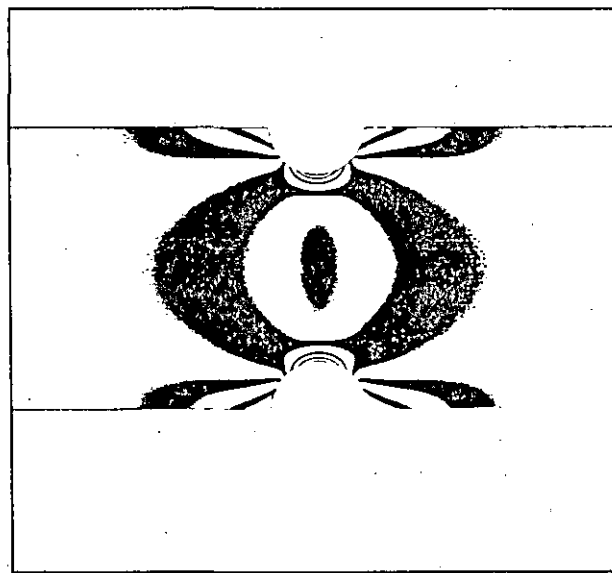
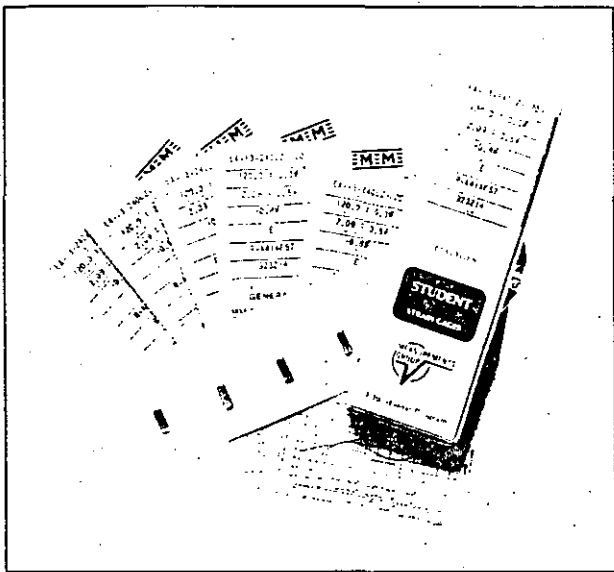
DEL 28 DE FEBRERO AL 4 DE MARZO

IRAPUATO, GTO.

A N E X O

DR. LUIS FERRER ARGOTE
ING. ALFREDO OLIVARES PONCE

1994



Teaching/Learning Aids for Experimental Stress Analysis

Education Division

Teaching/Learning Aids

Through its Micro-Measurements, Instruments, and Photolastic Divisions, the Measurements Group is dedicated to developing, manufacturing, and marketing high-quality materials and equipment for precision strain measurement and stress analysis testing. In addition to offering a broad range of products, the Measurements Group also provides extensive collateral support for those practicing experimental stress analysis. Training programs in the techniques of stress analysis, a full-time staff of applications engineers, and an extensive selection of up-to-date technical and

product literature are available to assist you in the application of experimental stress analysis technology.

The Measurements Group is equally dedicated to serving the special needs of the educational community. The Education Division was established with a commitment to providing an outlet for the resources of the Measurements Group to engineering and technology students and teachers at schools, colleges and universities around the world. In addition to offering a unique line of high-quality instructional materials and equipment, the Education Division serves as your chan-

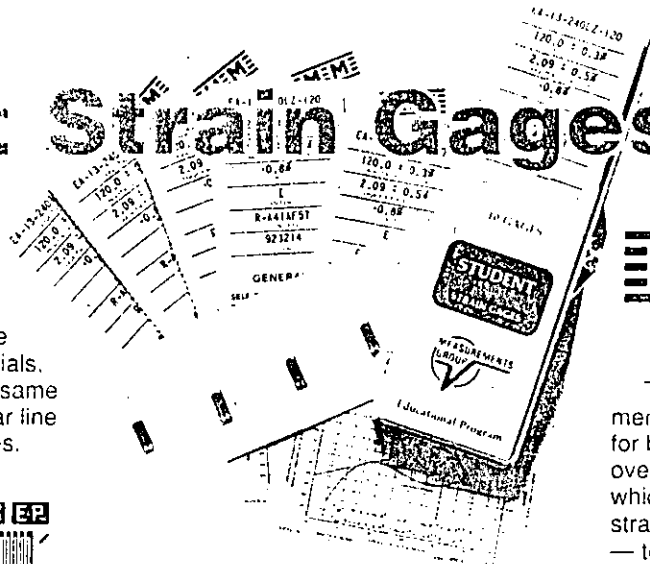
nel to the full range of Measurements Group experimental stress analysis products and services.

This brochure describes a selection of Measurements Group products with exceptional utility as teaching and learning aids. These technically sound and academically effective instructional materials and equipment are now in use in hundreds of technical high schools, technical institutes, engineering colleges, and universities.

The teaching and learning aids described in this brochure are fully compatible with the entire range of Measure-

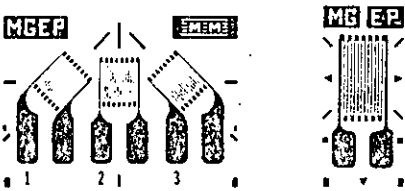
Student Strain Gages

Student Gages are a group of ten Micro-Measurements EA-Series and CEA-Series strain gage types specially designed for student use. These strain gages are manufactured from the same materials, by the same processes, and to the same high-quality standards as the regular line of Micro-Measurements strain gages.



MEME Strain Gages

The complete line of Micro-Measurements precision strain gages is available for both teaching and research uses. With over 250,000 possible gage types from which to select, a Micro-Measurements strain gage for every measurement need — teaching or research — can be found in Catalog 500.



resistance and all include a polyimide encapsulation of the grid. The CEA-Series gages feature extra-large copper-coated solder tabs.

Student Gages are supplied in a standard package quantity of ten gages. Each package of gages contains ten engineering data forms with gage type, resistance, gage factor, transverse sensitivity, and thermal output data which have been compiled specifically for the gages in the package.

Because costs are heavily subsidized, Student Gages are provided exclusively for use in those teaching and learning activities which are an integral part of a formal course of study.

For information on how to qualify for Student Gages, ask for Bulletin 307 or write to the Education Program Coordinator.

Like others in the EA Series, Student Gages have constantan metal foil grids and tough, flexible polyimide backings. Student Gages are produced in three single-element linear patterns (LZ) and in a three-element rectangular rosette (RZ). The LZ patterns are available with 0.060-, 0.120-, and 0.240-in (1.5-, 3-, and 6-mm) active gage lengths. The RZ rosette is designed with 0.060 in (1.5 mm) active grid lengths. CEA-Series Student Gages are available only in a linear pattern (UZ) with 0.240-in (6-mm) active gage length. All patterns of Student Gages are produced in 06 and 13 ppm/°F self-temperature-compensations for use on steels and on aluminum alloys, respectively. All gages are 120Ω in

MEME Practice Patterns

Practice Patterns are uniquely designed for developing strain gage bonding and soldering techniques. They are similar in appearance to EA-Series strain gages and are constructed of the same materials. Because they contain inactive grids, Practice Patterns cannot be used to measure strain.

These training aids are ideally suited to first-time strain gage users. Write to the Education Program Coordinator for more details.

ments Group products for strain measurement and stress analysis testing. In fact, they are differentiated only by their usefulness in teaching and learning activities.

Student Understanding

Measurements Group teaching and learning aids are directed toward improving and deepening student understanding of stresses and strains by emphasizing:

- how, why, and where they occur
- their relevance to the design of safe, economical components, machines, and structures
- how to measure them
- how to control and limit them

Such understanding is critical for students who will become technicians or engineers. Therefore, these educational aids are particularly relevant and

beneficial to those courses in:

- mechanics of deformable solids (strength of materials)
- machine design
- experimental stress analysis
- materials science
- measurements and instrumentation
- structures and structural design
- design for safety and reliability
- value engineering
- failure analysis

Teaching/Learning Aids

Measurements Group instructional products have been designed for maximum adaptability in supplementing and enriching established courses without revamping or restructuring them.

The educational products utilize strain gage and photoelastic stress analysis techniques as vehicles for accomplishing their tutorial purposes. Basic products for

strain gage and photoelastic techniques are also available separately.

Learning is Faster and More Complete

Learning is faster, easier, and in greater depth when the principles of mechanics, mechanical design, structures, and stress analysis are actually experienced by the student.

Measurements Group teaching/learning aids are intended to generate student interest, provide motivation, and develop comprehension of stress and strain concepts which otherwise tend to remain abstractions.

The learning aids described in this brochure are flexible and can be employed in a purely illustrative or demonstrative fashion or as fundamental components of course content. Most of them are also open-ended, and provide the means for the imaginative teacher (or student) to explore advanced areas.



The Student Strain Gage Application Kit contains an assortment of those Micro-Measurements *M-LINE* Accessories necessary for making successful strain gage installations in the laboratory. In addition to the materials for preparing the specimen surface for bonding, the kit includes both the popular, fast-curing M-Bond 200 cyanoacrylate and the durable, creep-free M-Bond AE-10 epoxy strain gage adhesive systems. All the tools and materials for bonding and soldering strain gages — including a controlled-temperature soldering iron — are provided. Designed with the student in mind, each kit comes complete with practice materials for developing strain gage installation techniques. Up to four students can work from one kit. The Student Strain Gage Application Kit is

packaged in a durable storage box. All items are fully compatible with, and may be supplemented by, the complete line of Micro-Measurements *M-LINE* Strain Gage Accessories. All consumables in the kit are replaceable from standard Micro-Measurements stock. For a complete list of contents, ask for Bulletin 310.

M-LINE Accessories

Making accurate and reliable measurements with electrical resistance strain gages in the classroom or laboratory requires installation with high-quality accessory tools, materials, and supplies qualified for making strain gage installations. Ask for Catalog A-110 which describes the complete line of Micro-Measurements *M-LINE* Strain Gage Accessories.

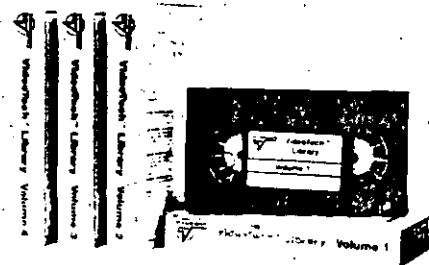
VideoTech™ Libraries

The VideoTech Library is a series of instructional VHS videotapes for strain gage installation.

The procedures outlined in the VideoTech Library will help both novice and experienced strain gage users to make reliable, professional-caliber strain gage installations every time.

The videotape presentation format of these dependable, proven, state-of-the-art methods can be adapted with equal success to individual, self-taught programs, or to group training sessions. Each tape contains instruction for general-purpose surface preparation, gage bonding, leadwire attachment, and typical environmental protections. Organized in detailed, fully illustrated steps, each tape concludes with an example of a successful strain gage installation.

With the VideoTech Library at hand, the student *learns by doing* each of the prescribed steps to reproduce the actual installation. For additional details concerning these instructional videotapes, request Bulletin 318.



Experiments In Mechanics

Experiments In Mechanics — Strain Gage Series are six complete experiments designed by C.C. Perry around the simple cantilever beam. (They are intended to teach mechanics, using experimental stress analysis technology as the teaching medium.) Presented in a logical, easy-to-follow format on 8-1/2 x 11 in (216 x 279 mm) pages, each experiment will yield consistently accurate and meaningful results when the instructions are carefully followed. Necessary supplemental information such as wiring diagrams, work sheets, graphs, and illustrations is included. Additionally, a list of the learning opportunities embodied in the experiment, as well as sources of errors and estimates of time required to perform the experiment, are contained in separate "Notes to the Instructor" provided with each set of experiments.

Experiments In Mechanics are complete exercises requiring a minimum of preparation time for the instructor. The experiments employ conventional strain gage technology and are coordinated with the beams described below.

Experiments In Mechanics are available separately or in complete sets.

Experiment E-101

Modulus of Elasticity — Flexure

Designed for use with Pregaged Beam B-101.

With a single strain gage mounted along the axis and near the fixed end of a cantilever beam, the student determines modulus of elasticity of the beam material by:

1. Measuring the beam dimensions.
2. Applying a known load to the free end of the beam.
3. Calculating the stress at the strain gage location from (1) and (2) with the flexure formula.
4. Measuring the strain along the beam axis.
5. Calculating the modulus of elasticity from (3) and (4), using Hooke's law.

Experiment E-102

Poisson's Ratio — Flexure

Designed for use with Pregaged Beam B-102.

In this experiment, two strain gages are used, one along the axis on the upper surface of the beam, and one transverse-ly oriented at the same section on the lower surface on the beam.

After applying an arbitrary displacement or load to the beam, the two strains are measured, and the Poisson's ratio of the beam material is calculated from these data.

Experiment E-103 Principal Strains and Stresses — Flexure

Designed for use with Pregaged Beam B-103.

A three-element strain gage rosette is mounted on a cantilever beam for this experiment. The rosette is oriented so that none of the element axes coincide with the axes of symmetry of the beam.

After applying a known load to the beam, the student measures the strains along the three rosette axes and calculates the principal strains from the strain transformation relationships. Using the biaxial Hooke's law, the student calcu-

Cantilever Beams

Cantilever Beams, designed for use with the Flexor, are coordinated with **Experiments In Mechanics**, but can be used separately for other demonstrations or experiments. All beams are manufactured from 2024-T6 high-strength aluminum alloy and are 1 in (25.4 mm) wide by 12.5 in (317.5 mm) long. Beams designed for Experiments E-101 and E-103 are 0.125 in (3.18 mm) thick. All others are 0.250 in (6.35 mm) thick.

Ungaged Beams

Ungaged Beams permit specialized instruction and are particularly valuable when instructional time is sufficient to allow students to mount their own strain gages.

Catalog No.	Description	For Use With Experiment No.
UB-01	0.125 in (3.18 mm) thick rectangular beam	E-101, E-103
UB-02	0.250 in (6.35 mm) rectangular beam	E-102, E-105

Special Configuration Beams

Special Configuration Beams are designed for advanced work in measuring stress concentrations. They are engaged to afford students the opportunity to position and mount their own strain gages.

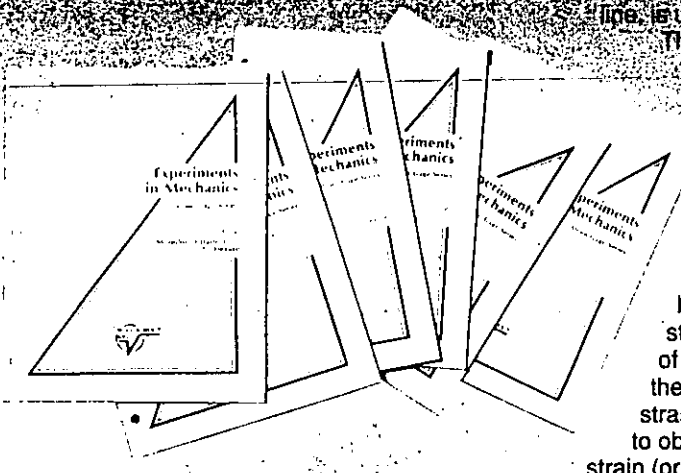
Catalog No.	Description	For Use With Experiment No.
UBS-01	Stress Concentration — with a 1/4 in (6.35 mm) drilled and reamed hole	E-104
UBS-02	Stress Concentration — with accurately milled symmetrical U-Notches	E-104
UBS-03	Constant Stress — two-stage tapered beam with two constant-stress levels	E-106

Pregaged Beams

Pregaged Beams are instrumented with Micro-Measurements temperature-compensated foil strain gages. The strain gage installations are fully wired and are covered with a clear protective coating. In addition, all installations are factory tested for resistance, stability, and freedom from creep.

Catalog No.	For Use With Experiment No.	Number Of Gages	Gage Type	Gage Length (in)
B-101	E-101	1	Linear	0.125
B-102	E-102	2	Linear	0.125
B-103	E-103	1	3-Element Rosette	0.125
B-104	E-104	3	Linear	0.030
		1	Linear	0.125
B-105	E-105	3	Linear	0.125
B-106	E-106	4	Linear	0.125





line, is used in this experiment. Three very small strain gages are mounted at varying distances from the edge of the hole to permit measuring the local increase in strain due to the presence of the hole. The student is shown how to extrapolate the strain data to the edge of the hole, and compare the result to the nominal strain at the same section to obtain a measure of the strain (or stress) concentration factor.

The slope of the moment distribution with the strain gages mounted at various points along the beam is related to the slope of the strain distribution. This arrangement of the constant stress indicator is flexible enough to measure the vertical shear force. This technique can be used to make a load or force transducer for which the output is independent of the point of load application, as long as it is not between the two strain gages.

**Experiment E-106
Constant Stress Beams**
Designed for use with Pregaged Beam B-106.

The constant stress beam is employed in this experiment as a vehicle for teaching the relationships among bending moment, section modulus, and stress or strain in a beam while at the same time introducing the student to the concept of efficient beam design.

lates the principal stresses from the principal strains. These results are compared with the stress calculated from the flexure equations for the known load and measured beam dimensions.

**Experiment E-104
Stress and Strain Concentration**
Designed for use with Pregaged Beam B-104.

A cantilever beam with a hole through the thickness of the beam, on the center-

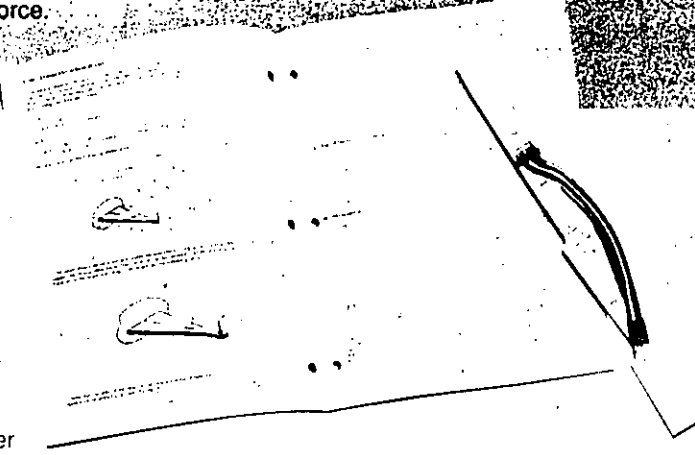
**Experiment E-105
Cantilever Flexure**
Designed for use with Pregaged Beam B-105

This experiment provides a practical demonstration of the relationship between the vertical shear force and bending moment distributions in a beam. It exploits the fact that the derivative (slope) of the bending moment distribution is equal to the vertical shear force.

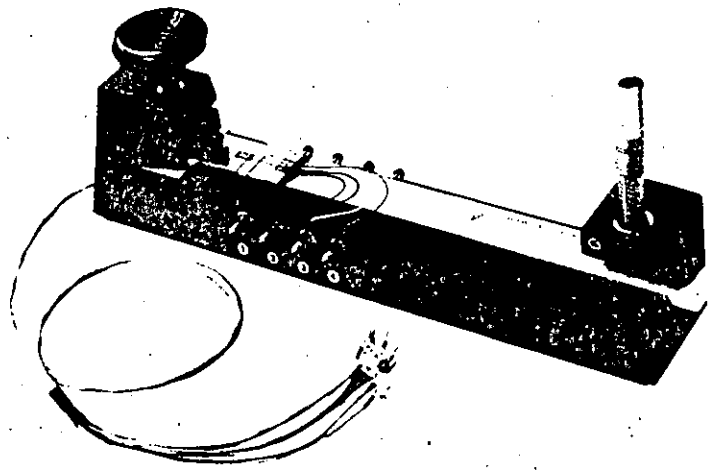
Flexor

The Flexor, a cantilever flexure frame, is a simple, versatile, and portable all-in-one fixture for loading beams. The cantilever-beam principle is particularly appropriate for measuring basic materials properties, and for performing strain gage and other stress analysis experiments. The test specimens are inexpensive and simple to fabricate, and

only modest forces are required to develop large strains and high stresses. Since the cantilever beam is a fundamental and widely used structural element, the Flexor offers numerous associated advantages as a technical teaching aid.



Deflections are produced and measured by a micrometer, and strains of up to 2500 $\mu\epsilon$ can be obtained on a 0.250 in (6.35 mm) thick beam. The Flexor can also be used with deadweights. Eight integral push-clamp binding posts on the side of the Flexor are used for intermediate connections to the gaged beams. The binding posts are prewired to an attached instrument cable which conveniently connects to a strain indicator. The Flexor is 13-1/4 in (335 mm) long, 4-3/4 in (120 mm) high and 2-1/2 in (65 mm) deep. It weighs 3-1/2 lb (1.6 kg). Three ungaged high-strength aluminum alloy beams, a weight hook, and user's manual are provided with each Flexor. The Flexor is recommended for all Experiments in Mechanics.

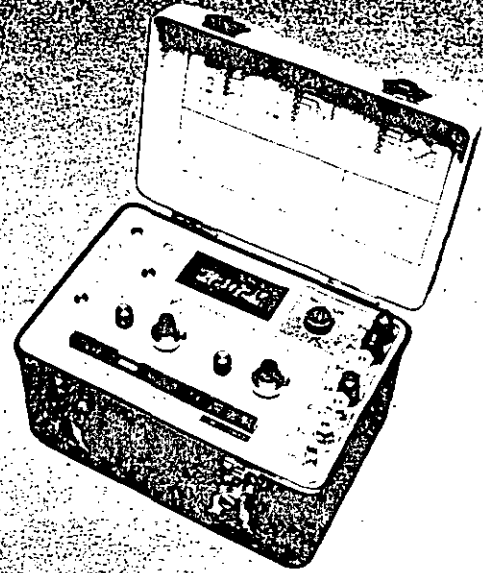


Strain Gage Instrumentation

A wide range of state-of-the-art strain gage instrumentation is available from the Measurements Group Instruments Division. Many of these instruments are ideally suited for use in the classroom or teaching laboratory. The **Model P-3500 Strain Indicator**, for example, is a portable, lightweight, rugged instrument which can be used both for stress analysis testing and strain-gage-based transducers. Featuring an LCD (or optional LED) readout, the P-3500 will accept full-, half-, or quarter-bridge strain gage inputs, and provides direct readings of strain, pressure, torque, load, and other engineering variables. An auxiliary analog output for driving an external oscilloscope or recorder is also provided. The

bridge excitation potential of 2 Vdc results in low bridge operating power and negligible drift due to gage self-heating. The P-3500 Strain Indicator is the most easy-to-use instrument of its kind. By following a logical sequence of set-up steps and activating color-coded push-button controls, even the most inexperienced user can rapidly prepare the instrument for making accurate and reliable measurements.

For making dynamic measurements, the **2100 System** is designed to accept inputs from strain gages; load, pressure, and dc-displacement transducers; and nickel temperature sensors. With a standard bandpass of dc to 5 kHz minimum at -0.5 dB, the 2100 System accepts low-



level signals, and conditions and amplifies them into high-level outputs suitable for multi-channel simultaneous dynamic recording. The system is com-

Teaching Polariscope

Photoelastic methods of stress analysis provide a complete "picture" of the stress distributions in a structure. As a result, they have become increasingly important elements in the design of modern products. The **080 Series Teaching Polariscope System** will enable you to give your students a firm foundation in this valuable technology and will add new understanding to courses in design and strength of materials.

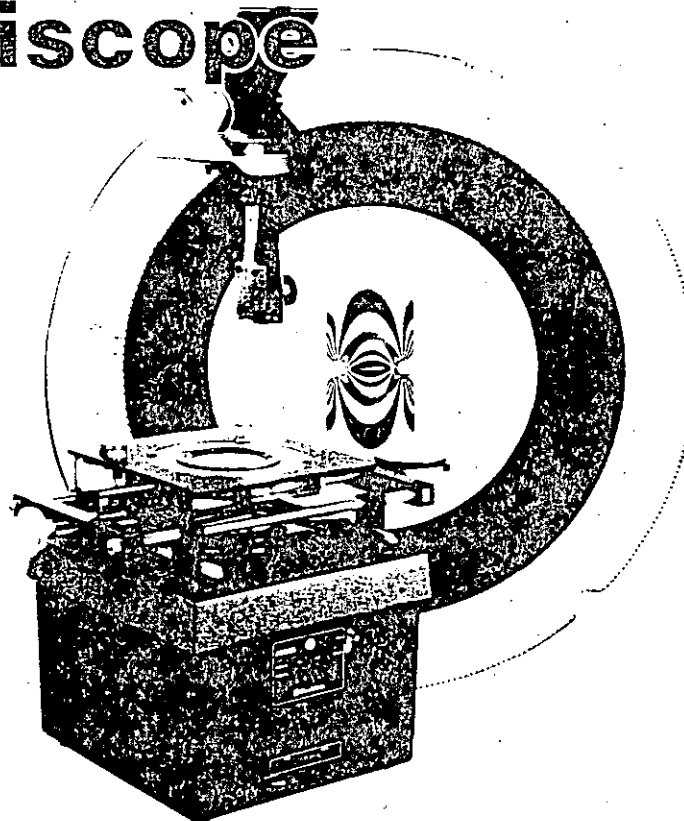
The Model 081 Teaching Polariscope is a complete working polariscope which can be used to graphically demonstrate and teach the principles of photoelasticity and its application to stress analysis. Because it has all the elements of a bench-mounted laboratory instrument, the 081 is also an excellent device for teaching the theory and operation of a polariscope.

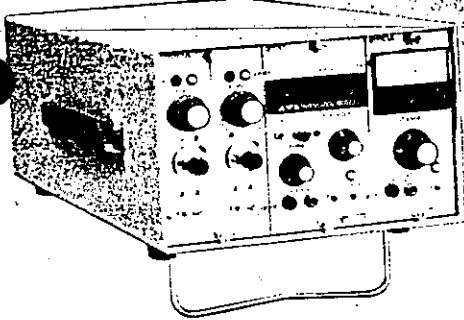
The 081 can be easily carried to the classroom and quickly set up for use. It is designed to be placed on an overhead projector and allows students to observe the different measuring operations necessary to determine the stress directions and magnitudes of the projected photoelastic pattern. Quantitative measurements are made through the use of a transparent dial which surrounds the projected pattern.

The Polariscope consists of a sturdy anodized metal frame, two plane polarizing filters, two removable quarter-wave filters, and the transparent numbered dial. A mechanical drive system is provided

for rotating all four filters simultaneously. The filters are laminated in glass for excellent light transmission as well as durability.

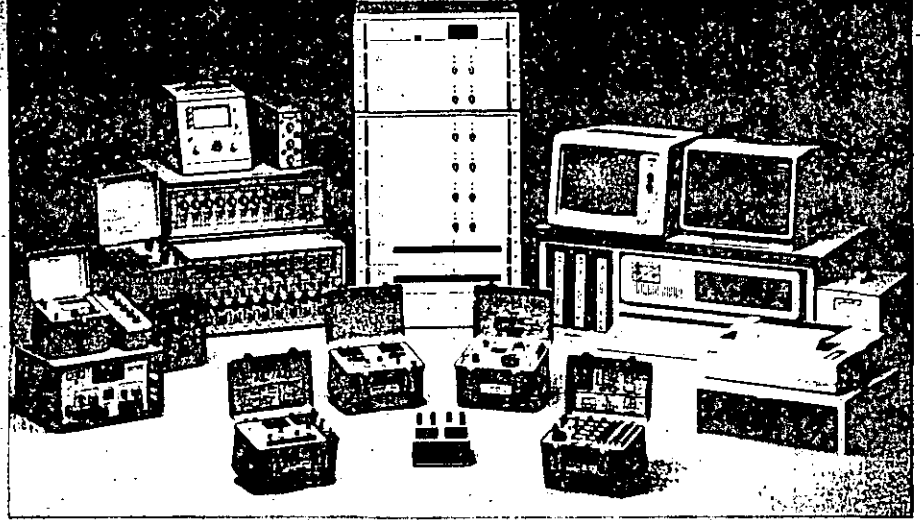
A full line of accessories is also available to extend the usefulness of the polariscope in teaching and research. The recommended 080 System would include a straining frame with mechanical force dial indicator, support stage for stress-frozen models, uniform-field digital compensator, monochromator, and a set of educational models. For additional information on the 080 Series Teaching Polariscope System, ask for Bulletin 306. For information about other reflection and transmission polariscopes and photoelastic materials and supplies, ask for short form catalog SFC-300.





patible with galvanometers, computers, and strip-chart, magnetic tape, and X-Y recorders. Each 2110A power supply module will power up to five 2120A dual channel conditioner/amplifier modules (ten channels total). With the optional 2130/2131 digital readout module, the 2100 System can also function as a direct-reading static strain indicator.

Also available is a complete line of accessories and auxiliary instruments, including strain-indicator calibrators and

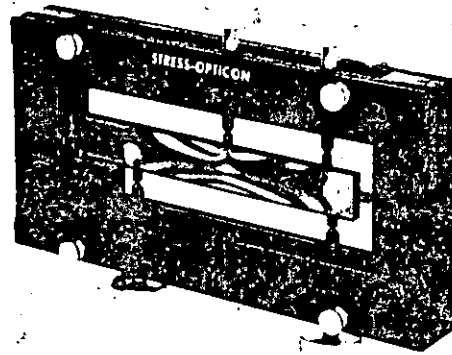


a gage installation tester.
For information about the complete line of strain gage instrumentation — including the System 4000 computer-

based stress analysis data system — consult your Strain Gage Technology Master Binder or ask for short-form catalog SFC-600.

Stress-Opticon

The Stress-Opticon is a unique, textbook size instrument which can be used to demonstrate the fundamental principles of stress analysis, mechanics of materials and the general nature of stress distribution in various structural



shapes. Its five movable loading screws allow an infinite variety of loading

modes — e.g., cantilever bending, column, statically indeterminate beam, and eccentrically loaded column — to be studied on a single prismatic model.

Each of the eight models available for the Stress-Opticon is a separate structural shape which can be easily correlated to standard textbook examples.

The Stress-Opticon is effective in room lighting, requiring no special light source. For lecture purposes, it can be used with an overhead projector for particularly dramatic presentations. In addition, it is lightweight, yet rugged enough to be passed from student to student during laboratory courses.

The Stress-Opticon is 9 in (229 mm) long, 6 in (150 mm) high and 1-1/2 in (38 mm) deep. The device comes complete with a detailed instruction manual and structural Model No. M-241.

Each Stress-Opticon model is a specific structural shape which can be subjected to a variety of different loading arrangements.

The models are machined from Type PSM-1 Plastic, a durable, non-brittle photoelastic material that is high in photoelastic sensitivity and free from time-edge effects.

PSM-1 Plastic is also available for custom designing photoelastic models and comes complete with machining instructions for producing models without initial fringes.

The accompanying photographs show the stress distribution for only one of the many loading conditions possible with each model.

Stress-Opticon Models



Model M-241: Standard prismatic model for teaching beam and column theories, St Venant's principle, and others



Model M-242: Standard model with 3/16 in (4.8 mm) diameter central hole for teaching stress concentration. Elastic stress concentration factor (K_t) approximately 2.43 for axial load.



Model M-243: Standard model with 3/8 in (9.5 mm) diameter central hole for teaching stress concentration. Elastic stress concentration factor (K_t) approximately 2.16 for axial load.



Model M-244: Model with symmetrical semicircular notches for teaching stress concentration. Elastic stress concentration factor approximately 1.9, axial; 1.6, bending.



Model M-245: Dual section structural member for teaching relationship between stress and cross-sectional properties, as well as stress concentration in fillets.



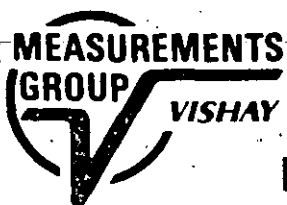
Model M-246: Representative mechanical component configuration for teaching photoelastic stress measurement in arbitrary shapes.



Model M-247: Knee frame for teaching stress distribution in typical structural shapes.



Model M-248: Arch for teaching stress distribution in classical structural member.

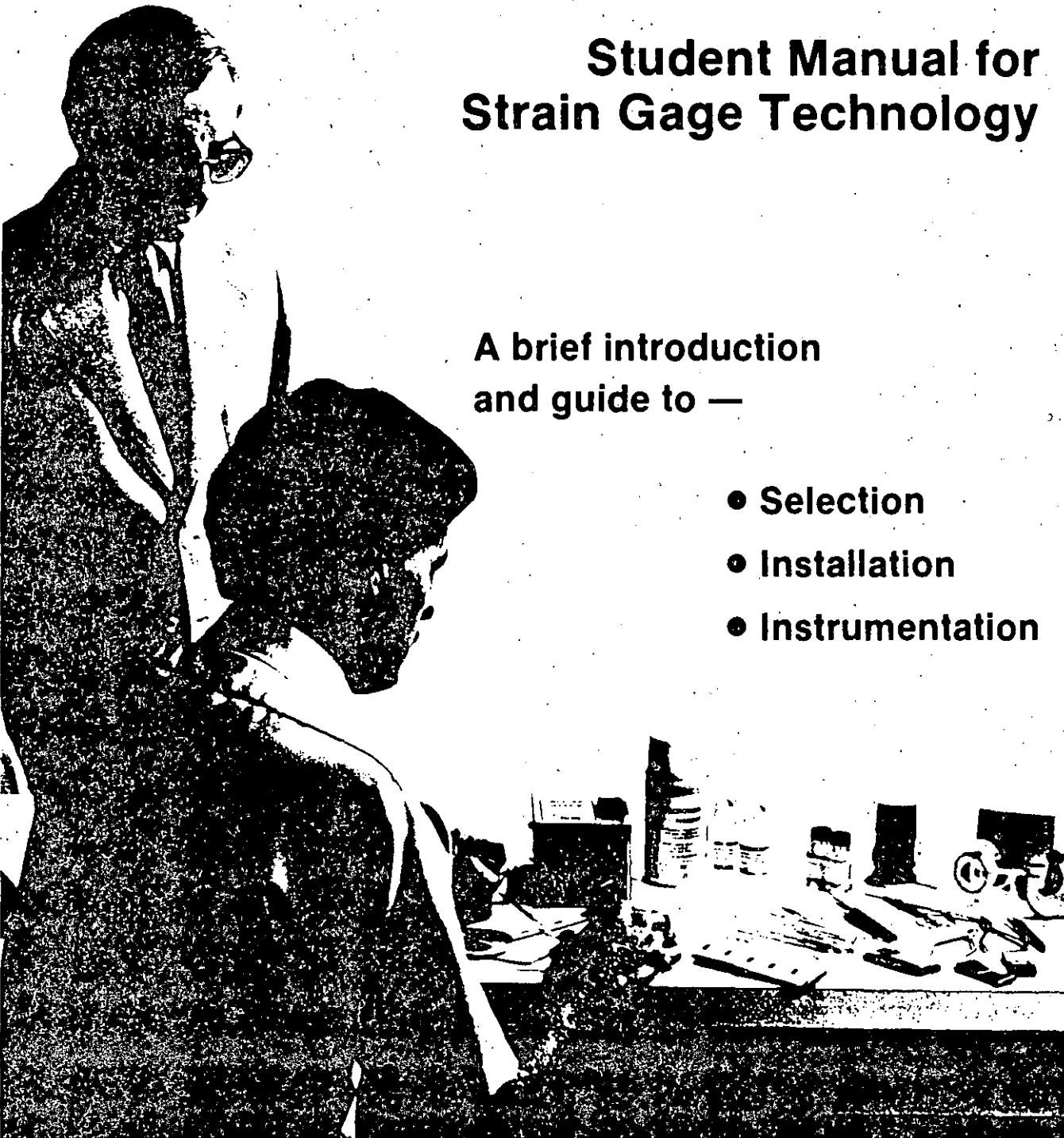


Education Division

Student Manual for Strain Gage Technology

A brief introduction
and guide to —

- Selection
- Installation
- Instrumentation



Introduction to Strain Gage Technology

Experimental Stress Analysis is an established, popular engineering tool, routinely used in the design of safe and reliable products and engineering structures. The techniques of experimental stress analysis may be applied at different stages in the life of a product; from preliminary design concepts to testing of the finished product; in proof and overload testing; and in failure analysis of products already in service. Within the broad field of experimental stress analysis, several practical techniques are available, including photoelastic coatings and models, moiré, and electrical resistance strain gages.

Of these techniques, the modern bonded electrical resistance strain gage is widely recognized as the most practical technology for testing of load-bearing parts, members, and structures. Because both excellent accuracy and repeatability can be achieved, strain gages are also becoming increasingly important as primary sensing elements in load cells as well as in pressure, force, torque, displacement, and other specialized transducers.

To make strain measurements of acceptable quality — whether for structural testing or for transducer applications

— requires the consideration of several well-defined parameters: quality of the strain gage itself; proper selection of the strain gage, bonding adhesive, environmental protection, and other strain gage accessories; proper circuit design, proper installation of the strain gage; and quality of the strain gage instrumentation. While the importance of these parameters is well understood by the experienced stress analyst, their significance may be less obvious to those unfamiliar with strain gage technology. The purpose of this manual is to familiarize students with the proper techniques of strain measurements with electrical resistance strain gages.

In addition to providing high-quality, state-of-the-art strain gages and strain gage instrumentation, the Measurements Group maintains an extensive selection of technical and product literature describing the techniques, equipment, and practical application of strain gage technology. This manual is a compendium of the Measurements Group strain gage literature, specially selected to provide the student with a sound introduction to the hardware and procedures of strain gage methods. It includes the following topics:

- **Strain Gage Selection Criteria, Procedures, Recommendations:** The parameters for gage selection — including strain sensing alloy, backing material, gage length and pattern, self-temperature compensation, gage resistance, and gage options — are detailed. Examples are given of gage selections made in actual application.
- **Strain Gage Installations with M-Bond 200 and AE-10 Adhesive Systems:** Steps used by professional stress analysts in preparing the test specimen and making gage installations with both M-Bond 200 cyanoacrylate and M-Bond AE-10 epoxy adhesive systems are described in detail. Also included is a section of two- and three-leadwire strain gage circuits and a troubleshooting guide. By following the detailed, illustrated steps, the first-time strain gage user can make dependable installations.

In the later sections, the hardware of strain gage technology is described:

- **Description of Strain Gages and Accessories:** Partial listings of Micro-Measurements strain gages show the range of modern foil strain gage sizes and geometries. Included are linear patterns, three-element rosettes, pressure diaphragm gages, shear patterns, and others. Also included is a description of the accessory materials and equipment necessary for making good, sound installations.
- **Description of Strain Gage Instrumentation:** The range of instrumentation — including static, dynamic, and computer-controlled stress analysis systems — is shown. A selection chart is provided as a guide in determining the type of instrumentation best suited to a specific measurement application.
- **Reading List:** Additionally, a reading list of recommended references is provided for supplemental study.

MEASUREMENTS GROUP

TECH NOTE

Strain Gage Selection Criteria, Procedures, Recommendations

1.0 Introduction

The initial step in preparing for any strain gage installation is the selection of the appropriate gage for the task. It might at first appear that gage selection is a simple exercise, of no great consequence to the stress analyst; but quite the opposite is true. Careful, rational selection of gage characteristics and parameters can be very important in: optimizing the gage performance for specified environmental and operating conditions, obtaining accurate and reliable strain measurements, contributing to the ease of installation, and minimizing the *total* cost of the gage installation.

The installation and operating characteristics of a strain gage are affected by the following parameters, which are selectable in varying degrees:

- strain-sensitive alloy
- backing material (carrier)
- gage length
- gage pattern
- self-temperature-compensation number
- grid resistance
- options

Basically, the gage selection process consists of determining the particular available combination of parameters which is most compatible with the environmental and other operating *conditions*, and at the same time best satisfies the installation and operating *constraints*. These constraints are generally expressed in the form of requirements such as:

- accuracy
- stability
- temperature
- elongation
- test duration
- cyclic endurance
- ease of installation
- environment

The cost of the strain gage itself is not ordinarily a prime consideration in gage selection, since the significant economic measure is the total cost of the complete installation, of which the gage cost is usually but a small fraction. In many cases, the selection of a gage series or optional feature which increases the gage cost serves to decrease the total installation cost.

It must be appreciated that the process of gage selection generally involves compromises. This is because parameter choices which tend to satisfy one of the constraints or requirements may work against satisfying others. For example, in the case of a small-radius fillet, where the space available for gage installation is very limited, and the strain gradient extremely high, one of the shortest available gages might be the obvious choice. At the same time, however, gages shorter than about 0.125 in (3 mm) are generally characterized by lower maximum elongation, reduced fatigue life, less stable behavior, and greater installation difficulty. Another situation which often influences gage selection, and leads to compromise, is the stock of gages at hand for day-to-day strain measurements. While compromises are almost always necessary, the stress analyst should be fully aware of the effects of such compromises on meeting the requirements of the gage installation. This understanding is necessary to make the best overall compromise for any particular set of circumstances, and to judge the effects of that compromise on the accuracy and validity of the test data.

The strain gage selection criteria considered here relate primarily to stress analysis applications. The selection criteria for strain gages used on transducer spring elements, while similar in many respects to the considerations presented here, may vary significantly from application to application and should be treated accordingly. The Measurements Group's Transducer Applications Department can assist in this selection.



MEASUREMENTS GROUP, INC.
P.O. Box 27777
Raleigh, North Carolina 27611, USA

(919) 365-3800
Telex 802-502
FAX (919) 365-3945

2.0 Gage Selection Parameters

2.1 Strain-Sensing Alloys

The principal component which determines the operating characteristics of a strain gage is the strain-sensitive alloy used in the foil grid. However, the alloy is not in every case an independently-selectable parameter. This is because each of Micro-Measurements strain gage series (identified by the first two, or three, letters in the alphanumeric gage designation — see diagram on page 11) is designed as a complete system. That system is comprised of a particular foil and backing combination, and usually incorporates additional gage construction features (such as encapsulation, integral leadwires, or solder dots) specific to the series in question.

Micro-Measurements supplies a variety of strain gage alloys as follows (with their respective letter designations):

- A: Constantan in self-temperature-compensated form.
- P: Annealed constantan.
- D: Iso-Elastic.
- K: Nickel-chromium alloy, a modified Karma in self-temperature-compensated form.

2.1.1 Constantan Alloy

Of all modern strain gage alloys, constantan is the oldest, and still the most widely used. This situation reflects the fact that constantan has the best overall combination of properties needed for many strain gage applications. This alloy has, for example, an adequately high strain sensitivity, or *gage factor*, which is relatively insensitive to strain level and temperature. Its resistivity is high enough to achieve suitable resistance values in even very small grids, and its temperature coefficient of resistance is not excessive. In addition, constantan is characterized by good fatigue life and relatively high elongation capability. It must be noted, however, that constantan tends to exhibit a continuous drift at temperatures above +150° F (+65° C); and this characteristic should be taken into account when zero stability of the strain gage is critical over a period of hours or days.

Very importantly, constantan can be processed for self-temperature-compensation (see box at right) to match a wide range of test material expansion coefficients. Micro-Measurements A alloy is a self-temperature-compensated form of constantan. A alloy is supplied in self-temperature-compensation (S-T-C) numbers 00, 03, 05, 06, 09, 13, 15, 18, 30, 40 and 50, for use on test materials with corresponding thermal expansion coefficients (expressed in ppm/° F).

For the measurement of very large strains, 5% (50 000 $\mu\epsilon$) or above, annealed constantan (P alloy) is the grid material normally selected. Constantan in this form is very ductile; and, in gage lengths of 0.125 in (3 mm) and longer, can be strained to >20%. It should be borne in mind, however, that under high cyclic strains the P alloy will exhibit some permanent resistance change with each cycle, and cause a corresponding zero shift in the strain gage. Because of this characteristic, and the tendency for premature grid failure with repeated straining, P alloy is not ordinarily recommended for cyclic strain applications. P alloy is available with S-T-C numbers of 08 and 40 for use on metals and plastics, respectively.

2.1.2 Iso-Elastic Alloy

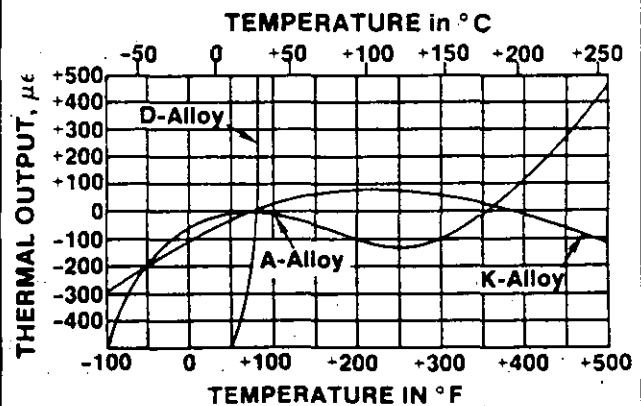
When purely dynamic strain measurements are to be made — that is, when it is not necessary to maintain a stable reference zero — Iso-Elastic (D alloy) offers certain advantages. Principal among these are superior fatigue life, compared to A alloy, and a high gage factor (approximately 3.2) which improves the signal-to-noise ratio in dynamic testing.

Self-Temperature-Compensation

An important property shared by constantan and modified Karma strain gage alloys is their responsiveness to special processing for self-temperature-compensation. Self-temperature-compensated strain gages are designed to produce minimum thermal output (temperature-induced apparent strain) over the temperature range from about -50° to +400° F (-45° to +200° C). When selecting either constantan (A-alloy) or Karma (K-alloy) strain gages, the self-temperature-compensation (S-T-C) number must be specified. The S-T-C number is the approximate thermal expansion coefficient in ppm/° F of the structural material on which the strain gage will display minimum thermal output.

The accompanying graph illustrates typical thermal output characteristics for A and K alloys. The thermal output of uncompensated Iso-Elastic alloy is included in the same graph for comparison purposes. In normal practice, the S-T-C number for an A- or K-alloy gage is selected to most closely match the thermal expansion coefficient of the test material. However, the thermal output curves for these alloys can be rotated about the room-temperature reference point to favor a particular temperature range. This is done by intentionally mismatching the S-T-C number and the expansion coefficient in the appropriate direction. When the selected S-T-C number is lower than the expansion coefficient, the curve is rotated counterclockwise. An opposite mismatch produces clockwise rotation of the thermal output curve. Under conditions of S-T-C mismatch, the thermal output curves for A and K alloys (supplied with each package of strain gages) do not apply, of course, and it will generally be necessary to calibrate the installation for thermal output as a function of temperature.

For additional information on strain gage temperature effects, see Measurements Group Tech Note TN-504.



D alloy is not subject to self-temperature-compensation. Moreover, as shown in the graph (see box), its thermal output is so high [about $80\mu\epsilon/^\circ F$ ($145\mu\epsilon/^\circ C$)] that this alloy is not normally usable for static strain measurements. There are times, however, when D alloy finds application in special-purpose transducers where a high output is needed, and where a full-bridge arrangement can be used to achieve reasonable temperature compensation within the circuit.

Other properties of D alloy should also be noted when considering the selection of this grid material. It is, for instance, magnetoresistive; and its strain-sensitive response is somewhat nonlinear, becoming significantly so at strains beyond $\pm 5000\mu\epsilon$.

2.1.3 Karma Alloy

Modified Karma, or K alloy, with its wide areas of application, represents an important member in the family of strain gage alloys. This alloy is characterized by good fatigue life and excellent stability; and is the preferred choice for accurate static strain measurements over long periods of time (months or years) at room temperature, or lesser periods at elevated temperature. It is recommended for extended static strain measurements over the temperature range from -452° to $+500^\circ F$ (-269° to $+260^\circ C$). For short periods, encapsulated K-alloy strain gages can be exposed to temperatures as high as $+750^\circ F$ ($+400^\circ C$). An inert atmosphere will improve stability and extend the useful gage life at high temperatures.

Among its other advantages, K alloy offers a much flatter thermal output curve than A alloy, and thus permits more accurate correction for thermal output errors at temperature extremes. Like constantan, K alloy can be self-temperature-compensated for use on materials with different thermal expansion coefficients. The available S-T-C numbers in K alloy are limited, however, to the following: 00, 03, 05, 06, 09, 13, and 15. K alloy is the normal selection when a temperature-compensated gage is required that has environmental capabilities and performance characteristics not attainable in A-alloy gages.

Due to the difficulty of soldering directly to K alloy, the duplex copper feature, which was formerly offered as an option, is now standard on all Micro-Measurements open-faced strain gages produced with K alloy. The duplex copper feature is a precisely formed copper soldering pad (DP) or dot (DD), depending on the available tab area. All K-alloy gages which do not have leads or solder dots are specified with DP or DD as part of the designation (in place of, or in addition to, the option specifier). The specific style of copper treatment will be advised when the Order Service Department is contacted. Open-faced K-alloy gages may also be ordered with solder dots.

2.2 Backing Materials

Conventional foil strain gage construction involves a photoetched metal foil pattern mounted on a plastic backing or carrier. The backing serves several important functions:

- provides a means for handling the foil pattern during installation
- presents a readily bondable surface for adhering the gage to the test specimen
- provides electrical insulation between the metal foil and the test object

Backing materials supplied on Micro-Measurements strain gages are of two basic types: polyimide and glass-fiber-reinforced epoxy-phenolic. As in the case of the strain sensitive alloy, the backing is not completely an independently specifiable parameter. Certain backing and alloy combinations, along with special construction features, are designed as systems, and given gage series designations. As a result, when arriving at the optimum gage type for a particular application, the process does not permit the arbitrary combination of an alloy and a backing material, but requires the specification of an available gage series. Micro-Measurements gage series and their properties are described in the following Section 2.3. Each series has its own characteristics and preferred areas of application; and selection recommendations are given in the table on page 5. The individual backing materials are discussed here, as the alloys were in the previous section, to aid in understanding the properties of the series in which the alloys and backing materials occur.

The Micro-Measurements polyimide E backing is a tough and extremely flexible carrier, and can be contoured readily to fit small radii. In addition, the high peel strength of the foil on the polyimide backing makes polyimide-backed gages less sensitive to mechanical damage during installation. With its ease of handling and its suitability for use over the temperature range from -320° to $+350^\circ F$ (-195° to $+175^\circ C$), polyimide is an ideal backing material for general-purpose static and dynamic stress analysis. This backing is capable of large elongations, and can be used to measure plastic strains in excess of 20%. Polyimide backing is a feature of Micro-Measurements EA-, CEA-, EP-, EK-, S2K-, N2A-, J2A- and ED-Series strain gages.

For outstanding performance over the widest range of temperatures, the glass-fiber-reinforced epoxy-phenolic backing material is the most suitable choice. This backing can be used for static and dynamic strain measurement from -452° to $+550^\circ F$ (-269° to $+290^\circ C$). In short-term applications, the upper temperature limit can be extended to as high as $+750^\circ F$ ($+400^\circ C$). The maximum elongation of this carrier material is limited, however, to about 1 to 2%. Reinforced epoxy-phenolic backing is employed on the following gage series: WA, WK, SA, SK, WD, and SD.

2.3 Gage Series

As noted in Sections 2.1 and 2.2, the strain-sensing alloy and backing material are not subject to completely independent selection and arbitrary combination. Instead, a selection must be made from among the available gage systems, or series, where each series generally incorporates special design or construction features, as well as a specific combination of alloy and backing material. For convenience in identifying the appropriate gage series to meet specified test requirements, the information on gage series performance and selection is presented here, in condensed form, in two tables.

The table on the following page gives brief descriptions of all general-purpose Micro-Measurements gage series — including in each case the alloy and backing combination and the principal construction features. This table defines the performance of each series in terms of operating temperature range, strain range, and cyclic endurance as a function of strain level. It must be noted, however, that the performance data are *nominal*, and apply primarily to gages of 0.125 in (3 mm) or longer gage length.

EA	Constantan foil in combination with a tough, flexible, polyimide backing. Wide range of options available. Primarily intended for general-purpose static and dynamic stress analysis. Not recommended for highest accuracy transducers.	Normal: -100° to $+350^{\circ}$ F. (-75° to -175° C) Special or Short-Term: -320° to -400° F (-195° to $+205^{\circ}$ C)	$\pm 3\%$ for gage lengths under 1/8 in (3.2 mm) $\pm 5\%$ for 1/8 in and over	± 1800 ± 1500 ± 1200	10^5 10^6 10^8
CEA	Universal general-purpose strain gages. Constantan grid completely encapsulated in polyimide, with large, rugged copper-coated tabs. Primarily used for general-purpose static and dynamic stress analysis. 'C'-Feature gages are specially highlighted throughout the gage listing sections of Catalog 500, Part A — Strain Gage Listings.	Normal: -100° to $+350^{\circ}$ F. (-75° to $+175^{\circ}$ C) Stacked rosettes limited to $+150^{\circ}$ F ($+65^{\circ}$ C)	$\pm 3\%$ for gage lengths under 1/8 in (3.2 mm) $\pm 5\%$ for 1/8 in and over	± 1500 ± 1500	10^5 10^6 *Fatigue life improved using low-modulus solder.
N2A	Open-faced constantan foil gages with a thin, laminated, polyimide-film backing. Primarily recommended for use in precision transducers, the N2A Series is characterized by low and repeatable creep performance. Also recommended for stress analysis applications employing large gage patterns, where the especially flat matrix eases gage installation.	Normal Static Transducer Service: -100° to $+200^{\circ}$ F (-75° to $+95^{\circ}$ C)	$\pm 3\%$	± 1700 ± 1500	10^6 10^7
J2A	Constantan foil gages with a thin, laminated, polyimide backing and encapsulating film. Exposed solder tabs for direct leadwire attachment. Primarily recommended for precision transducers; the encapsulating film provides a more rugged gage than the N2A Series, but may increase reinforcement of thin transducer flexures.	Normal Static Transducer Service: -100° to $+200^{\circ}$ F (-75° to $+95^{\circ}$ C)	$\pm 2\%$	± 1700 ± 1500	10^6 10^7
ED	Iso-Elastic foil in combination with tough, flexible polyimide film. High gage factor and extended fatigue life excellent for dynamic measurements. Not normally used in static measurements due to very high thermal-output characteristics.	Dynamic: -320° to $+400^{\circ}$ F (-195° to $+205^{\circ}$ C)	$\pm 2\%$ Nonlinear at strain levels over $\pm 0.5\%$	± 2500 ± 2200	10^6 10^7
WA	Fully encapsulated constantan gages with high-endurance leadwires. Useful over wider temperature ranges and in more extreme environments than EA Series. Option W available on some patterns, but restricts fatigue life to some extent.	Normal: -100° to -400° F (-75° to -205° C) Special or Short-Term: -320° to -500° F (-195° to -260° C)	$\pm 2\%$	± 2000 ± 1800 ± 1500	10^5 10^6 10^7
EK	Karma foil in combination with a tough, flexible polyimide backing. Primarily used where a combination of higher grid resistances, stability at elevated temperature, and greatest backing flexibility are required.	Normal: -320° to -350° F (-195° to -175° C) Special or Short-Term: -452° to -400° F (-269° to -205° C)	$\pm 1.5\%$	± 1800	10^7
WK	Fully-encapsulated K-alloy gages with high-endurance leadwires. Widest temperature range and most extreme environmental capability of any general-purpose gage when self-temperature-compensation is required. Option W available on some patterns, but restricts both fatigue life and maximum operating temperature.	Normal: -452° to $+550^{\circ}$ F (-269° to $+290^{\circ}$ C) Special or Short-Term: -320° to $+750^{\circ}$ F (-269° to $+400^{\circ}$ C)	$\pm 1.5\%$	± 2400 ± 2200 ± 2000	10^6 10^7 10^8
EP	Special annealed constantan foil with tough, high-elongation polyimide backing. Used primarily for measurements of large post-yield strains in metals or on low-modulus materials (polymers). Available with Options E, L, and LE (may restrict elongation capability).	-100° to $+400^{\circ}$ F (-75° to $+205^{\circ}$ C)	$\pm 10\%$ for gage lengths under 1/8 in (3.2 mm) $\pm 20\%$ for 1/8 in and over	± 1000	10^4 EP gages show zero shift under high-cyclic strains.
SA	Fully encapsulated constantan gages with solder dots. Same matrix as WA Series. Same uses as WA Series but derated somewhat in maximum temperature and operating environment because of solder dots.	Normal: -100° to -400° F (-75° to -205° C) Special or Short-Term: -320° to -450° F (-195° to -230° C)	$\pm 2\%$	± 1800 ± 1500	10^6 10^7
S2K	Karma foil laminated to 0.001 in (0.025 mm) thick, high-performance polyimide backing, with a laminated polyimide overlay fully encapsulating the grid and solder tabs. Provided with large solder pads for ease of leadwire attachment.	Normal: -100° to $+250^{\circ}$ F (-75° to $+120^{\circ}$ C) Special or Short-Term: -300° to $+300^{\circ}$ F (-185° to $+150^{\circ}$ C)	$\pm 1.5\%$	± 1800 ± 1500	10^6 10^7
SK	Fully encapsulated K-alloy gages with solder dots. Same uses as WK Series, but derated in maximum temperature and operating environment because of solder dots.	Normal: -452° to $+450^{\circ}$ F (-269° to $+230^{\circ}$ C) Special or Short-Term: -452° to -500° F (-269° to -260° C)	$\pm 1.5\%$	± 2200 ± 2000	10^6 10^7
WD	Fully encapsulated Iso-Elastic gages with high-endurance leadwires. Used in wide-range dynamic strain measurement applications in severe environments.	Dynamic: -320° to $+500^{\circ}$ F (-195° to $+260^{\circ}$ C)	$\pm 1.5\%$ — non-linear at strain levels over $\pm 0.5\%$	± 3000 ± 2500 ± 2200	10^5 10^7 10^8
SD	Equivalent to WD Series, but with solder dots instead of leadwires.	Dynamic: -320° to $+400^{\circ}$ F. (-195° to $+205^{\circ}$ C)	$\pm 1.5\%$ See above note	± 2500 ± 2200	10^6 10^7

Strain Gage Series and Adhesive Selection Reference Table

TYPE OF TEST OR APPLICATION	OPERATING TEMPERATURE RANGE	TEST DURATION IN HOURS	ACCURACY REQUIRED*	ENDURANCE**		GAGE SERIES	ADHESIVE
				Maximum Strain, %	Number of Cycles		
GENERAL STATIC OR STATIC-DYNAMIC STRESS ANALYSIS*	-50° to +150° F (-45° to +65° C)	<10 ⁴	Moderate	±1300	<10 ⁶	CEA, EA	200 or AE-10
		>10 ⁴	Moderate	±1300	<10 ⁶	CEA, EA	AE-10 or AE-15
		>10 ⁴	High	±1600	>10 ⁶	WA, SA	AE-15 or 610
		>10 ⁴	Very High	±2000	>10 ⁶	WK, SK	AE-15 or 610
	-50° to +400° F (-45° to +205° C)	<10 ³	Moderate	±1600	<10 ⁶	WA, SA	600 or 610
		>10 ³	High	±2000	<10 ⁶	WK, SK	600 or 610
	-452° to +450° F (-269° to +230° C)	>10 ³	Moderate	±2000	>10 ⁶	WK, SK	610
	<600° F (<315° C)	<10 ²	Moderate	±1800	<10 ⁶	WK	610
<700° F (<370° C)	<10	Moderate	±1500	<10 ⁶	WK	610	
HIGH-ELONGATION (POST-YIELD)	-50° to +150° F (-45° to +65° C)	<10	Moderate	±50 000	1	CEA, EA	AE-10
		>10 ³	Moderate	±100 000	1	EP	AE-15
		>10 ³	Moderate	±200 000	1	EP	A-12
	0° to +500° F (-20° to +260° C)	<10 ²	Moderate	±15 000	1	SA, SK, WA, WK	610
-452° to +500° F (-269° to +260° C)	<10 ³	Moderate	±10 000	1	SK, WK	600 or 610	
DYNAMIC (CYCLIC) STRESS ANALYSIS	-100° to +150° F (-75° to +65° C)	<10 ⁴	Moderate	±2000	10 ⁷	ED	200 or AE-10
		<10 ⁴	Moderate	±2400	10 ⁷	WD	AE-10 or AE-15
	-320° to +500° F (-195° to +260° C)	<10 ⁴	Moderate	±2000	10 ⁷	WD	600 or 610
		<10 ⁴	Moderate	±2300	<10 ⁵	WD	600 or 610
TRANSDUCER GAGING	-50° to +150° F (-45° to +65° C)	<10 ⁴	1 to 5%	±1300	<10 ⁶	CEA, EA	AE-10 or AE-15
		<10 ⁶	1 to 5%	±1300	<10 ⁶	CEA	AE-15
	-50° to +200° F (-45° to +95° C)	<10 ⁴	Better than 0.2%	±1500	10 ⁶	N2A	600, 610 or 43-B
	-50° to +300° F (-45° to +150° C)	<10 ⁴	0.2 to 0.5%	±1600	10 ⁶	WA, SA	610
	-320° to +350° F (-195° to +175° C)	<10 ⁴	Better than 0.5%	±1800	10 ⁶	WK, SK	610

* This category includes most testing situations where some degree of stability under static test conditions is required. For absolute stability with constant gages over long periods of usage and temperatures above +150° F (+65° C), it may be necessary to employ half- or full-bridge configurations. Protective coatings may also influence stability in cases other than transducer applications where the element is hermetically sealed.

** It is inappropriate to quantify "accuracy" as used in this table without consideration of various aspects of the actual test program and the instrumentation used. In general, "moderate" for stress analysis purposes is in the 2 to 5% range, "high" in the 1 to 3% range, and "very high" 1% or better.

The above table gives the recommended gage series for specific test "profiles," or sets of test requirements, categorized by the following criteria:

- type of strain measurement (static, dynamic, etc.)
- operating temperature of gage installation
- test duration
- accuracy required
- cyclic endurance required

This table provides the basic means for preliminary selection of the gage series for most conventional applications. It also includes recommendations for adhesives, since the adhesive in a strain gage installation becomes part of the gage system, and correspondingly affects the performance of

the gage. This selection table, supplemented by the information in the table on page 4, is used in conjunction with Catalog 500, Part A — *Strain Gage Listings* to arrive at the complete gage selection. The procedure for accomplishing this is described in *Section 3.0* of this Tech Note.

When a test profile is encountered that is beyond the ranges specified in the above table, it can usually be assumed that the test requirements approach or exceed the performance limitations of available gages. Under these conditions, the interactions between gage performance characteristics become too complex for presentation in a simple table. In such cases, the user should consult the Applications Engineering Department of Micro-Measurements for assistance in arriving at the best compromise.

Strain Gage Series and Adhesive Selection Reference Table

TYPE OF TEST OR APPLICATION	OPERATING TEMPERATURE RANGE	TEST DURATION IN HOURS	ACCURACY REQUIRED	RECOMMENDED GAGES		ADHESIVE	REMARKS
				Minimum Strain, $\mu\epsilon$	Maximum of Cycle		
GENERAL STATIC OR STATIC-DYNAMIC STRESS ANALYSIS*	-50° to -150°F (-45° to -65°C)	<10 ⁴	Moderate	±1300	<10 ⁶	CEA, EA	200 or AE-10
		>10 ⁴	Moderate	±1300	<10 ⁶	CEA, EA	AE-10 or AE-15
		>10 ⁴	High	±1600	>10 ⁶	WA, SA	AE-15 or 610
		>10 ⁴	Very High	±2000	>10 ⁶	WK, SK	AE-15 or 610
	-50° to -400°F (-45° to -205°C)	<10 ³	Moderate	±1600	<10 ⁶	WA, SA	500 or 610
		>10 ³	High	±2000	<10 ⁶	WK, SK	600 or 610
	-452° to -450°F (-269° to -230°C)	>10 ³	Moderate	±2000	>10 ⁶	WK, SK	610
<600°F (<315°C)	<10 ²	Moderate	±1800	<10 ⁶	WK	610	
<700°F (<370°C)	<10	Moderate	±1500	<10 ⁶	WK	610	
HIGH-ELONGATION (POST-YIELD)	-50° to -150°F (-45° to -65°C)	<10	Moderate	±50 000	1	CEA, EA	AE-10
		>10 ³	Moderate	±100 000	1	EP	AE-15
		>10 ³	Moderate	±200 000	1	EP	A-12
	-0° to -500°F (-20° to -260°C)	<10 ²	Moderate	±15 000	1	SA, SK, WA, WK	610
-452° to -500°F (-269° to -250°C)	<10 ³	Moderate	±10 000	1	SK, WK	600 or 610	
DYNAMIC (CYCLIC) STRESS ANALYSIS	-100° to -150°F (-75° to -65°C)	<10 ⁴	Moderate	±2000	10 ⁷	ED	200 or AE-10
		<10 ⁴	Moderate	±2400	10 ⁷	WD	AE-10 or AE-15
	-320° to -500°F (-195° to -260°C)	<10 ⁴	Moderate	±2000	10 ⁷	WD	600 or 610
		<10 ⁴	Moderate	±2300	<10 ⁵	WD	600 or 610
TRANSDUCER GAGING	-50° to -150°F (-45° to -65°C)	<10 ⁴	1 to 5%	±1300	<10 ⁶	CEA, EA	AE-10 or AE-15
		<10 ⁶	1 to 5%	±1300	<10 ⁶	CEA	AE-15
	-50° to -200°F (-45° to -95°C)	<10 ⁴	Better than 0.2%	±1500	10 ⁶	N2A	600, 610 or 43-B
	-50° to -300°F (-45° to -150°C)	<10 ⁴	0.2 to 0.5%	±1600	10 ⁶	WA, SA	610
	-320° to -350°F (-195° to -175°C)	<10 ⁴	Better than 0.5%	±1800	10 ⁶	WK, SK	610
<p>* This category includes most testing situations where some degree of stability under static test conditions is required. For absolute stability with constantan gages over long periods of usage and temperatures above +150°F (+65°C), it may be necessary to employ half- or full-bridge configurations. Protective coatings may also influence stability in cases other than transducer applications where the element is hermetically sealed.</p> <p>** It is inappropriate to quantify "accuracy" as used in this table without consideration of various aspects of the actual test program and the instrumentation used. In general, "moderate" for stress analysis purposes is in the 2 to 5% range, "high" in the 1 to 3% range, and "very high" 1% or better.</p>							

The above table gives the recommended gage series for specific test "profiles," or sets of test requirements, categorized by the following criteria:

- type of strain measurement (static, dynamic, etc.)
- operating temperature of gage installation
- test duration
- accuracy required
- cyclic endurance required

This table provides the basic means for preliminary selection of the gage series for most conventional applications. It also includes recommendations for adhesives, since the adhesive in a strain gage installation becomes part of the gage system, and correspondingly affects the performance of

the gage. This selection table, supplemented by the information in the table on page 4, is used in conjunction with Catalog 500, Part A — *Strain Gage Listings* to arrive at the complete gage selection. The procedure for accomplishing this is described in *Section 3.0* of this Tech Note.

When a test profile is encountered that is beyond the ranges specified in the above table, it can usually be assumed that the test requirements approach or exceed the performance limitations of available gages. Under these conditions, the interactions between gage performance characteristics become too complex for presentation in a simple table. In such cases, the user should consult the Applications Engineering Department of Micro-Measurements for assistance in arriving at the best compromise.

the representative strain in the structure. In other words, it is usually the *average* strain that is sought in such instances, not the severe local fluctuations in strain occurring at the interfaces between the aggregate particles and the cement. In general, when measuring strains on structures made of composite materials of any kind, the gage length should normally be large with respect to the dimensions of the inhomogeneities in the material.

As a generally applicable guide, when the foregoing considerations do not dictate otherwise, gage lengths in the range from 0.125 to 0.25 in (3 to 6 mm) are preferable. The largest selection of gage patterns and stock gages is available in this range of lengths. Furthermore, larger or smaller sizes generally cost more, and larger gages do not noticeably improve fatigue life, stability, or elongation, while shorter gages are usually inferior in these characteristics.

2.5 Gage Pattern

The gage pattern refers cumulatively to the shape of the grid, the number and orientation of the grids in a multiple-grid gage, the solder tab configuration, and various construction features which are standard for a particular pattern. All details of the grid and solder tab configurations are illustrated in the "Gage Pattern" columns of Catalog 500, Part A — *Strain Gage Listings*. The wide variety of patterns in the list is designed to satisfy the full range of normal gage installation and strain measurement requirements.

With single-grid gages, pattern suitability for a particular application depends primarily on the following:

Solder tabs — These should, of course, be compatible in size and orientation with the space available at the gage installation site. It is also important that the tab arrangement be such as to not excessively tax the proficiency of the installer in making proper leadwire connections.

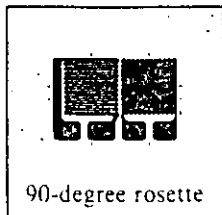
Grid width — When severe strain gradients perpendicular to the gage axis exist in the test specimen surface, a narrow grid will minimize the averaging error. Wider grids, when available and suitable to the installation site, will improve the heat dissipation and enhance gage stability — particularly when the gage is to be installed on a material or specimen with poor heat transfer properties.

Gage resistance — In certain instances, the only difference between two gage patterns available in the same series is the grid resistance — typically 120 ohms vs. 350 ohms. When the choice exists, the higher-resistance gage is preferable in that it reduces the heat generation rate by a factor of three (for the same applied voltage across the gage). Higher gage resistance also has the advantage of decreasing leadwire effects such as circuit desensitization due to leadwire resistance, and unwanted signal variations caused by leadwire resistance changes with temperature fluctuations. Similarly, when the gage circuit includes switches, slip rings, or other sources of random resistance change, the signal-to-noise ratio is improved with higher resistance gages operating at the same power level.

In experimental stress analysis, a single-grid gage would normally be used only when the stress state at the point of measurement is known to be uniaxial and the directions of the principal axes are known with reasonable accuracy ($\pm 5^\circ$).

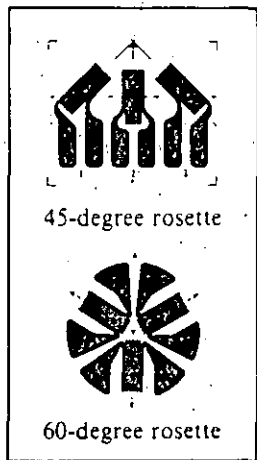
These requirements severely limit the meaningful applicability of single-grid strain gages in stress analysis; and failure to consider biaxiality of the stress state can lead to large errors in the stress magnitude inferred from measurements made with a single-grid gage.

For a biaxial stress state — a common case necessitating strain measurement — a two- or three-element rosette is required in order to determine the principal stresses. When the directions of the principal axes are known in advance, a two-element 90-degree (or "tee") rosette can be employed with the gage axes aligned to coincide with the principal axes. The directions of the principal axes can sometimes be determined with sufficient accuracy from one of several considerations. For example, the shape of the test object and the mode of loading may be such that the directions of the principal axes are obvious from the symmetry of the situation, as in a cylindrical pressure vessel. The principal axes can also be defined by testing with photoelastic coating.



90-degree rosette

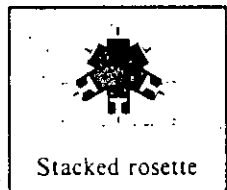
In the most general case of surface stresses, when the directions of the principal axes are not known from other considerations, a three-element rosette must be used to obtain the principal stress magnitudes. The rosette can be installed with any orientation, but is usually mounted so that one of the grids is aligned with some significant axis of the test object. Three-element rosettes are available in both 45-degree rectangular and 60-degree delta configurations. The usual choice is the rectangular rosette since the data-reduction task is somewhat simpler for this configuration.



45-degree rosette

60-degree rosette

When a rosette is to be employed, careful consideration should always be given to the difference in characteristics between single-plane and stacked rosettes. For any given gage length, the single-plane rosette is superior to the stacked rosette in terms of heat transfer to the test specimen, generally providing better stability and accuracy for static strain measurements. Furthermore, when there is a significant strain gradient perpendicular to the test surface (as in bending), the single-plane rosette will produce more accurate strain data because all grids are as close as possible to the test surface. Still another consideration is that stacked rosettes are generally less conformable to contoured surfaces than single-plane rosettes.



Stacked rosette

On the other hand, when there are large strain gradients in the plane of the test surface, as is often the case, the single-plane rosette can produce errors in strain indication because the grids sample the strain at different points. For these applications the stacked rosette is ordinarily preferable. The stacked rosette is also advantageous when the space for mounting the rosette is limited.

2.6 Optional Features

Micro-Measurements offers a selection of optional features for its strain gages and special sensors. The addition of options to the basic gage construction usually increases the cost, but this is generally offset by the benefits. Examples are:


- Significant reduction of installation time and costs
- Reduction of the skill level necessary to make dependable installations
- Increased reliability of applications
- Simplified installation of sensors in difficult locations on components or in the field
- Increased protection, both in handling during installation and shielding from the test environment
- Achievement of special performance characteristics


Availability of each option varies with gage series and pattern. Standard options are noted for each sensor in Catalog 500, Part A — *Strain Gage Listings*.

Shown below is a summary of the optional features offered.

Standard Catalog Options

OPTION	BRIEF DESCRIPTION
W	Integral Terminals and Encapsulation
E	Encapsulation with Exposed Tabs
SE	Solder Dots and Encapsulation
L	Preattached Leads
LE	Preattached Leads and Encapsulation

Option <i>W</i>	Series Availability: EA, EP, WA, ED, EK, WK	
<p>General Description: This option provides encapsulation, and thin, printed circuit terminals at the tab end of the gage. Beryllium copper jumpers connect the terminals to the gage tabs. The terminals are 1.4 mil [0.0014 in (0.036 mm)] thick copper on polyimide backing about 1.5 mil [0.0015 in (0.038 mm)] thick. Option W gages are rugged and well protected, and permit the direct attachment of larger leadwires than would be possible with open-faced gages. This option is primarily used on EA-Series gages for general-purpose applications. Solder: +430° F (+220° C) tin-silver alloy solder joints on E-backed gages; +570° F (+300° C) lead-tin-silver alloy solder joints on W-backed gages. Temperature Limit: +400° F (+200° C) for E-backed gages, +500° F (+260° C) for W-backed gages. Grid Protection: Entire grid and part of terminals are encapsulated with polyimide. Fatigue Life: Some loss in fatigue life unless strain levels at the terminal location are below $\pm 1000 \mu\epsilon$. Size: Option W extends from the soldering tab end of the gages and thereby increases gage size. With some patterns width is slightly greater. Strain Range: With some gage series, notably E-backed gages, strain range will be reduced. This effect is greatest with EP gages, and Option W should be avoided with them if possible. Flexibility: Option W adds encapsulation, making gages slightly thicker and stiffer. Conformance to curved surfaces will be somewhat reduced. In the terminal area itself, stiffness is markedly increased. Resistance Tolerance: On E-backed gages, resistance tolerance is normally doubled.</p>		

Option <i>E</i>	Series Availability: EA, ED, EK, EP	
<p>General Description: Option E consists of a protective encapsulation of polyimide film approximately 1 mil [0.001 in (0.025 mm)] thick. This provides ruggedness and excellent grid protection, with little sacrifice in flexibility. Soldering is greatly simplified since the solder is prevented from tinning any more of the gage tab than is deliberately exposed for lead attachment. Option E contributes significantly to long-term gage stability, because the grid cannot be contaminated by fingerprints or other agents during installation. Heavier leads may be attached directly to the gage tabs for simple static load tests. Supplementary protective coatings should still be applied after lead attachment in most cases. Temperature Limit: No degradation. Grid Protection: Entire grid and part of tabs are encapsulated. Fatigue Life: When gages are properly wired with small jumpers, maximum endurance is easily obtained. Size: Gage size is not affected. Strain Range: Strain range of gages will be reduced because the additional reinforcement of the polyimide encapsulation can cause bond failure before the gage reaches its full strain capability. Flexibility: Option E gages are almost as conformable on curved surfaces as open-faced gages, since no internal leads or solder are present at the time of installation. Resistance Tolerance: Resistance tolerance is normally doubled when Option E is selected.</p>		

Option SE**Series Availability: EA, ED, EK, EP**

General Description: Option SE is the combination of solder dots on the gage tabs with a 1-mil [0.001-in (0.025-mm)] polyimide encapsulation layer that covers the entire gage. The encapsulation is removed over the solder dots, providing access for lead attachment. These gages are very flexible, and well protected from handling damage during installation. Option SE is primarily intended for small gages that must be installed in restricted areas, since leadwires can be routed to the exposed solder dots from any direction. The option does not increase overall gage dimensions, so the matrix may be field-trimmed very close to the actual pattern size. Option SE is sometimes useful on miniature transducers of medium or low accuracy class, or in stress analysis work on miniature parts. **Solder:** +570° F (+300° C) lead-tin-silver alloy. To prevent loss of long-term stability, gages with Option SE must be soldered with noncorrosive (rosin) flux, and all flux residue should be carefully removed with *M-LINE* Rosin Solvent after wiring. Protective coatings should then be used. **Temperature Limit:** No degradation. **Grid Protection:** Entire gage is encapsulated. **Fatigue Life:** When gages are properly wired with small jumpers, maximum endurance is easily obtained. **Size:** Gage size is not affected. **Strain Range:** Strain range of gages will be reduced because the additional reinforcement of the polyimide encapsulation can cause bond failure before the gage reaches its full strain capability. **Flexibility:** Option SE gages are almost as conformable on curved surfaces as open-faced gages. **Resistance Tolerance:** Resistance tolerance is normally doubled when Option SE is selected.

**Option L****Series Availability: EA, ED, EK, EP**

General Description: Option L is the addition of soft copper lead ribbons to open-faced polyimide-backed gages. The use of this type of ribbon results in a thinner and more conformable gage than would be the case with round wires of equivalent cross section. At the same time, the ribbon is so designed that it forms almost as readily in any desired direction. **Leads:** Nominal ribbon size is 0.012 wide x 0.004 thick in (0.30 x 0.10 mm). Leads are approximately 0.8 in (20 mm) long. **Solder:** +430° F (+220° C) tin-silver alloy. The solder is confined to small, well-defined areas at the end of each ribbon. **Temperature Limit:** +400° F (+200° C). **Fatigue Life:** Fatigue life will normally be degraded by Option L. This occurs primarily because the copper ribbon has limited cyclic endurance. When it is possible to carefully dress the leads so that they are not bonded in a high strain field, the performance limitation will not apply. Option L is not often recommended for very high endurance gages such as the ED Series. **Size:** Matrix size is unchanged. **Strain Range:** Strain range will usually be reduced by the addition of Option L. **Flexibility:** Gages with Option L are not as conformable as standard gages. **Resistance Tolerance:** Not affected.

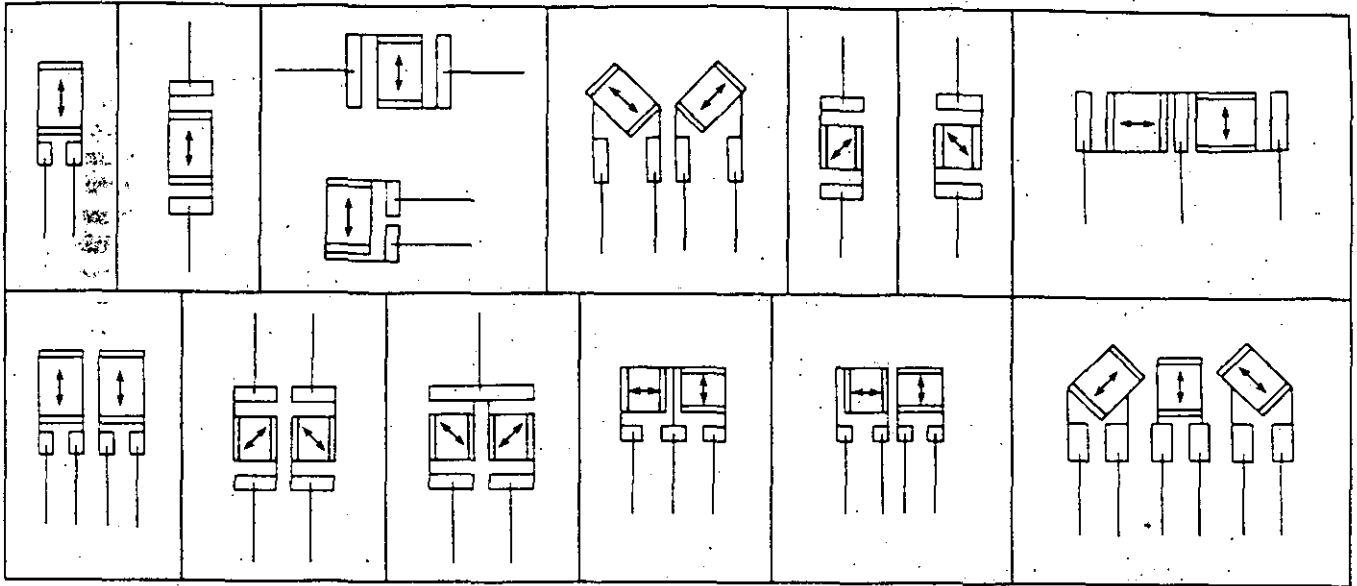
**Option LE****Series Availability: EA, ED, EK, EP**

General Description: This option provides the same conformable soft copper lead ribbons as used in Option L, but with the addition of a 1-mil [0.001-in (0.025-mm)] thick encapsulation layer of polyimide film. The encapsulation layer provides excellent protection for the gage during handling and installation. It also contributes greatly to environmental protection, though supplementary coatings are still recommended for field use. Gages with Option LE will normally show better long-term stability than open-faced gages which are "waterproofed" only after installation. A good part of the reason for this is that the encapsulation layer prevents contamination of the grid surface from fingerprints or other agents during handling and installation. The presence of such contaminants will cause some loss in gage stability, even though the gage is subsequently coated with protective compounds. **Leads:** 0.012 wide x 0.004 thick in (0.30 x 0.10 mm) copper ribbons. Leads are approximately 0.8 in (20 mm) long. **Solder:** +430° F (+220° C) tin-silver alloy. The solder is confined to small, well-defined areas at the end of each ribbon. **Temperature Limit:** +400° F (+200° C). **Grid Protection:** Entire gage is encapsulated. A short extension of the backing is left uncovered at the leadwire end to prevent contact between the leadwires and the specimen surface. **Fatigue Life:** Fatigue life will normally be degraded by Option LE. This occurs primarily because the copper ribbon has limited cyclic endurance. Option LE is not often recommended for very high endurance gages such as the ED Series. **Size:** Matrix size is unchanged. **Strain Range:** Strain range will usually be reduced by the addition of Option LE. **Flexibility:** Gages with Option LE are not as conformable as standard gages. **Resistance Tolerance:** Resistance tolerance is normally doubled by the addition of Option LE.



Leadwire Orientation for Options L and LE

These illustrations show the standard orientation of leadwires relative to the gage pattern geometry for Options L and LE. The general rule is that the leads are parallel to the longest dimension of the pattern. The illustrations also apply to leadwire orientation for WA-, WK-, and WD-Series gages, when the pattern shown is available in one of these series.



2.7 Characteristics of Standard Catalog Options on EA-Series Gages

As in other aspects of strain gage selection, the choice of options ordinarily involves a variety of compromises. For instance, an option which maximizes a particular gage performance parameter such as fatigue life may at the same time require greater skill in installing the gage. Because of the many interactions between installation attributes and performance parameters associated with the options, the relative merits of all standard options are summarized qualitatively in the chart below as an aid to option selection. For comparison purposes, the corresponding characteristics of the CEA Series are given in the right-most column of the table.

Since, in strain measurement for stress analysis, the standard options are most frequently applied to EA-Series strain gages, the information supplied in this section is directed primarily toward such option applications.

When contemplating the application of an EA-Series gage with an option, the first consideration should usually be whether there is an equivalent CEA-Series gage that will satisfy the test requirements. Comparing, for example, an EA-Series gage equipped with Option W and a similar CEA-Series pattern, it will be found that the latter is characterized by lower cost, greater flexibility and conformability, and superior fatigue life. The only possible advantages for the selection of Option W are the wider variety of available patterns and the occasional need for large soldering terminals.

It should also be noted that many standard strain gage types, without options, are normally available from stock; while gages with options are commonly manufactured to order, and may thus involve a minimum order requirement.

In the table below, the respective performance parameters for an open-faced EA-Series gage without options are arbitrarily assigned a value of 5. Numbers greater than 5 indicate a particular parameter is improved by addition of the option, while smaller numbers indicate a reduction in performance.

INSTALLATION ATTRIBUTE OR PERFORMANCE PARAMETER	STANDARD OPTIONS					CEA SERIES
	W	E	SE	L	LE	
Overall Ease of Gage Installation	8	7	6	5	6	10
Ease of Leadwire Attachment	10	8	7	7	8	10
Protection of Grid from Environmental Attack	8	8	8	5	8	8
Cyclic Strain Endurance	2	7	8	3	4	4
Elongation Capability	2	3	3	4	3	3
Resistance Tolerance	3	3	3	5	3	3
Reinforcement Effects	2	3	3	5	3	3

3.0 Gage Selection Procedure

The performance of a strain gage in any given application is affected by every element in the design and manufacture of the gage. Micro-Measurements offers a great variety of gage types for meeting the widest range of strain measurement needs. Despite the large number of variables involved, the process of gage selection can be reduced to only a few basic steps. From the diagram below that explains the gage designation code, it is evident that there are but five parameters to select, not counting options. These are: the gage series, the S-T-C number, the gage length and pattern, and the resistance.

Of the preceding parameters, the gage length and pattern are normally the first and second selections to be made, based on the space available for gage mounting and the nature of the stress field in terms of biaxiality and expected strain gradient. A good starting point for initial consideration of gage length is 0.125 in (3 mm). This size offers the widest variety of choices from which to select remaining gage parameters such as pattern, series and resistance. The gage and its solder tabs are large enough for relatively easy handling and installation. At the same time, gages of this length provide performance capabilities comparable to those of larger gages.

The principal reason for selecting a longer gage would commonly be one of the following: (a) greater grid area for better heat dissipation; (b) improved strain averaging on inhomogeneous materials such as fiber-reinforced composites; or (c) slightly easier handling and installation [for gage lengths up to 0.50 in (13 mm)]. On the other hand, a shorter gage length may be necessary when the object is to measure localized peak strains in the vicinity of a stress concentration, such as a hole or shoulder. The same is true, of course, when the space available for gage mounting is very limited.

In selecting the gage pattern, the first consideration is whether a single-grid gage or rosette is required (see Section 2.5). Single-grid gages are available with different aspect (length-to-width) ratios and various solder tab arrangements for adaptability to differing installation requirements. Two-element 90-degree rosettes, when applicable, can also be selected from a number of different grid and solder tab configurations. With three-element rosettes (rectangular or delta), the primary choice in pattern selection, once the gage length has been determined, is between planar and stacked construction, as described in Section 2.5.

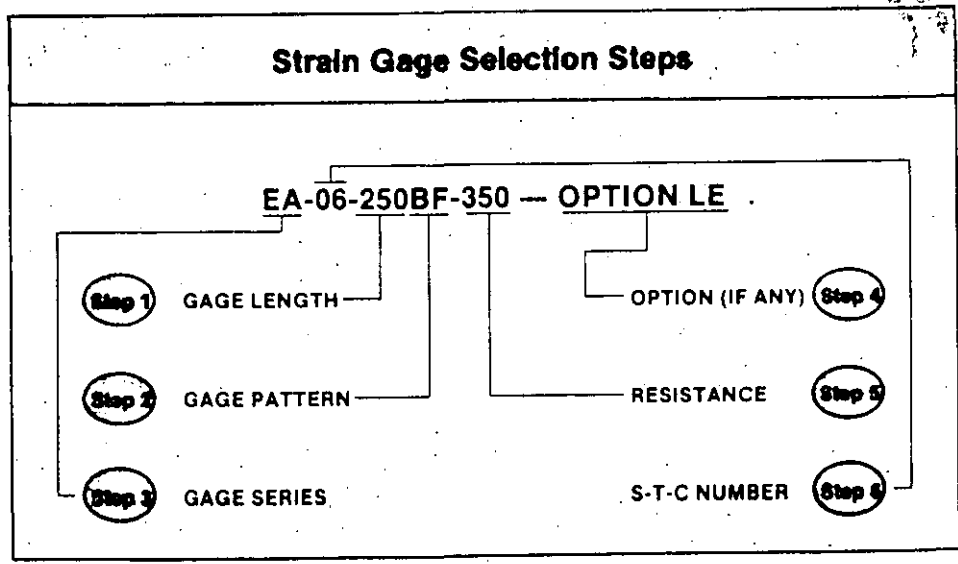
The format of Catalog 500, Part A — *Strain Gage Listings* is designed to simplify selection of the gage length and pattern. Similar patterns available in each gage length are grouped together, and listed in order of size. The strain gages in the Super Stock section of the catalog are the most widely used for stress analysis applications. This section should always be reviewed first to locate an appropriate gage.

With an initial selection of the gage size and pattern completed, the next step is to select the gage series, thus determining the foil and backing combination, and any other features common to the series. This is accomplished by referring to the chart on page 5, which gives the recommended gage series for specific test "profiles", or sets of test requirements. If the gage series is to have a standard option applied, the option should be tentatively specified at this time, since the availability of the desired option on the selected gage pattern in that series requires verification during the procedure outlined in the following paragraph.

After selecting the gage series (and option, if any), reference is made again to Catalog 500, Part A — *Strain Gage Listings* to record the gage designation of the desired gage size and pattern in the recommended series. If this combination is not listed as available in the catalog, a similar gage pattern in the same size group, or a slightly different size in an equivalent pattern, can usually be selected for meeting the installation and test requirements. In extreme cases, it may be necessary to select an alternate series and repeat this process. Quite frequently, and especially for routine strain measurement, more than one gage size and pattern combination will be suitable for the specified test conditions. In these cases, it is wise to select a gage from the Super Stock Listings to eliminate the likelihood of extended delivery time or a minimum order requirement.

As noted under the gage pattern discussion on page 7, there are often advantages from selecting the 350-ohm resistance if this resistance is compatible with the instrumentation to be used. This decision may be influenced, however, by cost considerations, particularly in the case of very small gages. Some reduction in fatigue life can also be expected for the high-resistance small gages. Finally, in recording the complete gage designation, the S-T-C number should be inserted from the list of available numbers for each alloy given on page 4 of Catalog 500, Part A — *Strain Gage Listings*.

This completes the gage selection procedure. In each step of the procedure, the Strain Gage Selection Checklist on page 12 should be referred to as an aid in accounting for the test conditions and requirements which could affect the selection.



4.0 Strain Gage Selection Checklist

This checklist is provided as a convenient, rapid means for helping make certain that no critical requirement of the test profile which could affect gage selection is overlooked. It should be borne in mind in using the checklist that the "considerations" listed apply to relatively routine and conventional stress analysis situations, and do not embrace exotic applications involving nuclear radiation, intense magnetic fields, extreme centrifugal forces, and the like.

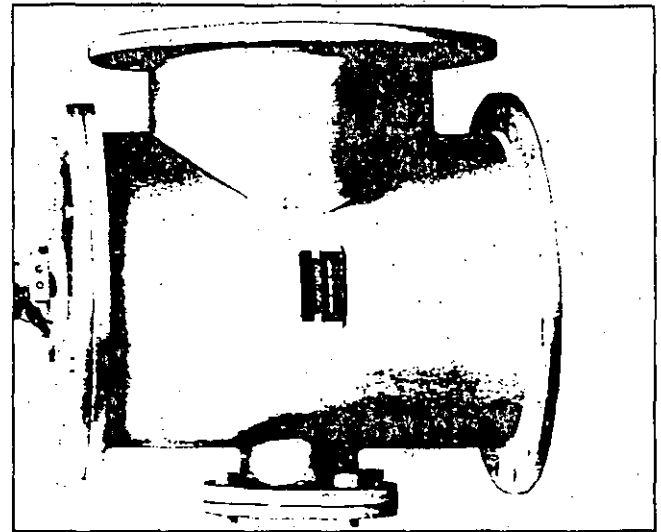
CONSIDERATIONS FOR PARAMETER SELECTION	
<p>Selection Step: 1 Parameter: Gage Length</p>	<input type="checkbox"/> strain gradients <input type="checkbox"/> area of maximum strain. <input type="checkbox"/> accuracy required <input type="checkbox"/> static strain stability <input type="checkbox"/> maximum elongation <input type="checkbox"/> cyclic endurance <input type="checkbox"/> heat dissipation <input type="checkbox"/> space for installation <input type="checkbox"/> ease of installation
<p>Selection Step: 2 Parameter: Gage Pattern</p>	<input type="checkbox"/> strain gradients (in-plane and normal to surface) <input type="checkbox"/> biaxiality of stress <input type="checkbox"/> heat dissipation <input type="checkbox"/> space for installation <input type="checkbox"/> ease of installation <input type="checkbox"/> gage resistance availability.
<p>Selection Step: 3 Parameter: Gage Series</p>	<input type="checkbox"/> type of strain measurement application (static, dynamic, post-yield, etc.) <input type="checkbox"/> operating temperature <input type="checkbox"/> test duration <input type="checkbox"/> cyclic endurance <input type="checkbox"/> accuracy required <input type="checkbox"/> ease of installation
<p>Selection Step: 4 Parameter: Options</p>	<input type="checkbox"/> type of measurement (static, dynamic, post-yield, etc.) <input type="checkbox"/> installation environment — laboratory or field <input type="checkbox"/> stability requirements <input type="checkbox"/> soldering sensitivity of substrate (plastic, bone, etc.) <input type="checkbox"/> space available for installation <input type="checkbox"/> installation time constraints
<p>Selection Step: 5 Parameter: Gage Resistance</p>	<input type="checkbox"/> heat dissipation <input type="checkbox"/> leadwire desensitization <input type="checkbox"/> signal-to-noise ratio
<p>Selection Step: 6 Parameter: S-T-C Number</p>	<input type="checkbox"/> test specimen material <input type="checkbox"/> operating temperature range <input type="checkbox"/> accuracy required

5.0 Gage Selection Examples

In this section, three examples are given of the gage-selection procedure in representative stress analysis situations. An attempt has been made to provide the principal reasons for the particular choices which are made. It should be noted, however, that an experienced stress analyst does not ordinarily proceed in the same step-by-step fashion illustrated in these examples. Instead, simultaneously keeping in mind the test conditions and environment, the gage installation constraints, and the test requirements, the analyst reviews Catalog 500, Part A — *Strain Gage Listings*, and quickly segregates the more likely candidates from among the available gage-pattern and series combinations in the appropriate sizes. The selection criteria are then refined in accordance with the particular strain-measurement task to converge on the gage or gages to be specified for the test program. Whether formally or otherwise, the knowledgeable practitioner does so in the light of parameter selection considerations such as those itemized in the preceding checklist.

A. Design Study of a Pressure Vessel

Strain measurements are to be made on a scaled-down plastic model of a pressure vessel. The model will be tested statically at, or near, room temperature; and, although the tests may be conducted over a period of several months, individual tests will take only a few hours to run.



Gage Selection:

1. **Gage Length** — Very short gage lengths should be avoided in order to minimize heat dissipation problems caused by the low thermal conductivity of the plastic. The model is quite large, and apparently free of severe strain gradients; therefore, a 0.25-in (6.3-mm) gage length is specified, because the widest selection of gage patterns is available in this length.
2. **Gage Pattern** — In some areas of the model, the directions of the principal axes are obvious from considerations of symmetry, and single-grid gages can be employed. Of the patterns available in the selected gage length, the 250BF pattern is a good compromise because of its high grid resistance which will help minimize heat dissipation problems.

In other areas of the model, the directions of the principal axes are not known, and a three-element rosette will be required. For this purpose, a "planar" rosette should be selected, since a stacked rosette would contribute significantly to reinforcement and heat dissipation problems. Because of its high-resistance grid, the 250RD pattern is a good choice.

- Gage Series** — The polyimide (E) backing is preferred because its low elastic modulus will minimize reinforcement of the plastic model. Because the normal choice of grid alloy for static strain measurement at room temperature is the A alloy, the EA Series should be selected for this application.
- Options** — Excessive heat application to the test model during leadwire attachment could damage the material. Option L (preattached leads) is therefore selected so that the instrument cable can be attached directly to the leads without the application of a soldering iron to the gage proper. Option L is preferable over Option LE because the encapsulation in the latter option would add reinforcement.
- Resistance** — In this case, the resistance was determined in Step 2 when the higher resistance alternative was selected from among the gage patterns; i.e., in selecting the 250BF over the 250BG, and the 250RD over the 250RA. The selected gage resistance is thus 350 ohms.
- S-T-C Number** — Ideally, the gages should be self-temperature-compensated to match the model material, but this is not always feasible, since plastics — particularly reinforced plastics — vary widely in thermal expansion coefficient. For unreinforced plastic, S-T-C 30, 40 or 50 should usually be selected. If a mismatch between the model material and the S-T-C number is necessary, S-T-C 13 should be selected (because of stock status), and the test performed at constant temperature.

Gage Designations:

From the above steps, the strain gages to be used are:

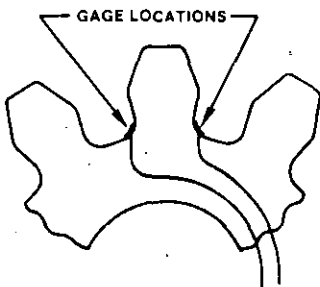
EA-30-250BF-350/Option L (single-grid)

EA-30-250RD-350/Option L (rosette)

See page 15 for a description of the strain gage types mentioned in this section.

B. Dynamic Stress Analysis Study of a Spur Gear in a Hydraulic Pump

Strain measurements are to be made at the root of the gear tooth while the pump is operating. The fillet radius at the tooth root is 0.125 in (or about 3 mm) and test temperatures are expected to range from 0° to +180° F (-20° to +80° C).



Gage Selection:

- Gage Length** — A gage length which is small with respect to the fillet radius should be specified for this application. A length of 0.015 in (0.38 mm) is preferable, but reference to Catalog 500, Part A — *Strain Gage Listings*, indicates that such a choice severely limits the available gage patterns and grid alloys. Anticipating problems which would otherwise be encountered in Steps 2 and 3, a gage length of 0.031 in (0.8 mm) is selected.
- Gage Pattern** — Because the gear is a spur gear, the directions of the principal axes are known, and single-grid gages can be employed. A gage pattern with both solder tabs at the same end should be selected so that leadwire connections can be located in the clearance area along the root circle between adjacent teeth. In the light of these considerations, the 031CF pattern is chosen for the task.
- Gage Series** — Low strain levels are expected in this application; and, furthermore, the strain signals must be transmitted through slip rings or through a telemetry system to get from the rotating component to the stationary instrumentation. Iso-Elastic (D alloy) is preferred for its higher gage factor (nominally 3.2, in contrast to 2.1 for A and K alloys). Because the gage must be very flexible to conform to the small fillet radius, the E backing is the most suitable choice. The maximum test temperature is not a consideration in this case, since it is well within the recommended temperature range for any of the standard backings. The combination of the E backing and the D alloy defines the ED gage series.
- Options** — For protection of the gage grid in the test environment, Option E, encapsulation, should be specified. Because of the limited clearance between the outside diameter of one gear and the root circle of the mating gear, a particularly thin gage installation must be made; and very small leadwires will be attached to the gage tabs at 90° to the grid direction, and run over the sides of the gear for connection to larger wires. This requirement necessitates attachment of the small leadwires after gage bonding, and prevents the use of preattached leads.
- Resistance** — In the ED-Series version of the 031CF gage pattern, Catalog 500, Part A — *Strain Gage Listings*, lists the resistance as 350 ohms. The higher resistance should usually be selected whenever the choice exists, and will be advantageous in this instance in improving the signal-to-noise ratio when slip rings are used.
- S-T-C Number** — D alloy is not subject to self-temperature-compensation, nor is compensation needed for these tests since only dynamic strain is to be measured. In the ED-Series designation the two-digit S-T-C number is replaced by the letters DY for "dynamic."

Gage Designation:

Combining the results of the above selection procedure, the gage to be employed is:

ED-DY-031CF-350/Option E

**C. Flight-Test Stress Analysis
of a Titanium Aircraft Wing Tip Section —
With, and Without, a Missile Module Attached**

The operating temperature range for strain measurements is from -65° to $+450^{\circ}$ F (-55° to $+230^{\circ}$ C), and will be a dominant factor in the gage selection.



Gage Selection:

1. *Gage Length* — Preliminary design studies using the Photo-Stress[®] photoelastic coating technique indicate that a gage length of 0.062 in (1.6 mm) represents the best compromise in view of the strain-gradients, areas of peak strain, and space for gage installation.
2. *Gage Pattern* — With information about the stress state and directions of principal axes gained from the photoelastic coating studies, there are some areas of the wing tip where single-grid gages and two-element "tee" rosettes can be employed. In other locations, where principal strain directions vary with the nature of the flight maneuver, 45°-degree rectangular rosettes are required.

The strain gradients are sufficiently steep that stacked rosettes should be selected. From Catalog 500, Part A — *Strain Gage Listings*, the foregoing requirements suggest the selection of 060WT and 060WR gage patterns for the stacked rosettes, and the 062AP pattern for the single-grid gage. In making this selection, attention was given to the fact that all three patterns are available in the WK Series, which is compatible with the specified operating temperature range.

3. *Gage Series* — The maximum operating temperature, along with the requirement for static as well as dynamic strain measurement, clearly dictates use of K alloy for the grid material. Either the SK or WK Series could be selected, but the WK gages are preferred because they have integral leadwires.
4. *Options* — For ease of gage installation, Option W, with integral soldering terminals, is advantageous. This option is not applicable to stacked rosettes, however, and is therefore specified for only the single-grid gages.
5. *Resistance* — When available, as in this case, 350-ohm gages should be specified because of the benefits associated with the higher gage resistance.
6. *S-T-C Number* — The titanium alloy used in the wing tip section is the 6Al-4V type, with a thermal expansion coefficient of 4.9×10^{-6} per $^{\circ}$ F (8.8×10^{-6} per $^{\circ}$ C). K alloy of S-T-C number 05 is the appropriate choice.

Gage Designations:

WK-05-062AP-350 Option W

WK-05-060WT-350

WK-05-060WR-350

GAGE PATTERN Actual Size Shown.
Enlarged When Necessary
For Definition.

ES = Each Section
S = Section (S1 = Sec 1)
CP = Complete Pattern
M = Matrix

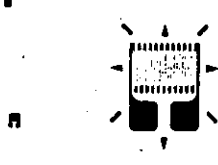
inches
millimetres

GAGE PATTERN Actual Size Shown.
Enlarged When Necessary
For Definition.

ES = Each Section
S = Section (S1 = Sec 1)
CP = Complete Pattern
M = Matrix

inches
millimetres


031CF



1X 6X

GAGE LENGTH	OVERALL LENGTH	GRID WIDTH	OVERALL WIDTH
0.031	0.076	0.062	0.062
0.79	1.93	1.57	1.57
Matrix Size		0.19L x 0.14W	4.8L x 3.5W


062AP



1X 2X

GAGE LENGTH	OVERALL LENGTH	GRID WIDTH	OVERALL WIDTH
0.062	0.114	0.062	0.062
1.57	2.90	1.57	1.57
Matrix Size		0.26L x 0.15W	6.6L x 4.1W

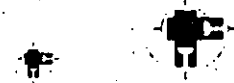
250BF



1X 2X

GAGE LENGTH	OVERALL LENGTH	GRID WIDTH	OVERALL WIDTH
0.250	0.375	0.125	0.125
6.35	9.53	3.18	3.18
Matrix Size		0.52L x 0.22W	13.2L x 5.6W

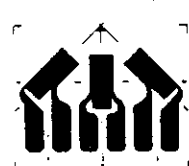
060WT



1X 2X

GAGE LENGTH	OVERALL LENGTH	GRID WIDTH	OVERALL WIDTH
0.060 ES	0.240 M	0.060 ES	0.300 M
1.52 ES	6.1 M	1.52 ES	7.6 M
Matrix Size		0.24L x 0.30W	6.1L x 7.6W

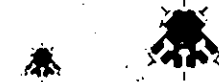
250RD



1X 2X

GAGE LENGTH	OVERALL LENGTH	GRID WIDTH	OVERALL WIDTH
0.250 ES	0.550 CP	0.125 ES	0.847 CP
6.35 ES	13.79 CP	3.18 ES	21.51 CP
Matrix Size		0.78L x 0.93W	19.8L x 23.6W

060WR



1X 2X

GAGE LENGTH	OVERALL LENGTH	GRID WIDTH	OVERALL WIDTH
0.060 ES	0.24 M	0.060 ES	0.030 M
1.52 ES	6.1 M	1.52 ES	7.6 M
Matrix Size		0.24L x 0.30W	6.1L x 7.6W

Strain Gage Installations with M-Bond 200 and AE-10 Adhesive Systems

1.0 INTRODUCTION

Because the strain gage is an extremely sensitive device capable of registering the smallest effects of an imperfect bond, considerable attention to detail must be taken to assure stable, creep-free installations. However, the techniques involved are very simple, and readily mastered.

This manual gives explicit step-by-step instructions for making consistently successful strain gage installations with M-Bond 200 and M-Bond AE-10 Adhesives. These directions should be followed precisely. More detailed information may be found in the Measurements Group VideoTech™ Library and in the following publications:

- Instruction Bulletin B-129, *Surface Preparation for Strain Gage Bonding.*
- Instruction Bulletin B-127, *Strain Gage Installations with M-Bond 200 Adhesive.*
- Instruction Bulletin B-137, *Strain Gage Installations with M-Bond AE-10/15 and M-Bond GA-2 Adhesive Systems.*

All operations described in this manual can be performed with the use of the Student Strain Gage Application Kit. The procedures outlined here are ideally suited to the classroom or teaching laboratory. For most teaching/learning activities involving strain gage technology, the specially priced, first-quality *Student Gages* manufactured by Micro-Measurements Division of the Measurements Group may be used with excellent results.



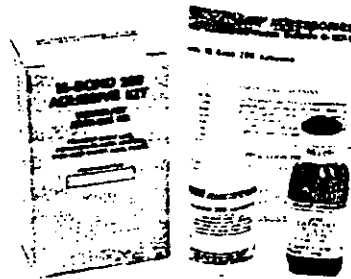
2.0 STRAIN GAGE ADHESIVES

Because consistently successful installation of strain gages requires the use of an adhesive certified for strain gage use, Micro-Measurements *M-LINE* adhesives undergo extensive laboratory testing to ensure reliability and consistency of those properties required in strain gage bonding. To assure

accurate and reliable strain gage measurements, it is strongly recommended that a certified adhesive such as M-Bond 200 methyl-2-cyanoacrylate or M-Bond AE-10 epoxy adhesive be selected for most general laboratory installations.

2.1 M-Bond 200

Micro-Measurements certified M-Bond 200 is an excellent general-purpose laboratory adhesive because of its fast room-temperature cure and ease of application. It is compatible with all Micro-Measurements strain gages and all common structural materials. M-Bond 200 Adhesive can be used for high-elongation tests (+60 000µε), for fatigue studies, and for one-cycle proof tests within a normal operating temperature range of -25° to +150° F (-32° to +65° C).

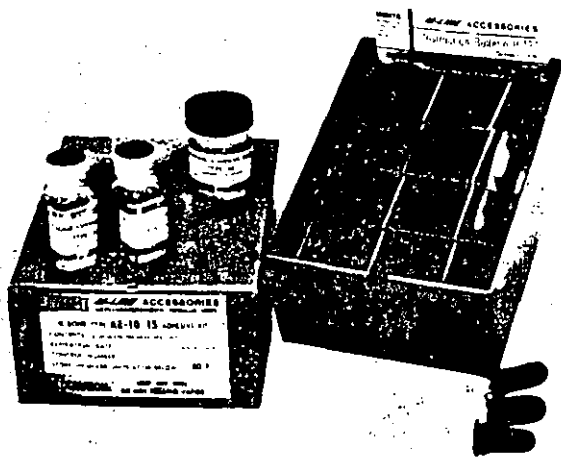


The catalyst supplied with M-Bond 200 is specially formulated to control the reactivity rate. For best results, the catalyst should be used sparingly. Since M-Bond 200 bonds are weakened by exposure to high humidity, adequate protective coatings are essential. Because this adhesive will become harder and more brittle with time, M-Bond 200 is not generally recommended for permanent installations over one or two years in duration.

HANDLING PRECAUTIONS

M-Bond 200 is a cyanoacrylate compound. *Immediate bonding of eye, skin, or mouth may result upon contact. Causes irritation.* The user is cautioned to (1) *avoid contact with skin;* (2) *avoid prolonged or repeated breathing of vapors;* and (3) *use with adequate ventilation.* For additional health and safety information, consult the material safety data sheet which is available upon request.

The shelf life of M-Bond 200 is six months when stored under normal laboratory conditions. Life of *unopened* material can be extended by refrigeration [+40° F (+5° C)]. Due to possible condensation problems, care should be taken to allow the unopened bottle to return to room temperature before opening. Refrigeration after opening is not recommended.



Micro-Measurements certified M-Bond AE-10 is a 100% solids epoxy system for use with strain gages. It offers the advantages of high elongation (10%) and wider operating temperature range [-320° to +200° F (-195° to +95° C)]. Because it is highly resistant to moisture and most chemicals, M-Bond AE-10 is recommended for permanent installations over one year in duration.

M-Bond AE-10 Adhesive is supplied in kit form with pre-weighed resin and sufficient curing agent for six separate mixes of adhesive. Allow the materials to attain room temperature before opening the containers. Each of the individual units of resin can be separately activated by filling one of the calibrated droppers with curing agent *exactly* to the number 10 and dispensing the contents into the center of the jar of resin. *Immediately cap the bottle of curing agent to avoid moisture absorption.* Mix the resin and curing agent for five minutes, using one of the plastic stirring rods. The pot life or working time after mixing is 15 to 20 minutes at +75° F (+24° C). The pot life can be somewhat extended by occasionally stirring the mixture, by cooling the jar, or by spreading the adhesive on a chemically clean aluminum plate. Discard the dropper and stirring rod after use.

HANDLING PRECAUTIONS

While M-Bond AE-10 is considered relatively safe to handle, *contact with skin and inhalation of its vapors should be avoided.* Immediately washing with ordinary soap and water is effective in cleansing should skin contact occur. For eye contact, rinse thoroughly with copious amounts of water and consult a physician. For additional health and safety information, consult the material safety data sheet which is available upon request.

The shelf life of unmixed components is one year at room temperature. During storage, crystals may form in the resin. These crystals do not affect adhesive performance, but should be reliquefied prior to mixing by warming the resin jar to +120° F (+50° C) for approximately one-half hour. Because excess heat will shorten pot life, allow the resin to return to room temperature before adding the curing agent.

3.0 SURFACE PREPARATION

Strain gages can be bonded satisfactorily to almost any solid material if the material surface is properly prepared. While there are many surface preparation techniques available, the specific procedures and techniques described here are a carefully developed and thoroughly proven system. They are ideal for both M-Bond 200 and M-Bond AE-10 Strain Gage Adhesives.

The purpose of surface preparation is to develop a chemically clean surface having a roughness appropriate to the gage installation requirements, a surface alkalinity of the correct pH, and visible gage layout lines for locating and orienting the strain gage. The Micro-Measurements system of surface preparation will accomplish these objectives for aluminum alloys and steels in five basic operations:

- Solvent degreasing
- Surface abrading
- Application of gage layout lines
- Surface conditioning
- Neutralizing

To ensure maximum cleanliness and best results, the following should be avoided in all steps:

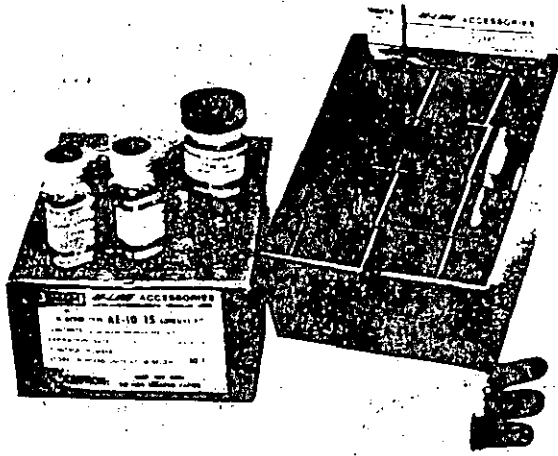
- Touching the surface with the fingers
- Wiping back and forth or reusing swabs or sponges
- Dragging contaminants into the cleaned area from the uncleaned boundary of that area
- Allowing a cleaning solution to evaporate on the surface
- Allowing partially prepared surface to sit between steps in the preparation process or a prepared surface to sit before bonding

Consult Instruction Bulletin B-129 for other test materials and for special precautions and considerations for surface preparation.

3.1 Solvent Degreasing



Degreasing is performed to remove oils, greases, organic contaminants, and soluble chemical residues. Degreasing should *always* be the first operation.



Micro-Measurements certified M-Bond AE-10 is a 100% solids epoxy system for use with strain gages. It offers the advantages of high elongation (10%) and wider operating temperature range [-320° to +200° F (-195° to +95° C)]. Because it is highly resistant to moisture and most chemicals, M-Bond AE-10 is recommended for permanent installations over one year in duration.

M-Bond AE-10 Adhesive is supplied in kit form with pre-weighed resin and sufficient curing agent for six separate mixes of adhesive. Allow the materials to attain room temperature before opening the containers. Each of the individual units of resin can be separately activated by filling one of the calibrated droppers with curing agent *exactly* to the number 10 and dispensing the contents into the center of the jar of resin. *Immediately cap the bottle of curing agent to avoid moisture absorption.* Mix the resin and curing agent for five minutes, using one of the plastic stirring rods. The pot life or working time after mixing is 15 to 20 minutes at +75° F (+24° C). The pot life can be somewhat extended by occasionally stirring the mixture, by cooling the jar, or by spreading the adhesive on a chemically clean aluminum plate. Discard the dropper and stirring rod after use.

HANDLING PRECAUTIONS

While M-Bond AE-10 is considered relatively safe to handle, *contact with skin and inhalation of its vapors should be avoided.* Immediately washing with ordinary soap and water is effective in cleansing should skin contact occur. For eye contact, rinse thoroughly with copious amounts of water and consult a physician. For additional health and safety information, consult the material safety data sheet which is available upon request.

The shelf life of unmixed components is one year at room temperature. During storage, crystals may form in the resin. These crystals do not affect adhesive performance, but should be reliquefied prior to mixing by warming the resin jar to +120° F (+50° C) for approximately one-half hour. Because excess heat will shorten pot life, allow the resin to return to room temperature before adding the curing agent.

Strain gages can be bonded satisfactorily to almost any solid material if the material surface is properly prepared. While there are many surface preparation techniques available, the specific procedures and techniques described here are a carefully developed and thoroughly proven system. They are ideal for both M-Bond 200 and M-Bond AE-10 Strain Gage Adhesives.

The purpose of surface preparation is to develop a chemically clean surface having a roughness appropriate to the gage installation requirements, a surface alkalinity of the correct pH, and visible gage layout lines for locating and orienting the strain gage. The Micro-Measurements system of surface preparation will accomplish these objectives for aluminum alloys and steels in five basic operations:

- Solvent degreasing
- Surface abrading
- Application of gage layout lines
- Surface conditioning
- Neutralizing

To ensure maximum cleanliness and best results, the following should be avoided in all steps:

- Touching the surface with the fingers
- Wiping back and forth or reusing swabs or sponges
- Dragging contaminants into the cleaned area from the uncleaned boundary of that area
- Allowing a cleaning solution to evaporate on the surface
- Allowing partially prepared surface to sit between steps in the preparation process or a prepared surface to sit before bonding

Consult Instruction Bulletin B-129 for other test materials and for special precautions and considerations for surface preparation.

3.1 Solvent Degreasing

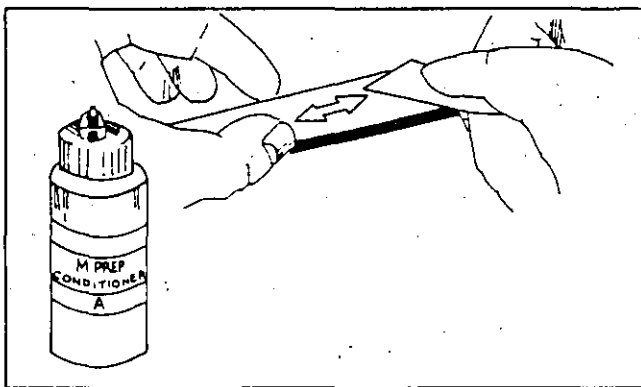


Degreasing is performed to remove oils, greases, organic contaminants, and soluble chemical residues. Degreasing should *always* be the first operation.

Degreasing can be accomplished using a solvent such as CSM-1 Degreaser. Spray applicators are preferred to avoid back-contamination of the parent solvent. Use a clean gauze sponge to clean the entire specimen, if possible, or an area covering 4 to 6 in (100 to 150 mm) on all sides of the gage location.

3.2 Surface Abrading

The surface is abraded to remove any loosely bonded adherents (scale, rust, paint, coatings, oxides, etc.), and to develop a surface texture suitable for bonding. For rough or coarse surfaces it may be necessary to start with a grinder, disc sander, or file; but, for most specimens a suitable surface can be produced with only silicon-carbide paper of the appropriate grit.



Place a liberal amount of M-Prep Conditioner A in the gaging area and wet-lap with clean 320-grit silicon-carbide paper for aluminum, or 220-grit for steel. Add Conditioner A as necessary to keep the surface wet during the lapping process.

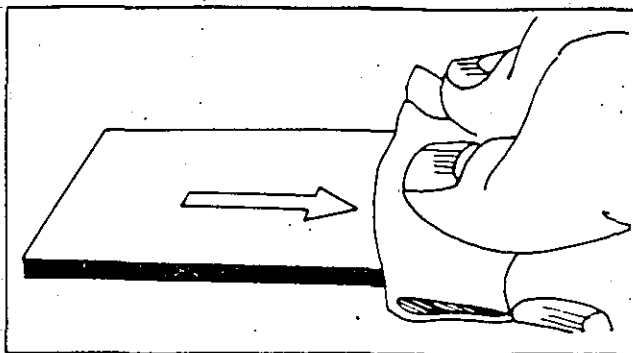
When a bright surface is produced, wipe the surface dry with a clean gauze sponge. A clean surface of the gauze should be used with each wiping stroke. A sufficiently large area should be cleaned to ensure that contaminants will not be dragged back into the gaging area during the steps to follow.

Repeat the above step, using 400-grit silicon-carbide paper for aluminum, or 320-grit for steel.

3.3 Layout Lines

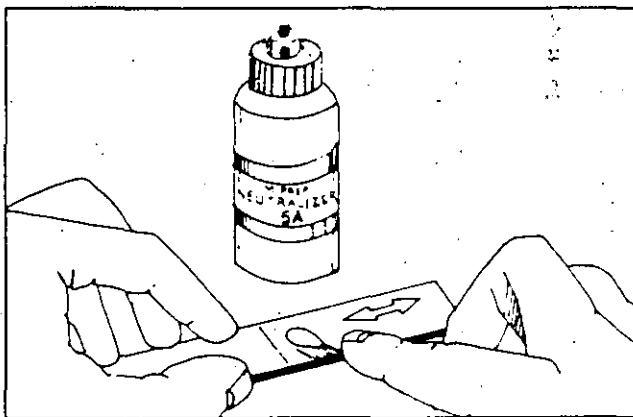
The desired location and orientation of the strain gage on the test surface should be marked with a pair of crossed, perpendicular reference lines. The reference or layout lines should be *burnished*, rather than scored or scribed, on the surface. For aluminum, a medium-hard drafting pencil is satisfactory. For most steels, a ball-point pen or a tapered brass rod may be used. All residue from the burnishing operations should be removed in the following step.

3.4 Surface Conditioning



After the layout lines are marked, Conditioner A should be applied repeatedly, and the surface scrubbed with cotton-tipped applicators until a clean tip is no longer discolored by scrubbing. The surface should be kept constantly wet with Conditioner A until the cleaning is completed. When clean, the surface should be dried by wiping through the cleaned area with a *single* slow stroke of a gauze sponge. The stroke should begin inside the cleaned area to avoid dragging contaminants in from the surrounding area. Throw the used gauze away and, with a fresh gauze, make a *single* slow stroke in the opposite direction. Throw the second gauze away.

3.5 Neutralizing



To provide optimum alkalinity for Micro-Measurements strain gage adhesives, the cleaned surfaces must be neutralized. This can be done by applying M-Prep Neutralizer 5A liberally to the cleaned surface, and scrubbing the surface with a clean cotton-tipped applicator. The cleaned surface should be kept completely wet with Neutralizer 5A throughout this operation. When neutralized, the surface should be dried by wiping through the cleaned area with a *single* slow stroke of a clean gauze sponge. Throw the gauze away and with another fresh gauze sponge, make a *single* stroke in the opposite direction. Always begin within the cleaned area to avoid recontamination from the uncleaned boundary.

If the foregoing instructions have been followed precisely, the surface is now properly prepared for gage bonding. The gages should be installed within 30 minutes on aluminum or 45 minutes on steel.

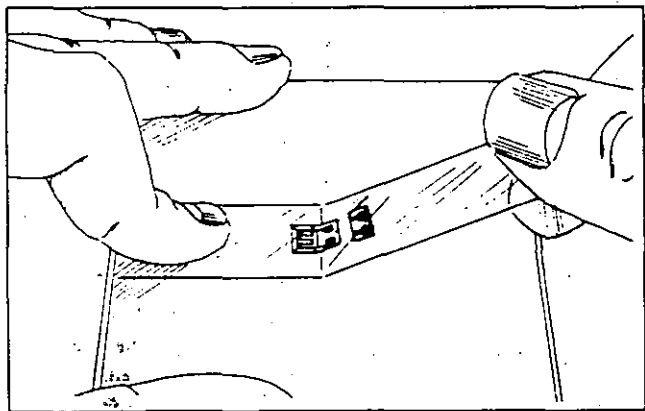
4.0 STRAIN GAGE BONDING

The electrical resistance strain gage is capable of making accurate and sensitive indications of strains on the surface of the test part. Its performance is absolutely dependent on the bond between itself and the test part. The procedures outlined below will help ensure satisfactory bonds when using M-Bond 200 or AE-10 Adhesives. While the steps may appear unduly elaborate, these techniques have been used repeatedly in strain gage installations which have yielded consistent and accurate results. The steps shown assume that a terminal strip will be used. When CEA-Series gages are used, no strip is required.

4.1 Handling and Preparation

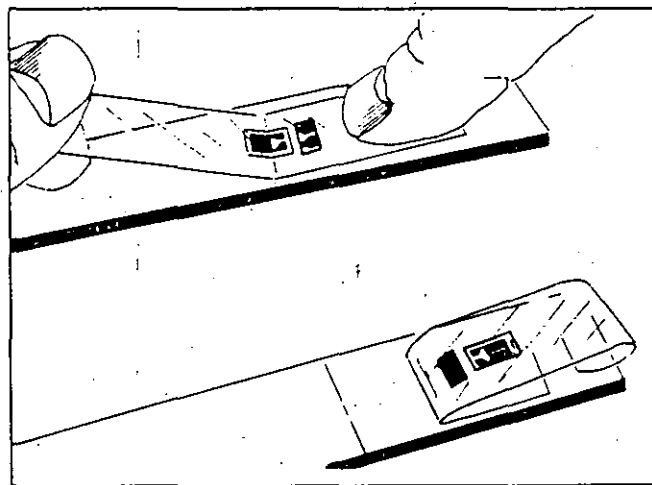
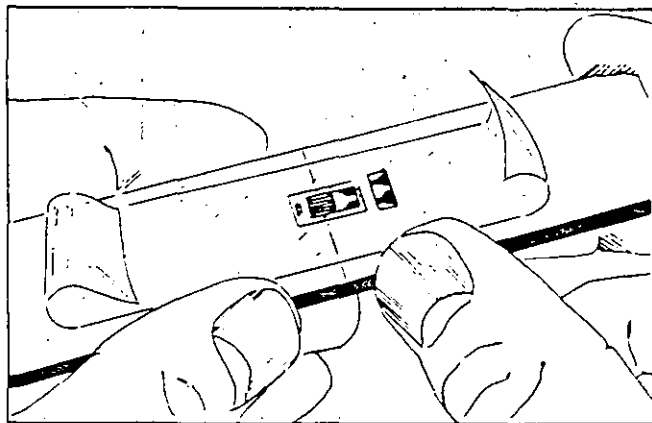
Micro-Measurements strain gages are specially treated for optimum bond formation with all appropriate gage adhesives. No further cleaning is necessary if contamination of the prepared bonding surface is avoided during handling. (Should contamination occur, clean with a cotton swab moistened with a low residue solvent such as *M-LINE* Neutralizer 5A or GC-6 Isopropyl Alcohol. Allow the gage to dry for several minutes before bonding.) Gages should never be touched with the hands.

Remove the strain gage from its acetate envelope by grasping the edge of the gage backing with tweezers, and place on a chemically clean glass plate (or empty gage box) with the bonding side of the gage down. Place the appropriate terminals (if any) next to the strain gage solder tabs, leaving a space of approximately $1/16$ in (1.5 mm) between the gage backing and terminal.



Using a 4-to-6-in (100 -to- 150 -mm) length of *M-LINE* PCT-2A cellophane tape, anchor one end of the tape to the glass plate behind the gage and terminal. Wipe the tape firmly down over the gage and terminals. Pick the gage and terminals up by carefully lifting the tape at a shallow angle (30 to 45 degrees) until the tape comes free with the gage and terminal attached. (The shallow angle is important to avoid over-stressing the gage and causing permanent resistance changes.) **Caution: Some tapes may contaminate the bonding surface or react with the bonding adhesive. Use only tapes certified for strain gage installations.**

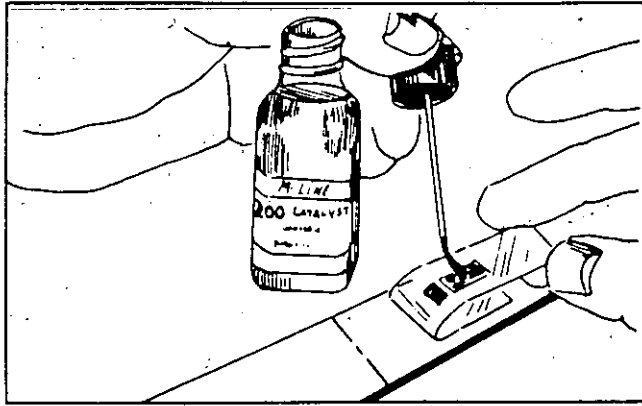
The strain gage is now prepared for positioning on the test specimen. Position the gage; tape assembly so the triangle alignment marks on the gage are over the layout lines on the specimen. Holding the tape at a shallow angle, wipe the assembly onto the specimen surface. If the assembly is misaligned, lift the tape again at a shallow angle until the assembly is free of the specimen. Reposition and wipe the assembly again with a shallow angle.



In preparation for applying the adhesive, lift the end of the tape opposite the solder tabs at a shallow angle until the gage and terminal are free of the specimen. Tack the loose end of the tape under and press to the surface so the gage lies flat with the bonding side exposed.

The appropriate adhesive may now be applied. The procedures for M-Bond 200 and M-Bond AE-10 are described in the two sections which follow.

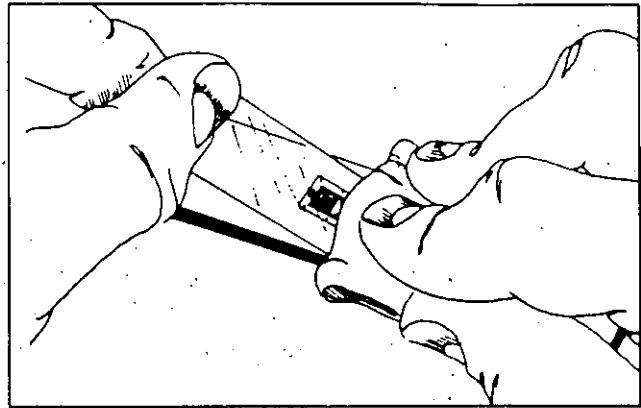
4.2 Bonding with M-Bond 200



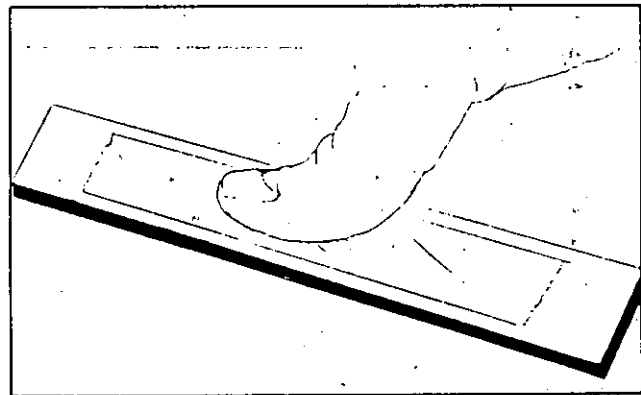
M-Bond 200 Catalyst should be applied sparingly in a thin uniform coat. Wipe the brush against the lip of the bottle approximately ten times to remove most of the catalyst. Set the brush down on the gage and swab the gage backing by sliding — not brushing in the painting style — the brush over the entire gage surface. Move the brush to an adjacent tape area prior to lifting from the surface. Allow the catalyst to dry at least one minute under normal ambient laboratory conditions.

The next three steps must be completed in sequence within three to five seconds. Read these steps before proceeding.

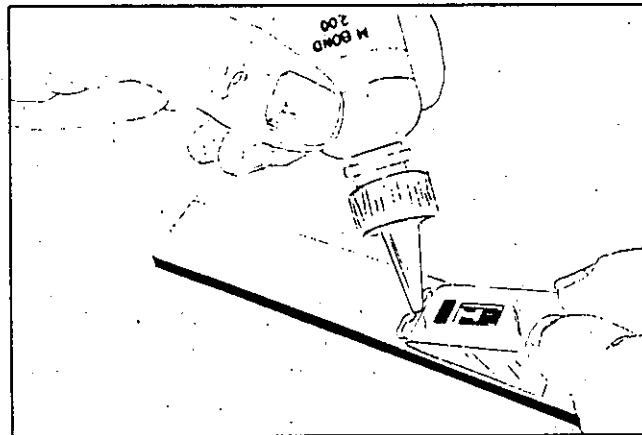
Holding the tape slightly taut and beginning from the tab end of the gage, slowly and *firmly* make a single wiping stroke over the gage/tape assembly with a clean gauze sponge to bring the gage back down over the alignment marks on the specimen. Release the tape.



Immediately upon completion of the above step, *discard the gauze* and apply firm thumb pressure to the gage and terminal area. This pressure should be held for at least one minute. Wait two minutes before the next step (tape removal).

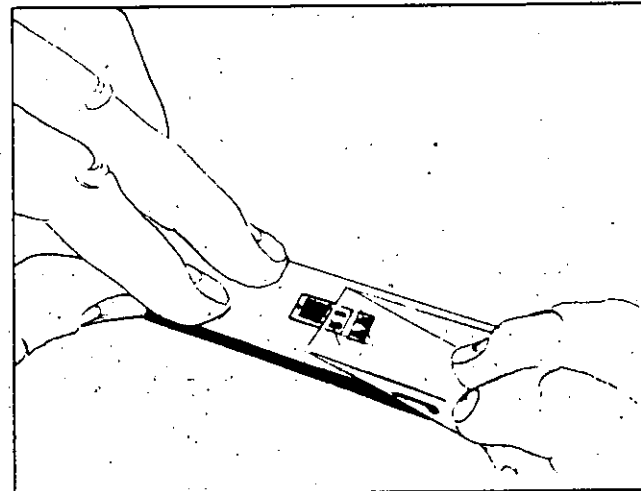


The gage and terminals should now be bonded to the specimen. To remove the tape, pull it back directly over itself, *peeling* it slowly and steadily off the surface.



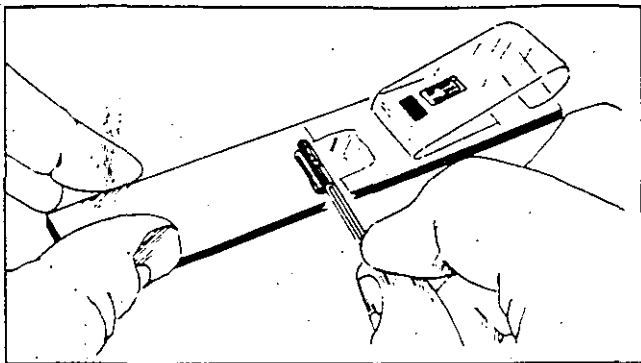
Lift the tucked-under tape. Holding the gage/tape assembly in a fixed position, apply one or two drops of M-Bond 200 Adhesive at the junction of the tape and specimen surface, about $1/2$ in (13 mm) outside the actual gage installation area.

Immediately rotate the tape to approximately a 30-degree angle so that the gage is bridged over the installation area.

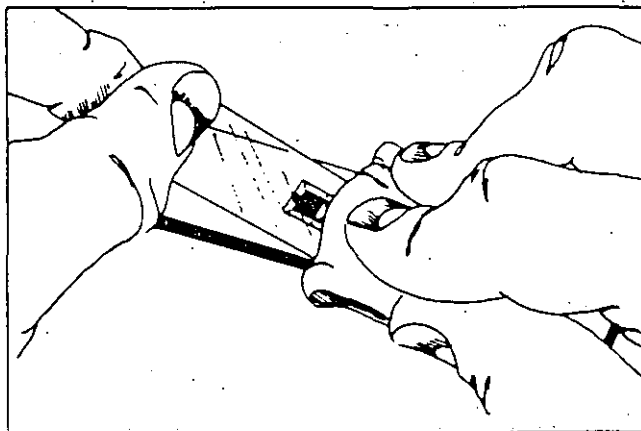


4.3 Bonding with M-Bond AE-10

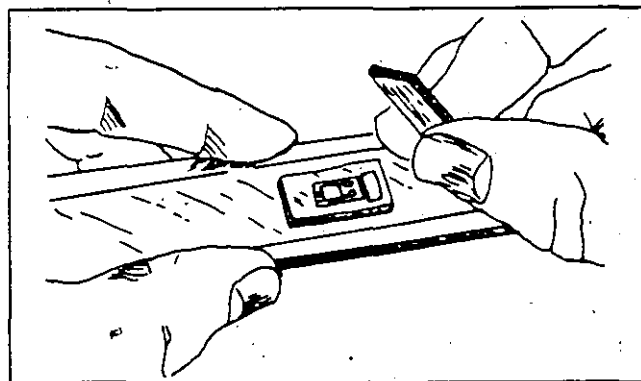
(This section follows 4.1 when using M-Bond AE-10 Adhesive.) Mix the Resin AE with Curing Agent Type 10 per the instructions in Instruction Bulletin B-137 supplied with the adhesive.



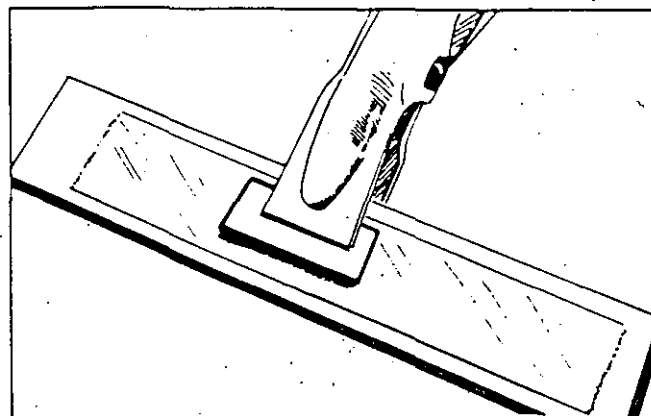
Coat the specimen and back of the gage and terminal with the prepared M-Bond AE-10 Adhesive. The mixing rod may be used to apply a thin layer of adhesive over both surfaces. *Be careful not to pick up any unmixed components of the adhesive.* To ensure this, wipe the mixing rod clean and then pick up a very small amount of adhesive from the central area of the adhesive jar. After applying the adhesive, proceed immediately to the next step.



Lift the tuckered-over end of the tape and bridge over the specimen installation area at approximately a 30-degree angle. Beginning from the tab end of the gage and using a clean gauze sponge, slowly and firmly make a single wiping stroke over the gage/tape assembly to bring the gage back down over the alignment marks on the specimen.

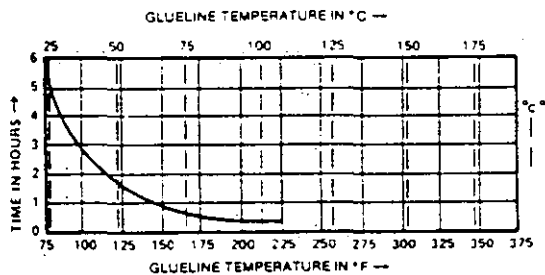


Place a silicone rubber pad and a back-up plate over the gage installation. Apply force by dead weight or spring clamp until a pressure of 5 to 20 psi (35 to 135 kN/M²) is attained. Take care to ensure the pressure is equal over the entire gage surface.



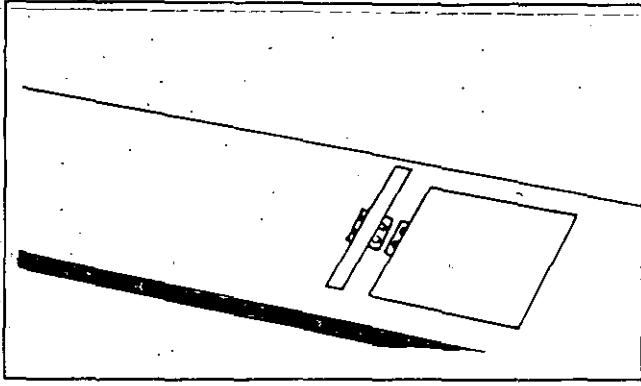
The M-Bond AE-10 Adhesive will develop adequate bonding strength in six hours at room temperature [-75°F (+24°C)]. The time may be reduced by increasing the temperature of the glue line per the schedule below. **Warning:** For curing temperature above +150°F (+66°C) a special mylar tape must be used for gage handling, and a Teflon® strip should be placed between the gage and the silicone rubber pad.

RECOMMENDED CURE SCHEDULE



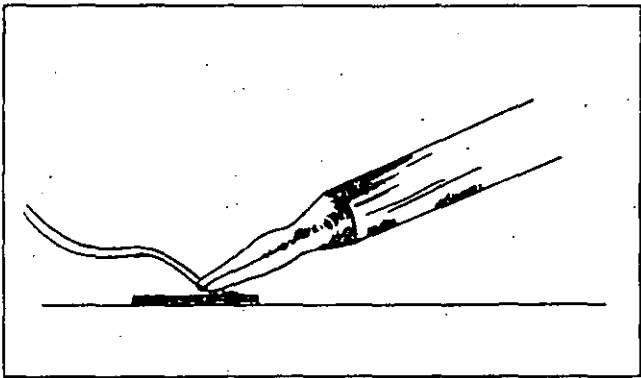
After the adhesive is cured, remove the clamps or weights, the silicone pads and Teflon strip (if used). To remove the tape, pull it back directly over itself, *peeling* it slowly and steadily off the surface.

5.0 SOLDERING TECHNIQUES



If the strain gage is without encapsulation or preattached lead ribbons, mask the gage grid area with drafting tape, leaving only the tabs exposed.

After the soldering iron has reached operating temperature, clean the tip with a gauze sponge and tin it with fresh solder. Tin the gage tabs and terminal tabs (if used). Melt a small amount of solder on the tip of the soldering iron, lay the rosin-core solder wire across the gage tab or copper terminal. Firmly apply the iron tip for one second, then *simultaneously* lift both solder and tip. A bright, shiny, even mound of solder should have been deposited on the tab. If not, repeat the process. If spikes are formed rather than smooth beads, it is a sign of inadequate flux, dwelling too long with the iron, and/or an improper iron temperature. Feeding the cored solder into the tab area during heat application will increase the amount of flux available.

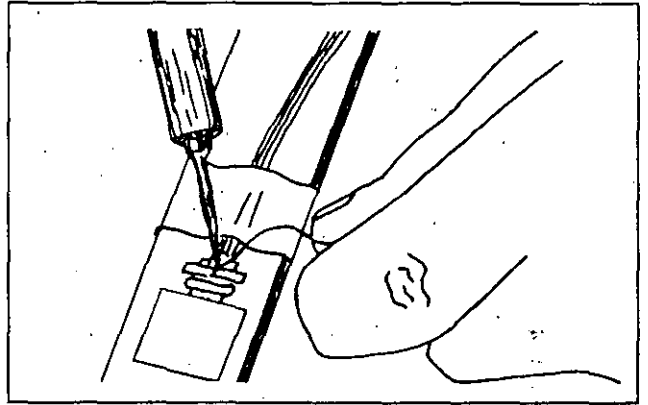


For a three-conductor lead-in wire, separate the individual leads for $3/4$ in (20 mm). Strip away $1/2$ in (13 mm) of insulation by using the soldering tip to melt the insulation on both sides of each end of the wire $1/2$ in (13 mm) from the ends and quickly pulling off the insulation. **Warning: Do not use a knife or other blade to cut the insulation.** When the main leadwire is stranded and terminal strips are used, it is often convenient to cut all strands but one to fit the size of the copper pad. The long strand can then be used as the jumper wire. Soldering is made considerably easier by this method. This is unnecessary when the leadwires are bonded directly to the solder tabs on CEA-Series strain gages.

Holding the tip of a finger on the tip of the tinned wire for safety, cut each wire with diagonal wire cutters leaving $1/8$ in (3 mm) of exposed, tinned wire.

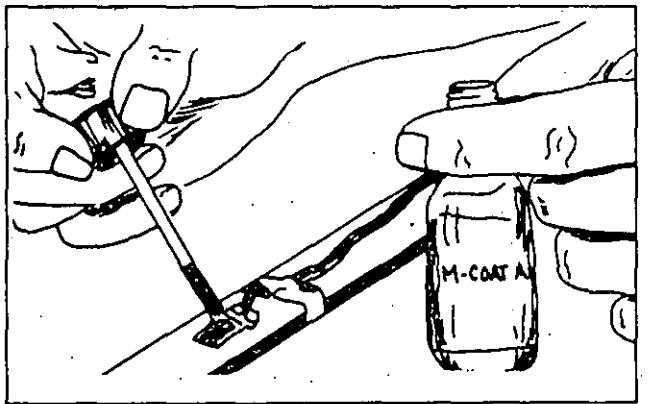
Tack the lead-in wires to the specimen with drafting tape so the tinned end of the wire is spring-loaded in contact with the solder bead. Complete the solder connection as before by applying solder and iron tip for one second and removing simultaneously.

Apply rosin solvent liberally to the solder joints. Drafting tape may be removed by loosening the mastic with rosin solvent. Remove all solvent with a gauze sponge, using a dabbing action. Repeat.



Tape or otherwise secure the lead-in wires to the specimen to prevent the wires from being accidentally pulled from the tabs. A stress relief "loop" should be placed between the tape and the solder connections.

Apply a protective coating over the entire gage and terminal area. For most laboratory uses, M-Coat A will provide adequate long-term protection. The coating should be continuous up to and over at least the first $1/8$ in (3 mm) of leadwire insulation.

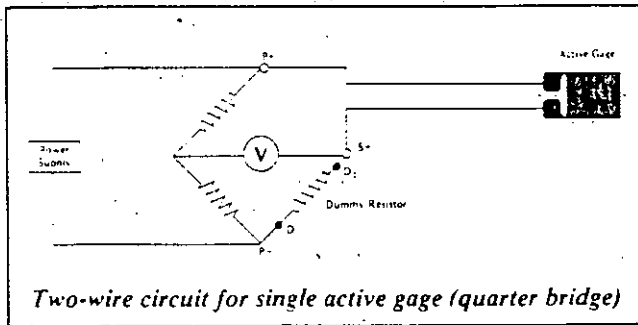


The properly installed strain gage will have a resistance to ground of at least 10 000 to 20 000 megohms. Checking leakage resistance with the Model 1300 Gage Installation Tester is highly recommended.

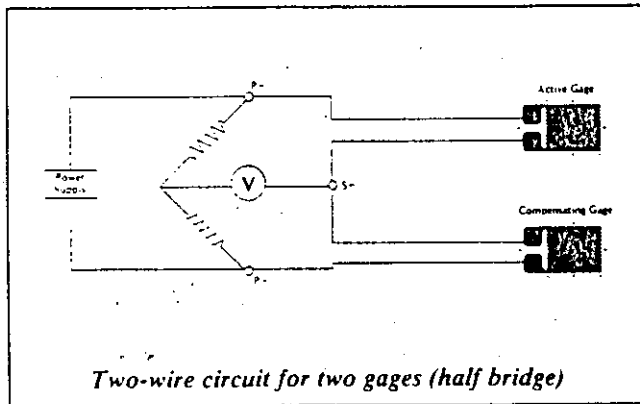
6.0 TWO-AND THREE-WIRE CIRCUITS

All commercial static strain indicators employ some form of the Wheatstone bridge circuit to detect the resistance change in the gage with strain.

When a single active gage is connected to the Wheatstone bridge with only two wires, as shown in the accompanying schematic, both the wires will be in series with the gage in the same arm of the bridge circuit. One of the effects of this arrangement is that temperature-induced resistance changes in the leadwires are manifested as thermal output by the strain indicator.



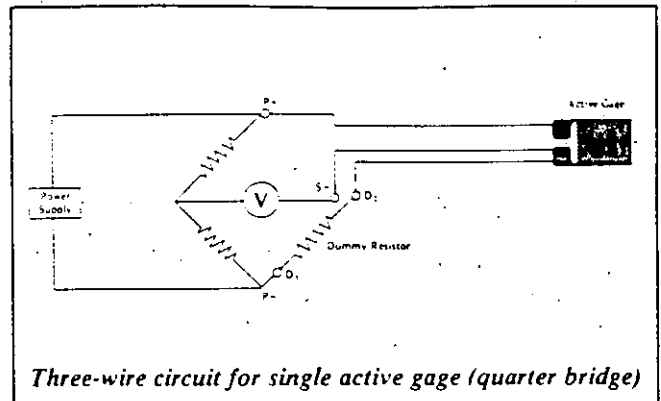
The errors due to leadwire resistance changes in single-gage installations with two-wire circuits can be minimized by minimizing the total leadwire resistance; that is, by using short leadwires of the largest practicable cross-section.



When two matched gages are connected as adjacent arms of the bridge circuit (with the same length leadwires, maintained at the same temperature), the temperature effects cancel since they are the same in each arm, and "like" resistance changes in adjacent arms of the bridge circuit are self-nullifying.

Leadwire effects can be virtually eliminated in single active gage installations by use of the "three-wire" circuit. In this case a third lead, representing the centerpoint connection of the bridge circuit, is brought out to one of the gage terminals. Resistance changes in the bridge centerpoint lead do not affect bridge balance.

For this method of leadwire compensation to be effective, the two leadwires in the adjacent bridge arms should be the same length, and should be maintained at the same temperature. The three-wire circuit is the standard method of connection for a single active temperature-compensated strain-gage in a quarter-bridge arrangement.



Contact resistance at mechanical connections within the Wheatstone bridge circuit can lead to errors in the measurement of strain. Connections should be snugly made. Following bridge balance, a "wiggle" test should be made on wires leading to mechanical connections. No change in balance should occur if good connections have been made.

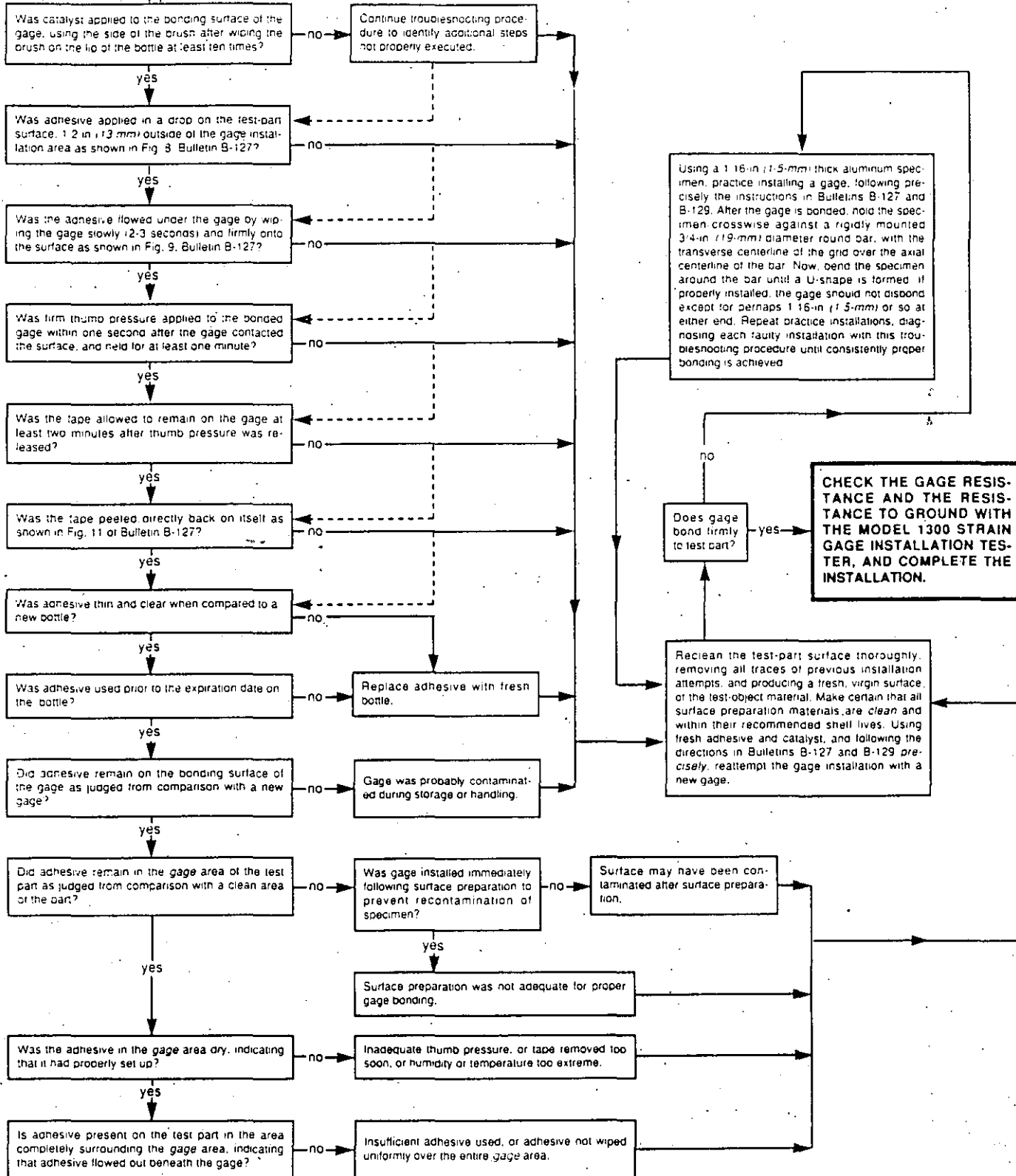
If necessary, contact surfaces may be cleaned of oils with a low residue solvent such as isopropyl alcohol. If long periods of disuse have caused contact surfaces to tarnish, clean them by scraping lightly with a knife blade.

7.0 TROUBLESHOOTING PROCEDURE

M-Bond 200 Gage Installation

I attempted to install a strain gage with M-Bond 200 Adhesive, but the gage unbonded from the test surface when I removed the handling tape. What should I do?

When the gage fails to adhere to the test-part surface, it is necessary, of course, to reprepare the surface and install a new gage. Before doing so, however, follow through this troubleshooting procedure to isolate the cause or causes of bond failure. Among the first seven questions, any question which cannot be answered precisely and firmly with YES or NO for its answer. Irrespective of encountering one or more NO answers, the troubleshooting procedure should be continued via the dashed lines to identify additional installation steps which may not have been performed properly. In any case, a careful review of Micro-Measurements Instruction Bulletin B-127, *Strain Gage Installations with M-Bond 200 Adhesive*, is recommended before attempting to install a new gage. See also the VideoTech™ Library.

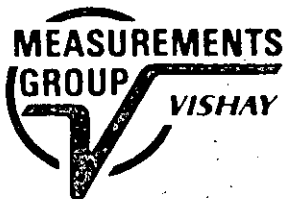
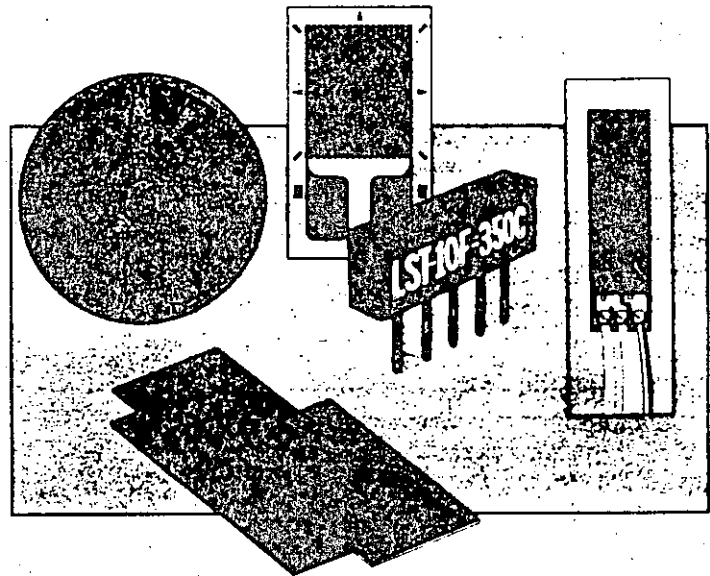
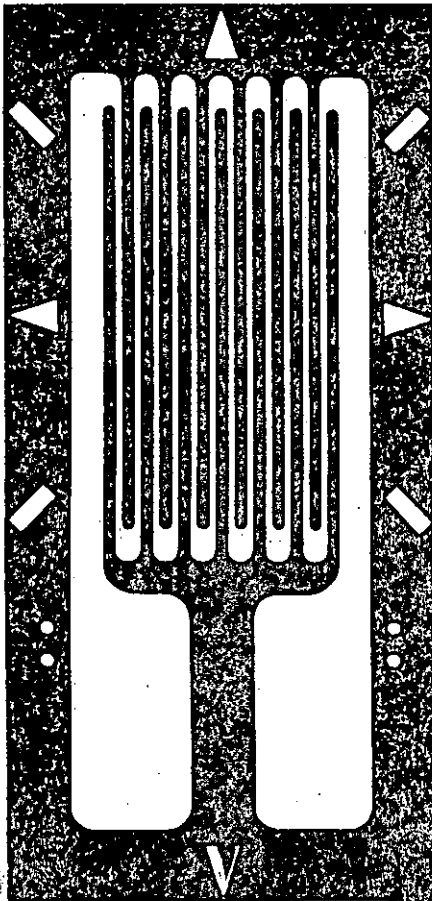


An Introduction to . . .

Micro-Measurements

MEME

- Strain Gages
- Special Sensors
- Installation Accessories



The Broadest Range Of Strain Gages And Accessories Available

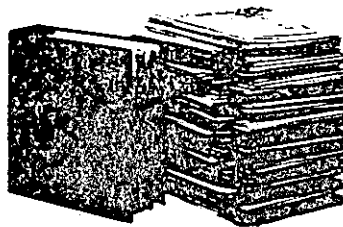
Micro-Measurements has been a trusted name in the field of Strain Gage Technology for many years. We are proud of our worldwide reputation as a premier supplier of high-quality precision strain gages and strain gage accessories, and are fully committed to maintaining our position as the leader in this field. This short-form catalog of Micro-Measurements strain gages and related products is intended to provide a condensed overview of the sensors, supplies, and tools commonly needed for typical strain gage applications.

Micro-Measurements was independently founded and operated in the early 1960's. A few years later it became a part of Vishay Intertechnology, Inc. and, in late 1973, was incorporated with the other stress analysis divisions of Vishay into a single entity — The Measurements Group. All divisions of the Measurements Group are now located in our world headquarters facility near Raleigh, North Carolina. Micro-Measurements maintains an additional strain gage production facility in Romulus, Michigan.

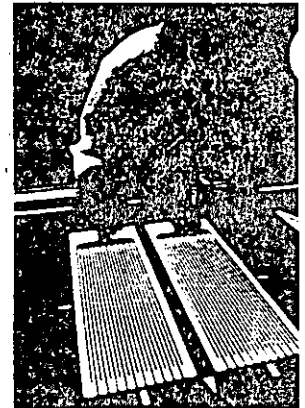
Customer Support Services

The common denominator in all Micro-Measurements products and services is our dedication to helping you achieve consistently accurate and reliable strain measurements. And we've made some significant commitments to help ensure your success:

We publish the widest range of technical reference literature in the strain gage field — available through the Measurements Group's Technical Data Mailing Program.



We respond quickly to requests for "specials" to suit individual requirements.



An experienced and friendly Applications Engineering staff is readily available by phone or letter.



We offer a variety of comprehensive technical training programs from beginner to advanced levels in strain gage technology. The Measurements Group regularly conducts workshops and technical seminars in our Technical Training Center in Raleigh, North Carolina and at locations throughout the U.S. and the world.



At Micro-Measurements, Your Success Is Our Goal

Master Strain Gage Catalog

Catalog 500



This introductory catalog contains abridged strain gage listings which are representative of the types and sizes most widely used in stress analysis applications. For those involved in extensive stress/strain measurement programs, it is advantageous to request a copy of Micro-Measurements Catalog 500. The gage listings in Catalog 500 include essentially all standard types and pattern configurations manufactured by Micro-Measurements. Considering the variations in pattern design, grid alloys, self-temperature-compensation (S-T-C) numbers, backing materials, and optional features, there are over 100,000 possible gage types from which to select.

Catalog 500 contains a broad range of pattern configurations and sizes, designed to meet the many and varied test requirements encountered throughout the field of experimental stress analysis.

A special group of strain gages — *Transducer-Class*® — has been developed specifically for transducer applications. *Transducer-Class* strain gages, described in separate Micro-Measurements literature, are a select group of standard and special gage patterns designed for optimum cost/performance ratio (in transducer service) in high-volume production quantities.

GAGE PATTERN	GAGE DESIGNATION	RES. IN OHMS	OPTIONS AVAILABLE
125AD	EA-XX-125AD-120 ED-DY-125AD-350 EK-XX-125AD-350 WA-XX-125AD-120 WK-XX-125AD-350 EP-08-125AD-120 SA-XX-125AD-120 SK-XX-125AD-350 SD-DY-125AD-350 WD-DY-125AD-350	120 ± 0.15% 350 ± 0.3% 350 ± 0.15% 120 ± 0.3% 350 ± 0.3% 120 ± 0.15% 120 ± 0.3% 350 ± 0.3% 350 ± 0.6% 350 ± 0.6%	W, E, SE, L, LE
125AW	EA-XX-125AW-120 ED-DY-125AW-350 EK-XX-125AW-350 WA-XX-125AW-120 WK-XX-125AW-350 EP-08-125AW-120 SA-XX-125AW-120 SK-XX-125AW-350 SD-DY-125AW-350 WD-DY-125AW-350	120 ± 0.15% 350 ± 0.3% 350 ± 0.15% 120 ± 0.3% 350 ± 0.3% 120 ± 0.15% 120 ± 0.3% 350 ± 0.3% 350 ± 0.6% 350 ± 0.6%	W, E, SE, L, LE
125AM	EA-XX-125AM-120 ED-DY-125AM-350 EK-XX-125AM-350 WA-XX-125AM-120 WK-XX-125AM-350 EP-08-125AM-120 SA-XX-125AM-120 SK-XX-125AM-350 SD-DY-125AM-350 WD-DY-125AM-350	120 ± 0.15% 350 ± 0.3% 350 ± 0.15% 120 ± 0.3% 350 ± 0.3% 120 ± 0.15% 120 ± 0.3% 350 ± 0.3% 350 ± 0.6% 350 ± 0.6%	W, E, SE, L, LE

Gage Listings

Reproduced below is a sample Catalog 500 listing for a single, representative gage pattern. The listing includes a tabulation of all gage series in which the pattern is available, as well as optional features applicable to each series. Complete descriptions of the gage series, options, etc. are provided in the introductory section of Catalog 500.

GAGE PATTERN	GAGE DESIGNATION	RES. IN OHMS	OPTIONS AVAILABLE					
			W	E	SE	L	LE	
ES = Each Section S = Section (S1 = Sec 1) CP = Complete Pattern M = Matrix	Insert Desired S-T-C No. in Spaces Marked XX							

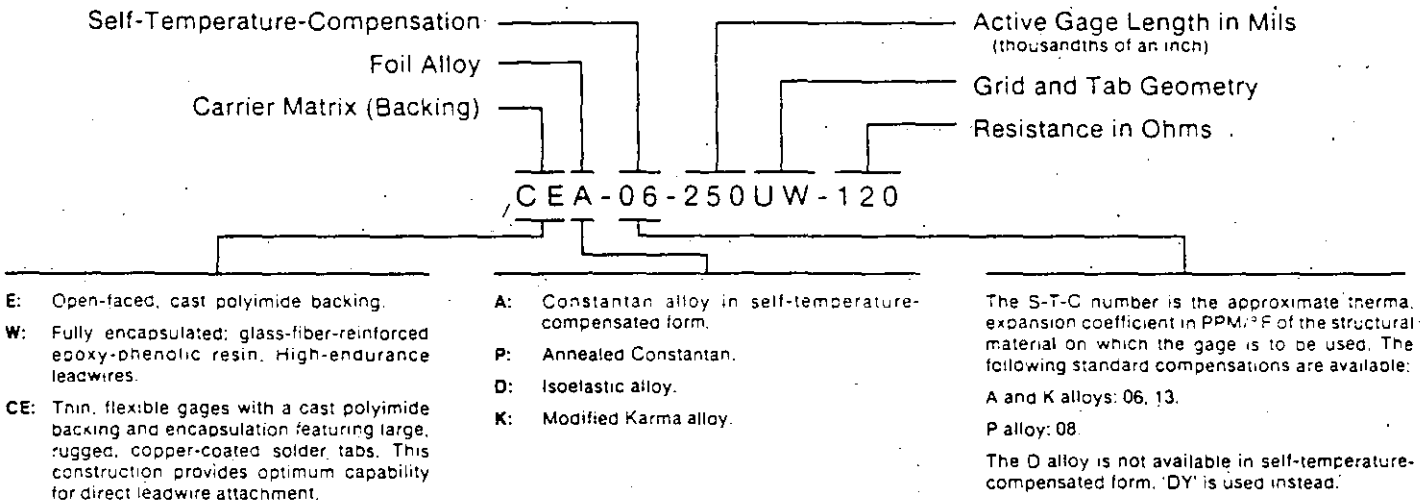
125AD				Widely used general-purpose gage. See also 125AC pattern. EK-Series gages are supplied with duplex copper pads (DP) when optional feature W or SE is not specified.						
				EA-XX-125AD-120	A	120 ± 0.15%				
				ED-DY-125AD-350	A	350 ± 0.3%				
				EK-XX-125AD-350	A	350 ± 0.15%				
				WA-XX-125AD-120	A	120 ± 0.3%				
				WK-XX-125AD-350	A	350 ± 0.3%				
				EP-08-125AD-120	A	120 ± 0.15%				
				SA-XX-125AD-120	A	120 ± 0.3%				
				SK-XX-125AD-350	A	350 ± 0.3%				
				SD-DY-125AD-350	A	350 ± 0.6%				
				WD-DY-125AD-350	A	350 ± 0.6%				
GAGE LENGTH	OVERALL LENGTH	GRID WIDTH	OVERALL WIDTH							
0.125	0.250	0.125	0.125							
3.18	6.35	3.18	3.18							
Matrix Size	0.40L x 0.22W	10.2L x 5.8W								

Strain Gage Designation System and Selection Chart

In selecting the most suitable strain gage for each application, consideration must be given to the variations in pattern design, grid alloy, self-temperature-compensation (S-T-C), backing material; and optional features. The gage designation system and standard strain gage selection chart shown on this page present a partial summary of the many combinations of these factors available in Micro-Measurements strain gages. For brevity, this summary is limited to those gage series and optional features listed in this catalog only. When selecting or ordering a strain gage from this catalog, these charts will provide a key to choosing the appropriate gage for your application.

A complete, detailed designation system and selection chart are included in Catalog 500.

When test conditions are severe, or when there are unusually stringent demands on accuracy and stability, selection of the optimum gage parameters to satisfy the test specifications can involve a number of subtle considerations. As an aid in systematically arriving at the most appropriate gage type, given a specific measurement task, Measurements Group Tech Note TN-505, "Strain Gage Selection Criteria, Procedures, Recommendations", available on request from the Measurements Group's Applications Engineering Department, will provide a valuable reference for use in conjunction with these selection criteria and charts.



Gage Series	DESCRIPTION AND PRIMARY APPLICATION	TEMPERATURE RANGE	STRAIN RANGE	FATIGUE LIFE	
				Strain Level in $\mu\epsilon$	Number of Cycles
EA	General-purpose static and dynamic stress analysis. Wide range of options available.	Normal: -100° to +350° F (-75° to +175° C) Special or Short Term: -320° to +400° F (-195° to +205° C)	±3% for gage lengths under 1/8 in (3.2 mm). ±5% for 1/8 in & over.	±1800 ±1500 ±1200	10 ⁶ 10 ⁶ 10 ⁶
CEA	Universal general-purpose strain gages. Constantan grid completely encapsulated in polyimide, with large, rugged, copper-coated tabs. Primarily used for general-purpose static and dynamic stress analysis.	Normal: -100° to +350° F (-75° to +175° C) Stacked rosettes limited to +150° F (+65° C)	±3% for gage lengths under 1/8 in (3.2 mm). ±5% for 1/8 in & over.	±1500 ±1500	10 ⁶ 10 ⁶ *
ED	Excellent for dynamic measurements. High gage factor and extended fatigue life.	Dynamic: -320° to +400° F (-195° to +205° C)	±2% Nonlinear at strain levels over ±0.5%.	±2500 ±2200	10 ⁶ 10 ⁷
WA	Stress analysis and transducer applications. Wide temperature range and extreme environmental capability. High-endurance leadwires.	Normal: -100° to +400° F (-75° to +205° C) Special or Short-Term: -320° to +500° F (-195° to +260° C)	±2%	±2000 ±1800 ±1500	10 ⁶ 10 ⁶ 10 ⁷
WK	Widest temperature range and most extreme environmental capability. High-endurance leadwires.	Normal: -452° to +550° F (-269° to +290° C) Special or Short-Term: -452° to +750° F (-269° to +400° C)	±1.5%	±2400 ±2200 ±2000	10 ⁶ 10 ⁷ 10 ⁶
EP	High-elongation measurements (post yield). Only available in 08 S-T-C value.	-100° to +400° F (-75° to +205° C)	±10% for gage lengths under 1/8 in (3.2 mm). ±20% for 1/8 in & over.	±1000	10 ⁴ EP gages show zero shift under high-cyclic strains.
WD	For wide-range dynamic strain measurements in severe environments. High-endurance leadwires.	Dynamic: -320° to +500° F (-195° to +260° C)	±1.5% Nonlinear at strain levels over ±0.5%.	±3000 ±2500 ±2200	10 ⁶ 10 ⁷ 10 ⁶
















*Fatigue life improved using low-modulus solder.




















The gages listed on this and the following page represent the most widely used types for general-purpose experimental stress analysis. Gage lengths range from 0.015 to 0.500 in (0.4 to 13 mm) in a wide range of pattern configurations. In addition to single-element gages in a variety of sizes and aspect ratios, the list includes two- and three-element rosettes for use in biaxial stress fields. There are also twin-element chevron patterns for measuring shear strain or torque. Grid resistances of 120, 350, and 1000 ohms are available.

Selection of gages from this list will generally lead to the best delivery and, in many cases, to a price advantage as well. The "C"-feature, or CEA-Series, strain gages are normally the first choice because of the ease of installation. These gages have rugged, copper-coated solder tabs, permitting direct leadwire attachment.

All gages in this list are classified as *Super Stock*. This means that Micro-Measurements guarantees to maintain stock for off-the-shelf delivery of at least 10 packages of any type listed in 06 and 13 self-temperature-compensation numbers (except 08 S-T-C for P alloy and DY for Isoelastic). There are no Minimum Order Requirements for gages selected under the above conditions.

If your application requires a gage that is not listed here, you should refer to Micro-Measurements Catalog 500, which includes all standard, general-purpose Micro-Measurements strain gages. All gage patterns are shown at actual size except where enlargement is necessary for geometry definition.

GAGE DESIGNATION AND PATTERN	GAGE DESIGNATION AND PATTERN	GAGE DESIGNATION AND PATTERN
<p>CEA-XX-015UW-120</p> <p>Micro-miniature pattern with large exposed solder tabs for high-strain-gradient applications. Exposed tab area is 0.06 x 0.04 in (1.5 x 1.0 mm).</p>  <p>4X</p>	<p>EA-XX-062AP-120 WK-XX-062AP-350</p> <p>Compact small general-purpose pattern. Select WK gage for wide temperature range applications.</p>  <p>2X</p>	<p>EA-XX-125AC-350</p> <p>Widely used general-purpose pattern with high-resistance grid.</p> 
<p>CEA-XX-032UW-120</p> <p>Short gage length pattern with large exposed solder tabs for high-strain-gradient applications. Exposed tab area is 0.07 x 0.04 in (1.8 x 1.0 mm).</p>  <p>2X</p>	<p>EA-XX-062AQ-350</p> <p>Same size as 062AP pattern but with high-resistance grid in EA Series.</p>  <p>2X</p>	<p>EA-XX-125AD-120 ED-DY-125AD-350 WD-DY-125AD-350 WK-XX-125AD-350</p> <p>Widely used, general-purpose pattern. Select ED- or WD-DY gages for fatigue applications; WK for wide temperature range static or dynamic measurements.</p> 
<p>EA-XX-031DE-120</p> <p>Miniature pattern for positioning adjacent to high stress concentrations, e.g., holes, fillets, etc.</p>  <p>4X</p>	<p>CEA-XX-062UW-120 CEA-XX-062UW-350</p> <p>Small general-purpose gage with large exposed solder tabs. Exposed tab area is 0.07 x 0.04 in (1.8 x 1.0 mm).</p>  <p>2X</p>	<p>CEA-XX-125UN-120 CEA-XX-125UN-350</p> <p>Narrow general-purpose gage pattern. Exposed tab area is 0.06 x 0.05 in (1.5 x 1.1 mm).</p> 
<p>WA-XX-060WR-120</p> <p>Small 3-element 45° rectangular stacked rosette.</p>  <p>2X</p>	<p>EA-XX-062TV-350</p> <p>Small 2-element 90° torque gage.</p>  <p>2X</p>	<p>CEA-XX-125UW-120 CEA-XX-125UW-350</p> <p>Most widely used general-purpose gage in CEA Series. Exposed tab area is 0.10 x 0.07 in (2.5 x 1.8 mm).</p> 
<p>EA-XX-062AK-120</p> <p>Small general-purpose pattern with elongated solder tabs.</p>  <p>2X</p>	<p>EA-XX-062TT-120</p> <p>Small general-purpose 90° 'tee' rosette. Sections are electrically independent.</p>  <p>2X</p>	<p>EA-XX-125BB-120</p> <p>Narrow general-purpose pattern with elongated tabs.</p> 

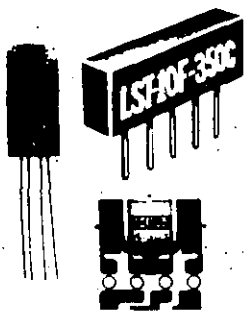
GAGE DESIGNATION AND PATTERN	GAGE DESIGNATION AND PATTERN	GAGE DESIGNATION AND PATTERN
<p>EA-XX-125BT-120</p> <p>General-purpose pattern with narrow grid and compact geometry.</p>  <p>2X</p>	<p>CEA-XX-187UV-120 CEA-XX-187UV-350</p> <p>2-element 90° rosette for torque and shear-strain measurements. Sections have a common electrical connection. Exposed tab area is 0.13 x 0.08 in (3.3 x 2.0 mm).</p> 	<p>EA-XX-250BK-10C</p> <p>Very high-resistance (1000Ω) pattern. Recommended for high bridge voltages or for use on plastics.</p> 
<p>EA-XX-125BZ-350</p> <p>Narrow high-resistance pattern with compact geometry.</p>  <p>2X</p>	<p>EA-XX-250AE-350</p> <p>Large general-purpose gage. Used when high power-dissipation is required.</p> 	<p>CEA-06-W250A-120 CEA-06-W250A-350</p> <p>Lowest-cost, most flexible and conformable linear weldable gage pattern. See page 8 for more details.</p> 
<p>EA-XX-125RA-120</p> <p>General-purpose 3-element 45° rectangular rosette. Compact geometry.</p> 	<p>EA-XX-250AF-120</p> <p>Large general-purpose gage. Used when high power-dissipation is required.</p> 	<p>CEA-XX-250UR-120 CEA-XX-250UR-350</p> <p>Large 3-element 45° single-plane rosette. Exposed tab area is 0.13 x 0.08 in (3.3 x 2.0 mm).</p> 
<p>CEA-XX-125UR-120 CEA-XX-125UR-350</p> <p>General-purpose 45° single-plane rosette. Compact geometry. Exposed tab area is 0.08 x 0.06 in (2.0 x 1.5 mm).</p> 	<p>EA-XX-250BG-120 EP-08-250BG-120 WA-XX-250BG-120 WK-XX-250BG-350</p> <p>Widely used general-purpose pattern. EP Series capable of elongation > 20%.</p> 	<p>EA-XX-500BH-120</p> <p>Long general-purpose gage in a compact geometry.</p> 
<p>EA-XX-125TM-120</p> <p>General-purpose 2-element 30° tee rosette. Sections are electrically independent.</p> 	<p>EA-XX-250BF-350</p> <p>General-purpose pattern with high-resistance grid. Compact geometry. Similar to 250BG pattern except for resistance.</p> 	<p>CEA-XX-500UW-120</p> <p>Widely used long gage pattern. Exposed tab area is 0.10 x 0.07 in (2.5 x 1.8 mm).</p> 
<p>CEA-XX-125UT-120 CEA-XX-125UT-350</p> <p>2-element 90° tee rosette for general-purpose use. Exposed tab area is 0.10 x 0.07 in (2.5 x 1.8 mm).</p> 	<p>CEA-XX-250UN-120 CEA-XX-250UN-350</p> <p>Narrow general-purpose gage pattern. Exposed tab area is 0.08 x 0.05 in (2.0 x 1.1 mm).</p> 	
<p>EA-XX-125TK-350</p> <p>High-resistance 2-element 90° gage for torque applications.</p> 	<p>CEA-XX-250UW-120 CEA-XX-250UW-350</p> <p>Larger grid and tab than 250UN pattern. Exposed tab area is 0.10 x 0.07 in (2.5 x 1.8 mm).</p> 	

Special-Purpose Gages, Sensors, and Equipment

In addition to providing the stress analyst with a vast selection of standard strain gage types, Micro-Measurements offers a variety of products designed to meet special needs and perform special functions in experimental stress analysis. Although space in this introductory catalog permits neither a full listing of these products, nor complete descriptions, a few types of special sensors are briefly noted.

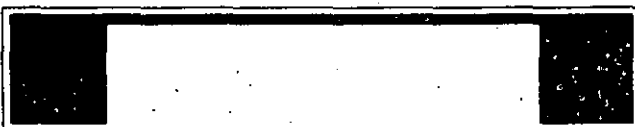
Full information on any of these products, along with detailed technical specifications, can be obtained by requesting Catalog 500, or by contacting the Measurements Group's Applications Engineering Department.

Temperature Sensors



TG Temperature Sensors, with a grid of ultra-pure nickel foil, are recommended for general-purpose temperature measurement from -320°F to $+500^{\circ}\text{F}$ (-195°C to $+260^{\circ}\text{C}$). For application at extremely low temperatures, two alloys — nickel and manganin — are combined to produce the CLTS-2B (cryogenic linear temperature sensor). The duplex construction of this sensor results in an essentially linear change of overall resistance with temperature, from -452°F to $+100^{\circ}\text{F}$ (-269°C to $+40^{\circ}\text{C}$).

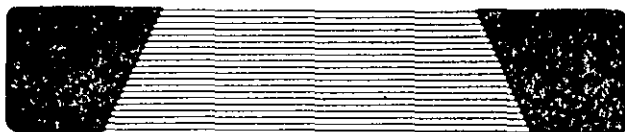
Reusable LST matching networks are available for half-bridge connection of temperature sensors to strain indicators. With these accessories, the strain indicator registers temperature directly, at a scale factor of 10 or 100 microstrain per $^{\circ}\text{F}$ or $^{\circ}\text{C}$.



Crack Detection

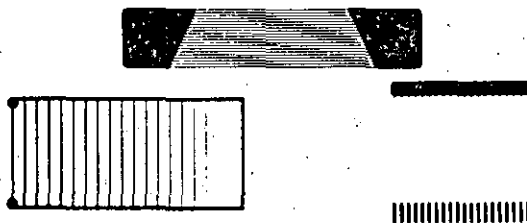
CD-Series Crack Detection Gages are designed to provide a convenient, economical method of indicating the presence of a crack, or indicating when a crack has progressed to a predetermined location on a test part or structure. By employing several CD gages, it is also possible to monitor the rate of crack growth.

Crack detection gages are available with various strand lengths; from 0.4 to 2.0 in (10 to 50 mm).



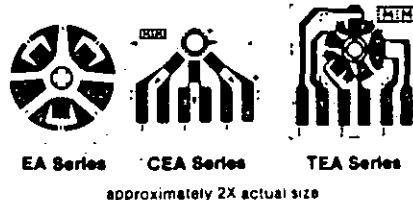
Crack Propagation

Crack Propagation Gages accurately indicate rate of crack propagation in a specimen material over a very small distance. These sensors are often used adjacent to notches, fillets, or other types of discontinuities in structures. Several sizes and geometries are available.



Strain Gages for Residual Stress Determination

The most widely used practical technique for measuring residual stresses is the hole-drilling strain gage method described in ASTM Standard E837. With this method, a specially configured electrical resistance strain gage rosette is bonded to the surface of the test object, and a small, shallow hole is introduced through the center of the gage, using a precision drilling apparatus such as the Measurements Group's RS-200 Milling Guide. After drilling, the strain in the immediate vicinity of the hole is measured, and the relaxed residual stresses are computed from these measurements.



approximately 2X actual size

For further details, request Bulletin 304.

Weldable Strain Gages and Temperature Sensors

Weldable gages are precision foil sensors bonded to a metal carrier for spot welding to structures and components. These sensors are easy to install and require minimal surface preparation. Installation is accomplished without adhesives, eliminating heat curing problems on massive structures. They are also well suited to laboratory test programs requiring elevated-temperature testing and minimal installation time.

SPECIFICATIONS

Sensor	Standard S-T-C	Resistance in Ohms	Gage Factor	Temperature Range
CEA	06.09	120 ± 0.4% 350 ± 0.4%	2.0	-100° to +200° F. (-75° to +95° C)
LWK	06.09	350 ± 0.4%	2.1	-320° to +500° F. (-195° to +260° C)
WWT	N/A	50 ± 0.4% @ +75° F (+24° C)	N/A	-320° to +500° F. (-195° to +260° C)

SENSOR DESCRIPTIONS

CEA-Series Weldable Strain Gage: Constantan alloy sensing grid completely encapsulated in polyimide. Very flexible. In most cases can be contoured to radii as small as 1/2 in (13 mm). Rugged, copper-coated tabs for convenient leadwire attachment.



W250A

LWK-Series Weldable Strain Gage: Modified Karma (K-alloy) sensing grid completely encapsulated in a fiberglass-reinforced epoxy-phenolic matrix. Integral three-wire lead system consists of 10 in (250 mm) flexible etched Teflon[®]-insulated leadwires. Installation radius generally limited to 2 in (50 mm) or larger in the direction of the grid axis.



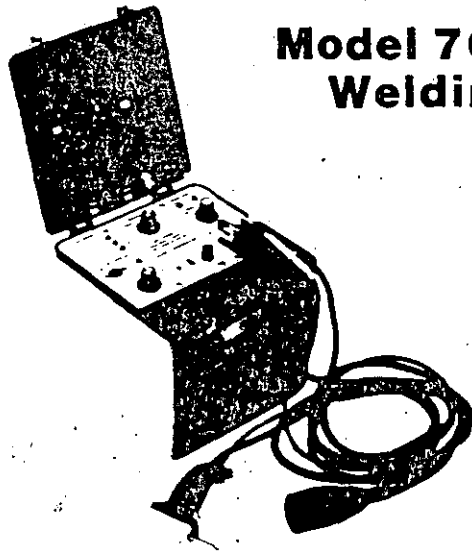
W250B

WWT-Series Weldable Temperature Sensor: High-purity nickel sensing grid completely encapsulated in a fiberglass-reinforced epoxy-phenolic matrix. Integral three-tab printed circuit terminals for convenient leadwire attachment.



W200B

*Registered Trademark of DuPont



Model 700 Portable Strain Gage Welding and Soldering Unit

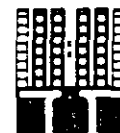
The Model 700 is a completely portable, capacitance-discharge spot welder, designed for efficient installation of weldable strain gages and temperature sensors. Supplied in a rugged, gasketed case, the battery-powered unit can be used under field conditions where no power lines are available.

A temperature-controlled soldering pencil, operated from the main battery supply, is an integral part of the Model 700. The lightweight pencil can be adjusted to a wide range of tip temperatures for both gage soldering and leadwire splicing.

For further details, request Bulletin 302.

Bondable Resistors

Micro-Measurements manufactures a variety of fixed, adjustable, and combination bondable resistors for use in many applications where precise resistance is required. Appropriate patterns are available in both low and high temperature-coefficient-of-resistance types. Widest use is in transducer bridge circuits to compensate for small temperature-induced errors and to adjust bridge balance.



Various alloys, sizes, and patterns are available, allowing selection of the optimum resistor for specific applications. Resistors are normally produced open-faced on a polyimide carrier. The recommended temperature range is from 0° to +300° F (-20° to +175° C). For further details, request Transducer-Class Catalog TC-116.

Micro-Measurements Strain Gage Accessories

Micro-Measurements strain gages are produced under rigidly controlled manufacturing conditions, with the utmost care and attention given to ensuring the high level of quality and precision for which these gages have gained world-wide recognition. However, the gages' full potential for accurate strain measurement can be realized only when they are properly installed. There are, in fact, three principal components in every strain gage installation: (1) the strain gage itself, (2) the tools, materials, and supplies (accessories) needed to install the gage, and (3) the techniques employed in performing the installation. Professional stress analysts have learned from experience that compromising any of these may lead to compromising the quality of the installation and the accuracy of the strain data.

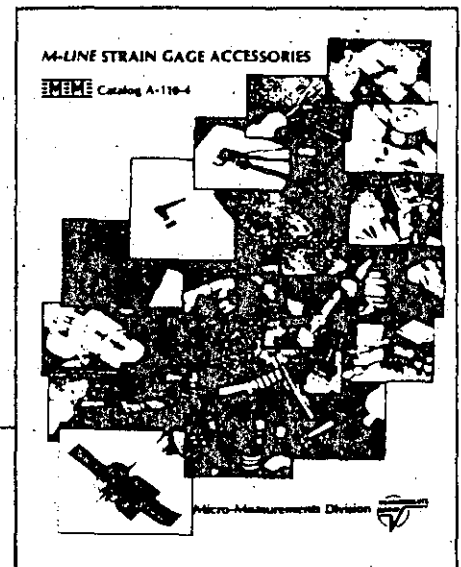
The well-established formula for making consistently successful strain gage installations is quite simple:

- select high-quality precision strain gages.
- select professional-caliber accessories which have been laboratory-tested and field-proven for effectiveness and compatibility with the strain gages.
- follow the installation procedures recommended by the manufacturer of the gages and accessories.

Featured on the following two pages is a small sample of Micro-Measurements *M-LINE* strain gage installation accessories. As indicated, the appropriate materials, supplies, and tools are provided for each important step in the gage installation process — from preparing the surface of the test piece to applying a protective coating over the bonded and wired gage. All accessory items, whether manufactured directly by Micro-Measurements or specified for purchase from an outside supplier, are of the highest quality, and have been designed or selected specifically to help ensure successful installation of Micro-Measurements strain gages.

Regular users of strain gages will want to request a copy of Catalog A-110. This 40-page, fully illustrated catalog describes the complete line of gage installation accessories and related equipment. In addition to detailed product descriptions and specifications, it includes, where applicable, extensive recommendations for the appropriate selection and application of the accessories.

Catalog A-110 is available on request from our Applications Engineering Department.



6 Simple Steps To Successful S

Surface Preparation



CSM-1 Degreaser
 M-Prep Conditioner
 M-Prep Neutralizer
 Silicon Carbide Paper
 Cotton Swabs
 Gauze Sponges

Adhesive Selection



M-Bond 200
 M-Bond AE-10
 M-Bond AE-15
 M-Bond 600
 M-Bond 610

Gage Handling and Bonding



Adhesive Film

Leadwire Attachment



Protective Coating Application

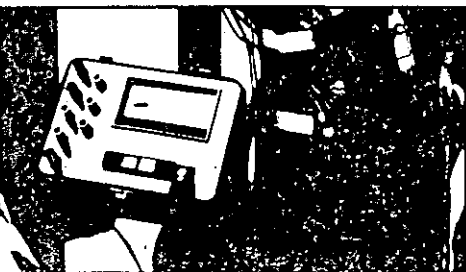
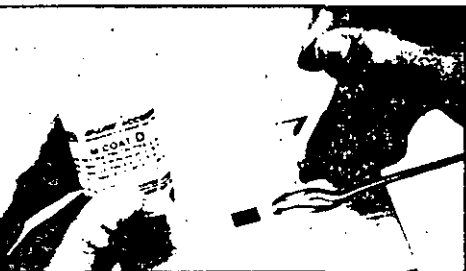
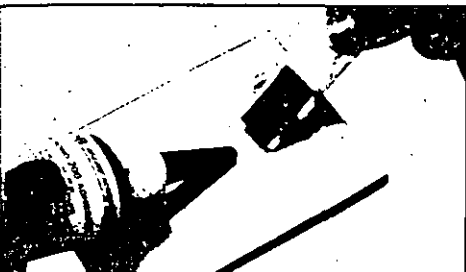


Gage Installation Tester



... With **M-LINE** Accessories —

Strain Gage Installations . . .



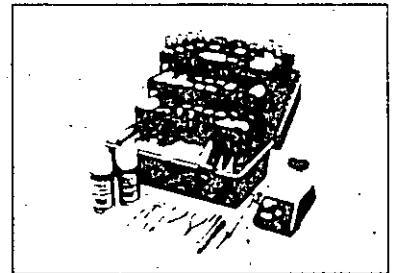
General Application Kits



It is often of greatest convenience for the strain gage user to purchase all of the needed accessory supplies and materials in a single package.

GAK-2 Series Kits provide specific selections of *M-LINE* accessories for making basic strain gage installations with the M-Bond 200, AE-10/15, or 610 adhesives.

The ultimate in gage installation capability is provided by the **MAK-1, Master Strain Gage Application Kit**. The MAK-1 includes all of the supplies and special tools necessary for making a wide range of gage installations for both laboratory and field applications.

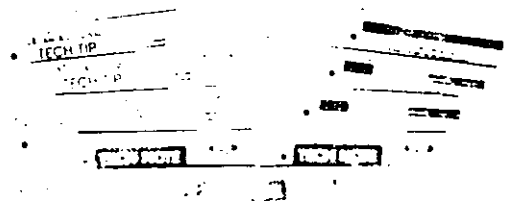


Because technique is such an important ingredient in successful strain gage installation, detailed **Instruction Bulletins** have been prepared for virtually all Micro-Measurements strain gage installation products.

In addition, a library of **Tech Notes** and **Tech Tips** is available for reference on a broad range of subjects within Strain Gage Technology.

Tech Tips present practical strain gage application techniques for "out-of-the-ordinary" situations, and represent, as much as possible, a practical "how-to" approach to strain gage installation.

Tech Notes contain in-depth technical treatments of specific subjects having direct or indirect bearing on the successful application of stress/strain measurement technology.

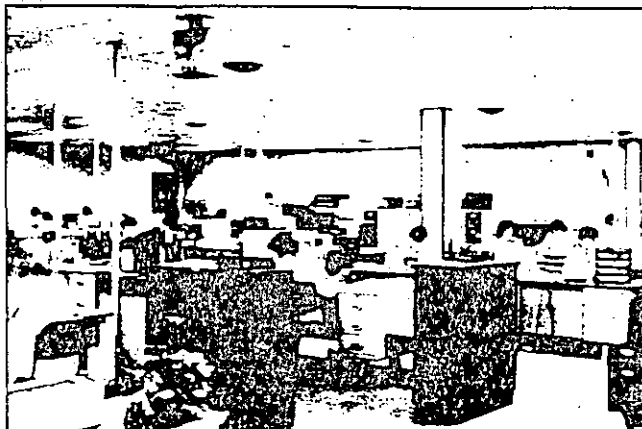


Lab-Tested — Field-Proven

Ordering Information

The Measurements Group Order Service Department can provide immediate stock and delivery information. Most products are available for same-day shipment or can be produced on short delivery cycles. Measurements Group, Inc. maintains regional sales representatives throughout the world to further assist you. For additional information on any of our product lines, contact us or our representative serving your area.

Quantity discounts are available on strain gages and special sensors. All other items are sold on a net basis only. All prices are subject to change without notice.



Micro-Measurements Warranty Policy

The Micro-Measurements Division of Measurements Group, Inc., warrants that the products sold under its name, are fit for the purpose for which they were intended by the supplier and guarantees said items against defects in workmanship or material for a period of ninety (90) days, or otherwise specified limits, from date of delivery. Every reported case of non-standard material is thoroughly investigated by our Quality Assurance Department. It should be recognized that there is no method to 100% test our type of products since many tests would be destructive. Both Micro-Measurements and the purchasers must depend upon statistical sampling techniques that have in the past proved to be reliable and economical in respect to the cost of the product.

This warranty is in lieu of any other warranties, expressed or implied, including any implied warranties of merchantability or fitness for a particular purpose. There are no warranties which extend beyond the description on the face hereof. Purchaser acknowledges that all goods purchased from Measurements Group are purchased as is, and buyer states that no salesman, agent, employee or other person has made any such representations or warranties or otherwise assumed for Measurements Group any liability in connection with the sale of any goods to the Purchaser. Buyer hereby waives all rights buyer may have arising out of any breach of contract or breach of warranty on the part of Measurements Group, to any incidental or consequential damages, including but not limited to damages to property, damages for injury to the person, damages for loss of use, loss of time, loss of profits or income, or loss resulting from personal injury.

Some states do not allow the exclusion or limitation of incidental or consequential damages for consumer products, so the above limitations or exclusions may not apply to you.

The Purchaser agrees that the Purchaser is responsible for notifying any subsequent buyer of goods manufactured by Measurements Group of the warranty provisions, limitations, exclusions and disclaimers stated herein prior to the time any such goods are purchased by such buyers, and the Purchaser hereby agrees to indemnify and hold Measurement Group harmless from any claim asserted against or liability imposed on Measurements Group occasioned by the failure of the Purchaser to so notify such buyer. This provision is not intended to afford subsequent purchasers any warranties or rights not expressly granted to such subsequent purchasers under the law.

The Measurements Group is solely a manufacturer and assumes no responsibility of any form for the accuracy or adequacy of any test results, data, or conclusions which may result from the use of its equipment.

The manner in which the equipment is employed and the use to which the data and test results may be put are completely in the hands of the purchaser. Measurements Group, Inc. shall in no way be liable for damages consequential or incidental to defects in any of its products.

LIMITATION OF REMEDY: In the event any discrepancy is found to be Micro-Measurements' responsibility, the buyer's sole and exclusive remedy will be the replacement of, or full credit for the discrepant product.

We will provide immediate assistance to the best of our ability in locating and identifying the source of any difficulties involving our product.

MEASUREMENTS GROUP, INC.

P.O. Box 27777

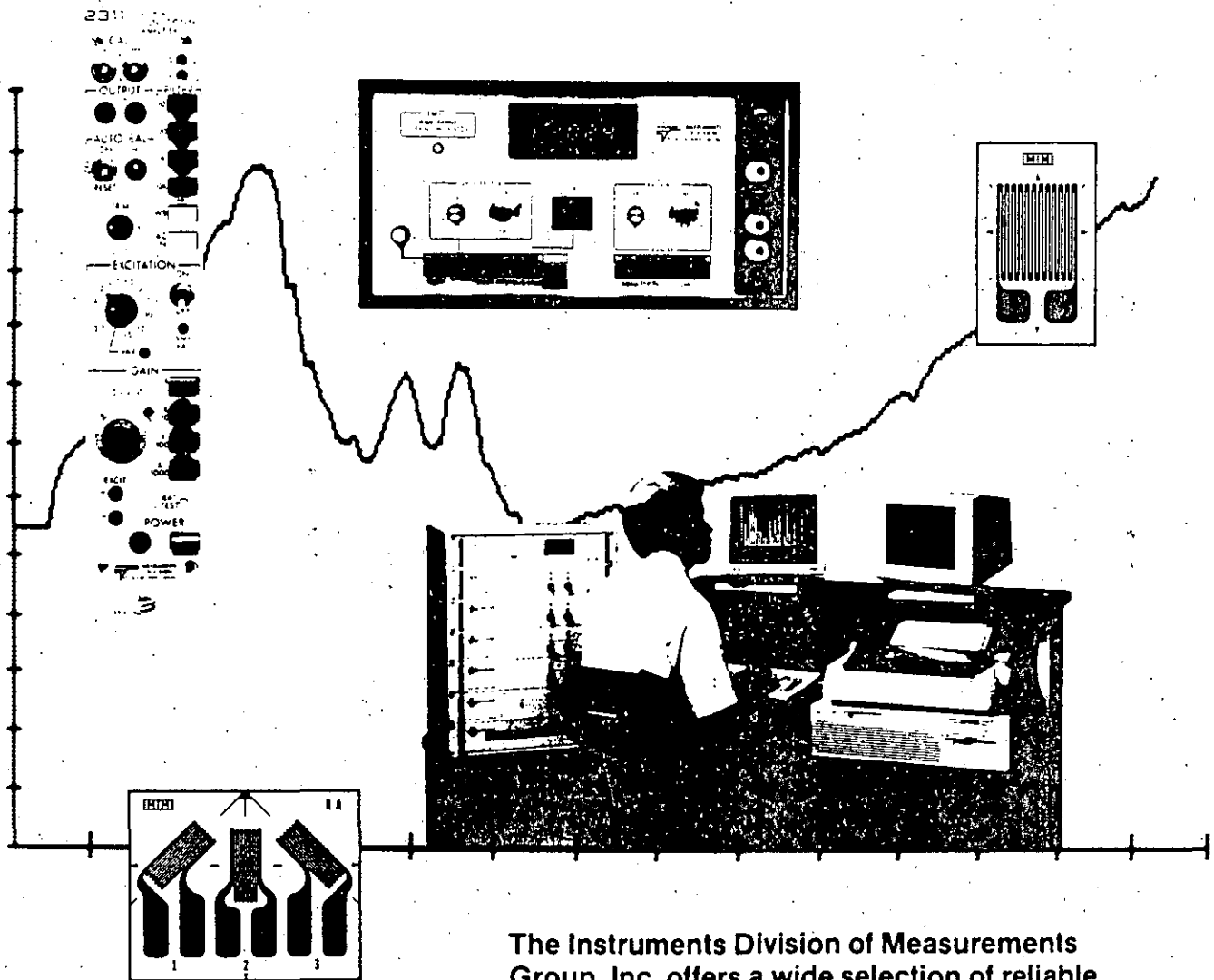
Raleigh, NC 27611, USA

(919) 365-3800

Telex 802-502 • FAX (919) 365-3945



STRAIN GAGE INSTRUMENTATION

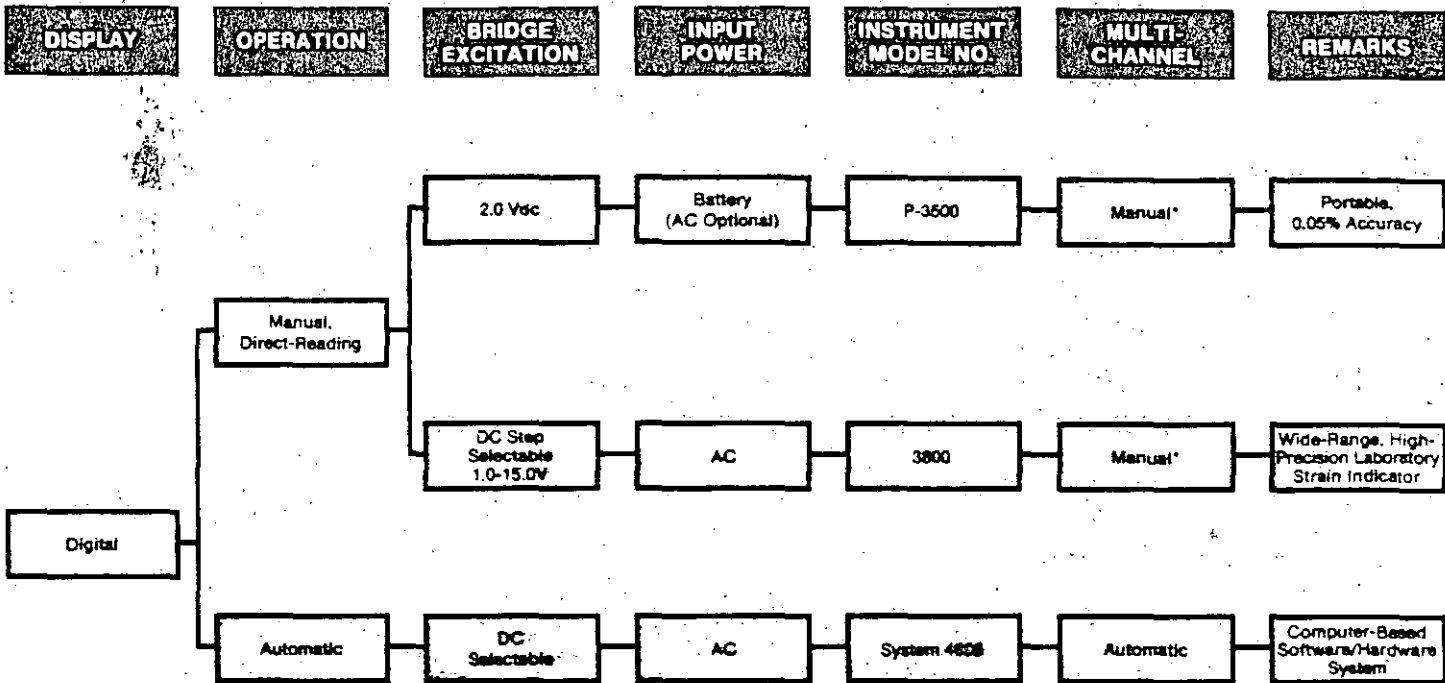


The Instruments Division of Measurements Group, Inc. offers a wide selection of reliable, precision strain gage instrumentation for stress analysis, structural, and materials testing.

This short-form catalog will introduce you to our instruments, and assist you in selecting those most appropriate for your measurement needs.

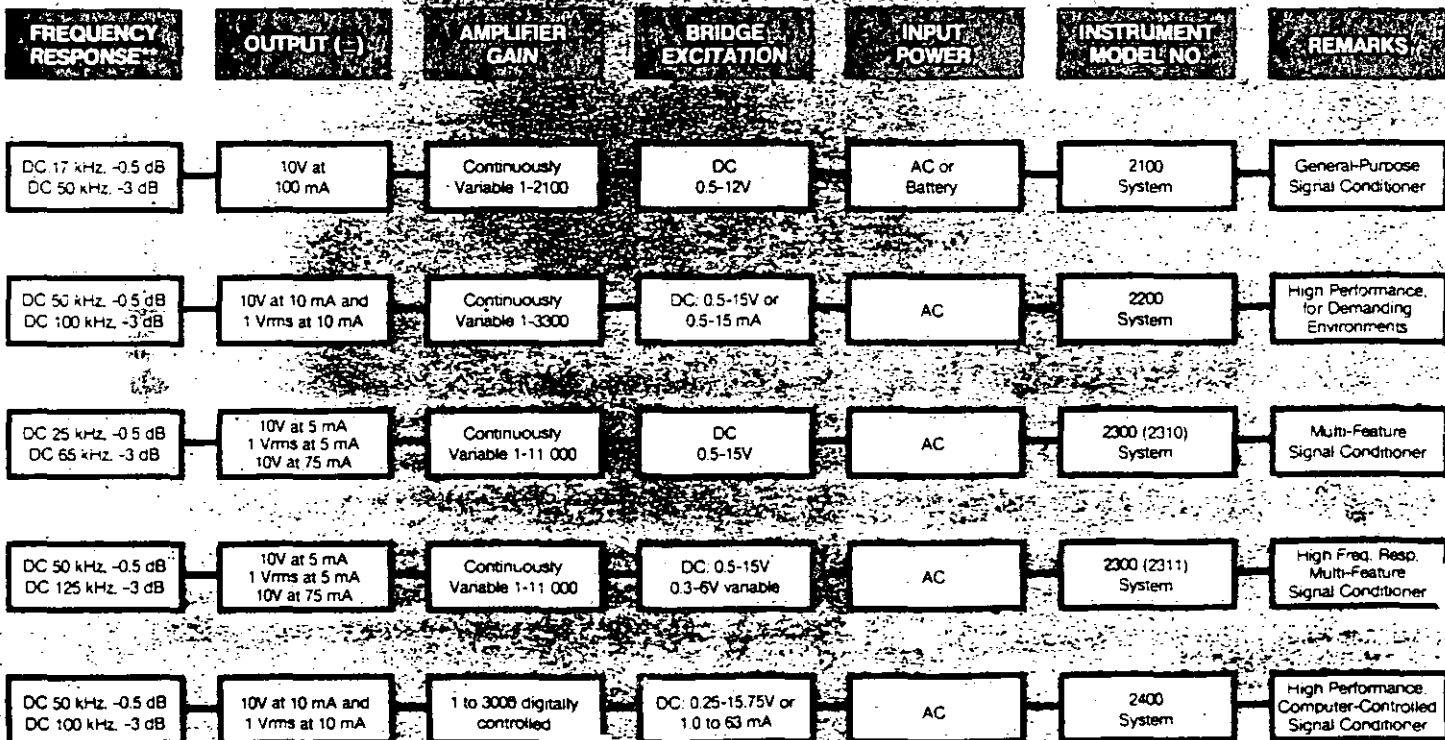


STATIC MEASUREMENTS

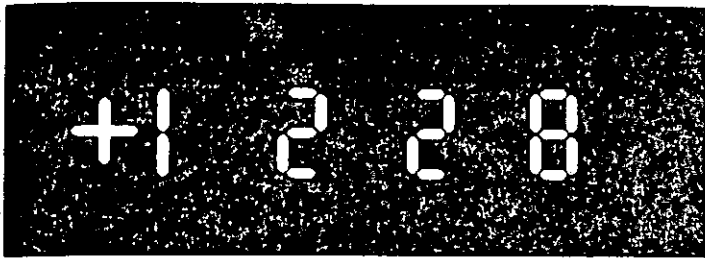


*Switch and balance units are used to read sequentially the outputs of two or more strain gages on a single indicator. See Special-Purpose Instrumentation on back cover.

DYNAMIC MEASUREMENTS



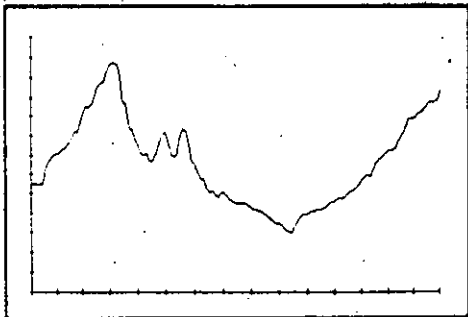
**Typical — see product bulletin and/or instruction manual for detailed performance specifications.



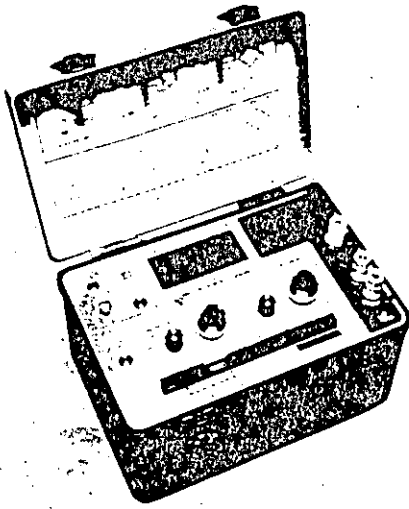
Static signals are essentially constant, while quasi-static signals vary slowly, typically at a few cycles per minute (e.g., 0.1 Hz). Basic instrumentation requirements call for stability, accuracy and high resolution, particularly where measurements are to be taken over long periods of time.

If test conditions involve predominantly static or quasi-static measurements, the first choice for a measuring instrument will ideally incorporate a digital or analog display, direct or null-balance reading, and, depending on the degree of sophistication, output to a printer, microprocessor or computer. Multi-channel capability can be provided by manual or automatic switching/multiplexing units, which may include balance and/or span control facilities.

Many static strain measuring instruments have an analog output available for making single-channel dynamic measurements in conjunction with, for example, an oscilloscope, recorder, or peak-read indicator. However, this dynamic capability may have limitations with respect to frequency response and amplifier gain compared to an instrument designed specifically for dynamic measurements.



Dynamic signals vary continuously at frequencies above 0.1 Hz, or are transients. Under these conditions, measuring instrumentation requires adequate frequency response, and a wide amplifier gain range for output to the appropriate recording or display instrument. A dynamic instrument consists of an amplifier and signal conditioner with a built-in or shared power supply. Individual units are normally required for each channel when simultaneous recording or multiple channels are needed. With the output sent to a suitable display device, dynamic instrumentation can be used for making static measurements, when maximum stability and accuracy are not primary considerations.

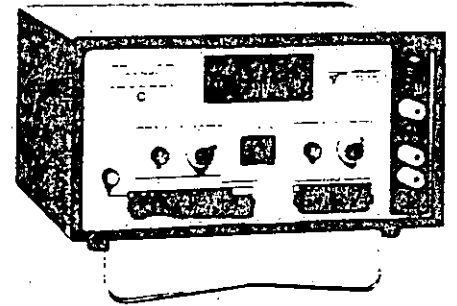


P-3500

The P-3500 is a portable, battery-powered precision instrument featuring a 4-1/2 digit LCD readout (optional LED available). Color-coded push-button controls provide an easy-to-follow, logical sequence of setup and operational steps. A transducer input connector facilitates connection of strain gage based transducers. *Request Bulletin 245.*

3800

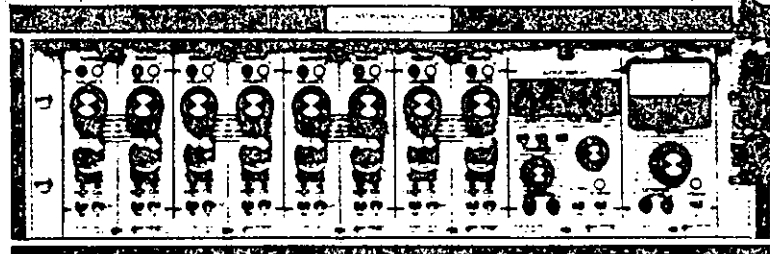
The 3800 is a high-precision, laboratory-type digital display strain indicator. It features extremely wide-range gage factor, balance, and bridge excitation controls. The wide-range feature enables measurement resolution of $0.1 \mu\epsilon$. The 3800 can also be used as a high-performance transducer indicator. *Request Bulletin 249.*



The 2100, 2200, 2300, and 2400 Systems accept low-level signals, and condition and amplify them into high-level outputs suitable for multiple-channel simultaneous dynamic recording. These systems can be used in conjunction with various recording devices.

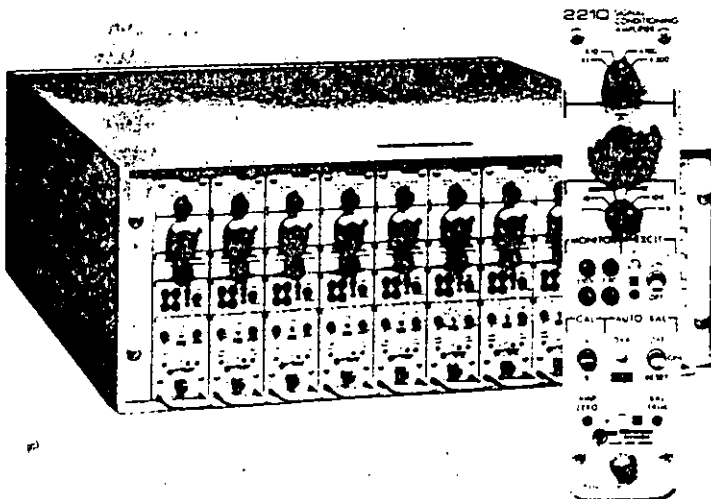
2100

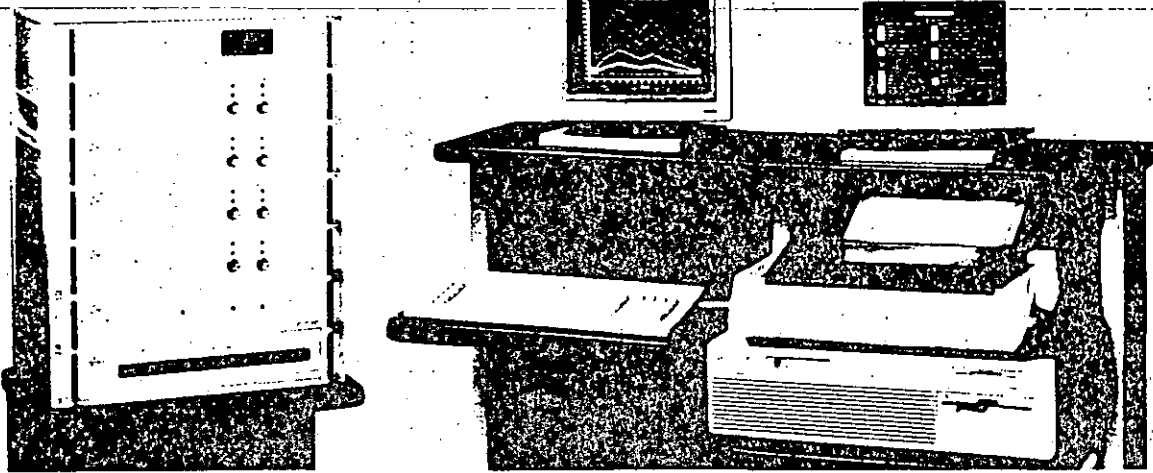
The 2100 is an economical system with a central power supply, and two active channels per unit module. *Request Bulletin 250.*



2200

The 2200 System offers high performance in the most severe operating environments. Among its features are isolated constant-voltage/constant-current excitation, guarded input structure with $\pm 350V$ common-mode capability, automatic wide-range bridge-balance, and four-pole Bessel low-pass filter. The plug-in amplifiers are removable from the rack mount without having to disconnect the input wiring. *Request Bulletin 252.*





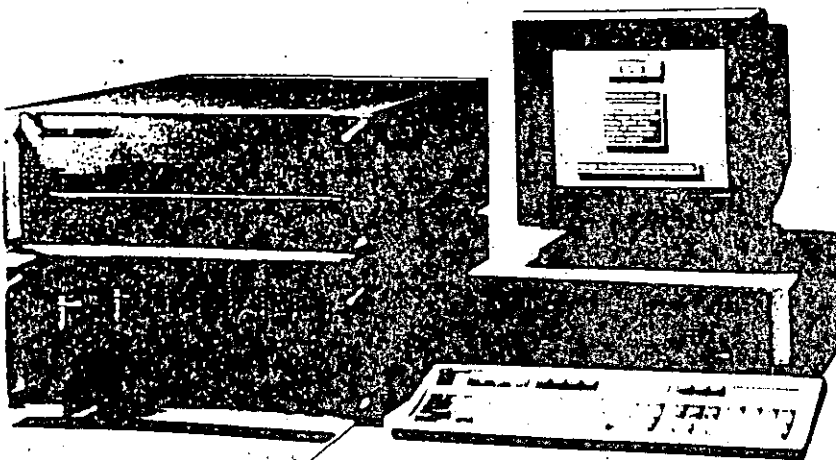
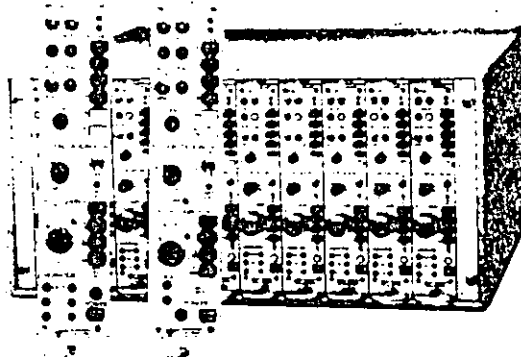
SYSTEM 4000

Featuring an extensive, preprogrammed software package, System 4000 is a state-of-the-art computer-based data system for stress analysis and structural materials testing. The most significant feature of System 4000 is its unique 4216 Executive Unit, including the system's comprehensive operating software which addresses virtually every variable that must be considered in stress analysis testing — from initial data entry, to data acquisition and conditioning, to on-line and off-line presentation of results. System 4000 will accept inputs from strain gages, thermocouples, LVDT's, load cells, and other transducers. Simple to operate, System 4000 provides maximum stress analysis testing capability with minimum investment. *Request Bulletin 235.*

2300

The 2300 is a sophisticated system incorporating such advanced features as an individual power supply per channel, active filtering, three simultaneous outputs, tape playback mode, wide frequency response, and electronic bridge balance.

Request Bulletin 251.



2400

The 2400 System is an expandable strain gage signal conditioning/amplifier system which allows the user to configure individual signal conditioners from any host computer with IEEE-488 or RS-232 capability. Programmed functions include amplifier gain, excitation, filter selection, and auto-balancing. *Request Bulletin 253.*

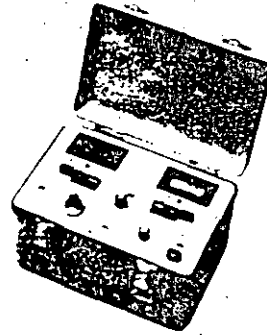
SPECIAL-PURPOSE INSTRUMENTATION

SB-10



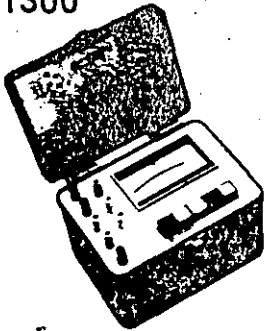
The SB-10 is a high-quality, 10-channel switch and balance unit for use with strain indicators. It features gold-plated binding posts for reliable connection of input circuits, and incorporates fine-balance control with turns-counting dials for each individual channel. *Request Bulletin 247.*

3650



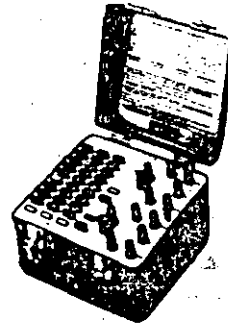
The 3650 Peak-Read Indicator is a portable, battery-powered instrument for capturing peak values of dynamic signals. The instrument is designed to be used in conjunction with any static strain gage indicator, transducer indicator, or signal conditioning system. The 3650 features dual LCD readouts for simultaneously displaying the most positive and most negative readings, and easy-to-use color-coded push-button controls. *Request Bulletin 246.*

1300



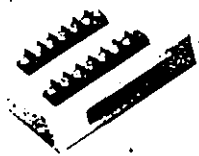
The 1300 Gage Installation Tester is used to verify the quality of an installed strain gage, as well as the complete gage installation, including leadwires. A carefully selected individualized test voltage is used for each measurement mode. Operation is by push buttons. *Request Bulletin 301.*

1550A



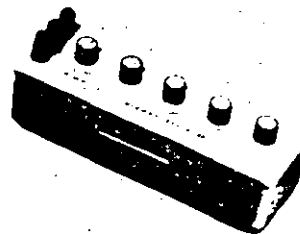
A true Wheatstone-bridge simulator, the 1550A Strain Indicator Calibrator presents known and repeatable resistance changes to the input of the indicator. Three decades of push buttons are used to produce incremental resistance changes. The 1550A is NIST-traceable. *Request Bulletin 313.*

1601 LVDT ADAPTER MODULE

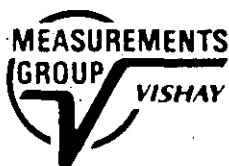


The 1601 Adapter Module provides an interface and direct compatibility between the strain indicator and a wide variety of LVDT displacement transducers.

V/E-40



This decade resistor/strain gage simulator can be used as a resistance standard, decade box, instrumentation calibrator, strain simulator, or investigative tool. It is also useful in measurement of arbitrary resistances and large strains. *Request Bulletin 316.*



MEASUREMENTS GROUP, INC.

P.O. Box 27777

Raleigh, NC 27611, USA

Telephone (919) 365-3800

Telex 802-502 • FAX (919) 365-3945

RECOMMENDED REFERENCE LITERATURE

The Strain Gage Primer, by C.C. Perry and H.R. Lissner.

Explains the use of bonded wire and foil resistance strain gages for solving problems in experimental stress analysis. Covers all phases, from selecting the proper gage through interpreting readings in terms of significant stresses.

Strain Gauge Technology, edited by A.L. Window and G.S. Holister.

Thorough, practical review of contemporary strain gage technology. Includes a chapter on gage use in hostile environments, and one on errors and uncertainties in strain measurements.

Handbook on Experimental Mechanics, edited by A.S. Kobayashi.

Twenty-one chapters contributed by twenty-five prominent authors cover well-known traditional disciplines as well as new experimental techniques. Extensive lists of references are provided.

Experimental Stress Analysis, by J.W. Dally and W.F. Riley.

Prepared to serve as a teaching text for courses in experimental stress analysis. Topics covered include elementary elasticity, brittle coatings, photoelasticity, strain gages, and related instrumentation.

Formulas for Stress and Strain, by R.J. Roark and W.C. Young.

A comprehensive summary of the formulas, facts, and principles pertaining to the strength of materials, for the design engineer and stress analyst.

Experimental Stress Analysis and Motion Measurement, by R.C. Dove and P.H. Adams.

A thorough discussion of stress analysis and strain measurement, with proper attention to new experimental methods including moiré fringes and semiconductor gages. Part two covers techniques and instruments used for measuring and analyzing displacements, velocities, and accelerations.

Stress Concentration Factors, by R.E. Peterson.

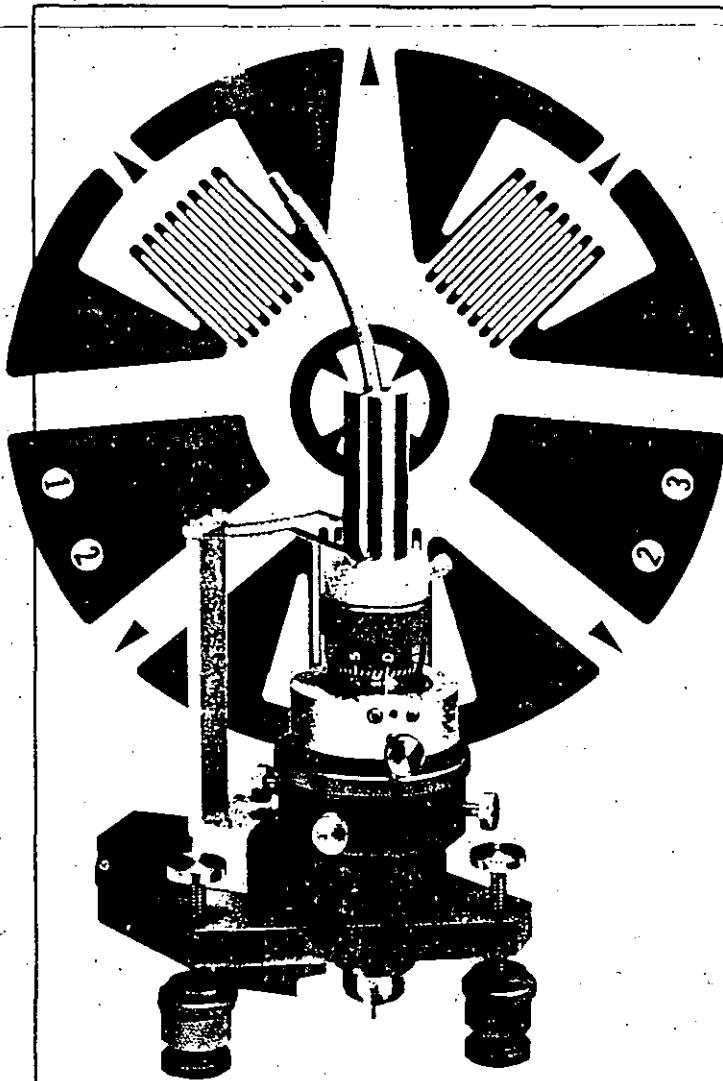
The most complete and authoritative compilation of stress concentration factors available in the published literature. Data are included for most commonly encountered geometric configurations and design details.

A broader selection of Experimental Stress Analysis related literature is available from:

Society for Experimental Mechanics
7 School Street
Bethel, Connecticut 06801
Telephone (203) 790-6373

MEME

Strain Gages and Instrumentation for Residual Stress Measurements



A predominant factor contributing to the structural failure of machine parts, pressure vessels, framed structures, etc., may be the residual "locked-in" stresses that exist in the object prior to its being put into service. These residual stresses are usually introduced during manufacturing, and are caused by processes such as casting, welding, machining, heat treating, molding, etc.

Residual stress can neither be detected nor evaluated by conventional surface measurement techniques, since the strain sensor (strain gage, photoelastic coating, etc.) can only respond to strain changes that occur after the sensor is installed.

The most widely used practical technique for measuring residual stresses is the hole-drilling strain gage method described in ASTM Standard E837. With this method, a specially configured electrical resistance strain gage rosette is bonded to the surface of the test object, and a small shallow hole is drilled through the center of the rosette. The local changes in strain due to introduction

of the hole are measured, and the relaxed residual stresses are computed from these measurements. Measurements Group Tech Note TN-503, *Measurement of Residual Stresses By The Hole-Drilling Strain Gage Method*, presents a detailed discussion of the theory and application of this technique.

The hole-drilling method is generally considered semi-destructive, since the drilled hole may not noticeably impair the structural integrity of the part being tested. Depending on the type of rosette gage used, the drilled hole is typically 0.062 or 0.125 in (about 1.5 or 3.0 mm), both in diameter and depth. In many instances, the hole can also be plugged, if necessary, to return the part to service after the residual stresses have been measured.

The practicality and accuracy of this method is directly related to the precision with which the hole is drilled through the center of the strain gage rosette. The Measurements Group RS-200 optical milling guide described herein provides a practical means to accomplish this task.

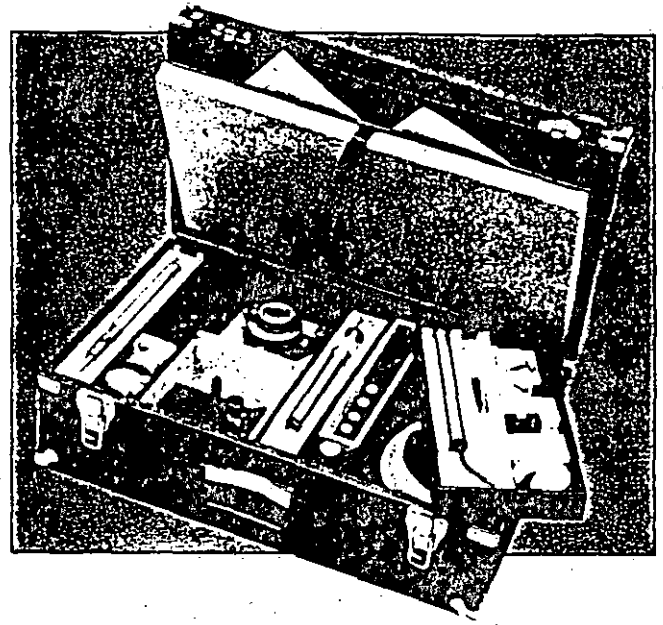
Equipment

The RS-200 Milling Guide is a precision fixture for the accurate positioning and drilling of a hole through the center of the strain gage rosette. Principal features and components of the milling guide assembly are shown in the photos below. When installed on the workpiece, the guide is supported by three leveling screws which are footed with swivel mounting pads to facilitate attachment to uneven surfaces.

Alignment of the milling guide relative to the strain gage rosette is accomplished by inserting a special-purpose microscope into the guide's centering journal, and then positioning the guide precisely over the center of the rosette by means of four X-Y adjusting screws. The microscope assembly, consisting of a polished steel housing with eyepiece, reticle, and objective lens, permits alignment to within 0.0015 in (0.038 mm) of the gage center. The microscope is also used to measure the diameter of the hole after it is drilled. An illuminator attaches to the base of the guide to aid in the optical alignment procedure.

After alignment is achieved, the microscope is removed from the guide, and the milling bar inserted in its place for slow-speed drilling of the hole. Two standard milling cutters are supplied: 0.062 and 0.125 in (1.6 and 3.2 mm) diameter. The milling bar is equipped with a universal joint for flexible connection to a drill motor.

Conventional slow-speed milling may be satisfactory on some mild steels and aluminum alloys. But high-speed drilling is generally the most convenient and practical method for introducing the hole in all test materials. (When residual stresses are to be measured on materials such as stainless steels, nickel-based alloys, etc., ultra-high-speed drilling techniques are preferred.) For this purpose, a high-speed air-turbine assembly is supplied for use with the milling guide, along with a supply of tungsten carbide-tipped cutters [ten each 0.031 in (0.8 mm) diameter and 0.062 in

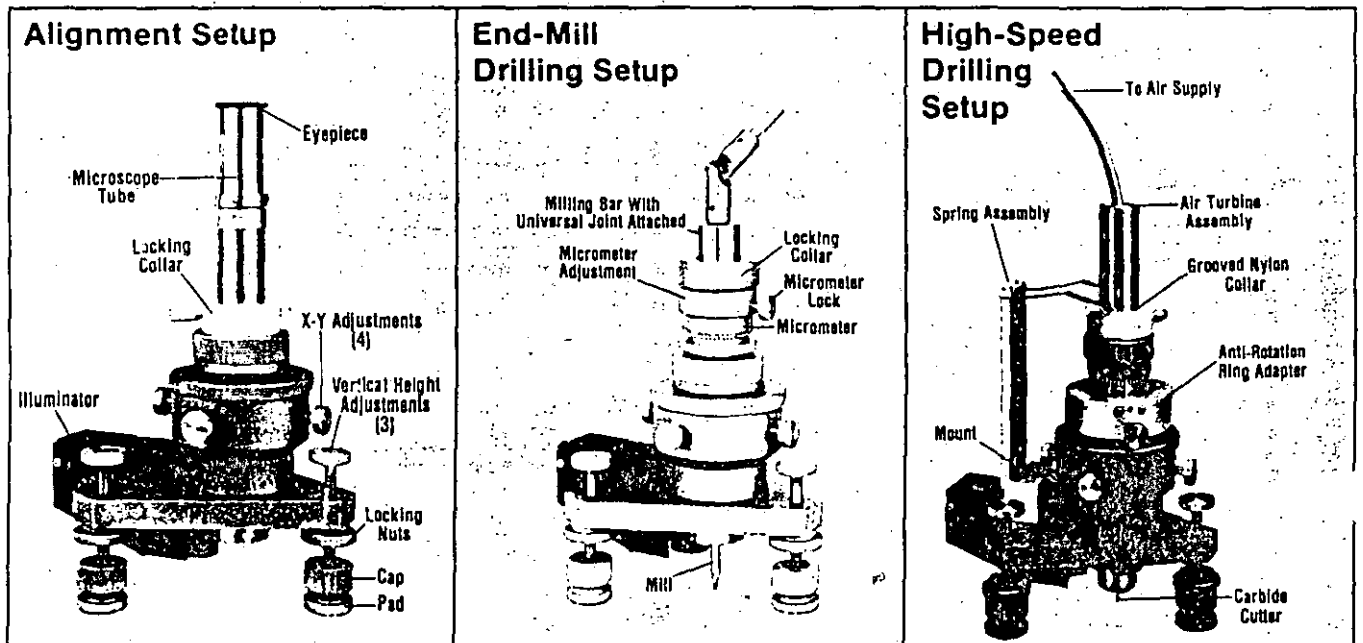


(1.6 mm) diameter]. A foot pedal control is included for operating the air turbine.

Also part of the milling guide assembly is a micrometer depth set attachment. This device is used for incremental drilling in those cases when information on the variation of residual-stress-with-depth is considered essential.

Other items supplied include a plastic template for the proper location of the milling guide foot pads on the test part and a special break-off tool which is used to remove the foot pads from the part after the test is completed. All components are housed in a sturdy carrying case. The guide is approximately 9 in (230 mm) high, and 4.5 in (114 mm) wide at the base.

A fast-setting-cement kit, used to firmly attach the guide to the test part, is available as an accessory item.



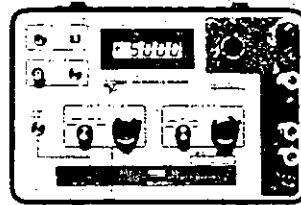
Residual Stress Measurement Procedure

Making residual stress measurements with the RS-200 Milling Guide consists of the following steps:

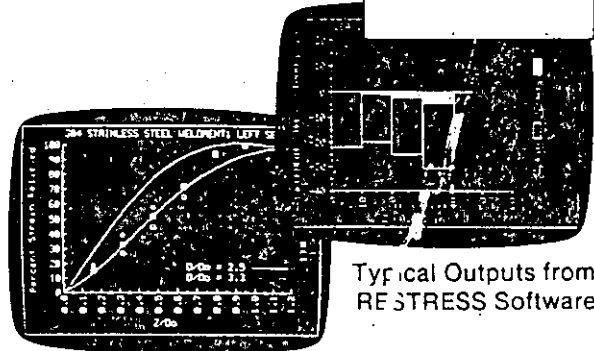
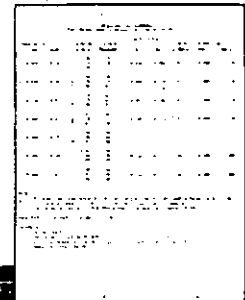
1. A special three-element Micro-Measurements strain gage rosette is bonded to the test part at points where residual stresses are to be determined.
2. Each rosette grid element is connected to a strain measuring instrument and "zero" readings are recorded.
3. The RS-200 Milling Guide is positioned over the center of the gage and securely attached to the test part.
4. The RS-200 is optically aligned so that its drilling axis is precisely positioned over the target at the center of the strain gage rosette.
5. A hole is drilled through the center of the rosette and into the test part.
6. Strain gage instrumentation is used to obtain strain readings.



7. Residual stresses are then computed, either manually or by using the Measurements Group's RESTRESS software program. RESTRESS is available on either 5-1/4 inch or 3-1/2 inch disks for use with most MS-DOS PC-compatible computers. RESTRESS provides data reduction in accordance with ASTM Standard Method E837, as well as approximate determination of residual stress variation with depth. (Refer to TN-503).



Model P-3500 Strain Indicator for Manual Data Acquisition



Typical Outputs from RESTRESS Software

Accessories and Replacement Parts for the RS-200

Listed below are accessory items and replacement parts for the RS-200 Milling Guide.

Double-Ended Boring Mills

Although boring mills are supplied as standard equipment with the basic guide, replacement will be necessary after prolonged usage. These mills, of high-speed steel, are available in two sizes:

HS-200-125, 0.125 in (3.2 mm) diameter.

HS-200-062, 0.062 in (1.6 mm) diameter.

Cutters For High-Speed Air Turbine

Cutters are inverted-cone, carbide-tipped:

ATC-200-062, 0.062 in (1.6 mm) diameter.

ATC-200-031, 0.031 in (0.8 mm) diameter.

Type RM-1 Motor for High-Speed Air Turbine

Cement Kit

A fast-setting (15 minutes) two-component resinous-type dental cement especially suited for firmly attaching the milling guide to the test part. Standard packaging is approximately two ounces. One package is sufficient for ten guide mountings.

A full line of strain gage instruments for measuring the strain magnitude is also available from the Measurements Group.

MEME Special Rosette Strain Gages






All gages are constructed of self-temperature-compensated constantan foil, mounted on a flexible polyimide carrier. Since their application is generally associated with a precision alignment milling guide, each incorporates a centering target. The unique features of each construction are:

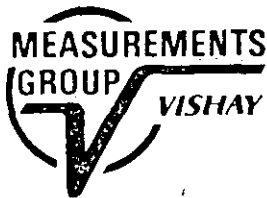
EA Series: Normally supplied "open-faced", but also available with solder dots and encapsulation (Option SE).

TEA Series: Fully encapsulated with easily accessible copper terminals to facilitate installation.

CEA Series: Incorporates all the advantages of Micro-Measurements' popular 'C' Feature gages. Pattern is specifically designed for applications where it is impractical to use RE or RK configurations (i.e., adjacent to weldments, corners, and intersecting surfaces). Care must be exercised when using this pattern, however, as limitations may exist in data reduction equations.

Refer to Micro-Measurements Catalog A-110 for detailed information concerning strain gage installation accessories. Refer to Catalog 500 for detailed information about rosette specifications.

GAGE PATTERN AND DESIGNATION	RES IN OHMS	DIMENSIONS					
		GAGE LENGTH	GRID CTR LINE DIA.	TYPICAL HOLE DIA.		MATRIX	
				Min.	Max.	Length	Width
EA-XX-031RE-120 EA-XX-031RE-120/Option SE 	120 ±0.2% 120 ±0.4%	0.031	0.101	0.03	0.04	0.29	0.29
		0.79	2.56	0.8	1.0	7.4	7.4
Due to small pattern size, measurement error can be magnified by slight mistocation of drill hole. Pattern not recommended for general-purpose applications.							
EA-XX-062RE-120 EA-XX-062RE-120/Option SE 	120 ±0.2% 120 ±0.4%	0.062	0.202	0.06	0.08	0.42	0.42
		1.57	5.13	1.5	2.0	10.7	10.7
Most widely used RE pattern for general-purpose residual stress measurement applications.							
EA-XX-125RE-120 EA-XX-125RE-120/Option SE 	120 ±0.2% 120 ±0.4%	0.125	0.404	0.12	0.16	0.78	0.78
		3.18	10.26	3.0	4.1	19.8	19.8
Larger version of the 062RE pattern.							
TEA-XX-062RK-120 	120 ±0.4%	0.062	0.202	0.06	0.08	0.60	0.60
		1.57	5.13	1.5	2.0	15.2	15.2
Fully encapsulated, with copper terminals for ease of soldering. Same pattern geometry as 062RE pattern.							
CEA-XX-062UM-120 	120 ±0.4%	0.062	0.202	0.06	0.08	0.38	0.48
		1.57	5.13	1.5	2.0	9.6	12.2
Fully encapsulated with large copper-coated soldering tabs and special trim alignment marks. Trim line spaced 0.068 in (1.73 mm) from hole center.							



EDIC, S. A. DE C. V.
 EQUIPOS DIDACTICOS INDUSTRIALES
 Y CIENTIFICOS, S. A. DE C. V.
 R. F. C. EDI-891208-PGA
 CAIRO No. 251 COL. EL RECREO
 C. P. 02070 MEXICO, D. F.
 TEL. 561-80-04 FAX 343-59-51

MEASUREMENTS GROUP, INC.
 P.O. Box 27777
 Raleigh, North Carolina 27611, USA
 Telephone (919) 365-3800
 Telex 802-502 • FAX (919) 365-3945

MODEL 1550A

S. A. DE C. V.
 EQUIPOS DIDACTICOS INDUSTRIALES
 Y CIENTIFICOS, S. A. DE C. V.
 P. O. BOX 264 COL. EL RECREO
 MEXICO, D. F. MEX.
 TEL. 543-0231 FAX 543-0231



STRAIN INDICATOR CALIBRATOR

A laboratory standard for verifying the calibration of strain and transducer indicators.

- True Wheatstone Bridge Circuitry
- Simulates Quarter, Half & Full Bridge — both $120\Omega/350\Omega$
- 3 Decades of Push Buttons
 - Strain Range Direct Reading: $\pm 99\ 900\mu\epsilon$. . . Increments of $100\mu\epsilon$
 - Transducer Range: $\pm 49.95\text{ mV/V}$. . . Increments of 0.05 mV/V
- Reversing Switch for Plus and Minus Calibration
- High Precision Vishay Resistors used throughout to ensure Excellent Stability
- Accuracy 0.025 Percent — Traceable to the U.S. National Institute of Standards and Technology



MEASUREMENTS GROUP, INC.

P.O. Box 27777
 Raleigh, North Carolina 27611, USA
 (919) 365-3800

DESCRIPTION

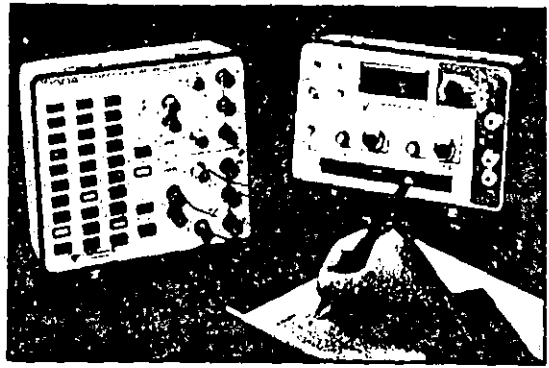
Sound engineering and laboratory practices require that the instrumentation used to make critical strain measurements be periodically calibrated to verify that it is within the manufacturer's original specifications. Additionally, each type of strain indicator exhibits some degree of nonlinearity, especially for large strains during quarter-bridge operation. Since this is the most common stress analysis application of strain gages, it is important that the strain indicator be calibrated in this mode. Instrumentation span should also be checked at a number of points before each important test to avoid inaccurate data.

The Model 1550A calibrator is a Wheatstone bridge and generates a true change of resistance in one or two arms of the bridge. It simulates the actual behavior of a strain gage in both positive and negative strain.

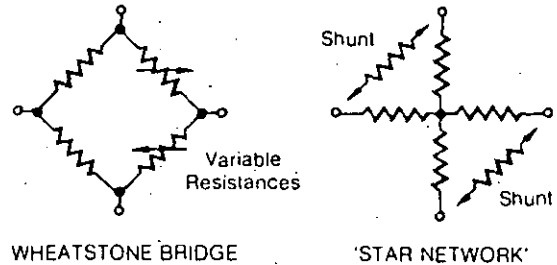
The 'star network' used in certain other commercial calibrators provides a substantially lower cost instrument design, because component specifications are less critical, and fewer components are required.

However, the 'star network' cannot simulate quarter-bridge strain gage behavior, and cannot simulate positive strain. Another serious problem with this circuit is that the bridge input and output resistances change in an abnormal manner, leading to inaccuracies in calibration under some conditions.

A calibrator based on the Wheatstone bridge principle requires stable components. A total of 66 ultra-stable Vishay precision resistors are used in the Model 1550A calibrator to provide the stability, repeatability, accuracy and incremental steps required in a laboratory standards instrument.

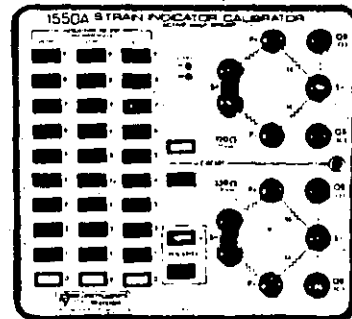


Calibration verification of a P-3500 Portable Strain Indicator before an important test.



SPECIFICATIONS

Accuracy:	0.025% of setting $\pm 1 \mu\epsilon$ (0.0005 mV/V), max. Traceable to United States National Institute of Standards and Technology.	Output @ 000:	50 $\mu\epsilon$ (0.025 mV/V), max. in full-bridge mode.
Repeatability:	$\pm 1 \mu\epsilon$ (0.0005 mV/V), max.	Environment:	Temperature: 0° to +120° F (-18° to +49° C). Humidity: Up to 70% RH, non-condensing.
Stability:	(0.001% of setting $\pm 1 \mu\epsilon$)/°C, max.	Size:	Aluminum case (separable lid). 5-3/4 H x 8-1/4 W x 7-3/4 D in (145 x 210 x 195 mm).
Thermal EMF:	0.5 $\mu\text{V/V}$ of excitation, max.	Weight:	4.8 lbs (2.2 kg).
Bridge Resistances:	120 Ω and 350 Ω . Input resistance: $\pm 0.05\%$, max., from nominal at all output settings. Output resistance: $\pm 0.05\%$, max., from nominal at "000" $\mu\epsilon$, -0.25% at $\pm 99\ 900 \mu\epsilon$.		
Circuit:	True $\pm \Delta R$ in two adjacent arms (opposite signs), plus two fixed arms for bridge completion.		
Simulation:	Quarter bridge, one active arm. Half bridge, one or two active arms. Full bridge, two active arms.		
Range:	Two active arms: 0 to $\pm 99\ 900 \mu\epsilon$ in steps of 100 $\mu\epsilon$ @ GF=2.00. 0 to ± 49.95 mV/V in steps of 0.05 mV/V. One active arm: 0 to $\pm 49\ 950 \mu\epsilon$ in steps of 50 $\mu\epsilon$ @ GF=2.00.		
Excitation:	To meet accuracy and repeatability specifications: 120 Ω : 0-10V ac or dc. 350 Ω : 0-15V ac or dc. Maximum permissible: 120 Ω : 25V ac or dc. 350 Ω : 30V ac or dc.		



A Certificate of Calibration is provided with each Model 1550A Calibrator.

MEASUREMENTS GROUP, INC.

P.O. Box 27777, Raleigh, N.C. 27611, USA

(919) 365-3800 • FAX (919) 365-3945 • Telex 802-502

01-1514TD
Printed in USA

MODEL V/E-40



STRAIN GAGE SIMULATOR

A precision decade resistor for accurately simulating the behavior of strain gages and RTD's.

- 5 Decade Selector Switches
- Resistance Range: 30.00 to 1111.10 Ω in 0.01 Ω steps
- High Precision Vishay Resistors used throughout to ensure Excellent Stability
- Accuracy 0.02% of Setting
- Simulates Tension and Compression Strain for most widely used Strain Gage Resistance Values
- Simulates a Broad Range of RTD's for Instrumentation Set Up and Calibration



EDIC, S. A. DE C. V.
EQUIPOS DIDACTICOS INDUSTRIALES
Y CIENTIFICOS, S. A. DE C. V.
R. F. C. EDI-891208-PGA
CAIRO No. 251 COL. EL RECREO
C. P. 02070 MEXICO, D. F. ATZ.
TEL. 561-80-04 FAX 343-59-51

MEASUREMENTS GROUP, INC.

P.O. Box 27777
Raleigh, North Carolina 27611, USA
(919) 365-3800

©Copyright Measurements Group, Inc., 1992
All Rights Reserved.

DESCRIPTION

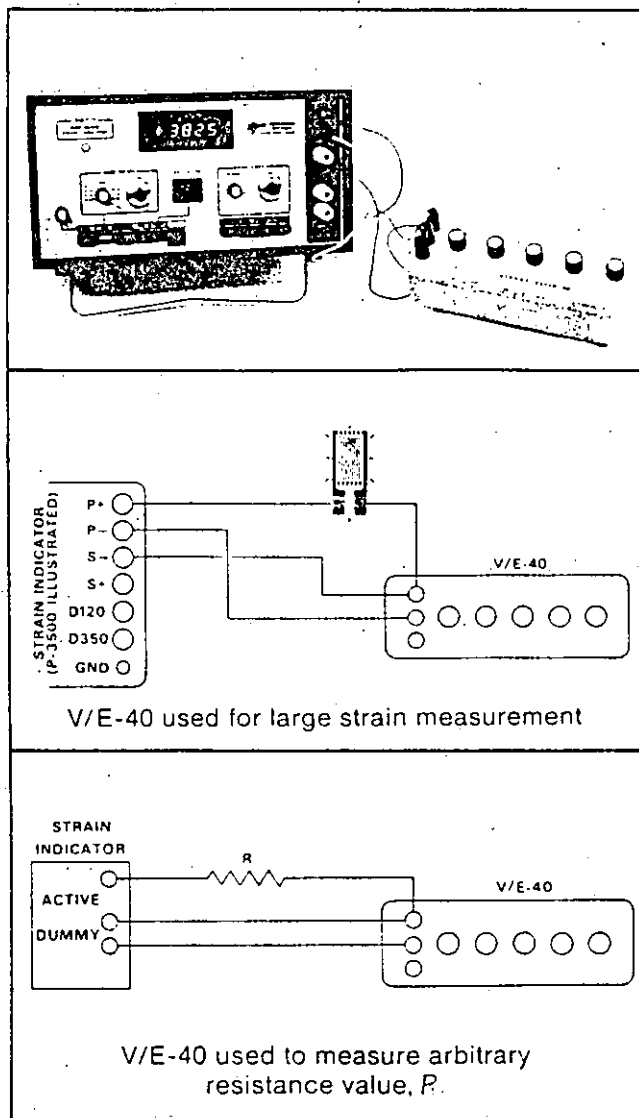
The V/E-40 Strain Gage Simulator is an accurate, stable, compact, five-decade resistor specially designed to simulate the behavior of strain gages and RTD's, and for use in a broad range of measurement and calibration applications.

As a precision strain gage simulator, the V/E-40 can be used to **measure nonlinearity of the instrumentation** in quarter-bridge operation, or to **verify instrument calibration** over the anticipated measurement range. It is also well-suited to **measuring desensitization of the strain gage circuit** due to the finite resistance of the strain gage leadwire system.

In a similar manner, the V/E-40 can be temporarily substituted for an RTD over a resistance range of 30.00 to 1111.10 ohms to **verify calibration of temperature measurement instrumentation**.

The V/E-40 can also be used in conjunction with a conventional Wheatstone bridge strain indicator to **measure arbitrary resistances** between 30.00 and 1111.10 ohms, or to **eliminate Wheatstone bridge nonlinearity effects when measuring high post-yield strains in quarter-bridge operation**. In this mode, the resistance or strain gage to be measured is connected as one arm of a Wheatstone bridge, the V/E-40 is used as a decade resistor in an adjacent arm, and the strain measuring instrument as a null detector.

Other applications include use as an investigative tool to troubleshoot faulty strain gage installations, or as a precision decade resistor.



SPECIFICATIONS

Accuracy: 0.02% of reading.
 Maximum Current: To meet accuracy and repeatability specifications: 120Ω: 65 mA; 350Ω: 55 mA; 1000Ω: 25 mA.
 Stability: ±3 ppm/°C max.
 Resistance Range: 30.00 to 1111.10Ω in 0.01Ω steps.

Environment: 0° to +120°F (-18° to +49° C), up to 70% relative humidity, non-condensing.

Size: 3-7/8 H x 9-1/8 W x 3-1/8 D in (98 x 232 x 89 mm).

Weight: 1.9 lb (0.85 kg).

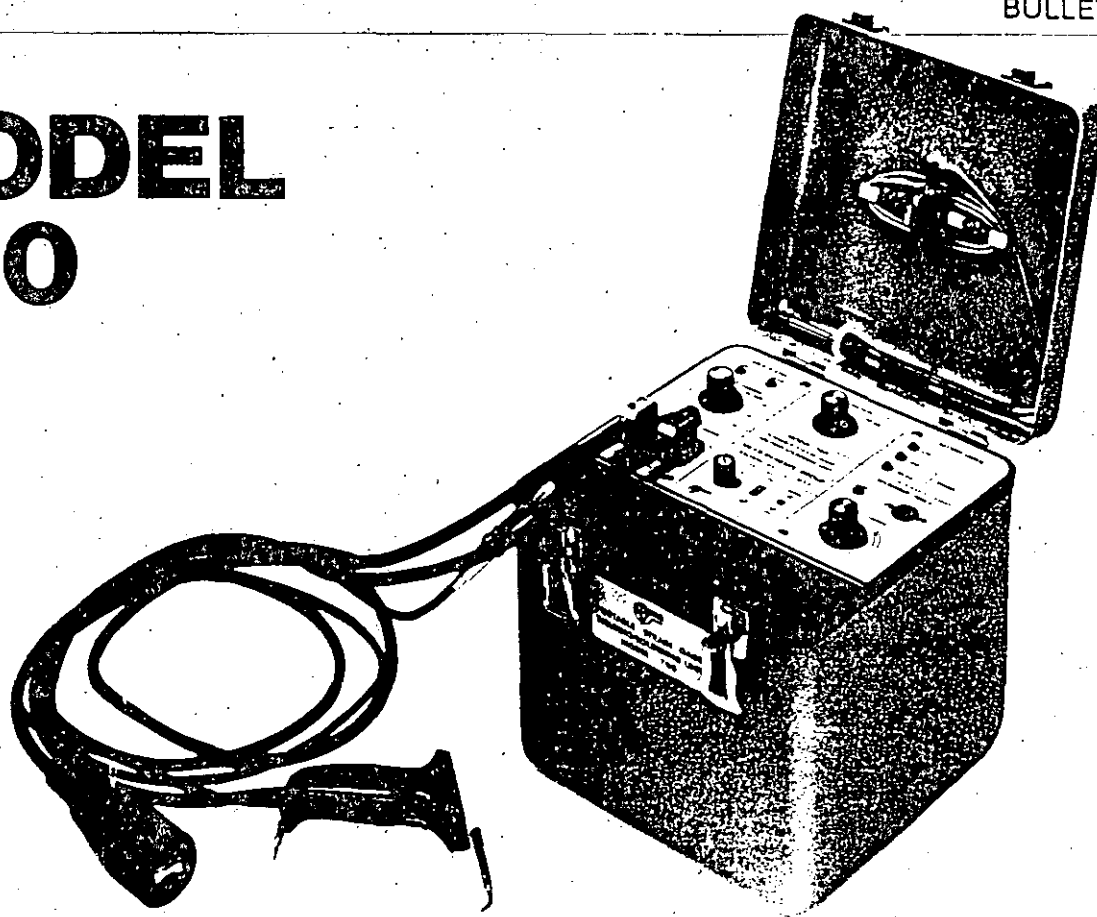
All specifications are nominal or typical at +23° C (+73° F).

MEASUREMENTS GROUP, INC.

P.O. Box 27777, Raleigh, NC 27611, USA
 (919) 365-3800 • Telex 802-502 • FAX (919) 365-3945

02114TD
 Printed in USA

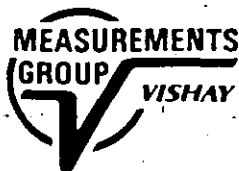
MODEL 700



PORTABLE STRAIN GAGE WELDING AND SOLDERING UNIT

A battery-operated capacitive discharge spot welder for attaching and wiring weldable strain gages and temperature sensors.

- **Separate visual and audible indicators monitor welder status** — Weld energy is continuously adjustable from 3 to 50 joules, making the Model 700 an excellent choice for installing weldable strain gages and temperature sensors, as well as small thermocouples and light-gauge metal.
- **Supplied with a lightweight soldering pencil** — A front-panel control adjusts soldering tip temperature for a wide range of soldering applications in the field or in the laboratory.
- **"Low-battery" light to warn the user when the internal, sealed lead-acid battery requires charging** — A built-in charger operates automatically when plugged into 115 or 230 Vac, to ensure full battery charge with no danger of overcharging. Indicator lights monitor battery charge rate.
- **Convenient storage space for cables and instruction manual.**



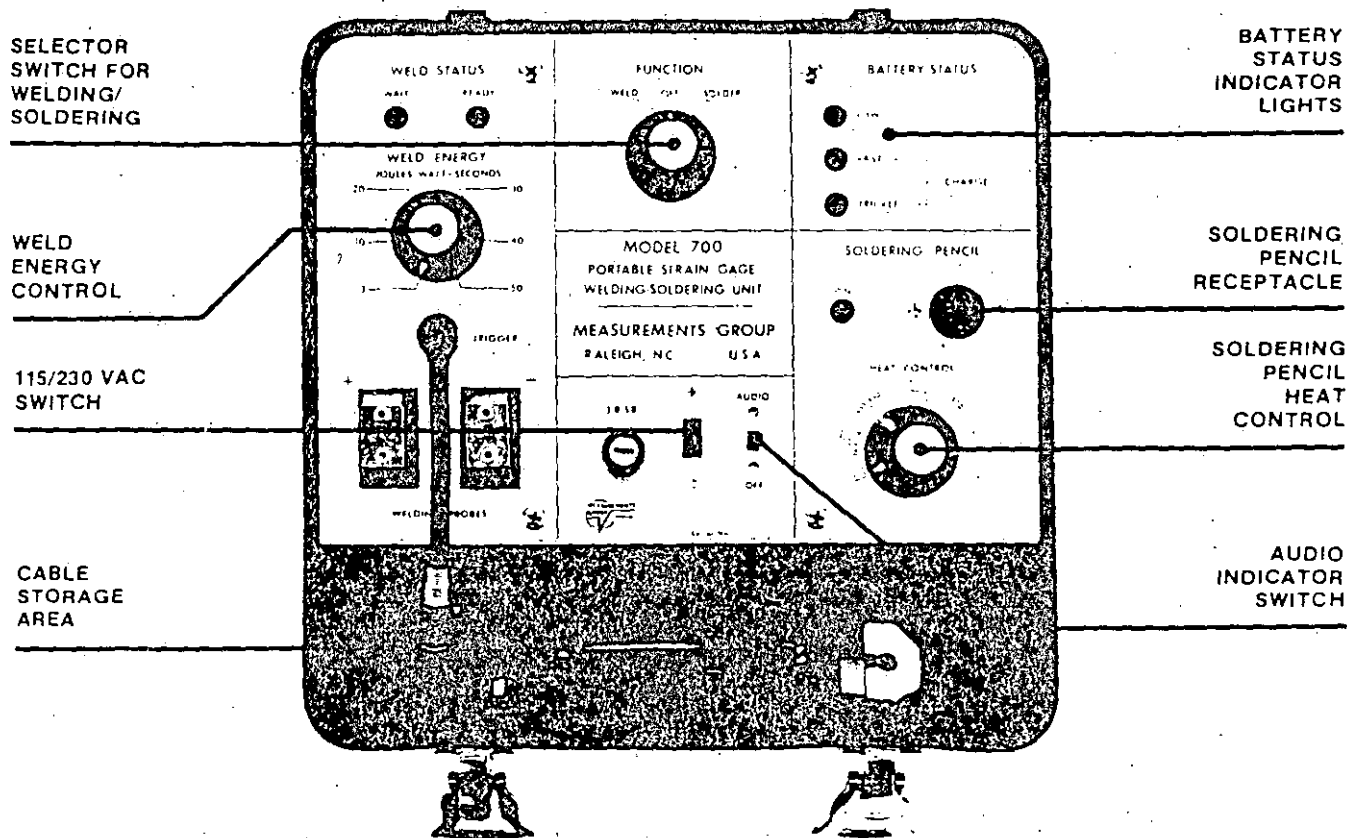
EDIC, S. A. DE C. V.
EQUIPOS DIDACTICOS INDUSTRIALES
Y CIENTIFICOS, S. A. DE C. V.
R. F. C. EDI-891208-PGA
CAIRO No. 251 COL. EL RECREO
C. P. 02070 MEXICO, D. F. MEX.
TEL. 521 20 04 FAX 521 20 51

MEASUREMENTS GROUP, INC.

P.O. Box 27777
Raleigh, North Carolina 27611, USA
(919) 365-3800

©Copyright Measurements Group, Inc., 1981
All Rights Reserved.

PANEL CONTROL FEATURES



SPECIFICATIONS

WELDING

- WELD ENERGY RANGE**
3 to 50 joules, continuously adjustable by front-panel control.
- MAXIMUM WELD REPETITION RATE**
20 per minute at 30 joules, typical.
- NUMBER OF WELDS PER BATTERY CHARGE**
Approximately 2000 at weld energy setting of 30 joules. This is equivalent to 40 Micro-Measurements weldable gage installations.
- BATTERY CHARGE TIME (from full discharge)**
12 hours to 75% full charge; 18 hours to full charge.
- BATTERY**
One sealed, rechargeable lead-acid (non-liquid) type, 12 volt, 5 ampere-hour.
- WELDING PROBE**
Manually fired with trigger control and "steady-rest."
- WELDING CABLES**
Two 5 ft (1.5 m), fully flexible.
- WELD ENERGY MONITOR**
Calibrated front-panel control with READY and WAIT indicators; audible indication selectable.

SOLDERING

- TEMPERATURE CONTROL**
Continuously variable with bands indicating melting range of solders.
- SOLDERING PENCIL**
1.1 oz (31 gm), rated at 25 watts, 12 volt operation. Tip temperature adjustable from +200° to +900° F (+90° to +480° C).
- SOLDERING DURATION**
4 hours using +361° F (+183° C) melting point solders (with initial full charge).

GENERAL

- OVERALL SIZE**
9 L x 9 W x 9-3/4 H in (230 x 230 x 250 mm).
- WEIGHT**
21 lb (9.5 kg).
- INPUT POWER FOR RECHARGING**
115 Vac or 230 Vac, 50-60 Hz.
- OPERATING AND STORAGE TEMPERATURE RANGE**
0° to +120° F (-20° to +50° C).

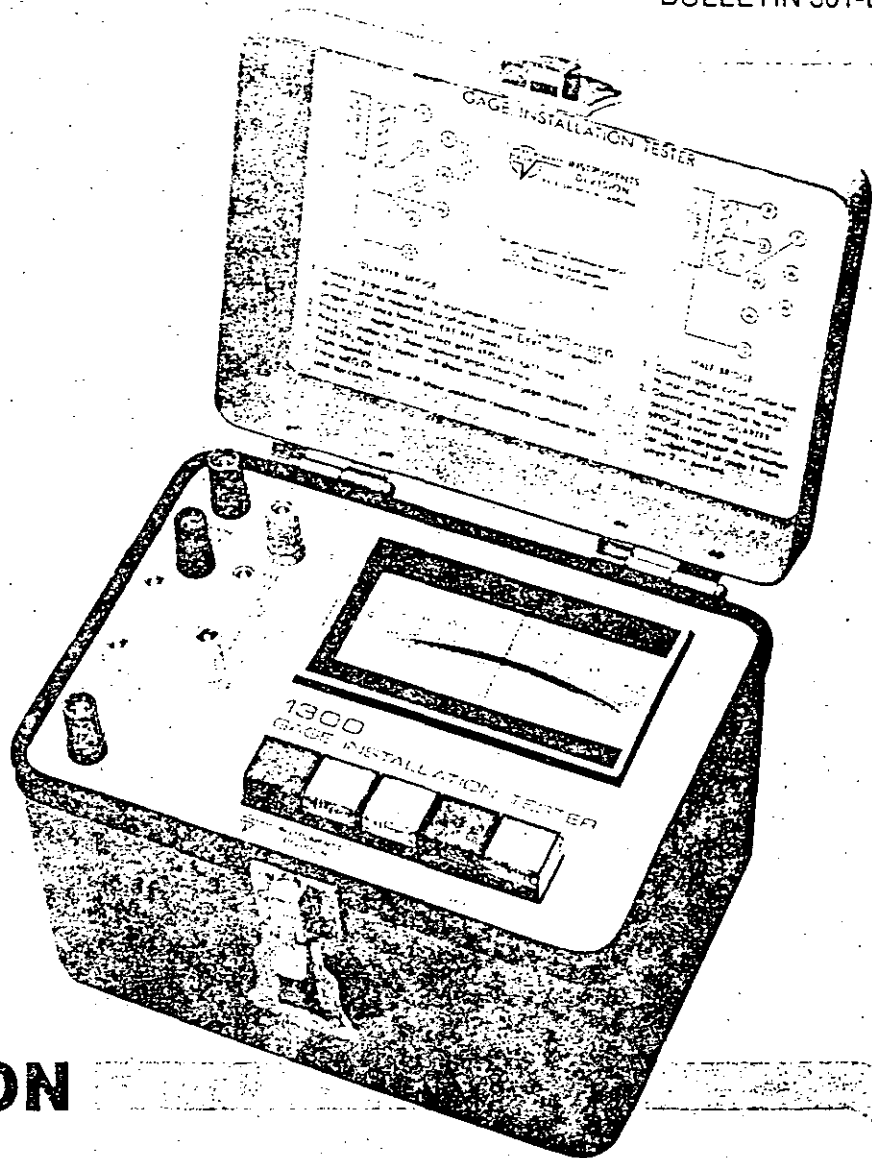
MEASUREMENTS GROUP, INC.

P.O. Box 27777, Raleigh, N.C. 27611, USA
(919) 365-3800 • FAX (919) 365-3945 • Telex 802-502

991118TD

Printed in USA

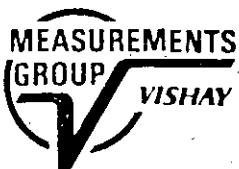
MODEL 1300



GAGE INSTALLATION TESTER

A compact, battery-powered instrument used to verify the electrical quality of a strain gage installation BEFORE it is placed in service.

- Reads with the Push of a Button: No Warm-Up.
- Reads Insulation Resistance (Leakage) to 20 000 Megohms with 15 Vdc.
- Measures Deviation of Installed Gage Resistance from Precise Standards to a Resolution of 0.02 Percent.
- Ohmmeter Scale for Troubleshooting Questionable Installations.
- Verifies the Complete Gage Circuit Including Leadwires.



EDIC, S. A. DE C. V.
EQUIPOS DIDACTICOS INDUSTRIALES
Y CIENTIFICOS, S. A. DE C. V.
R. F. C. EDI-891208-PGA
CAIRO No. 251 COL. EL RECREO
C. P. 02070 MEXICO, D. F. ATZ.
TEL. 561-80-04 FAX 342-50-51

MEASUREMENTS GROUP, INC.

P.O. Box 27777
Raleigh, North Carolina 27611, USA
(919) 365-3800

©Copyright Measurements Group, Inc., 1980
All Rights Reserved.

DESCRIPTION

Two of the most important measurements used to verify the quality of a strain gage installation are insulation resistance (leakage to ground) and shift in gage resistance due to installation procedures. While these two measurements are not a complete guarantee of eventual proper strain gage performance, any installation which produces questionable values should not be relied upon where accuracy of results is necessary.

Several sources of variations in insulation resistance and shifts in gage resistance are:

Insulation resistance in excess of 20 000 megohms should be expected for foil strain gages when installed under laboratory conditions. A value of 10 000 megohms should be considered minimum. A reading below this value generally indicates trapped foreign matter, moisture, residual flux or backing damage due to soldering, as well as incomplete solvent evaporation from an overcoating.

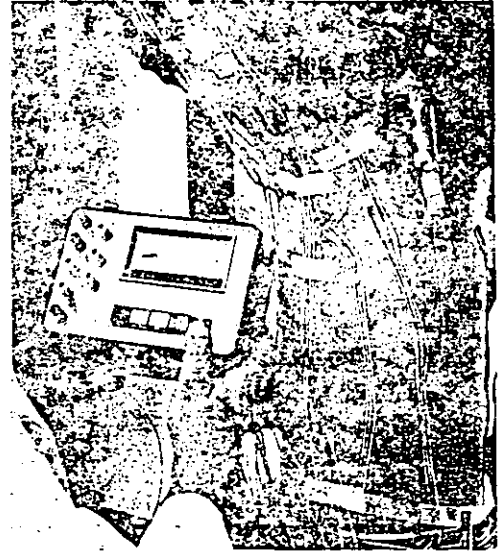
Deterioration of the insulation resistance with time may be an indication of an improperly coated installation.

At higher test temperatures, particularly above +300°F (+150°C), it is normal to expect lesser values. Ten megohms is considered to be the lower allowable value.

A voltage difference between the specimen and strain gage frequently exists. A very high insulation resistance will help keep this voltage differential from introducing extraneous signals during strain measurement.

Shifts in gage resistance during installation should not normally exceed 0.5% when using room-temperature-curing adhesives. Resistance shifts greater than 0.5% generally indicate damage to the gage due to improper handling or clamping. However, strain gages installed using elevated-temperature-curing adhesives may exhibit greater shifts in resistance due to adhesive lock-up at elevated temperatures (difference in linear coefficient of thermal expansion between the strain gage and specimen). These shifts will vary depending upon the specific cure temperature and materials used. The shifts should never exceed 2% and should be uniform within 0.5%.

The Model 1300 was jointly designed by the Micro-Measurements and Instruments Divisions of the Measurements Group for maximum usability. The unit's payback is very short as it will identify faulty gage installations that could ruin a costly test program.



Complete strain gage installation is easily verified using the Model 1300. Once initial wire connections are made, measurements are accomplished simply by pushing the appropriate buttons.

SPECIFICATIONS

INPUT CIRCUITS

Gages: 3-wire quarter bridge (120 and 350 Ω) and half bridge. Other value quarter bridges using customer's reference, at readily accessible panel terminals. As ohmmeter: 2 leads (500 Ω and 500 M Ω mid-scale).

INPUT LEADS

4-ft (1.2-m) 4-conductor AWG #26 (0.4-mm dia.) twisted Teflon[®]-insulated cable supplied (with ground clip and 3 tinned leads).

METER

3.5-in size [3.00-in (76-mm) scale length] with mirror. Tracking accuracy $\pm 1\%$ full range.

MODE SWITCH

5 momentary push buttons: battery check, $\pm 5\%$ deviation, $\pm 1\%$ deviation, gage resistance (ohms), and insulation resistance (megohms).

DEVIATION MODE

Two ranges, $\pm 1\%$ and $\pm 5\%$ F.S. (50 graduations either side of zero).

Accuracy: 1% range: 0.04% ΔR (2 meter graduations)

5% range: 0.2% ΔR (2 meter graduations)

Excitation: 1.0 Vdc per gage.

INSULATION RESISTANCE MODE

Graduated 5 M Ω to 20 000 M Ω (500 M Ω mid-scale).

Accuracy: 1 scale div.

Test Voltage: 15 Vdc open circuit.

OHM MODE

Graduated 5 Ω to 20 k Ω (500 Ω mid-scale).

Accuracy: 1 scale div.

Test Voltage: 2 Vdc open circuit (0.4 Vdc @ 120 Ω).

ENVIRONMENTAL

+15° to +125°F (-10° to +50°C); up to 90% relative humidity, non-condensing.

SIZE

Aluminum case (separable lid)

5 H x 7 W x 5 D in with lid

(125 x 180 x 125 mm).

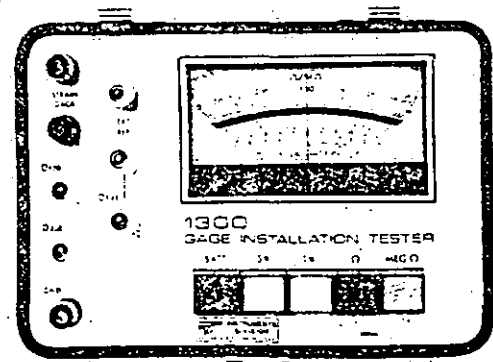
WEIGHT

3.6 lb (1.6 kg) with batteries

POWER SUPPLY

Four 9V NEDA 1604 batteries (Eveready 216 or equiv.)

Life: Will fully test 1000-3000 installations.



Momentary action, color-coded push-button switches enable easy selection of meter scales—ohms/megohms, $\pm 1\%$ deviation, $\pm 5\%$ deviation and battery check.

MEASUREMENTS GROUP, INC.

P.O. Box 27777, Raleigh, N.C. 27611, USA

(919) 365-3800 • FAX (919) 365-3945 • Telex-802-502

991118TD

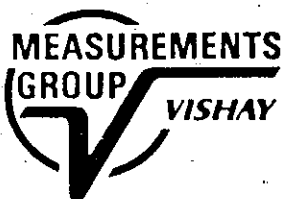
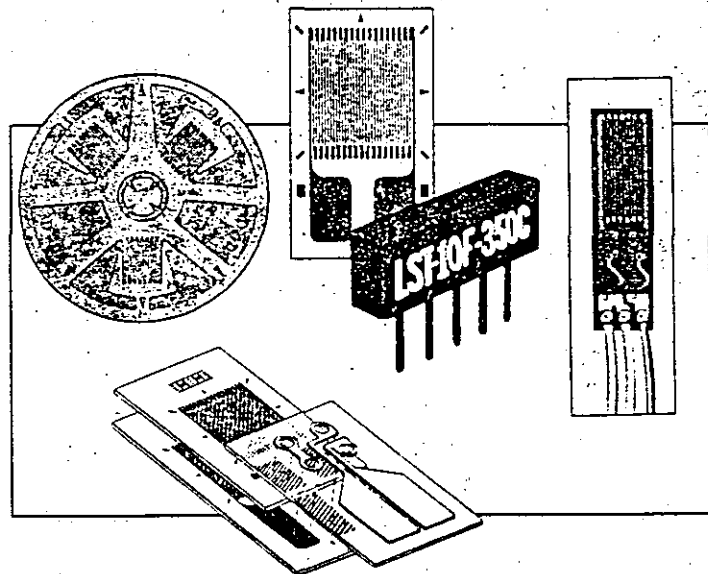
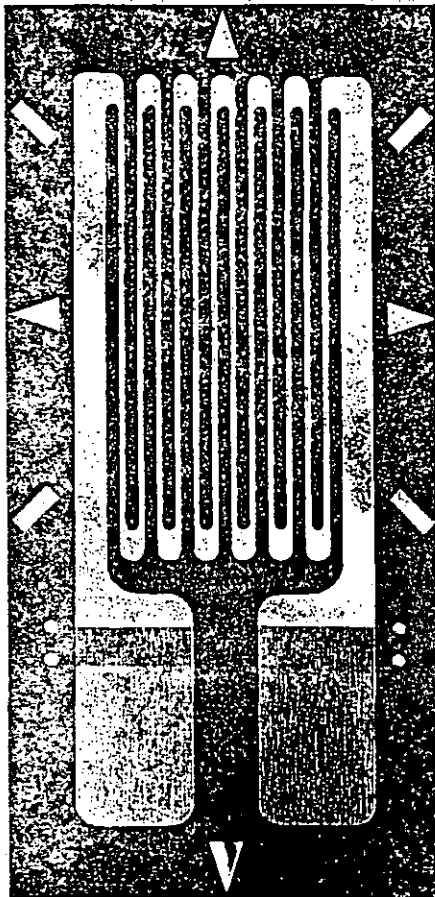
Printed in USA

An Introduction to . . .

Micro-Measurements

MEME

- Strain Gages
- Special Sensors
- Installation Accessories



The Broadest Range Of Strain Gages And Accessories Available

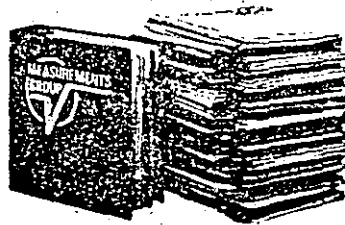
Micro-Measurements has been a trusted name in the field of Strain Gage Technology for many years. We are proud of our worldwide reputation as a premier supplier of high-quality precision strain gages and strain gage accessories, and are fully committed to maintaining our position as the leader in this field. This short-form catalog of Micro-Measurements strain gages and related products is intended to provide a condensed overview of the sensors, supplies, and tools commonly needed for typical strain gage applications.

Micro-Measurements was independently founded and operated in the early 1960's. A few years later it became a part of Vishay Intertechnology, Inc. and, in late 1973, was incorporated with the other stress analysis divisions of Vishay into a single entity — The Measurements Group. All divisions of the Measurements Group are now located in our world headquarters facility near Raleigh, North Carolina. Micro-Measurements maintains an additional strain gage production facility in Romulus, Michigan.

Customer Support Services

The common denominator in all Micro-Measurements products and services is our dedication to helping you achieve consistently accurate and reliable strain measurements. And we've made some significant commitments to help ensure your success:

We publish the widest range of technical reference literature in the strain gage field — available through the Measurements Group's Technical Data Mailing Program.



We respond quickly to requests for "specials" to suit individual requirements.



An experienced and friendly Applications Engineering staff is readily available by phone or letter.



We offer a variety of comprehensive technical training programs from beginner to advanced levels in strain gage technology. The Measurements Group regularly conducts workshops and technical seminars in our Technical Training Center in Raleigh, North Carolina and at locations throughout the U.S. and the world.



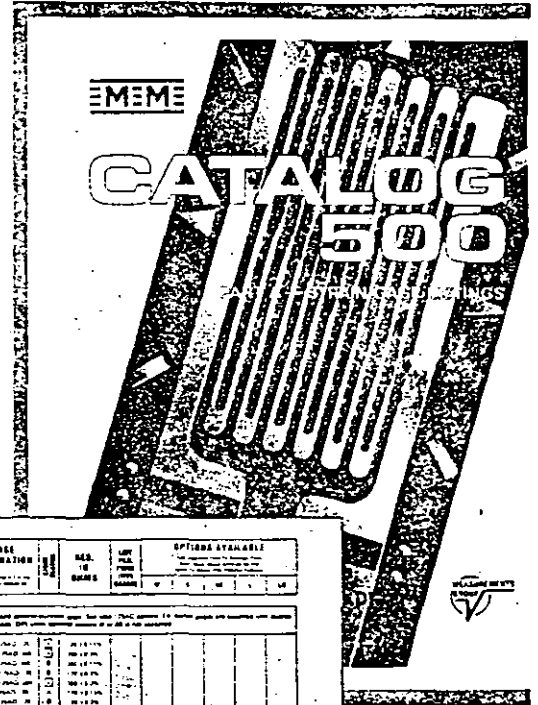
At Micro-Measurements, Your Success Is Our Goal

Master Strain Gage Catalog

Catalog 500

This introductory catalog contains abridged strain gage listings which are representative of the types and sizes most widely used in stress analysis applications. For those involved in extensive stress/strain measurement programs, it is advantageous to request a copy of Micro-Measurements Catalog 500. The gage listings in Catalog 500 include essentially all standard types and pattern configurations manufactured by Micro-Measurements. Considering the variations in pattern design, grid alloys, self-temperature-compensation (S-T-C) numbers, backing materials, and optional features, there are over 100,000 possible gage types from which to select.

Catalog 500 contains a broad range of pattern configurations and sizes, designed to meet the many and varied test requirements encountered throughout the field of experimental stress analysis.



A special group of strain gages — *Transducer-Class*® — has been developed specifically for transducer applications. *Transducer-Class* strain gages, described in separate Micro-Measurements literature, are a select group of standard and special gage patterns designed for optimum cost/performance ratio (in transducer service) in high-volume production quantities.

Gage Listings

Reproduced below is a sample Catalog 500 listing for a single, representative gage pattern. The listing includes a tabulation of all gage series in which the pattern is available, as well as optional features applicable to each series. Complete descriptions of the gage series, options, etc. are provided in the introductory section of Catalog 500.

GAGE PATTERN	GAGE DESIGNATION	RES. IN OHMS	LIST PKG. PRICE (FIVE GAGES)	OPTIONS AVAILABLE
125AD	Widely used general-purpose gage. See also 125AC pattern. EK-Series gages are supplied with duplex copper pads (DP) when optional feature W or SE is not specified.			
125AW	Widely used general-purpose gage. See also 125AC pattern. EK-Series gages are supplied with duplex copper pads (DP) when optional feature W or SE is not specified.			
125AM	Widely used general-purpose gage. See also 125AC pattern. EK-Series gages are supplied with duplex copper pads (DP) when optional feature W or SE is not specified.			

GAGE PATTERN <small>Actual Size Shown. Enlarged When Necessary For Definition.</small>	GAGE DESIGNATION Insert Desired S-T-C No. in Spaces Marked XX	STOCK STATUS	RES. IN OHMS	LIST PKG. PRICE (FIVE GAGES)	OPTIONS AVAILABLE				
					W	E	SE	L	LE
ES = Each Section S = Section (S1 = Sec 1) CP = Complete Pattern M = Matrix Inches millimetres									

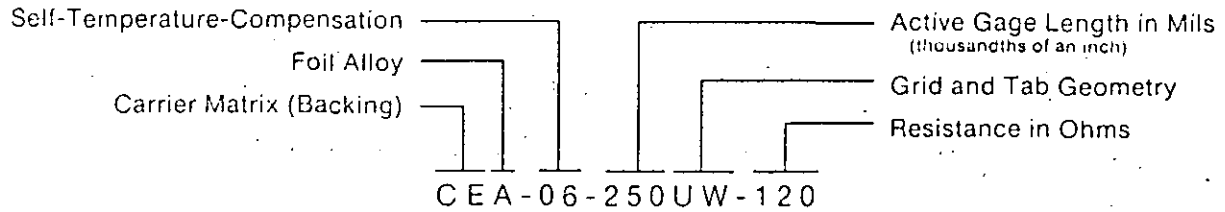
125AD				Widely used general-purpose gage. See also 125AC pattern. EK-Series gages are supplied with duplex copper pads (DP) when optional feature W or SE is not specified.						
GAGE LENGTH	OVERALL LENGTH	GRID WIDTH	OVERALL WIDTH							
0.125	0.250	0.125	0.125	EA-XX-125AD-120	A	120 ± 0.15%				
				ED-DY-125AD-350	A	350 ± 0.3%				
				EK-XX-125AD-350	B	350 ± 0.15%				
				WA-XX-125AD-120	B	120 ± 0.3%				
				WK-XX-125AD-350	A	350 ± 0.3%				
				EP-08-125AD-120	A	120 ± 0.15%				
				SA-XX-125AD-120	B	120 ± 0.3%				
				SK-XX-125AD-350	A	350 ± 0.3%				
				SD-DY-125AD-350	B	350 ± 0.6%				
				WD-DY-125AD-350	A	350 ± 0.6%				
Matrix Size				0.40L x 0.22W	10.2L x 5.6W					

Strain Gage Designation System and Selection Chart

In selecting the most suitable strain gage for each application, consideration must be given to the variations in pattern design, grid alloy, self-temperature-compensation (S-T-C), backing material, and optional features. The gage designation system and standard strain gage selection chart shown on this page present a partial summary of the many combinations of these factors available in Micro-Measurements strain gages. For brevity, this summary is limited to those gage series and optional features listed in this catalog only. When selecting or ordering a strain gage from this catalog, these charts will provide a key to choosing the appropriate gage for your application.

A complete, detailed designation system and selection chart are included in Catalog 500.

When test conditions are severe, or when there are unusually stringent demands on accuracy and stability, selection of the optimum gage parameters to satisfy the test specifications can involve a number of subtle considerations. As an aid in systematically arriving at the most appropriate gage type, given a specific measurement task, Measurements Group Tech Note TN-505, "Strain Gage Selection Criteria, Procedures, Recommendations", available on request from the Measurements Group's Applications Engineering Department, will provide a valuable reference for use in conjunction with these selection criteria and charts.



- E: Open-faced, cast polyimide backing.
- W: Fully encapsulated; glass-fiber-reinforced epoxy-phenolic resin. High-endurance leadwires.
- CE: Thin, flexible gages with a cast polyimide backing and encapsulation featuring large, rugged, copper-coated solder tabs. This construction provides optimum capability for direct leadwire attachment.

- A: Constantan alloy in self-temperature-compensated form.
- P: Annealed Constantan.
- D: Isoelastic alloy.
- K: Modified Karma alloy.

The S-T-C number is the approximate thermal expansion coefficient in PPM/°F of the structural material on which the gage is to be used. The following standard compensations are available:
 A and K alloys: 06, 13.
 P alloy: 08.
 The D alloy is not available in self-temperature-compensated form. 'DY' is used instead.

Gage Series	DESCRIPTION AND PRIMARY APPLICATION	TEMPERATURE RANGE	STRAIN RANGE	FATIGUE LIFE	
				Strain Level In $\mu\epsilon$	Number of Cycles
EA	General-purpose static and dynamic stress analysis. Wide range of options available.	Normal: -100° to $+350^{\circ}$ F (-75° to $+175^{\circ}$ C) Special or Short Term: -320° to $+400^{\circ}$ F (-195° to $+205^{\circ}$ C)	$\pm 3\%$ for gage lengths under 1/8 in (3.2 mm). $\pm 5\%$ for 1/8 in & over.	± 1800 ± 1500 ± 1200	10^5 10^6 10^7
CEA	Universal general-purpose strain gages. Constantan grid completely encapsulated in polyimide, with large, rugged, copper-coated tabs. Primarily used for general-purpose static and dynamic stress analysis.	Normal: -100° to $+350^{\circ}$ F (-75° to $+175^{\circ}$ C) Stacked rosettes limited to $+150^{\circ}$ F ($+65^{\circ}$ C)	$\pm 3\%$ for gage lengths under 1/8 in (3.2 mm). $\pm 5\%$ for 1/8 in & over.	± 1500 ± 1500	10^5 10^6
ED	Excellent for dynamic measurements. High gage factor and extended fatigue life.	Dynamic: -320° to $+400^{\circ}$ F (-195° to $+205^{\circ}$ C)	$\pm 2\%$ Nonlinear at strain levels over $\pm 0.5\%$.	± 2500 ± 2200	10^6 10^7
WA	Stress analysis and transducer applications. Wide temperature range and extreme environmental capability. High-endurance leadwires.	Normal: -100° to $+400^{\circ}$ F (-75° to $+205^{\circ}$ C) Special or Short-Term: -320° to $+500^{\circ}$ F (-195° to $+260^{\circ}$ C)	$\pm 2\%$	± 2000 ± 1800 ± 1500	10^5 10^6 10^7
WK	Widest temperature range and most extreme environmental capability. High-endurance leadwires.	Normal: -452° to $+550^{\circ}$ F (-269° to $+290^{\circ}$ C) Special or Short-Term: -452° to $+750^{\circ}$ F (-269° to $+400^{\circ}$ C)	$\pm 1.5\%$	± 2400 ± 2200 ± 2000	10^6 10^7 10^8
EP	High-elongation measurements (post yield). Only available in 08 S-T-C value.	-100° to $+400^{\circ}$ F (-75° to $+205^{\circ}$ C)	$\pm 10\%$ for gage lengths under 1/8 in (3.2 mm). $\pm 20\%$ for 1/8 in & over.	± 1000	10^4 EP gages show zero shift under high-cyclic strains.
WD	For wide-range dynamic strain measurements in severe environments. High-endurance leadwires.	Dynamic: -320° to $+500^{\circ}$ F (-195° to $+260^{\circ}$ C)	$\pm 1.5\%$ Nonlinear at strain levels over $\pm 0.5\%$.	± 3000 ± 2500 ± 2200	10^5 10^7 10^8










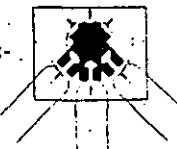





*Fatigue life improved using low-modulus solder.

The gages listed on this and the following page represent the most widely used types for general-purpose experimental stress analysis. Gage lengths range from 0.015 to 0.500 in (0.4 to 13 mm) in a wide range of pattern configurations. In addition to single-element gages in a variety of sizes and aspect ratios, the list includes two- and three-element rosettes for use in biaxial stress fields. There are also twin-element chevron patterns for measuring shear strain or torque. Grid resistances of 120, 350, and 1000 ohms are available.








Selection of gages from this list will generally lead to the best delivery and, in many cases, to a price advantage as well. The "C"-feature, or CEA-Series, strain gages are normally the first choice because of the ease of installation. These gages have rugged, copper-coated solder tabs, permitting direct leadwire attachment.








All gages in this list are classified as *Super Stock*. This means that Micro-Measurements guarantees to maintain stock for off-the-shelf delivery of at least 10 packages of any type listed in 06 and 13 self-temperature-compensation numbers (except 08 S-T-C for P alloy and DY for Isoelastic). There are no Minimum Order Requirements for gages selected under the above conditions.






If your application requires a gage that is not listed here, you should refer to Micro-Measurements Catalog 500, which includes all standard, general-purpose Micro-Measurements strain gages. All gage patterns are shown at actual size except where enlargement is necessary for geometry definition.

GAGE DESIGNATION AND PATTERN	GAGE DESIGNATION AND PATTERN	GAGE DESIGNATION AND PATTERN
<p>CEA-XX-015UW-120</p> <p>Micro-miniature pattern with large exposed solder tabs for high-strain-gradient applications. Exposed tab area is 0.06 x 0.04 in (1.5 x 1.0 mm).</p>  <p>4X</p>	<p>EA-XX-062AP-120 WK-XX-062AP-350</p> <p>Compact small general-purpose pattern. Select WK gage for wide temperature range applications.</p>  <p>2X</p>	<p>EA-XX-125AC-350</p> <p>Widely used general-purpose pattern with high-resistance grid.</p> 
<p>CEA-XX-032UW-120</p> <p>Short gage length pattern with large exposed solder tabs for high-strain-gradient applications. Exposed tab area is 0.07 x 0.04 in (1.8 x 1.0 mm).</p>  <p>2X</p>	<p>EA-XX-062AQ-350</p> <p>Same size as 062AP pattern but with high-resistance grid in EA Series.</p>  <p>2X</p>	<p>EA-XX-125AD-120 ED-DY-125AD-350 WD-DY-125AD-350 WK-XX-125AD-350</p> <p>Widely used, general-purpose pattern. Select ED- or WD-DY gages for fatigue applications; WK for wide temperature range static or dynamic measurements.</p> 
<p>EA-XX-031DE-120</p> <p>Miniature pattern for positioning adjacent to high stress concentrations, e.g., holes, fillets, etc.</p>  <p>4X</p>	<p>CEA-XX-062UW-120 CEA-XX-062UW-350</p> <p>Small general-purpose gage with large exposed solder tabs. Exposed tab area is 0.07 x 0.04 in (1.8 x 1.0 mm).</p>  <p>2X</p>	<p>CEA-XX-125UN-120 CEA-XX-125UN-350</p> <p>Narrow general-purpose gage pattern. Exposed tab area is 0.06 x 0.05 in (1.5 x 1.1 mm).</p> 
<p>WA-XX-060WR-120</p> <p>Small 3-element 45° rect-angular stacked rosette.</p>  <p>2X</p>	<p>EA-XX-062TV-350</p> <p>Small 2-element 90° torque gage.</p>  <p>2X</p>	<p>CEA-XX-125UW-120 CEA-XX-125UW-350</p> <p>Most widely used general-purpose gage in CEA Series. Exposed tab area is 0.10 x 0.07 in (2.5 x 1.8 mm).</p> 
<p>EA-XX-062AK-120</p> <p>Small general-purpose pattern with elongated solder tabs.</p>  <p>2X</p>	<p>EA-XX-062TT-120</p> <p>Small general-purpose 90° 'tee' rosette. Sections are electrically independent.</p>  <p>2X</p>	<p>EA-XX-125BB-120</p> <p>Narrow general-purpose pattern with elongated tabs.</p> 

Super Stock Gage Listings Section

GAGE DESIGNATION AND PATTERN	
<p>CEA-XX-125BT-120</p> <p>General-purpose pattern with narrow grid and compact geometry.</p>  <p>2X</p>	
<p>CEA-XX-125BZ-350</p> <p>Narrow high-resistance pattern with compact geometry.</p>  <p>2X</p>	
<p>CEA-XX-125RA-120</p> <p>General-purpose 3-element 45° rectangular rosette. Compact geometry.</p> 	
<p>CEA-XX-125UR-120 CEA-XX-125UR-350</p> <p>General-purpose 45° single-plane rosette. Compact geometry. Exposed tab area is 0.08 x 0.05 in (2.0 x 1.5 mm).</p> 	
<p>CEA-XX-125TM-120</p> <p>General-purpose 2-element 90° 'tee' rosette. Sections are electrically independent.</p> 	
<p>CEA-XX-125UT-120 CEA-XX-125UT-350</p> <p>2-element 90° 'tee' rosette for general-purpose use. Exposed tab area is 0.10 x 0.07 in (2.5 x 1.8 mm).</p> 	
<p>CEA-XX-125TK-350</p> <p>High-resistance 2-element 90° gage for torque applications.</p> 	

GAGE DESIGNATION AND PATTERN	
<p>CEA-XX-187UV-120 CEA-XX-187UV-350</p> <p>2-element 90° rosette for torque and shear-strain measurements. Sections have a common electrical connection. Exposed tab area is 0.13 x 0.08 in (3.3 x 2.0 mm).</p> 	
<p>CEA-XX-250AE-350</p> <p>Large general-purpose gage. Used when high power-dissipation is required.</p> 	
<p>CEA-XX-250AF-120</p> <p>Large general-purpose gage. Used when high power-dissipation is required.</p> 	
<p>CEA-XX-250BG-120 EP-06-250BG-120 WA-XX-250BG-120 WK-XX-250BG-350</p> <p>Widely used general-purpose pattern. EP Series capable of elongation > 20%.</p> 	
<p>CEA-XX-250BF-350</p> <p>General-purpose pattern with high-resistance grid. Compact geometry. Similar to 250BG pattern except for resistance.</p> 	
<p>CEA-XX-250UN-120 CEA-XX-250UN-350</p> <p>Narrow general-purpose gage pattern. Exposed tab area is 0.08 x 0.05 in (2.0 x 1.1 mm).</p> 	
<p>CEA-XX-250UW-120 CEA-XX-250UW-350</p> <p>Larger grid and tab than 250UN pattern. Exposed tab area is 0.10 x 0.07 in (2.5 x 1.8 mm).</p> 	

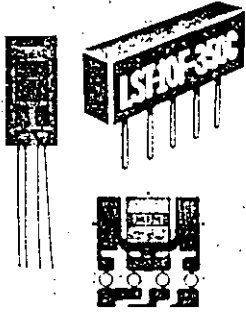
GAGE DESIGNATION AND PATTERN	
<p>EA-XX-250BK-10C</p> <p>Very high-resistance (1000Ω) pattern. Recommended for high bridge voltages or for use on plastics.</p> 	
<p>CEA-06-W250A-120 CEA-06-W250A-350</p> <p>Lowest-cost, most flexible and conformable linear weldable gage pattern. See page 8 for more details.</p> 	
<p>CEA-XX-250UR-120 CEA-XX-250UR-350</p> <p>Large 3-element 45° single-plane rosette. Exposed tab area is 0.13 x 0.08 in (3.3 x 2.0 mm).</p> 	
<p>EA-XX-500BH-120</p> <p>Long general-purpose gage in a compact geometry.</p> 	
<p>CEA-XX-500UW-120</p> <p>Widely used long gage pattern. Exposed tab area is 0.10 x 0.07 in (2.5 x 1.8 mm).</p> 	

Special-Purpose Gages, Sensors, and Equipment

In addition to providing the stress analyst with a vast selection of standard strain gage types, Micro-Measurements offers a variety of products designed to meet special needs and perform special functions in experimental stress analysis. Although space in this introductory catalog permits neither a full listing of these products, nor complete descriptions, a few types of special sensors are briefly noted.

Full information on any of these products, along with detailed technical specifications, can be obtained by requesting Catalog 500, or by contacting the Measurements Group's Applications Engineering Department.

Temperature Sensors



TG Temperature Sensors, with a grid of ultra-pure nickel foil, are recommended for general-purpose temperature measurement from -320° to $+500^{\circ}$ F (-195° to $+260^{\circ}$ C). For application at extremely low temperatures, two alloys — nickel and manganin — are combined to produce the CLTS-2B (cryogenic linear temperature sensor). The duplex construction of this sensor results in an essentially linear change of overall resistance with temperature, from -452° to $+100^{\circ}$ F (-269° to $+40^{\circ}$ C).

Reusable LST matching networks are available for half-bridge connection of temperature sensors to strain indicators. With these accessories, the strain indicator registers temperature directly, at a scale factor of 10 or 100 microstrain per $^{\circ}$ F or $^{\circ}$ C.

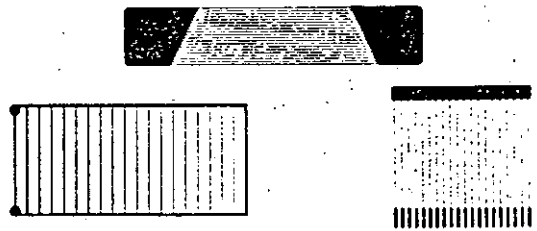
Crack Detection

CD-Series Crack Detection Gages are designed to provide a convenient, economical method of indicating the presence of a crack, or indicating when a crack has progressed to a predetermined location on a test part or structure. By employing several CD gages, it is also possible to monitor the rate of crack growth.

Crack detection gages are available with various strand lengths; from 0.4 to 2.0 in (10 to 50 mm).

Crack Propagation

Crack Propagation Gages accurately indicate rate of crack propagation in a specimen material over a very small distance. These sensors are often used adjacent to notches, fillets, or other types of discontinuities in structures. Several sizes and geometries are available.



Strain Gages for Residual Stress Determination

The most widely used, practical technique for measuring residual stresses is the hole-drilling strain gage method described in ASTM Standard E837. With this method, a specially configured electrical resistance strain gage rosette is bonded to the surface of the test object, and a small, shallow hole is introduced through the center of the gage, using a precision drilling apparatus such as the Measurements Group's RS-200 Milling Guide. After drilling, the strain in the immediate vicinity of the hole is measured, and the relaxed residual stresses are computed from these measurements.



EA Series CEA Series TEA Series

approximately 2X actual size

For further details, request Bulletin 304.

Weldable Strain Gages and Temperature Sensors

Weldable gages are precision foil sensors bonded to a metal carrier for spot welding to structures and components. These sensors are easy to install and require minimal surface preparation. Installation is accomplished without adhesives, eliminating heat curing problems on massive structures. They are also well suited to laboratory test programs requiring elevated-temperature testing and minimal installation time.

SPECIFICATIONS

Sensor	Standard S-T-C	Resistance In Ohms	Gage Factor	Temperature Range
CEA	06,09	120 ± 0.4% 350 ± 0.4%	2.0	-100° to +200° F (-75° to +95° C)
LWK	06,09	350 ± 0.4%	2.1	-320° to +500° F (-195° to +260° C)
WWT	N/A	50 ± 0.4% @ +75° F (+24° C)	N/A	-320° to +500° F (-195° to +260° C)

SENSOR DESCRIPTIONS

CEA-Series Weldable Strain Gage: Constantan alloy sensing grid completely encapsulated in polyimide. Very flexible. In most cases can be contoured to radii as small as 1/2 in (13 mm). Rugged, copper-coated tabs for convenient leadwire attachment.



W250A

LWK-Series Weldable Strain Gage: Modified Karma (K-alloy) sensing grid completely encapsulated in a fiberglass-reinforced epoxy-phenolic matrix. Integral three-wire lead system consists of 10 in (250 mm) flexible etched Teflon[®]-insulated leadwires. Installation radius generally limited to 2 in (50 mm) or larger in the direction of the grid axis.



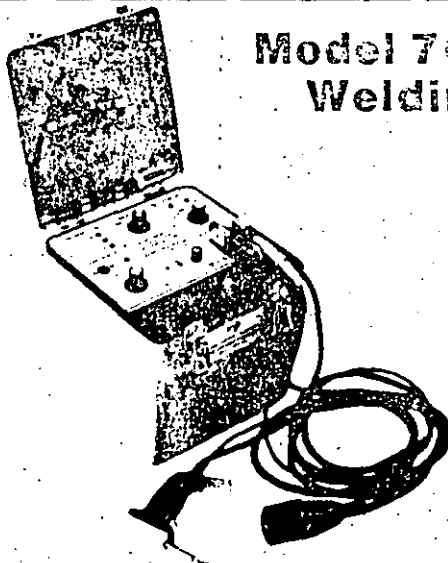
W250B

WWT-Series Weldable Temperature Sensor: High-purity nickel sensing grid completely encapsulated in a fiberglass-reinforced epoxy-phenolic matrix. Integral three-tab printed circuit terminals for convenient leadwire attachment.



W200B

®Registered Trademark of DuPont



Model 700 Portable Strain Gage Welding and Soldering Unit

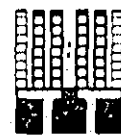
The Model 700 is a completely portable, capacitance-discharge spot welder, designed for efficient installation of weldable strain gages and temperature sensors. Supplied in a rugged, gasketed case, the battery-powered unit can be used under field conditions where no power lines are available.

A temperature-controlled soldering pencil, operated from the main battery supply, is an integral part of the Model 700. The lightweight pencil can be adjusted to a wide range of tip temperatures for both gage soldering and leadwire splicing.

For further details, request Bulletin 302.

Bondable Resistors

Micro-Measurements manufactures a variety of fixed, adjustable, and combination bondable resistors for use in many applications where precise resistance is required. Appropriate patterns are available in both low and high temperature-coefficient-of-resistance types. Widest use is in transducer bridge circuits to compensate for small temperature-induced errors and to adjust bridge balance.



Various alloys, sizes, and patterns are available, allowing selection of the optimum resistor for specific applications. Resistors are normally produced open-faced on a polyimide carrier. The recommended temperature range is from 0° to +300° F (-20° to +175° C). For further details, request Transducer-Class Catalog TC-116.

Micro-Measurements Strain Gage Accessories

Micro-Measurements strain gages are produced under rigidly controlled manufacturing conditions, with the utmost care and attention given to ensuring the high level of quality and precision for which these gages have gained world-wide recognition. However, the gages' full potential for accurate strain measurement can be realized only when they are properly installed. There are, in fact, three principal components in every strain gage installation: (1) the strain gage itself, (2) the tools, materials, and supplies (accessories) needed to install the gage, and (3) the techniques employed in performing the installation. Professional stress analysts have learned from experience that compromising any of these may lead to compromising the quality of the installation and the accuracy of the strain data.

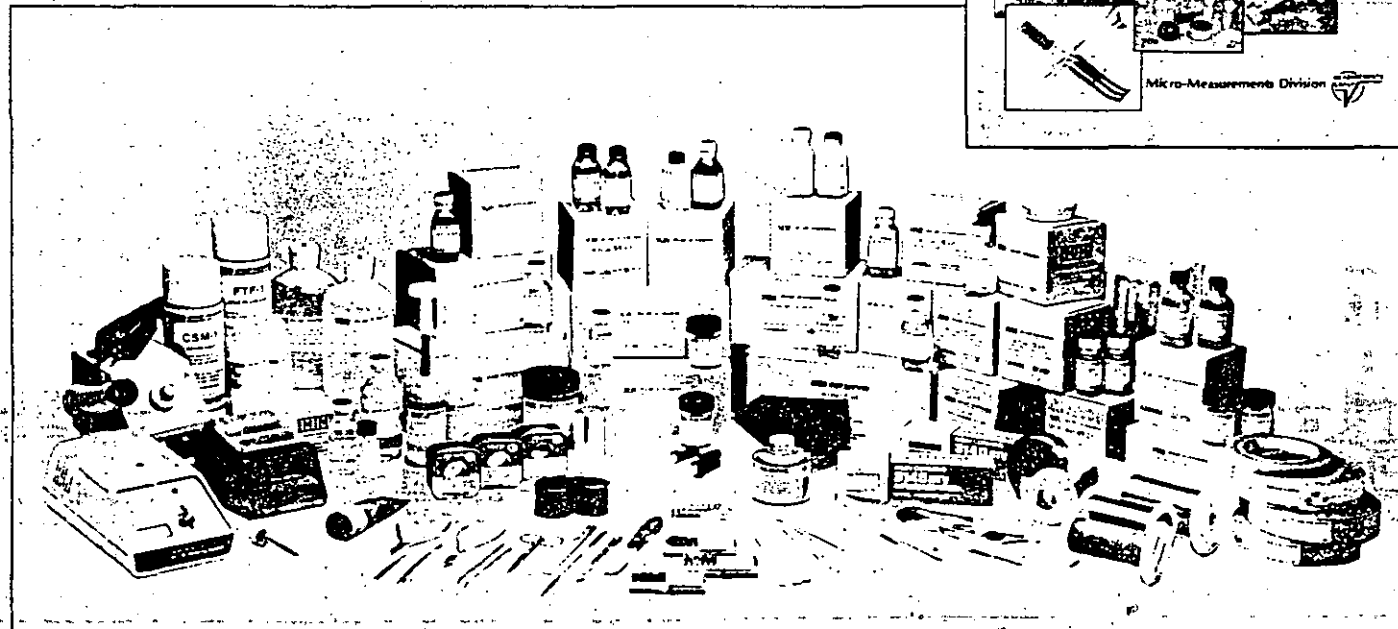
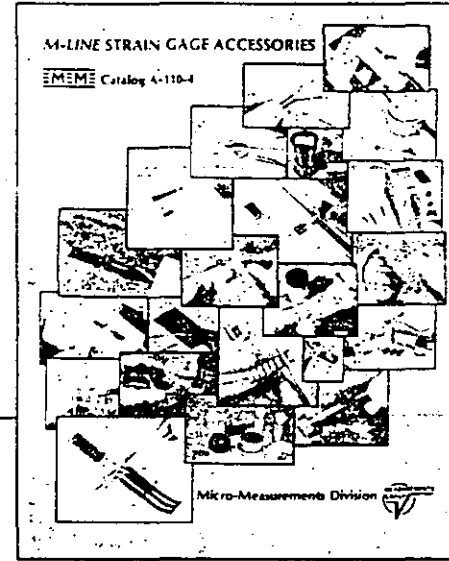
The well-established formula for making consistently successful strain gage installations is quite simple:

- select high-quality precision strain gages.
- select professional-caliber accessories which have been laboratory-tested and field-proven for effectiveness and compatibility with the strain gages.
- follow the installation procedures recommended by the manufacturer of the gages and accessories.


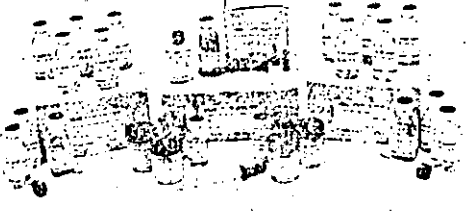
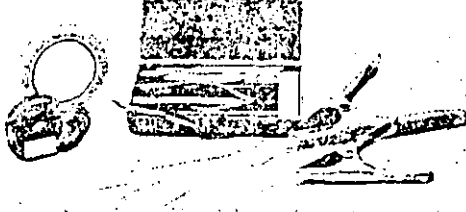



Featured on the following two pages is a small sample of Micro-Measurements *M-LINE* strain gage installation accessories. As indicated, the appropriate materials, supplies, and tools are provided for each important step in the gage installation process — from preparing the surface of the test piece to applying a protective coating over the bonded and wired gage. All accessory items, whether manufactured directly by Micro-Measurements or specified for purchase from an outside supplier, are of the highest quality, and have been designed or selected specifically to help ensure successful installation of Micro-Measurements strain gages.

Regular users of strain gages will want to request a copy of Catalog A-110. This 40-page, fully illustrated catalog describes the complete line of gage installation accessories and related equipment. In addition to detailed product descriptions and specifications, it includes, where applicable, extensive recommendations for the appropriate selection and application of the accessories.

Catalog A-110 is available on request from our Applications Engineering Department.

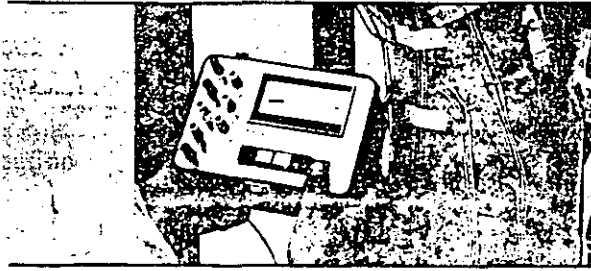
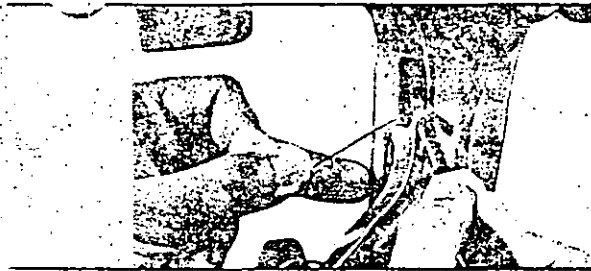
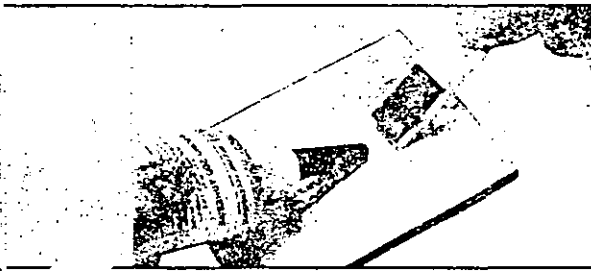
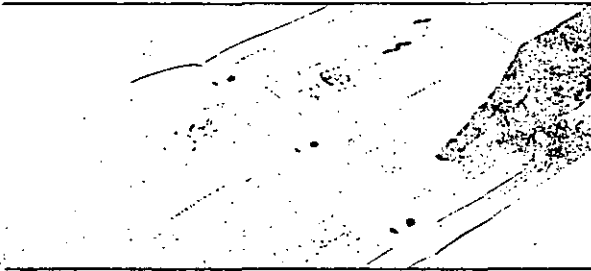


6 Simple Steps To Successful

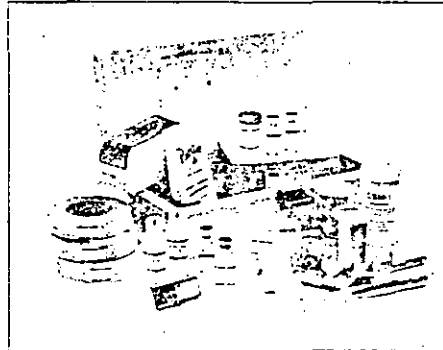
<p>Surface Preparation</p>		<p>CSM-1 Degreaser M-Prep Conditioner A M-Prep Neutralizer 5A Silicon-Carbide Paper Cotton Swabs Gauze Sponges</p>
<p>Adhesive Selection</p>		<p>M-Bond 200 M-Bond AE-10 M-Bond AE-15 M-Bond 600 M-Bond 610</p>
<p>Gage Handling and Bonding</p>		<p>Cellophane Tape Mylar JG Tape Spring Clamps Teflon Film Silicone Rubber Application Tools</p>
<p>Leadwire Attachment</p>		<p>Solder Terminals Wires, Cables — Solid, Stranded, Tinned Solders Soldering Station Wiring Tools</p>
<p>Protective Coating Application</p>		<p>M-Coat A Polyurethane M-Coat B Nitrile Rubber M-Coat C Silicone Rubber M-Coat D Acrylic M-Coat W-1 Microcrystalline Wax</p>
<p>Gage Installation Tester</p>		<ul style="list-style-type: none"> • Reads insulation resistance (leakage) to 20 000 MΩ with 15 Vdc. • Measures deviation of installed gage resistance from precise standards to a resolution of 0.02%. • Auxiliary ohmmeter scale for troubleshooting questionable installations. • Reads with the push of a button. • Verifies the complete gage circuit including leadwires.

... **With M-LINE Accessories**

Strain Gage Installations . . .



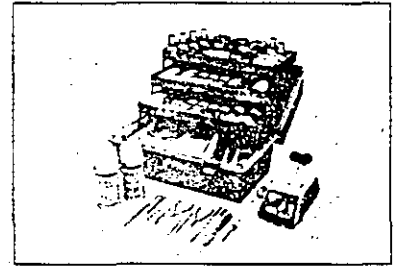
General Application Kits



It is often of greatest convenience for the strain gage user to purchase all of the needed accessory supplies and materials in a single package.

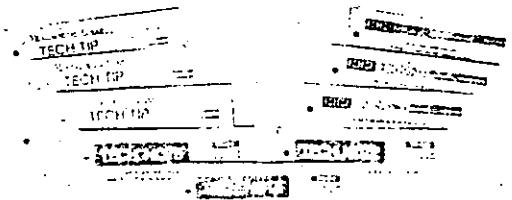
GAK-2 Series Kits provide specific selections of *M-LINE* accessories for making basic strain gage installations with the M-Bond 200, AE-10/15, or 610 adhesives.

The ultimate in gage installation capability is provided by the **MAK-1, Master Strain Gage Application Kit**. The MAK-1 includes all of the supplies and special tools necessary for making a wide range of gage installations for both laboratory and field applications.



Instructional Materials

Because technique is such an important ingredient in successful strain gage installation, detailed **Instruction Bulletins** have been prepared for virtually all Micro-Measurements strain gage installation products.



In addition, a library of **Tech Notes** and **Tech Tips** is available for reference on a broad range of subjects within Strain Gage Technology.

Tech Tips present practical strain gage application techniques for "out-of-the-ordinary" situations, and represent, as much as possible, a practical "how-to" approach to strain gage installation.

Tech Notes contain in-depth technical treatments of specific subjects having direct or indirect bearing on the successful application of stress/strain measurement technology.

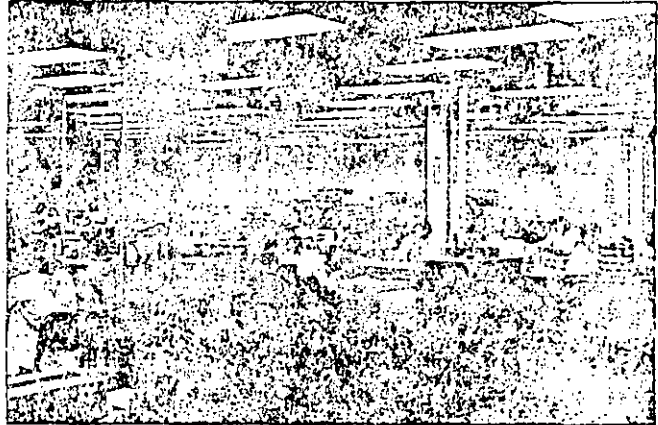
— Lab-Tested — Field-Proven

Ordering Information

All Micro-Measurements products shown in this catalog can be ordered from the accompanying price list.

The Measurements Group Order Service Department can provide immediate stock and delivery information. Most products are available for same-day shipment or can be produced on short delivery cycles. Measurements Group, Inc. maintains regional sales representatives throughout the world to further assist you. For additional information on any of our product lines, contact us or our representative serving your area.

Quantity discounts are available on strain gages and special sensors. All other items are sold on a net basis only. All prices are subject to change without notice.



Micro-Measurements Warranty Policy

The Micro-Measurements Division of Measurements Group, Inc., warrants that the products sold under its name, are fit for the purpose for which they were intended by the supplier and guarantees said items against defects in workmanship or material for a period of ninety (90) days, or otherwise specified limits, from date of delivery. Every reported case of non-standard material is thoroughly investigated by our Quality Assurance Department. It should be recognized that there is no method to 100% test our type of products since many tests would be destructive. Both Micro-Measurements and the purchasers must depend upon statistical sampling techniques that have in the past proved to be reliable and economical in respect to the cost of the product.

This warranty is in lieu of any other warranties, expressed or implied, including any implied warranties of merchantability or fitness for a particular purpose. There are no warranties which extend beyond the description on the face hereof. Purchaser acknowledges that all goods purchased from Measurements Group are purchased as is, and buyer states that no salesman, agent, employee or other person has made any such representations or warranties or otherwise assumed for Measurements Group any liability in connection with the sale of any goods to the Purchaser. Buyer hereby waives all rights buyer may have arising out of any breach of contract or breach of warranty on the part of Measurements Group, to any incidental or consequential damages, including but not limited to damages to property, damages for injury to the person, damages for loss of use, loss of time, loss of profits or income, or loss resulting from personal injury.

Some states do not allow the exclusion or limitation of incidental or consequential damages for consumer products, so the above limitations or exclusions may not apply to you.

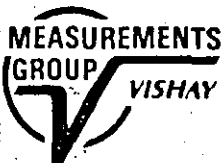
The Purchaser agrees that the Purchaser is responsible for notifying any subsequent buyer of goods manufactured by Measurements Group of the warranty provisions, limitations, exclusions and disclaimers stated herein prior to the time any such goods are purchased by such buyers, and the Purchaser hereby agrees to indemnify and hold Measurements Group harmless from any claim asserted against or liability imposed on Measurements Group occasioned by the failure of the Purchaser to so notify such buyer. This provision is not intended to afford subsequent purchasers any warranties or rights not expressly granted to such subsequent purchasers under the law.

The Measurements Group is solely a manufacturer and assumes no responsibility of any form for the accuracy or adequacy of any test results, data, or conclusions which may result from the use of its equipment.

The manner in which the equipment is employed and the use to which the data and test results may be put are completely in the hands of the purchaser. Measurements Group, Inc. shall in no way be liable for damages consequential or incidental to defects in any of its products.

LIMITATION OF REMEDY: In the event any discrepancy is found to be Micro-Measurements' responsibility, the buyer's sole and exclusive remedy will be the replacement of, or full credit for the discrepant product.

We will provide immediate assistance to the best of our ability in locating and identifying the source of any difficulties involving our product.



EDIC, S. A. DE C. V.
EQUIPOS DIDACTICOS INDUSTRIALES
Y CIENTIFICOS, S. A. DE C. V.
R. F. C. EDI-891203-PGA
CAIRO No. 251 COL. EL RECREO
C. P. 02070 MEXICO, D. F. ATZ.
TEL. 561-89-04 FAX 343-59-51

MEASUREMENTS GROUP, INC.

P.O. Box 27777

Raleigh, NC 27611, USA

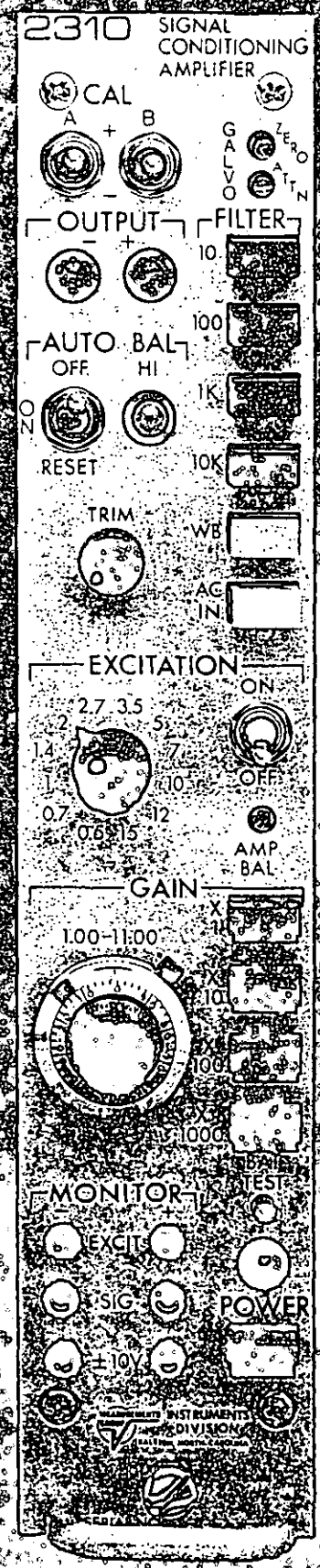
(919) 365-3800

Telex 802-502 • FAX (919) 365-3945

2300 SYSTEM

SIGNAL CONDITIONING AMPLIFIER

A versatile, multi-channel, dynamic instrumentation system that generates high-level signals from strain gages (or strain gage based transducers) for display or recording of data on external equipment.



Sophisticated/Uncomplicated

The 2300 Signal Conditioning Amplifier System combines the latest in electronic sophistication with simplicity in setup and operation

The 2300 System conditions and amplifies low-level signals to high-level outputs for multiple-channel, simultaneous dynamic recording or display on external devices.

Among its advanced features, each 2310/2311 Module includes a built-in power supply, active filtering, three simultaneous outputs, playback mode, wide frequency response, and electronic bridge balance. Socket-mounted integrated circuits and discrete components achieve the demanding specifications listed while providing ease of serviceability.

Up to ten 2310/2311 Modules can be mounted in a Model 2350 Rack Adapter; or up to four modules in a Model 2360 Portable Enclosure; or, a single 2310/2311 can serve as a stand-alone unit.

While the Model 2311 provides wider frequency response and more versatile excitation, the basic 2310 and 2311 Signal Conditioner/Amplifier

Modules accept inputs from strain gages, load/pressure/dc displacement transducers, potentiometers, thermocouples (with Model 1611 Adapter), RTD's and nickel temperature sensors, without any internal modification.

Controls on the 2310/2311 are arranged in sections, permitting easy setup. Clearly marked push-button and single-purpose switches minimize the possibility of operator error during use. With the exception of the playback switch, all operational and monitor controls are on the front panel. Switches for selecting remote sense and specific shunt calibration configurations are located on the printed circuit board inside the unit.

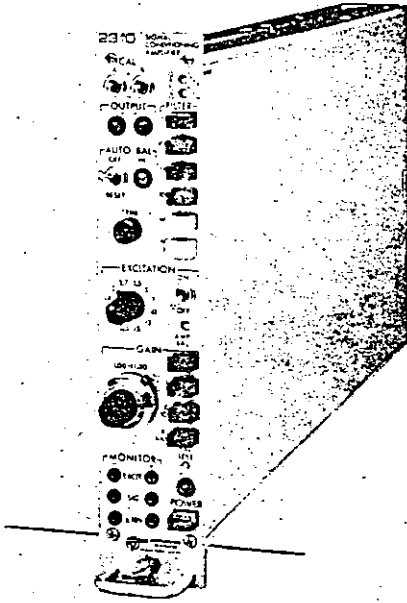
Typical 2300 System configurations are shown on the facing page. The operating features of the basic 2310 and 2311 Modules (shown actual size) are illustrated and described on pages 4 and 5. Complete specifications are given on page 7.

Features

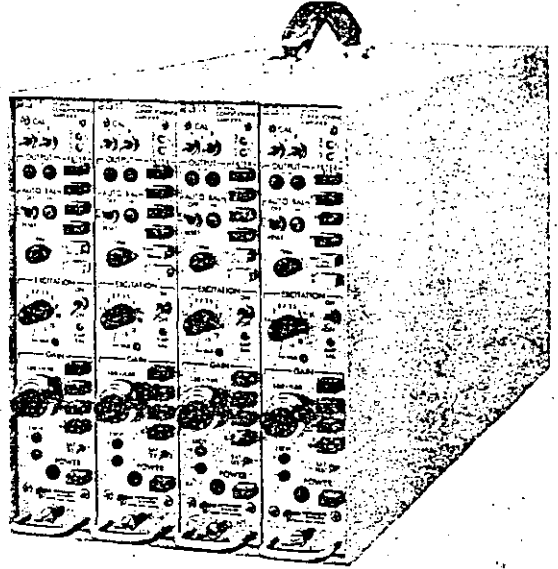
- Selectable bridge excitation, 0.5 to 15 Vdc (0.3 to 15 Vdc for Model 2311)
- Fully adjustable calibrated gain from 1 to 11 000.
- Dual-range (± 5000 and $\pm 25\ 000 \mu\epsilon$) automatic bridge balance, with "keep-alive" power to preserve balance for months without external power.
- All bridge completion built in, including 120 and 350 ohm dummies.
- Dual polarity, two-step double-shunt calibration.
- Bandpass:
 - 2310: 25 kHz (-0.5 dB)
65 kHz (-3.0 dB)
 - 2311: 50 kHz (-0.5 dB)
125 kHz (-3.0 dB).
- Switchable active filter — up to six poles.
- Three simultaneous buffered outputs.
- Playback mode to filter and observe or re-record previously recorded magnetic tape data.
- Input Impedance above 10 megohms at all times.

Configurations

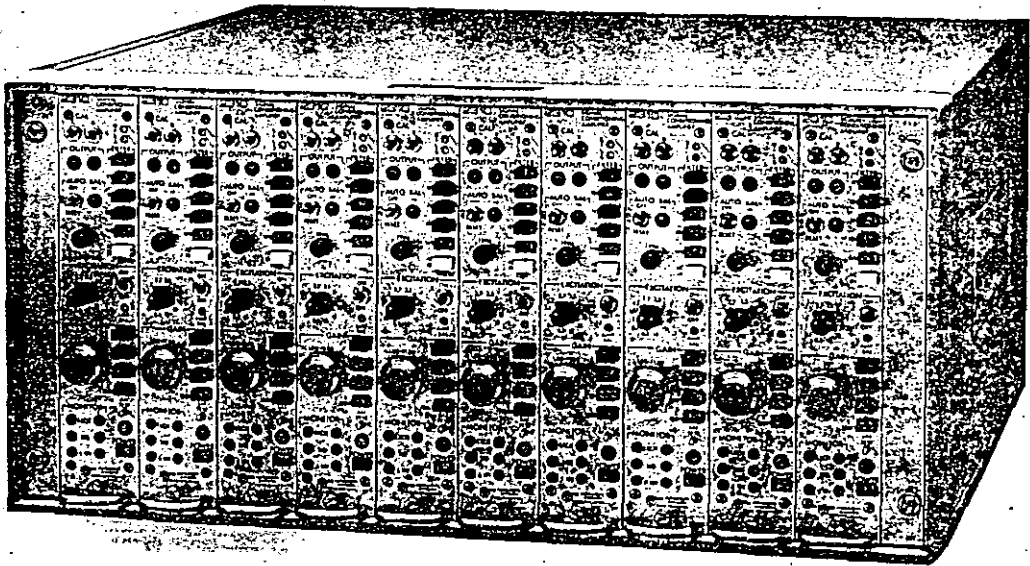
The 2310/2311 Amplifier Modules can be used as stand-alone, single-channel instruments, or can be configured into racks for multi-channel testing.



Stand-alone, single-channel instrument used with the Model 2310-A20 line cord and stabilizer bar accessory package.



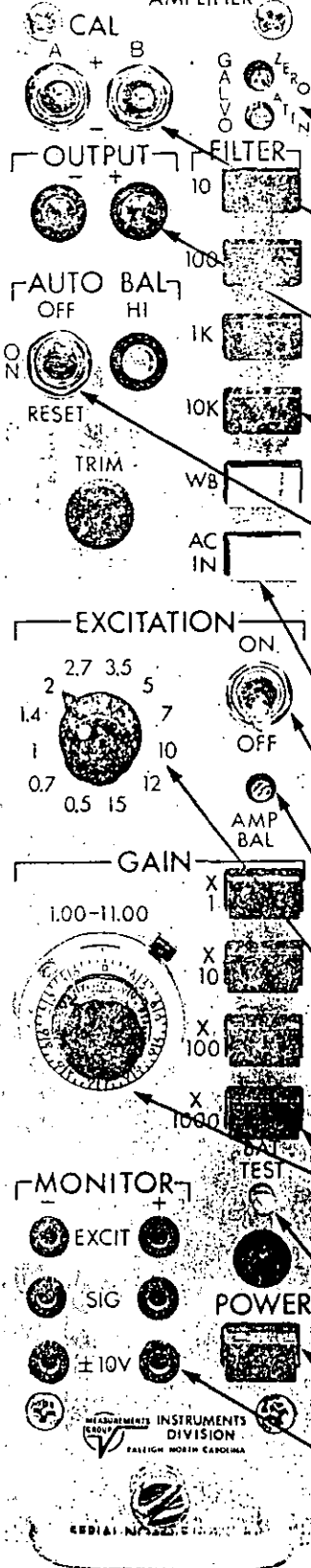
Model 2360 Portable Enclosure includes all ac wiring. Accepts up to four amplifier modules.



Ten-Channel System (including Model 2350 Rack Adapter) shown with the Model 2355 Enclosure. The Model 2350 Rack Adapter fits standard 19-in (483-mm) electronic equipment rack. All wiring is built-in to accept adjacent ten-channel systems.

Front-Panel Controls

2310 SIGNAL CONDITIONING AMPLIFIER



The principal differences between the 2310 and 2311 amplifiers are the 2311's wider frequency response and broader range of excitation settings. See specifications on page 7.

GALVANOMETER: Electronic adjustment for zero positioning and span of the galvanometer, remote from recorder.

CALIBRATION: Momentary two-position switches, $\pm A$ and $\pm B$, control shunt calibration levels; 4 point.

LED DISPLAY: Set up indicator for amplifier balance, bridge balance and for monitoring the output level.

FILTER SECTION: Push-button controls for activating appropriate low-pass active filter, or selecting wide-band operation (WB).

ELECTRONIC BRIDGE BALANCE SECTION: Three-position switch — OFF, ON, RESET — for electronic bridge balance; auto ranging up to $\pm 25\ 000\ \mu\epsilon$ with nonvolatile zero storage; yellow light indicates high-range operation or overrange condition. Vernier TRIM control is used to refine bridge balance when desired.

AC IN: Capacitive coupling in the amplifier; eliminates static component of the signal.

BRIDGE EXCITATION: ON-OFF switch for removing bridge excitation from the strain gage or transducer.

AMPLIFIER BALANCE: Adjusts any amplifier offset.

EXCITATION LEVEL: Twelve-position switch; values arranged for doubling power with each step.

2311 — Same as 2310 except 0.5 replaced by variable setting: 0.3 to 6 Vdc.

AMPLIFIER GAIN SECTION: Continuously variable potentiometer (1.00 to 11.00) plus push-button multipliers control amplifier gain; direct-reading.

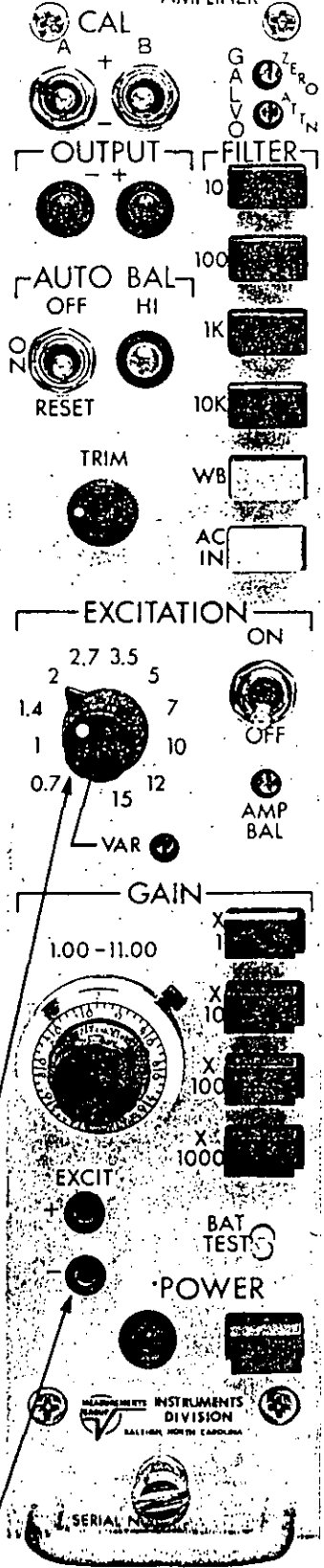
BATTERY TEST: Momentary push button determines battery level for bridge zero storage.

MAIN POWER: Turns unit on/off; LED pilot light.

PIN JACKS: Monitoring of EXCITATION, UNAMPLIFIED INPUT, AMPLIFIED OUTPUT.

Excitation pin jacks only for Model 2311.

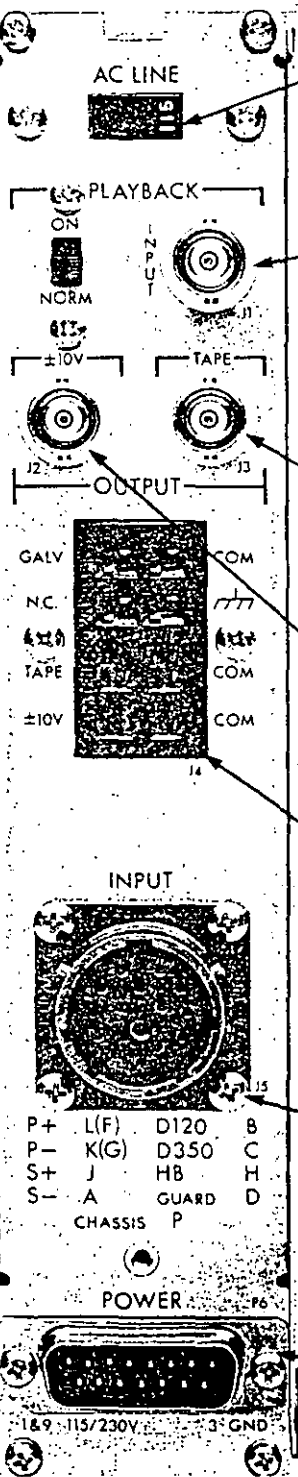
2311 SIGNAL CONDITIONING AMPLIFIER



Shown actual size

Shown actual size

Back-Panel Controls — 2310/2311



AC LINE SWITCH: Selects nominal 115 or 230 Vac operation. Recessed to eliminate inadvertent movement.

TAPE PLAYBACK SECTION: Slide switch activates magnetic tape-playback operating mode. Connects the input to the filter circuits and post amplifiers. BNC input connector.

MAGNETIC TAPE OUTPUT: Full-scale $\pm 1.4V$ level available at this BNC connector for driving magnetic tape recorder.

HIGH-LEVEL OUTPUT: Full-scale $\pm 10V$ level available at this BNC connector for driving an oscilloscope, DPM, etc.

OUTPUT RECEPTACLE: All three outputs available at this connector for those who prefer to hard wire their connections (*mating plug included*). Outputs are 75 mA for galvanometers, $\pm 1.4V$, and $\pm 10V$.

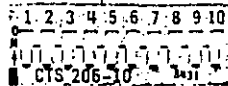
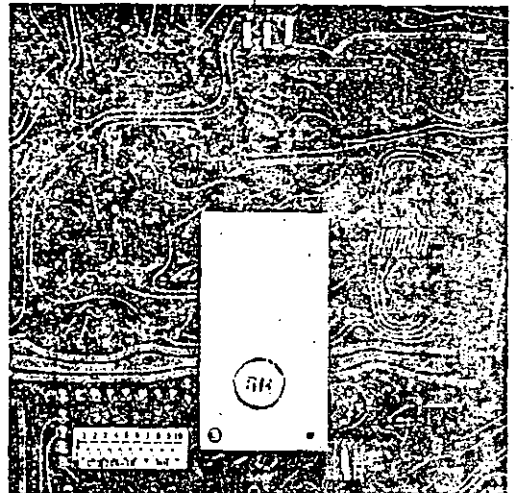
INPUT RECEPTACLE: All sensor inputs made through this 15-pin quarter-turn connector. Pin selection determines mode of operation (*mating plug included*).

POWER CONNECTOR: Main power input from the rack adapter, portable enclosure or individual line plug. Additional pins for optional remote operation of shunt calibration; bridge excitation (ON/OFF), and electronic bridge balance.

PC-Board Controls

Conveniently located switches on the printed circuit board permit easy setup for filtering of outputs, shunt calibration, and remote sense selection.

FILTER SELECTION (output)



SHUNT CALIBRATION SELECTION

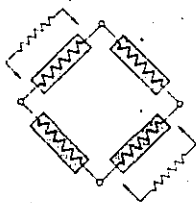


REMOTE SENSE SELECTION

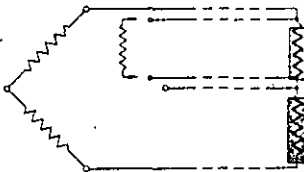
Technical Notes

CALIBRATION

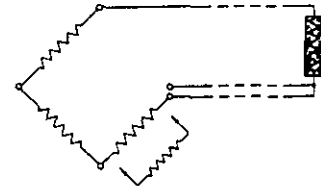
The shunt calibration technique is customarily used to calibrate and introduce gage factor into the system. Two front-panel switches, A and B, activate two pairs of fixed resistors mounted in sockets on the printed circuit (PC) board. These are the shunt calibration resistors, and their values determine the calibration levels. Additionally, a multiple switch assembly on the PC board controls which Wheatstone bridge arm(s) is being shunted, and selects local or remote wiring to these arms. Multiple shunt configurations are possible by simply moving the selector switches — rewiring is not necessary. The specific test conditions dictate the best configuration. Several of the more important configurations are illustrated below:



FULL BRIDGE: Double shunt; recommended for high-accuracy transducer applications.



HALF BRIDGE: Shunt active gage with dedicated leads; used on some transducers and some stress analysis applications; eliminates leadwire influences on calibration.



QUARTER BRIDGE: Shunt dummy gage; recommended for stress analysis applications to compensate for leadwire desensitization.

EXCITATION

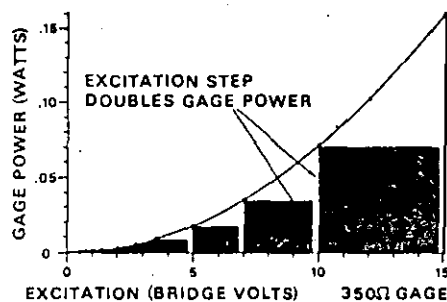
Power dissipation is an important consideration for obtaining optimum stability and performance from strain gages, strain gage based transducers and similar devices.

The excitation steps on the 2310/2311 have been carefully chosen and arranged to provide power doubling with each step, starting with an extremely low excitation. The power-versus-voltage graph illustrates this important feature. The step excitation switch allows quick and certain repositioning of the excitation level; and, in combination with a continuously variable gain, provides excellent measurement flexibility.

REMOTE SENSE: Serious full-bridge measurement inaccuracies can be caused by voltage losses due to cable resistance and variations of that resistance. To minimize this problem the 2310/2311 is equipped with a REMOTE SENSE feature. When used, it automatically senses the voltage at the transducer and regulates the voltage of the power supply to achieve the preset level at the transducer.

OPTION Y — REMOTE OPERATION: Remote calibration by external command is an optional feature for the 2300 System. This option adds six internal relays enabling the user to remotely operate: Shunt Calibration (+A, -A, +B, and -B), Auto Balance Reset, and Bridge Excitation ON/OFF (to check amplifier balance).

For single-channel applications, the internal power supply may be used to energize these relays. More than one 2310/2311 can be operated with a single set of switches (or external relays); an external 5 Vdc power supply is required (250 mA for each ten channels). If Option Y is specified for the 2310/2311, it must also be specified for the accompanying Rack Adapter (2350), or Portable Enclosure (2360), to ensure that the necessary internal cabling, receptacle and mating connector are supplied.



ELECTRONIC BRIDGE BALANCE

Setting the initial test condition to zero output (balance) is normally done before each test. With the 2310/2311, balance is automatically achieved by pushing the momentary switch to the RESET position. The OFF position disables the auto balance circuit.

The voltage injection technique is used to set zero. With this technique a voltage is generated which is essentially equal (but of opposite sign) to the unbalanced bridge output; this voltage is injected into the amplifier to produce zero net output voltage. The main advantage of this technique over the conventional potentiometer-resistive-balance method is that it does not load the bridge — a necessary requirement for accurate full-bridge operation and good common-mode rejection. The injection voltage, although analog in form, is digitally generated and digitally stored. Internal batteries preserve the zero when the main power to the unit is interrupted or turned off.

When balance cannot be achieved on the low range, the 2310/2311 will auto range to the high range, which is indicated by a steady yellow panel light. The high range provides greater range with less resolution.

Although not normally used, a TRIM control is provided for that demanding measurement where zero must be precisely set.

Balance by external command is an optional feature.

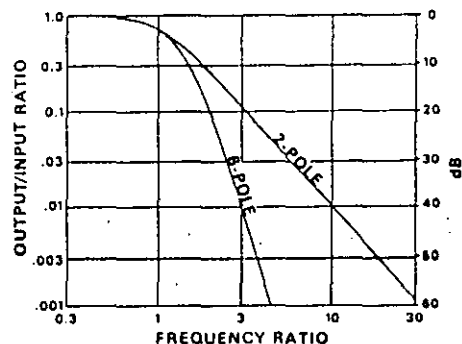
FILTERING

When the measurement does not require the full bandwidth, a built-in low-pass filter can be used to suppress high-frequency components of the input signal. The standard 2310/2311 has a two-pole low-pass active Butterworth filter with selectable frequencies. Greater suppression above the cutoff frequency can be obtained by specifying Option V. This option increases the standard two-pole filter to a four- or six-pole filter with characteristics similar to the Butterworth.

A graph illustrating the roll-off characteristics of the 2- and 6-pole filters is shown.

Push buttons control the cutoff frequency, while the wide band (WB) position allows the amplifier to operate at its fullest capacity.

The ac position is used to eliminate the static (dc) component of the signal and pass only the dynamic component. In this circuit configuration, the amplifier is capacitively coupled after the preamplifier.



Specifications

2310/2311 SIGNAL CONDITIONING AMPLIFIER

INPUT

Strain Gages: Quarter (120 and 350 Ω), half or full bridge (50 to 1000 Ω). Dummy resistors installed.

Transducers: Foil or piezoresistive strain gage types.

Potentiometer.

DCDT displacement transducer.

EXCITATION

2310 — 12 settings: 0.5, 0.7, 1, 1.4, 2, 2.7, 3.5, 5, 7, 10, 12 and 15 Vdc \pm 1%, max.

2311 — Same as 2310 except 0.5 replaced by variable setting: 0.3 to 6 Vdc.

Current: 0-100 mA, limited at 175 mA, max.

Regulation (0-100 mA, \pm 10% line change): \pm 0.5 mV \pm 0.04%, max measured at remote sense point. (Local sense: -5 mV, typical, @ 100 mA, measured at plug.)

Remote Sense Error: 0.0005%/ Ω of lead resistance (350 Ω load).

Noise and Ripple: 0.05% p-p, max (dc to 10 kHz).

Stability: 0.02%/ $^{\circ}$ C.

Level: Normally symmetrical about ground; either side can be grounded with no effect on performance.

BRIDGE BALANCE

Method: Counter-emf injection at preamp; automatic electronic; dual range; can be disabled on front panel.

Ranges (auto ranging):

\pm 5000 $\mu\epsilon$ (1% bridge unbalance or 2.5 mV/V), resolution

2.5 $\mu\epsilon$ (0.0012 mV/V).

\pm 25 000 $\mu\epsilon$ (5% bridge unbalance or 12.5 mV/V), resolution

12.5 $\mu\epsilon$ (0.006 mV/V).

Balance Time: 2 seconds, typical.

Manual Vernier Balance: \pm 50 $\mu\epsilon$ (\pm 0.025 mV/V).

Interaction: Essentially independent of excitation and amplifier gain.

Storage: Digital; up to 2 years without line power.

SHUNT CALIBRATION

Circuit (2-level, dual polarity):

Single-shunt (for stress analysis) across any bridge arm, including dummy gage.

Double-shunt (for transducer) across opposite bridge arms.

Provision for 4 dedicated leads to shunt external arms.

Cal circuit selected by switches on PC board.

Standard Factory-Installed Resistors (\pm 0.1%) Simulate:

\pm 200 and \pm 1000 $\mu\epsilon$ @ GF=2 across dummy half bridge;

+1000 $\mu\epsilon$ @ GF=2 across dummy gage (120 and 350 Ω);

\pm 1 mV/V (double-shunt) for 350 Ω transducer.

Remote-Operation Relays (Option Y): 4 relays (plus remote-

reset relay for bridge balance and relay for excitation on/off). Each requires 10 mA @ 5 Vdc, except excitation on/off 25 mA.

AMPLIFIER

Gain: 1 to 11 000 continuously variable. Direct-reading.

2310: \pm 1% max. of reading

\pm 0.5% max. of full scale vernier setting.

2311: \pm 1% max. of reading.

Ten-turn counting knob (X1 to X11) plus decade multiplier (X1 to X1000).

2310 Frequency Response (all gains $>$ 5, full output):

dc coupled: dc to 25 kHz, -0.5 dB max.

dc to 65 kHz, -3 dB; (typical at 40% output).

ac coupled: 5 Hz to 25 kHz, -0.5 dB.

2311 Frequency Response (all gains, full output):

dc coupled: dc to 50 kHz, -0.5 dB max.

dc to 125 kHz, -3 dB max.

ac coupled: 1.7 Hz to 125 kHz, -3 dB max.

2311 Frequency Response, Reduced Output (2 Vrms max):

Bandwidth (-3 dB) @ Gain of: 1-11, 200 kHz; 10-110,

170 kHz; 100-1100, 135 kHz; 1000-11000, 125 kHz.

All Specifications are nominal or typical at +23 $^{\circ}$ C unless noted.

Input Impedance: 100 M Ω , min, differential or common-mode, including bridge balance circuit.

Bias Current: \pm 50 nA, typical each input.

Source Impedance: 0 to 1000 Ω each input.

Common-Mode Voltage: \pm 10V.

Common-Mode Rejection (gain over X100):

Shorted input: 100 dB, min, at dc; 90 dB, min, dc to 1 kHz.

350 Ω balanced input: 90 dB, typical, at 1 kHz.

Stability (gain over X100): \pm 2 μ V/ $^{\circ}$ C, max, referred to input

(RTI).

Noise (gain over X100, all outputs):

0.01 to 10 Hz: 1 μ V p-p RTI.

0.5 Hz to 125 kHz: 5 μ Vrms, max, RTI.

FILTER

Characteristic: Low-pass active 2-pole Butterworth standard.

Frequencies (-3 \pm 1 dB): 10, 100, 1000 and 10 000 Hz and wide-band.

Outputs Filtered: Any 1 or 2 or all (switch-selected on PC board).

NOTE: Consult Applications Engineering Department concerning optional filter characteristics and frequencies.

AMPLIFIER OUTPUTS

Standard Output: \pm 10V @ 5 mA, min.

Tape Output: \pm 1.414V (1 Vrms) @ 5 mA, min.

Galvanometer Output: \pm 10V at 75 mA, min, current-limited at 100 mA, max (minimum load resistance for 0.05% linearity: 50 Ω).

Galvanometer attenuator (0-100%) and zero adjust (\pm 1V) on front panel.

Linearity @ dc: 0.02%.

Any output can be short-circuited with no effect on others.

PLAYBACK

Input: \pm 1.414V full scale; input impedance 20 k Ω .

Gain: X1 to tape output; X7.07 to standard output.

Filter Selection: As specified above.

Outputs: All three as specified above.

POWER

105 to 125V or 210 to 250V (switch-selected), 50/60 Hz, 10 watts, max.

Keep-Alive Supply (for bridge balance): 2 Eveready S76E or equal. Shelf-life (approx. 2 years).

SIZE & WEIGHT

Panel: 8.75 H x 1.71 W in (222 x 43.3 mm).

Case Depth Behind Panel: 15.9 in (404 mm).

Weight: 6 lb (2.7 kg).

2350 RACK ADAPTER

POWER

2-ft (0.6-m) 3-wire line cord; 10-ft (3-m) extension cord supplied.

Fuse: 1A size 3AG (32 x 6.4 dia mm).

Receptacle to accept line cord from adjacent 2350 Rack Adapter.

Wiring for remote calibration with Option Y.

SIZE & WEIGHT

8.75 H x 19 W x 19.06 D in (222 x 483 x 484 mm).

13.5 lb (6.1 kg).

2360 PORTABLE ENCLOSURE

POWER

8-ft (2.4-m) detachable 3-wire cord.

Fuse: 1/2A size 3AG (32 x 6.4 dia mm).

Wiring for remote calibration with Option Y.

SIZE & WEIGHT

9.06 H x 7.20 W x 18.90 D in (229 x 183 x 480 mm).

6.75 lb (3.1 kg).

2400 SYSTEM

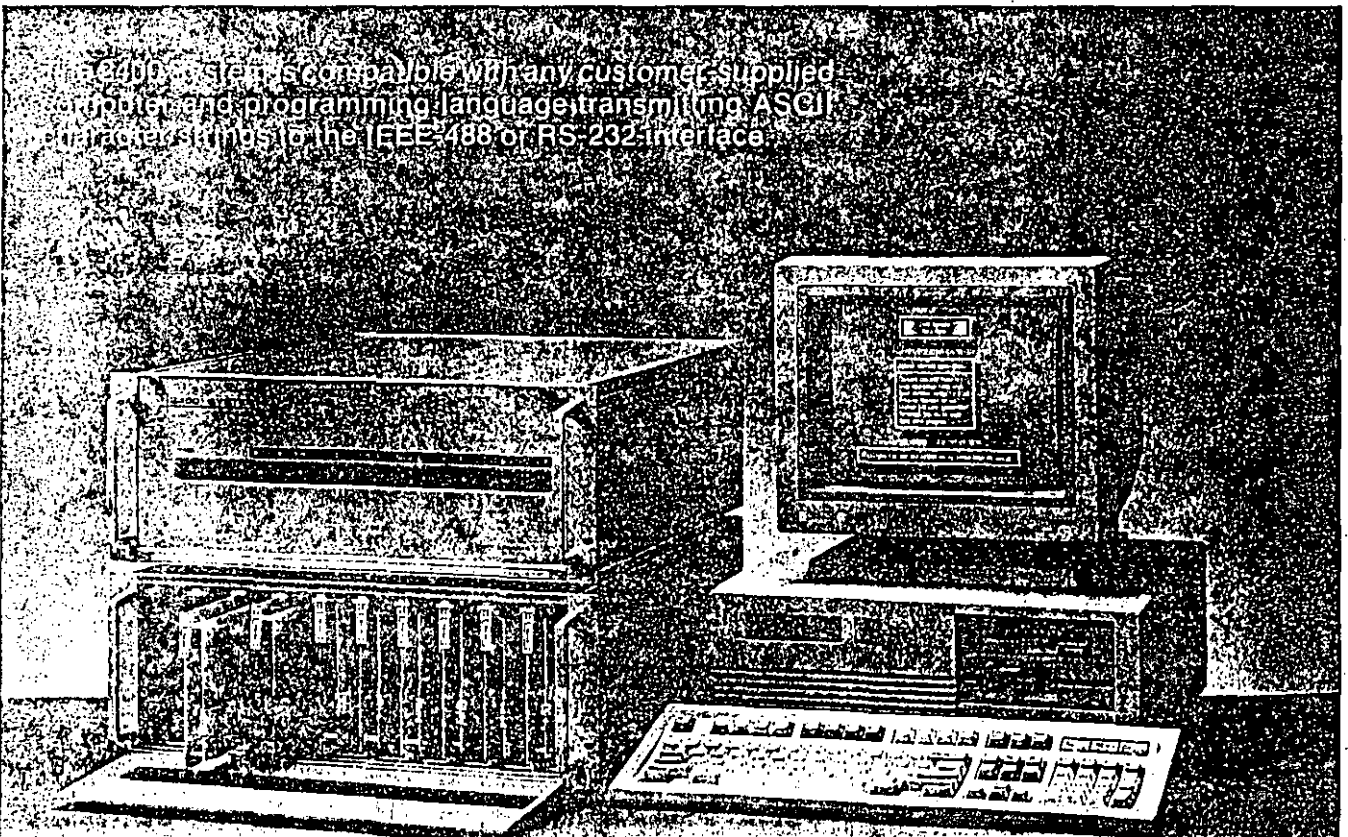
The computer-controlled 2400 Signal Conditioning Amplifier System offers high performance in the most demanding environments

The 2400 Signal Conditioning System incorporates, as standard, all the features necessary for precise conditioning of strain gage and transducer inputs combined with the convenience and speed of computer-controlled setup. The 2400 System allows the user to configure individual signal conditioners from any host computer with an IEEE-488 or RS-232 communications link.

Among the features of the 2410 Amplifier are isolated constant-voltage/constant-current excitation; guarded input structure with $\pm 350V$ common-mode capability, $\pm 10V$ and tape outputs; automatic wide-range bridge balance and four-pole Bessel low-pass filters.

A basic system consists of a Model 2401 Master Unit which accommodates up to eight (8) Model 2410 Signal Conditioning Amplifiers. The system may be expanded to 256 channels by adding a Model 2402 Expansion Unit for each additional eight-channel rack. The system may be expanded beyond 256 channels by using an additional IEEE-488 address or RS-232 port.

Each master and expansion unit is housed in a standard 19-in (483-mm) rack adapter which occupies 7 in (178 mm) of rack space. Attractive panels are supplied with each rack unit for those applications where tabletop mounting is desirable. Expansion units may be separated from the master unit and from succeeding expansion units by up to 100 ft (30.5 m).



Input/output signal, control, and power connectors are mounted on the rear panel of the rack mounting assembly. All mating connectors (except signal output) and power cords are supplied. Installation or removal of individual channel modules is accomplished from the front of the rack without requiring rear access or removal of mating connectors. An optional rack-mounted power control panel is available to provide front-panel access to the power switch.

Programmable functions and status outputs are compatible with the IEEE-488 and/or RS-232 protocols. No additional hardware is required to operate in either mode. Individual channels may be addressed, or an "all-channel" command may be utilized to address every channel simultaneously for fast initial setup.

All programmed functions may be read back from individual signal conditioners at any time without altering any programmed setting.

In addition to the user-selected settings described below, the following flags are provided

to enable the operator to easily determine the channel status:

- Excitation ON or OFF
- Autobalance ON or OFF
- Autobalance Range Low or High
- Autobalance Sequence Inrange or Overrange
- Excitation Constant-Voltage or Constant-Current
- Input dc-coupled or ac-coupled
- Addressed Channel Valid or Invalid
- Power Interrupt

A hardware reset capability is provided so that the amplifier will power up with the excitation reduced to zero. This capability guarantees that sensitive strain gages or other input devices will not be damaged by high excitation voltages (or currents). Likewise, a power interruption will cause all programmable functions to reset to the off state and will set the power-interrupt flag.

Features

- Set-up and monitoring of all channel input parameters from any host computer with IEEE-488 or RS-232 communications link.
- Plug-in amplifier design; amplifiers are removable from the master unit without affecting input/output connections.
- Programmable constant-voltage or constant-current excitation; 0.25 to 15.75V or 1.0 to 63 mA.
- Programmable gain from 1 to 3000.
- Electronically injected, automatic wide-range bridge balance with battery backup to retain balance in power-off condition.
- Input coupling; hardware selectable ac or dc.
- Fully guarded input amplifier; $\pm 350\text{Vdc}$ or peak ac common-mode operating voltage.
- Full-power bandwidth of 100 kHz at all gain settings; slew rate of $6.3\text{ V}/\mu\text{sec}$.
- Programmable four-pole Bessel low-pass filters with cutoff frequencies of 1 Hz, 10 Hz, 100 Hz, 1 kHz and 10 kHz.
- Two simultaneous buffered outputs; $\pm 10\text{V}$ and tape 1.0 Vrms; will drive up to $0.15\ \mu\text{F}$ without instability.
- Stable, proprietary bridge completion module for quarter- and half-bridge 120- and 350-ohm strain gage and transducer circuits.
- 120-ohm dummy easily configured for 1000-ohm completion.
- Built-in programmable shunt calibration circuits; internal user-selectable configurations to provide two-point shunting of any bridge component or two-point double shunt calibration of transducers.
- Documented system software commands for maximum flexibility of user programming.
- Initial set-up programs provided for system checkout.

Model 2410 Signal

SPI

INPUT

Input Impedance:

- dc-coupled: 22 M Ω .
- ac-coupled: 1.1 μ F in series with 20 k Ω ;
low frequency cutoff (3 dB) 8 Hz nom.

Source Current: ± 10 nA typical; ± 20 nA max.

Configuration: 2- to 10-wire plus guard shield to accept quarter-, half-, or full-bridge strain gage or transducer inputs. Internal bridge completion with temperature stability better than 3.0 ppm/ $^{\circ}$ C for dummy 120 Ω , 350 Ω , and 1000 Ω completion gages and internal half bridge. Accepts inputs from ground-referenced or isolated devices.

Differential Input: Maximum differential input voltage of ± 30 Vdc or peak ac.

Common-Mode Input: Maximum common-mode input voltage of ± 350 Vdc or peak ac.

Guard Impedance: >250 k Ω to output common; >1000 M Ω to power and rack ground.

AMPLIFIER

Gain: 1 to 3000. Coarse Gain Steps X1, X10, X100, X200. Fine Gain 0 to 15, 16 steps incremental. Overall accuracy $\pm 0.2\%$.

Linearity: $\pm 0.02\%$ of full scale at dc.

Frequency Response:

- dc to 100 kHz: 3 ± 0.2 dB at all gain settings and full output;
- dc to 50 kHz: 0.5 dB max at all gain settings and full output.

Slew Rate: 6.3 V/ μ sec min at all gain settings.

Noise: (350 Ω source impedance, dc-coupled).

Referred-to-Input (RTI):

- 1 μ V 0.1 Hz to 10 Hz p-p;
- 2 μ V 0.1 Hz to 100 Hz p-p;
- 3 μ V 0.1 Hz to 100 kHz rms.

Referred-to-Output (RTO):

- FG = fine gain setting
- 200 μ V + (FG x 100 μ V) 0.1 Hz to 10 Hz p-p;
- 500 μ V + (FG x 200 μ V) 0.1 Hz to 100 Hz p-p;
- 600 μ V + (FG x 300 μ V) 0.1 Hz to 100 kHz rms.

Zero Stability: ± 2 μ V RTI, ± 200 μ V RTO at constant temp.

Temperature Coefficient of Zero: ± 1 μ V/ $^{\circ}$ C RTI
 ± 200 μ V/ $^{\circ}$ C RTO; -10° to 60° C.

Common-Mode Rejection:

GAIN	CMR (dB)	GAIN	CMR (dB)
X1	82	X100	122
X10	102	X200	128

Common-Mode Voltage: ± 350 Vdc or peak ac, max operating.

Standard Output: ± 10 V @ 10 mA max.

Tape Output: 1.0 Vrms @ 10 mA max.

Output Isolation: Isolated from power and rack ground;
 >1000 M Ω .

Output Protection: Protected against continuous short.

Capacitive Loading: Up to 0.15 μ F.

Filter: Four-pole Bessel low-pass filter with selectable 3 dB bandwidths of 1 Hz, 10 Hz, 100 Hz, 1 kHz and 10 kHz.

CONSTANT-VOLTAGE EXCITATION

Range: 0.25 to 15.75 Vdc @ 85 mA max, 0.25V increments.

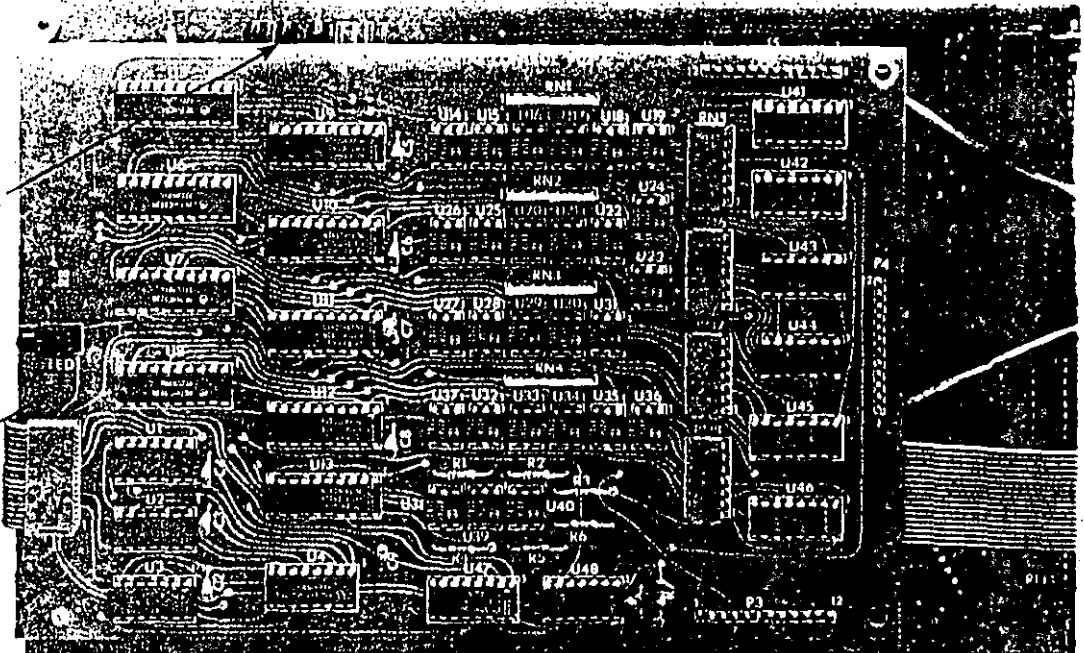
Accuracy: $\pm 0.10\%$ ± 5 mV.

Noise: 100 μ V $\pm 0.002\%$ p-p dc to 20 kHz.

Line Regulation: ± 200 μ V $\pm 0.01\%$ max for line voltage change of 10% from nom.

Input Coupling ac/dc Select

Digital Control Board



"Piggyback-mounting" of the Model 2410's printed circuit boards affords compact design, yet provides for easy access when internal configuration changes are required to meet specific test applications.

Conditioning Amplifier

FIG 3

Load Regulation: $\pm 200 \mu\text{V} \pm 0.01\%$ max for load variation of 10% to 90% of full load.

Remote Sense: Excitation error $< 0.0005\%$ of lead resistance.

Temperature Stability: $\pm 0.01\%/^{\circ}\text{C}$.

Monitoring: Front-panel monitoring jacks.

Isolation: Isolated from power ground and output common; floats with Guard.

CONSTANT-CURRENT EXCITATION

Range: 1.00 to 63.0 mA dc. 1.0 mA increments. Compliance voltage 15.75V; max open circuit voltage 21.0V.

Accuracy: $\pm 0.10\% \pm 5 \mu\text{A}$.

Noise: $(1 \mu\text{A} + 10 \mu\text{V})$ p-p; dc to 20 kHz.

Line Regulation: $\pm 1 \mu\text{A} \pm 0.01\%$ max for line voltage change of $\pm 10\%$ from nom.

Load Regulation: $\pm 1 \mu\text{A} \pm 0.01\%$ max for 100% load change.

Monitoring: Front-panel monitoring jacks.

Isolation: Isolated from power ground and output common; floats with Guard.

Temperature Stability: $\pm 0.01\%/^{\circ}\text{C}$

AUTOMATIC BALANCE

Method: Electronically injected automatic balance.

Activation: Programmable.

Storage: Digital storage with battery backup. Battery life 2 to 4 years.

Balance Time: 4 seconds typical; 8 seconds max.

Range: $\pm 15,000 \mu\epsilon$ (7.5 mV/V) RTI Low Range; $\pm 45,000 \mu\epsilon$ (22.5 mV/V) RTI High Range.

Resolution: $0.5 \mu\epsilon$ RTI Low Range; $1.5 \mu\epsilon$ RTI High Range.

Accuracy: ± 3 mV RTO; $\pm 3 \mu\epsilon$ RTI.

NOTE: Range, Resolution, and Accuracy specifications apply to gain ranges of X10, X100, X200. On gain range of X1, all RTI specifications are multiplied X10.

CALIBRATION

Four internal shunt calibration resistors, $\pm 0.1\%$ tolerance:

174.8K 1000 $\mu\epsilon$ (0.50 mV/V) 350 Ω ; (2 each)

874.8K 200 $\mu\epsilon$ (0.10 mV/V) 350 Ω ;

59.94K 1000 $\mu\epsilon$ (0.50 mV/V) 120 Ω .

Internal selector switches for selection of two-point unipolar, bipolar, or two-point double-shunt calibration circuits.

External static or dynamic calibration signals are also program selectable.

ENVIRONMENTAL

Temperature:

Operating Range -10°C to 60°C ;

Storage Range -20°C to 70°C ;

Humidity to 95% without condensation.

SIZE

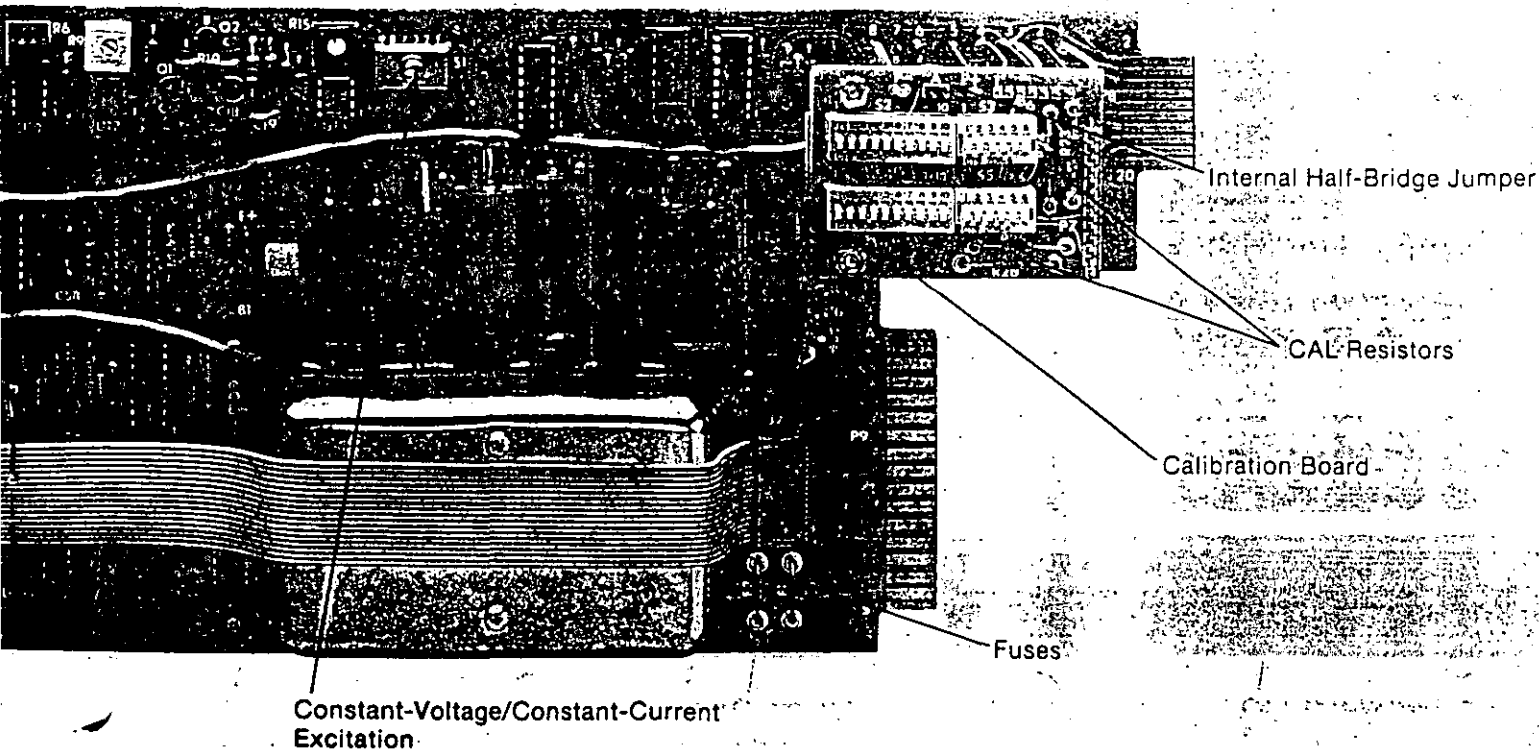
5.69 H x 1.87 W x 20.37 D in (145 x 48 x 518 mm).

WEIGHT

2.6 lb (1.17 kg).

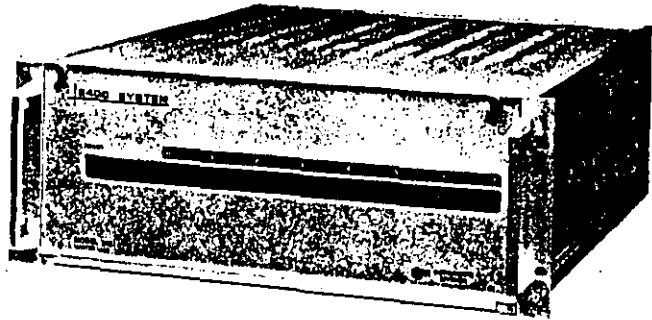
All references to microstrain assume a gage factor of 2.00.

All specifications nominal or typical at $+25^{\circ}\text{C}$ unless noted.



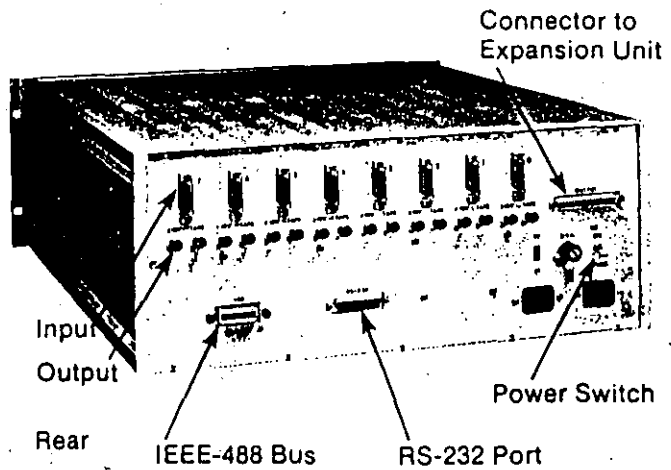
Model 2401 Master Unit

The Model 2401 Master Unit contains the system control circuitry. It accepts up to eight (8) Model 2410 Signal Conditioning Amplifiers and provides the required input/output rear-panel connections. The front panel has silk-screened channel identification (0 to 7). The master unit is attractively styled for tabletop mounting, or it can be rack mounted in a standard 19-in (483-mm) equipment rack.



Front

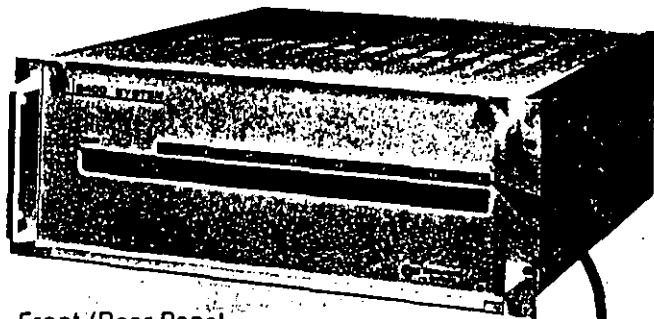
Specifications	
Input:	Input plugs are provided for eight Model 2410 Amplifiers.
Output:	Standard ($\pm 10V$) and tape (1.0 Vrms) output for each channel; BNC receptacle.
Computer Interface:	Connector for interfacing to RS-232 port. Connector for interfacing to IEEE-488 bus.
Power:	115/230 Vac, 50-60 Hz, 120W max Fuse: 1.5A, 3AG (115V) or 3/4 A, 3AG (230V).
Size:	7 H x 19 W x 21.5 D in (178 x 483 x 546 mm).
Weight:	17 lb (7.7 kg).



EDIC, S. A. DE C. V.
 EQUIPOS DIDACTICOS INDUSTRIALES
 Y CIENTIFICOS, S. A. DE C. V.
 R. F. C. EDI-891208-PGA
 CAIRO No. 251 COL. EL RECREO
 C. P. 02070 MEXICO, D. F. APT.
 TEL. 561-80-04 FAX 343-59-51

Model 2402 Expansion Unit

The Model 2402 Expansion Unit allows the addition of up to eight (8) Model 2410 Amplifiers to a system. All required control and interface circuits are included. This unit can be stacked for tabletop mounting with the Model 2401, or rack mounted. The Model 2402 is supplied with pre-numbered, reusable "customer-installed", self-adhesive channel identification strips.



Front (Rear Panel Input/Output Arrangement Similar to Master Unit)

Specifications	
Input:	Input plugs are same as the Model 2401.
Output:	Same as the Model 2401.
Specifications for Power, Size, and Weight are same as the Model 2401.	

Reusable Self-Adhesive Channel Identification Strips — Provided for Both Front and Rear Panel on Expansion Units.



Programmable Functions

Communication with the 2400 System is accomplished by sending simple ASCII commands to the Model 2401 Master Unit. All commands are well documented to provide sufficient information for developing user-written programs.*

INPUT

Selectable input configurations are:

- Standard — connected to the external S+, S- bridge input;
- AUX 1 — connected to the external auxiliary input #1;
- AUX 2 — connected to the external auxiliary input #2.

The auxiliary inputs are connected through the rear-panel input connector. Inputs may be dynamic signals for calibration of recorders, oscilloscopes and other devices, or direct current calibration voltages within specified accuracy limits. Also, an auxiliary input can be shorted to provide a reliable amplifier zero reference point.

AMPLIFIER GAIN

Coarse Gain (CG) steps of X1, X10, X100, X200.

Fine Gain (FG) steps of 0 to 15.

Total amplifier gain is the product of CG and FG. Overall accuracy $\pm 0.2\%$.

A fine gain setting of zero allows operator to observe output noise independent of the input circuit.

CALIBRATION

Two low-thermal EMF, shielded, guarded relays are utilized. Selectable configurations are:

- Calibration OFF
- Shunt Cal A
- Shunt Cal B
- Shunt Cal A & B simultaneously

Four shunt calibration resistors are provided for calibration of 350 Ω and 120 Ω bridges. These resistors are easily changeable (without soldering) so that user-selected values can be substituted as desired.

Board-mounted dip switches allow the user to select any desired calibration configuration for Shunt Cal A and Shunt Cal B; i.e., shunt dummy resistor, shunt active gage, shunt internal half bridge, etc. Also, the relays can be configured to shunt remote or local resistors across external bridge components of transducers as in double-shunt calibration of transducers.

External calibration sources can be used by connection to the auxiliary inputs.

*A demonstration program for initial setup and control of all programmable functions, through the RS-232 port, is provided with each system.

EXCITATION

Constant voltage or constant current excitation is selected by a board-mounted toggle switch. A status bit is set to allow operator monitoring of the existing setting.

Constant voltage, 0.25 to 15.75 Vdc in 0.25V increments, 85 mA max.

Constant current, 1.0 to 63 mA in 1.0 mA increments, 15.75V compliance voltage, 21.0V max.

A separate on/off function reduces excitation to zero without altering the previously programmed excitation level, with the on/off status available for review.

FILTER AND OUTPUT

Selectable four-pole Bessel low-pass filters of 1 Hz, 10 Hz, 100 Hz, 1 kHz and 10 kHz are provided. The wideband (WB) output can also be selected.

Outputs of $\pm 10V$ and Tape (1 Vrms) are standard. The filtered or WB output can be independently routed to the $\pm 10V$ and/or the Tape output by the filter program command. For example, a wideband tape output may be viewed or recorded while the $\pm 10V$ output is used for monitoring quasi-static or filtered signals.

Both outputs are capable of driving large capacitive loads as in the case of long coaxial output cables.

AUTOMATIC BALANCE

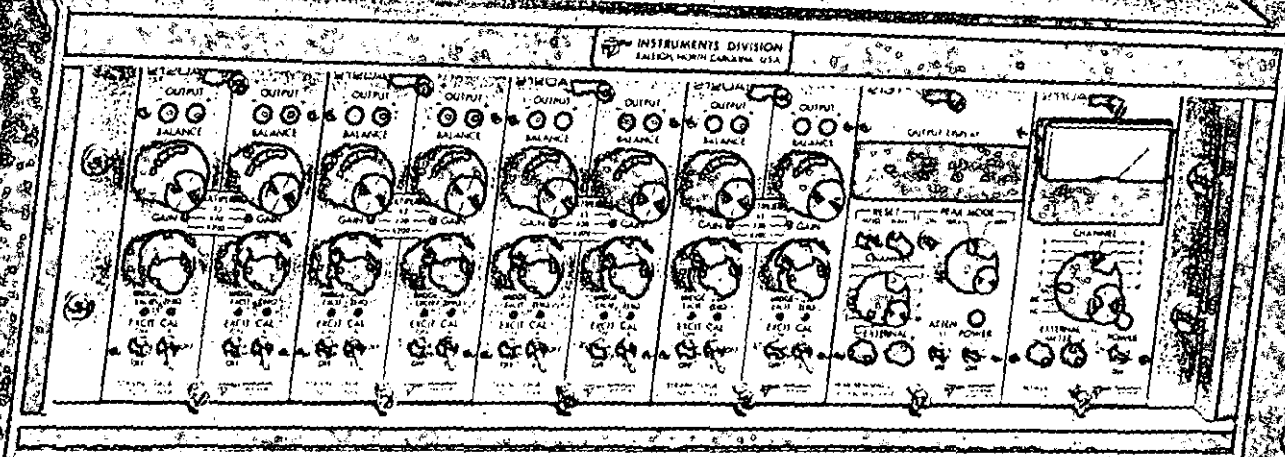
The autobalance circuit provides balance ranges of $\pm 15\ 000\ \mu\epsilon$ (7.5 mV/V) and $\pm 45\ 000\ \mu\epsilon$ (22.5 mV/V), with resolutions of 0.50 $\mu\epsilon$ and 1.50 $\mu\epsilon$, respectively. The autobalance circuit is fully programmable as follows:

- | | |
|------------|---|
| OFF | Autobalance injection voltages are removed. In this mode, raw input unbalances may be read and the input circuit evaluated. |
| ON-LOW | Autobalance voltages are injected and the low ($\pm 15\ 000\ \mu\epsilon$) range is selected. |
| ON-HIGH | Autobalance voltages are injected and the high ($\pm 45\ 000\ \mu\epsilon$) range is selected. |
| ON-Restart | The autobalance voltage is reset to zero, and a new autobalance sequence is initiated. |

The autobalance circuit is fully ratiometric. Injected voltages are derived from the sensed (local or remote) voltages. Also, when constant current excitation is used, the autobalance circuit remains fully ratiometric and undesirable fixed offset voltages are not used.

Status "flags" are provided to allow monitoring of autobalance range (low/high), autobalance on/off, and autobalance overrange.

Autobalance readings are stored and memory is battery backed. Battery life is 2 to 4 years.



Eight channel system
with digital output display

2100 SYSTEM

MULTI-CHANNEL SIGNAL CONDITIONER/AMPLIFIER

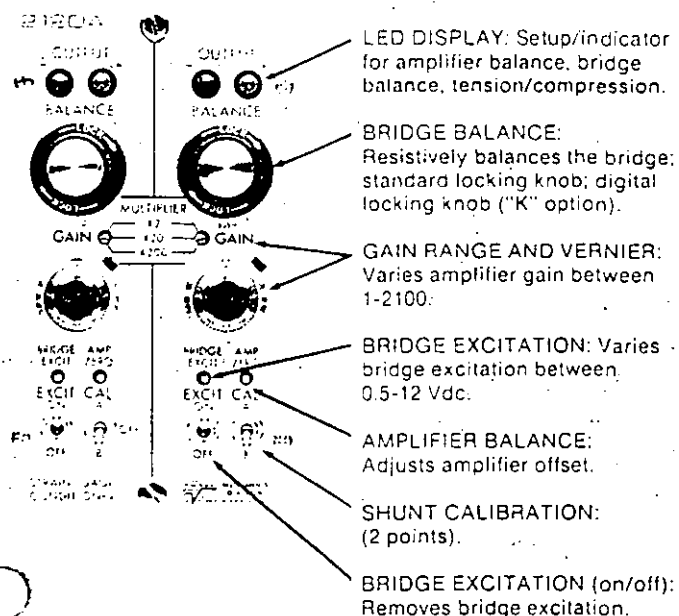
Conditions signals from strain gages and transducers when
multiple channel simultaneous dynamic recordings are required



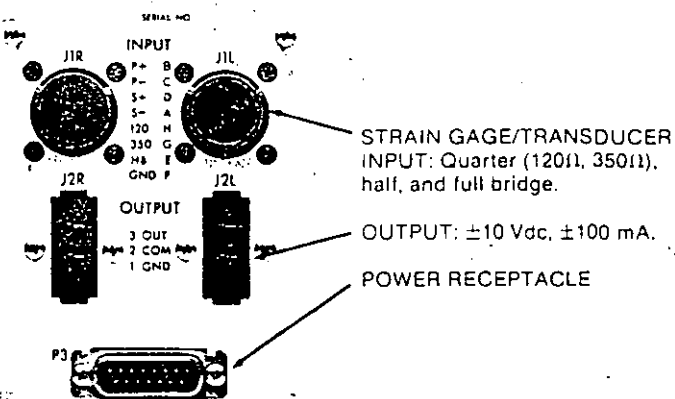
Model 2120A Strain Gage Conditioner/Amplifier

A two-channel plug-in module which includes bridge completion, bridge balance, amplifier, amplifier balance, excitation regulator and shunt calibration.

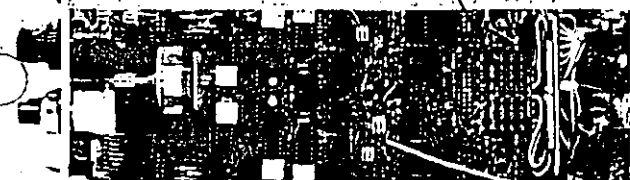
FRONT



REAR



SPECIAL PORTION OF PRINTED CIRCUIT BOARD FOR SHUNT CALIBRATION RESISTORS AND JUMPERS



Specifications

These specifications apply for each of two independent channels per module.

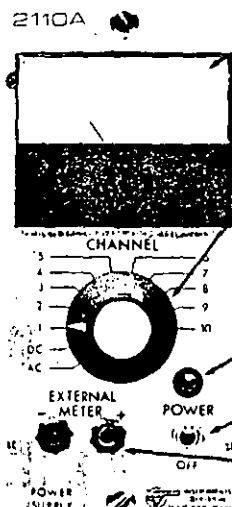
INPUTS	Quarter (120Ω and 350Ω), half and full bridge (50-1000Ω). Quarter-bridge dummy gages provided.								
BRIDGE EXCITATION	0.5 to 12 Vdc (adjustable for each channel) with 120Ω full-bridge load. Short-circuit current: <40 mA. Ripple, noise, and 10% line change: ±2 mV max. Load regulation: ±0.2% no-load to 120Ω load (10% line change).								
BRIDGE BALANCE	±2000μe (quarter, half, or 350Ω full bridge), range can be changed by internal jumper to ±4000μe or ±6000μe.								
CALIBRATION	Two-position (center off) toggle switch. Standard factory-installed resistors (±0.1%) simulate ±1000μe at GF=2.								
AMP GAIN	1 to 2100 continuously adjustable, ±0.5%.								
BANDPASS	DC to 5 kHz (min): -0.5 dB (-5%). DC to 15 kHz: -3 dB. Can be extended by internal jumper to: DC to 17 kHz -0.5 dB; DC to 50 kHz -3 dB.								
AMP INPUT	Temperature Coefficient of Zero: ±1 μV/°C RTI*, ±210 μV/°C RTO**; -10° to +60° C (after 30 minute warm-up). Noise RTI: (350Ω source impedance) 1 μV p-p at 0.1 Hz to 10 Hz; 2 μV p-p at 0.1 Hz to 100 Hz; 2 μVrms at 0.1 Hz to 50 kHz. Noise RTO: 50 μV p-p at 0.1 Hz to 10 Hz; 80 μV p-p at 0.1 Hz to 100 Hz; 100 μVrms at 0.1 Hz to 100 kHz; 200 μVrms at 0.1 Hz to 50 kHz. Input Impedance: >100 MΩ (balance limit resistor disconnected). Common-Mode Rejection: (dc to 60 Hz).								
	<table border="1"> <thead> <tr> <th>Gain Multiplier</th> <th>CMR (dB)</th> </tr> </thead> <tbody> <tr> <td>X2</td> <td>67</td> </tr> <tr> <td>X20</td> <td>87</td> </tr> <tr> <td>X200</td> <td>100</td> </tr> </tbody> </table>	Gain Multiplier	CMR (dB)	X2	67	X20	87	X200	100
Gain Multiplier	CMR (dB)								
X2	67								
X20	87								
X200	100								
	Source Current: ±10 nA typical; ±40 nA max.								
OUTPUT	±10V (min) at ±100 mA. Current limit: 140 mA.								
OPTIONAL FEATURE	May be ordered with, or be field upgraded for, remote-operation relays for control of shunt calibration and excitation (off). Remote-operation capability is required in the Model 2150 or 2160 also. Contact Measurements Group for details.								
SIZE	5.25 H x 2.94 W x 10.97 D in (133 x 75 x 279 mm).								
WEIGHT	2.2 lb (1.0 kg).								

* Referred to input

** Referred to output

All specifications in this bulletin are nominal or typical at +23° C unless noted.

Model 2110A Power Supply



BRIDGE-VOLTS METER:
Used to set up/monitor bridge excitation, also line and power supply levels.

CHANNEL SELECTOR:
AC monitors AC line input. DC monitors the power supplies. Positions 1-10 select and display bridge excitation for each channel.

PILOT LAMP:
Indicates main power.

POWER SWITCH: Main power on-off.

EXTERNAL METER:
Used with an external digital voltmeter to precisely adjust bridge excitation.

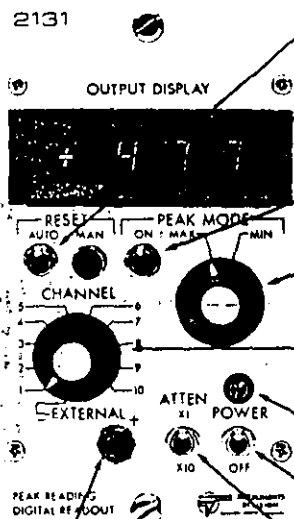
A plug-in module capable of powering up to ten channels (five Model 2120A modules) at maximum rated voltage or current. Provides initial bridge and amplifier voltages. All supplies are current-limited against amplifier malfunction.

Specifications

OUTPUTS	$\pm 15V$ at 1.2A and $+17.5V$ at 1.1A; all regulators current-limited against overload.
INPUT	107, 115, 214, 230 Vac $\pm 10\%$ 50/60 Hz (selected internally). Power: 40W typical, 100W max.
METER	0 to 12 Vdc (with switch) to read bridge excitation. Also AC input and DC output go/no-go monitor.
SIZE	5.25 H x 2.44 W x 12.34 D in (133 x 62 x 313 mm).
WEIGHT	6.7 lb (3.1 kg).

Model 2130/2131 Digital Display

A plug-in module that provides real-time digital readout on channel-by-channel basis. Will accept and switch up to 10 inputs. Peak hold/retention capability is provided with the Model 2131. (The Model 2131 is shown below.)



PEAK RESET: Provides manual or automatic reset.

DIGITAL DISPLAY:
3-1/2 Digit LED, ± 1999 counts.

PEAK MODE ON:
On/off switch.

PEAK MODE MAX/MIN:
Selector for maximum or minimum peak mode.

CHANNEL SELECTOR:
Positions 1-10 select input channel for display.

PILOT LAMP: Indicates main power.

POWER SWITCH: Main power on-off.

ATTENUATOR:
Attenuates input signal to increase measurement range.

EXTERNAL:
Front-panel jacks accept input, typically bridge voltage from 2110A external meter jacks.

Specifications

2130/2131 SPECIFICATIONS

INPUT CAPACITY	10 channels, BNC (rear panel). 1 channel, banana jacks (front panel).
SWITCH OUTPUT	Not attenuated, BNC (rear panel).
UPDATE RATE	3 readings/sec, nominal.
INPUT VOLTAGE RANGE	± 1999 mV (X1 range) — 2130/2131. ± 19990 mV (X10 range) — 2130. $\pm 10V$ (X10 range) — 2131.
INPUT IMPEDANCE	100 k Ω — 2130. Greater than 1 M Ω — 2131.
COMMON MODE INPUT RANGE	± 100 mV (rear-panel input) min — 2130. $\pm 10V$ (rear-panel input) — 2131.
ACCURACY	$\pm (0.05\% \text{ reading} + 0.05\% \text{ full scale})$ or better (Peak Mode Off — 2131).
SIZE	5.25 H x 2.94 W x 10.97 D in (133 x 75 x 279 mm).
WEIGHT	2 lb (0.8 kg).

2131 SPECIFICATIONS

STEP/INPUT RESPONSE	± 5 counts for 10 msec full-scale step input (worst case).
STORAGE STABILITY	± 3 counts/min (max).
PEAK MODES	MAX (usually positive) excursion and MIN (usually negative) excursion.
PEAK RESET	Manual or Automatic.

Model 2111 DC-Operated Power Supply

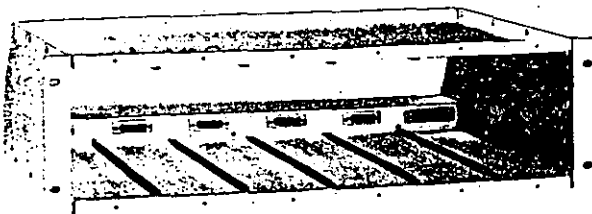
A plug-in module capable of powering up to eight channels (four Model 2120A modules) at maximum rated bridge voltage and output current, or up to ten channels when maximum bridge voltage and output current are not required. The 2111 functions similarly to the 2110A Power Supply, with the exception of the 12 Vdc nominal input which supports battery operation only. The front panel is similar in appearance to the Model 2110A.

Specifications

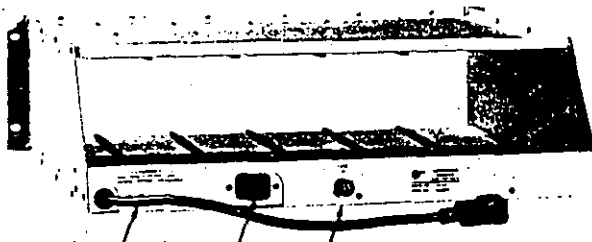
OUTPUTS	±15 Vdc at 1.0A and +17.5 Vdc at 1.0A; outputs are protected against overload.
INPUT	12 Vdc nominal (9 to 18 Vdc range). Power: 60W max; 78% efficiency at full load. Reverse polarity protection: Internal shunt diode.
METER	0 to 12 Vdc (with switch) to read bridge excitation. DC output go/no-go monitor.
SIZE	5.25 H x 2.44 W x 12.34 D in (133 x 62 x 313 mm).
WEIGHT	3.0 lb (1.4 kg).

Model 2150 Rack Adapter, Model 2155 Enclosure, and Model 2160 Portable Enclosure

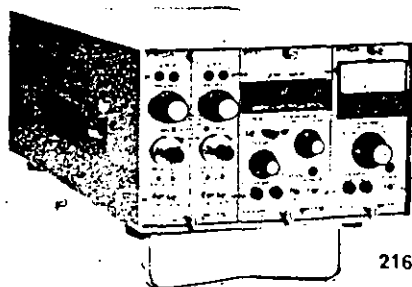
Model 2150: A prewired rack adapter which accepts one Model 2110A or 2111, and any combination of five Model 2120A, 2130, or 2131 plug-in modules. It has its own fuse and power cord and can be housed in any standard 19-in (483-mm) electronic equipment rack.



2150-FRONT



2150 REAR
LINE CORD FUSE
AUXILIARY RECEPTACLE



2160

Model 2155: A sturdy cabinet (shown on front cover) for enclosing a complete eight- or ten-channel system for free-standing operation, while providing additional mechanical protection and increased portability. A Model 2150 is required.

Model 2160: A prewired, fused enclosure which houses one Model 2110A or 2111, one 2130 or 2131, and one 2120A module. A carrying handle ensures maximum portability. An additional snap-down bail support on the bottom can be used to elevate the 2160 for excellent work efficiency during bench-top operation. The Model 2160 (shown with the 2110A, 2131, and 2120A modules) would be substituted for the Model 2150 when two or four channels and maximum portability are required.

Specifications

2150 SPECIFICATIONS

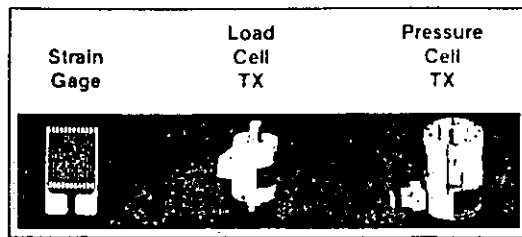
POWER	2-ft (0.6-m) 3-wire line cord; 10-ft (3-m) extension available. Fuse: 1A size 3 AG (32 x 6.5 dia. mm). Receptacle to accept line cord from adjacent 2150 Rack Adapter.
SIZE	5.25 H x 19 W x 14.17 D in (133 x 483 x 360 mm).
WEIGHT	6.6 lb (3.0 kg).

2155 SPECIFICATIONS

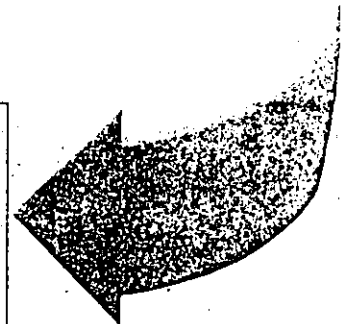
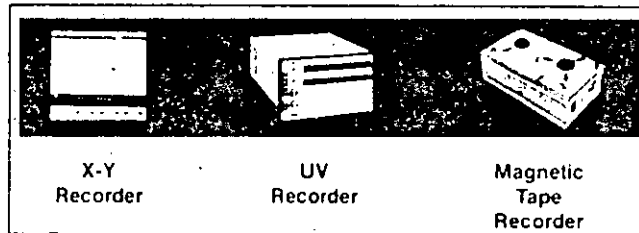
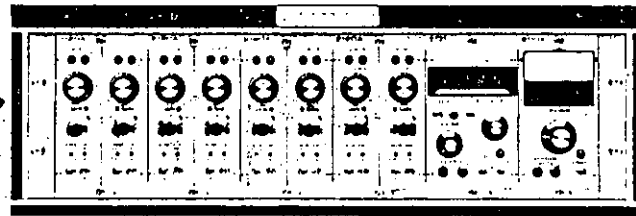
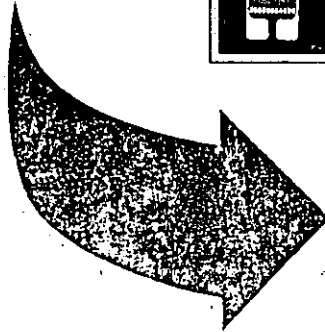
SIZE	5.25 H x 19 W x 13 D in (133 x 483 x 330 mm).
WEIGHT	18.8 lb (9.5 kg).

2160 SPECIFICATIONS

SIZE	5.55 H x 8.75 W x 13.80 D in (141 x 222 x 350 mm).
WEIGHT	5.2 lb (2.4 kg).



2100 System with I/O Devices



The 2100 System provides better data . . .

A separate bridge power switch removes bridge excitation, enabling the operator to detect unwanted signals due to electrical interference and/or noise, thermocouple effects, and shifts of the instrument zero during a long-term test. This feature is an absolute must for dynamic testing, and for validating test results.

An adjustable bridge excitation control on each channel permits excitation to be set as specified by the strain gage or transducer manufacturer. It also allows for any special consideration which may be dictated by the test material; for example, the poor thermal conductivity normally associated with plastics.

In addition to adjustable bridge excitation, each channel has its own regulator circuit. This prevents interaction of adjacent channels during setup or operation.

Each channel has a continuously variable gain control. In combination with recommended excitation, the independent gain control can provide a large output signal so that small signals can be resolved without overpowering the strain gage or transducer.

An LED display for each channel gives positive indication of amplifier and resistive balance. This capability accelerates setup, minimizes the risk of destroying galvanometers, and verifies tension/compression loading.

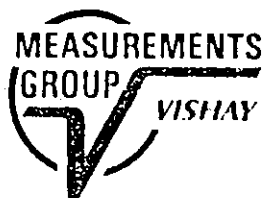
Easily read reference marks on the setup meter indicate acceptable line voltage and proper operation of internal power supplies.

A switch contained in the Model 2110A Power Supply allows adjustment when the line voltage is too high or too low.

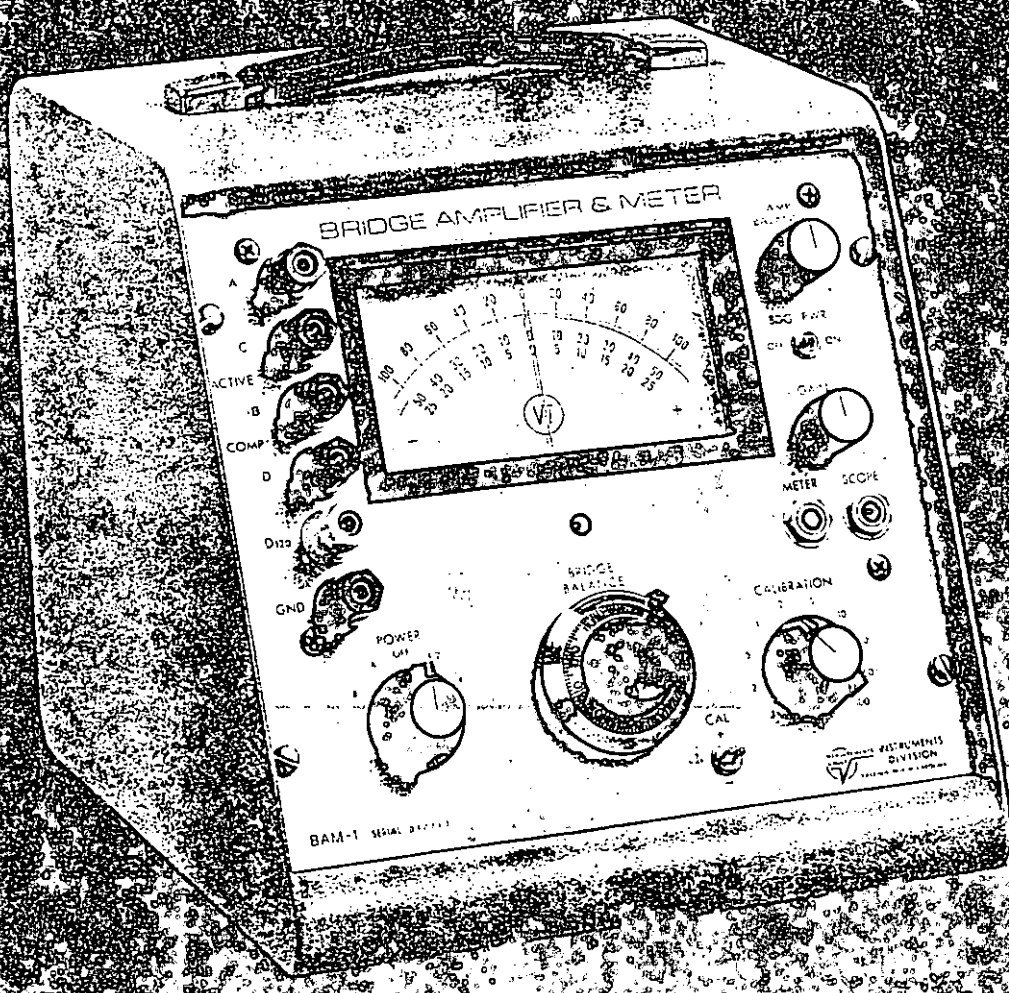
The 2100 System provides true quarter-bridge, three-leadwire capability, including internal dummies and sufficient plug connections for remote shunt calibration.

A convenient network in the Model 2120A Strain Gage Conditioner/Amplifier allows the operator to change the factory-supplied shunt values, as well as shunt any arm of the bridge, as required.

EDIC, S. A. DE C. V.
EQUIPOS DIDACTICOS INDUSTRIALES
Y CIENTIFICOS, S. A. DE C. V.
R. F. C. EDI-891208-PGA
CAIRO No. 251 COL. EL RECREO
C. P. 02070 MEXICO, D. F. ATZ.
TEL. 561-80-04 FAX 343-59-51



MEASUREMENTS GROUP, INC.
P.O. Box 2771
Raleigh, NC 27611, USA
Telephone (919) 365-3800
Telex 802-502 • FAX (919) 365-3945



BAM-1

A portable battery-powered
universal strain measuring instrument

DESCRIPTION

The BAM-1 is a battery-powered universal strain measuring instrument and signal conditioner containing a DC amplifier, bridge completion, and indicating meter. Additional features include a separate bridge excitation switch, variable gain control, initial bridge balance control, shunt calibration switch, and amplifier balance control.

Static measurements are made directly on the instrument's analog meter. If desired, a standard digital voltmeter can be used with the BAM-1 to provide a digital output.

For dynamic testing, two outputs are provided: The SCOPE signal provides DC to 20 000 Hz at high source impedance, while the METER signal is a low source impedance output for oscillographs. The dynamic range can be increased to 100 000 Hz by specifying Option B (BAM-1B).

An independent bridge power switch makes the BAM-1 an excellent instrument for long-term testing. With this feature, amplifier balance can be checked and corrections made at any time during a test by temporarily turning off bridge power and resetting the amplifier balance if the output has deviated from zero. Thus, during long-term measurements, the user has the ability to electrically maintain the original zero of the instrument, and separate any instrumentation drift from the desired test measurement signal.

Calibration of the BAM-1 for static or dynamic work is accomplished by using a ten-point shunt CALIBRATION switch, and system GAIN (span) control. The GAIN control is adjustable over a wide range by changing bridge excitation and, in the case of static measurements, by attenuating the meter signal. The BAM-1 can be adjusted to read directly in strain, psi, or any other desired engineering unit.

Applications with the BAM-1 or BAM-1B include measuring or monitoring signals from strain gages, transducers, temperature sensors, and thermocouples on an oscilloscope, oscillographic recorder, or directly on the meter of the instrument.

FEATURES

- Static and Dynamic Measuring Capability
- Battery Operation with AC Option
- Separate Bridge Excitation Switch plus Variable Gain Control
- DC to 20 000 Hz std.
100 000 Hz with "B" Option
- Built-in Ten-point Shunt Calibration Switch

SPECIFICATIONS

INPUT CIRCUITS

- Strain gages/transducers, 50 to 2000 Ω , and thermocouples.
- Half or full bridges: 120 Ω quarter-bridge operation with the provided 120 Ω dummy (internal) resistor.
- Bridge Balance: Ten-turn potentiometer with counting dial, $\pm 8\%$ for half bridge, or $\pm 7\%$ for 350 Ω full bridge.

BRIDGE EXCITATION

- Half or Quarter Bridge (excitation per gage): 120 Ω , 0.25 to 2.5 Vdc;
350 Ω , 0.7 to 5.6 Vdc.
- Full Bridge: 120 Ω , 0.5 to 6 Vdc; 350 Ω , 1.4 to 9 Vdc.
- Gage Current: Max 25 mA depending on gage resistance and GAIN setting using recommended procedures.

AMPLIFIER

- Direct-coupled, solid state.
- Balanced differential input, approximately 20k Ω impedance.
- Noise: 2 μ Vrms RTI.
- Stability: $\pm 1\mu$ V/hr max at input after 1/2 hour warm-up.
Drift: $\pm 0.5\mu$ V/ $^{\circ}$ F max at input (32 $^{\circ}$ to 77 $^{\circ}$ F)
($\pm 0.9\mu$ V/ $^{\circ}$ C max at input (0 $^{\circ}$ to 25 $^{\circ}$ C)).
 $\pm 25\mu$ V max at input from turn-on and 32 $^{\circ}$ to 77 $^{\circ}$ F
(0 $^{\circ}$ to 25 $^{\circ}$ C) change.
- Gain: 125 at SCOPE jack; 250 at METER jack.
- Bandpass (-0.5 dB or 5%): SCOPE jack DC to 20 000 Hz;
METER jack DC to 2000 Hz.
- Output Impedance: SCOPE 30k Ω single ended; METER 250 Ω differential.
- Linear Output: SCOPE ± 3 V into 500k Ω load;
METER ± 5 V into 100k Ω load, or ± 0.5 mA into 1k Ω or less.

CALIBRATION

- Ten 1% shunt-calibration resistors.
- Half or Quarter Bridge: Simulates ± 20 to 20 000 $\mu\epsilon$ (GF=2) by shunting internal 400 Ω half bridge.
- Full Bridge: Shunts one arm of external bridge.

METER

- Taut Band Movement, Linearity: ± 1 graduation.
- Scale 3.5 in (89 mm), 100 total graduations; with mirror.
- Sensitivity attenuated 15:1 with GAIN control.

SYSTEM SENSITIVITY USING METER

- Half or Quarter Bridge, 120 Ω , 1 active gage, GF=2: ± 100 to ± 15 000 $\mu\epsilon$ F.S.
- Full Bridge: 120 Ω , ± 0.1 to 10 mV/V F.S.
350 Ω , ± 0.05 to ± 4 mV/V F.S.
- DC Input: ± 350 to 5000 μ V F.S.

POWER SUPPLY

- Internal Batteries (standard): Two 6V NEDA No. 920, 200 hr;
One 22-1/2V NEDA No. 710, 500 hr.

PHYSICAL

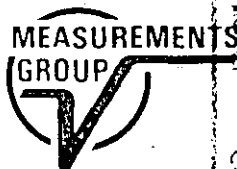
- Weight: 12 lb (5.4 kg) with batteries.
- Case Dimensions: 9 L x 9 W x 10 H in (228.6 x 228.6 x 254 mm).

ACCESSORY

- AC Power Pack (replaces batteries): Model 4008, 115 Vac, 50-60 Hz, 2W;
Model 4008Z, 230 Vac, 50-60 Hz, 2W.

All specifications nominal or typical at +23 $^{\circ}$ C unless noted.

The Measurements Group is a leading supplier of strain gage instrumentation. Available instruments include portable indicators, signal conditioners/amplifiers, strain gage installation tester, instrument calibrator, and sophisticated computer-controlled systems for the acquisition, storage and reduction of test data. Call or write for all of your strain gage instrumentation needs.



MEUDIC, S. A. DE C. V.
EQUIPOS DIDACTICOS INDUSTRIALES
Y CIENTIFICOS, S. A. DE C. V.
R. F. C. EDI-891206 P.G. (919) 365-3800 • Telex 802-502 • FAX (919) 365-3945
CAMINO No. 251 COL. EL RECREO
C. P. 02070 MEXICO, D. F. AT
TEL. 361 80-04 FAX 361 80-04

MEASUREMENTS GROUP, INC.
P.O. Box 27777
Raleigh, NC 27611, USA

MODEL 3650

DUAL PEAK-READ INDICATOR

This instrument is designed to simultaneously display both the maximum (most positive excursion) and minimum (most negative excursion) values of a transient waveform. The primary application is to display the peak values of dynamic mechanical strains measured by strain indicators such as the Measurements Group's P-3500 and Model 3800.

A typical example of such usage is the measurement of maximum forces developed in the structure of mechanical presses during each load cycle. In this case, strain gages are installed at appropriate locations on the press, and the Model 3650 utilizes the analog output signal from the strain indicator as its input signal. The Model 3650 is equipped with an extremely versatile system of meter display and reset, which allows easy and accurate monitoring of the variable force occurring with each strike of the press.

While the Model 3650 is primarily intended to operate from the DC analog output signal obtained from suitable strain gage indicators or conditioners, it may also be used to capture and display dynamic voltage signals obtained from other sources, so long as these signals lie within its operating range (typically, instruments that provide an analog output in the 1.0 to 11.0-volt range).

The Model 3650 features dual LCD digital displays with a full-scale range of ± 19999 counts. Color-coded push-button controls are easy to use, and allow the operator to determine the operating mode at a glance.

The instrument is powered from an internal battery pack consisting of six alkaline "C" cells, which are readily available anywhere in the world when replacement is required. Battery life is approximately 250 hours of continuous use. An external line-voltage adapter is also available (115 or 230 Vac, 50 to 60 Hz).

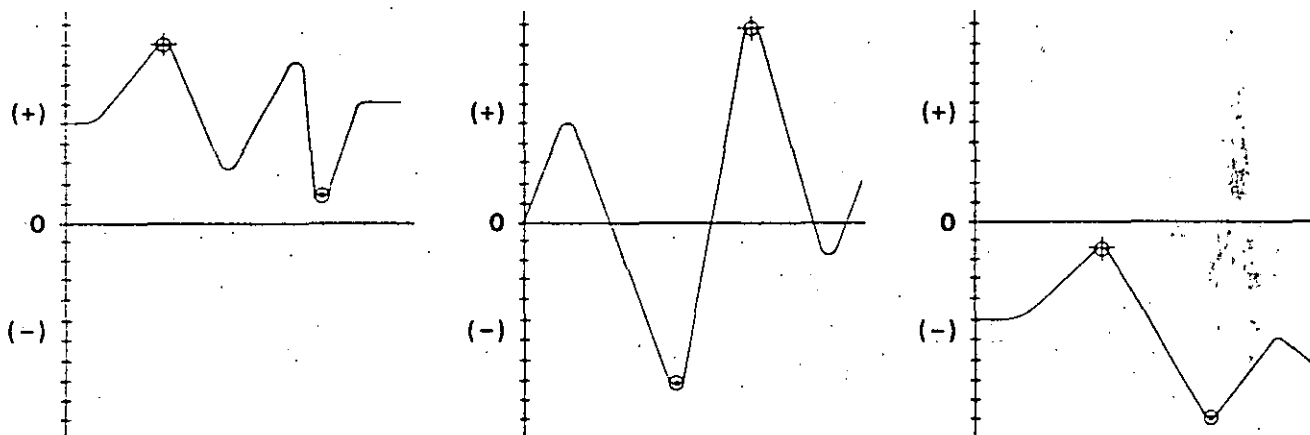
As a dynamic analog signal is fed into the Model 3650, an instantaneous comparison is made to the previously stored values. When the stored values are exceeded, they are immediately replaced with updated values and displayed. The new values are retained until they are exceeded, or reset occurs.

Reset is accomplished either manually with a push-button switch, automatically by a selectable timing circuit, or externally by contact closure or TTL low-logic level. Reset simply changes the stored values to the values of the input signal.

For suppression of voltage transients (noise), often encountered during strain gage measurements in shop environments, a four-pole Bessel low-pass filter with switchable cutoff frequencies from 2 to 4000 Hz is built into the instrument.

To measure the amplitude of dynamic voltages, the use of peak-capturing meters, such as the 3650, often requires special precautions to ensure that the input signal is sufficiently "clean" (free of noise), and that the signal duration is sufficient to permit proper measurement accuracy. While the Model 3650 demonstrates repetitive accuracies approaching 0.1% during calibration on ideal waveforms, such accuracies should not be expected in practical dynamic strain measurement. Because of parasitic strains from loose or badly fitting parts of a moving structure, excessive electrical noise, etc., practical repetitive peak measurement accuracies may range from 0.5% to 5%, or even 10%, of the transient maximum strain value.

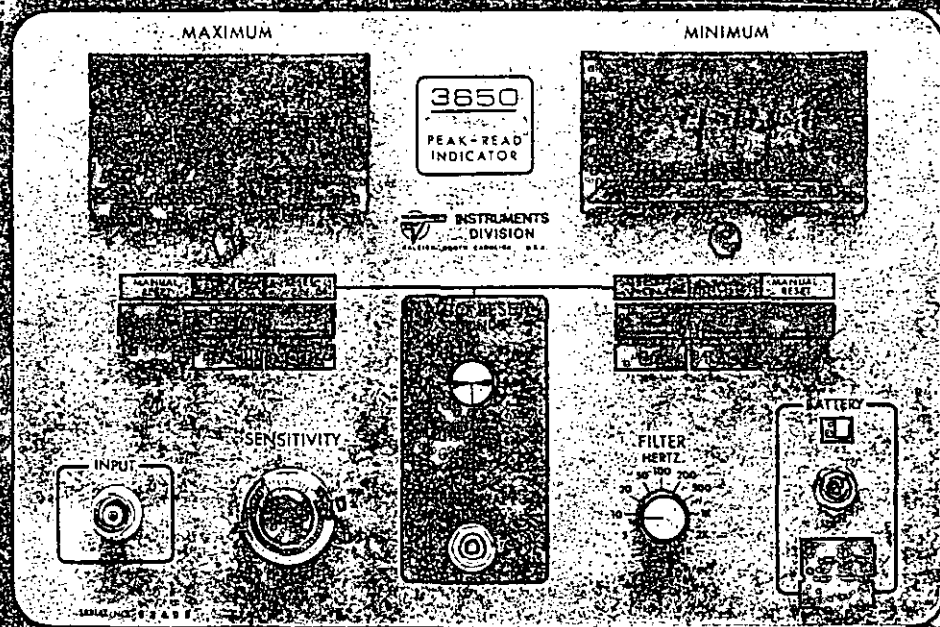
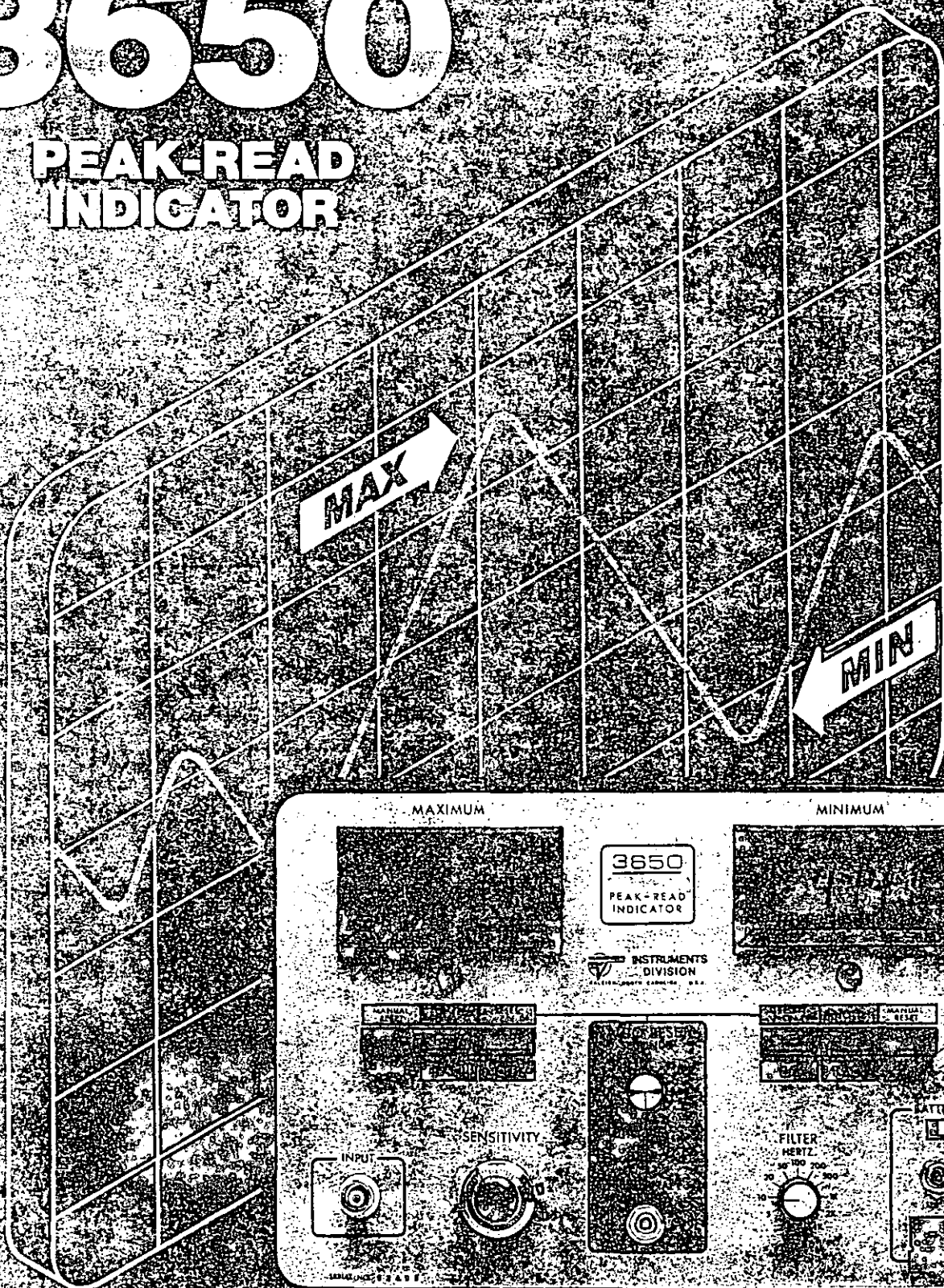
It should also be noted that the "response time" of this instrument, which determines the minimum duration of the pulse that can be measured with suitable accuracy, has been designed for typical dynamic mechanical phenomena. The Model 3650 is therefore not generally intended for high-speed electrical waveforms that are of interest in various electronic circuit developments.



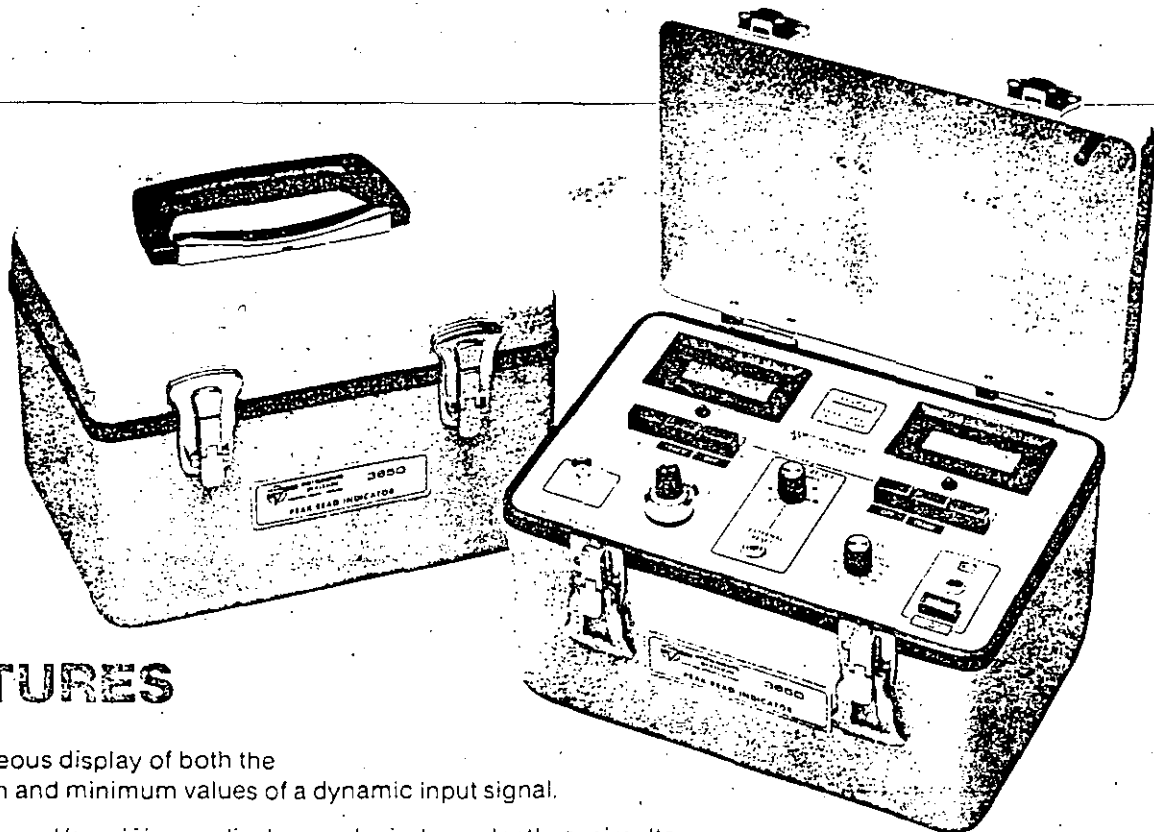
The Model 3650 simultaneously displays both the maximum (most positive excursion) and minimum (most negative excursion) values of a transient waveform, as illustrated in the above diagram.

3650

PEAK-READ INDICATOR



A portable battery-powered instrument
for capturing peak values of dynamic signals.



FEATURES

- Simultaneous display of both the maximum and minimum values of a dynamic input signal.
- Maximum and/or minimum display can be independently or simultaneously reset by manual push buttons, externally generated reset pulse, or periodic automatic internal reset.
- Selectable four-pole Bessel low-pass filter to discriminate against undesirable high-frequency interference.
- Color-coded push-button controls for simple operation and minimum operator training.
- Compatibility with most instruments that provide an analog output signal.

SPECIFICATIONS

Range and Display:

Dual direct-reading liquid crystal display. ± 19999 counts full scale.

Overload Indication: All-zero display with two flashing columnar indicators.

Sensitivity:

± 1.0 to $\pm 11V$ nominal for full-scale indication (± 19999 counts).

Resolution:

1 count, 50 to 550 μV .

Accuracy:

Step Input: $\pm 0.1\% \pm 4$ counts for step input of > 4 milliseconds duration.

Repetitive Step Input: $\pm 0.2\% \pm 4$ counts for repetitive step inputs of > 200 microseconds duration. Number of steps required

$$\frac{4 \text{ milliseconds}}{\text{Pulse Duration}}$$

Input Circuit:

Isolated; input impedance $> 20000\Omega$; either side may be connected to system ground.

Hold Stability:

4 counts/minute maximum, averaged over 5-minute period.

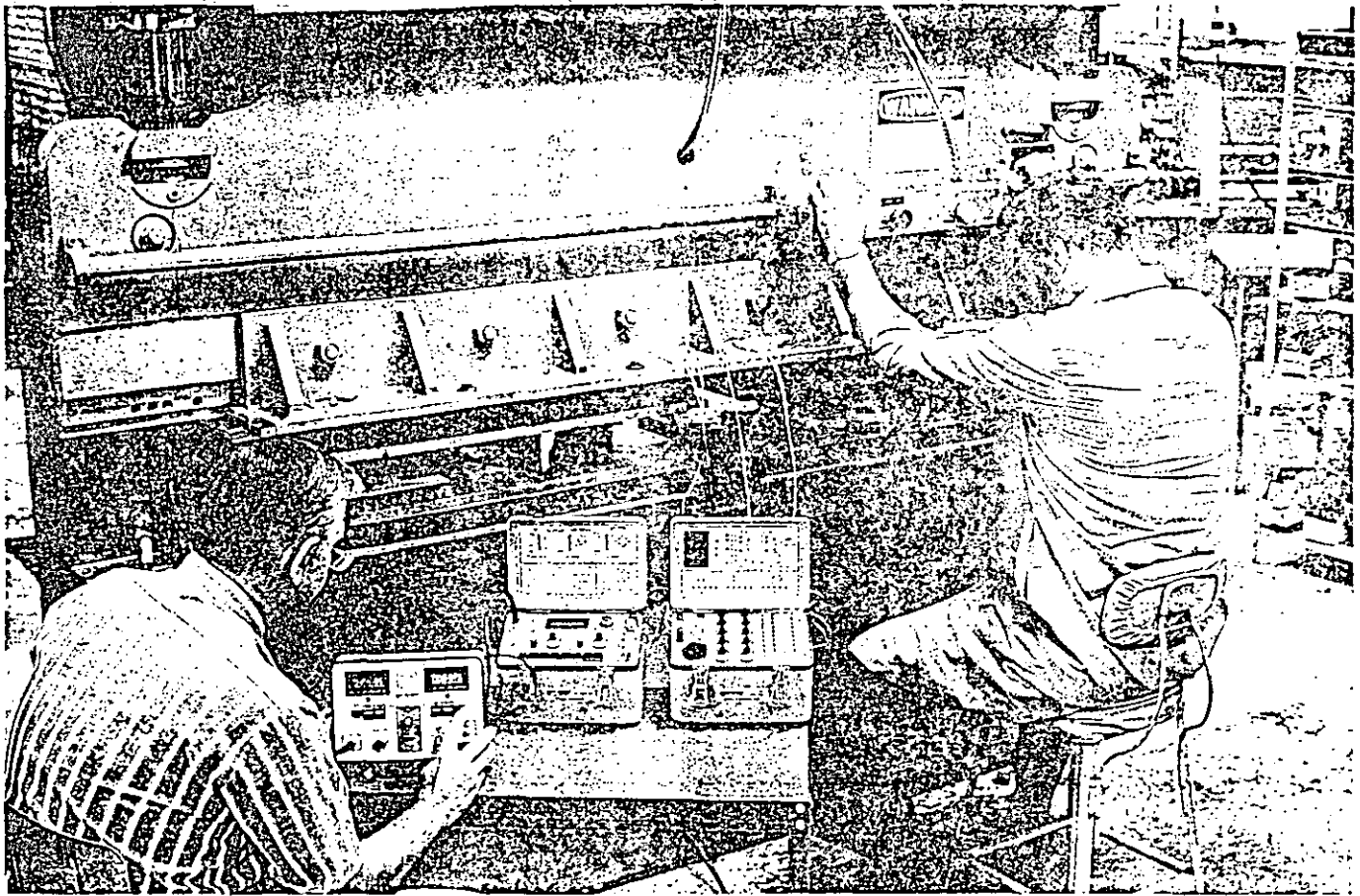
Reset Capability:

Independent or simultaneous reset of maximum and/or minimum by manual push buttons; automatic timed reset; or external contact closure or low TTL level.

Size and Weight:

6 H x 9 W x 6 D in (152 x 228 x 152 mm).
5.5 lb (2.5 kg).

All specifications nominal or typical at $+23^\circ C$ unless noted.



Model 3650 Peak-Read Indicator, used in conjunction with P-3500 Strain Indicator and SB-10 Switch and Balance Unit, to measure peak strains on press platen during metal punching operation.

Other applications include, but are not limited to:

- Rolling Mills
- Ship Propellers
- Production Machinery
- Vehicle Testing
- Aircraft Landing Gear
- Hydraulic Systems
- Structures Testing
- Cranes, Derricks
- Off-The-Road Machinery
- And More ...

The Measurements Group is a leading supplier of strain gage instrumentation. Available instruments include portable indicators, signal conditioners/amplifiers, strain gage installation tester, instrument calibrator, and sophisticated computer-controlled systems for the acquisition, storage and reduction of test data. Call or write for all of your strain gage instrumentation needs.

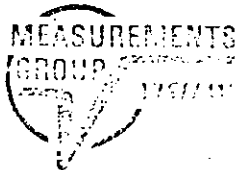
EDIC, S. A. DE C. V.
 EQUIPOS DIDACTICOS INDUSTRIALES
 Y CIENTIFICOS, S. A. DE C. V.
 R. F. C. EDI-891208-PGA
 CAIRO No. 251 COL. EL REFORMA
 C. P. 02070 MEXICO, D. F. MEX.
 TEL. 561-80-04 FAX 343-59-61

MEASUREMENTS GROUP, INC.

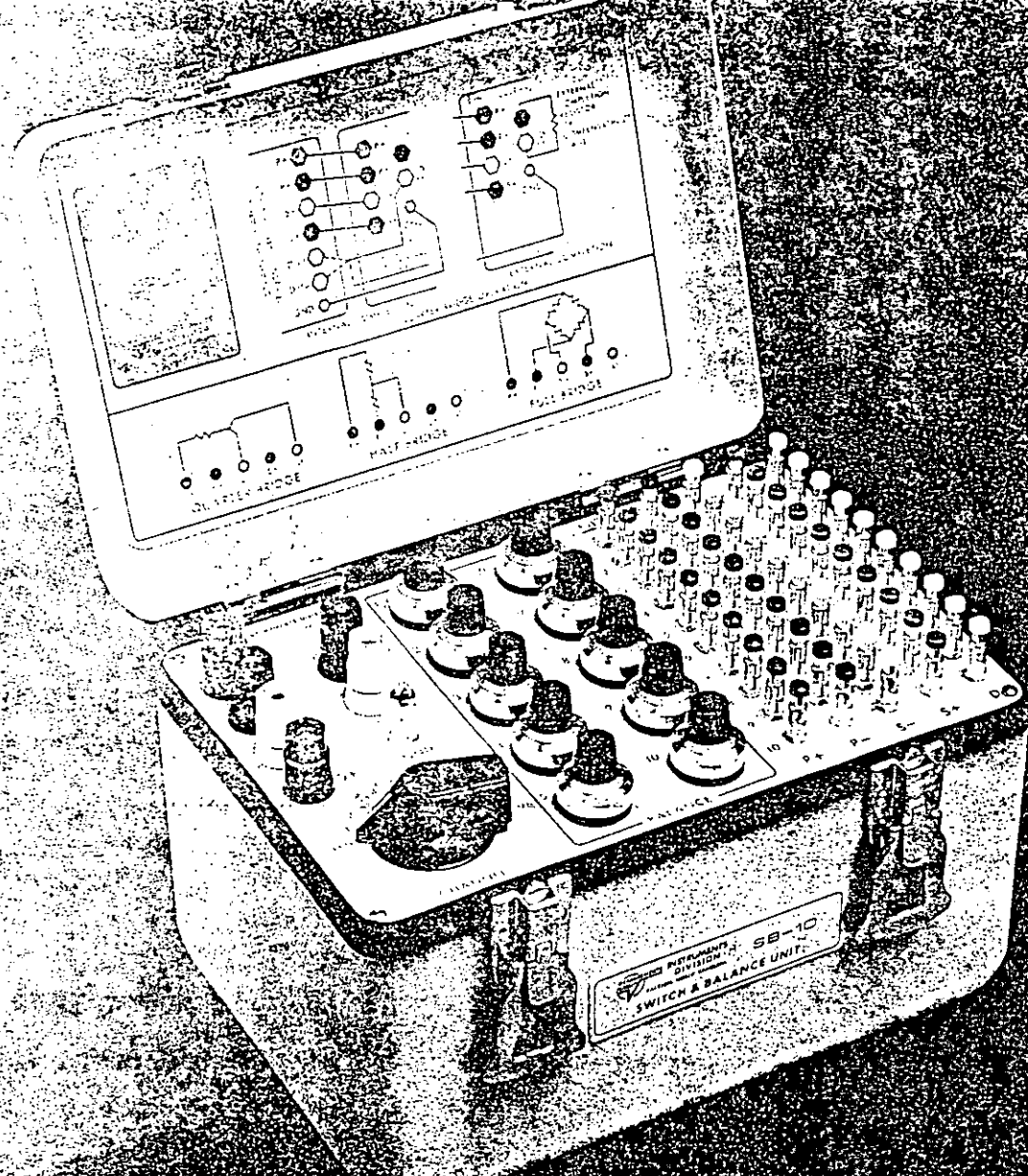
P.O. Box 27777

Raleigh, NC 27611, USA

919-365-3800 • Telex 802-502 • FAX (919) 365-3945



022216HP
 Printed in USA



SB-10

SWITCH AND BALANCE UNIT

Provides portable, ten-channel switching and balancing capability for strain indicators

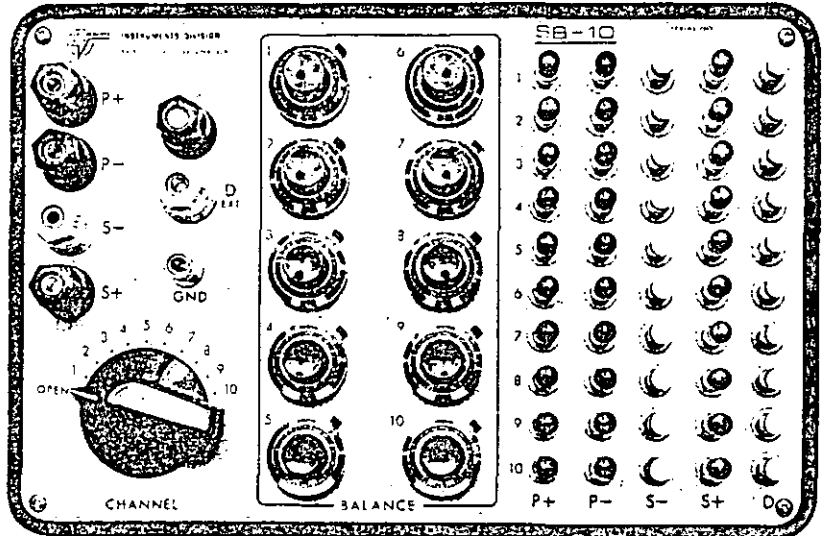
MODEL SB-10 SWITCH AND BALANCE UNIT

The SB-10 Switch and Balance Unit provides a convenient means for strain measurement when more than one strain gage is involved. While designed for use primarily with the Measurements Group P-3500 Strain Indicator, the SB-10 can also be used with other types of strain indicators.

An updated version of the time-proven SB-1K Switch-and-Balance Unit, the SB-10 features gold-plated push/clamp binding posts to allow fast, convenient, and reliable connection of input circuits, and individual ten-turn locking potentiometers with turns-counting dials for fine-balance adjustment. Also available is the SB-10L, a basic version of the SB-10. It also features locking potentiometers, but without turns-counting dials. (SB-10 front panel is shown.)

The channel selector switch of the SB-10 has negligible switch resistance, and provides an open position to allow the use of additional SB-10's with a single strain indicator. The SB-10 also incorporates a common dummy position for use with other than 120- or 350-ohm strain gages.

Ruggedly built and lightweight, the SB-10 is ideal for use in harsh field environments.

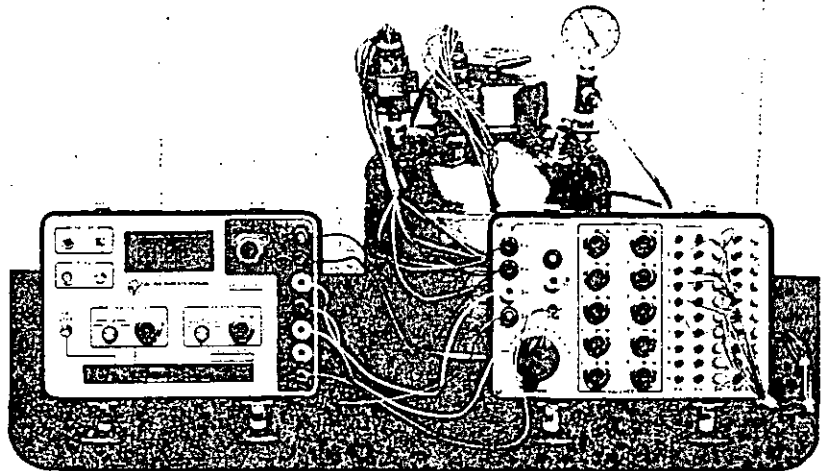


SPECIFICATIONS

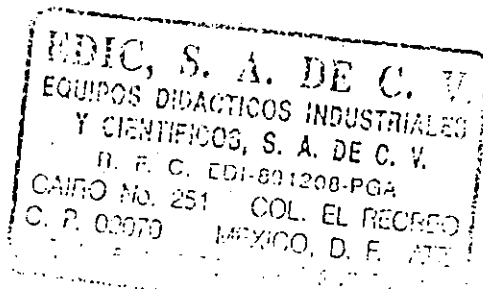
- Circuits:** 10 channels plus OPEN position.
- Inputs:** Will accept quarter-, half- or full-bridge circuits in any combination, including three-wire quarter bridges.
- Balance Range:**
Quarter and Half Bridge: $\pm 2000 \mu\epsilon$ with 350 Ω half bridge in strain indicator.
Full Bridge: $\pm 2000 \mu\epsilon$ for 350 Ω bridge. Range proportional to bridge resistance.
- Switching**
Repeatability: Better than 1% for gage resistance of 120 Ω or higher.
- Size & Weight:** 9" x 6" x 6 in (230 x 150 x 150 mm), 5.5 lb (2.5 kg).

* when used with Model P-3500

All specifications nominal or typical at -23°C unless noted.



The Measurements Group is a leading supplier of strain gage instrumentation. Available instruments include portable indicators, signal conditioners/amplifiers, strain gage installation tester, instrument calibrator, and sophisticated computer-controlled systems for the acquisition, storage and reduction of test data. Call or write for all of your strain gage instrumentation needs.



MEASUREMENTS GROUP, INC.

P.O. Box 27777

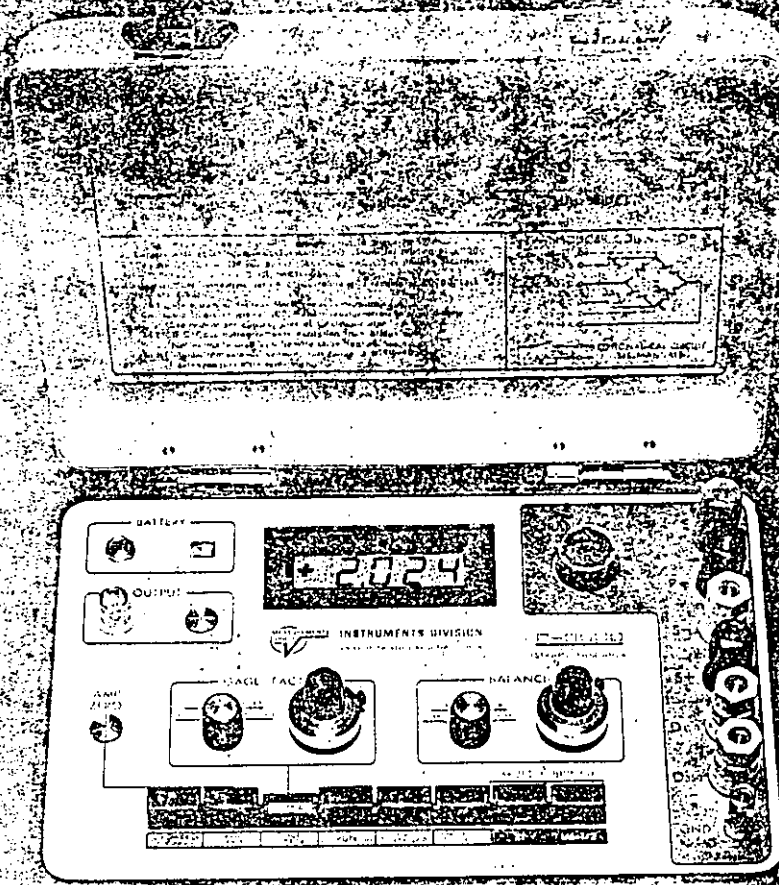
Raleigh, NC 27611, USA

Telephone (919) 365-3800

Telex 802-502 • FAX (919) 365-3945

992712HP

Printed in USA

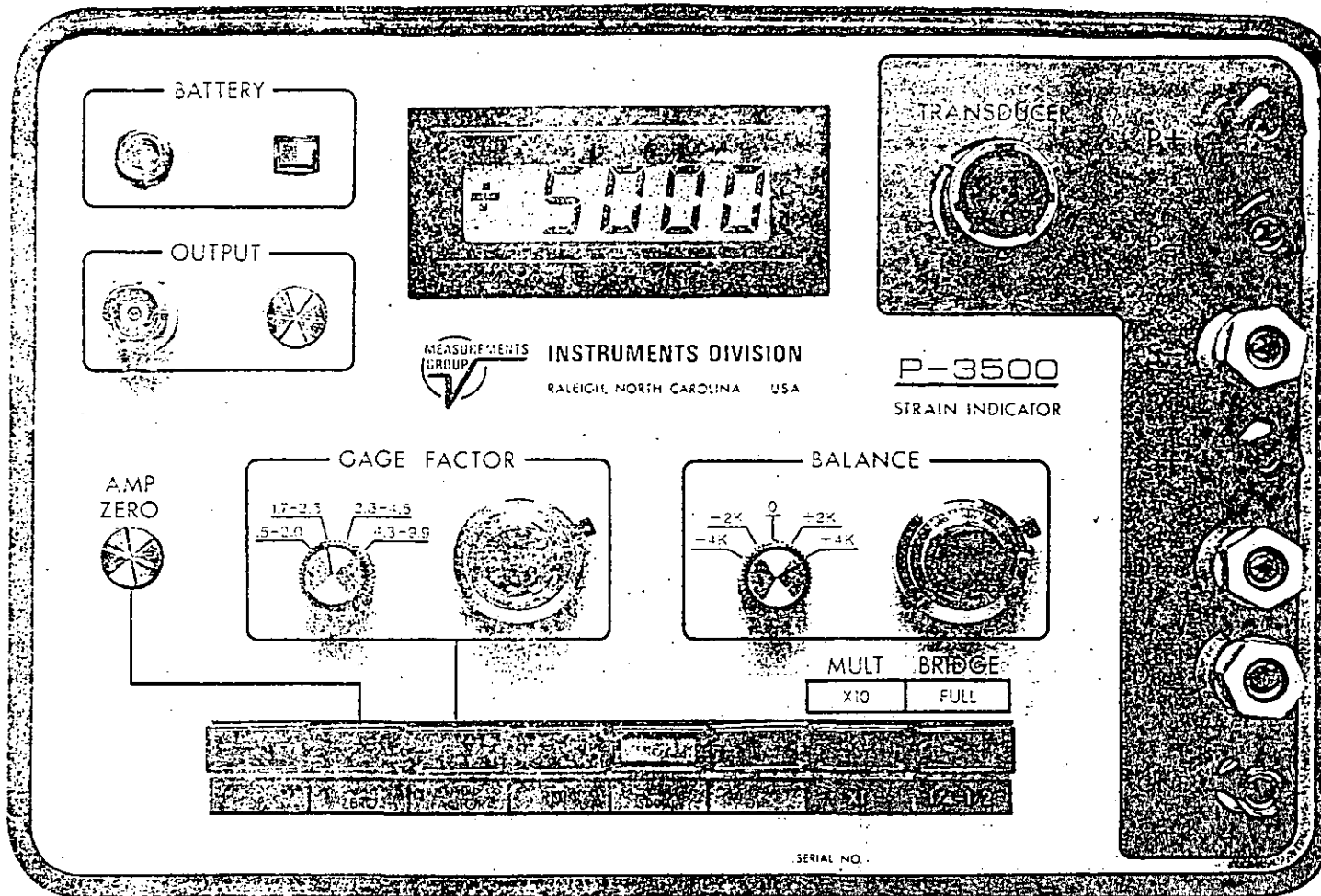


P-3500

PORTABLE STRAIN INDICATOR

Featuring advanced electronic design and
unique easy-to-understand operating controls
for making accurate and reliable measurements.





The Model P-3500 Strain Indicator is a portable, battery-powered instrument with unique features for use in stress analysis testing, and for use with strain gage based transducers. The P-3500 offers a choice of LCD or LED readouts, and incorporates many unique operating features that make it the most advanced and easy-to-use instrument of its kind. In use, the operator follows a logical sequence of setup steps by activating color-coded push-button controls to prepare the instrument for making accurate and reliable measurements.

The P-3500 also incorporates a highly stable DC amplifier, precisely regulated bridge excitation supply, and precisely settable gage factor controls.

Static measurements are displayed directly on the indicator's readout with $1\mu\epsilon$ resolution. An analog output with a -3 dB bandwidth of 4 kHz is provided to drive an external oscilloscope or recorder for dynamic measurements. The instrument will accept full-, half-, or quarter-bridge strain gage inputs, and all required bridge completion components for 120, 350 and 1000 Ω gages are built in.

Bridge excitation is 2 Vdc, resulting in low gage power and negligible drift due to gage self-heating. The P-3500 operates in fully ratiometric mode. Minute changes in bridge excitation due to drift or battery deterioration do not affect accuracy of reading.

Gage factor is precisely settable (to a resolution of 0.001) by a front-panel 10-turn potentiometer, and is displayed on the digital readout when the gage factor push button is depressed.

The P-3500 operates from an internal battery pack consisting of six "D" cells, which are readily available worldwide when replacement is required. Battery life is approximately

250 to 300 hours of continuous use (approximately 200 hours with LED readout). Battery condition is monitored by a miniature front-panel meter while the instrument is on. An external line-voltage adapter is also available (115 or 230 Vac, 50 to 60 Hz).

An optional transducer input connector facilitates connection of four- or six-wire strain gage based transducers. The P-3500's unique remote-sense feature is operational whenever the remote-sense leads are connected, and no switching is required. A remote calibration resistor is also accessible via a contact closure at the transducer connector.

FEATURES

- Choice of 4-1/2 Digit LCD or LED Readout
- Direct Reading of Strain, Pressure, Torque, Load, and Other Engineering Variables
- Battery or Line-Voltage Operation
- Convenient Color-Coded Push-Button Controls
- Gage Factor Setting (to four significant digits) Displayed on Readout
- Quarter-, Half-, and Full-Bridge Circuits
- Built-in 120, 350 and 1000 Ω Bridge Completion
- Separate Bridge Excitation On/Off Control
- Transducer Connector with Remote-Sense
- Balance by Voltage Injection
- Analog Output
- ANSI/SEM Color-Coded Bridge Connection Terminals
- Portable, Lightweight, Rugged for Field Use

MODEL SB-10 COMPANION SWITCH AND BALANCE UNIT FOR THE MODEL P-3500

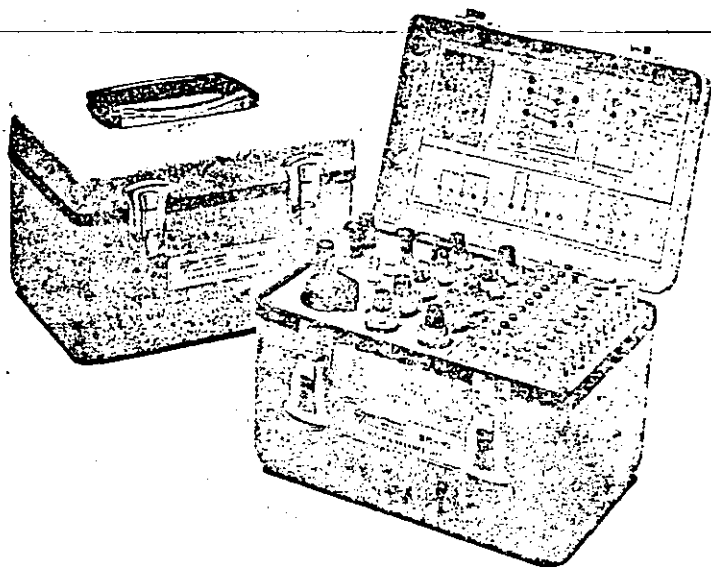
The SB-10 Switch and Balance Unit features gold-plated push/clamp binding posts to allow fast, convenient, and reliable connection of input circuits, and individual 10-turn potentiometers with turns-counting dial for fine-balance adjustments.

The channel switch of the SB-10 has an OPEN position to allow the use of additional SB-10's with a single P-3500 Strain Indicator. The SB-10 also incorporates a common dummy position for use with other than 120, 350 or 1000 Ω gages.

The combination of a P-3500 and SB-10 allows the operator to intermix, in a single 10-channel system, quarter-, half-, and full-bridge circuits. This feature is not found in most portable strain gage instrumentation.

Quarter and half bridges of the same resistance (e.g., all 120 or all 350 Ω) can be intermixed in any combination without alteration of either instrument. If the installation makes use of both 120 and 350 Ω gages, it is necessary only to connect to the dummy binding post corresponding to the selected gage resistance as the channel is changed.

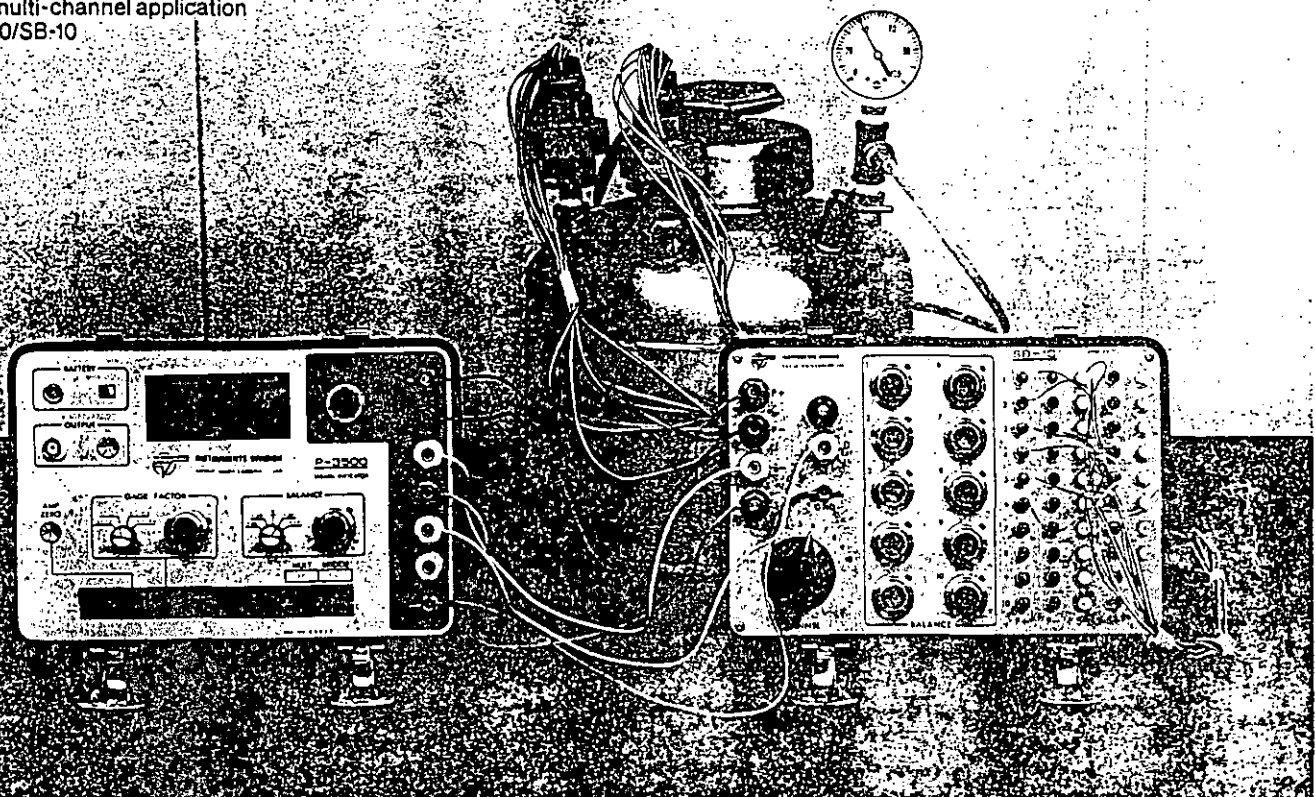
Full bridges can also be intermixed in any combination. In this case, the operator needs only to depress the P-3500 BRIDGE push button to FULL position when a full-bridge channel is selected.

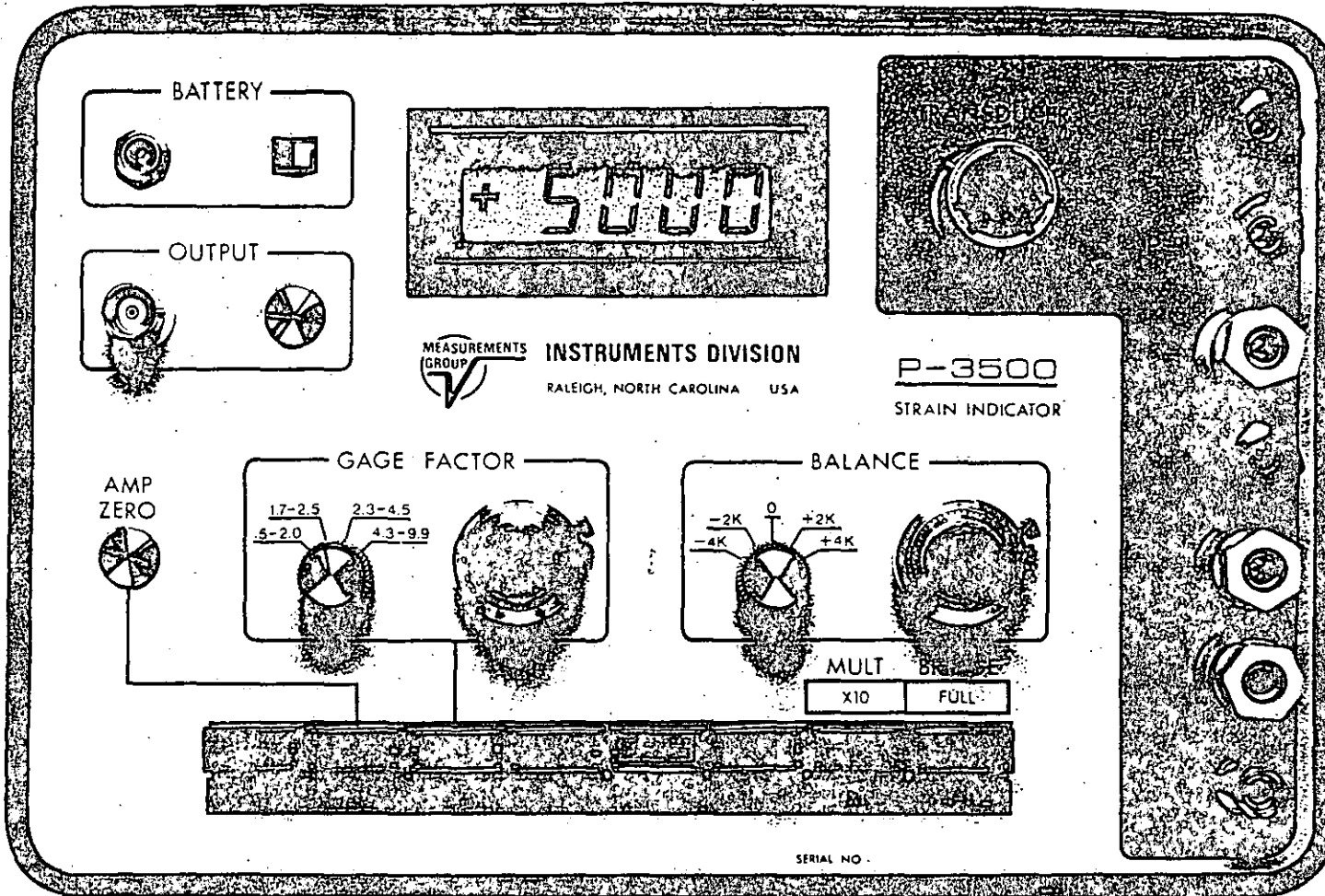


FEATURES

- 10 Channels plus OPEN Position
- Gold-Plated Push/Clamp Binding Posts
- Rugged, Lightweight
- Intermix Quarter, Half and Full Bridges
- Negligible Switching Resistance
- Switching Repeatability Better than 1 $\mu\epsilon$

Typical multi-channel application
of P-3500/SB-10





The Model P-3500 Strain Indicator is a portable, battery-powered instrument with unique features for use in stress analysis testing, and for use with strain gage based transducers. The P-3500 offers a choice of LCD or LED readouts, and incorporates many unique operating features that make it the most advanced and easy-to-use instrument of its kind. In use, the operator follows a logical sequence of setup steps by activating color-coded push-button controls to prepare the instrument for making accurate and reliable measurements.

The P-3500 also incorporates a highly stable DC amplifier, precisely regulated bridge excitation supply, and precisely settable gage factor controls.

Static measurements are displayed directly on the indicator's readout with $1\mu\epsilon$ resolution. An analog output with a -3 dB bandwidth of 4 kHz is provided to drive an external oscilloscope or recorder for dynamic measurements. The instrument will accept full-, half-, or quarter-bridge strain gage inputs, and all required bridge completion components for 120, 350 and 1000Ω gages are built in.

Bridge excitation is 2 Vdc, resulting in low gage power and negligible drift due to gage self-heating. The P-3500 operates in fully ratiometric mode. Minute changes in bridge excitation due to drift or battery deterioration do not affect accuracy of reading.

Gage factor is precisely settable (to a resolution of 0.001) by a front-panel 10-turn potentiometer, and is displayed on the digital readout when the gage factor push button is depressed.

The P-3500 operates from an internal battery pack consisting of six "D" cells, which are readily available worldwide when replacement is required. Battery life is approximately

250 to 300 hours of continuous use (approximately 200 hours with LED readout). Battery condition is monitored by a miniature front-panel meter while the instrument is on. An external line-voltage adapter is also available (115 or 230 Vac, 50 to 60 Hz).

An optional transducer input connector facilitates connection of four- or six-wire strain gage based transducers. The P-3500's unique remote-sense feature is operational whenever the remote-sense leads are connected, and no switching is required. A remote calibration resistor is also accessible via a contact closure at the transducer connector.

FEATURES

- Choice of 4-1/2 Digit LCD or LED Readout
- Direct Reading of Strain, Pressure, Torque, Load, and Other Engineering Variables
- Battery or Line-Voltage Operation
- Convenient Color-Coded Push-Button Controls
- Gage Factor Setting (to four significant digits) Displayed on Readout
- Quarter-, Half-, and Full-Bridge Circuits
- Built-in 120, 350 and 1000Ω Bridge Completion
- Separate Bridge Excitation On/Off Control
- Transducer Connector with Remote-Sense
- Balance by Voltage Injection
- Analog Output
- ANSI/SEM Color-Coded Bridge Connection Terminals
- Portable, Lightweight, Rugged for Field Use

MODEL SB-10

COMPANION SWITCH AND BALANCE UNIT FOR THE MODEL P-3500

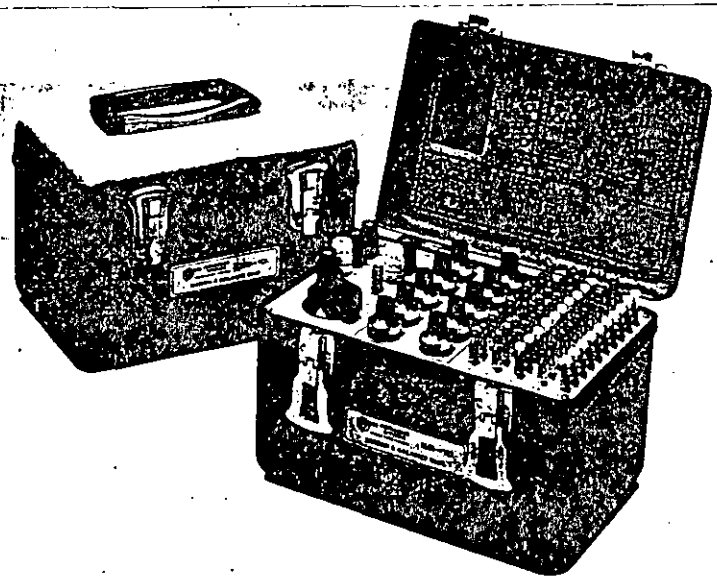
The SB-10 Switch and Balance Unit features gold-plated push/clamp binding posts to allow fast, convenient, and reliable connection of input circuits, and individual 10-turn potentiometers with turns-counting dial for fine-balance adjustments.

The channel switch of the SB-10 has an OPEN position to allow the use of additional SB-10's with a single P-3500 Strain Indicator. The SB-10 also incorporates a common dummy position for use with other than 120, 350 or 1000Ω gages.

The combination of a P-3500 and SB-10 allows the operator to intermix, in a single 10-channel system, quarter-, half-, and full-bridge circuits. This feature is not found in most portable strain gage instrumentation.

Quarter and half bridges of the same resistance (e.g., all 120 or all 350Ω) can be intermixed in any combination without alteration of either instrument. If the installation makes use of both 120 and 350Ω gages, it is necessary only to connect to the dummy binding post corresponding to the selected gage resistance as the channel is changed.

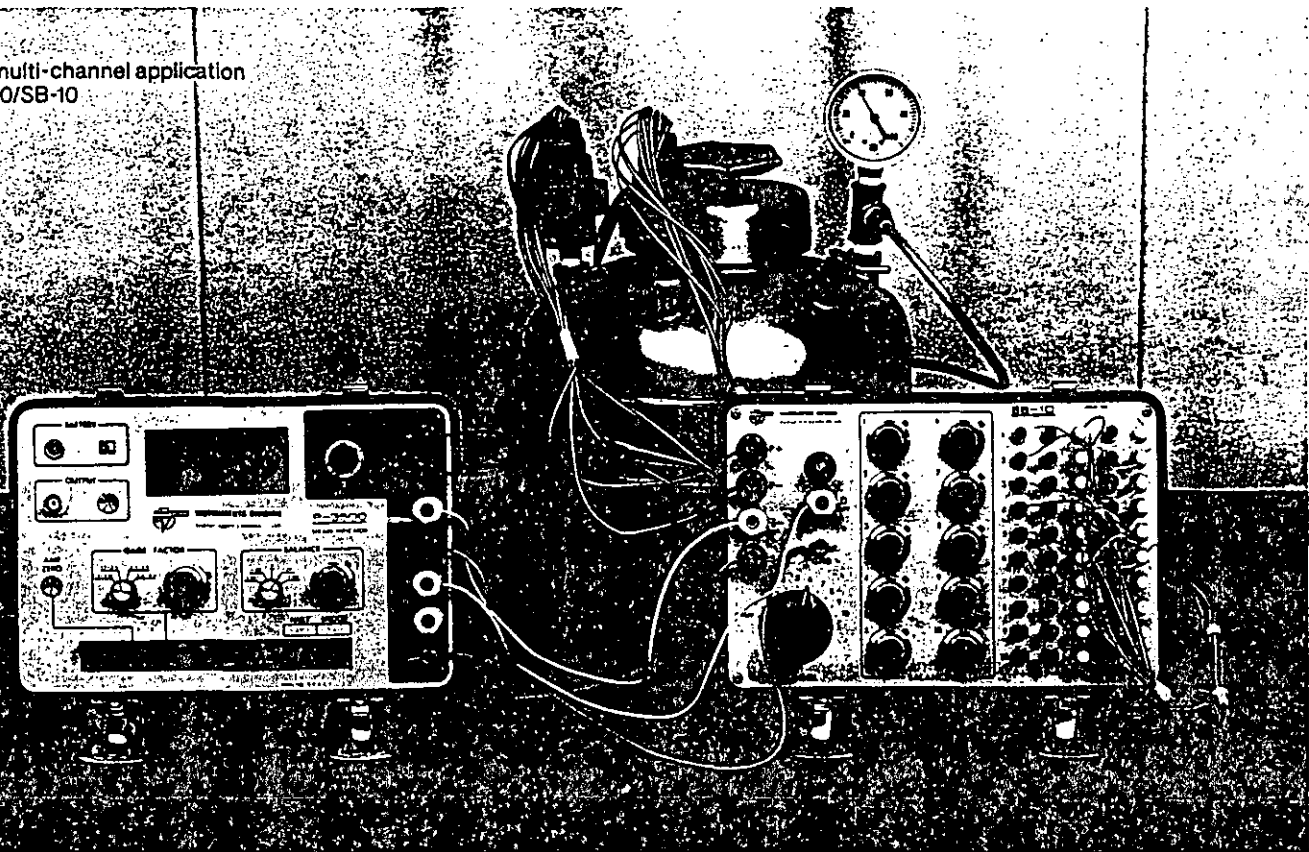
Full bridges can also be intermixed in any combination. In this case, the operator needs only to depress the P-3500 BRIDGE push button to FULL position when a full-bridge channel is selected.



FEATURES

- 10 Channels plus OPEN Position
- Gold-Plated Push/Clamp Binding Posts
- Rugged, Lightweight
- Intermix Quarter, Half and Full Bridges
- Negligible Switching Resistance
- Switching Repeatability Better than 1με

Typical multi-channel application
of P-3500/SB-10



SPECIFICATIONS

MODEL P-3500

Range:

$\pm 19\,999\mu\epsilon$ at Gage Factor < 6.000 .

$\pm \frac{6.000}{G.F.} \times 19\,999\mu\epsilon$ at Gage Factor > 6.000 .

Above ranges increased by factor of 10 when using X10 multiplier switch; Example: $\pm 199\,990$ at Gage Factor < 6.000 .

Accuracy:

$\pm 0.05\%$ of reading $\pm 3\mu\epsilon$ for Gage Factor settings of 1.000 to 9.900.

$\pm 0.05\%$ of reading $\pm 10\mu\epsilon$ for Gage Factor settings of 1.000 to 9.900 when using X10 multiplier.

Sensitivity (Resolution):

$\pm 1\mu\epsilon$ at all Gage Factor settings.

$\pm 10\mu\epsilon$ when using X10 multiplier.

Gage Factor:

Range 0.500 to 9.900. Precisely settable to a resolution of 0.001 by 10-turn potentiometer and four-position switch. Gage Factor accuracy $\pm 0.02\%$ at all settings. Displayed on digital readout.

Balance:

Coarse: 5 switch positions: Off, $\pm 2000\mu\epsilon$, and $\pm 4000\mu\epsilon$ (GF=2.000). Tolerance $\pm 1\%$ nominal.

Fine: 10-turn potentiometer with turns-counting dial, $\pm 1050\mu\epsilon$ min. range (GF=2.000). Zero position of potentiometer calibrated for zero $\pm 2\mu\epsilon$.

All balance voltages are electronically injected at input of amplifier. No bridge loading by balance controls, and no compromise of measurement range.

Bridge Excitation:

2.0 Vdc $\pm 0.1\%$. Temperature stability better than $\pm 0.02\%$ per $^{\circ}\text{C}$. Readings are fully ratiometric, and not degraded by variation in excitation voltage.

Bridge Configurations:

Quarter-, half-, and full-bridge circuits. Internal bridge completion provided for 120, 350, and 1000 Ω quarter bridges. 60 to 2000 Ω half or full bridge.

Amplifier:

Warm-up drift: Less than ± 3 counts at GF=2.000, cold start to ten min.

Random drift at constant ambient temperature: Less than ± 1 count at GF=2.000.

Common-mode rejection: Greater than 90 dB, 50 to 60 Hz.

Temperature effect on zero: Less than $1\mu\text{V}/^{\circ}\text{C}$ referred to input.

Temperature effect on span: Less than $0.005\%/^{\circ}\text{C}$.

Input impedance: Greater than 30 M Ω .

Calibration:

Shunt calibration across 120 and 350 Ω dummy gages to simulate 5000 $\mu\epsilon$ ($\pm 0.05\%$).

Analog Output:

Linear $\pm 2.50\text{V}$ max. Adjustable from 40 $\mu\text{V}/\mu\epsilon$ to 440 $\mu\text{V}/\mu\epsilon$, nominal. Output load 2 K Ω min. Bandwidth, DC to 4 kHz, -3 dB nominal. Noise: Less than 400 μV rms at 40 $\mu\text{V}/\mu\epsilon$ output level.

Remote Sense:

Provided at the transducer connector. Remote-sense error less than $0.001\%/ \Omega$ of lead resistance.

Power:

Internal battery pack using six "D" cells. Battery life 300 hours nominal (200 hours with LED readout).

Case:

Aluminum.

Size and Weight:

9 x 6 x 6 in (228 x 152 x 152 mm). 6.3 lb (2.9 kg) including batteries.

Accessories:

Line voltage adapter for 115V or 230V, 50 or 60 Hz operation.

Transducer input connector.

MODEL SB-10

(when used with Model P-3500)

Circuits:

10 channels plus OPEN position.

Inputs:

Will accept quarter-, half- or full-bridge circuits in any combination, including three-wire quarter bridges.

Balance Range:

$\pm 5800\mu\epsilon$ for quarter-, half-, and 350 Ω full-bridge inputs.

$\pm 2000\mu\epsilon$ for 120 Ω full-bridge inputs.

Switching Repeatability:

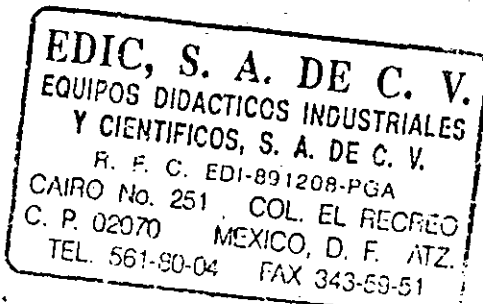
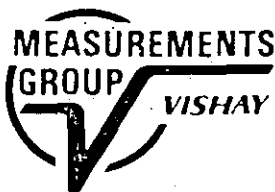
Better than $1\mu\epsilon$.

Size and Weight:

9 x 6 x 6 in (228 x 152 x 152 mm). 5.5 lb (2.5 kg).

All specifications nominal or typical at $+23^{\circ}\text{C}$ unless noted.

The Measurements Group is a leading supplier of strain gage instrumentation. Available instruments include portable indicators, signal conditioners/amplifiers, strain gage installation tester, instrument calibrator, and sophisticated computer-controlled systems for the acquisition, storage and reduction of test data. Call or write for all of your strain gage instrumentation needs.



MEASUREMENTS GROUP, INC.

P.O. Box 27777

Raleigh, NC 27611, USA

Telephone (919) 365-3800

Telex 802-502 • FAX (919) 365-3945

021621HP
Printed in USA

NEW HORIZONS IN RANGE • RESOLUTION NEVER BEFORE ACHIEVED IN A LABORATORY INSTRUMENT

The Model 3800 *Wide Range Strain Indicator* is a versatile, high-precision laboratory-type instrument designed for use with strain gages and strain-gage-based transducers.

Principal features of the Model 3800 are wide-range control of gage factor; excitation precisely settable over 1–15 volt range; and wide balance range with no bridge loading effect.

With these extended operating capabilities, the Model 3800 can be used for the most demanding measurement tasks which are not possible with conventional strain measuring instruments and general-purpose transducer indicators. Resolutions achievable with the Model 3800 are $0.10\mu\epsilon$ when used as a strain indicator, and $0.10\mu V/V$ when used as a transducer indicator ($0.025\mu V/V$ with suppressed zero).

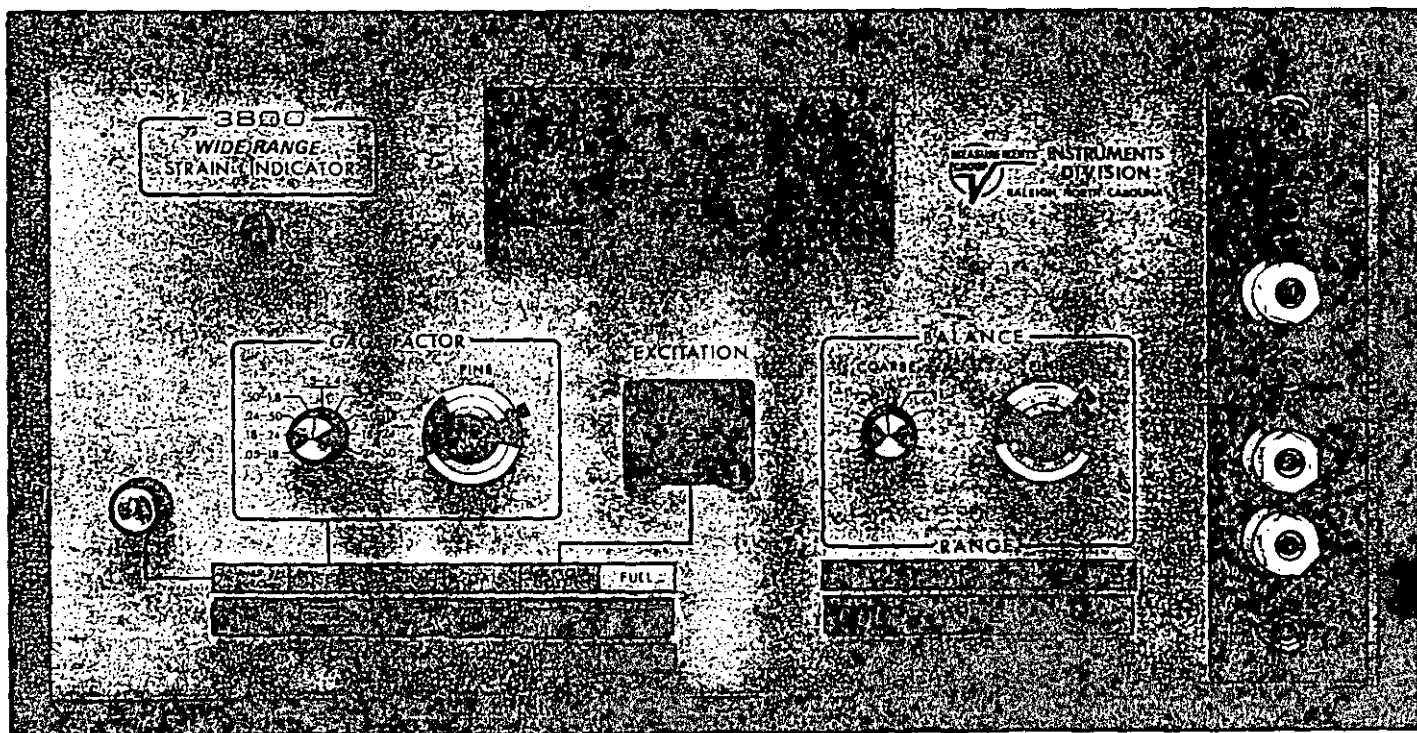
In addition to the wide-range features, the Model 3800 incorporates simplified operating controls that minimize set-up time, and promote measurement accuracy. The operator follows a logical sequence of steps to configure the instrument for the desired measurement. Color-coded interlocked push-button controls minimize operator errors, and make the operating mode instantly recognizable.

Gage factor on the Model 3800 is settable by front panel controls over a range of 0.0500 to 50.00, and is displayed by the LED readout when in the SET position. The instrument allows full range display (± 19999 counts) over the complete gage factor range.

Excitation voltage is precisely settable over a range of 1–15 volts in 1-volt increments by a front-panel thumbwheel switch. The output display automatically tracks the excitation setting so that gage factor does not vary with bridge voltage.

The balance system in the Model 3800 has four ranges which are selected by the BALANCE RANGE push buttons. Each range is further divided into four sub-ranges by the COARSE balance switch. The FINE balance control provides an additional adjustment range that overlaps the COARSE balance switch positions. This unique system provides a total of 32 overlapping ranges for achieving precise balance settings and resolution. All balance voltages are electronically injected into the input amplifier to eliminate bridge loading errors and preserve full measurement range.

FRONT PANEL



TION • VERSATILITY

Input circuitry includes an ultra-stable internal half-bridge, as well as internal 120- and 350-ohm dummy gages for bridge completion. Shunt-calibration resistors across the internal dummy gages are provided on the rear panel. Two remote calibration resistors, also mounted on the rear panel, are automatically actuated by the front-panel calibration button.

Virtually all strain-gage-based transducers can be used with the Model 3800 via the rear-panel transducer connector. This connector provides precision remote-sense capability, as well as access to the remote calibration resistors. Full-scale resolutions of $0.10 \mu\text{V/V}$ are routinely possible. By using the wide-range balance controls to suppress zero, resolutions to $0.025 \mu\text{V/V}$ can be achieved.

In addition to the digital LED display, the Model 3800 provides an analog output available at the rear panel. A separate analog level control totally independent of the digital display is also provided.

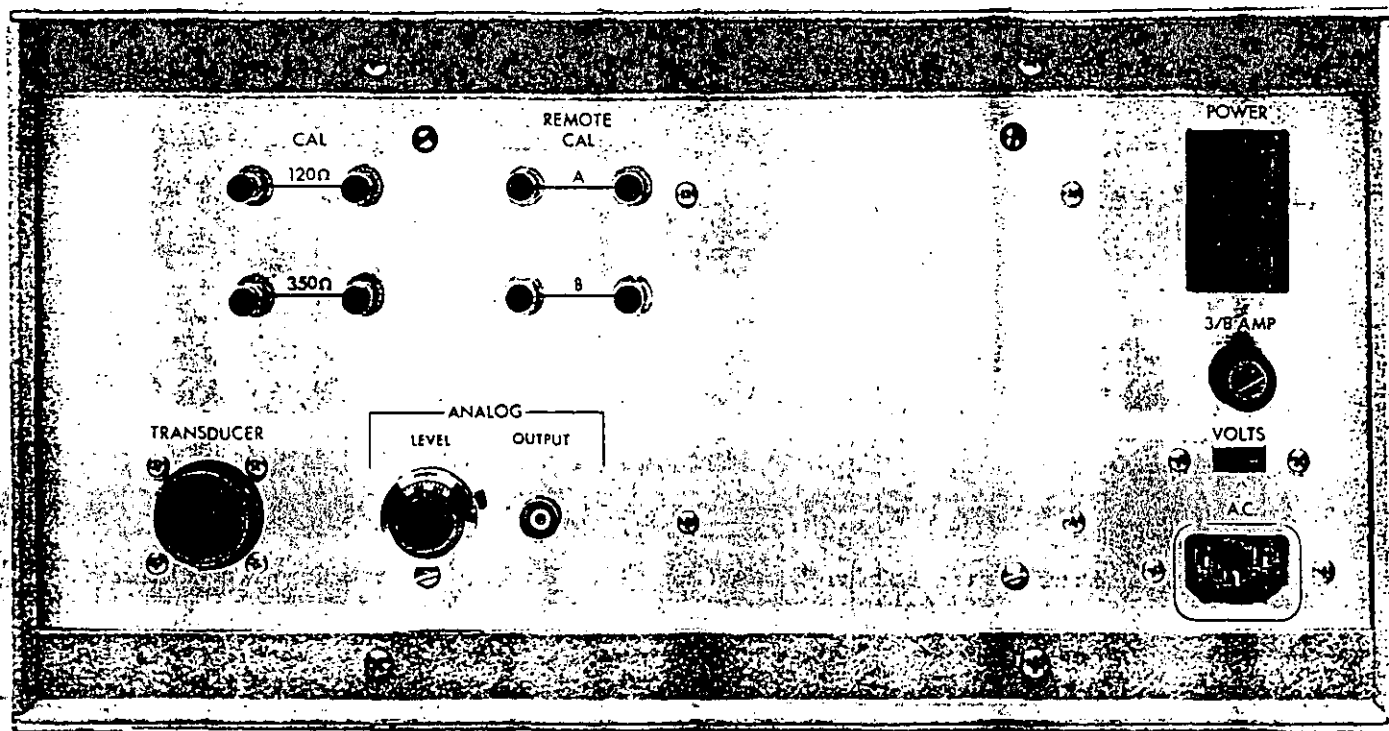
The Model 3800 *Wide Range* Strain Indicator is an exceptional, high-resolution instrument that will make a valuable contribution to any experimental stress analysis or transducer development laboratory.

FEATURES

- 4-1/2 Digit LED Display
- ANSI/SEM Color-Coded Bridge Connection Terminals
- Analog Output
- Transducer Connector with Remote Sense
- Direct Reading of Strain, Pressure, Torque, Load, and other Engineering Variables
- Convenient Color-Coded Push-Button Controls
- Gage Factor Range from 0.0500 to 50.00 Displayed on LED Readout (to four significant digits)
- Bridge Excitation Range from 1.000 to 15.000 Vdc
- Extremely Wide Balance Range. Balance by Voltage Injection.
- Quarter-, Half-, and Full-Bridge Circuits
- Separate Bridge Excitation On/Off Control
- Built-in 120- and 350-ohm Dummy Gages

Complete specifications for the Model 3800 are given on the back of this bulletin.

REAR PANEL



SPECIFICATIONS

Range and Display:

$\pm 19\,999$ counts direct-reading LED display.

Resolution:

$1\mu\epsilon$ at any Gage Factor from 0.0500 to 50.00.
 $0.10\mu V/V$ as a transducer indicator.

Linearity:

$\pm 0.01\%$ of full scale.

Balance Range:

Coarse Balance: $\pm 2.5\%$ to $\pm 100\%$ of full scale per step,
in 32 total steps.

Fine Balance: $\pm 1.25\%$ to $\pm 50\%$ of full scale; overlaps each
coarse balance step.

Balance Method:

Electronically injected counter-emf.

Gage Factor:

Range: 0.0500 to 50.00; displayed by LED readout when
in the SET position.

Resolution: 0.0001 from GF of 0.0500 to 0.5000.
0.001 from GF of 0.500 to 5.000.
0.01 from GF of 5.00 to 50.00.

Linearity: $\pm 0.05\%$ of full scale.

Accuracy: ± 1 least significant digit.

Excitation Voltage:

1.000 to 15.000 Vdc ± 1 mV $\pm 0.02\%$. Settable in 1V
increments by front-panel thumbwheel switch.

Temperature Stability: $\pm 0.01\%/^{\circ}\text{C}$.

Amplifier:

Temperature Effect on Zero: $\pm 1.0\mu V/^{\circ}\text{C}$ RTI \dagger max.;
 $\pm 0.50\mu V/^{\circ}\text{C}$ RTI \dagger typical.

Temperature Effect on Span: $\pm 0.005\%/^{\circ}\text{C}$ max.

Warm-up Drift: Less than $\pm 3\mu V$ RTI \dagger from turn-on to 5
minutes.

Random Drift at Constant Ambient Temperature:
Less than $\pm 1\mu V$ RTI \dagger .

Common-Mode Rejection: Greater than 100 dB at 50-60 Hz.

Common-Mode Voltage: $\pm 8\text{V}$ max.

\dagger Referred to input

All specifications are nominal or typical at $+23^{\circ}\text{C}$ unless noted.

Input Impedance:

Greater than 100 M Ω differential and common mode.

Input Circuits:

60 to 10 000 Ω half or full bridge. Internal dummy gages
are provided for 120 Ω and 350 Ω quarter bridges.

Calibration:

Shunt calibration resistors are provided across internal
120 Ω and 350 Ω dummy gages to simulate 5000 $\mu\epsilon$ $\pm 0.05\%$.
Calibration resistors are located on the rear of instrument
and may be changed to suit specific requirements.

Contact closures are provided for two rear-panel-
mounted resistors to facilitate any calibration
configuration. Typical use is double-shunt calibration
of transducers.

Analog Output:

Linear Output: $\pm 10.00\text{V}$ max; adjustable over 11:1 range by
a ten-turn potentiometer mounted on the
rear panel.

Output Load: 2 k Ω min.

Bandwidth: GF > 0.500 , DC to 4.5 kHz (-3 dB nominal).
GF < 0.500 , DC to 2.0 kHz (-3 dB nominal).

Output Noise: Less than 2.5 μV peak to peak 0.10 to 10 Hz,
RTI \dagger . Less than 2 μV rms dc to 5 kHz, RTI \dagger ,
plus 0.005% of full scale, RTO (referred to
output).

Remote Sense:

Remote sense connections provided at transducer connector.

Remote Sense Error: Less than 0.0005%/ Ω of lead
resistance. Maximum lead resistance
40 Ω or less.

Power:

115/230 Vac, 50-60 Hz, less than 10 volt-amperes.

Size and Weight:

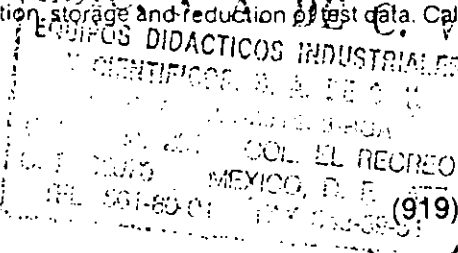
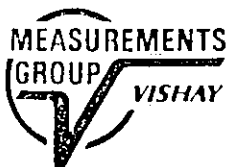
6.5 H x 11.0 W x 12.5 D in (165 x 280 x 318 mm).
10.2 lb (4.6 kg).

Companion instruments for use with the Model 3800

Model SB-10—A high-quality 10-channel Switch and Balance
Unit that allows multiple gage hook-up to the Model 3800 Strain
Indicator.

**Model V/E-40 Decade Resistor Strain Gage Simulator, and Model
1550A Strain Indicator Calibrator**—with these specialized instru-
ments, the capabilities and sensitivity of the Model 3800 can be
further extended by making critical measurements through
precise strain simulation.

The Measurements Group is a leading supplier of strain gage instrumentation. Available instruments include portable indicators, signal conditioners/amplifiers, strain gage installation tester, instrument calibrator, and sophisticated computer-controlled systems for the acquisition, storage and reduction of test data. Call or write for all of your strain gage instrumentation needs.



MEASUREMENTS GROUP, INC.

P.O. Box 27777

Raleigh, NC 27611, USA

(919) 365-3800 • Telex 802-502 • FAX (919) 365-3945

System 4000

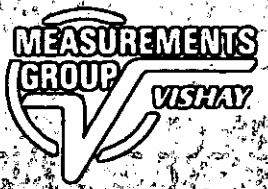
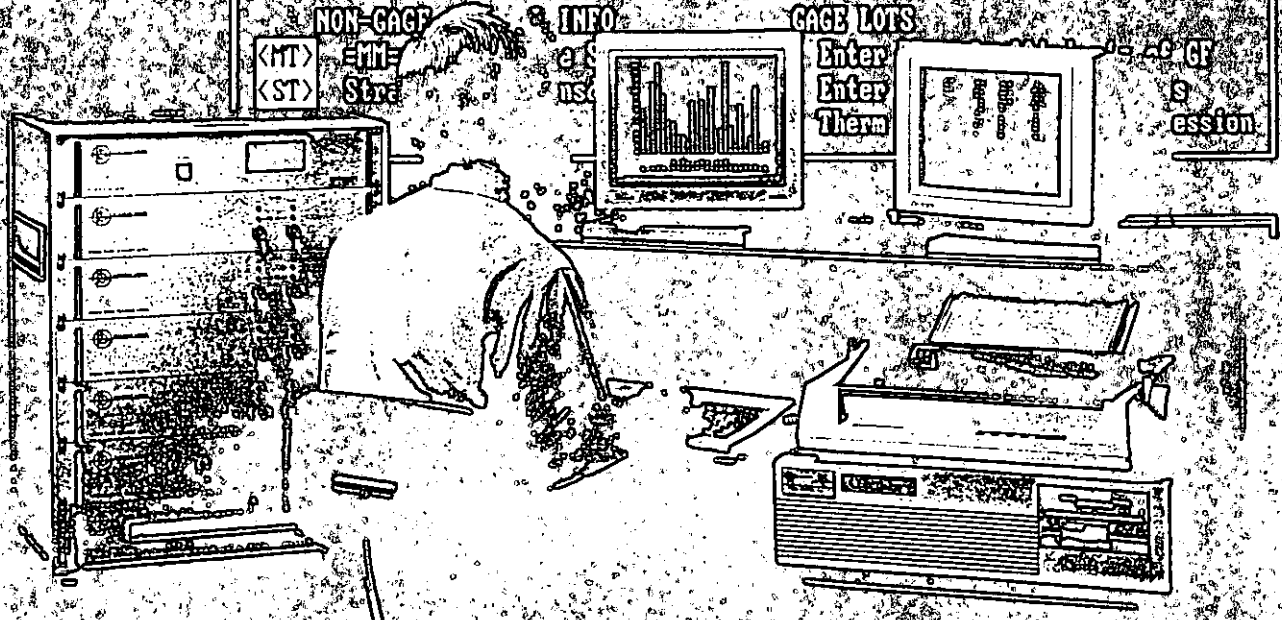
Unique Power and Simplicity in a Data System for Stress Analysis, Structural and Materials Testing

SENSOR INFO-ENTRY MENU

9:24:24 AM

Strain Gage Scanner 1

STRAIN GAGE CHANNEL INFO		ROSETTES	
<GF>	Gage Factor	<RO>	Rosette Types and Elements
<TC>	Temperature Corrections	<KT>	Kt (Transverse Sensitivity)
<SH>	Shunt Calibration (ue)	<MP>	Material Properties
<AA>	Active Arms	<MA>	Material Assignment to Channels
NON-GAGE CHANNEL INFO		GAGE LOTS	
<MT>	Enter	Enter	Enter
<ST>	Strain	Enter	Therm



DISTRIBUIDO POR
EDIC SA DE CV.
 EQUIPO PARA INDUSTRIAS
 Y CENTROS DE INVESTIGACION
 (CARTAGENA) COLIMA (MEXICO)
 (C.A. MEX) ATZCAPOTZACO
 MEXICO DF
 TEL 55 52 52 52
 FAX 55 52 52 52

System 4000 — It Pays

... with dividends like weight reduction and material savings, performance improvements and failure prevention, and shortened design-to-development time. In today's demanding world of product and structural design, payoffs like these can make a big difference.

Experimental Stress Analysis (ESA) is often called the **quality control of design** because it assures maximum reliability with minimum material and weight. Even with recent advances in analytical methods using finite-element analysis and high-speed computers, essential data which can affect not only design results but also product life, liability, and profitability, can be provided only by ESA technology.

The leaders in nearly every industry depend on the Measurements Group for the equipment and expertise to apply the quality-control benefits of ESA to their designs. And the System 4000 approach to stress analysis provides these benefits more effectively — and economically — than ever before.

Unique Power and Simplicity

... to meet today's measurement challenges. System 4000 is completely preprogrammed to perform all system functions. It accepts and stores test parameters, controls the scanning operations, records input signals, and corrects and reduces the data to provide directly usable engineering information.

The System's hardware incorporates all of those features that strain gage users have come to expect from the Measurements Group for more than 30 years, including precision bridge completion for quarter- and half-bridge circuits, and selectable bridge excitation. And, for maximum stability and noise rejection, System 4000 incorporates a 14-bit (plus sign), dual-slope integrating A/D converter, synchronized to line frequency for data acquisition.

In addition to its many special features which simplify the acquisition and reduction of strain gage data, System 4000 is also equipped to handle inputs from the other types of sensors commonly used in stress analysis and structural testing, including thermocouples, RTD's, LVDT's, load cells, DCDT's, potentiometers and other transducers.

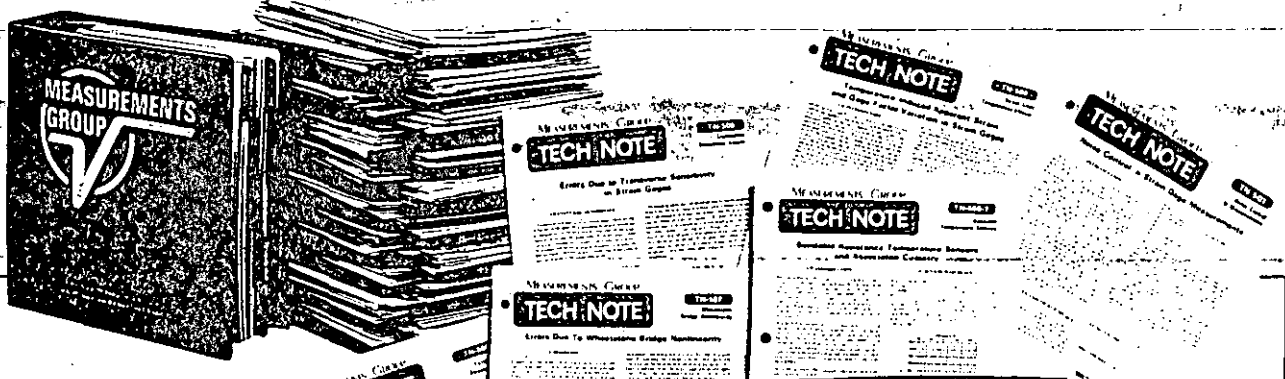
The Premier Data System

... today and tomorrow. System 4000 has been acknowledged by hundreds of users as the world's premier data system for stress analysis, structural and materials testing since its introduction in 1981. In the years since, both hardware and software have been enhanced and refined, through significant commitments we've made to ensure that System 4000 remains the world's premier data system.

About This Brochure

The Measurements Group's commitment to System 4000 is long term. In this brochure, you will read about some of our ongoing programs and development efforts which we believe will keep System 4000 the world's premier data system for stress analysis and structural testing. Operating software enhancements and new hardware developments are but a few of the programs in place to keep System 4000 expansion in pace with the needs of its users.

Because of the ongoing nature of these programs, this brochure can serve only as an introduction to the concept behind System 4000. To keep System 4000 users informed of important developments, *System 4000 Update — the Users Group Newsletter*, is published periodically and distributed to all System 4000 users throughout the world. As you are reading this, chances are that new and more powerful aspects of System 4000 are *already* available.



$$\frac{\Delta R}{R} = F_a \epsilon_a + F_t \epsilon_t$$

where: ϵ_a, ϵ_t = strain parallel to and perpendicular to the gage axis
 F_a = axial
 F_t = transverse

SENSOR INFO-ENTRY MENU 9:24:24 AM

Strain Gage Scanner

STRAIN GAGE CHANNEL INFO

(GF)	Gage Factor	(RO)	Rosette Types and Elements
(TC)	Temperature Corrections	(KT)	Kt (Transverse Sensitivity)
(SH)	Shunt Calibration (ue)	(MP)	Material Properties
(AA)	Active Arms	(MA)	Material Assignment to Channels

MON-GAGE CHANNEL INFO

(MT)	RTD Temperature Sensor	(CC)	Enter Temp Coefficients of CT
(ST)	Strain Gage Transducer	(AC)	Enter Thermal Output Coef's
		(AD)	Therm Output Coef's by Regression

ROSETTES

(RO)	Rosette Types and Elements
(KT)	Kt (Transverse Sensitivity)
(MP)	Material Properties
(MA)	Material Assignment to Channels

GAGE LOTS

(CC)	Enter Temp Coefficients of CT
(AC)	Enter Thermal Output Coef's
(AD)	Therm Output Coef's by Regression

Universal Scanner

(HT)	High-Level Transducer	(CR)	Special RTD Coef's by Regression
(LU)	LUOT (AC)		
(DC)	DCDT (DC LUOT)		
(RT)	RTD or Thermistor		
(PO)	Potentiometer		
(UD)	Volts or mV		

ENTER LETTER

(M) = Main Menu

Below the monitor, there are several printed outputs: a graph titled 'PERCENT STRAIN RELATIVE TO STRESS', a data table, a graph showing a peak, and another graph titled '1500 TEST AT 1500 PSI'.

Strain gage technology has developed into the world's most widely used precision stress/strain measurement technique. Over the years, through our Technical Data Mailing Program, we have treated technical matters relating to stress analysis in a practical, usable fashion that we hope most benefits you, the user, in your stress analysis applications. The primary factors affecting strain gage and instrumentation performance are covered in the *Tech Note* portion of the Measurements Group's Strain Gage Technology literature binder, recognized and used as the authoritative reference for strain gage measurement by practitioners throughout the world.

Virtually all of the materials included in the Measurements Group's Strain Gage Technology *Tech Note* library are incorporated into System 4000's extensive software package, designed by Measurements Group engineers. Now, you can apply these techniques directly to your test measurements.

Computer technology has impacted virtually all disciplines of engineering, primarily through the greatly expanded potential for computational speed, accuracy, and flexibility provided by software. While the System 4000 hardware is designed for the highest performance/cost ratio possible, it is the software that provides the true power behind System 4000.

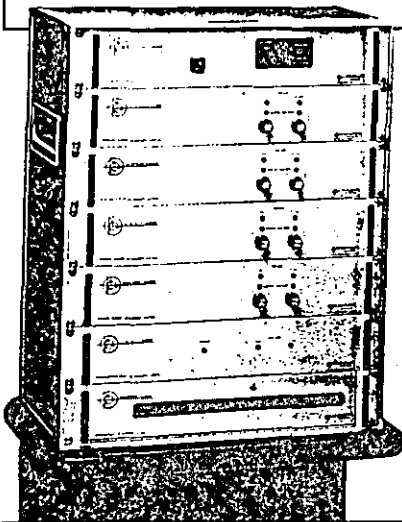
The System

4220 CONTROLLER

Serves as the interface between the Executive Unit and the System's scanners, providing primary system power, channel display, and analog-to-digital conversion.

4270A STRAIN GAGE SCANNER

Each scanner accommodates 20 channels of strain gage inputs (quarter, half, or full bridge). Switch-selectable bridge excitation is provided for each block of 10 channels.



4280 UNIVERSAL SCANNER

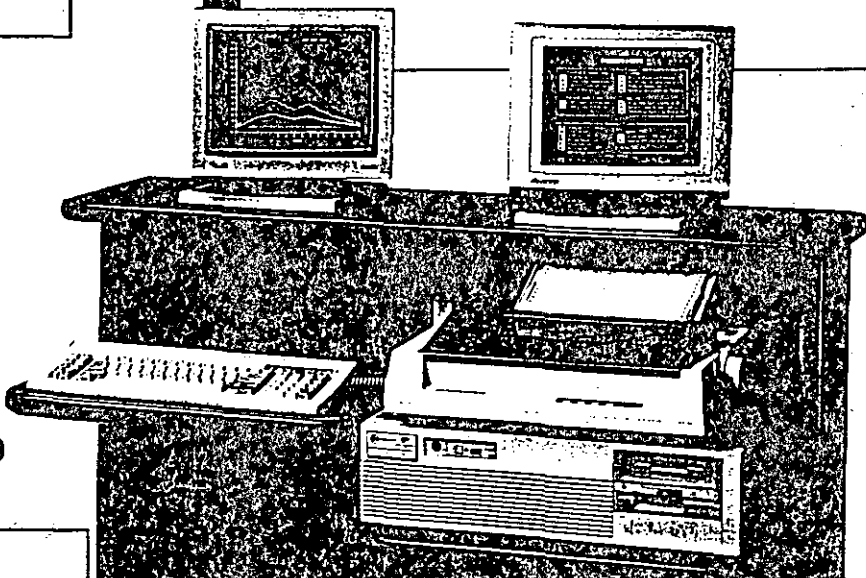
Capacity for 10 channels of mixed inputs, including thermocouples, LVDT's, RTD's, DCDT's, semiconductor transducers, potentiometers and voltage inputs.

SOFTWARE/HARDWARE CONFIGURATIONS

The heart of System 4000 is the extensive software that organizes, processes, and presents test data in various modes as required by the user. **Model 610 Standard System Software** operates on a wide range of customer-supplied, general-purpose personal computers, including laptops.

For tests requiring more modest capabilities, the lower cost **Model 605 Data Logger Software** is also available. *A listing of specific hardware component requirements for both software packages is available, upon request, from our Applications Engineering Department.*

Additionally, the **Model 4216 Executive Unit** (shown here), consisting of Model 510 Standard System Software and Model 4202 Computer Hardware Components, is available to those wishing to purchase a complete, dual-monitor turn-key system.



4290 THERMOCOUPLE SCANNER

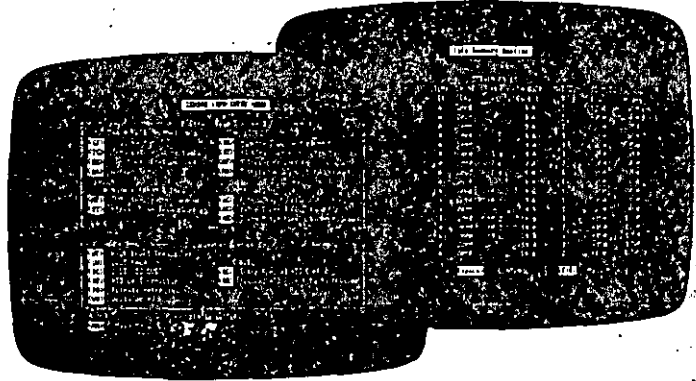
Provides dedicated capability for 20 channels of thermocouple inputs (Types J, K, T, E, R, S, B). Type is selectable for each block of 10 channels.

PRINCIPAL FEATURES

- Complete, preprogrammed software
- Inputs accepted from strain gages, strain gage based transducers, LVDT's, DCDT's, potentiometers, thermocouples, and RTD's
- Input capacity from 1 to 1000 channels — expandable as needed at any time
- Scanning speed up to 30 channels per second (25 channels per second for 50 Hz operation)
- Automatic bridge balance (offset values stored in memory and/or permanently recorded)
- Switch-selectable excitation voltage (1, 2, 5, 10 Vdc)
- Built-in bridge completion for all 120 and 350 Ω strain gage channels (quarter and half bridges)
- PC-compatible for user-preferred off-line data handling

TEST INFORMATION ENTRY

- Channel assignment
- Gage Factor
- Thermal output coefficients
- Gage factor temperature coefficient
- Transducer input/output specifications
- Control limits (by channel or by groups) (except Model 605)
- Active bridge arms
- Transverse sensitivity
- Modulus of elasticity
- Poisson's ratio



SOFTWARE CAPABILITIES

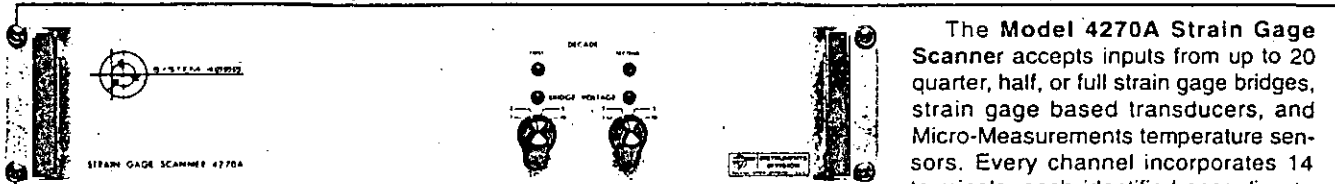
The scope and capabilities of System 4000's standard, preprogrammed stress analysis software far exceed those of other commercially available packages, which are generally designed for narrowly defined applications only.

- Rosette data reduction (delta, rectangular, biaxial) and conversion of strains to stress
- Thermal output correction
- Correction for gage factor temperature coefficient
- Scaling for number of active bridge arms
- Wheatstone bridge nonlinearity correction
- RTD linearization
- Transverse sensitivity correction
- Thermocouple linearization
- Alarm or control limits (print or initiate scan) (except Model 605)
- On-line monitoring of key channels and/or rosette solutions in numeric and graphic (except Model 605) formats
- Reduced data can be printed for up to 1000 channels
- Automatic or manual data scan and record
- Data storage for later analysis or processing
- Off-line plot generation on color monitor or optional plotter (except Model 605)

Optional software packages for specialized test requirements are also available.

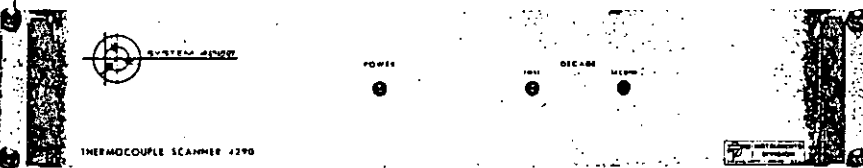
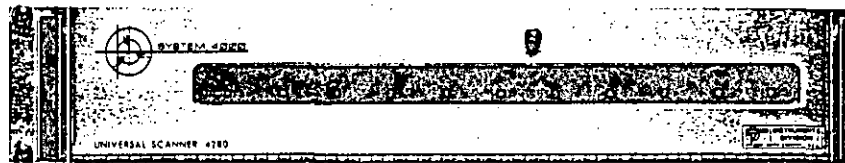
What System 4000 Can

FLEXIBLE, COST-EFFECTIVE INPUT AND SIGNAL CONDITIONING CAPABILITY



The Model 4270A Strain Gage Scanner accepts inputs from up to 20 quarter, half, or full strain gage bridges, strain gage based transducers, and Micro-Measurements temperature sensors. Every channel incorporates 14 terminals, each identified according to standard wiring codes. The 4270A provides switch-selectable bridge excitation voltage, bridge completion for 120- and 350-ohm circuits, and shunt calibration for individual channels or common banks of 10 channels. Intermixing of input types within each scanner is accommodated by the 4270A.

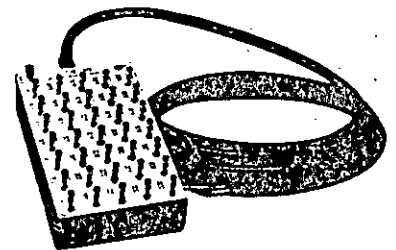
The Model 4280 Universal Scanner accepts up to 10 inputs from LVDT's, thermocouples (Types K, J, T, E, R, S, and B), DCDT's, rotary and linear potentiometers, RTD's, and other devices commonly used in conjunction with strain gages for structural testing.



The Model 4290 Thermocouple Scanner accepts inputs from up to 20 thermocouples (Types K, J, T, E, R, S, and B) and provides ice-point compensation and signal conditioning. Thermocouple type is set in banks of 10 channels. A precision Micro-Measurements

temperature sensor bonded directly to a specially designed isothermal mounting strip ensures accurate, electronic ice-point compensation.

The Model RTB-35 Terminal Block provides 35 gold-plated push posts for convenient connect-disconnect input capability for the Model 4270A Strain Gage Scanner. Each terminal block has the capacity for 10 three-wire quarter- and half-bridge installations; or 8 four-wire or 5 six-wire full-bridge installations. A standard cable length of 10 ft (3.05 m) is provided, with different lengths available on a custom basis.



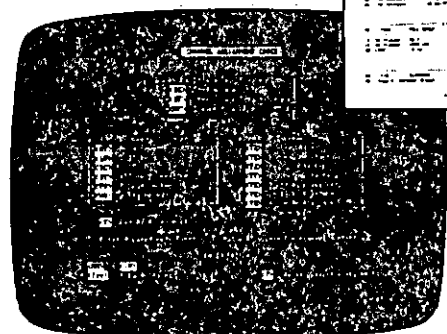
SPEED AND EASE OF TEST SETUP

Sensor input connections are quickly made to System 4000 through easy-access terminals at the rear of each scanner module. Input terminals for the 4270A Strain Gage Scanner, for example, are identified by channel number and clearly marked for quarter-, half-, and full-bridge hookup — using built-in precision bridge-completion resistors as required. After connecting all sensors, the desired bridge voltage is set.

Through the Executive Unit, the appropriate constants — gage factor, modulus of elasticity, Poisson's ratio, transducer sensitivity, etc. — are entered, and System 4000 automatically outputs test data directly in engineering units. The system records input information entries for permanent retention and displays or prints them in summary form on command.

Test setup for multi-channel measurements has never been easier.

Info Setup for 4270A

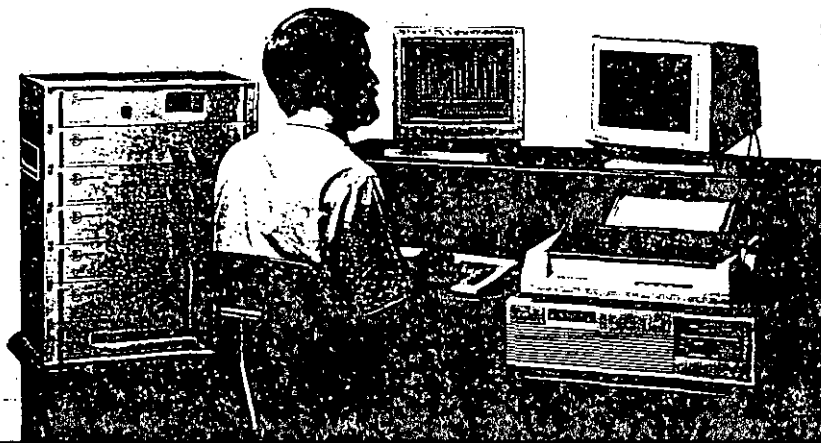


Add to Your Test Program

TRAINING

Although a complete set of reference manuals is supplied with every System, we believe there is no substitute for "hands-on" training for orientation to the System's fullest capabilities. Each purchase of System 4000 includes one full day of training by an experienced technical staff member at our World Headquarters in Raleigh, North Carolina. Our training facility has available a complete range of sensor inputs for the System so that maximum effectiveness can be built into each training session.

And, your personalized training session is designed to take into account your specific requirements and applications.



APPLICATIONS ENGINEERING SUPPORT



A full-time staff of Applications Engineers is available to you for System 4000 consultation. Several complete Systems maintained within our Applications Engineering Department are used to simulate user applications. Whether your questions or comments involve the System's hardware, software, or general application, our staff of Applications Engineers is always "on call" and available to assist with your problems or simply provide a sounding board for your specific test application or program.

YOUR FUTURE WITH SYSTEM 4000

The operating software of System 4000 carries the value of your investment in System 4000 far into the future. As your needs expand, so can your system — through the addition of input scanner modules to increase channel capacity, or by adding specialized off-line software.

Announced through *System 4000 Update — the Users Group Newsletter*, these new software developments are made available to System 4000 users for their evaluation through the β -TEST Program.

Incorporating System 4000 into your test program not only brings you today's state-of-the-art data system — it represents your investment in the future.

Add to Your Test Program

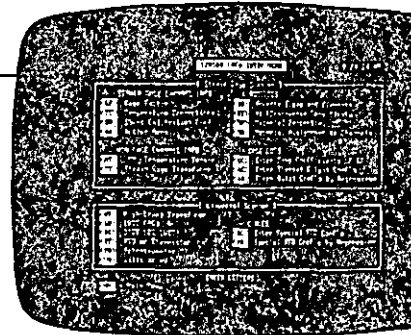
ACCURACY

Accurate strain gage measurements require that attention be paid to characteristics unique to the strain gage itself — characteristics such as thermal output, transverse sensitivity, nonlinearity of output from the Wheatstone bridge, temperature coefficient of gage factor, and grid power dissipation. In addition, care must be taken to apply corrections at the appropriate stage in the measurement process. System 4000 can take into account as many — or as few — of these potential error sources as your test requires.

For thermocouple measurements, a unique, isothermal strip eliminates temperature gradients between input terminals.

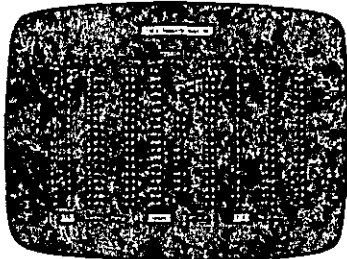
The System's specially selected analog-to-digital converter uses a dual-slope conversion technique to integrate the analog signal over a complete powerline cycle, making it possible to achieve the high resolution and excellent noise rejection essential for accurate strain measurements.

Through its unique software and hardware, System 4000 provides the test operator with the tools to obtain the most accurate test data possible.

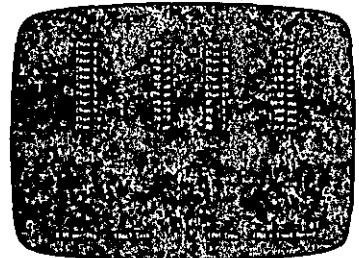


ON-LINE MONITORING

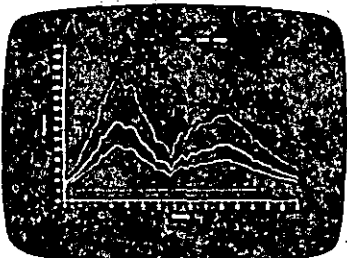
System 4000 provides a wide range of options for monitoring test parameters and data, including:



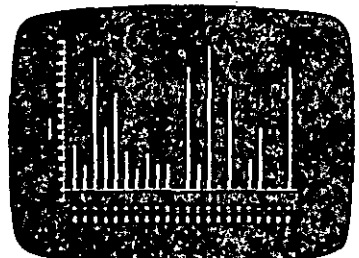
Test parameters reviewed through a screen display before testing is begun.



Up to 44 key channels of corrected and reduced data simultaneously displayed and updated.



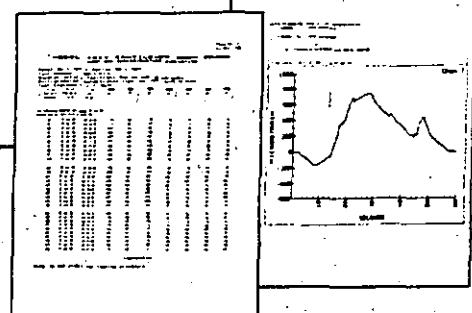
Up to 12 line plots of data (vs. data or time) displayed (except Model 605).



Up to 44 bar graphs that change color when user-defined trip levels are exceeded — allowing for fast recognition of critical test conditions (except Model 605).

FLEXIBILITY IN DATA PRESENTATION

Through the System's Data Translation Program, data files can be transformed into ASCII, DIF, or WKS formats, allowing for easy manipulation and presentation of data with commercial software packages or user-developed programs.



Worldwide, System 4000 Users* Are Putting Power, Accuracy, and Simplicity Into Their Stress/Strain Measurement Programs

In Industry and Research . . .

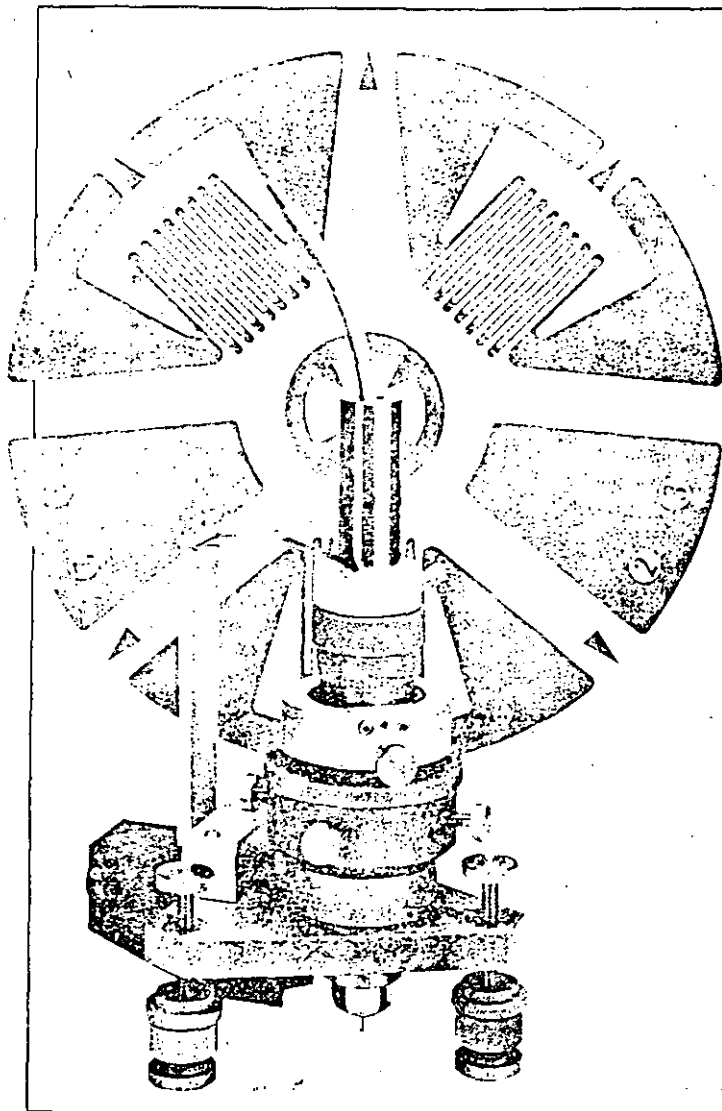
AM General	General Dynamics	Ontario Hydro	Ecole Centrale de Lyon
AT&T Bell Laboratories	General Electric Company	PPG Industries	Ecole D'Ingenieurs de Yamoussoukro
Admiralty Marine Technology Est.	Gilbarco	Pettibone-Tiffin	Ecole Supérieure D'Ingenieurs des Techniques du Bois
Aérospatiale	Gradall Company	Piasecki Aircraft	Electronics & Telecommunication Research Institute
Agency for Defense Development	Graviner Limited	Picker International	Enit Tunisia University
Alcoa Technical Center	Groupe P.S.A.	Pratt & Whitney Aircraft Co.	General Motors Institute
Alfa Romeo S.P.A.	Grove Manufacturing	Precision Medical Instruments	Howard University
Alsthom Atlantique La Rochelle	Grumman	Pullman Technology	Indian Institute of Technology
American Sterilizer	Hamilton Standard	Research & Development Establishment (India)	Institut Francais de Petrole
Amp	Harris Corporation	Richards Medical	Institut National de Genie Mecanique Algiers
Armco Steel	Hindustan Motors	Rockwell Intl. Rocketdyne Div.	Institut Nationale de Toulouse
Astech	Hughes Aircraft	SEMAT	Institut Universitaire de Bordeaux
Avions Hurel/Dubois	Hughes Offshore	SNECMA Villaroche	Institut Universitaire de Bourges
Baker Tubular Services	Hunting Oilfield Services	SPAR Aerospace	Institut Universitaire de Reims
Beech Aircraft	Hyundai	STE Alkan Aeronautique	Kuwait University
Bender Machine Services	IBM	STE Beta	Metropolitan Medical Center
Bendix Aerospace	IMPA, SPA	STE Elmex Paris	Michigan State University
Blue Bird Body Company	Institute for Industrial Research & Standards, Ireland	STE Eternit	Nan Yang Technical Institute
Boeing	Israel Aircraft Industries	STE Hermex	Oklahoma State University
Borg-Warner	Isringhausen Railroad Products	STE Messier Aeronautique	Rochester Institute of Technology
British Nuclear Fuels	J.A. Jones Applied Research	STE Thomson	Southern Illinois University
British Steel Corporation	Jim Haé Machine Depot	Samsung	Swanmore College
Brookhaven Laboratories	Korea Institute of Mining & Metals	Shell Development Company	U.S. Naval Post-graduate School
L.J. Broutman & Associates	Knolls Atomic Power Labs	A.O. Smith	Universidad de Oviedo
CASA	Koch Fiberglass	Southwest Research Institute	Universite de Lille
CNERIB Alger	Kon Mij de Schelde	Specialty Measurements	University of Bari
Cameron Iron Works	Laboratoire du Balltimont et Travaux Publics a Libreville	Steiger Tractor	University of Bridgeport
Canoecean Resources	Laboratorio Ensayo Investigacion Industrial	Stress Engineering Services	University of California
Chrysler Corporation	Laboratoire des Ponts et Chaussées de Toulouse	Tadran	University of Dayton
Clark Michigan Company	McDonnell Douglas	Tennessee Eastman	University of Delaware
Crown-Zellerbach	Marshalls of Cambridge Engr.	Thrall Car Manufacturing Co.	University of Grenobles
Cummins Engine	Martin Marietta Aerospace Co.	Trinity Engineering	University of Illinois
Daimler-Benz AG	Martin Marietta Energy Systems	U.S. Air Force	University of Louisville
Defense Product Assurance Agency	Massachusetts General Hospital	U.S. Army	University of Maryland
Delas Weir	Menasco	U.S. Marine Corps	University of Miami
Dominion Engineering	Metalastik Vibration Control Sys.	U.S. Navy	University of Michigan
Dow Chemical	Metallurgical Engineers	VME America	University of Nova Scotia
Dow Corning Wright	Michelin Tire	Volvo Flymotor AB	University of Petroleum & Minerals
Dunlop Aviation Division	Ministry of Defence, France	WSM Industries	University of Pittsburgh
E. I. DuPont Company	Motor Wheel Corporation	Water Research Center	University of South Florida
E.C.A.N.	NASA	Waukesha Engine	University of Toledo
ETSI Industriales	National Aeronautical Lab (India)	Weber Aircraft	University of Trieste
Eaton Axle Division	National Crane Company	Westinghouse Electric	University of Wisconsin
Electricité de France	National Forge Company	Whitehead Motofides S.P.A.	Villanova University
Equipos Nucleares	National Research Council of Canada		Virginia Polytechnic Institute and State University
Etablissement Central de L'Armement Naval de Nantes	Naval Ocean Systems Ctr. (U.S.)		Washington University
Exxon	Naval Science & Technological Lab (India)		Youngstown State University
Fiberglas	Naval Surface Weapons Ctr. (U.S.)		
Fisher Controls	Navistar International		
Fixible Corporation	Neil F. Lamson		
Ford Aerospace	Newport News Shipbuilding		
Ford Motor Company	O'Donnell & Associates		
GEC Research Centre	Oilkon Corporation		
GM, Allison Gas Turbine Division	Omark Industries		
GM, Chevrolet Division			
GM Technical Center			
Garrett Turbine Engine Company			

In Education . . .

American University of Beirut
 Auburn University
 Beijing Aeronautical Institute
 California Polytechnic State Univ.
 Carleton University
 The Citadel
 Columbia University
 Dublin College of Technology

*The listing represents a selection of organizations using System 4000 at the time this brochure was printed. Inclusion does not imply endorsement.

... Shouldn't You?



MEME

Strain Gages and Instrumentation for Residual Stress Measurements

A predominant factor contributing to the structural failure of machine parts, pressure vessels, framed structures, etc., may be the residual "locked-in" stresses that exist in the object prior to its being put into service. These residual stresses are usually introduced during manufacturing, and are caused by processes such as casting, welding, machining, heat treating, molding, etc.

Residual stress can neither be detected nor evaluated by conventional surface measurement techniques, since the strain sensor (strain gage, photoelastic coating, etc.) can only respond to strain changes that occur after the sensor is installed.

The most widely used practical technique for measuring residual stresses is the hole-drilling strain gage method described in ASTM Standard E837. With this method, a specially configured electrical resistance strain gage rosette is bonded to the surface of the test object, and a small shallow hole is drilled through the center of the rosette. The local changes in strain due to introduction

of the hole are measured, and the relaxed residual stresses are computed from these measurements. Measurements Group Tech Note TN-503, *Measurement of Residual Stresses By The Hole-Drilling Strain Gage Method*, presents a detailed discussion of the theory and application of this technique.

The hole-drilling method is generally considered semi-destructive, since the drilled hole may not noticeably impair the structural integrity of the part being tested. Depending on the type of rosette gage used, the drilled hole is typically 0.062 or 0.125 in (about 1.5 or 3.0 mm), both in diameter and depth. In many instances, the hole can also be plugged, if necessary, to return the part to service after the residual stresses have been measured.

The practicality and accuracy of this method is directly related to the precision with which the hole is drilled through the center of the strain gage rosette. The Measurements Group RS-200 optical milling guide described herein provides a practical means to accomplish this task



**FACULTAD DE INGENIERIA U.N.A.M.
DIVISION DE EDUCACION CONTINUA**

"METODOS EXPERIMENTALES DE ANALISIS DE ESFUERZOS"

Comisión Federal de Electricidad

Del 28 de febrero al 4 de marzo de 1994.

Irapuato, Gto.

**Curso Institucional
febrero de 1994.**

OPTIMIZATION OF PLUGS FOR THE DIVERSION TUNNELS OF DAMS

LUIS FERRER, ALFREDO OLIVARES and OSCAR HERNANDEZ

School of Engineering National Autonomous, University of Mexico, Mexico City, Mexico

Abstract—The construction of dams on narrow rivers with great volume of flow has forced the construction of diversion tunnels of great diameter (15 meters or larger). After the dam has been built, the tunnels have to be plugged to begin the filling process of the storage reservoir. The large size of the plugs has led to the idea that their shape should be optimized in order to obtain a structure with the desirable characteristics of being lighter and stronger. The optimization process for such plug was conducted using twenty one photoelastic models and the validation of the results from the 2D models was achieved using four 3D models. The results of the work reported here are shown in dimensionless form so they can be used in the design process of plugs with similar geometry.

NOMENCLATURE

d	diameter of the cavity
D	diameter of the plug
E	modulus of elasticity
f_s	stress fringe value
F_s	stress fringe value for the model
L	total length of the plug
n	fringe order
p	hydrostatic pressure
S	effective width
t	model thickness
θ	angle formed by the principal axes and the coordinate axes (x, y)
σ_1, σ_2	principal stresses
σ_e	elastic limit
σ_u	ultimate strength
τ_{max}	maximum shear stress
τ_{xy}	shear stress along the x, y axes

1. INTRODUCTION

THE CONSTRUCTION of dams on narrow rivers with great volume of flow has forced the construction of diversion tunnels of great diameter (15 meters or larger). After the dam has been built, the tunnels have to be plugged so that the filling process of the storage reservoir can begin.

The large size of the plugs has led to the idea that their shape should be optimized in order to obtain a lighter and stronger structure. This, in turn, would save considerable amount of time and money in their construction.

2. GENERAL ASPECTS OF THE PROBLEM

The problem to be solved was that of a tunnel perforated in a rock medium, which had a reinforced concrete plug somewhere along its length (Fig. 1). The tunnel as well as the upstream-side of the plug were subjected to the hydrostatic pressure from the dam; the downstream-side of the plug and the rest of the tunnel were free from external forces.

The prototype tunnel runs inside a mountain and the plug is located at a considerable distance from its ends (Fig. 1). Based on this, the following assumptions were made:

(i) Taking the plug and its vicinity as the region of interest, it can be considered to be surrounded by an infinite media.

(ii) If the boundaries for the model are taken as those given by the contour line e on Fig. 1, it is observed that, both the radial as well as the longitudinal displacements are restricted by an

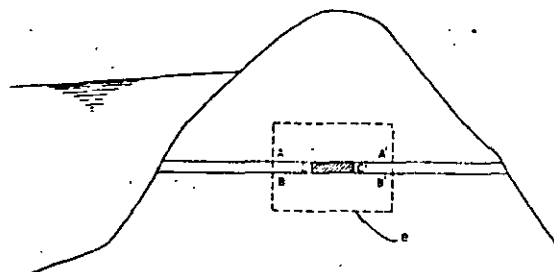


Fig. 1. Location of the plug inside the tunnel.

infinite amount of material which surrounds the area under study. This justifies the assumption made to clamp the plastic model to an infinitely rigid media beyond the border e .

(iii) As far as the load is concerned, both, the loaded side of the tunnel as well as side e of the plug are going to withstand the pressure due to the maximum depth of water in the dam for the most critical possible loading conditions.

(iv) The analogy between plane stress and plane strain (refs[1,2]) has been used with great frequency and advantage in the solution of many engineering problems such as dams, tunnels, inspection galleries, rockets, pressure vessels, etc. (refs[3,4]). This analogy allows the use of two dimensional plane stress models for the solution of problems where it is reasonable to assume that the corresponding region in the prototype is subjected to a state of plane strain. For the problem at hand, meridional planes of the plug, subjected to a plane stress field with the boundary conditions shown in Fig. 2, were studied.

3. OBJECTIVE

The objective of this study was that of finding a simple and practical geometry for a two-dimensional model, which reduced substantially the tension stresses on the plug surfaces. With this goal in mind, 21 models with different geometric configurations were analysed.

4. ANALYSIS OF GEOMETRIC CONFIGURATIONS

In order to obtain an optimal shape for the plug, the following geometrical configurations were analysed:

(i) Cylindrical plug (Fig. 3, geometric figures A). The ratio of effective plug width (S) to tunnel diameter (D), [ratio (S/D)], was varied from 0.27 to 2.

(ii) Long plug with cylindrical cavity and hemispherical end (Fig. 3, geometric figures B). For this group of models, the specific width of the plugs (S) was held constant to $S = 4/15D$. The cavity diameter d was varied from $d = 0.25D$ to $d = D$. The total length of the plug (L) was $L = 2D$.

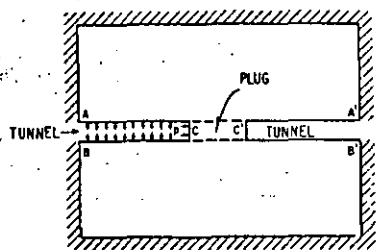


Fig. 2. Boundary conditions for the model.

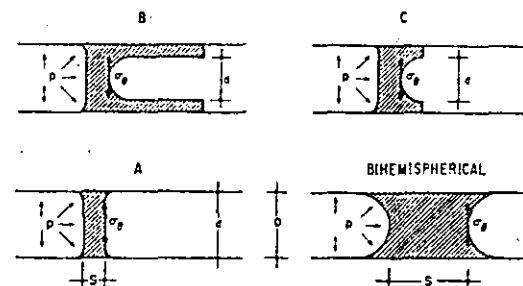


Fig. 3. Geometries analysed.

(iii) Short plug with hemispheric cavity (Fig. 3, geometric figures C). For this group of models, the only variation was the total length (L), which was made $L = 23/30D$. The cavity diameter variations and the effective width were the same as those for group (ii).

(iv) Bihemispherical plug. The bihemispherical plug has the geometry shown in Fig. 3. The specific width (S) was varied from $S = 0.28D$ to $S = 1.07D$.

5. MODEL MANUFACTURING AND LOAD SYSTEMS

5.1. Model manufacturing

The material used for the model fabrication was (CR-39) Columbia Resin, which is manufactured by the Homalite Corporation. This transparent plastic material has the following mechanical and optical properties (ref.[5]).

σ_u	ultimate strength	420 kg/cm ²
σ_e	elastic limit	210 kg/cm ²
E	modulus of elasticity	21,000 kg/cm ²
F_s	stress fringe value	6.1 kg/cm ² -cm/fringe.

The ratio fringe-stress is linear up to the elastic limit for a given time and the material is homogeneous and isotropic.

The models were machined from 90 × 90 × 0.63 cm plates. The machining was made with the use of a high speed router.

5.2. Load systems

The boundary conditions for the two-dimensional models were given in the following way:

(i) The perimetral restriction was achieved binding the CR-39 to a rigid frame made of steel (Fig. 4).

(ii) The pressure on the surface A-C-B (Fig. 2) was applied with nitrogen inside a rubber membrane, which acted upon the surface as shown in Fig. 5. This mechanism allowed the application to the surface of the model the same pressure p as that of the nitrogen held inside the membrane (see ref.[6]).

6. METHOD OF ANALYSIS

The experimental method used was photoelasticity. This method yields two photoelastic patterns:

(i) The isochromatics (Fig. 6) are the loci of points with the same value τ_{max}

$$\left(\tau_{max} = \frac{\sigma_1 - \sigma_2}{2} \right)$$

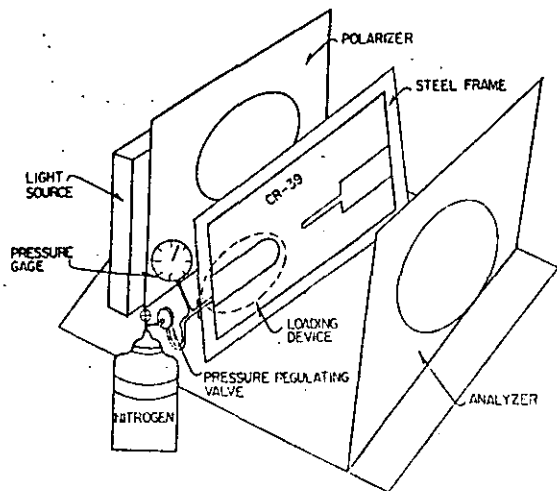


Fig. 4. Loading set-up for two-dimensional models.

(ii) The isoclinics (Fig. 7) are the loci of points with the same inclination for their principal axes.

The maximum shear stresses in a plane are those associated to the isochromatics in that plane.

Calling our plane (x, y) , the shear stresses associated to the coordinate directions (τ_{xy}) can be obtained by means of the following formula:

$$(\tau_{\max})_{x,y} = \frac{\tau_{xy}}{\sin 2\theta} = n f_s \frac{1}{t}$$

Where: τ_{\max} is the maximum shear stress; τ_{xy} , the shear stress along the x, y axes; θ the angle formed by the principal axes and the coordinate axes (x, y) ; n the fringe order; f_s the stress fringe value; and t the model thickness.

On free boundaries of two dimensional thin models (plane stress), (for our problem on A'-C'-B'), two of the principal stresses are zero (the one perpendicular to the plane of the plate

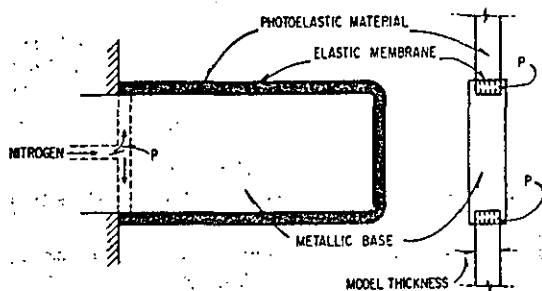


Fig. 5. Loading device for two-dimensional models.

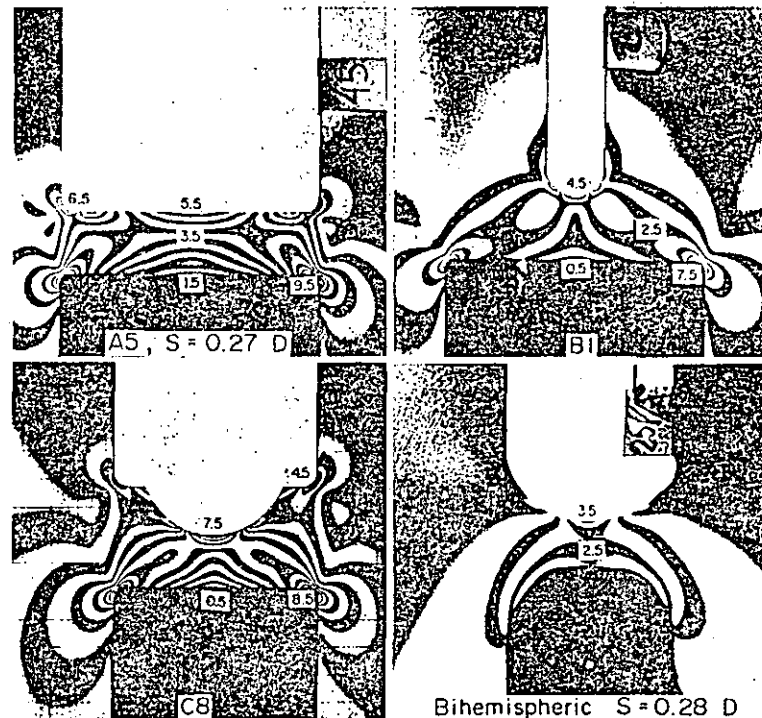


Fig. 6. Isochromatic fringe patterns for different geometries.

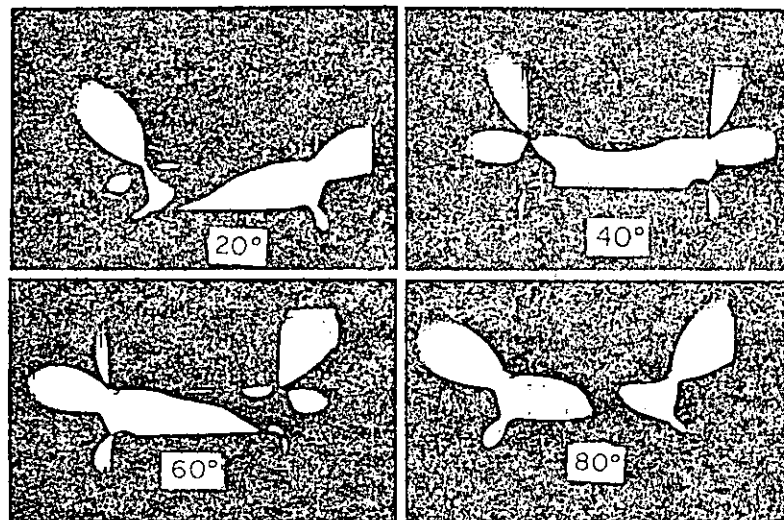


Fig. 7. Isochromatic patterns for geometry A5.

and the normal one to the free edge); therefore the isochromatics yield the value of the third principal stress directly on those borders.

$$\tau_{\max} = \frac{\sigma_1 - \sigma_2}{2} = nF_s.$$

If: $\sigma_1 = 0$

$$\frac{-\sigma_2}{2} = nF_s.$$

Or: $\sigma_2 = 0$

$$\frac{\sigma_1}{2} = nF_s.$$

If the only applied stress to the boundary is perpendicular to the border and different from zero, the applied stress is a principal one and its value is known to be $-p$ for our problem.

In such a case, the isochromatic fringes yield the value of the third principal stress directly on those borders.

Again:

$$\tau_{\max} = \frac{\sigma_1 - \sigma_2}{2} = nF_s.$$

If: $\sigma_1 = -p$

$$\frac{-p - \sigma_2}{2} = nF_s.$$

Or: $\sigma_2 = -p$

$$\frac{\sigma_1 - (-p)}{2} = nF_s.$$

For the problem at hand, the study was conducted along the boundaries A-C-B and A'-C'-B' of the plugs and the neighboring region of the tunnel. One of them (A'-C'-B') is free, and the other (A-C-B) is subjected to the known hydrostatic pressure ($-p$). For both cases, photoelasticity directly yields the stress value of the component tangent to the border. This component is contained on the plane of the model.

7. RESULTS

7.1. Geometric configuration A

For the first series of geometric figures, which consisted of cylindrical plugs, the effective width S was gradually reduced until a value for S was reached which corresponded to that of a circular thick plate.

The analysis of the results from the models corresponding to this geometric figure showed that the maximum tensile stresses on the loaded side (which always appeared in the region of the joint between the tunnel and the plug), and the maximum tensile ones on the unloaded border (which always appeared on the central part of the plug), augmented with the reduction of the specific width S of the plug. Figure 8 shows the stress distribution and the corresponding isochromatic pattern for the smaller specific width.

7.2. Geometric configuration B

For this case, a cylindrical plug with $L = 2D$, fixed S and a cavity with a hemispherical end, whose diameter was gradually augmented until it reached the value of tunnel diameter, was studied.

The stress distribution on both the up and downstream faces of the plug for the larger diameter are shown on Fig. 9. Figure 10 shows the maximum tangential stress $(\sigma_t)_{\max}$ on each of the plug faces as a function of the cavity radius. In all cases, the maximum tangential stress is shown on the loaded side in a region immediate to the joint between the plug and the tunnel.

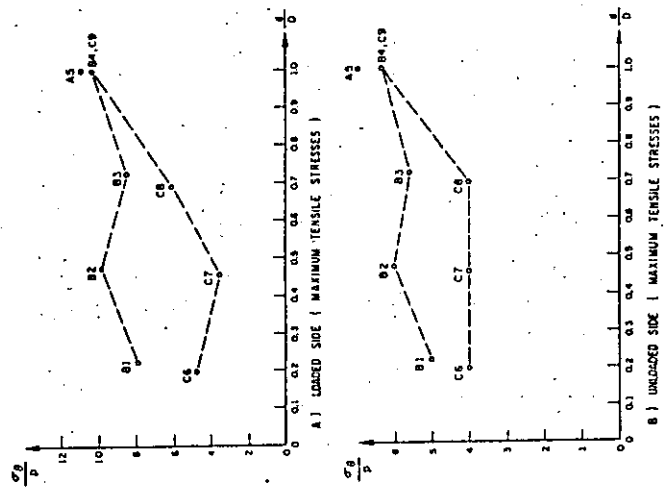


Fig. 10. Stress variation of σ_θ as a function of plug geometry.

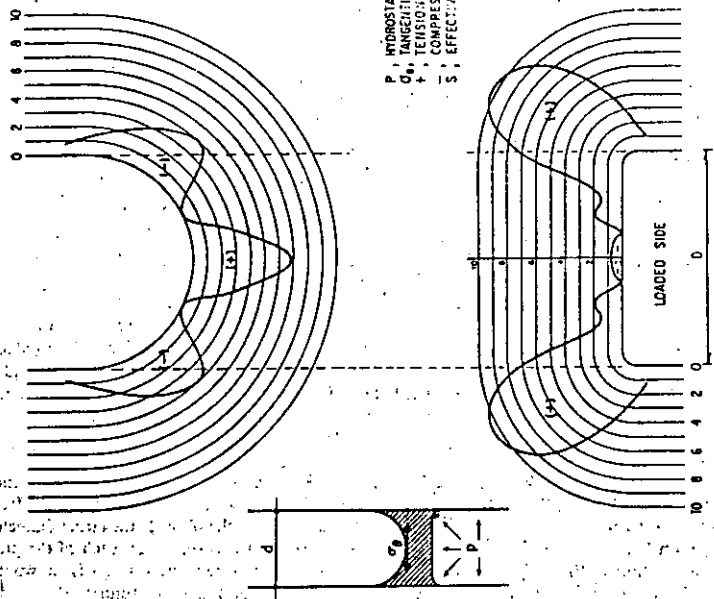


Fig. 9. Stress distribution in geometries B4 and C9. $D = d$.

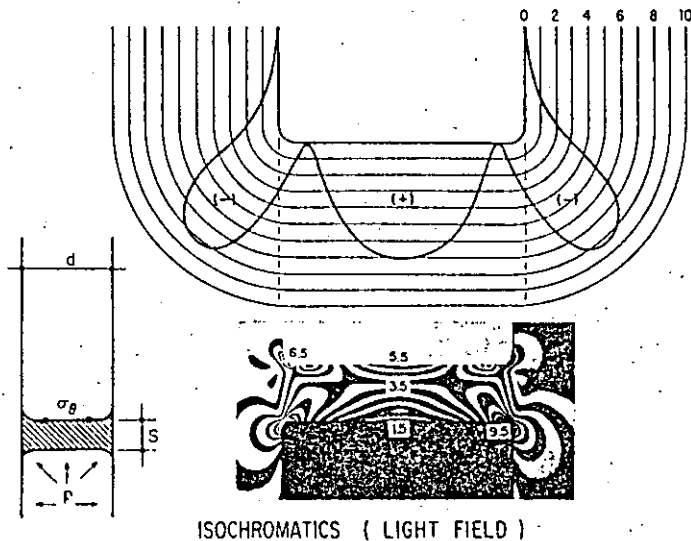


Fig. 8. Stress distribution in the cylindrical plug. $S = 0.27D$.

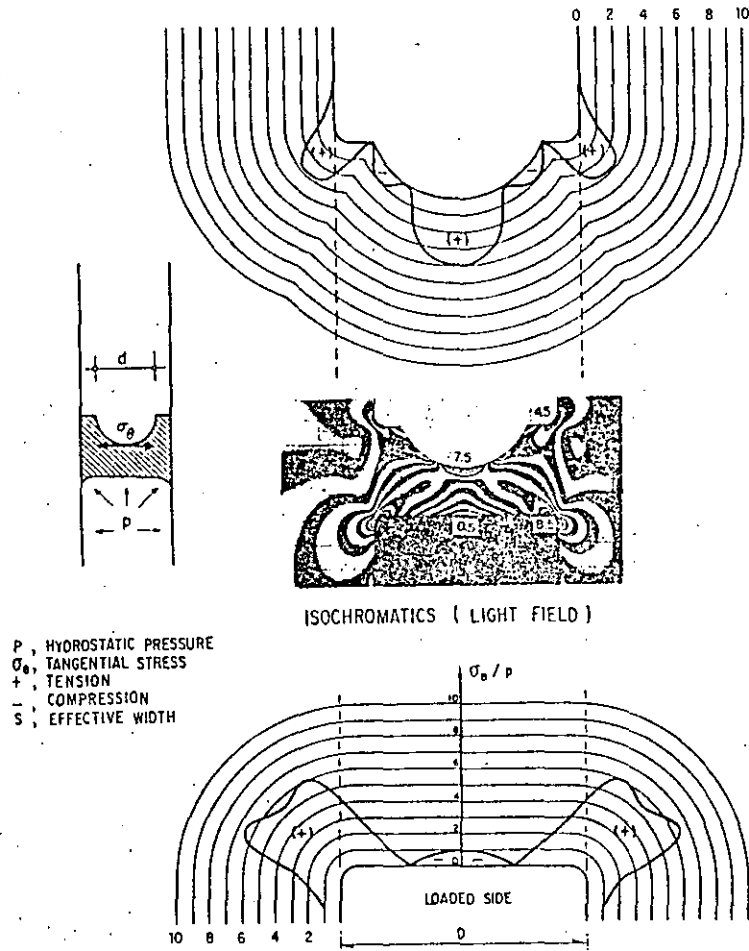


Fig. 11. Stress distribution in geometry CR, $d = 0.7D$.

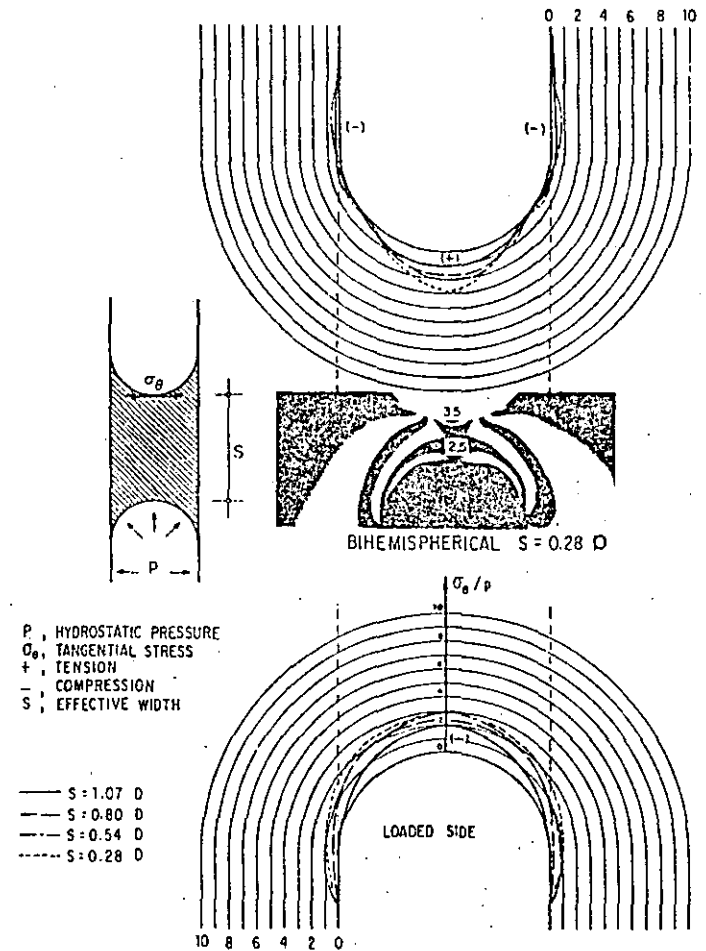


Fig. 12. Stress distribution in the bihemispherical plug, $S = 1.07D$; $S = 0.80D$; $S = 0.54D$; $S = 0.28D$.

Fig. 14. Two-dimensional models loaded up to failure.

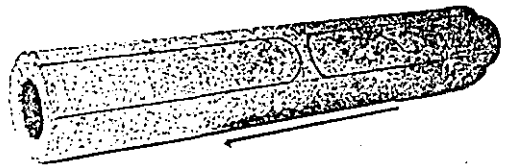
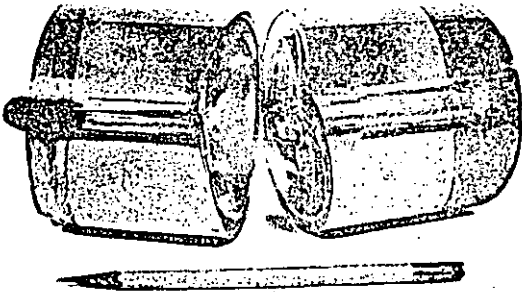
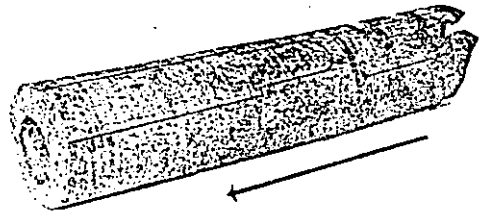
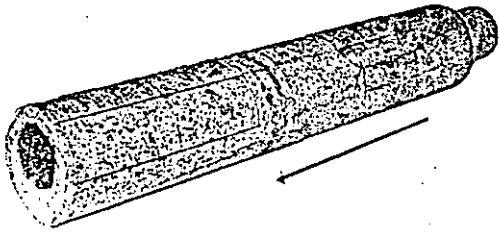
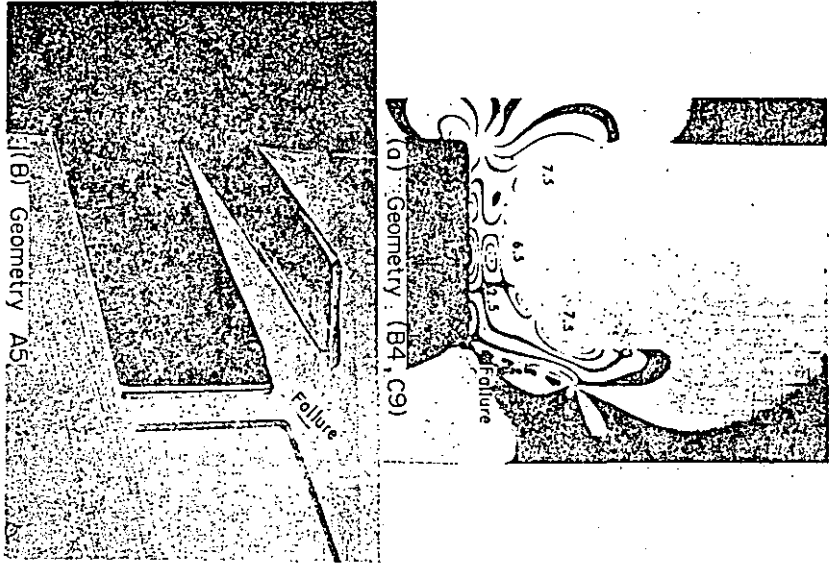


Fig. 15. Three-dimensional models loaded to failure.

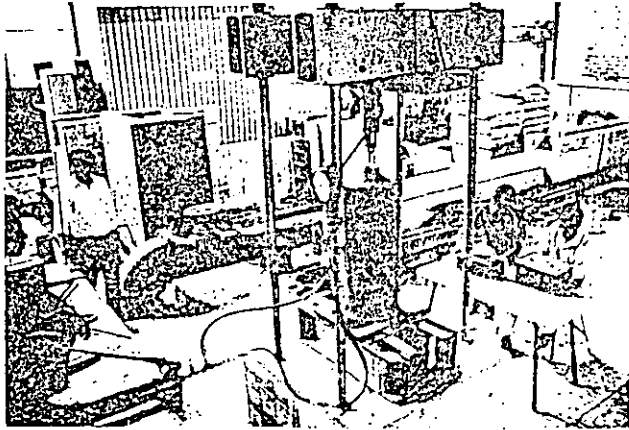


Fig. 16. Test set-up for the three-dimensional concrete models.

7.3. Geometric configuration C

For the models in this group, the plug studied had $L = 23/30D$, and fixed S . As in the previous case, a cavity whose diameter varied from $d = 0.2D$ to $d = D$ was introduced.

The stress distribution on both ends of the plug are shown on Fig. 11 for the geometric configuration C8.

Figure 10 shows the variation of the maximum tangential stress $(\sigma_{\theta})_{max}$ on both faces of the plug as a function of the cavity radius. As with the previous geometric figures, it can be observed that the maximum value for the tensile stress appears on the loaded side in the region of junction of the tunnel with the plug.

8. THE BIHEMISPHERICAL PLUG (GEOMETRIC CONFIGURATION D)

The evidence for the geometric figures previously studied, which shows that the maximum tensile stress consistently appeared on the loaded side in the region of the junction of the plug with the tunnel, led us to consider the need for geometry variations on the loaded side of the plug.

Due to the simplicity in its geometry, the bihemispherical one was chosen for this stage of the study.

In this case, both ends of the plug have a hemispherical cavity with $d = D$, varying only the effective width S .

The stress distributions for both ends of the plug are shown in Fig. 12.

Figure 13 shows the maximum tangential stress on the plug faces as a functional variation of the effective width S .

An interesting feature to be noticed is that for $S/D = 1$, the maximum tensile stress on the free surface of the plug is equal in magnitude to the hydrostatic pressure applied (p).

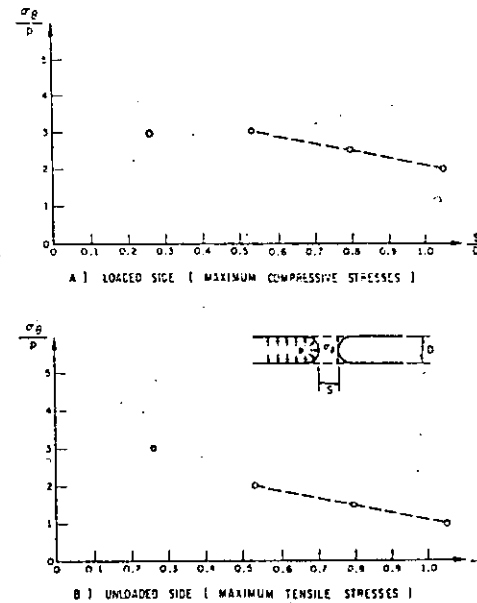
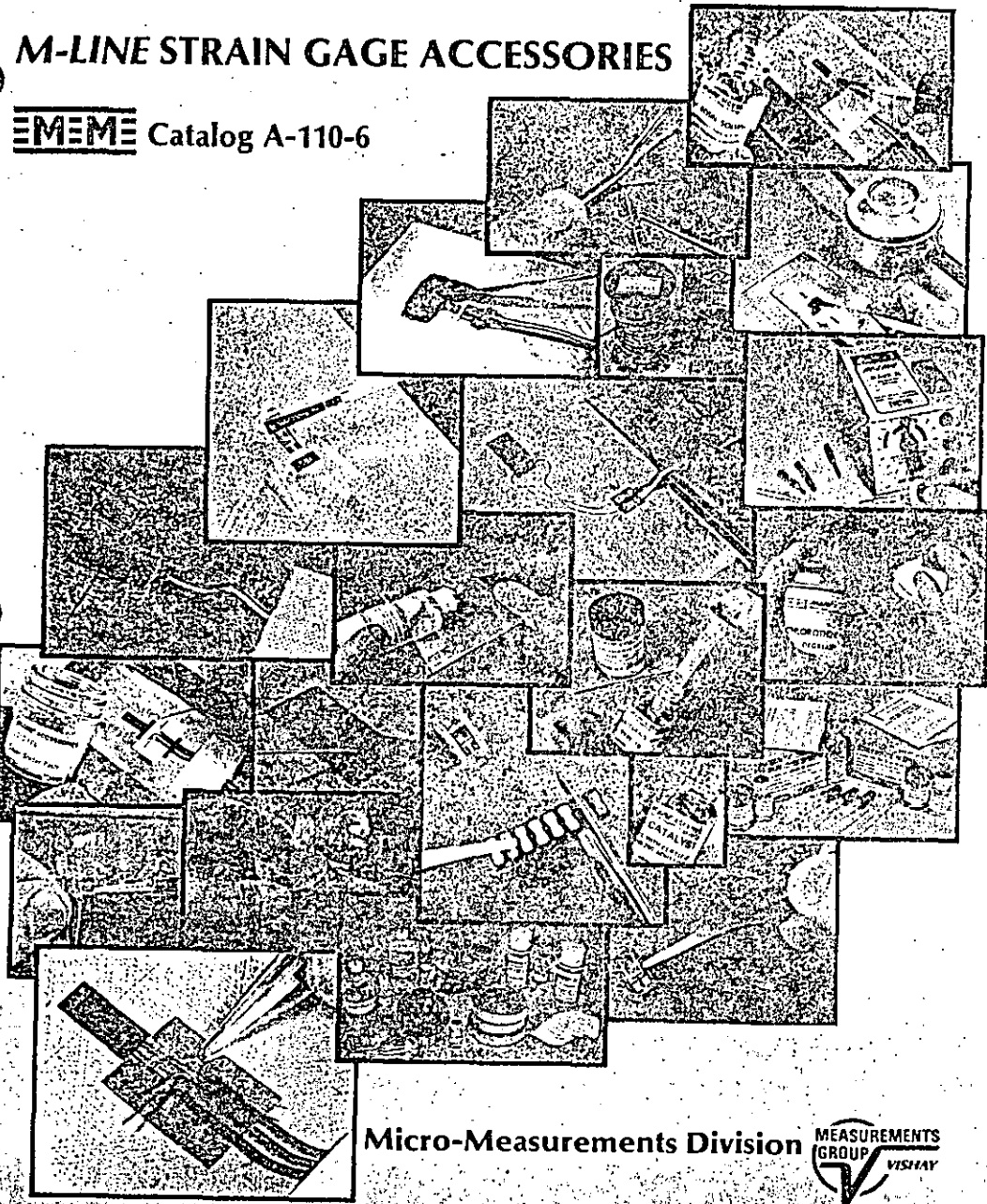


Fig. 13. Variations of the maximum tangential stress (σ_{θ}) as a function of the S/D ratio.

M-LINE STRAIN GAGE ACCESSORIES

MEME Catalog A-110-6



Micro-Measurements Division



INTRODUCTION

This catalog describes a wide range of accessories used for installation of electrical resistance strain gages. These accessories have been developed and selected specifically for their effectiveness and ease of use in making strain gage installations. They have also been carefully tested for their reliability and consistency of properties. The range of products offered in this catalog covers the full spectrum of typical gage installation requirements.

Making accurate and reliable strain gage measurements does not depend on the quality of the strain gage alone. The gage can perform to its fullest potential only if the installation is of comparable quality. To accomplish this requires strict adherence to the recommended installation procedure, including use of the proper accessory tools and supplies.

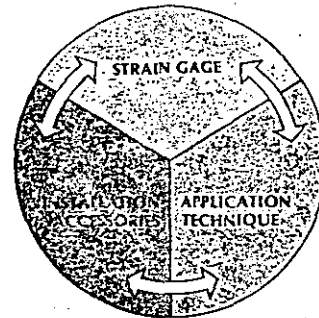
As shown in the accompanying diagram, there are three principal components in every strain gage installation: 1) the strain gage, 2) the tools, materials, and supplies (accessories) used in installing the gage, and 3) the techniques employed in performing the installation. The well-documented formula for making consistently successful strain gage installations is really very simple—

- select high quality, precision strain gages.
- select professional-caliber accessories, laboratory- and field-proven for effectiveness and compatibility with the strain gages.
- pay careful attention to the installation procedures recommended by the manufacturer of the gages and accessories.

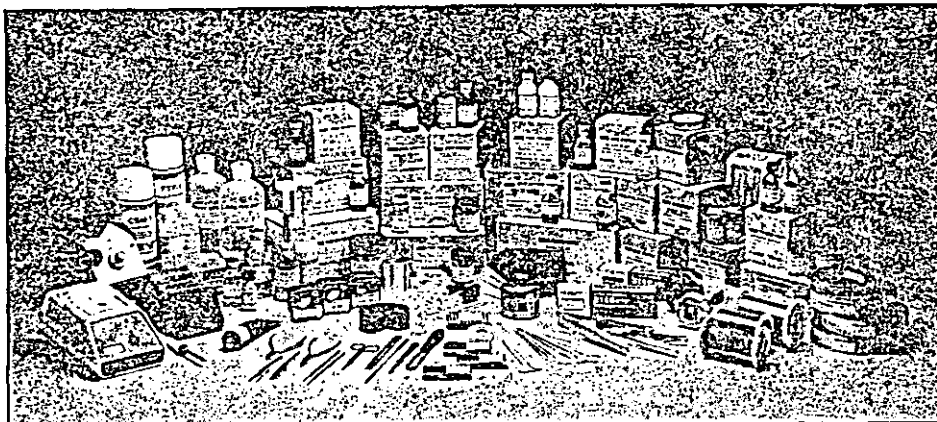
There are, as indicated by the double-ended arrows in the diagram, three sets of interface reactions—between the gage and accessories, between the gage and application techniques, and between the accessories and installation procedures.

Because technique is such an important ingredient in strain gage installation, *M-LINE* accessories are always accompanied by detailed instructions for their proper use. The importance of attention to detail, and of precise adherence to the application instructions supplied, cannot be overemphasized when installing strain gages.

Additionally, to help ensure your success in installing strain gages, Micro-Measurements maintains an experienced and highly trained Applications Engineering staff. Our Applications Engineers are as close as your telephone, and we urge you to call them for recommendations in the strain gage/accessory selection process, installation technique, or to discuss any problems you may encounter when using our products.



COMPONENTS OF A
STRAIN GAGE INSTALLATION



When a decision is made to purchase a strain gage, it is imperative that the appropriate accessories be most carefully selected to complement the quality installation of the strain gage. The chart on the next page is designed as a guide to help in the selection process.

To your convenience, in order to help you find the accessories you need, the catalog is divided into sections by type of accessory. The gages, adhesives, soldering supplies, wire, etc. In addition, the order forms sections in the catalog correspond generally to the order accessories used in making a strain gage installation. Thus, the first section is devoted to surface cleaning materials, then second to adhesive, and so on. A table of contents on page 4 and the associated color-coded index at the end of the page are intended to serve as a valuable guide to the catalog contents. Also included in the catalog is information on products and accessories for use in the strain gage installation process, including: portable welder for installing weldable strain gages and strain measuring instruments.

Each product entry in the catalog includes both the product description and its stock designation. Product selection guides and buy recommendations are also provided where applicable. Prices for all products in the catalog, along with further ordering information, are given in the Micro-Measurements Catalog A-100 Price List.

Remember, your success in making a reliable strain gage installation is important to us. Whenever you encounter any difficulty in the installation process, or are unsure of selecting the proper accessories for a given application, call our Applications Engineers at 1-800-451-7861.

(919) 365-3800

PLANNING FOR RELIABLE STRAIN GAGE INSTALLATIONS

SEQUENCE RELEVANT QUESTIONS AND CONSIDERATIONS

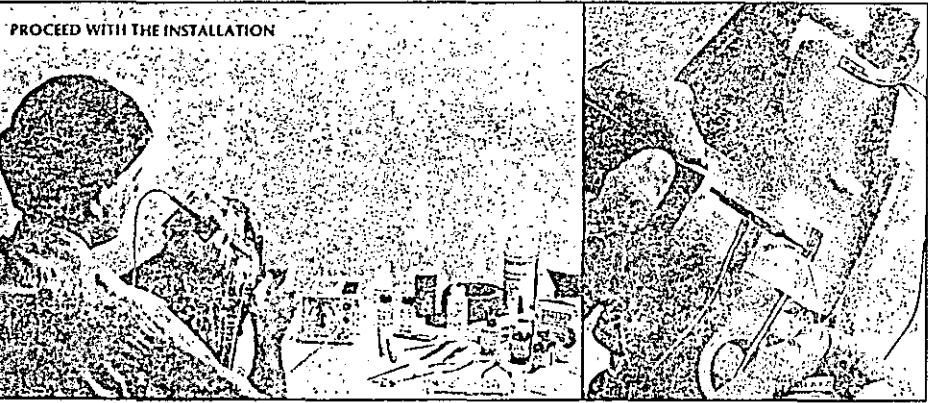
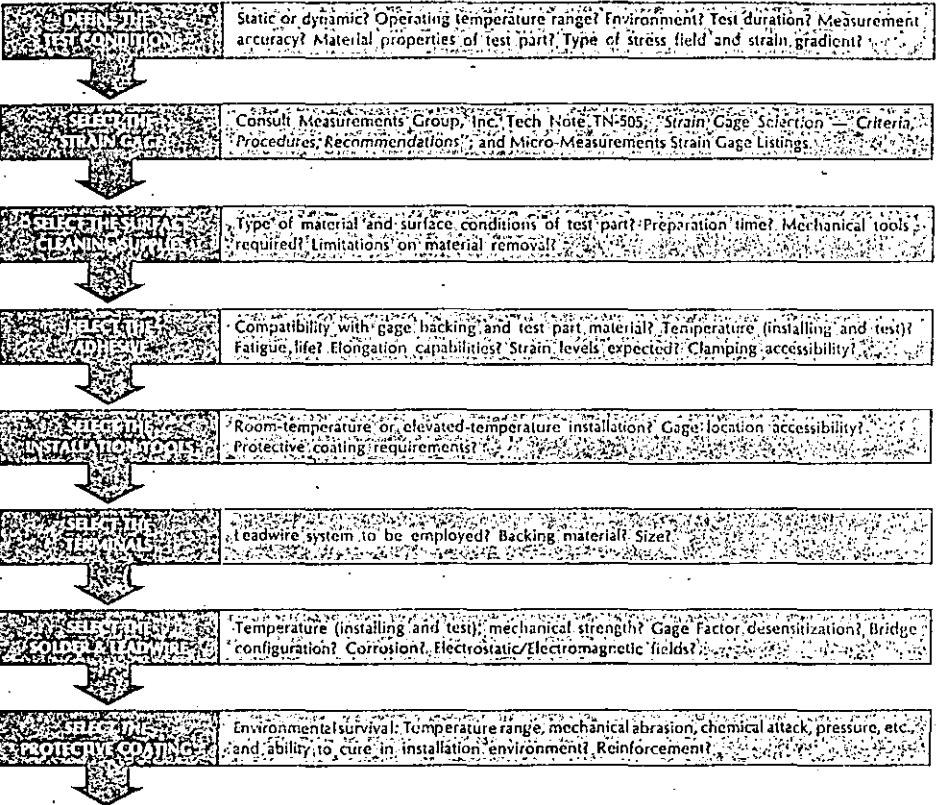


Table of Contents

Surface Cleaning Supplies

Adhesives

Installation Tools

Bondable Terminals

Soldering Supplies

Wire and Cable

Protective Coatings

Application Kits

Precision Resistors

Instrumentation and Special-Purpose Equipment

Training and Technical Support

M-PREP

SURFACE CLEANING SUPPLIES

For proper bonding of strain gages and temperature sensors, the workpiece surface must be chemically clean and totally free of contaminants before applying the adhesive. Recommended surface cleaning procedures for all common structural materials are described in Micro-Measurements Instruction Bulletin B-129, *Surface Preparation for Strain Gage Bonding*.

In the case of steel and aluminum parts with finish-machined or formed surfaces, the surface cleaning procedure can be summarized briefly as follows:

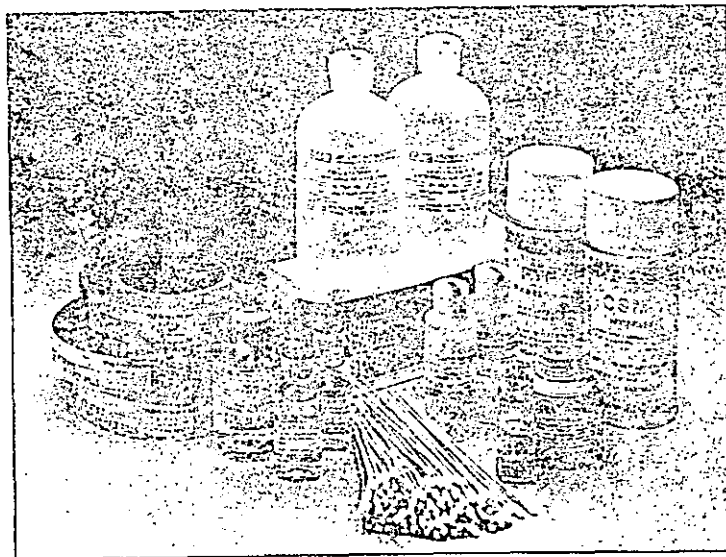
1. Removal of oily contaminants with a solvent cleaner. Note: Immersion of the workpiece in a degreaser is, by itself, inadequate; and, if done as a preliminary step, must be followed by cleaning with an uncontaminated solvent (one which is never returned to the container or otherwise reapplied after contact with the workpiece).

2. Light abrasion in the presence of a mildly acidic wash, to dislodge and remove oxides and mechanically bound contaminants.

3. Thorough surface scrubbing with an alkaline solution, to finish the cleaning process and leave the surface at the appropriate pH level for optimum bonding.

When the cleaning procedure is performed strictly according to the instructions in Bulletin B-129, and when the proper high-quality cleaning agents are used, the surface will be left in a condition best suited for bonding.

Described on the following page is a complete assortment of M-Prep cleaning supplies, compounded and selected specifically for surface preparation in the installation of strain gages and temperature sensors.



DESCRIPTION

PACKAGING INFORMATION

ORD
CO

SOLVENT CLEANERS

Degreaser: A powerful chlorinated hydrocarbon. Readily attacks general-purpose lubricating and hydraulic oils. Nonflammable.	12-oz (0.35-kg) pressurized spray can. <i>Dispensing solvents from "one-way" containers prevents contamination buildup.</i>	CSN
Isopropyl Alcohol: Frequently used as a solvent degreaser where chlorinated solutions are restricted, such as with most plastics. Flammable.	4-oz (120-ml) bottle.	GC

WATER-BASED CLEANERS

<i>Final surface preparation for most materials is accomplished with M-Prep Conditioner A immediately followed by M-Prep Neutralizer 5A.</i>		
Conditioner A: A mild phosphoric acid compound. Acts as a mild etchant and accelerates the cleaning process.	*2-oz (60-ml) plastic squeeze bottle with on/off dispenser nozzle cap.	MCA
	16-oz (0.5-l) plastic squeeze bottle with on/off dispenser nozzle cap.	MCA
Neutralizer 5A: An ammonia-based material. Neutralizes any chemical reaction introduced by the Conditioner A, and produces optimum surface conditions for most strain gage adhesion.	*2-oz (60-ml) plastic squeeze bottle with on/off dispenser nozzle cap.	MNS
	16-oz (0.5-l) plastic squeeze bottle with on/off dispenser nozzle cap.	MNS
*Note: The 2-oz (60-ml) size is recommended for bench use and is easily refilled from the 16-oz (0.5-l) bottle.		

SURFACE ABRASION MATERIALS

<i>Abrading is often necessary to dislodge contaminants and to remove rust, scale, etc. When grit-blasting is necessary, use fine alumina powder and high-quality filters, and never recycle used grit. In general, wet-or-dry silicon-carbide paper is most convenient.</i>		
Wet-or-Dry Silicon-Carbide Paper: 220- and 320-grit: Suited to most steels. 320- and 400-grit: Suited to aluminum alloys and other soft metals.	220 grit, 1-in-x-100-ft (25-mm-x-30-m) roll	SCP-1
	320 grit, 1-in-x-100-ft (25-mm-x-30-m) roll	SCP-2
	400 grit, 1-in-x-100-ft (25-mm-x-30-m) roll	SCP-3
Pumice Powder: Produces a dull, matte finish. Recommended for minimal removal of surface material.	1/2-oz (15-ml) bottle	GC

SPECIAL-PURPOSE MATERIALS

M-LINE Rosin Solvent: Used for removal of rosin soldering flux residue. (Does not contain halogens.)	Kit — 12 1-oz (30-ml) brush-cap bottles	RSK-1
Tetra-Etch Compound: Used for etching Teflon® to render the surface bondable.	2-oz (60-ml) can	TEC-1
Cotton Swabs	100 single-ended applicators per package [6-in (150-mm) long, wooden stick]	CSP-1
Gauze Sponges	200 3-x-3-in (75-x-75-mm) sponges per package	CSP-2

M-BOND STRAIN GAGE ADHESIVES

Because a strain gage can perform no better than the adhesive with which it is bonded to the test member, the adhesive is a vitally important component in every strain gage installation. Although there is no single adhesive which is ideally suited to all applications, Micro-Measurements offers a wide selection of adhesives to cover the spectrum of stress analysis testing, and for use in transducer manufacturing. Micro-Measurements adhesives are specially formulated for highest performance under the recommended environmental conditions, and are packaged to provide the user with maximum control in mixing and application.

Each adhesive is accompanied by specific instructions for its proper handling—storage, mixing, application, curing, and, if appropriate, post-curing. The adhesive containers are also dated to assure freshness of the contents.

Note: It is usually misguided economy to attempt installing strain gages with outdated adhesive, or adhesive that has not been stored as recommended. It should also be noted that conventional industrial and consumer adhesives are not generally suitable for bonding strain gages.

BASIC STRAIN GAGE ADHESIVES

Since different adhesives are intended for different types of applications and different environmental conditions, it is obviously important to select the most appropriate adhesive for each strain measurement task. The table at right lists all of the Micro-Measurements M-Bond adhesives in their order of popularity and ease of use, while the table on the facing page is provided as a guide for selecting the most appropriate adhesive for compatibility with a particular strain gage series and test environment.

For the majority of applications, gages will be installed with one of the six basic adhesives shown in the table at right—with the choice depending primarily on the relative weights given to the ease of and speed of application versus performance and resistance to environmental extremes. When the application requires it, selection can be made from among the six special-purpose adhesives described.

TYPE	PRINCIPAL FEATURES
200	Most widely used general-purpose adhesive. Easiest to handle. Fast room-temperature curing.
AE-10	General-purpose adhesive that is highly resistant to moisture and most chemicals. Room-temperature curing.
AE-15	Similar to AE-10. Recommended for more critical applications, including transducer gaging. Elevated-temperature curing.
610	Used primarily in applications over wide temperature range. Widely used in transducer gaging. Elevated-temperature curing.
600	Similar to 610, but faster reacting. Can be cured at lower temperatures than 610.
43-B	Normally used in transducer gaging. Highly resistant to moisture and chemical attack. Elevated-temperature curing.

SPECIAL-PURPOSE ADHESIVES

GA-2	General-purpose adhesive primarily used on very rough or irregular surfaces. Room-temperature curing.
GA-61	Similar to GA-2, but more viscous. Also used to fill irregular surfaces and to anchor leadwires. Elevated-temperature curing.
GA-100	Ceramic cement for use with special design strain gages operating at high temperatures. Elevated-temperature curing.
A-12	Very high elongation adhesive. Used only when other adhesives cannot meet elongation requirements. Elevated-temperature curing.
300	Polyester adhesive used primarily when low-temperature curing is required. Sensitive to solvents. Not recommended as a general-purpose adhesive.
450	High-performance epoxy for high-temperature transducer applications.

The two most important considerations for proper adhesive selection are compatibility with the backing material of the strain gage and the operating temperature range over which the bond is expected to perform.

To assist you in your selection, the chart below defines the recommended adhesive(s) for use with a particular strain gage series over various operating temperature ranges. When more than one adhesive is listed for a particular gage/test condition, preference would be given to that adhesive which is easiest to apply while still meeting all of the other performance criteria.

In addition to the primary adhesive selection criteria presented here, other factors (such as test time duration, cyclic endurance required, and accuracy required) may have to be considered in the test profile. Factors such as these are addressed in Measurements Group, Inc. Tech Note TN-505, *Strain Gage Selection—Criteria, Procedures, Recommendations*. There are also many times when the interaction of test characteristics is too complex for selecting the proper adhesive from a chart with a high degree of confidence. In these cases, we suggest that you contact our Applications Engineering Department for recommendations.

RECOMMENDED ADHESIVES FOR DIFFERENT STRAIN GAGE SERIES

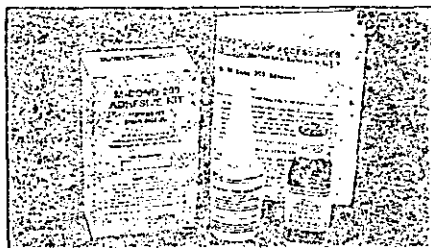
TYPE OF TEST OR APPLICATION	OPERATING TEMPERATURE RANGE	M-M GAGE SERIES	M-BOND ADHESIVE
General Static or Static-Dynamic Stress Analysis	-50° to +150°F (-45° to +65°C)	CFA, FA	200 or AE-10 or AE-15
	-50° to +100°F (-45° to +205°C)	WA, SA, WK, SK	AE-15 or 610
	-452° to +450°F (-269° to +239°C)	WK, SK	610
	<600°F (<315°C)	WK	610
High Elongation (Post-Yield)	-50° to +150°F (-45° to +65°C)	CEA, EA	200 or AE-10
		EP	AE-15 or A-12
Dynamic (cyclic) Stress Analysis	-100° to +150°F (-75° to +65°C)	ED	200 or AE-10
		WD	AE-10 or AE-15
Transducer Gaging	-320° to +500°F (-195° to +260°C)	WD	600 or 610
	-50° to +150°F (-45° to +65°C)	CEA, EA	AE-10 or AE-15
	-50° to +200°F (-45° to +95°C)	N2A, J2A	600 or 610 or 43-B
	-50° to +300°F (-45° to +150°C)	WA, SA, TA, TK, JSK	610, 450
	-320° to +350°F (-195° to +175°C)	WK, SK, TK, JSK	610, 450

On the following pages is a complete guide to M-Bond adhesives, detailing specific characteristics and further application considerations for each type.

M-BOND 200

For routine experimental stress analysis applications under temperate environmental conditions, M-Bond 200 adhesive is ordinarily the best choice. This adhesive is very easy to handle, and cures almost instantly to produce an essentially creep-free, fatigue-resistant bond, with elongation capability of five percent or more.

M-Bond 200 is a special cyanoacrylate which has been pretested and certified for use in bonding strain gages. It is an excellent general-purpose adhesive for laboratory and short-term field applications. The procedure for installing a strain gage with



ORDERING INFORMATION

KIT: (as shown above) 1 bottle (1 oz./28 g) Adhesive
1 brush-cap bottle (30 ml) Catalyst
polyethylene dispenser cap

BULK: Adhesive—16 bottles (1 oz./28 g each)
Catalyst—12 brush-cap bottles (30 ml each)

M-Bond 200 is summarized in the illustrations below, and described in detail in Micro-Measurements Instruction Bulletin B-127, a copy of which accompanies each kit of adhesive.

The user should note that the performance of the adhesive can be degraded by the effects of time, humidity conditions, elevated temperature, and moisture absorption. Because of the latter effect, strain gage installations should always be covered with a suitable protective coating. When necessitated by more rigorous test requirements and/or environmental conditions, consideration should be given to one of the epoxy adhesives described on the following pages, using the chart on page 7 as a guide in making the selection.

CHARACTERISTICS

CURE REQUIREMENTS

One-minute thumb pressure, followed by a minimum two-minute delay before tape removal. Bond strength increases rapidly during first five minutes. Cure time must be extended under conditions of low temperature (<50°F (<10°C)) or low humidity (<40%RH).

OPERATING TEMPERATURE RANGE

SHORT TERM: -300° to +200°F (-185° to +95°C)
LONG TERM: -25° to +150°F (-32° to +65°C)

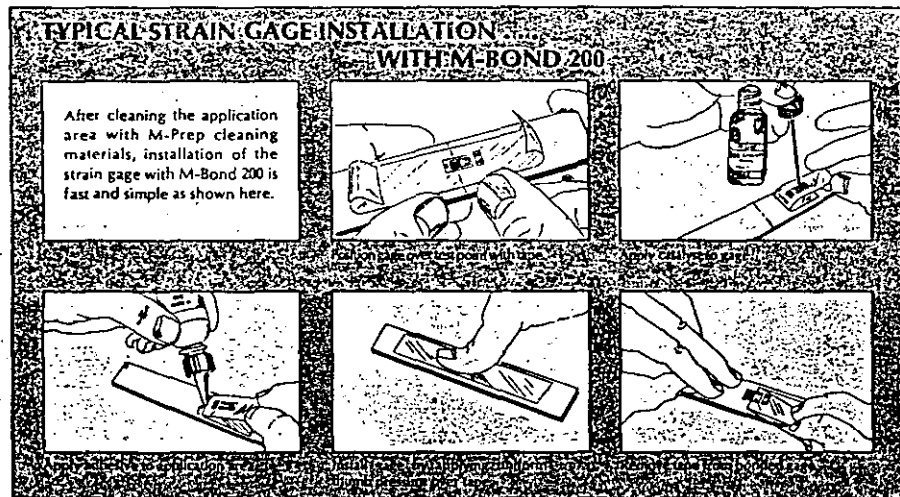
ELONGATION CAPABILITIES

>6% at +75°F (+24°C), [3% at +75°F (+24°C) when used with CEA- or EA-/Option E strain gages].

SHELF LIFE*

6 mo at +75°F (+24°C). (After opening and properly sealing after each application.)

9 mo at +75°F (+24°C); 12 mo at +40°F (+5°C)
(unopened adhesive only)

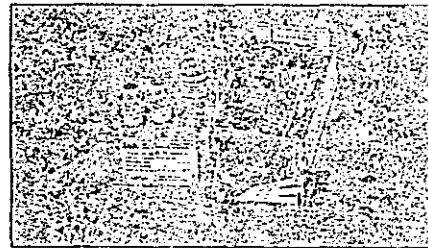


*Shelf life refers to the duration of time, beginning on date of shipment, over which the item, when properly stored, should be expected to meet published specifications.

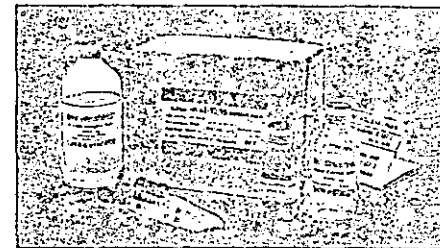
M-BOND AE-10/15

Two-component, 100%-solid epoxy system for general-purpose stress analysis. Transparent, medium viscosity. With AE-10, a cure time as low as six hours at +75°F (+24°C) may be used; with AE-15, as low as six hours at +125°F (+50°C). AE-15 is recommended for more critical applications, including transducers. It has a longer pot life than AE-10 which allows more time for multiple gage installations. For both AE-10/15 resin

systems, elevated-temperature postcure is recommended for maximum stability, and/or tests above room temperature. Both adhesives are highly resistant to moisture and most chemicals, particularly when postcured. For maximum elongation, bonding surface must be rough. Cryogenic applications require very thin gluelines.



Kit: 6 mixing jars (10 g ea) Resin • 1 bl (15 ml) Curing Agent 10
1 bl (15 ml) Curing Agent 15 • 3 calibrated pipettes
6 stirring rods



Bulk: 200 g Resin • 40 g Curing Agent 10
25 g Curing Agent 15 • 3 calibrated pipettes

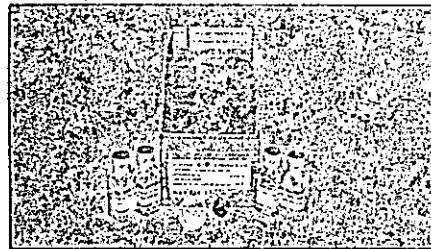
CHARACTERISTICS

	AE-10	AE-15
OPERATING TEMPERATURE RANGE	LONG TERM: -320° to +200°F (-195° to +95°C)	LONG TERM: -452° to +200°F (-269° to +95°C) TRANSDUCERS: to +175°F (+80°C)
ELONGATION CAPABILITIES	• 3% at -320°F (-195°C) • 6% to 10% at +75°F (+24°C) • 15% at +200°F (+95°C)	• 2% at -320°F (-195°C) • 10% to 15% at +75°F (+24°C) • 15% at +200°F (+95°C)
SHELF LIFE	12 mo at +75°F (+24°C); 18 mo at +20°F (-7°C) If crystals form in resin bottle, heat to +120°F (+50°C) for 30 minutes. Cool before mixing.	Same
POT LIFE	15 to 20 minutes at +75°F (+24°C) Can be extended by cooling air or by spreading adhesive on clean aluminum plate.	1-1/2 hr at +75°F (+24°C)
CLAMPING PRESSURE	5 to 20 psi (35 to 140 kN/m ²)	Same
CURE REQUIREMENTS	<p>PREFERRED ROOM-TEMPERATURE CURE 24 hr at +75°F (+24°C) RECOMMENDED POSTCURE 2 hr at 25° (75°C) above max. operating temp.</p>	<p>RECOMMENDED POSTCURE 1 hr at 25° (75°C) above max. operating temp. OPTIMUM PERFORMANCE TRANSDUCER POSTCURE 1 hr at +200°F (+95°C)</p>

References: M-M Instruction Bulletin B-137, Strain Gage Applications with M-Bond AE-10/15 and M-Bond GA-2 Adhesive Systems.

M-BOND 610

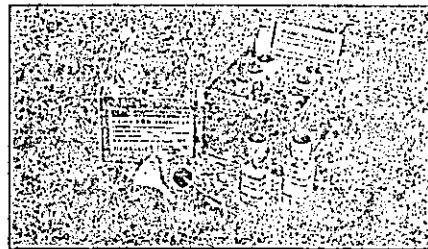
Two-component, solvent-thinned, epoxy-phenolic adhesive for high-performance applications, including high-precision transducers. Solids content 22%. Widest temperature range general-purpose adhesive available. Low viscosity, capable of glue-lines $\lt; 0.0002\text{ in } (0.005\text{ mm})$. Extremely thin, hard, void-free glue-lines minimize creep, hysteresis, and linearity problems. Life limited by oxidation and sublimation effects at elevated temperatures.



Kit: 4 bottles (11 g ea) Curing Agent
4 bottles (14 g ea) Resin
4 brush caps for dispensing mixed adhesive
4 disposable mixing funnels

M-BOND 600

Similar to M-Bond 610 except with more reactive curing agent. Shorter shelf life, pot life, and working time than M-Bond 610, but has lower temperature cures and faster reaction time. Cure must begin within 30 minutes of application (up to 10 hr for M-Bond 610).



Kit: 4 bottles (11 g ea) Curing Agent
4 bottles (8 g ea) Resin
4 brush caps for dispensing mixed adhesive
4 disposable mixing funnels

CHARACTERISTICS

610

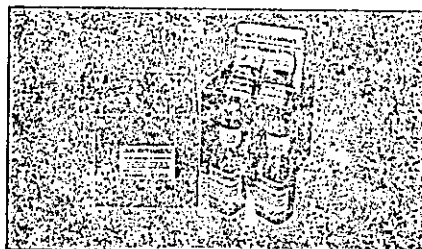
600

OPERATING TEMPERATURE RANGE	SHORT TERM: -452° to $+700^{\circ}\text{F}$ (-269° to $+370^{\circ}\text{C}$) LONG TERM: -452° to $+500^{\circ}\text{F}$ (-269° to $+260^{\circ}\text{C}$) TRANSDUCERS: to $+450^{\circ}\text{F}$ ($+230^{\circ}\text{C}$)	SHORT TERM: -452° to $+700^{\circ}\text{F}$ (-269° to $+370^{\circ}\text{C}$) LONG TERM: -452° to $+500^{\circ}\text{F}$ (-269° to $+260^{\circ}\text{C}$)
ELONGATION CAPABILITIES	<ul style="list-style-type: none"> • 1% at -452°F (-269°C) • 3% at $+75^{\circ}\text{F}$ ($+24^{\circ}\text{C}$) • 3% at $+500^{\circ}\text{F}$ ($+260^{\circ}\text{C}$) 	Same
SHELF LIFE	9 mo at $+75^{\circ}\text{F}$ ($+24^{\circ}\text{C}$); 15 mo at $+40^{\circ}\text{F}$ ($+5^{\circ}\text{C}$)	3 mo at $+75^{\circ}\text{F}$ ($+24^{\circ}\text{C}$); 9 mo at $+40^{\circ}\text{F}$ ($+5^{\circ}\text{C}$)
POT LIFE	6 wk at $+75^{\circ}\text{F}$ ($+24^{\circ}\text{C}$); 11 wk at $+40^{\circ}\text{F}$ ($+5^{\circ}\text{C}$)	2 wk at $+75^{\circ}\text{F}$ ($+24^{\circ}\text{C}$); 4 wk at $+40^{\circ}\text{F}$ ($+5^{\circ}\text{C}$)
CLAMPING PRESSURE	10 to 70 psi (70 to 490 kN/m ²) 30 to 40 psi optimum (200 to 275 kN/m ²)	Same
CURE REQUIREMENTS	<p>GLUELINE TEMPERATURE IN $^{\circ}\text{C}$</p> <p>RECOMMENDED POSTCURE: 2 hr at 50° to 75°C (20 to 40°C) above operating temp. or cure temp., whichever is higher. HIGH PRECISION TRANSDUCER POSTCURE: 1 hr at $+400^{\circ}$ to $+450^{\circ}\text{F}$ ($+200^{\circ}$ to $+230^{\circ}\text{C}$) after curing.</p>	<p>GLUELINE TEMPERATURE IN $^{\circ}\text{C}$</p> <p>MODERATELY ELEVATED TEMPERATURE CURE REQUIRED: 1 hr at 50° to 75°C (20 to 40°C) above max operating temp. RECOMMENDED POSTCURE: 1 hr at 50° to 75°C (20 to 40°C) above max operating temp.</p>

References: M-M Instruction Bulletin B-130, Strain Cage Installations with M-Bond 43-B, 600 and 610 Adhesive Systems.

M-BOND 43-B

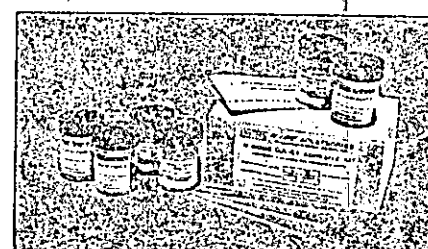
Single-component, solvent-thinned, epoxy adhesive normally used in transducer applications; solids content 25%. May be used both as an adhesive and as a protective coating. Capable of forming very thin, hard, void-free glue-lines similar to M-Bond 610. Highly resistant to moisture and chemical attack.



Kit: 4 brush-cap bottles (30 ml ea) premixed adhesive

M-BOND GA-61

Two-component, partially filled, 100%-solids epoxy adhesive for general-purpose stress analysis. Very high viscosity. Widely used to fill irregular surfaces and to anchor leadwires. Forms a very hard, chemical-resistant material when fully cured. Glue-line thickness is generally $\lt; 0.002\text{ in } (0.05\text{ mm})$.



Kit: 3 jars (10 g ea) Resin
3 jars (5 g ea) Hardener
3 stirring rods

CHARACTERISTICS

43-B

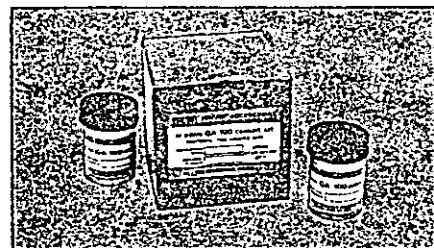
GA-61

OPERATING TEMPERATURE RANGE	SHORT TERM: -452° to $+350^{\circ}\text{F}$ (-269° to $+175^{\circ}\text{C}$) LONG TERM: -452° to $+300^{\circ}\text{F}$ (-269° to $+150^{\circ}\text{C}$) TRANSDUCERS: to $+250^{\circ}\text{F}$ ($+120^{\circ}\text{C}$)	SHORT TERM: -100° to $+600^{\circ}\text{F}$ (-75° to $+315^{\circ}\text{C}$) LONG TERM: -100° to $+500^{\circ}\text{F}$ (-75° to $+260^{\circ}\text{C}$) TRANSDUCERS: to $+250^{\circ}\text{F}$ ($+120^{\circ}\text{C}$)
ELONGATION CAPABILITIES	<ul style="list-style-type: none"> • 1% at -452°F (-269°C) • 4% at $+75^{\circ}\text{F}$ ($+24^{\circ}\text{C}$) • 7% at $+300^{\circ}\text{F}$ ($+150^{\circ}\text{C}$) 	<ul style="list-style-type: none"> • 1% at -100°F (-75°C) • 2% at $+75^{\circ}\text{F}$ ($+24^{\circ}\text{C}$) • 1% at $+500^{\circ}\text{F}$ ($+260^{\circ}\text{C}$)
SHELF LIFE	9 mo at $+75^{\circ}\text{F}$ ($+24^{\circ}\text{C}$); 18 mo at $+40^{\circ}\text{F}$ ($+5^{\circ}\text{C}$)	12 mo at $+75^{\circ}\text{F}$ ($+24^{\circ}\text{C}$); 18 mo at $+40^{\circ}\text{F}$ ($+5^{\circ}\text{C}$)
POT LIFE	9 mo at $+75^{\circ}\text{F}$ ($+24^{\circ}\text{C}$); 18 mo at $+40^{\circ}\text{F}$ ($+5^{\circ}\text{C}$)	10 hr at $+75^{\circ}\text{F}$ ($+24^{\circ}\text{C}$); increased by refrigeration
CLAMPING PRESSURE	15 to 100 psi (100 to 700 kN/m ²) 40 to 50 psi (275 to 350 kN/m ²) optimum	10 to 30 psi (70 to 200 kN/m ²)
CURE REQUIREMENTS	<p>GLUELINE TEMPERATURE IN $^{\circ}\text{C}$</p> <p>MINIMUM: 2 hr at 250°F (125°C) RECOMMENDED: 1 hr at 375°F (190°C) RECOMMENDED FOR TRANSDUCER POSTCURE: 2 hr at 400°F (205°C)</p>	<p>GLUELINE TEMPERATURE IN $^{\circ}\text{C}$</p> <p>ELEVATED TEMPERATURE CURE REQUIRED: 1 hr at 50° to 75°C (20 to 40°C) above max operating temp. not to exceed $+400^{\circ}\text{F}$ ($+215^{\circ}\text{C}$)</p>

References: M-M Instruction Bulletin B-130, Strain Cage Installations with M-Bond 43-B, 600, and 610 Adhesive Systems.
M-M Instruction Bulletin B-128, Strain Cage Applications with M-Bond GA-61 Adhesive.

M-BOND GA-100

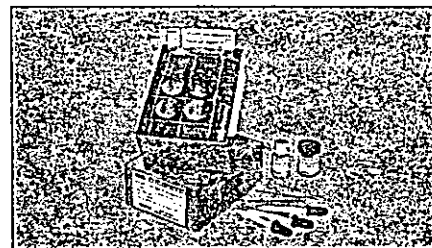
Single-component, ceramic cement. Principal ingredients aluminum phosphate and silica. Primarily used with free-film strain gages above +600°F (+315°C). Difficult to use without prior experience. Leakage to ground resistance with a >0.0012 in (0.03 mm) base coat is >10⁶ ohms at +1200°F (+650°C), and >0.3 x 10⁶ ohms at +1400°F (+760°C). Must be cured in air. Very hygroscopic.



Kit: 2 jars (25 g ea) premixed ceramic cement

M-BOND GA-2

Two-component, partially filled, 100%-solids epoxy system for general-purpose stress analysis. Higher viscosity than AE systems. Elevated-temperature cure recommended for best performance and resistance to chemical attack. Often used to fill irregular surfaces. Uneven glue lines easily detectable by non-uniformity of bond color.



Kit: 6 mixing jars (15 g ea) Resin • 6 calibrated pipettes
1 bl (15 ml) Curing Agent 10-A • 6 stirring rods

CHARACTERISTICS

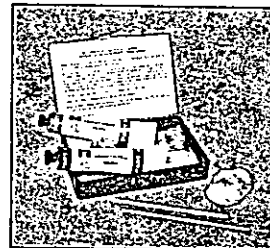
GA-100

GA-2

OPERATING TEMPERATURE RANGE	SHORT TERM: -452° to +1500°F (-269° to +815°C) LONG TERM: -452° to +1300°F (-269° to +705°C)	LONG TERM: -320°F to +200°F (-195° to +95°C)
ELONGATION CAPABILITIES	Approximately 0.5% depending on linear expansion coefficient of specimen material	• 4% at -320°F (-195°C) • 10% to 15% at +75°F (+24°C) after 40 hr RT cure or 6 hr RT cure with postcure • 15% to 20% at +200°F (+95°C)
SHELF LIFE	12 mo at +75°F (+24°C)	12 mo at +75°F (+24°C); 18 mo at +20°F (-7°C)
POT LIFE	1 day continuous use (Keep covered when not in actual use)	15 min at +75°F (+24°C) Can be extended by cooling jar or by spreading adhesive on clean aluminum plate
CLAMPING PRESSURE	None	5 to 20 psi (35 to 140 kN/m ²) The black filler provides a visual indication of non-uniform bond areas caused by uneven clamping pressure
CURE REQUIREMENTS	<p>PRECOAT: 15 min at +350°F (+175°C)</p> <p>FINAL: 60 min at +600°F (+315°C)</p> <p>Recommended max. heat increase rate from room temperature to +275°F (+135°C) is +200°F (+110°C) per hour</p>	<p>PREFERRED ROOM-TEMPERATURE CURE: 40 hr at +75°F (+24°C)</p> <p>RECOMMENDED POSTCURE: 2 hr at 25°F (15°C) above max. operating temp.</p>

M-BOND A-12

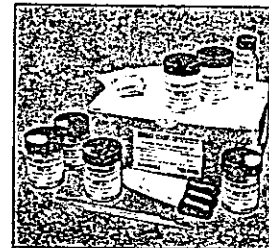
Two-component, 100%-solids epoxy system. Not intended as a general-purpose strain gage adhesive. Should be used only when maximum elongation requirements of a test exceed the capabilities of other M-Bond adhesive systems. Mixed adhesive gritty with large solid particles present; large particles must be removed prior to gage installation.



Kit: 1 tube each Part A and Part B
5 disposable mixing cups
5 wood stirring sticks

M-BOND 300

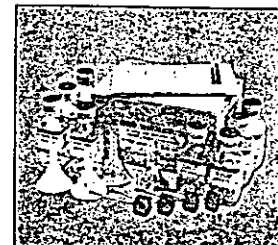
Special-purpose, two-component polyester adhesive. Not recommended as a general-purpose strain gage adhesive, but useful when a low-temperature-curing adhesive is required. While possessing the high shear strength required of a strain gage adhesive, peel strength and solvent sensitivity are relatively poor. Should not be used for impact strain measurements, or with solvent-thinned protective coatings.



Kit: 6 mixing jars (10 g ea) Resin
6 calibrated pipettes
1 bl (6 g) Catalyst
6 stirring rods

M-BOND 450

High-performance, two-component, solvent-thinned epoxy system specially formulated for high accuracy, elevated temperature transducer applications. M-Bond 450 is compatible with all Micro-Measurements strain gage series.



Kit: 4 bls (12.5 g ea) Curing Agent
4 bls (12.5 g ea) Resin
4 brush caps for applying adhesive
4 disposable mixing funnels

CHARACTERISTICS

A-12

300

450

OPERATING TEMPERATURE RANGE	LONG TERM: -50° to +180°F (-45° to +80°C)	LONG TERM: -40° to +300°F (-40° to +150°C)	SHORT TERM: -452° to +750°F (-269° to +400°C) LONG TERM: -452° to +500°F (-269° to +260°C)
ELONGATION CAPABILITIES	15% to 20% at +75°F (+24°C)	1 to 2% at +75°F (+24°C)	>5% at +75°F (+24°C)
SHELF LIFE	1 yr at +75°F (+24°C)	4 mo at +75°F (+24°C)	6 mo at +75°F (+24°C)
POT LIFE	Approximately 1 hr	15 to 20 min at +40°F (+5°C) 5 to 8 min at +75°F (+24°C)	6 wk at +75°F (+24°C)
CLAMPING PRESSURE	5 to 20 psi (35 to 140 kN/m ²)	5 to 20 psi (35 to 140 kN/m ²)	60 to 100 psi (415 to 690 kN/m ²)
CURE REQUIREMENTS	2 hr at +165°F (+75°C) or 2 weeks at +75°F (+24°C)	24 hrs at +40°F (+5°C) or 18 hrs at +60°F (+15°C) or 12 hrs at +75°F (+24°C)	<p>STEP 1: Air dry at +75°F (+24°C) 10 to 30 min</p> <p>B-STAGE: +225°F (+105°C) for 30 min</p> <p>CURE: +350°F (+175°C) for 1 hr</p> <p>RECOMMENDED POSTCURE: 1 hr at 50°F (30°C) above max. operating temp. in 50°F (30°C) increments from +350°F (+175°C), dwelling 1 hr at each step.</p>

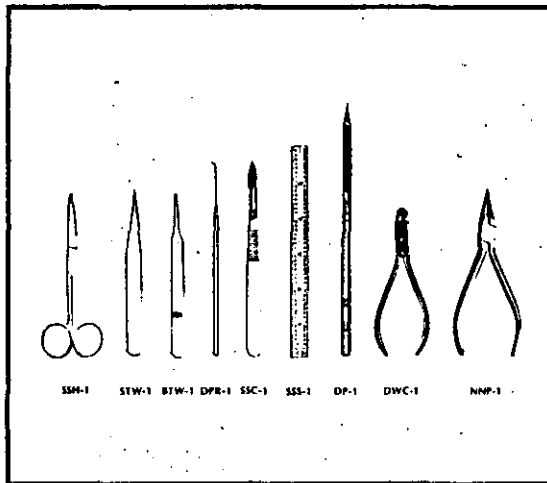
Note: Application instructions for M-Bond A-12 are included in each kit.
References: M-M Instruction Bulletin B-133, Strain Gage Installations with M-Bond 300 Adhesive.
M-M Instruction Bulletin B-152, Instructions for the Application of Micro-Measurements M-Bond 450 Adhesive.

References: M-M Instruction Bulletin B-132, Strain Gage Installations with M-Bond GA-100 Cement.
M-M Instruction Bulletin B-137, Strain Gage Applications with M-Bond AE-10/15 and M-Bond GA-2 Adhesive Systems.

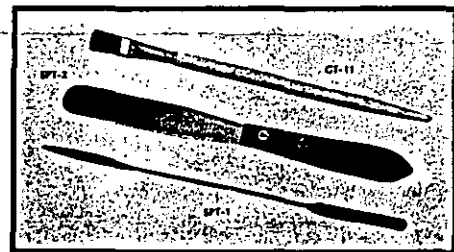
INSTALLATION TOOLS & ACCESSORIES

There is a strong element of craftsmanship involved in making consistently successful strain gage installations. As for any other field, this craft has its own special tools and working materials—found by seasoned professionals to be most effective for achieving the desired results. The installation accessories described on this and the following page represent the distillation of many years' experience in determining the most appropriate tool or material for each task in the gage installation process.

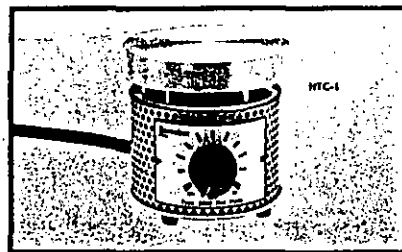
Every accessory item listed here has been thoroughly tested and evaluated in the Measurements Group Applications Engineering Laboratory for quality and reliability, for ease of use, and for compatibility with all other Micro-Measurements products. It should be noted that the instruction bulletins supplied for gages, adhesives, protective coatings, etc. assume the availability of these accessories to the user, since such is generally the case for an experienced practitioner in a well-equipped laboratory.



- SSH-1 **SURGICAL SHEARS** — Chromium steel, 4-1/2 in (115 mm) long, with one sharp pointed blade and one blunt-end blade.
- STW-1 **TWEEZERS** — Stainless steel, 4-1/2 in (115 mm) long. Rugged, precision ground. Primarily used for handling leadwires.
- BTW-1 **TWEEZERS** — Stainless steel, 4-1/2 in (115 mm) long. Antimagnetic; acid and corrosion resistant. Thin, flat blunt ends ideal for safe handling of strain gages.
- DPR-1 **DENTAL PROBE** — Stainless steel "pick". Flexible 75° pointed tip.
- SSC-1 **SURGICAL SCALPEL AND BLADE** — Stainless steel, uses SSC-2 snap-in replacement blade.
- SSC-2 **REPLACEMENT SCALPEL BLADES** — Five/package.
- SSS-1 **STEEL SCALE** — 6 in (150 mm) long, satin-chromed finish. Graduated in inches — 1/32, 1/64, 1/10, 1/100.
- DP-1 **4-H DRAFTING PENCIL** — for gage layout.
- DWC-1 **DIAGONAL CUTTERS** — Nickel-chrome plated, 4-1/2 in (115 mm) long, precision cutter for wire up to AWG No. 18 (1 mm) diameter.
- NNP-1 **NEEDLE-NOSED PLIERS** — Nickel-chrome plated, 4-1/2 in (115 mm) long, with serrated needle-nosed jaws.
- ATS-2 **GAGE APPLICATION TOOL SET** — Includes one of each item plus one additional DPR-1 Dental Probe, and one pkg SSC-2. Durable, polypropylene box.



- GT-11 **CAMEL'S HAIR BRUSH** — 3/8 in (9.5 mm). Shed-proof.
- STAINLESS STEEL MIXING SPATULAS**
- SPT-1 **Double blade. Overall length 8 in (200 mm).**
- SPT-2 **Single blade. Overall length 7-3/4 in (195 mm). Wooden handle.**



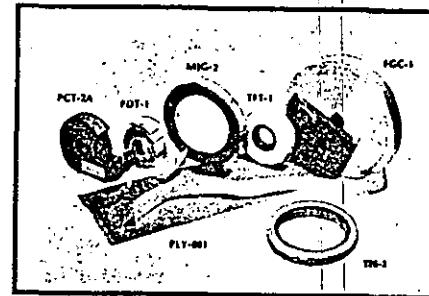
- MYC-1 **TEMPERATURE CONTROLLED HOTPLATE**
Temperature range +100° to +600°F (+40° to +315°C). Calibrated bimetallic thermostat. 3-1/2 in (90-mm) diameter aluminum alloy top plate. Embedded heating elements for high thermal conductivity. 120 Vac 6-ft (1.8-m) linecord. 3-wire plug.

GENERAL-PURPOSE TAPES & MATERIALS

- PCT-2A **Cellophane Tape**. For gage installation. 3/4 in x 108 ft (19 mm x 33 m).
- PDT-1 **Paper Drafting Tape**. For soldering mask, and lead positioning. 3/4 in x 400 in (19 mm x 10 m).
- PLY-001 **Kapton Film**. For electrical insulation. 4 x 10 x 0.001 in thick (100 x 250 x 0.02 mm thick).

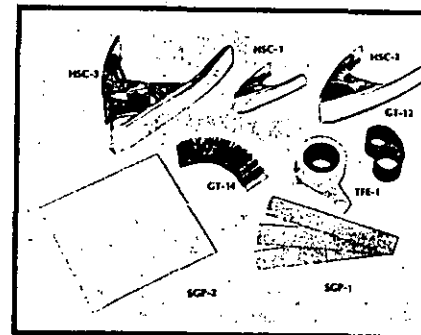
HIGH-TEMPERATURE TAPES & MATERIALS

- MJC-2 **Mylar JG Tape**. For gage installation with heat-curing resin systems. 1/2 in x 216 ft (13 mm x 66 m).
- TFT-1 **Thermosetting [340°F (170°C)] Fiberglass Tape**. For electrical insulation at high temperatures. 1/2 in x 66 ft (13 mm x 20 m).
- FGC-1 **Woven Fiberglass Cloth**. Bound edges. For lead anchoring when used in conjunction with M-Bond adhesives and M-Coat protective coatings.
- TFE-2 **High modulus TFE teflon with silicone mastic**. 1/2 in x 108 ft (13 mm x 33 m).



CLAMPING SUPPLIES

	Max. Opening	Max. Rec. Opening	Approx. Force at 1/2 in (13 mm) Opening
HSC-1 Spring Clamp	1 in (25 mm)	1/2 in (13 mm)	18 lb (80 N)
HSC-2 Spring Clamp	2 in (51 mm)	1 in (25 mm)	18 lb (80 N)
HSC-3 Spring Clamp	3 in (76 mm)	1-1/2 in (38 mm)	22 lb (100 N)
GT-12	NEC'ATOR Constant Force Extension Spring Clamp. 1 x 0.006 x 38 in (25 mm x 0.4 mm x 0.97 m) stainless steel band, drum I.D. 1.16 in (30 mm), 10.6 lb (47 N) load.		
TFE-1	TFE Teflon film. 0.003 in x 1 in x 50 ft (0.08 mm x 25 mm x 15 m).		
GT-14	Pressure Pads and Backup Plates. Kit of 12 Silicone Rubber Pads 3/32 x 1/2 x 1-1/4 in (2.5 x 13 x 32 mm), and 12 aluminum plates, 1/8 x 1/2 x 1-1/4 in (3 x 13 x 32 mm).		
SGP-1	Silicone Rubber. Three pieces, each 3/32 x 1 x 6 in (2.5 x 25 x 150 mm).		
SGP-2	Silicone Rubber. One piece, 3/32 x 6 x 6 in (2.5 x 150 x 150 mm).		

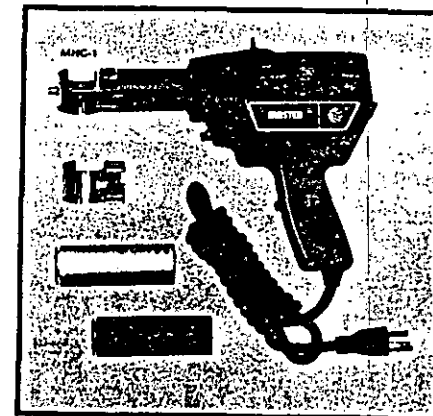


MHG-1 MASTER MITE HEAT GUN

Lightweight, compact, perfectly balanced. 2 lb (0.9 kg) with nozzle attached. 8-7/8 x 7 in (225 x 180 mm). Quiet, brushless-type shaded pole motor rated for continuous duty. Three interchangeable nozzle heating elements control average outlet temperature 1/2 in (13 mm) from nozzle at 900°F (260°C), 650°F (345°C), or 800°F (425°C). Air-cooled barrel. Three-conductor grounded linecord. Slip-on deflector completely surrounds shrinkable tubing (HST-1) with heat. Pinpoint adapter directs heat without affecting adjacent areas. 120 Vac, 60 Hz. Maximum current draw 5.4 amps.

MHG-2 Same as above, except 220 Vac.

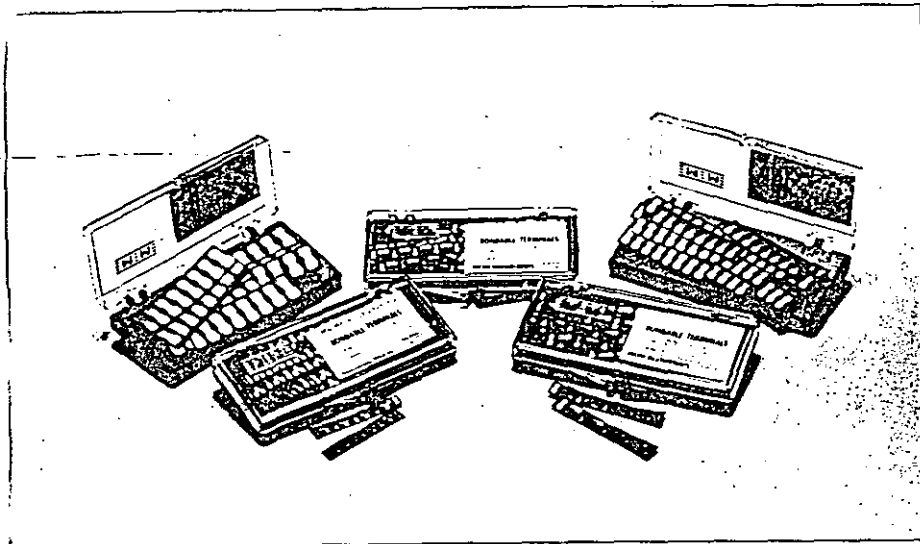
NOTE: Additional types of installation tools particular to a specific accessory group are presented elsewhere in this catalog.



BONDABLE TERMINALS

For many types of strain gages (such as Micro-Measurements EA-Series), it is not generally intended that instrument leadwires be attached directly to the solder tabs of the gage. The normal practice, instead, is to install bondable terminals adjacent to the gage, and solder the instrument leadwires to these. Small, flexible jumper wires, curved to form strain-relief loops,

are then connected from the terminals to the gage solder tabs. The accompanying drawings on the facing page show typical strain gage terminal installations (see also M-M Tech Tip TT-603, *The Proper Use of Bondable Terminals in Strain Gage Applications*).



TERMINAL CONSTRUCTION

BACKING MATERIALS

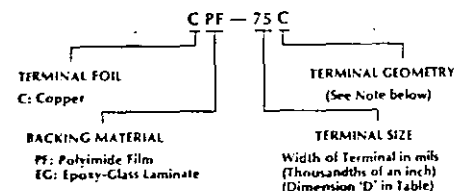
Micro-Measurements bondable terminals are especially designed for use in strain gage circuits. They are produced from 0.014-in (0.036-mm) thick copper foil, electro-deposited on one of two types of backing material. Both backings are fully bondable with strain gage adhesives. Terminals are available in four different geometries, and in a range of sizes to suit varying gage installation needs.

Type PF — Polyimide film: 0.003 in (0.08 mm) thick.

This is the preferred general-purpose backing material. It is more flexible and conformable than the Type EG (below); although not as strong. Type PF backing combines high-temperature capability, resistance to soldering damage and good electrical properties. It is suitable for long-term use at +450° to +500°F (+230° to +260°C), limited primarily by gradual oxidation of the copper foil interface. The relatively high thermal expansion coefficient of unfilled polyimide can cause loss of bond at temperatures below -100°F (-75°C).

Type EG — Epoxy-glass laminate: 0.005 in (0.13 mm) thick.

This special laminate provides a strong but flexible backing for terminals. It is suitable for long-term use at +300°F (+150°C), and is recommended for cryogenic applications at temperatures down to -452°F (-269°C). The radius of curvature of the mounting surface should generally be greater than 1/16 in (1.6 mm).



Note: Patterns with the 'C', 'D', or 'L' suffix show actual number of terminals per strip, and are packaged and priced as strips per package. 'S' patterns are packaged pairs per package; pairs per strip will vary.

References: M-M Tech Tip TT-603, *The Proper Use of Bondable Terminals in Strain Gage Applications*.

TERMINAL DETAIL AND DESCRIPTIONS	TERMINAL PATTERN (Actual Size) — See Notes —	DIMENSIONS					ORDER NUMBERS	Pkg	
		Inches millimetres							
		A*	B	C	D	E			
 SUFFIX C: General purpose. Widely used between gage jumper wires and main leadwire system. Suitable for many bridge intracconnection applications.		0.11 2.7	0.065 1.65	0.025 0.64	0.025 0.64	N/A	CEG-25C CPF-25C	70**	
		0.14 3.4	0.095 2.41	0.030 0.76	0.038 0.97	N/A	CEG-38C CPF-38C	60**	
		0.18 4.5	0.125 3.18	0.036 0.91	0.050 1.27	N/A	CEG-50C CPF-50C	50**	
		0.25 6.4	0.190 4.83	0.040 1.02	0.075 1.91	N/A	CEG-75C CPF-75C	30**	
		0.33 8.4	0.250 6.35	0.070 1.78	0.100 2.54	N/A	CEG-100C CPF-100C	20**	
		0.48 12.1	0.375 9.53	0.070 1.78	0.150 3.81	N/A	CEG-150C CPF-150C	10**	
	 SUFFIX D: Designed for installations with 2-wire jumper arrangement to gage and a 3-wire main lead system.		0.18 4.5	0.125 3.18	0.036 0.91	0.050 1.27	N/A	CEG-50D CPF-50D	30**
			0.21 5.3	0.150 3.81	0.038 0.97	0.060 1.52	N/A	CEG-60D CPF-60D	25**
			0.25 6.4	0.190 4.83	0.040 1.02	0.075 1.91	N/A	CEG-75D CPF-75D	20**
			0.33 8.4	0.250 6.35	0.050 1.27	0.100 2.54	N/A	CEG-100D CPF-100D	15**
		0.21 5.3	0.150 3.81	0.040 1.02	0.060 1.52	N/A	CEG-60L CPF-60L	25**	
		0.25 6.4	0.190 4.83	0.050 1.27	0.075 1.91	N/A	CEG-75L CPF-75L	20**	
TERMINAL ASSORTMENT: Contains 2 strips of all above patterns, except 1 strip of the 150C and 100D designs.							CEG-AST CPF-AST	22**	
 SUFFIX S: Primarily used where soldering and desoldering may be encountered. Hole in center produces thermal isolation at each end of terminal. Not recommended for high cyclic endurance. Available only in epoxy-glass backing.		0.13 3.2	0.063 1.60	0.021 0.53	0.021 0.53	0.042 1.07	CEG-215	200†	
		0.21 5.2	0.125 3.18	0.042 1.07	0.042 1.07	0.084 2.13	CEG-425	100†	
		0.29 7.4	0.190 4.83	0.063 1.60	0.063 1.60	0.126 3.20	CEG-635	100†	
		0.37 9.4	0.250 6.35	0.083 2.11	0.083 2.11	0.166 4.22	CEG-835	60†	
		0.54 13.6	0.375 9.53	0.125 3.18	0.125 3.18	0.250 6.35	CEG-1255	30†	

*"A" dimensions are nominal

**Strips of 4 pairs

†Pairs

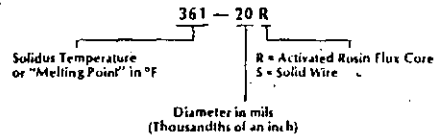
M-LINE SOLDERING SUPPLIES & ACCESSORIES

The quality of the solder joints is a critical element in the performance of any strain gage installation. Because of special requirements associated with strain gage circuitry, many commercial solders and fluxes are not satisfactory for this purpose. Micro-Measurements stocks and distributes a selection of solders and fluxes which have been carefully tested and qualified for use with strain gages.

SOLDERS — M-LINE strain gage solders are listed below, along with their compositions, principal properties, and recommended applications. For ordering purposes, the solders are specified according to the coding system shown at right. All solders are supplied on spools, except for the 1240-FPA paste which is supplied in a jar.

FLUXES — Although some of the solders described in the table below have rosin-flux cores, it is often necessary to use separate, externally applied fluxes. This may be the case, for instance, when soldering fine jumper wires to gage tabs or printed-circuit terminals, because not enough flux is released from the cored solder. It may also be necessary to supplement the cored flux in high-temperature solders such as Type 570.

Two fluxing compounds are available for strain gage soldering applications. M-Flux AR is an active but noncorrosive rosin flux which is effective on constantan, copper, and nickel. M-Flux SS

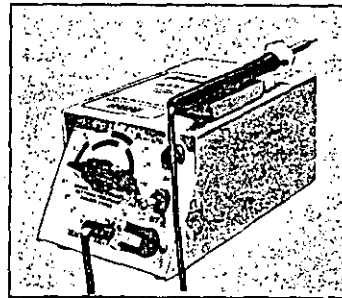


is a very active acid flux which is used primarily with solid-wire solders applied to Isoelastic and K-alloy gages, and to stainless steel. The two fluxes should never be mixed. Whether the rosin or acid flux is used, it must be completely removed immediately after soldering to prevent degradation of protective coatings and corrosion of the metals, and to eliminate conductive flux residues. Rosin residues are best removed with M-LINE Rosin Solvent. Removal of M-Flux SS requires two steps: liberal applications of M-Prep Conditioner A, which must be blotted dry; and then M-Prep Neutralizer SA, also to be blotted dry.

SOLDER TYPE	PACKAGING		SOLIDUS/LIQUIDUS TEMP.	Wetting & Flow	Mechanical Strength	Corrosion Resistance	PRIMARY USES
	ORDER NO.	UNIT SIZE					
361A-20R 67% Tin 36.65% Lead 0.35% Antimony	361A-20R-25	25 ft (7.6 m)	361°/361°F (183°/183°C)	Excellent	Very Good	Good	Best all-around solder for general use. Also capable of use at cryogenic temperature.
	361A-20R	1 lb (450 g)					
361-40R 63% Tin 37% Lead	361-40R-15	15 ft (4.6 m)	361°/361°F (183°/183°C)	Excellent	Very Good	Good	All-around solder for general use. Convenient for instrument work and with heavy leadwires.
	361-40R	1 lb (450 g)					
430-20S 96% Tin 4% Silver	430-20S-25	25 ft (7.6 m)	430°/430°F (221°/221°C)	Very Good	Very Good	Excellent	Recommended for critical work, particularly where high electrical conductivity is required. Good mechanical fatigue properties. Do not use at cryogenic temperatures.
	430-20S	1 lb (450 g)					
450-20S 93% Tin 3% Antimony	450-20S-25	25 ft (7.6 m)	450°/460°F (232°/238°C)	Excellent	Very Good, Hard	Good	Higher temperature solder with very good handling properties. Supplied in solid form; can be used with either M-Flux AR or M-Flux SS. Presence of antimony prevents "tin disease"; can be used in cryogenic environments, although quite brittle at low temperatures.
	450-20S	1 lb (450 g)					
570-28R 93% Lead 5.2% Tin 1.8% Silver	570-28R-20	20 ft (6.1 m)	565°/574°F (286°/301°C)	Very Good	Very Good	Fair	High-lead content. For high-temperature connections and long-term cryogenic temperature tests.
	570-28R	1 lb (450 g)					
1240-FPA 40% Silver 20% Zinc 30% Copper 2% Nickel	1240-FPA	1 oz (28 g)	1220°/1435°F (660°/780°C)	Excellent	Excellent	Good	For very high temperature solder joints, generally with WK-Series strain gages. The WRS-1 Resistance Soldering Unit is an ideal tool for use with this solder.

FLUX AND ROSIN SOLVENT	M-FLUX AR KIT — Order No. FAR-1	M-LINE ROSIN SOLVENT KIT — RSN-1	M-FLUX SS KIT — Order No. FSS-1
	2 1-oz (30-ml) dispenser btl M-Flux AR 2 1-oz (30-ml) brush-cap btl M-LINE Rosin Solvent	12 1-oz (30-ml) btl	1 1-oz (30-ml) dispenser btl M-Flux SS 1 1-oz (30-ml) brush-cap btl M-Prep Conditioner A 1 1-oz (30-ml) brush-cap btl M-Prep Neutralizer SA

MARK V SOLDERING STATION



A time-proven precision soldering instrument for miniature and/or delicate soldering applications. Full 25-watt rating in 17 selector positions to handle all M-LINE solder alloys except 1240-FPA. Magnetic solder pencil holder and flexible, burn-resistant cord. Lightweight soldering pencil [1.1 oz (31 g)]. Specify 115 or 230 Vac, 50 or 60 Hz operation.

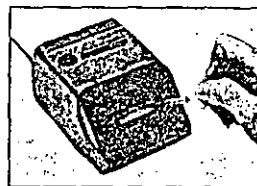
- MSS-1 Mark V Soldering Station, Complete
- MSS-2 Mark V Control Unit Only
- MSS-3 Mark V Soldering Pencil Only

SOLDERING TIPS FOR MARK V

- MSS-A Type A, general-purpose 1/16 in (1.5 mm), screwdriver
- MSS-B Type B, miniature 1/16 in (1.5 mm), chisel
- MSS-C Type C, heavy duty 1/8 in (3 mm), screwdriver
- MSS-D Type D, high-temperature 3/32 in (2.5 mm), chisel

Types A, B, and C tips are pre-tinned, ironclad copper, overlapped with nickel/chromium to retard oxidation. Type D is nickel-plated copper, particularly suited to high-temperature soldering.

MODEL STC-1 SOLDERING IRON TIP CLEANER

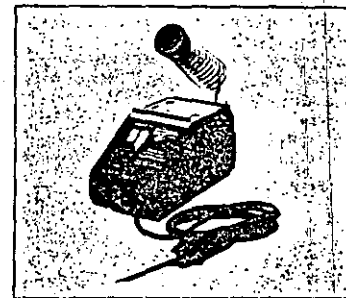


A clean soldering iron tip is important to ensure reliable solder connections and maximum electrical integrity of strain gage installations. The Model STC-1 provides important features not previously available for this often overlooked stage of the soldering operation. Eight spare sponge rollers are included with the STC-1, 100 to 130 Vac.

- STC-1 Soldering Iron Tip Cleaner
- STC-1RS Package of 8 replacement sponges

References: M-M Tech Tip TT-606, Soldering Techniques for Lead Attachment to Strain Gages with Solder Dots.
M-M Tech Tip TT-602, Silver Soldering Technique for Attachment of Leads to Strain Gages.
M-M Tech Tip TT-609, Strain Gage Soldering Techniques.

MARK VII SOLDERING UNIT



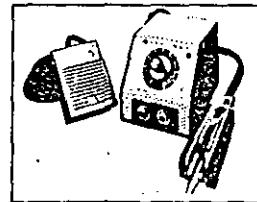
Manufactured for Measurements Group, Inc., the Mark VII is configured and calibrated specifically for strain gage applications. Tip temperature range of +500° to +800°F (+260° to +425°C) is ideal for most laboratory and field strain gage applications. The Mark VII incorporates closed-loop temperature control with no overshoot; high-performance, replaceable ceramic heating element; comfortable, cushioned iron handle. Includes one each M75-A and M75-B high-thermal-capacity tips. Color-coded temperature ranges indicate proper tip temperatures for all Micro-Measurements soft solders.

- M75-1-XXX Mark VII Soldering Unit, Complete, XXX = Voltage 115 or 230 (Vac)

SOLDERING TIPS FOR MARK VII

- M75-A Narrow tip 0.015 in (0.38 mm) screwdriver
- M75-B Wide tip 0.03 in (0.76 mm) screwdriver
- M75-RS Package of 1 replacement sponge

RESISTANCE SOLDERING UNIT



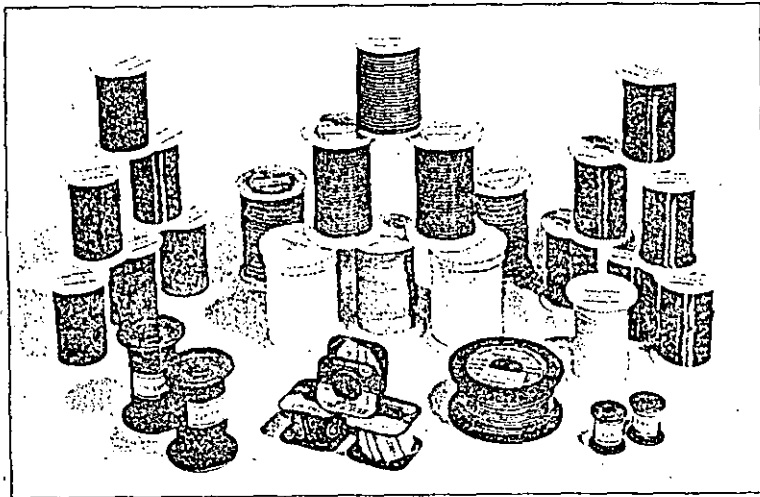
When used in combination with 1240-FPA silver-solder paste, this unit makes an excellent lead attachment system for strain gage operation above +500°F (+260°C). The infinitely variable power control allows adjustment from zero to 100 watts and zero to 3 Vac. The power control is fused, and a pilot light is incorporated. The foot switch and tweezer soldering handpiece give excellent operator control over each solder joint.

- WRS-1 (110 Vac) — includes power unit and foot switch, both with 3-wire NEMA plug, tweezer soldering handpiece, and replacement electrodes.
- WRS-2 (220 Vac) — same as WRS-1, but 220 Vac.

- REPLACEMENT ELECTRODES
- WRS-A Package of 6 electrodes

M-LINE WIRE, CABLE & ACCESSORIES

Different strain gage installation conditions and test specifications often necessitate the use of different types or sizes of leadwires. For accurate, reliable strain measurements, it is important to use the right type of leadwire for each installation. Micro-Measurements stocks a wide variety of wires and cables, cataloged in tabular form on the following pages. All wires and cables listed in the tables have been thoroughly field-tested and found to give excellent sensor performance when properly used in the specified environment. Special gage wiring problems may require the use of wires not listed here. In such cases, our Applications Engineering Department can recommend appropriate wire types, and can suggest suppliers.



WIRE AND CABLE CODING SYSTEM

Number of Conductors **3 2 6** — **D F V**
 AWG (American Wire Gauge) Wire Size

- TYPES OF WIRE**
- A: Solid copper
 - B: Stranded copper
 - C: Tinned solid copper
 - D: Tinned stranded copper
 - E: Silver-plated solid copper
 - F: Silver-plated stranded copper
 - G: Nickel-clad solid copper
 - H: Solid Manganin
 - I: Solid Balco*

- CONSTRUCTION**
- F: Flat cable
 - I: Twisted cable with jacket
 - S: Shielded/twisted with jacket
 - T: Twisted cable without jacket
 - W: Round single wire

- INSULATION**
- E: Etched TFE Teflon**
 - F: Fiberglass braid
 - K: Kapton** (polyimide) wrap
 - N: Nylon/polyurethane enamel
 - P: Polyurethane enamel
 - Q: Polyimide enamel
 - T: TFE Teflon
 - V: Vinyl (PVC)

AWG	Diameter†		AWG	Diameter†	
	(in)	(mm)		(in)	(mm)
22	0.0253	0.643	34	0.0063	0.160
26	0.0159	0.404	36	0.0050	0.127
27	0.0142	0.361	37	0.0045	0.114
30	0.0100	0.254	42	0.0025	0.064

†Nominal

*W.R. Driver Company trade name
 **DuPont trade name

The Wire and Cable Coding System shown in the box at left gives the unique designation of each wire type for ordering purposes. This system applies to all M-M wire types except the uninsulated flat ribbon leads which are independently identified in the charts that follow. The leadwire and cabling selection charts presented on the next three pages are organized according to number of conductors. All M-LINE wires and cables are supplied on spools for user convenience. Some types may not be continuous length.


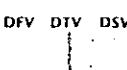

WIRE SELECTION CHARTS


		SINGLE-CONDUCTOR TYPES: SOLID WIRE		
		M-M TYPE	PACKAGING Foot/Metre	DESCRIPTION
AWP	AWN	134-AWP	500 ft/150 m	Solid copper wire, polyurethane enamel: General-purpose intragage hookup wire. Useful from -100° to +300°F (-75° to +150°C). Enamel coating easily removed by applying heat from soldering iron.
		136-AWP	500 ft/150 m	
AWQ	GWF	127-AWN	500 ft/150 m	Solid copper wire, nylon/polyurethane enamel: Identical in use to Type AWP above, but with superior abrasion resistance and slightly reduced insulation resistance at elevated temperatures. 134-AWN is available in four colors; specify: -R (red), -W (white), -B (black), -G (green).
		130-AWN	500 ft/150 m	
		134-AWN	500 ft/150 m	
AWQ	GWF	127-AWQ	500 ft/150 m	Solid copper wire, polyimide enamel: Intragage hookup wire. Temperature range -452° to +600°F (-269° to +315°C) short term. Enamel is extremely tough and abrasion resistant, with excellent electrical properties; generally removed by mechanical scraping or sanding.
		130-AWQ	500 ft/150 m	
		134-AWQ	500 ft/150 m	
AWQ	GWF	126-GWF	100 ft/ 30 m	Solid nickel-clad copper wire, fiberglass braid insulation: Useful from -452° to +900°F (-269° to +480°C). Recommended for use with WK-Series gages when silver solder is used for lead attachment.
		126-GWF	1000 ft/300 m	
HWN	JWN	137-HWN	200 ft/ 60 m	Solid manganin wire, nylon/polyurethane enamel: Used for bridge balance and span set in transducer circuits. Nominal resistance: 15 ohms/ft (50 ohms/m). Temperature range: +10° to +125°F (-10° to +50°C).
		142-JWN	500 ft/150 m	





		SINGLE-CONDUCTOR TYPES: STRANDED WIRE		
		M-M TYPE	PACKAGING Foot/Metre	DESCRIPTION
DWW	FWK	126-DWW	100 ft/ 30 m	Stranded tinned copper wire, vinyl insulation: General-purpose leadwire. Useful to +180°F (+80°C). Vinyl insulation becomes brittle at low temperature; not normally used below -60°F (-50°C). Specify red, white, black, or green.
		126-FWK	25 ft/ 7.5 m	
DWW	FWK	126-FWK	25 ft/ 7.5 m	Stranded silver-plated copper wire, Kapton polyimide insulation: High-performance. Recommended for unusually severe service from -452° to over +600°F (-269° to +315°C) short term. Excellent resistance to abrasion, radiation, and outgassing in high vacuum. Treated for bondability.
		130-FWK	25 ft/ 7.5 m	
DWW	FWK	130-FWT	100 ft/ 30 m	Stranded silver-plated copper wire, Teflon insulation: Wide temperature range. Useful from -452° to +500°F (-269° to +260°C). When bonding to Teflon-insulated wire, insulation must be treated with Tetra-Etch compound (see "Special-Purpose Materials," page 5). Specify red, white, black, or green.
		130-FWT	100 ft/ 30 m	

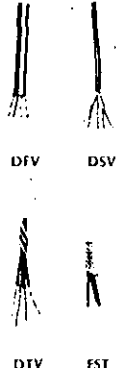
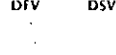


References: M-M Tech Tip TT-601, Techniques for Bonding Leadwires to Surfaces Experiencing High Centrifugal Forces.
 M-M Tech Tip TT-604, Leadwire Attachment Techniques for Obtaining Maximum Fatigue Life of Strain Gages.
 M-M Tech Tip TT-608, Techniques for Attaching Leadwires to Unbonded Strain Gages.


CABLE SELECTION CHARTS

	THREE-CONDUCTOR CABLE		
	M-M TYPE	PACKAGING Foot/Metre	DESCRIPTION
 DFV DTV DSV	326-DFV	100 ft/ 30 m	Stranded tinned-copper wire, 3-conductor flat cable, vinyl insulation: Convenient general-purpose cable. For use from -60° to +180°F (-50° to +80°C). Flat construction requires minimum space. Color-coded red/white/black.
	326-DFV	1000 ft/300 m	
	330-DFV	100 ft/ 30 m	
 DTV DTV	326-DTV	100 ft/ 30 m	Stranded tinned-copper wire, 3-conductor twisted cable, vinyl insulation: Convenient general-purpose cable for low electrical noise pickup. For use from -60° to +180°F (-50° to +80°C). Color-coded red/white/black.
	326-DTV	1000 ft/300 m	
 DSV DSV	326-DSV	100 ft/ 30 m	Stranded tinned-copper wire, 3-conductor twisted cable, vinyl insulation, braided shield, vinyl jacket: Special-purpose cable to minimize electrical noise interference. Useful from -60° to +180°F (-50° to +80°C). Color-coded red/white/black.
	326-DSV	1000 ft/300 m	

 FFE FFE	330-FFE	100 ft/ 30 m	Stranded silver-plated copper wire, 3-conductor flat cable, etched Teflon insulation: For use from -452° to +500°F (-269° to +260°C). Color-coded red/white/black. Insulation treated for bonding.
	330-FFE	1000 ft/300 m	

 FJT FTE GJF	330-FJT	100 ft/ 30 m	Stranded silver-plated copper wire, 3-conductor twisted cable, Teflon insulation, Teflon jacket: Small, flexible. For use from -452° to +500°F (-269° to +260°C). Color-coded red/white/black. When bonding Teflon-insulated wire, insulation must be treated with Tetra-Etch compound (see "Special-Purpose Materials," page 5).
	330-FJT	1000 ft/300 m	
 FJT FTE GJF	336-FTE	50 ft/ 15 m	Stranded silver-plated copper wire, 3-conductor twisted cable, etched Teflon insulation: Small, flexible cable. For use from -452° to +500°F (-269° to +260°C). Color-coded red/white/black. Insulation treated for bonding.
	330-FTE	100 ft/ 30 m	
 FJT FTE GJF	330-FTE	100 ft/ 30 m	Stranded silver-plated copper wire, 3-conductor, twisted cable, etched Teflon insulation: For use from -452° to +500°F (-269° to +260°C). Color-coded red/white/black. Insulation treated for bonding.
	330-FTE	500 ft/150 m	
 FJT FTE GJF	326-GJF	100 ft/ 30 m	Solid nickel-clad copper wire, 3-conductor twisted cable, fiberglass braid insulation and jacket: For use from -452° to +900°F (-269° to +480°C). Recommended with WK-series pages when silver solder is used for lead attachment. Color-coded red/white/black.
	326-GJF	1000 ft/300 m	

	FOUR-CONDUCTOR CABLE		
	M-M TYPE	PACKAGING Foot/Metre	DESCRIPTION
 DFV DSV DTV FST	426-DFV	100 ft/ 30 m	Stranded tinned-copper wire, 4-conductor flat cable, vinyl insulation: For use from -60° to +180°F (-50° to +80°C). Conductors easily separated for stripping and wiring. Color-coded red/white/black/green.
	426-DFV	1000 ft/300 m	
	430-DFV	100 ft/ 30 m	
	430-DFV	1000 ft/300 m	
 DSV DSV	422-DSV	100 ft/30 m	Stranded tinned-copper wire, 4-conductor polypropylene insulated: Twisted shielded pairs (red/black and white/green) with a drain wire, PVC jacket. For use from -60° to +180°F (-50° to +80°C).
	422-DSV	1000 ft/300 m	
 DTV DTV	426-DTV	100 ft/ 30 m	Stranded tinned-copper wire, 4-conductor twisted cable, vinyl insulation: For use from -60° to +180°F (-50° to +80°C). Color-coded red/white/black/green.
	426-DTV	1000 ft/300 m	
 FST FST	430-FST	100 ft/ 30 m	Stranded silver-plated copper wire, 4-conductor twisted cable, Teflon insulation, braided shield, Teflon jacket: Small, flexible cable. For use from -452° to +500°F (-269° to +260°C). Color-coded red/white/black/green. When bonding Teflon-insulated wire, insulation must be treated with Tetra-Etch compound (see "Special-Purpose Materials," page 5).
	430-FST	1000 ft/300 m	

	FLAT RIBBON LEADS (UNINSULATED)		
	M-M TYPE	PACKAGING Foot/Metre	DESCRIPTION
 CL-92R-50	CL-92R-50	50 ft/ 15 m	Uninsulated flat ribbon ni-clad copper: For use from -452° to +900°F (-269° to +480°C). Can be easily soldered or spot welded. 0.001 x 1/64 in (0.025 x 0.4 mm).

HEAT-SHRINKABLE WIRE SPLICE SEALANT

Fast, easy-to-use method for protecting wire splice connections. Constructed of irradiated polyolefin plastic tubing with a heat-flowable inner liner sealant. Forms an immediate and tight seal to splice connection at a shrink temperature of +275°F (+135°C). Inside diameter before heating is 0.125 in (3.2 mm); after heating, 0.023 in (0.6 mm). Large range of shrinkage allows use with leadwire insulation diameters from 0.03 to 0.11 in (0.75 to 2.8 mm). The operating temperature range is -55° to +500°F (-55° to +260°C).

Order No. HST-1 — pkg. of eight 6-in (150-mm) lengths.

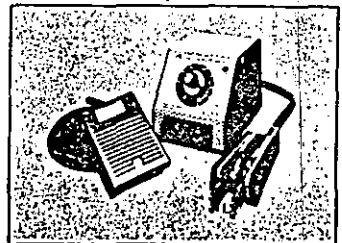


THERMAL WIRE STRIPPER

The ease and simplicity of operation of the Thermal Wire Stripper make it ideal for most strain gage leadwire stripping. The variable heat control allows stripping of all thermoplastic insulations, including Teflon, in sizes No. 18 to No. 36 AWG (7 to 0.1 mm diameter). The foot switch and tweezer handpiece give excellent operator control over the stripping operation.

Order No. WTS-1 — (110 Vac) includes power unit and foot switch, both with 3-wire NEMA plugs, and tweezer handpiece.

Order No. WTS-2 — (220 Vac) same as WTS-1, but 220 Vac.



REPLACEMENT ELEMENTS

Order No. WTS-A — set of two.

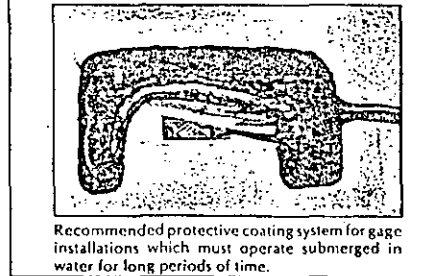
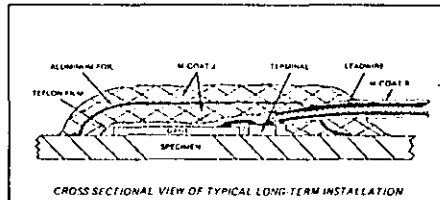
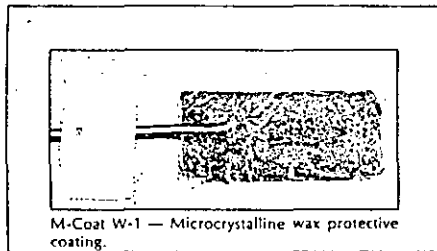
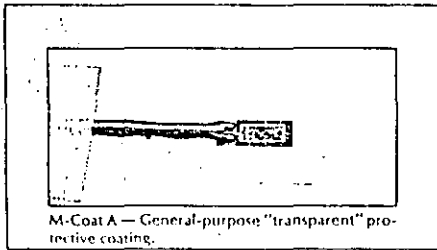
M-COAT PROTECTIVE COATINGS

Strain gage performance is easily degraded by the effects of moisture, chemical attack, or mechanical damage. As a result, gages require varying degrees of protection according to the severity of the environment in which they must operate. While it is often practical, in laboratory applications, to operate fully encapsulated gages without additional protection, open-faced gages should always be covered with a suitable coating as soon as possible after installation.

The M-Coat compounds described on the following pages have been formulated specifically for use in protecting strain gage installations from destabilizing and damaging environmental conditions. The range of materials offered is adequate for handling the majority of gage protection requirements. In the benign atmosphere of an air-conditioned laboratory, for instance, a single layer of M-Coat A would ordinarily provide

sufficient protection against moisture, fingerprints, and other degrading contaminants. When the gage installation must operate in a more severe environment, alternate coatings or combinations of coatings can be employed as illustrated in the photographs below.

To serve as a preliminary guide for coating selection, the chart on the facing page gives recommended coating systems for a variety of typical environments. The effectiveness of these materials and procedures has been experimentally validated on numerous occasions. However, application technique is also an important factor in the performance of any gage protection system. It is therefore good practice, particularly in the case of long-term installations, to verify by test that the system performs as required.

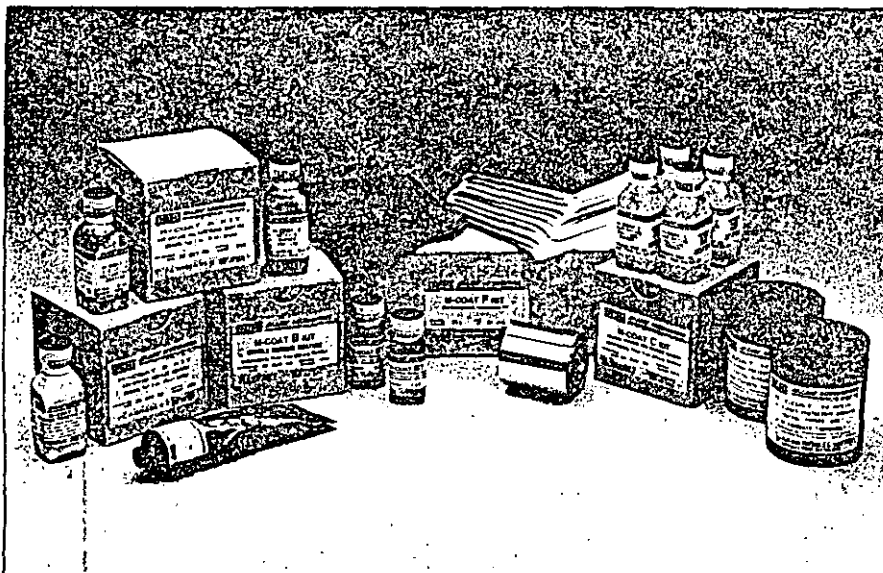


APPLICATION NOTES FOR PROTECTIVE COATINGS

- For long-term tests, or in particularly hostile environments, carefully clean the surface before applying any protective coating. Coating extending into uncleaned areas will eventually loosen.
- When several layers of coating are required, extend each overcoat beyond the previous layer.
- Incomplete protection around leadwires is a common cause of moisture penetration into gage installations. (Many commercial leadwire insulations contain pinholes.)
- Seal wire splices with HST-1 Heat Shrinkable Tubing.
- Before applying any protective coating to an unprotected installation which has been exposed to high humidity, dry the installation thoroughly.
- If the coating is a room-temperature-curing type, the moisture absorption rate can be decreased by postcuring at an elevated temperature.
- Generally, a thick coating offers a more resistant path to moisture absorption than a thin one.
- For a further vapor barrier, apply an intermediate layer of metal foil (aluminum, such as M-Coat JA-2, or stainless steel), or TFE Teflon film (first treated with TEC-1 Tetra-Etch compound for optimum bond). Since moisture can only penetrate around the edges of the foil or film, the path to the gage is much longer.
- To evaluate protective coatings for long-term testing, monitor the zero-shift of the gage. Resistance to ground measurements can also indicate deterioration.

COATING SELECTION CHART

ENVIRONMENT	RECOMMENDATION
TYPICAL LABORATORY 50%, or lower, relative humidity	M-Coat A, or M-Coat C; or M-Coat D; or M-Coat F
FIELD APPLICATIONS Outdoor installations, shielded from rain and snow	M-Coat F, or M-Coat J
HIGH HUMIDITY, WATER SPLASH Laboratory and field applications under damp or wet conditions	3140 RTV or 3145 RTV for short term; or W-1 Wax or M-Coat F for long term.
WATER IMMERSION Short-term, fresh water or salt water Long-term, fresh water Long-term, salt water High-pressure water	Teflon + M-Coat B (on vinyl-insulated leadwires) + J; or W-1 Wax; Per diagram and photo (page 24); or W-1 Wax; or M-Coat F Per diagram and photo (page 24); plus metal cap and conduit for leadwires Per diagram and photo (page 24); or M-Coat F; or W-1 Wax for short-term.
STEAM 212°F (100°C), long-term installation	Hermetically sealed metal cap, and conduit for leadwires
CONCRETE SURFACES Long-term	Per diagram and photo (page 24); preceded by AE-10 or GA-61 to seal concrete surface
OILS AND GASOLINE Commercial oils, to +180°F (+80°C), gasoline, and kerosene Synthetic oils, to +200°F (+95°C)	M-Coat D plus two or three layers of M-Coat B; or 3145 RTV, + B Two or three layers of M-Bond 43-B or GA-61
HIGH-TEMPERATURE AIR To +500°F (+260°C), with good mechanical protection	M-Bond GA-61 (short term); or 3145 RTV



M-COAT DESCRIPTION AND APPLICATIONS	CURE REQUIREMENTS	SHELF LIFE	OPERATING TEMP. RANGE
<p>M-COAT A Air-drying solvent-thinned (xylene) polyurethane. Transparent. Moderate hardness; good flexibility. Can be removed with M-LINE Rosin Solvent or toluene. Film thickness 0.005-0.01 in (0.1-0.25 mm) per coat. General-purpose coating for lab use, and as base coating for field applications. Must be fully cured before addition of other coatings. Good moisture resistance. Not readily attacked by many solvents. Convenient to use. Kit Pkg: 4 brush-cap bits [1 oz (30 ml) ea]</p>	<p>Dries tack-free at room temperature in 20 min. Completely dry in 2 hr. Normal cure 24 hr at room temperature. Chemical resistance and coating hardness increase for 6 to 7 days.</p>	<p>1 yr at +75°F (+24°C)</p>	<p>SHORT TERM -100° to +300°F (-75° to +150°C) LONG TERM -100° to +250°F (-75° to +120°C)</p>
<p>M-COAT B Air-drying solvent-thinned (MEK) nitrile rubber. Forms flexible rubbery coating. Do not use directly on exposed foil or bare leads. If used as primer on leads, thin 50:50 with MEK. Generally used to prime vinyl-insulated wire to improve bondability to other coatings. Flexible at cryogenic temperatures. Excellent resistance to gasoline, kerosene, commercial oils. Electrical properties poorer than other M-Coats, particularly at high temperatures. Kit Pkg: 4 brush-cap bits [1 oz (30 ml) ea]</p>	<p>Air-dries in 1 hr at +75°F (+24°C). Do not apply subsequent protective coatings for at least 2 hr from time of application. Further improve chemical resistance with 1 hr bake at +200°F (+95°C).</p>	<p>1 yr at +75°F (+24°C)</p>	<p>SHORT TERM -320° to +300°F (-195° to +150°C) LONG TERM -320° to +200°F (-195° to +95°C)</p>
<p>M-COAT C Solvent-thinned (naphtha) RTV silicone rubber. Cures to tough rubbery transparent film. Good all-around mechanical and electrical properties. Completely noncorrosive. Film thickness 0.015-0.02 in (0.4-0.5 mm) per coat. Recommended for lab and field installations which require a high degree of protection in thin coatings. Good water-splash protection. Good chemical resistance. Kit Pkg: 4 brush-cap bits [1 oz (30 ml) ea]</p>	<p>Solvents evaporate in about 60 min at room temperature. Allow 20 min drying time between coats. Cures in 24 hr at +75°F (+24°C) and 50% RH. Longer cure at lower humidity.</p>	<p>9 mos at +75°F (+24°C) kept tightly sealed</p>	<p>SHORT TERM -75° to +550°F (-60° to +290°C) LONG TERM -75° to +500°F (-60° to +260°C)</p>

M-COAT DESCRIPTION AND APPLICATIONS	CURE REQUIREMENTS	SHELF LIFE	OPERATING TEMP. RANGE
<p>M-COAT D Air-drying solvent-thinned (toluene) acrylic. Dense white color for easy visual inspection of coverage. Forms hard thin coating capable of high elongation. Can be removed with M-LINE Rosin Solvent or toluene. Apply in thin coats to prevent solvent entrapment. Film thickness 0.005-0.01 in (0.1-0.25 mm) per coat. Good general laboratory moisture barrier. Electrical leakage negligible even when uncured. Good base coating for subsequent applications of M-Coat B. Convenient for anchoring and insulating intrabridge wiring and jumper leads. Chemical resistance only fair but can be improved by postcure at +175°F (+80°C) for 30 min. Kit Pkg: 4 brush-cap bits [1 oz (30 ml) ea]</p>	<p>Solvents evaporate in 30 min at +75°F (+24°C). Fully cured in 24 hr. Overcoats can be applied 30 min from time of application. Coating binder begins to sublimate at +280°F (+140°C), but residue is inorganic and will not become conductive.</p>	<p>1 yr at +75°F (+24°C) kept tightly sealed</p>	<p>SHORT TERM -100° to +325°F (-75° to +160°C) LONG TERM -100° to +250°F (-75° to +120°C)</p>
<p>M-COAT F Kit of selected materials easily applied in various combinations. Provides environmental and mechanical protection. Particularly well-suited to field applications where conditions are not ideal. Typical applications include pipelines, tunnels, bridges, reinforcement bars in concrete structures, heavy machinery, ships, aircraft, motor vehicles, and pressure vessels. Kit Pkg: 12 pcs [3-3/4 in (95 mm) sq, 1/8 in (3.2 mm) T] ea M-Coat FB Butyl Rubber Sealant and M-Coat FN Neoprene Rubber Sheets 1 roll [0.003 in (0.08 mm) T x 2 in (50 mm) W x 20 ft (6 m) L] M-Coat FA Aluminum Foil Tape 2 brush-cap bits [1/2 oz (15 ml) ea] M-Coat B Air-Drying Nitrile Rubber Coating 1 M-Coat FT 4-x-4-x-0.003-in (101-x-101-x-0.08-mm) Teflon Film Bulk Pkg: M-Coat FB-2 Butyl Rubber Sealant — 25 pcs M-Coat FN-2 Neoprene Rubber Sheets — 25 pcs M-Coat FA-2 Aluminum Foil Tape — 20 ft (6 m) roll M-Coat B Air-Drying Nitrile Rubber Coating — 4 brush-cap bits [1 oz (30 ml) ea] M-Coat FT 4-x-4-x-0.003-in (101-x-101-x-0.08-mm) Teflon film — 10 pcs</p>	<p>No mixing or curing required.</p>	<p>2 yr at +75°F (+24°C)</p>	<p>SHORT TERM -70° to +250°F (-55° to +120°C) LONG TERM -20° to +175°F (-30° to +80°C)</p>
<p>M-COAT FBT Solvent-thinned butyl rubber designed to provide excellent moisture protection with low reinforcement effects. Principally used in transducers. Exhibits a paste-like consistency and is normally applied with a spatula. Thickness over 0.1 in (2.5 mm) not recommended. Kit Pkg: 75 gm collapsible tubes, 4 ea</p>	<p>Air dry 8 hr, followed by an elevated temperature cure of +150° to +175°F (+65° to +80°C).</p>	<p>12 mos at +75°F (+24°C)</p>	<p>0° to +175°F (-20° to +80°C)</p>
<p>M-COAT J Two-part polysulfide liquid polymer compound. Can be applied in coating thickness to 1/8 in (3 mm) without flowing on vertical surfaces. Tough flexible coating. No weighing required. Uncured coating can be removed with CSM-1 Degreaser, Rosin Solvent, or MEK. General-purpose coating. Good protection against oil, grease, most acids and alkalis, and most solvents. Strong solvents may cause swelling and softening with time. Concentrated acids eventually break down coating. Good salt-water immersion coating. Kit Pkg: M-Coat J-1: 1 mixing dispenser (70 g ea) 1 pc M-Coat FT 4-x-4-x-0.003 in (101-x-101-x-0.85 mm) Teflon Film M-Coat J-3: 3 mixing dispensers (70 g ea) 3 pcs M-Coat FT 4-x-4-x-0.003 in (101-x-101-x-0.85 mm) Teflon Film</p>	<p>Mixed pot life 30 min at +75°F (+24°C). Normal cure in 24 hr at +75°F (+24°C). To accelerate cure and improve properties, cure 2 hr at +150°F (+65°C).</p>	<p>9 mos at +75°F (+24°C)</p>	<p>SHORT TERM -50° to +250°F (-45° to +120°C) LONG TERM -50° to +200°F (-45° to +95°C)</p>

M-COAT DESCRIPTION AND APPLICATIONS	CURE REQUIREMENTS	SHelf LIFE	OPERATING TEMP. RANGE
<p>M-COAT W-1 Microcrystalline wax. Has very low water-vapor transmission rate. Attacked by most solvents. Coating thickness 0.015-0.06 in (0.4-1.5 mm). Excellent water-immersion coating. Poor mechanical protection. Often used as intermediate coating.</p> <p>Kit Pkg: 5 tins [1 oz (29 g) ea]</p> <p>Bulk Pkg: 1 pkg [5 lb (2.25 kg)]</p>	<p>Heat to at least +120°F (+75°C) to melt. For best wetting and sealing, heat specimen surface to at least +100°F (+45°C) before applying.</p> <p>No cure required.</p>	No Limit	0° to +150°F (-20° to +65°C)
<p>3140 RTV Single-component 98%-solids RTV silicone rubber. Room temperature cure (humidity-reactive). Completely noncorrosive. Forms tough rubbery coating. Excellent properties. Translucent; permits full inspection of installation. Self-leveling; forms fairly thick coats 0.03-0.06 in (0.75-1.5 mm).</p> <p>Easy-to-apply general-purpose coating. Lab and field use. Low reinforcing effects. High-elongation capabilities. Good for short-term water immersion. Resists many chemicals. Bonds to contaminated surfaces for short-term tests; for best long-term, chemically clean surface and prime with AI-11 RTV Primer No. 1.</p> <p>Pkg: 1 collapsible metal tube [3 oz (85 g)]</p> <p>Accessory: 4 brush-cap bits [1 oz (30 ml) ea] RTV Primer No. 1</p>	<p>Tack-free in approximately 2 hr.</p> <p>Cure 24 hr for each 0.02 in (0.5 mm) thickness at +75°F (+24°C), 50% RH. Longer cure at lower humidity levels.</p> <p>Note: Will not cure properly if coating is not exposed to atmosphere.</p>	6 mos at +75°F (+24°C)	<p>SHORT TERM -100° to +600°F (-75° to +315°C)</p> <p>LONG TERM -65° to +500°F (-55° to +260°C)</p>
<p>3145 RTV Identical to 3140, except opaque gray coating of higher strength and toughness. Not self-leveling.</p> <p>Uses same as 3140 except very thick coatings can be applied without sag or runoff. Tear strength much higher than 3140. Good cable anchor.</p> <p>Pkg: 1 collapsible metal tube [3 oz (85 g)]</p> <p>Accessory: 4 brush-cap bits [1 oz (30 ml) ea] RTV Primer No. 1</p>	Same as 3140.	6 mos at +75°F (+24°C)	<p>SHORT TERM -100° to +600°F (-75° to +315°C)</p> <p>LONG TERM -65° to +500°F (-55° to +260°C)</p>

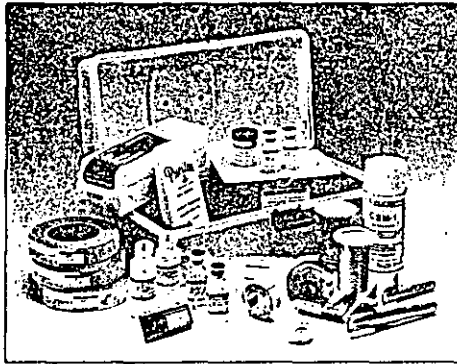


M-COAT DESCRIPTION AND APPLICATIONS	CURE REQUIREMENTS	SHelf LIFE	OPERATING TEMP. RANGE
<p>M-BOND AE-10/15 Two-component 100%-solids epoxy systems. Primarily used as adhesives. Often used as protective coating because of low vapor-transmission rate. AE-15 is superior but requires heat cure. Single coating thickness 0.005-0.015 in (0.1-0.4 mm).</p> <p>Primarily used where thin hard coating is required to resist water immersion for short time. Good electrical/mechanical protection where high velocity fluids are present and minimum disturbance to flow is necessary. Good leadwire anchor. Often used as precoat for sealing concrete.</p> <p>Kit Pkg: 6 mixing jars AE Resin (10 g ea) 1 bit Hardener 10 [1/2 oz (15 ml)] 1 bit Hardener 15 [1/2 oz (15 ml)]</p> <p>Bulk Pkg: 1 bit AE Resin (200 g) 1 bit Curing Agent 10 (40 g) 1 bit Curing Agent 15 (25 g)</p>	<p>AE-10 minimum cure 6 hr at +75°F (+24°C); AE-15 6 hr at +125°F (+50°C). To accelerate cure at higher temperatures, see cure schedules in the Adhesives Section.</p> <p>AE-10 mixed pot life 15-20 min; AE-15 1-1/2 hr at +75°F (+24°C).</p>	<p>12 mos at +75°F (+24°C) >18 mos at +20°F (-5°C)</p>	-100° to +200°F (-75° to +95°C)
<p>M-BOND 43-B Solvent-thinned (MEK and xylene) single-component epoxy resin compound. Primarily used as adhesive. Very compatible with MA-Series gages as both adhesive and protective coating. Cured coating 0.002-0.01 in (0.05-0.25 mm) thick.</p> <p>Provides excellent chemical, electrical, and mechanical properties when fully cured. Film is hard, with high heat-distortion temperature. Excellent in transducer service.</p> <p>Kit Pkg: 4 brush-cap bits [1 oz (30 ml) ea].</p>	<p>Air-dries in about 10 min at +75°F (+24°C). Minimum cure 2 hr at +325°F (+160°C). Pre-cured 2 hr at +375°F (+190°C).</p>	<p>9 mos at +75°F (+24°C) 18 mos at +40°F (+5°C)</p>	<p>SHORT TERM -452° to +400°F (-269° to +205°C)</p> <p>LONG TERM -452° to +275°F (-269° to +135°C)</p>
<p>M-BOND GA-61 Two-component 100%-solids, elevated-temperature-curing epoxy system. Very high viscosity, generally applied with spatula. Contains a filler and can be contoured to the surface. Coating thickness 0.005-0.03 in (0.1-0.75 mm).</p> <p>Commonly used for mechanical protection at elevated temperatures and in highly reactive hot synthetic oils such as in aircraft engines. Very good leadwire anchor to high g-fields (see M-M Tech Tip TT-601). Can be used to fill slots or grooves. Can be machined after cure.</p> <p>Kit Pkg: 3 mixing jars ea Resin and Hardener (45 g)</p>	<p>Mixed pot life 10 hr at +75°F (+24°C). Cure for 6 hr at +250°F (+120°C), or for 3 hr at +300°F (+150°C), or for 2 hr at +350°F (+175°C), or for 1 hr at +400°F (+205°C).</p>	>1 yr at +75°F (+24°C)	<p>SHORT TERM -100° to +500°F (-75° to +260°C)</p> <p>LONG TERM -100° to +400°F (-75° to +205°C)</p>

STRAIN GAGE APPLICATION KITS

It is often of greatest convenience for the strain gage user to purchase all of the needed accessory supplies and materials in a single package. For this purpose, Micro-Measurements offers two levels of strain gage application kits. The first level consists of the three GAK-2 Series kits described on this page. With either of these kits, the user can immediately start making simple strain gage installations for routine applications.

The ultimate in gage installation capability is provided by the MAK-1, Master Strain Gage Application Kit, shown on the facing page. This includes all of the supplies and special tools for making a wide range of gage installations for both laboratory and field applications. Kit contents are systematically stored in a compartmented tool box for convenience and portability.

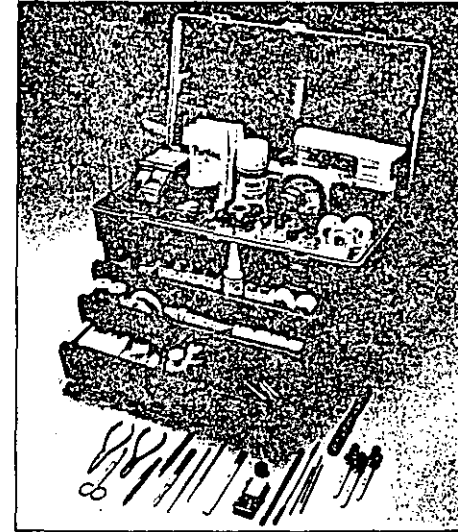


KIT CONTENTS		
GAK-2-200	GAK-2-AE-10/15	GAK-2-610
M-Bond 200 Kit	M-Bond AE-10/15 Kit	M-Bond 610 Kit
CSM-1 Degreaser, 1 can	CSM-1 Degreaser, 1 can	CSM-1 Degreaser, 1 can
MCA-1 Conditioner A, 1 bl	MCA-1 Conditioner A, 1 bl	MCA-1 Conditioner A, 1 bl
MNSA-1 Neutralizer 5A, 1 bl	MNSA-1 Neutralizer 5A, 1 bl	MNSA-1 Neutralizer 5A, 1 bl
SCP-1 220 grit, 1 roll, 100 ft (30 m)	SCP-1 220 grit, 1 roll, 100 ft (30 m)	SCP-1 220 grit, 1 roll, 100 ft (30 m)
SCP-2 320 grit, 1 roll, 100 ft (30 m)	SCP-2 320 grit, 1 roll, 100 ft (30 m)	SCP-2 320 grit, 1 roll, 100 ft (30 m)
SCP-3 400 grit, 1 roll, 100 ft (30 m)	SCP-3 400 grit, 1 roll, 100 ft (30 m)	SCP-3 400 grit, 1 roll, 100 ft (30 m)
CSP-1 Cotton Swabs, 1 pkg	CSP-1 Cotton Swabs, 1 pkg	CSP-1 Cotton Swabs, 1 pkg
GSP-1 Gauze Sponges, 1 pkg	GSP-1 Gauze Sponges, 1 pkg	GSP-1 Gauze Sponges, 1 pkg
PCT-2A Cellophane Tape, 1 roll	PCT-2A Cellophane Tape, 1 roll	MJG-2 Mylar Tape, 1 roll
PDT-1 Paper Drafting Tape, 1 roll	PDT-1 Paper Drafting Tape, 1 roll	PDT-1 Paper Drafting Tape, 1 roll
361A-20R-25 Solder, 1 roll, 25 ft (7.6 m)	361A-20R-25 Solder, 1 roll, 25 ft (7.6 m)	361A-20R-25 Solder, 1 roll, 25 ft (7.6 m)
Rosin Solvent, 1 oz (30 ml)	Rosin Solvent, 1 oz (30 ml)	Rosin Solvent, 1 oz (30 ml)
CPF-AST Bondable Terminals, 1 box	CPF-AST Bondable Terminals, 1 box	CPF-AST Bondable Terminals, 1 box
326-DFV, 3-Conductor Leadwire, 100 ft (30 m)	326-DFV, 3-Conductor Leadwire, 100 ft (30 m)	326-DFV, 3-Conductor Leadwire, 100 ft (30 m)
M-Coat A, 1 oz (30 ml)	M-Coat A, 1 oz (30 ml)	M-Coat C, 1 oz (30 ml)
134-AWP Solid Copper Wire, 500 ft (150 m)	134-AWP Solid Copper Wire, 500 ft (150 m)	134-AWP Solid Copper Wire, 500 ft (150 m)
Plastic Tool Box	SCP-2 Silicone Rubber, 1 pc	SCP-2 Silicone Rubber, 1 pc
	HSC-1 No. 1 Spring Clamp, 1 ea	HSC-1 No. 1 Spring Clamp, 1 ea
	HSC-2 No. 2 Spring Clamp, 1 ea	HSC-2 No. 2 Spring Clamp, 1 ea
	Plastic Tool Box	TFE-1 Teflon Film, 1 roll
		Plastic Tool Box

Note: All kit contents are available separately. Refer to the appropriate sections in this catalog for specific component details.

MAK-1 MASTER STRAIN GAGE APPLICATION KIT

The MAK-1 Master Strain Gage Application Kit contains all the materials necessary to successfully complete any organic strain gage installation for operation from -452° to $+500^{\circ}$ F (-269° to $+260^{\circ}$ C). In addition to M-Bond 200 and M-Bond AE-10/15, the MAK-1 includes M-Bond 610, a high-performance, two-component, solvent-thinned epoxy-phenolic adhesive system. All materials, including complete instructions, are conveniently packaged in a molded, crush-proof, copolymer toolbox. Adhesive operating characteristics are covered in the "M-Bond Strain Gage Adhesives" section, pages 6-13.



SURFACE PREPARATION MATERIALS

- CSM-1, Degreaser, 1 can
- MCA-1, M-Prep Conditioner A, 1 bl
- MNSA-1, M-Prep Neutralizer 5A, 1 bl
- Silicon-Carbide Paper: 220, 320, 400 grit, 1 10-ft (3-m) roll ea
- CSP-1, Cotton Swabs, 4 pkgs
- GSP-1, Gauze Sponges, 2 pkgs
- RSK-1, Rosin Solvent, two 1-oz (30-ml) bls

APPLICATION TOOLS

- SSH-1, Surgical Shears
- STW-1, Tweezers
- BTW-1, Tweezers
- DPR-1, Dental Probe (2)
- SSC-1, Surgical Scalpel & Blade
- SPT-1, Spatula (small)
- SSC-2, Scalpel Blades (5)
- DP-1, 4-H Drafting Pencil
- DWC-1, Diagonal Cutters
- NNP-1, Needle-Nosed Pliers
- SSS-1, Steel Scale
- SPT-2, Spatula (large)

HARDWARE

- PCT-2A, Cellophane Tape, 2 dispenser rolls
- PDT-1, Drafting Tape, 2 dispenser rolls
- MJG-2, Mylar IG Tape, 1 roll
- HSC-1, No. 1 Spring Clamps (4)
- HSC-2, No. 2 Spring Clamps (2)
- HSC-3, No. 3 Spring Clamp (1)
- TFE-1, Teflon Film, 1 roll
- GF-14, Pressure Pads & Plates Kit

KIT CONTENTS

ADHESIVES

- M-Bond 200 Kit
- M-Bond AE-10/15 Kit
- M-Bond 610 Kit

SOLDERING SUPPLIES

- M7S-1-XXX, Mark VII Soldering Unit (specify 115 or 230 Vac)
- 361A-20R, 1 lb (0.45 kg)
- 361A-20K-25, 1 roll
- 450-20S-25, 1 roll
- 570-28R-20, 1 roll
- FAR-1, M-Flux AR Kit
- CPF-AST, Terminal Strip Assortment

LEADWIRE

- 134-AWP, 100 ft (30 m)
- 126-DWV: Red, White, Black, Green, 1 100-ft (30-m) roll ea
- 326-DFV, 100 ft (30 m)
- 130-FWT: Red, White, Black, Green, 1 50-ft (15-m) roll ea

PROTECTIVE COATINGS

- M-Coat A, two 1-oz (30-ml) bls
- M-Coat B, two 1-oz (30-ml) bls
- M-Coat C, 1-oz (30-ml) bl
- M-Coat D, 1-oz (30-ml) bl
- M-Coat E, 1 kit
- 314S RTV Silicone Rubber, 3-oz (85-g) tube

Note: All kit contents are available separately. Refer to the appropriate sections in this catalog for specific component details.

PRECISION RESISTORS

Fixed resistors have several different uses in strain gage circuits. One of these is for shunt calibration of strain-measuring instrumentation. In this procedure, a fixed resistor is temporarily shunted across a bridge arm to produce a known resistance change in the bridge circuit. The resulting instrument indication is then compared to the calculated strain corresponding to the resistance change.

Another common use of fixed resistors is in bridge-completion applications. When a single active strain gage is connected in a quarter-bridge arrangement, a fixed resistor may be used in the adjacent arm of the bridge to complete the external half-bridge circuit. Similarly, when it is necessary that the full-bridge circuit be formed outside the instrument, a matched pair of fixed resistors can serve as a balanced half-bridge.

In each of these applications, the accuracy of the strain measurement is affected, directly or indirectly, by the accuracy and stability of the fixed resistor(s) used in the circuit. It is important, therefore, that only precision, high-stability resistors be selected for these purposes.

Micro-Measurements offers three types of precision resistors which are specifically designed for use in strain gage circuits:

STANDARD S-TYPE (Prefix "S"): Epoxy-encapsulated Vishay resistors, noted for long-term stability and low temperature-coefficient-of-resistance. Used for shunt calibration (below 100 000 ohms) and bridge completion.

WIRE-WOUND (Prefix "W"): Good quality wire-wound resistors, used for high-value shunt resistance requirements (above 100 000 ohms).

HERMETIC (Prefix "H"): Hermetically sealed Vishay resistors, for best long-term stability under adverse environmental conditions. These premium resistors are used for bridge completion where highest accuracy and stability are required.

PRECISION RESISTOR SPECIFICATIONS

Standard S-Type (Prefix "S")

SIZE:
0.295 x 0.120 x 0.10 in
(7.5 x 3.1 x 2.5 mm)

TEMP. COEFFICIENT:
±0.1 ppm/°F; 22 to 140°F
(±0.1 ppm/°C; 0° to 60°C)

STABILITY:
25 ppm/year maximum drift

WATTAGE:
0.3 @ 75°F (24°C)

LEADWIRES:
No. 22 AWG tinned copper

CONSTRUCTION:
Encapsulated in epoxy case for use in normal laboratory environment.

Wire-Wound (Prefix "W")

SIZE:
0.23 in dia. x 0.75 in long
(5.8 x 19.1 mm)

TEMP. COEFFICIENT:
±12 ppm/°F; 32° to 140°F
(±20 ppm/°C; 0° to 60°C)

STABILITY:
30 ppm/year maximum drift

WATTAGE:
0.3 @ 75°F (24°C)

LEADWIRES:
No. 20 AWG tinned copper

CONSTRUCTION:
Noninductive windings. Encapsulated for use in normal laboratory environment.

Hermetic (Prefix "H")

SIZE:
0.4 in square x 0.15 in thick
(10 x 4 mm)

TEMP. COEFFICIENT:
±0.6 ppm/°F; 32° to 140°F
(±1 ppm/°C; 0° to 60°C)

STABILITY:
5 ppm/year maximum drift

WATTAGE:
0.25 @ 75°F (24°C)

LEADWIRES:
No. 22 AWG tinned copper

CONSTRUCTION:
Hermetically sealed in metal case. Excellent long-term stability.

BRIDGE COMPLETION MODULES

In addition to precision resistors, Micro-Measurements offers a selection of bridge completion modules. Bridge completion modules combine small size, light weight and convenience with the tight resistance tolerance, low temperature coefficient of resistance and the stability necessary for strain gage bridge completion.

For additional information, please contact our Applications Engineering Department.

SELECTION CHARTS

	Order No.	Resistance in Ohms	Tolerance in %	Equivalent Microstrain
FOR 120-OHM GAGE CIRCUIT	W-59980-02	599 800	±0.02	1000
	W-119880-02	119 880	±0.02	500
	S-59980-01	59 880	±0.01	1000
	S-29980-01	29 880	±0.01	2000
	S-19880-01	19 880	±0.01	3000
	S-14880-01	14 880	±0.01	4000
FOR 350-OHM GAGE CIRCUIT	W-349650-02	349 650	±0.02	500
	W-174650-02	174 650	±0.02	1000
	S-87150-01	87 150	±0.01	2000
	S-57983-01	57 983	±0.01	3000
	S-43400-01	43 400	±0.01	4000
	S-34650-01	34 650	±0.01	5000
FOR 1000-OHM GAGE CIRCUIT	W-999000-02	999 000	±0.02	500
	W-499000-02	499 000	±0.02	1000
	W-249000-02	249 000	±0.02	2000
	W-165666-02	165 666	±0.02	3000
	W-124000-02	124 000	±0.02	4000
	S-99000-01	99 000	±0.01	5000

The "Equivalent Microstrain" column shows the true compression strain simulated by shunting each calibration resistor across an active strain gage arm of the circuit indicated resistance. This is based on a circuit gage factor setting of 2.000. See References below.

SHUNT-CALIBRATION RESISTORS

Order No.	Resistance in Ohms	Tolerance in %
S-50-01	50.0	±0.01
S-60-01	60.0	±0.01
S-100-01	100.0	±0.01
S-120-01	120.0	±0.01
S-175-01	175.0	±0.01
S-240-01	240.0	±0.01
S-350-01	350.0	±0.01
S-500-01	500.0	±0.01
S-1000-01	1000.0	±0.01
S-2000-01	2000.0	±0.01
S-5000-01	5000.0	±0.01
H-100-01	100.0	±0.01
H-120-01	120.0	±0.01
H-350-01	350.0	±0.01
H-1000-01	1000.0	±0.01

BRIDGE-COMPLETION RESISTORS

Order No.	Resistance in Ohms	Tolerance in %	Pairs Matched To
S2-120-01	120/ 120	±0.01	50 ppm
S2-240-01	240/ 240	±0.01	50 ppm
S2-350-01	350/ 350	±0.01	50 ppm
S2-500-01	500/ 500	±0.01	50 ppm
S2-1000-01	1000/1000	±0.01	50 ppm
S2-2000-01	2000/2000	±0.01	50 ppm
S2-5000-01	5000/5000	±0.01	50 ppm
H2-120-01	120/ 120	±0.01	20 ppm
H2-350-01	350/ 350	±0.01	20 ppm
H2-1000-01	1000/1000	±0.01	20 ppm
H2-5000-01	5000/5000	±0.01	20 ppm

50 ppm = 0.005%
Resistors are matched at ±75°F (±24°C)

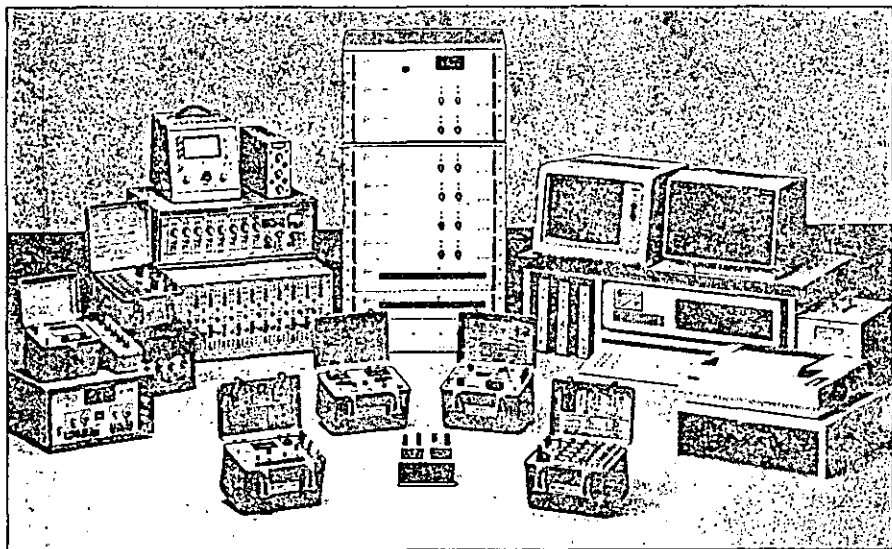
20 ppm = 0.002%
Resistors are matched at ±75°F (±24°C)

NOTES

- The wattage rating of these resistors is adequate for most strain gage excitation levels; i.e., a dissipation of 0.3 watts per arm corresponds to 12 Vdc bridge excitation in an equal-arm 120-ohm circuit. When unusually high excitation levels are involved, the resistors can be connected in series, parallel, or series-parallel configurations to increase power-handling capability.
- Many resistor values listed here are appropriate for use in resistance temperature sensor circuits. See References below.
- The shunt-calibration resistors are chosen to accurately simulate resistance change in a strain gage subjected to specified levels of compressive strain. However, strain indicators generally produce a linear output from the input of a fully active half-bridge or full-bridge circuit, and will be slightly in error when a single active arm is used. The same nonlinearity occurs whether the gage is actually strained in compression or simulated by shunting the gage with the corresponding calibration resistor; and, in either case, the error increases with strain level. See References below.

References: M-M Catalog 500, Part A — Strain Gage Listings, pgs 80-82, *Temperature Sensors and LST Matching Networks*, *Measurement Group, Inc. Tech Notes TN-506, Bondable Resistance Temperature Sensors and Associated Circuitry*; TN-507, *Errors Due to Wheatstone Bridge Nonlinearity*; and TN-514, *Shunt Calibration of Strain Gage Instrumentation*.

INSTRUMENTATION AND SPECIAL-PURPOSE EQUIPMENT



The Instruments Division of the Measurements Group (sister division to Micro-Measurements) is the only organization of its kind devoted exclusively to the design and manufacture of high-quality strain gage instrumentation. The result of such specialization is an instrument line engineered specifically for use with strain gages, in contrast to general-purpose instruments which have been adapted (usually with some undesirable compromises) to strain gage use.

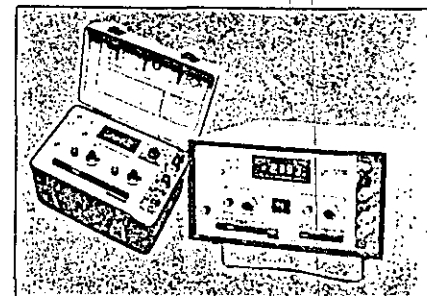
The instruments briefly described on pages 34 through 37 are representative of the Instruments Division's complete line which encompasses the full range of strain measurement needs. Because these instruments were designed by stress analysts, for stress analysts, they characteristically have the level of performance and the operating features valued by professional practitioners. Typically, the instruments offer high resolution, coupled with excellent accuracy and stability. Whether it is connectors for external circuits, displays, controls, panel markings, or other elements of the operator interface, they are designed for easy, error-free use, convenient setup and adjustment.

Instrumentation produced by the Instruments Division of the Measurements Group is in daily use in thousands of test and stress analysis laboratories throughout the world. For an overview of the complete line of strain gage instrumentation, request our short-form catalog, Bulletin SFC-600. To obtain a detailed description and specifications for any of the instruments shown here, request the bulletin number given for that item.



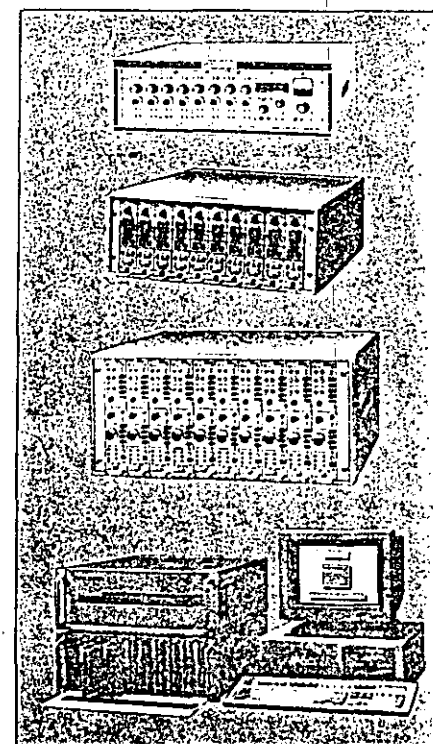
STRAIN INDICATORS

- P-3500**
 The P-3500 is a rugged, portable, battery-powered instrument featuring a 4-1/2 digit LCD readout. Color-coded push-button controls provide an easy-to-follow and logical sequence of setup and operation steps. A transducer input connector facilitates connection of strain gage based transducers. (Bulletin 245).
- 3800**
 The 3800 is a high-precision, laboratory-type digital display strain indicator. It features extremely wide-range gage factor, balance, and bridge excitation controls. The wide-range feature enables measurement resolution of 0.1µε. The 3800 can also be used as a high-performance transducer indicator. (Bulletin 249).



MULTI-CHANNEL SIGNAL CONDITIONER/AMPLIFIERS

- 2100 SYSTEM**
 Multi-channel utility signal-conditioning amplifier. Converts low-level signals from strain gages and other sensors to high-level outputs for recording or computer analysis. Accepts 1/4, 1/2, and full bridges, with 120-ohm, 350-ohm, and 1000-ohm bridge-completion resistors built in. (Bulletin 250).
- 2200 SYSTEM**
 Incorporates all the features necessary for precise conditioning of strain gage and transducer inputs in the most severe operating environments. Standard features include: switch-selectable constant voltage/constant current excitation; ±350V common mode capability; automatic bridge balance; wide frequency response; switch selectable 4-pole Bessel low-pass filter. (Bulletin 252).
- 2300 SYSTEM**
 Sophisticated multi-channel signal-conditioning amplifier for more exacting instrumentation tasks. Among advanced features are: individual regulated power supply for each channel, active filtering selectable by push-button control, three simultaneous outputs per channel, playback operating mode, wide frequency response, and automatic electronic bridge balance. (Bulletin 251).
- 2400 SYSTEM**
 A high-performance computer-controlled dynamic instrumentation system. Incorporates, as standard, all the features necessary for precise conditioning of strain gage and transducer inputs combined with the speed and convenience of computer-controlled setup. The 2400 System allows the user to configure individual signal conditioners from any host computer with an IEEE-488 or RS-232 communications link. (Bulletin 253).

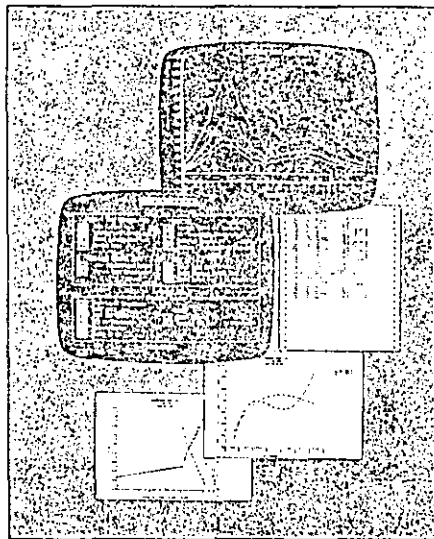


COMPUTER-BASED DATA ACQUISITION SYSTEM

• SYSTEM 4#BB

Unique combination of power and simplicity in a computer-based stress analysis data system. No previous computer experience or programming knowledge is needed to use the system. Includes preprogrammed software to provide fast, accurate acquisition of data, and automatic reduction to engineering units. Simple, four-step operation:

1. Connect sensors — strain gages, transducers, thermocouples, etc. — to easy-access terminals at rear of each scanning unit.
2. Enter circuit parameters and elastic constants by computer keyboard. Friendly, interactive program that asks for all inputs, and tests entered quantities for validity.
3. Press clearly marked keys for whatever operation is desired — scan, record, display, reduce data, etc. System automatically balances and shunt-calibrates all bridge circuits before scanning.
4. Print out test results, fully reduced to specified engineering units — and precorrected for error effects such as apparent strain and transverse sensitivity. Automatically calculates and tabulates principal strains and stresses from strain gage rosette data. (Bulletin 235).



SPECIAL-PURPOSE INSTRUMENTATION

• 1550-A

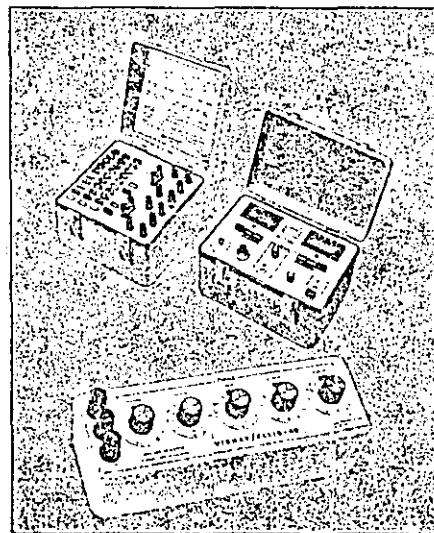
Precision calibrator for determining the accuracy of strain gage and transducer instrumentation. Embodies a true Wheatstone bridge simulator which presents known, repeatable resistance changes to input of strain gage instrument. Easy push-button operation; accurate to 0.025% of setting, $\pm 1\mu\epsilon$. (Bulletin 313).

• 3650

The 3650 Peak-Read Indicator is a portable, battery-powered instrument for capturing peak values of dynamic signals. The instrument is designed to be used in conjunction with any static strain gage indicator, transducer indicator, or signal conditioning system. The 3650 features dual LCD readouts for simultaneously displaying the most positive and most negative readings, and easy-to-use color-coded push-button controls. (Bulletin 246).

• V/E-40

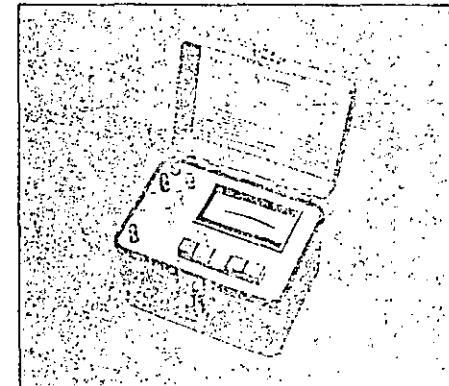
Strain gage simulator. Multi-purpose decade resistor for use with strain gage circuits. Applications include: resistance standard, decade box, instrument calibrator, strain simulator, and investigative tool for identifying circuit problems. $\pm 0.02\%$ accuracy, with 0.01-ohm resistance steps. (Bulletin 316).



MODEL 1300 GAGE INSTALLATION TESTER

The Measurements Group Model 1300 Gage Installation Tester is an instrument designed specifically to test the quality of strain gage installations. With this special-purpose instrument the user can quickly make several electrical measurements on an installed strain gage and determine whether the installation process has degraded the potential gage performance (or even rendered the gage nonfunctional). On new gage installations, it is obviously good practice to perform such tests before completing the wiring and attempting to measure strain. And, of course, the capabilities of the Gage Installation Tester are equally valuable in pinpointing the cause for malfunction in an existing gage installation.

Two of the most important measurements for assessing the quality of a strain gage installation are the insulation resistance between the grid and ground (the test surface), and the shift in gage resistance due to installation procedures. The Model 1300 is specially designed to measure both of these parameters accurately and easily. While the satisfactory outcome of these two measurements does not guarantee all aspects of proper strain gage performance, any installation characterized by other-than-satisfactory values should not be relied upon for accurate strain data.



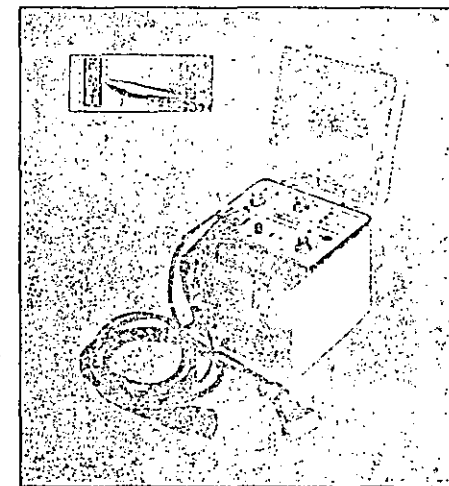
The 1300 is a compact, lightweight battery-operated instrument — equally at home in the laboratory or in the field. (Bulletin 301).

MODEL 700 PORTABLE STRAIN GAGE WELDING AND SOLDERING UNIT

A battery-operated capacitive discharge spot welder for attaching and wiring weldable strain gages and temperature sensors.

In strain gage testing, there are instances when the gages cannot be bonded to the test specimen or structure by conventional adhesive bonding. The solution to this problem is to install Micro-Measurements weldable strain gages. These gages are attached by spot welding, and the Model 700 Portable Welder has been designed to efficiently and conveniently perform this function. The unit also features a battery-operated soldering pencil for attaching leadwires to the strain gage.

The Model 700 Welder is compact and lightweight. Separate visual and audible indicators monitor the welding status. A low-battery light alerts the user when the internal, sealed lead-acid battery requires charging. Other features include a weld energy control, soldering pencil heat control, and storage area for the welding cables. (Bulletin 302).



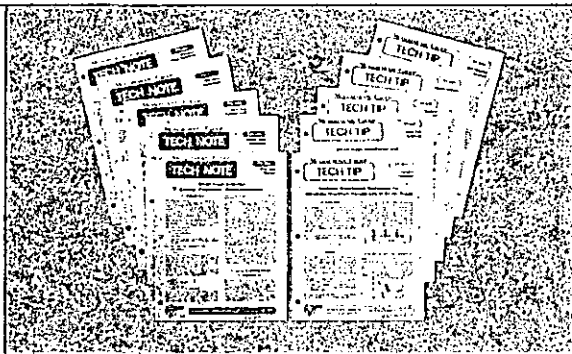
TECHNICAL SUPPORT AND TRAINING FOR PROFESSIONAL CALIBER STRAIN GAGE INSTALLATIONS

In the previous sections of this catalog we have described the necessary tools, materials, and supplies required for successful strain gage installation. Once the proper selection of application accessories is made, the next and most important step in installing the gage is the application technique itself. To this end Micro-Measurements offers a full range of technical support which includes an extensive set of instructional literature, regularly sched-

uled training programs on the procedures and techniques for making high quality strain gage installations, and self-teaching aids to help trainees quickly gain skill and proficiency in application techniques. Additionally, we maintain a full-time Applications Engineering staff to assist the customer with any particular strain gage installation problem he may encounter.

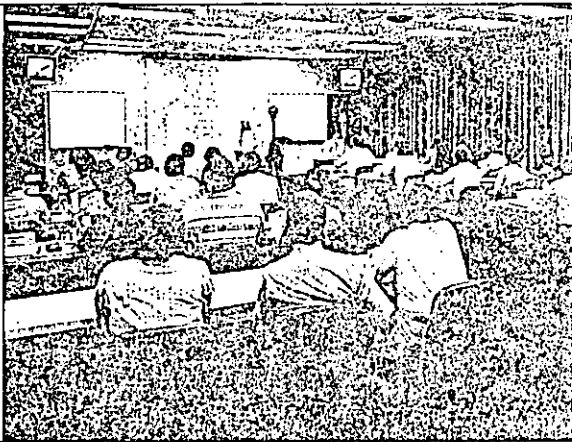
TECHNICAL PUBLICATIONS

Micro-Measurements has published an extensive set of technical notes and detailed instructional literature on practical strain gage application techniques. Most of this technical literature is unique in that the content cannot be found in engineering textbooks or other published sources. The Micro-Measurements library of strain gage reference material is continuously updated to reflect the latest technology in application techniques, and is available at no charge.



TRAINING PROGRAMS

Micro-Measurements training programs cover all levels of strain gage technology. Our specially designed Technical Training Center in Raleigh, North Carolina is complete with the latest in visual-aid equipment including closed-circuit television, and features custom-built, fully equipped work stations for hands-on learning. Our two-day strain gage workshop (Course W65) is a hands-on program where each participant completes gage installations using materials selected for suitability in a majority of gage operating environments. For a detailed description of Course W65 and other Measurements Group courses, ask for our Stress Analysis Training Brochure and schedule of dates offered.



APPLICATIONS ENGINEERING STAFF

In keeping with Micro-Measurements customer-service policies, help is never farther away than your telephone when you encounter a problem in strain gage application. A staff of trained Applications Engineers is always on duty at Measurements Group headquarters in Raleigh, North Carolina during regular office hours, to answer your questions and provide whatever assistance you may need. Telephone (919) 365-3800.



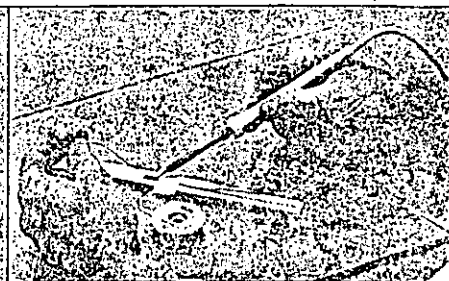
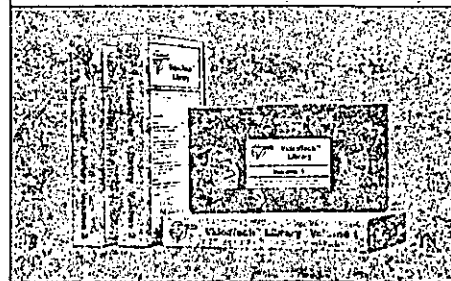
SELF-TEACHING VIDEOTAPE SYSTEM

The VideoTech™ library is a series of instructional VHS videotapes for strain gage installation. The first three volumes cover installations for general-purpose strain measurements. Other tapes involving special-purpose measurement techniques are planned.

The procedures outlined in the VideoTech Library will help both novice and experienced strain gage users to make reliable, professional-caliber strain gage installations every time.

The videotape presentation format of these dependable, proven, state-of-the-art methods can be adapted with equal success to individual, self-taught programs, or to group training sessions. Each tape contains instruction for general-purpose surface preparation, gage bonding, leadwire attachment, and typical environmental protections. Organized in detailed, fully illustrated steps, each tape concludes with an example of a successful strain gage installation.

With the VideoTech Library at hand, the trainee learns by doing each of the prescribed steps to reproduce the actual installation. For additional details concerning these instructional videotapes, request Bulletin 378 or contact our Applications Engineering Department.



ORDERING INFORMATION

Prices: See Micro-Measurements Catalog A-110 Price List

Purchase orders and requests for quotation should be made out to Measurements Group, Inc., Micro-Measurements Division, P.O. Box 27777, Raleigh, North Carolina 27611, USA

Terms: F.O.B. Wendell, North Carolina, USA

All items described in this catalog are normally carried in stock for fast delivery.

UPDATES

Micro-Measurements continually tests existing accessory items as well as new products for possible inclusion in our Accessories line.

When significant changes, deletions, or additions to M-ERM Accessories are made, you will be advised through our Technical Data Mailing Program with supplement sheets to this Catalog. Our Accessories Price Sheet is also periodically updated and made available through this program.

If you have any questions as to the current status of the literature you have on hand, or to the availability of a specific product, please contact our Customer Service Department.

WARRANTY POLICY

The Micro-Measurements Division of Measurements Group, Inc., warrants that the products sold under its name, are fit for the purpose for which they were intended by the supplier and guarantee said items against defects in workmanship or material for a period of ninety (90) days, or otherwise specified limits, from date of delivery. Every reported case of non-standard material is thoroughly investigated by our Quality Assurance Department. It should be recognized that there is no method to 100% test our type of products since many tests would be destructive. Both Micro-Measurements and the Purchasers must depend upon statistical sampling techniques that have in the past proved to be reliable and economical in respect to the cost of the product.

This warranty is in lieu of any other warranties, expressed or implied, including any implied warranties of merchantability or fitness for a particular purpose. There are no warranties which extend beyond the description of the face hereof. Purchaser acknowledges that all goods purchased from Measurements Group are purchased as is, and Buyer states that no salesman, agent, employee or other person has made any such representations or warranties or otherwise assumed for Measurements Group any liability in connection with the sale of any goods to the

Purchaser. Buyer hereby waives all rights Buyer may have arising out of any breach of contract or breach of warranty on the part of Measurements Group, to any incidental or consequential damages, including but not limited to damages to property, damages for injury to the person, damages for loss of use, loss of time, loss of profits or income, or loss resulting from personal injury.

Some states do not allow the exclusion or limitation of incidental or consequential damages for consumer products, so the above limitations or exclusions may not apply to you.

The Purchaser agrees that the Purchaser is responsible for notifying any subsequent buyer of goods, manufactured by Measurements Group of the warranty provisions, limitations, exclusions and disclaimers stated herein, prior to the time any such goods are purchased by such buyer, and the Purchaser hereby agrees to indemnify and hold Measurements Group harmless from any claim asserted against or liability imposed on Measurements Group occasioned by the failure of the Purchaser to so notify such buyer. This provision is not intended to afford subsequent purchasers any warranties or rights not expressly granted to such subsequent purchasers under the law.

The Measurement Group is solely a manufacturer and assumes no responsibility of any form for the accuracy or adequacy of any test results, data, or conclusions which may result from the use of its equipment.

The manner in which the equipment is employed and the use to which the data and test results may be put are completely in the hands of the Purchaser. Measurements Group, Inc., shall in no way be liable for damages consequential or incidental to defects in any of its products.

LIMITATION OF REMEDY: In the event any discrepancy is found to be Micro-Measurements' responsibility, the Buyer's sole and exclusive remedy will be the replacement of, or full credit for the discrepant product.

We will provide immediate assistance to the best of our ability in locating and identifying the source of any difficulties involving our product.



MICRO-MEASUREMENTS DIVISION
MEASUREMENTS GROUP, INC.

P.O. Box 27777

Raleigh, North Carolina 27611, USA

Telephone: (919) 365-3800 • Telex: 802-502 • FAX: (919) 365-3945

World's Leading Supplier of Precision Strain Gages and Accessories

Surface Preparation for Strain Gage Bonding

1.0 INTRODUCTION

Strain gages can be satisfactorily bonded to almost any solid material if the material surface is prepared *properly*. While a properly prepared surface can be achieved in more than one way, the specific procedures and techniques described here offer a number of advantages. To begin with, they constitute a carefully developed and thoroughly proven system; and, when the instructions are followed precisely (along with those for gage and adhesive handling), the consistent result will be strong stable bonds. The procedures are simple to learn, easy to perform, and readily reproducible.

Furthermore, the surface preparation materials used in these procedures are, unless otherwise noted, generally low in toxicity, and do not require special ventilation systems or other stringent safety measures. Of course, as with any materials containing solvents or producing vapors, adequate ventilation is necessary.

The importance of attention to detail, and precise adherence to instructions, cannot be overstressed in surface preparation for strain gage bonding. Less thorough, or even casual, approaches to surface preparation may sometimes yield satisfactory gage installations; but for *consistent* success in achieving high-quality bonds, the methods given here can be recommended without qualification. Fundamental to the Micro-Measurements system of surface preparation is an understanding of *cleanliness* and *contamination*. All open surfaces not thoroughly and freshly cleaned must be considered contaminated, and require cleaning immediately prior to gage bonding. Similarly, it is imperative that the materials used in the surface preparation be fresh, clean, and uncontaminated. It is worth noting that strain gages as received from Micro-Measurements are chemically clean, and specially treated on the underside to promote adhesion. Simply touching the gages with the fingers (which are always contaminated) can be detrimental to bond quality.

The Micro-Measurements system of surface preparation includes five basic operations.* These are, in the usual order of execution:

- solvent degreasing
- abrading
- application of gage layout lines
- conditioning
- neutralizing

These five operations are varied and modified for compatibility with different test material properties, and exceptions are introduced as appropriate for certain special materials and situations.

The surface preparation operations are described individually in *Section 2.0*, following a summary of the general principles applicable to the entire process. *Section 3.0* discusses special precautions and considerations which should be borne in mind when working with unusual materials and/or surface conditions.

As a convenience to the gage installer in quickly determining the specific surface preparation steps applicable to any particular test material, *Section 4.0* includes a chart listing approximately 75 common (and uncommon) materials and the corresponding surface preparation treatments.

On the back cover of this Instruction Bulletin, a blank form is provided so that the laboratory supervisor, or the instructor in an educational institution, can prepare individual procedure sheets for particular materials of interest. The form can be copied, and the relevant information from this Instruction Bulletin transferred to the blank spaces to produce a completely spelled-out surface preparation procedure for any material listed in *Section 4.0*.

2.0 BASIC SURFACE PREPARATION OPERATIONS AND TECHNIQUES

2.1 General Principles of Surface Preparation for Strain Gage Bonding

The purpose of surface preparation is to develop a chemically clean surface having a roughness appropriate to the gage installation requirements, a surface alkalinity corresponding to a pH of 7 or so, and visible gage layout lines for locating and orienting the strain gage. It is toward this purpose that the operations described here are directed.

*Note: Basic surface preparation procedures and techniques are presented and described in detail in Micro-Measurements' VideoTech™ Library. These videotape sequences provide thorough, step-by-step procedures for making successful strain gage installations. For more information, request Bulletin 318.

As noted earlier, cleanliness is vital throughout the surface preparation process. It is also important to guard against recontamination of a once-cleaned surface. Following are several examples of surface recontamination to be avoided:

- Touching the cleaned surface with the fingers.
- Wiping back and forth with a gauze sponge, or reusing a once-used surface of the sponge (or of a cotton swab).
- Dragging contaminants into the cleaned area from the uncleaned boundary of that area.
- Allowing a cleaning solution to evaporate on the surface.
- Allowing a cleaned surface to sit for more than a few minutes before gage installation, or allowing a partially prepared surface to sit between steps in the cleaning procedure.

Beyond the above, it is good practice to approach the surface preparation task with freshly washed hands, and to wash hands as needed during the procedure.

2.2 Solvent Degreasing

Degreasing is performed to remove oils, greases, organic contaminants, and soluble chemical residues. Degreasing should always be the first operation. This is to avoid having subsequent abrading operations drive surface contaminants into the surface material. Porous materials such as titanium, cast iron, and cast aluminum may require heating to drive off absorbed hydrocarbons or other liquids.

Degreasing can be accomplished using a hot vapor degreaser, an ultrasonically agitated liquid bath, aerosol type spray cans of CSM-1 Degreaser, or wiping with GC-6 Isopropyl Alcohol. One-way applicators, such as the aerosol type, or cleaning solvents are always preferable because dissolved contaminants cannot be carried back into the parent solvent. Whenever possible, the entire test piece should be degreased. In the case of large bulky objects which cannot be completely degreased, an area covering 4 to 6 in (100 to 150 mm) on all sides of the gage area should be cleaned. This will minimize the chance of recontamination in subsequent operations, and will provide an area adequately large for applying protective coatings in the final stage of gage installation.

2.3 Surface Abrading

General

In preparation for gage installation the surface is abraded to remove any loosely bonded adherents (scale, rust, paint, galvanized coatings, oxides, etc.), and to develop a surface texture suitable for bonding. The abrading operation can be performed in a variety of ways, depending upon the initial condition of the surface and the desired finish for gage installation. For rough, or coarse surfaces, it may be necessary to start with a grinder, disc sander, or file. (Note: Before performing any abrading operations, see Section 3.1 for safety precautions.) Finish abrading is done with silicon-carbide paper of the appropriate grit, and recommended grit sizes for specific materials are given in Section 4.0.

If grit blasting is used instead of abrading, either clean alumina or silica (100 to 400 grit) is satisfactory. In any case, the air supply should be well filtered to remove oil and other contaminant vapors coming from the air compressor. The grit used in blasting should not be recycled or used again in surface preparation for bonding strain gages.

The optimum surface finish for gage bonding depends somewhat upon the nature and purpose of the installation. For general stress analysis applications, a relatively smooth surface (in the order of 100 μ m, or 2.5 μ m, rms) is suitable, and has the advantage over rougher surfaces that it can be cleaned more easily and thoroughly. Smoother surfaces, compatible with the thin "gluelines" required for minimum creep, are used for transducer installations. In contrast, when very high elongations must be measured, a rougher (and preferably cross-hatched) surface should be prepared. The recommended surface finishes for several classes of gage installations are summarized in Table I, below.

TABLE I

CLASS OF INSTALLATION	SURFACE FINISH, rms	
	μ m	μ m
General stress analysis	63 — 125	1.6 — 3.2
High elongation	>250 cross-hatched	>6.4
Transducers	16 — 63	0.4 — 1.6
Ceramic cement	>250	>6.4

Wet Abrading

Whenever M-Prep Conditioner A is compatible with the test material (see Section 4.0), the abrading should be done while keeping the surface wet with this solution, if physically practicable. Conditioner A is a mildly acidic solution which generally accelerates the cleaning process and, on some materials, acts as a gentle etchant. It is not recommended for use on magnesium, synthetic rubber, or wood.

2.4 Gage-Location Layout Lines

The normal method of accurately locating and orienting a strain gage on the test surface is to first mark the surface with a pair of crossed reference lines at the point where the strain measurement is to be made. The lines are made perpendicular to one another, with one line oriented in the direction of strain measurement. The gage is then installed so that the triangular index marks defining the longitudinal and transverse axes of the grid are aligned with the reference lines on the test surface.

The reference or layout lines should be made with a tool which burnishes, rather than scores or scribes, the surface. A scribed line may raise a burr or create a stress concentration. In either case, such a line can be detrimental to strain gage performance and to the fatigue life of the test part. On aluminum and most other nonferrous alloys, a 4H drafting pencil is a satisfactory and convenient burnishing tool. However, graphite pencils should never be used on high-temperature alloys where the operating temperature might cause a carbon embrittlement problem. On these and other hard alloys, burnished alignment marks can be made with a ballpoint pen or a round-pointed brass rod. Layout lines are ordinarily applied following the abrading operation and before final cleaning. All residue from the burnishing operation should be removed by scrubbing with Conditioner A as described in the following section.

2.5 Surface Conditioning

After the layout lines are marked, Conditioner A should be applied repeatedly, and the surface scrubbed with cotton-tipped applicators until a clean tip is no longer discolored by the scrubbing. During this process the surface should be kept constantly wet with Conditioner A until the cleaning is completed. *Cleaning solutions should never be allowed to dry on the surface.* When clean, the surface should be dried by wiping through the cleaned area with a single slow stroke of a gauze sponge. The stroke should begin inside the cleaned area to avoid dragging contaminants in from the boundary of the area. Then, with a fresh sponge, a single slow stroke is made in the opposite direction. The sponge should never be wiped back and forth, since this may redeposit the contaminants on the cleaned surface.

2.6 Neutralizing

The final step in surface preparation is to bring the surface condition back to an optimum alkalinity of 7.0 to 7.5 pH, which is suitable for all Micro-Measurements strain gage adhesive systems. This should be done by liberally applying M-Prep Neutralizer 5A to the cleaned surface, and scrubbing the surface with a clean cotton-tipped applicator. The cleaned surface should be kept completely wet with Neutralizer 5A throughout this operation. When neutralized, the surface should be dried by wiping through the cleaned area with a single slow stroke of a clean gauze sponge. With a fresh sponge, a single stroke should then be made in the opposite direction, beginning with the cleaned area to avoid recontamination from the uncleaned boundary.

If the foregoing instructions are followed precisely, the surface is now properly prepared for gage bonding, and the gage or gages should be installed as soon as possible.

3.0 SPECIAL PRECAUTIONS AND CONSIDERATIONS

3.1 Safety Precautions

As in any technical activity, safety should always be a prime consideration in surface preparation for strain gage bonding. For example, when grinding, disc sanding, or filing, the operator should wear safety glasses and take such other safety precautions as specified by his organization or by the Occupational Safety and Health Administration (OSHA).

When dealing with toxic materials such as beryllium, lead, uranium, plutonium, etc., all procedures and safety measures should be approved by the safety officer of the establishment before commencing surface preparation.

3.2 Surfaces Requiring Special Treatment

Concrete

Concrete surfaces are usually uneven, rough, and porous. In order to develop a proper substrate for gage bonding, it is necessary to apply a leveling and sealing precoat of epoxy

adhesive to the concrete. Before applying the precoat, the concrete surface must be prepared by a procedure which accounts for the porosity of this material.

Contamination from oils, greases, plant growth, and other soils should be removed by vigorous scrubbing with a stiff-bristled brush and a mild detergent solution. The surface is then rinsed with clean water. Surface irregularities can be removed by wire brushing, disc sanding, or grit blasting, after which all loose dust should be blown or brushed from the surface.

The next step is to apply M-Prep Conditioner A generously to the surface in and around the gaging area, and scrub the area with a stiff-bristled brush. Contaminated Conditioner A should be blotted with gauze sponges, and then the surface should be rinsed thoroughly with clean water. Following the water rinse, the surface acidity must be reduced by scrubbing with M-Prep Neutralizer 5A, blotting with gauze sponges, and rinsing with water. A final thorough rinse with distilled water is useful to remove the residual traces of water-soluble cleaning solutions. Before precoat-ing, the cleaned surface must be thoroughly dried. Warming the surface gently with a propane torch or electric heat gun will hasten evaporation.

Micro-Measurements M-Bond AE-19 room-temperature-curing epoxy adhesive is an ideal material for precoat-ing the concrete. For those cases in which the test temperature may exceed the specified maximum operating temperature of AE-10 (+200°F, or +93°C), it will be necessary to fill the surface with a higher temperature resin system such as M-Bond GA-61.

In applying the coating to the porous material, the adhesive should be worked into any voids, and leveled to form a smooth surface. When the adhesive is completely cured, it should be abraded until the base material begins to be exposed again. Following this, the epoxy surface is cleaned and prepared conventionally, according to the procedure specified in Section 4.0 for bonding gages to epoxies.

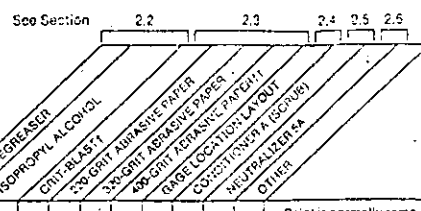
Plated Surfaces

In general, plated surfaces are detrimental to strain gage stability, and it is preferable to remove the plating at the gage location, if this is permissible. Cadmium and nickel plating are particularly subject to creep, and even harder platings may creep because of the imperfect bond between the plating and the base metal. When it is not permissible to remove the plating, the surface should be prepared according to the procedure given in Section 4.0 for the specific plating involved. Note that it may be necessary to adjust testing procedures to minimize the effects of creep.

Use of Solvents on Plastics

Plastics vary widely in their reactivity to solvents such as those employed in the surface preparation procedures described here. Before applying a solvent to any plastic, Section 4.0, which includes most common plastics, should be referred to for the recommended compatible solvent. For plastics not listed in Section 4.0, the manufacturer of the material should be consulted, or tests should be performed to verify nonreactivity between the solvent and the plastic.

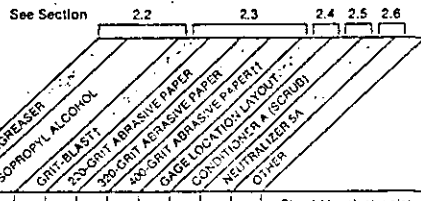
TABLE II
Index of Test Materials
and
Surface Preparation Procedures
(Sheet 2 of 3)



SPECIAL NOTES
*Heating specimen will help drive out oils, moisture, and solvent.
**Rinse with distilled water, and wipe dry.
†Use clean (filtered), dry air. Do not recycle alumina or silica gages.
††Wet lap with Conditioner A when compatibility is indicated by "Conditioner A (Scrub)" column.
() Parentheses indicate alternate step(s).

SPECIMEN MATERIAL	See Section					REMARKS		
	2.2	2.3	2.4	2.5	2.6			
ENAMEL PAINTS			2	3	4	1	Paint is normally removed for gage installation. Baked enamels may be left on surface if essential to test.	
EPOXIES	1	(1)	2	3	(3)	4	Surface may require several initial cleanings with Conditioner A if silicates are present.	
FIBERGLASS LAMINATES	1		2	3	4	5	Coarser abrasive may be necessary. In Step 2 to remove all surface gloss.	
GRAPHITE AND GRAPHITE COMPOSITES	1, 3, 5*		2	4		(5)		
GLASS	1	(1)	No		2	3	Abrasion not usually necessary. Engineering approval for abrading is generally required.	
GOLD	1	(1)			2	3		
INCONEL	1	2	(2a) (2b)	3	4	5	Repeat Steps 4 and 5 if gages cannot be installed within 45 min.	
INDIUM	1			2	3	3		
INVAR	1	2	(2a) (2b)	3	4	5	Repeat Steps 4 and 5 if gages cannot be installed within 45 min.	
IRON, CAST OR WROUGHT	1*	2	(2a) (2b)	3	4	5	Repeat Steps 2 through 5 if gages cannot be installed within 30 min.	
ISOELASTIC	1	No	2	3	4	5	Repeat Steps 4 and 5 if gages cannot be installed within 45 min.	
KAPTON	1	(1)	(2)	2	3	4		
LEAD	1	No	2	3	4	5		
MAGNESIUM	1	(1)		3	No	4	2	Do not abrade magnesium (i.e., avoid producing fine particles). Scrape gage site with deburring knife or file. Do not use Conditioner A on magnesium.
MANGANIN	1	(1), 5		2	3	4		
MASONRY	1, 4*			3	5	6	2	Wire-brush or disc-sand, and remove dust with dry paint brush. Fill and seal surface with epoxy adhesive, such as M-M AE-10, and sand smooth after adhesive is cured.
MODELTECH® (aluminum-filled cast epoxy)	1			2	3	4	5	
MOLYBDENUM	1	(1)		2	3	4	5	
MONEL	1	(1)		2	3	4	5	
MYLAR	1	(2)		2	3		4	
NICHROME	1	(1)	(2)	2	3	4	5	
NICKEL AND NICKEL PLATE	1	(1)		2	3	4	5	If permissible, nickel plating should be removed at gage installation site.
NI-SPAN C	1	(1)	(2)	2	3	4	5	
NYLON	1	(2)		2	3		4	
PHENOLIC COMPOSITES	1	1, 5*		2	3	4	(5)	Step 2 may require coarser abrasive to remove all surface gloss.
PHOSPHOR BRONZE	1	(6)**		2	3	4	5**	
PLATINUM	1			2	3	4		

TABLE II
Index of Test Materials
and
Surface Preparation Procedures
(Sheet 3 of 3)



SPECIAL NOTES
*Heating specimen will help drive out oils, moisture, and solvent.
**Rinse with distilled water, and wipe dry.
†Use clean (filtered), dry air. Do not recycle alumina or silica gages.
††Wet lap with Conditioner A when compatibility is indicated by "Conditioner A (Scrub)" column.
() Parentheses indicate alternate step(s).

SPECIMEN MATERIAL	See Section					REMARKS			
	2.2	2.3	2.4	2.5	2.6				
PLUTONIUM	1			3	4	5	2	Should be electroplated with nickel before gage installation. Contact M-M Applications Engineering Department for specific instructions.	
POLYCARBONATES	1	No		2	3	4	5		
POLYETHYLENE	1			(2)	3	No	4	2	Scour with household cleanser and rinse with water, or flame-burnish surface.
POLYURETHANE	1			2	3		4		
POLYVINYL CHLORIDE	1			(2)	3		4	2	Scour with household cleanser and rinse with water.
PORCELAIN	1				2	3			
QUARTZ	1				2	3			
RENE 41	1	(2)	2	3	4	5			
RUBBER, NATURAL OR SYNTHETIC	1		2	3	4	(2)		Scour with household cleanser and rinse with water.	
SILVER	1			3	4	2		Scrub with slurry of pumice powder and isopropyl alcohol.	
SINTERED METALS	1		2	3	4	5	6	(1)	Hot-vapor degrease.
STEEL (Carbon and Stainless)	1	2	(2a) (2b)	3	4	5		Repeat Steps 4 and 5 if gages cannot be bonded within 45 min of final surface preparation.	
STEEL, 4000 SERIES	1	(2)	2	3	No	4		Conditioner A tends to produce black residue on surface.	
STEEL SURFACE HARDENED	1			2	3, 4	5		Removal of surface material may alter residual stress conditions and/or fatigue life and wear resistance.	
STONE	1	2*			3	4	1	Wire-brush, grind, or disc-sand, and dust surface with dry paint brush. Fill and seal surface with epoxy adhesive, such as M-M AE-10, and sand smooth after adhesive is cured.	
TANTALUM	1	(1)		2	3	4	5		
TEFLON	1	(1)			3	4	2	Etch surface with M-M Tetra-Etch, rinse with isopropyl alcohol, and then with water.	
TIN	1	(1)		2	3	4	5		
TITANIUM	1	2	(2)	3	4	5		It may be necessary to heat-cycle the specimen two or three times to -350°F (-175°C) as initial step in surface preparation. Halogens should never be used for degreasing if the specimen is to be tested at temperatures above +760°F (+370°C). Install gages within 10 min of final surface preparation.	
TITANIUM SILICATE	1	(1)	2	3	4	5			
TUNGSTEN CARBIDE	1	(1)	2	3	4	5			
URANIUM	1	No		3	4	5	2	Should be electroplated with nickel before gage installation. Contact M-M Applications Engineering Department for specific instructions.	
WOOD	1	No	(2)	2	3		1	It may be necessary to kiln-dry wood of more than 20% moisture content. After abrasion, dust surface with dry paint brush.	
ZINC	1	No	2	3	4	5			
ZIRCONIUM	1	(1)	2	3	4	5		It may be necessary to repeat Step 5 until proper surface pH is achieved.	

Noise Control in Strain Gage Measurements

INTRODUCTION

Strain measurements must often be made in the presence of electric and/or magnetic fields which can superimpose electrical noise on the measurement signals. If not controlled, the noise can lead to inaccurate results and incorrect interpretation of the strain signals; and, in severe cases, can obscure the strain signals altogether. In order to control the noise level, and maximize the signal-to-noise ratio, it is necessary first to understand the types and characteristics of electrical noise, as well as the sources of such noise. With this understanding, it is then possible to apply the most effective noise-reduction measures to any particular instrumentation problem.

This technical note identifies some of the more common noise sources, and describes the routes by which the noise is induced into strain gage circuits. It should be noted that the treatment here is limited to noise from external electrical and magnetic sources. This note does not cover effects from nuclear or thermal sources, nor does it consider the effects of variable wiring or contact resistance caused by slip rings, connectors, switches, etc. Following the discussion of noise sources, specific methods are given, varying with the noise-coupling mechanism, for noise avoidance. The information in this technical note is equally applicable to both analog and digital systems employing DC amplifiers. It also applies to systems using carrier excitation and carrier amplifiers, although noise problems are usually less severe in such systems.

NOISE SOURCES AND PICKUP MEDIA

Virtually every electrical device which generates, consumes, or transmits power is a potential source for causing noise in strain gage circuits. And, in general, the higher the voltage or current level, and the closer the strain gage circuit to the electrical device, the greater will be the induced noise. Following is a list of common electrical noise sources:

- AC power lines
- motors and motor starters
- transformers
- relays
- generators
- rotating and reciprocating machinery
- arc welders
- vibrators
- fluorescent lamps
- radio transmitters
- electrical storms
- soldering irons

Electrical noise from these sources can be categorized into two basic types: electrostatic and magnetic. The two types of noise are fundamentally different, and thus require different noise-reduction measures. Unfortunately, most of the common noise sources listed above produce combinations of the two noise types, which can complicate the noise-reduction problem.

Electrostatic fields are generated by the presence of voltage—with, or without current flow. Alternating electrical fields inject noise into strain gage systems through the phenomenon of *capacitive coupling*, by which charges of correspondingly alternating sign are developed on any electrical conductors subjected to the field (Fig. 1). Fluorescent lighting is one of the more common sources of electrostatic noise.

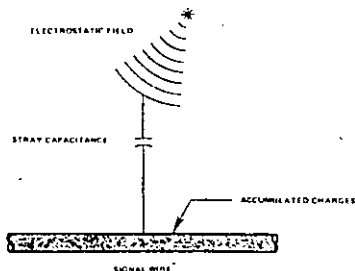


Fig. 1—Electrostatic noise coupling.

Magnetic fields are ordinarily created either by the flow of electric current or by the presence of permanent magnetism. Motors and transformers are examples of the former, and the earth's magnetic field is an instance of the latter. In order for noise voltage to be developed in a conductor, magnetic lines of flux must be "cut" by the conductor. Electric generators function on this basic principle. In the presence of an alternating field, such as that surrounding a 50/60-Hz power line, voltage will be induced into any stationary conductor as the magnetic field expands and collapses (Fig. 2). Similarly, a conductor moving through the earth's magnetic field has a noise voltage

generated in it as it cuts the lines of flux. Since most iron and steels are ferromagnetic, moving machine members redirect existing lines of flux, and may cause them to be cut by adjacent sensitive conductors. As a result, signal conductors in the vicinity of moving or rotating machinery are generally subject to noise voltages from this source.

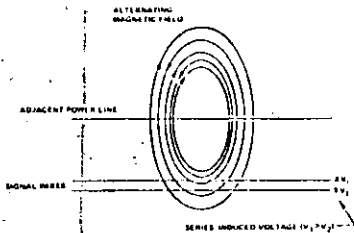


Fig. 2—Electromagnetic noise coupling.

DETECTING AND TROUBLESHOOTING

In order to effectively assess the presence and magnitude of noise, the strain gage instrument selected for use should incorporate a simple, but very significant feature—a control for removing the excitation from the Wheatstone bridge. With such a control, the instrument output can be easily checked for noise, independently of any strain signal. This represents a very powerful tool for evaluating the effectiveness of shields and ground, and for experimentally modifying these methods to minimize the effects of noise. All Measurements Group strain gage signal conditioners are equipped with this important control.

The following procedure can be used to troubleshoot a system for noise:

1. If not already known, determine the tolerable levels of noise in output units (millivolts, inches of deflection, etc.) as observed on a readout such as an oscilloscope or recorder.
2. With no strain gage input, terminate the S/S—amplifier input with about the same input impedance that the amplifier normally senses (typically 120 or 350 ohms). If excessive noise exists:
 - a) Check for ground loops (more than one connection of the system to ground).
 - b) Check for line ("mains")—radiated noise.
 - c) If feasible, reduce amplifier gain and compensate by increasing bridge voltage.
3. With excitation switch set to off, connect the gage (or transducer) to the instrument, and observe noise. Any noise picked up in this step is attributed, of course, to lead-wire and/or gage pickup. If the output changes when the instrument chassis is touched with a finger, this is an indication of a poor ground and/or radio-frequency interference.
4. Apply a load to the part under test (excitation still off). If additional noise is observed, the noise is due to something associated with the loading mechanism such as a motor creating a magnetic field, or the motion of the gage or wiring (generating emf).
5. Remove the load from the test part, if possible, and apply excitation voltage to the bridge circuit. After balancing the bridge, any subsequent gradual zero drift may be due to gage self-heating effects (see Micro-Measurements Tech Note TN-127, *Strain Gage Excitation Levels*).

The procedures of this Tech Note give recommended noise-reduction procedures for electrostatic noise, and for magnetic noise.

ELECTROSTATIC NOISE REDUCTION

The simplest and most effective barrier against electrostatic noise pickup is a conductive shield, sometimes referred to as a *Faraday cage*. It functions by capturing the charges that would otherwise reach the signal wiring. Once collected, these charges must be drained off to a satisfactory ground (or reference potential). If not provided with a low-resistance drainage path, the charges can be coupled into the signal conductors through the shield-to-cable capacitance (Fig. 3).

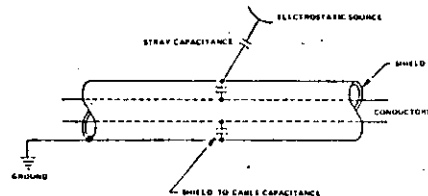


Fig. 3—Electrostatic shielding.

The two most popular types of cable shields are braided wire and conductive foil. The braided shield construction provides about 95 percent coverage of the cable, and is characteristically low in resistance. Foil shields, although commonly higher in resistance, give 100 percent cable coverage, and are also easier to terminate. Following are commercially available examples of the two types of shielded cable:

- braided: Micro-Measurements Type 430-FST (four conductors, twisted)
- foil: Belden No. 8434

When long reaches of multiple conductors are run adjacent to each other, problems with crosstalk between conductors can be encountered. With runs of 50 feet (15m) or more, significant levels of noise can be induced into sensitive conductors through both magnetic and electrostatic coupling. Even though bridge-excitation conductors may carry only a millivolt of noise, there can be significant coupling to signal conductors to produce potentially troublesome microvolt-level noise in those conductors. The noise transfer can be minimized by employing an instrumentation cable composed of individually shielded pairs—one pair for excitation, and one pair for the signal. This type of construction is embodied in Belden No. 8434 cable. When using such cable, having separate shields, both shields should be grounded at the instrument end of the cable. Electrostatic coupling between excitation and signal pairs can be reduced somewhat by using a cable that has its conductor pairs twisted on separate axes. Belden No. 8730 cable has the conductor pairs both separately twisted and shielded with foil.

The shield-to-conductor capacitance can also become significant for long runs, since the capacitance is proportional to the cable length. Therefore, a significant portion of the residual noise can be coupled from even a well-grounded shield to the sensitive conductors. To minimize this effect, some strain gage instruments (for example, Measurements Group Instruments Division's 2300 System) incorporate a feature called a *driven guard*. A driven guard (also known as a *driven shield*) functions by maintaining the shield at a voltage equal to the average signal, or common-mode voltage. Since, with this arrangement, the voltage difference between the conductors and shield is essentially zero, the effective capacitance is decreased, and

in severe magnetic fields, especially those with steep gradients in field intensity, additional measures may be required. For this purpose, Micro-Measurements has developed a special gage configuration consisting of two identical grids, with one stacked directly above, and insulated from the other. By connecting the upper and lower gage elements in series so that the current flows in opposite directions through the two grids, the noise induced in the assembly tends to be self-cancelling. This arrangement is particularly effective against magnetic field gradients and their components parallel to the test surface. The dual-element gage is intended to function as one arm of a Wheatstone bridge circuit; and the bridge is usually completed with another gage of the same type, or with a fixed precision resistor. Standard practices are followed when installing the gages; but Micro-Measurements M-Bond 600/610 adhesive system is recommended for bonding, since this will result in the thinnest "glue line", and placement of the grids as close as possible to the specimen surface.

In addition to the strain gage size and pattern, the selection of the gage grid alloy should be given careful consideration. If the grid alloy is magnetic, it will be subject to extraneous physical forces in a magnetic field; and, if magnetostrictive, will undergo spurious resistance changes. Similarly, if the alloy

is magnetostrictive, the grid will try to change length in the magnetic field. Inelastic alloy, for example, should not be used in magnetic fields, since it is both strongly magnetostrictive and magnetoelastic. Stemming from their comparative freedom from magnetic effects, constantan and Karma-type alloys are usually selected for such applications. Constantan, however, at cryogenic temperatures and in high magnetic fields (7–70 Tesla) becomes severely magnetostrictive. The Karma alloy is ordinarily preferred for cryogenic service because of its generally superior performance in magnetic fields at very low temperatures. Available from Micro-Measurements are two types of dual-element stacked gages—WA-XX-125WJ-240 and WK-XX-125WJ-700—in constantan and Karma-type alloys, respectively.

When necessary, strain gages can also be shielded, to some degree, from electromagnetic fields with a magnetic shielding material such as mu-metal. Two or more layers of the shielding material may be required to effect a noticeable improvement; and, of course, even this will be ineffective if the source of the magnetic field is beneath the strain gage. When high frequency (audio) fields are encountered, be sure that the material is suitable (high permeability) at the anticipated frequency.

SUGGESTED ADDITIONAL READING

Aronson, Milton H., "Low-Level Measurements," *Measurements & Control*, Measurements & Data Corporation, Pittsburgh, PA pp. C1–C16.

Coffey, M. B., "Common-mode Rejection Techniques for Low-level Data Acquisition," *Instrumentation Technology*, pp. 45–49, July 1977.

Ficchi, R. F., *Practical Design for Electromagnetic Compatibility*, Hayden Book Co., New York, 1971.

Freynek, H. S., et al., "Nickel-Chromium Strain Gages for Cryogenic Stress Analysis of Super-Conducting Structures in High Magnetic Fields," *Proceedings of the 7th Symposium on Engineering Problems of Fusion Research*, October 1977.

Hayt Jr., W. H., *Engineering Electromagnetics*, McGraw-Hill, New York, 1967.

Klipeck, B., "How To Avoid Noise Pickup on Wire and Cable," *Instruments & Control Systems*, December 1977.

McDermott, Jim, "EMI Shielding and Protective Components," *EDN Magazine*, pp. 165–176, September 1979.

Morrison, Ralph, *Grounding and Shielding Techniques in Instrumentation*, 2nd Ed., John Wiley & Sons, Inc., New York, 1977.

Severinsen, J., "Gaskets That Block EMI," *Machine Design*, August 7, 1975.

Sitter, R. P., "What It Is and How to Control It," *Instrumentation Technology*, pp. 59–65, September-October 1978.

*Stein, Peter K., "Spurious Signals Generated in Strain Gages, Thermocouples and Leads," *LfMSE Publ. No. 69*, April 1977.

*Stein, Peter K., "The Response of Transducers to Their Environment, The Problem of Signal and Noise," *LfMSE Publ. No. 17*, October 1969.

White, D. R. J., *Electromagnetic Interference and Compatibility*, Vol. 3, Don White Consultants, Germantown, MD, 1973.

*Available from: Stein Engineering Services
5602 E. Monte Ross
Phoenix, AZ 85018

there is minimal noise transfer. The result is a very quiet shield. It is important to note that, for proper operation, the driven shield is connected at only one end to the driven-guard pin on the instrument input connector. The driven shield is ordinarily surrounded by a second shield, which should be grounded at one end.

Another often-overlooked source of noise is leakage to ground through the strain gage and/or the cabling. This leakage, if excessive, can cause noise transfer from the specimen to the gage circuit, since even supposedly well-grounded specimens may carry some noise. It is not uncommon to have strain gages installed on nominally grounded test objects which, in fact, have noise levels expressible in volts. And, of course, any strain gage installation on a conductive specimen forms a classic capacitor which can couple noise from the specimen to the gage. In the light of these considerations, it is no more than good practice to make certain that the specimen is properly grounded and that leakage between the gage circuit and the specimen is well within bounds.

Prior to connecting leadwires to the strain gage, the insulation resistance from the gage to the specimen should be measured with a megohm meter such as the Instruments Division Model 1300 Gage Installation Tester. A reading of 10,000 megohms is normally considered a minimum for satisfactory system operation. Readings below this level are indicative of a possibly troublesome bond-line condition which can deteriorate with time and strain. It should also be kept in mind, for gage installations which will operate at elevated temperatures, that leakage resistance tends to decrease as the temperature increases.

After cable placement, and connection at the gage-end of the cable, the following resistance measurements should be made, preferably from the instrument-end of the cable: conductor-to-ground, shield-to-ground, and conductor-to-shield. Because of distributed leakage, these resistances may be somewhat lower than the gage-to-specimen resistance; but cables with significantly lower resistances should be investigated, and the excessive leakage eliminated to avoid potential noise problems.

ELECTROMAGNETIC NOISE REDUCTION

The most effective approach to minimizing magnetically-induced noise is not to attempt magnetic shielding of the sensitive conductors; but, instead, to ensure that noise voltages are induced equally in both sides of the amplifier input (Fig. 4). When analyzed, all conventional strain gage bridge

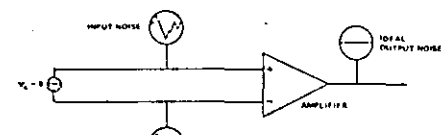


Fig. 4—Noise cancellation by amplifier common-mode rejection.

arrangements—quarter bridge (two- or three-leadwire), half bridge, and full bridge—reduce to the same basic circuit shown in Fig. 4. This is also true for systems such as Instruments Division Models V/E-20A, BAM-1, etc., which employ the "rotated" or non-symmetrical bridge circuit. Achievement of noise cancellation by the method shown in Fig. 4 requires that the amplifier exhibit good common-mode rejection characteristics. Attention must also be given, however, to the strain gage wiring, and to the effects of nearby power lines. For example, it is evident from Fig. 2 that a gradient in magnetic

field intensity exists with respect to distance from the current-carrying power line. The series noise voltages (V_1 and V_2) induced in the signal wires will therefore depend greatly upon their distances from the offending current. Twisting the signal conductors together tends to make the distances equal, on the average, thereby inducing equal noise voltages which will cancel each other. Correspondingly effective, the magnetic field strengths radiated by power lines can be reduced by twisting the power conductors.

In theory, at least, the more twists per unit conductor length, the better. Standard twisted-conductor cables, such as Belden No. 8771, have sufficient twisting for most applications. However, in environments with high magnetic field gradients, such as those found close to motors, generators, and transformers, tighter twisting may be required. For particularly severe applications, conventional twisting may be inadequate, and it may be necessary to use a special woven cable as described later.

When attaching leadwires to a strain gage for operation in a magnetic field, connections should be made directly to the solder tabs on the gage, rather than through auxiliary terminals. Micro-Measurements type CEA gages, with copper-coated solder tabs, are particularly suited to this type of application. As shown in Fig. 5, the gage selection and the wiring arrangements can greatly affect the sensitivity to magnetic pickup. It will be noticed that the preferred arrangement minimizes the susceptible loop area between the wires. For the same reason, flat ribbon cable is very prone to noise pickup, and its use in magnetic fields should be avoided. When necessary to use this type of cable, optimal conductor assignment, as shown in Fig. 6, can help reduce the pickup. In addition, excess lengths of input cable should be eliminated; and under no circumstances should the extra length be disposed of by winding into a coil as illustrated in Fig. 7a. If excess cable length cannot be avoided, it should be folded in half and coiled as indicated in Fig. 7b so that each clockwise current loop is intimately accompanied by a counterclockwise loop. The same cabling considerations apply to both the excitation leads and the signal leads.

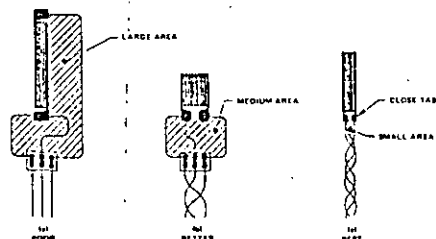


Fig. 5—Gage selection and wiring technique.

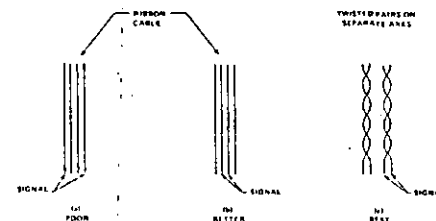


Fig. 6—Cable comparison.

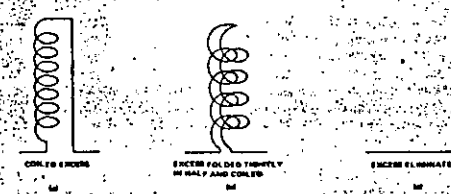


Fig. 7—Handling excess cable.

Unlike the case for electrostatic noise, a simple, grounded conductive shield does not function as a barrier to magnetic noise. Magnetic shields operate on a different principle, and serve to bend or shunt the magnetic field around the conductor rather than eliminate it. Effective magnetic shields are made from high-permeability materials such as iron and other ferromagnetic metals. Special high-permeability alloys ("mu-metal"®) for instance) have been developed specifically for magnetic shielding purposes. At the relatively low 50/60-Hz power line frequencies often encountered in magnetic noise problems, shield thicknesses in the order of 0.1 in. (2.5mm) must be used before any significant noise reduction is achieved. Heavy-walled iron conduit can also be used to provide some reduction in magnetic noise pickup. When faced with the apparent necessity for magnetic shielding, attention should always be given to reducing the noise at its source. As an example, transformers can readily be designed to minimize the leakage flux.

SEVERE NOISE ENVIRONMENTS

The preceding two sections have treated the standard methods of noise reduction applicable to the majority of instrumentation problems. This section describes techniques which may become necessary when very high noise levels are anticipated or experienced.

Generally, when shielding against audio-frequency electrostatic noise, it is not good practice to ground the shield at more than one point. The reason for this is that the ground points may be at different voltage levels, causing current to flow through the shield. Current flow in such ground loops can induce noise in the signal-carrying conductors through the same phenomenon that occurs in a transformer.

However, for long cables in severe noise environments, the shield impedance from one end to the other can become significant, particularly with high-frequency noise sources. When this occurs, the noise charges captured by the shield no longer find a low-resistance drain to ground, and the result is a noisy shield. Improved shield performance under such circumstances can often be obtained by grounding the shield at both ends, and/or at intermediate points—preferably at points near any localized sources of electrostatic noise. Multiple-point ground connections may also be necessary when radio-frequency interference (RFI) problems are encountered. At these frequencies the shield, or segments of the shield between grounded points, can display antenna behavior. By experimentally grounding the shield at numerous points along its length, the optimum grounding scheme can be determined.

Although the leadwires are ordinarily by far the dominant medium for noise induction in a strain gage circuit, noise pickup can also occur in the gage itself. When needed, a simple electrostatic shield can be fabricated by forming an aluminum foil box over the gage and the unshielded leadwire terminations. If the gaged specimen is small and electrically conductive, aluminum tape with conductive adhesive should be used to connect the cable shield, the gage shield, and the specimen together. Conductive epoxy compounds can also be used for this purpose.

On the other hand, when gages are installed on machinery or other large, conductive test objects, care must be exercised to prevent the occurrence of ground current loops in the shield. In such cases, the foil should be electrically insulated from the machine. But the machine should be grounded with a heavy-gauge wire connected to the single-point ground near the instrument. Care must also be taken to make certain that the shield does not form a short circuit to the gage wiring. If the cable has two shields, then ideally, at least, a double-foil shield should be used over the strain gage. The two shields should be connected together only at the instrument end of the cable.

A word about ground connections is in order. It is important to remember that all conductors are characterized by resistance, inductance, and shunt capacitance. As a result, attention should always be given to the quality of the ground connections. A connection to ground, to be effective, should be made with heavy-gauge copper wire, and should be as short as practicable. If the nearest earth ground is too remote, a 6-ft (2-m) copper rod can be driven into the earth to establish a local ground.

As with electrostatic noise pickup, the leadwires commonly represent the principal source of magnetic noise induction in strain gage circuits. In intense electromagnetic fields with steep gradients (near motors, generators, and similar equipment), ordinary wire-twisting techniques may prove inadequate. An end view of a conventionally twisted pair can reveal the reason for pickup. Even if the induced noise were precisely equal in both wires, as indicated in Fig. 4, the amplifier noise output would be zero only if the amplifier had infinite common-mode rejection characteristics—an impossibility. In order to minimize common-mode noise voltages, a special, woven, four-wire cable has been designed which, as seen from the wire end, eliminates the spiral inductive loops (Fig. 8). For maximum field cancellation, pairs of wires (composed of one wire from each plane) are connected in parallel. Referring to the figure, wires 1 and 2 are paralleled to form one conductor; and wires 3 and 4, to form the other. This type of cable, so connected, is largely insensitive to magnetic field gradients, both parallel and perpendicular to the cable length. The cable is known as *Inter-Weave*, and is available from: Magnetic Shield Division, Perfection Mica, 740 Thomas Drive, Bensenville, Illinois 60106.

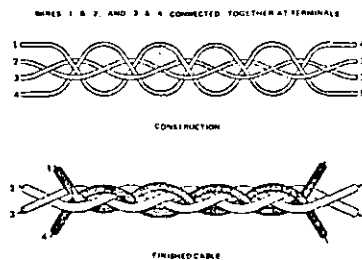


Fig. 8—Woven cable to reduce severe electromagnetic radiation and pickup.

Even though the strain gage is much less frequently the significant medium for magnetic noise induction than the leadwires, different gage patterns have differing sensitivities to noise pickup. If the gage has both solder tabs at one end, for instance, the net noise pickup is less than for a gage with one tab at each end. As shown in Fig. 5, the difference in noise sensitivity results from the relative size of the inductive loop area in each case. It is also worth noting that smaller gages, with more closely spaced grid lines, are intrinsically quieter than large gages.

Optimizing Strain Gage Excitation Levels

Introduction

A common request in strain gage work is to obtain the recommended value of bridge excitation voltage for a particular size and type of gage. A simple, definitive answer to this question is not possible, unfortunately, because factors other than gage type are involved. The problem is particularly difficult when the maximum excitation level is desired.

This Tech Note is intended to outline the most significant considerations which apply, and to suggest specific approaches to optimizing excitation levels for various strain gage applications.

It is important to realize that strain gages are seldom damaged by excitation voltages considerably in excess of proper values. The usual result is performance degradation, rather than gage failure; and the problem therefore becomes one of meeting the total requirements of each particular installation.

Thermal Considerations

The voltage applied to a strain gage bridge creates a power loss in each arm, all of which must be dissipated in the form of heat. Only a negligible fraction of the power input is available in the output circuit. This causes the sensing grid of every strain gage to operate at a higher temperature than the substrate to which it is bonded. With exceptions, which are discussed later, it can be considered that the heat generated within a strain gage must be transferred by conduction to the mounting surface. The heat flow through the specimen causes a temperature rise in the substrate, which is a function of its heat-sink capacity and the gage power level.

Consequently, both sensing grid and substrate operate at temperatures higher than ambient. When the temperature rise is excessive, gage performance will be affected as follows:

1. A loss of self-temperature compensation (S-T-C) occurs when the grid temperature is considerably above the specimen temperature. All manufacturers' data on S-T-C are necessarily obtained at low excitation levels.
2. Hysteresis and creep effects are magnified, since these are dependent on backing and glue-line temperatures. A gage

backing normally rated at +250° F (+120° C) in transducer service might have to be derated by 20° to 50° F (10° to 30° C) under high-excitation conditions.

3. Zero (no-load) stability is strongly affected by excessive excitation. This is particularly true in strain gages with high thermal output characteristics, and when inherent half-bridge or full-bridge compensation is relied upon to meet a low zero-shift vs. temperature specification. The zero-shift occurs because of variation in heat-sink conditions between gages in the bridge circuit.

Another point should be emphasized. Any tendency for localized areas of the grid to operate at higher temperatures than the rest of the grid will restrict the allowable excitation levels. Creep and instability are particularly susceptible to these "hot-spot" effects, which are usually due to voids or bubbles in the glue-line or discontinuities in the substrate. Imperfections in the gage itself can cause hot spots to develop, and only gages of the highest quality should be considered for high-excitation applications.

When other factors are constant, the power-dissipation capability of a strain gage varies approximately with the area of the grid (active gage length x active grid width). The amount or type of waterproofing compound or encapsulant is relatively unimportant. Open-face gages mounted on metal show only 10 to 15% less power-handling capacity than fully encapsulated gages with the same grid area. Note, however, that proper waterproofing materials must always be applied to open-face gages to prevent loss of performance through grid corrosion.

It is sometimes stated that gage adhesives of high thermal conductivity can considerably improve the power-handling capability of strain gage installations. Generally, this is not correct. These adhesives incorporate high-conductivity fillers such as aluminum oxide and metal powders. This produces an adhesive of high viscosity, resulting in excessively thick glue-lines and a longer thermal path from gage to substrate. Any net gain in thermal conductivity is more than offset by the performance degradation due to thicker glue-lines. It is much better, for high gage excitation as well as normal gage applications, to use high-functionality adhesives that permit thin, void-free glue-lines. On smooth mounting surfaces, ideal glue-line thicknesses range from 0.0001 to 0.0003 in. (0.0025 to 0.0075 mm).

Factors Affecting Optimum Excitation

Following are factors of primary importance in determining the optimum excitation level for any strain gage application:

1. **Strain gage grid area.** (Active gage length x active grid width)
2. **Gage resistance.** High resistances permit higher voltages for a given power level.
3. **Heat-sink properties of the mounting surface.** Heavy sections of high-thermal-conductivity metals, such as copper or aluminum, are excellent heat sinks. Thin sections of low-thermal-conductivity metals, such as stainless steel or titanium, are poor heat sinks. Also, the shape of the gaged part may create thermal stresses in portions of the structure due to gage self-heating. Long warm-up times and apparent gage instability can result. The situation often arises in low-force transducers, where thin sections and intricate machining are fairly common.
4. **Strain measurement on plastic requires special consideration.** Most plastics act as thermal insulators rather than heat sinks. Extremely low values of excitation are required to avoid serious self-heating effects. The modulus of elasticity of the common plastics drops rapidly as temperature rises, increasing visco-elastic effects. This can significantly affect the material properties in the area under the strain gage. Plastics which are heavily loaded with inorganic fillers in powder or fibrous form present a lesser problem, because such fillers reduce expansion coefficients, increase the elastic modulus, and improve thermal conductivity.
5. **Environmental operating temperature range of the gage installation.** Creep in the gage backing and adhesive will occur at lower ambient temperatures when grid and substrate temperatures are raised by self-heating effects. Thermal output due to temperature will also be altered when grid and substrate temperatures are significantly different.
6. **Required operational specifications.** Gages for normal stress analysis can be excited at a higher level than under transducer conditions, where the utmost in stability, accuracy, and repeatability is needed.

A significant distinction exists between gages used in dynamic strain measurement and those used in static measurement applications. All the various performance losses due to gage self-heating affect static characteristics of the gage much more seriously than the dynamic response. Therefore, it is practical to "drive" the dynamic installations much harder, and thus take advantage of the higher signal-to-noise ratio which results.

6. **Installation and wiring technique.** If the gage is damaged during installation, if solder tabs are partially unbonded due to soldering heat, or if any discontinuities are formed in the glue line, high levels of excitation will create serious problems. Proper technique is essential in obtaining consistent performance in all strain gage work, but particularly under high-excitation conditions.

In addition to the preceding, secondary factors exist which affect maximum permissible excitation levels. Poor grid design, such as improper line-to-space ratio, will reduce the heat transfer effectiveness. The type of gage matrix, in terms of resin and filler, determines the thermal conductivity of the backing. The backing is usually more important than the adhesive selected because the backing is thicker than the adhesive layer in proper installations.

Stacked Rosette Gages

These represent a special case, because the thermal path length is much greater from the upper grid to the substrate, and because the temperature rise of the lower grids adds directly to those above. For a three-element stacked rosette in which the three grids are completely superimposed, the top grid will have six times the temperature rise of a similar single gage, if all grids receive the same input power. To keep the temperature rise of the top grid equal to that of a similar single gage, the three rosette sections should each receive 1/6 of the power applied to the single gage. This corresponds to a reduction factor of 2.5 for bridge excitation voltage, since power varies as the square of the applied voltage. For two-element stacked rosettes, the comparable derating factor is 3 for power, and 1.7 for bridge voltage.

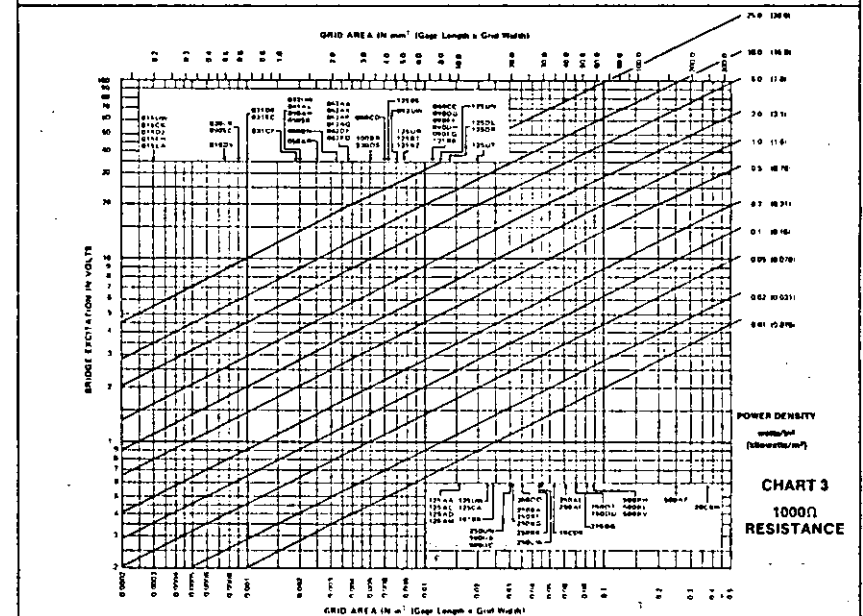
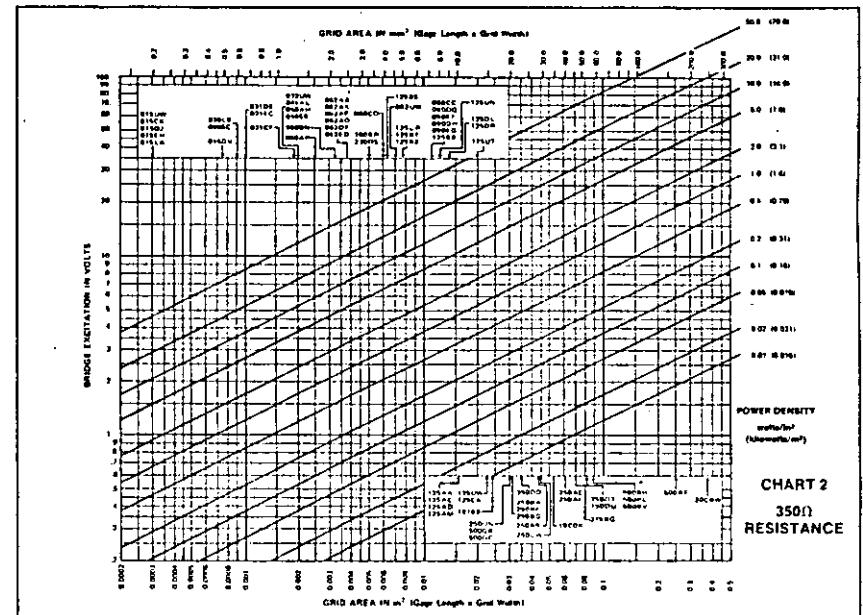
This discussion is based on rosettes of square grid geometry, where each grid covers essentially all of the grid(s) in the assembly. When substantial areas of the grids are not superimposed, the derating factors mentioned above will be somewhat conservative.

Cryogenic Gage Applications

Many strain gage measurements are now made under direct submersion in liquefied gases such as nitrogen, hydrogen, and helium. Since these liquids are electrically nonconductive, open-face gages have been used occasionally without a protective or waterproofing coating. An interesting effect has been reported under these conditions. If excitation voltages are not kept sufficiently low, grid self-heating will cause gas bubbles to form on the gridlines, and thus partially insulate the grid from the cold liquid. Larger bubbles are then created by increased grid temperatures, and bubbles periodically break loose and rise toward the surface. The relative motion of these insulating bubbles with respect to the gridlines produces local temperature changes, which appear in the output signal as noise. Grid alloys which display very high values of thermal output at cryogenic temperatures (most constantan alloys, for example) are particularly susceptible to this effect. The remedy is to utilize very low excitation levels, and/or to use protective coatings over the grid to prevent direct liquid contact. Such coatings must necessarily retain sufficient flexibility at cryogenic temperatures to prevent cracking of the protective layer.

Experimental Determination of Maximum Gage Excitation

To be certain that the excitation level chosen for a given strain gage application is not excessive, it is necessary to run performance tests at the maximum environmental temperature. In many cases, however, this rather complicated procedure can be greatly simplified by gradually increasing the bridge excitation under zero-load conditions until a definite zero instability is observed. The excitation should then be reduced until the zero reading becomes stable again, without a significant offset from the low-excitation zero reading. For most applications in experimental stress analysis, this value of bridge voltage is the highest that can be used safely without significant performance degradation. Conducting this test at the maximum operating temperature instead of room temperature will increase the likelihood that the maximum safe bridge voltage has been established.



The rigid operating requirements for precision transducers make the above procedure useful primarily as a first approximation; and further verification is usually required. The performance tests most sensitive to excessive excitation voltage are: (1) zero-shift vs. temperature and (2) stability under load at the maximum operating temperature.

Excitation Levels for Resistance Temperature Sensors

It has become increasingly common to measure specimen temperatures in strain gage work by the use of bondable nickel-grid temperature sensors such as the ETG-50 and WTG-50. These sensors are fabricated in the same manner as strain gages, and consequently experience environmental temperature changes in the same way. By eliminating many of the measurement errors often encountered with thermocouples, temperature sensors are ideal for correcting strain gage data under rapidly changing temperature conditions.

Like strain gages, temperature sensors are adversely affected by excessive excitation levels. Variation in heat-sink conditions and accuracy requirements make universally applicable excitation recommendations impossible, but a single test procedure is available. The excitation level should be increased until the readout device indicates an excessive grid temperature rise; it should then be reduced as necessary. Since the readout in this case shows temperature measurement error directly, the determination is straightforward.

Since temperature sensors are most often used with linearization networks of the LST type, it is not normally necessary to check for errors due to excitation level. These networks greatly attenuate the input bridge voltage, and the sensors are therefore operated at very low power levels.

Typical Strain Gage Excitation Values

The following data curves represent general recommendations or starting points for determining optimum excitation levels. These curves are plots of bridge excitation voltage vs. grid area (active gage length x grid width) for constant power-density levels in watts/in² (or kilowatts/m²).^{*} A large

^{*}The power density is expressed here in terms of kilowatts per square metre, in accordance with recommended SI practice. It is numerically equal to milliwatts per square millimetre.

Table I — Heat Sink Conditions
watts/in² kilowatts/m²

	Accuracy Requirements	EXCELLENT		GOOD	FAIR	POOR	VERY POOR
		Heavy Aluminum or Copper Specimen	Thick Steel				
STATIC	High	2-5 3.1-7.8	1-2 1.6-3.1	0.5-1 0.78-1.6	0.1-0.2 0.16-0.31	0.01-0.02 0.016-0.031	
	Moderate	5-10 7.8-16	2-5 3.1-7.8	1-2 1.6-3.1	0.2-0.5 0.31-0.78	0.02-0.05 0.031-0.078	
	Low	10-20 16-31	5-10 7.8-16	2-5 3.1-7.8	0.5-1 0.78-1.6	0.05-0.1 0.078-0.16	
DYNAMIC	High	5-10 7.8-16	5-10 7.8-16	2-5 3.1-7.8	0.5-1 0.78-1.6	0.01-0.05 0.016-0.078	
	Moderate	10-20 16-31	10-20 16-31	5-10 7.8-16	1-2 1.6-3.1	0.05-0.2 0.078-0.31	
	Low	20-50 31-78	20-50 31-78	10-20 16-31	2-5 3.1-7.8	0.2-0.5 0.31-0.78	

number of standard measurements single-element gage patterns are listed at the various grid areas they represent. Separate plots are provided for gage resistances of 120, 350, and 1000 ohms. For other grid areas and/or other gage resistances, calculations can be made according to the following formulas for recommended power-density levels:

$$\text{Power Dissipated in Grid (watts)} = \frac{E_b^2}{4R_0} = P_G$$

$$\text{Power Density in Grid (watts/in}^2 \text{ or kW/m}^2\text{)} = \frac{P_G}{A_G} = P'_G$$

where: R_0 = Gage resistance in ohms

A_G = Grid area (active gage length x grid width)

E_b = Bridge excitation in volts

Note that bridge voltage (E_b) is based on an equal-arm bridge arrangement, where the voltage across the active arm is one-half the bridge voltage.

When grid area (A_G), gage resistance (R_0), and grid power density (P'_G) are known:

$$E_b = 2\sqrt{R_0 \times P'_G \times A_G}$$

Grid Power-Density Curves

Selecting the most appropriate power-density lines on the following charts depends, primarily, on two considerations: degree of measurement accuracy required, and substrate heat-sink capacity. A series of general recommendations follows, but should be verified by the procedures previously described for critical applications.

Typical Power-Density Levels in Watts/in² (kW/m²)

It is of interest that some commercial strain indicators utilize constant excitation voltage of 3 to 5 volts. The power densities created in gages of various sizes and resistances by these bridge voltages can be taken directly from the charts and compared with Table I. For very small gages, it is evident that commercial instruments may require voltage reduction for proper results. A simple circuit modification, which can be utilized when the instrument voltage is not adjustable, involves the insertion of "dead" resistance in the form of high-precision resistors of the Vishay type in series with the active and dummy gages in the external half bridge. Power density is then reduced by (multiplied by) the factor $[R_0/(R_0 + R_G)]^2$, where R_0 is the inactive series resistance in

ohms, and R_G is the active gage resistance in ohms. Note that the adjacent bridge arm must be increased by the same R_0 to maintain bridge balance under these conditions. The sensitivity of the bridge will be decreased by this procedure, and the readings must be multiplied by the ratio of $(R_0 + R_G)/R_0$ to correct for this desensitization.

Examples of Chart Use

Case 1: What excitation level can safely be applied to an EA-09-125AD-120 strain gage, mounted on a 1/2 x 1/16 x 6 in (12.5 x 1.5 x 150 mm) stainless-steel bar, for a static stress analysis test with moderate accuracy (3% to 5%)?

From Table I, determine the typical power density level [1 to 2 W/in² (1.6 to 3.1 kW/m²)] corresponding to a fair heat-sink condition in stainless steel. Refer to Chart 1:

- Enter on the horizontal axis at the arrowhead for the 125AD gage [0.0156 in² (10.06 mm²)].
- Mark the intersection of the vertical line with the 1 and 2 W/in² (1.6 and 3.1 kW/m²) sloped lines.
- Read horizontally to the left ordinate for Bridge Excitation of 2.7 and 3.8 volts, respectively. A strain indicator with a maximum bridge excitation of 3.8 volts can be used.

Case 2: Can an instrument with a fixed 4.5V excitation be used? If not, what correction of data points must be made?

To determine the power density in a 125AD gage at a given excitation level, refer to Chart 1:

- Enter the left ordinate at 4.5 volts until intersecting the abscissa value equivalent to the 125AD gage. The power density is 2.7 W/in² (4.2 kW/m²), which is in excess of the maximum power determined in Case 1. If low accuracy (i.e., 5 to 10% data) is acceptable, the higher P'_G can be used. If greater accuracy must be maintained, several alternatives are available: (1) select a higher resistance gage, (2) select a gage with a larger area, or (3) reduce the bridge voltage with an inactive series resistor, R_0 .

The inactive resistor (R_0) required to reduce the power density to the desired 2 W/in² (3.1 kW/m²), with a given E_b , can be determined from the following relationship:

$$\left(\frac{E_b^2}{R_0 A_G}\right) \left(\frac{R_0}{R_0 + R_G}\right)^2 = P'_G \text{ (desired)}$$

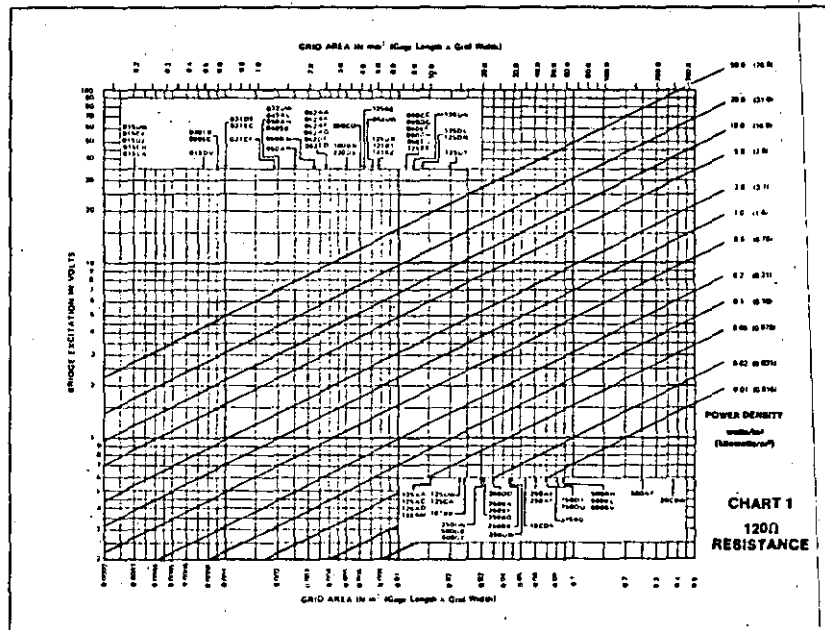
For a desired P'_G of 2 W/in² (3.1 kW/m²):

$$R_0 = \frac{E_b}{2} \sqrt{\frac{R_G}{A_G P'_G}} - R_G = 19.5 \text{ ohms}$$

Select the nearest precision resistor value greater than 19.5 ohms for R_0 .

For actual strain values, accounting for the inserted inactive resistor, all indicated strain readings must be multiplied by:

$$\frac{R_0 + R_G}{R_G} = \frac{19.5 + 120}{120} = 1.16$$



TECH NOTE

TN-506-1

Bondable Temperature Sensors

Bondable Resistance Temperature Sensors and Associated Circuitry

1.0 Introduction

Resistance thermometry is a widely employed method of measuring temperature, and is based on using a material whose resistivity changes as a function of temperature. Resistance Temperature Detectors (RTD's) have fast response time, provide absolute temperature measurement (since no reference junctions are involved), and are very accurate. Their measurement circuits are relatively simple, and the sensors, when properly installed, are very stable over years of use.

2.0 Sensor Materials

The resistance of Balco and of high-purity nickel, copper, and platinum increases rapidly with temperature, following repeatable and stable curves to over +500° F (+260° C). As shown in Fig. 1, the resistance changes are quite large, resulting in high signal levels. Platinum is not normally used in bondable temperature sensors because it is very easily and severely damaged by stresses. Nickel is a commonly used RTD material because of its large resistance change with temperature; and, in its pure form, it is very stable and repeatable.

This Tech Note discusses the operational characteristics and various methods of data readout for special bondable-resistance-temperature-detectors (TG-Series) manufactured by Micro-Measurements. These bondable RTD's have certain distinct advantages over wirewound sensors: they are less expensive, not as fragile in use, and their time-temperature response is similar to a strain gage. Standard strain gage instrumentation is ideal for use with these RTD's.

Micro-Measurements TG resistance temperature sensors are constructed much like wide-temperature-range strain gages. The standard sensors, described in Product Bulletin PB-105, utilize high-purity nickel sensing grids, though special-purpose gages are also available in Balco® alloy or copper foil grids. TG temperature sensors are bonded to structures using standard strain gage installation techniques, and can measure surface temperatures from -320° to approximately +500° F (-195° to +260° C), or +250° F (+120° C) with the copper sensors. Because of their extremely low thermal mass and the large bonded area, TG sensors follow temperature changes in the structural mounting surface with negligible time lag.

The standard lines of Micro-Measurements temperature sensors, LST matching networks, and calibration resistors are listed in Product Bulletin PB-105.

*Trademark — W.B. Driver Co.

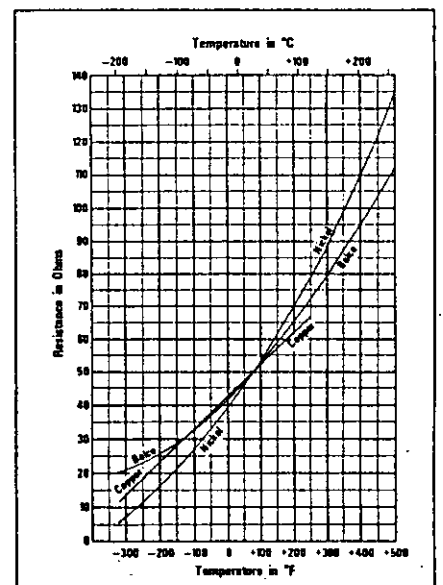


Fig. 1 — Data for 50Ω sensors mounted on 1018 Steel.

TABLE 12

Resistance vs. Temperature in Degrees Celsius											
Balco Sensors mounted on 2024-T4 Aluminum — Lot No. B03											
°C	R	°C	R	°C	R	°C	R	°C	R	°C	R
-195	19.97	-135	24.86	-75	32.31	-15	42.27	40	53.47	100	67.68
-190	20.28	-130	25.18	-70	31.04	-10	43.21	45	54.54	105	68.95
-185	20.61	-125	25.92	-65	33.80	-5	44.16	50	55.70	110	70.23
-180	20.95	-120	26.48	-60	34.57	0	45.13	55	56.84	115	71.52
-175	21.31	-115	27.06	-55	35.36	5	46.12	60	57.99	120	72.82
-170	21.70	-110	27.65	-50	36.16	10	47.13	65	59.15	125	74.13
-165	22.09	-105	28.26	-45	36.98	15	48.14	70	60.33	130	75.45
-160	22.51	-100	28.89	-40	37.82	20	49.18	75	61.53	135	76.79
-155	22.94	-95	29.54	-35	38.68	25	50.00	80	62.73	140	78.13
-150	23.40	-90	30.21	-30	39.55	25	50.23	85	63.95	145	79.48
-145	23.86	-85	30.89	-25	40.44	30	51.29	90	65.18	150	80.85
-140	24.35	-80	31.59	-20	41.35	35	52.37	95	66.42	155	82.22
										200	94.92
										215	99.37
										220	100.72
										225	102.19
										230	103.65
										235	105.12
										240	106.60
										245	108.07
										250	109.55
										255	111.03
										260	112.51

TABLE 13

Resistance vs. Temperature in Degrees Celsius											
ED Copper Sensors mounted on 1018 Steel											
°C	R	°C	R	°C	R	°C	R	°C	R	°C	R
-195	11.55	-150	19.67	-105	27.68	-60	35.58	-15	43.38	25	50.22
-190	12.46	-145	20.56	-100	28.56	-55	36.45	-10	44.24	30	51.06
-185	13.36	-140	21.46	-95	29.45	-50	37.32	-5	45.10	35	51.91
-180	14.27	-135	22.35	-90	30.33	-45	38.19	0	45.95	40	52.76
-175	15.17	-130	23.24	-85	31.21	-40	39.06	5	46.81	45	53.60
-170	16.07	-125	24.13	-80	32.08	-35	39.93	10	47.66	50	54.45
-165	16.98	-120	25.02	-75	32.96	-30	40.79	15	48.51	55	55.29
-160	17.87	-115	25.91	-70	33.84	-25	41.66	20	49.37	60	56.13
-155	18.77	-110	26.80	-65	34.71	-20	42.52	25	50.00	65	56.97
										70	57.81
										75	58.64
										80	59.48
										85	60.31
										90	61.15
										95	61.98
										100	62.81
										105	63.64
										110	64.46

TABLE 14

Resistance vs. Temperature in Degrees Celsius											
ED Copper Sensors mounted on 2024-T4 Aluminum											
°C	R	°C	R	°C	R	°C	R	°C	R	°C	R
-195	11.37	-150	19.49	-105	27.53	-60	35.47	-15	43.32	25	50.23
-190	12.28	-145	20.39	-100	28.42	-55	36.35	-10	44.19	30	51.08
-185	13.18	-140	21.29	-95	29.30	-50	37.22	-5	45.06	35	51.94
-180	14.09	-135	22.18	-90	30.19	-45	38.10	0	45.92	40	52.80
-175	14.99	-130	23.08	-85	31.07	-40	38.97	5	46.78	45	53.65
-170	15.89	-125	23.97	-80	31.95	-35	39.85	10	47.65	50	54.50
-165	16.80	-120	24.86	-75	32.83	-30	40.72	15	48.51	55	55.36
-160	17.70	-115	25.75	-70	33.71	-25	41.59	20	49.37	60	56.21
-155	18.60	-110	26.64	-65	34.59	-20	42.46	25	50.00	65	57.06
										70	57.91
										75	58.75
										80	59.60
										85	60.44
										90	61.29
										95	62.13
										100	62.97
										105	63.81
										110	64.65



MEASUREMENTS GROUP, INC.
 P.O. Box 27777
 Raleigh, North Carolina 27611, USA
 (919) 365-3900
 Telex 802-502
 FAX (919) 365-3945

Balco, an alloy of nickel and iron, although more nonlinear than nickel, has demonstrated equal stability and repeatability over the temperature range in which bondable RTD's are used. In addition, Balco sensors are easier to fabricate, and have 2.4 times the resistivity of pure nickel sensors. The result is lower cost sensors and the ability to make higher resistances in smaller sizes. Copper displays very good linearity but has low resistivity. However, in applications where linearity is important and where size or high resistance is not critical, copper is often the best choice. Oxidation of copper proceeds very rapidly at elevated temperature, and these sensors are usually limited to maximum temperatures on the order of +250° to +300° F (+120° to +150° C). Table 1 gives chord-slope temperature coefficients of resistivity from +32° to +212° F (0° to +100° C) for these materials mounted on 1018 Steel.

Table 1

Material	Chord Slope T.C.R. (Typical)	
	$\Omega/\Omega^\circ F$	$\Omega/\Omega^\circ C$
Nickel T04	0.0036	0.0064
Balco B03	0.0027	0.0049
ED Copper	0.0019	0.0034

Selection of the appropriate type for each application is governed by performance requirements and cost. But, in cases where the temperature gage is to be used in conjunction with strain gages, nickel TG's, combined with LST networks (see Section 6.0) are usually selected. When using the Measurements Group System 4000 data acquisition system with universal scanners, any RTD can be read without additional circuitry, and the indicated temperature can be automatically corrected for linearity, and presented in the temperature units desired. Data reduction is discussed in detail in Section 10.0. Common error sources for bondable RTD's are reviewed in the following sections: self-heating, Section 4.0; leadwire problems, Section 5.0; nonlinearity, Section 6.0; strain effects, Section 7.0; instability, Section 8.0.

3.0 Sensor Installation

Type TG temperature sensors and temperature-sensitive resistors are installed with the same techniques and materials used for installation of wide-temperature-range strain gages. M-Bond 600 or 610 adhesives are usually employed because they are useful over the entire temperature range of the sensor itself. Surface preparation techniques are given in Micro-Measurements Instruction Bulletin B-129, and specific installation procedures are included in the selected adhesive kit.

Leadwires of RTD's are normally handled in the same way as strain gage leadwires with one significant difference. The three-wire system used with strain gages to eliminate errors due to temperature-induced resistance changes in the leadwires is not effective in many cases with bondable temperature sensors. This subject is treated at greater length in Sections 5.0 and 6.0. Normally, temperature gages need protective coatings of the same types as strain gages. For recommendations, refer to Micro-Measurements Accessory Catalog A-110.

4.0 Self-Heating

In order to obtain a useful output from passive transducers such as TG temperature sensors, it is necessary to apply an excitation voltage; which results in self-heating of the sensor. This will cause a certain temperature rise in the surface to which the sensor is bonded, thus creating an error signal. Since TG sensors have a very high temperature coefficient of resistance, it is not necessary to use high excitation levels to develop large outputs, and self-heating errors can easily be kept to insignificant values. When it is necessary to use high excitation levels to obtain maximum output signals, it should be noted that the largest practical sensor grid size should be chosen. The thermal conductivity and thermal capacity of the specimen will then determine the highest excitation level that can be used for a given self-heating error. It is usually very simple to measure self-heating errors directly with TG sensors because the excitation can be varied under constant ambient temperature conditions while observing the change in output indication in degrees. A bridge excitation of 0.25V or less will usually produce self-heating errors of only a fraction of one degree for standard sensors mounted on metallic specimens. Special attention should be given to self-heating when accurate measurements must be made on low thermal conductivity materials such as plastic or glass.

The attenuation factor incorporated in LST networks (see Section 6.0) greatly reduces the strain indicator excitation voltage, and self-heating errors are seldom encountered when this readout method is used with TG sensors.

5.0 Readout Methods

One method of reading temperature with TG sensors is to connect the sensor to a Wheatstone resistance bridge, and convert the resistance readings to equivalent temperature with the tables given in this Tech Note. This method is cumbersome and therefore seldom used. Also, the leadwires cause two different types of errors with Wheatstone bridges. The resistance of the leads, which can be appreciable with remote gages, produces an initial offset error, and desensitizes the arm of the bridge containing the temperature sensor. The second error is a result of resistance change in the leads caused by temperature variations. Except under unusual conditions, errors of this type are very small. In cases where long leadwires are necessary, special calibration techniques or compensation systems can be used.^{1,2*}

A variation of the above method is of interest because it is capable of providing accurate compensation for leadwire errors with a three-wire system. The circuit is shown in Fig. 2 (on the following page), in which the precision decade box is used instead of a conventional Wheatstone resistance bridge. The decade box in this circuit is varied to keep the output at null, and the indicated decade resistance is therefore the same as the sensor resistance. Provided leads 1 and 3 are of the same effective length and size, and are routed together through the same environment, resistance variations in the leadwire circuit caused by temperature changes common to all wires will not create errors in the reading. Three-wire compensation is effective in this case because this is a true null-balance system, with the decade box in the bridge arm

*Superscript numbers refer to references appended to this tech note.

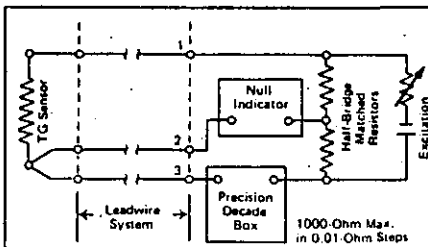


Fig. 2

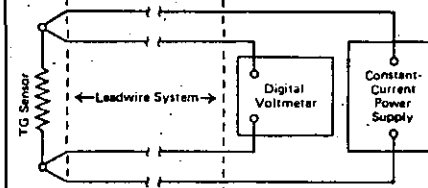


Fig. 3

adjacent to the sensor always set to the sensor resistance at the time of readout. Excitation power can be either dc or ac, depending upon the null indicator chosen.

A more sophisticated readout system which eliminates the need for manual rebalance is shown in Fig. 3. This arrangement eliminates leadwire errors by use of a four-wire system. If the digital voltmeter has a high enough input impedance, the readings will be a known function of sensor resistance regardless of resistance change in any of the leadwires. A current level of one milliamperere will allow the voltmeter to read sensor resistance in terms of millivolts (50.0 ohms reads as 50.0 millivolts). The Measurements Group System 4000 with universal scanners uses essentially the circuit of Fig. 3 for leadwire-error-free temperature readings.

6.0 Linearity

The readout methods shown in Figs. 2 and 3 can be extremely accurate, but are somewhat awkward in that they read sensor resistance directly. The nonlinear characteristic of sensor resistance versus temperature requires the use of tabulated data to convert resistance values to the equivalent temperature. A very simple method exists for converting the nonlinear response of pure nickel sensors to a linear resistance change with temperature, with good practical accuracy. This is accomplished by shunting the sensor with a fixed resistor.

The value of the resistor is selected to provide the best linearization over a given temperature range. For example, the effect of a 187.5-ohm resistor shunting a 50-ohm nickel TG temperature sensor [50 ohm at +75° F (+23.9° C)] is shown in Fig. 4.

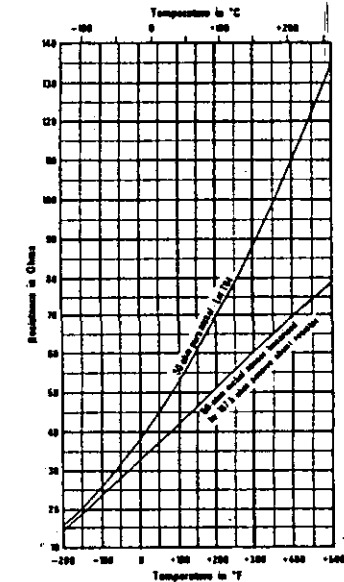
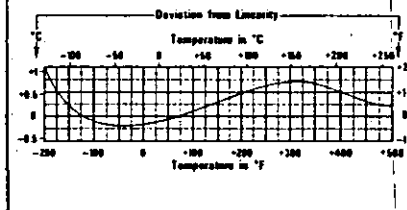


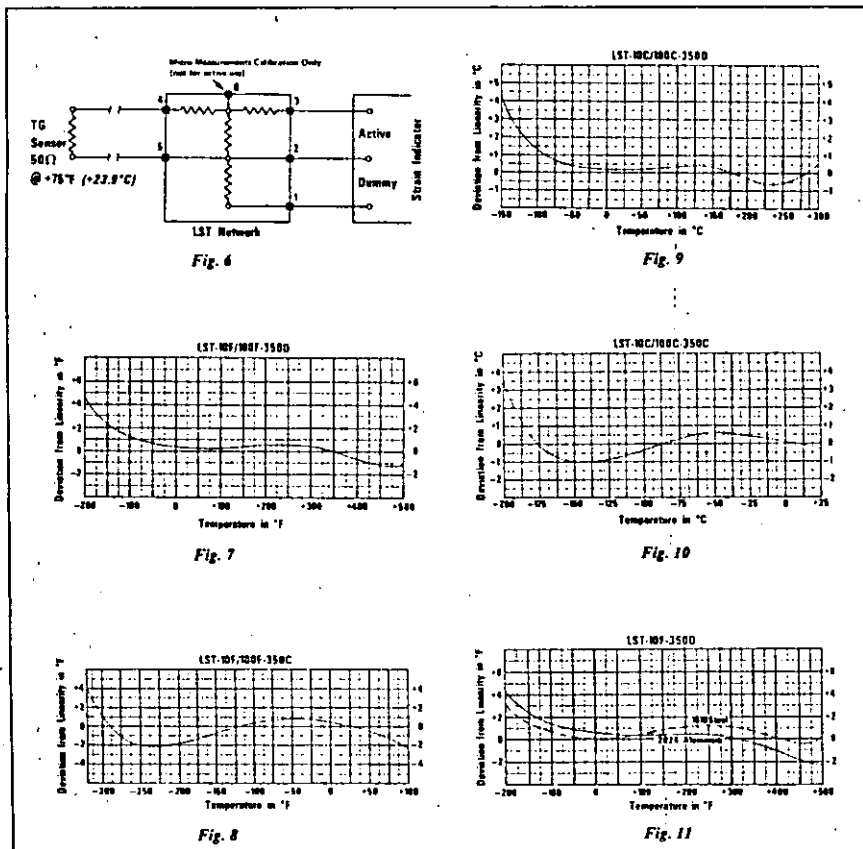
Fig. 4 — Data for sensors mounted on 1018 Steel.



The resultant change has a lower slope versus temperature, of course, but is quite linear with temperature. Figure 5 is a plot of deviation from linearity for this circuit and provides much higher error readability than Fig. 4.

Commercial single- or multiple-channel strain indicators are excellent readout devices for TG temperature sensors, and are particularly convenient when combinations of strain and temperature are to be measured or recorded simultaneously. This readout method requires the use of an interface signal-conditioning network, referred to as an LST network, to "match" the temperature sensor to the strain indicator. The arrangement is shown in Fig. 6 (on the following page).

The LST network is a small, completely encapsulated unit consisting of four special precision resistors. When used with standard 50-ohm nickel TG temperature sensors, it performs the following three functions:



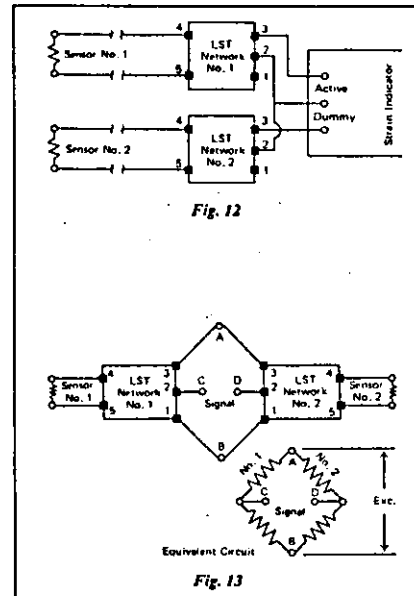
- Provides a linear resistance change at the output terminals. To assure optimum correction for nonlinearity of the nickel, the user may select from four temperature ranges: -200° to $+500^{\circ}$ F (LST-10/100F-350D); -320° to $+100^{\circ}$ F (LST-10/100F-350C); -150° to $+260^{\circ}$ C (LST-10/100C-350D); or -200° to $+25^{\circ}$ C (LST-10/100C-350C). Deviations from linearity for these networks are shown in Figs. 7 through 10. The expansion coefficient of the structure to which the temperature sensor is bonded will affect linearity. Figure 11 shows the deviation of TG sensors with LST-10F-350D conditioning networks on 1018 Steel and 2024 Aluminum. For optimum accuracy it is necessary to calibrate gage/LST systems on the material to be used. In most work, however, the average curves of Figs. 7 through 10 are satisfactory.
- Attenuates the resistance change slope to the equivalent of 10 or 100 $\mu\Omega/\text{deg}$ for a gage factor setting of 2.00 on the strain indicator. It is usually most practical to use 10 $\mu\Omega/\text{deg}$ networks when a large temperature range is

involved, and 100 $\mu\Omega/\text{deg}$ networks for high resolution of small temperature spans.

- Presents a balanced 350-ohm half-bridge circuit to the strain indicator at the sensor reference temperature of 0° F (Fahrenheit networks) or 0° C (Celsius networks).

Differential temperature measurements can be made by combining two TG sensors and two LST networks as shown in Fig. 12. This provides a half-bridge circuit to the strain indicator in which the active arm responds to sensor 1, and the dummy arm to sensor 2. An alternate method is to arrange the networks to form a full-bridge circuit as shown in Fig. 13, and this arrangement may be preferred for some types of readout equipment.

Calibration and balancing of circuits containing LST networks can be handled in various ways. Initial balance is usually obtained by setting the BALANCE dial of the strain indicator so that the instrument reading corresponds to the initial temperature of the sensor.



When it is not possible to control or measure the initial temperature of the sensor, it can be temporarily replaced by a precision 50.0-ohm resistor. The BALANCE dial is then set to create an equivalent readout of $+75.0^{\circ}$ F (Fahrenheit networks) or $+23.9^{\circ}$ C (Celsius networks). The sensor can then be reconnected to the network. The first procedure has the obvious advantage of correcting for the error due to tolerance limits on initial TG-sensor resistance.

Resistance shunt calibration can be applied to the output terminals of the LST network in order to verify linearity and span accuracy of the associated instrumentation. It is also useful in setting the GAGE FACTOR dial or in correcting for leadwire desensitization when the LST network is remote from the readout instrument. In this latter case, note that shunt resistors must be placed across the leadwire terminals at the network end, not at the instrument end.

Because of significant resistance changes in the active arm with temperature, shunt calibration across network terminals 2 and 3 will be correct only when the sensor temperature is near $+75^{\circ}$ F ($+24^{\circ}$ C). So, it is preferable that calibration resistors be shunted across the dummy arm (network terminals 1 and 2). When it is desired to calibrate across both arms to simulate both plus and minus temperature changes, and it is not convenient to stabilize sensor temperature near $+75^{\circ}$ F ($+24^{\circ}$ C), the sensor can be replaced by a precision 50.0-ohm resistor during calibration.

When applying shunt calibration to the differential temperature measurement circuit shown in Fig. 12, it will be necessary to calibrate across the active arms (network terminals 2 and 3). Shunting network 1 will simulate a temperature decrease for sensor 1 or an increase for sensor 2. Under

these conditions, the nominal or common-mode temperature for both sensors must be near $+75^{\circ}$ F ($+24^{\circ}$ C) if desired to calibrate across both networks. If this cannot be conveniently arranged, the sensors should be temporarily replaced by 50.0-ohm resistors during calibration. If the alternate full-bridge connection of Fig. 13 is used for a differential operation, shunt calibration steps can be applied to either dummy arm, terminals 1 and 2, regardless of temperature.

For best accuracy, it is always advisable to select shunt calibration values which are close to the temperature span of greatest interest. When the instrument readings are not in agreement with the simulated calibration temperature, the GAGE FACTOR dial can be adjusted to eliminate the error.

With modern computer technology, it is a relatively easy job to design and build special LST networks, tailored to special temperature ranges, output slopes and impedance matching. Consult the Measurements Group Applications Engineering Department for details.

Leadwires are a source of error in all circuits using TG sensors, except those of the types shown in Figs. 2 and 3. To minimize these errors, leadwires between the sensor and the readout device (or LST network) should be of low resistance and no longer than necessary. A total two-wire resistance of 0.5 ohm will introduce a shift or offset of about $+4^{\circ}$ F ($+2^{\circ}$ C) at room temperature. This leadwire resistance corresponds to 25 ft (7.5 m) of AWG No. 20 (0.8 mm diameter) copper double leads, or 100 ft (30 m) of AWG No. 14 (1.6 mm diameter) double leads.

Changes in leadwire temperature are normally a minor source of error. A change of $+50^{\circ}$ F ($+28^{\circ}$ C) over the entire length of a 0.5-ohm copper leadwire circuit will create an offset error of approximately $+0.4^{\circ}$ F ($+0.2^{\circ}$ C) when the sensor temperature is near $+75^{\circ}$ F ($+24^{\circ}$ C). This error decreases at higher sensor temperatures and increases at lower sensor temperatures. Accurate measurements in the cryogenic temperature region may require the approach of Figs. 2 and 3 when long lengths of small leadwire must be employed. For other lead compensating circuits, see Refs. 1 and 2.

"Initial-zero" errors, or offsets due to the tolerances applicable to LST networks and the TG sensors themselves, can be eliminated by stabilizing the sensor installation at any known temperature close to $+75^{\circ}$ F ($+24^{\circ}$ C), and then setting the instrument BALANCE dial so that the reading corresponds to this known temperature. This procedure also eliminates offset error caused by initial leadwire resistance.

In certain circumstances it may be necessary to locate the instrumentation at an extreme distance from the sensor installations. When LST networks are employed under these conditions, it is preferable to position the network close to its associated sensor and to use a three-wire lead circuit between the network and the remote indicator. However, this should not be done if the ambient temperature at the network location will exceed about $+200^{\circ}$ F ($+93^{\circ}$ C). This type of hookup will eliminate first-order offset errors due to leadwire resistance and leadwire temperature changes. Desensitization or slope-change error is greatly reduced and can be eliminated by setting the strain indicator GAGE FACTOR dial properly. The correct setting can be calculated on the

basis of known leadwire resistance in a 350-ohm bridge arm or, preferably, can be directly determined by applying shunt calibration to the remote network terminals.

7.0 Strain Effects

The strain sensitivity of RTD alloys can create error signals when the sensors are installed in areas of high strain. Magnitude of this effect is fairly small, however, as shown for nickel in Fig. 14, Balco in Fig. 15, and copper in Fig. 16.

The shape of the curve in Fig. 14 is caused by the nonlinear response of pure nickel. The strain-sensitivity coefficient has a high negative value in the central portion of the elastic region and tends toward a much smaller, positive value on either side of this region. It will be observed that compressive strains result in smaller error signals, and this strain field orientation should therefore be selected for sensor placement when possible. The center of "symmetry" of this curve is located at approximately +750 $\mu\epsilon$ because the manufacturing process leaves the sensor with a residual compression of this value. This point of symmetry, as well as gage temperature response, can be shifted somewhat by installing the gage on materials of different thermal expansion coefficients, and/or with different adhesive cure temperatures. As a result of this shift, gage response, when mounted on a given material, will differ slightly from that obtained when mounted on another. Therefore, to take full advantage of the repeatability (typically $\pm 0.05\%$ of applied temperature span) and other intrinsic features of TG temperature sensors, it is advisable to conduct a calibration run of the sensor mounted on the specific test material.

The tables of Section 11.0 demonstrate how the resistance-versus-temperature characteristic of TG sensors mounted on aluminum differs from that with the sensors mounted on steel.

8.0 Stability

In common with most other organic resin systems, the matrix of TG sensors will slowly sublime and lose strength when aged at elevated temperatures. When properly installed, life will be essentially infinite below +250° F (+120° C), and will be approximately 10 000 hours at +400° F (+205° C). At +500° F (+260° C), life can be estimated at 1000 hours in the presence of air, and will be considerably extended if an inert atmosphere is used.

The sensing grids are very stable under the aging conditions described above [+250° F (+120° C) for copper]. If exposed to temperatures above +500° F (+260° C), however, a slight shift in resistivity will occur, together with a small change in temperature coefficient. For example, if the WTG-Series sensor is exposed to a temperature of +600° F (+315° C) for one hour, the +75.0° F (+23.9° C) resistance will shift from 50 ohms to approximately 50.6 ohms. On a normalized basis, the resistance increase from +75.0° to +450° F (+23.9° to +232° C) will become 140% instead of the previous 143%. Operation at temperatures below +550° F (+290° C) will thereafter be stable and repeatable.

9.0 Special Sensors

In addition to the standard line of TG sensors described in Product Bulletin PB-105, Micro-Measurements can furnish almost any type of sensor pattern desired, in a wide range

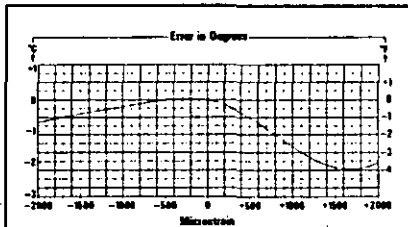


Fig. 14—Typical error signal caused by strain applied to Lot T04 TG sensor. Data applies to sensor temperatures near +75° F (+24° C).

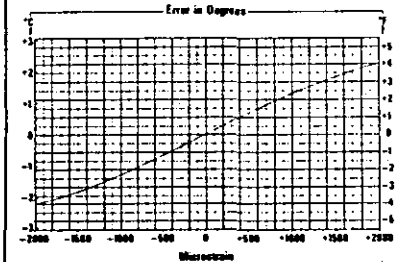


Fig. 15—Typical error signal caused by strain applied to Lot B83 Balco sensor. Data applies to sensor temperatures near +75° F (+24° C).

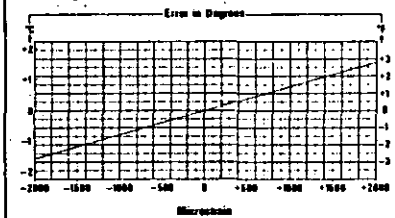


Fig. 16—Typical error signal caused by strain applied to ED copper sensor. Data applies to sensor temperatures near +75° F (+24° C).

of resistances. Setup charges will be minimized when the special design corresponds either to an A-Pattern resistor or to one of the patterns in the line of EA-Series strain gages; although resistances available are sometimes limited.

Nickel, Balco, and copper are frequently used for temperature compensation of transducer gage circuits. One or two bondable resistors are commonly inserted in the excitation arms of the bridge to provide automatic compensation for the combined effects of elastic modulus variation (in the transducer) and gage factor variation (in the strain gage) with

temperature. Although fixed resistors can be used for such compensation, a series of adjustable bondable resistor patterns is also available, and these permit trimming to the exact value of resistance required. Both resistor types are available in all three alloys and are also used to compensate other temperature effects in transducers.

While Balco has a slightly lower temperature coefficient of resistivity than pure nickel, its lower cost and high resistivity often permit smaller size and better economy. Figure 1 shows the resistance-versus-temperature characteristics of Balco and copper compared to that of pure nickel.

10.0 Calibration

Nickel, Balco, and copper temperature sensors are calibrated with specially designed test equipment consisting of a carefully controlled, uniform temperature bath, and a platinum resistance standard having calibration results traceable to the National Institute of Standards and Technology. Accuracy of calibration during these tests is 0.5° F (0.3° C). The temperature range used during calibration is -320° to +500° F (-195° to +260° C). Readout of both the platinum standard and the test gages is by means of a Measurements Group System 4000 which provides for leadwire-error-free data by using the circuit in Fig. 3. The test data from TG sensors shows that their behavior can be described well by a polynomial equation of the form:

$$R = A + BT + CT^2 + DT^3 + ET^4 + FT^5 + GT^6 \quad (1)$$

where: R = Resistance of the gage
 T = Temperature

A through G = Constants determined using regression analysis curve fitting.

REFERENCES

1. Robert B. Watson, James Dorsey, James E. Starr, "Conditioning Circuits for Bondable RTD's," 30th International Instrumentation Symposium, Instrument Society of America, Denver, Colorado, May 1984.
2. American National Standard ASTM E-644, "Standard Methods for Testing Industrial Resistance Thermometers," American Society for Testing and Materials, 1916 Race Street, Philadelphia, Pennsylvania 19103, 1978.

When the RTD's are being used with the System 4000, the equation must be entered in the transposed form:

$$T = A' + BR' + CR'^2 + DR'^3 + ER'^4 + FR'^5 + GR'^6 \quad (2)$$

(Note: The constants A' through G' in Eq. 2 are not the same as A through G in Eq. 1.)

Values of the coefficients for Eqs. 1 and 2 for 50-ohm (at +75° F (+23.9° C)) nickel TG sensors, and Balco and copper resistors, are listed in Tables 2a and 2b on page 8.

Finally, as discussed in Section 7.0, results will be slightly affected by the substrate to which the sensor is bonded.

11.0 Resistance-vs-Temperature Tables

The following section gives the resistance of standard Micro-Measurements 50-ohm type TG temperature sensors at all temperatures from the boiling point of liquid nitrogen [-320.4° F (-195.8° C)] to +500° F (+260° C). Tables are provided for both Fahrenheit (in 10-deg increments) and Celsius (in 5-deg increments) scales. Because of the slight difference in sensor response caused by the thermal expansion of the mounting surface, data are presented separately for sensors mounted on steel and aluminum. Tabular values are also given for copper and Balco sensors.

The tables are based upon an initial sensor resistance of precisely 50.0 ohms at +75° F (+23.9° C).

If the tabulated resistance readings are multiplied by 2.0, the tables can be used to express the resistance of sensors with other resistance values as a percentage of their resistance value at +75° F (+23.9° C).

TABLE 2a

Coefficients for Equation (1)						
Coef.	Lot T04 Nickel		Lot B03 Balco		Copper	
	1018	2024	1018	2024	1018	2024
A	39.46795	39.39097	41.94175	41.75797	42.89993	42.84167
	43.84157	43.78630	45.24435	45.13489	45.95225	45.92059
B	0.133972	0.134525	0.100229	0.102435	9.56482 x 10 ⁻⁷	9.64392 x 10 ⁻⁷
	0.250996	0.252373	0.191234	0.195874	0.171218	0.172788
C	8.31445 x 10 ⁻³	8.63411 x 10 ⁻³	9.53280 x 10 ⁻³	1.01253 x 10 ⁻²	-8.23169 x 10 ⁻⁴	-6.96694 x 10 ⁻⁴
	2.84885 x 10 ⁻⁴	2.95290 x 10 ⁻⁴	2.98942 x 10 ⁻⁴	3.18796 x 10 ⁻⁴	-2.66707 x 10 ⁻⁵	-2.25729 x 10 ⁻⁵
D	4.72396 x 10 ⁻¹	5.02142 x 10 ⁻¹	-3.14647 x 10 ⁻⁴	-2.89501 x 10 ⁻¹	0	0
	3.00807 x 10 ⁻¹	2.84453 x 10 ⁻¹	-1.91916 x 10 ⁻²	-1.94198 x 10 ⁻¹	0	0
E	4.93933 x 10 ⁻¹¹	1.21108 x 10 ⁻¹¹	-1.05422 x 10 ⁻¹¹	-3.42715 x 10 ⁻¹¹	0	0
	2.03720 x 10 ⁻¹⁰	2.13625 x 10 ⁻¹⁰	-1.11432 x 10 ⁻¹⁰	-3.69063 x 10 ⁻¹⁰	0	0
F	-2.16840 x 10 ⁻¹¹	-2.51606 x 10 ⁻¹¹	0	0	0	0
	-2.95460 x 10 ⁻¹²	-2.97514 x 10 ⁻¹²	0	0	0	0
G	3.15935 x 10 ⁻¹⁰	4.88934 x 10 ⁻¹⁰	0	0	0	0
	1.07663 x 10 ⁻¹⁰	1.65922 x 10 ⁻¹⁰	0	0	0	0

Coefficients in screened areas are °C.

TABLE 2b

Coefficients for Equation (2)						
Coef.	Lot T04 Nickel		Lot B03 Balco		Copper	
	1018	2024	1018	2024	1018	2024
A'	-3.87148 x 10 ¹	-3.85275 x 10 ²	-9.51899 x 10 ²	-9.09076 x 10 ²	-4.31693 x 10 ²	-4.30297 x 10 ²
	-2.32852 x 10 ²	-2.31809 x 10 ²	-5.46785 x 10 ²	-5.23095 x 10 ²	-2.57610 x 10 ²	-2.56831 x 10 ²
B'	14.37356	14.23312	44.73235	42.24911	9.65987	9.71064
	7.98384	7.90495	24.87051	23.50261	5.36677	5.39480
C'	-0.206576	-0.196463	-0.794763	-0.735627	9.38198 x 10 ⁻³	7.76763 x 10 ⁻³
	-0.114693	-0.109006	-0.44223	-0.409818	5.21012 x 10 ⁻³	4.31535 x 10 ⁻³
D'	3.47019 x 10 ⁻¹	3.14370 x 10 ⁻¹	7.60825 x 10 ⁻³	6.93316 x 10 ⁻¹	0	0
	1.92684 x 10 ⁻¹	1.74321 x 10 ⁻¹	4.23649 x 10 ⁻³	3.86758 x 10 ⁻¹	0	0
E'	-3.70193 x 10 ⁻¹	-3.23587 x 10 ⁻¹	-2.76346 x 10 ⁻¹	-2.47837 x 10 ⁻¹	0	0
	-2.05640 x 10 ⁻¹	-1.79412 x 10 ⁻¹	-1.53976 x 10 ⁻¹	-1.38422 x 10 ⁻¹	0	0
F'	2.05767 x 10 ⁻¹	1.75570 x 10 ⁻¹	0	0	0	0
	1.14362 x 10 ⁻¹	9.73545 x 10 ⁻²	0	0	0	0
G'	-4.55192 x 10 ⁻¹⁰	-3.82500 x 10 ⁻¹⁰	0	0	0	0
	-2.53118 x 10 ⁻¹⁰	-2.12139 x 10 ⁻¹⁰	0	0	0	0

Coefficients in screened areas are °C.

TABLE 3

Resistance vs. Temperature in Degrees Fahrenheit															
TG Nickel Sensors mounted on 1018 Steel — Lot No. T04AH															
°F	R	°F	R	°F	R	°F	R	°F	R	°F	R	°F	R		
-320	5.15	-210	14.77	-100	26.86	10	40.82	110	55.28	220	73.51	330	94.58	440	119.10
-310	5.88	-200	15.79	-90	28.05	20	42.18	120	56.83	230	75.30	340	96.65	450	121.54
-300	6.64	-190	16.82	-80	29.26	30	43.56	130	58.40	240	77.11	350	98.75	460	124.03
-290	7.44	-180	17.87	-70	30.48	40	44.96	140	59.99	250	78.95	360	100.88	470	126.55
-280	8.27	-170	18.94	-60	31.72	50	46.38	150	61.61	260	80.82	370	103.05	480	129.12
-270	9.12	-160	20.03	-50	32.97	60	47.82	160	63.24	270	82.71	380	105.24	490	131.73
-260	10.01	-150	21.13	-40	34.24	70	49.27	170	64.90	280	84.62	390	107.46	500	134.39
-250	10.92	-140	22.24	-30	35.52	80	50.00	180	66.57	290	86.56	400	109.72		
-240	11.85	-130	23.38	-20	36.82	90	50.74	190	68.27	300	88.52	410	112.01		
-230	12.80	-120	24.52	-10	38.14	100	52.24	200	70.00	310	90.51	420	114.34		
-220	13.78	-110	25.69	0	39.47	110	53.75	210	71.74	320	92.51	430	116.70		

TABLE 4

Resistance vs. Temperature in Degrees Fahrenheit															
TG Nickel Sensors mounted on 2024-T4 Aluminum — Lot No. T04AH															
°F	R	°F	R	°F	R	°F	R	°F	R	°F	R	°F	R		
-320	5.04	-210	14.65	-100	26.76	10	40.74	110	55.30	220	73.65	330	94.78	440	119.43
-310	5.76	-200	15.67	-90	27.95	20	42.12	120	56.86	230	75.45	340	96.86	450	121.90
-300	6.51	-190	16.70	-80	29.16	30	43.51	130	58.45	240	77.28	350	98.96	460	124.42
-290	7.31	-180	17.76	-70	30.38	40	44.91	140	60.05	250	79.12	360	101.18	470	126.99
-280	8.13	-170	18.83	-60	31.62	50	46.34	150	61.67	260	80.99	370	103.27	480	129.62
-270	8.99	-160	19.91	-50	32.87	60	47.78	160	63.32	270	82.89	380	105.46	490	132.30
-260	9.87	-150	21.02	-40	34.14	70	49.25	170	64.99	280	84.81	390	107.70	500	135.05
-250	10.78	-140	22.13	-30	35.43	80	50.00	180	66.68	290	86.75	400	109.97		
-240	11.72	-130	23.27	-20	36.73	90	50.73	190	68.39	300	88.72	410	112.27		
-230	12.67	-120	24.41	-10	38.05	100	52.23	200	70.12	310	90.71	420	114.61		
-220	13.65	-110	25.58	0	39.39	110	53.76	210	71.88	320	92.73	430	117.00		

TABLE 5

Resistance vs. Temperature in Degrees Fahrenheit															
Balco Sensors mounted on 1018 Steel — Lot No. B03															
°F	R	°F	R	°F	R	°F	R	°F	R	°F	R	°F	R		
-320	20.55	-210	25.37	-100	32.90	10	42.95	110	54.08	220	68.25	330	84.14	440	101.42
-310	20.87	-200	25.94	-90	33.72	20	43.98	120	55.29	230	69.62	340	85.66	450	103.05
-300	21.22	-190	26.54	-80	34.55	30	45.03	130	56.51	240	71.02	350	87.19	460	104.68
-290	21.59	-180	27.16	-70	35.40	40	46.10	140	57.75	250	72.42	360	88.73	470	106.33
-280	21.98	-170	27.80	-60	36.28	50	47.19	150	59.01	260	73.84	370	90.29	480	107.98
-270	22.39	-160	28.47	-50	37.17	60	48.29	160	60.28	270	75.28	380	91.85	490	109.63
-260	22.83	-150	29.15	-40	38.09	70	49.41	170	61.57	280	76.72	390	93.42	500	111.30
-250	23.29	-140	29.86	-30	39.02	80	50.00	180	62.88	290	78.18	400	95.00		
-240	23.78	-130	30.59	-20	39.98	90	50.55	190	64.20	300	79.66	410	96.99		
-230	24.29	-120	31.34	-10	40.95	100	51.71	200	65.53	310	81.14	420	98.19		
-220	24.82	-110	32.11	0	41.94	110	52.89	210	66.88	320	82.64	430	99.80		

TABLE 6

Resistance vs. Temperature in Degrees Fahrenheit							
Balco Sensors mounted on 2024-T4 Aluminum — Lot No. B03							
*F	R	*F	R	*F	R	*F	R
-320	19.94	-210	24.91	-100	32.55	10	42.79
-310	20.28	-200	25.50	-90	33.38	20	43.85
-300	20.64	-190	26.10	-80	34.22	30	44.92
-290	21.03	-180	26.73	-70	35.09	40	46.02
-280	21.44	-170	27.38	-60	35.98	50	47.13
-270	21.87	-160	28.06	-50	36.89	60	48.26
-260	22.32	-150	28.75	-40	37.82	70	49.41
-250	22.80	-140	29.47	-30	38.78	75	50.00
-240	23.29	-130	30.21	-20	39.75	80	50.58
-230	23.81	-120	30.97	-10	40.74	90	51.77
-220	24.35	-110	31.75	0	41.76	100	52.98
				100	52.98	210	67.40
						320	83.60
						430	101.05

TABLE 7

Resistance vs. Temperature in Degrees Fahrenheit							
ED Copper Sensors mounted on 1018 Steel							
*F	R	*F	R	*F	R	*F	R
-320	11.45	-240	19.47	-160	27.39	-80	35.20
-310	12.46	-230	20.47	-150	28.37	-70	36.16
-300	13.46	-220	21.46	-140	29.35	-60	37.13
-290	14.47	-210	22.45	-130	30.33	-50	38.10
-280	15.47	-200	23.44	-120	31.30	-40	39.06
-270	16.47	-190	24.43	-110	32.28	-30	40.02
-260	17.47	-180	25.42	-100	33.25	-20	40.98
-250	18.47	-170	26.40	-90	34.22	-10	41.94
				0	42.90	75	50.00
				150	57.06	230	64.66
				300	77.99	340	83.99
				450	104.31		

TABLE 8

Resistance vs. Temperature in Degrees Fahrenheit							
ED Copper Sensors mounted on 2024-T4 Aluminum							
*F	R	*F	R	*F	R	*F	R
-320	11.27	-240	19.29	-160	27.23	-80	35.08
-310	12.28	-230	20.29	-150	28.22	-70	36.06
-300	13.28	-220	21.29	-140	29.20	-60	37.03
-290	14.29	-210	22.28	-130	30.19	-50	38.00
-280	15.29	-200	23.28	-120	31.17	-40	38.97
-270	16.30	-190	24.27	-110	32.15	-30	39.94
-260	17.30	-180	25.26	-100	33.13	-20	40.91
-250	18.30	-170	26.25	-90	34.11	-10	41.88
				0	42.84	75	50.00
				150	57.15	230	64.65
				300	77.99	340	83.99
				450	104.31		

TABLE 9

Resistance vs. Temperature in Degrees Celsius											
TG Nickel Sensors mounted on 1018 Steel — Lot No. T04H											
*C	R	*C	R	*C	R	*C	R	*C	R	*C	R
-195	5.22	-135	14.67	-75	26.51	-15	40.14	40	54.36	100	72.09
-190	5.88	-130	15.59	-70	27.58	-10	41.36	45	55.74	105	73.69
-185	6.56	-125	16.51	-65	28.66	-5	42.59	50	57.14	110	75.30
-180	7.28	-120	17.45	-60	29.75	0	43.84	55	58.56	115	76.93
-175	8.01	-115	18.41	-55	30.85	5	45.10	60	59.99	120	78.58
-170	8.78	-110	19.38	-50	31.97	10	46.38	65	61.44	125	80.26
-165	9.56	-105	20.36	-45	33.10	15	47.67	70	62.91	130	81.95
-160	10.37	-100	21.35	-40	34.24	20	48.98	75	64.40	135	83.66
-155	11.19	-95	22.36	-35	35.39	23.9	50.00	80	65.90	140	85.39
-150	12.04	-90	23.38	-30	36.56	25	50.30	85	67.42	145	87.14
-145	12.90	-85	24.41	-25	37.74	30	51.64	90	68.96	150	88.92
-140	13.78	-80	25.45	-20	38.93	35	52.99	95	70.52	155	90.71
										210	112.01
										215	114.11

TABLE 10

Resistance vs. Temperature in Degrees Celsius											
TG Nickel Sensors mounted on 2024-T4 Aluminum — Lot No. T04H											
*C	R	*C	R	*C	R	*C	R	*C	R	*C	R
-195	5.11	-135	14.55	-75	26.40	-15	40.07	40	54.37	100	72.23
-190	5.76	-130	15.46	-70	27.47	-10	41.29	45	55.77	105	73.83
-185	6.44	-125	16.39	-65	28.55	-5	42.53	50	57.18	110	75.45
-180	7.15	-120	17.33	-60	29.64	0	43.79	55	58.61	115	77.09
-175	7.88	-115	18.29	-55	30.75	5	45.06	60	60.05	120	78.75
-170	8.64	-110	19.26	-50	31.87	10	46.34	65	61.51	125	80.43
-165	9.43	-105	20.24	-45	33.00	15	47.64	70	62.99	130	82.13
-160	10.23	-100	21.24	-40	34.15	20	48.95	75	64.49	135	83.84
-155	11.06	-95	22.25	-35	35.30	23.9	50.00	80	66.00	140	85.58
-150	11.91	-90	23.27	-30	36.47	25	50.30	85	67.53	145	87.34
-145	12.77	-85	24.30	-25	37.66	30	51.63	90	69.08	150	89.11
-140	13.65	-80	25.34	-20	38.85	35	52.99	95	70.65	155	90.91
										210	112.37
										215	114.38

TABLE 11

Resistance vs. Temperature in Degrees Celsius											
Balco Sensors mounted on 1018 Steel — Lot No. B03											
*C	R	*C	R	*C	R	*C	R	*C	R	*C	R
-195	20.58	-135	21.31	-75	32.66	-15	42.44	40	53.36	100	67.15
-190	20.87	-130	22.83	-70	33.39	-10	43.36	45	54.44	105	68.38
-185	21.18	-125	23.36	-65	34.13	-5	44.30	50	55.53	110	69.63
-180	21.51	-120	23.91	-60	34.89	0	45.24	55	56.63	115	70.88
-175	21.86	-115	24.48	-55	35.66	5	46.21	60	57.75	120	72.14
-170	22.22	-110	25.06	-50	36.45	10	47.19	65	58.88	125	73.42
-165	22.61	-105	25.67	-45	37.26	15	48.18	70	60.03	130	74.70
-160	23.01	-100	26.29	-40	38.09	20	49.19	75	61.18	135	76.00
-155	23.44	-95	26.93	-35	38.93	23.9	50.00	80	62.35	140	77.31
-150	23.88	-90	27.59	-30	39.78	25	50.21	85	63.54	145	78.62
-145	24.34	-85	28.26	-25	40.65	30	51.25	90	64.73	150	79.95
-140	24.81	-80	28.95	-20	41.54	35	52.30	95	65.94	155	81.29
										210	112.01
										215	114.11

Strain Gage Selection Criteria, Procedures, Recommendations

1.0 Introduction

The initial step in preparing for any strain gage installation is the selection of the appropriate gage for the task. It might at first appear that gage selection is a simple exercise, of no great consequence to the stress analyst; but quite the opposite is true. Careful, rational selection of gage characteristics and parameters can be very important in: optimizing the gage performance for specified environmental and operating conditions, obtaining accurate and reliable strain measurements, contributing to the ease of installation, and minimizing the *total* cost of the gage installation.

The installation and operating characteristics of a strain gage are affected by the following parameters, which are selectable in varying degrees:

- strain-sensitive alloy
- backing material (carrier)
- gage length
- gage pattern
- self-temperature-compensation number
- grid resistance
- options

Basically, the gage selection process consists of determining the particular available combination of parameters which is most compatible with the environmental and other operating *conditions*, and at the same time best satisfies the installation and operating *constraints*. These constraints are generally expressed in the form of requirements such as:

- accuracy
- stability
- temperature
- elongation
- test duration
- cyclic endurance
- ease of installation
- environment

The cost of the strain gage itself is not ordinarily a prime consideration in gage selection, since the significant economic measure is the total cost of the complete installation, of which the gage cost is usually but a small fraction. In many cases, the selection of a gage series or optional feature which increases the gage cost serves to decrease the total installation cost.

It must be appreciated that the process of gage selection generally involves compromises. This is because parameter choices which tend to satisfy one of the constraints or requirements may work against satisfying others. For example, in the case of a small-radius fillet, where the space available for gage installation is very limited, and the strain gradient extremely high, one of the shortest available gages might be the obvious choice. At the same time, however, gages shorter than about 0.125 in (3 mm) are generally characterized by lower maximum elongation, reduced fatigue life, less stable behavior, and greater installation difficulty. Another situation which often influences gage selection, and leads to compromise, is the stock of gages at hand for day-to-day strain measurements. While compromises are almost always necessary, the stress analyst should be fully aware of the effects of such compromises on meeting the requirements of the gage installation. This understanding is necessary to make the best overall compromise for any particular set of circumstances, and to judge the effects of that compromise on the accuracy and validity of the test data.

The strain gage selection criteria considered here relate primarily to stress analysis applications. The selection criteria for strain gages used on transducer spring elements, while similar in many respects to the considerations presented here, may vary significantly from application to application and should be treated accordingly. The Measurements Group's Transducer Applications Department can assist in this selection.



MEASUREMENTS GROUP, INC.
P.O. Box 27777
Raleigh, North Carolina 27611, USA

(919) 365-3500
Telex 802-502
FAX (919) 365-3945

©Copyright Measurements Group, Inc., 1989
All Rights Reserved.

2.0 Gage Selection Parameters

2.1 Strain-Sensing Alloys

The principal component which determines the operating characteristics of a strain gage is the strain-sensitive alloy used in the foil grid. However, the alloy is not in every case an independently selectable parameter. This is because each of Micro-Measurements strain gage series (identified by the first two, or three, letters in the alphanumeric gage designation — see diagram on page 11) is designed as a complete system. That system is comprised of a particular foil and backing combination, and usually incorporates additional gage construction features (such as encapsulation, integral leadwires, or solder dots) specific to the series in question.

Micro-Measurements supplies a variety of strain gage alloys as follows (with their respective letter designations):

- A: Constantan in self-temperature-compensated form.
- P: Annealed constantan.
- D: Iso-Elastic.
- K: Nickel-chromium alloy, a modified Karma in self-temperature-compensated form.

2.1.1 Constantan Alloy

Of all modern strain gage alloys, constantan is the oldest, and still the most widely used. This situation reflects the fact that constantan has the best overall combination of properties needed for many strain gage applications. This alloy has, for example, an adequately high strain sensitivity, or *gage factor*, which is relatively insensitive to strain level and temperature. Its resistivity is high enough to achieve suitable resistance values in even very small grids, and its temperature coefficient of resistance is not excessive. In addition, constantan is characterized by good fatigue life and relatively high elongation capability. It must be noted, however, that constantan tends to exhibit a continuous drift at temperatures above +150° F (+65° C), and this characteristic should be taken into account when zero stability of the strain gage is critical over a period of hours or days.

Very importantly, constantan can be processed for self-temperature-compensation (see box at right) to match a wide range of test material expansion coefficients. Micro-Measurements A alloy is a self-temperature-compensated form of constantan. A alloy is supplied in self-temperature-compensation (S-T-C) numbers 00, 03, 05, 06, 09, 13, 15, 18, 30, 40 and 50, for use on test materials with corresponding thermal expansion coefficients (expressed in ppm/°F).

For the measurement of very large strains, 5% (50 000µε) or above, annealed constantan (P alloy) is the grid material normally selected. Constantan in this form is very ductile; and, in gage lengths of 0.125 in (3 mm) and longer, can be strained to >20%. It should be borne in mind, however, that under high cyclic strains the P alloy will exhibit some permanent resistance change with each cycle, and cause a corresponding zero shift in the strain gage. Because of this characteristic, and the tendency for premature grid failure with repeated straining, P alloy is not ordinarily recommended for cyclic strain applications. P alloy is available with S-T-C numbers of 08 and 40 for use on metals and plastics, respectively.

2.1.2 Iso-Elastic Alloy

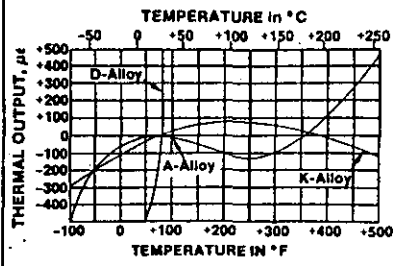
When purely dynamic strain measurements are to be made — that is, when it is not necessary to maintain a stable reference zero — Iso-Elastic (D alloy) offers certain advantages. Principal among these are superior fatigue life, compared to A alloy, and a high gage factor (approximately 3.2) which improves the signal-to-noise ratio in dynamic testing.

Self-Temperature-Compensation

An important property shared by constantan and modified Karma strain gage alloys is their responsiveness to special processing for self-temperature-compensation. Self-temperature-compensated strain gages are designed to produce minimum thermal output (temperature-induced apparent strain) over the temperature range from about -50° to +400° F (-45° to +200° C). When selecting either constantan (A-alloy) or Karma (K-alloy) strain gages, the self-temperature-compensation (S-T-C) number must be specified. The S-T-C number is the approximate thermal expansion coefficient in ppm/°F of the structural material on which the strain gage will display minimum thermal output.

The accompanying graph illustrates typical thermal output characteristics for A and K alloys. The thermal output of uncompensated Iso-Elastic alloy is included in the same graph for comparison purposes. In normal practice, the S-T-C number for an A- or K-alloy gage is selected to most closely match the thermal expansion coefficient of the test material. However, the thermal output curves for these alloys can be rotated about the room-temperature reference point to favor a particular temperature range. This is done by intentionally mismatching the S-T-C number and the expansion coefficient in the appropriate direction. When the selected S-T-C number is lower than the expansion coefficient, the curve is rotated counterclockwise. An opposite mismatch produces clockwise rotation of the thermal output curve. Under conditions of S-T-C mismatch, the thermal output curves for A and K alloys (supplied with each package of strain gages) do not apply, of course, and it will generally be necessary to calibrate the installation for thermal output as a function of temperature.

For additional information on strain gage temperature effects, see Measurements Group Tech Note TN-504.



D alloy is not subject to self-temperature-compensation. Moreover, as shown in the graph (see box), its thermal output is so high (about 80µε/°F (145µε/°C)) that this alloy is not normally usable for static strain measurements. There are times, however, when D alloy finds application in special-purpose transducers where a high output is needed, and where a full-bridge arrangement can be used to achieve reasonable temperature compensation within the circuit.

Other properties of D alloy should also be noted when considering the selection of this grid material. It is, for instance, magnetoresistive; and its strain-sensitive response is somewhat nonlinear, becoming significantly so at strains beyond ±5000µε.

2.1.3 Karma Alloy

Modified Karma, or K alloy, with its wide areas of application, represents an important member in the family of strain gage alloys. This alloy is characterized by good fatigue life and excellent stability; and is the preferred choice for accurate static strain measurements over long periods of time (months or years) at room temperature, or lesser periods at elevated temperature. It is recommended for extended static strain measurements over the temperature range from -452° to +500° F (-269° to +260° C). For short periods, encapsulated K-alloy strain gages can be exposed to temperatures as high as +750° F (+400° C). An inert atmosphere will improve stability and extend the useful gage life at high temperatures.

Among its other advantages, K alloy offers a much flatter thermal output curve than A alloy, and thus permits more accurate correction for thermal output errors at temperature extremes. Like constantan, K alloy can be self-temperature-compensated for use on materials with different thermal expansion coefficients. The available S-T-C numbers in K alloy are limited, however, to the following: 00, 03, 05, 06, 09, 13, and 15. K alloy is the normal selection when a temperature-compensated gage is required that has environmental capabilities and performance characteristics not attainable in A-alloy gages.

Due to the difficulty of soldering directly to K alloy, the duplex copper feature, which was formerly offered as an option, is now standard on all Micro-Measurements open-faced strain gages produced with K alloy. The duplex copper feature is a precisely formed copper soldering pad (DP) or dot (DD), depending on the available tab area. All K-alloy gages which do not have leads or solder dots are specified with DP or DD as part of the designation (in place of, or in addition to, the option specifier). The specific style of copper treatment will be advised when the Order Service Department is contacted. Open-faced K-alloy gages may also be ordered with solder dots.

2.2 Backing Materials

Conventional foil strain gage construction involves a photoetched metal foil pattern mounted on a plastic backing or carrier. The backing serves several important functions:

- provides a means for handling the foil pattern during installation
- presents a readily bondable surface for adhering the gage to the test specimen
- provides electrical insulation between the metal foil and the test object

Backing materials supplied on Micro-Measurements strain gages are of two basic types: polyimide and glass-fiber-reinforced epoxy-phenolic. As in the case of the strain sensitive alloy, the backing is not completely an independently specifiable parameter. Certain backing and alloy combinations, along with special construction features, are designed as systems, and given gage series designations: As a result, when arriving at the optimum gage type for a particular application, the process does not permit the arbitrary combination of an alloy and a backing material, but requires the specification of an available gage series. Micro-Measurements gage series and their properties are described in the following Section 2.3. Each series has its own characteristics and preferred areas of application; and selection recommendations are given in the table on page 5. The individual backing materials are discussed here, as the alloys were in the previous section, to aid in understanding the properties of the series in which the alloys and backing materials occur.

The Micro-Measurements polyimide E backing is a tough and extremely flexible carrier, and can be contoured readily to fit small radii. In addition, the high peel strength of the foil on the polyimide backing makes polyimide-backed gages less sensitive to mechanical damage during installation. With its ease of handling and its suitability for use over the temperature range from -320° to +350° F (-193° to +173° C), polyimide is an ideal backing material for general-purpose static and dynamic stress analysis. This backing is capable of large elongations, and can be used to measure plastic strains in excess of 20%. Polyimide backing is a feature of Micro-Measurements EA-, CEA-, EP-, EK-, S2K-, N2A-, J2A- and ED-Series strain gages.

For outstanding performance over the widest range of temperatures, the glass-fiber-reinforced epoxy-phenolic backing material is the most suitable choice. This backing can be used for static and dynamic strain measurement from -452° to +550° F (-269° to +290° C). In short-term applications, the upper temperature limit can be extended to as high as +750° F (+400° C). The maximum elongation of this carrier material is limited, however, to about 1 to 2%. Reinforced epoxy-phenolic backing is employed on the following gage series: WA, WK, SA, SK, WD, and SD.

2.3 Gage Series

As noted in Sections 2.1 and 2.2, the strain-sensing alloy and backing material are not subject to completely independent selection and arbitrary combination. Instead, a selection must be made from among the available gage systems, or series, where each series generally incorporates special design or construction features, as well as a specific combination of alloy and backing material. For convenience in identifying the appropriate gage series to meet specified test requirements, the information on gage series performance and selection is presented here, in condensed form, in two tables.

The table on the following page gives brief descriptions of all general-purpose Micro-Measurements gage series — including in each case the alloy and backing combination and the principal construction features. This table defines the performance of each series in terms of operating temperature range, strain range, and cyclic endurance as a function of strain level. It must be noted, however, that the performance data are nominal, and apply primarily to gages of 0.125 in (3 mm) or longer gage length.

GAGE SERIES	DESCRIPTION AND PRIMARY APPLICATION	TEMPERATURE RANGE	STRAIN RANGE	FATIGUE LIFE	
				Strain Level in $\mu\epsilon$	Number of Cycles
EA	Constantan foil in combination with a tough, flexible, polyimide backing. Wide range of options available. Primarily intended for general-purpose static and dynamic stress analysis. Not recommended for highest accuracy transducers.	Normal: -100° to +350°F (-75° to +175°C) Special or Short-Term: -320° to +400°F (-195° to +205°C)	±3% for gage lengths under 1/8 in (3.2 mm) ±5% for 1/8 in and over	±1800 ±1500 ±1200	10 ⁶ 10 ⁶ 10 ⁶
CEA	Universal general-purpose strain gages. Constantan grid completely encapsulated in polyimide, with large, rugged copper-coated tabs. Primarily used for general-purpose static and dynamic stress analysis. C-Feature gages are specially highlighted throughout the gage listing sections of Catalog 500, Part A — Strain Gage Listings.	Normal: -100° to +350°F (-75° to +175°C) Stacked rosettes limited to +150°F (+65°C)	±3% for gage lengths under 1/8 in (3.2 mm) ±5% for 1/8 in and over	±1500 ±1500 ±1000	10 ⁶ 10 ⁶ 10 ⁶ *Fatigue life improved using low-modulus solder.
N2A	Open-faced constantan foil gages with a thin, laminated, polyimide-film backing. Primarily recommended for use in precision transducers, the N2A Series is characterized by low and repeatable creep performance. Also recommended for stress analysis applications employing large gage patterns, where the especially flat matrix eases gage installation.	Normal Static Transducer Service: -100° to +200°F (-75° to +95°C)	±3%	±1700 ±1500	10 ⁶ 10 ⁷
J2A	Constantan foil gages with a thin, laminated, polyimide backing and encapsulating film. Exposed solder tabs for direct leadwire attachment. Primarily recommended for precision transducers; the encapsulating film provides a more rugged gage than the N2A Series, but may increase reinforcement of thin transducer flexures.	Normal Static Transducer Service: -100° to +200°F (-75° to +95°C)	±2%	±1700 ±1500	10 ⁶ 10 ⁷
ED	Iso-Elastic foil in combination with tough, flexible polyimide film. High gage factor and extended fatigue life excellent for dynamic measurements. Not normally used in static measurements due to very high thermal-output characteristics.	Dynamic: -320° to +400°F (-195° to +205°C)	±2% Nonlinear at strain levels over ±0.5%	±2500 ±2200	10 ⁶ 10 ⁷
WA	Fully encapsulated constantan gages with high-endurance leadwires. Useful over wider temperature ranges and in more extreme environments than EA Series. Option W available on some patterns, but restricts fatigue life to some extent.	Normal: -100° to +400°F (-75° to +205°C) Special or Short-Term: -320° to +500°F (-195° to +260°C)	±2%	±2000 ±1800 ±1500	10 ⁶ 10 ⁶ 10 ⁷
EK	Karma foil in combination with a tough, flexible polyimide backing. Primarily used where a combination of higher grid resistances, stability at elevated temperature, and great backing flexibility are required.	Normal: -320° to +350°F (-195° to +175°C) Special or Short-Term: -452° to +400°F (-269° to +205°C)	±1.5%	±1800	10 ⁷
WK	Fully encapsulated K-alloy gages with high-endurance leadwires. Widest temperature range and most extreme environmental capability of any general-purpose gage when self-temperature-compensation is required. Option W available on some patterns, but restricts both fatigue life and maximum operating temperature.	Normal: -452° to +550°F (-269° to +290°C) Special or Short-Term: -452° to +750°F (-269° to +400°C)	±1.5%	±2400 ±2200 ±2000	10 ⁶ 10 ⁷ 10 ⁶
EP	Special annealed constantan foil with tough, high-elongation polyimide backing. Used primarily for measurements of large post-yield strains in metals or on low-modulus materials (polymers). Available with Options E, L, and LE (may restrict elongation capability).	-100° to +400°F (-75° to +205°C)	±10% for gage lengths under 1/8 in (3.2 mm) ±20% for 1/8 in and over	±1000	10 ⁴
SA	Fully encapsulated constantan gages with solder dots. Same matrix as WA Series. Same uses as WA Series but derated somewhat in maximum temperature and operating environment because of solder dots.	Normal: -100° to +400°F (-75° to +205°C) Special or Short-Term: -320° to +450°F (-195° to +230°C)	±2%	±1800 ±1500	10 ⁶ 10 ⁷
B2K	Karma foil laminated to 0.001 in (0.025 mm) thick, high-performance polyimide backing, with a laminated polyimide overlay fully encapsulating the grid and solder tabs. Provided with large solder pads for ease of leadwire attachment.	Normal: -100° to +250°F (-75° to +120°C) Special or Short-Term: -300° to +300°F (-185° to +150°C)	±1.5%	±1800 ±1500	10 ⁶ 10 ⁷
BK	Fully encapsulated K-alloy gages with solder dots. Same uses as WK Series, but derated in maximum temperature and operating environment because of solder dots.	Normal: -452° to +450°F (-269° to +230°C) Special or Short-Term: -452° to +500°F (-269° to +260°C)	±1.5%	±2200 ±2000	10 ⁶ 10 ⁷
WD	Fully encapsulated Iso-Elastic gages with high-endurance leadwires. Used in wide-range dynamic strain measurement applications in severe environments.	Dynamic: -320° to +500°F (-195° to +260°C)	±1.5% — nonlinear at strain levels over ±0.5%	±3000 ±2500 ±2200	10 ⁶ 10 ⁷ 10 ⁶
SD	Equivalent to WD Series, but with solder dots instead of leadwires.	Dynamic: -320° to +400°F (-195° to +205°C)	±1.5% See above note	±2500 ±2200	10 ⁶ 10 ⁷

Strain Gage Series and Adhesive Selection Reference Table

TYPE OF TEST OR APPLICATION	OPERATING TEMPERATURE RANGE	TEST DURATION IN HOURS	ACCURACY REQUIRED**	CYCLIC ENDURANCE REQ'D		TYPICAL SELECTION	
				Maximum Strain, $\mu\epsilon$	Number of Cycles	Gage Series	M-Bond Adhesive
GENERAL STATIC OR STATIC-DYNAMIC STRESS ANALYSIS*	-50° to +150°F (-45° to +65°C)	<10 ⁴	Moderate	±1300	<10 ⁴	CEA, EA	200 or AE-10
		>10 ⁴	Moderate	±1300	<10 ⁶	CEA, EA	AE-10 or AE-15
		>10 ⁴	Very High	±1800	>10 ⁶	WA, SA	AE-15 or 610
	-50° to +400°F (-45° to +205°C)	<10 ⁴	Moderate	±1800	<10 ⁴	WA, SA	800 or 610
		>10 ⁴	High	±2000	<10 ⁶	WK, SK	AE-15 or 610
		>10 ⁴	Moderate	±2000	>10 ⁶	WK, SK	800 or 610
HIGH-ELONGATION (POST-YIELD)	-50° to +150°F (-45° to +65°C)	<10	Moderate	±50 000	1	CEA, EA	AE-10
		>10 ⁴	Moderate	±100 000	1	EP	AE-15
		>10 ⁴	Moderate	±200 000	1	EP	A-12
	0° to +500°F (-20° to +260°C)	<10 ⁶	Moderate	±15 000	1	SA, SK, WA, WK	610
	-452° to +500°F (-269° to +260°C)	<10 ⁴	Moderate	±10 000	1	SK, WK	800 or 610
		<10 ⁴	Moderate	±2000	10 ⁷	ED	200 or AE-10
<10 ⁴		Moderate	±2400	10 ⁷	WD	AE-10 or AE-15	
DYNAMIC (CYCLIC) STRESS ANALYSIS	-100° to +150°F (-75° to +65°C)	<10 ⁴	Moderate	±2000	10 ⁷	WD	800 or 610
		<10 ⁴	Moderate	±2000	<10 ⁶	WD	800 or 610
		<10 ⁴	Moderate	±2000	<10 ⁶	WD	800 or 610
TRANSDUCER GAGING	-50° to +150°F (-45° to +65°C)	<10 ⁴	1 to 5%	±1300	<10 ⁶	CEA, EA	AE-10 or AE-15
		<10 ⁴	1 to 5%	±1300	<10 ⁶	CEA	AE-15
	-50° to +200°F (-45° to +95°C)	<10 ⁴	Better than 0.2%	±1500	10 ⁶	N2A	800, 610 or 43-B
		<10 ⁴	0.2 to 0.5%	±1800	10 ⁶	WA, SA	610
	-320° to +300°F (-195° to +175°C)	<10 ⁴	Better than 0.5%	±1800	10 ⁶	WK, SK	610
		<10 ⁴	Better than 0.5%	±1800	10 ⁶	WK, SK	610

* This category includes most testing situations where some degree of stability under static test conditions is required. For absolute stability with constantan gages over long periods of usage and temperatures above +150°F (+65°C), it may be necessary to employ half- or full-bridge configurations. Protective coatings may also influence stability in cases other than transducer applications where the element is hermetically sealed.

** It is inappropriate to quantify "accuracy" as used in this table without consideration of various aspects of the actual test program and the instrumentation used. In general, "moderate" for stress analysis purposes is in the 2 to 5% range, "high" in the 1 to 3% range, and "very high" 1% or better.

The above table gives the recommended gage series for specific test "profiles," or sets of test requirements, categorized by the following criteria:

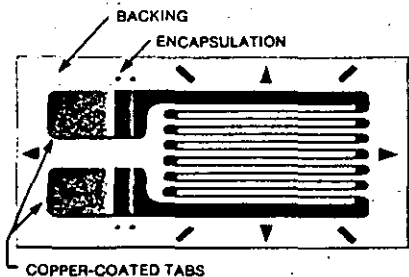
- type of strain measurement (static, dynamic, etc.)
- operating temperature of gage installation
- test duration
- accuracy required
- cyclic endurance required

This table provides the basic means for preliminary selection of the gage series for most conventional applications. It also includes recommendations for adhesives, since the adhesive in a strain gage installation becomes part of the gage system, and correspondingly affects the performance of

the gage. This selection table, supplemented by the information in the table on page 4, is used in conjunction with Catalog 500, Part A — Strain Gage Listings to arrive at the complete gage selection. The procedure for accomplishing this is described in Section 3.0 of this Tech Note.

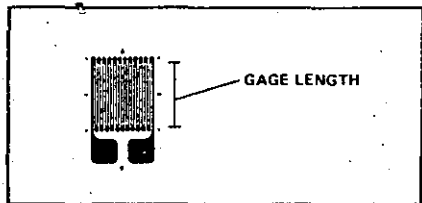
When a test profile is encountered that is beyond the ranges specified in the above table, it can usually be assumed that the test requirements approach or exceed the performance limitations of available gages. Under these conditions, the interactions between gage performance characteristics become too complex for presentation in a simple table. In such cases, the user should consult the Applications Engineering Department of Micro-Measurements for assistance in arriving at the best compromise.

As indicated in the previous table, the CEA-Series is usually the preferred choice for routine strain-measurement situations, not requiring extremes in performance or environmental capabilities (and not requiring the very smallest in gage lengths, or specialized grid configurations). CEA-Series strain gages are polyimide-encapsulated A-alloy gages, featuring large, rugged, copper-coated tabs for ease in soldering leadwires directly to the gage (photograph below). These thin, flexible gages can be contoured to almost any radius. In overall handling characteristics, for example, convenience, resistance to damage in handling, etc., CEA-Series gages are outstanding.



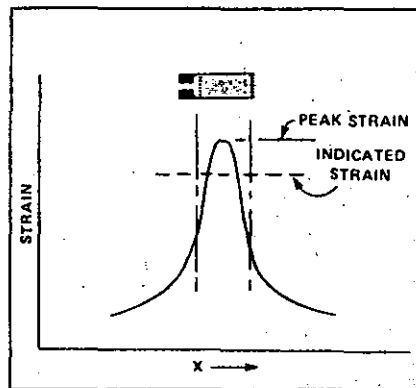
2.4 Gage Length

The gage length of a strain gage is the active or strain-sensitive length of the grid, as shown below. The endloops and solder tabs are considered insensitive to strain because of their relatively large cross-sectional area and low electrical resistance. To satisfy the widely varying needs of experimental stress analysis and transducer applications, the Micro-Measurements Division offers gage lengths ranging from 0.008 in (0.2 mm) to 4 in (100 mm).



Gage length is often a very important factor in determining the gage performance under a given set of circumstances. For example, strain measurements are usually made at the most critical points on a machine part or structure — that is, at the most highly stressed points. And, very commonly, the highly stressed points are associated with stress concentrations, where the strain gradient is quite steep and the area of maximum strain is restricted to a very small region. The strain gage tends to integrate, or average, the strain over the area covered by the grid. Since the average of any nonuniform strain distribution is always less than the maximum, a strain gage which is noticeably larger than the maximum strain region will indicate a strain magnitude which is too

low. The sketch below illustrates a representative strain distribution in the vicinity of a stress concentration, and demonstrates the error in strain indicated by a gage which is too long with respect to the zone of peak strain.



As a rule of thumb, when practicable, the gage length should be no greater than 0.1 times the radius of a hole, fillet, or notch, or the corresponding dimension of any other stress raiser at which the strain measurement is to be made. With stress-raiser configurations having the significant dimension less than, say, 0.5 in (13 mm), this rule of thumb can lead to very small gage lengths. Because the use of a small strain gage may introduce a number of other problems, it is often necessary to compromise.

Strain gages of less than about 0.125 in (3 mm) gage length tend to exhibit degraded performance — particularly in terms of the maximum allowable elongation, the stability under static strain, and endurance when subjected to alternating cyclic strain. When any of these considerations outweigh the inaccuracy due to strain averaging, a larger gage may be required.

When they can be employed, larger gages offer several advantages worth noting. They are usually easier to handle (in gage lengths up to, say, 0.5 in or 13 mm) in nearly every aspect of the installation and wiring procedure than miniature gages. Furthermore, large gages provide improved heat dissipation because they introduce, for the same nominal gage resistance, lower wattage per unit of grid area. This consideration can be very important when the gage is installed on a plastic or other substrate with poor heat transfer properties. Inadequate heat dissipation causes high temperatures in the grid, backing, adhesive, and test specimen surface, and may noticeably affect gage performance and accuracy (see Measurements Group Tech Note TN-502, *Optimizing Strain Gage Excitation Levels*).

Still another application of large strain gages — in this case, often very large gages — is in strain measurement on nonhomogeneous materials. Consider concrete, for example, which is a mixture of aggregate (usually stone) and cement. When measuring strains in a concrete structure it is ordinarily desirable to use a strain gage of sufficient gage length to span several pieces of aggregate in order to measure

the representative strain in the structure. It is usually the average strain that is sought in such instances, not the severe local fluctuations in strain occurring at the interfaces between the aggregate particles and the cement. In general, when measuring strains on structures made of composite materials of any kind, the gage length should normally be large with respect to the dimensions of the inhomogeneities in the material.

As a generally applicable guide, when the foregoing considerations do not dictate otherwise, gage lengths in the range from 0.125 to 0.25 in (3 to 6 mm) are preferable. The largest selection of gage patterns and stock gages is available in this range of lengths. Furthermore, larger or smaller sizes generally cost more, and larger gages do not noticeably improve fatigue life, stability, or elongation, while shorter gages are usually inferior in these characteristics.

2.5 Gage Pattern

The gage pattern refers cumulatively to the shape of the grid, the number and orientation of the grids in a multiple-grid gage, the solder tab configuration, and various construction features which are standard for a particular pattern. All details of the grid and solder tab configurations are illustrated in the "Gage Pattern" columns of Catalog 500, Part A — *Strain Gage Listings*. The wide variety of patterns in the list is designed to satisfy the full range of normal gage installation and strain measurement requirements.

With single-grid gages, pattern suitability for a particular application depends primarily on the following:

Solder tabs — These should, of course, be compatible in size and orientation with the space available at the gage installation site. It is also important that the tab arrangement be such as to not excessively tax the proficiency of the installer in making proper leadwire connections.

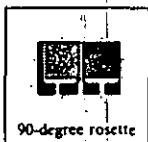
Grid width — When severe strain gradients perpendicular to the gage axis exist in the test specimen surface, a narrow grid will minimize the averaging error. Wider grids, when available and suitable to the installation site, will improve the heat dissipation and enhance gage stability — particularly when the gage is to be installed on a material or specimen with poor heat transfer properties.

Gage resistance — In certain instances, the only difference between two gage patterns available in the same series is the grid resistance — typically 120 ohms vs. 350 ohms. When the choice exists, the higher-resistance gage is preferable in that it reduces the heat generation rate by a factor of three (for the same applied voltage across the gage). Higher gage resistance also has the advantage of decreasing leadwire effects such as circuit desensitization due to leadwire resistance, and unwanted signal variations caused by leadwire resistance changes with temperature fluctuations. Similarly, when the gage circuit includes switches, slip rings, or other sources of random resistance change, the signal-to-noise ratio is improved with higher resistance gages operating at the same power level.

In experimental stress analysis, a single-grid gage would normally be used only when the stress state at the point of measurement is known to be uniaxial and the directions of the principal axes are known with reasonable accuracy ($\pm 5^\circ$).

These requirements severely limit the meaningful applicability of single-grid strain gages in stress analysis; and failure to consider biaxiality of the stress state can lead to large errors in the stress magnitude inferred from measurements made with a single-grid gage.

For a biaxial stress state — a common case necessitating strain measurement — a two- or three-element rosette is required in order to determine the principal stresses. When the directions of the principal axes are known in advance, a two-element 90-degree (or "tee") rosette can be employed with the gage axes aligned to coincide with the principal axes. The directions of the principal axes can sometimes be determined with sufficient accuracy from one of several considerations. For example, the shape of the test object and the mode of loading may be such that the directions of the principal axes are obvious from the symmetry of the situation, as in a cylindrical pressure vessel. The principal axes can also be defined by testing with photoelastic coating.



In the most general case of surface stresses, when the directions of the principal axes are not known from other considerations, a three-element rosette must be used to obtain the principal stress magnitudes. The rosette can be installed with any orientation, but is usually mounted so that one of the grids is aligned with some significant axis of the test object. Three-element rosettes are available in both 45-degree rectangular and 60-degree delta configurations. The usual choice is the rectangular rosette since the data-reduction task is somewhat simpler for this configuration.



When a rosette is to be employed, careful consideration should always be given to the difference in characteristics between single-plane and stacked rosettes. For any given gage length, the single-plane rosette is superior to the stacked rosette in terms of heat transfer to the test specimen, generally providing better stability and accuracy for static strain measurements. Furthermore, when there is a significant strain gradient perpendicular to the test surface (as in bending), the single-plane rosette will produce more accurate strain data because all grids are as close as possible to the test surface. Still another consideration is that stacked rosettes are generally less conformable to contoured surfaces than single-plane rosettes.



On the other hand, when there are large strain gradients in the plane of the test surface, as is often the case, the single-plane rosette can produce errors in strain indication because the grids sample the strain at different points. For these applications the stacked rosette is ordinarily preferable. The stacked rosette is also advantageous when the space for mounting the rosette is limited.

2.6 Optional Features

Micro-Measurements offers a selection of optional features for its strain gages and special sensors. The addition of options to the basic gage construction usually increases the cost, but this is generally offset by the benefits. Examples are:


- Significant reduction of installation time and costs
- Reduction of the skill level necessary to make dependable installations
- Increased reliability of applications
- Simplified installation of sensors in difficult locations on components or in the field
- Increased protection, both in handling during installation and shielding from the test environment
- Achievement of special performance characteristics


Availability of each option varies with gage series and pattern. Standard options are noted for each sensor in Catalog 500, Part A — *Strain Gage Listings*.


Shown below is a summary of the optional features offered.


Standard Catalog Options


OPTION	BRIEF DESCRIPTION
W	Integral Terminals and Encapsulation
E	Encapsulation with Exposed Tabs
SE	Solder Dots and Encapsulation
L	Preattached Leads
LE	Preattached Leads and Encapsulation

Option W	Series Availability: EA, EP, WA, ED, EK, WK
<p>General Description: This option provides encapsulation, and thin, printed circuit terminals at the tab end of the gage. Beryllium copper jumpers connect the terminals to the gage tabs. The terminals are 1.4 mil [0.0014 in (0.036 mm)] thick copper on polyimide backing about 1.5 mils [0.0015 in (0.038 mm)] thick. Option W gages are rugged and well protected, and permit the direct attachment of larger leadwires than would be possible with open-faced gages. This option is primarily used on EA-Series gages for general-purpose applications. Solder: +430° F (+220° C) tin-silver alloy solder joints on E-backed gages, +570° F (+300° C) lead-tin-silver alloy solder joints on W-backed gages. Temperature Limit: +400° F (+200° C) for E-backed gages, +500° F (+260° C) for W-backed gages. Grid Protection: Entire grid and part of terminals are encapsulated with polyimide. Fatigue Life: Some loss in fatigue life unless strain levels at the terminal location are below ±1000µε. Size: Option W extends from the soldering tab end of the gages and thereby increases gage size. With some patterns width is slightly greater. Strain Range: With some gage series, notably E-backed gages, strain range will be reduced. This effect is greatest with EP gages, and Option W should be avoided with them if possible. Flexibility: Option W adds encapsulation, making gages slightly thicker and stiffer. Conformance to curved surfaces will be somewhat reduced. In the terminal area itself, stiffness is markedly increased. Resistance Tolerance: On E-backed gages, resistance tolerance is normally doubled.</p>	
	

Option E	Series Availability: EA, ED, EK, EP
<p>General Description: Option E consists of a protective encapsulation of polyimide film approximately 1 mil [0.001 in (0.025 mm)] thick. This provides ruggedness and excellent grid protection, with little sacrifice in flexibility. Soldering is greatly simplified since the solder is prevented from finning any more of the gage tab than is deliberately exposed for lead attachment. Option E contributes significantly to long-term gage stability, because the grid cannot be contaminated by fingerprints or other agents during installation. Heavier leads may be attached directly to the gage tabs for simple static load tests. Supplementary protective coatings should still be applied after lead attachment in most cases. Temperature Limit: No degradation. Grid Protection: Entire grid and part of tabs are encapsulated. Fatigue Life: When gages are properly wired with small jumpers, maximum endurance is easily obtained. Size: Gage size is not affected. Strain Range: Strain range of gages will be reduced because the additional reinforcement of the polyimide encapsulation can cause bond failure before the gage reaches its full strain capability. Flexibility: Option E gages are almost as conformable on curved surfaces as open-faced gages, since no internal leads or solder are present at the time of installation. Resistance Tolerance: Resistance tolerance is normally doubled when Option E is selected.</p>	
	

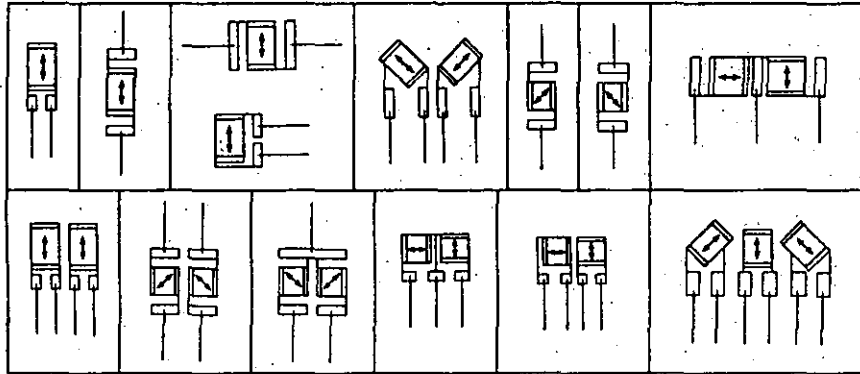
Option SE	Series Availability: EA, ED, EK, EP
<p>General Description: Option SE is the combination of solder dots on the gage tabs with a 1-mil [0.001-in (0.025-mm)] polyimide encapsulation layer that covers the entire gage. The encapsulation is removed over the solder dots, providing access for lead attachment. These gages are very flexible, and well protected from handling damage during installation. Option SE is primarily intended for small gages that must be installed in restricted areas, since leadwires can be routed to the exposed solder dots from any direction. The option does not increase overall gage dimensions, so the matrix may be field-trimmed very close to the actual pattern size. Option SE is sometimes useful on miniature transducers of medium or low accuracy class, or in stress analysis work on miniature parts. Solder: +570° F (+300° C) lead-tin-silver alloy. To prevent loss of long-term stability, gages with Option SE must be soldered with noncorrosive (rosin) flux, and all flux residue should be carefully removed with <i>M-LINE</i> Rosin Solvent after wiring. Protective coatings should then be used. Temperature Limit: No degradation. Grid Protection: Entire gage is encapsulated. Fatigue Life: When gages are properly wired with small jumpers, maximum endurance is easily obtained. Size: Gage size is not affected. Strain Range: Strain range of gages will be reduced because the additional reinforcement of the polyimide encapsulation can cause bond failure before the gage reaches its full strain capability. Flexibility: Option SE gages are almost as conformable on curved surfaces as open-faced gages. Resistance Tolerance: Resistance tolerance is normally doubled when Option SE is selected.</p>	
	

Option L	Series Availability: EA, ED, EK, EP
<p>General Description: Option L is the addition of soft copper lead ribbons to open-faced polyimide-backed gages. The use of this type of ribbon results in a thinner and more conformable gage than would be the case with round wires of equivalent cross section. At the same time, the ribbon is so designed that it forms almost as readily in any desired direction. Leads: Nominal ribbon size is 0.012 wide x 0.004 thick in (0.30 x 0.10 mm). Leads are approximately 0.8 in (20 mm) long. Solder: +430° F (+220° C) tin-silver alloy. The solder is confined to small, well-defined areas at the end of each ribbon. Temperature Limit: +400° F (+200° C). Fatigue Life: Fatigue life will normally be degraded by Option L. This occurs primarily because the copper ribbon has limited cyclic endurance. When it is possible to carefully stress the leads so that they are not bonded in a high strain field, the performance limitation will not apply. Option L is not often recommended for very high endurance gages such as the ED Series. Size: Matrix size is unchanged. Strain Range: Strain range will usually be reduced by the addition of Option L. Flexibility: Gages with Option L are not as conformable as standard gages. Resistance Tolerance: Not affected.</p>	
	

Option LE	Series Availability: EA, ED, EK, EP
<p>General Description: This option provides the same conformable soft copper lead ribbons as used in Option L, but with the addition of a 1-mil [0.001-in (0.025-mm)] thick encapsulation layer of polyimide film. The encapsulation layer provides excellent protection for the gage during handling and installation. It also contributes greatly to environmental protection, though supplementary coatings are still recommended for field use. Gages with Option LE will normally show better long-term stability than open-faced gages which are "waterproofed" only after installation. A good part of the reason for this is that the encapsulation layer prevents contamination of the grid surface from fingerprints or other agents during handling and installation. The presence of such contaminants will cause some loss in gage stability, even though the gage is subsequently coated with protective compounds. Leads: 0.012 wide x 0.004 thick in (0.30 x 0.10 mm) copper ribbons. Leads are approximately 0.8 in (20 mm) long. Solder: +430° F (+220° C) tin-silver alloy. The solder is confined to small, well-defined areas at the end of each ribbon. Temperature Limit: +400° F (+200° C). Grid Protection: Entire gage is encapsulated. A short extension of the backing is left uncovered at the leadwire end to prevent contact between the leadwires and the specimen surface. Fatigue Life: Fatigue life will normally be degraded by Option LE. This occurs primarily because the copper ribbon has limited cyclic endurance. Option LE is not often recommended for very high endurance gages such as the ED Series. Size: Matrix size is unchanged. Strain Range: Strain range will usually be reduced by the addition of Option LE. Flexibility: Gages with Option LE are not as conformable as standard gages. Resistance Tolerance: Resistance tolerance is normally doubled by the addition of Option LE.</p>	
	

Leadwire Orientation for Options L and LE

These illustrations show the standard orientation of leadwires relative to the gage pattern geometry for Options L and LE. The general rule is that the leads are parallel to the longest dimension of the pattern. The illustrations also apply to leadwire orientation for WA-, WK-, and WD-Series gages, when the pattern shown is available in one of these series.



2.7 Characteristics of Standard Catalog Options on EA-Series Gages

As in other aspects of strain gage selection, the choice of options ordinarily involves a variety of compromises. For instance, an option which maximizes a particular gage performance parameter such as fatigue life may at the same time require greater skill in installing the gage. Because of the many interactions between installation attributes and performance parameters associated with the options, the relative merits of all standard options are summarized qualitatively in the chart below as an aid to option selection. For comparison purposes, the corresponding characteristics of the CEA Series are given in the right-most column of the table.

Since, in strain measurement for stress analysis, the standard options are most frequently applied to EA-Series strain gages, the information supplied in this section is directed primarily toward such option applications.

When contemplating the application of an EA-Series gage with an option, the first consideration should usually be whether there is an equivalent CEA-Series gage that will satisfy the test requirements. Comparing, for example, an EA-Series gage equipped with Option W and a similar CEA-Series pattern, it will be found that the latter is characterized by lower cost, greater flexibility and conformability, and superior fatigue life. The only possible advantages for the selection of Option W are the wider variety of available patterns and the occasional need for large soldering terminals.

It should also be noted that many standard strain gage types, without options, are normally available from stock; while gages with options are commonly manufactured to order, and may thus involve a minimum order requirement.

In the table below, the respective performance parameters for an open-faced EA-Series gage without options are arbitrarily assigned a value of 5. Numbers greater than 5 indicate a particular parameter is improved by addition of the option, while smaller numbers indicate a reduction in performance.

INSTALLATION ATTRIBUTE OR PERFORMANCE PARAMETER	STANDARD OPTIONS					CEA-SERIES
	W	E	SE	L	LE	
Overall Ease of Gage Installation	8	7	6	5	6	10
Ease of Leadwire Attachment	10	8	7	7	8	10
Protection of Grid from Environmental Attack	8	8	8	5	8	8
Cyclic Strain Endurance	2	7	8	3	4	4
Elongation Capability	2	3	3	4	3	3
Resistance Tolerance	3	3	3	5	3	3
Reinforcement Effects	2	3	3	5	3	3

3.0 Gage Selection Procedure

The performance of a strain gage in any given application is affected by every element in the design and manufacture of the gage. Micro-Measurements offers a great variety of gage types for meeting the widest range of strain measurement needs. Despite the large number of variables involved, the process of gage selection can be reduced to only a few basic steps. From the diagram below that explains the gage designation code, it is evident that there are but five parameters to select, not counting options. These are: the gage series, the S-T-C number, the gage length and pattern, and the resistance.

Of the preceding parameters, the gage length and pattern are normally the first and second selections to be made, based on the space available for gage mounting and the nature of the stress field in terms of biaxiality and expected strain gradient. A good starting point for initial consideration of gage length is 0.125 in (3 mm). This size offers the widest variety of choices from which to select remaining gage parameters such as pattern, series and resistance. The gage and its solder tabs are large enough for relatively easy handling and installation. At the same time, gages of this length provide performance capabilities comparable to those of larger gages.

The principal reason for selecting a longer gage would commonly be one of the following: (a) greater grid area for better heat dissipation; (b) improved strain averaging on inhomogeneous materials such as fiber-reinforced composites; or (c) slightly easier handling and installation [for gage lengths up to 0.50 in (13 mm)]. On the other hand, a shorter gage length may be necessary when the object is to measure localized peak strains in the vicinity of a stress concentration, such as a hole or shoulder. The same is true, of course, when the space available for gage mounting is very limited.

In selecting the gage pattern, the first consideration is whether a single-grid gage or rosette is required (see Section 2.5). Single-grid gages are available with different aspect (length-to-width) ratios and various solder tab arrangements for adaptability to differing installation requirements. Two-element 90-degree rosettes, when applicable, can also be selected from a number of different grid and solder tab configurations. With three-element rosettes (rectangular or delta), the primary choice in pattern selection, once the gage length has been determined, is between planar and stacked construction, as described in Section 2.5.

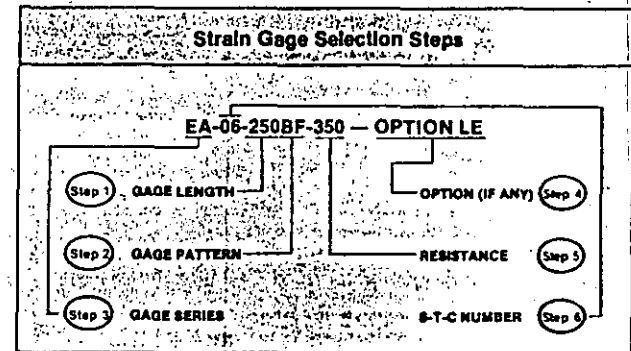
The format of Catalog 500, Part A — Strain Gage Listings is designed to simplify selection of the gage length and pattern. Similar patterns available in each gage length are grouped together, and listed in order of size. The strain gages in the Super Stock section of the catalog are the most widely used for stress analysis applications. This section should always be reviewed first to locate an appropriate gage.

With an initial selection of the gage size and pattern completed, the next step is to select the gage series, thus determining the foil and backing combination, and any other features common to the series. This is accomplished by referring to the chart on page 5, which gives the recommended gage series for specific test "profiles", or sets of test requirements. If the gage series is to have a standard option applied, the option should be tentatively specified at this time, since the availability of the desired option on the selected gage pattern in that series requires verification during the procedure outlined in the following paragraph.

After selecting the gage series (and option, if any), reference is made again to Catalog 500, Part A — Strain Gage Listings to record the gage designation of the desired gage size and pattern in the recommended series. If this combination is not listed as available in the catalog, a similar gage pattern in the same size group, or a slightly different size in an equivalent pattern, can usually be selected for meeting the installation and test requirements. In extreme cases, it may be necessary to select an alternate series and repeat this process. Quite frequently, and especially for routine strain measurement, more than one gage size and pattern combination will be suitable for the specified test conditions. In these cases, it is wise to select a gage from the Super Stock Listings to eliminate the likelihood of extended delivery time or a minimum order requirement.

As noted under the gage pattern discussion on page 7, there are often advantages from selecting the 350-ohm resistance if this resistance is compatible with the instrumentation to be used. This decision may be influenced, however, by cost considerations, particularly in the case of very small gages. Some reduction in fatigue life can also be expected for the high-resistance small gages. Finally, in recording the complete gage designation, the S-T-C number should be inserted from the list of available numbers for each alloy given on page 4 of Catalog 500, Part A — Strain Gage Listings.

This completes the gage selection procedure. In each step of the procedure, the Strain Gage Selection Checklist on page 12 should be referred to as an aid in accounting for the test conditions and requirements which could affect the selection.



4.0 Strain Gage Selection Checklist

This checklist is provided as a convenient, rapid means for helping make certain that no critical requirement of the test profile which could affect gage selection is overlooked. It should be borne in mind in using the checklist that the "considerations" listed apply to relatively routine and conventional stress analysis situations, and do not embrace exotic applications involving nuclear radiation, intense magnetic fields, extreme centrifugal forces, and the like.

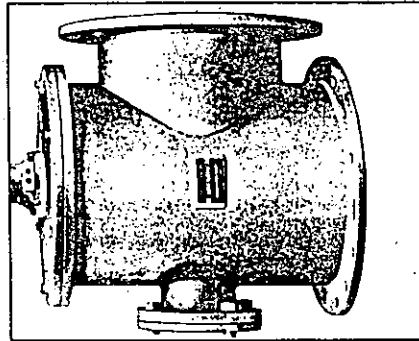
CONSIDERATIONS FOR PARAMETER SELECTION	
<p>Selection Step: 1 Parameter: Gage Length</p>	<input type="checkbox"/> strain gradients <input type="checkbox"/> area of maximum strain <input type="checkbox"/> accuracy required <input type="checkbox"/> static strain stability <input type="checkbox"/> maximum elongation <input type="checkbox"/> cyclic endurance <input type="checkbox"/> heat dissipation <input type="checkbox"/> space for installation <input type="checkbox"/> ease of installation
<p>Selection Step: 2 Parameter: Gage Pattern</p>	<input type="checkbox"/> strain gradients (in-plane and normal to surface) <input type="checkbox"/> biaxiality of stress <input type="checkbox"/> heat dissipation <input type="checkbox"/> space for installation <input type="checkbox"/> ease of installation <input type="checkbox"/> gage resistance availability
<p>Selection Step: 3 Parameter: Gage Series</p>	<input type="checkbox"/> type of strain measurement application (static, dynamic, post-yield, etc.) <input type="checkbox"/> operating temperature <input type="checkbox"/> test duration <input type="checkbox"/> cyclic endurance <input type="checkbox"/> accuracy required <input type="checkbox"/> ease of installation
<p>Selection Step: 4 Parameter: Options</p>	<input type="checkbox"/> type of measurement (static, dynamic, post-yield, etc.) <input type="checkbox"/> installation environment — laboratory or field <input type="checkbox"/> stability requirements <input type="checkbox"/> soldering sensitivity of substrate (plastic, bone, etc.) <input type="checkbox"/> space available for installation <input type="checkbox"/> installation time constraints
<p>Selection Step: 5 Parameter: Gage Resistance</p>	<input type="checkbox"/> heat dissipation <input type="checkbox"/> leadwire desensitization <input type="checkbox"/> signal-to-noise ratio
<p>Selection Step: 6 Parameter: S-T-C Number</p>	<input type="checkbox"/> test specimen material <input type="checkbox"/> operating temperature range <input type="checkbox"/> accuracy required

5.0 Gage Selection Examples

In this section, three examples are given of the gage-selection procedure in representative stress analysis situations. An attempt has been made to provide the principal reasons for the particular choices which are made. It should be noted, however, that an experienced stress analyst does not ordinarily proceed in the same step-by-step fashion illustrated in these examples. Instead, simultaneously keeping in mind the test conditions and environment, the gage installation constraints, and the test requirements, the analyst reviews Catalog 500, Part A — *Strain Gage Listings*, and quickly segregates the more likely candidates from among the available gage-pattern and series combinations in the appropriate sizes. The selection criteria are then refined in accordance with the particular strain-measurement task to converge on the gage or gages to be specified for the test program. Whether formally or otherwise, the knowledgeable practitioner does so in the light of parameter selection considerations such as those itemized in the preceding checklist.

A. Design Study of a Pressure Vessel

Strain measurements are to be made on a scaled-down plastic model of a pressure vessel. The model will be tested statically at, or near, room temperature; and, although the tests may be conducted over a period of several months, individual tests will take only a few hours to run.



Gage Selection:

- Gage Length** — Very short gage lengths should be avoided in order to minimize heat dissipation problems caused by the low thermal conductivity of the plastic. The model is quite large, and apparently free of severe strain gradients; therefore, a 0.25-in (6.3-mm) gage length is specified, because the widest selection of gage patterns is available in this length.
- Gage Pattern** — In some areas of the model, the directions of the principal axes are obvious from considerations of symmetry, and single-grid gages can be employed. Of the patterns available in the selected gage length, the 250BF pattern is a good compromise because of its high grid resistance which will help minimize heat dissipation problems.

In other areas of the model, the directions of the principal axes are not known, and a three-element rosette will be required. For this purpose, a "planar" rosette should be selected, since a stacked rosette would contribute significantly to reinforcement and heat dissipation problems. Because of its high-resistance grid, the 250RD pattern is a good choice.

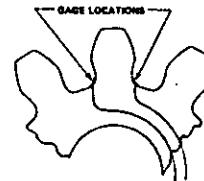
- Gage Series** — The polyimide (E) backing is preferred because its low elastic modulus will minimize reinforcement of the plastic model. Because the normal choice of grid alloy for static strain measurement at room temperature is the A alloy, the EA Series should be selected for this application.
- Options** — Excessive heat application to the test model during leadwire attachment could damage the material. Option L (preattached leads) is therefore selected so that the instrument cable can be attached directly to the leads without the application of a soldering iron to the gage proper. Option L is preferable over Option LE because the encapsulation in the latter option would add reinforcement.
- Resistance** — In this case, the resistance was determined in Step 2 when the higher resistance alternative was selected from among the gage patterns; i.e., in selecting the 250BF over the 250BG, and the 250RD over the 250RA. The selected gage resistance is thus 350 ohms.
- S-T-C Number** — Ideally, the gages should be self-temperature-compensated to match the model material, but this is not always feasible, since plastics — particularly reinforced plastics — vary widely in thermal expansion coefficient. For unreinforced plastic, S-T-C 30, 40 or 50 should usually be selected. If a mismatch between the model material and the S-T-C number is necessary, S-T-C 13 should be selected (because of stock status), and the test performed at constant temperature.

Gage Designations:

From the above steps, the strain gages to be used are:
 EA-30-250BF-350/Option L (single-grid)
 EA-30-250RD-350/Option L (rosette)

B. Dynamic Stress Analysis Study of a Spur Gear in a Hydraulic Pump

Strain measurements are to be made at the root of the gear tooth while the pump is operating. The fillet radius at the tooth root is 0.125 in (or about 3 mm) and test temperatures are expected to range from 0° to +180° F (-20° to +80° C).



Gage Selection:

- Gage Length** — A gage length which is small with respect to the fillet radius should be specified for this application. A length of 0.015 in (0.38 mm) is preferable, but reference to Catalog 500, Part A — *Strain Gage Listings*, indicates that such a choice severely limits the available gage patterns and grid alloys. Anticipating problems which would otherwise be encountered in Steps 2 and 3, a gage length of 0.031 in (0.8 mm) is selected.
- Gage Pattern** — Because the gear is a spur gear, the directions of the principal axes are known, and single-grid gages can be employed. A gage pattern with both solder tabs at the same end should be selected so that leadwire connections can be located in the clearance area along the root circle between adjacent teeth. In the light of these considerations, the 031CF pattern is chosen for the task.
- Gage Series** — Low strain levels are expected in this application; and, furthermore, the strain signals must be transmitted through slip rings or through a telemetry system to get from the rotating component to the stationary instrumentation. Iso-Elastic (D alloy) is preferred for its higher gage factor (nominally 3.2, in contrast to 2.1 for A and K alloys). Because the gage must be very flexible to conform to the small fillet radius, the E backing is the most suitable choice. The maximum test temperature is not a consideration in this case, since it is well within the recommended temperature range for any of the standard backings. The combination of the E backing and the D alloy defines the ED gage series.
- Options** — For protection of the gage grid in the test environment, Option E, encapsulation, should be specified. Because of the limited clearance between the outside diameter of one gear and the root circle of the mating gear, a particularly thin gage installation must be made; and very small leadwires will be attached to the gage tabs at 90° to the grid direction, and run over the sides of the gear for connection to larger wires. This requirement necessitates attachment of the small leadwires after gage bonding, and prevents the use of preattached leads.
- Resistance** — In the ED-Series version of the 031CF gage pattern, Catalog 500, Part A — *Strain Gage Listings*, lists the resistance as 350 ohms. The higher resistance should usually be selected whenever the choice exists, and will be advantageous in this instance in improving the signal-to-noise ratio when slip rings are used.
- S-T-C Number** — D alloy is not subject to self-temperature-compensation, nor is compensation needed for these tests since only dynamic strain is to be measured. In the ED-Series designation the two-digit S-T-C number is replaced by the letters DY for "dynamic."

Gage Designation:

Combining the results of the above selection procedure, the gage to be employed is:

ED-DY-031CF-350/Option E

**C. Flight-Test Stress Analysis
of a Titanium Aircraft Wing Tip Section —
With, and Without, a Missile Module Attached**

The operating temperature range for strain measurements is from -65° to $+450^{\circ}$ F (-35° to $+230^{\circ}$ C), and will be a dominant factor in the gage selection.



Gage Selection:

1. **Gage Length** — Preliminary design studies using the Photo-Stress[®] photoelastic coating technique indicate that a gage length of 0.062 in (1.6 mm) represents the best compromise in view of the strain gradients, areas of peak strain, and space for gage installation.
2. **Gage Pattern** — With information about the stress state and directions of principal axes gained from the photoelastic coating studies, there are some areas of the wing tip where single-grid gages and two-element "tee" rosettes can be employed. In other locations, where principal strain directions vary with the nature of the flight maneuver, 45° -degree rectangular rosettes are required.

The strain gradients are sufficiently steep that stacked rosettes should be selected. From Catalog 500, Part A — *Strain Gage Listings*, the foregoing requirements suggest the selection of 060WT and 060WR gage patterns for the stacked rosettes, and the 062AP pattern for the single-grid gage. In making this selection, attention was given to the fact that all three patterns are available in the WK Series, which is compatible with the specified operating temperature range.

3. **Gage Series** — The maximum operating temperature, along with the requirement for static as well as dynamic strain measurement, clearly dictates use of K alloy for the grid material. Either the SK or WK Series could be selected, but the WK gages are preferred because they have integral leadwires.
4. **Options** — For ease of gage installation, Option W, with integral soldering terminals, is advantageous. This option is not applicable to stacked rosettes, however, and is therefore specified for only the single-grid gages.
5. **Resistance** — When available, as in this case, 350-ohm gages should be specified because of the benefits associated with the higher gage resistance.
6. **S-T-C Number** — The titanium alloy used in the wing tip section is the 6Al-4V type, with a thermal expansion coefficient of 4.9×10^{-6} per $^{\circ}$ F (8.8×10^{-6} per $^{\circ}$ C). K alloy of S-T-C number 05 is the appropriate choice.

Gage Designations:

- WK-05-062AP-350/Option W
- WK-05-060WT-350
- WK-05-060WR-350

Measurement of Residual Stresses by the Hole-Drilling* Strain-Gage Method

RESIDUAL STRESSES AND THEIR MEASUREMENT

Residual (locked-in) stresses in a structural material or component are those stresses which exist in the object without (and usually prior to) the application of any service or other external loads. Manufacturing processes are the most common causes of residual stress. Virtually all manufacturing and fabricating processes—casting, welding, machining, molding, heat treatment, etc.—introduce residual stresses into the manufactured object. In some instances, residual (or *in situ*) stress may also be induced later in the life of the structure by installation or assembly procedures, by occasional overloads, by ground settlement effects on underground structures, or by dead loads which may ultimately become an integral part of the structure. Another common cause of residual stress is in-service repair or modification.

The effects of residual stress may be either beneficial or detrimental, depending upon the magnitude, sign, and distribution of the stress with respect to the load-induced stresses. Very commonly, the residual stresses are detrimental, and there are many documented cases in which these stresses were the predominant factor contributing to fatigue and other structural failures when the service stresses were superimposed on the already present residual stresses. The particularly insidious aspect of residual stress is that its presence generally goes unrecognized; and, until recently, there were no simple methods for measuring the stress without completely destroying the component or structural member.

*Drilling implies all methods of introducing the hole (i.e., drilling, milling, air abrasion, etc.).

Measurement of residual stress cannot be accomplished by conventional procedures for experimental stress analysis, since the strain sensor (strain gage, photoelastic coating, etc.) is totally insensitive to the history of the part, and measures only *changes* in strain after installation of the sensor. In order to measure residual stress with these standard sensors, the locked-in stress must be relieved in some fashion (with the sensor present) so that the sensor can register the change in strain caused by removal of the stress. This was usually done destructively in the past—by cutting and sectioning the part, by removal of successive surface layers, or by trepanning and coring (Figs. 1a, 1b). With strain sensors judiciously placed before dissecting the part, the sensors measure the relaxed strains, from which the initial residual stresses can be inferred by conventional methods. As ordinarily practiced, these destructive techniques frequently produce a semi-quantitative understanding of residual stresses, rather than accurate local measurements of principal stress magnitudes.

X-ray diffraction strain measurement offers a non-destructive alternative to the foregoing methods, but has its own severe limitations. Aside from the bulk and complexity of the equipment, which frequently precludes field applications, the technique is limited to strain measurements in only very shallow surface layers.

The most widely used modern technique for measuring residual stresses is the hole-drilling strain gage method (Fig. 1c). With this method, after installing strain sensors on the part surface, a small, shallow hole is drilled in the surface. After drilling, the change in strain in the immediate vicinity of the hole is measured, and the relaxed residual stresses are computed from these data. The hole-drilling method can be described as "semidestructive," since the small hole will not, in many cases, noticeably impair the structural integrity of the part being tested [the hole



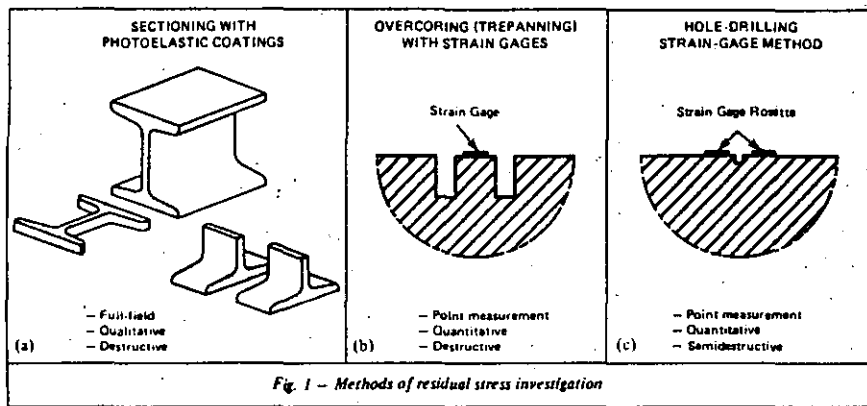


Fig. 1 - Methods of residual stress investigation

is typically 1/16 to 1/8 in (about 1.5 or 3.0 mm) in both diameter and depth). If desired, the hole can be removed after testing is completed by lightly blending or smoothing the surface with a small hand-held grinder. Using commercially available equipment and supplies, the hole-drilling method can be applied routinely by any practicing stress analysis technician, since no special expertise is required.

PRINCIPLE AND THEORY OF THE HOLE-DRILLING STRAIN-GAGE METHOD

The introduction of a hole (even of very small diameter) into a residually stressed body relaxes the stresses at that location by virtue of the fact that the stress on any free surface (the hole surface in this case) must of necessity be zero. The elimination of the radial stresses on the hole surface changes the stress in the immediately surrounding region, causing the local surface strains to change correspondingly.

This principle is the foundation for the blind-hole-drilling method; and its applications to residual stress measurement was first proposed by Mathar.¹ Subsequently, Rendler and Vigness² investigated the method very thoroughly and established the basic parameters for reducing it to a practical technique.

When a hole of small diameter ($D_0 = 2R_0$, Fig. 2) is drilled in a region initially containing residual stresses, the magnitudes of strain relieved at any point P are functions of the local principal stresses σ_x and σ_y , and of the geometric relationships between the point and the hole, and the point and the principal axes. Consider, for example, the strains relieved at the point when only one of the principal stresses, σ_x , is present:

$$\epsilon_r = -\sigma_x \frac{1+\nu}{2E} \left[\frac{1}{r^2} - \frac{3}{r^4} \cos 2\alpha + \left(\frac{4\nu}{1+\nu} \right) \frac{1}{r^2} \cos 2\alpha \right] \quad (1a)$$

$$\epsilon_\theta = -\sigma_x \frac{1+\nu}{2E} \left[-\frac{1}{r^2} + \frac{3}{r^4} \cos 2\alpha - \left(\frac{4\nu}{1+\nu} \right) \frac{1}{r^2} \cos 2\alpha \right] \quad (1b)$$

(Equations 1a and 1b are derived from the Kirsch solution first reported in 1898.)

where:

- $\epsilon_r, \epsilon_\theta$ = radial and tangential normal strains (respectively) relieved at point P
- σ_x, σ_y = principal stresses; however, neither is yet defined as maximum or minimum
- $r = R/R_0$ = dimensionless radius to point P from center of hole
- E, ν = elastic modulus, and Poisson's ratio of test material, respectively

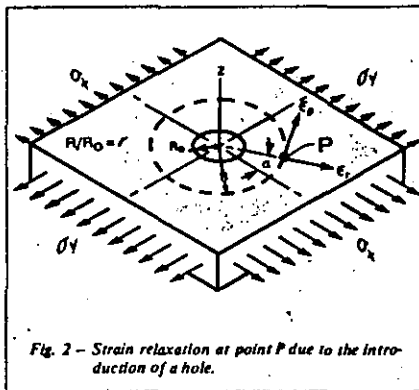


Fig. 2 - Strain relaxation at point P due to the introduction of a hole.

The relieved strains expressed by Eqs. (1) are plotted in Fig. 3 for $\alpha = 0^\circ$ and $\alpha = 90^\circ$ to illustrate their variations along the principal axes with distance from the center of the hole. As distance from the hole increases, the relieved strains decrease very rapidly. Because of this, it is desirable to measure the strains as close as practicable to the hole in order to maximize the output signal of the strain sensor. On the other hand, parasitic effects also increase in the immediate vicinity of the hole. These considerations necessitate a compromise in the selection of the optimum measurement radius.

Equations (1) demonstrate that the relieved radial and tangential normal strains vary sinusoidally along a circle of radius R , and can be expressed generally as:

$$\epsilon_r = \sigma_x (A + B \cos 2\alpha) \quad (2a)$$

$$\epsilon_\theta = \sigma_x (-A + C \cos 2\alpha) \quad (2b)$$

$$\text{where: } A = -\frac{1+\nu}{2E} \left(\frac{1}{r^2} \right)$$

$$B = -\frac{1+\nu}{2E} \left[\left(\frac{4}{1+\nu} \right) \frac{1}{r^2} - \frac{3}{r^4} \right]$$

$$C = -\frac{1+\nu}{2E} \left[-\left(\frac{4\nu}{1+\nu} \right) \frac{1}{r^2} + \frac{3}{r^4} \right]$$

If the stress state is biaxial, with both σ_x and σ_y present simultaneously, the expression for the relieved strain in the radial direction (the only direction relevant to the following discussion) becomes:

$$\epsilon_r = \sigma_x (A + B \cos 2\alpha) + \sigma_y [A + B \cos 2(\alpha + 90^\circ)] \quad (3)$$

Coefficients A and B can be calculated directly for any radius, R , on any material, from the relationships accompanying Eqs. (2). It is important to realize that these calculated values are applicable for Kirsch's theoretical solution for the stress distribution around a circular hole through a thin wide plate subjected to plane stress. Further, Kirsch's solution does not consider the strain-averaging (or integrating) effect of strain gages which have finite dimensions. More appropriate values A and B can be established by additional analytical and/or experimental calibration procedures as discussed in the section, *Determining Coefficients A and B*.

Since both A and B are negative, a tensile (+) residual stress will produce a compressive (-) relieved strain.

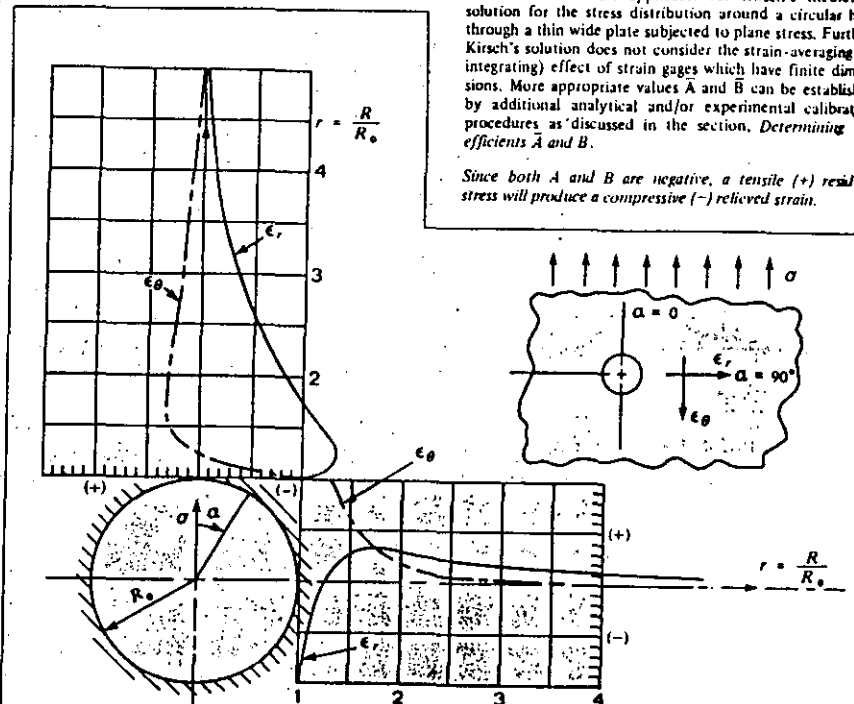


Fig. 3 - Variation of relieved strains with distance (along the principal axes) from the center of the drilled hole-uniaxial residual stress

In order to determine the principal residual stresses and their directions with respect to any reference axis, three independent strain measurements must be made. These three measurements will permit the solution of three equations from which the stresses σ_x and σ_y and the direction β can be readily calculated. The most common procedure for measuring the relieved strains is to mount three resistance strain gages in the form of a rosette around the site of the hole before drilling.

ANALYSIS OF THE RESIDUAL STRESS ROSETTE

As shown in Fig. 4, three radially oriented strain gages are installed with their centers at the radius R from the center of the hole site, and located at the angles:

$$\alpha_1 = \beta \text{ (arbitrary)}$$

$$\alpha_2 = \beta + 45^\circ$$

$$\alpha_3 = \beta + 90^\circ$$

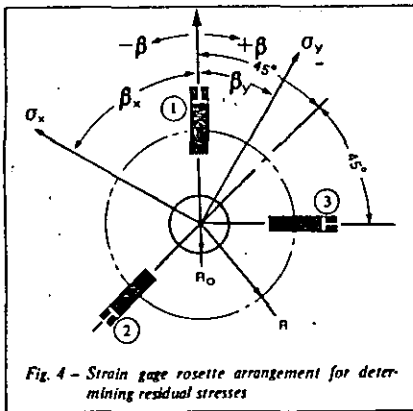


Fig. 4 - Strain gage rosette arrangement for determining residual stresses

Substituting these three angles successively into Eq. (3) produces three simultaneous equations in σ_x , σ_y , β and the measured strains ϵ_3 , ϵ_2 , ϵ_1 . Solving for the principal stresses and direction yields:

$$\sigma_x = \frac{\epsilon_1 + \epsilon_3}{4\bar{A}} + \frac{\sqrt{2}}{4\bar{B}} \sqrt{(\epsilon_1 - \epsilon_3)^2 + (\epsilon_2 - \epsilon_3)^2} \quad (4a)$$

$$\sigma_y = \frac{\epsilon_1 + \epsilon_3}{4\bar{A}} - \frac{\sqrt{2}}{4\bar{B}} \sqrt{(\epsilon_1 - \epsilon_3)^2 + (\epsilon_2 - \epsilon_3)^2} \quad (4b)$$

$$\tan 2\beta = \frac{\epsilon_1 - 2\epsilon_2 + \epsilon_3}{\epsilon_3 - \epsilon_1} \quad (4c)$$

where \bar{A} and \bar{B} (both of which are negative) are determined by experimental calibration or from Fig. 7. Equations (4a) and (4b) define the minimum (σ_x) and maximum (σ_y) principal stresses. Note that the direction angle β is referenced to gage 1 where clockwise is the positive (+) direction and:

$$\beta = \beta_x \text{ if } (\epsilon_1 + \epsilon_3)/2 < \epsilon_2$$

$$\beta = \beta_y \text{ if } (\epsilon_1 + \epsilon_3)/2 > \epsilon_2$$

$$\beta = 45^\circ \text{ if } \epsilon_1 = \epsilon_3$$

EFFECT OF HOLE DEPTH

Figure 5 illustrates the results of several investigators, and shows the increase in measured strain as the depth of the hole increases. The strains in the immediate vicinity of the hole are relieved (that is, the curves tend to an asymptotic value) when the depth reaches 1.0 to 1.2 hole diameters. These graphs apply to the carefully controlled case where the stress was uniaxial and did not vary with depth. While the shapes of these graphs for strain versus the ratio of hole depth to diameter are similar, it is clear that the strain output is also dependent on the gage circle diameter (D). Indeed, the constants \bar{A} and \bar{B} in Eqs. (4a) and (4b) are functions of the gage circle diameter D , the hole diameter D_0 , hole depth Z , and strain gage geometry, as well as the test material.

The ASTM Standard Method E837² states that the hole depth should be increased in small increments (ΔZ) and that strain measurements should be made at each increment of depth. Graphs of the measured strains versus depth (Z/D_0) should be reasonably similar to those of Fig. 5. Graphs differing substantially from those of Fig. 5 indicate

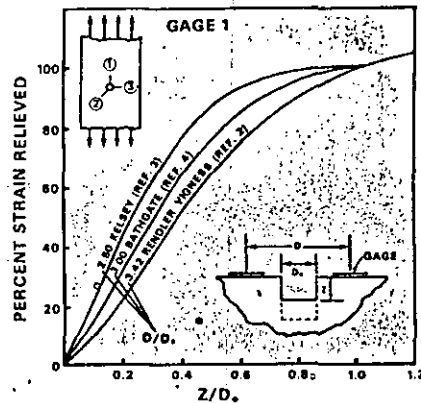


Fig. 5 - Percent strain relieved versus ratio of hole depth to diameter

a measurable stress gradient through the depth of the hole. For these cases, it may be desirable to consider approximate methods of data reduction as discussed by Kelsey,³ Bathgate,⁴ Birley and Owens,⁵ Scaramangas, Goff, and Leggett,⁷ or Schajer.⁸

DETERMINING COEFFICIENTS \bar{A} AND \bar{B}

The Kirsch solution defines \bar{A} and \bar{B} by the relations accompanying Eq. (2). It is important to recognize that this theoretical solution is restricted to:

- a small circular through-hole in a thin, wide plate
- stress (or strain) at a point and does not account for the strain-averaging effect under the finite area of a strain gage grid
- constant stress through the plate thickness

In most instances, the hole drilling method is used on thicker sections and the hole is "blind" rather than "through". Fortunately, it has been demonstrated² that Eqs. (4) also describe the stress field around a blind hole; and further, coefficients \bar{A} and \bar{B} can be readily determined by experimental calibration^{2,3}. Experimental calibration is particularly attractive since it automatically accounts for the mechanical properties of the test material, strain gage rosette geometry, hole depth and diameter, and the strain-averaging effect of the strain gage grid.

Experimental Calibration

Calibration for \bar{A} and \bar{B} is accomplished by installing a residual stress rosette on a uniaxially loaded tensile specimen which is made from the same material as the test part. The rosette should be oriented to align grid 3 parallel to the direction of loading. Care must be taken to insure that bending stresses are minimal. End effects must also be minimized, and it is suggested that specimen width (w)

be equal to, or greater than, ten times the hole diameter ($10D_0$). Also, the length, between grips, should exceed five times the width ($5w$). When determining \bar{A} and \bar{B} for "blind-hole" applications, a specimen thickness (t) of at least five times the hole diameter ($5D_0$) is suggested. "Through-hole" applications should, of course, be calibrated using through-hole calibration specimens. Calibration tensile stresses (σ_c) should not exceed one-half of the proportional limit stress of the test material [$\sigma_c = \text{Force}/(wt)$]. Load is applied both before and after drilling the hole and strain measurements are made before (ϵ_b) and after (ϵ_a) as well. Calibration strain (ϵ_c) is defined as ($\epsilon_a - \epsilon_b$):

$$\epsilon_c = (\epsilon_a - \epsilon_b)$$

Calibration procedures are normally improved by loading incrementally and graphing σ_c versus ϵ_{c1} and ϵ_{c3} as illustrated in Fig. 6. Best-fit straight lines are generally more representative of behavior than single-point or one-load data points. Calibration values of \bar{A} and \bar{B} can be calculated from:^{2,3}

$$\bar{A} = \frac{\epsilon_{c3} + \epsilon_{c1}}{2\sigma_c}$$

$$\bar{B} = \frac{\epsilon_{c3} - \epsilon_{c1}}{2\sigma_c}$$

As shown in Fig. 6, ϵ_{c1} and ϵ_{c3} are +39 and $-90\mu\epsilon$, respectively, when σ_c is 10 000 psi (69 MPa).

Then,

$$\bar{A} = -0.25 \times 10^{-8} \text{ psi}^{-1} \quad (-0.36 \times 10^{-13} \text{ Pa}^{-1})$$

$$\bar{B} = -0.65 \times 10^{-8} \text{ psi}^{-1} \quad (-0.94 \times 10^{-13} \text{ Pa}^{-1})$$

Through-hole
304 Stainless Steel

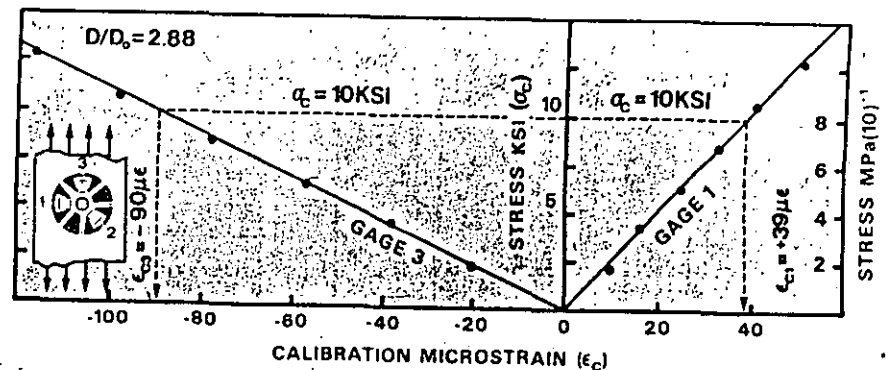


Fig. 6 - Stress versus relieved strain for calibration of coefficients \bar{A} and \bar{B} on 304 Stainless Steel (through-hole)

Numerical Analysis

Calibration is, of course, a reliable method of determining coefficients \bar{A} and \bar{B} ; however, it does require additional time, expense, and effort. Schajer⁸ redefined coefficients \bar{A} and \bar{B} as:

$$\bar{A} = -\frac{1+\nu}{2E} \cdot \bar{a} \quad (5a)$$

$$\bar{B} = -\frac{1}{2E} \cdot \bar{b} \quad (5b)$$

Coefficients \bar{a} and \bar{b} (for through-holes) have been established by computer analysis using a numerical integrating program. The program considered the actual geometry of the strain gage filaments within the grid, including the reduced sensitivity of the wider (and lower resistance)

outermost filaments. Coefficient \bar{a} is independent of the mechanical properties (E and ν) of the test material, and \bar{b} has only a very slight dependence on Poisson's ratio (ν).

The strain response of through-hole and blind-hole applications differ; consequently, the computer-determined values of \bar{a} and \bar{b} , for through-holes, are not directly applicable to the more common blind-hole applications. Finite element analyses and experimental calibrations^{8,9} have been used to define the data reduction coefficients \bar{a} and \bar{b} for blind-hole applications. Figure 7 shows typical data reduction coefficients \bar{a} and \bar{b} plotted versus D/D_0 for two types of gage arrangements.

Values of data reduction coefficients \bar{a} and \bar{b} are supplied with each package of Micro-Measurements strain gage rosettes for residual stress measurements.

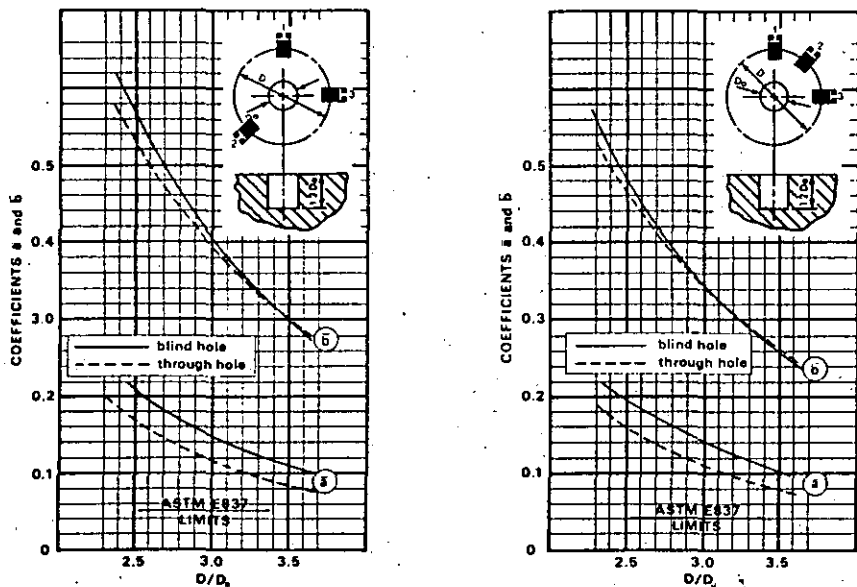


Fig. 7 - Data reduction coefficients \bar{a} and \bar{b} versus dimensionless hole diameter (typical). The left-hand graph is generally representative of the UM gage; and the right-hand graph, of the RE and RK gages

EXPERIMENTAL TECHNIQUES

As in all experimental methods, proper materials, instrumentation, and application procedures are essential if accurate results are to be obtained. The accuracy of the hole-drilling method is dependent chiefly upon:

- strain gage selection and installation
- strain-indicating instrumentation
- hole alignment and boring
- understanding the mechanical properties of the test material

Strain Gage Selection and Installation

Installing three individual strain gages accurately spaced and oriented on a small circle is not easy or advisable. Special-purpose rosette configurations (Fig. 8) have been designed and developed by the Micro-Measurements Division for residual stress measurement. Among other

features, these rosette designs incorporate centering marks for aligning the boring tool precisely at the center of the gage circle. All configurations are available with different temperature compensations; however, only the "RE" design is available in different sizes (031RE, 062RE, 125RE). The "RE" design is available open-faced or with Option SE (solder dots and encapsulation).

The RK and UM configurations are supplied in 1/16 in gage length, and both are fully encapsulated. Easily accessible copper solder terminals are incorporated in the RK design, while the UM configuration has integral copper terminals and offers all features of the popular C-Feature strain gage series.

Residual stress measurements are not normally conducted at elevated temperatures and Micro-Measurements M-Bond 200 adhesive is generally used to install the strain gage rosettes. However, it is important to recognize that the measured relieved strains, produced by a known residual stress, will be approximately ten times less than those produced by the same magnitude of mechanical stress during conventional testing (see *Experimental Calibration* section). For this reason, it is mandatory that all surface preparation and gage installation procedures be of the highest quality. Drift, associated with inferior installations, has a more serious influence on residual stress measurements because of the generally low value of the measured strains.

EA-XX-062RE-120

This geometry conforms to the early Rendler and Vigness design⁴ and has been used in most reported technical articles (see references). It is available in different sizes, and therefore facilitates increased or decreased hole depth during measurement.



TEA-XX-062RK-120

This is a rugged, encapsulated design incorporating heavy copper solder terminals which greatly reduce installation time and expense. It is compatible with all methods of introducing the hole, and the strain-gage grid geometry is identical to the 062RE pattern.

CEA-XX-062UM-120

All practical advantages of the CEA strain gage series are maintained in this design (integral copper soldering tabs, encapsulation, conformability, etc.). The grid widths have been reduced to facilitate positioning all three grids on one side of the measurement point as shown. With this geometry, and appropriate trimming, it is possible to position the hole closer to welds and other irregularities. The user should be reminded, however, that the data reduction equations are theoretically valid only when the holes are well removed from free boundaries, discontinuities, abrupt geometric changes, etc. The UM design is compatible with all methods of introducing the hole.



Fig. 8 - Residual stress rosettes

Strain-Indicating Instrumentation

A portable, battery-operated precision strain indicator, augmented by a high-quality switch-and-balance unit, is ordinarily the most effective and convenient instrumentation for measuring the relieved strains. The Measurements Group Model P-3500 Strain Indicator and SB-10 Switch-and-Balance Unit are ideally suited for this application.

Hole Alignment and Boring

Introducing the hole requires careful consideration of:

- **hole alignment** - it is clear from analytical considerations that the hole must be accurately positioned at the center of the three gages.
- **hole shape** - ideally, the hole should be cylindrical, uniform in diameter, have a flat bottom, with square corners at the outside top and inside bottom of the hole.
- **machining technique** - machining should be stress-free; that is, the method of material removal should not induce residual stress/strain of its own.

With these considerations satisfied, the measured relaxed strains can be substituted into Eqs. (4) and the residual stresses, at the hole location prior to introducing the hole, can be determined.

Alignment

Rendler and Vigness² noted that "the accuracy of the (hole-drilling) method for field applications will be directly related to the operator's ability to position the milling cutter precisely in the center of the gage rosette." More recent efforts have quantified the error in the calculated stress^{10,11}. For example, with a hole ± 0.001 in (± 0.025 mm) off-center of the 062RE, 062RK, or 062UM rosette, the error in calculated stress* will not exceed 3%. In practice, the required alignment of ± 0.001 in (± 0.025 mm) is accomplished using the RS-200 Milling Guide as shown in Fig. 9a. The Milling Guide is normally secured to the test item by bonding its three pads (Fig. 9a) with a quick-setting adhesive. A microscope is then installed, and visual alignment is accomplished using the four X-Y adjustments on the exterior of the guide.

Boring

Numerous studies on the effects of hole size, shape and machining procedures have been published. Rendler and Vigness² were the first to specify a specially-dressed end mill which is compatible with the residual stress rosettes of Fig. 8. The end mill is ground to remove the side cutting edges, and then relieved immediately behind the cutting face to avoid rubbing on the hole surface. It is imperative that the milling cutter be rigidly guided during the drilling operation so that the cutter progresses in a straight line, without side pressure on the hole, or friction at the non-cutting edge. These end mills generate the desired flat bottomed and square cornered hole shape at initial surface contact and maintain the desired shape until the hole is completed. In doing so, they fulfill the incremental drilling needs as stipulated in ASTM Standard E837³. Specially-dressed end mills offer a direct and simple approach when measuring residual stresses on readily machinable materials (aluminum, mild steels, etc.).

Figure 9b shows the RS-200 Milling Guide with the microscope removed and the end mill assembly in place. The end mill is driven by either a hand drill or variable-speed electric drill which is attached to the universal joint at the top of the assembly.

In 1980, Flamin¹² first reported excellent results of residual stress measurement using a high speed (up to 400 000 rpm) air turbine and carbide cutters. This approach maintained all of the advantages (good hole shape, adaptability to incremental drilling, etc.) of the specially-dressed end mill, while demonstrating some very desirable additional features. Materials difficult to machine, such as 304 Stainless Steel, can be tested in an acceptable stress-free manner using the high speed air turbine/carbide cutter combination. Further, the high speed approach is essentially free of operator dependency and is generally more convenient to use than the earlier end mill procedure. Figure 9c shows the air turbine/carbide cutter assembly in the same basic RS-200 Milling Guide. Carbide cutters are not effective in penetrating glass, most ceramics, very hard metals, etc.; however, diamond cutters have shown promise, and additional investigative efforts continue.

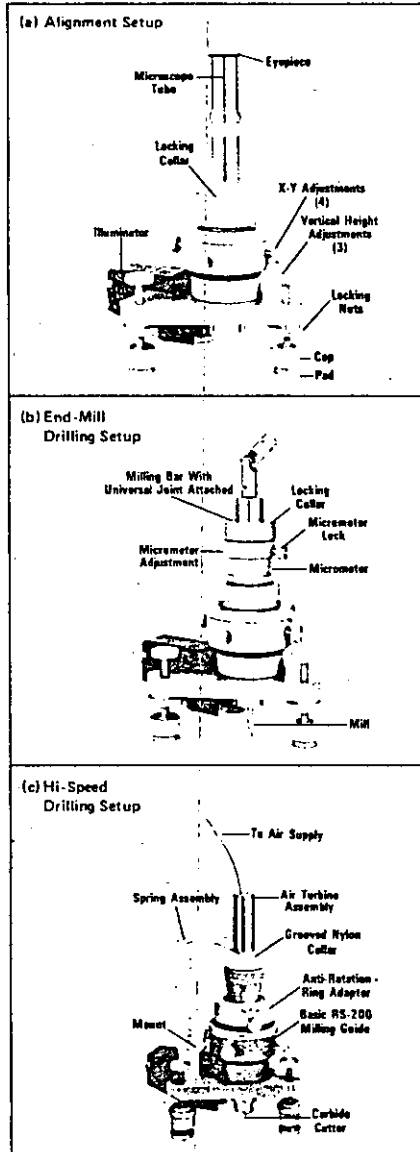


Fig. 9 - RS-200 Milling Guide used for machining a precisely located flat-bottomed hole

Bush and Kromer,¹² in 1972, reported that stress-free holes are achieved using abrasive jet machining (AJM). Modifications and adjustments to AJM were made by other investigators,^{11,13} and Wnuk¹³ experienced good results by physically adapting AJM apparatus to his RS-200 Milling Guide. The chief advantage of AJM is its reported ability to generate stress-free holes in virtually all materials. Its chief limitations center about the considerable changes in hole shape as a function of hole depth. The initial shape is saucer-like and the final is cylindrical with slightly rounded corners. During drilling there is also uncertainty of the actual hole depth. These factors make AJM a less practical technique to establish strain versus hole depth data (Fig. 5) as required in ASTM Standard Method E837.³

Mechanical Properties

It is clear from Equations (4) and (5) that the accuracy of residual stress determination is limited by the accuracies of the elastic modulus (E) and the Poisson's ratio (ν). Uncertainties in mechanical properties of $\pm 2\%$ are not at all uncommon in conventional stress analysis; and these uncertainties are common to residual stress analysis as well.

It is reasonable that the stress concentration at the hole can produce localized yielding around the hole. When this occurs, it influences the measured relieved strains and introduces uncertainty in the calculated residual stresses. This effect has been considered both experimentally^{11,15,16} and analytically,^{7,11,16} and there is substantial agreement among the different investigators. That is, errors are negligible when the residual stresses are less than 70% of the yield stress (proportional limit) of the test material. When internal residual stresses equal the yield stress, Proctor and Beany¹¹ and Bynum's¹⁵ experimental studies indicate positive errors of 10% to 30% in the experimentally determined residual stress calculations. These results are applicable to thicker test sections where blind holes are the case. Nickola's¹⁶ experimental studies, for through-holes, also show negligible error when residual stresses are less than 70% of the proportional limit. However, these data suggest measurably greater errors when residual stresses equal the yield stress. The data also show a definite relationship between error magnitude and the shape of the post-yield (or plastic) portion of the stress-strain diagram. That is, materials approaching the perfect "elastic-plastic" concept have the greater error.

NUMERICAL EXAMPLE OF DATA REDUCTION PROCEDURES*

A Micro-Measurements strain gage rosette, type TEA-06-062RK-120 was applied to a cold-rolled steel bar. Elastic properties of the material are: $E = 29.5 \times 10^6$ psi, and $\nu = 0.29$. With a gage circle diameter of 0.202 in, and a hole diameter of 0.070 in, $D/D_0 = 2.89$.

Using a RS-200 Milling Guide and the High-Speed Accessory, a 0.070 in diameter hole was drilled incrementally to a depth of 0.080 in. The depth and recorded strain data

are shown in the first three columns of Table 1 on page 13. In accordance with the ASTM Standard Method,³ the measured strains at full depth ($Z/D_0 = 1.14$) are used to determine the percent strain relieved. For example, at $Z/D_0 = 1.14$:

$$\left. \begin{aligned} \epsilon_1 &= -152 \mu\epsilon \\ \epsilon_2 &= -42 \mu\epsilon \\ \epsilon_3 &= -85 \mu\epsilon \end{aligned} \right\} \begin{array}{l} \text{Column 3} \\ \text{Table 1} \end{array}$$

and the percent strains relieved at $Z/D_0 = 0.86$ are:

$$\left. \begin{aligned} \epsilon_1 &= \frac{146}{152} \times 100 = 96\% \\ \epsilon_2 &= \frac{40}{42} \times 100 = 95\% \\ \epsilon_3 &= \frac{79}{75} \times 100 = 93\% \end{aligned} \right\} \begin{array}{l} \text{Column 4} \\ \text{Table 1} \end{array}$$

these and all other percent relieved strains are tabulated in Column 4 of Table 1 on page 13. The ASTM Standard Method³ suggests that percent strain be plotted versus hole depth (Z/D_0) and compared with the strain response curve for uniform stress (no stress gradient with depth below the surface). Rosette element number 1 experienced the largest released strain and its response is shown in Fig. 10 where it can be compared with the responses for uniform stress cases. For this example, $D/D_0 = 2.89$ and the test values may be compared with the $D/D_0 = 3.0$ curve. The experimental values are seen to lie well above the $D/D_0 = 3.0$ curve and indicate the presence of a stress gradient with hole depth.

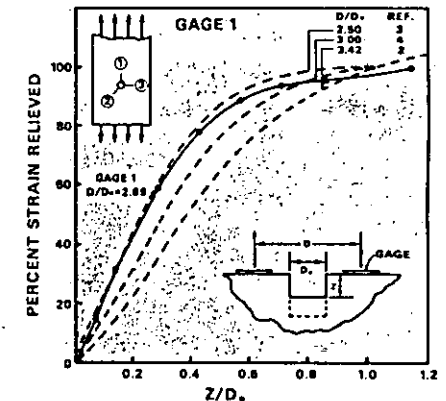


Fig. 10 - Percent Strain relieved compared to response from uniform stress field

* Uniaxial stress test case.

* For greater clarity in the presentation of this example, numerical values are given in U. S. customary units only. The procedure is, of course, unaffected by the units used.

In the following, for demonstration purposes, the average residual stress will first be calculated, using only the maximum measured strains at full hole depth (0.080 in. or 2.0 mm). This corresponds to complete stress relief, if the assumption is made that the stress is uniform with depth. Then, as a comparison, the residual stress will be calculated from incremental strain measurements. This latter exercise will underscore the fact that when the plotted curve for cumulative strain relieved differs noticeably from the standard curve in Fig. 10, the stress state is also markedly different from that calculated using only the maximum strain at full hole depth.

ASSUMED UNIFORM RESIDUAL STRESS

The experimental parameters at full depth $Z/D_0 = 1.14$ are:

$$\begin{aligned} \epsilon_1 &= -152 \mu\epsilon; E = 29.5(10)^6 \text{ psi} \\ \epsilon_2 &= -42 \mu\epsilon; \nu = 0.29 \\ \epsilon_3 &= -85 \mu\epsilon; D/D_0 = 2.89 \end{aligned}$$

From the strain gage package Engineering Data Sheet:

$$\bar{a} = 0.155 \text{ and } \bar{b} = 0.370$$

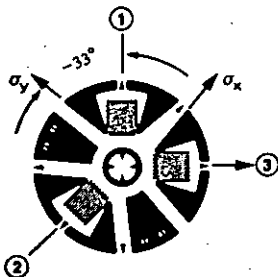
Using Eqs. (5):

$$4\bar{A} = -4 \times \frac{1+\nu}{2E} \times \bar{a}; 4\bar{B} = -4 \times \frac{1}{2E} \times \bar{b}$$

$$4\bar{A} = -1.36(10)^{-8} \text{ psi}^{-1}; 4\bar{B} = -2.50(10)^{-8} \text{ psi}^{-1}$$

Substituting $4\bar{A}$, $4\bar{B}$, and the three measured strains into Eqs. (4) yield:

$$\begin{aligned} \beta_y &= -33^\circ \\ \alpha_x &= +11 \text{ KSI} \\ \alpha_y &= +24 \text{ KSI} \end{aligned}$$



Residual Stress Approximation Via Incremental Drilling

Schajer's finite element studies⁸ of the uniform stress field (no gradient in the Z direction) offer useful understanding of coefficients \bar{a} and \bar{b} as functions of hole depth. Figure 11 shows these relations, as determined from Schajer's work, where coefficients \bar{a} and \bar{b} are plotted versus Z/D_0 for different values of D/D_0 . These graphs can be used to gain a much improved understanding of stress gradients as a function of hole depth.

For this example, values of Z/D_0 have been tabulated (Column 2 of Table 1, on page 13) for each increment of depth (Z), and it is already established that $D/D_0 = 2.89$. This value of D/D_0 (2.89) does not appear on Fig. 11, however, reasonable estimates can be made by interpolation. Consider the first depth increment where $Z/D_0 = 0.07$:

- Enter the Z/D_0 axis of Fig. 11 at 0.07 and project vertical past the 2.9 curve.
- $D/D_0 = 2.89$ would be only slightly above the 2.9 curve.
- Estimate values of \bar{a} and \bar{b} as:

$$\bar{a} = 0.016$$

$$\bar{b} = 0.031$$

and record these values in the spaces provided in Columns 5 and 6 of Table 1.

- Use Eqs. (5) to determine $4\bar{A}$ and $4\bar{B}$:

$$\bar{A} = -\frac{1+\nu}{2E} \times \bar{a}; \bar{B} = -\frac{1}{2E} \times \bar{b}$$

$$\bar{A} = -0.035(10)^{-8} \text{ psi}^{-1}; \bar{B} = -0.052(10)^{-8} \text{ psi}^{-1}$$

$$4\bar{A} = -0.140(10)^{-8} \text{ psi}^{-1}; 4\bar{B} = -0.210(10)^{-8} \text{ psi}^{-1}$$

and record these values in the spaces provided in Columns 5 and 6 of Table 1.

Continue the above procedure until $4\bar{A}$ and $4\bar{B}$ are established for other Z/D_0 increments. The direction (β) and principal stress magnitudes are determined, for each increment, using Eqs. (4):

$$\sigma_{x,y} = \frac{\epsilon_1 + \epsilon_3}{4\bar{A}} \pm \frac{\sqrt{2}}{4\bar{B}} \sqrt{(\epsilon_1 - \epsilon_2)^2 + (\epsilon_2 - \epsilon_3)^2}$$

$$\tan 2\beta = \frac{\epsilon_1 - 2\epsilon_2 + \epsilon_3}{\epsilon_3 - \epsilon_1}$$

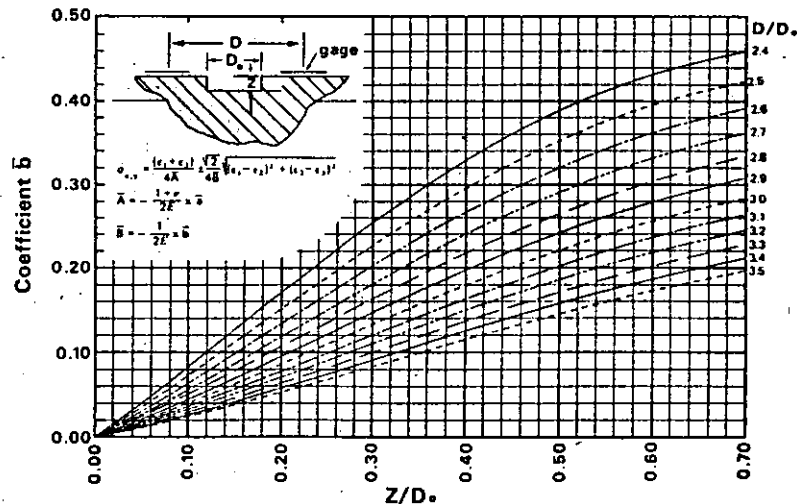
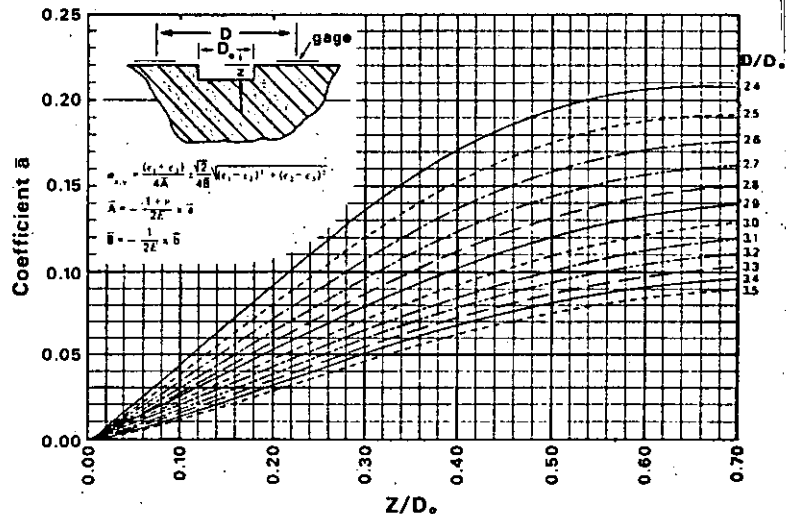


Fig. 11 - Data Reduction Coefficients \bar{a} and \bar{b} as a Function of Hole Depth for RE and RK Rosettes. Developed from Schajer, G.S., "Application of Finite Element Calculations to Residual Stress Measurements," *Journal of Engineering Materials and Technology*, Vol. 103(1981), pp. 157-163.

and are tabulated in Columns 7, 8, and 9 of Table 1*. It is important to recognize that these calculated values represent the *average* stress values between the top surface and the depth (Z). For example:

- | Between | Average Stress | |
|------------------------------------|----------------|------------|
| | σ_x | σ_y |
| (1) 0 and 0.005 in (0.13 mm) . . . | +16 KSI | +36 KSI |
| (2) 0 and 0.010 in (0.25 mm) . . . | +15 KSI | +34 KSI |
| (3) 0 and 0.020 in (0.51 mm) . . . | +12 KSI | +31 KSI |
| etc. . . | | |

Figure 12 shows the average stresses plotted versus depth. Note that the *average stresses* are plotted at the *mid points* of their respective increments. It can be seen from the foregoing that the average surface residual stresses are about 50 percent greater than those calculated from the maximum measured strains at the full hole depth. This example illustrates the necessity for incremental drilling (with proper hole geometry) when residual stresses near the surface are important—as they usually are.

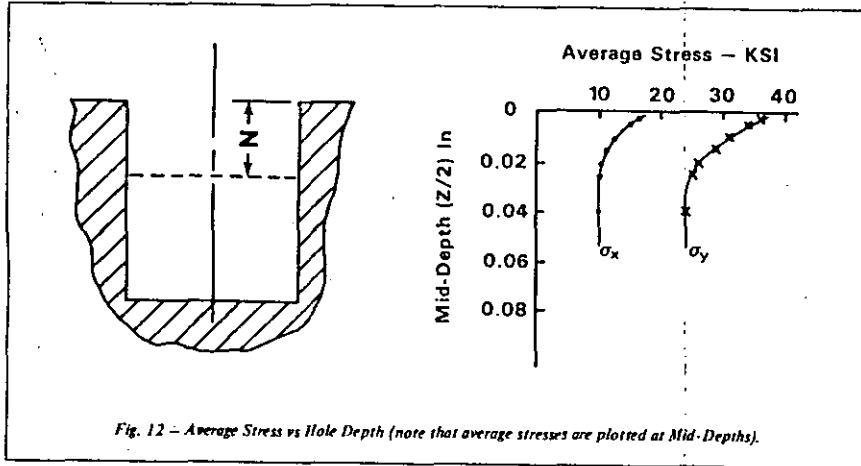
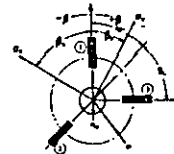


Fig. 12 - Average Stress vs Hole Depth (note that average stresses are plotted at Mid-Depths).

*For the convenience of the RS-200 user, a blank copy of the form for Table 1 is reproduced on page 14. The form can be copied for use in recording measured and calculated data during residual stress testing.

TABLE 1

DEPTH	Z	Z/D _o	MEASURED STRAIN $\mu\epsilon$	PERCENT STRAIN RELIEVED	COEFFICIENTS Exponent of (10) ⁻⁸ with \bar{A} and \bar{B}			β_y	σ_x KSI	σ_y KSI
					\bar{a}	\bar{b}	$4\bar{B}$			
0	0	0	ϵ_1 0	0	\bar{a} —	\bar{b} —	$4\bar{B}$ —	—	—	—
			ϵ_2 0	0	\bar{A} —	\bar{B} —	$4\bar{B}$ —			
			ϵ_3 0	0	$4\bar{A}$ —	$4\bar{B}$ —	$4\bar{B}$ —			
0.005	0.07	0.07	ϵ_1 -23	15	\bar{a} 0.016	\bar{b} 0.031	$4\bar{B}$ -0.210	-32°	+16	+36
			ϵ_2 -9	21	\bar{A} -0.035	\bar{B} -0.052	$4\bar{B}$ -0.210			
			ϵ_3 -14	16	$4\bar{A}$ -0.140	$4\bar{B}$ -0.210	$4\bar{B}$ -0.210			
0.010	0.14	0.14	ϵ_1 -49	32	\bar{a} 0.037	\bar{b} 0.067	$4\bar{B}$ -0.453	-32°	+15	+34
			ϵ_2 -21	50	\bar{A} -0.081	\bar{B} -0.113	$4\bar{B}$ -0.453			
			ϵ_3 -31	36	$4\bar{A}$ -0.324	$4\bar{B}$ -0.453	$4\bar{B}$ -0.453			
0.020	0.29	0.29	ϵ_1 -90	59	\bar{a} 0.077	\bar{b} 0.147	$4\bar{B}$ -0.994	-34°	+12	+31
			ϵ_2 -30	71	\bar{A} -0.169	\bar{B} -0.248	$4\bar{B}$ -0.994			
			ϵ_3 -55	65	$4\bar{A}$ -0.675	$4\bar{B}$ -0.994	$4\bar{B}$ -0.994			
0.030	0.43	0.43	ϵ_1 -118	78	\bar{a} 0.109	\bar{b} 0.215	$4\bar{B}$ -1.453	-34°	+11	+29
			ϵ_2 -33	79	\bar{A} -0.228	\bar{B} -0.363	$4\bar{B}$ -1.453			
			ϵ_3 -68	80	$4\bar{A}$ -0.911	$4\bar{B}$ -1.453	$4\bar{B}$ -1.453			
0.040	0.57	0.57	ϵ_1 -136	89	\bar{a} 0.131	\bar{b} 0.271	$4\bar{B}$ -1.832	-33°	+10	+26
			ϵ_2 -36	86	\bar{A} -0.287	\bar{B} -0.458	$4\bar{B}$ -1.832			
			ϵ_3 -73	86	$4\bar{A}$ -1.148	$4\bar{B}$ -1.832	$4\bar{B}$ -1.832			
0.050	0.71	0.71	ϵ_1 -143	94	\bar{a} 0.142	\bar{b} 0.315	$4\bar{B}$ -2.129	-32°	+10	+25
			ϵ_2 -38	90	\bar{A} -0.311	\bar{B} -0.532	$4\bar{B}$ -2.129			
			ϵ_3 -78	89	$4\bar{A}$ -1.244	$4\bar{B}$ -2.129	$4\bar{B}$ -2.129			
0.060	0.88	0.88	ϵ_1 -146	96	\bar{a} —	\bar{b} —	$4\bar{B}$ —	Beyond Range of Fig. 11	—	—
			ϵ_2 -40	95	\bar{A} —	\bar{B} —	$4\bar{B}$ —			
			ϵ_3 -79	93	$4\bar{A}$ —	$4\bar{B}$ —	$4\bar{B}$ —			
.080	1.14	1.14	ϵ_1 -152	100	\bar{a} 0.155	\bar{b} 0.370	$4\bar{B}$ -2.501	-33°	+11	+24
			ϵ_2 -42	100	\bar{A} -0.339	\bar{B} -0.625	$4\bar{B}$ -2.501			
			ϵ_3 -85	100	$4\bar{A}$ -1.358	$4\bar{B}$ -2.501	$4\bar{B}$ -2.501			
			ϵ_1 —		\bar{a} —	\bar{b} —	$4\bar{B}$ —			
			ϵ_2 —		\bar{A} —	\bar{B} —	$4\bar{B}$ —			
			ϵ_3 —		$4\bar{A}$ —	$4\bar{B}$ —	$4\bar{B}$ —			
1	2		3	4	5	6	7	8	9	



$D_o = 0.070$; $E = 29.5$;
 $D/D_o = 2.89$; $\nu = 0.29$;
 $\frac{1+\nu}{2E} = 2.19 (10)^{-8}$

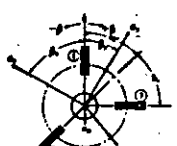
$\frac{1}{2E} = 1.69 (10)^{-8}$
 Material: Cold Rolled Steel

MEASUREMENTS GROUP RS-200 DATA FORM

REFERENCES

DEPTH		MEASURED STRAIN $\mu\epsilon$	PERCENT STRAIN RELIEVED	COEFFICIENTS Exponent of $(10)^{-6}$ with A and B		β	σ_x KSI	σ_y KSI
Z	Z/D ₀			\bar{a}	\bar{b}			
		ϵ_1		\bar{a}	\bar{b}			
		ϵ_2		\bar{A}	\bar{B}			
		ϵ_3		4 \bar{A}	4 \bar{B}			
		ϵ_1		\bar{a}	\bar{b}			
		ϵ_2		\bar{A}	\bar{B}			
		ϵ_3		4 \bar{A}	4 \bar{B}			
		ϵ_1		\bar{a}	\bar{b}			
		ϵ_2		\bar{A}	\bar{B}			
		ϵ_3		4 \bar{A}	4 \bar{B}			
		ϵ_1		\bar{a}	\bar{b}			
		ϵ_2		\bar{A}	\bar{B}			
		ϵ_3		4 \bar{A}	4 \bar{B}			
		ϵ_1		\bar{a}	\bar{b}			
		ϵ_2		\bar{A}	\bar{B}			
		ϵ_3		4 \bar{A}	4 \bar{B}			
		ϵ_1		\bar{a}	\bar{b}			
		ϵ_2		\bar{A}	\bar{B}			
		ϵ_3		4 \bar{A}	4 \bar{B}			
		ϵ_1		\bar{a}	\bar{b}			
		ϵ_2		\bar{A}	\bar{B}			
		ϵ_3		4 \bar{A}	4 \bar{B}			
		ϵ_1		\bar{a}	\bar{b}			
		ϵ_2		\bar{A}	\bar{B}			
		ϵ_3		4 \bar{A}	4 \bar{B}			

- Mathar, J., "Determination of Initial Stresses by Measuring the Deformation Around Drilled Holes." *Trans. ASME* 56, No. 4: 249-254 (1934).
- Rendler, N.J. and I. Vigness, "Hole-drilling Strain-gage Method of Measuring Residual Stresses." *Proc. SESA XXIII*, No. 2: 577-586 (1966).
- Kelsey, R.A., "Measuring Non-uniform Residual Stresses by the Hole-drilling Method." *Proc. SESA XIV*, No. 1: 181-194 (1956).
- Bathgate, R.G., "Measurement of Non-uniform Bi-axial Residual Stresses by the Hole drilling Method." *Strain, Journal of BSSM*, 4, No. 2: 20-29 (1968).
- "Determining Residual Stresses by the Hole-drilling Strain-Gage Method." ASTM Standard E837.
- Birley, S.S. and A. Owens, "Blind Hole Drilling Technique for Residual Stress Measurement: Application in NDT." *NDT International*, pp. 3-9 (February 1980).
- Scaramangas, A.A., R.F.D. Porter Goff, and R.H. Leggatt, "On the Correction of Residual Stress Measurements Obtained Using the Centre-hole Method." *Strain, Journal of BSSM*, 18, No. 3: 88-97 (1982).
- Schajer, G.S., "Application of Finite Element Calculations to Residual Stress Measurements." *Journal of Engineering Materials and Technology* 103: 157-163 (1981).
- Redner, S. and C.C. Perry, "Factors Affecting the Accuracy of Residual Stress Measurements Using the Blind-Hole Drilling Method." *Proc., 7th International Conference on Experimental Stress Analysis*. Haifa, Israel: Israel Institute of Technology, 1982.
- Sandifer, J.P. and G.E. Bowie, "Residual Stress by Blind-hole Method with Off-Center Hole." *Experimental Mechanics* 18: 173-179 (May 1978).
- Procter, E. and E.M. Beaney, "Recent Developments in Centre-hole Technique for Residual-stress Measurement." *Experimental Techniques* 6: 10-15 (December 1982).
- Bush, A.J. and F.J. Kromer, "Simplification of the Hole-drilling Method of Residual Stress Measurements." *Trans. ISA* 112, No. 3: 249-260 (1973).
- Flaman, M.T., "Brief Investigation of Induced Drilling Stresses in the Center-hole Method of Residual-stress Measurement." *Experimental Mechanics* 22: 26-30 (January 1982).
- Wnuk, S.P., "Residual Stress Measurements in the Field Using the Airbrasive Hole Drilling Method." Presented at the Technical Committee for Strain Gages, Spring Meeting of SESA, Dearborn, Michigan, June, 1981.
- Bynum, J.E., "Modifications to the Hole-drilling Technique of Measuring Residual Stresses for Improved Accuracy and Reproducibility." *Experimental Mechanics* 21: 21-33 (January 1981).
- Delameter, W.R. and T.C. Mamaros, "Measurement of Residual Stresses by the Hole-drilling Method." *Sandia National Laboratories Report SAND-77-8006* (1977), 27 pp. (NTIS).
- Nawwar, A.M., K. McLachlan and J. Shewchuk, "A Modified Hole-drilling Technique for Determining Residual Stresses in Thin Plates." *Experimental Mechanics* 16: 226-232 (June 1976).
- Nickola, W.E., "Post-Yield Effects on Center Hole Residual Stress Measurements." *Proc. 5th International Congress on Experimental Mechanics*, pp. 126-136. Brookfield Center, Connecticut: Society for Experimental Mechanics, 1984.
- Ajovalasit, A., "Measurement of Residual Stresses by the Hole-Drilling Method: Influence of Hole Eccentricity." *Journal of Strain Analysis* 14, No. 4: 171-178 (1979).
- Beaney, E.M. and E. Procter, "A Critical Evaluation of the Centre-hole Technique for the Measurement of Residual Stresses." *Strain, Journal of BSSM* 10, No. 1: 7-14 (1974).
- Nickola, W.E., "Weld Induced Residual Stress Measurements via the Hole-Drilling Strain Gage Method." Presented at the Winter Annual Meeting, ASME, New Orleans, Louisiana, December 9-14, 1984.
- Witt, F., F. Lee, and W. Rider, "A Comparison of Residual Stress Measurements Using Blind-hole Drill, Abrasive Jet Trepan Ring." *Experimental Techniques* 7: 41-45 (February 1983).



$D_0 =$ _____ $E =$ _____
 $D/D_0 =$ _____ $\nu =$ _____ $\frac{1}{2E} =$ _____ $(10)^{-6}$
 $\frac{1+\nu}{2E} =$ _____ $(10)^{-6}$ Material: _____



Fatigue Characteristics of Micro-Measurements Strain Gages

All metals are subject to fatigue damage when strained cyclically at sufficiently high amplitudes; and the foils used in strain gages are no exception. Fatigue damage in a strain gage is first evidenced as a permanent change in unstrained resistance of the gage, ordinarily expressed in terms of equivalent indicated strain, and referred to as "zero-shift". As damage increases in strain gages, cracks eventually begin to develop and these can result in data that is seriously in error.

Micro-Measurements monitors three parameters of strain gages during fatigue life testing: "super-sensitivity", gage factor change, and zero-shift. Super-sensitivity results from cracks that are just forming, and that are open only during the tension portion of the loading cycle. If output of a strain gage is monitored continuously on an oscilloscope during a fatigue test, the waveform observed for an undamaged gage will be a sine wave. As cracking starts, the sine wave will distort during the tension portion of the cycle. Monitoring for onset of cracking is necessary because, at zero load, cracks often close and their presence can be hidden. Experimental stress analysts who unexpectedly encounter large strain signals from strain gages in cyclic applications should check signal waveform for any indications of super-sensitivity.

Fatigue damage in strain gages can also cause gage factor changes, although substantial differences are rare. If cracking has started, however, it will cause an apparent increase in tension gage factor, easily detected because the compression value will be much lower.

Procedures for fatigue testing of Micro-Measurements gages start with the very best installations that can be made (see Appendix A). No strain gage application requirement is more demanding than cyclic endurance. Micro-Measurements uses NAS-942 test rigs with modified beams to achieve strain levels of different magnitudes*. Zero of each gage is recorded

*The NAS-942 beam is designed for constant stress, producing a single $\pm 1500\mu\epsilon$ strain level.

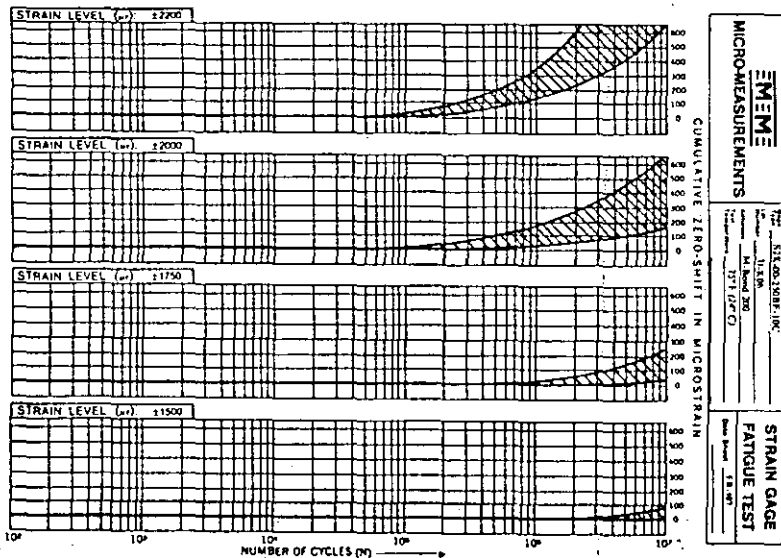
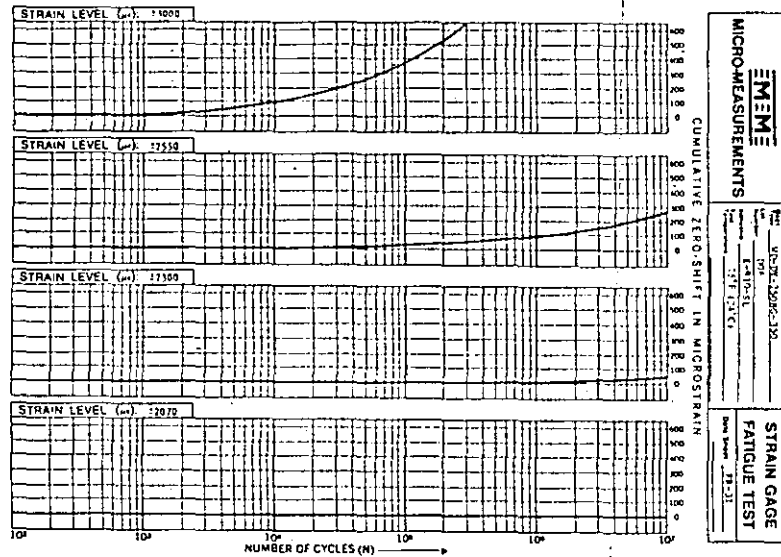
along with output for both tension and compression static strains of the same magnitude as will be encountered during cycling. Throughout dynamic loading, gage outputs are monitored for super-sensitivity.

Strain gages can be considered to "fail" over a wide range of damage levels, depending on the application and the required accuracy. For example, in static-dynamic strain measurement, varying with the particular situation, there is some level of damage at which zero-shifts may impair the utility of strain gages for that application. Such zero-shifts thus represent "failure" under those conditions, even though the strain gages could still endure many thousands or millions of additional cycles before fatigue cracks became evident. On the other hand, for purely dynamic strain measurement, zero-shift is relatively incidental, and strain gages can be considered functionally adequate until fatigue damage has progressed almost to the stage of super-sensitivity.

Normal behavior of strain gages is illustrated by the graphs in Fig. 1 (on page 2), data from WK-05-250BG-350 gages. Note that as the strain level is reduced, and life extended, spread in data increases markedly. Prediction of gage life in high cycle fatigue (over 5×10^5 cycles) is difficult because test data displays large variations. Using the data in Fig. 1, a nominal fatigue life curve can be drawn for WK-05-250BG-350 gages as shown in Fig. 2 (on page 2), based on a $100\mu\epsilon$ zero-shift failure criterion. Other typical data are shown in Appendix B.

Table 1 (on page 3) is a summary of the fatigue characteristics of Micro-Measurements strain gages. "Fatigue Life" in the table generally refers to the approximate number of cycles at which a zero-shift of $100\mu\epsilon$ can be expected. W1) gages, normally used only for dynamic testing, have values for a $300\mu\epsilon$ zero-shift (approximately).

The data in Table 1 and graphs of Appendix B were obtained using 1/4-in (6.4-mm) gage length strain gages. Gage selection is an important criterion in achieving maximum cyclic life and many different parameters affect the



MEASUREMENTS GROUP, INC.
 P.O. Box 27777
 Raleigh, North Carolina 27611, USA
 (919) 345-3000
 Telex 802-542
 FAX (919) 345-3045

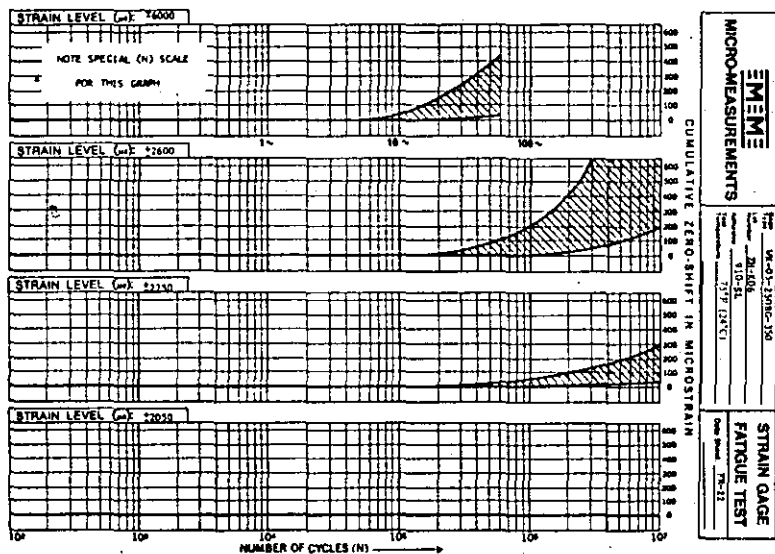


Fig. 1 — Strain Gage Fatigue Test Results.

endurance of strain gages. A study of Table I will provide information on how the different series (backing/alloy combinations) relate to each other in fatigue life. In addition, a number of other criteria have marked effects and each compromise made deteriorates life to some degree. While there are many aspects to selection of appropriate gages for any application, there are some general "rules" concerning what will improve or deteriorate fatigue life. (Refer to Measurements Group Tech Note TN-505, *Strain Gage Selection Criteria, Procedures, Recommendations.*) The larger the grid area of a foil strain gage, the higher its fatigue life, but the higher the gage's resistance, the lower its fatigue life. Encapsulation (such as 'E' or 'SE' on E-backed gages) is helpful while solder and copper have a negative affect; so CEA gages or gages with Options L, LE, or W on EA gages should be used with caution. Some very small Micro-Measurements gages, and some very high resistance gages, are made using ultra-thin foil. These gages should be avoided where cyclic endurance is important. While such gages can't be identified from catalogs, estimated fatigue life for any of our gages can be obtained from the Measurements Group Applications Engineering Department.

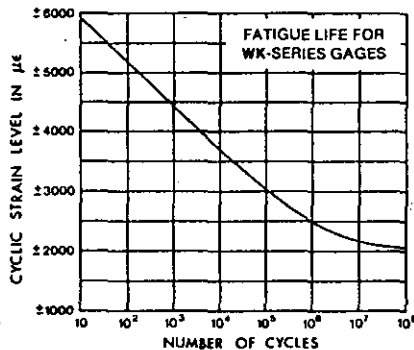


Fig. 2 — Average Cyclic Endurance of WK Strain Gages.

Table I

Nominal Fatigue Life — 100 $\mu\epsilon$ Zero-Shift					
M-M Gage Series	Strain Level, $\mu\epsilon$	Number of Cycles	M-M Gage Series	Strain Level, $\mu\epsilon$	Number of Cycles
CEA	± 1500	10^1	SA	± 1800	10^6
	± 1300	10^6		± 1500	10^7
EA	± 1500	10^4	SK	± 2200	10^6
	± 1200	10^6		± 2000	10^7
ED	± 2500	10^6	S2K	± 1800	10^6
	± 2200	10^7		± 1500	10^7
EK	± 1800	10^7	SD	± 2500	10^6
	± 1500	10^8		± 2200	10^6
EP	± 1500	10^2	TA	± 1700	10^6
	± 1000	10^4		± 1500	10^7
J2A	± 1700	10^6	TK	± 2200	10^7
	± 1500	10^7		± 2000	10^8
J5K	± 2000	10^1	TD	± 2400	10^7
	± 1800	10^6			
N2A	± 1700	10^6	WA	± 1800	10^6
	± 1500	10^7		± 1500	10^7
N2K	± 1800	10^7	WK	± 2400	10^6
	± 1500	10^8		± 2200	10^7
N3K	± 1500	10^8	WD	± 3000	10^{2*}
				± 2500	10^{3*}

*300 $\mu\epsilon$ zero-shift (approximately) for WD strain gages.

The above fatigue life data is based on fully reversed strain levels. As a generalized approximation, this table can be used for unidirectional strains, or various mean-strains, by taking the indicated peak-to-peak amplitude and derating by 10 percent. As an example, $\pm 1500\mu\epsilon$ would be approximately equivalent in gage fatigue damage to strain levels of

$$+2700 \begin{matrix} 2700 \\ 0 \end{matrix} \mu\epsilon, \quad \text{or} \quad 0 \begin{matrix} 0 \\ -2700 \end{matrix} \mu\epsilon, \quad \text{or} \quad +2500 \begin{matrix} 2500 \\ -200 \end{matrix} \mu\epsilon.$$

A mean-strain which increases in a tensile direction during cycling will lead to much earlier failure, however.

REFERENCE

"Strain Gages, Bonded Resistance"; Classification Specification NAS-942 (National Aerospace Standard 942) 1963. Aerospace Industries Association of America, Inc. Published by National Standards Association, Inc., 1315 Fourteenth Street, N.W., Washington, D.C., 20005 U.S.A.

APPENDIX A

Installation Recommendations for Maximum Strain Gage Fatigue Life

When designing structures for maximum fatigue endurance, special care should be employed to avoid rapid changes in section, stress concentrations, and excess inertial loading, to name a few considerations. When stress concentrations are unavoidable, they should be in a minimum strain field. The same considerations apply to strain gage installations in a fatigue environment.

Ideally, bonding agents used to adhere gages should be unfilled, thin-film-setting adhesives such as M-Bond 200, M-Bond 600 or 610, or M-Bond AE-10/15. All excess adhesive around the edge of gages should be removed to prevent this unnecessarily thick film of cement from cracking and initiating failure of the gage bond.

Solder connections present the greatest stress concentrations at the gage location, and solder is poor in fatigue, and therefore must be applied sparingly. Controlling solder flow on gage tabs can be accomplished by carefully masking the tab with drafting tape. The masked area should expose only a section of the tab slightly wider than the leadwire diameter. An alternative for limiting solder flow is selection of gages with solder dots and encapsulation. EA gages with Option SE, and SA/SK-Series gages provide very controlled solder masses for leadwire attachment. (Refer to Measurements Group Tech Tip TT-606, *Soldering Techniques for Lead Attachment to Strain Gages with Solder Dots*.) Also, specialty soft solders such as 50-50% Tin-Indium* alloy minimize stress concentration factors at the solder/tab interface, and will maximize the fatigue life of any user-soldered gage installation. Data presented in this Tech Note for gages without leads was obtained using 63-36.7-0.3% Lead-Tin-Antimony alloy solder (Micro-Measurements Type 361A-20R). This solder is recommended for its ease of use and minimum shrinkage.

All heavy instrument leadwires must be soldered to intermediate terminal strips; terminal strips and gages should be interconnected with small diameter wires. Proper handling procedures for using terminal strips are described in Measurements Group Tech Tip TT-603, *The Proper Use of Bondable Terminals in Strain Gage Applications*. Any leadwires located in high strain fields should not be rigidly constrained because cyclic stress will fail soft copper wires well before gages fail; a flexible restraint should be provided to prevent peeling leadwires and gage tabs from the gage backing. If the strain field at gage locations has been defined, it is good practice to route leads onto solder tabs in the minimum strain direction. After soldering the leads, a flexible restraint should be positioned on them as close as possible to the gage backing. This restraint may be a piece of drafting or aluminum tape (FA-2), a small drop of adhesive such as M-Bond AE-10, or a protective coating like M-Coat J or JL.

The WK and WD Series, with preattached beryllium copper leads, exhibit the highest fatigue life of any Micro-Measurements strain gages. When using WK- or WD-Series strain gages in a cyclic strain field, refer to Measurements Group Tech Tip TT-604, *Leadwire Attachment Techniques for Obtaining Maximum Fatigue Life of Strain Gages*, for

the recommended method of leadwire attachment. An EA gage with Option LE should not be used in a fatigue environment.

Most fatigue failures in the strain gage occur in the solder tab and transition area — the area between the tab and the outer gridline. When the strain field has been predefined, it is good practice to position the gage tabs in the lowest possible strain area.

CEA gages may require special attention, although CEA installations can have the same life as reported for an open-faced EA gage if each installation is carefully made. But some characteristics which make CEA gages so convenient for static test must be carefully managed when maximum fatigue life is required. The large, soft-copper-coated tabs, bonded in the strain field, are subject to cracking at lower cycles than the high endurance A-foil beneath. The act of tinning the tabs can affect the ultimate life of the installations, because adding solder to tin the copper coating introduces additional loading on the tabs.

The natural tendency, when presented with the large copper tabs of the CEA, is to apply solder to the whole tab. This markedly deteriorates the fatigue life. When cyclic loads are applied to the structure, copper, having lower strength than the A-foil, begins to crack. These cracks effectively create notch stress concentrations at the copper and foil interface. Such a concentrated strain at the interface causes the foil to fail prematurely. Solder has greater stiffness and even poorer fatigue endurance than copper; hence, the notch concentration effect will propagate to earlier failure of the whole installation. The CEA has a soft encapsulating layer and where this encapsulant ends, a natural solder stop exists. Adding solder fully to this encapsulant concentrates the structure's strain directly onto the softer copper coating assuring failure at the encapsulant/solder/copper interface. By placing a minimum amount of solder in only the bottom one-third of the CEA tab area, cyclic life may be markedly improved.

Such solder control may be achieved by masking the solder location with a piece of drafting tape in the lower one-third tab area. Then apply a second piece of drafting tape below the first piece making a gap about the diameter of the solder wire. This exposes a sufficient area of the tab copper for tinning and ultimately lead attachment.

Available solders have a variety of characteristics. While melt temperatures are most familiar, solders also vary in their stiffness, shrinkage and their resistance to cyclic loads. The higher the melt temperature, the greater the solder's stiffness and shrinkage. Eutectic solders, regardless of composition, provide for the best cyclic endurance for that composition. The solders listed in Micro-Measurements Catalog A-110 are all eutectic or nearly eutectic, and may be selected based on a given fatigue test's thermal conditions. When the test is to be run below +350°F (+177°C), 361A-20R offers the least stiffness and shrinkage. With lower stiffness, less stress concentration occurs at the solder/copper interface; and, the less shrinkage a solder has, the lower the peel stress that is imposed on the tab during solder solidification. When the maximum fatigue life of a CEA installation is required,

INDALLOY® 50/50 Tin-Indium solder should be used. This is a very soft solder which melts at +242°F (+117°C) and has very low stiffness and shrinkage. The solder requires some practice to apply as its wetting and flow characteristics are poor.

Regardless of the solder chosen, apply only a minimum amount of solder to tin the exposed tab area between the pieces of drafting tape.

When the soldering iron is too hot, tabs may become separated from the backing. Soldering iron temperature should be controlled, and only as high as necessary to melt the solder. If an auxiliary flux is necessary, such as when solid solder wire is used, use the flux sparingly. Auxiliary fluxes contain volatile solvents which also contribute to tabs lifting. Dip the solder wire into the flux, allow the excess to drain a few seconds, then wipe the wire on the exposed

copper to put a thin film of flux across the tab area. Lay the solder wire on the exposed copper, then firmly press a temperature-adjusted soldering iron onto the solder wire. Lift both the iron and solder wire as soon as the solder wire melts. If the tab tinning was not complete, repeat the operation until the exposed tab is tinned.

Gage to terminal wiring may use either solid copper or stranded leads, and should not be larger than 34-AWG. Solid wires are insulated with various varnishes. Stranded leads are available with Teflon® insulations. Support all leads as close to the solder connection as practicable. This prevents inertial loads from peeling the gage tabs from the gage backing. Micro-Measurements Catalog A-110 lists both types of wires which can be chosen for the intrabridge connections.

®Registered Trademark of DuPont.

®Registered Trademark of Indium Corporation of America.

*Indium solders, available from Indium Company of America, are difficult to apply and expensive.

Temperature-Induced Apparent Strain and Gage Factor Variation in Strain Gages

1.0 INTRODUCTION

Ideally, a strain gage bonded to a test part would respond only to the applied strain in the part, and be unaffected by other variables in the environment. Unfortunately, the resistance strain gage, in common with all other sensors, is somewhat less than perfect. The electrical resistance of the strain gage varies not only with strain, but with temperature as well. In addition, the relationship between strain and resistance change, the *gage factor*, itself varies with temperature. These deviations from ideal behavior can be important under certain circumstances, and can cause significant errors if not properly accounted for. When the underlying phenomena are thoroughly understood, however, the errors can be controlled or virtually eliminated by compensation or correction.

In Section 2.0 of this Tech Note, apparent strain is defined, and the causes of this effect are described. Typical apparent strain magnitudes as functions of temperature are then given, followed by the commonly used methods for compensation and correction. Section 3.0 treats gage factor variations with temperature in a similar but briefer manner since this error source is generally much less significant. Methods for the simultaneous correction of both apparent strain and gage factor errors are given in Section 4.0, accompanied by numerical examples.

2.0 APPARENT STRAIN

Once an installed strain gage is connected to a strain indicator and the instrument balanced, a subsequent change in the temperature of the gage installation will generally produce a resistance change in the gage. Because this purely temperature-induced resistance change will be registered by the strain indicator as strain, the indication is referred to (in the United States) as *apparent strain* to distinguish it from strain in the test part due to applied stress.

The apparent strain caused by temperature change is potentially the most serious error source in the practice of static strain measurement with strain gages. In fact, when measuring strains at temperatures remote from room temperature, the error due to apparent strain, if not controlled, can be much greater than the magnitude of the strain to be measured. At any temperature, or in any temperature range, this error source requires careful consideration; and it is usually necessary to either provide compensation for apparent strain or make a correction for it.

Apparent strain is caused by two concurrent and algebraically additive effects in the strain gage installation. First, the electrical resistivity of the grid conductor is temperature dependent, and any resistance change with temperature due to this effect appears as strain to a strain indicator. The second contribution to apparent strain is caused by the differential thermal expansion between the grid conductor and the test part or substrate material to which the gage is bonded. With temperature change, the substrate expands or contracts; and, since the strain gage is firmly bonded to the substrate, the gage grid is forced to undergo the same expansion or contraction. To the extent that the thermal expansion coefficient of the grid differs from that of the substrate, the grid is mechanically strained in conforming to the free expansion or contraction of the substrate. Since the grid is, by design, strain sensitive, the resultant resistance change appears to the strain indicator as strain in the substrate.

The net temperature-induced apparent strain can be expressed as the sum of the resistivity and differential expansion effects:

$$\epsilon_{APP(G/S)} = \left[\frac{\rho_G}{F} + (\alpha_S - \alpha_G) \right] \Delta T \quad (1)$$

where, in consistent units:

$\epsilon_{APP(G/S)}$ = apparent strain of grid material *G*
on substrate material *S*

ρ_G = thermal coefficient of resistance of
grid conductor

F = gage factor

$(\alpha_S - \alpha_G)$ = difference in thermal expansion coefficients between substrate and grid, respectively

ΔT = temperature change from arbitrary
initial reference temperature

It should not be assumed from the form of Eq. (1) that the apparent strain is linear with temperature, because all of the coefficients within the brackets are themselves functions of temperature. The equation clearly demonstrates, however, that the apparent strain exhibited with temperature change depends not only upon the nature of the strain gage, but also upon the material to which the gage is bonded. Because of this, apparent strain data are meaningful only when referred to a particular grid alloy bonded to a specified substrate material.

supply used to power the strain gage bridge. In both cases, the nonlinearity errors are identical if the amplifiers have high input impedances, and if the power supplies are of the constant-voltage type. Note also that in both circuits the "balance" control is used only to establish initial bridge balance before the gages are strained, and that the balance controls do not form part of the readout circuit. This type of "balance" circuit is normally provided with a very limited range so as not to cause problems in resolution and setting-stability; and therefore does not greatly influence the nonlinearity errors as described in this Tech Note. To permit a rigorous treatment of the errors without introducing other considerations, it is assumed throughout the following discussion that the "balance" circuit is either completely disconnected, or that the control is left at the midpoint of its range. It is also assumed that the bridge arms are nominally resistively symmetrical about an axis joining the output corners of the bridge; i.e. that $(R_1/R_2)_{nom} = 1 = (R_3/R_4)_{nom}$.

As a result of the circuit arrangements described above, obtaining a reading from the static strain indicator (whether or not the process involves nulling a meter) has no effect on the state of resistive balance within the Wheatstone bridge circuit. Even if the Wheatstone bridge is initially balanced resistively so that $R_1/R_2 = R_3/R_4$, this will no longer be

true, in general, when one or more of the strain gages in the bridge arms are strained. Consequently, the Wheatstone bridge is ordinarily operated in a resistively unbalanced state. In this mode of operation, resistance changes in the bridge arms may cause changes in the currents through the arms, depending upon the signs and magnitudes of the resistance changes in all four arms. When current changes occur, the voltage output of the bridge is not proportional to the resistance changes, and thus the output is nonlinear with strain, and the instrument indication is in error.

III. Error Magnitudes and Corrections

Table I gives, for the class of instruments described in Section II, the output voltage as a function of the applied strain for a variety of cases, representing different strain states and different arrangements of gages on the structural member and within the Wheatstone bridge. While the magnitudes of the nonlinearities are difficult to judge from the table, it can be seen from the column of bridge and strain arrangements that only when the resistance changes are such that the currents in the bridge arms remain constant—that is, when $\Delta R_1/R_1 + \Delta R_2/R_2 = 0$ and $\Delta R_3/R_3 + \Delta R_4/R_4 = 0$ (the third, sixth, and seventh cases)—is the output a linear function of the strain. The table also includes, for each

case, the ratio of the actual strain (ϵ) to the indicated strain ($\hat{\epsilon}$), permitting correction of indicated strains with these formulas in the nonlinear cases.

The first case in Table I is applicable whenever a single active strain gage is used in a quarter-bridge arrangement; and occurs very commonly in the practice of strain measurement for experimental stress analysis purposes. Because of its basic importance, this case will later be used in several numerical examples to demonstrate the procedure for making nonlinearity corrections. The character of the nonlinearity associated with the quarter-bridge arrangement can be illustrated by writing the bridge output equation in the following form:

$$\frac{E_o}{E} = \frac{F\epsilon \times 10^{-3}}{4} \left(\frac{2}{2 + F\epsilon \times 10^{-6}} \right) \quad (1)$$

where:

E_o/E = dimensionless bridge output, mV/V

E_o = output voltage, mV

E = bridge supply voltage, V

F = gage factor of strain gage

ϵ = strain, $\mu\epsilon$ (microstrain)

In Eq. (1), the term in parentheses represents the nonlinearity. It is evident from the form of the nonlinearity term that its magnitude will be less than unity for tensile strains and greater than unity for compressive strains. And the errors in strain indication due to the nonlinearity will correspond. In other words, indicated tensile strains will be too small and indicated compressive strains too large. For subsequent convenience, the incremental nonlinearity error, or correction, (n), is defined as the amount which must be added algebraically to the indicated strain to obtain the actual strain. That is,

$$\epsilon = \hat{\epsilon} + n \quad (2)$$

where:

ϵ = actual strain causing a resistance change in one arm of the Wheatstone bridge, $\mu\epsilon$

$\hat{\epsilon}$ = indicated strain (corresponding to ϵ) as read from a strain indicator with the specifications given in Fig. 1, $\mu\epsilon$

n = incremental error in indicated strain, $\mu\epsilon$

For the single active gage in a quarter-bridge arrangement, it can be shown that the incremental error (in $\mu\epsilon$) is represented by the following expression:

$$n = \frac{F(\hat{\epsilon})^2 \times 10^{-6}}{2 - F\hat{\epsilon} \times 10^{-6}} \quad (3)$$

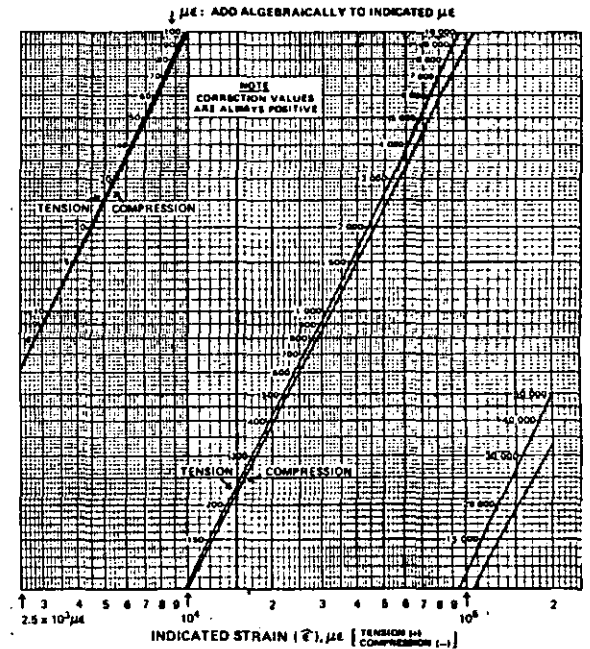


Figure 2

Equation (3) has been plotted in Figure 2 (for $F = 2.0$) to illustrate the magnitude of the error and to permit making corrections simply and accurately. To use the graph, enter the abscissa at the value of the indicated strain, project vertically to the proper curve for tensile or compressive strain, then read the value of the correction from the scale provided adjacent to the curves. The correction (which, from Eq. (3), always has a positive sign, irrespective of the sign of the indicated strain) is to be added algebraically to the indicated strain. That is, the magnitude of an indicated tensile strain is always increased by adding the correction, while that of a compressive strain is always reduced.

IV. Numerical Examples

As a first example, assume that the Wheatstone bridge was initially balanced resistively, after which the gaged test member was loaded until the strain indicator registered 15 000 $\mu\epsilon$ in tension. Entering the graph along the abscissa at 15 000 $\mu\epsilon$, and projecting upward to the "Tension" line, yields the correction as 230 $\mu\epsilon$. The actual strain is thus 15 230 $\mu\epsilon$. By following directions given in the "Comments" column and in the footnotes of Table I, Figure 2 can be used to correct any of the nonlinear cases listed in the table (when $F = 2.0$). For other gage factors in the vicinity of 2.0, the correction obtained from Figure 2 can be multiplied

Table I

BRIDGE/STRAIN ARRANGEMENT (Note 1)	DESCRIPTION	OUTPUT EQUATION— E_o/E IN mV/V (Notes 2, 3)	ACTUAL STRAIN INDICATED STRAIN = $\frac{\epsilon}{\hat{\epsilon}}$	COMMENTS
	Single active gage in uniaxial tension or compression.	$\frac{E_o}{E} = \frac{F\epsilon \times 10^{-3}}{4 + 2F\epsilon \times 10^{-6}}$	$\frac{\epsilon}{\hat{\epsilon}} = 1 + \frac{F\epsilon \times 10^{-6}}{2 - F\epsilon \times 10^{-6}}$	Nonlinear. Incremental correction can be read directly from Fig. 2.
	Two active gages in uniaxial stress field—one aligned with max. principal strain, one "Poisson" gage.	$\frac{E_o}{E} = \frac{F\epsilon(1+\nu) \times 10^{-3}}{4 + 2F\epsilon(1-\nu) \times 10^{-6}}$	$\frac{\epsilon}{\hat{\epsilon}} = 1 + \frac{F\epsilon(1-\nu) \times 10^{-6}}{2 - F\epsilon(1-\nu) \times 10^{-6}}$	Nonlinear. Apply incremental correction from Fig. 2, using indicated strain equal to $\hat{\epsilon}(1-\nu)$. (Note 4)
	Two active gages with equal & opposite strains—typical of bending beam arrangement.	$\frac{E_o}{E} = \frac{F\epsilon}{2} \times 10^{-3}$	$\frac{\epsilon}{\hat{\epsilon}} = 1$	Linear.
	Two active gages with equal strains of same sign—used on opposite sides of column with low temperature gradient (bending cancellation, for instance).	$\frac{E_o}{E} = \frac{F\epsilon \times 10^{-3}}{2 + F\epsilon \times 10^{-6}}$	$\frac{\epsilon}{\hat{\epsilon}} = 1 + \frac{F\epsilon \times 10^{-6}}{2 - F\epsilon \times 10^{-6}}$	Nonlinear. Incremental correction can be read directly from Fig. 2.
	Four active gages in uniaxial stress field—two aligned with max. principal strain, two "Poisson" gages (column).	$\frac{E_o}{E} = \frac{F\epsilon(1+\nu) \times 10^{-3}}{2 + F\epsilon(1-\nu) \times 10^{-6}}$	$\frac{\epsilon}{\hat{\epsilon}} = 1 + \frac{F\epsilon(1-\nu) \times 10^{-6}}{2 - F\epsilon(1-\nu) \times 10^{-6}}$	Nonlinear. Apply incremental correction from Fig. 2, using indicated strain equal to $\hat{\epsilon}(1-\nu)$. (Note 5)
	Four active gages in uniaxial stress field—two aligned with max. principal strain, two "Poisson" gages (beam).	$\frac{E_o}{E} = \frac{F\epsilon(1+\nu) \times 10^{-3}}{2}$	$\frac{\epsilon}{\hat{\epsilon}} = 1$	Linear.
	Four active gages with pairs subjected to equal and opposite strains (beam in bending or shaft in torsion).	$\frac{E_o}{E} = F\epsilon \times 10^{-3}$	$\frac{\epsilon}{\hat{\epsilon}} = 1$	Linear.

NOTES: 1. $(R_1/R_2)_{nom} = 1; (R_3/R_4)_{nom} = 1$ when two or less active arms are used.
 2. Constant voltage power supply is assumed.
 3. ϵ and $\hat{\epsilon}$ (strain) are expressed in microstrain units (10^{-6}).
 4. With the gage factor dial of the strain indicator set to the gage factor of the gages in use, the indicator will read the quantity: $\hat{\epsilon}(1+\nu)$. Multiply this by $(1-\nu)/(1+\nu)$ to obtain $\hat{\epsilon}(1-\nu)$. Enter Fig. 2 at $\hat{\epsilon}(1-\nu)$ on the abscissa and read the incremental correction from the appropriate curve. Add the correction (always a positive number) algebraically to $\hat{\epsilon}(1-\nu)$ and divide the result by $(1-\nu)$ to obtain the actual strain, ϵ .
 5. With the gage factor dial of the strain indicator set to the gage factor of the gages in use, the indicator will read the quantity: $2\hat{\epsilon}(1+\nu)$. Multiply this by $(1-\nu)/(1+\nu)$ to obtain $\hat{\epsilon}(1-\nu)$. Proceed as in Note 4 to complete the correction.

Figure 1 shows the variation of apparent strain with temperature for a variety of strain gage alloys bonded to steel. These data are illustrative only, and not for use in making corrections. It should be noted, in fact, that the curves for constantan and Karma are for non-self-temperature-compensated alloys. With self-temperature compensation (Section 2.1.2), as employed in Micro-Measurements strain gages, the apparent strain characteristics of these alloys are adjusted to minimize the error over the normal range of working temperatures.

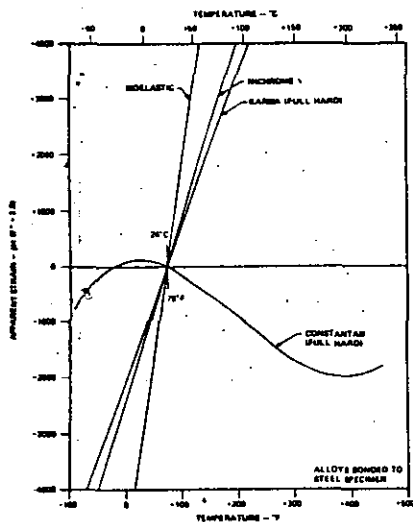


FIG. 1

As indicated by Fig. 1, the errors due to apparent strain can become extremely large as temperatures deviate from the arbitrary reference temperature (ordinarily, room temperature) with respect to which the apparent strain is measured. The illustration shows distinctly the necessity for compensation or correction if accurate static strain measurements are to be made in an environment involving temperature changes.

With respect to the latter statement, it should be remarked that if it is feasible to bring the gaged test part to the test temperature in the test environment, maintaining the test part completely free of mechanically or thermally induced stresses, and balance the strain indicator for zero strain under these conditions, no apparent strain error exists when subsequent strain measurements are made at this temperature. In other words, when no temperature change occurs between the stress-free and stressed conditions, strain measurements can be made without compensating or correcting for apparent strain. In practice, however, it is rare that the foregoing requirements can be satisfied, and the stress analyst ordinarily finds it necessary to take full account of apparent strain effects.

Also, in the case of purely dynamic strain measurements, where there is no need to maintain a stable zero-strain reference, temperature-induced apparent strain may be of no consequence. This is because the frequency of the dynamic strain signal is usually very high with respect to the frequency of temperature change, and the two signals are readily separable. If, however, there is combined static/dynamic strain, and the static component must also be measured, or if the frequency of temperature change is of the same order as the strain frequency, apparent strain effects must again be considered.

2.1 Compensation for Apparent Strain

2.1.1 Compensating (Dummy) Gage

In theory, at least, the error due to apparent strain can be completely eliminated by employing, in conjunction with the "active" strain gage, but connected in an adjacent arm of the Wheatstone bridge circuit, an identical compensating or "dummy" gage—mounted on an unstrained specimen made from the identical material as the test part, and subjected always to the same temperature as the active gage. Under these hypothetical conditions, the apparent strains manifested by the two gages should be identical. And, since identical resistance changes in adjacent arms of the Wheatstone bridge do not unbalance the circuit, the apparent strains in the active and dummy strain gages should cancel exactly—leaving only the stress-induced strain in the active strain gage to be registered by the strain indicator. For this to be precisely true requires additionally that the leadwires to the active and dummy gages be the same length and be routed together so that their temperature changes identically.

The principal problems encountered in this method of temperature compensation are those of establishing and maintaining the three sets of identical conditions postulated above. To begin with, it is sometimes very difficult to arrange for the placement of an unstrained specimen of the test material in the test environment; and even more difficult to make certain that the specimen remains unstrained under all test conditions. There is a further difficulty in ensuring that the temperature of the compensating gage on the unstrained specimen is always identical to the temperature of the active gage. This problem becomes particularly severe whenever there are temperature gradients or transients in the test environment. And, as indicated in the preceding paragraph, the same considerations apply to the leadwires. Finally, it must be recognized that no two strain gages—even from the same lot or package—are precisely identical. For most static strain measurement tasks in the general neighborhood of room temperature, the difference in apparent strain between two gages from the same lot is negligible; but the difference may become evident (and significant) when measuring strains at temperature extremes such as those involved in high-temperature or cryogenic work. In these instances, point-by-point correction for apparent strain will usually be necessary. With non-self-temperature-compensated gages, the gage-to-gage differences in apparent strain may be so great as to preclude dummy compensation for temperatures which are remote from room temperature.

In general, when the three identity criteria already mentioned can be well satisfied, the method of compensating with a dummy gage is a very effective technique for controlling the apparent strain error. There is, moreover, a special class of strain measurement applications which is particularly adaptable to compensation of apparent strain with a second

gage. This class consists of those applications in which the ratio of the strains at two different but closely adjacent (or at least thermally adjacent) points on the test object are known a priori. Included in this class are bars in torsion, beams in bending, columns, diaphragms, etc., all stressed within their respective proportional limits. In these applications, the compensating gage can often be located strategically on the test member itself so as to provide two active gages which undergo the same temperature variations while sensing strains that are preferably opposite in sign and of known ratio. The two gages in adjacent arms of the Wheatstone bridge circuit then function as an active half-bridge.

For example, when strain measurements are to be made on a beam which is thin enough so that under test conditions the temperatures on the two opposite surfaces normal to the plane of bending are the same, the two strain gages can be installed directly opposite each other on these surfaces (Fig. 2a). The active half-bridge thus formed will give effective temperature compensation over a reasonable range of temperatures and, since the strains sensed by the gages are equal in magnitude and opposite in sign, will double the output signal from the Wheatstone bridge. Similarly, for a bar in torsion (Fig. 2b), the two gages can be installed adjacent to each other and aligned along the principal axes of the bar (at 45 deg to the longitudinal axis). As in the case of the beam, excellent temperature compensation can be achieved, along with a doubled output signal.

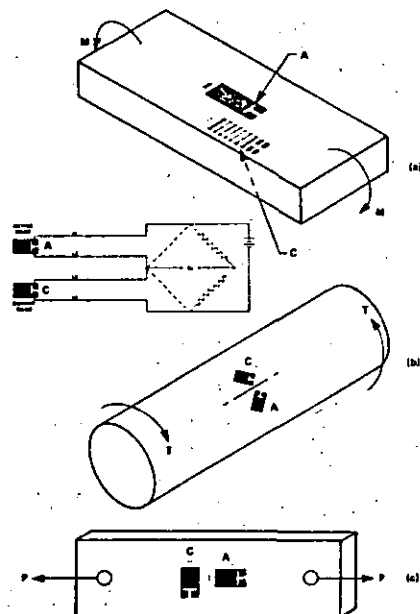


FIG. 2

When making strain measurements along the axis of a column or tension link, the compensating gage can be mounted on the test member adjacent to the axial gage and

aligned transversely to the longitudinal axis to sense the Poisson strain (Fig. 2c). The result, again, is compensation of the apparent strain, accompanied by an augmented output signal [by the factor $(1 + \nu)$ in this case]. It should be borne in mind in this application, however, that the accuracy of the strain measurement is somewhat dependent upon the accuracy with which the Poisson's ratio of the test material is known. For most common structural materials, the percent error in strain measurement is about one-fourth the percent error in Poisson's ratio. A further caution is necessary when strain gages are mounted transversely on small-diameter rods (or, for that matter, in small-radius fillets or holes). Hines has shown (see Appendix) that under these conditions the apparent strain characteristics of a strain gage are different than when the gage is mounted on a flat surface of the same material.

In all strain-measurement applications which involve mounting the compensating gage on the test object itself, the relationship between the strains at the two locations must be known with certainty. In a beam, for example, there must be no indeterminate axial or torsional loading; and the bar in torsion must not be subject to indeterminate axial or bending loads. This requirement for a priori knowledge of the strain distribution actually places these and most similar applications in the class of transducers. And the same method of compensation is universally employed in commercial strain gage transducers. Such transducers, however, ordinarily employ full-bridge circuits and special arrangements of the strain gages to eliminate the effects of extraneous forces or moments.

2.1.2 Self-Temperature-Compensated Strain Gages

The metallurgical properties of certain strain gage alloys—in particular, constantan and modified Karma (Micro-Measurements A- and K-alloys, respectively)—are such that these alloys can be processed to minimize the apparent strain over a wide temperature range when bonded to test materials with thermal expansion coefficients for which they are intended. Strain gages employing these specially processed alloys are referred to as self-temperature-compensated.

Since the advent of the self-temperature-compensated strain gage, the requirement for a matching unstrained dummy gage in the adjacent arm of the Wheatstone bridge has been relaxed considerably. It is now normal practice when making strain measurements at or near room temperature to use a single self-temperature-compensated gage in a quarter-bridge arrangement, completing the bridge circuit with a stable fixed resistor in the adjacent arm (Fig. 3). Such "bridge-completion" resistors, with temperature coefficients of resistance not exceeding 1×10^{-6} per °C, are supplied by Micro-Measurements and are incorporated in most modern strain indicators.

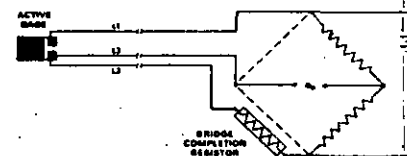


FIG. 3

Figure 4 illustrates the apparent strain characteristics of typical A- and K-alloy self-temperature-compensated strain gages. As demonstrated by the figure, the gages are designed to minimize the apparent strain over the temperature range from about 0°F to +400°F (-20°C to +203°C). When the self-temperature-compensated strain gage is bonded to a material having the thermal expansion coefficient for which the gage is intended, and when operated within the temperature range of effective compensation, strain measurements can usually be made without the necessity of correcting for apparent strain. If correction for apparent strain is needed, it can be made as shown in the following sections.

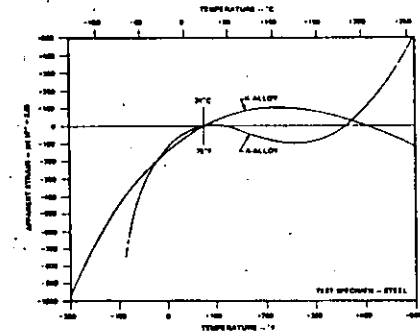


FIG. 4

Self-temperature-compensated strain gages can also be used in the manner described in Section 2.1.1. That is, when circumstances are such that a pair of matched gages can be used in adjacent arms of the bridge circuit, with both gages maintained at the same temperature, and with one of the gages unstrained (or strained at a determinate ratio to the other gage), excellent temperature compensation can be achieved over a wide temperature range.

The designations of Micro-Measurements self-temperature-compensated strain gages include a two-digit S-T-C number identifying the nominal thermal expansion coefficient (in PPM/°F) of the material on which the gage will exhibit optimum apparent strain characteristics as shown in Fig. 4. Micro-Measurements A-alloy is available in the following S-T-C numbers: 00, 03, 05, 06, 09, 13, 15, 18, 30 and 35. The very large S-T-C numbers, 30 and 35, are intended primarily for plastics. In K-alloy, the range of S-T-C numbers is more limited, and consists of 00, 03, 05, 06, 09, 13, and 15. For reference convenience, Table 1 lists a number of common materials, and gives the Fahrenheit and Celsius expansion coefficients for each, along with the recommended S-T-C number.

If a strain gage with a particular S-T-C number is installed on a material with a nonmatching coefficient of expansion, the apparent strain characteristics will be altered from those shown in Fig. 4 by a general rotation of the curve about the room-temperature reference point (see Section 2.2.5). When the S-T-C number is lower than the material expansion coefficient, the rotation is counterclockwise; and

when higher, clockwise. Rotation of the apparent strain curve by intentionally mismatching the S-T-C number and expansion coefficient can be used to bias the apparent strain characteristics so as to favor a particular working temperature range.

TABLE 1
Thermal Expansion Coefficients
of Common Materials

Material	Expansion Coefficient		Recommended S-T-C Number
	Per °F	Per °C	
ALUMINA, FIRED	3.0 x 10 ⁻⁶	5.4 x 10 ⁻⁶	03
ALUMINUM, 2024-T4*, 7075-T6	12.8	23.2	13*
BERYLLIUM	6.4	11.5	08
BERYLLIUM COPPER 25	9.3	16.7	09
BRASS, 30-70	11.1	20.0	13
BRONZE, PHOSPHOR (10%)	10.2	18.4	09
COPPER	9.3	16.7	09
GLASS, SODA LIME	5.1	9.2	05
INCONEL WROUGHT	7.0	12.6	06
INCONEL X	6.7	12.1	06
INVAR	0.8	1.4	00
IRON, GRAY CAST	6.0	10.8	06
MAGNESIUM, AZ-31B*	14.5	26.1	15*
MOLYBDENUM*	2.2	4.0	00*
MONEL	7.5	13.6	06
NICKEL A	6.6	11.9	06
QUARTZ, FUSED	0.28	0.8	00
STEEL, 1008, 1018*	6.7	12.1	06*
STEEL, 4340	6.3	11.3	06
STEEL, 17-4 PH	6.0	10.8	06
STEEL, 17-7	5.7	10.3	06
STEEL, 15-7 MO. PH	5.0	9.0	05
STEEL, 304 STAINLESS*	9.8	17.3	09*
STEEL, 310 STAINLESS	8.0	14.4	09
STEEL, 316 STAINLESS	8.9	16.0	09
STEEL, 410 STAINLESS	5.9	9.9	05
TIN, PURE	13.0	23.4	13
TITANIUM, PURE*	4.8	8.6	06*
TITANIUM*, 6AL-4V	4.9	8.8	06*
TITANIUM*, SILICATE	0.017	0.00	00*
TUNGSTEN	2.4	4.3	03
ZIRCONIUM	2.1	3.8	03

*Indicates type of material used in determining apparent strain curves.

2.2 Correction for Apparent Strain

Depending upon the test temperature and the degree of accuracy required in the strain measurement, it will sometimes be necessary to make corrections for apparent strain, even though self-temperature-compensated gages are used.

2.2.1 Simple Procedure

Correction for apparent strain can be accomplished most directly and easily using the technical data sheet found in each package of self-temperature-compensated Micro-Measurements strain gages. Figure 5 is a typical graph of apparent strain data (for A-alloy) as supplied with the gages.

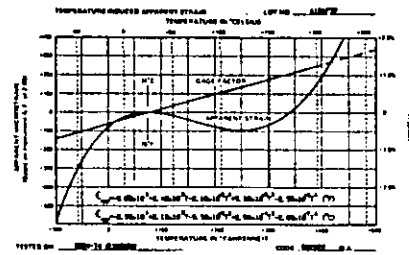


FIG. 5

The first step in the correction procedure is to refer to the graph and read the apparent strain corresponding to the test temperature. Then, assuming that the strain indicator was balanced for zero strain at room temperature (the reference temperature with respect to which the apparent strain data were measured), subtract the apparent strain given on the graph from the strain measurement at the test temperature, carrying all signs. This procedure can be expressed analytically as follows:

$$\epsilon = \epsilon' - \epsilon_{APP} \quad (2)$$

where: ϵ' = uncorrected strain measurement as registered by the strain indicator

ϵ = partially corrected strain indication—that is, corrected for apparent strain, but not for gage factor variation with temperature (see Sections 3.0 and 4.0)

ϵ_{APP} = apparent strain, from the package technical data sheet

As an example, assume that, with the test part under no load and at room temperature, the strain indicator was balanced for zero strain. At the test temperature of +200°F (+93°C), the indicated strain is +2300 $\mu\epsilon$. Referring to Fig. 5, assuming that this graph was the one in the gage package, the apparent strain at test temperature is -100 $\mu\epsilon$. From Eq. (2), the corrected strain is thus 2300 - (-100) = 2400 $\mu\epsilon$. Had the indicated strain been negative, the corrected strain would be: -2300 - (-100) = -2200 $\mu\epsilon$.

2.2.2 Adjusting Apparent Strain for Gage Factor

It should be noted that the gage factor employed in obtaining the apparent strain data is standardized at 2.0 for all Micro-Measurements A- and K-alloy strain gages. An

improvement in the accuracy of the correction can be made by adjusting the apparent strain data to the gage factor of the gage as given on the technical data sheet. This is done as follows:

$$\epsilon_{APP} = \epsilon_{APP} \frac{2.0}{F} \quad (3)$$

where: ϵ_{APP} = apparent strain data adjusted for room-temperature gage factor

ϵ_{APP} = apparent strain from data sheet (gage factor = 2.0)

F = room-temperature gage factor of strain gage in use

Continuing the example, and assuming that the data sheet gives a room-temperature gage factor of 2.10 for the gage, the adjusted apparent strain is calculated from Eq. (3):

$$\epsilon_{APP} = -100 \frac{2.0}{2.1} = -95$$

And the corrected strain measurements become:

$$2300 - (-95) = 2395 \mu\epsilon$$

and,

$$-2300 - (-95) = -2205 \mu\epsilon$$

A further improvement in the accuracy of the apparent strain correction can be obtained by accounting for the fact that the test-temperature gage factor is slightly different from the room-temperature value, as described in Section 3.0 (see also Fig. 5). This effect can easily be introduced by first correcting the room-temperature gage factor to the test temperature in the manner shown in Section 3.1. The test-temperature gage factor is then substituted for F in Eq. (3) to obtain the gage-factor-adjusted apparent strain, which is subtracted algebraically from the indicated strain, as in Eq. (2), to obtain the corrected strain measurement.

2.2.3 Extensive Data Acquisition

If desired, for extensive strain measurement programs, the apparent strain curve in Fig. 5 can be replotted with the gage factor adjustment—either room-temperature or test-temperature—already incorporated. Upon completion, the apparent strain read from the replotted curve can be used directly to correct the indicated strain. This procedure may be found worth the effort if many strain readings are to be taken with one gage or a group of gages from the same lot.

For convenience in computerized correction for apparent strain, Micro-Measurements supplies, for each lot of A-alloy and K-alloy gages, a regression-fitted (least squares) polynomial equation representing the apparent-strain curve for that lot. The polynomial is of the following form:

$$\epsilon_{APP} = A_0 + A_1 T + A_2 T^2 + A_3 T^3 + A_4 T^4 \quad (4)$$

where: T = Temperature

If not included directly on the graph, as shown in Fig. 5, the coefficients A_1 for Eq. (4) can be obtained from Micro-Measurements on request by specifying the lot number.

It should be borne in mind that the regression-fitted equations, like the data from which they are derived, are based upon a gage factor of 2.0; and apparent-strain values calculated from the equations must be adjusted for gage factor if the added accuracy is needed. And, of course, the apparent-strain data and equations are applicable only to the specified lot of gages, bonded to the same material as used by Micro-Measurements in performing the apparent-strain test.

2.2.4 Accuracy and Practicality — First-Hand Measurement of Apparent Strain

There is a limit as to just how far it is practical to go in adjusting the manufacturer's apparent strain data in an attempt to obtain greater accuracy. In the first place, the apparent strain curve provided on the technical data sheet (or by the polynomial equation) represents an average, since there is some variation in apparent strain characteristics from gage to gage within a lot. And the width of the scatter band increases as the test temperature departs further and further from the room-temperature reference. The spreading of the scatter band is approximately linear with deviation from room temperature, at least over the temperature range from +32°F (0°C) to +350°F (+175°C) for which scatter data are available. At the 2σ (95%) confidence level, the variability for A-alloy can be expressed as ±0.15 με/°F (±0.27 με/°C), and that of K-alloy as ±0.25 με/°F (±0.45 με/°C). Thus, at a test temperature of 275°F (+135°C), the 2σ width of the scatter band is ±30 με for A-alloy, and ±50 με for K-alloy.

Furthermore, the apparent strain data given in the gage package were necessarily measured on a particular lot of a particular material (see Table I). Different materials with the same or closely similar nominal expansion coefficients, and different lots and forms of the same material, have different thermal expansion characteristics.

From the above considerations, it should be evident that in order to achieve the most accurate correction for apparent strains it is generally necessary to obtain the apparent strain data with the actual test gage installed on the actual test part. For this purpose, a thermocouple or resistance-temperature sensor is installed immediately adjacent to the strain gage. The gage is then connected to the strain indicator and, with no loads applied to the test part, the instrument is balanced for zero strain. Subsequently, the test part is subjected to the test temperature(s), again with no loads applied, and the temperature and indicated strain are recorded under equilibrium conditions. If throughout this process, the part is completely free of mechanical and thermal stresses, the resulting strain indication at any temperature is the apparent strain at that temperature. The observed apparent strain should be subtracted algebraically from any subsequent strain measurements at the same temperature to arrive at the corrected strain.

In order to correct for apparent strain in the manner described here, it is necessary, of course, to measure the temperature at the strain gage installation each time a strain measurement is made. The principal disadvantage of this procedure is that two channels of instrumentation are pre-empted for each strain gage — one for the strain gage proper, and one for the thermocouple or resistance temperature sensor.

2.2.5 S-T-C Mismatch

When a strain gage is employed on a material other than that used in obtaining the manufacturer's apparent strain data for that lot of gages, an S-T-C mismatch occurs. In such cases, the apparent strain output of the gage will differ from the curve supplied in the gage package. Consider, for example, strain measurements made at an elevated temperature on Monel with a strain gage of 06 S-T-C number, calibrated for apparent strain on 1018 steel (Table I). The thermal expansion characteristics of Monel are somewhat different from 1018 steel, and the strain gage will produce a correspondingly different apparent strain indication. Thus, if accurate strain measurement is required, the apparent strain characteristics of the gage bonded to Monel must be measured over the test temperature range as described in Section 2.2.4. For small temperature excursions from room

temperature, the effect of the difference in expansion properties between Monel and 1018 steel is not very significant, and would commonly be ignored.

On the other hand, when the difference in thermal expansion properties between the apparent strain calibration material and the material to which the gage is bonded for stress analysis is great, the published apparent strain curve cannot be used directly for making corrections. Examples of this occur in 30 and 35 S-T-C A-alloy strain gages. The principal application of these gages would normally be strain measurement on high-expansion-coefficient plastics. But the thermal (and other) properties of plastics vary significantly from lot to lot and, because of formulation differences, even more seriously from manufacturer to manufacturer of nominally the same plastic. This fact, along with the general instability of plastics properties with time, temperature, humidity, etc., creates a situation in which there are no suitable plastic materials on which to test 30 or 35 S-T-C strain gages for their apparent strain characteristics. As an admittedly less-than-satisfactory alternative, the apparent strain data provided with these gages are measured on 1018 steel specimens because of the stability and repeatability of this material.

As a result of the foregoing, it is always preferable when measuring strains on plastics with 30 or 35 S-T-C gages at other than room temperature to first experimentally determine the apparent strain output of the gages on the test material as described in Section 2.2.4. Using these data, corrections are then made as usual by subtracting algebraically the apparent strain from the measured strain.

As a quick first approximation, the apparent strain characteristics of 30 and 35 S-T-C gages on a plastic or any other material of known coefficient of expansion can be estimated by reversing the clockwise rotation of the apparent strain curve which occurred when measuring the characteristics on a steel specimen. Assume, for example, that strain measurements are to be made on a plastic with a constant expansion coefficient of $35 \times 10^{-6}/°F$ ($81 \times 10^{-6}/°C$) over the test temperature range, and that 1018 steel has a constant coefficient of $6.7 \times 10^{-6}/°F$ ($12.1 \times 10^{-6}/°C$) over the same temperature range. To find the approximate apparent strain characteristics of the 30 S-T-C gage when installed on the plastic instead of the steel, Eq. (1) can be reexpressed as follows:

$$\epsilon_{APP(G/S)} = \left(\frac{BC}{F} - \alpha_G \right) \Delta T + \alpha_S \Delta T \quad (5)$$

(Note: Although the remainder of this example is carried through in only the Fahrenheit system to avoid over-complicating the notation, the same procedure produces the equivalent result in the Celsius system.)

Rewriting Eq. (5) to apply specifically to 6.7 and 45 × 10⁻⁶/°F materials,

$$\epsilon_{APP(G/7)} = \left(\frac{BC}{F} - \alpha_G \right) \Delta T + 6.7 \Delta T \quad \begin{matrix} 30 \text{ S-T-C} \\ \text{gage} \\ \text{installed on} \\ 1018 \text{ steel} \end{matrix} \quad (6a)$$

$$\epsilon_{APP(G/35)} = \left(\frac{BC}{F} - \alpha_G \right) \Delta T + 35 \Delta T \quad \begin{matrix} 30 \text{ S-T-C gage} \\ \text{installed on} \\ 35 \times 10^{-6}/°F \\ \text{plastic} \end{matrix} \quad (6b)$$

Solving Eq. (6a) for $\left(\frac{BC}{F} - \alpha_G \right) \Delta T$, and substituting into Eq. (6b),

$$\epsilon_{APP(G/35)} = \epsilon_{APP(G/7)} + (35 - 6.7) \Delta T \quad (7)$$

In words, Eq. (7) states that the apparent strain curve for the 30 S-T-C gage mounted on 1018 steel can be converted to that for the same gage mounted on a $35 \times 10^{-6}/°F$ plastic by adding to the original curve the product of the difference in expansion coefficients and the temperature deviation from room temperature (always carrying the proper sign for the temperature deviation). Figure 6 shows the apparent strain curve for a 30 S-T-C gage as originally measured on a 1018 steel specimen, and as rotated counterclockwise to approximate the response on a plastic with an expansion coefficient of $35 \times 10^{-6}/°F$.

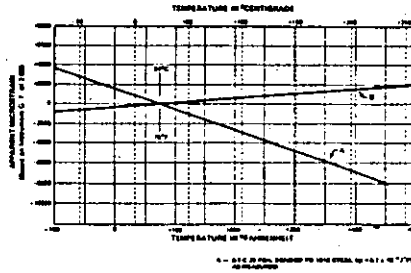


Fig. 6

The procedure just demonstrated is quite general, and can be used to predict the approximate effect of any mismatch between the expansion coefficient used for obtaining the apparent strain curve on the gage package data sheet and the expansion coefficient of some other material on which the gage is to be installed. Although generally applicable, the procedure is also limited in accuracy because the expansion coefficients in Eq. (5) are themselves functions of temperature for most materials. A further limitation in accuracy can occur when measuring strains on plastics or other materials with poor heat transfer characteristics. If, due to self heating, the temperature of the strain gage is significantly higher than that of the test part, the apparent strain data supplied in the gage package cannot be applied meaningfully.

3.0 GAGE FACTOR VARIATION WITH TEMPERATURE

The alloys used in resistance strain gages typically exhibit a change in gage factor with temperature. In some cases, the error due to this effect is small and can be ignored. In others, depending upon the alloy involved, the test temperature, and the required accuracy in strain measurement, correction for the gage factor variation may be necessary.

Figure 7 shows the variation of gage factor with temperature for constantan, Incoelastic, and an iron-chromium-aluminum alloy (Micro-Measurements A-, D-, and C-alloys, respectively). It can be seen from the graph that the effect

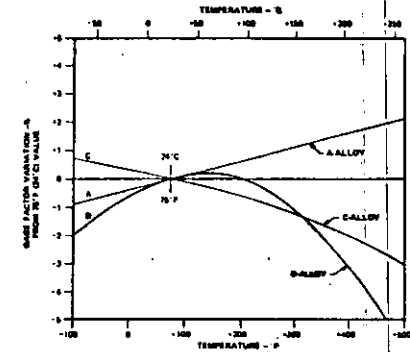


FIG. 7

in the A-alloy is essentially linear, and quite small at any temperature, typically being in the order of 1% or less per 100°F (about 2% per 100°C). Thus, for a temperature range of, say, ±100°F or (±50°C), about room temperature, correction may not be necessary. At more extreme temperatures, when justified by accuracy requirements, the correction can be made as shown in Section 3.1, or combined with the apparent strain correction as in Section 4.0.

The variation of gage factor in the D-alloy, while very modest and flat between room temperature and +200°F (+90°C), steepens noticeably outside of this range. However, even for temperatures where the gage factor deviation is several percent, correction may not be practical. This is because D-alloy is used primarily for purely dynamic strain measurement, under which conditions other errors in the measurement system may greatly overshadow the gage factor effect. The magnitude of the gage factor variation in C-alloy is similar to that of the A-alloy, but the sign of the variation is negative, and the gage factor drops as the temperature rises.

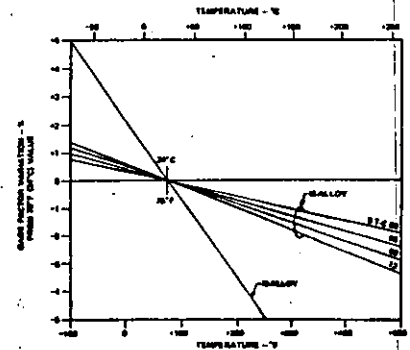


FIG. 8

As shown in Fig. 8, the gage factor variation with temperature for modified Karma (K-alloy) is distinctly different from that of the A- and D-alloys. The gage factor variation is nearly linear with temperature, as it is for A-alloy, but the slope is negative and is a function of the S-T-C number, becoming steeper with higher numbers.

Also shown in Fig. 8 is the gage factor variation with temperature of Micro-Measurements N-alloy (similar to Nichrome V). This alloy is characterized by severe gage factor changes, and correction is necessary for strain measurements made at temperatures more than about 50°F (10°C) from room temperature.

3.1 Correcting Strain Measurements for Gage Factor Variation with Temperature

The standard procedure for measuring the gage factor of a lot of any particular type of strain gage is performed at room temperature. It is this value of the gage factor, along with its tolerance, which is given on the technical data sheet in each package of Micro-Measurements strain gages. Thus, at any temperature other than room temperature the gage factor is different, and a correction may be needed, according to the circumstances. Also given on each data sheet is the applicable graph of gage factor variation with temperature, such as those in Figs. 7 and 8. This information is all that is required to make the correction.

In general, any strain measurement data can be corrected (or adjusted) from one gage factor to another with a very simple relationship. Assume, for instance, that a strain, ϵ_1 , was registered with the gage factor setting of the strain indicator at F_1 , and it is desired to correct the data to a gage factor of F_2 . The corrected strain, ϵ_2 , is calculated from:

$$\epsilon_2 = \epsilon_1 \cdot \frac{F_1}{F_2} \quad (8)$$

When correcting for gage factor variation with temperature, F_1 can be taken as the package-data room-temperature gage factor at which the strain indicator may have been set, and F_2 the gage factor at the test temperature. Of course, when the test temperature is known with reasonable accuracy in advance, the gage factor control of the strain indicator can be set at F_2 initially, and no correction is necessary. Note, however, that if apparent strain corrections are to be made from the graph on the technical data sheet in the gage package, the apparent strain data must be corrected from a gage factor of 2.0 (at which the apparent strain was measured) to the test temperature gage factor, F_1 .

The following relationship is used to determine the gage factor at the test temperature from the tabular and graphical data supplied in the gage package:

$$F_2 = F_1 \left(1 + \frac{\Delta F(\%) }{100} \right) \quad (9)$$

where: $\Delta F(\%)$ = percent variation in gage factor with temperature as shown in Figs. 7 and 8. (Note: the sign of the variation must always be included.)

As a numerical example, using Eqs. (8) and (9), assume that the room-temperature gage factor of a 13 S-T-C K-alloy gage is 2.05 and, with the instrument set at this value, the strain indication at +450°F (+230°C) is 1820 $\mu\epsilon$. Referring to Fig. 8, $\Delta F(\%)$ for this case is -3, and, from Eq. (9),

$$F_2 = 2.05(1 - 0.03) = 1.99$$

Substituting into Eq. (8),

$$\epsilon_2 = 1820 \frac{2.05}{1.99} = 1875 \mu\epsilon$$

Since gage factor variation with temperature affects both the apparent strain and the stress-induced strain, and because confusion may arise in making the corrections individually and then combining them, the following section gives equations for performing both corrections simultaneously.

4.0 SIMULTANEOUS CORRECTION OF APPARENT STRAIN AND GAGE FACTOR ERRORS

Relationships are given in this section for correcting indicated strains for apparent strain and gage factor variation with temperature. The forms these relationships can take depend upon the measuring circumstances—primarily upon the strain indicator gage factor setting and the temperature at which the instrument was balanced for zero strain.

The strain indicator gage factor can be set at any value within its control range, but one of the following three is most likely:

1. Gage factor used by Micro-Measurements ($F^* = 2.0$) in determining apparent strain data
2. Room-temperature gage factor as given on the gage package technical data sheet
3. Gage factor of gage at test temperature or at any arbitrary temperature other than room or test temperature

No single gage factor is uniquely correct for this situation; but, of the foregoing, it will be found that selecting the first alternative generally leads to the simplest form of correction expression. Because of this, the procedure developed here requires that the gage factor of the instrument be set at $F = F^* = 2.0$, the gage factor at which the apparent strain data were recorded.

Similarly, the strain indicator can be balanced for zero strain at any one of several strain gage temperatures:

1. Room temperature
2. Test temperature
3. Arbitrary temperature other than room or test temperature

The second and third of the above choices can be used for meaningful strain measurements only when the test object is known to be completely free of mechanical and thermal stresses at the balancing temperature. Because this requirement is usually difficult or impossible to satisfy, the first alternative is generally preferable, and is thus selected for the following procedure.

As an example, assume that the strain indicator is balanced with the gage at room temperature, and with the gage factor control set at F^* , the value used by Micro-Measurements in recording the apparent strain data. Assume also that a strain ϵ_1 is subsequently indicated at a temperature T_1 which is different from room temperature. The indicated strain ϵ_1 is generally in error due both to temperature-induced apparent strain and to variation of the gage factor with temperature—and hence the double circumflex over the strain symbol.

Consider first the correction for apparent strain. Since the gage factor setting of the strain indicator coincides with that used in measuring the apparent strain, this correction can be made by direct subtraction of the gage package data apparent strain from the indicated strain. That is,

$$\epsilon_1 = \hat{\epsilon}_1 - \epsilon_{APP}(T_1)$$

where: $\hat{\epsilon}_1$ = indicated strain, uncorrected for either apparent strain or gage factor variation with temperature

ϵ_1 = semicorrected strain; i.e., corrected for apparent strain only

$\epsilon_{APP}(T_1)$ = apparent strain at temperature T_1 (functional notation is used to avoid double and triple subscripts)

Next, correction is made for the gage factor variation with temperature. Since the strain measurement was made at a gage factor setting of F^* , the correction to the gage factor at the test temperature is performed with Eq. (8) as follows:

$$\epsilon_1 = \hat{\epsilon}_1 \frac{F^*}{F(T_1)}$$

where: ϵ_1 = strain magnitude corrected for both apparent strain and gage factor variation with temperature

$F(T_1)$ = gage factor at test temperature

Combining the two corrections,

$$\epsilon_1 = [\hat{\epsilon}_1 - \epsilon_{APP}(T_1)] \frac{F^*}{F(T_1)} \quad (10)$$

When the prescribed conditions on the gage factor setting and the zero balance temperature have been met, the strain ϵ_1 from Eq. (10) is the strain induced by mechanical and/or thermal stresses in the test object at the test temperature. As a numerical example of the application of Eq. (10), assume the following:

Strain gage	WK-06-250BG-120
Test material	Steel
†Room-temperature gage factor, F_0	2.07
Test temperature	-50°F (-45°C)
$\hat{\epsilon}_1$, indicated strain at test temperature	-1850 $\mu\epsilon$
† $\epsilon_{APP}(T_1)$, apparent strain at test temperature	-200 $\mu\epsilon$
† $\Delta F(T_1)$, deviation at test temperature from room-temperature gage factor	+0.6%

†From technical data sheet in gage package.

Using Eq. (9) to obtain $F(T_1)$, the gage factor of the gage at test temperature,

$$F(T_1) = F_0 \left(1 + \frac{0.6}{100} \right) = 2.07 \times 1.006$$

$$F(T_1) = 2.08$$

Substituting into Eq. (10), with $F^* = 2.0$,

$$\epsilon_1 = \left[-1850 - (-200) \right] \frac{2.0}{2.08} = -1587 \mu\epsilon$$

For what might appear to be a more complex case, consider a strain-gage-instrumented centrifugal compressor, operating first at speed N_1 , with the temperature of the gage installation at T_1 . Under these conditions, the indicated strain is $\hat{\epsilon}_1$. The compressor speed is then increased to N_2 , with a resulting gage installation temperature of T_2 ; and an indicated strain $\hat{\epsilon}_2$. The engineer wishes to determine the change in stress-induced strain caused by the speed increase from N_1 to N_2 .

This problem is actually no more difficult than the previous example. Applying Eq. (10) to each condition:

$$\epsilon_1 = \left[\hat{\epsilon}_1 - \epsilon_{APP}(T_1) \right] \frac{F^*}{F(T_1)}$$

$$\epsilon_2 = \left[\hat{\epsilon}_2 - \epsilon_{APP}(T_2) \right] \frac{F^*}{F(T_2)}$$

The same numerical substitution procedure is followed as before, and the results subtracted to give $(\epsilon_2 - \epsilon_1)$, the change in stress-induced strain caused by the speed increase. The subtraction can also be done algebraically to yield a single equation for the strain change:

$$\epsilon_2 - \epsilon_1 = F^* \left[\frac{\hat{\epsilon}_2 - \epsilon_{APP}(T_2)}{F_2} - \frac{\hat{\epsilon}_1 - \epsilon_{APP}(T_1)}{F_1} \right] \quad (11)$$

When computerized data reduction is used, analytical expressions for the functions $\epsilon_{APP}(T)$ and $F(T)$ can be introduced into the program to permit direct calculation of corrected strains from indicated strains.

Equations (11), (14), and (15) will now be applied to an example in order to demonstrate the magnitudes of the errors encountered.

Consider first a thin-walled cylindrical pressure vessel. In this case, the hoop stress or circumferential stress is twice the longitudinal stress, and of the same sign.

Thus,

$$\frac{\sigma_p}{\sigma_q} = R_G = 2$$

And Eqs. (11), (14), and (15) become:

$$n_{T_{MAX}} = -(1 - \cos 2\beta) \times 100 \quad (11a)$$

$$n_{\sigma_p} = -1/4 (1 - \cos 2\beta) \times 100 \quad (14a)$$

$$n_{\sigma_q} = 1/2 (1 - \cos 2\beta) \times 100 \quad (15a)$$

Equations (11a), (14a), and (15a) are plotted in Fig. 5. From the figure, it can be seen that the errors introduced by rosette misalignment in this instance are quite small. For example, with a 5° mounting error, T_{MAX} , σ_p , and σ_q are in error by only -1.5%, -0.38%, and 0.75%, respectively.

In order to correct for a known misalignment by reading the value of n from Fig. 5, or any similar graph derived from the basic error equations [Eqs. (7), (9), (11), (14), (15)], it is only necessary to solve Eqs. (6), (8), and (10) for σ_p , σ_q , and T_{MAX} , respectively, and substitute the value of n from Fig. 5, including the sign. That is,

$$\sigma_p = \frac{\hat{\sigma}_p}{1 + \frac{n_{\sigma_p}}{100}} \quad (16)$$

$$\sigma_q = \frac{\hat{\sigma}_q}{1 + \frac{n_{\sigma_q}}{100}} \quad (17)$$

$$T_{MAX} = \frac{\hat{T}_{MAX}}{1 + \frac{n_{T_{MAX}}}{100}} \quad (18)$$

where:

$\hat{\sigma}_p$ = maximum principal stress as calculated from gage readings

$\hat{\sigma}_q$ = minimum principal stress as calculated from gage readings

\hat{T}_{MAX} = maximum shear stress as calculated from

$$\hat{T}_{MAX} = \frac{\hat{\sigma}_p - \hat{\sigma}_q}{2}$$

While the errors in the above case were very small, this is not true for stress fields involving extremes of R_G . In general, n_{σ_p} becomes very large for $|R_G| \ll 1.0$, as does n_{σ_q} for $|R_G| \gg 1.0$. The error in shear stress is independent of the stress state.

The above generalities can be demonstrated by extending the previous case of the pressurized cylinder. Consider an internally pressurized cylinder with an axial compressive load applied externally to the ends. If, for example, the load were $0.8 \pi r^2 p$, where r is the inside radius of the cylinder, and p is the internal pressure, the principal stress ratio would become,

$$R_G = 10$$

Equations (14) and (15) become:

$$n_{\sigma_p} = -0.45 (1 - \cos 2\beta) \times 100 \quad (14b)$$

$$n_{\sigma_q} = 4.5 (1 - \cos 2\beta) \times 100 \quad (15b)$$

For this case, a 5° error in mounting the rosette produces a -0.68% error in σ_p and a 6.75% error in σ_q .

The errors defined and evaluated in the foregoing occur, in each case, due to misalignment of a single strain gage or of an entire rosette. The effect of misalignment among the individual gages within a rosette is the subject of a separate study.

MEASUREMENTS GROUP TECH NOTE

TN-511

Strain Gage
Misalignment Errors

Errors Due to Misalignment of Strain Gages

Single Gage in a Uniform Biaxial Strain Field

When a strain gage is bonded to a test surface at a small angular error with respect to the intended axis of strain measurement, the indicated strain will also be in error due to the gage misalignment. In general, for a single gage in a uniform biaxial strain field, the magnitude of the misalignment error depends upon three factors (ignoring transverse sensitivity):

1. The ratio of the algebraic maximum to the algebraic minimum principal strain, ϵ_p / ϵ_q .
2. The angle ϕ between the maximum principal strain axis and the intended axis of strain measurement.
3. The angular mounting error, β , between the gage axis after bonding and the intended axis of strain measurement.

These quantities are defined in Figs. 1 and 2 for the particular but common case of the uniaxial stress field. Figure 1 is a polar diagram of strain at the point in question, and Fig. 2 gives the concentric Mohr's circles for stress and strain for the same point. In Fig. 1, the distance to the boundary of the diagram along any radial line is

proportional to the normal strain along the same line. The small lobes along the Y axis in the diagram represent the negative Poisson strain for this case. It can be seen qualitatively from Fig. 1 that when ϕ is 0° or 90°, a small angular misalignment of the gage will produce a very small error in the strain indication, since the polar strain diagram is relatively flat and passing through zero-slope at these points.

However, for angles between 0° and 90°, Fig. 1 shows that the error in indicated strain due to a small angular misalignment can be surprisingly large because the slope of the polar strain diagram is very steep in these regions. More specifically, it can be noticed from Fig. 2, when $\phi = 45^\circ$, or $2\phi = 90^\circ$, that the same small angular misalignment will produce the maximum error in indicated strain, since ϵ is changing most rapidly with angle at this point. The same result could be obtained by writing the analytical expression for the polar strain diagram, and setting the second derivative equal to zero to solve for the angle at which the maximum slope occurs. In fact, the general statement can be made that in any uniform biaxial strain field the error due to gage misalignment is always greatest when measuring strain at 45° to a principal axis, and is always least when

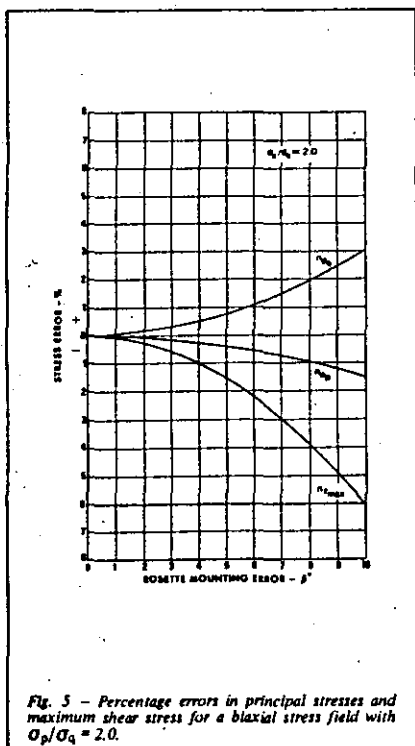


Fig. 5 - Percentage errors in principal stresses and maximum shear stress for a biaxial stress field with $\sigma_p/\sigma_q = 2.0$.

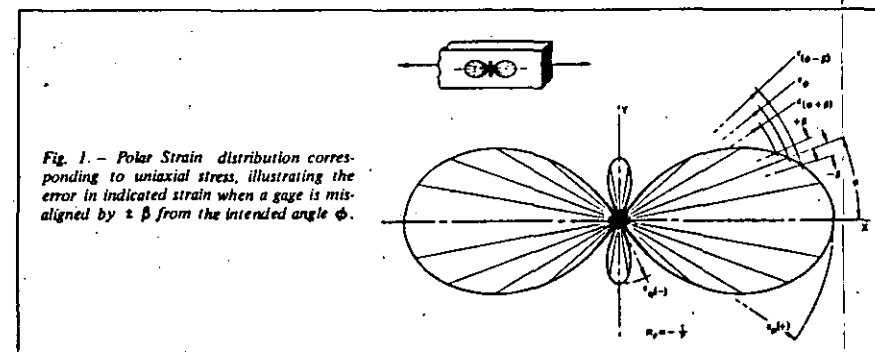


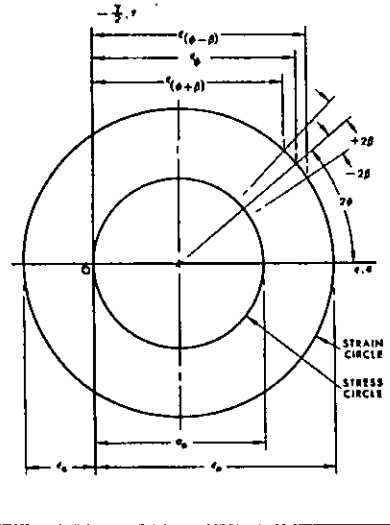
Fig. 1 - Polar Strain distribution corresponding to uniaxial stress, illustrating the error in indicated strain when a gage is misaligned by β from the intended angle ϕ .



MEASUREMENTS GROUP, INC.

P. O. Box 27777 (919) 365-3800
Raleigh, North Carolina 27611, USA

Fig. 2 - Mohr's circles of stress and strain for uniaxial stress, an alternative representation of the misalignment errors.



measuring the principal strains.* The error in strain indication due to angular misalignment of the gage can be expressed as follows:

$$n = \epsilon_{(\phi \pm \beta)} - \epsilon_{\phi} \quad (1)$$

where: n = Error, $\mu\epsilon$

ϵ_{ϕ} = Strain along axis of intended measurement at angle ϕ from principal axis, $\mu\epsilon$

$\epsilon_{(\phi \pm \beta)}$ = Strain along gage axis with angular mounting error of $\pm \beta$, $\mu\epsilon$

Or,

$$n = \frac{\epsilon_p - \epsilon_q}{2} [\cos 2(\phi \pm \beta) - \cos 2\phi] \quad (2)$$

where: ϵ_p, ϵ_q = Maximum and minimum principal strains, respectively

The error can also be expressed as a percentage of the intended strain measurement, ϵ_{ϕ} :

$$n' = \frac{\epsilon_{(\phi \pm \beta)} - \epsilon_{\phi}}{\epsilon_{\phi}} \times 100 \quad (3)$$

$$n' = \frac{\cos 2(\phi \pm \beta) - \cos 2\phi}{\frac{R\epsilon + 1}{R\epsilon - 1} + \cos 2\phi} \times 100 \quad (4)$$

where: $R_{\epsilon} = \frac{\epsilon_p}{\epsilon_q}$

However, from Eq. (3) it can be seen that n becomes unmeaningfully large for small values of ϵ_{ϕ} , and infinite when ϵ_{ϕ} vanishes. In order to better illustrate the order of magnitude of the error due to gage misalignment, Eq. (2) will be evaluated for a more-or-less typical case.

In a uniaxial stress field, $\epsilon_q = -\nu\epsilon_p$. And, for steel, $\nu = 0.285$.

Assume $\epsilon_p = 1000\mu\epsilon$

Then, $\epsilon_q = -285\mu\epsilon$

And, $n = 642.5 [\cos 2(\phi \pm \beta) - \cos 2\phi]$ (5)

Equation (5) is plotted in Fig. 3 over a range of ϕ from 0° to 90° , and over a range of mounting errors from 1° to 10° .

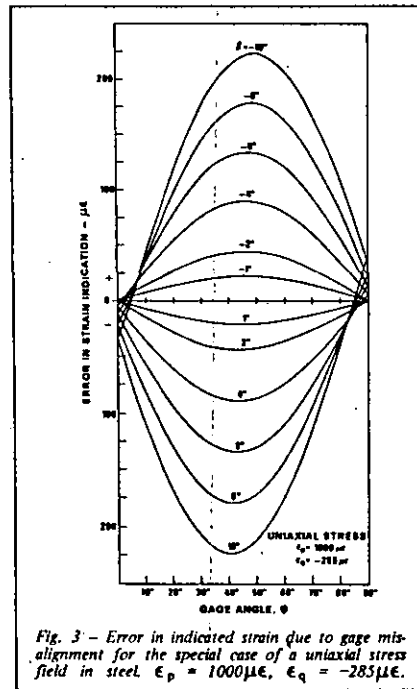
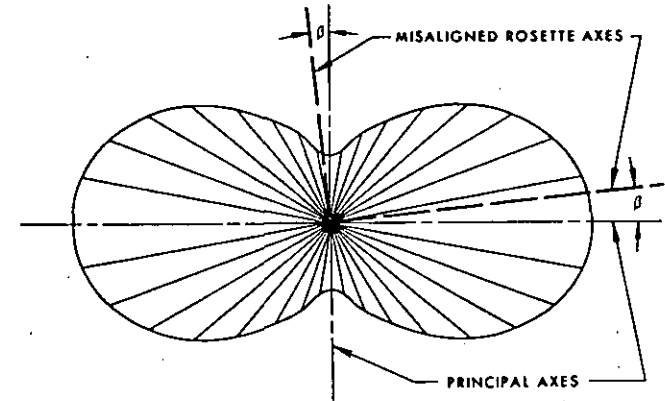


Fig. 3 - Error in indicated strain due to gage misalignment for the special case of a uniaxial stress field in steel $\epsilon_p = 1000\mu\epsilon$, $\epsilon_q = -285\mu\epsilon$.

*The exception to this statement is the singular case when $\epsilon_p \equiv \epsilon_q$, as on the surface of a pressurized sphere. In this instance, the strain is everywhere the same and independent of direction.

Fig. 4 - Biaxial strain field with rosette axes misaligned by the angle β from the principal axes.



In order to correct for a known misalignment by reading the value of n from Fig. 3, it is only necessary to solve Eq. (1) for ϵ_{ϕ} and substitute the value of n , including the sign as given by Fig. 3. This figure is given only as an example, and applies only to the case in which $\epsilon_q = -0.285\epsilon_p$ (uniaxial stress in steel). Equation (2) can be used to develop similar error curves for any biaxial strain state.

Two-Gage Rectangular Rosette

While the above analysis of the errors due to misalignment of a single gage may help in understanding the nature of such errors, the 90-degree, two-gage rosette is of considerably greater practical interest.

A two-gage rectangular rosette is ordinarily used by stress analysts for the purpose of determining the principal stresses when the directions of the principal axes are known from other sources. In this case, the rosette should be bonded in place with the gage axes coincident with the principal axes. Whether there is an error in orientation of the rosette with respect to the principal axes, or in the locations of the principal axes themselves, there will be a corresponding error in the principal stresses as calculated from the strain readings.

In Fig. 4, a general biaxial strain field is shown, with the axes of a two-gage rosette, misaligned by the angle β , superimposed. The percentage errors in the principal stresses and maximum shear stress due to the misalignment are:

$$n_{\sigma_p} = \frac{\hat{\sigma}_p - \sigma_p}{\sigma_p} \times 100 \quad (6)$$

$$n_{\sigma_q} = \frac{(1-R_{\epsilon})(1-\nu)(1-\cos 2\beta)}{2(R_{\epsilon} + \nu)} \times 100 \quad (7)$$

$$n_{\sigma_q} = \frac{\hat{\sigma}_q - \sigma_q}{\sigma_q} \times 100 \quad (8)$$

$$n_{\sigma_q} = \frac{(R_{\epsilon} - 1)(1 - \nu)(1 - \cos 2\beta)}{2(1 + \nu R_{\epsilon})} \times 100 \quad (9)$$

$$n_{T_{MAX}} = \frac{\hat{T}_{MAX} - T_{MAX}}{T_{MAX}} \times 100 \quad (10)$$

$$n_{T_{MAX}} = -(1 - \cos 2\beta) \times 100 \quad (11)$$

where:

$\hat{\sigma}_p, \hat{\sigma}_q, \hat{T}_{MAX}$ are the principal stresses and maximum shear stress inferred from the indicated strains when the rosette is misaligned by the angle β .

$R_{\epsilon} = \epsilon_p/\epsilon_q$, the ratio of the algebraic maximum to the algebraic minimum principal strain, as before.

When the principal strain ratio is replaced by the principal stress ratio, where:

$$R_{\sigma} = \frac{R_{\epsilon} + \nu}{1 - \nu R_{\epsilon}} = \frac{\sigma_p}{\sigma_q} \quad (12)$$

Or,

$$R_{\epsilon} = \frac{R_{\sigma} - \nu}{1 - \nu R_{\sigma}} = \frac{\epsilon_p}{\epsilon_q} \quad (13)$$

$$n_{\sigma_p} = \frac{1 - R_{\sigma}}{2R_{\sigma}} (1 - \cos 2\beta) \times 100 \quad (14)$$

$$n_{\sigma_q} = \frac{R_{\sigma} - 1}{2} (1 - \cos 2\beta) \times 100 \quad (15)$$

The historical practice of quoting gage factors which, in effect, mask the presence of transverse sensitivity, and which are correct in themselves for only a specific stress field in a specific material, is an unfortunate one. This approach has generally complicated the use of strain gages, while leading to errors and confusion. Although the uniaxial stress field is very common, it is not highly significant to the general field of experimental stress analysis. There is no particular merit, therefore, in combining the axial and transverse sensitivities for this case.

In general, then, a strain gage actually has two gage factors, F_a and F_t , which refer to the gage factors as determined in a uniaxial strain field (not uniaxial stress) with, respectively, the gage axes aligned parallel to and perpendicular to the strain field. For any strain field, the output of the strain gage can be expressed as:

$$\frac{\Delta R}{R} = F_a \epsilon_a + F_t \epsilon_t \quad (1)$$

where: ϵ_a, ϵ_t = strains parallel to and perpendicular to the gage axis, or the grid lines in the gage.

F_a = axial gage factor.

F_t = transverse gage factor.

Or,

$$\frac{\Delta R}{R} = F_a (\epsilon_a + K_t \epsilon_t) \quad (2)$$

where: $K_t = \frac{F_t}{F_a}$ = transverse sensitivity coefficient, referred to from here on as the "transverse sensitivity."

When the gage is calibrated for gage factor in a uniaxial stress field on a material with Poisson's ratio, ν_a ,

$$\epsilon_t = -\nu_a \epsilon_a$$

Therefore,

$$\frac{\Delta R}{R} = F_a (\epsilon_a - K_t \nu_a \epsilon_a)$$

Or,

$$\frac{\Delta R}{R} = F_a (1 - \nu_a K_t) \epsilon_a \quad (3)$$

The strain gage manufacturers commonly write this as:

$$\frac{\Delta R}{R} = F \epsilon \quad (3a)$$

where: F = manufacturers' gage factor.

which is deceptively simple in appearance, since, in reality:

$$F = F_a (1 - \nu_a K_t) \quad (4)$$

Furthermore, ϵ is actually ϵ_a , the strain along the gage axis (and only one of two strains sensed by the gage during calibration) when the gage is aligned with the maximum principal stress axis in a uniaxial stress (not uniaxial strain) field, on a material with $\nu_a = 0.285$. Errors and confusion occur through failure to fully comprehend and always account for the real meanings of F and ϵ as used by the manufacturers.

It is imperative to realize that for any strain field except that corresponding to a uniaxial stress field (and even in the latter case, with the gage mounted along any direction except the maximum principal stress axis, or on any material with Poisson's ratio other than 0.285), there is always an error in strain indication if the transverse sensitivity of the strain gage is other than zero. In some instances, this error is small enough to be neglected. In others, it is not. The error due to transverse sensitivity for a strain gage oriented at any angle, in any strain field, on any material, can be expressed as:

$$n_t = \frac{K_t \left(\frac{\epsilon_t}{\epsilon_a} + \nu_a \right)}{1 - \nu_a K_t} \times 100 \quad (5)$$

where: n_t = the error as a percentage of the actual strain along the gage axis.

ν_a = the Poisson's ratio of the material on which the manufacturer's gage factor, F , was measured (usually 0.285).

ϵ_a, ϵ_t = respectively, the actual strains parallel and perpendicular to the primary sensing axis of the gage.*

From the above equation, it is evident that the percentage error due to transverse sensitivity increases with the absolute values of K_t and ϵ_t/ϵ_a , whether these parameters are positive or negative. Equation (5) has been plotted in Figure 1 for convenience in judging whether the magnitude of the error may be significant for a particular strain field. Figure 1 also yields an approximate rule-of-thumb for quickly estimating the error due to transverse sensitivity — that is,

$$n_t \approx K_t \frac{\epsilon_t}{\epsilon_a} \times 100 \quad (\text{percent})$$

As Equation (5) shows, this approximation holds quite well as long as the absolute value ϵ_t/ϵ_a is not close to ν_a . For an example, assume the task of measuring Poisson (transverse) strain in a uniaxial stress field. In this case, the Poisson strain is represented by ϵ_a , the strain along

*Subscripts (a) and (t) always refer to the axial and transverse directions with respect to the gage (without regard to directions on the test surface), while subscripts (x) and (y) refer to an arbitrary set of orthogonal axes on the test surface, and subscripts (p) and (q) refer to the principal axes.

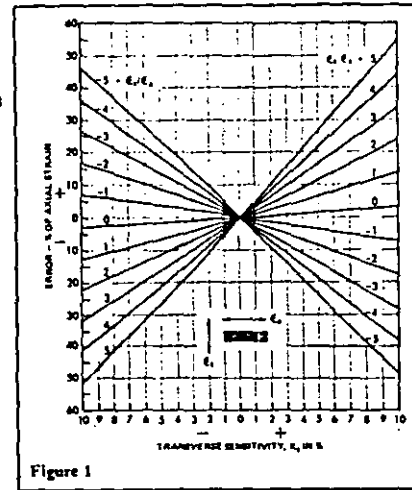


Figure 1

the gage axis, and the longitudinal strain in the test member by ϵ_a , since the latter is transverse to the gage axis (see sketch below, and footnote on preceding page).

$$\epsilon_a = -\nu_a \epsilon_t$$

$$\epsilon_t/\epsilon_a = -\frac{1}{\nu_a}$$



If the test specimen is an aluminum alloy, with $\nu = 0.32$, then $\epsilon_t/\epsilon_a = -1/\nu = -3.1$. Assuming that the transverse sensitivity of the strain gage is -3% (i.e., $K_t = -0.03$), the rule of thumb gives an approximate error of +9.3%. The actual error, calculated from Equation (5), is +8.5%.

CORRECTING FOR TRANSVERSE SENSITIVITY

The effects of transverse sensitivity should always be considered in the experimental stress analysis of a biaxial stress field with strain gages. Either it should be demonstrated that the effect of transverse sensitivity is

negligible and can be ignored or, if not negligible, the proper correction should be made. Since a two- or three-gage rosette will ordinarily be used in such cases, simple correction methods are given here for the two-gage 90-degree rosette, the three-gage rectangular rosette, and the delta rosette. Unless otherwise noted, these corrections apply to rosettes in which the transverse sensitivities of the individual gage elements in the rosettes are equal to one another, or approximately so. Generalized correction equations for any combination of transverse sensitivities are given in the Appendix.

Consider first the two-gage 90-degree rosette, with the gage axes aligned with two orthogonal axes, x and y , on the test surface. When using this type of rosette, the x and y axes would ordinarily be the principal axes, but this need not necessarily be so. The correct strains along any two perpendicular axes can always be calculated from the following equations in terms of the indicated strains along those axes:

$$\epsilon_x = \frac{(1 - \nu_a K_t) (\hat{\epsilon}_x - K_t \hat{\epsilon}_y)}{1 - K_t^2} \quad (6)$$

$$\epsilon_y = \frac{(1 - \nu_a K_t) (\hat{\epsilon}_y - K_t \hat{\epsilon}_x)}{1 - K_t^2} \quad (7)$$

where: $\hat{\epsilon}_x = \hat{\epsilon}_{ax}$, the indicated (uncorrected) strain from gage no. 1.

$\hat{\epsilon}_y = \hat{\epsilon}_{ay}$, the indicated (uncorrected) strain from gage no. 2.

ϵ_x, ϵ_y = corrected strains along the x and y axes respectively.

The $(1 - K_t^2)$ term in the denominators of Equations (6) and (7) is generally in excess of 0.995, and can be taken as unity:

$$\epsilon_x = (1 - \nu_a K_t) (\hat{\epsilon}_x - K_t \hat{\epsilon}_y) \quad (6a)$$

$$\epsilon_y = (1 - \nu_a K_t) (\hat{\epsilon}_y - K_t \hat{\epsilon}_x) \quad (7a)$$

Data reduction can be further simplified by setting the gage factor control on the strain-indicating instrumentation at F_a instead of F , the manufacturer's gage factor. Since,

$$F_a = \frac{F}{1 - \nu_a K_t}$$

Equations (6a) and (7a) can be rewritten:

$$\epsilon_x = \hat{\epsilon}_x - K_t \hat{\epsilon}_y \quad (6b)$$

$$\epsilon_y = \hat{\epsilon}_y - K_t \hat{\epsilon}_x \quad (7b)$$

where: $\hat{\epsilon}_x, \hat{\epsilon}_y$ = strains as indicated by instrumentation with gage factor control set at

$$\frac{F}{1 - \nu_a K_t}$$

As an alternative to the preceding methods, a quick graphical correction for the transverse sensitivity can be made through the use of Figure 2. To use the graph, the first step is to calculate:

$$\left(\frac{\hat{\epsilon}_1}{\hat{\epsilon}_a}\right)_1 = \frac{\hat{\epsilon}_1}{\hat{\epsilon}_1} = \frac{\hat{\epsilon}_y}{\hat{\epsilon}_x} \quad (\text{Gage No. 1})$$

$$\left(\frac{\hat{\epsilon}_1}{\hat{\epsilon}_a}\right)_2 = \frac{\hat{\epsilon}_1}{\hat{\epsilon}_2} = \frac{\hat{\epsilon}_x}{\hat{\epsilon}_y} \quad (\text{Gage No. 2})$$

Having done this, it is only necessary to enter the graph at the appropriate value of K_t , move upward to the line (or interpolated line) representing the observed (indicated) strain ratio, $\hat{\epsilon}_1/\hat{\epsilon}_a$ for that particular rosette element, and horizontally to the vertical scale on the left to read the correction factor.

Then,

$$\epsilon_x = \epsilon_1 = C_1 \hat{\epsilon}_1$$

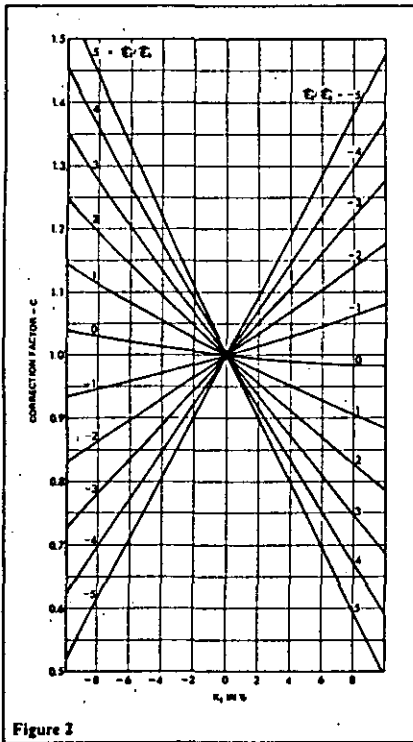


Figure 2

Similarly,

$$\epsilon_y = \epsilon_2 = C_2 \hat{\epsilon}_2$$

Following is a numerical example utilizing first Equations (6a) and (7a), and then Figure 2.

Assume that the indicated strains for rosette elements (1) and (2) along the x and y axes are, respectively:

$$\hat{\epsilon}_1 = +1530 \mu\epsilon$$

$$\hat{\epsilon}_2 = +920 \mu\epsilon$$

Assume also that $K_t = -0.06$. Substituting into Equations (6a) and (7a), with $\nu_0 = 0.285$,

$$\epsilon_x = (1 + 0.285 \times 0.06)(1530 + 0.06 \times 920) = 1612 \mu\epsilon$$

$$\epsilon_y = (1 + 0.285 \times 0.06)(920 + 0.06 \times 1530) = 1029 \mu\epsilon$$

For use with the correction graph, Figure 2,

$$\left(\frac{\hat{\epsilon}_1}{\hat{\epsilon}_a}\right)_1 = \frac{920}{1530} = 0.601 \approx 0.6$$

$$\left(\frac{\hat{\epsilon}_1}{\hat{\epsilon}_a}\right)_2 = \frac{1530}{920} = 1.663 \approx 1.65$$

Following the line for $K_t = -0.06$ upward, interpolating the location of $(\hat{\epsilon}_1/\hat{\epsilon}_a)_1 = 0.6$, and $(\hat{\epsilon}_1/\hat{\epsilon}_a)_2 = 1.65$, and reading the respective values of the correction factor,

$$C_1 = 1.06; C_2 = 1.12$$

From which,

$$\epsilon_x = C_1 \hat{\epsilon}_1 = 1.06 \times 1530 = 1620 \mu\epsilon$$

$$\epsilon_y = C_2 \hat{\epsilon}_2 = 1.12 \times 920 = 1030 \mu\epsilon$$

CORRECTION FOR SHEAR STRAIN

A two-gage, 90-degree rosette, or "T"-rosette, is sometimes used for the direct indication of shear strain. It can be shown that the shear strain along the bisector of the gage axes is, in this case, numerically equal to the difference in normal strains on these axes. Thus, when the two gage elements of the rosette are connected in adjacent arms of a Wheatstone bridge, the indicated strain is equal to the indicated shear strain along the bisector, requiring at most correction for the error due to transverse sensitivity. The latter error can be corrected for very easily if both gages have the same transverse sensitivity,

since the error is independent of the state of strain. The correction factor for this case is:

$$C_s = \frac{1 - \nu_0 K_t}{1 - K_t} \quad (8)$$

The actual shear strain is obtained by multiplying the indicated shear strain by the correction factor. Thus,

$$\gamma = C_s \hat{\gamma} = C_s (\hat{\epsilon}_x - \hat{\epsilon}_y) = \frac{1 - \nu_0 K_t}{1 - K_t} (\hat{\epsilon}_x - \hat{\epsilon}_y)$$

For convenience, the shear strain correction factor is plotted in Figure 3 against K_t , with $\nu_0 = 0.285$. Since this correction factor is independent of the state of strain, it can again be incorporated in the gage factor setting on the strain-indicating instrumentation if desired. This can be done by setting the gage factor control at:

$$F_s = F \frac{1 - K_t}{1 - \nu_0 K_t} \quad (9)$$

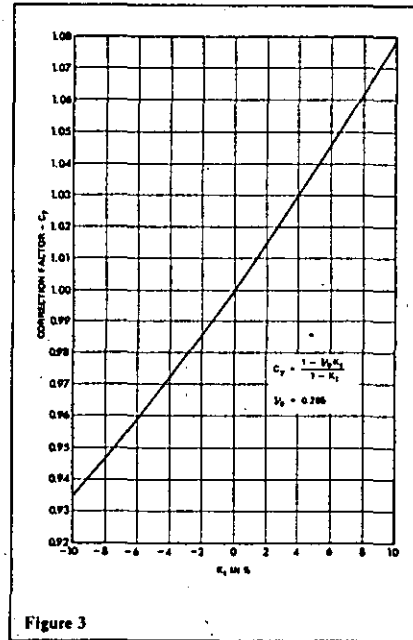


Figure 3

With this change, the strain indicator will indicate the actual shear strain along the bisector of the gage axis, already corrected for transverse sensitivity in the strain gages.

THREE-GAGE RECTANGULAR (45°) ROSETTE

When the directions of the principal axes are unknown, three independent strain measurements are required to completely determine the state of strain. For this purpose, a three-gage rosette should be used, and the rectangular rosette is generally the most convenient form.

If the transverse sensitivity of the gage elements in the rosette is other than zero, the individual strain readings will be in error, and the principal strains and stresses calculated from these data will also be incorrect.

Correction for the effects of transverse sensitivity can be made either on the individual strain readings or on the principal strains or principal stresses calculated from these. Numbering the gage elements consecutively, elements (1) and (3) correspond directly to the two-gage, 90-degree rosette, and correction can be made with Equations (6) and (7), or (6a) and (7a), or (by properly setting the gage factor control on the strain indicator) with Equations (6b) and (7b). The center gage of the rosette requires a special correction relationship since there is no direct measurement of the strain perpendicular to the grid. The correction equations for all three gages are listed here for convenience:

$$\epsilon_1 = \frac{1 - \nu_0 K_t}{1 - K_t} (\hat{\epsilon}_1 - K_t \hat{\epsilon}_2) \quad (10)$$

$$\epsilon_2 = \frac{1 - \nu_0 K_t}{1 - K_t} [\hat{\epsilon}_2 - K_t (\hat{\epsilon}_1 + \hat{\epsilon}_3 - \hat{\epsilon}_2)] \quad (11)$$

$$\epsilon_3 = \frac{1 - \nu_0 K_t}{1 - K_t} (\hat{\epsilon}_3 - K_t \hat{\epsilon}_1) \quad (12)$$

where: $\hat{\epsilon}_1, \hat{\epsilon}_2, \hat{\epsilon}_3$ = indicated strains from the respective gage elements.

$\epsilon_1, \epsilon_2, \epsilon_3$ = corrected strains along the gage axes.

It should be noted that Equations (10), (11), and (12) are based upon the assumption that the transverse sensitivity is the same, or effectively so in all gage elements, as it is in stacked rosettes. This may not be true for planar foil rosettes, since the individual gage elements do not all have the same orientation with respect to the direction in which the foil was rolled. It is common practice, however, to etch the rosette in a position of symmetry about the foil rolling direction, and therefore the transverse sensitivities of gage elements (1) and (3) will be nominally the same, while that of element (2) may differ. Correction equations for rosettes with nonuniform transverse sensitivities among the gage elements are given in the Appendix.

DELTA ROSETTES

A delta strain gage rosette consists of three gage elements in the form of an equilateral triangle or a "Y" with equally spaced branches. The delta rosette offers a very slight potential advantage over the three-gage rectangular rosette in that the lowest possible sum of the strain readings obtainable in a particular strain field is somewhat higher than for a three-gage rectangular rosette. This is because the three gage elements in the delta rosette are at the greatest possible angle from one another. However, the data reduction for obtaining the principal strains or correcting for transverse sensitivity is also more involved and lengthy than for rectangular rosettes.

As in the case of rectangular rosettes, plane foil delta rosettes are manufactured symmetrically with respect to the rolling direction of the foil. Thus, two of the gage elements will ordinarily have the same nominal transverse sensitivity, and the third may differ. Correction equations for this condition are given in the Appendix. In the stacked delta rosette, all three gages have the same nominal transverse sensitivity.

The individual strain readings from a delta rosette can be corrected for transverse sensitivity with the following relationships when a single value of K_t can be used for the transverse sensitivity:

$$\epsilon_1 = \frac{1 - \nu_0 K_t}{1 - K_t^2} \left[\left(1 + \frac{K_t}{3}\right) \bar{\epsilon}_1 - \frac{2}{3} K_t (\bar{\epsilon}_2 + \bar{\epsilon}_3) \right] \quad (13)$$

$$\epsilon_2 = \frac{1 - \nu_0 K_t}{1 - K_t^2} \left[\left(1 + \frac{K_t}{3}\right) \bar{\epsilon}_2 - \frac{2}{3} K_t (\bar{\epsilon}_1 + \bar{\epsilon}_3) \right] \quad (14)$$

$$\epsilon_3 = \frac{1 - \nu_0 K_t}{1 - K_t^2} \left[\left(1 + \frac{K_t}{3}\right) \bar{\epsilon}_3 - \frac{2}{3} K_t (\bar{\epsilon}_1 + \bar{\epsilon}_2) \right] \quad (15)$$

As before, simplification can be achieved by treating $(1 - K_t)$ as unity, and by incorporating the quantity $(1 - \nu_0 K_t)$ into the gage factor setting of the strain instrumentation. When doing this, the gage-factor control is set at:

$$F_0 = \frac{F}{1 - \nu_0 K_t}$$

CORRECTION OF PRINCIPAL STRAINS

With any rosette, rectangular, delta, or otherwise, it is always possible (and often most convenient) to calculate the indicated principal strains directly from the completely uncorrected gage readings, and then apply

corrections to the principal strains. This is true because of the fact that the errors in principal strains due to transverse sensitivity are independent of the kind of rosette employed, as long as all gage elements in the rosette have the same nominal transverse sensitivity. Since Equations (6) and (7) apply to any two indicated orthogonal strains, they must also apply to the indicated principal strains. Thus, if the indicated principal strains have been calculated from strain readings uncorrected for transverse sensitivity, the actual principal strains can readily be calculated from the following:

$$\epsilon_p = \frac{1 - \nu_0 K_t}{1 - K_t^2} (\bar{\epsilon}_p - K_t \bar{\epsilon}_q) \quad (16)$$

$$\epsilon_q = \frac{1 - \nu_0 K_t}{1 - K_t^2} (\bar{\epsilon}_q - K_t \bar{\epsilon}_p) \quad (17)$$

Furthermore, Equations (16) and (17) can be rewritten to express the actual principal strain in terms of the indicated principal strain and a correction factor. Thus,

$$\epsilon_p = \bar{\epsilon}_p \left[\frac{(1 - \nu_0 K_t)}{1 - K_t^2} \right] \left(1 - K_t \frac{\bar{\epsilon}_q}{\bar{\epsilon}_p} \right) \quad (18)$$

$$\epsilon_q = \bar{\epsilon}_q \left[\frac{(1 - \nu_0 K_t)}{1 - K_t^2} \right] \left(1 - K_t \frac{\bar{\epsilon}_p}{\bar{\epsilon}_q} \right) \quad (19)$$

Since Equations (18) and (19) are the same relationship used to plot the correction graph of Figure 2, this graph can be used directly to correct indicated principal strains by the procedure described earlier, merely noting that:

$$\frac{\bar{\epsilon}_1}{\bar{\epsilon}_2} = \frac{\bar{\epsilon}_q}{\bar{\epsilon}_p} \text{ when correcting } \bar{\epsilon}_p$$

and

$$\frac{\bar{\epsilon}_2}{\bar{\epsilon}_3} = \frac{\bar{\epsilon}_p}{\bar{\epsilon}_q} \text{ when correcting } \bar{\epsilon}_q$$

In fact, the indicated strains from three gages with any relative angular orientation define an "indicated" Mohr's circle of strain. When employing a data-reduction scheme that produces the distance to the center of Mohr's circle of strain, and the radius of the circle, still another simple correction method is applicable. To correct the indicated Mohr's circle to the actual Mohr's circle, the distance to the center of the indicated circle should be multiplied by $(1 - \nu_0 K_t)/(1 + K_t)$, and the radius of the circle by $(1 - \nu_0 K_t)/(1 - K_t)$. The maximum and minimum principal strains are the sum and difference, respectively, of the distance to the center and the radius of Mohr's circle of strain.

BIBLIOGRAPHY

ASTM Standard E251, Part III. "Standard Test Method for Performance Characteristics of Bonded Resistance Strain Gages."

Avril, J. "L'Effet Latéral des Jauges Électriques." GAMAC Conference. April 25, 1967.

Baumberger, R. and F. Hines. "Practical Reduction Formulas for Use on Bonded Wire Strain Gages in Two-Dimensional Stress Fields." *Proceedings of the Society for Experimental Stress Analysis II*: No. 1, 113-127, 1944.

Bossart, K. J. and G. A. Brewer. "A Graphical Method of Rosette Analysis." *Proceedings of the Society for Experimental Stress Analysis IV*: No. 1, 1-8, 1946.

Campbell, W. R. "Performance Tests of Wire Strain Gages: IV - Axial and Transverse Sensitivities." *NACA TN1042*, 1946.

Gu, W. M. "A Simplified Method for Eliminating Error of Transverse Sensitivity of Strain Gage." *Experimental Mechanics* 22: No. 1, 16-18, January 1982.

Meier, J. H. "The Effect of Transverse Sensitivity of SR-4 Gages Used as Rosettes." *Handbook of Experimental Stress Analysis*, ed. by M. Hetényi, John Wiley & Sons, pp. 407-411, 1950.

Meier, J. H. "On the Transverse-strain Sensitivity of Foil Gages." *Experimental Mechanics* 1: 39-40, July 1961.

Meyer, M. L. "A Unified Rational Analysis for Gauge Factor and Cross-Sensitivity of Electric-Resistance Strain Gages." *Journal of Strain Analysis* 2: No. 4, 324-331, 1967.

Meyer, M. L. "A Simple Estimate for the Effect of Cross-Sensitivity on Evaluated Strain-gage Measurement." *Experimental Mechanics* 7: 476-480, November 1967.

Murray, W. M. and P. K. Stein. *Strain Gage Techniques*. Massachusetts Institute of Technology, Cambridge, Massachusetts, pp. 56-81, 1959.

Nasudevan, M. "Note on the Effect of Cross-Sensitivity in the Determination of Stress." *STRAIN* 7: No. 2, 74-75, April 1971.

Starr, J. E. "Some Untold Chapters in the Story of the Metal Film Strain Gages." *Strain Gage Readings* 3: No. 5, 31, December 1960-January 1961.

Wu, Charles T. "Transverse Sensitivity of Bonded Strain Gages." *Experimental Mechanics* 2: 338-344, November 1962.

APPENDIX

The following relationships can be used to correct for transverse sensitivity when the gage elements in a rosette do not all have the same value of K_t .

TWO-GAGE, 90-DEGREE ROSETTE

$$\epsilon_1 = \frac{\bar{\epsilon}_1(1 - \nu_0 K_{t1}) - K_{t1} \bar{\epsilon}_2(1 - \nu_0 K_{t2})}{1 - K_{t1} K_{t2}} \quad (20)$$

$$\epsilon_2 = \frac{\bar{\epsilon}_2(1 - \nu_0 K_{t2}) - K_{t2} \bar{\epsilon}_1(1 - \nu_0 K_{t1})}{1 - K_{t1} K_{t2}} \quad (21)$$

where: $\bar{\epsilon}_1, \bar{\epsilon}_2$ = indicated strains from gages (1) and (2), uncorrected for transverse sensitivity.

K_{t1}, K_{t2} = transverse sensitivities of gages (1) and (2).

ϵ_1, ϵ_2 = actual strains along gage axes (1) and (2).

THREE-GAGE RECTANGULAR (45-DEGREE) ROSETTE

$$\epsilon_1 = \frac{\bar{\epsilon}_1(1 - \nu_0 K_{t1}) - K_{t1} \bar{\epsilon}_2(1 - \nu_0 K_{t2})}{1 - K_{t1} K_{t2}} \quad (22)$$

$$\epsilon_2 = \frac{\bar{\epsilon}_2(1 - \nu_0 K_{t2}) - K_{t2} [\bar{\epsilon}_1(1 - \nu_0 K_{t1})(1 - K_{t1}) + \bar{\epsilon}_3(1 - \nu_0 K_{t3})(1 - K_{t3})]}{(1 - K_{t1} K_{t2})(1 - K_{t3})} \quad (23)$$

$$\epsilon_3 = \frac{\bar{\epsilon}_3(1 - \nu_0 K_{t3}) - K_{t3} \bar{\epsilon}_1(1 - \nu_0 K_{t1})}{1 - K_{t1} K_{t3}} \quad (24)$$

When the two quadrants are connected as adjacent legs of a Wheatstone bridge circuit (Fig. 7a), so that their difference appears as a signal, the combined output is:

$$E_o \propto \frac{2\gamma_{xy}}{H} \quad (16)$$

An alternate method of canceling the unwanted normal-strain term in Eq. (14) is shown in Fig. 7b. In this case, two half gage-length linear elements are oriented along the X and Y axes, respectively, and connected in series to form one leg of a Wheatstone bridge. When a single circular-arc quadrant is used for the adjacent bridge leg, the output signal becomes:

$$E_o \propto \frac{\gamma_{xy}}{H} \quad (17)$$

Figure 8 illustrates a variety of gage-element configurations and their respective outputs. It is evident that the simplest approach to shear-strain measurement is the 90-deg rosette. When the maximum shear stress or the principal stresses are required, and the principal axes are unknown, the three-gage 45-deg rosette is the most convenient choice.

CORRECTION FOR TRANSVERSE SENSITIVITY

Up to this point, the effect of transverse sensitivity on shear-strain indication has been neglected. However, the correction for transverse sensitivity is particularly simple in the case of shear strain, and consists of multiplying the indicated shear strain by the factor $[(1 - \nu_o K_x) / (1 - K_x)]$, where K_x represents the transverse sensitivity of the strain gages used to generate the indicated shear-strain output, and ν_o is the Poisson's ratio of the material on which the manufacturer measured the gage factor.

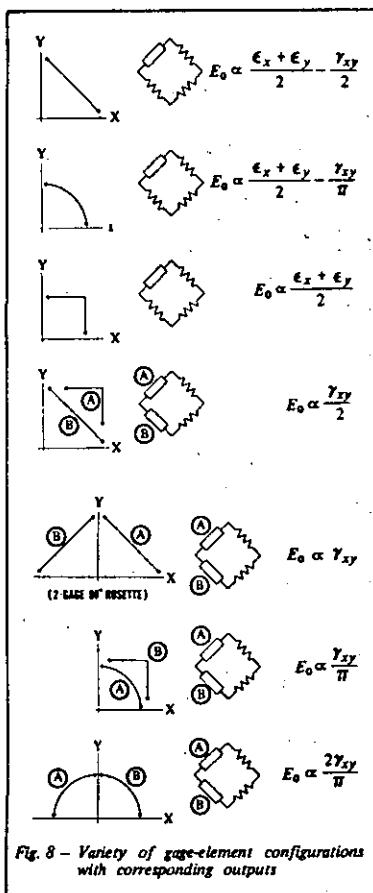


Fig. 8 - Variety of gage-element configurations with corresponding outputs

MEASUREMENTS GROUP TECH NOTE

TN-512

Plane-Shear
Measurement

Plane-Shear Measurement With Strain Gages

It is sometimes convenient to obtain a direct indication of shear strain from strain gages. Examples include shear-buckling studies and shear sensing in flexural transducers to provide load indication which is independent of the point of load application.

INTRODUCTION

Although a strain gage does not respond to shear strain as such, shear and normal strains are related through the laws of elasticity; and it is thus possible, by proper orientation of gages on the strained surface, and proper disposition of the gages in a Wheatstone bridge circuit, to produce an indication which is directly proportional to shear strain in the surface.

SHEAR STRAIN FROM NORMAL STRAINS

Consider an array of two strain gages oriented at arbitrarily different angles with respect to an X-Y coordinate system which, in turn, is arbitrarily oriented with respect to the principal axes, as in Fig. 1. From elementary mechanics of materials, the strain along the gage axes can be written as:

$$\epsilon_1 = \frac{\epsilon_x + \epsilon_y}{2} + \frac{\epsilon_x - \epsilon_y}{2} \cos 2\theta_1 + \frac{\gamma_{xy}}{2} \sin 2\theta_1 \quad (1)$$

$$\epsilon_2 = \frac{\epsilon_x + \epsilon_y}{2} + \frac{\epsilon_x - \epsilon_y}{2} \cos 2\theta_2 + \frac{\gamma_{xy}}{2} \sin 2\theta_2 \quad (2)$$

Subtracting (2) from (1) and solving for γ_{xy} ,

$$\gamma_{xy} = \frac{2(\epsilon_1 - \epsilon_2) - (\epsilon_x - \epsilon_y)(\cos 2\theta_1 - \cos 2\theta_2)}{\sin 2\theta_1 - \sin 2\theta_2} \quad (3)$$

It is now noticeable that if $\cos 2\theta_1 = \cos 2\theta_2$, the term in ϵ_x and ϵ_y vanishes, and

$$\gamma_{xy} = \frac{2(\epsilon_1 - \epsilon_2)}{\sin 2\theta_1 - \sin 2\theta_2} \quad (4)$$

Since the cosine function is symmetrical about the zero argument, and about all integral multiples of π , $\cos 2\theta_1 = \cos 2\theta_2$ when,

$$\theta_1 + \alpha = -\pi/2, 0, \pi/2, \pi \dots \frac{n\pi}{2} = \theta_2 - \alpha \quad (5)$$

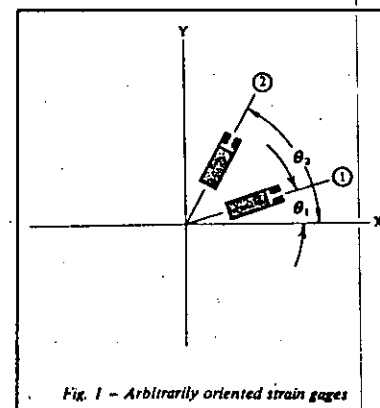


Fig. 1 - Arbitrarily oriented strain gages

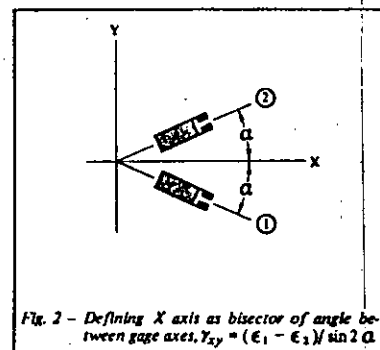


Fig. 2 - Defining X axis as bisector of angle between gage axes. $\gamma_{xy} = (\epsilon_1 - \epsilon_2) / \sin 2\alpha$



MEASUREMENTS GROUP, INC.

P. O. Box 27777 (919) 365-3800
Raleigh, North Carolina 27611, USA

© Copyright Measurements Group, Inc., 1983
All Rights Reserved.

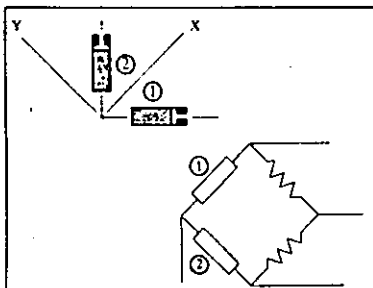


Fig. 3a - 90-deg rosette for direct indication of shear strain, γ_{xy}

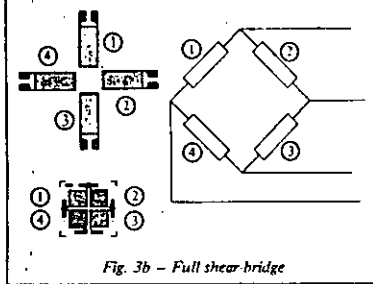


Fig. 3b - Full shear-bridge

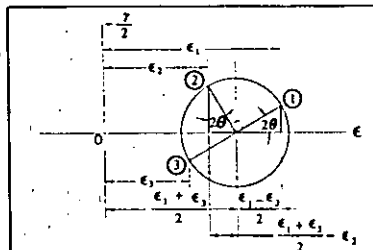


Fig. 4 - Mohr's circle for strain used to determine maximum shear strain

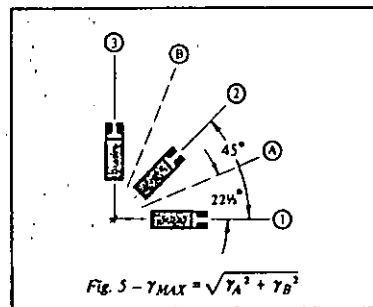


Fig. 5 - $\gamma_{MAX} = \sqrt{\gamma_A^2 + \gamma_B^2}$

It is thus evident that, if the gage axes are oriented symmetrically with respect to, say, the X axis (Fig. 2),

$$\theta_1 = -\theta_2$$

and,

$$\gamma_{xy} = -\frac{\epsilon_1 - \epsilon_2}{\sin 2\theta_1} = \frac{\epsilon_1 - \epsilon_2}{\sin 2\theta_1} \quad (6)$$

The preceding results can be generalized as follows: *The difference in normal strain sensed by any two arbitrarily oriented strain gages in a uniform strain field is proportional to the shear strain along an axis bisecting the strain gage axes, irrespective of the included angle between the gages.*

When the two gages are 90 deg apart, the denominator of Eq. (6) becomes unity and the shear strain along the bisector is numerically equal to the difference in normal strains. Thus, a conventional 90-deg two-gage rosette constitutes an ideal shear half bridge because the required subtraction, $\epsilon_1 - \epsilon_2$, is performed automatically for two gages in adjacent legs of the bridge circuit (Fig. 3a). When the gage axes of a two-gage 90-deg rosette are aligned with the principal axes, the output of the half bridge is numerically equal to the maximum shear strain. A full shear-bridge (with twice the output signal) is then composed of four gages as shown in Fig. 3b. The gages may have any of several configurations, including the cruciform arrangement and the compact geometry illustrated in the figure.

PRINCIPAL STRAINS

It should be kept in mind that with the shear bridges described above, the indicated shear strain exists along the bisector of any adjacent pair of gage axes, and it is not possible to determine the maximum shear strain or the complete state of strain from any combination of gage outputs unless the orientation of the gage axes with respect to the principal axes is known. In general, when the directions of the principal axes are unknown, a three-gage 45-deg rectangular rosette can be used.

Referring to Mohr's circle for strain (Fig. 4), it is apparent that the two shaded triangles are always identical for a 45-deg rosette, and therefore the maximum shear strain is equal to the "vector sum" of the shear strains along any two axes which are 45 deg apart on the strained surface. Looking at the 45-deg rosette as shown in Fig. 5, it can be seen that the shear strains along the bisectors of the gage pairs ①-② and ②-③ are in fact 45 deg apart and, thus, the maximum shear strain is,

$$\gamma_{MAX} = \sqrt{\gamma_A^2 + \gamma_B^2}$$

and, considering Eq. (6),

$$\gamma_{MAX} = \sqrt{\left(\frac{\epsilon_1 - \epsilon_2}{\sin 45^\circ}\right)^2 + \left(\frac{\epsilon_2 - \epsilon_3}{\sin 45^\circ}\right)^2}$$

or,

$$\gamma_{MAX} = \sqrt{2} \sqrt{(\epsilon_1 - \epsilon_2)^2 + (\epsilon_2 - \epsilon_3)^2} \quad (7)$$

and, from Mohr's circle again, the principal strains are obviously

$$\epsilon_p, \epsilon_q = \frac{\epsilon_1 + \epsilon_2}{2} \pm \frac{1}{\sqrt{2}} \sqrt{(\epsilon_1 - \epsilon_2)^2 + (\epsilon_2 - \epsilon_3)^2} \quad (8)$$

CIRCULAR-ARC GAGE ELEMENTS

A number of different grid-element configurations can be used, with varying degrees of practicability, for shear-strain measurement. Consider, for example, one quadrant of a circular arc (Fig. 6). The change in length of an element, dl , upon the application of an arbitrary uniform strain field can be expressed as:

$$\Delta dl = \epsilon_\theta R d\theta \quad (9)$$

where ϵ_θ refers to the normal strain at the angle θ which acts parallel to the element, since this is the only strain to which the element can respond if transverse sensitivity effects are ignored.

The change in length of the complete quadrant is:

$$\Delta l = \int_0^{\pi/2} \epsilon_\theta R d\theta \quad (10)$$

and the net strain over the quadrant becomes,

$$\bar{\epsilon}_1 = \frac{\Delta l}{l} = \frac{1}{(\pi/2)R} \int_0^{\pi/2} \epsilon_\theta R d\theta = \frac{2}{\pi} \int_0^{\pi/2} \epsilon_\theta d\theta \quad (11)$$

It is apparent from Fig. 6 that an element of the arc at an angle θ from the X axis actually senses the strain $\epsilon(\theta + \pi/2)$ in terms of Eq. (1), from which:

$$\epsilon = \epsilon(\theta + \pi/2) = \frac{\epsilon_x + \epsilon_y}{2} + \frac{\epsilon_x - \epsilon_y}{2} \cos 2(\theta + \pi/2) + \frac{\gamma_{xy}}{2} \sin 2(\theta + \pi/2) \quad (12)$$

but,

$$\cos(2\theta + \pi) = -\cos 2\theta$$

$$\sin(2\theta + \pi) = -\sin 2\theta$$

Therefore,

$$\epsilon_\theta = \frac{\epsilon_x + \epsilon_y}{2} - \frac{\epsilon_x - \epsilon_y}{2} \cos 2\theta - \frac{\gamma_{xy}}{2} \sin 2\theta \quad (13)$$

Substituting Eq. (13) into Eq. (11) and integrating,

$$\bar{\epsilon}_1 = \frac{\epsilon_x + \epsilon_y}{2} - \frac{\gamma_{xy}}{\pi} \quad (14)$$

If a similar arc is placed in the second quadrant, the same analysis will demonstrate that the output is:

$$\bar{\epsilon}_2 = \frac{\epsilon_x + \epsilon_y}{2} + \frac{\gamma_{xy}}{\pi} \quad (15)$$

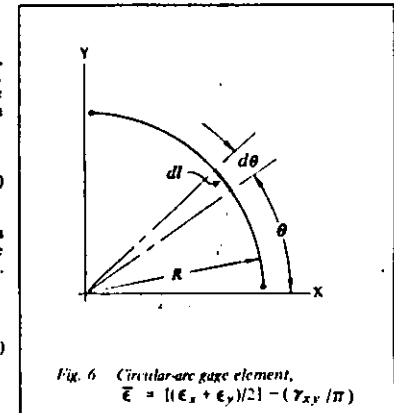


Fig. 6 - Circular-arc gage element, $\bar{\epsilon} = [(\epsilon_x + \epsilon_y)/2] - (\gamma_{xy}/\pi)$

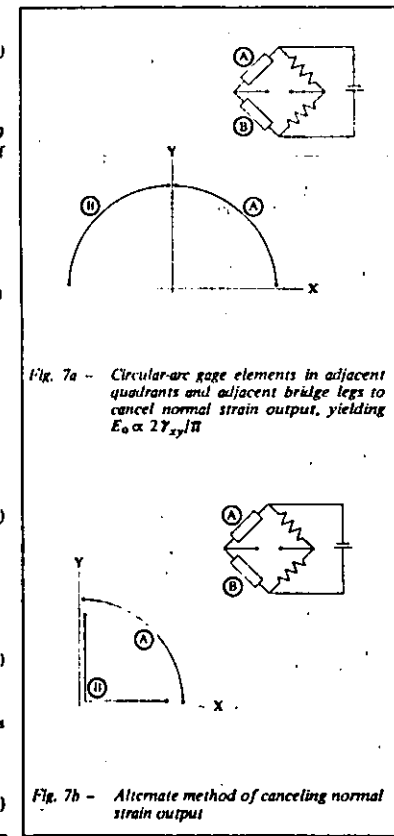


Fig. 7a - Circular-arc gage elements in adjacent quadrants and adjacent bridge legs to cancel normal strain output, yielding $\epsilon_0 \propto 2\gamma_{xy}/\pi$

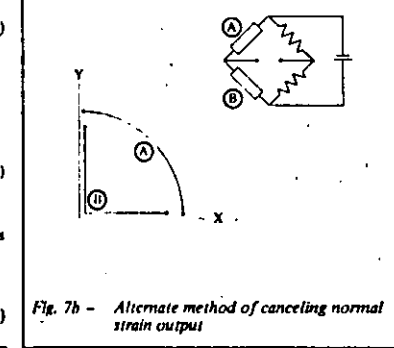


Fig. 7b - Alternate method of canceling normal strain output

Measurement of Thermal Expansion Coefficient Using Strain Gages

The thermal expansion coefficient is a very basic physical property which can be of considerable importance in mechanical and structural design applications of a material. Although there are many published tabulations of expansion coefficients for the common metals and standard alloys, the need occasionally arises to measure this property for a specific material over a particular temperature range. In some cases (e.g., new or special alloys, composites, etc.), there is apt to be no published data whatsoever on expansion coefficients. In others, data may exist (and eventually be found), but may encompass the wrong temperature range, apply to somewhat different material, or be otherwise unsuited to the application.

Historically, the classical means for measuring expansion coefficients has been the "dilatometer". In this type of instrument, the difference in expansion between a rod made from the test material and a matching length of quartz or vitreous silica is compared^{1,2}. Their differential expansion is measured with a sensitive dial indicator, or with an electrical displacement transducer. When necessary, the expansion properties of the quartz or silica can be calibrated against the accurately known expansion of pure platinum or copper. The instrument is normally inserted in a special tubular furnace or liquid bath to obtain the required temperatures. Making measurements with the dilatometer is a delicate, demanding task, however, and is better suited to the materials science laboratory than to the typical experimental stress analysis facility. This Tech Note provides an alternate method for easily and quite accurately measuring the expansion coefficient of a test material with respect to that of any reference material having known expansion characteristics.

The technique described here uses two well-matched strain gages, with one bonded to a specimen of the reference material, and the second to a specimen of the test material. The specimens can be of any size or shape compatible with the available equipment for heating and refrigeration (but specimens of uniform cross section will minimize potential problems with temperature gradients). Under stress-free conditions, the differential output between the gages on the two specimens, at any common temperature, is equal to the differential unit expansion ($\mu\text{in/in}$, or m/m). Aside from the basic simplicity and relative ease of making thermal expansion measurements by this method, it has the distinct advantage of requiring no specialized instruments beyond those normally found in a stress analysis laboratory. This technique can also be applied to the otherwise difficult task of determining directional expansion coefficients of materials with anisotropic thermal properties.

Because typical expansion coefficients are measured in terms of a few parts per million, close attention to procedural detail is required with any measurement method to obtain accurate results; and the strain gage method is not an exception to the rule. This Tech Note has been prepared as an aid to the gage user in utilizing the full precision of the modern foil strain gage for determining expansion coefficients. Given in the first of the following sections is an explanation of the technical principles underlying the method. The next section describes, in some detail, the strain-gage-related materials and procedures in making the measurement. Basically, the latter consists of essentially the same techniques required for any high-precision strain measurement in a variable thermal environment. Suggested refinements for achieving maximum accuracy are then given in the following section; after which, the principal limitations of the method are described.



MEASUREMENTS GROUP, INC.
P.O. Box 27777
Raleigh, North Carolina 27611, USA

(919) 365-3800
Telex 802-502
FAX (919) 365-3845

PRINCIPLE OF THE MEASUREMENT METHOD

When a resistance strain gage is installed on a stress-free specimen of any test material, and the temperature of the material is changed, the output of the gage changes correspondingly. This effect, present in all resistance strain gages, was formerly referred to as "temperature-induced apparent strain", but is currently defined as thermal output¹. It is caused by a combination of two factors. To begin with, in common with the behavior of most conductors, the resistivity of the grid alloy changes with temperature. An additional resistance change occurs because the thermal expansion coefficient of the grid alloy is usually different from that of the test material to which it is bonded. Thus, with temperature change, the grid is mechanically strained by an amount equal to the difference in expansion coefficients. Since the gage grid is made from a strain-sensitive alloy, it produces a resistance change proportional to the thermally induced strain. The thermal output of the gage is due to the combined resistance changes from both sources. The net resistance change can be expressed as the sum of resistivity and differential expansion effects as follows:

$$\frac{\Delta R}{R} = [\beta_G + (\alpha_S - \alpha_G)F_G] \Delta T \quad (1)$$

where: $\Delta R/R$ = unit resistance change

β_G = thermal coefficient of resistivity of grid material

$\alpha_S - \alpha_G$ = difference in thermal expansion coefficients between specimen and grid, respectively

F_G = gage factor of the strain gage

ΔT = temperature change from arbitrary initial reference temperature

The indicated strain due to a resistance change in the gage is:

$$\epsilon_i = \frac{\Delta R/R}{F_i} \quad (2)$$

where: F_i = instrument gage factor setting

Then, the thermal output in strain units can be expressed as:

$$\epsilon_{T(OGIS)} = \frac{[\beta_G + (\alpha_S - \alpha_G)F_G] \Delta T}{F_i} \quad (3)$$

where: $\epsilon_{T(OGIS)}$ = thermal output for grid alloy G on specimen material S

Or, in the usual case, with the instrument gage factor set equal to that of the strain gage, so that $F_i = F_G$,

$$\epsilon_{T(OGIS)} = \left[\frac{\beta_G}{F_G} + (\alpha_S - \alpha_G) \right] \Delta T \quad (4)$$

It should not be assumed from the form of Eq. (4) that the thermal output is linear with temperature, since all of the coefficients within the brackets are themselves functions of temperature. As an example, typical thermal output characteristics for a Micro-Measurements A-alloy gage (self-temperature-compensated constantan grid), bonded to steel, are represented by

the solid curve in Fig. 1. The lot of foil identified in the upper right corner of the graph was specially processed to minimize the thermal output over the temperature range from about -50° to $+300^\circ\text{F}$ (-45° to $+150^\circ\text{C}$). Strain gages fabricated from this lot of foil are intended for use only on material such as steel with a coefficient of expansion of approximately $6 \times 10^{-6}/^\circ\text{F}$ ($11 \times 10^{-6}/^\circ\text{C}$). If the gages are installed on some other material with a different coefficient of expansion, the result is to effectively rotate the curve in Fig. 1 about its reference point at

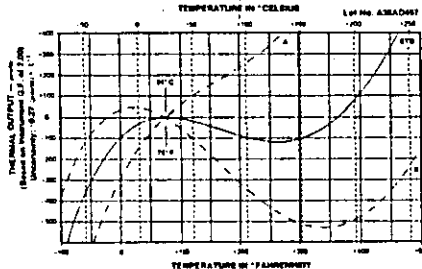


Fig. 1 — Rotation of the thermal output from a strain gage when installed on materials with differing thermal expansion coefficients.

$+75^\circ\text{F}$ ($+24^\circ\text{C}$). Installation on a material with a higher coefficient of expansion than steel will rotate the curve counterclockwise, while a material with a lower expansion coefficient than steel will cause clockwise rotation. For example, the broken curve labeled A in the figure illustrates the general effect of installing a gage from the subject lot on a beryllium alloy having an expansion coefficient of about $9 \times 10^{-6}/^\circ\text{F}$ ($16 \times 10^{-6}/^\circ\text{C}$). Similarly, if a gage from this lot were bonded to a titanium alloy with a somewhat lower expansion coefficient than steel, the thermal output would be shifted in the manner of the broken curve labeled B.

The principle of measuring expansion coefficients with strain gages then becomes evident from Fig. 1, since the rotation from one thermal output curve to the other is due only to the difference in thermal expansion properties between the materials represented by the two curves. An algebraic demonstration of the principle can be obtained by rewriting Eq. (4) twice; once for the gage installed on a specimen of the test material of unknown expansion coefficient α_S , and again for the same type of gage installed on a standard reference material with a known expansion coefficient α_R :

$$\epsilon_{T(OGIS)} = \left[\frac{\beta_G}{F_G} + (\alpha_S - \alpha_G) \right] \Delta T \quad (5a)$$

$$\epsilon_{T(OGIR)} = \left[\frac{\beta_G}{F_G} + (\alpha_R - \alpha_G) \right] \Delta T \quad (5b)$$

Subtracting Eq. (5b) from (5a), and rearranging,

$$\alpha_S - \alpha_R = \frac{(\epsilon_{T(OGIS)} - \epsilon_{T(OGIR)})}{\Delta T} \quad (6)$$

Thus, the difference in expansion coefficients, referred to a particular temperature range, is equal to the unit difference in thermal output for the same change in temperature. Although this technique for measuring expansion coefficients is widely applicable, and often the most practical approach, there is relatively little information about it in the technical literature. Representative applications are described in the bibliography to this Tech Note^{4,5}.

MEASUREMENT PROCEDURES

Reference Material

Selection of the material to be used as a reference standard is naturally an important factor in the accuracy of the method, as it is for any other form of differential dilatometry. In principle, the reference material could be any substance for which the expansion properties are accurately known over the temperature range of interest. In practice, however, it is often advantageous to select a material with expansion properties as close to zero as possible. Doing this will provide an output signal that closely corresponds to the "absolute" expansion coefficient of the test material, and permits a more straightforward test procedure. The thermal expansion of the reference material should also be highly repeatable, and stable with time at any constant temperature. In addition, the elastic modulus of the material should be great enough that mechanical reinforcement by the strain gage is negligible.

An excellent reference material with these and the other desirable properties is ULE™ Titanium Silicate Code 7971, available from Corning Glass Company, Corning, NY 14831.* As illustrated in Fig. 2, this special glass has an extremely low thermal expansion coefficient, particularly over the temperature range from about -50° to $+350^\circ\text{F}$ (-45° to $+175^\circ\text{C}$). It should be noted, however, that the material also has a very low coefficient of thermal conductivity. As a result, particular care should be exercised to achieve full thermal equilibrium when making measurements following a temperature change. Another potential disadvantage of titanium silicate as a reference material is its brittleness, since it will fracture readily if dropped on a hard surface. Because of the foregoing, a low-expansion metal (such as Invar or a similar alloy) may offer a preferable alternative if

*Also available from Micro-Measurements as Part No. TSB-1. See Appendix for specimen dimensions.

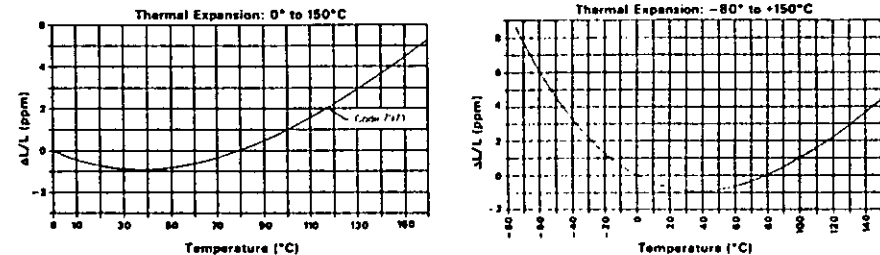


Fig. 2 — Thermal expansion characteristics of the titanium silicate reference material (data source: Corning Glass Company).

the alloy has repeatable and accurately known expansion properties over the temperature range of interest.

Strain Gage Selection

The type of strain gage selected for use in measuring expansion coefficients is also an important consideration, just as it is for stress analysis and transducer applications. Gage selection usually requires weighing a variety of factors which can directly or indirectly affect the suitability of a particular gage type to a specified measurement task. To assist gage users in this process, Measurements Group Tech Note TN-505 provides extensive background data for gage selection, along with procedures, recommendations, and application examples⁶. The subject Tech Note should serve as the primary reference on gage selection, supplemented here by special considerations applicable to the measurement of expansion coefficients.

For good accuracy, combined with ease of installation, a gage from Micro-Measurements CEA Series is ordinarily a suitable choice. This assumes that the temperature extremes for the measurements fall within the range of greatest stability and precision for the constantan foil in this type of gage [about -50° to $+150^\circ\text{F}$ (-45° to $+65^\circ\text{C}$)]. If a wider temperature range is involved, a gage from the WK Series becomes the preferred choice. The latter gage type is somewhat stiffer, however, and consideration of reinforcement effects may be necessary if the test material has a low modulus of elasticity, or the test specimen is thin and narrow.

In each of the foregoing cases, a 350Ω gage is preferable in order to minimize self-heating by the excitation current. The 350Ω gage is also advantageous in reducing the effects of small imbalances which may occur due to unsymmetric resistance changes in the leads with temperature. In addition, it is good practice, when feasible, to employ a medium gage length — say, 1/8 in. (3 mm) or larger — for more stable operation and improved heat transfer to the substrate.

Another gage parameter to be specified is the self-temperature-compensation (S-T-C) number. In principle, as indicated by Eq. (6), it should not matter what S-T-C number is selected. (Only the difference in thermal output, for the same gage type on two different materials, is involved in the expansion calculations. Practically, however, there are two considerations which may influence the choice. One of these is the availability of the selected gage in the desired series, gage pattern, and resistance.

numerical example

U.S. CUSTOMARY AND METRIC (SI) UNITS

Assume that a diaphragm pressure transducer is to be designed for a maximum rated pressure of 1000 psi (6.89 MPa), under which pressure the output (ϵ_o) from a steel diaphragm should be 2 mV/V. If the diaphragm diameter is to be 0.670 in (17.02 mm), find the following:

- (a) Diaphragm thickness
 (b) Center deflection
 (c) Resonant frequency
 (d) Approximate maximum diaphragm strain level

CONSTANTS*

U.S. Customary

$P = 1000 \text{ lbs/in}^2$
 $\epsilon_o = 2 \text{ mV/V}$
 $R_o = 0.335 \text{ in}$
 $E = 30 \times 10^6 \text{ psi}$
 $\gamma = 0.283 \text{ lbs/in}^3$
 $g = 386.4 \text{ in/sec}^2$

Metric (SI)

$P = 6.89 \text{ MPa}$
 $\epsilon_o = 2 \text{ mV/V}$
 $R_o = 8.51 \text{ mm}$
 $E = 207 \text{ GPa}$
 $D = 7.83 \times 10^{-3} \text{ kg/cm}^3 = \gamma/g$

- (a) From Eq. (4), solve for t

$$t = \sqrt{\frac{0.82 P R_o^2 (1-\nu^2) \times 10^3}{\epsilon_o E}}$$

$$t = \sqrt{\frac{0.82 \times 1000 \times (0.335)^2 [1-(0.285)^2] \times 10^3}{2 \times 30 \times 10^6}}$$

$$t = 0.0375 \text{ in}$$

$$t = \sqrt{\frac{0.82 \times 6.89 \times (8.51)^2 [1-(0.285)^2] \times 10^3}{2 \times 207 \times 10^9}}$$

$$t = 0.9529 \text{ mm}$$

- (b) From Eq. (5),

$$Y_c = \frac{3 P R_o^4 (1-\nu^2)}{16 \nu^3 E}$$

$$Y_c = \frac{3 \times 1000 \times (0.335)^4 [1-(0.285)^2]}{16 \times (0.0375)^3 \times 30 \times 10^6}$$

$$Y_c = 0.0014 \text{ in}$$

$$Y_c = \frac{3 \times 6.89 \times (8.51)^4 [1-(0.285)^2] \times 10^6}{16 \times (0.9529)^3 \times 207 \times 10^9}$$

$$Y_c = 0.0348 \text{ mm}$$

- (c) From Eq. (6),

$$f_n = \frac{0.469 t}{R_o^2} \sqrt{\frac{R E}{\gamma (1-\nu^2)}}$$

$$f_n = \frac{0.469 \times 0.0375}{(0.335)^2} \sqrt{\frac{386.4 \times 30 \times 10^6}{0.283 [1-(0.285)^2]}}$$

$$f_n = 33\,090 \text{ Hz}$$

$$f_n = \frac{0.469 \times 0.9529}{(8.51)^2} \sqrt{\frac{207 \times 10^9}{7.83 \times 10^{-3} [1-(0.285)^2]}}$$

$$f_n = 33\,102 \text{ Hz}$$

- (d) From Eq. (2),

$$\epsilon_{R_o} = -\frac{3 P R_o^3 (1-\nu^2)}{4 t^3 E}$$

$$\epsilon_{R_o} = -\frac{3 \times 1000 \times (0.335)^3 [1-(0.285)^2]}{4 \times (0.0375)^3 \times 30 \times 10^6}$$

$$\epsilon_{R_o} = -1832 \mu\text{in/in}$$

$$\epsilon_{R_o} = -\frac{3 \times 6.89 \times (8.51)^3 [1-(0.285)^2] \times 10^6}{4 \times (0.9529)^3 \times 207 \times 10^9}$$

$$\epsilon_{R_o} = -1830 \mu\text{m/m}$$

*The small differences occurring in comparable U.S. Customary and Metric results arise from rounding numbers in both sets of calculations.

MEASUREMENTS GROUP

TECH NOTE

TN-510

Diaphragm
Pressure Transducers

Design Considerations For Diaphragm Pressure Transducers

The following notes are intended only as general guidance for the preliminary design of diaphragm pressure transducers. The actual design and development process involves arriving at the best compromise (relative to the performance specifications) of sensitivity, linearity, and frequency response, as determined primarily by the diaphragm diameter and thickness.

The formulas included here are based upon one or more of the following assumptions:

- Uniform diaphragm thickness
- Small deflections
- Infinitely rigid clamping around the diaphragm periphery

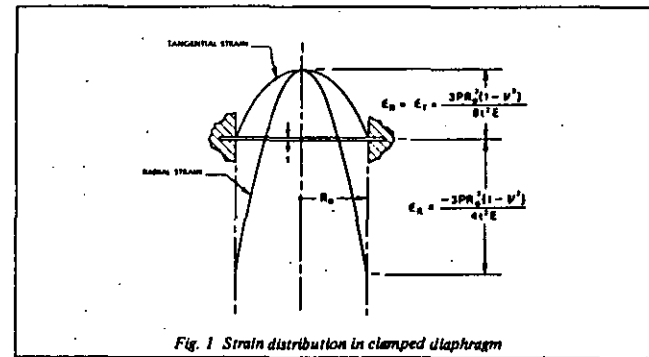
- Perfectly elastic behavior

- Negligible stiffening and mass effects due to the presence of the strain gage on the diaphragm

To the degree that the actual transducer fails to satisfy all of the above assumptions, the formulas will be inaccurate. Because of this, the formulas should be used only in the initial stages of transducer development to determine the approximate proportions of the transducer.

SENSITIVITY

The strain distribution in a rigidly clamped diaphragm under uniform pressure distribution is shown in Fig. 1.



MEASUREMENTS GROUP, INC.
 P.O. Box 27777
 Raleigh, North Carolina 27611, USA

(919) 365-3800
 Telex 802-502
 FAX (919) 365-3945

© Copyright Measurements Group, Inc., 1982
 All Rights Reserved

The radial and tangential strains at the center of the diaphragm are identical, and expressed by:

$$\epsilon_{R_c} = \epsilon_{T_c} = \frac{3PR_o^2(1-\nu^2)}{8t^3E} \quad \text{Eq. (1)}$$

where:

	U.S. CUSTOMARY UNITS	METRIC UNITS
P = pressure	psi	Pa
R_o = diaphragm radius	in	mm
t = diaphragm thickness	in	mm
ν = Poisson's ratio	dimensionless	
E = modulus of elasticity	psi	Pa

The radial strain decreases rapidly as the radius increases, becoming negative, and equal to twice the center strain at the edge. The tangential strain decreases from the center value to zero around the periphery of the diaphragm. Thus,

$$\epsilon_{R_o} = -\frac{3PR_o^2(1-\nu^2)}{4t^3E} \quad \text{Eq. (2)}$$

$$\epsilon_{T_o} = 0 \quad \text{Eq. (3)}$$

Reference to Fig. 2 will demonstrate that the Micro-Measurements "JB" strain gage pattern has been designed to take maximum advantage of the diaphragm strain distribution described above. Since the tangential strain falls off from the center value at only one-third the rate of the radial strain, the central sensing elements of the gage are oriented tangentially. Similarly, the radial sensing elements are located near the edge of the diaphragm because of the high radial strain in the region. Taking account of the sign difference in the strains sensed by the radial and tangential elements, and dividing the elements into symmetrical pairs, permits incorporating a full bridge into a single strain gage. In terms of optimizing the strain gage design, it can also be noticed from Fig. 2 that the solder tabs have been located in a region of low strain.

Averaging the strain over the region covered by each sensing element (assuming a gage factor of 2.0), and averaging the outputs of all sensing elements, the total gage output (ϵ_o) in millivolts per volt can be expressed approximately by the following formula:

$$\epsilon_o = 0.82 \frac{PR_o^2(1-\nu^2)}{t^3E} \times 10^3, \text{ mV/V} \quad \text{Eq. (4)}$$

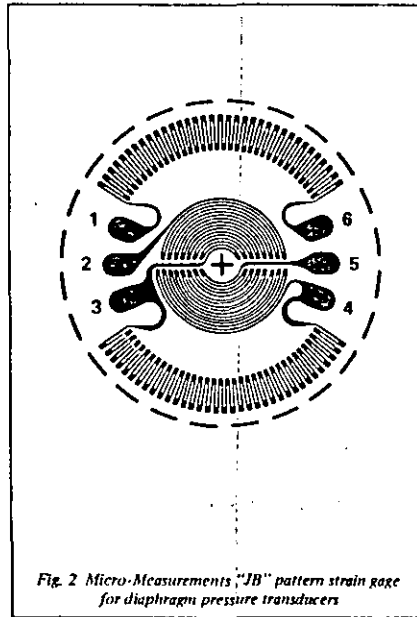


Fig. 2 Micro-Measurements "JB" pattern strain gage for diaphragm pressure transducers

LINEARITY

The preceding equations for diaphragm strain and output indicate that the output is proportional to the applied pressure. This precise linearity applies, however, only for vanishingly small deflections. In the case of finite deflections, the diaphragm pressure transducer is inherently nonlinear, and, becomes more so, the larger the deflection. As a general rule, the deflection of the diaphragm at the center must be no greater than the diaphragm thickness; and, for linearity in the order of 0.3%, should be limited to one quarter the diaphragm thickness.

Following is the formula for diaphragm deflection, based upon small-deflection theory:

$$Y_c = \frac{3PR_o^4(1-\nu^2)}{16t^3E} \quad \text{Eq. (5)}$$

where: Y_c = center deflection, in (mm)

FREQUENCY RESPONSE

In order to faithfully respond to dynamic pressures, it is necessary that the resonant frequency of the diaphragm be considerably higher than the highest applied frequency. Depending strongly upon the degree of damping in the diaphragm-strain gage assembly and in the fluid in contact with the diaphragm, the resonant frequency should be at least three to five times as high as the highest applied frequency. The subject of proper design for accurate dynamic response is too complex and extensive to be included here. However, for transducers subject to high frequencies or to sharp pressure wave fronts involving high-frequency components, careful consideration must be given to frequency response, both in terms of amplitude and phase-shift.

For reference purposes only, and subject to the assumptions listed earlier, the undamped resonant frequency of a rigidly clamped diaphragm can be expressed as follows:

$$f_n = \frac{0.469t}{R_o^2} \sqrt{\frac{gE}{\gamma(1-\nu^2)}} \cdot \text{Hz} \quad \text{Eq. (6)}$$

where:

	U.S. CUSTOMARY UNITS	METRIC UNITS
--	----------------------	--------------

g = acceleration of gravity	386.4 in/sec ²	
γ = specific weight of diaphragm material	lbs/in ³	kg/cm ³
$\gamma/g = \rho$		

CONSTRUCTION

For maximum accuracy and minimum hysteresis, it is common practice to design pressure transducers so that the diaphragm is an integral part of the transducer body (Fig. 3).

It is neither necessary nor desirable to try to machine the body of the transducer to a sharp internal corner at the junction with the diaphragm. The presence of the fillet radius, however, is merely one of the ways in which practical transducer construction differs from the idealized concept corresponding to the earlier assumptions and the equations given here. Because of this and the other differences, the transducer behavior will necessarily differ from the ideal; and experimental development will obviously be required to optimize the performance of a particular transducer.

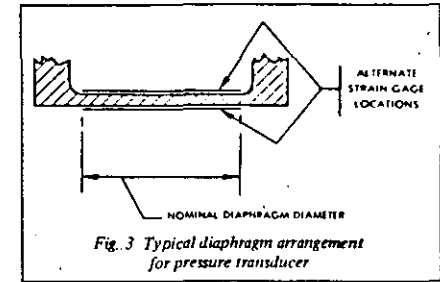


Fig. 3 Typical diaphragm arrangement for pressure transducer

WIRING

It will be noticed that the internal circuit of the "JB" pattern strain gage has two adjacent corners of the full bridge left open (Fig. 4). The open bridge corners are left for the introduction of zero-shift vs. temperature correction, and subsequent restoration of zero balance.

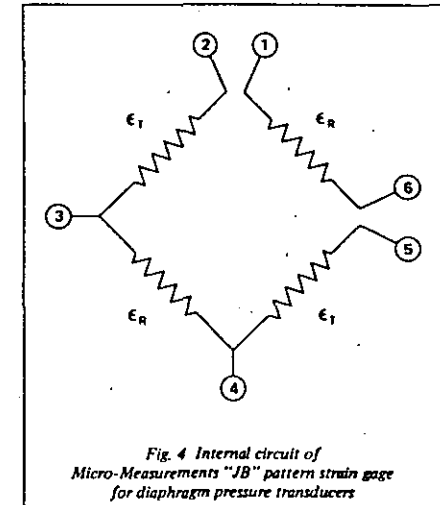


Fig. 4 Internal circuit of Micro-Measurements "JB" pattern strain gage for diaphragm pressure transducers

NOTE: See Micro-Measurements Catalog 500 for "JB" pattern dimensions and price and ordering information. Note also the "JC" patterns, which are similar except for gage resistance.

Diaphragms larger than 1/2 in (12.5 cm) in diameter generally require the use of special "linear" patterns. For additional information, contact our Applications Engineering Department.

Figure 1 shows the variation of apparent strain with temperature for a variety of strain gage alloys bonded to steel. These data are illustrative only, and not for use in making corrections. It should be noted, in fact, that the curves for constantan and Karma are for non-self-temperature-compensated alloys. With self-temperature compensation (Section 2.1.2), as employed in Micro-Measurements strain gages, the apparent strain characteristics of these alloys are adjusted to minimize the error over the normal range of working temperatures.

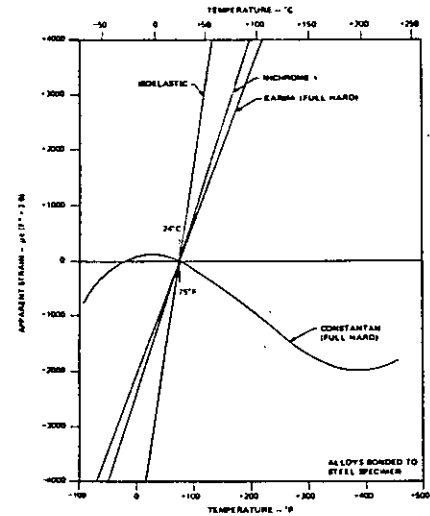


FIG. 1

As indicated by Fig. 1, the errors due to apparent strain can become extremely large as temperatures deviate from the arbitrary reference temperature (ordinarily, room temperature) with respect to which the apparent strain is measured. The illustration shows distinctly the necessity for compensation or correction if accurate static strain measurements are to be made in an environment involving temperature changes.

With respect to the latter statement, it should be remarked that if it is feasible to bring the gaged test part to the test temperature in the test environment, maintaining the test part completely free of mechanically or thermally induced stresses, and balance the strain indicator for zero strain under these conditions, no apparent strain error exists when subsequent strain measurements are made at this temperature. In other words, when no temperature change occurs between the stress-free and stressed conditions, strain measurements can be made without compensating or correcting for apparent strain. In practice, however, it is rare that the foregoing requirements can be satisfied, and the stress analyst ordinarily finds it necessary to take full account of apparent strain effects.

Also, in the case of purely dynamic strain measurements, where there is no need to maintain a stable zero-strain reference, temperature-induced apparent strain may be of no consequence. This is because the frequency of the dynamic strain signal is usually very high with respect to the frequency of temperature change, and the two signals are readily separable. If, however, there is combined static/dynamic strain, and the static component must also be measured, or if the frequency of temperature change is of the same order as the strain frequency, apparent strain effects must again be considered.

2.1 Compensation for Apparent Strain

2.1.1 Compensating (Dummy) Gage

In theory, at least, the error due to apparent strain can be completely eliminated by employing, in conjunction with the "active" strain gage, but connected in an adjacent arm of the Wheatstone bridge circuit, an identical compensating or "dummy" gage — mounted on an unstrained specimen made from the identical material as the test part, and subjected always to the same temperature as the active gage. Under these hypothetical conditions, the apparent strains manifested by the two gages should be identical. And, since identical resistance changes in adjacent arms of the Wheatstone bridge do not unbalance the circuit, the apparent strains in the active and dummy strain gages should cancel exactly — leaving only the stress-induced strain in the active strain gage to be registered by the strain indicator. For this to be precisely true requires additionally that the leadwires to the active and dummy gages be the same length and be routed together so that their temperatures change identically.

The principal problems encountered in this method of temperature compensation are those of establishing and maintaining the three sets of identical conditions postulated above. To begin with, it is sometimes very difficult to arrange for the placement of an unstrained specimen of the test material in the test environment; and even more difficult to make certain that the specimen remains unstrained under all test conditions. There is a further difficulty in ensuring that the temperature of the compensating gage on the unstrained specimen is always identical to the temperature of the active gage. This problem becomes particularly severe whenever there are temperature gradients or transients in the test environment. And, as indicated in the preceding paragraph, the same considerations apply to the leadwires. Finally, it must be recognized that no two strain gages — even from the same lot or package — are precisely identical. For most static strain measurement tasks in the general neighborhood of room temperature, the difference in apparent strain between two gages from the same lot is negligible; but the difference may become evident (and significant) when measuring strains at temperature extremes such as those involved in high-temperature or cryogenic work. In these instances, point-by-point correction for apparent strain will usually be necessary. With non-self-temperature-compensated gages, the gage-to-gage differences in apparent strain may be so great as to preclude dummy compensation for temperatures which are remote from room temperature.

In general, when the three identity criteria already mentioned can be well satisfied, the method of compensating with a dummy gage is a very effective technique for controlling the apparent strain error. There is, moreover, a special class of strain measurement applications which is particularly adaptable to compensation of apparent strain with a second

gage. This class consists of those applications in which the ratio of the strains at two different but closely adjacent (or at least thermally adjacent) points on the test object are known a priori. Included in this class are bars in torsion, beams in bending, columns, diaphragms, etc., all stressed within their respective proportional limits. In these applications, the compensating gage can, often be located strategically on the test member itself so as to provide two active gages which undergo the same temperature variations while sensing strains that are preferably opposite in sign and of known ratio. The two gages in adjacent arms of the Wheatstone bridge circuit then function as an active half-bridge.

For example, when strain measurements are to be made on a beam which is thin enough so that under test conditions the temperatures on the two opposite surfaces normal to the plane of bending are the same, the two strain gages can be installed directly opposite each other on these surfaces (Fig. 2a). The active half-bridge thus formed will give effective temperature compensation over a reasonable range of temperatures and, since the strains sensed by the gages are equal in magnitude and opposite in sign, will double the output signal from the Wheatstone bridge. Similarly, for a bar in torsion (Fig. 2b), the two gages can be installed adjacent to each other and aligned along the principal axes of the bar (at 45 deg to the longitudinal axis). As in the case of the beam, excellent temperature compensation can be achieved, along with a doubled output signal.

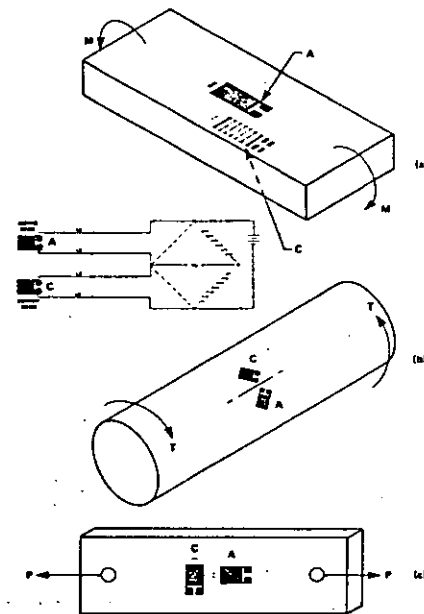


FIG. 2

When making strain measurements along the axis of a column or tension link, the compensating gage can be mounted on the test member adjacent to the axial gage and

aligned transversely to the longitudinal axis to sense the Poisson strain (Fig. 2c). The result, again, is compensation of the apparent strain, accompanied by an augmented output signal [by the factor $(1 + \nu)$ in this case]. It should be borne in mind in this application, however, that the accuracy of the strain measurement is somewhat dependent upon the accuracy with which the Poisson's ratio of the test material is known. For most common structural materials, the percent error in strain measurement is about one-fourth the percent error in Poisson's ratio. A further caution is necessary when strain gages are mounted transversely on small-diameter rods (or, for that matter, in small-radius fillets or holes). Lines has shown (see Appendix) that under these conditions the apparent strain characteristics of a strain gage are different than when the gage is mounted on a flat surface of the same material.

In all strain-measurement applications which involve mounting the compensating gage on the test object itself, the relationship between the strains at the two locations must be known with certainty. In a beam, for example, there must be no indeterminate axial or torsional loading; and the bar in torsion must not be subject to indeterminate axial or bending loads. This requirement for a priori knowledge of the strain distribution actually places these and most similar applications in the class of transducers. And the same method of compensation is universally employed in commercial strain gage transducers. Such transducers, however, ordinarily employ full-bridge circuits and special arrangements of the strain gages to eliminate the effects of extraneous forces or moments.

2.1.2 Self-Temperature-Compensated Strain Gages

The metallurgical properties of certain strain gage alloys — in particular, constantan and modified Karma (Micro-Measurements A- and K-alloys, respectively) — are such that these alloys can be processed to minimize the apparent strain over a wide temperature range when bonded to test materials with thermal expansion coefficients for which they are intended. Strain gages employing these specially processed alloys are referred to as self-temperature-compensated.

Since the advent of the self-temperature-compensated strain gage, the requirement for a matching unstrained dummy gage in the adjacent arm of the Wheatstone bridge has been relaxed considerably. It is now normal practice when making strain measurements at or near room temperature to use a single self-temperature-compensated gage in a quarter-bridge arrangement, completing the bridge circuit with a stable fixed resistor in the adjacent arm (Fig. 3). Such "bridge-completion" resistors, with temperature coefficients of resistance not exceeding 1×10^{-6} per °C, are supplied by Micro-Measurements and are incorporated in most modern strain indicators.

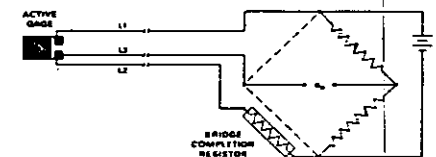


FIG. 3

As an alternative to the preceding methods, a quick graphical correction for the transverse sensitivity can be made through the use of Figure 2. To use the graph, the first step is to calculate:

$$\left(\frac{\hat{\epsilon}_t}{\hat{\epsilon}_a}\right)_1 = \frac{\hat{\epsilon}_2}{\hat{\epsilon}_1} = \frac{\hat{\epsilon}_y}{\hat{\epsilon}_x} \quad (\text{Gage No. 1})$$

$$\left(\frac{\hat{\epsilon}_t}{\hat{\epsilon}_a}\right)_2 = \frac{\hat{\epsilon}_1}{\hat{\epsilon}_2} = \frac{\hat{\epsilon}_x}{\hat{\epsilon}_y} \quad (\text{Gage No. 2})$$

Having done this, it is only necessary to enter the graph at the appropriate value of K_t , move upward to the line (or interpolated line) representing the observed (indicated) strain ratio, $\hat{\epsilon}_t/\hat{\epsilon}_a$ for that particular rosette element, and horizontally to the vertical scale on the left to read the correction factor.

Then,

$$\epsilon_x = \epsilon_1 = C_1 \hat{\epsilon}_1$$

Similarly,

$$\epsilon_y = \epsilon_2 = C_2 \hat{\epsilon}_2$$

Following is a numerical example utilizing first Equations (6a) and (7a), and then Figure 2.

Assume that the indicated strains for rosette elements (1) and (2) along the x and y axes are, respectively:

$$\hat{\epsilon}_1 = +1530 \mu\epsilon$$

$$\hat{\epsilon}_2 = +920 \mu\epsilon$$

Assume also that $K_t = -0.06$. Substituting into Equations (6a) and (7a), with $\nu_0 = 0.285$,

$$\epsilon_x = (1 + 0.285 \cdot 0.06)(1530 + 0.06 \cdot 920) = 1612 \mu\epsilon$$

$$\epsilon_y = (1 + 0.285 \cdot 0.06)(920 + 0.06 \cdot 1530) = 1029 \mu\epsilon$$

For use with the correction graph, Figure 2,

$$\left(\frac{\hat{\epsilon}_t}{\hat{\epsilon}_a}\right)_1 = \frac{920}{1530} = 0.601 \approx 0.6$$

$$\left(\frac{\hat{\epsilon}_t}{\hat{\epsilon}_a}\right)_2 = \frac{1530}{920} = 1.663 \approx 1.65$$

Following the line for $K_t = -0.06$ upward, interpolating the location of $(\hat{\epsilon}_t/\hat{\epsilon}_a)_1 = 0.6$, and $(\hat{\epsilon}_t/\hat{\epsilon}_a)_2 = 1.65$, and reading the respective values of the correction factor,

$$C_1 = 1.06; C_2 = 1.12$$

From which,

$$\epsilon_x = C_1 \hat{\epsilon}_1 = 1.06 \cdot 1530 = 1620 \mu\epsilon$$

$$\epsilon_y = C_2 \hat{\epsilon}_2 = 1.12 \cdot 920 = 1030 \mu\epsilon$$

CORRECTION FOR SHEAR STRAIN

A two-gage, 90-degree rosette, or "T"-rosette, is sometimes used for the direct indication of shear strain. It can be shown that the shear strain along the bisector of the gage axes is, in this case, numerically equal to the difference in normal strains on these axes. Thus, when the two gage elements of the rosette are connected in adjacent arms of a Wheatstone bridge, the indicated strain is equal to the indicated shear strain along the bisector, requiring at most correction for the error due to transverse sensitivity. The latter error can be corrected for very easily if both gages have the same transverse sensitivity,

since the error is independent of the state of strain. The correction factor for this case is:

$$C_s = \frac{1 - \nu_0 K_t}{1 - K_t} \quad (8)$$

The actual shear strain is obtained by multiplying the indicated shear strain by the correction factor. Thus,

$$\gamma = C_s \hat{\gamma} = C_s (\hat{\epsilon}_x - \hat{\epsilon}_y) = \frac{1 - \nu_0 K_t}{1 - K_t} (\hat{\epsilon}_x - \hat{\epsilon}_y)$$

For convenience, the shear strain correction factor is plotted in Figure 3 against K_t , with $\nu_0 = 0.285$. Since this correction factor is independent of the state of strain, it can again be incorporated in the gage factor setting on the strain-indicating instrumentation if desired. This can be done by setting the gage factor control at:

$$F_v = F \frac{1 - K_t}{1 - \nu_0 K_t} \quad (9)$$

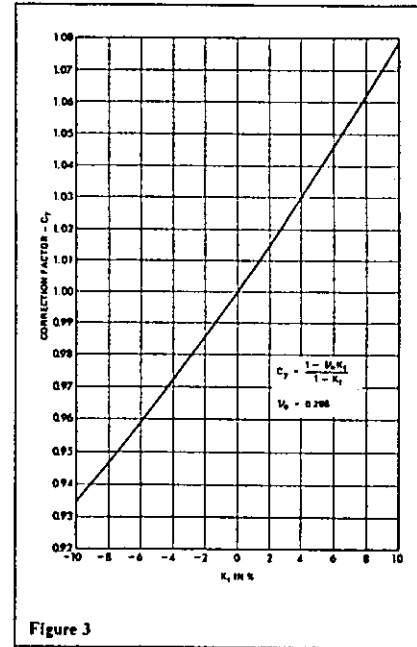


Figure 3

With this change, the strain indicator will indicate the actual shear strain along the bisector of the gage axis, already corrected for transverse sensitivity in the strain gages.

THREE-GAGE RECTANGULAR (45°) ROSETTE

When the directions of the principal axes are unknown, three independent strain measurements are required to completely determine the state of strain. For this purpose, a three-gage rosette should be used, and the rectangular rosette is generally the most convenient form.

If the transverse sensitivity of the gage elements in the rosette is other than zero, the individual strain readings will be in error, and the principal strains and stresses calculated from these data will also be incorrect.

Correction for the effects of transverse sensitivity can be made either on the individual strain readings or on the principal strains or principal stresses calculated from these. Numbering the gage elements consecutively, elements (1) and (3) correspond directly to the two-gage, 90-degree rosette, and correction can be made with Equations (6) and (7), or (6a) and (7a), or (by properly setting the gage factor control on the strain indicator) with Equations (6b) and (7b). The center gage of the rosette requires a special correction relationship since there is no direct measurement of the strain perpendicular to the grid. The correction equations for all three gages are listed here for convenience:

$$\epsilon_1 = \frac{1 - \nu_0 K_t}{1 - K_t} (\hat{\epsilon}_1 - K_t \hat{\epsilon}_3) \quad (10)$$

$$\epsilon_2 = \frac{1 - \nu_0 K_t}{1 - K_t} [\hat{\epsilon}_2 - K_t (\hat{\epsilon}_1 + \hat{\epsilon}_3 - \hat{\epsilon}_2)] \quad (11)$$

$$\epsilon_3 = \frac{1 - \nu_0 K_t}{1 - K_t} (\hat{\epsilon}_3 - K_t \hat{\epsilon}_1) \quad (12)$$

where: $\hat{\epsilon}_1, \hat{\epsilon}_2, \hat{\epsilon}_3$ = indicated strains from the respective gage elements.

$\epsilon_1, \epsilon_2, \epsilon_3$ = corrected strains along the gage axes.

It should be noted that Equations (10), (11), and (12) are based upon the assumption that the transverse sensitivity is the same, or effectively so in all gage elements, as it is in stacked rosettes. This may not be true for planar foil rosettes, since the individual gage elements do not all have the same orientation with respect to the direction in which the foil was rolled. It is common practice, however, to etch the rosette in a position of symmetry about the foil rolling direction, and therefore the transverse sensitivities of gage elements (1) and (3) will be nominally the same, while that of element (2) may differ. Correction sensitivities among the gage elements are given in the Appendix.

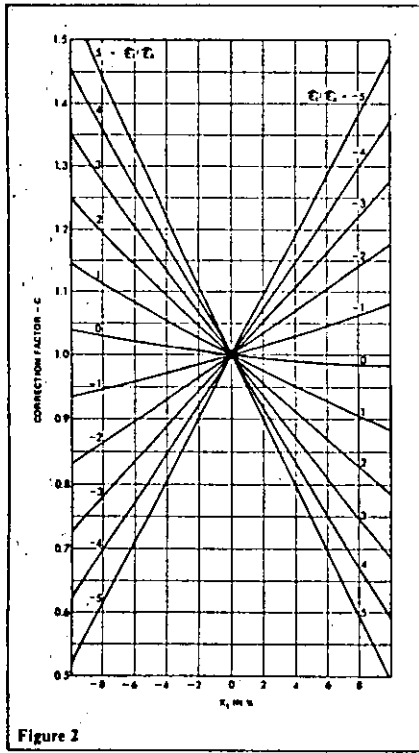


Figure 2

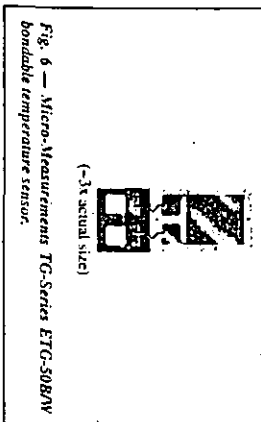


Fig. 6 — Micro-Measurements TG-Series ETG-508BN bondable temperature sensor.

Temperature measurement also requires care and consideration to obtain accurate expansion data. Typically, a temperature-sensing probe is placed immediately adjacent to the gage, and in intimate contact with the specimen surface, to indicate the specimen/gage temperature. This procedure assumes that previous verification has been made, by multiple temperature measurements on the specimen as necessary, to assure uniform specimen temperature under conditions of thermal equilibrium in the test chamber. Since the materials in the reference and test specimens normally differ in their thermal conductivity and specific heat, it is necessary that the temperatures at both gage sites be measured. The temperature must be the same, of course, whenever paired strain readings are made.

Depending primarily on personal preference and instrumentation availability, temperatures can be measured either with thermocouples or with resistance temperature sensors. If a thermocouple is employed on each specimen, Type J (iron-constantan) is preferred, assuming that the test temperature range is compatible with this type. The sensing junction should be small, as should the leads/wires (in the range of AWG 30 to AWG 26 (0.25 to 0.4 mm)), and premium grade thermocouple wire should be selected. Heat transfer from the specimen to the junction can be improved by laping the first 2 to 3 in (50 to 75 mm) of the extension wires to the specimen surface.

An alternate approach is to use resistance temperature sensors such as Micro-Measurements TG-Series (Fig. 6). The temperature sensor looks like a strain gage, and has essentially the same construction except that the grid is made from high-purity nickel foil. It is installed with standard strain gage installation procedures, and should be mounted side-by-side with the strain gage on the specimen surface. Because it is physically like the strain gage, and is attached to the specimen in the same way, the temperature sensor has about the same heat-transfer characteristics and thermal time constant as the strain gage. When used in conjunction with a specially designed passive resistance network for linearization and signal scaling (Micro-Measurements Type LST), it permits direct measurement of temperature with any conventional strain indicator. The small size and low stiffness of the TG-Series temperature sensor prevent minimum mechanical restraint to the free thermal expansion and contraction of the specimen.

Making Expansion Measurements

For any method of dilatometry, it is always necessary that the reference and test specimens be exposed to at least two different temperatures in measuring the expansion coefficient. The

actual means of achieving the desired temperatures in a particular case depends on the temperatures involved, and on the available facilities. These may consist, for instance, of ovens or liquid baths, or various other forms of environmental chamber. The strain gage method imposes no special restrictions on the nature or design of the chamber. On the contrary, the size and shape of the specimen can usually be adapted to suit the existing facilities. Since the available equipment varies widely from one laboratory to the next, the following remarks are limited to the general requirements for any dilatometric temperature chamber.

Two of the most desirable features of a chamber for measuring expansion coefficients are uniformity and stability of temperature. To avoid errors due to the development of thermal stresses in the specimen, the temperature should be uniform throughout the specimen at the time of measurement. This condition can be established only if the chamber temperature at equilibrium is essentially uniform — at least in the region containing the specimens. Temperature stability in the chamber is also necessary to permit measuring specimen temperatures and strains under static, nonvarying conditions.

Thermal equilibrium in the specimen can be achieved in a chamber equipped with a forced convection system to vigorously circulate the heat-transfer medium past the specimen surfaces. Heating and cooling rates should also be kept low to minimize temperature gradients perpendicular to the specimen surface. The required condition of uniform temperature throughout the specimen is difficult to judge, however, and is not necessarily assured by observing equal temperature readings at different points on the surface. One of the most effective ways to test for control over the uniformity of specimen temperature is to make a continuous plot of strain gage output versus temperature over the working temperature range — in both the heating and cooling directions. In this process, the temperature is changed incrementally, and, at each test temperature, after the specimen is evidently in thermal equilibrium, the temperature and thermal output are recorded and plotted. If uniformity of specimen temperature is actually achieved, the heating and cooling legs of the plotted curve should very nearly coincide. If, on the other hand, the two portions of the curve are significantly separated to form a hysteresis loop, a likely cause is nonuniform temperature distribution through the thickness of the specimen. In the latter case, the heating and cooling rates must be lowered, or thermal stabilization times increased, or other measures taken to essentially eliminate the temperature gradients.

Means must be provided for supporting the specimens in the chamber so that friction cannot impede expansion or contraction. In some cases, a simple way to accomplish this is to suspend the specimens from one end. Although the specimen may be strained slightly by its own weight, the strain is constant (as long as the elastic modulus is essentially constant), and does not affect the change in thermal output with temperature. If the elastic modulus of the test material changes significantly over the range of temperatures to be encountered, the error due to this effect must be evaluated to determine the suitability of the method. Another approach is to lay the specimens on the floor of the chamber or compartment, supported by a layer of fiber-glass cloth or some other low-friction medium. When this method is used, its effectiveness should be verified by observing the behavior of the thermal output as the specimen is cycled through the working temperature range. Erratic output hysteresis, or lack of repeatability may indicate excessive friction.

Briefly performing actual measurements to determine the coefficient of expansion, the entire system, including both specimens (with gages installed and power applied), should be stabilized by cycling several times to temperatures at least 100°F (50°C) above the highest, and below the lowest, test temperatures. One of the reasons for this procedure is that residual stresses are generally present in all of the components — the reference and test specimens, the gages as manufactured and installed, the leads/wires, etc. Thermal cycling is intended to relax and/or redistribute any residual stresses which might otherwise change during the test and cause the data to be nonreproducible. The cycling procedure should be performed at low enough rates of temperature change to minimize thermal stresses in the specimens due to temperature gradients. Otherwise, the thermal stress, superimposed on the residual stress, may cause yielding, and thus defeat the purpose of the cycling.

Normally, after the second or third stabilizing cycle, the thermal output at any given temperature should be highly repeatable. If not, and if the lack of repeatability is significant compared to the accuracy required from the test, the sources of the variability must be found. In such cases, the problem may be associated with the temperature, or the strain, or both. Careful re-reading of this Tech Note may provide the clue for finding and correcting the trouble. Further assistance, if needed, can be obtained from the Measurements Group Applications Engineering Department.

Following stabilization, verified by reproducible strain indications throughout the temperature range, the user is ready to perform the final measurements for determining the thermal expansion properties of the test material. When the oven or other chamber is such that only a single specimen can be accommodated the two specimens are tested one at-a-time, using the circuit of Fig. 5a. The resulting two sets of thermal output data are subtracted (and the difference divided by the temperature change) as indicated by Eq. (6) to give the differential thermal expansion coefficient. With the preferable arrangement, having both specimens together in the chamber, the measurements can be made separately as in Fig. 5a, or the differential thermal output can be read directly as shown in Fig. 5b.

Special Precautions and Refinements for Improving Accuracy

When attempting to achieve greater and greater accuracy with the strain gage method (or with any method), it is necessary to examine ever smaller effects which may introduce errors. In some instances, these second-order errors are well defined, systematic in nature, and responsive to routine procedures for correction or elimination. In others, the cause-and-effect relationship is more nebulous, and error reduction is accomplished primarily by technique refinement — i.e., by removing or minimizing all of the known possible sources of error.

An example of a readily correctable inaccuracy (in certain cases) is the error due to transverse sensitivity. This error arises because the strain field induced in the gage grid by the difference in thermal expansion between the specimen and grid [Eq. (1)] is generally different from that employed in gage factor calibration. When both the reference and test materials are isotropic in their thermal expansion properties, the transverse

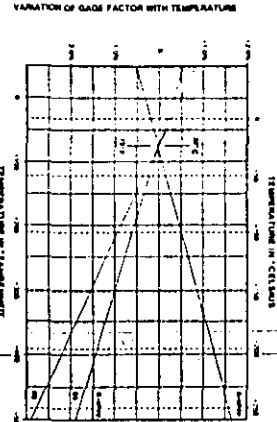


Fig. 7 — Gage factor variation with temperature (typical) for A- and K-dilute strain gages.

sensitivity error, which is ordinarily quite small, can be corrected for rather easily. Although not derived here, correction can be made by multiplying the difference in thermal outputs [Eq. (6)] by the factor $(1 - 0.288 K_1 / K_2 + K_1)$, where K_1 is the detransversely sensitive sensitivity of the gage in use. This correction factor is not applicable to anisotropic materials for which case differential thermal outputs between a reference gage and two perpendicularly oriented specimen gages are required to correct for transverse sensitivity.

Another minor error source is the variation of gage factor with temperature. The gage factor specified for Micro-Measurements strain gages is measured at +75°F (+2.3°C). At any other temperature it is slightly different. With constant gages, for example, the gage factor varies directly with temperature, at a rate of about 0.5% per 100°F (0.9% per 100°C). In contrast, the gage factor of K-dilute (modified Karma) gages varies inversely with temperature. The rate of change depends on the 5:1:1 number of the gage, but is generally in the range from -4.5 to -11.0% per 100°F (-0.9 to -1.8% per 100°C). Representative plots of gage factor variation with temperature are illustrated in Fig. 7 for both types of gages. The technical data sheet contained in each gage package includes a graph of the gage factor variation applicable to that gage type.

Complete elimination of the small error introduced by gage factor variation is not always feasible, but first-order correction, to remove most of the error, is relatively simple. When expansion measurements are made incrementally across the working temperature range, the differential thermal output for each increment in temperature can be corrected individually. This is done by multiplying the difference in indicated thermal outputs from the specimen and reference gages by the factor $(1 + \Delta F_1 / F_1)$. The term $\Delta F_1 / F_1$ in the foregoing is the decimalized change in gage factor (with sign) corresponding to the middle temperature of each measurement increment. It can usually be read with sufficient accuracy directly from the graph on the technical data sheet accompanying the gages.

Sometimes, the average differential expansion coefficient is to be determined over the full temperature range by making only two sets of measurements, at the temperature extremes. The same correction procedure can be applied, using the $\Delta F_1 / F_1$ for the mid-range temperature, but it will be much less effective because the thermal output is a nonlinear function of temperature.

When the two quadrants are connected as adjacent legs of a Wheatstone bridge circuit (Fig. 7a), so that their difference appears as a signal, the combined output is:

$$E_o \propto \frac{2\gamma_{xy}}{\pi} \quad (16)$$

An alternate method of canceling the unwanted normal-strain term in Eq. (14) is shown in Fig. 7b. In this case, two half gage-length linear elements are oriented along the X and Y axes, respectively, and connected in series to form one leg of a Wheatstone bridge. When a single circular-arc quadrant is used for the adjacent bridge leg, the output signal becomes:

$$E_o \propto \frac{\gamma_{xy}}{\pi} \quad (17)$$

Figure 8 illustrates a variety of gage-element configurations and their respective outputs. It is evident that the simplest approach to shear-strain measurement is the 90-deg rosette. When the maximum shear stress or the principal stresses are required, and the principal axes are unknown, the three-gage 45-deg rosette is the most convenient choice.

CORRECTION FOR TRANSVERSE SENSITIVITY

Up to this point, the effect of transverse sensitivity on shear-strain indication has been neglected. However, the correction for transverse sensitivity is particularly simple in the case of shear strain, and consists of multiplying the indicated shear strain by the factor $[(1 - \nu_o K_T) / (1 - K_T)]$, where K_T represents the transverse sensitivity of the strain gages used to generate the indicated shear-strain output, and ν_o is the Poisson's ratio of the material on which the manufacturer measured the gage factor.

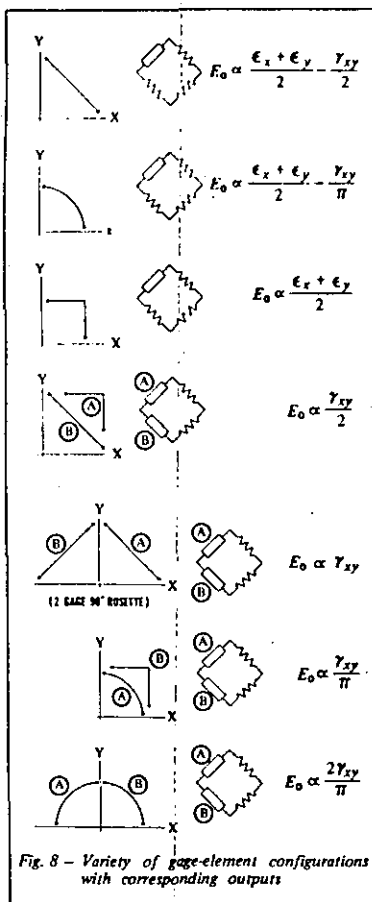


Fig. 8 - Variety of gage-element configurations with corresponding outputs

MEASUREMENTS GROUP TECH NOTE

TN-512

Plane-Shear
Measurement

Plane-Shear Measurement With Strain Gages

It is sometimes convenient to obtain a direct indication of shear strain from strain gages. Examples include shear-buckling studies and shear sensing in flexural transducers to provide load indication which is independent of the point of load application.

INTRODUCTION

Although a strain gage does not respond to shear strain as such, shear and normal strains are related through the laws of elasticity; and it is thus possible, by proper orientation of gages on the strained surface, and proper disposition of the gages in a Wheatstone bridge circuit, to produce an indication which is directly proportional to shear strain in the surface.

Shear Strain From Normal Strains

Consider an array of two strain gages oriented at arbitrarily different angles with respect to an X-Y coordinate system which, in turn, is arbitrarily oriented with respect to the principal axes, as in Fig. 1. From elementary mechanics of materials, the strain along the gage axes can be written as:

$$\epsilon_1 = \frac{\epsilon_x + \epsilon_y}{2} + \frac{\epsilon_x - \epsilon_y}{2} \cos 2\theta_1 + \frac{\gamma_{xy}}{2} \sin 2\theta_1 \quad (1)$$

$$\epsilon_2 = \frac{\epsilon_x + \epsilon_y}{2} + \frac{\epsilon_x - \epsilon_y}{2} \cos 2\theta_2 + \frac{\gamma_{xy}}{2} \sin 2\theta_2 \quad (2)$$

Subtracting (2) from (1) and solving for γ_{xy} ,

$$\gamma_{xy} = \frac{2(\epsilon_1 - \epsilon_2) - (\epsilon_x - \epsilon_y)(\cos 2\theta_1 - \cos 2\theta_2)}{\sin 2\theta_1 - \sin 2\theta_2} \quad (3)$$

It is now noticeable that if $\cos 2\theta_1 \equiv \cos 2\theta_2$, the term in ϵ_x and ϵ_y vanishes, and

$$\gamma_{xy} = \frac{2(\epsilon_1 - \epsilon_2)}{\sin 2\theta_1 - \sin 2\theta_2} \quad (4)$$

Since the cosine function is symmetrical about the zero argument, and about all integral multiples of π , $\cos 2\theta_1 \equiv \cos 2\theta_2$ when,

$$\theta_1 + \alpha = -\pi/2, 0, \pi/2, \pi \dots \frac{n\pi}{2} = \theta_2 - \alpha \quad (5)$$

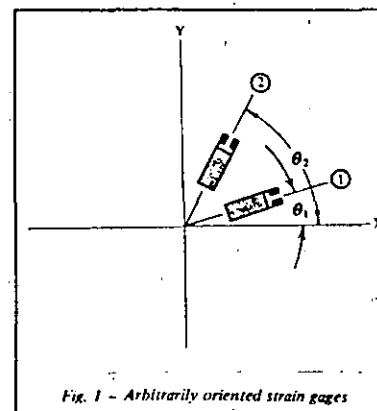


Fig. 1 - Arbitrarily oriented strain gages

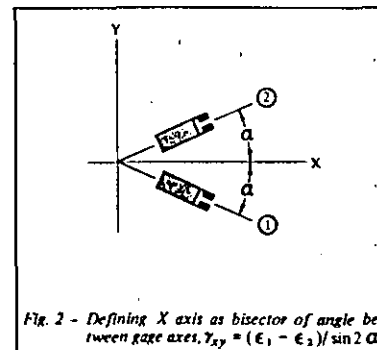


Fig. 2 - Defining X axis as bisector of angle between gage axes, $\gamma_{xy} = (\epsilon_1 - \epsilon_2) / \sin 2\alpha$



MEASUREMENTS GROUP, INC.

P. O. Box 27777 (919) 385-3800
Raleigh, North Carolina 27611, USA

Measurement of Thermal Expansion Coefficient Using Strain Gages

The thermal expansion coefficient is a very basic physical property which can be of considerable importance in mechanical and structural design applications of a material. Although there are many published tabulations of expansion coefficients for the common metals and standard alloys, the need occasionally arises to measure this property for a specific material over a particular temperature range. In some cases (e.g., new or special alloys, composites, etc.), there is apt to be no published data whatsoever on expansion coefficients. In others, data may exist (and eventually be found), but may encompass the wrong temperature range, apply to somewhat different material, or be otherwise unsuited to the application.

Historically, the classical means for measuring expansion coefficients has been the "dilatometer". In this type of instrument, the difference in expansion between a rod made from the test material and a matching length of quartz or vitreous silica is compared^{1,2}. Their differential expansion is measured with a sensitive dial indicator, or with an electrical displacement transducer. When necessary, the expansion properties of the quartz or silica can be calibrated against the accurately known expansion of pure platinum or copper. The instrument is normally inserted in a special tubular furnace or liquid bath to obtain the required temperatures. Making measurements with the dilatometer is a delicate, demanding task, however, and is better suited to the materials science laboratory than to the typical experimental stress analysis facility. This Tech Note provides an alternate method for easily and quite accurately measuring the expansion coefficient of a test material with respect to that of any reference material having known expansion characteristics.

The technique described here uses two well-matched strain gages, with one bonded to a specimen of the reference material, and the second to a specimen of the test material. The specimens can be of any size or shape compatible with the available equipment for heating and refrigeration (but specimens of uniform cross section will minimize potential problems with temperature gradients). Under stress-free conditions, the differential output between the gages on the two specimens, at any common temperature, is equal to the differential unit expansion (in/in, or m/m). Aside from the basic simplicity and relative ease of making thermal expansion measurements by this method, it has the distinct advantage of requiring no specialized instruments beyond those normally found in a stress analysis laboratory. This technique can also be applied to the otherwise difficult task of determining directional expansion coefficients of materials with anisotropic thermal properties.

Because typical expansion coefficients are measured in terms of a few parts per million, close attention to procedural detail is required with any measurement method to obtain accurate results; and the strain gage method is not an exception to the rule. This Tech Note has been prepared as an aid to the gage user in utilizing the full precision of the modern foil strain gage for determining expansion coefficients. Given in the first of the following sections is an explanation of the technical principles underlying the method. The next section describes, in some detail, the strain-gage-related materials and procedures in making the measurement. Basically, the latter consists of essentially the same techniques required for any high-precision strain measurement in a variable thermal environment. Suggested refinements for achieving maximum accuracy are then given in the following section; after which, the principal limitations of the method are described.



MEASUREMENTS GROUP, INC.
P.O. Box 27777
Raleigh, North Carolina 27611, USA

(919) 365-3800
Telex 802-512
FAX (919) 365-3945

As a rule, the greatest selection of gages is available in the 06 and 13 S-T-C groups, since these are the most widely used compensations for stress analysis and transducer applications. It will often be expedient, therefore, to specify one of the above for the S-T-C number.

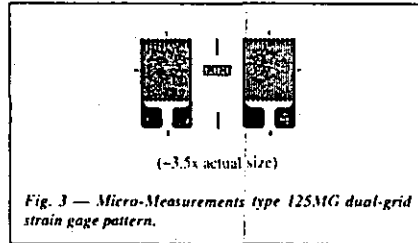
When expansion measurements must be made over an extended temperature range, or at high or low temperature extremes, the S-T-C number should be carefully selected to obtain the best measurement accuracy. It is evident from Fig. 1 that, with excessive mismatch between the S-T-C number of the gage and the expansion coefficient of the specimen, the slope of the thermal output curve can become very steep at one or both extreme temperatures. Under such circumstances, a small error in temperature (or temperature deviation between the reference and test materials) can produce a large error in the thermal output signal. Judicious selection of the S-T-C mismatch can be used to simultaneously keep the slopes of the thermal output curves for both the test and reference materials under reasonably good control in the temperature range of interest.

Almost any single-element "linear" grid pattern can be employed for measuring expansion coefficients. As indicated earlier, however, the two gages — one on the reference specimen, and one on the test material — must always be well-matched. That is, the gages must be identically the same type, and must be from the same manufacturing lot to assure closely related thermal output characteristic. Both requirements can be met by simply using a pair of gages taken from the same package. Gages of the identical type taken from different packages, but having the same lot number, will be equally close in their thermal outputs. When a still closer relationship is desired for greater measurement accuracy, a dual-grid gage pattern such as the 125MG (Fig. 3) can be selected, and the grids cut apart to form two individual gages. The resulting gages are, in effect, identical twins, and will provide the closest possible match in thermal output characteristics (as in all other properties).

Gage Installation

As noted, one of the advantages of this method is that the specimens of the reference and test materials can be of any convenient size or configuration suitable to the available heating or refrigeration equipment. In fact, the two specimens can even be different in size or shape if there is a reason to have them so. In general, however, specimens should be uniform in cross section to minimize temperature gradients induced during heating or cooling; and the use of flat specimens will make for easier and higher-quality gage and temperature sensor installations. The specimens should also be large enough in cross section so that the strain gage stiffness is negligible compared to the overall section stiffness. Beyond the foregoing, selection of the specimen dimensions for about the same thermal inertia will be helpful in most quickly achieving the same temperature when both specimens are heated or cooled together.

Specimen surfaces should be thoroughly cleaned and prepared for bonding as described in Micro-Measurements Instruction Bulletin B-129, which includes specific step-by-step procedures for a wide variety of materials⁷. For best accuracy, bonding should be done with a high performance adhesive such as M-Bond 600 or 610. Both adhesives are capable of forming thin, hard "gluelines" for maximum fidelity in transmitting strains from the specimen surface to the gage. These adhesives



are intended for use on relatively smooth, nonporous surfaces, and should not be used where the adhesive is required to fill surface irregularities or to seal pores. For the latter conditions, the recommended adhesive is M-Bond AE-10 or AE-15. In all cases, complete instructions for applying and curing the adhesive are included in the package with the material.

Extra care is required in the selection of leadwires and their attachment to the gages, in order to obtain the most accurate results. Thermally produced resistance changes in the leadwires will generate circuit outputs which are indistinguishable from the thermal outputs being measured. If these differ in any way between the reference and test specimens, the indicated differential expansion data will be in error accordingly. To minimize such effects, leadwire resistance should be kept as low as possible by employing a generous wire size, and by keeping the leads short. The wiring should also be the same for both specimens — in size, length, and routing. If measurements are to be made on both specimens in the same chamber or liquid bath at the same time, the leadwire should be kept physically together throughout as much of their length as practical. Leadwire insulation must be selected, of course, for compatibility with the temperature range and environment encountered in the measurements.

In attaching leadwires to the gage solder tabs or to solder terminals, the solder joints should be smooth, bright, and free of spikes or excess solder. The joints should also be as uniform as possible; and the leadwires should be dressed the same on both specimens. After lead attachment, the gage installations must be thoroughly cleaned with n-xin solvent to remove all traces of soldering flux and residues.

The final step in the installation is to apply a protective coating system which is appropriate to the expected test environment. Since these tests are normally conducted under short-term laboratory conditions, a coating is selected for basic protection against moisture, dew point condensation in cold tests and minimum/maximum operating temperature range. The coating recommendations in the following table also take into consideration low reinforcement of the specimen. Further details on these and other coatings can be found in Micro-Measurements M-LINE Strain Gage Accessories Catalog A-110.

The process of gage installation has been summarized very briefly here, since detailed instructions are supplied elsewhere in Measurements Group technical publications. It should be appreciated, however, that proper gage installation is a basic requirement for accurate measurement of expansion coefficients. In general, gage installations should be of the highest quality — comparable to those found in precision strain gage transducers. Care should also be taken that the two gage instal-

PROTECTIVE COATING		
Operating Temperature Range		Coating
°F	°C	
+60 to +250	+15 to +120	M-Coat A or C
0 to +150	-20 to +65	W-1 Wax
-100 to +500	-75 to +260	3140 or 3145 RTV
-452 to +400	-269 to +200	Two coats M-Bond 43B

lations, on the reference and test specimens, are as uniform as possible to minimize small physical differences which could affect the differential thermal response. If installation questions or problems arise, the user should consult the Measurements Group Applications Engineering Department for assistance. Figure 4 is a photograph of a properly installed strain gage on a metal specimen for thermal expansion measurements. A bondable resistance temperature sensor (see page 6) is installed adjacent to the gage to monitor the specimen temperature. This photograph shows the installation just prior to application of the protective coating over the gage and temperature sensor.

Strain and Temperature Instrumentation

Basically, any stable precision strain indicator can be used for the strain measurements needed in this procedure. Satisfactory instruments for this purpose include the Model P-3500 and Model 3800 Strain Indicators produced by the Instruments Division of the Measurements Group. Beyond the necessity for instrument precision and stability, it is important that the gage excitation voltage be kept low enough to avoid the effects of self-heating in the gage. Both the Models P-3500 and 3800 are high-gain instruments with low excitation voltages. Using these strain indicators, there is ordinarily no self-heating problem with a gage such as the 125MG pattern installed on a metal specimen with reasonably good heat-dissipating characteristics. When measurements are made with other instruments having higher excitation voltages, or with gages installed on specimens of low thermal conductivity, self-heating may be excessive, and the voltage applied to the gage must be reduced. Comprehensive background information and guidelines for setting excitation voltages are provided in Tech Note TN-502⁸.

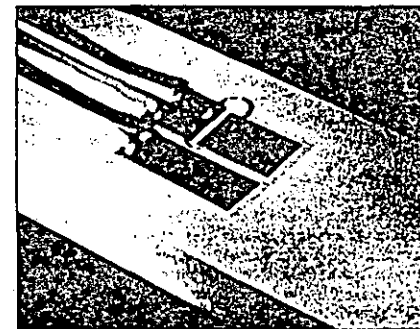


Fig. 4 — Strain gage (half of the 125MG dual-gage pattern, at top) and resistance temperature sensor, installed side-by-side on a specimen of test material.

Either of two basic circuit arrangements can be used in measuring expansion coefficients. One of these, shown in Fig. 5a, employs separate, three-wire, quarter-bridge circuits for the gages on the reference and test specimens. With this arrangement, the gage outputs are read individually, and subsequently subtracted to determine the differential strain for use with Eq. (6). Since the separate circuits permit monitoring the gages independently, it is relatively simple to identify the cause of any improper or anomalous strain readings which may occur when conducting the test. A disadvantage of this approach is that it requires a switch-and-balance unit (when used with a single-channel strain indicator) or a two-channel instrument.

The second arrangement (Fig. 5b) uses the properties of the half-bridge circuit to perform the subtraction electrically. When the two gages are connected as adjacent arms of the bridge circuit, the instrument output is equal to the difference in the individual thermal outputs. The circuit is obviously simpler in terms of both wiring and instrumentation, and is direct-reading. Its primary disadvantage lies in the difficulty of isolating the gage which may be malfunctioning when improper operation is suspected.

In both of the foregoing circuit arrangements, the leadwires to the gages should be as short as possible, and should be of the same wire size and length. Since leadwires #1 and #3 are always in adjacent arms of the bridge circuit, they should be particularly well-matched and maintained physically together throughout their lengths, to minimize differential resistance changes which could appear in the instrument output. With a half-bridge circuit such as shown in Fig. 5b, it is also necessary that leadwire #2 be connected at the midpoint of the jumper between the gages. This is done to place half of the jumper resistance in series with each gage in its respective bridge arm, and thus avoid a false output signal due to the thermally induced resistance change in the jumper wire. It is worth noting that a 6-in (~150-mm) dissymmetry in the wiring — whether in leadwires #1 and #3, or in the jumper — in AWG 30 (±0.25 mm) wire size will cause a false output of about 17µ per 100°F (per 55°C).

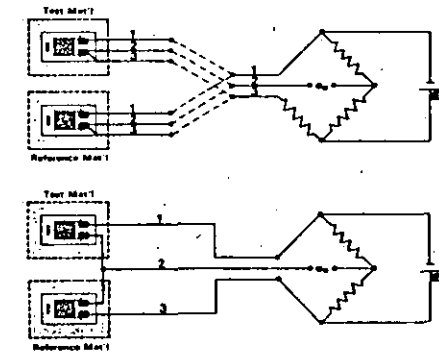


Fig. 5 — Strain gage circuits for measuring thermal expansion coefficients: (a) separate quarter-bridge circuits; (b) half-bridge circuit.

As a rule, the greatest selection of gages is available in the 06 and 13 S-T-C groups, since these are the most widely used compensations for stress analysis and transducer applications. It will often be expedient, therefore, to specify one of the above for the S-T-C number.

When expansion measurements must be made over an extended temperature range, or at high or low temperature extremes, the S-T-C number should be carefully selected to obtain the best measurement accuracy. It is evident from Fig. 1 that, with excessive mismatch between the S-T-C number of the gage and the expansion coefficient of the specimen, the slope of the thermal output curve can become very steep at one or both extreme temperatures. Under such circumstances, a small error in temperature (or temperature deviation between the reference and test materials) can produce a large error in the thermal output signal. Judicious selection of the S-T-C mismatch can be used to simultaneously keep the slopes of the thermal output curves for both the test and reference materials under reasonably good control in the temperature range of interest.

Almost any single-element "linear" grid pattern can be employed for measuring expansion coefficients. As indicated earlier, however, the two gages — one on the reference specimen, and one on the test material — must always be well-matched. That is, the gages must be identically the same type, and must be from the same manufacturing lot to assure closely related thermal output characteristic. Both requirements can be met by simply using a pair of gages taken from the same package. Gages of the identical type taken from different packages, but having the same lot number, will be equally close in their thermal outputs. When a still closer relationship is desired for greater measurement accuracy, a dual-grid gage pattern such as the 125MG (Fig. 3) can be selected, and the grids cut apart to form two individual gages. The resulting gages are, in effect, identical twins, and will provide the closest possible match in thermal output characteristics (as in all other properties).

Gage Installation

As noted, one of the advantages of this method is that the specimens of the reference and test materials can be of any convenient size or configuration suitable to the available heating or refrigeration equipment. In fact, the two specimens can even be different in size or shape if there is a reason to have them so. In general, however, specimens should be uniform in cross section to minimize temperature gradients induced during heating or cooling; and the use of flat specimens will make for easier and higher-quality gage and temperature sensor installations. The specimens should also be large enough in cross section so that the strain gage stiffness is negligible compared to the overall section stiffness. Beyond the foregoing, selection of the specimen dimensions for about the same thermal inertia will be helpful in most quickly achieving the same temperature when both specimens are heated or cooled together.

Specimen surfaces should be thoroughly cleaned and prepared for bonding as described in Micro-Measurements Instruction Bulletin B-129, which includes specific step-by-step procedures for a wide variety of materials. For best accuracy, bonding should be done with a high performance adhesive such as M-Bond 600 or 610. Both adhesives are capable of forming thin, hard "gluefilms" for maximum fidelity in transmitting strains from the specimen surface to the gage. These adhesives

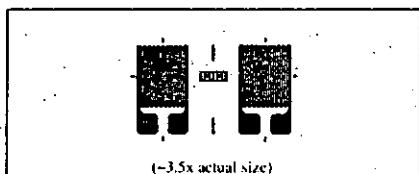


Fig. 3 — Micro-Measurements type 125MG dual-grid strain gage pattern.

are intended for use on relatively smooth, nonporous surfaces, and should not be used where the adhesive is required to fill surface irregularities or to seal pores. For the latter conditions, the recommended adhesive is M-Bond AE-10 or AE-15. In all cases, complete instructions for applying and curing the adhesive are included in the package with the material.

Extra care is required in the selection of leadwires and their attachment to the gages, in order to obtain the most accurate results. Thermally produced resistance changes in the leadwires will generate circuit outputs which are indistinguishable from the thermal outputs being measured. If these differ in any way between the reference and test specimens, the indicated differential expansion data will be in error accordingly. To minimize such effects, leadwire resistance should be kept as low as possible by employing a generous wire size, and by keeping the leads short. The wiring should also be the same for both specimens — in size, length, and routing. If measurements are to be made on both specimens in the same chamber or liquid bath at the same time, the leadwire should be kept physically together throughout as much of their length as practical. Leadwire insulation must be selected, of course, for compatibility with the temperature range and environment encountered in the measurements.

In attaching leadwires to the gage solder tabs or to solder terminals, the solder joints should be smooth, bright, and free of spikes or excess solder. The joints should also be as uniform as possible; and the leadwires should be dressed the same on both specimens. After lead attachment, the gage installations must be thoroughly cleaned with rosin solvent to remove all traces of soldering flux and residues.

The final step in the installation is to apply a protective coating system which is appropriate to the expected test environment. Since these tests are normally conducted under short-term laboratory conditions, a coating is selected for basic protection against moisture, dew point condensation in cold tests, and minimum/maximum operating temperature range. The coating recommendations in the following table also take into consideration low reinforcement of the specimen. Further details on these and other coatings can be found in Micro-Measurements M-LINE Strain Gage Accessories Catalog A-110.

The process of gage installation has been summarized very briefly here, since detailed instructions are supplied elsewhere in Measurements Group technical publications. It should be appreciated, however, that proper gage installation is a basic requirement for accurate measurement of expansion coefficients. In general, gage installations should be of the highest quality — comparable to those found in precision strain gage transducers. Care should also be taken that the two gage instal-

PROTECTIVE COATING		
Operating Temperature Range		Coating
°F	°C	
+60 to +250	+15 to +120	M-Coat A or C
0 to +150	-20 to +65	W-1 Wax
-100 to +500	-75 to +260	3140 or 3145 RTV
-452 to +400	-269 to +200	Two coats M-Bond 43B

lations, on the reference and test specimens, are as uniform as possible to minimize small physical differences which could affect the differential thermal response. If installation questions or problems arise, the user should consult the Measurements Group Applications Engineering Department for assistance. Figure 4 is a photograph of a properly installed strain gage on a metal specimen for thermal expansion measurements. A bondable resistance temperature sensor (see page 6) is installed adjacent to the gage to monitor the specimen temperature. This photograph shows the installation just prior to application of the protective coating over the gage and temperature sensor.

Strain and Temperature Instrumentation

Basically, any stable precision strain indicator can be used for the strain measurements needed in this procedure. Satisfactory instruments for this purpose include the Model P-3500 and Model 3800 Strain Indicators produced by the Instruments Division of the Measurements Group. Beyond the necessity for instrument precision and stability, it is important that the gage excitation voltage be kept low enough to avoid the effects of self-heating in the gage. Both the Models P-3500 and 3800 are high-gain instruments with low excitation voltages. Using these strain indicators, there is ordinarily no self-heating problem with a gage such as the 125MG pattern installed on a metal specimen with reasonably good heat-dissipating characteristics. When measurements are made with other instruments having higher excitation voltages, or with gages installed on specimens of low thermal conductivity, self-heating may be excessive, and the voltage applied to the gage must be reduced. Comprehensive background information and guidelines for setting excitation voltages are provided in Tech Note TN-502⁴.

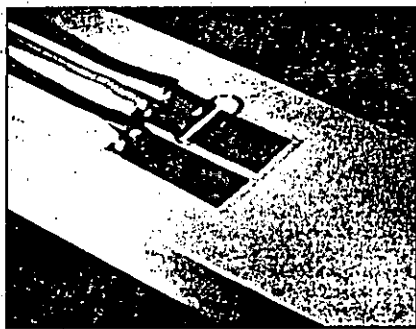


Fig. 4 — Strain gage (half of the 125MG dual-gage pattern, at top) and resistance temperature sensor, installed side-by-side on a specimen of test material.

Either of two basic circuit arrangements can be used in measuring expansion coefficients. One of these, shown in Fig. 5a, employs separate, three-wire, quarter-bridge circuits for the gages on the reference and test specimens. With this arrangement, the gage outputs are read individually, and subsequently subtracted to determine the differential strain for use with Eq. (6). Since the separate circuits permit monitoring the gages independently, it is relatively simple to identify the cause of any improper or anomalous strain readings which may occur when conducting the test. A disadvantage of this approach is that it requires a switch-and-balance unit (when used with a single-channel strain indicator) or a two-channel instrument.

The second arrangement (Fig. 5b) uses the properties of the half-bridge circuit to perform the subtraction electrically. When the two gages are connected as adjacent arms of the bridge circuit, the instrument output is equal to the difference in the individual thermal outputs. The circuit is obviously simpler in terms of both wiring and instrumentation, and is direct-reading. Its primary disadvantage lies in the difficulty of isolating the gage which may be malfunctioning when improper operation is suspected.

In both of the foregoing circuit arrangements, the leadwires to the gages should be as short as possible, and should be of the same wire size and length. Since leadwires #1 and #3 are always in adjacent arms of the bridge circuit, they should be particularly well-matched and maintained physically together throughout their lengths, to minimize differential resistance changes which could appear in the instrument output. With a half-bridge circuit such as shown in Fig. 5b, it is also necessary that leadwire #2 be connected at the midpoint of the jumper between the gages. This is done to place half of the jumper resistance in series with each gage in its respective bridge arm, and thus avoid a false output signal due to the thermally induced resistance change in the jumper wire. It is worth noting that a 6-in (150-mm) dissymmetry in the wiring — whether in leadwires #1 and #3, or in the jumper — in AWG 30 (0.25 mm) wire size will cause a false output of about 17µε per 100°F (per 55°C).

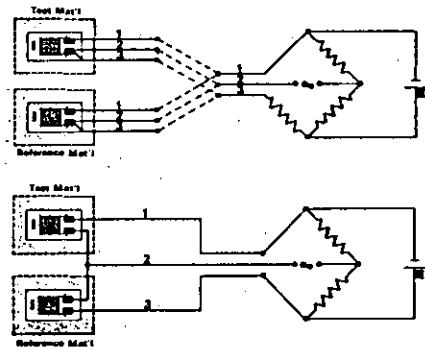


Fig. 5 — Strain gage circuits for measuring thermal expansion coefficients: (a) separate quarter-bridge circuits; (b) half-bridge circuit.



(-3x actual size)

Fig. 6 — Micro-Measurements TG-Series ETG-50B/W bondable temperature sensor.

Temperature measurement also requires care and consideration to obtain accurate expansion data. Typically, a temperature-sensing probe is placed immediately adjacent to the gage, and in intimate contact with the specimen surface, to indicate the specimen/gage temperature. This procedure assumes that previous verification has been made, by multiple temperature measurements on the specimen as necessary, to assure uniform specimen temperature under conditions of thermal equilibrium in the test chamber. Since the materials in the reference and test specimens normally differ in their thermal conductivity and specific heat, it is necessary that the temperatures at both gage sites be measured. The temperature must be the same, of course, when ever paired strain readings are made.

Depending primarily on personal preference and instrumentation availability, temperatures can be measured either with thermocouples or with resistance temperature sensors. If a thermocouple is employed on each specimen, type J (iron-constantan) is preferred, assuming that the test temperature range is compatible with this type. The sensing junction should be small, as should the leadwires [in the range of AWG 30 to AWG 26 (0.25 to 0.4 mm)], and premium grade thermocouple wire should be selected. Heat transfer from the specimen to the junction can be improved by taping the first 2 to 3 in (50 to 75 mm) of the extension wires to the specimen surface.

An alternate approach is to use resistance temperature sensors such as Micro-Measurements TG-Series (Fig. 6). The temperature sensor looks like a strain gage, and has essentially the same construction except that the grid is made from high-purity nickel foil. It is installed with standard strain gage installation procedures, and should be mounted side-by-side with the strain gage on the specimen surface. Because it is physically like the strain gage, and is attached to the specimen in the same way, the temperature sensor has about the same heat-transfer characteristics and thermal time constant as the strain gage. When used in conjunction with a specially designed passive resistance network for linearization and signal scaling (Micro-Measurements Type LST), it permits direct measurement of temperature with any conventional strain indicator. The small size and low stiffness of the TG-Series temperature sensor present minimum mechanical restraint to the free thermal expansion and contraction of the specimen.

Making Expansion Measurements

For any method of dilatometry, it is always necessary that the reference and test specimens be exposed to at least two different temperatures in measuring the expansion coefficient. The

actual means of achieving the desired temperatures in a particular case depends on the temperatures involved, and on the available facilities. These may consist, for instance, of ovens, or liquid baths, or various other forms of environmental chamber. The strain gage method imposes no special restrictions on the nature or design of the chamber. On the contrary, the size and shape of the specimen can usually be adapted to suit the existing facilities. Since the available equipment varies widely from one laboratory to the next, the following remarks are limited to the general requirements for any dilatometric temperature chamber.

Two of the most desirable features of a chamber for measuring expansion coefficients are uniformity and stability of temperature. To avoid errors due to the development of thermal stresses in the specimen, the temperature should be uniform throughout the specimen at the time of measurement. This condition can be established only if the chamber temperature at equilibrium is essentially uniform — at least in the region containing the specimens. Temperature stability in the chamber is also necessary to permit measuring specimen temperatures and strains under static, nonvarying conditions.

Thermal equilibrium in the specimen can be achieved in a chamber equipped with a forced convection system to vigorously circulate the heat-transfer medium past the specimen surfaces. Heating and cooling rates should also be kept low to minimize temperature gradients perpendicular to the specimen surface. The required condition of uniform temperature throughout the specimen is difficult to judge, however, and is not necessarily assured by observing equal temperature readings at different points on the surface. One of the most effective ways to test for control over the uniformity of specimen temperature is to make a continuous plot of strain gage output versus temperature over the working temperature range — in both the heating and cooling directions. In this process, the temperature is changed incrementally; and, at each test temperature, after the specimen is evidently in thermal equilibrium, the temperature and thermal output are recorded and plotted. If uniformity of specimen temperature is actually achieved, the heating and cooling legs of the plotted curve should very nearly coincide. If, on the other hand, the two portions of the curve are significantly separated to form a hysteresis loop, a likely cause is nonuniform temperature distribution through the thickness of the specimen. In the latter case, the heating and cooling rates must be lowered, or thermal stabilization times increased, or other measures taken to essentially eliminate the temperature gradients.

Means must be provided for supporting the specimens in the chamber so that friction cannot impede expansion or contraction. In some cases, a simple way to accomplish this is to suspend the specimens from one end. Although the specimen may be strained slightly by its own weight, the strain is constant (as long as the elastic modulus is essentially constant), and does not affect the change in thermal output with temperature. If the elastic modulus of the test material changes significantly over the range of temperatures to be encountered, the error due to this effect must be evaluated to determine the suitability of the method. Another approach is to lay the specimens on the floor of the chamber or compartment, supported by a layer of fiber-glass cloth or some other low-friction medium. When this method is used, its effectiveness should be verified by observing the behavior of the thermal output as the specimen is cycled through the working temperature range. Erratic output, hysteresis, or lack of repeatability may indicate excessive friction.

Before performing actual measurements to determine the coefficient of expansion, the entire system, including both specimens (with gages installed and power applied), should be stabilized by cycling several times to temperatures at least 10°F (5°C) above the highest, and below the lowest, test temperatures. One of the reasons for this procedure is that residual stresses are generally present in all of the components — the reference and test specimens, the gages as manufactured and installed, the leadwires, etc. Thermal cycling is intended to relax and/or redistribute any residual stresses which might otherwise change during the test and cause the data to be nonrepeatably. The cycling procedure should be performed at low enough rates of temperature change to minimize thermal stresses in the specimens due to temperature gradients. Otherwise, the thermal stress, superimposed on the residual stress, may cause yielding, and thus defeat the purpose of the cycling.

Normally, after the second or third stabilizing cycle, the thermal output at any given temperature should be highly repeatable. If not, and if the lack of repeatability is significant compared to the accuracy required from the test, the sources of the variability must be found. In such cases, the problem may be associated with the temperature, or the strain, or both. Careful re-reading of this Tech Note may provide the clue for finding and correcting the trouble. Further assistance, if needed, can be obtained from the Measurements Group Applications Engineering Department.

Following stabilization, verified by reproducible strain indications throughout the temperature range, the user is ready to perform the final measurements for determining the thermal expansion properties of the test material. When the oven or other chamber is such that only a single specimen can be accommodated, the two specimens are tested one-at-a-time, using the circuit of Fig. 5a. The resulting two sets of thermal output data are subtracted (and the difference divided by the temperature change) as indicated by Eq. (6) to give the differential thermal expansion coefficient. With the preferable arrangement, having both specimens together in the chamber, the measurements can be made separately as in Fig. 5a, or the differential thermal output can be read directly as shown in Fig. 5b.

Special Precautions and Refinements for Improving Accuracy

When attempting to achieve greater and greater accuracy with the strain gage method (or with any method), it is necessary to examine ever smaller effects which may introduce errors. In some instances, these second-order errors are well-defined, systematic in nature, and responsive to routine procedures for correction or elimination. In others, the cause-and-effect relationship is more nebulous, and error reduction is accomplished primarily by technique refinement — i.e., by removing or minimizing all of the known possible sources of error.

An example of a readily correctable inaccuracy (in certain cases) is the error due to transverse sensitivity. This error arises because the strain field induced in the gage grid by the difference in thermal expansion between the specimen and grid [Eq. (1)] is generally different from that employed in gage factor calibration. When both the reference and test materials are isotropic in their thermal expansion properties, the transverse-

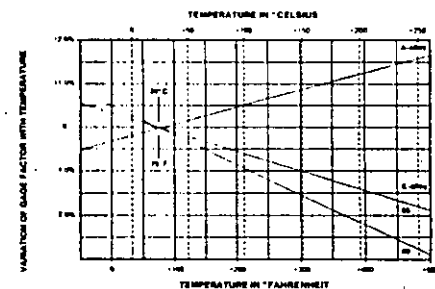


Fig. 7 — Gage factor variation with temperature (typical) for A- and K-alloy strain gages.

sensitivity error, which is ordinarily quite small, can be corrected for rather easily. Although not derived here, correction can be made by multiplying the difference in thermal outputs [Eq. (6)] by the factor $(1 - 0.285 K_1)/(1 + K_1)$, where K_1 is the decimalized transverse sensitivity of the gage in use. This correction factor is not applicable to orthotropic materials, for which case differential thermal outputs between a reference gage and two perpendicularly oriented specimen gages are required to correct for transverse sensitivity.

Another minor error source is the variation of gage factor with temperature. The gage factor specified for Micro-Measurements strain gages is measured at +75°F (+24°C). At any other temperature it is slightly different. With constantan gages, for example, the gage factor varies directly with temperature, at a rate of about 0.5% per 100°F (0.9% per 100°C). In contrast, the gage factor of K-alloy (modified Karma) gages varies inversely with temperature. The rate of change depends on the S.T.C. number of the gage, but is generally in the range from -0.5 to -1.0% per 100°F (-0.9 to -1.8% per 100°C). Representative plots of gage factor variation with temperature are illustrated in Fig. 7 for both types of gages. The technical data sheet contained in each gage package includes a graph of the gage factor variation applicable to that gage type.

Complete elimination of the small error introduced by gage factor variation is not always feasible, but first-order correction, to remove most of the error, is relatively simple. When expansion measurements are made incrementally across the working temperature range, the differential thermal output for each increment in temperature can be corrected individually. This is done by multiplying the difference in indicated thermal outputs from the specimen and reference gages by the factor $1/(1 + \Delta F/G)$. The term $\Delta F/G$ in the foregoing is the decimalized change in gage factor (with sign) corresponding to the middle temperature of each measurement increment. It can usually be read with sufficient accuracy directly from the graph on the technical data sheet accompanying the gages.

Sometimes, the average differential expansion coefficient is to be determined over the full temperature range by making only two sets of measurements, at the temperature extremes. The same correction procedure can be applied, using the $\Delta F/G$ for the mid-range temperature, but it will be much less effective because the thermal output is a nonlinear function of temperature.

When the leadwire resistance can be kept very low, as recommended in the preceding section, the signal attenuation ("desensitization") caused by the inert resistance in series with the gage should be negligible. If, on the other hand, the series resistance is greater than about 1 percent of the gage resistance, the user who is striving for maximum accuracy may wish to perform a correction. For this purpose, the indicated thermal outputs are multiplied by the factor $(R_G + R_L)/R_G$, where R_G is the gage resistance, and R_L is the leadwire resistance in series with the gage in the same arm of the bridge circuit. An alternative, for direct reading of corrected strains, is to set the gage factor control of the instrument at $F_G \times R_G/(R_G + R_L)$, where F_G is the specified gage factor of the gages in use.

The supposition is made, in the strain gage method of measuring expansion coefficients, that if the two gages (and gage circuits) behave identically, then any difference in their outputs can be due only to the difference in expansion properties between the reference and test specimens. It is obvious, therefore, that the highest accuracy will be achieved by minimizing all differences in gage behavior. For this reason, as noted earlier, the thermal output characteristics of the gages should be as nearly the same as possible. However, two nominally identical gages from the same manufacturing lot do not especially have identical thermal outputs. Instead, as shown in Fig. 8, there is a tolerance on the thermal output.* Almost all of the tolerance can be removed by splitting a dual-element gage (such as the 125MG pattern) to make a pair of twin gages, and this procedure is always recommended when high accuracy is the goal. The same reasoning underlies the repeated emphasis in this Tech Note on the uniformity of gage installations. Identical installation procedures should be used for both gages; and, ideally, there should be no visible differences in the completed installations.

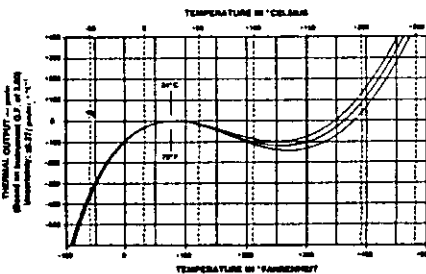


Fig. 8 — Tolerance band for the thermal output of randomly selected A-alloy strain gages from the same manufacturing lot.

The remaining areas of possible refinement for improved accuracy are primarily associated with the measurements procedures. Each of the items in the following checklist can be considered, and steps taken as necessary to satisfy the desired conditions:

- a) stable, accurate instrumentation, for both temperature and strain.

- b) high-quality, stable gage installations, exhibiting negligible drift over the operating temperature range.
- c) gage excitation at a level low enough to avoid self-heating effects.
- d) thermal stabilization of specimens, gages, and wiring prior to making expansion measurements.
- e) assurance of thermal equilibrium in the specimens when measurements are made.
- f) avoidance of significant thermal stresses during heating and cooling.
- g) elimination of frictional effects preventing free expansion and contraction.

Except for the absolute accuracy of the instrumentation, the degree to which the foregoing conditions have been met can be judged quite well by the repeatability of the data. Highly reproducible data generally indicate that the system is functioning properly, and that random error sources are well-controlled.

After it has been demonstrated that the measurement system and procedures are suitable for obtaining closely reproducible data from a single specimen, consideration should be given to the question of variation in thermal properties from specimen to specimen. The usual purpose of expansion-coefficient measurements is to determine the nominal value which is representative of a particular material. But the thermal and other physical properties of any material tend to vary randomly from specimen to specimen within a lot, and still more widely from lot to lot. Since such variation is not subject to the control of the user, it becomes necessary to use statistical sampling techniques, with a sample size large enough to provide an adequate estimate of the mean and standard deviation. Variability in thermal properties is apt to be particularly great in materials such as plastics and composites.

The mechanical and thermal properties of some materials (e.g., graphite, titanium 6Al4V, composites with oriented fiber reinforcement, etc.) are highly directional. In such cases, orientation of the strain gage on the specimen (with respect to the natural axes of the material, as determined by the rolling direction, fiber orientation or otherwise) is critical if the directional expansion coefficient is to be measured. When it is impossible to determine the directions of the natural material axes, it may be necessary to make measurements over a wide range of angles to define the distribution of the expansion coefficient, or to obtain a rough, integrated average value.

LIMITATIONS

The strain gage method of differential dilatometry has very few special limitations. Of these, the principal one for some types of studies may be the allowable temperature range. Constantan gages, for instance, should be used for high-accuracy measurements only within a temperature range from about -50° to $+150^{\circ}\text{F}$ (-45° to $+65^{\circ}\text{C}$). Higher temperatures normally require the use of K-alloy gages, which can provide accurate strain measurements from approximately -50° to $+400^{\circ}\text{F}$ (-45° to $+205^{\circ}\text{C}$). With special techniques, these temperature ranges can sometimes be extended, depending on the circumstances. Users should consult with the Measurements Group Applications Engineering Department for recommendations.

Mechanical reinforcement of the specimen by the strain gage can also be a limitation in some instances. When the test specimen is made from a material such as plastic, with a very low modulus of elasticity, the stiffness of the gage may perturb the local strain field and introduce a sizeable error. With metal specimens, the reinforcement effect is ordinarily negligible unless the specimen is so thin and narrow that the gage stiffness represents a significant fraction of the overall section stiffness.

Other limitations are generally those common to all methods of differential dilatometry. For example, the expansion coefficient of the test material can never be determined to greater accuracy than that of the reference material. Similarly, the measurements can be no more accurate than the instrumentation used to indicate the temperatures and strains.

SUMMARY

This Tech Note has described a simple, straightforward means of measuring the expansion coefficient of a test material relative to that of any reference material having known expansion properties. The method is particularly well-suited to the stress analysis laboratory, since it usually requires no special instrumentation, techniques, or materials not already available in such a facility. Considerable attention has been given here to procedural details aimed at extracting the utmost accuracy from the method. Most of the recommended procedures, however, should represent standard practices for a stress laboratory which is accustomed to making precision strain measurements in a variable thermal environment. Even when expedience dictates somewhat less rigorous procedures, the method can be used to quickly and easily measure thermal expansion coefficients with sufficient accuracy for many engineering purposes.

REFERENCES

1. American Society for Testing and Materials, "Standard Test Method for Linear Expansion of Metals", ASTM Standard No. B95-39.
2. American Society for Testing and Materials, "Linear Thermal Expansion of Rigid Solids with a Vitreous Silica Dilatometer", ASTM Standard No. E228-71.
3. Measurements Group, Inc., Tech Note TN-504, "Strain Gage Thermal Output and Gage Factor Variation with Temperature", 1989.
4. Finke, T. E., and T. G. Heberling, "Determination of Thermal Expansion Characteristics of Metals Using Strain Gages", *Proceedings, SESA* (now, SEM), Vol. XXV, No. 1, 1978, pp. 155-158.
5. Poore, M. W., and K. F. Kesterson, "Measuring the Thermal Expansion of Solids with Strain Gages", *Journal of Testing and Evaluation*, ASTM, Vol. 6, No. 2 (March 1978), pp. 98-102.
6. Measurements Group, Inc., Tech Note TN-505, "Strain Gage Selection Criteria, Procedures, Recommendations", 1989.
7. Measurements Group, Inc., Bulletin B-129, "Surface Preparation for Strain Gage Bonding", 1976.
8. Measurements Group, Inc., Tech Note TN-502, "Optimizing Strain Gage Excitation Levels", 1979.
9. Measurements Group, Inc., Tech Note TN-509, "Errors Due to Transverse Sensitivity in Strain Gages", 1982.

*See Tech Note TN-504, page 6.

APPENDIX

REFERENCE INFORMATION

I. Specification for CORNING GLASS WORKS Titanium Silicate, Code 7971 ULF™ thermal expansion coefficient

Control Limit:	5° to 35°C	0.00 ± 0.03 × 10 ⁻⁶ /°C
Typical Values:	0° to 200°C	0.03 ± 0.03 × 10 ⁻⁶ /°C
	-100° to 200°C	-0.03 ± 0.03 × 10 ⁻⁶ /°C

Tolerance within one specimen purchased from Micro-Measurements (Part No. TSB-1):

5° to 35°C	0.00 ± 0.015 × 10 ⁻⁶ /°C
------------	-------------------------------------

This tolerance also applies to typical values noted above.

Micro-Measurements Specimen Size: 155 x 30 x 6.5 mm (6 x 1 x 0.25 in)

Micro-Measurements Specimen Finish: 80 Grit

II. Thermal Output Scatter of Micro-Measurements Strain Gages

All data are based on a 2σ or 95% confidence level over the temperature range of 0° to +175°C (+32° to +350°F).

Catalog 500 single-element A-alloy gages: ±0.27 μm/m°C (±0.15 μin/in°F).

Catalog 500 single-element K-alloy gages: ±0.45 μm/m°C (±0.25 μin/in°F).

EA-XX-125MG-120 with one grid on Code 7971 and the other on unknown material: ±0.05 μm/m°C (±0.03 μin/in°F).

WK-XX-125MG-350 used as described with the EA gage: ±0.10 μm/m°C (±0.06 μin/in°F).

III. Correction for Transverse Sensitivity

With K_t in decimal form, multiply the parenthetic expression [$\epsilon_{T(X)GS} - \epsilon_{T(X)GR}$] in Eq. (6), page 2, by $(1 - 0.285 K_t)/(1 + K_t)$ — for isotropic materials only.

IV. Correction for Gage Factor vs. Temperature

For any temperature increment, multiply the parenthetic expression ($\epsilon_{T(X)GS} - \epsilon_{T(X)GR}$) in Eq. (6), page 2, by $1/(1 + \Delta F_G)$. The term ΔF_G , in decimal form, corresponds to the midpoint of the temperature increment over which thermal output measurements are made.

V. Correction for Leadwire Resistance (R_L) for a Single Gage in a Three-wire Configuration

R_L is the resistance of a single leadwire in the three-wire connection to the instrument. To avoid the tedious task of correcting all individual readings by the factor $(R_G + R_L)/R_G$ it is much simpler to adjust the gage factor setting of the instrument to $F_I = F_G \times R_G/(R_G + R_L)$.

To evaluate the need for this correction, the approximate lead resistances for typical Micro-Measurements cables are:

326-DFV, 326-DTV: 0.141 ohms/m (0.043 ohms/ft)

330-DFV, 330-FFE, 330-FJT, 330-FTE: 0.354 ohms/m (0.108 ohms/ft)

NOTES

Shunt Calibration of Strain Gage Instrumentation

I. Introduction

The need for calibration arises frequently in the use of strain gage instrumentation. Periodic calibration is required, of course, to assure the accuracy and/or linearity of the instrument itself. More often, calibration is necessary to scale the instrument sensitivity (by adjusting gage factor or gain) in order that the registered output correspond conveniently and accurately to some predetermined input. An example of the latter situation occurs when a strain gage installation is remote from the instrument, with measurable signal attenuation due to leadwire resistance. In this case, calibration is used to adjust the sensitivity of the instrument so that it properly registers the strain signal produced by the gage. Calibration is also used to set the output of any auxiliary indicating or recording device (oscilloscope, computer display, etc.) to a convenient scale factor in terms of the applied strain.

There are basically two methods of calibration available: direct and indirect. With direct calibration, a precisely known mechanical input is applied to the sensing element of the measurement system, and the instrument output is compared to this for verification or adjustment purposes. For example, in the case of transducer instrumentation, an accurately known load (pressure, torque, displacement, etc.) is applied to the transducer, and the instrument sensitivity is adjusted as necessary to register the corresponding output. Direct calibration of instrument systems in this fashion is highly desirable, but is not ordinarily feasible for the typical stress analysis laboratory because of the special equipment and facilities required for its valid implementation.

The more practical and widely used approach to either instrument verification or scaling is by indirect calibration; that is, by applying a simulated strain gage output to the input terminals of the instrument. It is assumed throughout this Tech Note that the input to the instrument is always through a Wheatstone bridge circuit as a highly sensitive means of detecting the small resistance changes which characterize strain gages. The behavior of a strain gage can then be simulated by increasing or decreasing the resistance of a bridge arm.

As a rule, strain gage simulation by increasing the resistance of a bridge arm is not very practical because of the small resistance changes involved. Accurate calibration would require inserting a small, ultra-precise resistor in series with the gage. Furthermore, the electrical contacts for inserting the resistor can introduce a significant uncertainty in the resistance change. On the other hand, decreasing the resistance of a bridge arm by shunting with a large resistor offers a simple, potentially accurate means for simulating the action of a strain gage. This method, known as *shunt calibration*, places no particularly severe tolerance requirements on the shunting resistor, and is relatively insensitive to modest variations in contact resistance. It is also more versatile in application and generally simpler to implement.

Because of its numerous advantages, shunt calibration is the normal procedure for verifying or setting the output of a strain gage instrument relative to a predetermined mechanical input at the sensor. The subject matter of this Tech Note encompasses a variety of commonly occurring bridge circuit arrangements and shunt-calibration procedures. In all cases, it should be noted, the assumptions are made that the excitation for the bridge circuit is provided by a constant-voltage power supply, and that the input impedance of any instrument applied across the output terminals of the bridge circuit is effectively infinite. The latter condition is approximately representative of most modern strain-measurement instruments in which the bridge output is "balanced" by injecting an equal and opposite voltage developed in a separate network. It is also assumed that there are no auxiliary resistors (such as those commonly used in transducers for temperature compensation, span adjustment, etc.) in either the bridge circuit proper or in the circuitry supplying bridge power.

Although simple in concept, shunt calibration is actually much more complex than is generally appreciated. The full potential of this technique for accurate instrument calibration can be realized only by careful consideration of the errors which can occur when the method is misused. Of primary

importance, the principles employed here are equally applicable to constant-current systems, but the shunt-calibration relationships will differ where nonlinearity considerations are involved.

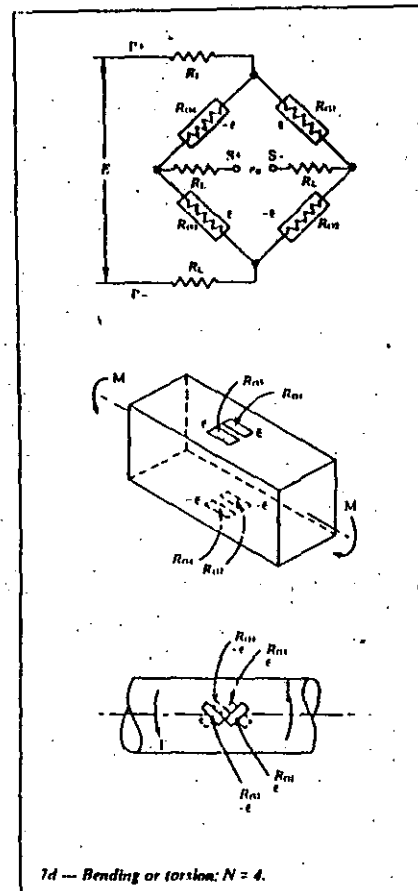


Fig. 2 — Bending or torsion: $N = 4$.

The cause of the nonlinear behavior (when it occurs) can be demonstrated by reexamining Eq. (1a), with reference to Fig. 1. The bridge output voltage under any initial condition can be expressed as:

$$\left(\frac{e_o}{E}\right)_1 = \frac{R_1}{R_1 + R_2} - \frac{R_4}{R_3 + R_4} \quad (10)$$

Considering, for the moment, resistance changes in \$R_1\$ and \$R_2\$ (composing the right-hand branch of the bridge circuit), the output voltage after such changes is:

$$\left(\frac{e_o}{E}\right)_2 = \frac{R_1 + \Delta R_1}{R_1 + R_2 + \Delta R_1 + \Delta R_2} - \frac{R_4}{R_3 + R_4} \quad (11)$$

The change in the output signal from the bridge (or the nulling voltage) is then:

$$\Delta\left(\frac{e_o}{E}\right) = \left(\frac{e_o}{E}\right)_2 - \left(\frac{e_o}{E}\right)_1 = \frac{R_1 + \Delta R_1}{R_1 + R_2 + \Delta R_1 + \Delta R_2} - \frac{R_1}{R_1 + R_2} \quad (12)$$

In the usual case, however, \$R_1 = R_2 = R_0\$, the nominal strain gage resistance. After making this substitution, and reducing,

$$\Delta\left(\frac{e_o}{E}\right) = \frac{\frac{\Delta R_1}{R_0} - \frac{\Delta R_2}{R_0}}{4 + 2\frac{\Delta R_1}{R_0} + 2\frac{\Delta R_2}{R_0}} \quad (13)$$

For the quarter-bridge circuit with only a single active gage (\$R_2, \Delta R_2 = 0\$) and:

$$\Delta\left(\frac{e_o}{E}\right) = \frac{\frac{\Delta R_1}{R_0}}{4 + 2\frac{\Delta R_1}{R_0}} \quad (14)$$

Or, introducing the relationship from Eq. (4),

$$\Delta\left(\frac{e_o}{E}\right) = \frac{F_{10} \epsilon}{4 + 2F_{10} \epsilon} \quad (15)$$

It is evident from Eqs. (14) and (15) that in a quarter-bridge circuit the output is a nonlinear function of the resistance change and the strain — due to the presence of the second term in the denominator. The nonlinearity reflects the fact that as the gage resistance changes, the current through \$R_0\$ and \$R_2\$ also changes, in the opposite direction of the resistance change. For typical working strain levels, the quantity \$2F_{10} \epsilon\$ in Eq. (15) is very small compared to 4, and the nonlinearity can usually be ignored. When measuring large strains, or when the greatest precision is required, the indicated strain must be corrected for the nonlinearity. The only known exception to the latter statement is the Measurements Group's System 4060, in which the correction can be made automatically, and at all strain levels.

Returning to the more general expression for the output of a half-bridge [Eq. (13)], it can be seen that the nonlinearity terms in the denominator can be eliminated only by setting \$\Delta R_2 = -\Delta R_1\$. Then, with the resistance changes in \$R_1\$ and \$R_2\$ numerically equal, but opposite in sign, Eq. (13) reduces to the linear expression:

$$\Delta\left(\frac{e_o}{E}\right) = \frac{2\frac{\Delta R_1}{R_0} - \frac{\Delta R_1}{R_0}}{4} = \frac{\Delta R_0}{2} \quad (16)$$

Thus, when the separate resistance changes in \$R_1\$ and \$R_2\$ are such that the total series resistance is unchanged, the current through \$R_1\$ and \$R_2\$ remains constant, and the bridge output is proportional to the resistance change. A common application of this condition occurs when a beam in bending is instrumented with a strain gage on the convex side and another, mounted directly opposite, on the concave side.

concern are: (1) the choice of the bridge arm to be shunted, along with the placement of the shunt connections in the bridge circuit; (2) calculation of the proper shunt resistance to simulate a prescribed strain level or to produce a prescribed instrument output; and (3) Wheatstone bridge non-linearity (when calibrating at high strain levels). Because of the foregoing, different shunt-calibration relationships are sometimes required for different sets of circumstances. It is particularly important to distinguish between two modes of shunt calibration which are referred to in this Tech Note, somewhat arbitrarily, as *instrument scaling* and *instrument verification*.

In what is described as *instrument scaling*, the reference is to the use of shunt calibration for *simulating the strain gage circuit output* which would occur during an actual test program when a particular gage in the circuit is subjected to a predetermined strain. The scaling is normally accomplished by adjusting the gain or gage-factor control of the instrument in use until the indicated strain corresponds to the simulated strain. This procedure is widely used to provide automatic correction for any signal attenuation due to leadwire resistance. In the case of half- and full-bridge circuits, it can also be employed to adjust the instrument scale factor to indicate the surface strain under a single gage, rather than some multiple thereof. When shunt calibration is used for instrument scaling, as defined here, the procedure is not directly related to verifying the accuracy or linearity of the instrument itself.

By *instrument verification*, in this context, is meant the process of using shunt calibration to *synthesize an input signal* to the instrument which should, for a perfectly accurate and linear instrument, produce a *predetermined output indication*. If the shunt calibration is performed properly, and the output indication deviates from the correct value, then the error is due to the instrument. In such cases, the instrument may require repair or adjustment of internal trimmers, followed by recalibration against a standard such as the Measurements Group Model 1350A Calibrator. Thus, shunt calibration for instrument verification is concerned only with the instrument itself; not with temporary adjustments in gain or gage factor, made to conveniently account for a particular set of external circuit conditions.

It is always necessary to maintain the distinction between *instrument scaling* and *verification*, both in selecting a calibration resistor and in interpreting the result of shunting. There are also several other factors to be considered in shunt calibration, some of which are especially important in scaling applications. The relationships needed to calculate calibration resistors for commonly occurring cases are given in the remaining sections of this Tech Note as follows:

Section	Content
II.	Basic Shunt Calibration Derivation of fundamental shunt-calibration equations.
III.	Instrument Scaling for Small Strains Simple quarter-bridge circuit — downscale, upscale calibration. Half- and full-bridge circuits.
IV.	Wheatstone Bridge Nonlinearity Basic considerations. Effects on strain measurement and shunt calibration.

- V. **Instrument Scaling for Large Strains**
Quarter-bridge circuit — downscale, upscale calibration. Half- and full-bridge circuits.
- VI. **Instrument Verification**
Small strains. Large strains.
- VII. **Accuracy Considerations**
Maximum error. Probable error.

For a wide range of practical applications, Sections II, III, and VI should provide the necessary information and relationships for routine shunt calibration at modest strain levels. When large strains are involved, however, reference should be made to Sections IV and V. Limitations on the accuracy of shunt calibration are investigated in Section VII. The Appendix to this Tech Note contains a logic diagram illustrating the criteria to be considered in selecting the appropriate shunt-calibration relationship for a particular application.

II. Basic Shunt Calibration

Illustrated in Fig. 1 is the Wheatstone bridge circuit in its simplest form. With the bridge excitation provided by the constant voltage E , the output voltage is always equal to the voltage difference between points A and B :

$$E_A = E \left(1 - \frac{R_4}{R_4 + R_1} \right)$$

$$E_B = E \left(1 - \frac{R_3}{R_3 + R_2} \right)$$

And,

$$e_o = E_A - E_B = E \left(\frac{R_1}{R_1 + R_2} - \frac{R_4}{R_4 + R_3} \right) \quad (1)$$

Or, in more convenient, nondimensional form:

$$\frac{e_o}{E} = \frac{R_1/R_2}{R_1/R_2 + 1} - \frac{R_4/R_3}{R_4/R_3 + 1} \quad (1a)$$

It is evident from the form of Eq. (1a) that the output depends only on the resistance ratios R_1/R_2 and R_4/R_3 , rather than on the individual resistances. Furthermore,

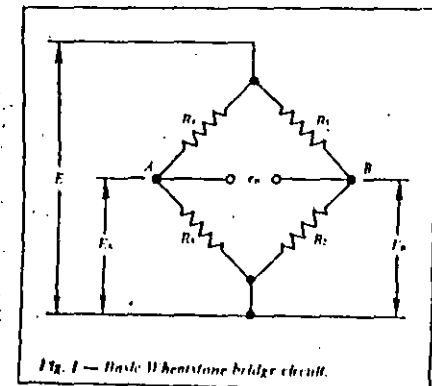


Fig. 1 — Basic Wheatstone bridge circuit.

when $R_4/R_3 = R_1/R_2$, the output is zero and the bridge is described as resistively balanced. Whether the bridge is balanced or unbalanced, Eq. (1a) permits calculating the change in output voltage due to decreasing any one of the arm resistances by shunting. The equation also demonstrates that the sign of the change depends on which arm is shunted. For example, decreasing R_1/R_2 by shunting R_1 , or increasing R_4/R_3 by shunting R_3 will cause a negative change in output. Correspondingly, a positive change in output is produced by shunting R_3 or R_4 (increasing R_4/R_3 , and decreasing R_1/R_2 , respectively).

Equation (1a) is perfectly general in application to constant-voltage Wheatstone bridges, regardless of the values of R_1 , R_2 , R_3 , and R_4 . In conventional strain gage instrumentation, however, at least two of the bridge arms normally have the same (nominal) resistance; and all four arms are often the same. For simplicity in presentation, without a significant sacrifice in generality, the latter case, known as the "equal-arm bridge", is assumed in the following, and pictured in Fig. 2. The diagram shows a single active gage, represented by R_1 , and an associated calibration resistor, R_c , for shunting across the gage to produce an output signal simulating strain. The bridge is assumed to be in an initial state of resistive balance; and all leadwire resistances are assumed negligibly small for this introductory development of shunt-calibration theory. Methods of accounting for leadwire resistance (or eliminating its effects) are given in Section III.

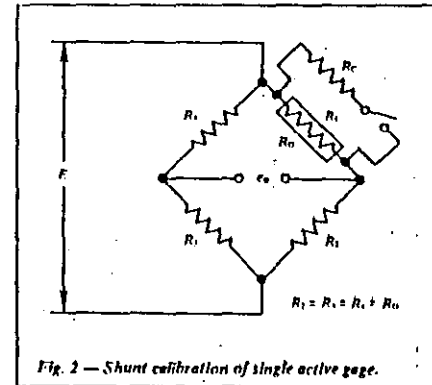


Fig. 2 — Shunt calibration of single active gage.

When the calibration resistor is shunted across R_1 , the resistance of the bridge arm becomes $R_1 R_c / (R_1 + R_c)$, and the change in arm resistance is:

$$\Delta R = \frac{R_1 R_c}{R_1 + R_c} - R_1 \quad (2)$$

Or,

$$\frac{\Delta R}{R_1} = \frac{-R_c}{R_1 + R_c} \quad (3)$$

Reexpressing the unit resistance change in terms of strain yields a relationship between the simulated strain and the shunt resistance required to produce it. The result is usually written here in the form $R_c = f(\epsilon_s)$, but the simulated strain for a particular shunt resistance can always be calculated by inverting the relationship.

The unit resistance change in the gage is related to strain through the definition of the gage factor, F_0 (see Footnote 2).

$$\frac{\Delta R}{R_0} = F_0 \epsilon \quad (4)$$

where: R_0 = the nominal resistance of the strain gage (e.g., 120 ohms, 350 ohms, etc.).

Combining Eqs. (3) and (4), and replacing R_1 by R_0 , since there is no other resistance in the bridge arm,

$$F_0 \epsilon_s = \frac{-R_c}{R_0 + R_c}$$

Or,

$$\epsilon_s = \frac{-R_0}{F_0 (R_0 + R_c)} \quad (5)$$

where: ϵ_s = strain (compressive) simulated by shunting R_0 with R_c . Solving for R_c ,

$$R_c = -\frac{R_0}{F_0 \epsilon_s} - R_0 \quad (6)$$

Since the simulated strain in this mode of shunt calibration is always negative, it is common practice in the strain gage field to omit the minus sign in front of the first term in Eq. (6), and write it as:

$$R_c = \frac{R_0}{F_0 \epsilon_s} - R_0 = \frac{R_0 \times 10^6}{F_0 \epsilon_{\mu m}} - R_0 \quad (7)$$

where: $\epsilon_{\mu m}$ = simulated strain, in microstrain units.

When substituting into Eq. (7), the user must always remember to substitute the numerical value of the compressive strain, without the sign.

TABLE I — Shunt Calibration Resistors

GAUGE CIRCUIT	RESISTANCE IN OHMS	EQUIVALENT MICROSTRAIN*
120-OHM	590 000	100
	119 000	500
	39 000	1000
	29 000	2000
	19 000	3000
	14 000	4000
350-OHM	11 000	5000
	5000	10 000
	349 000	500
	174 000	1000
	87 000	2000
	57 900	3000
1000-OHM	43 400	4000
	34 600	5000
	17 000	10 000
	990 000	500
	490 000	1000
	240 000	2000
1000-OHM	161 000	1000
	124 000	4000
	99 000	5000
	49 000	10 000

*In this Tech Note, the symbol F_0 represents the gage factor of the strain gage, while F_1 denotes the setting of the gage factor control on the strain indicator.

*The "Equivalent Microstrain" column gives the true compressive strain, in a quarter-bridge circuit, simulated by shunting each calibration resistor across an active strain gage arm of the exact indicated resistance. These values are based on a circuit gage factor setting of 2 000.

III. Instrument Scaling for Small Strains

Very commonly, when making practical strain measurements under typical test conditions, at least one active bridge arm is sufficiently remote from the instrument that the leadwire resistance is no longer negligible. Under these circumstances, the strain gage instrument is "desensitized", and the registered strain will be lower than the gage strain to an extent depending on the amount of leadwire resistance. In a three-wire quarter-bridge circuit, for instance, the signal will be attenuated by the factor $R_0/(R_0 + R_L)$, where R_L is the resistance of one leadwire in series with the gage. The usual way of correcting for leadwire desensitization is by shunt calibration — that is, by simulating a predetermined strain in the gage, and then adjusting the gage factor or gain of the instrument until it registers the same strain.

This section includes a variety of application examples involving quarter-, half-, and full-bridge strain gage circuits. In all cases treated here, it is assumed that strain levels are small enough relative to the user's permissible error limits that Wheatstone bridge nonlinearity can be neglected. Generalized relationships incorporating nonlinearity effects are given in subsequent sections.

Quarter-Bridge Circuit

Figure 4 illustrates a representative situation in which an active gage, in a three-wire circuit, is remote from the instrument and connected to it by leadwires of resistance R_L . If all leadwire resistances are nominally equal, then $R_1 = R_2 = R_3 = R_L + R_0$; i.e., the same amount of leadwire resistance is in series with both the active gage and the dummy. There is also leadwire resistance in the bridge output connection to the S-instrument terminal. The latter resistance has no effect, however, since the input impedance of the instrument applied across the output terminals of the bridge circuit is taken to be infinite. Thus, no current flows through the instrument leads.

To calibrate in compression, the active gage is shunted by a calibration resistor calculated from Eq. (7) or selected from Table I for the specified strain magnitude. After adjusting the sensitivity of the instrument to register the calibration strain, the effect of the leadwire resistance is eliminated from all subsequent strain measurements.

Unless additional leadwires are used (as demonstrated in Fig. 6), simulating compressive strain by directly shunting the remote active gage is usually difficult to implement in practice. Since the purpose of shunt calibration in this case is simply to scale the instrument sensitivity as a means of compensating for leadwire resistance, either upscale or downscale calibration is equally suitable. Thus, it is generally more convenient to shunt the adjacent dummy arm as shown in Fig. 4, because this can be done right at the instrument terminals. It should be apparent from the figure that the calibration resistor must be connected directly across the dummy to produce the desired result. (Calibration cannot be accurately simulated by shunting the active gage from S- to P+). Any shunt resistor connected across the dummy must be connected directly across the dummy to produce the desired result.

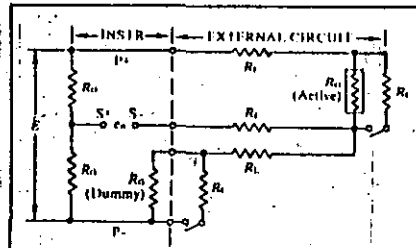


Fig. 4 — Quarter-bridge circuit with active gage remote from instrument.

Half-Bridge Circuits

In many stress analysis applications it is necessary (or at least advantageous) to employ two co-acting gages, connected as adjacent arms in the bridge circuit, to produce the required strain signal. A common example of this occurs when a second gage is installed on an unstressed specimen of the test material (and maintained in the same thermal environment as the test object) to provide temperature compensation for the active gage. In the special case of a purely uniaxial stress state, with the principal stress directions known, both gages can be mounted adjacent to each other, directly on the test part. One gage is aligned with the applied stress, and the other is installed in the perpendicular direction to sense the Poisson strain. This arrangement provides an augmented bridge output, along with excellent temperature compensation. Similar opportunities are offered by a beam in bending. One gage is mounted along the longitudinal centerline of the convex surface, with a mating gage at the corresponding point on the concave surface. When the two gages are connected as adjacent arms in the bridge circuit, and operating under uniform temperature conditions, the effect of the leadwire resistance is eliminated from all subsequent strain measurements.

III. Instrument Scaling for Small Strains

Very commonly, when making practical strain measurements under typical test conditions, at least one active bridge arm is sufficiently remote from the instrument that the leadwire resistance is no longer negligible. Under these circumstances, the strain gage instrument is "desensitized", and the registered strain will be lower than the gage strain to an extent depending on the amount of leadwire resistance. In a three-wire quarter-bridge circuit, for instance, the signal will be attenuated by the factor $R_0/(R_0 + R_L)$, where R_L is the resistance of one leadwire in series with the gage. The usual way of correcting for leadwire desensitization is by shunt calibration — that is, by simulating a predetermined strain in the gage, and then adjusting the gage factor or gain of the instrument until it registers the same strain.

This section includes a variety of application examples involving quarter-, half-, and full-bridge strain gage circuits. In all cases treated here, it is assumed that strain levels are small enough relative to the user's permissible error limits that Wheatstone bridge nonlinearity can be neglected. Generalized relationships incorporating nonlinearity effects are given in subsequent sections.

Quarter-Bridge Circuit

Figure 4 illustrates a representative situation in which an active gage, in a three-wire circuit, is remote from the instrument and connected to it by leadwires of resistance R_L . If all leadwire resistances are nominally equal, then $R_1 = R_2 = R_3 = R_L + R_0$; i.e., the same amount of leadwire resistance is in series with both the active gage and the dummy. There is also leadwire resistance in the bridge output connection to the S-instrument terminal. The latter resistance has no effect, however, since the input impedance of the instrument applied across the output terminals of the bridge circuit is taken to be infinite. Thus, no current flows through the instrument leads.

To calibrate in compression, the active gage is shunted by a calibration resistor calculated from Eq. (7) or selected from Table I for the specified strain magnitude. After adjusting the sensitivity of the instrument to register the calibration strain, the effect of the leadwire resistance is eliminated from all subsequent strain measurements.

Unless additional leadwires are used (as demonstrated in Fig. 6), simulating compressive strain by directly shunting the remote active gage is usually difficult to implement in practice. Since the purpose of shunt calibration in this case is simply to scale the instrument sensitivity as a means of compensating for leadwire resistance, either upscale or downscale calibration is equally suitable. Thus, it is generally more convenient to shunt the adjacent dummy arm as shown in Fig. 4, because this can be done right at the instrument terminals. It should be apparent from the figure that the calibration resistor must be connected directly across the dummy to produce the desired result. Gage strain cannot be accurately simulated by shunting from S- to P+ (or from S- to P+). After shunting the dummy with a calibration resistor selected to simulate the appropriate strain, the instrument sensitivity is adjusted to register the same strain. At low strain levels, the result is effectively the same as if the calibration had been performed by shunting the active gage.

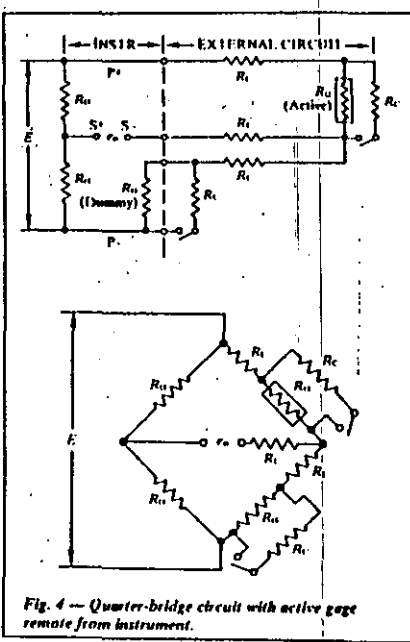


Fig. 4 — Quarter-bridge circuit with active gage remote from instrument.

Half-Bridge Circuits

In many stress analysis applications it is necessary (or at least advantageous) to employ two co-acting gages, connected as adjacent arms in the bridge circuit, to produce the required strain signal. A common example of this occurs when a second gage is installed on an unstressed specimen of the test material (and maintained in the same thermal environment as the test object) to provide temperature compensation for the active gage. In the special case of a purely uniaxial stress state, with the principal stress directions known, both gages can be mounted adjacent to each other, directly on the test part. One gage is aligned with the applied stress, and the other is installed in the perpendicular direction to sense the Poisson strain. This arrangement provides an augmented bridge output, along with excellent temperature compensation. Similar opportunities are offered by a beam in bending. One gage is mounted along the longitudinal centerline of the convex surface, with a mating gage at the corresponding point on the concave surface. When the two gages are connected as adjacent arms in the bridge circuit, and assuming uniform temperature through the thickness of the beam, the bridge output is doubled while maintaining temperature compensation.

All of the foregoing are examples of half-bridge circuits, since one-half of the Wheatstone bridge is external to the instrument. Aside from differences in the quality of the achievable temperature compensation, they differ principally in their degrees of signal increase. The factor of signal augmentation is usually expressed in terms of the "number

of active gages. N . When the gage in the adjacent bridge arm senses no applied strain, but serves solely for temperature compensation, $N = 1$. With two perpendicular gages, aligned along the principal axes in a uniaxial stress field, $N = 1 + \nu$, where ν is the Poisson's ratio of the test material. In the case of the beam, with gages on opposing surfaces, $N = 2$, since the gages sense equal and opposite strains, and the bridge output is doubled.

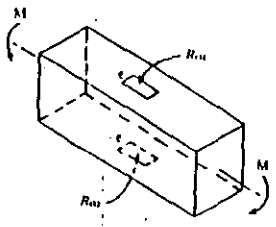
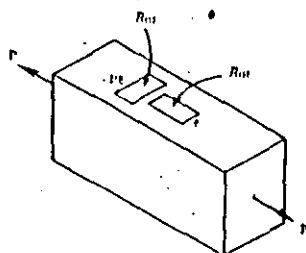
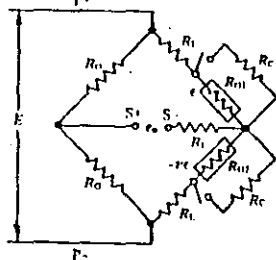
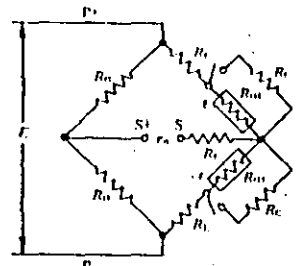
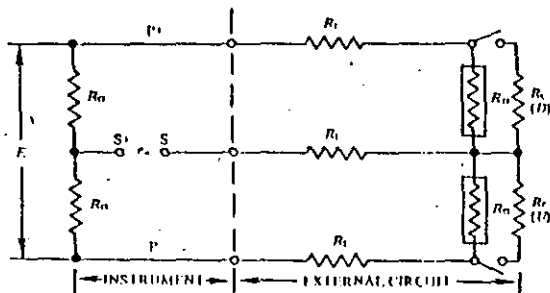
When N is greater than unity, it is obviously necessary to adjust the instrument sensitivity by the factor $1/N$ if the instrument is to directly register the actual surface strain sensed by the primary active gage. Furthermore, if the gage installations are at a distance from the instrument, additional adjustment of the sensitivity (in the opposite direc-

tion) is required to compensate for the signal loss due to leadwire resistance. Shunt calibration can correct for both effects simultaneously, and permit adjusting instrument sensitivity to register the correct surface strain at the primary active gage.

Figure 5a illustrates a typical half-bridge circuit, with the gages located away from the instrument, and with shunt resistors for downscale (D) and upscale (U) calibration. Figures 5b and 5c show the physical and circuit arrangements for $N = 1 + \nu$ and $N = 2$, respectively. The procedure for calibration is the same as for the quarter-bridge circuit. That is, a calibration resistor of the appropriate size is shunted across the gage, and the instrument sensitivity is adjusted to register the simulated strain.

Fig. 5 — Shunt calibration of external half-bridge circuits.

5a — Basic circuit.



5b — Uniform uniaxial stress: $N = 1 + \nu$

5c — Bending beam: $N = 2$

Confusion sometimes arises, however, in correlating the registered strain with the simulated strain (and with the calibration resistor) when N is greater than unity. The simplest way of handling this is to generalize Eq. (7) so that it includes the number of active gages. Thus,

$$R_c = \frac{R_n \times 10^6}{F_n \times N \times \epsilon_{sp}} - R_n \quad (8)$$

To calibrate, the strain gage is shunted with a resistor calculated from Eq. (8) and the instrument sensitivity adjusted to register ϵ_{sp} . The result is the same, except for the sign of the instrument output, no matter which of the two adjacent-arm gages in Fig. 5 is shunted. After calibration, the instrument output will correspond to the surface strain at the primary active gage. This procedure accounts for both the signal increase (when $N > 1$) and the leadwire desensitization.

When the gage installations are more than a few steps away from the instrument, it is usually inconvenient to connect a shunt-calibration resistor directly across the gage as shown in Fig. 5. For such cases, remote shunt calibration is a common practice. Figure 6 illustrates a half-bridge circuit with the calibration resistor positioned at the instrument. In this example, three extra leadwires and a switch permit connecting the shunt across either arm of the half bridge. Since shunt resistors are characteristically in the thousands of ohms, the resistances of the calibration leadwires, although shown in the figure, can usually be neglected in the strain simulation calculations. Equation (8) is then directly applicable to remote shunt calibration. If the leadwire resistance is large enough so that $100 \times R_l/R_c$ is greater than about 1/10 of the required calibration precision (expressed in percent), Eq. (8) can be modified as follows to calculate the correct calibration resistance:

$$R_c = \frac{R_n \times 10^6}{F_n \times N \times \epsilon_{sp}} - R_n - 2R_l \quad (9)$$

In Eq. (9), R_l represents the resistance of one leadwire between the calibration resistor and gage.

Full-Bridge Circuits

In strain-measurement (stress analysis) applications for which the half bridge is suitable, the output signal can be doubled by installing a full bridge, with four active strain gages on the test object. A representative circuit, including two supplementary leadwires for remote shunt calibration, is shown in Fig. 7a. In practice, the calibration leadwires can be connected across any arm of the bridge, and will always produce the same signal magnitude, but the sign of the signal depends on which arm is shunted. It will be noticed, in the case of the full-bridge circuit, that the leadwire resistance is now in the bridge power and output leads rather than in the bridge arms. With the assumption of infinite impedance at the bridge output, the resistance in the latter leads has no effect. (However, the resistance in the power leads reduces the voltage applied to the bridge proper, and attenuates the output signal accordingly.)

Three widely used full-bridge circuit arrangements are shown in Figs. 7b, 7c, and 7d. In the first two of these, for bending and direct stress, respectively, the number of active gages is expressed by $N = 2(1 + \nu)$. This value is substituted into Eq. (8) or Eq. (9) when calculating the calibration resistor to simulate a surface strain of ϵ_s . The physical arrangement of the gages is the same in both cases; but, as indicated by the equivalent-circuit diagrams, the gages are positioned differently in the bridge circuit to produce the desired signal in each instance. For applications involving pure bending or torsion, the bridge output signal can be increased further with the gage and circuit configurations illustrated in Fig. 7d. Since all four gages are fully active in these examples, $N = 4$ for substitution into Eqs. (8) or (9).

In general, the shunt-calibration relationships appearing in this section are limited in application to the simulation of low strain magnitudes, since nonlinearity effects in the Wheatstone bridge circuit have been ignored. The equations given here are intended primarily for scaling the output of an instrument to register the same strain magnitude that it

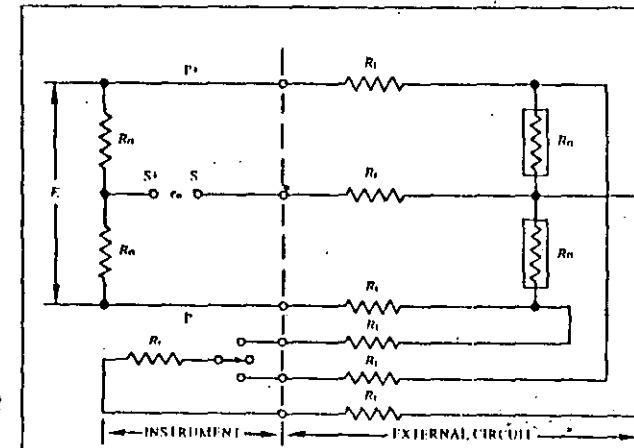


Fig. 6 — Remote shunt calibration of external half-bridge.

would if the selected gage were subjected to an actual strain equal to the simulated strain. This mode of shunt calibration offers a simple, convenient means for eliminating the effects of leadwire deactivation and accounting for more than one active gage ($N > 1$) in the bridge circuit.

For calibration at strain levels higher than about 2000 $\mu\epsilon$, or for precise evaluation of instrument accuracy, it is ordinarily necessary to incorporate the effects of Wheatstone bridge nonlinearity in the shunt-calibration relationships. Nonlinearity considerations are treated in Section IV, and application examples given in Section V.

IV. Wheatstone Bridge Nonlinearity

As described in TN-507, the common practice with modern strain gage instruments is to operate the Wheatstone bridge circuit in a resistively unbalanced mode during strain measurement. In some instruments, the resulting bridge output voltage is read directly as a measure of the strain-induced resistance change(s) in one or more of the bridge arms. In others, the bridge output signal is "balanced" (nulled) by injecting an equal and opposite voltage from a separate circuit which is powered by an equal supply voltage.

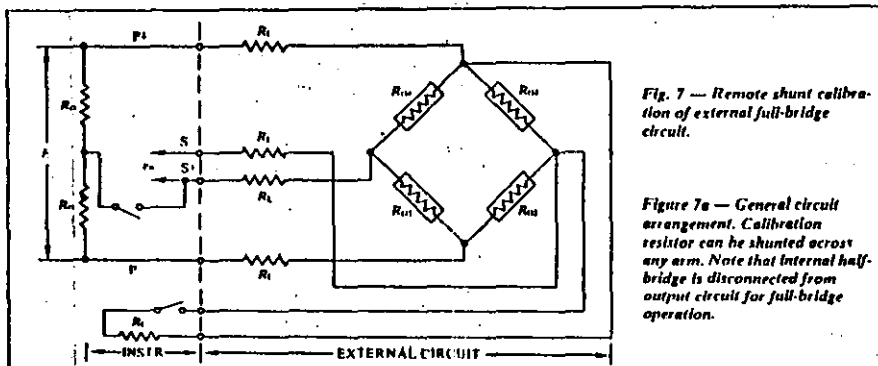
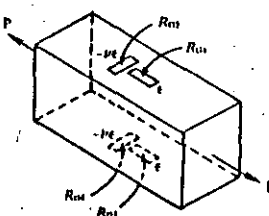
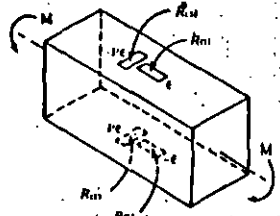
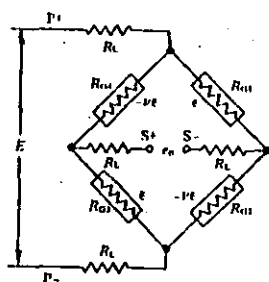
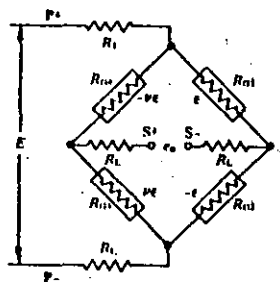


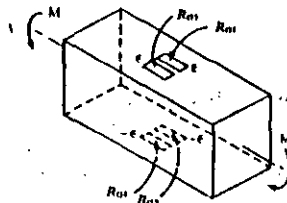
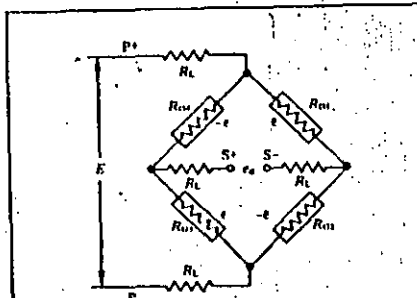
Fig. 7 — Remote shunt calibration of external full-bridge circuit.

Figure 7a — General circuit arrangement. Calibration resistor can be shunted across any arm. Note that internal half-bridge is disconnected from output circuit for full-bridge operation.



7c — Bending beam, with Poisson gage orientation: $N = 2(1 + \nu)$.

7d — Uniform uniaxial stress, with Poisson gage orientation: $N = 2(1 + \nu)$.



7d — Bending or torsion: $N = 4$.

The cause of the nonlinear behavior (when it occurs) can be demonstrated by reexamining Eq. (1a), with reference to Fig. 1. The bridge output voltage under any initial condition can be expressed as:

$$\left(\frac{\epsilon_0}{E}\right)_1 = \frac{R_1}{R_1 + R_2} - \frac{R_1}{R_2 + R_1} \quad (10)$$

Considering, for the moment, resistance changes in R_1 and R_2 (the output voltage after such changes is:

$$\left(\frac{\epsilon_0}{E}\right)_2 = \frac{R_1 + \Delta R_1}{R_1 + R_1 + \Delta R_1 + \Delta R_2} - \frac{R_1}{R_1 + R_2} \quad (11)$$

The change in the output signal from the bridge (or the nulling voltage) is then:

$$\begin{aligned} \Delta\left(\frac{\epsilon_0}{E}\right) &= \left(\frac{\epsilon_0}{E}\right)_2 - \left(\frac{\epsilon_0}{E}\right)_1 \\ &= \frac{R_1 + \Delta R_1}{R_1 + R_1 + \Delta R_1 + \Delta R_2} - \frac{R_1}{R_1 + R_2} \quad (12) \end{aligned}$$

In the usual case, however, $R_1 = R_2 = R_0$, the nominal strain gage resistance. After making this substitution, and reducing,

$$\Delta\left(\frac{\epsilon_0}{E}\right) = \frac{\frac{\Delta R_1}{R_0} - \frac{\Delta R_1}{R_0}}{4 + 2 \frac{\Delta R_1}{R_0} + 2 \frac{\Delta R_2}{R_0}} \quad (13)$$

For the quarter-bridge circuit with only a single active gage (R_1), $\Delta R_2 = 0$ and:

$$\Delta\left(\frac{\epsilon_0}{E}\right) = \frac{\frac{\Delta R_1}{R_0}}{4 + 2 \frac{\Delta R_1}{R_0}} \quad (14)$$

Or, introducing the relationship from Eq. (4),

$$\Delta\left(\frac{\epsilon_0}{E}\right) = \frac{F_1 \epsilon}{4 + 2F_0 \epsilon} \quad (15)$$

It is evident from Eqs. (14) and (15) that in a quarter-bridge circuit the output is a nonlinear function of the resistance change and the strain — due to the presence of the second term in the denominator. The nonlinearity reflects the fact that as the gage resistance changes, the current through R_1 and R_2 also changes, in the opposite direction of the resistance change. For typical working strain levels, the quantity $2F_0 \epsilon$ in Eq. (15) is very small compared to 4, and the nonlinearity can usually be ignored. When measuring large strains, or when the greatest precision is required, the indicated strain must be corrected for the nonlinearity. The only known exception to the latter statement is the Measurements Group's System 4000, in which the correction can be made automatically, and at all strain levels.

Returning to the more general expression for the output of a half-bridge [Eq. (13)], it can be seen that the nonlinearity terms in the denominator can be eliminated only by setting $\Delta R_2 = -\Delta R_1$. Then, with the resistance changes in R_1 and R_2 numerically equal, but opposite in sign, Eq. (13) reduces to the linear expression:

$$\Delta\left(\frac{\epsilon_0}{E}\right) = \frac{2 \frac{\Delta R_1}{R_0}}{4} = \frac{\Delta R_1}{2 R_0} \quad (16)$$

Thus, when the separate resistance changes in R_1 and R_2 are such that the total series resistance is unchanged, the current through R_1 and R_2 remains constant, and the bridge output is proportional to the resistance change. A common application of this condition occurs when a beam in bending is instrumented with a strain gage on the convex side and another, mounted directly opposite, on the concave side.

The strains sensed by the two gages are then equal in magnitude and opposite in sign ($\epsilon_2 = -\epsilon_1$). If the two gages are connected in a half-bridge circuit, as in Fig. 5c, the conditions required for Eq. (16) are satisfied, and the bridge output, expressed in strain units, is:

$$A \left(\frac{\epsilon_0}{E} \right) = \frac{E_0 \epsilon_1}{2} \quad \text{where } |\epsilon_1| \text{ represents the absolute value of strain in either gage.} \quad (17)$$

This demonstration has dealt with only bridge arms R_1 and R_2 in Fig. 1, but it applies equally to arms R_3 and R_4 . The principle can be generalized as follows: any combination of strains and resultant resistance changes in two active bridge arms (R_1 and R_2 , or R_3 and R_4) which causes the current in that branch of the bridge circuit to change will introduce nonlinearity into the output. Relationships giving the nonlinearity errors for a variety of commonly used circuit arrangements are given in TN-507.

With the foregoing principle in mind, we are now in a position to consider the effect of Wheatstone bridge nonlinearity on shunt calibration. It should first be noted that, in normal practice, only one arm of the bridge is shunted at a time; and it is never possible, by shunting, to produce equal and opposite resistance changes in R_1 and R_2 , or in R_3 and R_4 . Thus, the shunt-calibration procedure always results in nonlinear, quarter-bridge operation — regardless of how the bridge circuit functions during actual strain measurement. For instance, the bridge output during strain measurement is proportional to the surface strain, as indicated by Eq. (17). When either gage is shunted by a calibration resistor, however, the output is nonlinearly related to the simulated strain according to Eq. (15). As a result, shunting; say, R_1 in Fig. 5c does not exactly simulate, in terms of bridge output voltage, the behavior of the gage during strain measurement.

As noted earlier, the effect of the nonlinearity is small when the strains (actual or simulated) are small. For such cases, the relationships given in Section III are adequate to permit calculating the shunt resistor size to simulate a given strain magnitude. Because of this, it is preferable to perform instrument scaling at modest strain levels where the nonlinearity error is negligible.

When instrument scaling is done at higher strain levels, it is generally necessary to use special relationships, given in Section V, to precisely simulate gage behavior by shunt calibration. There is one notable exception to the latter statement, however. The bridge output due to shunting a single gage is indistinguishable from that of a quarter-bridge circuit with the gage shunted in compression. For this special (but common) case, the simulation is exact at all compressive strain levels because the nonlinearity due to shunting is the same as that caused by compressive strain in the gage. As shown in the Appendix, Eqs. (5) to (7) are thus appropriate for compressive scaling of quarter-bridge circuits at any level of strain.* The same is true, of course, for external half- and full-bridge circuits where there is only a single active gage, with the remaining bridge arms fitted for compensation and/or bridge-completion purposes.

Both Sections III and V are limited in scope to the subject of instrument scaling by gage simulation. Shunt calibration for instrument verification is treated separately in Section VI. For scaling applications, the size of the shunt-calibration resistor is selected so that the bridge output voltage is the same for both simulated and actual strains of the same magnitude. Therefore, when the Wheatstone bridge arrangement is intrinsically nonlinear (as in Fig. 5b, for instance), and the strain level is high, the instrument indication is accurate only at the simulated strain level. Subsequent correction may be needed if the instrument is to accurately register smaller or larger strains.

V. Instrument Scaling for Large Strains

It was demonstrated in the preceding section that Wheatstone bridge nonlinearity must generally be considered when shunt calibration is used for instrument scaling at high strain levels. Under such conditions, errors in gage simulation arise whenever the nonlinearity which is inherent in shunt calibration differs from that during actual strain measurement. The relationships given in this section for quarter-, half-, and full-bridge circuits provide for precisely simulating the strain gage output at any level of strain, low or high.† Thus, the instrument scaling will also be precise when the gain or gage factor control is adjusted to register the simulated strain. It must be kept in mind, however, that if the strain-measuring circuit arrangement is nonlinear (as in Figs. 4, 5b, and 7c), precise scaling is achieved only at the simulated strain level. At any other level of strain, some degree of error will be present due to the nonlinearity.

Quarter-Bridge Circuit

The quarter-bridge circuit, with a single active gage, is widely used in experimental stress analysis. When instrument scaling is done by connecting a shunt-calibration resistor directly across the gage, the simulation of compressive strain is exact at all strain levels. This is true because the nonlinearity in shunt calibration is the same as that during strain measurement. For such cases, the proper shunt-calibration resistor to simulate a given strain magnitude can be obtained directly from Table I, or calculated from Eq. (7) of Section II. After instrument scaling, the indicated strain will be correct at the magnitude of the calibration strain, but slightly in error at other strain levels because of the nonlinearity. For most practical applications, the corrected strain at any different strain level can be calculated from:

$$\epsilon = \frac{2\bar{\epsilon}}{2 + F_0(\epsilon_s - \bar{\epsilon})} \quad (18)$$

where: ϵ = corrected strain
 ϵ_s = calibration strain
 $\bar{\epsilon}$ = indicated strain
 F_0 = gage factor of strain gage

} with signs

Since the effect of leadwire resistance on bridge circuit nonlinearity is normally very small, terms involving R_L have been omitted from Eq. (18). If the leadwire resistance is a significant fraction of the gage resistance, however, Eq. (18) tends to overcorrect for the nonlinearity. In such cases, the following complete relationship can be used to obtain more accurate correction:

$$\epsilon = \frac{2 \left(1 + \frac{R_L}{R_0} \right) \bar{\epsilon}}{2 \left(1 + \frac{R_L}{R_0} \right) + F_0(\epsilon_s - \bar{\epsilon})} \quad (18a)$$

Shunting the dummy arm of the bridge (see Fig. 4) produces an upscale signal, and can be used to simulate a tensile strain in the active gage. For the simulation to be exact, however, a special shunt-calibration relationship is required, because the nonlinearity in tension is different from that in compression. If the active gage were subjected to an actual tensile strain, the resistance of the right-hand branch of the bridge in Fig. 4 would rise, and the current would decrease correspondingly. However, when the dummy arm of the bridge is shunted, the resistance of the branch decreases, and the current rises. This difference can be accounted for by calculating the calibration resistor so that the bridge output voltage due to shunting the dummy is the same as that for a preselected tensile calibration strain in the active gage. The procedure for doing so is demonstrated by the following derivation where, for the sake of simplicity, the effect of leadwire resistance is temporarily ignored ($R_L = 0$).

Equation (14) in Section IV gives the output voltage from a resistance change in the active gage (R_1). The negative of the same relationship applies to a change in the dummy arm, R_2 . Thus,

$$\left(\frac{\epsilon_0}{E} \right)_1 = \frac{\Delta R_1}{R_0} \quad (19)$$

$$\left(\frac{\epsilon_0}{E} \right)_2 = \frac{-\Delta R_2}{R_0} \quad (20)$$

The unit resistance change in the active gage due to a simulated tensile strain ϵ_{s1} is:

$$\frac{\Delta R_1}{R_0} = F_0 \epsilon_{s1}$$

Therefore,

$$\left(\frac{\epsilon_0}{E} \right)_1 = \frac{F_0 \epsilon_{s1}}{4 + 2F_0 \epsilon_{s1}} \quad (21)$$

On the other hand, the resistance change in the dummy, R_2 , is produced by shunting with a calibration resistor, R_c . From Eq. (3),

$$\frac{\Delta R_2}{R_0} = -\frac{R_0}{R_0 + R_c}$$

Substituting into Eq. (20),

$$\left(\frac{\epsilon_0}{E} \right)_2 = \frac{\frac{R_0}{R_0 + R_c}}{4 - 2 \frac{R_0}{R_0 + R_c}} = \frac{R_0}{2R_0 + 4R_c} \quad (22)$$

Equating the two expressions for output voltage,

$$\frac{F_0 \epsilon_{s1}}{4 + 2F_0 \epsilon_{s1}} = \frac{R_0}{2R_0 + 4R_c}$$

And, solving for R_c ,

$$R_c = \frac{R_0}{F_0 \epsilon_{s1}} - \frac{R_0}{2} \quad (23)$$

For the majority of routine applications, any desired tensile strain in the active gage can be simulated quite accurately by shunting the dummy gage with the calibration resistor specified by Eq. (23). This relationship can be compared to Eq. (7) to see the difference between simulating tensile and compressive strains in the active gage. After scaling for a given simulated tensile strain, the instrument indication will be correspondingly accurate for only that tensile strain magnitude. Measurements at other strain levels (tension or compression) can be corrected, if necessary, with Eq. (18) or (18a).

In extreme cases, when the simulated strain is very large, and the leadwire resistance is not a negligible fraction of the gage resistance, slightly greater accuracy in tensile strain simulation can be achieved by incorporating the leadwire resistance in the derivation of Eq. (23). The complete expression for the calibration resistor becomes:

$$R_c = \frac{R_0}{F_0 \epsilon_{s1}} - R_0 \left(\frac{R_L}{R_0} \right) \quad (23a)$$

The second term in Eq. (23a) can never be greater in magnitude than R_0 ; and, for typical strain levels, is negligible compared to the first term — irrespective of the leadwire resistance. Thus Eq. (23) is normally the appropriate relationship for the shunt resistor used in upscale calibration. The small error associated with Eq. (23) is plotted in Fig. 8 as a guide to the very rare circumstances when Eq. (23a) might be necessary.

It is worth noting, for quarter-bridge circuits, that scaling the instrument by shunting the internal dummy gage (which is usually a stable precision resistor) can offer distinct advantages in calibration accuracy. It is common practice, for instance, to calculate or select the value of the shunt-calibration resistor on the basis of the nominal gage resistance. But the resistance of the installed gage generally differs from the nominal, due both to its initial resistance tolerance and to a further change in resistance during installation. When this occurs, and the active gage is shunted for compression scaling, the simulated strain magnitude is in error accordingly. The extent of the error can be approximated by the method given in Section VII, "Accuracy Considerations".

*Since the nonlinearity due to a resistance increase is different than for a decrease, precise simulation of a high tensile strain requires a special relationship, as demonstrated in Section V.

†The subject relationships are "precise" or "exact" with respect to the specified parameters such as R_0 , R_c , and F_0 . The effects of tolerances on these quantities are discussed in Section VII, "Accuracy Considerations".

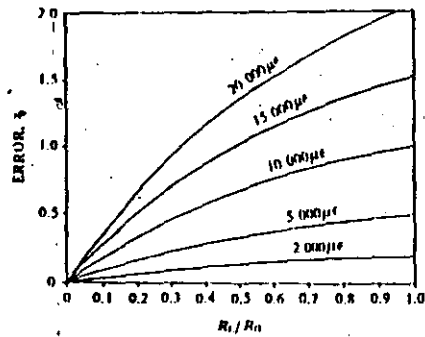


Fig. 8 — Percent error from using Eq. (23) instead of Eq. (7a). $F_0 = 2.0$.

One technique for avoiding most of the error due to deviation in the gage resistance is to temporarily replace the active gage in the bridge circuit with a precision resistor equal to the nominal resistance of the gage. The instrument is then scaled (in compression) by shunting the fixed resistor with a calibration resistor calculated from Eq. (7). After scaling, the active gage is reconnected to the bridge circuit. It is usually much more convenient, however, and about equally accurate, to scale in the tension direction by simply shunting the internal dummy with a resistor calculated from Eq. (23). When the leadwire resistance is negligible, this procedure is exact, and independent of the installed gage resistance. Even with modest leadwire resistance (say, less than $R_0/10$), the error due to a few ohms of gage resistance deviation is small enough to be ignored. In case of doubt, the installed gage resistance should be measured. If the resistance is significantly beyond the manufacturer's tolerance, one of the two foregoing procedures should always be used for shunt calibration.

Half-Bridge Circuits

When measuring the maximum principal strain in a known uniaxial stress state, a simple means for assuring effective temperature compensation is to mount a second gage adjacent and perpendicular to the primary gage, and connect the two gages in a half-bridge circuit as shown in Fig. 5b. Such an arrangement is said to have $N = 1 + \nu$ active gages, since the bridge output is increased by that factor. The circuit behavior is nonlinear, however, because the resistance changes in the two active gages are not equal and opposite.

It is assumed in the following that R_{01} in Fig. 5b represents the primary gage, and that the object is to scale the instrument to register the test-surface strain under that gage. Whether shunting R_{01} to simulate compression in the primary gage, or shunting R_{02} to simulate tension, the nonlinear error during scaling is different from that during actual strain measurement. Thus, two different shunt-calibration relationships are required for precise strain simulation, as in the case of the quarter-bridge circuit. These relationships are

developed in the same manner as before; that is, by enforcing the condition that the bridge output voltage be identical, whether scaling to a simulated strain level or measuring the same surface strain with the primary gage.

To simulate a compressive surface strain, ϵ_{c1} , by shunting R_{01} in Fig. 5b, the calibration resistor is calculated from:

$$R_c = \frac{R_0}{F_0 \epsilon_{c1} (1 + \nu)} - R_0 \left[1 - \frac{\nu}{(1 + \nu) \left(1 + \frac{R_L}{R_0} \right)} \right] \quad (24)$$

And, for a simulated tensile strain, ϵ_{t1} , generated by shunting R_{02} ,

$$R_c = \frac{R_0}{F_0 \epsilon_{t1} (1 + \nu)} - R_0 \left[1 - \frac{1}{(1 + \nu) \left(1 + \frac{R_L}{R_0} \right)} \right] \quad (25)$$

When substituting into Eqs. (24) and (25), the signs of the simulated strains must always be carried, of course. Also, it is apparent that leadwire resistance, if present, affects the nonlinear behavior, and must be known to permit exact simulation. Since the expressions are relatively insensitive to the quantity R_L/R_0 , precision measurement of the leadwire resistance is not ordinarily required. After scaling the instrument at a simulated strain, ϵ_s , the registered strain is precisely correct for only that same magnitude. When necessary, the corrected strain at any level can be calculated from:

$$\epsilon = \frac{2 \left(1 + \frac{R_L}{R_0} \right) \bar{\epsilon}}{2 \left(1 + \frac{R_L}{R_0} \right) + F_0 (1 - \nu) (\epsilon_s - \bar{\epsilon})} \quad (26)$$

The notation in Eq. (26) is the same as in Eq. (18) for the quarter-bridge circuit.

Another half-bridge application of interest is illustrated in Fig. 5c, where directly opposed strain gages are installed on the convex and concave sides of a rectangular-cross-section beam in bending. In this instance, the strains in R_{01} and R_{02} are always equal and opposite, if only bending occurs. As a result, the bridge behavior during strain measurement is linear; and, after scaling at a particular strain level, remains equally precise at all other strain magnitudes. Instrument scaling by shunt calibration is a nonlinear procedure, however, because there is a resistance change in only a single bridge arm. The simplest approach is to perform the scaling at a modest strain level where the error due to calibration nonlinearity is negligible. After scaling with Eq. (8), the instrument will register any other strain with the same relative precision.

If scaling at a high strain level is necessary, the calibration resistor can be calculated as follows to provide exact simulation of a surface strain, ϵ_s in R_{01} (when accompanied by the strain $-\epsilon_s$ in R_{02}):

$$R_c = \frac{R_0}{2F_0 |\epsilon_s|} - R_0 \left[1 - \frac{1}{2 \left(1 + \frac{R_L}{R_0} \right)} \right] \quad (27)$$

where: $|\epsilon_s|$ = absolute value of calibration strain

Equation (27) is suitable for either upscale or downscale shunt calibration. If the leadwire resistance is negligible, the relationship reduces to:

$$R_c = \frac{R_0}{2F_0 |\epsilon_s|} - \frac{R_0}{2} \quad (28)$$

Because the bridge output voltage varies linearly with strain when actual strains are being measured, no further correction is required.

Full-Bridge Circuits

When feasible, use of the full-bridge circuit offers several advantages, including a better signal-to-noise ratio. Typical applications are: beams in bending, shafts in torsion, and axially loaded columns and tension links. Although the simple examples described here do not incorporate the circuit refinements characteristic of commercial transducers, it is common practice to infer the magnitudes of mechanical variables such as bending moment, torque, and force from the full-bridge strain measurements.

Three representative full-bridge arrangements, illustrated in Figs. 7b, 7c, and 7d, are treated here. The circuits in Figs. 7b and 7d (for bending and torsion) have essentially the same characteristics, and can be grouped together for shunt-calibration purposes. In each of these circuits, the bridge output voltage varies linearly with strain, since equal and opposite resistance changes occur in arms 1 and 2, and in arms 3 and 4. The nonlinearity of shunt calibration must be accounted for, however, to achieve exact strain simulation at large strains. The proper calibration resistor to simulate a given surface strain (e.g., the longitudinal strain, in the case of the beam) can be calculated from the following:

$$R_c = \frac{R_0}{NF_0 |\epsilon_s|} - R_0 \left[\frac{1 + 3 \frac{R_L}{R_0}}{2 \left(1 + 2 \frac{R_L}{R_0} \right)} \right] \quad (29)$$

Once calibrated according to Eq. (29), an accurate instrument will register the correct strain at any other strain magnitude. As in the case of the half-bridge circuit, the leadwire resistance is present in the calibration relationship, but does not need to be known with high precision.

The arrangement shown in Fig. 7c for a centrally loaded column or tension member, is somewhat more complex. It can be seen from the figure that the bridge currents change with applied strain, and thus the output voltage is a nonlinear function of strain even before calibrating with a shunt resistor. Because the nonlinearity is different in tension and compression, separate calibration equations are required as follows:

To simulate compression in R_{01} ,

$$R_c = \frac{-R_0}{2(1 + \nu)F_0 \epsilon_{c1}} - R_0 \left[\frac{3(1 + \nu) \left(1 + 2 \frac{R_L}{R_0} \right) - 2\nu}{4(1 + \nu) \left(1 + 2 \frac{R_L}{R_0} \right)} \right] \quad (30)$$

And, for tension in R_{01} ,

$$R_c = \frac{R_0}{2(1 + \nu)F_0 \epsilon_{t1}} - R_0 \left[\frac{3(1 + \nu) \left(1 + 2 \frac{R_L}{R_0} \right) - 2\nu}{4(1 + \nu) \left(1 + 2 \frac{R_L}{R_0} \right)} \right] \quad (31)$$

Equations (30) and (31) provide for correctly simulating the longitudinal surface strain in compression and tension, respectively, at any strain magnitude. In conjunction with the corresponding half bridge (Fig. 5b), the instrument indication at the calibration strain level is precise, but operation at a different strain level will introduce a small error due to bridge-circuit nonlinearity. When necessary, the corrected strain can be calculated from [see Eq. (18) for notation]:

$$\epsilon = \frac{2 \left(1 + 2 \frac{R_L}{R_0} \right) \bar{\epsilon}}{2 \left(1 + 2 \frac{R_L}{R_0} \right) + F_0 (1 - \nu) (\epsilon_s - \bar{\epsilon})} \quad (32)$$

VI. Instrument Verification

The shunt-calibration procedures described in Sections III and V are intended specifically for instrument scaling purposes; that is, for adjusting the instrument output to match a given simulated surface strain. They are not directly related to the question of verifying the linearity and/or absolute accuracy of a strain-measuring instrument. It is implicitly assumed in the preceding sections of this Tech Note that the instrument involved is perfectly linear in its response characteristics and, if direct-indicating, is perfectly accurate. In practice, however, it is necessary to periodically verify the accuracy of the instrument by calibration; and methods for accomplishing this are given here.⁴

By far the most reliably accurate means for instrument verification is through the use of a laboratory-standard calibrator such as the Measurements Group Model 1550A. This instrument, which incorporates true tension and compression strain simulation, provides precision calibration of strain indicators to an accuracy of 0.025 percent. It also eliminates errors due to the tolerances on the strain gage and shunt resistances. The calibrator is equipped with three decades of switches, which permit rapid calibration in small steps over a very wide strain range (to $\sim 100,000 \mu\epsilon$).

Whether verification of the strain indicator is to be done with a precision calibrator or by shunt calibration, it is important that the procedure be unaffected by leadwire resistance. When verifying instrument accuracy with the Model 1550A, for instance, the calibrator should be connected to the strain indicator with short leads of generous wire size. Similarly, with shunt calibration, the leadwire resistance in the shunted bridge arm should be negligibly small. This can be accomplished, for calibration purposes, by connecting an installed strain gage or a stable precision resistor directly across the active gage terminals of the strain indicator. Either the active or dummy arm of the bridge circuit can then be shunted to produce, correspondingly, a downscale or upscale calibration signal. If the active arm is a strain gage, and is to be shunted, the installed resistance of the gage must be known accurately.

⁴As used in this section only, the term "calibration" thus refers exclusively to the process of instrument verification for linearity or accuracy.

An alternative approach, which eliminates the effect of leadwire resistance, is to shunt one arm of the internal half-bridge commonly found in conventional strain gage instruments. This procedure requires, of course, that the resistances of the internal bridge arms be known. In addition, it requires that the internal half-bridge be isolated from any balance circuitry which may be present, or that the effects of such circuitry be incorporated in the shunt-calibration calculations. In any case, the instruction manual and circuit diagrams for the instrument should be consulted before attempting to calibrate by shunting the internal half-bridge.

The calibration relationship for instrument verification is based on different reasoning than it is for instrument scaling. In scaling applications (Sections III and V), the calibration resistor is calculated to develop the same bridge output voltage that would occur when a strain gage of specified gage factor is subjected to a given strain. The instrument gage factor or gain control is then adjusted to register the simulated strain. The effects of signal loss due to leadwire resistance, or signal increase from multiple active gages, are thus compensated for. With this technique, the final setting of the gage factor or gain control is determined only by the external circuit parameters; and, in the case of a strain indicator, for example, the resulting gage factor setting of the instrument would normally be quite different from that of the strain gage.

In contrast, when calibrating for instrument verification purposes, the instrument gage factor or gain is ordinarily preset to some convenient value. The verification relationship is then written to express the registered strain (in a perfectly accurate instrument) as a function of the shunt resistor used to synthesize the strain signal. It will be seen that the gage factor of the strain gage itself is not involved in this process. Nor are other external circuit parameters, except the initial resistance of the shunted bridge arm, which is usually the nominal resistance of a strain gage.

In an ideal instrument, the registered strain is related to the bridge output voltage by:

$$\epsilon_r = C \times \frac{e_o}{E} \quad (33)$$

where: ϵ_r = strain magnitude indicated or registered by the ideal instrument.

C = instrument constant — at a fixed setting of the gain or gage-factor control.

But the bridge output caused by a unit resistance change in one arm can be expressed as:

$$\frac{\Delta R}{E} = \pm \frac{\frac{\Delta R}{R_0}}{4 + 2 \frac{\Delta R}{R_0}} \quad (34)$$

In Eq. (34), the choice of sign depends on which arm is being shunted. Referring to Fig. 1, the sign is positive for R_1 or R_2 , and negative for R_3 or R_4 . The unit resistance change in shunt calibration is always negative, however, and is calculated from Eq. (3):

$$\frac{\Delta R}{R_0} = \frac{-R_0}{R_0 + R_c}$$

Substituting into Eq. (34), and simplifying,

$$\frac{e_o}{E} = \mp \frac{R_0}{4R_c + 2R_0} \quad (35)$$

Thus, the bridge output is negative when shunting R_1 or R_2 , and positive for R_3 or R_4 .

Substituting Eq. (35) into Eq. (33),

$$\epsilon_r = \mp C \times \frac{R_0}{4R_c + 2R_0}$$

Or, in general, when shunting any arm of initial resistance R_0 ,

$$|\epsilon_r| = C \times \frac{R_0}{4R_c + 2R_0} \quad (36)$$

And,

$$R_c = \frac{C}{4} \times \frac{R_0}{|\epsilon_r|} - \frac{R_0}{2} \quad (37)$$

where: $|\epsilon_r|$ = absolute value of registered strain (ideal).

In the case of a strain indicator with a gage-factor control, the instrument is designed so that $C = A/F_0$, where F_0 is the instrument gage factor setting. Then,

$$R_c = \frac{R_0}{F_0 \times |\epsilon_r|} - \frac{R_0}{2} \quad (38)$$

When one arm of the bridge is shunted by a calibration resistor calculated from Eq. (38), the instrument should indicate the synthesized strain, ϵ_r . Failure to do so by more than the tolerances on R_0 and R_c is indicative of instrument error.

Instead of a strain indicator, the instrumentation may consist of a signal-conditioning amplifier. This type of instrument is normally equipped with a gain control rather than a gage-factor control. Its output is simply a voltage which can then be supplied to an oscilloscope or other device for recording. In the ideal instrument, the voltage at any gain setting should be strictly proportional to the bridge output signal. Thus, corresponding to Eq. (33),

$$V = C \frac{e_o}{E} \quad (39)$$

The object of calibration in this instance is to verify the instrument linearity; that is, to test whether C is, in fact, constant. Calibration is accomplished by comparing the measured instrument output voltage to the bridge output signal at a series of different signal levels. Substituting Eq. (35) into Eq. (39),

$$V = \mp C \times \frac{R_0}{4R_c + 2R_0}$$

Or, in general,

$$\frac{V}{\left(\frac{R_0}{4R_c + 2R_0}\right)} = C \quad (40)$$

After shunting one arm of the bridge with a calibration resistor, R_c , the instrument output voltage is measured, and the constant, C , calculated from Eq. (39). This operation is repeated at two or more different signal levels by successively shunting with appropriate calibration resistors. If the instrument is linear, variations in the calculated value of the instrument constant should not be greater than the tolerances on the parameters in Eq. (40).

VII. Accuracy Considerations

As described in the preceding sections, shunt calibration can be used for either system scaling or instrument verification purposes. In both cases, the greatest attainable accuracy with the procedure is limited by errors (deviations from the nominal or assumed value) in the variables which enter into the calibration calculations. The error sensitivity of the method can be demonstrated most easily with a generalized form of the basic shunt-calibration relationship [see Eqs. (3), (4), and (5)].

Let R_1 in Eq. (3) represent the actual resistance of the strain gage, after installation. The factor R_0 in Eq. (4) is replaced by a numerical constant, C , to emphasize the fact that the nominal resistance of the gage is not changed by gage installation. Then, the relationships in Eqs. (3) and (4) can be reexpressed as:

$$\Delta R = -\frac{R_1^2}{R_1 + R_c} \quad (3a)$$

$$\Delta R = CF_0 \epsilon \quad (4a)$$

Combining Eqs. (3a) and (4a), and solving for the simulated strain,

$$|\epsilon| = \frac{R_1^2}{CF_0(R_1 + R_c)} \quad (41)$$

The total differential of the simulated strain can be written:

$$d\epsilon = \frac{\partial \epsilon}{\partial R_1} dR_1 + \frac{\partial \epsilon}{\partial R_c} dR_c + \frac{\partial \epsilon}{\partial F_0} dF_0$$

After performing the partial differentiations and dividing through by $\epsilon = R_1^2 / CF_0(R_1 + R_c)$,

$$\frac{d\epsilon}{\epsilon} = \left(\frac{R_1 + 2R_c}{R_1 + R_c}\right) \frac{dR_1}{R_1} - \left(\frac{R_c}{R_1 + R_c}\right) \frac{dR_c}{R_c} - \frac{dF_0}{F_0} \quad (42)$$

For small deviations, the differentials can be replaced by finite differences, or:

$$\frac{\Delta \epsilon}{\epsilon} = \left(\frac{R_1 + 2R_c}{R_1 + R_c}\right) \frac{\Delta R_1}{R_1} - \left(\frac{R_c}{R_1 + R_c}\right) \frac{\Delta R_c}{R_c} - \frac{\Delta F_0}{F_0} \quad (43)$$

When multiplied by 100, Eq. (43) gives the percent error in the simulated strain as a function of the errors or deviations in R_1 (the actual gage resistance), R_c , and F_0 . Since R_c is ordinarily very large compared to R_1 , it can be seen that the percent error in simulated strain is about twice that in the gage resistance, and is approximately equal to that in the calibration resistor and gage factor (although the signs may differ). In practice, the errors in R_1 , R_c , and F_0 vary independently over their respective ranges of tolerance or uncertainty. Thus, they may tend to be self-cancelling on some

occasions; and, at other times, may be additive. The worst-case errors in simulated strain occur when ΔR_1 is positive while ΔR_c and ΔF_0 are negative, and vice versa. These conditions can be combined into a single expression by employing the absolute values of the errors:

$$\left| \frac{\Delta \epsilon}{\epsilon} \right|_{\text{MAX}} = \left(\frac{R_1 + 2R_c}{R_1 + R_c} \right) \left| \frac{\Delta R_1}{R_1} \right| + \left(\frac{R_c}{R_1 + R_c} \right) \left| \frac{\Delta R_c}{R_c} \right| + \left| \frac{\Delta F_0}{F_0} \right| \quad (44)$$

Equation (44) permits calculating the extreme error in simulated strain from the extreme errors in the other variables. Practically, however, the extreme errors in R_0 , R_c , and F_0 would occur only rarely at the same time, and with the required combination of signs, to be fully additive. A better measure of the approximate uncertainty (expected error range) in ϵ , as a function of the uncertainties or tolerances on the other three quantities can be obtained by an adaptation from the theory of error propagation. The latter theory is not strictly applicable in this case because the individual error distributions are unknown, are probably different from one another, and may otherwise violate statistical requirements of the method. However, if the uncertainties in each variable represent about the same number of standard deviations, the following expression should give a more realistic estimate of the uncertainty in ϵ than Eq. (44).

$$\frac{U_{\epsilon}}{\epsilon} = \sqrt{\left(\frac{R_1 + 2R_c}{R_1 + R_c}\right)^2 \left(\frac{U_{R_1}}{R_1}\right)^2 + \left(\frac{R_c}{R_1 + R_c}\right)^2 \left(\frac{U_{R_c}}{R_c}\right)^2 + \left(\frac{U_{F_0}}{F_0}\right)^2} \quad (45)$$

where: $\frac{U_x}{x}$ = percent uncertainty in variable x .

As a numerical example, assume that a 350-ohm gage with a gage factor of 2.0 is to be shunted to simulate a strain of 2000 $\mu\epsilon$. From Eq. (7),

$$R_c = \frac{350 \times 10^6}{2.0 \times 2000} - 350 = 87150 \text{ ohms}$$

This calibration resistor can be found in Table I; and, if supplied by Micro-Measurements, has a resistance tolerance of $\pm 0.01\%$. Assume also that the selected gage type has tolerances on its gage factor and resistance of $\pm 1\%$ and $\pm 0.3\%$, respectively. Since the gage resistance may have been shifted during installation, however, the uncertainty in the installed resistance should normally be taken somewhat larger — say, to be conservative, $\pm 1\%$. Substituting into Eq. (45),

$$\frac{U_{\epsilon}}{\epsilon} = \sqrt{(1.996)^2 \times (1.0)^2 + (0.996)^2 \times (0.01)^2 + (1.0)^2} = 4.23\%$$

Equations (44) and (45) will be found helpful guides in estimating the precision of shunt calibration. They can also serve in judging whether use of the large-strain relationships in Section V is warranted under any given set of circumstances. Thus, if the intrinsic uncertainty in shunt calibration is many times greater than the refinement obtained by considering large-strain effects, the simpler relationships in Section III may as well be employed.

When necessary, the overall uncertainty can be reduced somewhat by accurately measuring the installed gage resistance and employing this value in the shunt-calibration equations. Or, alternatively, the effect of resistance deviation in the gage can be largely eliminated by the methods described in Section V for quarter-bridge calibration.

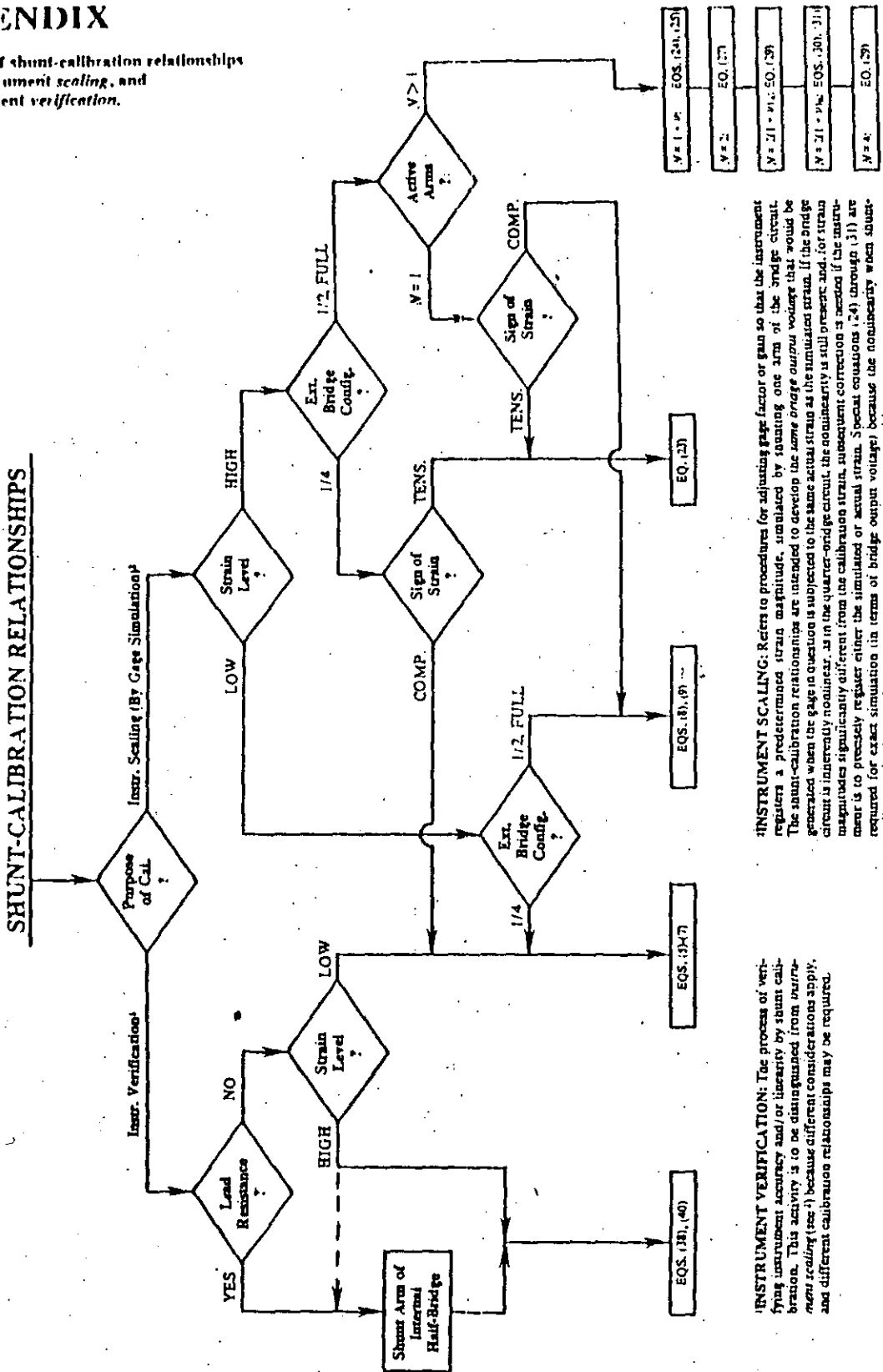
BACKGROUND REFERENCE

1. Measurements Group Tech Note TN-507, "Errors Due to Wheatstone Bridge Nonlinearity." Measurements Group, Inc., Raleigh, N.C., 1982.

APPENDIX

Selection of shunt-calibration relationships for (a) instrument scaling, and (b) instrument verification.

SHUNT-CALIBRATION RELATIONSHIPS



INSTRUMENT SCALING: Refers to procedures for adjusting gage factor or gain so that the instrument registers a predetermined strain magnitude, simulated by spanning one arm of the bridge circuit. The actual calibration relationships are intended to develop the same bridge output voltage that would be generated when the gage in question is subjected to the same actual strain as the simulated strain. If the bridge circuit is inherently nonlinear, as in the quarter-bridge circuit, the nonlinearity is null precorrection, for strain magnitudes significantly different from the calibration strain, subsequent correction is needed if the instrument is to precisely register either the simulated or actual strain. Special equations (24) through (31) are required for exact simulation (in terms of bridge output voltage) because the nonlinearity when shunt-calibrating is different from that under actual strain-measuring conditions.

INSTRUMENT VERIFICATION: The process of verifying instrument accuracy and/or linearity by shunt calibration. This activity is to be distinguished from *in-situ* scaling (see 1) because different considerations apply, and different calibration relationships may be required.

Strain Gage Rosettes — Selection, Application and Data Reduction

1.0 Introduction

A strain gage rosette is, by definition, an arrangement of two or more closely positioned gage grids, separately oriented to measure the normal strains along different directions in the underlying surface of the test part. Rosettes are designed to perform a very practical and important function in experimental stress analysis. It can be shown that for the not uncommon case of the general biaxial stress state, with the principal directions unknown, three independent strain measurements (in different directions) are required to determine the principal strains and stresses. And even when the principal directions are known in advance, two independent strain measurements are needed to obtain the principal strains and stresses.

To meet the foregoing requirements, the Micro-Measurements Division manufactures three basic types of strain gage rosettes (each in a variety of layouts):

- Tee: two mutually perpendicular grids.
- 45°-Rectangular: three grids, with the second and third grids angularly displaced from the first grid by 45° and 90°, respectively.
- 60°-Delta: three grids, with the second and third grids 60° and 120° away, respectively, from the first grid.

Representative gage patterns for the three rosette types are reproduced in Fig. 1.

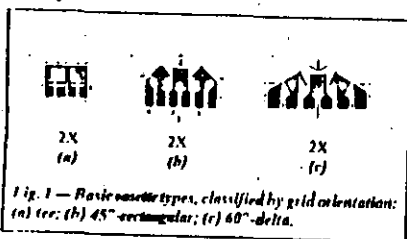


Fig. 1 — Basic rosette types, classified by grid orientation: (a) tee; (b) 45°-rectangular; (c) 60°-delta.

In common with single-element strain gages, rosettes are manufactured from different combinations of grid alloy and backing material to meet varying application requirements. They are also offered in a number of gage lengths, noting that the gage length specified for a rosette refers to the active length of each individual grid within the rosette. As illustrated in Fig. 2, rectangular and delta rosettes may appear in any of several geometrically different, but functionally equivalent, forms. Guidance in choosing the most suitable rosette for a particular application is provided in Section 2.0, where selection considerations are reviewed.

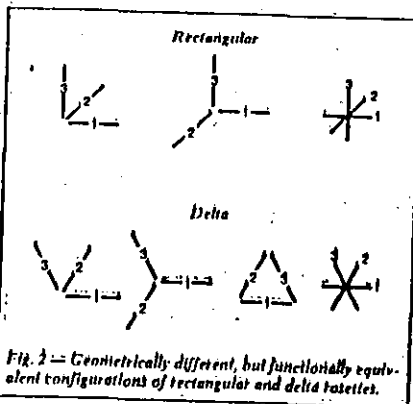


Fig. 2 — Geometrically different, but functionally equivalent configurations of rectangular and delta rosettes.

Since biaxial stress states occur very commonly in machine parts and structural members, it might be presumed that half or so of the strain gages used in experimental stress analysis would be rosettes. This does not seem to be the case, however, and ten percent (or less) rosette usage may be more nearly representative. To what degree this pattern of usage reflects an inclination for on-site makeup of rosettes from single-element gages, or simply an undue tendency to assume uniaxiality of the stress state, is an open question. At any

rate, neither practice can generally be recommended for the accurate determination of principal strains.

It must be appreciated that while the use of a strain gage rosette is, in many cases, a necessary condition for obtaining the principal strains, it is not a sufficient condition for doing so accurately. Knowledgeability in the selection and application of rosettes is critical to their successful use in experimental stress analysis; and the information contained in this Tech Note is intended to help the user obtain reliably accurate principal strain data.

2.0 Rosette Selection Considerations

A comprehensive guide for use in selecting Micro-Measurements strain gages is provided in Ref. 1. This publication should first be consulted for recommendations on the strain-sensitive alloy, backing material, self-temperature-compensation number, gage length, and other strain gage characteristics suitable in the expected application. In addition to basic parameters such as the foregoing, which must be considered in the selection of any strain gage, two other parameters are important in rosette selection. These are: (1) the rosette type — tee, rectangular, or delta; and (2) the rosette construction — planar (single-plane) or stacked (layered).

The tee rosette should be used only when the principal strain directions are known in advance from other considerations. Cylindrical pressure vessels and shafts in torsion are two classical examples of the latter condition. However, care must be exercised in all such cases that extraneous stresses (bending, axial stress, etc.) are not present, since these will affect the directions of the principal axes. Attention must also be given to nearby geometric irregularities, such as holes, ribs, or shoulders, which can locally alter the principal directions. The error magnitudes due to misalignment of a tee rosette from the principal axes are given in Ref. 2. As a rule, if there is uncertainty about the principal directions, a three-element rectangular or delta rosette is preferable. When necessary (and, using the proper data-reduction relationships), the tee rosette can be installed with its axes at any precisely known angle from the principal axes; but greatest accuracy will be achieved by alignment along the principal directions. In the latter case, except for the tediously corrected error due to transverse sensitivity, the two gage elements in the rosette indicate the corresponding principal strains directly.

Where the directions of the principal strains are unknown, a three-element rectangular or delta rosette is always required; and the rosette can be installed without regard to orientation. The data-reduction relationships given in Section 2.0 yield not only the principal strains, but also the directions of the principal axes relative to the reference grid (grid 1) of the rosette. Functionally, there is little choice between the rectangular and delta rosettes. Because the gage axes in the delta rosette have the maximum possible uniform angular separation (effectively 120°), this rosette is presumed to produce the optimum sampling of the underlying strain distribution. Rectangular rosettes have historically been the more popular of the two, primarily because the data reduction relationships are somewhat simpler. Currently, however, with the widespread access to computers

and programmable calculators, the computational advantage of the rectangular rosette is of little consequence. As a result of the foregoing, the choice between rectangular and delta rosettes is more apt to be based on practical application considerations such as availability from stock, compatibility with the space available for installation, convenience of holder lab arrangements, etc.

All three types of rosettes (tee, rectangular, and delta) are manufactured in both planar and stacked versions. As indicated (for the rectangular rosette) in Fig. 3, the planar rosette is etched from the strain-sensitive foil as an entity, with all gage elements lying in a single plane. The stacked rosette is manufactured by assembling and laminating two or three properly oriented single-element gages. When strain gradients in the plane of the test part surface are not too severe, the normal selection is the planar rosette. This form of rosette offers the following advantages in such cases:

- thin and flexible, with greater conformability to curved surfaces.
- minimal reinforcing effect.
- superior heat dissipation to the test part.
- available in all standard forms of gage construction, and generally accepts all standard optional features.
- optimal stability.
- maximum freedom in leadwire routing and attachment.

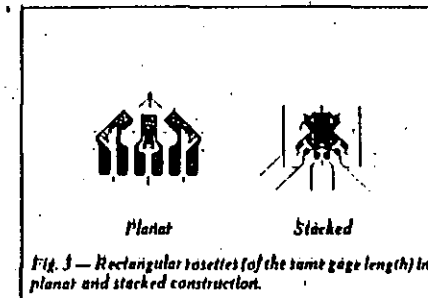


Fig. 3 — Rectangular rosettes (of the same gage length) in planar and stacked construction.

The principal disadvantages of the planar rosette arise from the larger surface area covered by the sensitive portion of the gage. When the space available for gage installation is small, a stacked rosette may fit, although a planar one will not. More importantly, where a steep strain gradient exists in the surface plane of the test part, the individual gage elements in a planar rosette may sense different strain fields and magnitudes. For a given active gage length, the stacked rosette occupies the least possible area, and has the centroids (geometric centers) of all grids lying over the same point on the test part surface. Thus, the stacked rosette more nearly approaches measurement of the strains at a point. Although normally a trivial consideration, it can also be noted that all gages in a stacked rosette have the same gage factor and transverse sensitivity, while the grids in a planar rosette will differ slightly in these properties, due to their different orientations relative to the rolling direction of the strain-sensitive foil. The technical data sheet accompanying the rosettes fully documents the separate properties of the individual grids.

It should be realized, however, that the stacked rosette is noticeably stiffer and less conformable than its planar counterpart. Also, because the heat conduction paths for the upper grids in a stacked rosette are much longer, the heat dissipation problem may be more critical when the rosette is installed on a material with low thermal conductivity. Taking into account their poorer heat dissipation and their greater reinforcement effects, stacked rosettes may not be the best choice for use on plastics and other nonmetallic materials. A stacked rosette can also give erroneous strain indications when applied to a thin specimen in bending, since the grid plane of the uppermost gage in a three-gage stack may be as much as 0.0045 in (0.11 mm) above the specimen surface. In short, the stacked rosette should ordinarily be reserved for applications in which the requirement for minimum surface area dictates its selection.

3.0 Gage Element Numbering

"Numbering", as used here, refers to the numeric (or alphabetic) sequence in which the gage elements in a rosette are identified during strain measurement, and for substitution of measured strains into data-reduction relationships such as those given in Section 4.0. Contrary to a widely held impression, the subject of gage numbering is not necessarily a trivial matter. It is, in fact, basic to the proper, and complete, interpretation of rosette measurements. With any three-element rosette, misinterpretation of the rotational sequence (CW or CCW), for instance, can lead to incorrect principal strain directions. In the case of the rectangular rosette, an improper numbering order will produce completely erroneous principal strain magnitudes, as well as directions. These errors occur when the gage user's numbering sequence differs from that employed in the derivation of the data-reduction relationships.

To obtain correct results using the data-reduction relationships provided in Section 4.0 (and in the Appendix), the grids in three-element rosettes must be numbered in a particular way. It is always necessary in a rectangular rosette, for instance, that grid numbers 1 and 3 be assigned to two mutually perpendicular grids. Any other arrangement will produce incorrect principal strains. Following are the general rules for proper rosette numbering. With a rectangular rosette, the axis of Grid 2 must be 45° away from that of Grid 1; and Grid 3 must be 90° away, in the same rotational direction. Similarly, with a delta rosette, the axes of Grids 2 and 3 must be 60° and 120° away, respectively, in the same direction from Grid 1.

In principle, the preceding rules could be implemented by numbering the grids in either the clock wise or counterclockwise direction, as long as the sequence is correct. Counterclockwise numbering is preferable, however, because it is consistent with the usual engineering practice of denoting counterclockwise angular measurement as positive in sign. The gage grids in all Micro-Measurements general-purpose, three-element planar rosettes (rectangular and delta) are numerically identified, and numbered in the counterclockwise direction. Examples of the grid numbering for several representative rosette types are illustrated in Fig. 4. At first glance, it might appear that gage patterns (b) and (c) are numbered clockwise instead of counterclockwise, but when these patterns are examined more closely, and when the axis

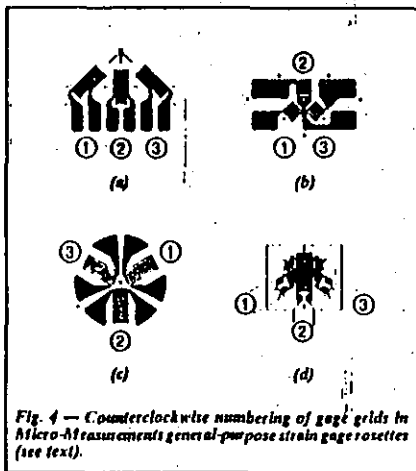


Fig. 4 — Counterclockwise numbering of gage grids in Micro-Measurements general-purpose strain gage rosettes (see text).

of Grid 2 is transposed across the grid-circle diameter to satisfy the foregoing numbering rules, it can be seen that the rosette numbering is counterclockwise in every case. Micro-Measurements stacked rosettes are not numbered, as a matter of manufacturing economy. The user should number the gages in stacked rosettes according to the rules given here and illustrated in Figs. 2 and 4.

4.0 Principal Strains and Directions from Rosette Measurements

The equations for calculating principal strains from three rosette strain measurements are derived from what is known as a "strain-transformation" relationship. As employed here, in its simplest form, such a relationship expresses the normal strain in any direction on a test surface in terms of the two principal strains and the angle from the principal axis to the direction of the specified strain. This situation can be envisioned most readily with the aid of the well-known Mohr's circle for strain, as shown in Fig. 5**. It can be seen from Fig. 5a (noting that the angles in Mohr's circle are double the physical angles on the test surface) that the normal strain at any angle θ from the major principal axis is simply expressed by:

$$\epsilon_x = \frac{\epsilon_1 + \epsilon_2}{2} + \frac{\epsilon_1 - \epsilon_2}{2} \cos 2\theta \quad (1)$$

** Micro-Measurements also supplies special-purpose planar rectangular rosettes designed exclusively for use with the hole-drilling method of residual stress analysis. Since these rosettes require different data-reduction relationships, procedures, and interpretation, they are numbered clockwise to distinguish them from general-purpose rosettes.

** The Mohr's circle in Fig. 5 is constructed with positive shear plotted downward. This is done so that the positive rotational direction in Mohr's circle is the same (CCW) as for the rosette, while maintaining the usual sign convention for shear (i.e., positive shear corresponds to reduction in the initial right angle of the origin of the X-Y axes as labeled in Fig. 5b).

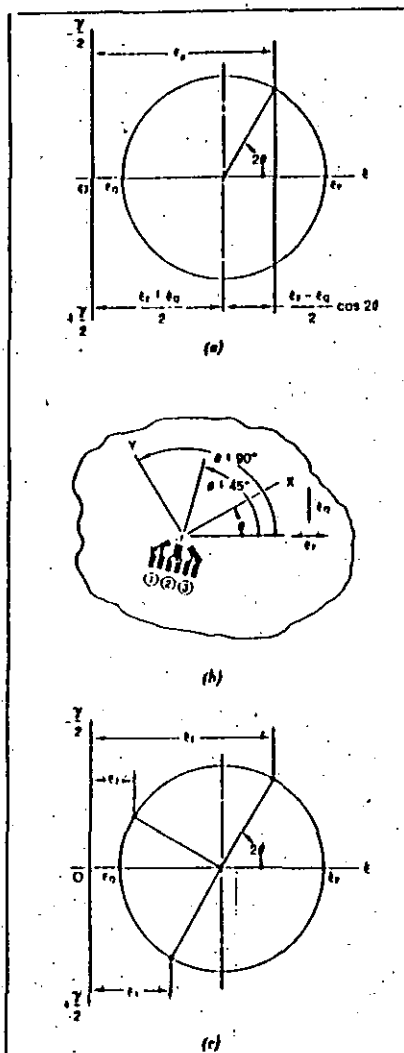


Fig. 5 — Strain transformation from the principal strains to the strain in any direction: (a) ϵ_x in terms of principal strains ϵ_1 and ϵ_2 , as shown by Mohr's circle for strain; (b) rectangular rosette installed on a test surface, with Grid 1 at the arbitrary angle θ from the major principal axis; (c) axes of the rectangular rosette superimposed on Mohr's circle for strain.

Figure 5b represents a small area of the test surface, with a rectangular rosette installed, and with the reference grid (#1) oriented at θ degrees from ϵ_1 . Mohr's circle, with the axes of the rosette superimposed, is shown in Fig. 5c.

By successively substituting into Eq. (1) the angles for the three grid directions, the strain sensed by each grid can be expressed as follows:

$$\epsilon_1 = \frac{\epsilon_x + \epsilon_y}{2} + \frac{\epsilon_x - \epsilon_y}{2} \cos 2\theta \quad (2a)$$

$$\epsilon_2 = \frac{\epsilon_x + \epsilon_y}{2} + \frac{\epsilon_x - \epsilon_y}{2} \cos 2(\theta + 45^\circ) \quad (2b)$$

$$\epsilon_3 = \frac{\epsilon_x + \epsilon_y}{2} + \frac{\epsilon_x - \epsilon_y}{2} \cos 2(\theta + 90^\circ) \quad (2c)$$

When the rosette is installed on a test part subjected to an arbitrary strain state, the variables on the right-hand side of Eqs. (2) are unknown. But the strains ϵ_1 , ϵ_2 , and ϵ_3 can be measured. Thus, by solving Eqs. (2) simultaneously for the unknown quantities ϵ_1 , ϵ_2 , and θ , the principal strains and angle can be expressed in terms of the three measured strains. Following is the result of this procedure:

$$\epsilon_{1,2} = \frac{\epsilon_1 + \epsilon_2}{2} \pm \frac{1}{2} \sqrt{(\epsilon_1 - \epsilon_2)^2 + (\epsilon_3 - \epsilon_1)^2} \quad (3)$$

$$\theta = \frac{1}{2} \tan^{-1} \left(\frac{\epsilon_1 - 2\epsilon_2 + \epsilon_3}{\epsilon_1 - \epsilon_2} \right) \quad (4)$$

If the rosette is properly numbered, the principal strains can be calculated from Eq. (3) by substituting the measured strains for ϵ_1 , ϵ_2 , and ϵ_3 . The plus and minus alternatives in Eq. (3) yield the algebraically maximum and minimum principal strains, respectively. Unambiguous determination of the principal angle from Eq. (4) requires, however, some interpretation, as described in the following. To begin with, the angle θ represents the acute angle from the principal axis to the reference grid of the rosette, as indicated in Fig. 5. In the practice of experimental stress analysis, it is somewhat more convenient, and easier to visualize, if this is re-expressed as the angle from Grid 1 to the principal axis. To change the sense of the angle requires only reversing the sign of Eq. (4). Thus:

$$\phi_{p,0} = -\theta = \frac{1}{2} \tan^{-1} \left(\frac{2\epsilon_2 - \epsilon_1 - \epsilon_3}{\epsilon_1 - \epsilon_2} \right) \quad (5)$$

The physical direction of the acute angle given by either Eq. (4) or Eq. (5) is always counterclockwise if positive, and clockwise if negative. The only difference is that θ is measured from the principal axis to Grid 1, while ϕ is measured from Grid 1 to the principal axis. Unfortunately, since $\tan 2\phi = \tan 2(\phi + 90^\circ)$, the calculated angle can refer to either principal axis; and hence the identification in Eq. (5) as $\phi_{p,0}$. This ambiguity can readily be resolved (for the rectangular rosette) by application of the following simple rules:

- If $\epsilon_1 > \epsilon_2$, then $\phi_{p,0} = \phi$.
- If $\epsilon_1 < \epsilon_2$, then $\phi_{p,0} = \phi + 90^\circ$.
- If $\epsilon_1 = \epsilon_2$ and $\epsilon_3 < \epsilon_1$, then $\phi_{p,0} = \phi - 45^\circ$.
- If $\epsilon_1 = \epsilon_2$ and $\epsilon_3 > \epsilon_1$, then $\phi_{p,0} = \phi + 45^\circ$.
- If $\epsilon_1 = \epsilon_2 = \epsilon_3$, then $\phi_{p,0}$ is indeterminate (equal biaxial strain).

The reasoning which underlies the preceding rules becomes obvious when a sketch is made of the corresponding Mohr's circle for strain, and the rosette axes are superimposed as in Fig. 5c. A similar technique for assuring correct interpretation of the angle is given in the form of a step-by-step algorithm in Ref. 3.

The preceding development has been applied to the rectangular rosette, but the same procedure can be used to derive corresponding data-reduction equations for the delta rosette shown in Fig. 6. When grid angles θ , $\theta + 60^\circ$, and $\theta + 120^\circ$ are successively substituted into Eq. (1), the resulting three equations can again be solved simultaneously for the principal strains and angle. Thus, for the delta rosette:

$$\epsilon_{r,o} = \frac{\epsilon_1 + \epsilon_2 + \epsilon_3}{3} \pm \frac{\sqrt{3}}{3} \sqrt{(\epsilon_1 - \epsilon_2)^2 + (\epsilon_2 - \epsilon_3)^2 + (\epsilon_3 - \epsilon_1)^2} \quad (6)$$

$$\theta = \frac{1}{2} \tan^{-1} \left[\frac{\sqrt{3}(\epsilon_2 - \epsilon_3)}{2\epsilon_1 - \epsilon_2 - \epsilon_3} \right] \quad (7)$$

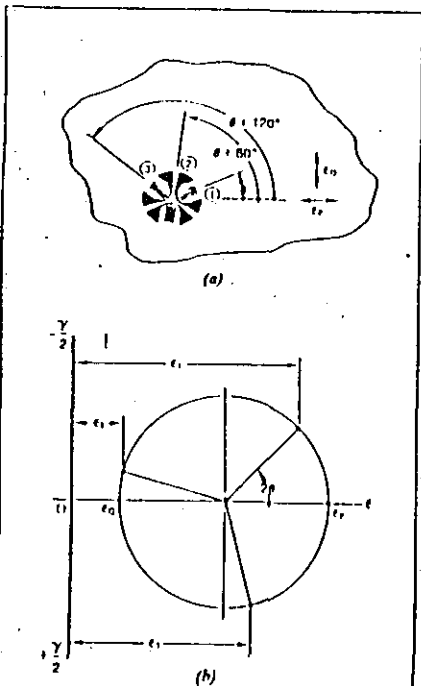


Fig. 4—Delta rosette: (a) installed on a test surface, with Grid 1 at the angle θ from the major principal strain direction; (b) rosette grid axes superimposed on Mohr's circle for strain. Note that Grid 2 is to be viewed as 60° (120°) from Grid 1 in the rosette, and 120° in Mohr's circle.

As in the case of Eq. (4), the angle θ calculated from Eq. (7) refers to the angular displacement of Grid 1 from the principal axis. The sense of the angle can again be changed by reversing its sign to give the angle from Grid 1 to a principal axis:

$$\phi_{r,o} = -\theta = \frac{1}{2} \tan^{-1} \left[\frac{\sqrt{3}(\epsilon_2 - \epsilon_3)}{2\epsilon_1 - \epsilon_2 - \epsilon_3} \right] \quad (8)$$

In every case [Eqs. (4), (5), (7), and (8)], the angles are to be interpreted as counterclockwise if positive, and clockwise if negative.

Equation (8) embodies the same ambiguity with respect to the $\tan 2\phi$ and $\tan 2(\phi + 90^\circ)$ as Eq. (5). As before, the ambiguity can easily be resolved (for the delta rosette) by considering the relative magnitudes (algebraically) among the individual strain measurements; namely:

- (a) if $\epsilon_1 > \frac{\epsilon_2 + \epsilon_3}{2}$, then $\phi_{r,o} = \phi_r$.
- (b) if $\epsilon_1 < \frac{\epsilon_2 + \epsilon_3}{2}$, then $\phi_{r,o} = \phi_o$.
- (c) if $\epsilon_1 = \frac{\epsilon_2 + \epsilon_3}{2}$ and $\epsilon_1 < \epsilon_2$, then $\phi_{r,o} = \phi_r = -45^\circ$.
- (d) if $\epsilon_1 = \frac{\epsilon_2 + \epsilon_3}{2}$ and $\epsilon_1 > \epsilon_2$, then $\phi_{r,o} = \phi_r = +45^\circ$.
- (e) if $\epsilon_1 = \epsilon_2 = \epsilon_3$, then $\phi_{r,o}$ is indeterminate (equal biaxial strain).

When the principal angle is calculated automatically by computer from Eq. (5) or Eq. (8), it is always necessary, of course, to avoid the condition of division by zero if $\epsilon_1 = \epsilon_2$ with a rectangular rosette, or $\epsilon_1 = (\epsilon_2 + \epsilon_3)/2$ with a delta rosette. For this reason, the computer should be programmed to perform the foregoing (c) and (d) tests, in each case, prior to calculating the arc-tangent.

Once the principal strains have been determined from Eq. (3) or Eq. (6), the strain state in the surface of the test part is completely defined. If desired, the maximum shear strain can be obtained directly from:

$$\gamma_{\max} = \epsilon_r - \epsilon_o \quad (9)$$

Intuitive understanding of the strain state can also be enhanced by sketching the corresponding Mohr's circle, approximately to scale. In Eqs. (3) and (6), the first term represents, in each case, the distance from the origin to the center of the circle, and the second term represents the radius, or $\gamma_{\max}/2$. With the angle ϕ calculated, further insight can be gained by superimposing the rosette grid axes on the Mohr's circle, as in Figs. 5c and 6b.

5.0 Principal Stresses from Principal Strains

As previously noted, a three-element strain gage rosette must be employed to determine the principal strains in a general biaxial stress state when the directions of the principal axes are unknown. The usual goal of experimental stress analysis, however, is to arrive at the principal stresses, for comparison with some criterion of failure. With the strain state fully established as described in Section 4.0, the complete state of stress (in the surface of the test part) can also be

obtained quite easily when the test material meets certain requirements on its mechanical properties. Since some types of strain gage instrumentation, such as the Measurements Group's System 4666, calculate both the principal strains and the principal stresses, the following material is provided as background information.

If the test material is homogeneous in composition, and is isotropic in its mechanical properties (i.e., the properties are the same in every direction), and if the stress/strain relationship is linear, with stress proportional to strain, then the biaxial form of Hooke's law can be used to convert the principal strains into principal stresses. This procedure requires, of course, that the elastic modulus (E) and Poisson's ratio (ν) of the material be known. Hooke's law for the biaxial stress state can be expressed as follows:

$$\sigma_r = \frac{E}{1 - \nu^2} (\epsilon_r + \nu \epsilon_o) \quad (10a)$$

$$\sigma_o = \frac{E}{1 - \nu^2} (\epsilon_o + \nu \epsilon_r) \quad (10b)$$

The numerical values of the principal strains calculated from Eq. (3) or Eq. (6) can be substituted into Eqs. (10), along with the elastic properties, to obtain the principal stresses. As an alternative, Eq. (3) or Eq. (6) (depending on the rosette type) can be substituted algebraically into Eq. (10) to express the principal stresses directly in terms of the three measured strains and the material properties. The results are as follows:

Rectangular:

$$\sigma_{r,o} = \frac{E}{2} \left[\frac{\epsilon_1 + \epsilon_2}{1 - \nu} \pm \frac{\sqrt{3}}{1 - \nu} \sqrt{(\epsilon_1 - \epsilon_2)^2 + (\epsilon_2 - \epsilon_3)^2} \right] \quad (11)$$

Delta:

$$\sigma_{r,o} = \frac{E}{3} \left[\frac{\epsilon_1 + \epsilon_2 + \epsilon_3}{1 - \nu} \pm \frac{\sqrt{3}}{1 - \nu} \sqrt{(\epsilon_1 - \epsilon_2)^2 + (\epsilon_2 - \epsilon_3)^2 + (\epsilon_3 - \epsilon_1)^2} \right] \quad (12)$$

When the test material is isotropic and linear-elastic in its mechanical properties (as required for the validity of the preceding strain-to-stress conversion), the principal stress axes coincide in direction with the principal strains. Because of this, the angle from Grid 1 of the rosette to the principal stress direction is given by Eq. (5) for rectangular rosettes, and by Eq. (8) for delta rosettes.

6.0 Errors, Corrections, and Limitations

The obvious aim of experimental stress analysis is to determine the significant stresses in a test object as accurately as necessary to assure product reliability under expected service conditions. As demonstrated in the preceding sections of this Tech Note, the process of obtaining the principal stresses involves three basic, and sequential, steps: (1) measurement of surface strains with a strain gage rosette; (2) transformation of measured strains to principal strains; and (3) conversion of principal strains to principal stresses. Each step in this procedure has its own characteristic error sources and limits of applicability; and the stress analyst must carefully consider these to avoid potentially serious errors in the resulting principal stresses.

Of first importance is that the measured strains be as free as possible of error. Strain measurements with rosettes are subject, of course, to the same errors (thermal output, transverse sensitivity, leadwire resistance effects, etc.) as those with single-element strain gages. Thus, the same controlling and/or corrective measures are required to obtain accurate data. For instance, signal attenuation due to leadwire resistance should be eliminated by shunt calibration, or by numerically correcting the strain data for the calculated attenuation, based on the known resistances of the leadwires and strain gages.

Because at least one of the gage grids in any rosette will in every case be subjected to a transverse strain which is equal to or greater than the strain along the grid axis, consideration should always be given to the transverse-sensitivity error when performing rosette data reduction. The magnitude of the error in any particular case depends on the transverse-sensitivity coefficient (K_t) of the gage grid, and on the ratio of the principal strains (ϵ_r/ϵ_o). In general, when $K_t \leq 1\%$, the transverse-sensitivity error is small enough to be ignored. However, at larger values of K_t , depending on the required measurement accuracy, correction for transverse sensitivity may be necessary. Detailed procedures, as well as correction equations for all cases and all rosette types, are given in Ref. 5.

When strain measurements must be made in a variable thermal environment, the thermal output of the strain gage can produce rather large errors, unless the instrumentation can be zero-balanced at the testing temperature, under strain-free conditions. In addition, the gage factor of the strain gage changes slightly with temperature. Reference 6 provides a thorough treatment of errors due to thermal effects in strain gages, including specific compensation and correction techniques for minimizing these errors.

After making certain that strain measurement errors such as the foregoing have been eliminated or controlled to the degree feasible, attention can next be given to possible errors in the strain-transformation procedure for obtaining the principal strains. A potentially serious source of error can be created when the user attempts to make up a rosette on the specimen from three conventional single-element gages. The error is caused by misalignment of the individual gages within the rosette. If, for example, the second and third gages in a rectangular rosette configuration are not accurately oriented at 45° and 90° , respectively, from the first gage, the calculated principal strains will be in error.

The magnitude of the error depends, of course, on the magnitude (and direction) of the misalignment; but it also depends on the principal strain ratio, ϵ_r/ϵ_o , and on the overall orientation of the rosette with respect to the principal axes. For certain combinations of principal strain ratio and rosette orientation, 3-degree alignment errors in Gages 2 and 3 relative to Gage 1 can produce an error of 20 percent or more in one of the principal strains.

Since it is very difficult for most persons to install a small strain gage with the required precision in alignment, the user is well-advised to employ commercially available rosettes. The manufacturing procedures for Measurements Group strain gage rosettes are such that errors due to grid alignment within the rosette need never be considered. For those cases in which it is necessary, for whatever reason, to assemble a

rossette from single-element gages, extreme care should be exercised to obtain accurate gage alignment. And when the principal strain directions can be predicted in advance, even approximately, alignment of (gage 1 or 2) in a rectangular rosette, or alignment of any gage in a delta rosette, with a principal axis, will minimize the error in that principal strain caused by inter-gage misalignment.

The strain-transformation relationships and data-reduction equations given in Section 4.0 assume a uniform state of strain at the site of the rosette installation. Since the rosette necessarily covers a finite area of the test surface, severe variations in the strain field over this area can produce significant errors in the principal strains - particularly with planar rosettes.⁷ For this type of application, the stacked rosette is distinctly superior; both because it covers a much smaller area (for the same gage length), and because the centroids of all three grids lie over the same point on the test surface.

The requirements for a homogeneous material and uniform strain state can be (and are) relaxed under certain circumstances. A case in point is the use of strain gage rosettes on fiber-reinforced composite materials. If the distance between inhomogeneities in the material (i.e., fiber-to-fiber spacing) is small compared to the gage length of the rosette, each grid will indicate the "macroscopic" or average strain in the direction of its axis. These measured strains (after the usual error corrections) can be substituted into Eq. (3) or Eq. (6) to obtain the macroscopic principal strains for use in the stress analysis of test objects made from composite materials.⁸ As noted later in this section, however, Eqs. (10) - (12) cannot be used for this purpose.

There is an additional limitation to the strain-transformation relationship in Eq. (1) which, although not frequently encountered in routine experimental stress analysis, should be noted. The subject of the strain distribution about a point, as universally treated in handbooks and in mechanics of materials textbooks, is developed from what is known as "infinitesimal-strain" theory. That is, in the process of deriving relatively simple relationships such as Eq. (1), the strain magnitudes are assumed to be small enough so that normal- and shear-strain approximations of the following types can be employed without introducing excessive error:

$$\epsilon_1 \epsilon^2 \approx \epsilon \quad (13)$$

$$\sin \gamma \approx \tan \gamma \approx \gamma \quad (14)$$

Although often unrecognized, these approximations are embodied in the equations used throughout the contemporary practice of theoretical and experimental stress analysis (where strain transformation is involved). This includes the concept of Mohr's circle for strain, and thus all of the equations in Section 4.0, which are consistent with the strain circle. Infinitesimal-strain theory has proven highly satisfactory for most stress analysis applications with conventional structural materials, since the strains, if not truly "infinitesimal", are normally very small compared to unity. Thus, for a not-untypical working strain level of 0.002 (2000 $\mu\epsilon$), the error in ignoring ϵ^2 compared to ϵ is only about 0.2 percent.

However, strain gage rosettes are sometimes used in the measurement of much larger strains, as in applications on plastics and elastomers, and in post-yield studies of metal behavior. Strain magnitudes greater than about 0.01

(10 000 $\mu\epsilon$) are commonly referred to as "large" or "finite"; and, for these, the strain-transformation relationship in Eq. (1) may not adequately represent the actual variation in strain about a point. Depending on the strain magnitudes involved in a particular application, and on the required accuracy for the principal strains, it may be necessary to employ large-strain analysis methods for rosette data reduction.⁹

The final step in obtaining the principal stresses is the introduction of Hooke's law [Eqs. (10)] for the biaxial stress state. To convert principal strains to principal stresses with Hooke's law requires, of course, that the elastic modulus and Poisson's ratio of the test material be known. Since the calculated stress is proportional to E , any error in the elastic modulus (for which a 3 to 5 percent uncertainty is common) is carried directly through to the principal stress. An error in Poisson's ratio has a much smaller effect because of the subordinate role of ν in the relationship.

It is also necessary for the proper application of Hooke's law that the test material exhibit a linear relationship between stress and strain (constant E) over the range of working stresses. There is normally no problem in satisfying this requirement when dealing with common structural materials such as the conventional steel and aluminum alloys. Other materials (e.g., some plastics, cast iron and magnesium alloys, etc.) may, however, be distinctly non-linear in their stress/strain characteristics. Since the process of transformation from measured strains to principal strains is independent of material properties, the correct principal strains in such materials can be determined from rosette measurements as described in this Tech Note. However, the principal strains cannot be converted accurately to principal stresses with the biaxial Hooke's law if the stress/strain relationship is perceptibly nonlinear.

A further requirement for the valid application of Hooke's law is that the test material be isotropic in its mechanical properties (i.e., that the elastic modulus and Poisson's ratio be the same in every direction). Although severely cold-worked metals may not be perfectly isotropic, this deviation from the ideal is commonly ignored in routine experimental stress analysis. In contrast, high-performance composite materials are usually fabricated with directional fiber reinforcement, and are thus strongly directional (orthotropic or otherwise anisotropic) in their mechanical properties. Hooke's law as expressed in Eqs. (10) is not applicable to these materials; and special "constitutive" relationships are required to determine principal stresses from rosette strain measurements.⁹

References

1. Measurements Group Tech Note TN-505, "Strain Gage Selection - Criteria, Procedures, Recommendations".
2. Measurements Group Tech Note TN-511, "Errors Due to Misalignment of Strain Gages".
3. Frey, C.C., "Data-Reduction Algorithms for Strain Gage Rosette Measurements", *Experimental Techniques*, May, 1989, pp. 13-18.
4. Measurements Group Tech Note TN-514, "Shunt Calibration of Strain Gage Instrumentation".
5. Measurements Group Tech Note TN-509, "Errors Due to Transverse Sensitivity in Strain Gages".
6. Measurements Group Tech Note TN-504, "Strain Gage Thermal Output and Gage Factor Variation with Temperature".
7. Troke, R.W., "Fial vs. Stacked Rosettes", *Experimental Mechanics*, May, 1967, pp. 24A-28A.
8. Tsai, S.W. and H.T. Hahn, *Introduction to Composite Materials*, Technomic Publishing Company, 1980.
9. Meyer, M.L., "Interpretation of Surface-Strain Measurements in Terms of Finite Homogeneous Strains", *Experimental Mechanics*, December, 1963, pp. 294-301.

APPENDIX

Derivation of Strain-Transformation Relationship [Eq. (1) in text] from Deformation Geometry

Consider a small area of a test surface, as sketched in Fig. A-1. The line O-P, of length l_0 , and at the angle θ from the X axis, is scribed on the surface in the unstrained state. When uniform principal strains ϵ_x and ϵ_y are applied in the directions of the X and Y axes, respectively, the point P moves to P' as a result of the displacements ΔX and ΔY (greatly exaggerated in the sketch).

It is evident from the figure that:

$$\Delta X = \epsilon_x (l_0 \cos \theta) \quad (A-1)$$

$$\Delta Y = \epsilon_y (l_0 \sin \theta) \quad (A-2)$$

It can also be seen (Fig. A-2), by enlarging the detail in the vicinity of points P and P', that for small strains:

$$\Delta l \approx \Delta X \cos \theta + \Delta Y \sin \theta \quad (A-3)$$

Substituting from Eqs. (A-1) and (A-2),

$$\Delta l \approx l_0 (\epsilon_x \cos^2 \theta + \epsilon_y \sin^2 \theta) \quad (A-4)$$

Or,

$$\epsilon_x = \frac{\Delta l}{l_0} = \epsilon_x \cos^2 \theta + \epsilon_y \sin^2 \theta \quad (A-5)$$

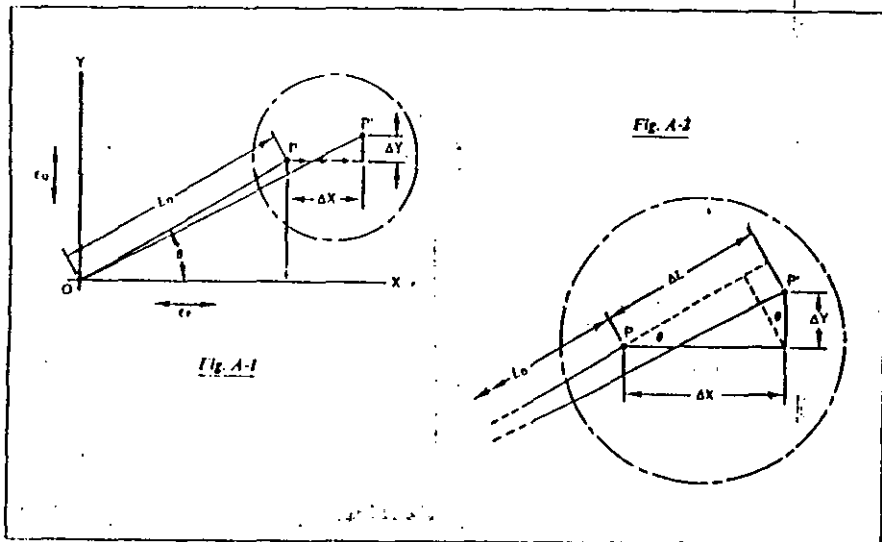
Thus,

$$\cos^2 \theta = \frac{1}{2} (1 + \cos 2\theta)$$

$$\sin^2 \theta = \frac{1}{2} (1 - \cos 2\theta)$$

After substituting the above identities,

$$\epsilon_x = \frac{\epsilon_x + \epsilon_y}{2} + \frac{\epsilon_x - \epsilon_y}{2} \cos 2\theta \quad (A-6)$$



Alternate Data Reduction Equations

In the extensive technical literature dealing with strain gage rosettes, the user will often encounter data-reduction relationships which are noticeably different from one another, and from those in the body of this Tech Note. As a rule, these published equations yield the same results, and differ only in algebraic format — although proving so in any given case may be rather time consuming. Since certain forms of the equations may be preferred for mnemonic reasons, or for computational convenience, several alternative expressions are given here. All of the following are equally correct when the gage elements in the rosette are numbered as described in this Tech Note.

Rectangular Rosette:

$$\epsilon_{r, \theta} = \frac{\epsilon_1 + \epsilon_2}{2} \pm \frac{1}{2} \sqrt{(\epsilon_1 - \epsilon_2)^2 + [2\epsilon_3 - (\epsilon_1 + \epsilon_2)]^2} \quad (A-7)$$

$$\epsilon_{r, \theta} = \frac{\epsilon_1 + \epsilon_2}{2} \pm \sqrt{[(\epsilon_1 - \epsilon_2)^2 + (\epsilon_3 - \epsilon_2)^2]}/2 \quad (A-8)$$

$$\epsilon_{r, \theta} = C \pm \sqrt{(C - \epsilon_1)^2 + (C - \epsilon_2)^2} \quad (A-9)$$

$$\text{where: } C = \frac{\epsilon_1 + \epsilon_2}{2}$$

Delta Rosette:

$$\epsilon_{r, \theta} = \frac{\epsilon_1 + \epsilon_2 + \epsilon_3}{3} \pm \sqrt{\left[\frac{2\epsilon_1 - (\epsilon_2 + \epsilon_3)}{3}\right]^2 + \frac{1}{3}(\epsilon_3 - \epsilon_2)^2} \quad (A-10)$$

$$\epsilon_{r, \theta} = \frac{\epsilon_1 + \epsilon_2 + \epsilon_3}{3} \pm \sqrt{2[(\epsilon_1 - \epsilon_2)^2 + (\epsilon_2 - \epsilon_3)^2 + (\epsilon_3 - \epsilon_1)^2]}/9 \quad (A-11)$$

$$\epsilon_{r, \theta} = C \pm \sqrt{2[(C - \epsilon_1)^2 + (C - \epsilon_2)^2 + (C - \epsilon_3)^2]}/3 \quad (A-12)$$

$$\text{where: } C = \frac{\epsilon_1 + \epsilon_2 + \epsilon_3}{3}$$

Cartesian Strain Components from Rosette Measurements

It is sometimes desired to obtain the Cartesian components of strain (ϵ_x , ϵ_y , and γ_{xy}) relative to a specified set of X-Y coordinate axes. This need can arise, for example, when making strain measurements on orthotropic composite materials. The Cartesian strain components are also useful when calculating principal strains from rosette data using matrix transformation methods.⁴

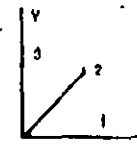
When the X axis of the coordinate system coincides with the axis of the reference grid (Grid 1) of the rosette, the Cartesian components of strain are as follows:

Rectangular Rosette:

$$\epsilon_x = \epsilon_1$$

$$\epsilon_y = \epsilon_2$$

$$\gamma_{xy} = 2\epsilon_3 - (\epsilon_1 + \epsilon_2)$$

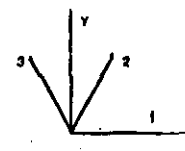


Delta Rosette:

$$\epsilon_x = \epsilon_1$$

$$\epsilon_y = [2(\epsilon_2 + \epsilon_3) - \epsilon_1]/3$$

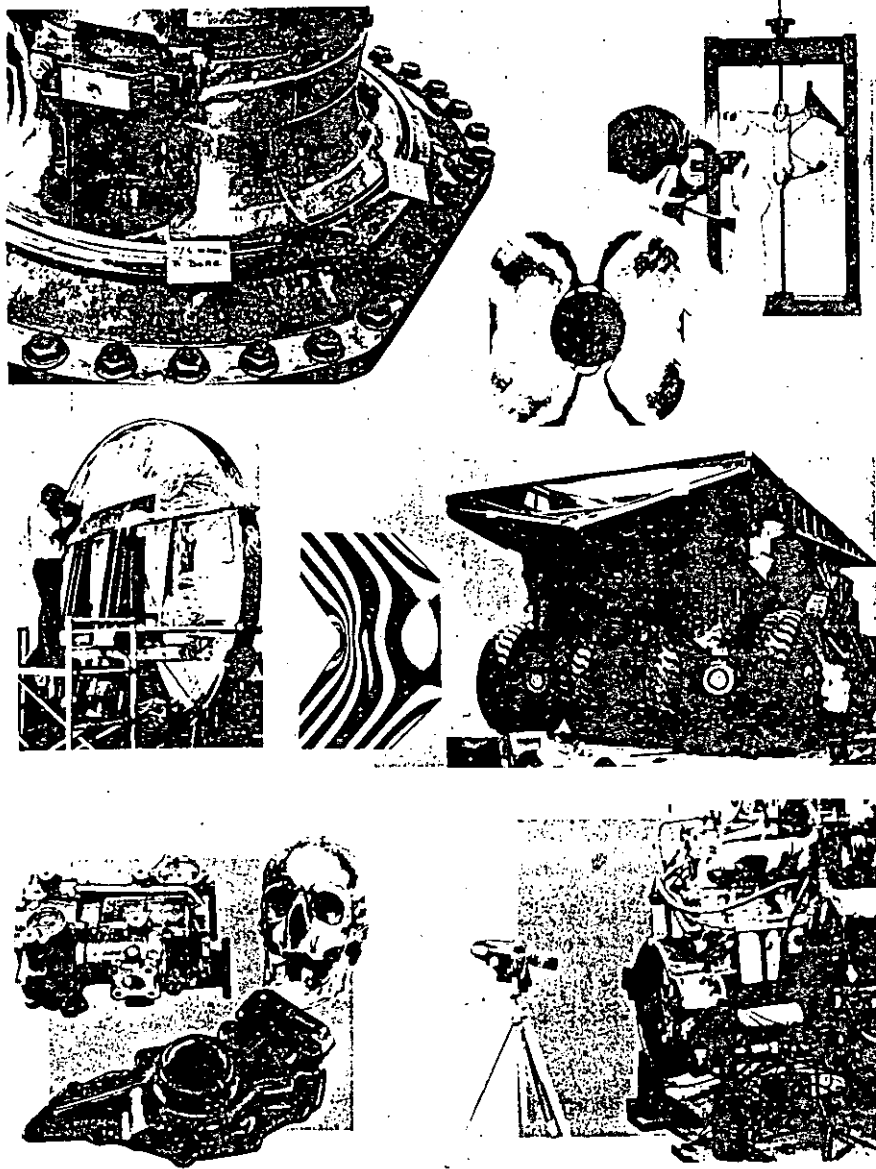
$$\gamma_{xy} = 2(\epsilon_3 - \epsilon_1)/\sqrt{3}$$



The foregoing assumes in each case that the gage elements in the rosette are numbered counterclockwise as indicated. When the calculated γ_{xy} is positive in sign, the initial right angle at the origin of the X-Y coordinate system is decreased by the amount of the shear strain.

⁴Atkes, P. R., "A Modern Approach to Principal Stresses and Strains", *Strain*, November, 1959, pp. 135-138.

TYPICAL APPLICATIONS OF PHOTOSTRESS



MEASUREMENTS GROUP
TECH NOTE

TN-702-1

PhotoStress® Method

Introduction to
Stress Analysis by the PhotoStress® Method

1.0 GENERAL DESCRIPTION

PhotoStress is a widely used full-field technique for accurately measuring surface strains to determine the stresses in a part or structure during static or dynamic testing.

With the PhotoStress method, a special strain-sensitive plastic coating is first bonded to the test part. Then, as test or service loads are applied to the part, the coating is illuminated by polarized light from a reflection polariscope. When viewed through the polariscope, the coating displays the strains in a colorful, informative pattern which immediately reveals the overall strain distribution and pinpoints highly strained areas. With an optical transducer (compensator) attached to the polariscope, quantitative stress analysis can be quickly and easily performed. Permanent records of the overall strain distribution can be made by photography or by video recording.

With PhotoStress, you can . . .

- Instantly identify critical areas, highlighting overstressed and understressed regions
- Accurately measure peak stresses and determine stress concentrations around holes, notches, fillets, and other potential failure areas
- Optimize the stress distribution in parts and structures for minimum weight and maximum reliability
- Measure principal stresses and directions at any point on the coated part
- Test repeatedly under varying load combinations without recoating the part
- Make stress measurements in the laboratory or in the field — unaffected by humidity or time
- Identify and measure assembly stresses and residual stresses
- Detect yielding, and observe redistribution of strains in the plastic range of deformation

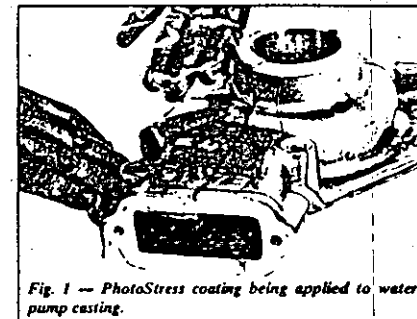


Fig. 1 — PhotoStress coating being applied to water pump casting.

PhotoStress coatings can be applied to the surface of virtually any test part regardless of its shape, size, or material composition. For coating complex shapes (Fig. 1), liquid plastic is cast on a flat-plate mold and allowed to partially polymerize. While still in a pliable state, the sheet is removed from the mold and formed by hand to the contours of the test part. When fully cured, the plastic coating is bonded in place with a special reflective cement, and the part is then ready for testing. For plane surfaces, premanufactured flat sheets are cut to size and bonded directly to the test part. Complete details covering the PhotoStress coating process are given in related Measurements Group publications listed in the bibliography.

PhotoStress has an established history of successful applications in virtually every field of manufacture and construction where stress analysis is employed, including: automotive — farm machinery — aircraft and aerospace — building construction — engines — pressure vessels — shipbuilding — office equipment — bridges — appliances — plus many, many others. A few applications of PhotoStress are shown on the back cover of this tech note.



MEASUREMENTS GROUP, INC.
P.O. Box 27777
Raleigh, North Carolina 27611, USA

(919) 365-3800
Telex 802-502
FAX (919) 365-3945

2.0 POLARIZED LIGHT — FUNDAMENTALS

Light or luminous rays are electromagnetic vibrations similar to radio waves. An incandescent source emits radiant energy which propagates in all directions and contains a whole spectrum of vibrations of different frequencies or wavelengths. A portion of this spectrum, wavelengths between 400 and 800 nm (15 and 30×10^8 in), is useful within the limits of human perception.

The vibration associated with light is perpendicular to the direction of propagation. A light source emits a train of waves containing vibrations in all perpendicular planes. However, by the introduction of a polarizing filter P (Fig. 2), only one component of these vibrations will be transmitted (that which is parallel to the privileged axis of the filter). Such an organized beam is called polarized light or "plane polarized" because the vibration is contained in one plane. If another polarizing filter A is placed in its way, complete extinction of the beam can be obtained when the axes of the two filters are perpendicular to one another.

Light propagates in a vacuum or in air at a speed C of 3×10^{10} cm/sec. In other transparent bodies, the speed V is lower and the ratio C/V is called the index of refraction. In a homogeneous body, this index is constant regardless of the direction of propagation or plane of vibration. However, in crystals the index depends upon the orientation of vibration with respect to index axis. Certain materials, notably plastics, behave isotropically when unstressed but become optically anisotropic when stressed. The change in index of refraction is a function of the resulting strain, analogous to the resistance change in a strain gage.

When a polarized beam a propagates through a transparent plastic of thickness t , where X and Y are the directions of principal strains at the point under consideration, the light vector splits and two polarized beams are propagated in planes X and Y (see Fig. 3). If the strain intensity along X and Y is ϵ_x and ϵ_y , and the speed of the light vibrating in these directions is V_x and V_y , respectively, the time necessary

to cross the plate for each of them will be t/V , and the relative retardation between these two beams is:

$$\delta = C \left(\frac{t}{V_x} - \frac{t}{V_y} \right) = t(n_x - n_y) \quad (1)$$

where: n = index of refraction

Brewster's law established that: "The relative change in index of refraction is proportional to the difference of principal strains", or:

$$(n_x - n_y) = K(\epsilon_x - \epsilon_y) \quad (2)$$

The constant K is called the "strain-optical coefficient" and characterizes a physical property of the material. It is a dimensionless constant usually established by calibration and may be considered similar to the "gage factor" of resistance strain gages. Combining the expressions above, we have:

$$\delta = tK(\epsilon_x - \epsilon_y) \quad \text{in transmission} \quad (3)$$

$$\delta = 2tK(\epsilon_x - \epsilon_y) \quad \text{in reflection (light passes through the plastic twice)} \quad (4)$$

Consequently, the basic relation for strain measurement using the PhotoStress (photoelastic coating) technique is:

$$(\epsilon_x - \epsilon_y) = \frac{\delta}{2tK} \quad (5)$$

Due to the relative retardation δ , the two waves are no longer in phase when emerging from the plastic. The analyzer A will transmit only one component of each of these waves (that parallel to A) as shown in Fig. 3. These waves will interfere and the resulting light intensity will be a function of:

- the retardation δ .
- the angle between the analyzer and direction of principal strains ($\beta - \alpha$)

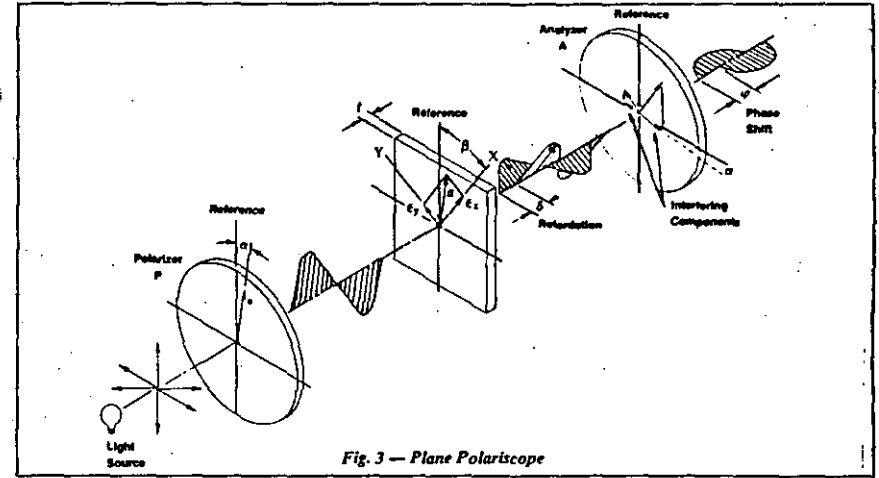


Fig. 3 — Plane Polariscopes

In the case of a plane polariscopes, the intensity of light emerging will be:

$$I = a^2 \sin^2 2(\beta - \alpha) \sin^2 \frac{\pi \delta}{\lambda} \quad (6)$$

The light intensity becomes zero when $\beta - \alpha = 0$, or when the crossed polarizer/analyzer is parallel to the direction of principal strains. Thus, a plane polariscopes setup is used to measure the principal strain directions.

Adding optical filters known as quarter-wave plates in the path of light propagation produces circularly polarized light, and the image observed is not influenced by the direction of

principal strains. The intensity of emerging light thus becomes:

$$I = a^2 \sin^2 \frac{\pi \delta}{\lambda} \quad (7)$$

In a circular polariscopes, the light intensity becomes zero when $\delta = 0, \delta = 1\lambda, \delta = 2\lambda, \dots$, or in general:

$$\delta = N\lambda$$

where N is 1, 2, 3, etc.

This number N is also called fringe order and expresses the size of δ . The wavelength selected is:

$$\lambda = 22.7 \times 10^3 \text{ in } (375 \text{ nm})$$

The retardation, or photoelastic signal, is then simply described by N . As an example:

$$\begin{aligned} \text{If } N = 2, (\delta) \text{ Retardation} &= 2 \text{ Fringes} \\ &\text{or } \delta = 2\lambda \\ &\text{or } \delta = 45.4 \times 10^3 \text{ in} \\ &\text{(1150 nm)} \end{aligned}$$

Once $\delta = N\lambda$ is known, the principal strain difference is obtained by:

$$\epsilon_x - \epsilon_y = \frac{\delta}{2tK} = N \frac{\lambda}{2tK} = Nf \quad (8)$$

where the fringe value, f , contains all constants, and N is the result of measurements.

For background reference as needed, the topic of polarized light, as used in conjunction with photoelasticity, is treated more comprehensively in the textbooks and other references listed in the bibliography.

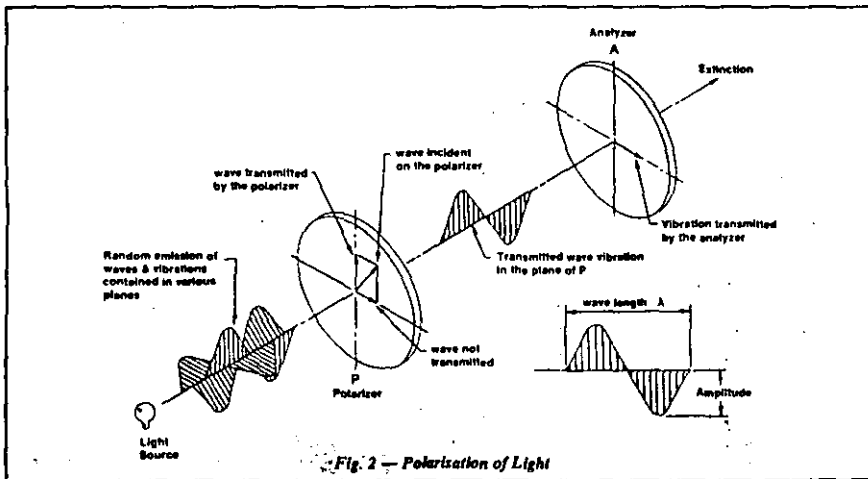


Fig. 2 — Polarisation of Light

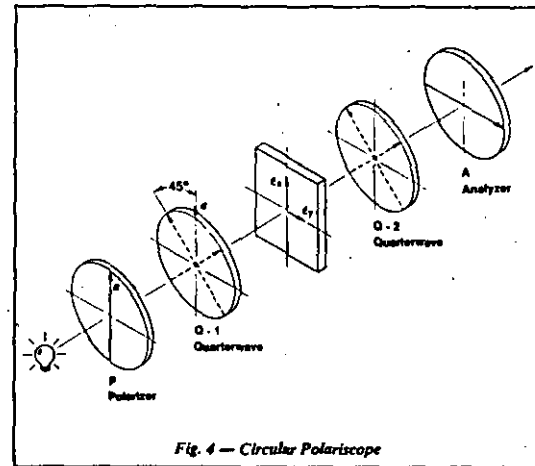


Fig. 4 — Circular Polariscopes

3.0 PHOTOSTRESS INSTRUMENTATION AND MATERIALS

3.1 Reflection Polariscopes

For PhotoStress analysis, a reflection polariscopes is used to observe and measure the surface strains on the photoelastically coated test part (Fig. 5). Two polariscopes systems are available. The 030 Series Modular System (Fig. 6) offers optional accessories to cover a wide range of strain measurement capabilities. For instance, measurements made on small parts or in regions of high stress concentration are both easier and more accurate when the optional telemicroscope accessory is attached. And the standard light source used for static measurements is readily replaceable with an optional stroboscopic light accessory for cyclical dynamic measurements. The Model 040 Reflection Polariscopes (Fig. 7) incorporates a built-in null-balance compensator and on-board electronics to permit fast and accurate measurements on statically loaded test parts. (For a complete description and specifications of both reflection polariscopes systems, see Bulletin S-134).

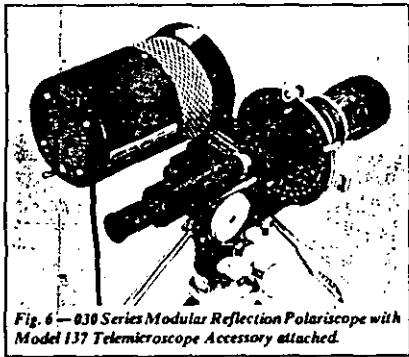


Fig. 6 — 030 Series Modular Reflection Polariscopes with Model 137 Telemicroscope Accessory attached.

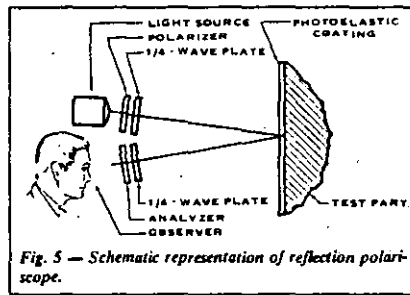


Fig. 5 — Schematic representation of reflection polariscopes.

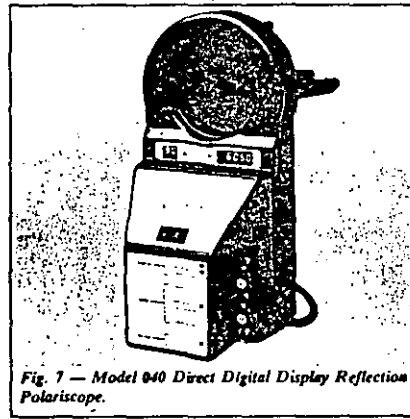


Fig. 7 — Model 040 Direct Digital Display Reflection Polariscopes.

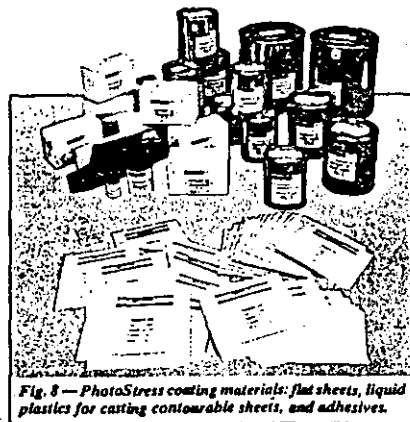


Fig. 8 — PhotoStress coating materials: flat sheets, liquid plastics for casting contourable sheets, and adhesives.

3.2 Coating Materials

The selection of PhotoStress coatings and their proper application to the test part are most essential to the success of PhotoStress analysis. A wide range of coating materials (Fig. 8) is available in both flat-sheet and liquid form for application to metals, concrete, plastics, rubber, and most other materials. The coatings are carefully controlled formulations of resins blended to provide known and repeatable photoelastic properties, and are supplied with detailed application and handling instructions. Also available are specially designed application kits, containing everything required for successful installation of the PhotoStress coating on the test part.

For complete information on PhotoStress coating materials, please refer to Bulletin S-116.

4.0 ANALYSIS OF PHOTOELASTIC FRINGE PATTERNS

PhotoStress offers the capability for the following types of analysis and measurement:

1. Full-field interpretation of fringe patterns, permitting overall assessment of nominal strain/stress magnitudes and gradients.
2. Quantitative measurements:
 - a. The directions of principal strains and stresses at all points on the photoelastic coating.
 - b. The magnitude and sign of the tangential stress along free (unloaded) boundaries, and in all regions where the state of stress is uniaxial.
 - c. In a biaxial stress state, the magnitude and sign of the difference in principal strains and stresses at any selected point on the coated surface of the test object.

4.1 Full-Field Interpretation of Strain Distribution

In addition to its capability for obtaining accurate strain measurements at preselected test points, PhotoStress provides another equally important capability to the stress analyst. This is the facility for immediate recognition of nominal strain (and stress) magnitudes, strain gradients, and overall strain distribution — including identification of overstressed and understressed areas. This extremely valuable attribute of PhotoStress, described as *full-field interpretation*, is unique to photoelastic methods of stress analysis. Its successful application depends only on the recognition of fringe orders by color, and an understanding of the relationship between fringe order and strain magnitude.

When a photoelastically coated test object is subjected to loads, the resulting stresses cause strains to exist generally throughout the part and over its surface. The surface stresses and strains are commonly the largest, and of the greatest importance. Because the photoelastic coating is intimately and uniformly bonded to the surface of the part, the strains in the part are faithfully transmitted to the coating. The strains in the coating produce proportional optical effects which appear as *isochromatic fringes* when viewed with a reflection polariscopes.

The photoelastic fringe pattern is rich with information and insights for the design engineer. If, for example, a part is being stress analyzed as a result of field service failures, the overall photoelastic pattern will usually suggest corrective measures for preventing the failures — often involving material removal and weight savings. Because of the full-field picture of stress distribution generated, it may be noted that the overstressed zone responsible for the failures is surrounded by an area of near-zero stress; and a slight change in shape will redistribute the stresses so as to eliminate the stress concentration, while forcing the understressed material to carry its share of the load.

Similarly, in prototype stress analysis for product development purposes, the photoelastic pattern can point the way toward design modifications to achieve the minimum-weight, functionally adequate part — i.e., the optimum design. In addition, full-field observation of the stress distribution

easily shows the effects of varying modes of loading, as well as the relative significance of individual loads and/or load directions. These examples are merely indicative of the many ways in which full-field fringe patterns in photoelastically coated test parts speak out to the knowledgeable stress analyst and provide a level of comprehension not achievable from "blind" strain measurements at a point.

4.2 Fringe Generation

Starting with the unloaded test part, and applying the load, or loads, in increments, fringes will appear first at the most highly stressed points (Fig. 9). As the load is increased and new fringes appear, the earlier fringes are pushed toward the areas of lower stress. With further loading, additional fringes are generated in the highly stressed regions and move toward regions of zero or low stress until the maximum load is reached. The fringes can be assigned ordinal numbers (first, second, third, etc.) as they appear, and they will retain their individual identities ("orders") throughout the loading sequence. Not only are fringes *ordered* in the sense of serial numbering, but they are also *orderly* — i.e., they are continuous, they never cross or merge with one another, and they always maintain their respective positions in the ordered sequence.

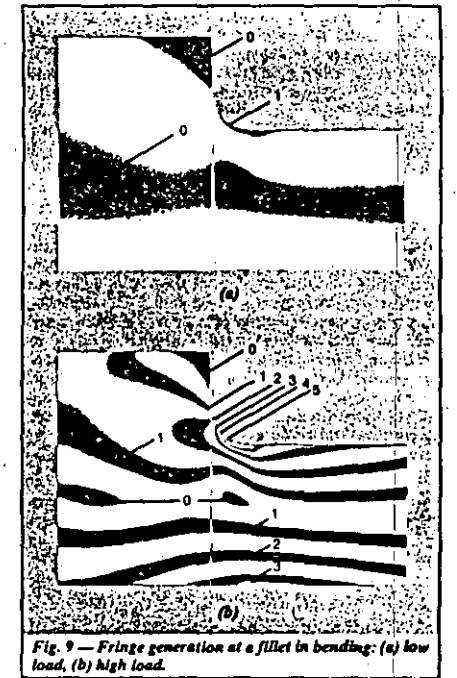


Fig. 9 — Fringe generation at a fillet in bending: (a) low load, (b) high load.

When observed with a reflection polariscope, the photoelastic fringe pattern appears as a series of successive and contiguous different-colored bands (isochromatics) in which each band represents a different degree of birefringence corresponding to the underlying strain in the test part. Thus, the color of each band uniquely identifies the birefringence, or fringe order (and strain level), everywhere along that band. With an understanding of the unvarying sequence in which the colors appear, the photoelastic fringe pattern can be read much like a topographical map to visualize the stress distribution over the surface of the coated test part.

The photoelastic effect is caused by alternately constructive and destructive interference between light rays which have undergone relative retardation, or phase shift, in the stressed photoelastic coating. When using monochromatic light, the magnitude of the relative retardation along any fringe is an integral multiple of the wavelength (λ , 2λ , 3λ , etc.), the rays are 180 degrees out of phase, and there is mutual cancellation, causing extinction of the light and producing a black band. On the other hand, when the relative retardation is an odd multiple of $\lambda/2$ ($\lambda/2$, $3\lambda/2$, $5\lambda/2$, etc.), the rays are perfectly in phase and combine to cause maximum brightness. Intermediate magnitudes of relative retardation produce intermediate light intensities. However, because the light intensity is a sine-squared function of the relative retardation, the resulting photoelastic pattern appears to be made up of alternate light and dark fringes.

White light, generally used for full-field interpretation of fringe patterns in PhotoStress testing, is composed of all wavelengths in the visible spectrum. Thus, the relative retardation which causes extinction of one wavelength (color) does not generally extinguish others. When, with increasing birefringence, each color in the spectrum is extinguished in turn according to its wavelength (starting with violet, the shortest visible wavelength), the observer sees the complementary color. It is these complementary colors which make up the visible fringe pattern in white light. The complete color sequence is given in Table I, including, for each color, the relative retardation and the numerical fringe order.

4.3 Fringe Identification

When observing an unloaded PhotoStress-coated test part with a reflection polariscope, the coating will appear uniformly black. As load is gradually applied to the part, the most highly stressed region begins to take on color — first gray, then white; and, when the violet is extinguished, yellow. With further load, the blue is extinguished to produce orange; and then green, to give red. The next color to vanish with increasing load is yellow, leaving a purple color; and this is followed by the extinction of orange, producing a deep blue fringe.

The purple fringe, which is easily distinguished from the red and blue on either side, and is very sensitive to a small change in strain level, is referred to as the *tint of passage*. Because of its distinctiveness and resolution, the purple tint of passage is selected to mark the increment in relative retardation equal to a fringe order of unity ($N = 1$). Subsequent recurrence of the tint of passage with greater relative retardation signifies the presence of higher integral fringe orders ($N = 2$, $N = 3$, etc.).

Continuing to increase the load on the test part and producing additional relative retardation, the red is extinguished from the white light spectrum, and the fringe color is

TABLE I
Isochromatic Fringe Characteristics

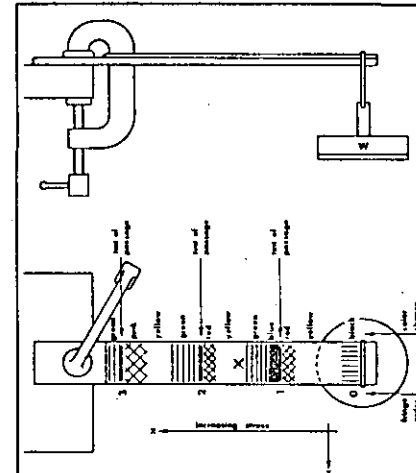
Color	Approximate Relative Retardation		Fringe Order N
	nm	in $\times 10^6$	
Black	0	0	0
Gray	160	6	0.28
White	260	10	0.45
Pale Yellow	345	14	0.60
Orange	460	18	0.80
Dull Red	520	20	0.90
Purple (Tint of Passage)	575	22.7	1.00
Deep Blue	620	24	1.08
Blue-Green	700	28	1.22
Green-Yellow	800	32	1.39
Orange	935	37	1.63
Rose Red	1050	42	1.82
Purple (Tint of Passage)	1150	45.4	2.00
Green	1350	53	2.35
Green-Yellow	1440	57	2.50
Red	1520	60	2.65
Red/Green Transition	1730	68	3.00
Green	1800	71	3.10
Pink	2100	83	3.65
Pink/Green Transition	2300	90.8	4.00
Green	2400	95	4.15

blue-green. With still greater load, the relative retardation reaches the level where it corresponds to twice the wavelength of violet, extinguishing this color for the second time and starting the fringe cycle over again. However, the deep red color at the far end of the white light spectrum also has twice the wavelength of violet, and thus undergoes its first extinction simultaneously with the second extinction of violet. The result is that the fringe color is the combination of two complementary colors, yellow and green. As the load and relative retardation continue to increase, the fringe color cycle is repeated, but the colors are not exactly the same as in the first cycle because of simultaneous extinction of two or more colors. With each successive complete color cycle the effect of increasingly complex simultaneous extinctions is to cause the fringe colors to become paler and less distinctive. Because of this effect, fringe orders above 4 or 5 are not distinguishable by color in white light. Although fringe orders higher than 3 are rarely encountered (or needed) in stress analysis with photoelastic coatings, fringes of very high order can always be detected by using the Model 036 Monochromator with the reflection polariscope.

Because of simultaneous multiple extinction of colors, the second-order tint of passage is fainter than the first, and falls in the transition area between red and green fringes. At fringe orders of 3 and 4 the tint of passage is not distinctly visible as a purple band, but the well-defined transition

between red and green in each case serves the same function and represents the integral fringe order.

A simple cantilever beam as shown in Fig. 10 provides a means for understanding fringe identification. The beam is coated on one side with photoelastic plastic and clamped (coated side up) to the edge of a bench or table. A weight is hung, using a wire or cable, on the free end of the beam. When observed with the polariscope (circular light operation), the retardation increases proportionally to the strain.



The fringes are related to increasing strain magnitude as summarized in the table. (See *Relationships Between Fringe Orders and Magnitudes of Strain and Stress* on page 10.) For this example (see Eq. (8)):

$$\begin{aligned} t &= 0.100 \text{ (2.54 mm)} \\ K &= 0.15 \\ \lambda &= 22.7 \times 10^{-6} \text{ in (575 nm)} \end{aligned} \quad \left. \vphantom{\begin{aligned} t \\ K \\ \lambda \end{aligned}} \right\} f = 757 \mu\text{in/in/fringe} \quad (\mu\text{m/m/fringe})$$

Fringe Order N	Strain $(\epsilon_1 - \epsilon_2) = Nf$
0 (Black Fringe)	0
1 (Red-Blue)	757 $\mu\text{in/in}$ ($\mu\text{m/m}$) (1 f)
2 (1st Red-Green)	1514 $\mu\text{in/in}$ ($\mu\text{m/m}$) (2 f)
3 (2nd Red-Green)	2271 $\mu\text{in/in}$ ($\mu\text{m/m}$) (3 f)

Fig. 10 — PhotoStress analysis of cantilever beam.

4.4 Quantitative Significance of Fringes

Photoelastic fringes have characteristic behaviors which are very helpful in fringe pattern interpretation. For instance, the fringes are ordinarily continuous bands, forming either closed loops or curved lines. The black zero-order fringes are usually isolated spots, lines, or areas surrounded by or adjacent to higher-order fringes. The fringes never intersect, or otherwise lose their identities, and therefore the fringe order and strain level are uniform at every point on a fringe. Furthermore, the fringes always exist in a continuous sequence by both number and color. In other words, if the first- and third-order fringes are identified, the second-order fringe must lie between them. The color sequence in any direction establishes whether the fringe order and strain level increase or decrease in that direction.

It turns out that the characteristics of photoelastic fringes are the same as those of constant-level contours on a colored topographic map. As a result, any photoelastic pattern can be considered, and visualized, as a contour map of the difference (without regard to sign) between principal strains or stresses over the surface of the test part. In other words, the magnitudes of the strain levels, as indicated by the fringe orders, correspond directly to constant-altitude levels on a topographic map. And the fringe pattern depicts peaks and valleys, plains and mesas — with "sea level" represented by the zero-order fringes.

If there is a zero-order fringe in the field of view, it will usually be obvious by its black color. Assuming that the coated test part has a free square corner or pointed projection, the stress there will always be zero, and a zero-order fringe (spot) will exist in the corner, irrespective of the load magnitude, but shrinking in size slightly as the load increases. When there is no zero-order fringe evident, the first-order fringe can often be recognized because of the bright colors adjacent to the purple tint of passage. As an alternative, when the test object can be loaded incrementally from an initially stress-free state, the starting zero-order fringe which covers the entire coating can usually be followed throughout the loading process as it recedes toward unstressed points, and regions where the difference in principal stresses is zero.

Once one fringe has been identified, orders can be assigned to the other fringes, making certain that the direction of increasing fringe order corresponds to the correct color sequence — i.e., yellow-red-green, etc. By this process the observer can quickly locate the highest fringe orders and, generally, the most highly strained regions. Areas of closely spaced fine fringes will usually attract the observer's attention, since regions of steep strain gradient ordinarily signify high strains as well. The stress analyst will also note any large areas where the pattern is almost uniformly black or gray, usually indicating a significantly understressed region.

Frequently, the process of locating the highest fringe orders will lead the observer to one or more critical points on a free boundary. When this occurs, the stress analyst knows that the non-zero principal stress at such a point is tangent to the boundary, and its magnitude can be obtained directly by multiplying the fringe order by a constant. The sign of the stress, plus or minus for tension or compression, can also be determined very easily on a free boundary with the reflection polariscope.

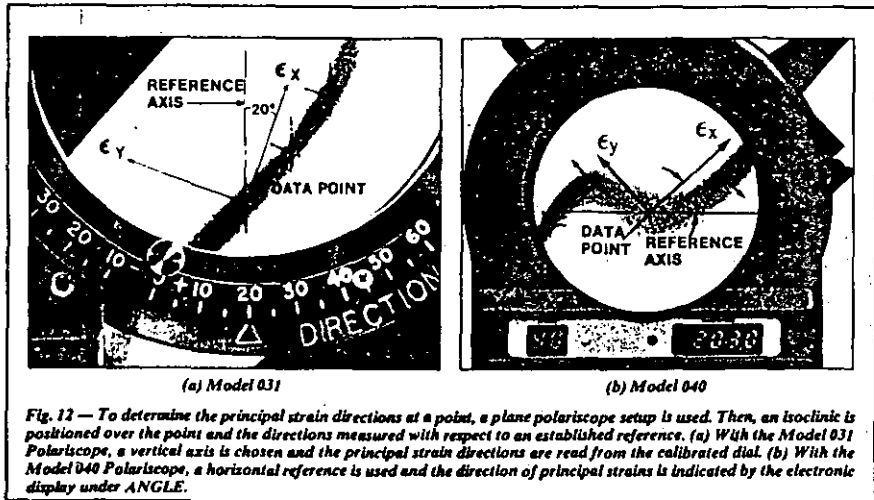
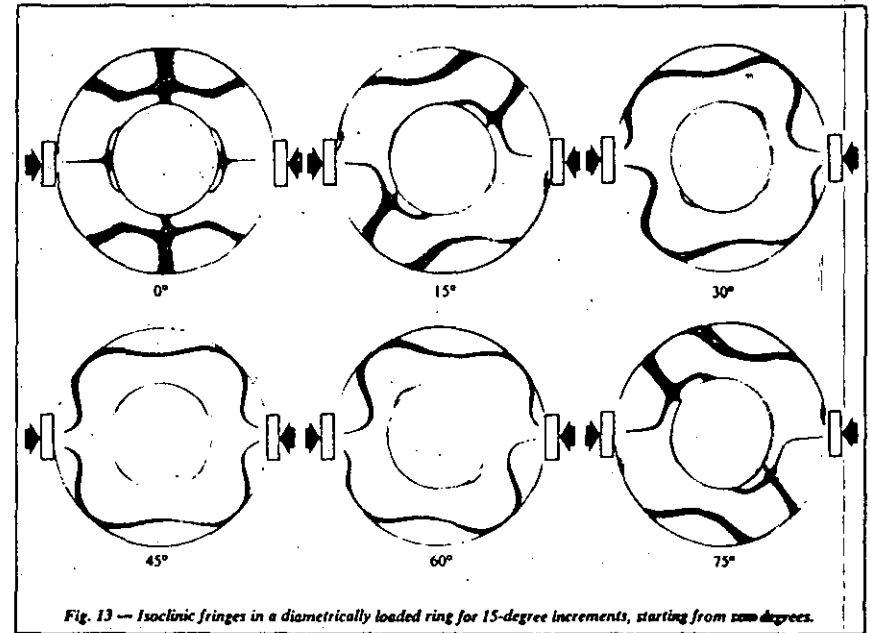
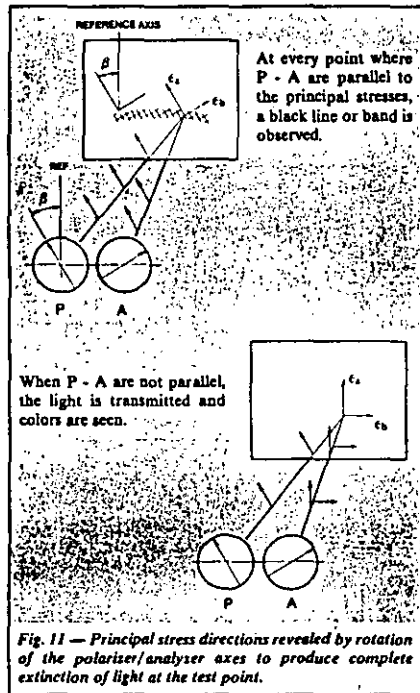
5.0 MEASUREMENT OF PRINCIPAL STRAIN DIRECTIONS

5.1 Measurement Principle

The principal strain directions are always measured with reference to an established line, axis, or plane. Therefore, the initial step for the determination of the direction of principal strains (or stresses) will be to select a convenient reference. In most cases, the reference direction is suggested immediately, like an axis of symmetry of the test part or structure; in other cases, a vertical or horizontal line will suffice.

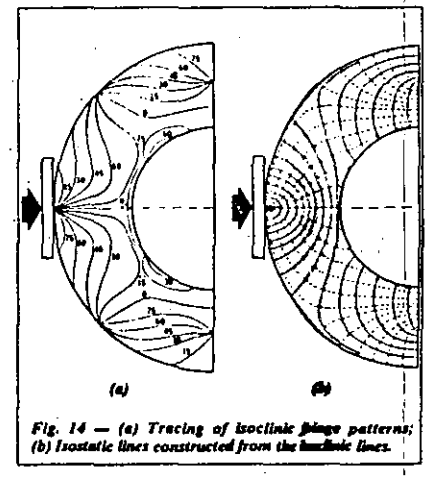
When a plane-polarized beam of light traverses a photoelastic coating on a part subjected to stress, it splits into waves propagating at different speeds along the direction of the principal strains. After emerging from the plastic, these two waves will be out of phase with one another and will not recombine into a single vibration parallel to the one entering the plastic. However, at points where the direction of the principal stresses are parallel to the axis of the polarizing filter, the beam will be unaffected and the emerging vibration will be parallel to the entering vibration. An analyzing filter *A* with its axis perpendicular to the polarizing filter *P* will produce extinction of the vibrations at these points (see Fig. 11).

Observing the stressed part through a reflection polariscope (Fig. 12), black lines (or even areas) appear. These lines are called *isoclinics*. At every point on an isoclinic, the directions of principal strains are parallel to the direction of polarization of *A* and *P*. With respect to the selected reference axis, the measurement of directions at a point is simply accomplished by the rotation of *A* and *P* together until a black isoclinic appears at the point where the directions are to be measured. When the strain directions are required over an entire area, the isoclinics are usually recorded by photography or by tracing directly on the coating.



If the isoclinics are narrow and sharply defined, it means that the directions of ϵ_x and ϵ_y vary rapidly from one location to the next. Isoclinics forming broad black lines or areas indicate that the ϵ_x and ϵ_y directions vary slowly in that region. When this occurs, the boundary surrounding the entire isoclinic should be marked (not merely the center). In the case of a tensile specimen with a constant cross section, an isoclinic will be seen to cover the entire area when the axes of polarization coincide with the specimen axes, since the direction of ϵ_x is the same at every point.

By rotating the polarizer and analyzer assemblies together (in small, uniform angular increments) over the range from 0 to 90 degrees, the complete family of isoclinics will be generated. An example of this procedure is shown photographically in Fig. 13, for a ring subjected to diametral compression. The isoclinics can be combined into a single drawing by tracing from the photographs onto a piece of paper, as illustrated in Fig. 14a (for only half of the ring, since the pattern is symmetric). Then, if desired, the family of isoclinics can be used to construct an *isostatic* diagram, as in Fig. 14b. Isostatic lines have the property of being everywhere tangent to the principal stress directions, and thus illustrate the "flow" of stress through the test object.



6.0 MEASUREMENT OF STRESS AND STRAIN MAGNITUDES

6.1 Relationships Between Fringe Orders And Magnitudes of Strain And Stress

The fringe orders observed in photoelastic coatings are proportional to the difference between the principal strains in the coating (and in the surface of the test part). This simple linear relationship is expressed as follows [repeating Eq. (8) here for convenient reference]:

$$\epsilon_x - \epsilon_y = Nf \quad (8)$$

where: ϵ_x, ϵ_y = principal strains; N = fringe order

$$f = \frac{\lambda}{2tK} \quad (\text{fringe value of coating})$$

λ = wavelength (in white light, 22.7×10^{-6} in or 373 nm)

t = thickness of coating

K = strain optical coefficient of coating

Equation (8) can also be written in terms of shear strain, γ_{xy} :

$$\gamma_{xy} = Nf \quad (9)$$

where: γ_{xy} = maximum shear strain (in the plane of the part surface) at any point.

The significance of the preceding is that the difference in the principal strains, or the maximum shear strain in the surface of the test part, can be obtained by simply recognizing the fringe order and multiplying by the fringe value of the coating.

Engineers and designers often work with stress rather than strain; and, for this purpose, Eqs. (8) and (9) can be transformed by introducing Hooke's law for the biaxial stress state in mechanically isotropic materials:

$$\sigma_x = \frac{E}{1-\nu^2} (\epsilon_x + \nu\epsilon_y) \quad (10)$$

$$\sigma_y = \frac{E}{1-\nu^2} (\epsilon_y + \nu\epsilon_x) \quad (11)$$

and,

$$\sigma_x - \sigma_y = \frac{E}{1+\nu} (\epsilon_x - \epsilon_y) \quad (12)$$

Substituting Eq. (8) into Eq. (12),

$$\sigma_x - \sigma_y = \frac{E}{1+\nu} Nf \quad (13)$$

where: σ_x, σ_y = principal stresses in test part surface

E = elastic modulus of test part

ν = Poisson's ratio of test part.

And, noting that the maximum shear stress, T_{MAX} , in the plane of the surface at any point is $(\sigma_x - \sigma_y)/2$,

$$T_{MAX} = \frac{1}{2} \left(\frac{E}{1+\nu} \right) Nf \quad (14)$$

Equations (8) and (13), which are the primary relationships used in photoelastic coating stress analysis, give only the difference in principal strains and stresses, not the individual

quantities. To determine the individual magnitudes and signs of either the principal strains or stresses generally requires, for biaxial stress states, a second measurement, such as the sum of the principal strains (see page 14). There are many cases, however, when these equations provide all of the information needed for stress analysis. For instance, when the ratio of principal stresses can be inferred from other considerations — a uniform shaft in torsion ($\sigma_x/\sigma_y = -1$), a thin walled pressure vessel ($\sigma_x/\sigma_y = 2$), etc. — this relationship can be combined with Eq. (13) to solve for the individual principal stresses. And, whenever the stress state is known to be uniaxial, with either σ_x or σ_y being zero, there is only one nonzero principal stress in the plane of the test part surface, and this can be obtained directly from Eq. (6). For example, if $\sigma_y = 0$,

$$\sigma_x = \frac{E}{1+\nu} Nf \quad (15)$$

The cases in which one of the principal surface stresses is zero include all straight, uniform-cross-section members in axial tension or compression (and bending), away from points of load application. Even for mildly tapered members, so loaded, the stress state is very nearly uniaxial, and Eq. (15) can often be applied as a very good approximation. A much more important class of cases from the viewpoint of practical stress analysis involves all points on the boundaries and free edges of the test part.

Consider, for example, an unloaded hole penetrating the test part. At every point on the edge of the hole the principal axes are normal and tangential, respectively, to the edge. Because the principal stress normal to the edge is necessarily zero, the stress state is uniaxial, and the only nonzero principal stress is everywhere tangent to the hole edge. There are many other cases, such as projecting flanges and ribs, and "two-dimensional" objects in general, in which the stress state on the unloaded edge is always uniaxial. For all such cases, the single nonzero principal stress, which is tangent to the edge, can be determined directly from the observed fringe order by substituting into Eq. (15); or, in effect, multiplying the fringe order by a constant.

Figure 15 shows a portion of the surface of a steel machine part to which a photoelastic coating has been applied. As indicated, the coating has been finished to accurately match the edge of the hole and that of the rib. The uniaxial stress state at points a and b is demonstrated by the enlarged free-body diagrams of elements of matter removed from the edges for examination. With the part under normal service loading, and viewing the coating with the reflection polariscope, a fringe order of 2 is observed at point a , and about 3/4 at point b . Previous calibration has established a fringe value of 1100 $\mu\epsilon$ per fringe for this coating. Thus, the stress at point a in the more critical region can be calculated directly from Eq. (15) assuming (for steel) that $E/(1+\nu) = 23.5 \times 10^4$ psi or 162 GPa:

$$\sigma_x = 23.5 \times 10^4 \times 1100 \times 10^{-6} \times 2 = 51\,700 \text{ psi or,}$$

$$\sigma_x = 162 \times 10^6 \times 1100 \times 10^{-6} \times 2 = 356 \text{ MPa}$$

*It should be kept in mind that the biaxial Hooke's law, involved in Eqs. (10)-(15), is strictly applicable only to homogeneous materials which are isotropic and linear-elastic in their mechanical properties.

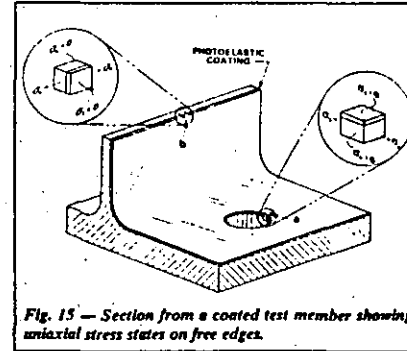


Fig. 15 — Section from a coated test member showing uniaxial stress states on free edges.

And similarly, the stress at the edge of the rib is about 19 400 psi, or 134 MPa.

Summarizing, the difference between principal strains can be determined from Eq. (8), and the difference between principal stresses from Eq. (13), at any point on a photoelastically coated surface. At points where the stress state is uniaxial, Eq. (15) gives the principal stress directly. In each case, the result is obtained by multiplying the observed fringe order by a constant. It remains, then, only to identify the fringe order at the point of measurement. Techniques for accomplishing this precisely and positively with the reflection polariscope follow.

6.2 Measurements at a Point

It has been shown that in the first step of measurement one observes the whole area and assigns to each fringe its order ($N=1, 2, 3$, etc.). At every point on a fringe, N is then known and therefore:

$$\epsilon_x - \epsilon_y = Nf$$

In general, the point of interest on the structure will fall between fringes, and it will be necessary to establish the "fractional order" or fraction of a fringe. The technique used is called "compensation". Two basic methods are used:

1. Tardy compensation using the rotatable analyzer built into the Model 031 Polaroscope.
2. Null-balance compensation using the Model 232 or 632, 030 Series Modular Accessories, or the Model 040 Polaroscope.

6.2.1 Tardy Compensation

Tardy compensation is a relatively fast and simple method. However, the method requires an experienced operator if measurements are to be foolproof. The principle of the method is as follows:

When the polarizer and analyzer are aligned with the direction of the principal strains/stresses, and the quarter-wave plates are at 45° (as shown in Fig. 4) a clockwise rotation α of the analyzer will move a fringe to a position where the fractional order r is $\alpha/180$.

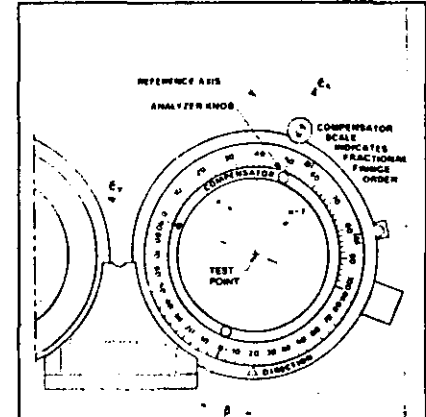


Fig. 16 — Tardy compensation: polarizer and analyzer aligned with principal strains ϵ_x and ϵ_y (β and $\beta + 90^\circ$ respectively). Rotate analyzer clockwise until fringe n (or $n + 1$) moves to test point. Read fraction r as indicated on compensator scale.

The analyzer dial is graduated in hundredths of a fringe from zero to 100 (see Fig. 16). The analyzer is rotated clockwise until a fringe arrives at the selected point of measurement (red on one side, green on the other side). The fractional fringe order r is then read directly from the analyzer dial.

If the lower order fringe moves to the point (fringe n), the total reading will be:

$$N = n + r$$

and, $\epsilon_x = \epsilon_1, \epsilon_y = \epsilon_2$

where: ϵ_1, ϵ_2 = maximum and minimum principal strains, respectively.

If the higher order fringe moves to the point (fringe $n + 1$) the total reading will be:

$$N = -[(n + 1) - r]$$

and, $\epsilon_x = \epsilon_1, \epsilon_y = \epsilon_2$

In either case:

$$\epsilon_x - \epsilon_y = Nf$$

and, $\sigma_x - \sigma_y = Nf \frac{E}{1+\nu}$

6.2.2 Measurements of Principal Stress at Free Boundaries Using Tardy Compensation

The sign and magnitude of the principal stresses in a uniaxial field, and also at a free edge or boundary, can be determined directly since one of the stresses is zero.

The procedure is as follows:

1. Align the ϵ_1 axis of the analyzer (Fig. 16) with the direction of the edge.
2. Identify the fringes n and $n + 1$ on either side of the point.
3. Rotate the analyzer in a clockwise direction. If the lower fringe order n moves toward the point of measurement, the sign of the stress is positive and the total reading will be $N = n + r$. If the higher order fringe $n + 1$ moves toward the point, the sign of the stress is negative and the total reading will be $N = -[(n + 1) - r]$. In either case the stress will be:

$$\sigma = Nf \frac{E}{1 + \nu}$$

where: σ = tension, if positive;
compression, if negative.

6.2.3 Measurements Using The Null-Balance Compensation Method

Null-balance compensation operates on the principle of introducing into the light path of the polariscope a calibrated variable birefringence of opposite sign to that induced in the photoelastic coating by the strain field. When the opposite-sign variable birefringence is adjusted to precisely match the magnitude of the strain-induced birefringence, complete cancellation will occur, and the net birefringence in the light

path will be zero. The condition of zero net birefringence is easily recognized because it produces a black fringe in the isochromatic pattern where, before introducing the compensating birefringence, a colored fringe existed (Fig. 17). The device for synthesizing a calibrated variable birefringence is known as a *null-balance compensator*.

The manner in which a null-balance compensator operates is illustrated schematically in Fig. 18 by analogy with the common knife-edge balance. The strain-induced birefringence (or optical "signal") is represented by an unknown mass on the left-hand pan of the scale, where it produces a counterclockwise moment, tipping the pointer off from center to the left. Known masses can be placed on the right-hand pan (introducing a clockwise moment) until the pointer is brought back to center again. When the pointer is centered, the sum of the known calibrated masses equals the unknown mass. The operation of the compensator directly parallels that of the balance — that is, compensating birefringence is added to the light path until it exactly balances the birefringence induced in the coating by the strain field on the surface of the coated part.

When using the 030 Series Reflection Polariscope, two versions of null-balance compensators are available. The Model 232 Compensator is a manual type whereby the fringe order is determined by a mechanical counter. The strain is then calculated from the numerical reading of the fringe order by introducing the calibration constant of the compensator (Figs. 19 and 20).

With the Model 632 System (Fig. 21), the compensator is electrically coupled to a strain indicator/printer instrument which provides a direct digital display of the strain magnitude $\epsilon_1 - \epsilon_2$ after achieving null-balance compensation at the point of measurement. The Model 632 System is also configured to electronically display the measured principal strain direction. This is accomplished by a transducer built into the compensator, which senses the angular orientation of the isochinic. A built-in printer also allows a hard copy of the measured quantitative strain values to be obtained. The printer is activated from the compensator.

In order for the null-balance measurement to be achieved when using either the Model 232 or Model 632 System, the compensator must first be aligned in the direction of the algebraically maximum principal strain. This is easily determined by establishing the directions of the two principal strains at the point of measurement with an isochinic measurement as described on pages 8 and 9.

The compensator is then aligned with one of these directions, and the compensation attempted. If null-balance cannot be achieved, it means the compensator is aligned with the minimum principal strain direction. Repositioning the compensator 90° away will allow the null-balance compensation to be performed.

When using the Model 040 Reflection Polariscope (Fig. 22), null-balance compensation can be achieved regardless of which principal strain the compensator is aligned with, since it has a special feature for introducing either positive or negative birefringence into the light path. And this introduces no ambiguity since the magnitude measurement made will always be displayed with the correspondingly correct sign. Also, the Model 040 Polariscope can be set up to read directly in units of fringe order, principal strain difference, principal stress difference, and the maximum principal stress at free boundaries.

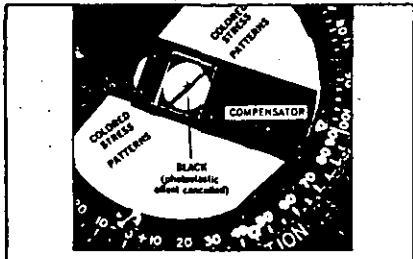


Fig. 17 — Initially colored fringe is rendered black by null-balance compensation.

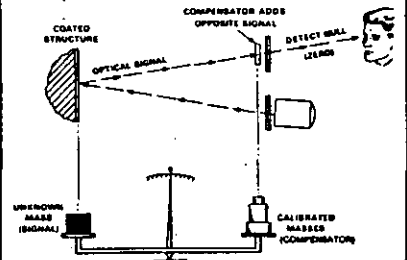


Fig. 18 — Principle of null-balance compensation.

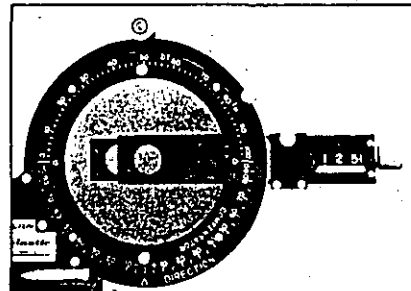


Fig. 19 — Model 232 Compensator mounted on the 030 Series Polariscope.

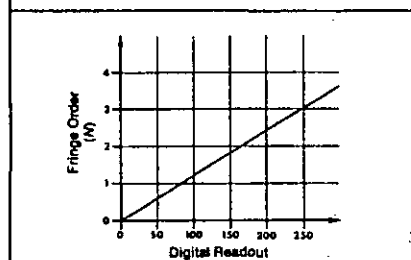


Fig. 20 — Typical calibration chart for Model 232 Compensator.

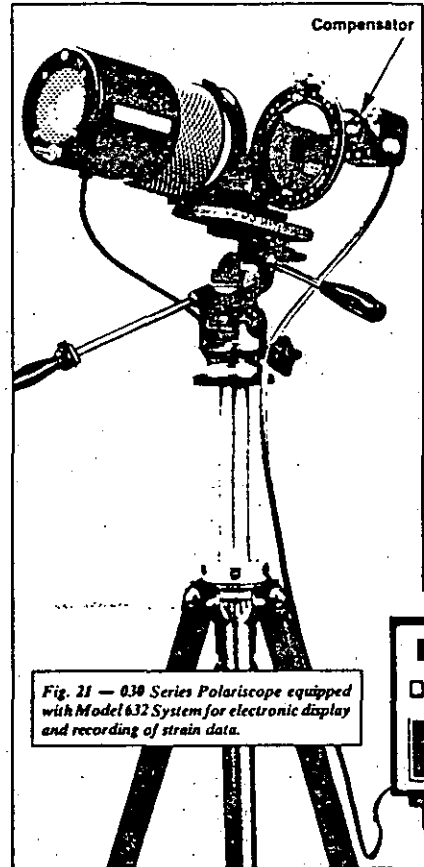
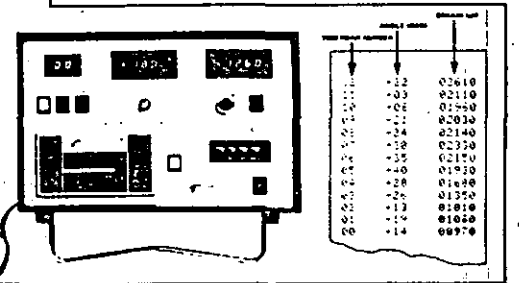


Fig. 21 — 030 Series Polariscope equipped with Model 632 System for electronic display and recording of strain data.



Fig. 22 — 040 Polariscope with on-board electronics.



7.0 PRINCIPAL STRAIN/STRESS SEPARATION METHODS

In the previous sections, it has been shown how to measure principal strain differences and then calculate the following stresses:

- The magnitude of the difference of the principal stresses $\sigma_x - \sigma_y$;
- The maximum shear stress $\tau_{MAX} = \frac{\sigma_x - \sigma_y}{2}$;
- The separate values of the nonzero principal stress on edges and free boundaries where the maximum stresses usually occur since at those points the other principal stress is zero.

In order to obtain the individual values of the principal stresses at points not located on free boundaries, additional measurements are required. There are two techniques available; the Oblique-Incidence Method, and the Strain Gage Separator Method. Oblique incidence is the more difficult to use, and is restricted to measurements at locations which afford mechanical access of the Oblique-Incidence Adapter. The oblique-incidence technique must be used on medium- and low-modulus PhotoStress coatings, since the separator strain gage method is only applicable to high-modulus coatings.

7.1 Oblique-Incidence Method

The term *oblique incidence* means that the light from the polarizer traverses the photoelastic coating at an angle, and the measured birefringence depends on the secondary principal strain in the plane perpendicular to the light path. Thus, an oblique-incidence reading (N_o), combined with the normal-incidence reading (N_n), provides the necessary information for determining the separate values of σ_x and σ_y at points other than free boundaries. The Oblique-Incidence Adapter (Model 033) has a fixed mirror angle which provides for simplified data reduction. The Model 033 is shown attached to the basic analyzer in Fig. 23. Figure 24 shows the path of light emerging from the polarizer, reflected by the oblique-incidence mirror, traversing the photoelastic coating, reflected back to the mirror, and finally back to the analyzer.

In normal incidence N_n , the measurement is:

$$N_n \lambda = \delta_{NORMAL} = 2tK(\epsilon_x - \epsilon_y)$$

In oblique incidence:

$$N_o \lambda = \delta_{OBLIQUE} = 2tK(A\epsilon_x - B\epsilon_y)$$

The coefficients A and B are dependent upon the Poisson's ratio of the coating, and the angle θ employed. This angle is preset in the Model 033 Oblique-Incidence Adapter. Solving these equations in terms of ϵ_x and ϵ_y :

$$\left. \begin{aligned} \epsilon_x &= f(1.5N_o - N_n) \\ \epsilon_y &= f(1.5N_o - 2N_n) \end{aligned} \right\} \text{for high-modulus coatings} \quad (16)$$

The numerical values of 1, 1.5, and 2 are coefficients derived from the development of equations for oblique-incidence measurements. (Reference 3 affords a more comprehensive technical description.)

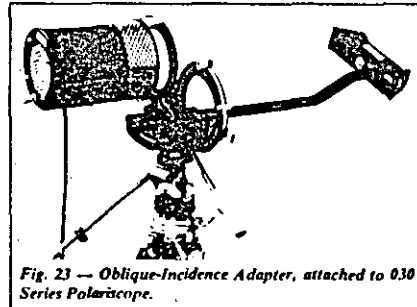


Fig. 23 — Oblique-Incidence Adapter, attached to 030 Series Polariscopes.

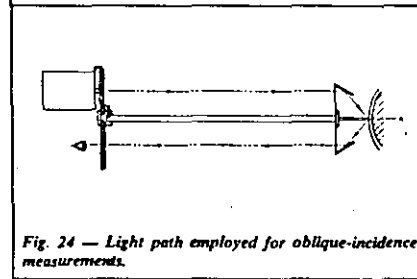


Fig. 24 — Light path employed for oblique-incidence measurements.

Once the principal strains have been determined, the principal stresses are calculated.

$$\sigma_x = \frac{E}{1 - \nu^2} (\epsilon_x + \nu\epsilon_y)$$

$$\sigma_y = \frac{E}{1 - \nu^2} (\epsilon_y + \nu\epsilon_x)$$

where E and ν are the modulus of elasticity and Poisson's ratio, respectively, of the test part.

7.2 Strain Gage Separator Method

If the sum of the principal strains can be determined at the same point where the difference of the principal strains is measured, then the separate principal strain values are obtainable by simply solving equations simultaneously.

The PhotoStress Separator Gage is based on this fundamental principle of mechanics. As shown in Fig. 25, the gage grid consists of two perpendicular elements connected in series. The indicated strain from the gage then corresponds to $(\epsilon_x + \epsilon_y)/2$ regardless of the gage orientation on the coated test surface. Representing the gage output signal by the symbol S_o for convenience in algebraic manipulation,

$$S_o = \frac{\epsilon_x + \epsilon_y}{2} \quad (18)$$

and $\epsilon_x + \epsilon_y = 2S_o$



Fig. 25 — PhotoStress Separator Gage

Adding to, and subtracting from, the measurement of the difference of principal strains,

$$\begin{aligned} \epsilon_x - \epsilon_y &= N_n f \\ \epsilon_x + \epsilon_y &= 2S_o \end{aligned} \quad (19)$$

$$\begin{aligned} \epsilon_x - \epsilon_y &= N_n f \\ \text{and } -\epsilon_x - \epsilon_y &= -2S_o \end{aligned} \quad (20)$$

In practical applications, the usual procedure is to first complete all PhotoStress observations and normal-incidence measurements (N_n) on the coated test object. Following this, separator gages are installed on the coating at the potentially critical points established by PhotoStress analysis. Loads are then reapplied to the test object, and the separator gage measurements are recorded.

The PhotoStress Separator Gage (for use on high-modulus coatings only) embodies a number of special features designed for ease of use and optimum performance in PhotoStress applications. First in importance, of course, is that the gage does not require any particular angular orientation. It is simply bonded at the point where separation measurements are desired. Preattached leadwires are provided to avoid the

problems that users may have in soldering the leads to the gage before installation, or attempting to do so after the gage is bonded to the photoelastic coating. The gage grid is also encapsulated in polyimide to eliminate the need for a protective coating in most PhotoStress applications.

Grid resistance of the separator gage is 200 ohms; and it is intended that the gage be connected to a Model P-3500 Static Strain Indicator through a specially designed interface module, the Model 330 (Fig. 26). The interface module is a four-channel switch-and-balance unit containing precision resistive circuits for attenuating gage excitation voltage and supplying appropriate bridge completion for the 200-ohm gage. The resulting gage current is approximately 1 mA, yielding a power level well below the threshold at which self-heating effects could destabilize the strain indication.

The complete technical background on the separator gage and its application can be found in Measurements Group Tech Note TN-708.

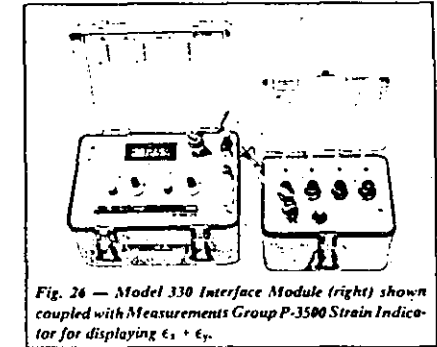


Fig. 26 — Model 330 Interface Module (right) shown coupled with Measurements Group P-3500 Strain Indicator for displaying $\epsilon_x + \epsilon_y$.

8.0 BIBLIOGRAPHY

1. Blum, A.E., "The Use and Understanding of Photoelastic Coatings," *Strain, Journal of the British Society for Strain Measurement* 13: 96-101 (July 1977).
2. Post, D. and F. Zandman, "Accuracy of Birefringent-coating Method for Coatings of Arbitrary Thickness," *Experimental Mechanics* 1: 21-32 (January 1961).
3. Redner, S., "New Oblique-incidence Method for Direct Photoelastic Measurement of Principal Strains," *Experimental Mechanics* 3: 67-72 (March 1963).
4. Redner, S., "Photoelastic Coatings," *Experimental Mechanics*, 20: 403-408 (November 1980).
5. Zandman, F., S. Redner, and J.W. Dally, *Photoelastic Coatings*. Ames, Iowa: Iowa State University Press, 1977.
6. Zandman, F., S. Redner, and D. Post, "Photoelastic-coating Analysis in Thermal Fields," *Experimental Mechanics* 3: 215-221 (September 1963).
7. Zandman, F., S. Redner, and E.I. Reigner, "Reinforcing Effect of Birefringent Coatings," *Experimental Mechanics* 2: 55-64 (February 1962).

Measurements Group Technical References

- Tech Note TN-701, "Calibration of Photoelastic Coatings".
 Tech Note TN-704, "How to Select Photoelastic Coatings".
 Tech Note TN-706, "Corrections to Photoelastic Coating Fringe-Order Measurements".
 Tech Note TN-708, "Principal Stress Separation in PhotoStress® Measurements".
 Bulletin IB-221, "Instructions for Casting and Contouring Photoelastic Sheets".
 Bulletin IB-223, "Instructions for Bonding Flat and Contoured Photoelastic Sheets to Test Part Surfaces".

THE USE OF CANDIED SUGAR AS A BRITTLE LACQUER

L. Ferrer*, J.F. Cardenas-Garcia**, J. Chaur* and E. Solis*

* Department of Mechanical Engineering, National Autonomous University of Mexico, DEPEFI, Mexico City, MEXICO 04510

** Department of Mechanical Engineering, Texas Tech University, Lubbock, Texas 79409-1021, USA

SUMMARY

The purpose of the present work is to introduce candied sugar as a brittle-coating. The chemistry of sugars and invert sugars is introduced, with an explanation of the role played by invert sugars in the manufacture of non-crystalline candy. The process of developing a brittle coating manufactured from sugar is briefly described, showing how the project evolved from using extra fine granulated cane sugar to a more systematic approach using laboratory supplied sugars. Experimental results for a circular disk and a circular ring coated with this new brittle lacquer³ and tested under diametral compression are presented. These results compare well with those obtained using commercially available brittle lacquers. Also, presented results show that the sensitivity of sugar based brittle-coatings can be varied over a wide range and some of the advantages to be found in their use are pointed out. Finally, some possible future areas of research are briefly discussed.

INTRODUCTION

The brittle-coating method is an experimental stress analysis non-destructive technique used for the determination of surface stresses on structural components. Its use relies on the coating adhering completely to the surface of the specimen to be analyzed. When the state of stress under the coating reaches a certain critical value, the brittle-coating fails. If the brittle-coating mechanical properties up to fracture have been properly characterized, then the state of stress on the surface under the failed coating can be determined. This experimental whole-field technique is used to obtain the magnitudes and the directions of the principal stresses on a free surface. As it can be directly applied to the machine or structural component under consideration, this allows the analysis of the element subjected to the actual working conditions, without necessarily knowing the loads acting on the specimen. The analysis of the data is done in a straight forward fashion [1].

LABORATORY EQUIPMENT.

The laboratory equipment used to pursue the outlined research

included: a controlled atmosphere moisture oven, a brittle coating calibrator, calibration beams, thermometers, psychrometers, and other miscellaneous items usually found in a brittle coating laboratory.

LITERATURE SURVEY

The available literature on brittle-coatings, although very profuse, for the purpose of the present work can be confined to the four chapters devoted to brittle-coatings in reference [1]. Information on candied sugar was obtained from references [2,3], and the information relevant to making brittle-coatings is reported here.

CANDY-SUGARS

Carbohydrates are a large group of chemical substances which occur widely in the vegetal and animal kingdom and conform to a general formula $C_x(H_2O)_y$, with x being generally a multiple of 6.

Cane or beet sugars - chemically speaking these are known as sucrose. Sucrose is referred to as a double sugar, and can be broken up into two single sugars by boiling it with a weak solution of acid, or by enzyme invertase. The two new sugars formed are called glucose (dextrose) and fructose (levulose). They are non-crystalline. They have been chemically changed into a product called "invert sugar", and the process is known as inversion. Lactose is the sugar present in milk, and maltose is a sugar produced by the hydrolysis of starch.

In making candy, the sugar is first dissolved with some solvent such as water. To this solution, an inverting substance such as dextrose, corn syrup, cream of tartar, vinegar or lemon juice is added. Then the mixture is subjected to high temperature. Boiling changes the mixture into a heavy syrup solution which becomes more and more concentrated, and, as the moisture evaporates, more and more supersaturated.

The temperatures, at sea level, to obtain candies of different consistencies are:

Soft ball	109-115°C
Hard ball	117-120°C
Crack stage	121-129°C
Hard crack	129-154°C
Caramel sugar, Sugar melts	158°C

SUGAR AS A BRITTLE COATING

The process of developing a brittle coating manufactured from sugar went through several stages. They were:

1. Use of extra fine granulated cane sugar

Extra fine granulated cane sugar was used on calibration beams which were covered with about one millimeter of sugar. The beams were placed in the oven at 185°C (the fusion temperature for cane

sugar is 158°C) for one hour, after which the oven was turned off and allowed to slowly cool to room temperature over a period of approximately two hours. The resulting golden brown, transparent coating on the calibration beams produced well defined cracks which were easy to detect. Figure 1 shows the resulting crack patterns on two calibration beams. The brittle coating had a sensitivity of the order of 500 microstrain.



Figure 1 - Calibration beam results using extra granulated cane sugar as a brittle coating.

2. Extra fine granulated cane sugar, corn syrup and water.

Next, a mixture by volume of 2 parts sugar, 1/2 part corn syrup (considered as an invert sugar) and 1 part of water was used. The use of an invert sugar allows the lowering of the caramelizing temperature of the mixture. The ingredients were thoroughly mixed in an aluminum container and then heated to temperatures ranging from 127-154°C together with the calibration beams. After fifteen minutes at the preset temperature the mixture was poured on top of the calibration beams, which were prepared so as not to allow the mixture to run off. The beams were then left in the oven at the preset temperature for an additional 45 minutes after which the oven was turned off and enabled to reach room temperature in about two hours. The obtained sensitivities ranged from 300-600 microstrain. Figure 2 shows the resulting coating which was crystal clear, with well defined and easily observable cracks. It appeared that the net effect of this particular invert sugar was to give to the resulting combination greater clarity, and, its use at a range of temperatures allowed for variations in the sensitivity of the brittle coating.

3. Confectionery sugar, brown sugar, maltose, dextrose, fructose, corn syrup and water.

The limited range of sensitivities previously obtained led to the consideration of other readily available sugars (confectionery sugar, brown sugar, maltose) and invert sugars (dextrose, fructose and corn syrup). Quick qualitative testing of the

resulting brittle coatings was made using these ingredients alone and also mixed with water. The results were very similar to those obtained when cane sugar or corn syrup were used alone.

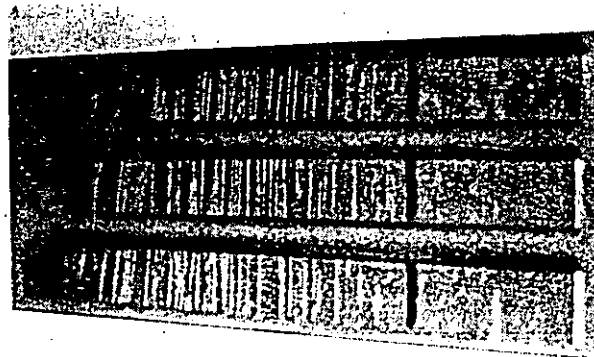


Figure 2 - Calibration beam results using a mixture of extra fine granulated cane sugar, corn syrup and water as a brittle coating

4. Cane sugar, beet sugar, confectionery sugar, brown sugar, maltose, fructose and water.

It was then decided to test the mixtures of the "most promising" sugars (cane sugar, beet sugar, confectionery sugar, brown sugar, maltose) with an invert sugar (fructose) and water. The choice of fructose was made due to the previous experience with corn syrup which is made up mostly of fructose and also because it is readily available. The idea of using a more homogeneous ingredient than corn syrup was also attractive. Mixtures by weight were made for all possible combinations of the sugars with the fructose, using 2 parts sugar, 1 part fructose and 1-1/2 parts water. Each mixture was placed in an aluminum foil cylindrical container of approximately 2.5 inches in diameter. The mixtures were placed in the oven at a temperature of 165°C, heated for 30 minutes and then allowed to cool to room temperature in about two hours. The qualitative results obtained showed no significant difference with previous results using cane sugar mixed with corn syrup and water.

5. A systematic approach.

Since no definite leads towards the best combinations of ingredients were emerging it was apparent that a more systematic approach was in order. To accomplish this it was decided to work with the following sugars: cane sugar, beet sugar, maltose, and lactose; and invert sugars: dextrose, fructose, corn syrup, and honey. The solvent in all cases was water.

The text matrix in table I was implemented. It shows that for

each combination tested three ratios of ingredients by weight were used (5:1), (3:3) and (1:5); the number on the left represents the corresponding ingredient in the vertical column, and that on the right, the corresponding ingredient in the top row. Each combination was identified by the number shown on the test matrix; a total of 84 samples were tested. The amount of water used for all combinations was held constant at 6 parts by weight out of the 12 total parts making up the mixture. Each mixture was placed in an aluminum foil cylindrical container of approximately 2.5 inches in diameter. The mixtures were placed in the preheated oven at a temperature of 165°C, cooked for 15 minutes and then allowed to cool to room temperature in about two hours. The thin coatings present at the bottom of the aluminum containers were then evaluated after cracking the coatings using finger pressure. The qualitative evaluation considered the sensitivity, adherence, fluidity, color and crack density of the brittle-coating.

Ingredients	Granulated Beet Sugar	Maltose	Lactose	Dextrose	Fructose	Corn Syrup	Honey
Extra Fine Cane Sugar	(1) (2) (3)	(4) (5) (6)	(7) (8) (9)	(10) (11) (12)	(13) (14) (15)	(16) (17) (18)	(19) (20) (21)
Granulated Beet Sugar		(22) (23) (24)	(25) (26) (27)	(28) (29) (30)	(31) (32) (33)	(34) (35) (36)	(37) (38) (39)
Maltose			(40) (41) (42)	(43) (44) (45)	(46) (47) (48)	(49) (50) (51)	(52) (53) (54)
Lactose				(55) (56) (57)	(58) (59) (60)	(61) (62) (63)	(64) (65) (66)
Dextrose					(67) (68) (69)	(70) (71) (72)	(73) (74) (75)
Fructose						(76) (77) (78)	(79) (80) (81)
Corn Syrup							(82) (83) (84)

* - The left digit corresponds to an ingredient in the vertical column; the right digit corresponds to an ingredient in the top row.

Table I - Test matrix showing all combinations tested using ratios of (5:1), (3:3) and (1:5) between components

Analysis of the results yielded three general tendencies: Beet and cane sugar have analogous behavior. Corn syrup has a behavior similar to fructose. And, lactose, when in large proportions, tends to granulate.

6. A systematic approach using laboratory supplied sugars.

It was then decided that it might be best to use sugars made for laboratory use. This would allow the close monitoring of their composition as most chemicals are manufactured under very high standards of quality control. The invert sugars and sugars included for the tests corresponding to this stage were: dextrose, fructose, lactose maltose and sucrose. The solvent was water.

Characteristics of the invert sugars and sugars used:

DEXTROSE. Reagent (D-Glucose, anhydrous). Dextrose, anhydrous, powder, 'Baker analyzed', HOCH₂CH(COH)₄O. Manufacturer J. T. Baker Inc., Phillipsburg, NJ 08865

FRUCTOSE. (D-Fructose) (Crystals) C₆H₁₂O₆. Manufacturer Mallinckrodt Inc., Paris, KY 40361

LACTOSE. Analytical reagent (powder) C₁₂H₂₂O₁₁ · H₂O. Manufacturer: Mallinckrodt Inc., Paris, KY 40361

MALTOSE. Hydrate grade I - Beta-anomer 96%, Alfa-anomer 4% CO₁₂H₂₂O₁₁ · H₂O. Manufacturer: Sigma Chemical Co., St. Louis, MO 63178

SUCROSE (Saccharose). C₁₂H₂₂O₁₁. Manufacturer: Fisher Scientific, Fair Lawn, NJ 07410

Ingredients	Fructose	Lactose	Maltose	Sucrose
Dextrose	(13) 1:5 (14) 3:3 (15) 5:1		(7) 1:5 (8) 3:3 (9) 5:1	(1) 1:5 (2) 3:3 (3) 5:1
Fructose			(10) 1:5 (11) 3:3 (12) 5:1	(4) 1:5 (5) 3:3 (6) 5:1
Lactose		(17) 5:1		(18) 1:5 (19) 3:3 (20) 5:1
Maltose				(22) 1:5 (23) 3:3 (24) 5:1

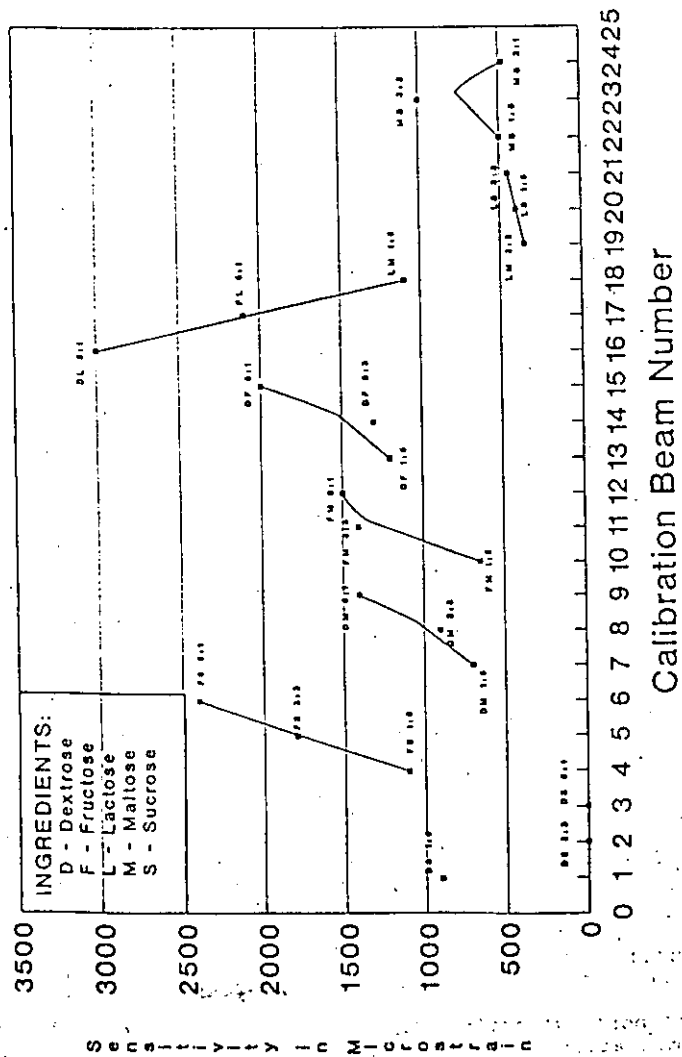
* - The left digit corresponds to an ingredient in the vertical column; the right digit corresponds to an ingredient in the top row.

Table II - Test matrix showing all combinations tested using ratios of (5:1), (3:3) and (1:5) between components

The test matrix used is shown in table II. For each combination tested three ratios, of sugars, by weight were used (5:1), (3:3) and (1:5). The numbers, as before, on the left represent the proportion of the corresponding ingredient in the vertical column; and on the right, the proportion of the corresponding ingredient in the top row. Each combination was identified by the number shown on the test matrix; a total of 24 samples were tested. Some combinations were not tested due to problems with granulation of the mixture. The amount of water used for all combinations was held constant at 6 parts by weight out of 12 total parts making up the mixture.

To more strictly assess the quality of the formulated combinations, the prepared mixtures were used to coat 24

Figure 3 Calibration beam sensitivity variation for 24 combinations of sugars, invert sugars and water.



calibration beams. As before, the oven was preheated to 165 °C and the coated beams introduced into the oven and kept for 30 minutes at that temperature and subsequently allowed to cool to room temperature in about two hours. The calibration beams were then taken from the oven, visually inspected and tested using the brittle coating calibrator.

Figure 3 shows a plot of beam number versus sensitivity for all tests. The range of sensitivities is from 300 to 3000 microstrain, i. e., an order of magnitude difference.

Figure 4 shows two beams covered with brittle coatings made up of maltose and sucrose in proportions of 1:5 and 3:3, respectively. From the test results is clear that the relative proportions have an effect on the sensitivity of the brittle-coating. From the data it is possible to conclude that sugars behave as resins and invert sugars as plasticizers. Thus, it can be postulated that with the appropriate combination of resin, plasticizer and solvent, brittle-coatings with almost any degree of sensitivity can be produced.

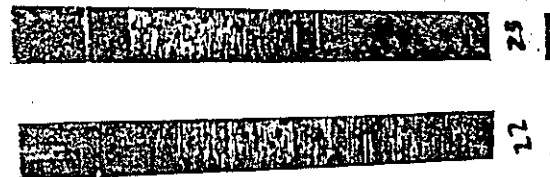


Figure 4 - Calibration beam sensitivity effects in a mixture of different proportions of maltose and sucrose: Beam 22(1:5) and beam 23 (3:3)

An additional test to corroborate the quality and reproducibility of the brittle coating manufactured using mixture 22 was performed. Figure 5 shows the results of testing four calibration beams which were coated and subjected to the same curing cycle as before. The results are reproducible and the qualities of the coatings are good.

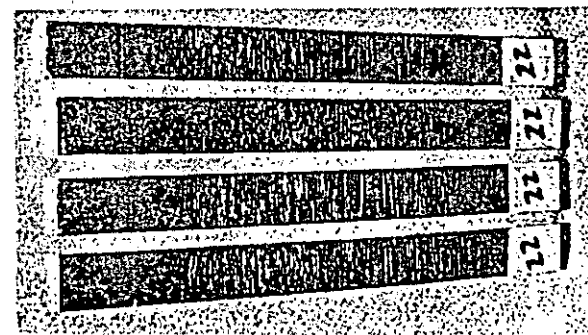


Figure 5 - Calibration beam results for a mixture of maltose and sucrose in a 1:5 proportion

7. The circular disk and ring subjected to diametral compression

To further assess the viability of mixture 22 obtained previously, it was decided to test it on the circular disk and ring as these have been thoroughly studied earlier, and the results could be easily compared to previously obtained results using commercially available brittle lacquers. A circular disk and ring with 177.8 millimeters (mm) in outside diameter (OD) were tested. The ring had an (OD/ID) ratio of 1/2. Both aluminum specimens were 12.7 mm thick. The disk was subjected to a compression load of 222,400 Newtons (50,000 pounds) and the ring was subjected to a compressive load of 111,200 Newtons (25,000 pounds). The resulting crack patterns are shown in Figures 6 and 7.

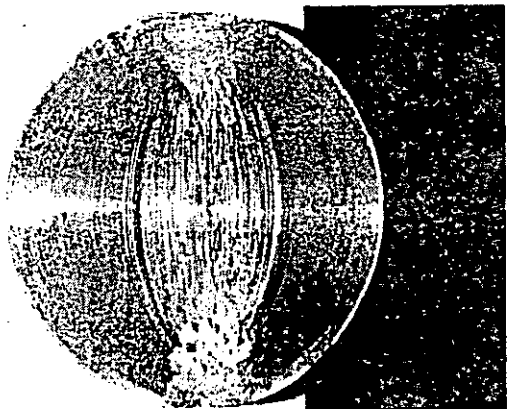


Figure 6 - Circular disk results for a mixture of maltose and sucrose in a 1:5 proportion.

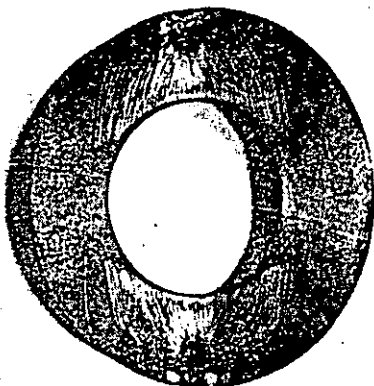


Figure 7 - Circular ring results for a mixture of maltose and sucrose in a 1:5 proportion.

DISCUSSION OF RESULTS

Progress to date shows that brittle coatings whose base is sugar have the following characteristics: The sensitivity of these brittle-coatings can be varied at will, keeping in mind that the sugars can be considered as the resin, the invert sugars as the plasticizer and the water as the solvent. Some of the advantages to be found in their use are their non-toxicity, non-flammability and non-explosivity; they are readily available and low in cost; they are easy to apply for the flat configurations considered, as little or no surface preparation is required, and easy to remove; they produce a well defined crack pattern and no crack enhancers are required.

FUTURE RESEARCH

The following areas of research need to be assessed more fully:

1. Methods of application. Probably this is the most critical area which still needs to be developed, specially for 3-D surfaces.
2. Physical characteristics of the coating. The coating thickness seems to have a strong influence on coating behavior.
3. Heat treatment of the coating. Variations in temperature and curing time may have strong influence on the coating behavior.
4. Elastic constants of the material. Both, the Modulus of Elasticity and Poisson's ratio for the different sugar based brittle-coatings have to be determined.
5. Test conditions. The effect of the temperature and relative humidity during testing also may have a very strong influence on the coating behavior.

BIBLIOGRAPHY

1. Durelli, A. J., Phillips E. A., and Tsao, C. H., "Introduction to the Theoretical and Experimental Analysis of Stress and Strain," McGraw-Hill Book Company, New York, 1958.
2. Bookmeyer, M. B., "Candy and Candy-making," The Manual Art Press, Peoria, Illinois, 1929.
3. DeGros, J. H., "Holiday Candy and Cookie Cook Book", Arco Publishing Co., Inc., New York, 1954.

9.3 Reconditioning the Frozen Sheet for Contouring

When a sheet of plastic is needed for contouring, remove it from the freezer and lay it on a flat surface for warming to room temperature. A nominal 20-minute waiting time is usually sufficient for the sheet to soften. The warming process can be accelerated, if necessary, by placing the frozen sheet on the Model 012-1H Heated Casting Plate, with the plate temperature set at about 95°F (35°C). A higher temperature is not recommended, since polymerization may advance too rapidly to leave sufficient time for contouring.

As soon as the plastic is restored to its soft, pliable state at room temperature, remove the waxed paper and immediately

contour the sheet to the test-part surface. From this point onward, all remaining steps in the PhotoStress procedure are the same as if the sheet has been cast at the job site and applied directly to the test part.

NOTE: For many beginning practitioners of the PhotoStress method, it may be advantageous to employ the thin Teflon carrier when making a sheet for contouring even if it is not intended to freeze the sheet for later use. By using the carrier, removal of the semi-polymerized sheet from the casting plate is easier, and handling of the sheet in preparation for contouring is more convenient.

PHOTOELASTIC COATING MATERIALS FOR CONTOURING APPLICATION

Resin Type	PL-1	PL-2	PL-3	PL-6	PL-8
Hardener	PLH-1	PLH-2	PLH-3	PLH-6	PLH-8
HANDLING DATA					
Amount of Hardener (pph)	18-20	100	150	70	14
Casting Plate Temperature °F (°C)*	90-110 [32-43]	115-125 [46-52]	125-135 [52-57]	125-135 [52-57]	90-110 [32-43]
Mixing Temperature °F (°C)*	90-110 [32-43]	115-125 [46-52]	125-135 [52-57]	125-135 [52-57]	90-110 [32-43]
Pouring Temperature °F (°C)	125-130 [52-55]	125-135 [52-57]	135-145 [57-63]	125 [50], Typical	125-130 [52-55]
Approximate Time on Casting Plate† to contourable stage (ready to remove from mold and shape)	1.5 hr	2-3 hr	2-3 hr	2.5	2 hr
Time to Complete Polymerization†	18-24 hr	18-24 hr	24 hr	12-18 hr	18-24 hr
FINISHED MATERIAL DATA, TYPICAL (Precise Values Determined by Calibration)					
"K" Factor	0.10	0.02	0.006	0.001	0.08
Modulus of Elasticity, psi [GPa]	0.42(10) ⁶ [2.9]	30,000 [0.27]	2,000 [0.014]††	100 [0.0007]††	0.42(10) ⁶ [2.9]
Maximum Elongation	3-5%	50%	over 50%	>100%	3-5%
Poisson's Ratio	0.36	0.42		0.50	0.36

* Proper selection of the casting plate temperature, and beginning mixing temperature of the resin/hardener combination, will depend on the overall size and thickness of the sheet to be cast. For thick sheets (nominally 0.080 to 0.120 in./2.0 to 3.0 mm), lower temperatures should be selected. For thinner sheets, higher temperatures can be selected. The selection criteria will become more obvious after some experience has been gained.

† Typical for room temperature of 77°F (22°C). Polymerization time is shortened by higher temperature and/or thicker sheets. Thin sheets and lower temperatures lengthen polymerization time.

†† After one minute at constant strain.

CAUTION

Epoxy resins and hardeners may cause dermatitis or other allergic reactions, particularly in sensitive persons. The user is cautioned to: (1) avoid contact with either the resin or hardener; (2) avoid prolonged or repeated breathing of the vapors; (3) use these materials only in well-ventilated areas. If skin contamination occurs, thoroughly wash the contaminated area with soap and water immediately. In case of eye contact, flush immediately and secure medical attention. Rubber gloves and aprons are recommended, and care should be taken not to contaminate working surfaces, tools, container handles, etc. Spills should be cleaned up immediately.

Supplemental instructions for each type of liquid plastic are provided with the liquid plastic package.

Refer to these Bulletins for detailed information on:

TN-704 How to Select Photoelastic Coatings.

S-116 Materials for Photoelastic Coatings and Models.

IB-223 Instructions for Bonding Flat and Contoured Photoelastic Sheets to Test-Part Surfaces.

Photolastic Division • Measurements Group, Inc.

Instruction
Bulletin
IB-221-C

Instructions for Casting and Contouring Photoelastic Sheets

INTRODUCTION

The PhotoStress® method is a very practical and versatile technique for experimental stress analysis. The method is particularly applicable to the complex three-dimensional configurations generally found in actual mechanical equipment, structural members, and machine components. The principal advantage of the PhotoStress method derives from the fact that it is a full-field technique—capable of showing the entire stress distribution over the surface of a part and thus highlighting the regions where the stresses are greatest. The direction of principal stresses, stress magnitudes (tangent to all free boundaries or edges), and maximum shear stresses can be determined quickly and easily. With proper instrumentation, and additional effort, individual principal stresses can be determined at internal locations which are removed from free boundaries or edges. Tech Note TN-702 presents a more complete treatment of the principles of the PhotoStress method.

The application of photoelastic coatings to irregular surfaces is a common requirement. Coatings may be applied by brushing, dipping, or spraying; however, with these methods it is generally impractical to accurately determine the nominal coating thickness. Further, the coating thickness varies markedly with position on the coated part; i.e., coatings in small fillets might be significantly thicker than in areas removed from sharp geometric irregularities. It is also impractical to achieve coating thicknesses sufficient for elastic analysis of many materials.

Knowledge of the coating thickness is necessary if quantitative strain measurements are to be established. The contoured sheet technique, described here, will produce coatings of uniform and measurable thickness for quantitative strain analysis on irregularly shaped parts.

Contouring is accomplished best in a reasonably clean area at ambient temperature between 65°F (18°C) and 85°F (30°C). Precautions should be taken to avoid or minimize:

- direct sunlight or direct radiant heat
- extreme drafts of hot or cold air
- dust or particle contamination
- moisture (rain or direct spray)
- contaminants in general

The techniques of contouring are not very difficult to learn, and the following procedures present an organized approach that will lead to a successful contouring operation. Approaches that are less than thorough can sometimes yield satisfactory results; however, for consistent success, the instructions given here should be followed.

The contouring procedure may be divided into seven principal steps:

1. Preparing the casting plate
2. Preparing the plastic (resin and hardener)
3. Pouring the plastic
4. Polymerization cycle
5. Removing the semi-polymerized sheet from the casting plate
6. Contouring the sheet to the test part surface
7. Removing the cured sheet from the test part.

Photolastic Division
MEASUREMENTS GROUP, INC.
P.O. Box 27777 • Raleigh, NC 27611, USA

Telephone (919) 365-3800
Telex 802-502
FAX (919) 365-3945



©Copyright Measurements Group, Inc., 1982
All Rights Reserved.

Printed in USA
022412GP

In this bulletin, each step is treated individually and a general chronological sequence is implied. All materials and supplies referred to have been carefully selected to produce high-quality contourable photoelastic coatings. They are readily available either in kit form (Figure 1) or as individual items. The contouring procedures described here were developed with respect to these particular materials and substitutions are not recommended. (See Bulletin P-01 for kits and Bulletin S-116 for materials).

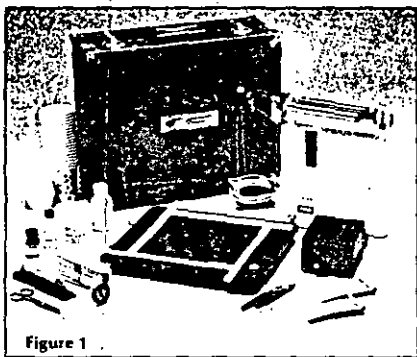


Figure 1

1.0 PREPARING THE CASTING PLATE

1.1 Work Table

Place the Model 012-1H temperature-controlled, Teflon[®]-coated heated casting plate on a rigid table.

1.2 Cleaning and Applying Releasing Agent

Clean the teflon surface with a gauze sponge wetted with isopropyl alcohol or acetone and wipe dry with a clean, dry gauze sponge. Apply a film of releasing agent (Photoelastic Part No. 012-183) to the teflon surface using a clean gauze sponge. The film of releasing agent must be very thin. Any evidence of beading or streaking should be wiped and removed using a clean, dry gauze sponge (Figure 2).

1.3 Leveling the Casting Plate

Carefully level the casting plate in two perpendicular directions with a machinist's level, using the three leveling screws provided (Figure 3). Do not move the casting plate from its leveled position while the cast sheet is curing.

1.4 Preparing and Assembling the Snap-Together Frame

The silicone rubber snap-together frame (Figure 4) should be cleaned, and a thin film of releasing agent applied to the narrow surfaces which will contact the

liquid plastic. Also, apply releasing agent to the bottom surfaces.

Assemble the frame on the teflon surface to the size of the desired sheet. The frame dimensions should be at least 0.25 in (6 mm) larger on all sides than the dimensions of the required sheet. This dimensional increase compensates for the meniscus which forms during polymerization of the liquid plastic. If calibration is required, an additional 1 in (25 mm) should be added to either the length or width. This increase provides for the 1-x-3-in (25-x-76-mm) calibration strip required for use with the Model 010 Calibrator. Recheck the level of the plate, as in Section 1.3, after assembling the snap-together frame.

1.5 Covering

Cover the plate with the plexiglas cover. This protects the prepared surface from dust and other contaminants.

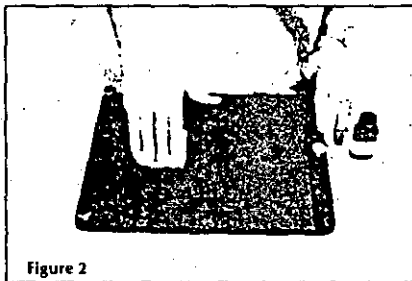


Figure 2

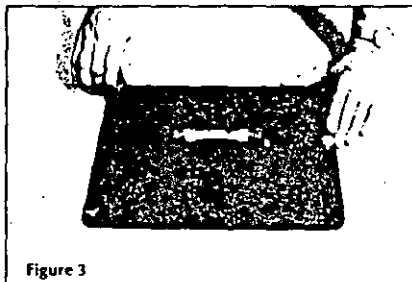


Figure 3

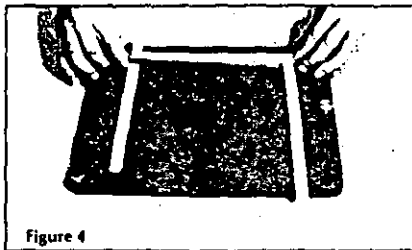


Figure 4

1.6 Warming the Casting Plate

During the casting process, the temperature of the casting plate is a critical factor in the production of high-quality contourable plastic sheets. For optimum results, the casting plate should be heated to within a prescribed temperature range (varying with the type of photoelastic plastic in use) prior to pouring the resin. Preheating to the specified temperature aids the flow-out of the resin on the casting plate, reduces humidity effects during curing, and significantly improves the surface quality of the cast sheet for contouring.

The new Model 012-1H Casting Plate, with its integral surface heater and thermostatic control, provides a uniform and closely regulated temperature over the entire plate area.

To warm the casting plate, proceed as follows: (see Figure 5)

1. Set voltage selector on the controller to the appropriate power (115 or 230 volts, 50/60 cycle).
2. Set the controller power switch to OFF.
3. Plug temperature sensor from the casting plate into the controller.
4. Plug heated casting plate power cord into controller.
5. Connect controller input power cord to proper voltage source.
6. Set the temperature control switch on the controller to the desired casting plate temperature for the particular photoelastic plastic being used. (See Coating Materials Chart on page 12 for recommended temperatures.)
7. Set the controller power switch to ON.
8. As the temperature of the casting plate begins to rise the heater indicator light will be illuminated.

until the set temperature has been reached. The heater light will then "blink" on and off as the pre-set casting plate temperature is being maintained.

2.0 PREPARING THE PLASTIC

If the resin and/or hardener were kept refrigerated, bring them to room temperature prior to opening the container. If the hardener was not refrigerated* and/or has been stored for extended periods, it is important to check its appearance. If the hardener is cloudy or contains foreign particles, discard in favor of a new bottle free of such impurities.

After removal from cold storage, the hardener (and resin) may be brought to room temperature with a heat lamp, or by placing on the surface of the heated casting plate. The lid should be loosened but not removed. Keeping the lid on during warm-up is necessary to avoid humidity condensation.

2.1 Determining Amount of Resin and Hardener

Calculate the amount of resin and hardener required. The total amount (weight) of plastic is determined by:

$$W = d \times A \times t$$

W = total amount needed (in grams)
d = plastic density, 18.5 gm/in³ (1.13 gm/cm³)
A = area of sheet to be cast (width x length)
t = desired thickness

Example: For a sheet 7 W x 8 L and 0.10 t in (180 x 200 x 2.50 mm), the total amount of plastic required is:

$$W = 18.5 \times 8 \times 7 \times 0.10 = 104 \text{ gm}$$

$$[W = 1.13(10)^3 \times 180 \times 200 \times 2.50 = 102 \text{ gm}]$$

*Hardener should be stored at 40°F (5°C).

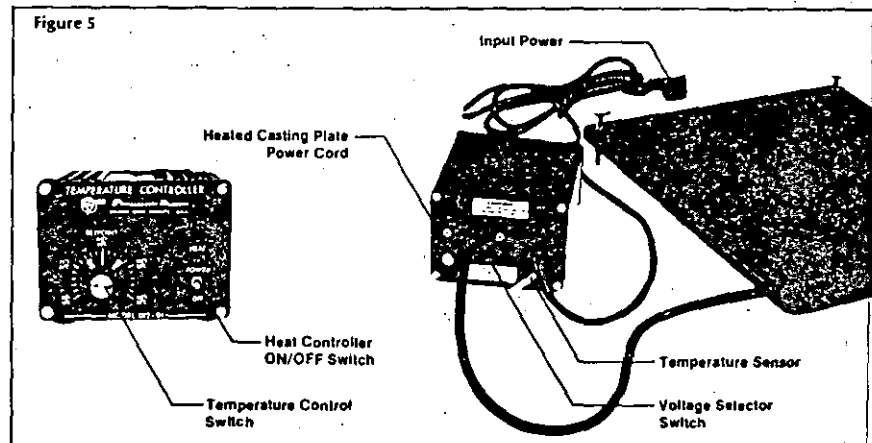


Figure 5

The amount of hardener is indicated in "parts per hundred" or "pph". For example, 20 pph of hardener means 20 grams of hardener for 100 grams of resin. Refer first to the Coating Materials Chart on page 12 to determine the proper proportion of hardener to resin. Then, continuing with the above example on page 3, for a total of 104 grams of Type PL-1 plastic, the resin and hardener calculations are made as follows:

$$\text{Resin: } 104 \times \frac{100}{120} = 86.7 \text{ gm}$$

$$\text{Hardener: } 104 \times \frac{20}{120} = 17.3 \text{ gm}$$

104 gm Total

2.2 Weighing the Resin and Hardener

Take an adequate size mixing cup and weigh out the needed amount of resin on a balance scale, such as the Photolastic Model 012-20. Remember to account for the weight of the mixing cup when weighing (see Figure 6). Six-ounce plastic coated cups are recommended for mixing the resin and hardener. Avoid using uncoated or wax-coated paper cups and shallow, large diameter containers. The proper amount of hardener can be preweighed, or it can be added to the preweighed resin as described in Section 2.4

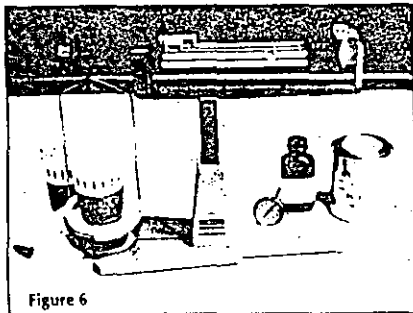


Figure 6

Plastic kits (80 gm), where the proper amounts of both resin and hardener have been preweighed, are available. In cases where 80 grams of plastic is sufficient for the sheet size required, the preweighed kits are both time saving and convenient.

2.3 Warming the Resin and Hardener

Prior to adding the hardener to the resin, warm the resin and hardener to the temperature indicated in the Coating Materials Chart on page 12. Intermittent, gentle stirring with a stem thermometer will help to maintain uniform resin temperature during warming. Warming the resin lowers its viscosity and facilitates a more uniform mix with the hardener. Warming can be accomplished by placing the resin-hardener containers on the surface of the Heated Casting Plate, or with a heat lamp.

2.4 Adding the Hardener to the Resin

Pour the hardener into the resin, being careful to avoid introduction of air bubbles during pouring. When mixing 80-gram preweighed kits, add all of the hardener to the resin container (Figure 7). When the hardener has not been preweighed in a separate container, the hardener can be measured by pouring it directly into the resin-filled cup while the cup is on the scale. In this case, the scale should be set to the total weight (cup + resin + hardener), and hardener added until the scale balances. The hardener will flow evenly on the top of the resin. If excess hardener is accidentally added, it can be conveniently withdrawn with a medicine dropper, or the excess can be absorbed using a paper towel or gauze sponge.

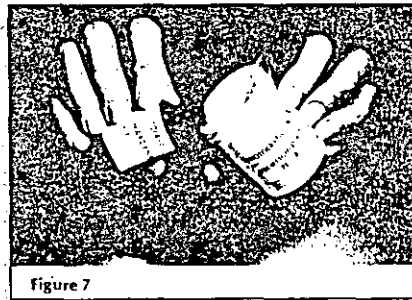


Figure 7

2.5 Mixing the Hardener and Resin

Mixing the resin and hardener is a very important step in obtaining a quality contoured sheet. It is essential to stir thoroughly but slowly. Do not use a whipping action which will introduce air bubbles. Stirring to produce a clear, non-streaking mixture is best accomplished using the technique illustrated in Figure 8. Nonuniform mixing will most likely occur at the inside surfaces of the mixing container. The stem thermometer (Part No. 0126) should be brought into line contact with the sides of the container several times during mixing. Line contact should be maintained while making several passes around the

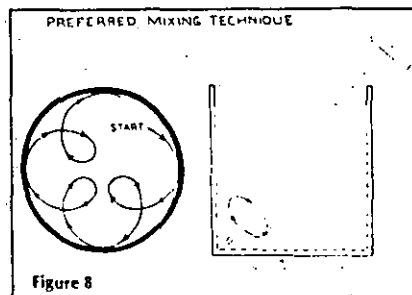


Figure 8

inside of the container. The temperature increase, produced by the exothermic chemical reaction during mixing, is easily observed on the stem thermometer (Figure 9). Continue stirring until the pouring temperature is obtained (see Coating Materials Chart on page 12 for correct pouring temperatures). The mixed plastic is now ready to be poured onto the previously prepared casting plate.

Note: Immediately prior to pouring the mixed plastic, set the temperature control switch on the casting plate heat controller to the OFF position.

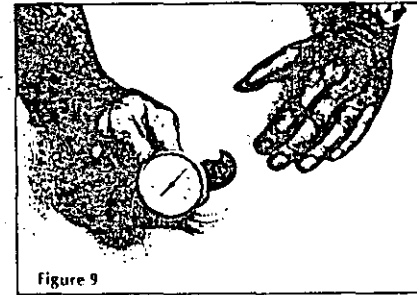


Figure 9

3.0 POURING THE PLASTIC

3.1 Pouring

Remove the cover from the casting plate and pour the plastic. When pouring, hold the mixing cup close to the casting plate surface and pour gently (Figure 10). This procedure will minimize bubble formation. While

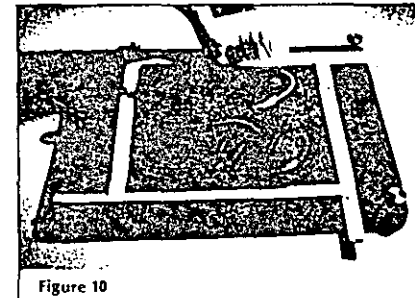


Figure 10

pouring, it is advisable to move the cup to form an "X" or "S" pattern which will improve flow to fill the mold. This is particularly advantageous when pouring thinner sheets (0.065 in (1.5 mm) or less). Thin sheets do not flow out and cover the casting plate as freely as thicker sheets. The final portion of the plastic should be poured along the outside boundary close to the frame.

DO NOT scrape excess plastic from the cup sides and bottom onto the casting plate. These are areas where a nonuniform mix is most likely to occur. The stem thermometer or a wooden tongue depressor (Figure 11) may be used to help spread the plastic over the entire plate surface (the liquid will level with time). Place the cover over the poured sheet to protect it from dust and other foreign matter during polymerization.

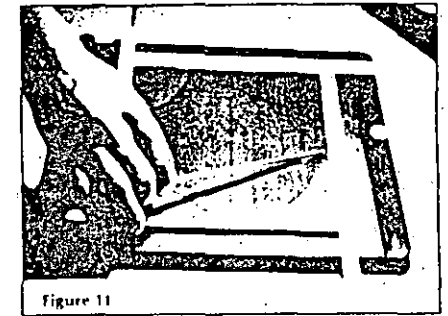


Figure 11

3.2 Bubble Removal

Wait several minutes for air bubbles, when present, to rise to the surface and burst. Surface bubbles which remain can be burst using a pointed scribe or dental probe. A medicine dropper can be used to vacuum air bubbles which might remain at the bottom of the sheet. Replace the cover.

4.0 POLYMERIZATION CYCLE

The liquid plastic will pass through several steps before arriving at the desired semi-polymerized condition for contouring. At the contouring stage it is semi-stable, but also highly flexible and formable. It has no geometric or photoelastic memory and can be readily contoured to conform to both simple and compound curved surfaces. The time span to reach this contourable state is dependent upon the:

- ambient room temperature
- casting plate temperature
- type of plastic
- thickness
- plastic temperature when poured onto the casting plate.

These parameters make it impractical to accurately predict the time span between pouring and removal of the sheet from the casting plate. However, guidelines do exist which make it possible to recognize when the sheet is ready for contouring. The time span is shortened with higher temperatures and/or thicker sheets; and is longer at lower temperatures and when casting thinner sheets. Information in the following table is typical when casting the more widely used Type PL-1 and PL-8 liquid plastics.

Conditions	PL-1	PL-8
Room Temperature	72°F (22°C)	72°F (22°C)
Casting Plate Temperature	100°F (38°C)	100°F (38°C)
Plastic Temperature When Poured	125°F (52°C)	125°F (52°C)
Sheet Thickness	0.090 in (2.3 mm)	0.10 in (2.5 mm)
Time Until Contourable	2 hr (typical)	2-1/2 hr (typical)

The following sections present a chronological sequence of the different states of polymerization leading to the time when the semi-polymerized sheet is ready for contouring.

4.1 Early Stage of Polymerization

Figure 12 shows the early stage of polymerization, with the plastic in a viscous liquid state. When probed, the plastic still behaves as a liquid. It adheres to the probe and a viscous string of plastic can be pulled up with the probe.

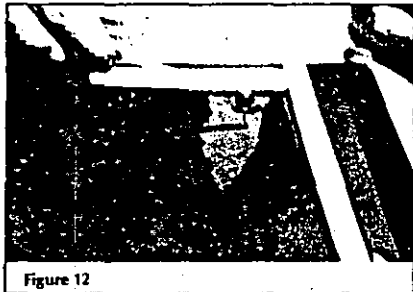


Figure 12

4.2 Second Stage of Polymerization

The plastic is no longer liquid but adheres to the probe. The surface is easily deformed with little or no pressure on the probe and feels very sticky to the touch (Figure 13).

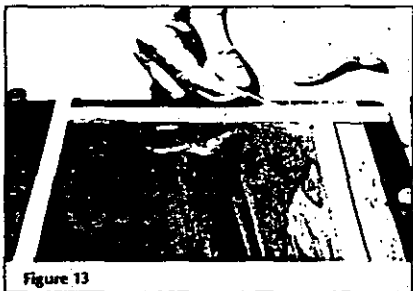


Figure 13

4.3 Approaching the Contourable Stage

The plastic can be depressed with light-to-moderate pressure on the probe. A corner of the snap-together frame can be removed with some difficulty but the edges of the sheet will remain square with no tendency to flow onto the casting plate. The corner can be raised using a quick snap-like finger action. The underside will feel slightly sticky to the touch. (If cut with scissors, the plastic tends to stick to the cutting edge and weld itself back together after cutting.) Left unsupported, the corner folds quickly back to the surface of the casting plate (Figure 14).



Figure 14

4.4 Optimum Stage for Contouring

The plastic can be depressed with moderate pressure on the probe. A corner of the sheet can be picked up easily from the mold, with little or no stretching. The plastic underside feels dry to the touch. The sheet can also be cut easily with scissors, without sticking to the cutting edge. The plastic at this time is flexible, mechanically stable, and in an ideal condition for contouring.

5.0 REMOVING THE SEMI-POLYMERIZED SHEET FROM THE CASTING PLATE

The surface of the test part should be prepared well in advance of sheet removal for contouring. All foreign matter such as paint, scale, rust, oxides, weld splatter, etc. must be removed (see Bulletin IB-223). Surface preparation prior to contouring consists of first degreasing and cleaning the surface with acceptable solvents; and second, applying mineral oil to the cleaned surface.

5.1 Snap-Together Frame Removal

Remove the silicone rubber frame from around the plastic (see Figure 15). If the frame does not release easily, the plastic is not yet ready for contouring.

5.2 Apply Mineral Oil

Lubricate both hands, scissor blades, and the surface of the part with mineral oil. Mineral oil should be applied to the top surface of the sheet as well. Do not press on or deform the sheet when spreading the mineral oil.

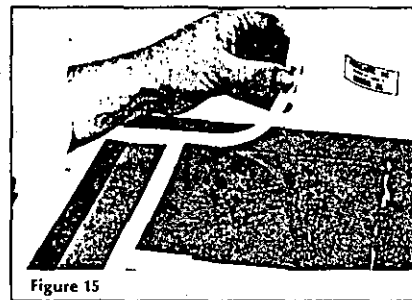


Figure 15

5.3 Lifting the Sheet

Lift one corner of the sheet using a flicking action with a finger (see Figure 16). Lift an area large enough to allow grasping between the thumb and fingers. Remove the entire sheet using a continuous, quick, smooth lifting motion as illustrated in Figure 17. Holding the casting plate is not normally required and many operators prefer to first lift two corners and then remove the sheet using two hands. In any case, the same lifting motion is required. Do not use a slow steady pull. This will cause stretching and produce unnecessary changes in sheet thickness. Invert the sheet and place it top side down on the casting plate. Now apply mineral oil to this side (bottom as cast) of the sheet.

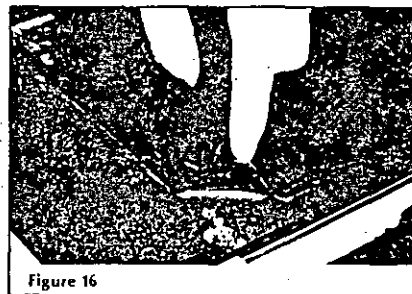


Figure 16

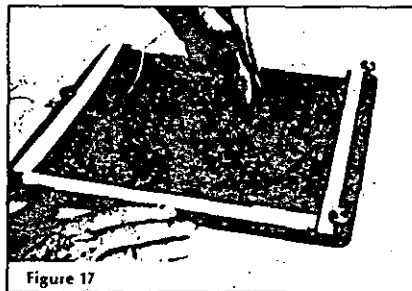


Figure 17

5.4 Cutting the Meniscus and Calibration Strip

Use sharp, lubricated scissors to cut off a 0.25-in (6-mm) border around the entire edge of the sheet. The thicker edge meniscus is contained along the border and should normally be discarded.

If calibration is required, cut a strip approximately 1 x 3 in (25 x 76 mm) from the sheet and place it flat on the casting plate as shown in Figure 18.

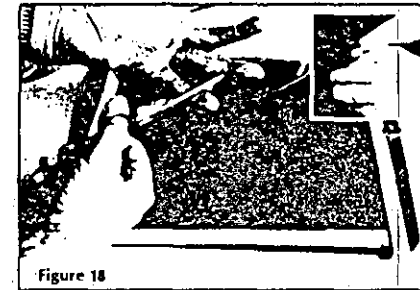


Figure 18

6.0 CONTOURING

It will be necessary to cut the sheet into smaller pieces when separate areas of the part are to be coated with plastic taken from a single sheet. Smaller pieces may also be needed if the part is very complex and irregularly shaped. Place the sheet on the part with the original (top) surface in contact with the test part. This is important because the bottom surface was in contact with the releasing agent on the casting plate, and it is desirable that the opposite (top) surface be in contact with the test part for eventual bonding.

When the part to be coated is not very complex (Figure 19), it is convenient to bring one edge of the sheet in contact with the part, and then gently and progressively contour the sheet to the remaining surface. Contouring is accomplished using a rather rapid stroking or light rubbing motion with the finger tips, working the plastic

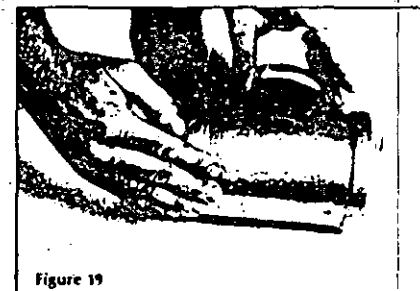


Figure 19

gently into place. If air pockets form under the plastic while contouring, lift the plastic in that area, add a little more mineral oil, if needed, and progressively contour a second time. The plastic, where contact has not yet been made on the test part, should be hand supported in a manner to negate sagging under its own weight. Do not press, push, or stretch the plastic into place. This will cause undesired changes in thickness. Small air pockets and localized "ponds" of mineral oil can be chased from beneath the plastic, for escape at the boundaries, by rapid stroking with the finger tips. Contouring soft sheets can be thought of as a supporting (lifting), folding, feeding, and stroking procedure.

Figure 20 shows a 10-x-10-in (254-x-254 mm) sheet which has been positioned for contouring over a complex casting. If the sheet were left unattended, it would stretch and sag under its own weight, tending to form into the unsupported areas and produce undesirable changes in thickness. Once the sheet has been roughly positioned, the operator should move quickly to the outside corner (front foreground of Figure 20), lift it and then gently feed and fold it inward toward the part. Rapid stroking with the finger tips must accompany the feeding and folding. As before, entrapped air or excess mineral oil can be chased to the outside by first lifting the plastic and then reforming in those areas.

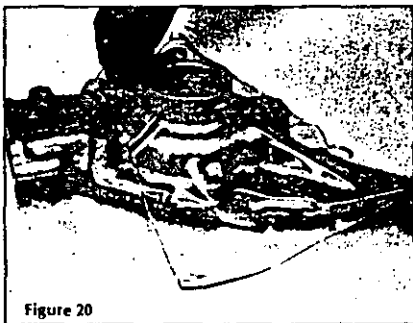


Figure 20

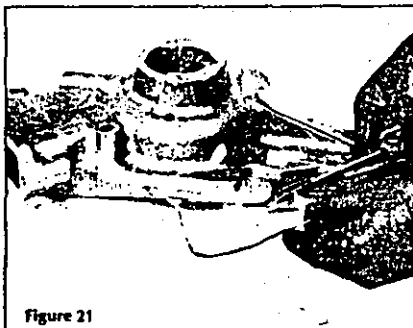


Figure 21

When contouring has been accomplished, the unused portion of plastic can be trimmed, as in Figure 21, to roughly match the boundary of the part. Final trimming can be accomplished after the plastic has fully polymerized using the methods and tools described in Bulletin IB-223. It should be recognized that some applications (Figures 20 and 21) may not require removal of a calibration sample before contouring, since there will be sufficient material left over to obtain the sample.

Note: The working time available for contouring the plastic after removal from the mold is approximately 10 to 20 minutes. After this time, the plastic will begin to get stiff, making it more difficult to manipulate and cut with scissors. After contouring has been completed, the formed sheet will retain its shape while final polymerization takes place. If the plastic has been contoured to a vertical or overhead surface, it may be necessary to mechanically hold it in place for complete cure. If so, this may be done with a few pieces of pressure sensitive tape. However, under no circumstances should the plastic be subjected to a clamping-type pressure. Clamping will introduce undesired birefringence in the plastic which will be retained after full polymerization.

6.1 Junctures Between Adjacent Sheet

Figure 22 illustrates the condition where a contoured sheet on the right is being applied and lapped over a previously applied adjacent sheet on the left. The edge of the adjacent sheet has been cut straight and crosses the fillets at a right angle.

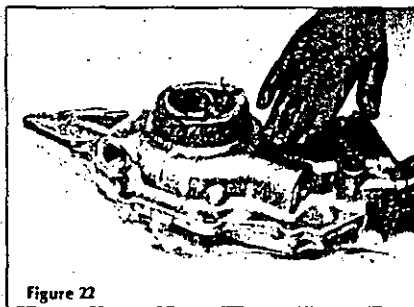


Figure 22

When the second sheet (right) has been contoured and properly cleared of entrapped air, etc., it is convenient to lift the overlap and carefully cut it to fit the pre-cut edge of the adjacent sheet (see Figure 23).

This procedure is normally followed when several pieces of plastic are needed to cover large areas, or when the surface to be coated is extremely complex. For complex parts, it is desirable, or necessary, to work with several smaller pieces rather than one or two large sheets. (See Bulletin IB-223 for additional technical considerations.)

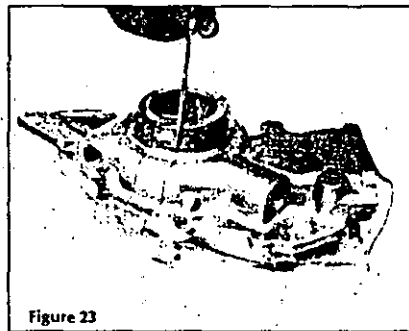


Figure 23

6.2 Final Polymerization

After the plastic has been contoured to the shape of the test part, it must be allowed to continue its polymerization cycle to full cure for an additional 18 hours or longer before removing it for trimming, cleaning and eventual bonding. At the end of this 18-hour period, or anytime thereafter, the plastic will be hard, and of the same size and shape as the surface of the test part.

7.0 REMOVING THE CURED SHEET FROM THE PART

The hardened sheets can be removed by carefully raising one edge or corner. This breaks the surface adhesion introduced by the mineral oil and the sheet will lift off freely. The sheet is then ready for final preparation for bonding in accordance with the instructions in Bulletin IB-223. Figure 24 shows the final results of the contoured sheet first illustrated in Figure 20.

"It sometimes happens that a contoured sheet, after hardening, has captured itself on the part and cannot be removed without some mechanical assistance. In many instances, release can be accomplished by simply filing or sanding edges of the plastic which have inadvertently been shaped around the edge of the part, locking it in place. In more extreme cases, the captured sheet may need to be cut into two or more sections before it releases. Small hand-held routers with fine point-shaped cutters are convenient for separating the captured sheet."

8.0 CONTOURING SHEETS TO LARGE AREAS

The preparation and contouring of a single photoelastic sheet as described herein is usually accomplished in a

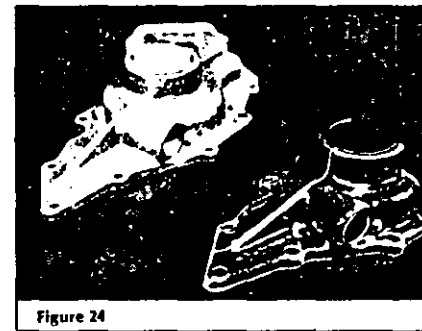


Figure 24

few hours of work [typical size 10 x 10 x 0.10 in thick (254 x 254 x 2.5 mm)].

On large structures, when several sheets are required, a carefully planned schedule must be outlined, not only for reasons of economy, but to ensure consistency of quality and calibration. The most essential steps leading to good results when casting multiple sheets are:

1. The liquid resin should be preweighed, preferably in identical containers, and stored in a drying oven until ready for mixing.
2. Sheets should be cast from the same lot material to a uniform size, allowing excess material for trimming. Maintaining casting uniformity helps with the efficient scheduling of work and provides for consistency in quality. Controlling the liquid level in the mixing container and careful monitoring of the speed of polymerization (time to harden) can eliminate potential casting problems.
3. A work station should contain three to five casting plates, and pouring and removing of the contourable sheets should be scheduled at fixed time intervals. This procedure will allow at least six sheets per work day. (See Chart on following page for typical work schedule.)
4. The coating should be contoured according to a planned pattern on the test part, providing for trim lines and a proper work-flow sequence. Sheets contoured on the first day should be trimmed for cementing on the next day.
5. Before cementing, scribing lines on the coating will help identify points of measurement and provide a means of reference for data-acquisition organization. Thickness measurements should also be performed before cementing. It is generally more advantageous to perform the cementing operation after all sheets are completed and all traces of oil and releasing agent are removed.

APPLICATION OF PHOTOELASTIC COATINGS TO LARGE AREAS—TYPICAL WORK SCHEDULE				
Time	Day 1	Day 2	Day 3	Day 4
8 AM	Weighing of resin & hardener	Remove & inspect #1 to #6	Remove & inspect #7, #8, #9	Remove & inspect #10, #11, #12
9	Mixing & pouring sheets #1, #2, #3, (at 15 to 20 minute intervals)	Mixing & pouring sheets #7, #8, #9	Mixing & pouring sheets #10, #11, #12	Finishing #10, #11, #12. Complete cleaning
10				
11	Contouring #1, #2, & #3 in preplanned locations.	Contouring #7, #8, #9	Contouring #10, #11, #12	Cementing of sheets to test part
12				
1 PM	Mixing and pouring sheets #4, #5, #6	Finishing #1 to #6 (making parting lines, scribing reference lines, measuring thickness)	Finishing #7, #8, #9	Cementing of sheets to test part
2			Surface preparation of test part for cementing	
3	Contouring #4, #5, #6			
4				

TEST PART

TYPICAL MATERIAL SPECIFICATION

All Sheets: 8 x 8 x 0.080 in
(200 x 200 x 2 mm)

Plastic Type: PL-8

Adhesive: PC-1

Sheet Placement Order: See illustration at left

9.0 MAKING FROZEN SHEETS FOR CONTOURING

As described in the previous sections of this Instruction Bulletin, the normal practice in using the PhotoStress method is to cast sheets of plastic directly at the test site, conveniently adjacent to the structure or part being stress-analyzed. When each sheet reaches the appropriate stage of polymerization at which it can be easily handled and formed, it is immediately contoured to the surface of the part, where polymerization continues until the coating has hardened.

There are occasions, however, when the standard procedure is inconvenient, or impractical, or not feasible at all. An outdoor test site, for instance, can sometimes cause severe problems in producing consistently high-quality sheets of plastic. If the test area is dusty, or the temperature below about 60°F (15°C), or the humidity very high, the quality and uniformity of the cast sheets may be degraded accordingly. In general, on-site casting of the sheets, whether indoors or outdoors, can often involve rather poor working conditions (dirt, noise, contaminating vapors, low lighting levels, inadequate work space, etc.) which are detrimental to the relatively delicate task of sheet casting.

In these and a variety of other cases, it would be preferable to cast the sheets in a clean, room-temperature laboratory environment; and then, at a convenient time, take the sheets to the test site and contour them to the workpiece. But the polymerization process continues during this period, and sheets will shortly become too rigid for contouring. An attractive alternative is to arrest the polymerization at the contourable stage and hold the sheets in that condition until they are needed. This can be done by removing the plastic sheet from the casting plate as soon as it reaches the contourable stage and quickly freezing at 0°F (-18°C). The plastic can be stored in the frozen state for later use up to 4 weeks at 0°F (-18°C), and for longer periods if stored at -40°F (-40°C) or below. When the plastic is removed from the freezer and brought back to room temperature, it will again be conformable for contouring, and the polymerization will continue until the sheet hardens. If the test site is remote from the freezer, the plastic can be transported to the workplace in a well-insulated container kept refrigerated with dry ice.

The frozen-sheet technique is advantageous in many industrial stress analysis applications. A typical example is the requirement to coat large areas of a structure which is outdoors or in an otherwise uncontrolled environ-

ment. The necessary number of frozen sheets can first be prepared in the laboratory and stored in the freezer until needed. When it is appropriate to apply the coating, the frozen sheets can be delivered to the test site, warmed to room temperature, and contoured in the usual manner. This procedure helps ensure consistency of quality and calibration from sheet to sheet. It also allows the structure to be coated much more rapidly than would be possible if the sheets had to be cast at the test site before contouring. The latter consideration may be the determining factor when the structure is in regular use or is otherwise inaccessible to the stress analyst except for short periods of time.

Numerous other examples can be cited; but, in general, the frozen-sheet technique adds another degree of freedom to the PhotoStress method. No special equipment is required to use the technique, since any conventional freezer will suffice for storing the frozen sheets. Laboratories working regularly with PhotoStress may even find it desirable to maintain a stock of frozen sheets for ready availability as the need arises.

9.1 Casting Procedure for Frozen Sheets

In most respects, preparation of the casting plate to receive the liquid resin is identical to that described in Section 1.0. When making a frozen sheet, however, the casting plate is initially covered with a thin sheet of Teflon (Part No. 012-190) to serve as a carrier for transporting the sheet to the freezer when it reaches the contourable stage. The carrier sheet is first placed over the casting plate, and carefully smoothed out (Figure 25). Then, the silicone rubber snap-together mold frame is assembled on top of the carrier sheet. Finally, with the resin and casting plate at the proper temperatures, the resin is poured into the mold as usual (Figure 26).

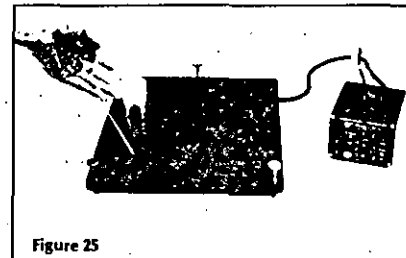


Figure 25

9.2 Preparation of the Contourable Sheet for Long-Term Storage

As soon as the cast sheet has reached the contourable stage, remove the snap-together mold frame, and pick up the sheet on its carrier (Figure 27). Place it im-

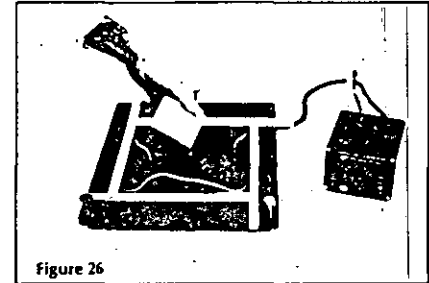


Figure 26

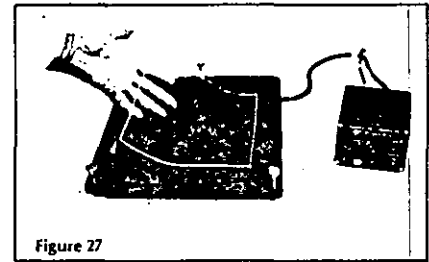


Figure 27

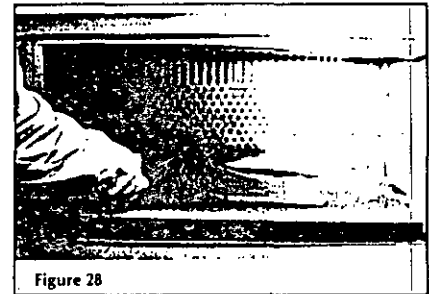


Figure 28

mediately in the freezer at 0°F (-18°C), making certain that the sheet lies flat (Figure 28). After two hours or so, when the sheet is frozen sufficiently for easy handling, remove it from the freezer and strip away the carrier. Next, place the frozen sheet between two pieces of waxed paper that have been lightly coated with mineral oil to prevent adhesion to the plastic. Promptly return the sheet (now sandwiched in waxed paper) to the freezer. The plastic sheet should not be kept out of the freezer for more than a few minutes in this final step of preparing it for long-term storage.

Summarizing the overall procedure for determining individual principal stresses by the PhotoStress/Separator-Gage Method, the basic steps are as follows:

1. Apply the appropriate PhotoStress coating to the test object, following the instructions for the selected type of photoelastic plastic.

Note: The PhotoStress Separator Gage is intended for use only with "high-modulus" coating materials (Types PS-1, PS-2, PS-8, PL-1, PL-8). It should not be used with medium- or low-modulus coatings.

2. Load the coated test object, and generally examine the fringe pattern with the Model 031 Reflection Polaroscope to identify significant or potentially critical areas.
3. Make accurate fringe-order measurements at all points of interest, numbering each point, and marking the location on the coating for subsequent reference.
4. If photographs of the photoelastic fringe pattern are desired, they should be made at this time.
5. Remove the load from the test object, and install PhotoStress Separator Gages (which can be arbitrarily oriented) at points where stress separation is required.
6. Connect Separator Gages to the four-channel Model 330 Interface, using 3-wire circuits in each case.
7. Connect the Model 330 output terminals to the corresponding input terminals of the Model P-3500 Static Strain Indicator. Set the gage-factor control of the strain indicator to the effective gage factor of the PhotoStress Separator Gages as specified on the accompanying technical data sheet.

Use the channel selector switch and balance controls on the Interface to establish initial balance for all gages.

8. Reapply the same test load, and use the channel selector switch of the Interface Module to successively read the indicated strains on all gages.
9. Review Figs. 5 and 6 of this Tech Note to judge whether correction for reinforcement or strain extrapolation is necessary. When correction is required, the appropriate correction factors can be read directly from the figures for coating Types PS-2, PS-8, PL-1, PL-8, and PS-1.
10. Substitute the fringe-order and strain data (corrected as necessary) into Eqs. (10) and (11) to calculate the principal strains.
11. Substitute the principal strains into Eqs. (16) and (17) to determine the principal stresses.

Although not described in detail here, the procedures for installing PhotoStress Separator Gages on the PhotoStress coating are essentially the same as for any other strain gage (having preattached leads) under the same circumstances. As a rule, gages can be bonded to the plastic coating most easily and quickly with M-Bond 200 (cyanoacrylate) adhesive. For detailed instructions on applying PhotoStress Separator Gages, refer to Photolastic Division Instruction Bulletin IB-237, *PhotoStress Separator Gage Installations with M-Bond 200 Adhesive*.

If questions or problems arise in applying this method of principal stress separation, users should contact the Measurements Group Applications Engineering Department.

References

1. "Introduction to Stress Analysis by the PhotoStress Method", Measurements Group Tech Note TN-702, Measurements Group, Inc., Raleigh, North Carolina.
2. Zandman, F., S. Redner, and J.W. Dally, *Photoelastic Coatings*, Society for Experimental Mechanics, Bethel, Connecticut.
3. *Strain Measurement with the 030-Series Reflection Polaroscope*, Measurements Group, Inc., Raleigh, North Carolina.
4. "Corrections to Photoelastic Fringe Order Measurements", Measurements Group Tech Note TN-706, Measurements Group, Inc., Raleigh, North Carolina.
5. Zandman, F., S. Redner, and E. Riegner, "Reinforcing Effect of Birefringent Coatings", Proceedings, SESA, 19, 1, pp. 55-64, Society for Experimental Mechanics, Bethel, Connecticut.
6. "Photoelastic Materials — Coatings/Models", Photolastic Bulletin S-116, Measurements Group, Inc., Raleigh, North Carolina.
7. Nickola, W.E., "A Summation Strain Gage — Alternative to Oblique Incidence in Photoelastic Coatings," *Proc. 1986 SEM Spring Conference on Experimental Mechanics*, Society for Experimental Mechanics, Bethel, Connecticut 1986.

MEASUREMENTS GROUP

TECH NOTE

TN-708-1

PhotoStress
Measurements

Principal Stress Separation in PhotoStress® Measurements

1.0 Introduction

In addition to its unique capability as a full-field technique for visualizing stress distribution, the PhotoStress method provides quantitative stress measurement at any selected point or points on the coated surface of the test object. In common with conventional transmission photoelasticity, the basic measurement is ordinarily made with the light directed perpendicular to the surface of the photoelastic plastic (referred to as *normal incidence*). When made in this manner, the measurement yields the difference of principal strains in the coating.

At interior locations, removed from a free edge, the stress state is commonly biaxial; and it is sometimes necessary to determine the separate principal stresses, as well as their difference. In the past, the usual method of accomplishing this was to perform a second, independent, photoelastic measurement at the test point, using the Model 033 Oblique-Incidence Adapter with the Model 031 Reflection Polaroscope.^{1,2,3} Considerable skill is required, however, to make reasonably accurate measurements under oblique incidence. In addition to its other practical limitations, the oblique-incidence adapter is sometimes rendered inoperable due to mechanical interference with projecting features of the part surface.

This Tech Note describes a new method of making the required additional measurement for determining the separate principal stresses from the photoelastically derived stress difference. The procedure uses a specially designed strain gage (*stress-separator gage*) which is applied to the coating surface after the normal-incidence reading has been made. Practical experience with the new method demonstrates that it offers several advantages over oblique-incidence measurements. It is quick, easy to use, and it completely eliminates the need for highly developed photoelastic skills. In most cases, it is also more accurate than oblique-incidence determinations.

2.0 Measurements of $\sigma_1 - \sigma_2$ with PhotoStress

The basic relationship for strain measurement in a photoelastic coating can be expressed as follows:

$$\epsilon_1 - \epsilon_2 = N_n \lambda / 2t \quad (1)$$

or,

$$\epsilon_1 - \epsilon_2 = N_n f \quad (2)$$

where: ϵ_1, ϵ_2 = principal strains in coating

N_n = normal-incidence fringe order

λ = wavelength of yellow light
(22.7 μ m, or 575 nm)

t = thickness of PhotoStress coating

k = strain-optic coefficient of coating

$f = \lambda / 2t =$ fringe value of coating

Assuming the strains in the coating precisely replicate those in the test-part surface, and assuming the part is stressed below its proportional limit, Hooke's law can be applied as follows to determine the difference of principal stresses:

$$\sigma_1 - \sigma_2 = \frac{E}{1 + \nu} (\epsilon_1 - \epsilon_2) \quad (3)$$

where: σ_1, σ_2 = principal stresses in test part

E = elastic modulus of test material

ν = Poisson's ratio of test material

The preceding relationships implicitly assume that the strains in the test part are unaffected by the presence of the bonded photoelastic coating, and that the strains in the coating are uniform through the coating thickness and equal to those in the surface of the test part. These assumptions are quite well satisfied for typical metal castings, forgings, and robust structural members, since the coating is much lower in elastic mod-



MEASUREMENTS GROUP, INC.
P.O. Box 27777
Raleigh, North Carolina 27611, USA

(919) 385-3800
Telex 802-502
FAX (919) 385-3945

ulus, and is usually thin compared to the section depth of the test part. However, with low-modulus test materials and/or thin sections, corrections for reinforcement effects and nonuniform strain in the coating may be necessary. Procedures for making such corrections are given in a later section of this Tech Note.

3.0 Principal Stress Separation with Strain Gages

Although the resistance strain gage does not offer a practical alternative to PhotoStress as a means for full-field stress analysis, there are several ways in which the strain gage can serve as a very useful adjunct to the photoelastic coatings method. One possibility, for example, is to use PhotoStress purely for the purpose of locating the most highly stressed points on the test part. A strain gage rosette can then be installed at each such point on an identical uncoated part (or on the same part, after removing the coating) to determine the complete strain state, from which the separate principal stresses can be calculated. This procedure is rarely practiced, however, since it discards the quantitative data carried by the photoelastic fringe pattern. It also creates uncertainties in the accuracy of the rosette locations.

An alternative method is to install conventional strain gage rosettes directly on the photoelastic coating at each point of interest. While conceptually simple, this technique involves a number of practical problems, and also introduces strain-measurement errors which cannot readily be quantified or corrected. The presence of the rosette, for instance, causes local reinforcement of the photoelastic coating, with the result that the strain indications tend to be too low. The degree of reinforcement is not definable, or subject to generalization, since the stiffness of the rosette varies with the gage construction, foil and backing thicknesses, grid and solder tab geometry, etc. Because the photoelastic plastic on which the gage is mounted is very low in thermal conductivity, there will also be problems with drift and instability of strain indication due to self-heating effects, unless extremely low gage-excitation voltage is employed. For many commercial strain indicators, this may be difficult to accomplish without introducing still other errors. These and similar problems arise primarily because neither the conventional rosette nor standard strain gage instrumentation is designed specifically for this highly specialized type of service. Perhaps of greatest importance in many practical cases would be the rather tedious task of reducing data from a number of strain gage rosettes, especially since the photoelastic analysis has already provided most of the necessary information.

The foregoing considerations suggest the possibility of developing a special-purpose strain gage, and circuitry, dedicated exclusively to the task of principal stress separation on PhotoStress coatings. With such an approach, the full capability of modern strain gage technology can be brought to bear in tailoring the gage parameters for optimum performance and ease of use in this single class of applications.

Gage construction details, for example, can be selected to minimize local reinforcement effects when installed on photoelastic plastic. Moreover, the residual reinforcement error can be entirely eliminated by calibrating the gage for its effective gage factor when installed on standard PhotoStress coatings. Other desirable characteristics such as preattached leads can similarly be built into the design to temper the inaccuracies and application problems commonly associated with the use of strain gages on plastics. Finally, the grid can be specially configured to produce an output which greatly simplifies data

reduction in calculating the separate principal stresses. All of the above features have been incorporated in a new special-purpose strain gage and instrument interface described in the following sections.

4.0 The PhotoStress Separator Gage

As noted earlier, a normal-incidence photoelastic measurement on the PhotoStress coating provides the difference in principal strains at the test point. If the sum of the principal strains can be measured at the same point, then the separate principal strains are obtainable by simply adding and subtracting the two measurements. It is evident from Mohr's circle of strain (Fig. 1) that the center of the circle corresponds to $(\epsilon_1 + \epsilon_2)/2$, where ϵ_1 and ϵ_2 are the principal strains. However, the center also corresponds to $(\epsilon_x + \epsilon_y)/2$, where ϵ_x and ϵ_y are the normal strains in any two perpendicular directions. Thus, for any point P on the coating surface (Fig. 2), the sum $\epsilon_x + \epsilon_y$ is constant, independent of the angle β , and equal to the sum $\epsilon_1 + \epsilon_2$. As a result, it is not necessary to measure the sum of the principal strains as such, but only the sum of any two perpendicular strains.

The PhotoStress Separator Gage is based on this fundamental principle of mechanics. As shown in Fig. 2, the gage grid consists of two perpendicular elements (for sensing ϵ_x and ϵ_y), connected in series. The indicated strain from the gage then corresponds to $(\epsilon_x + \epsilon_y)/2$, and thus to $(\epsilon_1 + \epsilon_2)/2$, regardless of the gage orientation on the test surface. Representing the gage output signal by the symbol S_G , for convenience in algebraic manipulation,

$$S_G = \frac{\epsilon_x + \epsilon_y}{2} = \frac{\epsilon_1 + \epsilon_2}{2} \quad (4)$$

$$\text{And, } \epsilon_1 + \epsilon_2 = 2S_G \quad (5)$$

Adding and subtracting with Eq. (2),

$$\begin{aligned} \epsilon_1 - \epsilon_2 &= N_s f \\ \epsilon_1 + \epsilon_2 &= 2S_G \\ \epsilon_1 &= S_G + \frac{N_s f}{2} \end{aligned} \quad (6)$$

$$\begin{aligned} \epsilon_1 - \epsilon_2 &= N_s f \\ -\epsilon_1 - \epsilon_2 &= -2S_G \\ \epsilon_2 &= S_G - \frac{N_s f}{2} \end{aligned} \quad (7)$$

In practical applications, the usual procedure is to first complete all PhotoStress observations and normal-incidence measurements (N_s) on the coated test object. Following this, separator gages are installed on the coating at the potentially critical points established by PhotoStress analysis. Loads are then reapplied to the test object, and the separator gage measurements are recorded. Individual principal strains can then be calculated as shown in Eqs. (6) and (7).

The PhotoStress Separator Gage (manufactured by Micro-Measurements Division of Measurements Group, Inc.) embodies a number of special features designed for ease of use and optimum performance in PhotoStress applications. First in importance, of course, is that the gage does not require any particular angular orientation. It is simply bonded at the point where separation measurements are desired. Preattached leadwires are provided to avoid the problems that users may have in soldering the leads to the gage before installation or, worse yet, attempting to do so after the gage is bonded to the photoelastic

coating. The gage grid is also encapsulated in polyimide to eliminate the need for protective coating in most PhotoStress applications. Gage characteristics are summarized in Table 1, and basic specifications are given in the technical data sheet enclosed in the gage package. The specifications include the effective gage factor when the gage is installed on a PhotoStress coating — accounting for the slight local reinforcement of the coating by the gage. To allow for variations in the elastic modulus and thickness of the coating, the gage factor is given with a $\pm 5\%$ tolerance. Setting the gage factor control of the strain indicator to this value automatically compensates for the local reinforcement.

Grid resistance of the separator gage is 200 ohms; and it is intended that the gage be connected to the P-3500 Static Strain Indicator through a specially designed interface module, the Model 330 (Fig. 4). The interface module is a four-channel switch-and-balance unit containing precision resistive circuits for attenuating gage excitation voltage and supplying appropriate bridge completion for the 200-ohm gage. The resulting gage current is approximately 1 mA, yielding a power level well below the threshold at which self-heating effects could destabilize the strain indication.

The Model 330 Interface Module attenuates the gage excitation voltage, and the gage output signal, by a factor of five. Designating the bridge output signal as R_s ,

$$R_s = \frac{S_G}{5} = \frac{\epsilon_1 + \epsilon_2}{10} \quad (8)$$

Thus, with the multiplier switch of the P-3500 set in the X1 position, if the unit digit of the display is interpreted as $10 \mu\epsilon$, instead of $1 \mu\epsilon$, the displayed strain equals the sum of the principal strains $(\epsilon_1 + \epsilon_2)$ directly. Letting $\Sigma \epsilon$ represent the displayed signal (with this interpretation),

$$\Sigma \epsilon = 10R_s = 2S_G = \epsilon_1 + \epsilon_2 \quad (9)$$

Substituting into Eqs. (6) and (7),

$$\epsilon_1 = \frac{\Sigma \epsilon + N_s f}{2} \quad (10)$$

$$\epsilon_2 = \frac{\Sigma \epsilon - N_s f}{2} \quad (11)$$

TABLE 1

Designation:	PSG-01-XX
Construction:	Constantan grid alloy, with polyimide backing and encapsulation.
Leadwires:	Preattached 6-in (150-mm), insulated, flexible leadwires.
Grid Configuration:	Two perpendicular linear elements, series-connected.
Gage Length:	0.063 in (1.60 mm).
Resistance:	200 ohms $\pm 0.4\%$.
Effective Gage Factor:	2.03 $\pm 5\%$.
Self-Temperature-Compensation:	Compensated for steel or aluminum — PSG-01-06 and PSG-01-13, respectively.

*The effective gage factor information supplied with the PhotoStress Separator Gage is applicable only when the gage is installed on a PhotoStress coating bonded to a test part. Because of this and its other special characteristics, the gage is intended for use only as described in this Tech Note, and is not suitable for general purpose strain measurement.

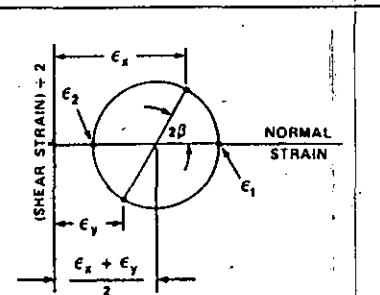


Fig. 1 — Mohr's circle of strain, illustrating the equivalence of $(\epsilon_x + \epsilon_y)/2$ and $(\epsilon_1 + \epsilon_2)/2$.

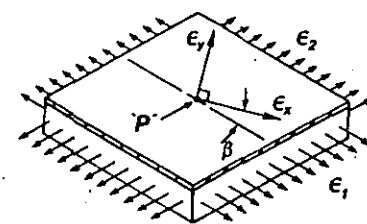


Fig. 2 — Coating surface at a selected test point, defining ϵ_x , ϵ_y , ϵ_1 , ϵ_2 .



Fig. 3 — PhotoStress Separator Gage.

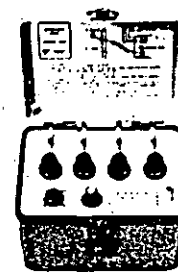


Fig. 4 — Model 330.

5.0 Corrections for Coating Effects

As noted in the preceding section, the reinforcement of the photoelastic coating by the strain gage is automatically compensated for when the gage factor control of the strain indicator is set at the value specified in the technical data sheet accompanying the PhotoStress Separator Gage. Consideration must still be given, however, to possible reinforcement effects of the coating on the test object; and, in the case of bending applications, to strain-extrapolation effects (nonuniform strain through the coating thickness).

When the test object is low in elastic modulus, or the test section is thin, a sensible fraction of the applied load may be borne by the coating, which thus acts as a reinforcement on the member. If this condition exists, strains in the test object are smaller (for a given applied load) with the photoelastic coating present than they would be without it. The resulting reinforcement error occurs both in the photoelastically measured principal strain difference ($\epsilon_1 - \epsilon_2$) and in the sum of the principal strains ($\epsilon_1 + \epsilon_2$) as measured by the PhotoStress Separator Gage.

For thin members in bending, not only is there reinforcement of the object (since the coating increases the section modulus), but the strain at the outer surface of the coating is necessarily greater than that at the test-part surface. This occurs because the strain increases linearly with distance from the neutral axis about which bending takes place. With these conditions, the observed photoelastic fringe order in the coating corresponds to the average strain through the coating thickness; i.e., to the strain at the mid-thickness. Similarly, the strain sensed by the PhotoStress Separator Gage is too great by the strain increment through the total coating thickness. This effect is referred to as a *strain-extrapolation error*, since the bending-induced strain gradient normal to the part surface is extrapolated outward through the coating.

In summary, when the elastic modulus of the test material is low, or the section thickness is small, corrections to both the photoelastic fringe order and the strain indicator reading may be required. These two sets of corrections are described separately in the following subsections.

A. Photoelastic Corrections

Well-established relationships are available to permit simple correction of measured fringe orders in either of two basic modes of loading: plane stress (flat objects with in-plane loads, thin-walled pressure vessels, etc.) and pure bending.^{4,5} The correction for plane stress can be expressed as:

$$C_{PS} = 1 + E^* t^* \quad (12)$$

where: C_{PS} = factor by which the observed fringe order in plane stress must be multiplied to obtain the corrected fringe order.

$$E^* = \frac{E_c}{E_s} = \text{ratio of the elastic modulus of the photoelastic coating to that of the specimen.}$$

$$t^* = \frac{t_c}{t_s} = \text{ratio of the coating thickness to the specimen thickness.}$$

The corresponding correction factor for applied bending moment is:

$$C_B = \frac{1 + E^* (4t^{*2} + 6t^{*2} + 4t^{*3}) + E^{*2} t^{*4}}{1 + t^*} \quad (13)$$

where: C_B = factor by which the observed fringe order in bending must be multiplied to obtain the corrected fringe order.

E^*, t^* = elastic modulus and thickness ratios as defined for Eq. (12).

Equations (12) and (13) apply specifically to cases of plane stress and pure bending, respectively. Correction methods for mixed plane stress and bending are described in References 4 and 5.

The relationships given in Figs. (12) and (13) are plotted in Figs. 5A and 5B for convenience in correcting measured fringe orders. Separate curves are provided for a number of structural materials, and for filled and unfilled plastics that are often used in structural models. Figure 5A shows C_{PS} and C_B for the epoxy family of photoelastic coatings (PS-2, PS-8, PL-1 and PL-8) where $E = 420,000$ psi (2.9 GPa). Figure 5B shows C_{PS} and C_B for polycarbonate coatings (Type PS-1) where $E = 360,000$ psi (2.5 GPa). After measuring fringe orders at selected test points on the coating, the appropriate correction factor is read directly from either Figs. 5A or 5B, and applied to the data. The corrected fringe order is then suitable for substitution into Eqs. (10) and (11). Equations (12) and (13) should be used to calculate C_{PS} and C_B when the elastic modulus of the coating differs from the values used in Figs. 5A and 5B.

B. Strain Gage Corrections

When reinforcement and strain-extrapolation errors are significant in the photoelastic measurements, they are also significant in the strains indicated by the PhotoStress Separator Gage. Separate correction factors have again been developed for the plane-stress and bending cases.

In plane stress, the correction factor for the indicated strain is the same as that for the fringe order; namely,

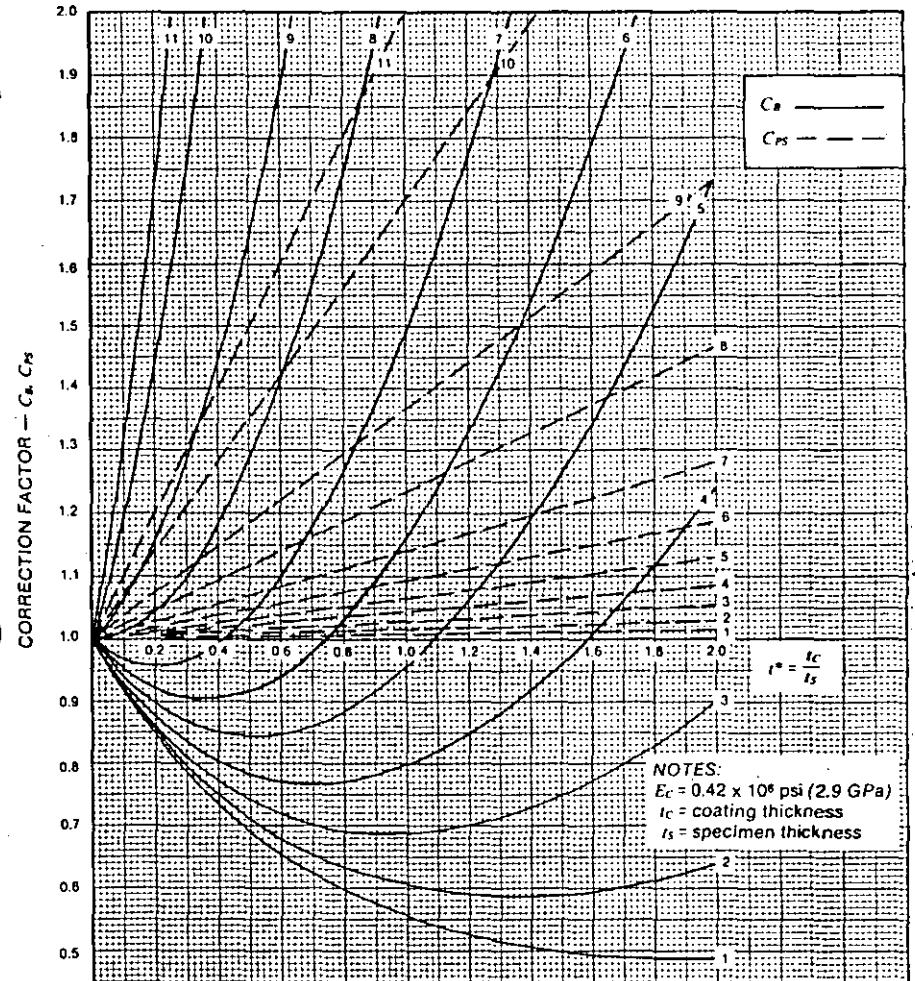
$$K_{PS} = C_{PS} = 1 + E^* t^* \quad (14)$$

where: K_{PS} = factor by which the indicated strain in plane stress is multiplied to obtain the corrected strain.

The correction factor for applied bending moment differs somewhat from the corresponding photoelastic correction because the measurement is made at the surface of the coating instead of its mid-thickness:

$$K_B = \frac{1 + E^* (4t^{*2} + 6t^{*2} + 4t^{*3}) + E^{*2} t^{*4}}{1 + 2t^* + E^* t^{*2}} \quad (15)$$

Correction is made, in either case, by multiplying the indicated strain ($\Sigma \epsilon$) by the appropriate factor. Equations (14) and (15) have been plotted in Figs. 6A and 6B (for the same materials as in Figs. 5A and 5B) to permit simple correction of the strain measurements. Figures 6A and 6B apply to the epoxy family and polycarbonate photoelastic coatings, respectively. Equations (14) and (15) should be used when the elastic



KEY:

	SPECIMEN ELASTIC MODULUS, E_s	
	in 10^6 psi;	in GPa
1 Tungsten	59	407
2 Steel	30	207
3 Cast Iron	16	110
4 Aluminum	10	69
5 Magnesium	6.5	45
6 Concrete	4.5	31
7 Reinforced Plastic	3.0	21
8 Wood	1.8	12.5
9 ModelTech — FR-10	1.15	7.9
10 ModelTech — FR-20	0.6	4.1
11 Rigid Vinyl	0.42	2.9

Fig. 5A — Correction factor C_B (bending) and C_{PS} (plane stress) for photoelastic epoxy coating Types PS-2, PS-8, PL-1, and PL-8. Multiply the observed birefringence by the appropriate factor to obtain the corrected fringe order.

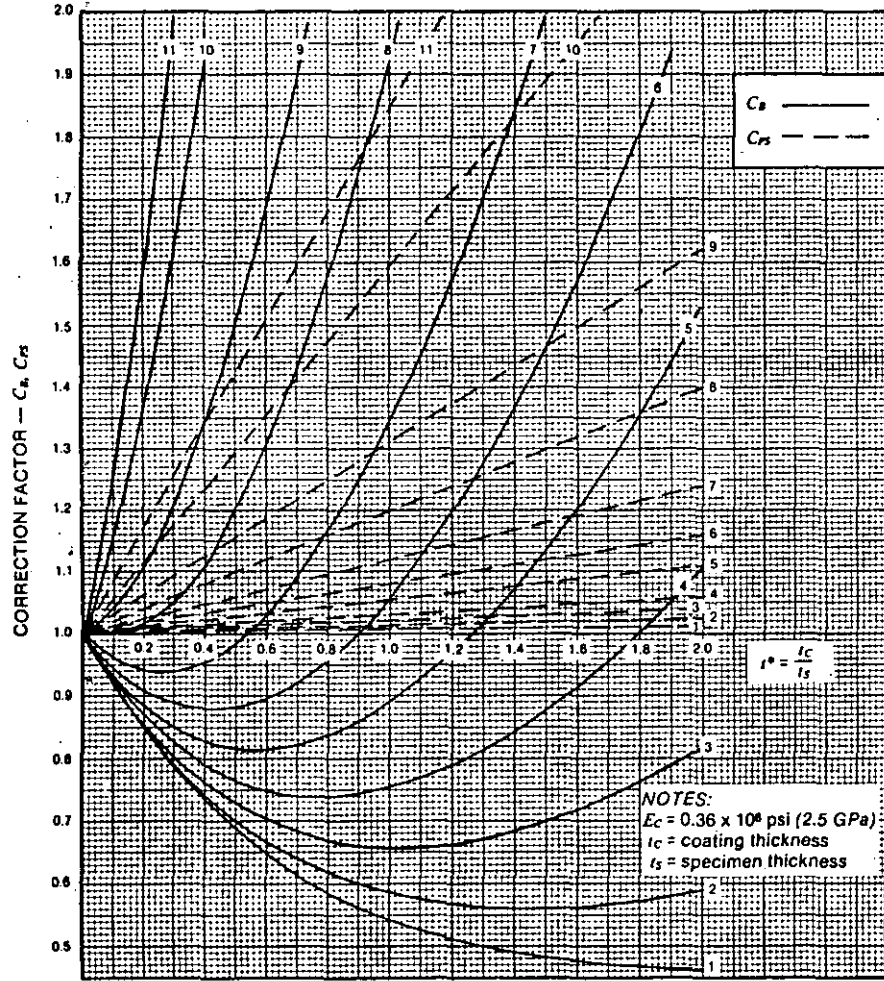


Fig. 5B — Correction factor C_B (bending) and C_{PS} (plane stress) for photoelastic polycarbonate coating Type PS-1. Multiply the observed birefringence by the appropriate factor to obtain the corrected fringe order.

KEY:

	SPECIMEN ELASTIC MODULUS, E_s	
	In 10^6 psi	In GPa
1 Tungsten	59	407
2 Steel	30	207
3 Cast Iron	18	110
4 Aluminum	10	69
5 Magnesium	6.5	45
6 Concrete	4.5	31
7 Reinforced Plastic	3.0	21
8 Wood	1.8	12.5
9 ModuTech — FR-10	1.15	7.9
10 ModuTech — FR-20	0.8	4.1
11 Rigid Vinyl	0.42	2.9

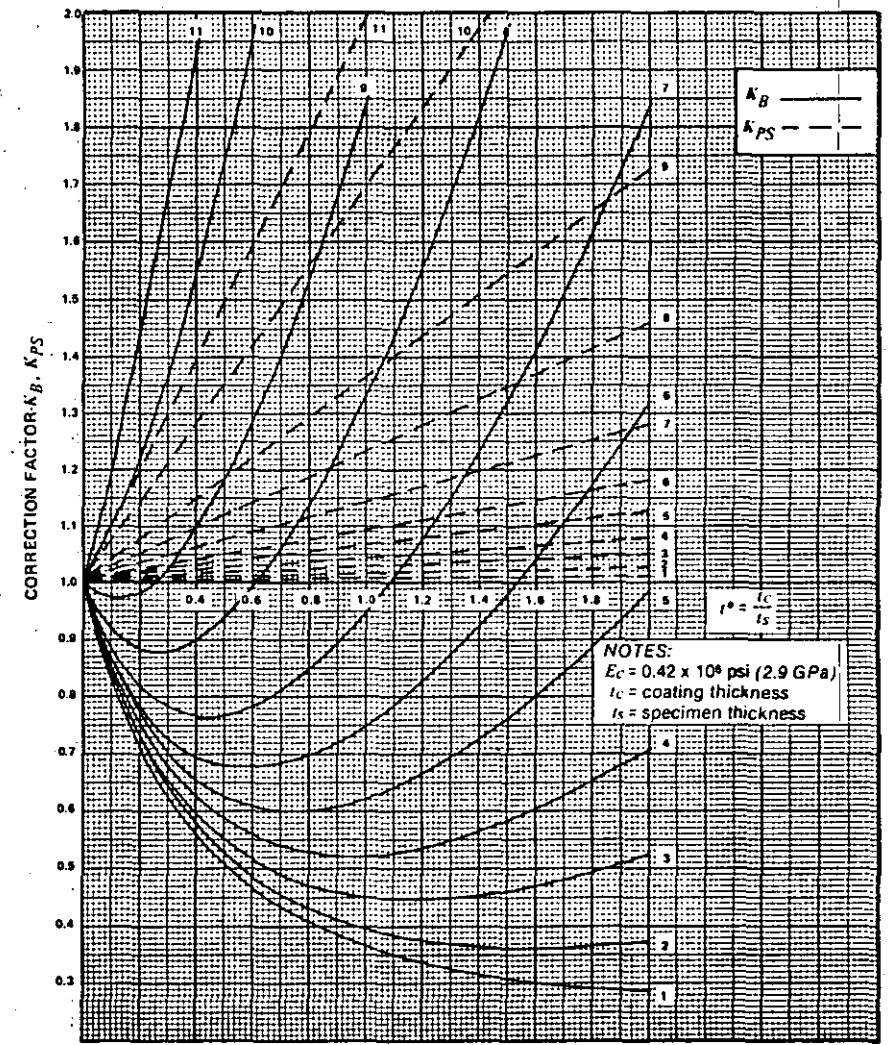
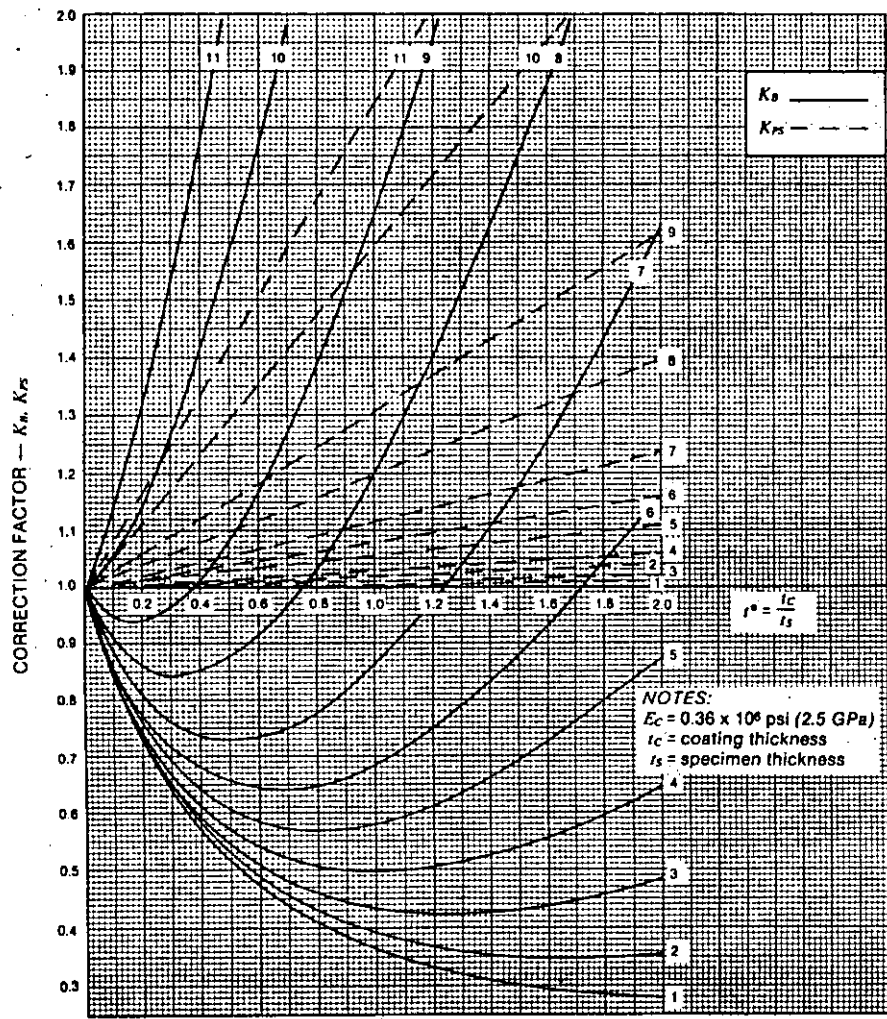


Fig. 6A — Correction factor K_B (bending) and K_{PS} (plane stress) for separator gage used with photoelastic epoxy coating Types PS-2, PS-3, PL-1, and PL-3. Multiply the measured reading by the appropriate correction factor to obtain the corrected measurement. Refer to KEY in Fig. 5B for Specimen Elastic Modulus, E_s .



NOTES:
 $E_c = 0.36 \times 10^6$ psi (2.5 GPa)
 t_c = coating thickness
 t_s = specimen thickness

KEY:	SPECIMEN ELASTIC MODULUS, E_s	
	in 10^6 psi;	in GPa
1 Tungsten	59	407
2 Steel	30	207
3 Cast Iron	18	110
4 Aluminum	10	69
5 Magnesium	6.5	45
6 Concrete	4.5	31
7 Reinforced Plastic	3.0	21
8 Wood	1.8	12.5
9 ModelTech — FR-10	1.15	7.9
10 ModelTech — FR-20	0.6	4.1
11 Rigid Vinyl	0.42	2.9

Fig. 6B — Correction factor K_B (bending) and K_{PS} (plane stress) for separator gage used with photoelastic polycarbonate coating Type PS-1. Multiply the measured reading by the appropriate correction factor to obtain the corrected measurement.

modulus of the coating differs from the values used in Figs. 6A and 6B.

After correcting both the measured fringe order and the indicated strain, the adjusted values of N_e and Σ_e are substituted into Eqs. (10) and (11) to obtain the separate principal strains. The separate principal stresses are then calculated from the biaxial Hooke's law as follows:

$$\sigma_1 = \frac{E_s}{1 - \nu_s^2} (\epsilon_1 + \nu_s \epsilon_2) \quad (16)$$

$$\sigma_2 = \frac{E_s}{1 - \nu_s^2} (\epsilon_2 + \nu_s \epsilon_1) \quad (17)$$

where: σ_1, σ_2 = principal stresses.

E_s, ν_s = elastic modulus and Poisson's ratio of test material.

C. Imposed Deformation Loading

Some structural components are loaded, or deformed, to prescribed shapes by imposing in-plane (plane stress) or out-of-plane (bending or flexural) deformations. When the imposed deformations are in-plane, the strain field is effectively the same in the coated and uncoated parts and no corrections to experimental measurements are required. However, when out-of-plane deformations are imposed, the new correction factors C_{BA} and K_{BA} differ from C_B and K_B as defined in Eqs. (13) and (14). From References 4 and 5:

$$C_{BA} = \frac{t_s}{t_c + 2\delta} \quad (18)$$

and by similar analysis:

$$K_{BA} = \frac{1}{2} \frac{t_s}{t_c + \delta} \quad (19)$$

where: t_c, t_s = coating and specimen thicknesses.

δ = distance from coating/part interface to neutral axis of coated part (calculable per Ref. 5).

Values of C_{BA} , per Eq. (18), are plotted in Fig. 7 for the same eleven specimen materials considered in Figs. 5 and 6. The broken lines show C_{BA} for polycarbonate photoelastic coatings (Type PS-1) and the solid lines are for the epoxy family of photoelastic coatings (PS-2, PS-8, PL-1, and PL-8). As shown in Fig. 7, C_{BA} is relatively independent of the type of coating applied to metal specimens; however, C_{BA} is dependent on the type of photoelastic coating when the test objects are made from the lower modulus plastics.

Separator Gage correction factors K_{BA} , per Eq. (19), are plotted in Fig. 8 and for practical engineering applications the K_{BA} for the epoxy family and polycarbonate coatings can be considered as equal. Calculation shows a worst case difference of only 3% for rigid vinyl and approximately a 1-1/2% difference for magnesium. No attempt is made in Fig. 8 to reflect these small variations. Equations (18) and (19) should be used when the elastic modulus of the coating differs from the values used in Figs. 7 and 8.

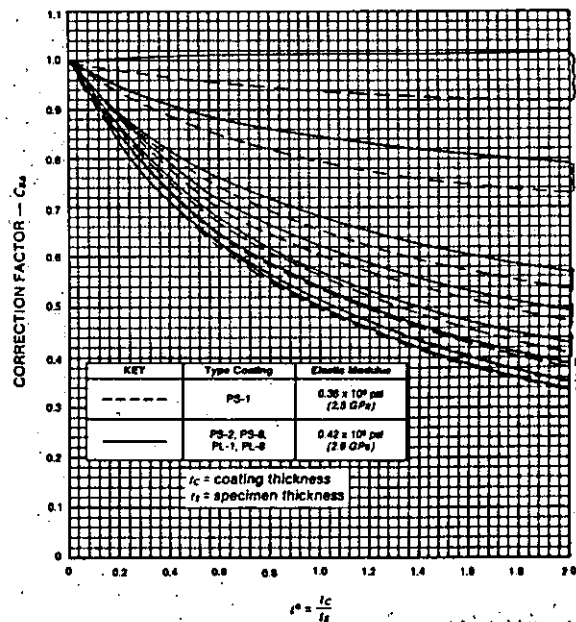


Fig. 7 — Correction factor C_{BA} (imposed curvature) for photoelastic coatings. Multiply the observed birefringence by the appropriate factor to obtain the corrected fringe order. Refer to KEY in Fig. 6B for Specimen Elastic Modulus, E_s .

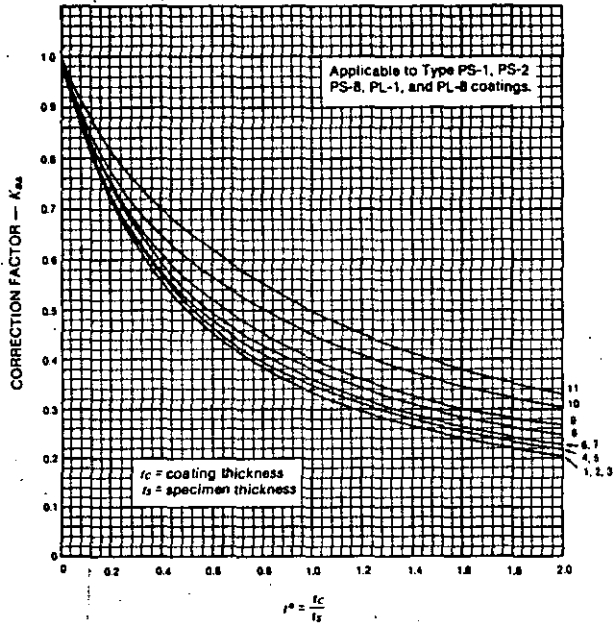


Fig. 8 — Correction factor K_{BA} (imposed curvature) for Separator Gage. Multiply the Separator Gage strain measurement by the appropriate factor to obtain the correct strain. Refer to KEY in Fig. 6B for Specimen Elastic Modulus, E_S .

6.0 Numerical Examples

The following numerical examples are provided to illustrate the data-reduction procedures for calculating the separate principal stresses from the combined photoelastic and separator strain gage measurements. The first example is representative of typical applications where there is no perceptible reinforcement of the test object by the PhotoStress coating. Two further examples show how to correct the measured photoelastic and strain gage data when reinforcement and strain-extrapolation effects are present.

Example 1

Assume that portions of a heavy steel structural member have been coated with Type PL-1 photoelastic plastic, 0.075 in (1.9 mm) thick. The fringe value (f) for the coating is 1513 $\mu\epsilon$ /fringe. Using the Model 031 Reflection Polariscopes, the normal-incidence measurement at a point of interest on the coating yields a reading of 2.1 fringes (N_n). The load is then removed from the member, and a PhotoStress Separator Gage is installed on the coating at the same point. Gage orientation is arbitrary, since the sum of any two perpendicular strains is equal to the sum of the principal strains.

The strain gage is connected to the P-3500 Strain Indicator through the Model 330 Interface Module and the instrument is

balanced to zero indication for the no-load condition. With the multiplier switch of the P-3500 set at X1, the same load is reapplied to the structural member, after which the indicated strain ($\Sigma_\epsilon = 10$ times the display reading) is 520 $\mu\epsilon$. In this case, it is not necessary to correct either N_n or Σ_ϵ for reinforcement or strain-extrapolation errors, since the effect of the coating on the elastic response of the structure is negligible. Substituting f , N_n , and Σ_ϵ into Eqs. (10) and (11),

$$\epsilon_1 = \frac{520 + 2.1 \times 1513}{2} = 1849 \mu\epsilon$$

$$\epsilon_2 = \frac{520 - 2.1 \times 1513}{2} = -1329 \mu\epsilon$$

These principal strains are then substituted into biaxial Hooke's law to determine the principal stresses:

$$\sigma_1 = \frac{E_S}{1 - \nu_S^2} (\epsilon_1 + \nu_S \epsilon_2)$$

With $E_S = 30.0 \times 10^6$ psi (207 GPa), and $\nu_S = 0.29$,

$$\sigma_1 = \frac{30 \times 10^6}{1 - (0.29)^2} (1849 - 0.29 \times 1329) \times 10^{-6}$$

And,

$$\sigma_1 = 47\,940 \text{ psi (330 MPa)}$$

$$\sigma_2 = \frac{30 \times 10^6}{1 - (0.29)^2} (-1329 + 0.29 \times 1849) \times 10^{-6}$$

And,

$$\sigma_2 = -25\,970 \text{ psi (-179 MPa)}$$

Example 2

Assume, for this example, a flat aluminum-alloy specimen 0.125 in (3.18 mm) thick, coated with PL-1 photoelastic plastic 0.090 in (2.3 mm) thick. The fringe value of the coating is 1261 $\mu\epsilon$ /fringe. With purely in-plane loads applied to the specimen (plane stress), the uncorrected normal-incidence photoelastic measurement (N_n) at the test point is 1.5 fringe. Following the procedure described in Example 1, a PhotoStress Separator Gage is installed on the coating at the same point, and the uncorrected indicated strain (Σ_ϵ), after reapplying the load, is +800 $\mu\epsilon$.

Since it can be suspected in this instance that the coating may sensibly reinforce the test specimen, the photoelastic and strain gage measurements should be corrected using the plane-stress correction factors C_{PS} and K_{PS} from Figs. 5A and 6A, respectively. For this purpose, it is first necessary to calculate the thickness ratio, r^* :

$$r^* = \frac{t_c}{t_s} = \frac{0.090}{0.125} = 0.72$$

Then, from Fig. 5A, the correction factor C_{PS} for the observed fringe order is 1.03, representing a modest 3% reinforcement effect. Since $K_{PS} = C_{PS}$, the same correction factor applies to the indicated strain from the PhotoStress Separator Gage as well.

Thus, $N_n = \hat{N}_n \times 1.03 = 1.5 \times 1.03 = 1.55$ fringe

$$\Sigma_\epsilon = \hat{\Sigma}_\epsilon \times 1.03 = 800 \times 1.03 = 824 \mu\epsilon$$

where: \hat{N}_n , $\hat{\Sigma}_\epsilon$ = observed (uncorrected) values of the variables.

Calculating the principal strains from Eqs. (10) and (11),

$$\epsilon_1 = \frac{824 + 1.55 \times 1261}{2} = 1389 \mu\epsilon$$

$$\epsilon_2 = \frac{824 - 1.55 \times 1261}{2} = -565 \mu\epsilon$$

And, substituting into Eqs. (16) and (17), with $E_S = 10 \times 10^6$ psi (69 GPa) and $\nu_S = 0.32$, the principal stresses are:

$$\sigma_1 = \frac{10 \times 10^6}{1 - (0.32)^2} (1389 - 0.32 \times 565) \times 10^{-6}$$

And,

$$\sigma_1 = 13\,460 \text{ psi (93 MPa)}$$

$$\sigma_2 = \frac{10 \times 10^6}{1 - (0.32)^2} (-565 + 0.32 \times 1389) \times 10^{-6}$$

And,

$$\sigma_2 = -1340 \text{ psi (9.2 MPa)}$$

Example 3

To permit ready comparison between coating effects in plane stress and those in bending, this example assumes the same specimen as in Example 2, with all of the same parameters, except that the specimen is subjected to pure bending. The observed photoelastic and strain gage measurements are also assumed the same.

With $r^* = 0.72$, reference to Fig. 5A gives the bending correction factor C_B for the fringe order as 0.76. The corrected fringe order is then:

$$N_n = \hat{N}_n \times C_B = 1.5 \times 0.76 = 1.14 \text{ fringe}$$

Similarly, the bending correction factor K_B for the strain indication is read from Fig. 6A as 0.54, from which:

$$\Sigma_\epsilon = \hat{\Sigma}_\epsilon \times K_B = 800 \times 0.54 = 432 \mu\epsilon$$

The principal strains are:

$$\epsilon_1 = \frac{432 + 1.14 \times 1261}{2} = 935 \mu\epsilon$$

$$\epsilon_2 = \frac{432 - 1.14 \times 1261}{2} = -503 \mu\epsilon$$

And the corresponding principal stresses become:

$$\sigma_1 = \frac{10 \times 10^6}{1 - (0.32)^2} (935 - 0.32 \times 503) \times 10^{-6}$$

And,

$$\sigma_1 = 8620 \text{ psi (59 MPa)}$$

$$\sigma_2 = \frac{10 \times 10^6}{1 - (0.32)^2} (-503 + 0.32 \times 935) \times 10^{-6}$$

And,

$$\sigma_2 = -2270 \text{ psi (-15.6 MPa)}$$

A comparison of Example 3 with Example 2 illustrates that, for this case, the coating effect in bending is much greater than in plane stress. That this is a common situation for low-modulus or thin test objects can be judged from the nature of the correction-factor curves in Figs. 5 and 6. It is also evident from these examples that the error can be quite large if not corrected.

7.0 Application Notes

Complete instructions for the proper use of the PhotoStress Separator Gage and the Model 330 Interface accompany these products. Careful attention to the recommendations in the instruction bulletins will help assure accurate, reliable data.